



IULTCS CONGRESS 2019

**“BENIGN BY DESIGN”
LEATHER — THE FUTURE THROUGH
SCIENCE AND TECHNOLOGY**

**JUNE 25–28, 2019
DRESDEN – GERMANY**

PROCEEDINGS

www.iultcs2019.org
www.iultcs.org



**INTERNATIONAL UNION
OF LEATHER TECHNOLOGISTS
AND CHEMISTS SOCIETIES**



Imprint

Publisher

Verein für Gerberei-Chemie und -Technik e. V.
Meißner Ring 1–5
D-09599 Freiberg

Designer and Editor

599media GmbH
Platz der Oktoberopfer 5
D-09599 Freiberg

FILK GmbH
Meißner Ring 1–5
D-09599 Freiberg

The authors acknowledged are responsible for the content of the contributions.
The publisher does not take any responsibility for the correctness of the abstracts
or for respecting the rights of third parties.

© 2019 VGCT

Email: info@vgct.de
www.iultcs2019.org



QR-Code:
Proceeding Book
of abstracts



HEIDEMANN LECTURE

AS TOUGH AS LEATHER: MACRO TO NANO SCALE PERSPECTIVES OF COLLAGEN STABILITY

K. L. Goh^{1,2,3}

*1 Newcastle Research & Innovation Institute, Singapore
80 Jurong East Street 21, #05-04, Singapore 609607.*

*2 Newcastle University in Singapore
172A Ang Mo Kio Avenue 8 #05-01, Singapore 567739*

*3 Faculty of Science, Agriculture and Engineering
Newcastle University, Newcastle Upon Tyne, NE1 7RU, UK*

a)Corresponding author: kheng-lim.goh@newcastle.ac.uk

Abstract. Leather is a fairly durable and flexible material. Created by tanning animal rawhides and skins, it can be found in many household and personal products. Collagen, one of the major components found in skin, serves an important function in leather—to provide mechanical support by withstanding loads acting on the material. The purpose of this paper is to discuss the basis of the mechanical stability of collagen from macro to nano scale that underpins the functional significance of collagen. There are several types of collagen but the one this paper is interested in are those that participate in higher-order assemblies such as networks, filaments, microfibrils, fibrils, fibres/fascicles. These assemblies collectively form a hierarchical architecture in the tissue from the molecular level to the macroscopic level. The functional significance of collagen is a subject of on-going research as the knowledge gained can direct the development of new technology, e.g. leather design and production. In this paper, the findings related to the mechanical stability of the biological material are highlighted with the help of a recently proposed structure-mechanical framework, underpinning the hierarchical architecture of the collagenous material.

1 Introduction

Biomechanical engineers tend to regard soft connective tissues such as tendons, ligaments and skin as biological examples of fibre reinforced composites comprising collagen fibrous structures embedded in a hydrated proteoglycan-rich extracellular matrix (ECM) [1]. With a remarkable high tensile stiffness and strength, these collagen fibrous structures are responsible for withstanding external loads that act on the tissue [2]. From a fibre composite perspective while the mechanical properties of the tissue are attributed to collagen, it is important to emphasize that the interfibrillar matrix (1) facilitates the load transfer from the hydrated PG-rich matrix (the weak phase) to collagen (the strong phase), (2) minimizes direct contact between fibres by ensuring that the individually fibres are separated, which can in turn prevent a brittle crack from passing completely across a section of the composite, (3) protects the surface of the individual fibres otherwise the fibre surface may experience abrasion by direct sliding contact and this could compromise the mechanical properties.

Animal hides and skins are tough and strong materials. Transforming these raw materials from into a variety of useful as well as desirable products involves a chain of processes. Several processes involve subjecting the collagen in the materials to chemical and mechanical modifications—to treat and soften the hides—while minimising possible damage to the properties of toughness and strength of the hide. There is also a need to design efficient methods that are environmentally sustainable for processing leather. At the tannery, often a significant amount of water, as well as chemicals which are toxic and environmentally undesirable, is used, but the carbon footprint is further enlarged as energy is also required to drive these chemical reactions [3].

Collagen molecule is composed of three polypeptide chains exhibiting a triple-helical structure, and the molecule is often referred to as tropocollagen molecule. How the tripeptides contribute to the stability of the collagen molecule has been a subject of great interest in the 70's from the perspective of fundamental research [4]. As pointed out by Professor Eckhart Heidemann, among the three areas of research in leather science, namely technique application, product/process development and fundamental research, the last is recognised as the necessary basis for the discovery of new products especially where it can produce relevant new insights in relation to the practice [5]. Professor John Ramshaw has addressed an up-to-date landscape of the key areas of the biochemistry and structural biology of collagen in a previous Heidemann lecture. As a continuation of this subject, this paper discusses recent findings on the role of collagen in regulating the mechanical stability of the biological material as follows

- (1) Physicochemical factors affecting collagen stability;
- (2) Mechanics of collagen: stability and cross-links;
- (3) Hierarchical architecture of collagen.

The recent findings are important because they have been carried out using new technology and more accurate methodology. This is expected to encourage further development of leather product to optimize for collagen stabilization and achieve a more sustainable future for the leather industry.

2 Physical and chemical factors affecting collagen stability

2.1 Overview

This section briefly highlights the similarities and differences between skin and leather in order to lend support to biomechanics-related arguments for establishing a simple picture of the mechanical stability in the leather. With regard to mechanical stability, the subjects of discussion are leather processing, and agents of deterioration namely heat and mechanical wear. With regard to heat, the discussion on deterioration effects is complemented by highlights on some recent findings on tanning process as a protection against heat. With regard to mechanical wear, the discussion is on structural changes and corresponding mechanical changes when leather is in service, complemented by differentiating these effects from mechanical treatment to leather during processing. Obviously deterioration due to heat and mechanical wear are two of the many factors; the other factors are oxidation, metals and salts, and water.

2.2 Extracellular matrix of skin versus leather

As you probably do not need reminding, collagen makes up the bulk of ECM of skin (as well as tendons and ligaments), amounting to about 70–80% of the dry weight of the skin [6, 7]. So how different is leather collagen structure from skin? The processing of skin leading to leather—the common stages being fresh green, salted, pickled, pretanned, wet blue, retanned, dry crust, dry crust staked[8]—removes many ECM components, e.g. epidermal cells, proteoglycans, elastin, but collagen appears not to be dramatically affected by the processing, even after liming, bating, and pickling are applied [9]. (NB: Elastin, an ECM component in skin well-known for providing the elastic properties of skin, may not have a significant effect on the leather mechanical properties as elastin degradation, e.g. elastin removal by elastase, in leather did not lead to a significant change in the stiffness, tensile strength and extensibility [10].) The collagen fibrils now become connected by synthetic chemical bonds as well as natural chemical bonds. These bonds may enhance the yield strength of the leather because the fibrils may be unable to slide past one another easily. However, these bonds may also undesirably stiffen the material; thus glycerol is introduced into the interfibrillar matrix during fat liquoring (Liu, 2003). The final product leads to two distinct layers in

the leather which are vaguely related to the dermis of skin: a fine densely packed fibrous layer and coarser layer which we refer to as the grain and corium layers respectively. Much of the organisation of collagen found in skin is retained in these layers; in skin the fibres (and fibrils) are oriented according to the Langer lines [11]. The other features of collagen fibrous structures in the skin namely high slenderness and characteristic light-dark bands referred to as the D-periods on the structure [6], are also retained in leather. Knowledge on the differences and similarities between skin and leather are important as it will enable us to know how structure of skin influence the properties and performance of leather.

2.3 Chemical processes

The general mechanical response of connective tissue when subjected to an external load follows the stress-strain profile that is depicted in Figure 1. As pointed out in previous section, there are 8 main stages of processing leather from skin, namely fresh green, salted, pickled, pretanned, wet blue, retanned, dry crust, dry crust staked. How do the stress-strain profiles look like for leather during the different stages of processing? It turns out that the stress-strain curve varies dramatically with the respective stages as reported by Sizeland and co-workers (Sizeland et al., 2015). Note that the analysis is not entirely complete as the authors did not carry out test on skin-related specimen, so it is not possible to know how much of the mechanical behaviour of skin has changed after leather processing.

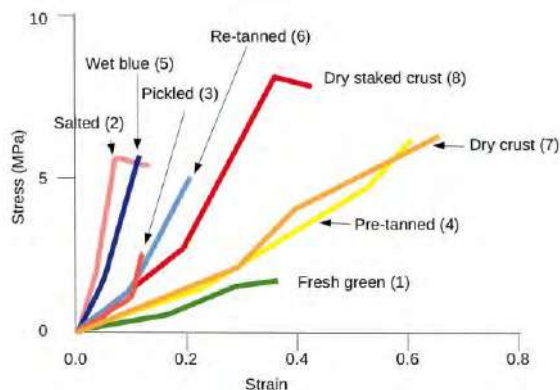


Fig. 1. Sketch of stress versus strain curves of leather material at different processing stages (labelled 1-8). Thereafter, all references to these stages in the main text are labelled as #1 (fresh green), #2 (salted), #3 (pickled), #4 (pre-tanned), #5 (wet blue), #6 (re-tanned), #7 (dry crust), #8 (dry staked crust). The stress-strain curves were derived from ovine skin. The curves were intended for a very general comparison of the shapes because the tests were carried out with no specific considerations for the orientation of the material to account for collagen fibril direction; an absolute comparison of the magnitudes of the stresses and strain is not possible [8]. Reprinted (adapted) with permission from Sizeland KH, Edmonds RL, Basil-Jones MM, Kirby N, Hawley A, Mudie S, Haverkamp RG: Changes to Collagen Structure during Leather Processing. *Journal of Agricultural and Food Chemistry* 2015, 63(9):2499-2500. Copyright (2015) American Chemical Society

Nevertheless, it is easy to point out the similarities with regard to the features, namely the existence of a toe region, non-linear (attributing to elasticity-related mechanisms) region in the low stress region, point of inflexion (attributing to failure mechanisms, such as yielding, leading to plasticity) at higher stress region and abrupt reduction in stress as the material breaks apart, beyond the maximum stress point. These features are reflected in skin [12] as well as ligaments [13] and tendons [14]. The more interesting observations are the effects from the various processing stages as reflected in the extents of the stress and strain, as well as the stiffness at low stress regions (Fig. 8). The different effects arising from the variety of processes underpin the collagen mechanical

stability at different hierarchical levels (section 0). Unfortunately, current findings of how the stress-strain behaviour leather changes during processing, by attributing to the collagen fibril alignment (fibrillar level) [8] and collagen D-spacing (molecular level) [8], does not lend to a complete understanding as the effects at the other hierarchical levels in leather are still not clear. These are important considerations for further study especially where newer findings, such as new fat liquoring agents [15], and recommendations to lower the amount of chromium use in stabilizing collagen [16], are recently proposed.

2.4 Thermal degradation

How does high temperature affect the mechanical stability of leather? There are many studies on high temperature effects, covering hydrothermal effects and shrinkage temperature {Kite, 2006 #5606}. Here, this section focuses on changes at the molecular level, addressing how the collagen molecular structure is affected. The basic mechanics at elevated temperature, e.g. at 120 °C, involves alteration (mainly shortening) to the D-period, as seen in dry collagen [17], possibly contributed by the shortening of the pitch of the collagen helix but predominated by axial sliding of molecules [17]. further shortening of the D period occurs [17]. The reversibility of the effects depends on the temperature: low temperatures produce effects (attributing to molecular unfolding occurring locally, i.e. possibly resulting from a small proportion of hydrogen bond ruptures) which are reversible [18]; high temperatures produce effects (the molecule unfolds into a random (coiled) structure) which are irreversible [18]. Elevated temperature effects appear to be time-dependent: the longer the duration in which it is subjected to elevated temperature, the higher the degree of randomness in the structure [18]. The mechanics of unfolding points to the disruption to the hydrogen bonds that binds the helices [18]. At the macroscopic level, the molecular changes may not affect the bulk mechanical properties appreciably at short heating duration [19]; interestingly, Weadock has reported that long duration results in increase extensibility, fracture strength and stiffness of the tissue [20].

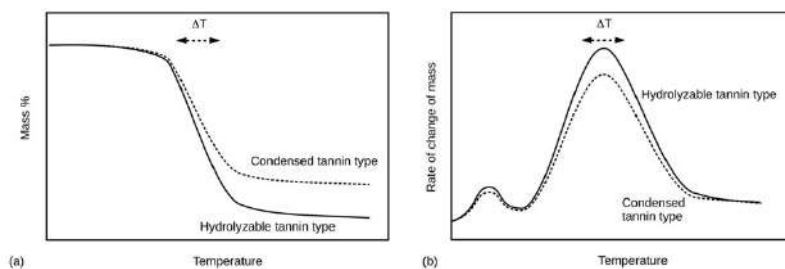


Fig. 2. Sketch of graphs of (a) mass loss and (b) rate of change of mass versus temperature to illustrate how tannin type affects the thermal stability of leather. Here ΔT represents a range of temperatures. For instance, in a previous study [21], $\Delta T = 300\text{-}400\text{ }^{\circ}\text{C}$ (for the details of the experimental findings see Sebestyen et al. [21]).

Tanning is intended to stabilise the collagen molecule by creating a more permanent bonding between the helices [21, 22]. The degree of stability depends on the tannin molecule with condensed tannin type being more superior than hydrolysed tannin type; the former yields lower mass loss (TGA curves) and smaller rate of mass loss (DSC curves) over a range of high temperatures [21] (**Fig. 2**). Currently findings of what really happened during heating by attributing to collagen molecular level effects, i.e. mechanics of bonding, does not lend to a complete understanding as the effects at the other hierarchical levels in leather are still not clear.

2.5 Mechanical wear and tear

How mechanical loading affects the mechanical stability of collagenous material such as leather has been dealt with in studies on (i) leather processing and (i) leather during service.

Repeated loading that form part of leather processing namely milling and staking is intended to yield the desired softness in leather [23]. Milling is likened to a preconditioning process to ensure consistency of results, borrowing from biomechanical testing of soft tissue [24], prior to the leather being deployed for use. At the macroscopic level, analysis of the hysteresis curve revealed that a milled leather results in smaller energy loss than unmilled leather [23]. As the number of cycles increases, the strength increases but the strain at fracture decreases [25] (Fig. 3 b). Clearly there is an optimal level to achieve high strength without compromising too much on reduction in the extensibility. At the fibrillar level, milling ensure that collagen fibrils are recruited into the desired orientation. At the tropocollagen molecular level, the cyclic stress experiences by a dry leather may minimise hydrogen bonding within the fibrils.

Static stretching of leather material, along its long axis (parallel to the backbone), to a desired length and maintaining the leather in this state over time has been proposed as part of a leather processing stage (namely during the wet blue stage) intended to achieve maximal area [26], which is important for optimising the profit, with consequential enhancement to collagen mechanical stability. At the macroscopic level, stretched leather stiffness is dramatically higher (particularly those treated to low angles with respect to the long axis) than those without pre-strain; the stiffness increase also depend on the amount of stretch applied during the pre-strain treatment [26]. At the fibrillar level, this is explained by the result of fibrils oriented predominantly along the pre-strain axis.

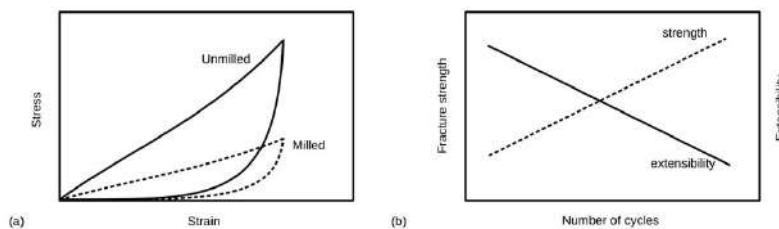


Fig. 3. Sketch of graphs of (a) stress versus strain (the stress is of the order of 10^6 Pa as reported elsewhere [23]) and (b) fracture strength versus number of loading cycling.

Tearing could occur when the leather is in service. In the latest attempts to understand the mechanical stability of collagenous materials, like leather, to resist tearing, Kelly and co-workers found that there was an appreciable difference in the tear strengths (whether torn in parallel or perpendicular to the backbone) in leather (tanned) processed without strain and leather prepared by tanning under strain; the tear strength increases in both direction [27]. This finding is important because it correlates to orientation changes at the fibrillar level whereby a greater degree of alignment was observed with pre-stretched leather compared with unstretched leather [27]. Of note, it has been pointed out that tannins may help to increase wear resistance. This is because hydrolysis of tannins, which can occur within the leather and is not desirable from the point of view as a loss of tanning material, results in carboxylic acid moieties by-products which is deposited in the tanning pits and this may contribute to the water resistance and wear properties of the leather [28].

3 Collagen mechanics in relation to stability and cross-links

3.1 Overview

This section is intended to highlight how the interfibrillar matrix, collagen volume fraction, fibril orientation as well as other individual fibril characteristics, and, finally, interfibrillar cross-links influence the mechanical stability of collagen.

3.2 Interfibrillar matrix

The interfibrillar matrix in ECM of tendons, ligaments, dermal skin may be regarded as a hydrated proteoglycan-rich ground substance which serves to hold the collagen fibrils together. Specifically, the interfibrillar matrix (1) protects the collagen fibrils from mechanical damage, (2) binds the fibrils and (3) provides a medium for load transfer from the interfibrillar matrix to the collagen fibrils [1, 2, 29]. Thus it is important to be able to measure the mechanical properties of the matrix to investigate the extent of some, if not all, of these assumptions.

A useful model for understanding the interfibrillar matrix is the rule-of mixture, complemented by the shear-lag model. Let E_{CT} and E_{cf} be the moduli of elasticity of the tissue and collagen fibril, G_m be the shear modulus of the interfibrillar matrix, V_f and V_m be the volume fractions of collagen and the interfibrillar matrix, L_f be the fibrillar length, and A_f , r_f and R be the fibrillar cross-sectional area, fibrillar radius and inter-fibrillar distance, respectively. To order-of-magnitude, according to the rule-of-mixtures for stiffness, estimates of the interfibrillar matrix stiffness (E_m) may be derived from the mathematical model,

$$E_{CT} = E_{cf}V_{cf}a + E_mV_m, \quad (1)$$

where the coefficients,

$$a = [1 - \tanh(bL_f)] / [bL_f], \quad (2)$$

is derived from the Cox shear-lag model [30], and

$$b = \sqrt{([G_m/E_{cf}][2\pi/A_f]/\log_e(R/r_f))}, \quad (3)$$

is an important parameter that is used to describe the effective length of the fibril, $L_f^1 = bL_f$ [31].

Of note, the larger the value of G_m/E_{cf} the more rapidly the stress in the fibril increases with distance from the fibril end and consequently, higher E_{CT} .

Moisture absorption by leather material confers flexibility to the material. In connective tissues such as tendons, deformation at the interfibrillar matrix level is correlated to the deformation at tissue level. [32-35]. Deformation at the interfibrillar matrix is regulated by interfibrillar shearing (by shear-lag mechanism or even shear-sliding mechanism); this involves transferring stress from the matrix to collagen fibrils [33, 34]. Since the interfibrillar matrix of tendon is highly hydrated, it suggests that water plays an important role in the flexibility of the tissue by provides a lubricating effect in collagen fibrils. A similar conclusion is recently established for leather: Kelly and co-workers further suggested that moisture absorption could result in a larger lateral spacing between collagen molecules in fibrils [36]. This conclusion should provide important consideration for leather processing, because it is known that salting (#2) causes dehydration to some extent.

But what is the nature of the interfibrillar matrix? To address this question we note that the various reactions occurring during the processing of leather would breakdown and remove a lot of the native interfibrillar matrix components, such as proteoglycans, and replaced by chemicals used in leather processing. For instance, glycosaminoglycans and other components are removed during the pickling stage (#3) [8]. Since some, not all, of these non-fibrous ECM protein molecules that were depleted from the ECM could be responsible for regulating the interfibrillar shear mechanics

and the stress transfer mechanisms [8], one would expect to introduce a compensatory approach to restore the material properties. This is covered in two ways: tannins and fat liquoring (tanning stage #6, the two components are introduced to soften the material), collagen cross links (pretanned stage #4, where collagen fibrils are cross-linked) [8], as well as water (when in service) and fats/oils and waxes (after tanning) [37]. At normal environmental conditions, water present in the leather may be categorised into two groups: multilayer water and molecularly bound water [37, 38]. The former, which is regarded also as free water, is believed (1) to be localized within the interfibrillar space in the form of multilayers; (2) to exist bound to proteins as monolayer layer; (3) to be held by mixture of strong and weak bonds (such as hydrogen and van Der Waals); (4) to be made up of about 15% volume fraction, at a relative humidity of 65% [37]. It is believed that loss of the free water may result in leather stiffness but this is reversible as long as the collagen structure is not significantly damaged during loading [37]. The latter, i.e. bound water, is present in the collagen in such a way that it is not available for dissolving electrolytes [37]. Thus, it is the multilayer water, tannins and other chemicals (i.e. present due to fabrication and use) in the interfibrillar matrix which may be regarded as substitutes for the original interfibrillar matrix, to facilitate the interfibrillar shear (i.e. shear-lag and shear-sliding, as described by eq.s (4) and (5), respectively in the following section). Deterioration of the interfibrillar matrix may occur when the leather is in service, e.g. attacked of the tanning agents by radical mechanisms during photochemical reactions [39]. This may compromise collagen stability: in the presence of a degraded interfibrillar matrix, when leather is subjected to external loads, high frictional stress could be generated between the fibrils as the fibrils attempt to slide pass one another.

3.3 Collagen

3.3.1 Collagen volume fraction

Collagen volume fraction, V_f , is a measure of the total volume of collagen in the tissue specimen with respect to the total volume of the tissue. V_f is an important parameter as it modulates the stiffness and strength of the tissue according to the rule of mixture for the respective mechanical properties. V_f could change with age and age-related changes as such could result in changes in the mechanical properties; in age-varying tendons, the strength and stiffness increase linearly with V_f [40]. These changes may be indirectly affected by sex hormones, such as estrogen and androgen, e.g. in the tissue of skin and gingival fibroblasts [41], which are responsible for (i) regulating proteoglycan turnover (which in turn may influence the fibril size) and (ii) hydroxyproline content; the latter is probably more important because it is a major component of collagen and any changes would directly influence collagen stability [41]. Indications of changes in V_f may be observed in changes in the fibril-bundle packing [41], fibril packing [41, 42], state of hydration [43] and Poisson's ratio of the collagenous material undergoing deformation under external load [44]. With regard to the collagen fibril-bundle, in young individuals, the bundles are tightly packed from the papillary to the deep dermis. With age, the bundle thickness increases and bundle packing density decreases in the dermis [41]; there is no appreciable change in the thickness of the bundles in the papillary dermis [41]. It is important to note the underpinning arguments for the changes in V_f in the physical feature (i.e. fibril packing) processes (state of hydration, and deformation mechanics parameterized by Poisson's ratio) arise from different causes: (1) the changes in fibril packing within bundles underpins changes in fibril-fibril interactions [42]; (2) the hydration process underpins the spacing between fibrils, as well as the gaps between the tropocollagen molecules, depending on how much water is expelled [43]; (3) the Poisson effect underpins the extent of cross-links between the collagen molecules in the lateral and longitudinal direction of the molecules [44].

3.3.2 Collagen fibril network

The network of collagen fibrils in dermal tissue features a somewhat randomly aligned state. However, when the tissue is deformed under a tensile load, the entire network can be recruited in tension by realigning the fibrils through a significantly large angular displacement, e.g. 50 degree, in the direction of the applied load [45]. Collagen is mechanically stabilised in this way for as long as the load does not exceed the fracture strength. Since the degree of fibril orientation determines the tear strength of the leather [27], high tensile strength may be achieved for the finished product which possessed highly aligned fibrils (if the strength is measured in the stretched direction of the load) [46]. The tensile strength depends on the direction of loading on the leather material in leather with highly aligned fibrils (Fig. 4a). The tensile strength, as well as stiffness, decreases as the angle of loading (with respect to the backbone) increases [26, 47],.

However, finished products of leather with highly aligned fibrils may not be desirable, especially if looseness occurs, a defect which (can be detected during quality control) decreases the product value because it does not make the leather look good. Some parts of a hide, namely shoulders and flanks, can give rise to looseness [46]. The highly aligned fibrils in loose leather occur throughout the thickness of leather, compared to tight leather [46]; loose leather is also found to have less densely packed fibrils, particularly in the lower grain region [46]. While the tear strength in the direction parallel to the aligned fibrils is high, the tear strength in the direction perpendicular to the aligned fibrils is low [27]. It is found that the looseness manifests during leather processing and exacerbates at different stages [8]. In particular, the fibril alignment is shown to develop during the wet blue stage (#5) [48]; the degree of fibril alignment follows a trending increase as the material undergoes different stages of processing. Unfortunately, what exactly causes looseness is still not clear.

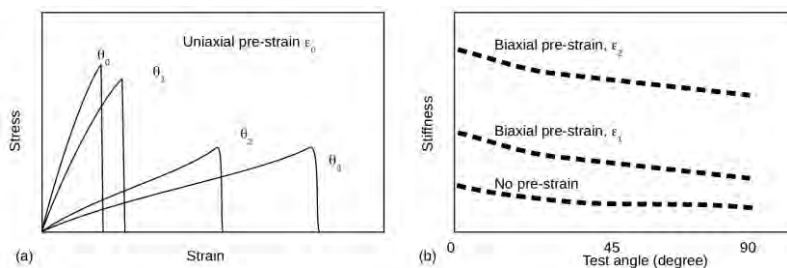


Fig. 4. Mechanical response of leather. (a) Sketch of stress-strain curves of leather treated to drying with a prestrain ϵ_0 , uniaxially tensile tested to rupture, stretched along long axis, i.e. parallel to the backbone (for instance, $\epsilon_0=0.3$ [26]). The angles are defined with respect to the backbone, $\theta_0, \theta_1, \theta_2$ and θ_3 . The angles reported in a previous study were $0^\circ, 15^\circ, 60^\circ$ and 90° , respectively; the stress was of the order of 10^6 Pa (MPa) [26]. (Adapted by permission from Springer Nature Customer Service Centre GmbH: Springer Nature, Journal of Materials Science, Boote C, Sturrock E J, Attenburrow G E, Meek K M, Pseudo-affine behaviour of collagen fibres during the uniaxial deformation of leather, **37**, 3651–3656 [COPYRIGHT] (2002).) (b) Sketch of stiffness of leather, treated to drying under varying pre-strains at different loading angles, with respect to the backbone. In a previous report [47], the pre-strains applied, ϵ_1 and ϵ_2 , corresponded to 0.1 and 0.2, respectively; the stiffness was of the order of 10^6 Pa (MPa). (Adapted by permission from Springer Nature Customer Service Centre GmbH: Springer Nature, Journal of Materials Science, Sturrock E J, Boote C, Attenburrow G E, Meek K M, The effects of the biaxial stretching of leather on fibre orientation and tensile modulus, **39**, 2481-2486 [COPYRIGHT] (2004))

Several factors can affect the alignment of collagen fibrils, namely hydration, leather thickness and pre-strain treatment. The fibrils in dehydrated leather materials are less aligned than hydrated ones [8]. Leather thickness also affects the fibril alignment in that the fibril orientation in the grain layer is vastly different from that in the corium layer [49]. The amount of pre-strain influences the stiffness; stiffness increases with increasing pre-strain values dramatically (Fig. 4b). It should be emphasized that changes in fibril alignment is not merely a 2D planar effect; a proportion of the

realignment of the fibrils also comes from the planes perpendicular to the surface of the leather during pre-strain and it is proposed that this proportion could also contribute to the increase stiffness [47].

3.3.3 Collagen fibril diameter

The mechanical stability of collagen at the fibrillar level addresses the stress uptake in the fibril during loading, described by

$$\sigma_{cf}(z) = \varepsilon_{ct} E_{cf} [1 - \cosh(bL_f z) / \cosh(bL_f)], \quad (4)$$

for the case of elastic stress transfer, which is associated with initial loading [2, 50]. Here b is given by Eq. (3). The mechanics of stress uptake changes during plastic stress transfer, which is associated with latter stages of (post-yield) loading, and this is described by

$$\sigma_{cf}(z) = 2\tau [L_f / r_f] (1 - z) \quad (5)$$

[1, 2, 51]. In all models, the cross-sectional size (e.g. radius (r_f) or diameter ($D_f = 2r_f$)) of the fibrils plays an important role in determining the stress uptake. Thus, understanding the size distribution and how radius changes could provide insight into how the fibril takes up stress.

The tear strength of some types of leather, e.g. bovine origin, is sensitive to D_f . The larger the D_f the higher the tear strength [52]. However, in other types, i.e. ovine, the tear strength is independent of D_f , suggesting that other factors could have confounded this relationship, e.g. τ , E_{cf} , G_m and L_f [53]. More research is needed to illuminate how each of these factors contribute to the overall strength of the leather.

Type V collagen may be important for regulating the initiation of collagen fibril assembly [54]. If this initiation were to be disrupted, e.g. when the type V collagen content is low, this may result in a mixture of two morphologically different fibrils, namely a population of fibrils (normal) cylinder-like cross-section and a population of fibrils with abnormally large irregular cross-section [54]; less fibrils are also formed and this results in lower collagen content [54]. Although bimodal distribution of D_f is found in young to old individuals, it is observed that with age, the cross section profile of the population with larger D_f appears to be more irregular [40]. While the resilience of the tissue increases with fibril diameter for both populations of fibril associated with small and large diameters only the fracture toughness of the tissue increases with fibril diameter for the large-diameter population (and the opposite effect occurs with the small-diameter population) [55].

Hides and skins containing defects such as lesions caused by demodex bovis mites-appearing as ragged fibrous cavities which are hard and unsightly [56]-are disposed leading to financial losses to farmers, traders and the tanning industry [57]. Abu-Samra and co-worker remarked that the fibres around the cavities were distorted, thinner (meaning, D_f is smaller) than normal [58]. They reported quantitative results showing that the tensile strength, tearing load, percentage elongation were significantly lower than non-infected ones [58]. However, no quantitative and qualitative evidence of the profile of the fibres (or fibrils) was shown; it was not possible to gain further insight about how the abnormal structure of the fibres (or fibrils) affect the mechanical properties of the leather material.

3.3.4 Fibril-matrix interface

When collagenous tissues deform under an external load, the deforming hydrated PG-rich ground substance shears on the collagen fibrils; the natural cross links between fibrils and between fibril-matrix are deformed and this generates an interfacial shear stress. Consequently, shear on the fibril causes the fibril to stretch and generate stresses to resist the external load that is attempting to pull the tissue apart. Fig. 5 a and b shows the profile of the shear stress as a function of distance

along the fibril from the centre ($Z=0$) to the end ($Z=L_f/2$) during elastic stress transfer (which corresponds to an elastically deforming tissue) [29] and during plastic stress transfer (tissue post-yield stage) [1, 2, 59]. Consequently, the non-linear profile in the former leads to a non-linear axial stress distribution described by Eq. (4) while the uniform stress profile in the latter leads to a simple linear axial distribution described by Eq. (5).

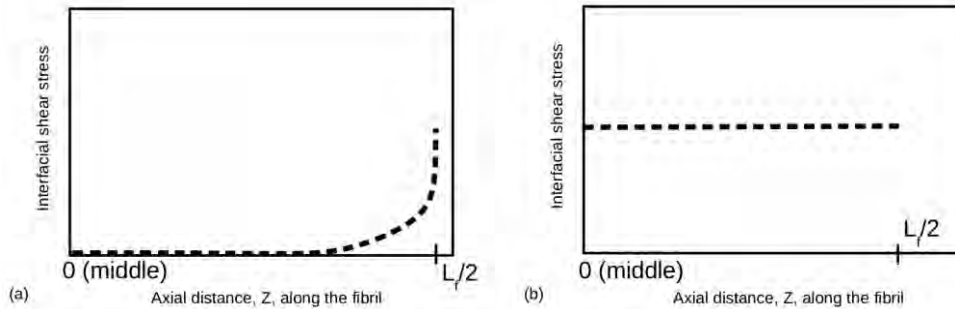


Fig. 5. Graphs of interfacial shear stress versus axial distance along the fibril during (a) elastic stress transfer, and (b) plastic stress transfer stages. The graph shows the stress level from the middle ($Z=0$) to the end ($Z=L_f/2$) of the fibril.

With regard to leather, during leather processing, various components of the hydrated proteoglycan-rich ground substance in ECM are removed (for instance, glycosaminoglycans (GAGs) are removed by liming and bating), and the intermediate product at the pickled stage (#3), would have fewer natural cross-links [8]. However, new cross-links are created during the pretanning (#4) and wet blue (#5) stages [8]. It was observed (**Fig. 6 a**) that the D-period of collagen during the pickled stage was much higher than that during the wet-blue stage, suggesting that the collagen fibrils were appreciably stretched in the former as compared to the latter [8]; this could compromise the collagen stability as shown by the small strain range in the former as compared to the latter. Nevertheless, the presence of new cross links in latter stages up to the finished product suggest that these shear stress response described in **Fig. 5 a** and **b** are expected to be applicable to the fibril-matrix interface in leather material. **Fig. 6 b** shows the results of an attempt to investigate whether GAGs are implicated in the cross-linking of fibrils to the matrix and between fibrils. With respect to native tissue, the absence of GAGs (removed by Chondroitinase ABC) showed no appreciable change to the orientation index. GAGs have been the 'usual suspect' for natural cross-links for quite a long time. These natural cross-links at the fibril-matrix interface facilitate the stress transfer within ECM, based on observation of micrographs of GAG side chain, associated with proteoglycans (PGs) bound on collagen fibrils, such as decorin PG-a member of the family of small leucine-rich PGs (SLRPs) [60-71].

But in the last 10 years or so, investigations to study how tissue mechanical properties are compromised by removing GAGs (by Chondroitinase ABC) has yielded negative results [24]. Although the exact nature of the natural cross links are not yet known, **Fig. 6 b** shows that introducing artificial crosslinks (using glutaraldehyde) into the collagenous tissue can result in a significant effect on the orientation index when the tissues are stretched, implicating that the artificial crosslinks actually works to anchor between fibrils, and to realign the fibrils in the direction of the applied load. Glutaraldehyde is a tanning agent that functions as collagen cross-linker, intermolecularly and intramolecularly, forming covalent bonds for interconnecting the collagen fibrils, as well as polymerisation of glutaraldehyde to increase the network density [72].

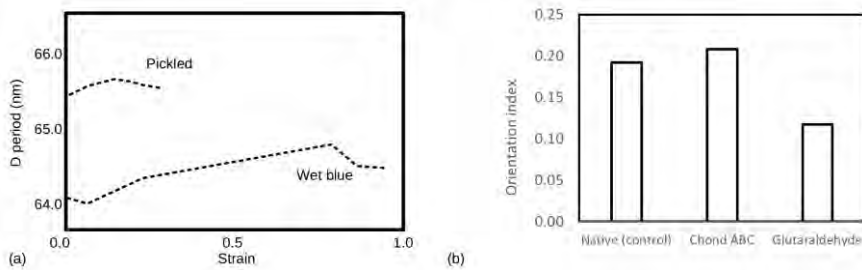


Fig. 6. Chemical treatment of collagen. (a) Sketch of graph of D period versus applied strain to partially processed skin [8] (Reprinted (adapted) with permission from Sizeland KH, Edmonds RL, Basil-Jones MM, Kirby N, Hawley A, Mudie S, Haverkamp RG: Changes to Collagen Structure during Leather Processing. *Journal of Agricultural and Food Chemistry* 2015, 63(9):2499-250. Copyright (2015) American Chemical Society) and (b) orientation index of native tissue versus tissue treated to Chondroitinase ABC (to remove GAGs) and glutaraldehyde (to introduce synthetic cross links), under tension. The values for the respective treatment were estimated from plots derived from a study reported elsewhere [72].

Alternatively, it has been proposed that collagen fibrils may interact directly without the help of extrafibrillar molecules by attributing the interaction to fibril branching [35]. During development, collagen fibrils grow in diameter and in length through both end-to-end and lateral fusion resulting in fibril branching; thus fibril branching is also regarded to facilitate interfibrillar load transfer between the small and large diameter fibrils [35]. Given that most tendons exhibit a distribution of small and large fibril diameters [55] small diameter fibrils may play an important function to connect and transmit force between the larger load-bearing fibrils in tendon [35].

3.4 Molecular level

At the molecular level, the mechanical stability of the fibrous structure may be better understood from studies of the assembly of the tropocollagen molecules into fibrils, which is regarded as a thermodynamically (entropy) driven process under ordinary/physiological conditions [73]. Tropocollagen molecule resembles a triple helical arrangement of three coiled collagen-protein chains, linked together by hydrogen bonds. When the molecule is stretched, at low displacement, the force generated in the molecule is low as the helix becomes uncoiled, but as the displacement increases, the force increases. These mechanical characteristics and structural bonding provide the cornerstone for understanding the ability of fibrous structures such as collagen fibrils to take up stress when stretched.

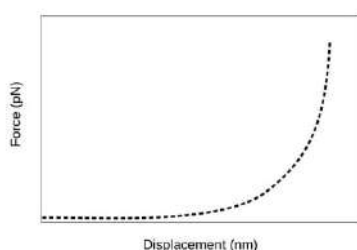


Fig. 7. Sketch of force versus displacement of tropocollagen molecule according to the worm-like-chain model.

The overall mechanical response of the molecule may be described by a worm-like chain (WLC) model [74] (**Fig. 7**). This force-displacement profile may be divided into three regimes, the low (near-constant) force regime is known as the entropic elastic regime while the linear regimes comprised of a low stiffness regime where the tropocollagen molecule continues to uncoil and a high stiffness regime where the molecule is fully stretched over the 'back-bone' so that further

stretching will result in rupture [75]. The mechanical stability of the molecule is parameterized by the molecular contour length and the persistence length [76] of the molecule at a predetermined absolute temperature. For a more detailed review of other modified WLC models (namely, extensible WLC, modified Marko-Siggia WLC, piecewise defined extended WLC, implicit elasticity WLC and twistable WLC) to describe the highly stretched regime, see Hillgarten's report [77]. One important highlight of these variant models is that they are underpinned by different contour lengths and persistence lengths.

How the changes at the molecular level, namely the D period in collagen, contribute to bulk level behaviour such as dehydration, tanning, and stretching, have been reported in several studies. You may need no reminding that in native tissues tropocollagen molecules in fibrils are staggered axially, resulting in a periodic light-dark bands with a D period of about 67 nm when viewed under an electron microscope. The light bands are associated with gaps (region of low-density collagen packing) between the ends of two molecules, while the dark bands arise from molecular overlaps [78, 79]. The nature of the D period has been well-explored for a long time using data from x-ray diffraction peak patterns of hides [80]. For instance, Professor Eckhart Heidemann has probed the x-ray diffraction peak patterns of hides and found that the intensity varied with water content, which may be attributed to changes in the crystallinity of the collagen molecular packing, namely at the side-chain spacing [80]. Recently, new studies carried out to exploit the sensitivity of the intensity of these diffraction peaks for investigating the effects of the respective tanning agents BCS, ZIR, or ALS in *post-tanning*, have revealed how the metal ions from the respective tanning agents penetrate into the fibrils and interact with the collagen [81]. Other tanning agents such as fat liquor can penetrate into the fibril and interact with the molecules to change the D-period [80]. Overall, D period is shown to decrease with progressive leather processing stages [81]. With regard to dehydration studies, it is well-known that the D period decreases on drying [17, 82]. The reduced D period reflects the overall reduction in the characteristic gap (where collagen packing density is low) and overlap regions, possibly associated with deformation of the collagen crystal structure [17, 82]. Upon re-hydration, swelling of the fibrils occurs but a critical point is reached beyond which the fibril volume remains constant [43]. Thereafter, only the interfibrillar matrix continues to swell [43]. In some, but not all, species, the D period is also dependent on the location in the leather (through-thickness), such as the corium and grain layers [49]. However the extent of the differences with respect to the location may be species-dependent [83]. Mechanical deformation of leather materials can influence the D period, which is likened to an internal strain gauge [72]. The D period increases with increase in the tensile strain of leather [83] as the tropocollagen molecules elongate, and slip with respect to adjoining molecules, along the fibril axis, which changes the length of the gap-overlap regions [83, 84].

It is important to emphasize that large-scale changes in a collagenous material, such as leather stretching from a relaxed state or past the point of yielding, cannot be properly understood in terms of what a single tropocollagen molecule is doing using the WLC model, although the WLC is a useful model for understanding how a molecule responds to an external load. Current interest in multiscale modelling of the collective 'many-molecule' behaviour (e.g. by incorporating the WLC model) at the molecular level, the collective 'many-fibril' behaviour (e.g. by incorporating stress transfer mechanisms) at the fibrillar level, and the correlations that must be established between the different levels across the full length scale as reported in several fundamental papers [75, 85-92], may be the answer to understanding the stability of collagen in leather. To address this approach would require establishing a conceptual framework underpinning organized information of the structure-function relationship of collagen. This is highlighted in the following (final) section of this paper.

4 Hierarchical architecture of collagen

Section 0 to 0 highlight the key findings on collagen stability from interfibrillar matrix level to tropocollagen molecular level. But can we fit these seemingly disparate pieces together to help us see the bigger picture better? In 2014, I proposed a strategy to help advance our understanding of the structure-function relationship of ECM. This strategy underpins a concept of organized information addressing a framework for the mechanisms of stress uptake in the structural units reinforcing the tissue at the respective levels of the hierarchical architecture [59]. The framework that I have constructed takes the form of a table initially but this eventually led to a schematic of structural levels versus loading stages, regulated by known mechanisms at each structural level and corresponding loading stage. A schematic of the framework is shown in Fig. 8. The framework was aimed at facilitating (1) comparison of individual stress uptake mechanisms between different tissue structural components of the same structural levels and across different structural levels, (2) comparison of mechanical pathways, and (3) prediction of new interconnection between existing mechanisms. A detailed description of the individual stress uptake mechanisms, mechanical pathways and interconnections is reported elsewhere [59, 93].

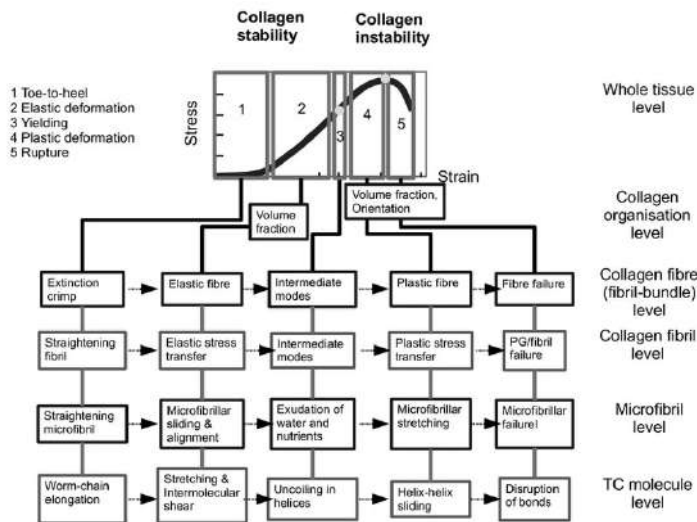


Fig. 8. Stress transfer mechanisms in ECM at various structural levels from macro to nano scale. The schematic diagram, proposed by Goh et al. [59], addresses both the structural organisation at different lengthscales and the different loading stages from initial until fracture. One may view the schematic diagram from left to right and from top to bottom. For the purpose of referencing, the structural lengthscales are labelled 1-6 and the stages of loading are labelled 1-5. The Inset shows a sketch of graph of load versus strain for (e.g. in vitro, uniaxial tensile test) of dermal skin, accompanied by schematics of the skin showing the collagen fibre orientation at various stages of the loading process. In a, collagen fibres appear disorganised with regards to direction, but becoming more aligned along the direction of the load acting on the skin. As the load increases further, the proportion of the collagen fibres becoming more aligned (and also straight) increases (part c). Finally, all collagen fibres are almost aligned and straight [94].

The framework for describing the hierarchical architecture can be applied to leather by organizing findings from experiments and predictions from analytical/computational models in leather studies. The findings would serve to aid researchers' understanding of the structure-function phenomena or to inform manufacturing decisions with socioeconomic consequences.

While many studies on collagen fundamentals have used computational biomechanics models such as those proposed by Buehler and co-workers [75, 86-88, 95-98], there is a dearth of reports from analytical/computational modelling in leather studies. It is likely that increased computer speed and better specialist software will enable collagen modelling, i.e. *in silico* leather, to be carried out, to be applied to an increasingly wide range of problems, and to be deployed in the manufacturing of leather where modelling could be incorporated as part of the process. On this

note, it is important to deal with model credibility where computational biomechanics models would be used for leather properties predictions. One such approach proposed by Patterson and Wheelan[99]-which is a simple 3x3 matrix for facilitating the categorization of models with respect to their testability-may be employed in order to guide the selection of an appropriate process of validation so that the leather researcher can obtain the evidence to establish credibility.

5 Conclusion

This paper has discussed recent findings on the role of collagen in regulating the mechanical stability of biological materials, covering three areas: physicochemical factors affecting collagen stability, mechanics of collagen stability and cross-links, and the hierarchical architecture of collagen. The recent findings highlighted here are likely to encourage further development of leather that addresses collagen stabilization and achieve a more sustainable future for the leather industry.

References

1. Goh KL, Meakin JR, Aspden RM, Hukins DWL: Influence of fibril taper on the function of collagen to reinforce extracellular matrix. *Proc R Soc Lond B Biol Sci* 2005, 272:1979-1983.
2. Goh KL, Meakin JR, Aspden RM, Hukins DWL: Stress transfer in collagen fibrils reinforcing connective tissues: Effects of collagen fibril slenderness and relative stiffness. *J Theor Biol* 2007, 245:305-311.
3. Chen K-W, Lin L-C, Lee W-S: Analyzing the Carbon Footprint of the Finished Bovine Leather: A Case Study of Aniline Leather. *Energy Procedia* 2014, 61:1063-1066.
4. Heidemann E, Neiss HG, Khodadadeh K, Heymer G, Sheikh EM, Saygin O: Structural studies of collagen-like sequential polypeptides. *Polymer* 1977, 18.
5. Heidemann E: *Fundamentals of leather manufacturing*. Darmstadt: Eduard Roether; 1993.
6. Tzaphlidou M: The role of collagen and elastin in aged skin: an image processing approach. *Micron* 2004, 35(3):173-177.
7. Silver FH, Siperko LM, Seehra GP: Review: Mechanobiology of force transduction in dermal tissue. *Skin Research and Technology* 2003, 9:3-23.
8. Sizeland KH, Edmonds RL, Basil-Jones MM, Kirby N, Hawley A, Mudie S, Haverkamp RG: Changes to Collagen Structure during Leather Processing. *Journal of Agricultural and Food Chemistry* 2015, 63(9):2499-2505.
9. Stephens LJ, Werkmeister JA, Ramshaw JAM: Changes to the bovine hides during leather processing. *Journal of the Society of Leather Technologists and Chemists* 1993, 77:71-74.
10. Schropfer M, Kluver E, Meyer M: Influence of elastin degradation on the mechanical properties of leather. *Journal of the American Leather Chemists Association* 2014, 109:306-313.
11. Meyer M: Processing of collagen based biomaterials and the resulting materials properties. *BioMedical Engineering Online* 2019, 18:24.
12. Wong WLE, Joyce TJ, Goh KL: Resolving the viscoelasticity and anisotropy dependence of the mechanical properties of skin from a porcine model. *Biomech Model Mechanobiol* 2016, 15:433-446.
13. Goh KL, Chen SY, Liao K: A thermomechanical framework for reconciling the effects of ultraviolet radiation exposure time and wavelength on connective tissue elasticity. *Biomech Model Mechanobiol* 2014.
14. Goh KL, Chen Y, Chou SM, Listrat A, Bechet D, Wess TJJ: Effects of frozen storage temperature on the elasticity of tendons from a small murine model. *Animal* 2010, 4:1613-1617.
15. Zhang Y, Wang L: Recent Research Progress on Leather Fatliquoring Agents. *Polymer-Plastics Technology and Engineering* 2009, 48:285-291.
16. Zhang Y, Mansel BW, Naffa R, Cheong S, Yao Y, Holmes G, Chen H-L, Prabakar S: Revealing Molecular Level Indicators of Collagen Stability: Minimizing Chrome Usage in Leather Processing. *ACS Sustainable Chemistry & Engineering* 2018, 6(5):7096-7104.
17. Wess TJ, Orgel JP: Changes in collagen structure: drying, dehydrothermal treatment and relation to long term deterioration. *Thermochimica Acta* 2000, 365:119-128.
18. Wright NT, Humphrey JD: Denaturation of collagen via heating: an irreversible rate process. *Annu Rev Biomed Eng* 2002, 4:109-128.
19. Yeo YL, Goh KL, Kin L, Wang HJ, Listrat A, Bechet D: Structure-property relationship of burn collagen reinforcing musculo-skeletal tissues. *Key Eng Mater* 2011, 478:87-92.
20. Weadock KS, Miller EJ, Bellincampi LD, Zawadsky JP, Dunn MG: Physical crosslinking of collagen fibers - comparison of ultraviolet irradiation and dehydrothermal treatment. *Journal of Biomedical Materials Research* 1995, 29:1373-1379.

21. Sebestyén Z, Jakab E, Badea E, Barta-Rajnai E, Şendrea C, Czégény Z: Thermal degradation study of vegetable tannins and vegetable tanned leathers. *Journal of Analytical and Applied Pyrolysis* 2019, 138:178-187.
22. Sebestyén Z, Czégény Z, Badea E, Carsote C, Şendrea C, Barta-Rajnai E, Bozi J, Miu L, Jakab E: Thermal characterization of new, artificially aged and historical leather and parchment. *Journal of Analytical and Applied Pyrolysis* 2015, 115:419-427.
23. Liu C-K, Latona NP, DiMaio G, Cooke P: Milling effects on mechanical behaviors of leather. *Journal of the American Leather Chemists Association* 2007, 102:191-197.
24. Fessel G, Snedeker JG: Evidence against proteoglycan mediated collagen fibril load transmission and dynamic viscoelasticity in tendon. *Matrix Biol* 2009, 28:503-510.
25. Huang JB, Liu J, Tang KY, Yang PY, Fan XL, Wang F, Du J, Liu CK: Effect of Cyclic Stress while Being Dried on the Mechanical Properties and Thermostability of Leathers. *Journal of the American Leather Chemists Association* 2018, 113:318-325.
26. Boote C, Sturrock EJ, Attenburrow GE, Meek KM: Psuedo-affine behaviour of collagen fibres during the uniaxial deformation of leather. *J Mater Sci* 2002, 37:3651-2656.
27. Kelly SJ, Wells HC, Sizeland KH, Kirby N, Edmonds RL, Ryan T, Hawley A, Mudie S, Haverkamp RG: Artificially modified collagen fibril orientation affects leather tear strength. *J Sci Food Agric* 2018, 98(9):3524-3531.
28. Covington T: *Tanning Chemistry: The Science of Leather*: Royal Society of Chemistry; 2009.
29. Goh KL, Meakin JR, Hukins DWL: Influence of fibre taper on the interfacial shear stress in fibre-reinforced composite materials during elastic stress transfer. *Compos Interface* 2010, 17:75-81.
30. Cox HL: The elasticity and strength of paper and other fibrous materials. *British Journal of Applied Physics* 1952, 3:72-79.
31. Kelly A, MacMillan NH: *Strong solids*, 3rd edn. Oxford: Clarendon Press; 1986.
32. Szczesny SE, Caplan JL, Pedersen P, Elliott DM: Quantification of interfibrillar shear stress in aligned soft collagenous tissues via notch tension testing. *Scientific Reports* 2015, 5:14649:1-9.
33. Szczesny SE, Elliott DM: Incorporating plasticity of the interfibrillar matrix in shear lag models is necessary to replicate the multiscale mechanics of tendon fascicles. *Journal of the Mechanical Behavior of Biomedical Materials* 2014, 40:325-338.
34. Szczesny SE, Elliott DM: Interfibrillar shear stress is the loading mechanism of collagen fibrils in tendon. *Acta Biomater* 2014, 10:2582-2590.
35. Szczesny SE, Fetchko KL, Dodge GR, Elliott DM: Evidence that interfibrillar load transfer in tendon is supported by small diameter fibrils and not extrafibrillar tissue components. *Journal of Orthopaedic Research* 2017, 35(10):2127-2134.
36. Kelly SJ, Weinkamer R, Bertinetti L, Edmonds RL, Sizeland KH, Wells HC, Fratzl P, Haverkamp RG: Effect of collagen packing and moisture content on leather stiffness. *Journal of the Mechanical Behavior of Biomedical Materials* 2019, 90:1-10.
37. Kite M, Thomson R: *Conservation of Leather and Related Materials*. Oxford: Butterworth-Heinemann; 2006.
38. Sato Y, Wada Y, Higo A: Relationship between monolayer and multilayer water contents, and involvement in gelatinization of baked starch products. *Journal of Food Engineering* 2010, 96(2):172-178.
39. Olle L, Jorba M, Castell JC, Font J, Bacardit A: Comparison of the weathering variables on both chrome-tanned and wet- white leather ageing. In: XXXI IULTCS Congress: September 27th-30th 2011; Valencia (Spain). IULTCS 2011.
40. Goh KL, Holmes DF, Lu HY, Richardson S, Kadler KE, Purslow PP, Wess TJ: Ageing changes in the tensile properties of tendons : influence of collagen fibril volume. *J Biomech Eng* 2008, 130:021011.
41. Gogly B, Godeau G, Gilbert S, Legrand JM, Kut C, Pellat B, Goldberg M: Morphometric analysis of collagen and elastic fibers in normal skin and gingiva in relation to age. *Clinical Oral Investigation* 1997, 1:147-152.
42. Liao J, Vesely I: A structural basis for the size-related mechanical properties of mitral valve chordae tendineae. *Journal of Biomechanics* 2003, 36(8):1125-1133.
43. Morin C, Hellmich C, Henits P: Fibrillar structure and elasticity of hydrating collagen: a quantitative multiscale approach. *J Theor Biol* 2013, 317:384-393.
44. Wells HC, Sizeland KH, Kaye HR, Kirby N, Hawley A, Mudie ST, Haverkamp RG: Poisson's ratio of collagen fibrils measured by small angle X-ray scattering of strained bovine pericardium. *J Appl Phys* 2015, 117:044701.
45. Wells HC, Sizeland KH, Kirby N, Hawley A, Mudie S, Haverkamp RG: Acellular dermal matrix collagen responds to strain by intermolecular spacing contraction with fibril extension and rearrangement. *J Mech Behav Biomed Mater* 2018, 79:1-8.
46. Wells HC, Holmes G, Haverkamp RG: Looseness in bovine leather: microstructural characterization. *J Sci Food Agric* 2016, 96(8):2731-2736.
47. Sturrock EJ, Boote C, Attenburrow GE, Meek KM: The effects of the biaxial stretching of leather on fibre orientation and tensile modulus. *J Mater Sci* 2004, 39:2481-2486.
48. Wells HC, Holmes G, Jeng US, Wu WR, Kirby N, Hawley A, Mudie S, Haverkamp RG: A small angle X-ray scattering study of the structure and development of looseness in bovine hides and leather. *J Sci Food Agric* 2017, 97(5):1543-1551.
49. Basil-Jones MM, Edmonds RL, Allsop TF, Cooper SM, Holmes G, Norris GE, Cookson DJ, Kirby N, Haverkamp RG: Leather structure determination by small-angle X-ray scattering (SAXS): cross sections of ovine and bovine leather. *J Agric Food Chem* 2010, 58(9):5286-5291.
50. Goh KL, Aspdren RM, Hukins DWL: Shear lag models for stress transfer from an elastic matrix to a fibre in a composite material. *International Journal of Materials and Structural Integrity* 2007, 1:180-189.
51. Goh KL, Aspdren RM, Mathias KJ, Hukins DWL: Effect of fibre shape on the stresses within fibres in fibre-reinforced composite materials. *Proc R Soc Lond A Math Phys Sci* 1999, 455:3351-3361.
52. Wells HC, Edmonds RL, Kirby N, Hawley A, Mudie ST, Haverkamp RG: Collagen fibril diameter and leather strength. *J Agric Food Chem* 2013, 61(47):11524-11531.

53. Goh KL, Hukins DWL, Aspden RM: Critical length of collagen fibrils in extracellular matrix. *J Theor Biol* 2003, 223:259-261.
54. Wenstrup RJ, Florer JB, Brunskill EW, Bell SM, Chervoneva I, Birk DE: Type V collagen controls the initiation of collagen fibril assembly. *J Biol Chem* 2004, 279(51):53331-53337.
55. Goh KL, Holmes DF, Lu Y, Purslow PP, Kadler KE, Bechet D, Wess TJ: Bimodal collagen fibril diameter distributions direct age-related variations in tendon resilience and resistance to rupture. *J Appl Physiol* 2012, 113:878-888.
56. Gbolagunet GD, Hambolu JO, Akpavie SO: Pathology and Leather Surface Appearance of Disease Afflicted Nigerian Small Ruminant Skins. *Australian Journal of Technology* 2009, 12:271-283.
57. Kahsay T, Negash G, Hagos Y, Hadush B: Pre-slaughter, slaughter and post-slaughter defects of skins and hides. *Onderstepoort Journal of Veterinary Research* 2015, 82.
58. Abu-Samrai TM, Shuaib Y: Bovine Demodicosis: Leather from the Raw Material to the Finished Product. *Journal of the Society of Leather Technologists and Chemists* 2015, 99:80-90.
59. Goh KL, Listrat A, Bechet D: Hierarchical mechanics of connective tissues: Integrating insights from nano to macroscopic studies. *J Biomed Nanotechnol* 2014, 10(10):2464-2507.
60. Scott JE: Proteoglycan: collagen interactions in connective tissues. *Ultrastructural, biochemical, functional and evolutionary aspects. Int J Biol Macromol* 1991, 13:157-161.
61. Scott JE: Extracellular matrix, supramolecular organisation and shape. *Journal of Anatomy* 1995, 187:259-269.
62. Scott JE: Structure and function in extracellular matrices depend on interactions between anionic. *Pathologie Biologie* 2001, 49:284-289.
63. Scott JE, Orford CR: Dermatan sulphate-rich proteoglycan associates with rat tail-tendon collagen at the d band in the gap region. *Biochemical Journal* 1981, 19:213-216.
64. Scott JE, Orford CR, Hughes EW: Proteoglycan-collagen arrangements in developing rat tail tendon. *Biochemical Journal* 1981, 195:573-581.
65. Liao J, Vesely I: Skewness angle of interfibrillar proteoglycans increases with applied load on mitral valve chordae tendineae. *J Biomech* 2007, 40(2):390-398.
66. Liao J, Vesely I: Relationship between Collagen Fibrils, Glycosaminoglycans, and Stress Relaxation in Mitral Valve Chordae Tendineae. *Annals of Biomedical Engineering* 2004, 32(7):977-983.
67. Parfitt GJ, Pinali C, Young RD, Quantock AJ, Knupp C: Three-dimensional reconstruction of collagen-proteoglycan interactions in the mouse corneal stroma by electron tomography. *J Struct Biol* 2010, 170(2):392-397.
68. Redaelli A, Vesentini S, Soncini M, Vena P, Mantero S, Montevecchi FM: Possible role of decorin glycosaminoglycans in fibril to fibril force transfer in relative mature tendons-a computational study from molecular to microstructural level. *Journal of Biomechanics* 2003, 36:1555-1569.
69. Vesentini S, Redaelli A, Montevecchi FM: Estimation of the binding force of the collagen molecule-decorin core protein complex in collagen fibril. *J Biomech* 2005, 38(3):433-443.
70. Gutsmann T, Fantner GE, Kindt JH, Venturoni M, Danielsen S, Hansma PK: Force Spectroscopy of Collagen Fibers to Investigate Their Mechanical Properties and Structural Organization. *Biophys J* 2004, 86:3186-3193.
71. Danielson KG, Baribault H, Holmes DF, Graham H, Kadler KE, Iozzo RV: Targeted disruption of decorin leads to abnormal collagen fibril morphology and skin fragility. *J Cell Biol* 1997, 136:729-743.
72. Kaye HR, Sizeland KH, Kirby N, Hawley A, Mudie T, Haverkamp RG: Collagen cross linking and fibril alignment in pericardium. *RSC Advances* 2015, 5:3611-3618.
73. Holmes DF, Watson RB, Chapman JA, Kadler KE: Enzymic control of collagen fibril shape. *J Mol Biol* 1996, 261:93-97.
74. Wiecezorek A, Rezaei N, Chan CK, Xu C, Panwar P, Bromme D, Merschrod SE, Forde NR: Development and characterization of a eukaryotic expression system for human type II procollagen. *BMC Biotechnol* 2015, 15:112.
75. Chang S-W, Buehler MJ: Molecular biomechanics of collagen molecules. *Materials Today* 2014, 17(2):70-76.
76. Ghavanloo E: Persistence length of collagen molecules based on nonlocal viscoelastic model. *Journal of Biological Physics* 2017, 43:525-534.
77. Hillgartner M, Linka K, Itskov M: Worm-like chain model extensions for highly stretched tropocollagen molecules. *Journal of Biomechanics* 2018, 2018:129-135.
78. Orgel JPRO, Miller A, Irving TC, Fischetti RF, Hammersley AP, Wess TJ: The in situ supermolecular structure of type I collagen. *Structure* 2001, 9:1061-1069.
79. Wess TJ, Hammersley AP, Wess L, Miller A: Molecular Packing of Type I Collagen in Tendon. *J Mol Biol* 1998, 275:255-267.
80. Heidemann E, Keller H: X-ray studies of tanned collagen. *Journal of the American Leather Chemists Association* 1970, 65(11):512.
81. Zhang Y, Ingham B, Cheong S, Ariotti N, Tilley RD, Naffa R, Holmes G, Clarke DJ, Prabakar S: Real-Time Synchrotron Small-Angle X-ray Scattering Studies of Collagen Structure during Leather Processing. *Industrial & Engineering Chemistry Research* 2017, 57(1):63-69.
82. Price RI, Lees S, Kirschner DA: X-ray diffraction analysis of tendon collagen at ambient and cryogenic temperatures: role of hydration. *Int J Biol Macromol* 1997, 20:23-33.
83. Sizeland KH, Wells HC, Kelly SJR, Edmonds RL, Kirby NM, Hawley A, Mudie ST, Ryan TM, Haverkamp RG: The influence of water, lanolin, urea, proline, paraffin and fatliquor on collagen D-spacing in leather. *RSC Advances* 2017, 7(64):40658-40663.
84. Sasaki N, Odajima S: Stress-strain curve and Young's modulus of a collagen molecule as determined by the x-ray diffraction technique. *Journal of Biomechanics* 1996, 29(5):655-658.

85. Andriotis OG, Chang SW, Vanleene M, Howarth PH, Davies DE, Shefelbine SJ, Buehler MJ, Thurner PJ: Structure–mechanics relationships of collagen fibrils in the osteogenesis imperfecta mouse model. *Journal of The Royal Society Interface* 2015, 12:20150701.
86. Buehler MJ: Nature designs tough collagen: explaining the nanostructure of collagen fibrils. *Proc Natl Acad Sci U S A* 2006, 103:12285-12290.
87. Buehler MJ, Keten S, Ackbarow T: Theoretical and computational hierarchical nanomechanics of protein materials: deformation and fracture. *Progress in Materials Science* 2008, 53:1101-1241.
88. Cranford SW, de Boer J, van Blitterswijk C, Buehler MJ: Materiomics: An -omics approach to biomaterials research. *Advanced Materials* 2013, 25:802-824.
89. Annovazzi L, Genna F: An engineering, multiscale constitutive model for fiber-forming collagen in tension. *Journal of Biomedical Materials Research* 2010, 92A:254-266.
90. Eekhoff JD, Fang F, Lake SP: Multiscale mechanical effects of native collagen cross-linking in tendon. *Connect Tissue Res* 2018, 59(5):410-422.
91. Malaspina DC, Szeifer I, Dhaher Y: Mechanical properties of a collagen fibril under simulated degradation. *Journal of the Mechanical Behavior of Biomedical Materials* 2017, 2017:549-557.
92. Depalle B, Qin Z, Shefelbine SJ, Buehler M, J.: Influence of cross-link structure, density and mechanical properties in the mesoscale deformation mechanisms of collagen fibrils. *Journal of the Mechanical Behaviour of Biomedical Materials* 2015, 52:1-13.
93. Goh KL, Holmes DF: Collagenous Extracellular Matrix Biomaterials for Tissue Engineering: Lessons from the Common Sea Urchin Tissue. *Int J Mol Sci* 2017, 18(5).
94. Jor JWY, Nash MP, Nielsen PMF, Hunter PJ: Estimating material parameters of a structurally based constitutive relation for skin mechanics. *Biomech Model Mechanobiol* 2011, 10:767-778.
95. Gronau G, Krishnaji ST, Kinahan ME, Giesa T, Wong JY, Kaplan DL, Buehler MJ: A review of combined experimental and computational procedures for assessing biopolymer structure-process-property relationships. *Biomaterials* 2012, 33:8240-8255.
96. Tang H, Buehler MJ, Moran B: A constitutive model of soft tissue: from nanoscale collagen to tissue continuum. *Annals of Biomedical Engineering* 2009, 37:1117-1130.
97. Tang Y, Ballarini R, Buehler MJ, Eppell SJ: Deformation micromechanisms of collagen fibrils under uniaxial tension. *Journal of the Royal Society, Interface* 2010, 7:839-850.
98. Uzel S, Buehler M: Molecular structure, mechanical behavior and failure mechanism of the C-terminal cross-link domain in type I collagen. *Journal of the Mechanical Behavior of Biomedical Materials* 2011, 4:153-161.
99. Patterson EA, Whelan MP: A framework to establish credibility of computational models in biology. *Progress in Biophysics and Molecular Biology* 2016.



KEY NOTES

BRAZILIAN LEATHER CERTIFICATION OF SUSTAINABILITY

A. Flores

Centre for the Brazilian Tanning Industry (CICB)

SAS quadra 1, Lote N, edifício Terra Brasília, sala 408/409 – Brasília – DF - Brazil.

contato@cscb.org.br

Abstract. Sustainability and transparency of the leather industry are increasingly important factors for the sector's clients as well as final consumers, looking for quality products that are also sustainable in all tiers of the production process. In this sense, certification and labelling processes are tools that grant visibility to the positive practices of manufacturers and their suppliers. In Brazil, through an unprecedented tanneries initiative conducted by the Centre for the Brazilian Tanning Industry (CICB), a certification for the leather production process was created. The Brazilian Leather Certification of Sustainability (CSCB) counts on the participation of the various links in the production chain. Using the concept of the sustainability tripod, CSCB considers the results of tanneries in economic, environmental and social aspects. A sustainable tannery develops its activities with positive economic results, seeking to reduce inherent environmental impact of its activities, providing better working conditions to employees and respecting the surrounding community. Since the starting point of its creation (2012), CSCB has reached many results concerning process' improvements in the industry, quitting wastage and getting efficiency in indicators. As the CSCB practices are inside more than 20 tanneries all over Brazil (some of them amongst the biggest in the country, covering a big part of the Brazilian leather production, which is one the hugest in the world) these findings are extremely important and must be shared with whole industry. The certification process is based on implementation and compliance with principles, criteria, and indicators established by standards developed by the Brazilian Association of Technical Standards (ABNT) and audited by certification institutes accredited by The National Metrology, Quality, and Technology Institute (Inmetro), signatory to the mutual recognition agreement within the framework of the International Accreditation Forum (IAF) and the International Laboratory Accreditation Cooperation (ILAC). These agreements guarantee the international validation and recognition of CSCB. Tanneries are certified according to how well they meet the standards, being granted an identification seal for sustainable processes, guaranteeing the transparency of Brazilian leather suppliers.

1 Introduction

Sustainability and transparency of the footwear supply chain are increasingly important factors for final consumers, looking for quality products that are also sustainable in all tiers of their production process. In this sense, certification and labelling processes are tools that grant visibility to the positive practices of manufacturers and their suppliers. Aligned to this reality, in Brazil, through an unprecedented tanneries initiative conducted by the Centre for the Brazilian Tanning Industry (CICB), a certification for the leather production process was created to demonstrate the capacity of the Brazilian tanning industry of producing leathers in a sustainable form.

The program of Brazilian Leather Certification of Sustainability ("Certificação de Sustentabilidade do Couro Brasileiro" - CSCB) had its beginning in 2012. The first step of the program consisted in the performance of the national and international references review, in terms of certification for leather as well as in certification of sustainability or of each of its dimensions. With this was tried to identify the state of art of this subject.

Alongside to this, one of the program most important aspects was the definition of which model to follow. There were various forms of certification possible, and it was identified the one that could guarantee the highest level of credibility. In this way, the program was aligned to the Brazilian System of Conformity Evaluation, an official format that indicates the need of having a normative basis, in other words, a standard that defines the requirements and the criteria, and a regulation of evaluating the conformity by the certifying organisms.

This model is ruled by the National Institute of Metrology, Standardization, and Industrial Quality (“Instituto Nacional de Metrologia, Normalização e Qualidade Industrial” - INMETRO), and is based on norms of the Brazilian Association of Technical Standards (“Associação Brasileira de Normas Técnicas” - ABNT), which are audited by organisms of a third party accredited by the Institute. INMETRO is known national and internationally in function of the articulations and partnerships that the organ has, such as the International Accreditation Forum (IAF) and the International Laboratory Accreditation Cooperation (ILAC).

At the end of May 2014, the Technical Standard “ABNT NBR 16.296 – Leathers - Principles, criteria, and indicators for the sustainable production” was published. On June 30th, 2015 the INMETRO ordinance 314/2015 was published with the Evaluation Requirements of Conformity (RAC – “Requisitos da Avaliação da Conformidade”). Following, INMETRO elaborated the program for accreditation of the certification companies, which are the third parties companies that perform the audits. Presently, two certification were already accredited by INMETRO and are conducting the audits.

Since the publishing of the normative basis, the tanneries have been preparing themselves for attending the requirements of the standard. CICB, through the program of Brazilian Leather Certification Sustainability (CSCB) has been rendering support to the tanneries, providing training and specific consultancy for the attendance of the standard. At this moment, we have three tanneries certified and another 24 in process of preparation.

The program is inserted in the scope of the Brazilian Leather project, which is a partnership between CICB and the Brazilian Trade and Investment Promotion Agency (Apex-Brasil).

2 The Normative Basis

The principles established on the normative base constitute the reference for the sustainable production of leather, in each of its dimensions: economic, environmental, and social. Besides this, we have a specific section to deal about the sustainability management by the company.

The principles of each dimension are unfolded in criteria, which are the expression of the requisites that describe the sustainable practices for the production of leathers and associated systems. The verification of the fulfillment of each criterion is established through the evaluation of the attendance of a set of specific indicators, which can be quantitative or qualitative.

Depending on the type of processing performed at the production unit (from raw hide to tanned leather, from tanned leather to finished leather, from raw leather to finished leather, etc.), not all indicators will be applicable or will be present. However, it will always be necessary to consider all those pertinent to the local situation.

Therefore, is defined a hierarchic structure of the principles, criteria, and indicators (see **Fig. 1**), for each one of the dimensions, which have the function of establishing the monitoring and the demonstration of the leather sustainable production.

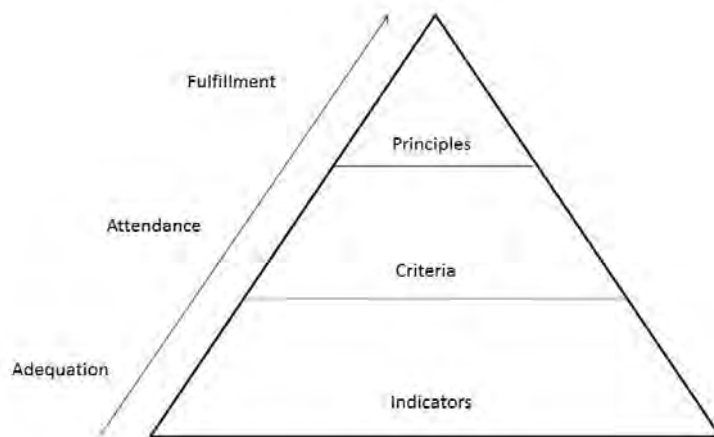


Fig. 1. Hierarchic structure of the principles, criteria, and indicators ^[1].

2.1 The Sustainability Principles

The following is an overview of the principles that are established for each of the dimensions of sustainability. To know more about the criteria and indicators it is recommended that you consult all of the norms.

2.1.1 Sustainability Management Dimension

This dimension has only one principle that says that the organization must efficiently manage issues of economic, environmental, and social nature, whether through a system of self management or, preferably, through a system certified in accordance with ISO 9001, ISO 14001, and ABNT NBR 16001.

2.1.2 Economic Dimension

The economic dimension approaches issues directed to the quality and productivity, as well as the results obtained by the company, and is made-up by three principles, which are:

- a) Production performance: the organization must establish and implement procedures that permit evaluation of production performance with regard to its productivity, operational controls, and workers.
- b) Product performance: the organization must establish and implement procedures that permit evaluation and analysis of product performance, as well as quality and development control.
- c) Economic impacts: the organization must establish and implement procedures - in all sectors – that have a positive economic impact.

2.1.3 Environmental Dimension

This dimension is the one that has the greatest number of principles, criteria, and indicators. This is due to the importance that the environmental issue has for the sustainable leather production. The principles are:

- a) Fulfillment of the applicable legal requisites: the organization must assure compliance of current environmental legislation and other regulations, and the tannery must also assure

- that any outsourced parties also meet current environmental legislation and other regulations.
- b) Traceability: the organization must have the means of assuring traceability of its raw material throughout its supply chain.
 - c) Control of restricted substances: the organization must guarantee that its products meet established limits in relation to restricted substances.
 - d) Water consumption management: the organization must properly manage water usage quantifying, monitoring, and adopting measures for rationing and reduction of consumption.
 - e) Energy consumption management: the organization must adequately manage energy usage- quantifying, selecting sources, monitoring, and adopting measures for rationing and reduction of consumption.
 - f) Production processes: the organization must conduct its productive processes so as to minimize its environmental impact.
 - g) Management of dangerous a non-dangerous waste: the organization must adequately manage dangerous and non-dangerous residues that are generated quantifying, monitoring, and adopting measures to minimize their generation.
 - h) Wastewater treatment: the organization must not only fulfill the regulatory requisites relative to residual water discharge, but must also implement an adequate management program and use advanced technologies to minimize the discharge of pollutants.
 - i) Atmospheric emissions management: the organization must adequately manage generated atmospheric emissions, not only by meeting regulatory requisites relative to emissions but also by implementing a preventative maintenance program for equipment and using technology to minimize pollutant emissions.

2.1.4 Social Dimension

The social dimension approaches the different stakeholders of the company, with highlight to the collaborators, suppliers, clients, competitors, community, and government. The principles are:

- a) Fulfillment of the applicable legal requisites: the organization must be managed through respect for basic human rights and on the fundamental principles and rights of labor, meeting all applicable legal requisites, specially no using child labor at any way, forced labor, or anything similar to slave labor, and must assure that any outsourcing parties also do not use child labor, forced labor, or anything similar to slave labor in their processes and operations.
- b) The organization must establish, implement, and maintain policies that are designated to the internal public, bearing all employees in mind, including health and safety, good working conditions, no discrimination and prejudice, promoting professional development and qualification.
- c) Suppliers: the organization must establish and maintain proper procedures for evaluating and selecting suppliers and subcontracted services, so that they meet the established criteria of social responsibility.
- d) Fair competition practices: the organization must establish practices of price and market competition, in accordance with current legislation, and in search of fair and significant positioning within the sector.
- e) Clients: the organization must establish and implement efficient means of communication and customer service, referring to: product development, client oriented services, and information for clients.

- f) Involvement with the community, government, and society: the organization must promote involvement with the community through developmental projects in order to improve quality of life, rescuing and preserving society in general.

2.2 Requirements of the Conformity Evaluation

The INMETRO Decree N. 314/2015 ^[2] establish the criteria for the Program of Evaluation of the Sustainability Conformity of the Leather Production Process, through certification mechanisms, attending the requirements specified in the ABNT NBR 16296:2014 standard. Besides establishing all aspects linked to the audit process, the regulation defines the levels of certification, and the system maintenance.

In the sense of promoting the inclusion of the companies in the process, were established different levels of certification. For each level was established a percentage of attendance of the indicator applicable of the sustainability management of each of the dimensions, including, necessarily, the obligatory criteria. The attendance percentages of the indicators are:

- a) Bronze: minimum attendance of 50%
- b) Silver: minimum attendance of 75%
- c) Gold: minimum attendance of 90%
- d) Diamond: Attendance of 100%

In accordance with the intended certification level, the Body Certifying Product evaluates the Integrated Management System of the supplier's production process, as well as performs auditing in the manufacturing unit, with the purpose of verifying the conformity of the production process with the documents sent, having as reference the ABNT NBR 16296:2014 standard.

The Conformity Certificate must specify the certification level, besides containing what is established in the General Requirements of Products Certification, and its validity must be of three years, from the date of its issue. The maintenance audit must follow with a periodicity of 12 (twelve) months.

3 Results for companies

The Brazilian Leather Sustainability Certification (CSCB) program has as one of its main tasks, to stimulate and support companies in implementing the actions necessary to meet the sustainability requirements established by the norm. This support is mainly provided through training and consulting in companies.

In the process of preparing companies, there is intense activity in the sense of identifying practices that already meet the norm, the issues that must be adjusted or adapted to guarantee the fulfillment of the requirements and those aspects that must be developed by the company. As the criteria is based on the best practices found in the leather industry, this process promotes the improvement of tannery processes.

To achieve certification companies end up promoting a comprehensive look at their processes and a critical analysis of the aspects that must be worked on. The comparison between the degree of fulfillment of the indicators of the norm at the moment the companies join the program and the level of attendance necessary to achieve certification demonstrates the growth potential that the company has in seeking certification.

Figure 2 shows the percentage of attendance to the indicators of each one of the dimensions at the moment the companies join the program (t₀).

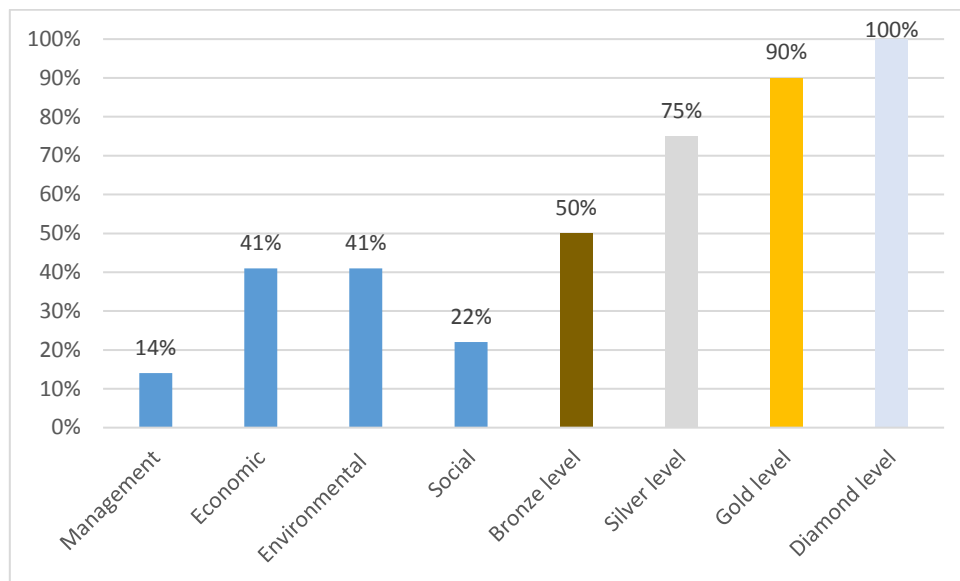


Fig. 2. Initial evaluation of indicators (t0) and level of attendance for certification. Average of 24 companies.

It can be seen that in the economic and environmental dimensions, the Brazilian tanneries, on average, already present an intermediate level of fulfillment of the sustainability requirements. However, in the management and social dimensions, companies usually need greater dedication to meet certification levels.

3.1 Application of management principles

The logic used to construct the Brazilian norm was based on some classic management tools, such as the PDCA Cycle and management by indicators. The application of these tools in a systematic way enables companies to continuously improve their processes for each of the dimensions of sustainability.

An analysis of the steps taken by companies during the consulting processes for the implementation of the requirements of the norm, highlights the main gains for companies in terms of management:

- a) dissemination of sustainability concepts, starting with top management which then permeates through all levels of the organization;
- b) seeing the company as a whole in order to facilitate the establishment of long-term strategic objectives;
- c) definition of performance indicators linked to the sustainability objectives, allowing for the evaluation of their evolution and actions taken to achieve the results;
- d) the establishment of formalized processes in order to guarantee the performance and standardization of the products;
- e) better definition of the organizational structure with a very positive impact on the communication between the parties;
- f) positive impact on the organization of the company in several aspects, thereby improving the working environment;
- g) inclusion or reinforcement of preventive actions and continuous improvement in processes, especially from the implementation of internal audits.

3.2 Economic, environmental and social gains

The gains obtained by the companies are individually quantifiable. In other words, each company has its own ways of identifying the returns obtained in each dimension. However, some aspects that have been detected in a general way for several participating companies can be highlighted, among them:

- a) gains in efficiency and optimization of the processes as well as those related to the quality of the products, due to the standardization, formalization and transparency of the processes;
- b) ensuring compliance with legal requirements not only by the certified company or the one that is seeking certification, but throughout the supply chain, with greater control over subcontracting;
- c) more safety in regards to compliance with the requirements for restricted substances;
- d) actions for the optimization of water and energy use;
- e) improvements to production processes through seeking the best production practices;
- f) reduction in waste generation and better control and management of waste;
- g) improved management of both liquid and atmospheric emissions;
- h) improving the health and safety conditions in the employees' work environment, thereby providing a positive impact on their performance and productivity;
- i) increased supplier qualification and customer satisfaction;
- j) integration with suppliers and customers as well as the community in which the company is inserted.

4 Productive Chain Integration Actions

As part of the certification program are being performed different alignment and integration actions with other actors of the productive chain. Following are highlighted the principal ones.

4.1 Presentation of the Certification to National and International Buyers

Different visits and conversations are taking place in Brazil as well as in other countries; for the presentation of criteria and format of the certification, so that all have knowledge and access to the attributes that the Brazilian leather certificate has with relation to the principles of sustainability. Public targets of this action are considered Brazilian brands, international brands, chemical companies, and footwear manufacturers.

The CSCB certification program also gains highlight in all promotional actions performed in the scope of the Brazilian leather program, a partnership between CICB and Apex-Brasil. There are more than ten international fairs in which the Brazilian tanneries participate and where the program is promoted.

4.2 Cooperation with Footwear Industries

Recently was established between CICB, Arezzo Co. and Calçados Bibi, and a cooperation agreement for the use of the sustainability certificate as criterion in the selection of leather suppliers by Arezzo Co. and Calçados Bibi. With this, the companies will have guaranteed that its suppliers are in agreement with the obligatory criteria of the standard and attending the majority of the indicators established by the ABNT NBR 16.296.

4.3 International Acknowledgment

An agreement of mutual acknowledgment was established between the Brazilian certification and the Italian certification. The document was signed by ICEC (the Italian Institute of Quality Certification for the Leathers Sector) and Brazilian Leather Certification of Sustainability (“Certificação de Sustentabilidade do Couro Brasileiro” - CSCB), signing the mutual acknowledgment of the certifications of the two countries. With this, new fronts of research shall be development by the two countries, as well as the strengthening of sustainability indicators, the valorization of leather close to the final consumer, and the acknowledgment of companies integrating the certification institutes that enter the agreement.

5 Conclusion

The Brazilian Leather Certification of Sustainability (CSCB) is an important form of externalizing the good practices of the Brazilian tanneries, which attend the environmental, social, economic, and management requirements of their productive process. This guarantees to the buyers and to the entire productive chain a high level of safety and best practices.

For being a model of official certification, performed with basis on national standards and certified by the organism of a third party accredited by INMETRO, it has total transparence in the process, aggregating the reliability necessary to transmit to the buyer the certainty of being a product that has its main raw material elaborated in an economically efficient, environmentally correct, and socially responsible form.

Significant gains are observed by companies that seek certification through the improvement of management process guided by the dimensions of Sustainability. Economic aspects are strengthened through a more comprehensive and in-depth look at environmental and social issues. The integration of the entire production chain to common objectives has been strengthening relationships throughout the leather sector.

References

1. ABNT NBR 16.296, *Leather – Principles, criteria, and indicators for sustainable production*. Rio de Janeiro, 2014
2. INMETRO Decree N. 314/2015, *Requirements of the conformity evaluation of the sustainability of the leather production process*

AUTOMOTIVE LEATHERS – EVALUATING THE PERFORMANCES LIMITS (PART II)

S. De Vecchi¹, J. Christner², A. Rama¹, S. Summa¹ and D. Rinaldi¹

1 TFL Italia S.p.A., Research&Development, Buscate, Italy a)

2 TFL Ledertechnik AG, Research&Application, Muttenz, Basel-Land, Switzerland b)

a)Corresponding author: sebastiano.devecchi@tfl.com

bjjorgen.christner@tfl.com

Abstract. Leather used in car interiors is sold as a premium product. Consumers perceive leather as a durable and natural product and to support this image original equipment manufacture (OEMs) manufacturers have set demanding performance profiles defined by mechanical wear, protection from the elements, low emissions and sustainable manufacture. High wear and protection can only be achieved with a polymeric coating and poor performance of coated leather becomes visible if polymer coat is wearing off or cracks over time. Therefore ageing property is seen as a representative key performance parameter and was determined by checking how flexible and strong a polymer coating remains after leather has been exposed to light, heat and humidity for a given time. In a first approach different type of crusts (wet blue ,wet white) were prepared and finished with a standard polyurethane coating. It turns out that the selection of the right fatliquors and tanning agents as well as the presence of vegetable tannins play an important role. On top of this the effective use of protective chemicals like anti-oxidants is needed for the production of crust to reach high aged flexing performances. In this work the polymer coating (matrix) was optimized without the impact of leather which means testing of the various polymer films with and without coating additives (pigments, fillers, waxes, feel agents etc.). Testing has been carried out through the analysis of the strain and stress curves of the polymer films before and after exposure to heat, light and hydrolysis. Parameters like polymer type, application technology, and impact of additives were investigated and tested after ageing when applied on chrome automotive leather. Results show that not only the right selection of polymers is critical but also the way the coat is being applied. Additives in coatings like dulling agents, feel agents, waxes and fillers obviously play an important role and cannot be easily dispensed although their presence in many cases would weaken the integrity of the polymer matrix and consequently reduce physical and chemical fastness properties. As to application, special emphasis is given to the transfer coating technology which potentially reduce the number of application steps, allow higher curing temperature and decrease the amount of additives while maintaining the aesthetic and haptic properties.

1 Introduction

Consumers consider automotive upholstery leather as a premium product, in particular they perceive car interior leather as a natural material which has to satisfy important aesthetic properties such as colour and surface touch but also be resistance to high mechanical wear and chemical during its lifetime. In order to support this concept, original equipment manufacturers (OEMs) set demanding performance profiles defined by mechanical properties, protection from the elements, low emission and sustainable manufacture.

Leather performances are generally evaluated after production, although a real judgement of quality can only be made after many year of service. Long term durability can be predicted by several methods like extended ageing tests. A very challenging test set up is to expose leather to several cycles of light at given heat and humidity (e.g. FAKRA test according to UNI ISO 105 B06-1) and after such exposure test the mechanical properties like flexibility of the coating.

In our previous work ¹, we focused our attention on testing the performance of different types of crust, alone and finished with a standard polyurethane basecoat. The chrome and chrome-free crust sample were subjected to various test cycles according to ISO 105 B06-1 and then evaluated in terms of flexes, dimensional changes, softness and mechanical properties. The results showed that selection of the right fat-liquors and tanning agents as well as the presence of vegetable

tannins and appropriate antioxidants play a key role in achieving best performances. In a second part of our work the interesting results achieved, directed our attention to the optimization of the finishing coating.

Finishing is the final step of leather processing and plays a pivotal role for achieving the final performance of automotive leather. Depending on the quality of the crust (as to defects) and the requirements set by OEM, the thickness and aspect of the finishing coat will vary from semi-aniline with lowest add-on quantity to corrected, embossed leather having the highest coating add-on.

From a chemical aspect, a typical automotive finishing coat consist mainly of polyurethane dispersion (PUDs) and acrylic emulsions, which are formulated by addition of pigments, organic and inorganic dulling agents and various other additives for feel, flow and rheological control. Those additives together with cross-linkers and the application procedure can greatly impact the performance of the final polymeric coating with major concern after ageing.

Polyurethane dispersions (PUDs) represent a large family of polymers and due to their excellent properties find a wide application in leather finishing. They are obtained from the reaction of a diisocyanate and a polyol. With the availability of different diisocyanates and polyols many tailor-made solutions are possible. Automotive upholstery leathers are generally finished by the use of PUDs based on aliphatic diisocyanate which, as widely reported, can support a long-term stability.^{2,3} On the other hand chemist resorts to a wide range of polyols which affect systematically the ageing behaviour of the final PUDs. Polyester polyols do not suffer severe degradation when they are exposed to UV-radiation, but heat and humidity can promote the hydrolytic cleavage of the ester group and lead to a loss of physical properties (hydrothermal aging).^{4,5} Polyether polyols show a better resistance to hydrothermal aging however they are susceptible to photo-oxidation phenomena which promote the cleavage of ether linkages resulting in a weakening of strength of the coating.⁶

Finally polycarbonate based polyols show the best resistance to both, UV and hydrothermal ageing, however their high costs prevent from a wide use in leather finishing.⁶

In this context, the co-use of acrylic binders offers interesting alternatives. It is not only the lower cost which make them interesting, but also their high resistance to light and hydrolysis whereas they are more thermoplastic and print retention when embossed is not as high as PUDs.

In the first part of this study the polymer coating (matrix) was optimized without the impact of leather which means testing of the various polymer films with and without coating additives (pigments, fillers, waxes, feel agents etc.). Testing has been carried out through the analysis of the strain and stress curves of the polymer films before and after exposure to heat, light and hydrolysis. In a second part of the work various polymer blends were applied on automotive crust leather which were then aged according to DIN EN ISO 105 B06-1 and tested for cracks in the finishing coat after a defined number of flexes. In a final optimization stage the impact of application was studied with an emphasis on transfer coating as an alternative to the more traditional spray and roller coat application.

In transfer coating the finishing coats (base and adhesion coat) are applied to a release (transfer) paper which has the desired surface texture (matt, gloss and embossed). Each coat is dried after application and the final polymer film is then transferred (laminated) via the carrier paper onto leather by applying heat and some pressure. Transfer coating technology reduces the number of application steps, allows higher curing temperatures and potentially reduces the amount of additives while maintaining the aesthetic and haptic properties.

2 Experimental Part

2.1 Materials and Methods

2.1.1 Film resin preparation

Films of various polymers and polymer combinations (PUDs and acrylics) were prepared by casting a defined amount of resin dispersion on a levelled petri dish and allowing them to dry at room temperature. The residual volatile matter was removed by drying for 12 hours in a static oven at 50 °C.

2.1.2 Leather preparation and finishing

Applicative tests have been carried out on commercial full grain automotive crust leather. The finishing procedure consists of three basic steps, first the polymer base coat was applied on release paper (film thickness 130 µm) and dried; then an adhesion coat was laminated to the base coat layer. The film coat on paper was then immediately laminated via a calender at a temperature of 100 °C to the leather substrate. The final top coat has been applied in two spray applications (total wet add-on of 5 g/ft²) and then dried for 2 minutes at 90 °C. Test pieces were allowed to rest for 5 days at room temperature before subjected to ageing test.

2.2 Accelerated ageing test

2.2.1 Ultraviolet (light) exposure – (xenon test)

Two specimens of leather (40 x 100 mm) were exposed to UV-irradiation using a Xenotest Alpha Light Exposure (Atlas Corporation) in accordance with ISO 105-B06-1. The exposure energy rate was 60 W/m² and chamber temperature was set to 65 °C at 30% of relative humidity, for a total radiant energy of 22000 KJ.

2.2.2 Hydrolysis test (exposure to humidity in climatic chamber)

Two specimens of leather (40 x 150 mm) were placed in a climate test chamber model WK3-180/40 (Weiss Technik) at a temperature of 70 °C and 90% of relative humidity for a total exposure of 400 hours. At the end of the tests the samples were removed from the chamber and allowed to equilibrate at 23 °C and 50% of humidity for 24 hours before further testing was executed.

2.2.3 Heat ageing test (exposure to heat in oven)

Two specimens of leather (40 x 150 mm) were placed in a ventilated oven model at a temperature of 100 °C for a total exposure of 400 hours. At the end of the tests the samples were removed from the chamber and allowed to equilibrate at 23 °C and 50% of humidity for 24 hours before further testing was executed.

2.2.4 Bally flexibility

Leather samples were cut into 45x70 mm pieces and mount on a Bally flexometer (Bally Matric 2182). Flexing tests have been carried out according to ISO 5402-1, each specimen was tested against 100000 flex cycles and examined after every 10000 flexes. Intensity of cracks was evaluated in a good light using, the following definitions were used to describe the final result:

- Cracks: Visible with naked eye.
- Fine crack: Visible with 6X magnifier.
- Micro cracks: Visible with 25X microscope.

2.2.5 Determination of gloss

Gloss has been measured with a BYK Gardner Micro Tri Gloss 20/60/85°, the measurement was carried out at 60° and the results were reported as an average of 5 different measures.

2.2.6 Strain and stress measurement

Strain and stress curve as well as modulus at 100% of elongation of polymer films were evaluated with a tensile strength machine (Instron Model 3343). From each sample at least five test specimens were tested. Table 1 shows dimension of the test specimen.

Table 1. Dimension in millimetre of the test specimen.

	L	L3	L2	b1	b	T
Measure (mm)	110	50	30	25	10	0.5 ± 0.05

Tensile strength measurements were recorded at a crosshead speed of 100 mm/min, with a maximum load capacity of 500 N; this method was used to determine the tensile strength at 100% of elongation with an experimental error lower than 1.5%.

3 Results and discussion

3.1 Effect of pigment on mechanical properties of polymer films

The number of parameters which influence physical properties of polymer film made from waterborne polyurethane and acrylic emulsion such as molecular weight, chemical nature and particle size distribution, introduce a considerable experimental uncertainty, leading to potential misunderstanding about the impact of difference variable on the polymer performances. In leather coating, this complexity is also increased by the use of different auxiliaries such as pigments, silica and dulling agents which increase the number of parameters involved in coating optimization.

In order to decrease the complexity, in the early stage of this project four different polymers, two polyurethane dispersions (PUD) and two acrylic resins (ACR) have been pre-selected by evaluating their physical and chemical properties as shown in table 2. The polymers exhibit high elongation and a rather low elastic modulus suited for their use in base coats. Polyester based PUD's in this case were not selected although there are interesting products available on the market which satisfy most important physical requirements (included hydrolysis resistance).

Table 2. Physical properties of pure polymer.

Designation	Chemistry	Modulus 100% (MPa)	Elongation (%)	SHORE A (°)
PUD 1*	Polyether	5.7	450	96
PUD 2*	Polyether/Polycarbonate	1.7	1000	74
ACR 1*	Polyacrilate	0.8	900	50
ACR 2*	Polyacrilate	1.6	750	62

Since pigments are the largest formulation component having an impact on physical properties of polymer films each of these polymers have been formulated with addition of 15% of inorganic black pigment. According to Fig. 1 all polymers under investigation show a significant increase in modulus (100% of elongation) when mixed with black pigment. The relative percentage increase is highest with acrylic binders (by average 22%). The pigment addition into polymer matrix lead to a composite material which maintains its elastic behaviour (no plastic deformation was observed)

but shows higher stiffness. More force is required to stretch the film to the same elongation. Interesting is the behaviour of PUD 2, in which case pigment addition lead to a 9% increase of modulus at 100%, which is the lowest change among the polymers tested.

These preliminary results point out that the effect of the pigment on physical properties of polymer matrix is not negligible leading to a systematic increase of stiffness which cannot be predicted with an ‘a priori’ model. Since pigments are fundamental in any leather coating all further work is done with pigmented films.

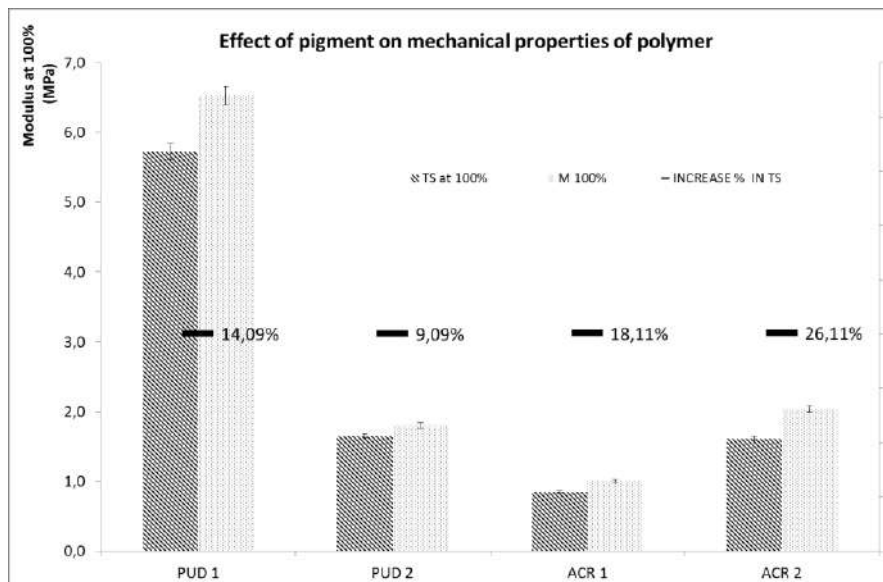


Fig. 1. Modulus at 100% of elongation of the polymer under investigation and the increase percent of the same due to the use of 15% black pigment.

3.2 Effect of additives on mechanical properties of polymer films

To further investigate the impact of pigments and additives on elastomeric properties of polymer films, two blends were designed (see table 3). Both blends are formulated with the pre-selected polymers as listed in table 2 whereas basecoat 1 is representative for a typical basecoat and pol-mix just contains the polymers and pigment but no further additives.

Table 3. Composition of blends under investigation.

Component	Basecoat 1 (%)	Pol-mix (%)
PUD 2	30	60
ACR 1	20	40
PARAFFIN WAX*	10	/
SILICONE	2	/
SILICA DISPERSION*	20	/
WATER	18	/
BLACK PIGMENT*	15	15

Films of basecoat 1 and pol-mix were tested via the strain and stress curves for their physical performances (Fig.3). The addition of 30% of additives lead to a 45% increase of modulus at 100% of elongation, moving from 1.8 MPa of the polymers mixture to 3.3 MPa for the ‘formulated’ basecoat. This result shows how the addition of additive changes completely the behaviour of the polymer matrix, the material (polymer film) becomes stiffer. The ‘additive-loaded’ film breaks at

around 134% of elongation while the ‘additive-free’ blend achieves 300% of elongation without any failure (break point could not be detected due to instrumental limits).

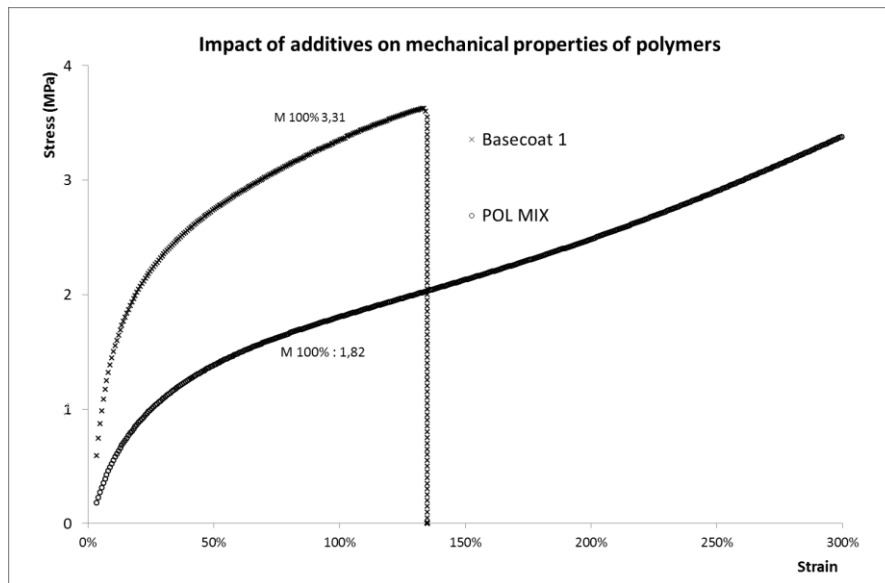


Fig. 3. Stress and strain curve of pol-mix and basecoat 1.

The influence of additives like waxes, feel additives and fillers is also visible in the behaviour of the material after exposure to light by the evaluation of the strain and stress curve in the low strain region (0-10 % elongation). In this region the material shows an ideal elastic deformation (Young Modulus). Both materials, before and after ageing maintain a linear elastic behaviour (Fig.4) however they show curves with different slopes. After aging basecoat 1 suffers a significant degradation by losing more than 25% of its initial modulus compared to the ‘additive-free’ blend (pol-mix) which also shows degradation but to a much lesser extent (appr.10%).

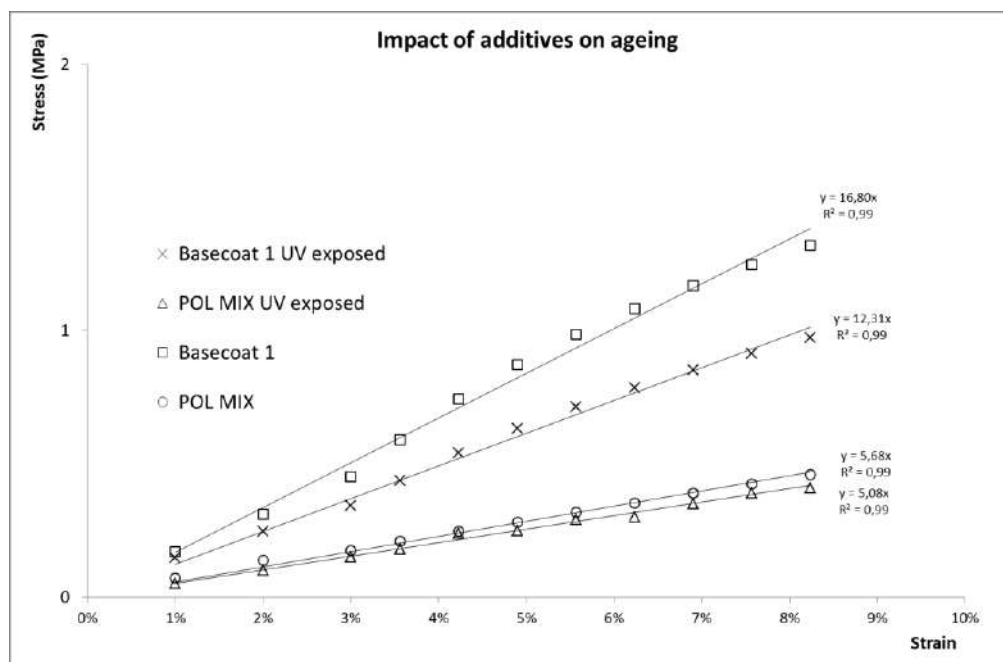


Fig. 4. Impact of light exposure (ISO 105B06-1) on Young Modulus.

3.3 Optimization of polymer matrix

The further optimization of the polymer films was carried by measuring the modulus of the films made with preselected polymers (see table 2) after exposure to light, heat and humidity.

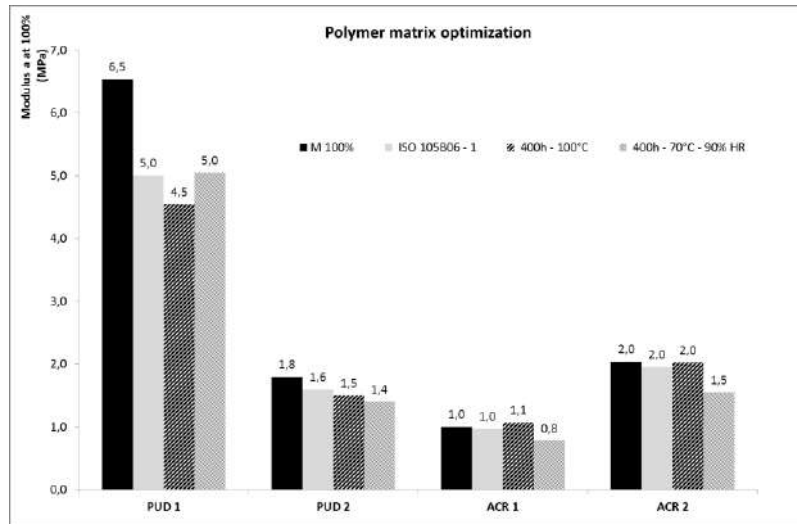


Fig. 5. Evaluation of modulus at 100% of various polymers after exposure to different ageing conditions.

The analysis of the data obtained after light exposure (ISO 105 B06-1) as shown in Fig.5 indicate a clear trend: the acrylic polymers almost maintain their mechanical properties with an average loss in modulus of only 3.3%, whereas PUDs show a significant decrease particularly PUD 1 losing 23% of its original value moving from 6.5 MPa to 5.0 MPa. Interesting is the behaviour of PUD 2, which shows a performance between PUD 1 and acrylic polymers by losing only 11% of its original modulus at 100%. The results obtained from heat ageing test (400 hrs, 100 °C) confirm above trend: acrylic emulsions maintain the same elastic moduli while PUD 1 and PUD 2 respectively lose 30% and 17% of their initial value. Results obtained after the hydrolysis test show how regardless of their chemical nature, the polymers when exposed for 400 hrs to 70 °C and 90% humidity show an average decrease of 22% in tensile strength value.

Based on these results the PUDs alone show inferior performances with regards to light and heat exposure than acrylic resins, with the exception of the hydrolysis test in which both resins suffered a loss of strength and elasticity. PUD 2, a polyether/polycarbonate polyurethane dispersion, shows a better overall behaviour than PUD 1 a polyether based PUD. In particular the good resistance to both UV-exposure and heat exposure could offer advantages when used as soft binder component. From this point of view the right ratio between PUD 2 and acrylic resins seems to offer the best solution to achieve an optimal cost/performance ratio. Therefore the idea for the next step of optimization was to improve PUD/acrylic blend while reducing the amount of additives via a different application approach.

3.4 Transfer coating technology as an innovative approach to high performance automotive leather

The results achieved by the stress testing of the film are an important part of the optimization but need to be fine-tuned when applied on crust leather. Already in part 1 of our studies it became evident that type of crust leathers has a significant impact on aging of the polymer coating. Particularly the flexing behaviour when tested after aging (checking for visible cracks in coating) of the finished crust leather gives a quite realistic view of real world conditions and how to best evaluate the performance limits of automotive leather.

Therefore, three different blends of PUD 2 and ACR 1 with pigments only (see table 4) were applied on a chrome tanned automotive crust via paper transfer coating technology following the process as outlined in materials and methods (see paragraph 2.1.2).

Table 4. Composition of the polymer blends used in transfer coating of automotive crust leather.

Component	MIX 1 (%)	MIX 2 (%)	MIX 3 (%)
PUD 2	50	80	20
ACR 1	50	20	80
BLACK PIGMENT	15	15	15

Coated leather were first subjected to accelerated ageing according to ISO 105 B06-1 conditions, then flexed for a defined number of times and finally checked for cracks in the coating (see table 5). The best performance for flexing after aging is achieved by mixing equal parts of ACR 1 and PUD 2 (MIX 1). The increase of polyurethane dispersion PUD 2 (MIX 2) leads to a drop of the performances after ageing (fine cracks). This result is consistent with previous findings, which showed the good weathering behaviour of acrylics polymer films. Thus the addition of ACR 1 to PUD 2 seems to provide a synergistic effect, improving the performance of the coating. Reversing the ratio towards acrylic (MIX 3) leads to a basecoat which cannot withstand 100k flexes before aging, a basic requirement in automotive leather upholstery.

Table 5. Flexing performances of the blends. Tests were performed according to ISO 5402-1.

Name	100k Dry Flexes	10k Dry Flexes 3x ISO 105B06-1
MIX 1	NO CRACKS	NO CRACKS
MIX 2	NO CRACKS	FINE CRACKS
MIX 3	MICRO CRACKS	/

This outcome is not unexpected and can be explained by refers to the 100% modulus of the polymeric films made from the three blends. As shown in **Fig.6**, MIX 3 has the lowest elastic modulus, which is the main cause why the coating fails to pass 100k flexes even before ageing. Also the performance of MIX 1 and MIX 2 can be explained by the analysis of the tensile strength properties of the polymer films: after one cycle of ISO 105B06-1, MIX 1 shows a 9% decrease of the modulus at 100% while MIX 2 loses more than 20% of its original value showing the worst ageing performances.

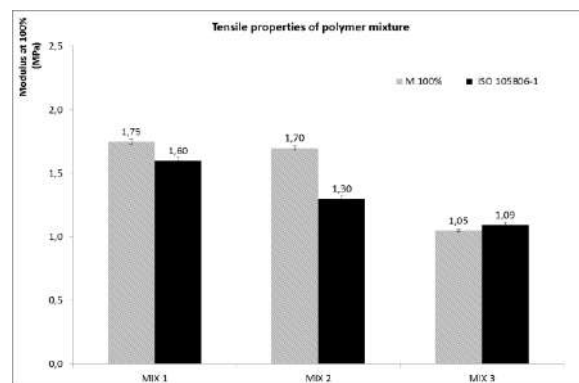


Fig. 6. Modulus (MPa) at 100% elongation of polymer blends films before and after one cycle of ISO 105B06-1.

In order to see potential benefits provided by transfer coating technology, a comparison with a classical finishing approach has been done. One piece of automotive leather was coated with

basecoat 1 (see composition in table 3) via roller-coating for total dry add on of 3.8 g/ft². In parallel, another specimen of same crust leather was coated with MIX 1 (only pigments no further additives) through transfer paper coating technology (see experimental part). The two pieces were dried and stored overnight; then a dull organic top coat, which composition is reported in table 6, has been sprayed two times with a total wet add on 5 g/ft². The final leathers were stored five days at room temperature before being subjected to the aging tests.

Table 6. Composition of the dull top coat

Component	(%)
ORGANIC DULL PU	70
PERFORMANCE SILICONE	8
WATER	17
ISOCYANATE CROSS LINKER	5

As shown in table 7 there is no significant difference in gloss between the two applications after exposure to heat and hydrolysis, although no silica dulling agent was used in basecoat of transfer coating application (TC). However there is a significant increase of gloss on both samples after they were exposed to three cycles (ISO 105B06-1). This loss of opacity is due to the degradation of the dull PUD particles and can be reduced by the co-use of suitable silica duller and optionally the use of antioxidants and UV stabilizers.

Table 7. Test results of final articles (TC = transfer coating of ‘additive-free’ basecoat; STD = roll coating application of basecoat 1; same total dry add on and finished with dull top coat by spraying).

Property	TC	STD
Gloss 60°	0.6	0.7
Gloss 60° after 3x ISO 105B06-1	2.5	2.1
Gloss 60° 400h 100°C	0.5	0.6
Gloss 60° 40h 70°C 90% HR	0.5	0.6
100k Dry Flexes	No Cracks	No Cracks
10k Flexes 3X ISO 105B06-1	No Cracks	Fine Cracks
100k Flexes 400h 100°C	No Cracks	No Cracks
100k Flexes 40h 70°C 90% HR	No Cracks	Fine Cracks
Dry Adhesion (N/cm)	12.0	7.2
Taber (CS 10)2000 cycles (10X Magnification)	Repolish-No Damage	Repolish-No Damage

With regards to flexing after aging the use of transfer coating offers clear advantages. According to table 7, the specimen of leather coated with the standard basecoat and standard application does not pass 10k flexes after three cycles of ISO 105B06-1 and at the same time it fails the hydrolysis test, showing cracks already at 60k flexes. With transfer paper coating technology, however the stringent flexing requirements after aging can be passed. This is mainly due to the reduction of additives and use of suitable papers along with selected polyurethane and acrylic polymers used in an optimized ratio.

4 Conclusions

The aim of this study was to examine the performance limits of automotive leather with regards to the flexibility of polymer coatings on automotive crust after being subjected to various aging conditions. In the first part of the work the impact of pigments and additives was shown via the

analysis of the strain and stress curves of polymer films. As a matter of fact pigments like carbon black and additives like fillers, dulling agents, waxes and feel additives increase modulus at 100% and thus the stiffness of the polymer coating. The comparison between a basecoat with typical coating additives and a 'additive-free' polymer blend show that auxiliaries not only increase the stiffness of the coating but after light exposure lead to a loss of the elastic modulus.

The coating polymer matrix consisting of selected PUDs and acrylic emulsions was further optimized with regards to resistance to heat, light and hydrolysis by testing the 100% modulus. Acrylic emulsions show the best fastness performances while PUDs provide strength to the polymer matrix. The final coating optimization has been achieved through the application of a polymer blend based on equal parts of a specific acrylic and polyurethane dispersions by using transfer coating technology. This technology allows reduction of coating additives (mainly dulling agents like silica) via use of a matte transfer papers. The results show that the critical step is not only the right selection of polymer but also the way the coat is being applied, from this point of view a significant improvement is offered by transfer coating technology which avoids the use of additives while maintaining aesthetic and haptic properties.

Trade Name

Designation	Trade Name
PUD 1	RODA©PUR MB
PUD 2	RODA©PUR 65
ACR 1	RODA©CRYL 5416
ACR 2	RODA©CRYL 2130

References

1. Christner, J : 'Automotive leathers where are the performance limits?' Oral contribution, 114th Annual ALCA convention, Eaglewood Resort, Itasca IL, June 19 22nd, 2018.
2. Allen, S., Dilhan, F., Stuart, C., 'Mechanical property changes and degradation during accelerated weathering of polyester-urethane coatings', JCT, Vol.3, 41-51, 2006.
3. Gite, V.V., Mahulika, P.P., Hundiwale, D.G., 'Preparation and properties of polyurethane coatings based on acrylic polyols and trimer diisocyanate', Progress in Organic Coating, Vol. 68, 307-312, 2010.
4. Oprea, S., Oprea, S., ' Mechanical behaviour during different weathering test of the polyurethane elastomers films', European Polymer Journal, Vol. 38, 1025-1210, 2002.
5. Aglan, H., Calhoun, M., Allie, L., 'Effect of UV and Hygrothermal Aging on the Mechanical Performance of Polyurethane Elastomers', Journal of Applied Polymer Science, Vol.108, 558-564, 2008.
6. Irusta, L., Fernandez-Berridi, M.J., 'Photooxidative Behaviour of Segmented Aliphatic Polyurethanes', Polymer Degradation and Stability, Vol.63, 113-119, 1999.

MINIMIZING EMISSIONS OF AUTOMOTIVE LEATHER

Dr. Volker Rabe, Dr. Rene Graupner-von Wolf, Dr. Martin Kleban

Business Unit Leather, Lanxess Deutschland GmbH, 51369 Leverkusen, Germany

Corresponding author: volker.rabe@lanxess.com

Abstract. Today, automotive leather has to meet a multitude of requirements. One of these parameters are the Volatile Organic Compounds (VOC) which the final leather article emits. The recurring question of how to further reduce the emissions of automotive leather is answered by presenting the latest crosslinker development as one focus of this article. Nowadays, the focus of the regulations has switched more and more from quantity of emissions to the properties of single substances emitted. Often the exact source of those single substances were initially unknown and consequently a specific solution to meet the limits was not available. The search for the sources is becoming increasingly complex and difficult as many of these substances are not applied directly but are often degradation products of other compounds. Often the measured low concentrations are in the range of the natural decomposition processes. Nevertheless, it is possible to identify some of the sources by evaluating the results of different analytical methods. Thus it is now possible to develop suitable countermeasures. The presentation of the source of acetaldehyde as well as the reduction of this component in leather forms a further focus of this article.

1 Introduction

Today, automotive leather has to meet a multitude of requirements of different automotive brands. In addition to the still important traditional aesthetic properties, such as the feel and appearance of the leather, a growing number of measurable specification parameters have been added over time. These analytically measurable specification variables can be subdivided into physical ones, such as rub fastness or light fastness and chemical requirements. The chemical restrictions can be further subdivided into substances that can be extracted from the leather with a solvent such as Cr(VI) or azo dyes and substances that are emitted from the leather. This latter group includes the subject area of this article, the Volatile Organic Compounds (VOC).

2 Background of VOC's

The starting point for the problem of interior emissions from vehicle interiors was so-called "fogging". This is a condensate of low-volatility compounds that can deposit on the inside of windscreens and thus restrict the driver's view. This topic was associated with a clear, safety-relevant aspect. To reduce this phenomenon, automobile brands introduced simple tests that measure either the weight of the condensate (gravimetric) or the effect on the light transmission of the precipitate (reflectometry). These methods were the starting point for the introduction of many other tests with the aim of determining the composition of the condensate more and more precisely.

Today, most VOC analyses are performed with gas chromatography and mass spectrometry detection, which leads both to the quantification of emissions and to the identification of many individual components. Over time the focus of the emissions issue has shifted from, as mentioned earlier, purely safety considerations to the general air quality of the vehicle interior and, as the latest in the field, the regulation of individual substances for toxicological reasons.

3 The Challenge

The fact that each individual automobile OEM has developed its own test program has led to the introduction of a variety of different emission regulations and limits. Today, this method and specification “jungle” poses a major challenge for the development of automotive leather [Fig 1].

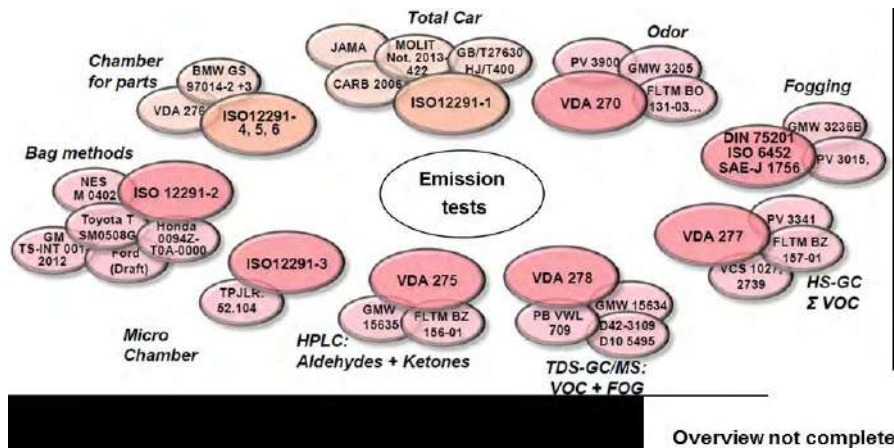


Fig. 1. Overview of emission tests.

Each of these methods has a slightly different substance focus and highlights a different group of volatile substances in the test result. For this reason, the individual methods cannot be compared. This is a big challenge, because nowadays one has to develop an automotive leather article with the very high demands on low emission values under consideration of the required test methods/limits. In order to be able to fulfil all the required parameters, it is necessary not only to have a sound knowledge of the required test methods, but also to have detailed knowledge of the products used.

4 The Trend

Due to the implementation of profound measurement of emissions over the last one and a half decades, it has been possible to reduce the emitted substances by a factor of 10 or more. As a result Total Volatile Organic Compounds (TVOC) have been reduced over time from grams to micrograms per kilogram of leather. This dramatic reduction in intensity has been made possible by the introduction of product solutions in the individual areas of both crusting and finishing products. This significant reduction is visualized in [Fig 2].

As a result, the emissions today are no longer determined solely by the products used, but are also increasingly influenced by natural, product-independent sources. These sources can be components of the hide or its degradation products or compounds which are introduced into the leather through the increasing use of sustainable processes such as fleet recycling. This means that nowadays, in addition to the still important aspects of the products used, the entire process for the production of automotive leather must also be taken into account to an increasing extent.

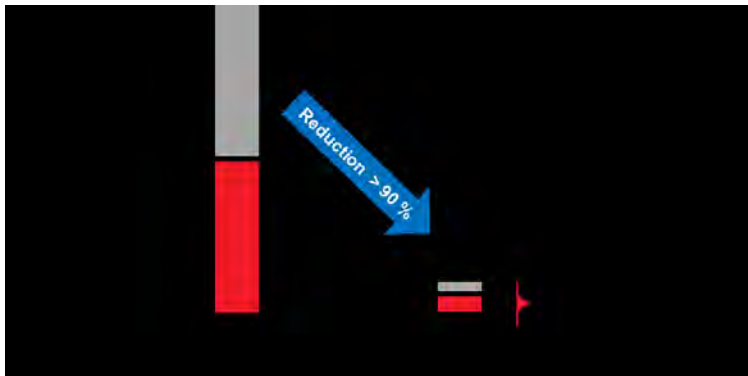


Fig. 2. Scheme of VOC contribution in different sectors.

5 Crosslinker: latest developments

Crosslinkers are an example of the range of solutions that are constantly being optimized to further reduce leather emissions. The content of solvents, which contribute to the emitted substances in the common test methods, has been further reduced in the course of time. As the latest development, the required content has been reduced to 0%, thus completely eliminating the solvent from the product. If one now prepares automotive leather with the different available crosslinkers, one measures in the usual emission test methods a clear reduction of the values. The TVOC of an automotive leather could be reduced in one example by measuring with the test method: ISO 12219-2 (10 l bag-test) from originally 66 g/sample when using a crosslinker with 50% solvent to 27 g/sample when using a crosslinker with 0% solvent content [Fig 3]. This strong reduction of 59% is more than one would normally expect. In order to understand this unusually large reduction, it is necessary to take a closer look at the individual regions of the spectrum. As expected, there is a significant decrease in emitted solvent molecules which can clearly be attributed to the solvent content of the crosslinkers used. In this example, however, this accounts for only about 72% of the measured TVOC decrease. The missing rest are mostly lower siloxanes-emissions. This is surprising as this group of substances has nothing to do with crosslinkers. The reduction of these substances can therefore only be explained by so-called "entrainment" of the siloxane molecules by solvent substances during the test. In the end, there is a synergistic effect in which other, less volatile substances are not measured in the emission test by reducing the solvents used in the crosslinkers and thus a disproportionate reduction in emissions is achieved.

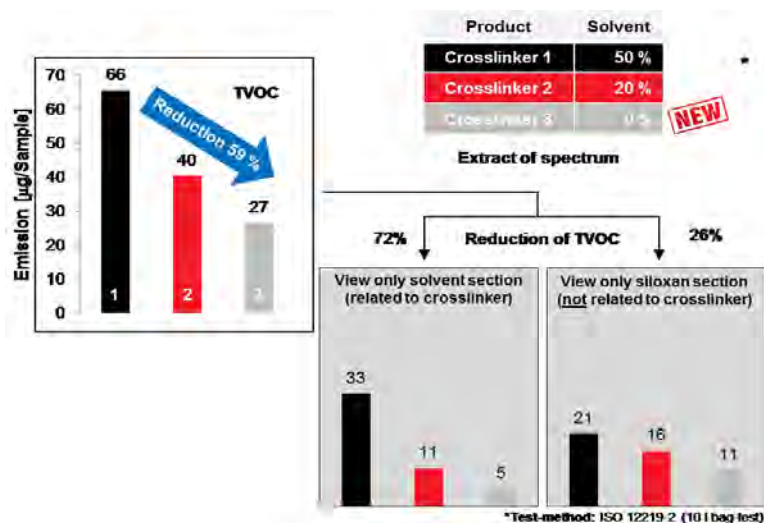


Fig. 3. TVOC values of automotive leathers using different ISO crosslinker with different solvent content.

6 Single substance regulations: Acetaldehyde

The new China Vehicle Interior Air Quality (VIAQ) standard can be regarded as one of the latest examples of the trend towards increased regulation of individual substances emitted from leather. This standard regulates 8 substances with limits and related test method for car interiors (Fig. 4). Following the publication of the first proposal a few years ago, OEMs have already taken these regulations as a basis and adapted their individual leather specifications with stricter limits and harsher test conditions. If you now take a closer look at the controlled substances, the limit value of 7 of the 8 substances for leather can be adhered to. The only exception was and still is acetaldehyde.

List of new Chinese VIAQ limits regulated 8 Substances for car interior	Substance	Limit [mg/m ³]
	Benzene	0.06
	Toluene	1.00
	Ethylbenzene	1.00
	Xylene	1.00
	Styrene	0.26
	Formaldehyde	0.10
	Acetaldehyde	0.20
	Acrolein	0.05

Fig. 4. Chinese new Vehicle Interior Air Quality (VIAQ) standard.

The problem was that the sources of this substance were initially completely unknown. Acetaldehyde is neither used directly in the leather production process nor indirectly, since it is not used in industry as a raw material for the manufacturing of chemicals for leather production. Consequently, due to the lack of knowledge where this molecule comes from, a solution to meet the limit was not available at that time.

7 The source

The interpretation of results from FILK gave the first hint about one source of acetaldehyde. This research institute found out that the highest acetaldehyde value is measured in the raw hide and the concentration decreases until the leather article is finished. One theory explaining this phenomena is the decomposition of proteins already in the raw hide^[1]. Nevertheless this means that the Acetaldehyde molecule is already present in the raw hide.

However, this may not be the only source for this molecule, as the measurement of a leather after 4 months of storage showed. A closer look at all emitted aldehydes shows that all concentrations increase and that all these substances are replicated after the leather is finished [Fig 5]. The later the compound is in the homologous series, the stronger is the increase percentage wise. This is understandable, since due to the higher molecular mass of the molecules the volatility becomes lower and the relationship between formation and emission shifts to higher concentrations. The source of all these aldehydes, from hexanal to nonanal, is known and can be traced back to the degradation of natural, unsaturated fatty acids. The increase in the concentration of acetaldehyde after storage also speaks for the degradation of fatliquors as another source. The high volatility explains why the increase is lower than for other aldehydes.



Fig. 5. Aldehyde values of a leather after storage.

To clarify the theory of whether this is really another source, 4 crust leathers were made, all from the same hide and produced in the same way. The only exception was the use of fatliquors. In one quarter no fatliquor was used and the other quarters used fatliquors with increasing natural content and therefore unsaturated fatty acids. Acetaldehyde concentrations were then measured using the VDA 277 emission method [Fig 6]. The measured concentrations increased compared to the crust leather without fatliquor and the value was more than doubled in one case. Since the samples all come from the same rawhide, the values should be similar if this were the only source. The increase in values can therefore only be explained by the degradation of fatty acids as a further source of acetaldehyde.

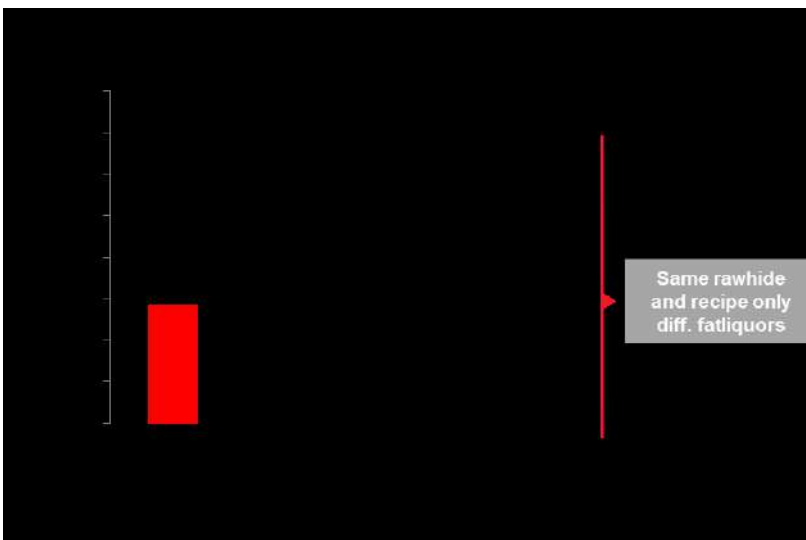


Fig. 6. Acetaldehyde values of a Crust-leather coming from one raw-hide and prepared with different fatliquors.

8 Independent confirmation

The trial series of the production of crust-leathers with different softening products was continued and, as expected, a relatively wide variation of acetaldehyde values can be found. To substantiate the theory of degradation of fatliquors as a another source, further independent confirmation by another measurement method would be desirable. For this reason, the undyed leather obtained was subjected to a heat yellowing test. In general, the results of the heat yellowing tests depend on various factors. The vegetable tanning agents, syntans, dyestuffs and fatliquors/polymers used

have an influence on the final result. In the case of the crust leather examined here, these influencing factors were limited purely to the influence of the softening products used, since all other products were the same.

In the case of fatliquors, it can be stated in general and somewhat simplified terms that a poor evaluation of heat yellowing indicates a high degradation rate or vice versa. A comparison of the values obtained for heat yellowing with the acetaldehyde concentration reveals a good correlation between the results [Fig. 7]. Crust leathers with a low heat yellowing rating, i.e. a fatliquor that is easier to degrade, also have high acetaldehyde concentrations. In contrast to this, a good heat yellowing rating is achieved when using more stable fatliquors/polymers softeners and a correspondingly lower acetaldehyde value is measured. Thus the theory is confirmed by a further, independent measurement. However, it must be emphasized again that the correlation of heat yellowing with acetaldehyde values is only possible within the framework of the selected test program, excluding the other influencing factors. Otherwise, this correlation is generally not possible due to the many existing variables.

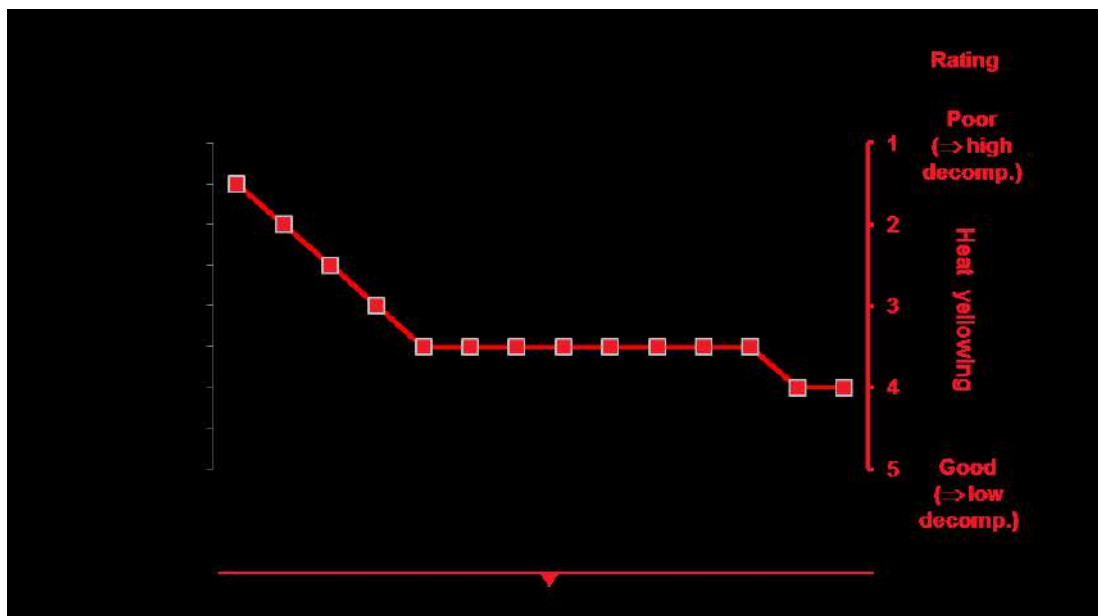


Fig. 7. Correlation of emission test and heat yellowing rating.

9 Available technical solutions

After identification of the two sources, suitable products could be developed to lower the measured concentrations of acetaldehyde and thus meet the required limits for this substance [Fig. 8]. Among others, special syntans are offered which can wash out aldehydes including acetaldehyde coming from the rawhide of the wet processes. In order to minimize the other source, the degradation of fatty acids, a special polymer softener can be used in the retannage to prevent the formation. Also special flesh side binders are offered to lower the substance coming from both sources directly. Such products can also be understood as a modular system.

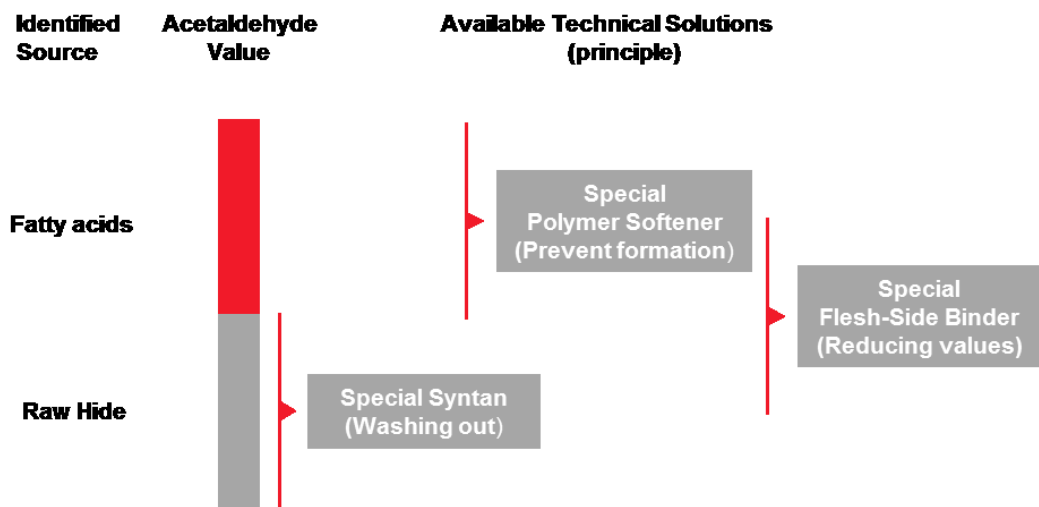


Fig. 8. Sources and possible solutions to reduce Acetaldehyde at a glance.

The following experimental concept was chosen to examine the extent to which the newly developed auxiliaries can reduce emittable substances [Fig. 9].

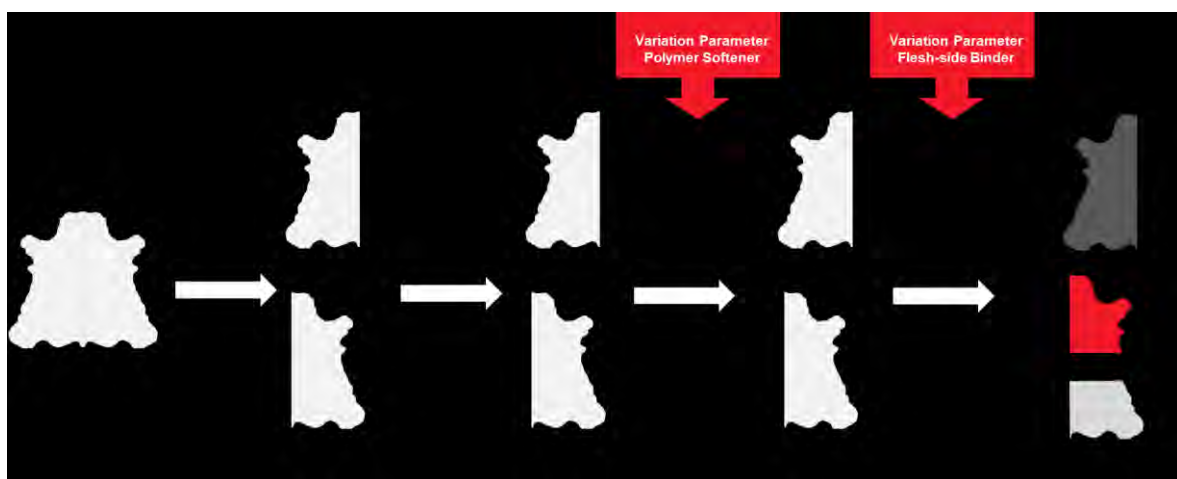


Fig. 9. Trial concept: to proof modular concept two possible parameter were changed.

The same wet blue was divided and retanned with the same recipe and products. The only exception was the softening products used. In one half the fatliquor was partially replaced with the special Polymer Softener. Subsequently, the two crust-leathers obtained were finished, whereby in one case the Flesh-side binder used was replaced by the specially developed one. Subsequently, the emissions of all samples were measured using the ISO 12219-2 method (10 l bag-test). The result shows that with the products not only the values for acetaldehyde and aldehydes in general are reduced, but also the total emission can be minimized [Fig 10].

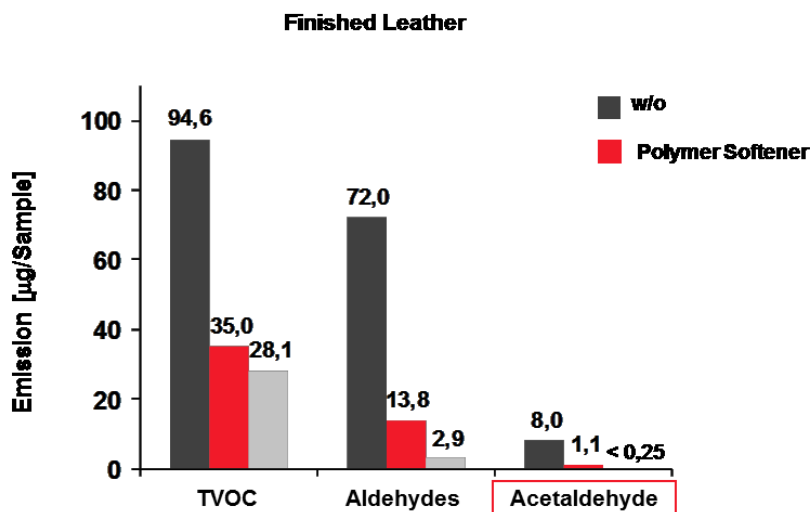


Fig. 10. Impact of auxiliaries integration in recipes.

10 How to minimize Emissions

Let us summarize the answers of how to minimize emissions from automotive leather. As is so often the case with leather issues, the entire manufacturing process must be taken into account to answer this question. The minimization of the VOC's starts already in the Beamhouse, continues with points that have to be considered in the retannage and finally the finishing system has to be considered [Fig. 11].

Field	Beamhouse	Crusting	Finishing
Minimum	<ul style="list-style-type: none"> Good degreasing Washing Proper preservation 	<ul style="list-style-type: none"> Low VOC softening agents Washing Unpolluted drying atmosphere 	<ul style="list-style-type: none"> Low solvent products Appropriate drying and good ventilation Cross contamination-free storage
Best (Ad-on)	<ul style="list-style-type: none"> Sulfide reduced unhairing Amine-free deliming Amine-free swell regulators 	<ul style="list-style-type: none"> Washing off of aldehydes (e.g. Special Syntan) Prevent aldehyde formation (e.g. Special polymer softener) Formaldehyde-free resins (e.g. natural based) 	<ul style="list-style-type: none"> Co-solvent free binders Solvent-free crosslinker Reduction of aldehydes (e.g. Special flesh side binder)

Fig. 11. Overview how to minimize emissions in automotive leather.

11 Conclusion

Nowadays, in the context of emissions, in order to meet the high requirements and all the required parameters, it is necessary to have a sound knowledge of the required tests and the associated focus of these methods. Furthermore, detailed know-how of the products used for the leather article is required. Through the development of ever better, VOC-optimized solutions, such as the solvent-free crosslinker presented in the article, the concentration of emitted substances from leather can be further reduced. In this case, the reduction is bigger than expected due to the

reduction of the solvent content alone. This trend towards reduction on the product side will continue. However, total emissions today are no longer determined solely by the products used but are also increasingly influenced by natural sources. Many of today's individual substance regulations are in the range of natural degradation processes. This complicates the search for sources, as many limited compounds are no longer used directly or for the production of leather chemicals. Many measurements and their conscientious evaluation are necessary for the detection in order to develop suitable solutions. This may take some time and, as in the case of acetaldehyde, may result in satisfactory solutions being available only after regulation of such substances. Nevertheless, the minimization of emissions from leather is a real success story in which the values found have been massively reduced in recent years.

References

1. Ammen, J. Wegner, B. Dannheim, B.: *Recent Findings in Acetaldehyde Emission from Leather*, JALCA, 112, 2017

CAPTURING THE ENVIRONMENTAL IMPACT OF LEATHER CHEMICALS

Michael Costello

Stahl Holdings

michael.costello@stahl.com

Abstract. Product Environmental Footprint Category Rules (PEFCRs) for calculating the environmental impact of leather manufacturing were approved by the European Commission in 2018. Chemicals are key input data for this methodology, given leather's chemically intensive makeup. The increasing use of non-petrochemical materials represents an important part of industry-wide efforts to reduce overall environmental impact. Though still in its infancy, research and commercial use of renewable raw materials for leather chemicals is expected to accelerate in the coming years, especially with regard to understanding the environmental impact of bio-based products. Indeed, when decisions are made to substitute fossil fuel-derived products with alternative bio-based versions, a common assumption is that a reduction in environmental footprint will accompany that substitution. However, reports have been published that challenge this view^{1,2,3}. The aim of this paper is to provide an overview of environmental impact data for bio-based polyurethanes and to interpret the data in order to make better decisions about further research and product design.

1 Introduction

Life Cycle Assessment Methodology (LCA) is widely recognized as the most effective way to calculate the environmental impact of a product, given that it tracks the impact of each element of the manufacture and transportation of that product from its origin to the end of life. The resulting data can be categorized and reported in an Environmental Product Declaration (EPD), which can be used by manufacturers to summarize the environmental impact of their products in a harmonized and standardized way.

The impact of chemicals is critical input when undertaking LCA methodology for leather manufacturing - a highly chemical-intensive process. This paper shows that the environmental impact data of different polyurethanes can vary within the same environmental category. It also suggests that the environmental impact of using renewable resources to reduce greenhouse gas emissions should not be evaluated in isolation.

2 Bio-based Polyurethane Dispersions

Polyurethane dispersions (also known as PUDs) are often used in the finishing step of leather manufacturing. They are typically formulated as the base resin for complex coatings formulations which are applied to the surface of the leather during in the final stages of its manufacture. These aqueous polyurethane coatings contribute to the long term durability, touch and aesthetic properties that characterize the finished leather that we know as consumers.

A typical PUD polymer is made up of many raw materials but in large part it is formed by the reaction of di-isocyanates with polyols to form a pre-polymer which is dispersed into water under controlled conditions. In recent years, new polyol raw materials have been made available that are derived from renewable resources instead of fossil fuels. These polyols are typically based on sugar, corn, rapeseed, soy, palm or other related plants which are processed by the biotechnology industry. Our research has developed to the point where the bio-based content of a PUD can reach levels of 40-60% of the solids of that polymer dispersion, while still maintaining the desired

performance in the final coating. Several such bio-based polyurethanes have been developed based on this principle.

Several cradle-to-gate environmental impact studies comparing bio-based PUDs and fossil fuel based PUD equivalents have been performed based on accepted LCA methodology and guidelines in which the manufacturing of the product, and that of its raw materials, were taken into account, ie: not the end of life. The data overview presented here is indicative, not conclusive, and is based on several of the LCA studies observed.

3 Main Findings

Given that they are derived from a natural and renewable resource, it could be assumed that a bio-based PUD will automatically have a lower environmental footprint than a fossil fuel based PUD. However, the findings show that this is not necessarily the case. The impact of using bio-based polyurethanes depends on the environmental category chosen, and on the source of the bio-based material used.

For example, in Fig. 1, it can be seen that the impact on climate change is lower (ie: better) for the bio-based PUDs than for the fossil fuel based PUDs. As expected, the LCA database allocates the manufacturing of fossil fuel based polyols as having a higher greenhouse gas emissions factor than their bio-based equivalents, hence the higher climate change impact.

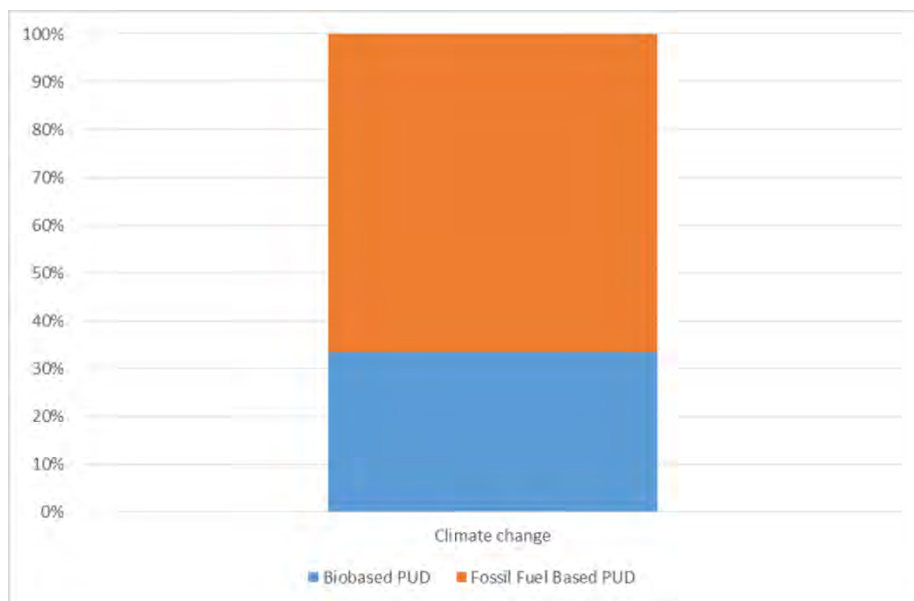


Fig. 1. Illustration of the relative impact on Climate Change of bio-based PUDs and fossil fuel based PUDs.

Conversely, Fig. 2 shows that the impact of manufacturing bio-based PUDs on land use is significantly higher than that of its fossil fuel equivalent. The likely reason for this is that most bio-based polyols are derived from plants which are grown for industrial use. This activity occupies areas of cropland that are farmed and irrigated - activities that have an impact on land use (and water quality). This latter point may also account for the relatively high impact on eutrophication of the bio-based PUDs shown in Fig. 3.

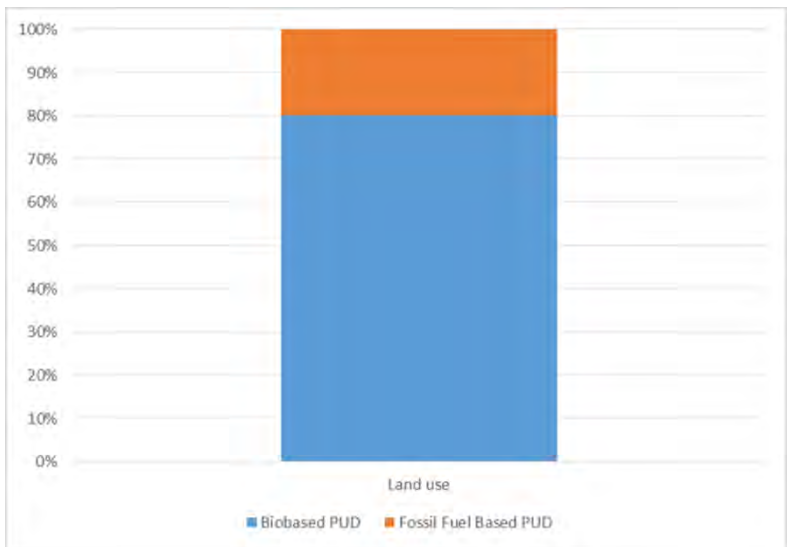


Fig. 2. Illustration of the relative impact on Land Use of bio-based PUDs and fossil fuel based PUDs.

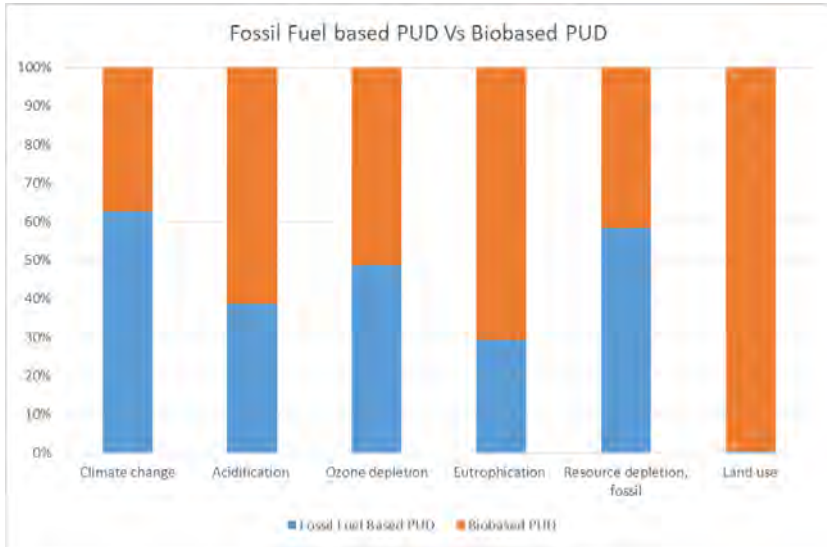


Fig. 3. Illustration of the environmental Impact comparison of fossil fuel based PUDs vs bio-based PUDs, for selected environmental categories.

Although the graphs are illustrations of indicative data, the impact of manufacturing bio-based polyurethanes is not consistently positive or negative across environmental categories. What is good for climate change is not necessarily good for land use, and so on.

Additional notes:

- a) The origin of plant-based biomaterials (ie: chemical or geographical origin) is a variable in the determination of their environmental impact and was not included in these illustrations, ie: different plants require different extraction methods and process techniques in order to be able to use their derivatives industrially. Similarly, if a polyol or its raw material is sourced from the other side of the world to where the polyurethane is manufactured, then the environmental impact of its transportation is taken into account in the calculation.
- b) Biotech industry processing: How renewable materials are processed (usually by the biotech industry) is also a determining factor in their environmental footprint, and much

research is being done in areas like carbon capture and alternative energy use for this reason.

- c) Waste streams: If a bio-based raw material were derived from a natural waste stream (eg: biomass), then its impact on land use will be significantly reduced when compared to that of a primary bio-based product that has been extracted from a plant that was exclusively cultivated for industrial use (as in this case). Research into waste stream technology like this has not yet reached a commercial stage in polyurethanes, but work has begun.
- d) C-14 content: The bio-based content (also known as C-14 content) of the PUDs in the graphs is 20-25%. Higher C-14 content will increase bio-based impact on the chosen environmental categories proportionally. Bio-based content of above 40% can now be achieved for PUDs of this type and are also being studied for their environmental impact.

4. Conclusions

Choosing bio-based raw materials over fossil fuel-based products does not necessarily reduce the overall environment footprint of polyurethane dispersions (PUD) used in leather finishing. However, if climate change is considered in isolation, there is a marked advantage in using bio-based polyurethanes, especially if their C-14 content is high. Conversely, if an improvement in land use impact is desired, using bio-based materials derived from plants that are grown exclusively for industrial purpose does not appear to be the best choice.

Given the ever-increasing importance of measuring and reducing the environmental impact of chemicals and leather, the opportunity for further research on this topic is high. It is hoped that the introduction of LCA methodology will trigger more focussed innovation, now that the environmental impact can be predicted before decisions on product design are made.

The development of bio-based raw materials for leather chemicals, though still in its infancy, represents a critical step in the move away from fossil fuels and towards a more circular economy. Developing a generation of even lower impact alternatives, based on biomass or other waste streams, appears to be the next move.

References

1. *Environmental Impacts of Innovative biobased products*, European Commission, March 12, 2019 (<https://publications.europa.eu/en/publication-detail/-/publication/15bb40e3-3979-11e9-8d04-01aa75ed71a1>)
2. *Environmental assessment of bio-based chemicals in early-stage development: a review of methods and indicators*, March 10, 2017. Martijn L.M. Broeren, Michiel C. Zijp, Susanne L. Waaijers-van der Loop, Evelyn H.W. Heugens, Leo Posthuma, Ernst Worrell, Li Shen.
3. *Sustainability Metrics: Life Cycle Assessment and Green Design in Polymers*, September 2, 2010.

1. Michaelangelo D. Tabone, James J. Cregg, Eric J. Beckman, Amy E. Landis.

SULFIDE UNHAIRING: RETHINKING THE RECEIVED WISDOM

W.R. Wise^{1a}, A.D. Ballantyne^{1b} and A.D. Covington^{1c}

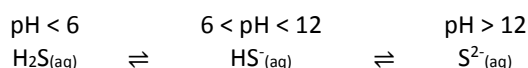
¹ Institute for Creative Leather Technologies (ICLT), University of Northampton, University Drive, Northampton, NN1 5PH, UK.

a) Corresponding author: will.wise@northampton.ac.uk

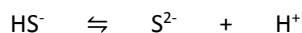
b) andrew.ballantyne@northampton.ac.uk

c) tony.covington3@northampton.ac.uk

Abstract. The removal of hair from a hide or skin by dissolving it with a mixture of lime and sulfide is a fundamentally understood feature of leather technology. Or is it? For a long time, it has been accepted within the leather literature that, in water, sulfide may be present as either hydrogen sulfide (H₂S), hydrosulfide (HS⁻) or sulfide (S²⁻), depending on the pH.



The generally accepted mechanism of hair burning is sulfide attack at the cystine disulfide linkages in keratin. Also, it is believed that the unhairing reaction only proceeds at an appreciable rate in the presence of the dianionic S²⁻ species, because that fits with the technological observation that unhairing reactions only proceed at pH greater than 12. However, recent publications have provided substantive proof that the S²⁻ species does not exist in aqueous media at any pH: researchers were unable to observe any evidence of the S²⁻ species in a solution of Na₂S dissolved in hyper-concentrated NaOH and CsOH using Raman spectroscopy. The assigned second pK_a for removal of the second proton has now been estimated to be 19, making the concentration of S²⁻ (see below) vanishingly small.

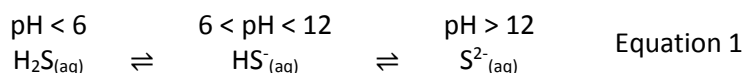


There is a clear contradiction between the currently accepted mechanism for sulfide unhairing with the evidenced speciation of sulfide species in aqueous environment. Here the implications for this important process are discussed and possible alternative mechanisms postulated that fit with the new knowledge.

1 Introduction

The subject of Leather Science is relatively young, certainly less than a century old, and has had relatively few practitioners. Consequently, certain myths about the mechanisms of processes fundamental to leather processing have been perpetuated: examples are the underlying principles of chromium(III) tanning and masking.¹ The process of hair burning unhairing with lime and sulfide is such an accepted part of leather technology that it might come as a surprise to be told that the understanding of the chemistry is flawed.

It has long been accepted that, in water, sulfide is speciated as follows (Equation 1).



Consequently, the previously accepted mechanism for sulfide degradation of keratin at pH>11, presented in Fig. 1, can be summarised as follows, defining what is known unequivocally.² At high pH, the reducing nucleophilic sulfide ion attacks the disulfide bond of cystine. The disulfide link is broken, creating cysteine moieties and the sulfide is converted to polysulfide.

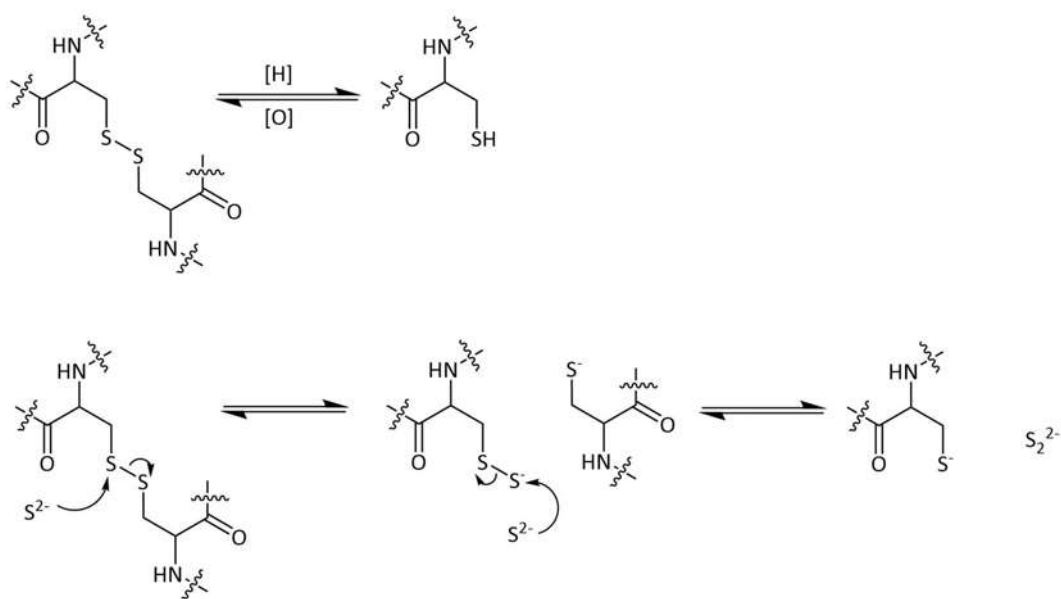


Fig. 1. The previously accepted mechanism of sulfide hair burning.

It is assumed the polymerisation of sulfur will not progress much further, because the bisulfide ion is a weaker nucleophile than sulfide and therefore is less effective in attacking the disulfide link. This can be seen in Table 1, setting out the oxidation potentials:³ note the reducing power of the reactions will depend on the precise chemical conditions, particularly pH.

Table 1. Standard reduction potentials for sulfide species.

Species	Standard reduction potential, E ⁰ (mV)
H ₂ S ⇌ S + 2H ⁺ + 2e ⁻	-0.142
HS ⁻ + OH ⁻ ⇌ S + H ₂ O + 2e ⁻	+0.478
S ²⁻ ⇌ S + 2e ⁻	+0.476
S ₂ ²⁻ ⇌ 2S + 2e ⁻	+0.428

The relative power of oxidising can be judged because of the following equation, which relates the Gibbs free energy to the standard electrode potential (Equation 2).

$$\Delta G^{\circ} = -nFE^{\circ} \quad \text{Equation 2}$$

where: n is the number of faradays (the number of electrons in the reaction) and F is the Faraday constant. A positive electrode potential results in a negative free energy, which means a spontaneous or favoured reaction.

The mechanism presented in Fig. 1 is based in part on the assumption of the relationships between the sulfide species, in particular the low pKa of the second ionisation, long thought to be ~13, which creates equilibria between hydrosulfide and sulfide at pH values familiar in lime buffer.²

2 The Problem

A large question mark has been raised over the chemistry of sulfide: the very existence of the S^{2-} species in aqueous solution has been queried.⁴

The problem lies in the value of the pKa of the dissociation of HS^- to S^{2-} : the previously assumed value of 13 has been revised upwards to 19, which means at pH 12.6 the concentration of sulfide ion in water can only be vanishingly small.³ The latest argument is based on high resolution Raman spectrometry, which could not confirm the presence of sulfide, whilst it was clear that hydrosulfide was still detectable at very high pH.⁴ The conclusion is not completely confirmed and accepted, but the evidence is compelling, so the new situation must be addressed and the implications reviewed.⁵

Up to 2014, the literature reported the value for the second dissociation constant of hydrogen sulfide at 12.9. The recent suggestion is that the value is not correct and a more accurate value for pKa2 should be about 17. There is controversy concerning the revised number and there appears to be some agreement that it should be 19: either way, this would in effect eliminate sulfide ion from consideration in aqueous medium. There is supporting evidence for this proposal in the literature; it is not as yet accepted chemistry, although current and recent editions of the 'Rubber Book' quote pKa2 as 19.3.³ Therefore, the possibility should be recognised and the implications for the leather industry assessed.

In 1946, Bowes assumed, without reference to pKa values, that sulfide was hydrolysed to completion at pH 12 (Equation 3):



and therefore, the unhairing agent is hydrosulfide.⁶ It may be noted from Table I that the quoted redox potentials for sulfide and hydrosulfide are the same in older reference sources² and in the latest definitive references.³

In 1956, Merrill reviewed the literature on unhairing,⁷ reporting that some sulfur is lost from degraded keratin and Bienkiewicz states that sulfide-based hair dissolving is negligible below pH 11.2. Sodium hydroxide is ineffective as a pulping agent below pH 13, so there is a clear pH effect on sulfide-based unhairing. The implication is that the rate can be expressed in the following generalised ways:

$$\text{rate } (S^{2-}) = k_s[S^{2-}]^a \quad \text{Equation 4a}$$

$$\text{rate } (HS^-) = k_{HS}[HS^-]^a[OH^-]^b \quad \text{Equation 4b}$$

But the order of the reaction has not been defined. If the revised case applies (Equation 4b), the mechanism of attack at the disulfide link and formation of polysulfide will also have to be redefined.

3 The solution?

The revised mechanism must incorporate the hydroxide ion and generate a polysulfide species as is observed practically. Assuming that the mechanism still involves a two-step process then addressing each step in isolation simplifies the issue. It is possible that the first step is analogous to the previously accepted sulfide mechanism but, instead, involves the attack of an activated hydrosulfide ion where the activity is increased by simultaneous abstraction of the proton as illustrated in Fig. 2.

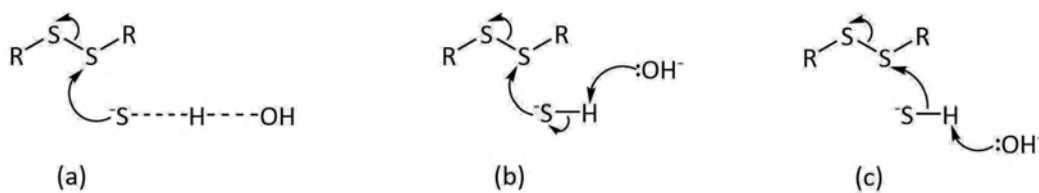


Fig. 2. Initial attack of the disulfide bond by the activated hydrosulfide species – a, b and c all illustrate subtle variations in way in which hydrosulfide activation could be imagined but lead to the same end result.

The second step involves conversion of the intermediate species to a cysteine residue generating the polysulfide species. This step too must be rethought due to the elimination of sulfide from the originally accepted mechanism; the authors of this paper propose two possible mechanisms by which this might be achieved shown in Fig. 3.

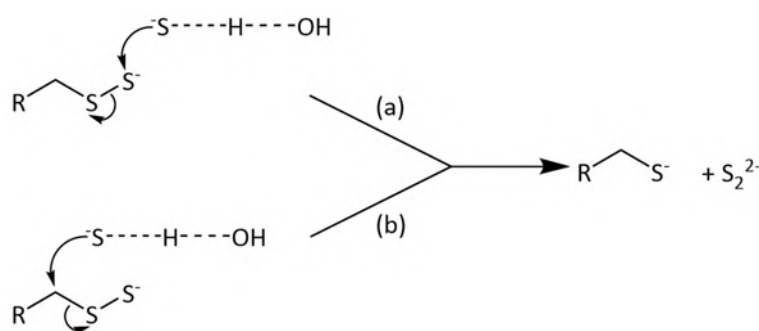


Fig. 3. Two proposed mechanisms (a – top and b – bottom) for conversion of the intermediate species to the cysteine residue.

The first of these mechanisms (Fig. 3a.) is analogous to step 1 where by the hydrosulfide ion undergoes some sort of activation by the hydroxide ion and subsequently attacks the primary sulfide in the intermediate species. However, studies would have to demonstrate that the activated ion is a strong enough nucleophile to attack an already negatively charged moiety.

Alternatively, the authors propose a different mechanism (Fig. 3b) where the hydrosulfide ion might attack the carbon adjacent to the disulfide. As illustrated this mechanism still produces the observed products (polysulfide and cysteine) but might be energetically favoured as it does not involve direct nucleophilic attack on an already negatively charged moiety.

4 The Consequences

The theoretically required amount of sulfide can be calculated to be 0.8% Na_2S or 0.6% $\text{NaHS} \equiv 1.1$ or 0.8% sulfide flake: where ‘flake’ is industrial sodium sulfide or sodium hydrosulfide, both quoted by the manufacturer as 70% Na_2S or NaHS respectively.⁵ The typical industrial offer is 2-3% ‘sulfide’ flake i.e. at least double the theoretical requirement and since this is considerably higher than the range quoted for calculated amounts, the doubt concerning the sulfide species does not affect the unhairing technology.

Regarding the relationship between hydrosulfide and hydrogen sulfide, there is no suggestion in the literature that there is any error in $\text{pK}_{\text{a}1}$ (accepted to be 7). The accepted conditions for hydrogen sulfide gas formation remain and are critical for safety.

5 Conclusion

This paper highlights the issues of preserved wisdom and the impact that this has on control of developments and improvements. In this case however whilst the new view of sulfide speciation does change the science and the mechanism of hair degradation, it does not change the observations made about the reaction nor does it change the current technology of the processing step. It was always an option to combine lime with hydrosulfide, since the equilibrium pH is 12.6, so there need be no process change there. However, it begs the question, what is the difference between reagents labelled NaSH and Na₂S? If the new findings are accepted, once dissolved in an aqueous medium the reagent labelled sodium sulfide is merely sodium hydrosulfide plus some sodium hydroxide.

The commercial consequence is: buy the cheaper version and carry on regardless!

Acknowledgements

The authors of this paper would like to thank Rachel Garwood, Director, The Institute for Creative Leather Technologies, University of Northampton, UK.

References

1. Covington, A.D.: *J. Amer. Leather Chem. Assoc.*, 2001, 96(12), 467.
2. Bienkiewicz, K.: *'Physical Chemistry of Leather Making'*, Krieger, Florida, 1983.
3. *Handbook of Chemistry and Physics*, 2016, CRC Press, Boca Rotan, USA.
4. May, P.M.: Batka, D.: Hefter, G.: Königsbergera, E.: Rowland, D.: *'Goodbye to S²⁻ in aqueous solution'*, *Chem. Comm.*, 54, 1980-1983, 2018.
5. Covington, A.D and Wise, W.R.: *Tanning Chemistry. The Science of Leather. 2nd ed.*, Royal Society of Chemistry Publishing, in press.
6. Bowes, J.H.: *Progress in Leather Science: 1920-45*, BLMRA, London, 1948.
7. O'Flaherty, F.: Roddy, W.T.: Lollar, R.M.: *'The Chemistry and Technology of Leather: Volume I Preparation for Tannage'*, Reinhold Publishing Corporation, New York (NY) USA, 1956.



ORAL PRESENTATIONS

TOWARDS A MOLECULAR LEVEL UNDERSTANDING OF CHROME TANNING: INTERPLAY BETWEEN COLLAGEN STRUCTURE AND REACTIVITY

Yi Zhang, Jenna K. Buchanan, Geoff Holmes and Sujay Prabakar

Leather and Shoe Research Association of New Zealand, P.O. Box 8094, Palmerston North, 4472, New Zealand

a) Corresponding author: sujay.prabakar@lasra.co.nz

Abstract. Synchrotron based small-angle X-ray scattering (SAXS) technique is a powerful technique that has helped us understand the changes in molecular-level collagen structure during tanning and denaturation (shrinkage). Based on SAXS results from real-time denaturation experiments on leather samples, we established a mechanistic model of chrome tanning indicated by the structural changes of collagen. It suggests that only low level of chromium species is effectively involved in the cross-linking with collagen, highlighting the overuse of chrome during conventional tanning processes. Any extra amount of chrome added, however, can support the stabilisation of collagen possibly via a non-covalent mechanism. Such mechanism points towards a more environment-friendly tanning method by using suitable supplementary reagents to benefit tanning effect non-covalently instead of chrome. Also, by pre-treating with complexing agents such as sodium formate and disodium phthalate, as well as nanoclay (sodium montmorillonite), the uniformity through bovine hide collagen matrix can be improved significantly. These pre-treatments effectively reduce the reactivity of chromium during its cross-linking reaction with collagen while retaining its bound water. However, collagen pre-treated with a covalent cross-linker (glutaraldehyde) results in a decrease in both chromium-collagen cross-linking and bound water while improving uniformity. These molecular-level insights can be developed into metrics to guide us towards a more sustainable future for the leather industry. Further, coating on collagen fibrils can provide a pseudo-stabilisation effect of increasing the heat resistance of collagen. Overall, synchrotron SAXS provides valuable information about collagen structure changes that could lead to more efficient use of chrome (or other tanning agents) in the global leather tanning industry.

1 Introduction

Conventional chrome tanning processes utilize 6% to 8% of basic chromium sulphate by weight relying on a concentration gradient to drive penetration.^{1,2} While an uptake of 40% to 70% is typical depending on the nature of animal hides and skins, the poor chrome uptake results in environmental stress relating to hexavalent chromium exposure, leading researchers to reassess the case of chromium sulphate in modern tanning.¹⁻⁴ Studying molecular level changes can reveal the mechanism by which chromium stabilizes collagen, and could lead to more efficient use of chrome during the tanning process.⁵⁻¹⁰ Collagen molecules are aligned in a quarter stagger structure, resulting in repeating gap/overlap regions within the fibrils.¹⁴ Because of its ordered arrangement, mechanistic information can be acquired by X-ray diffraction techniques from changes in the periodicity of the gap/overlap regions (D-period), fibril size and the intensity of the scattering peaks.¹¹⁻¹⁴ This paper will review some of our recent work on synchrotron based SAXS to minimize and effectively use chrome in leather processing.

2 Results and Discussion

Many studies have focused on the use of less chrome with higher uptake by involving nanocomposites, pre-tanning agents, or novel processing methodologies.¹⁵⁻²⁰ However, the evaluation of properties remains superficial with lack of molecular level insights, hindering researchers from finding comprehensive solutions to sustainable chrome tanning. Considering that collagen is the primary structural element in the extracellular matrix in animal hides and skins, the heat resistance of leather against shrinkage was determined by the hydrothermal denaturation temperature (T_d) of collagen molecules.

However, such a commonly used indicator is based on heat transfer and lacks molecular level observations of collagen structural changes during denaturation, which is essential to understand the chromium–collagen reaction and for improving the sustainability of chrome tanning.

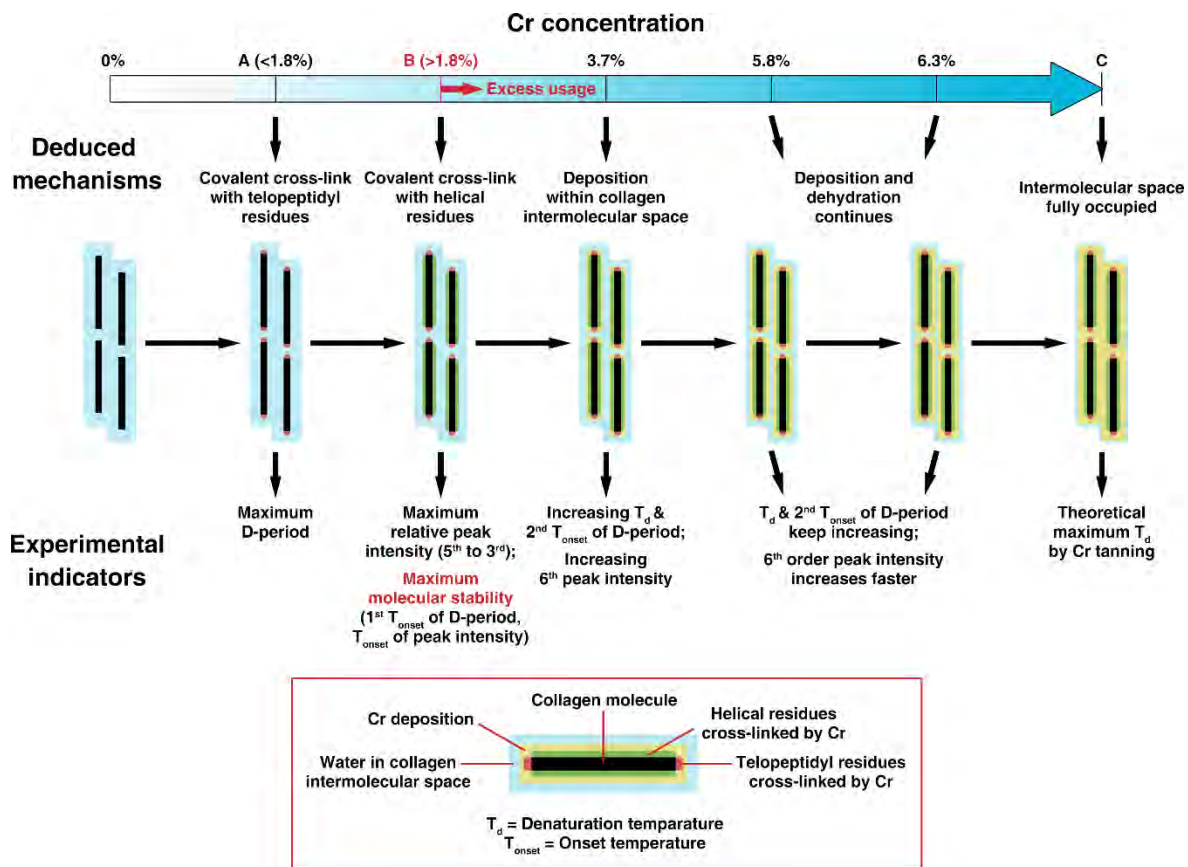


Fig. 1. Mechanistic model of the reaction between chromium and collagen at different concentrations, deduced from the molecular-level experimental indicators. © ACS Sustainable Chem. Eng. DOI: 10.1021/acssuschemeng.8b00954

The effect of chromium concentration in affecting the collagen structure in leather can be explained by a mechanistic model based on the observed molecular level indicators from SAXS measurements (Figure 1). At extremely low chrome concentration (A < 1.8%), chromium species form covalent bonds with telopeptidyl active sites causing the expansion of the axial staggering gaps, as indicated by the maximizing of the D-period.⁷ At slightly higher chrome concentration (1.8% < B < 3.7%), chromium species covalently occupied the active sites in both the telopeptidyl and helical regions, resulting in the maximized relative intensity of the fifth and the third order peaks. The intramolecular stability of collagen thereby reaches its upper limit using chrome tanning, revealed by the unchanged first T_{onset} of D-period and peak intensity at 90 °C from our real-time SAXS denaturation experiment. Upon exhaustion of the active covalent sites, the relative intensity of the fifth and the third order peaks would be reduced, indicating the prevalence of non-covalent deposition. Meanwhile, the intensity of the sixth order peak starts to increase at a higher rate, confirming the dehydration effect due to chromium deposition and the displacement of water. The non-covalent interaction only contributes to the apparent denaturation temperature (T_d), which rests once the intermolecular space is fully occupied.⁷

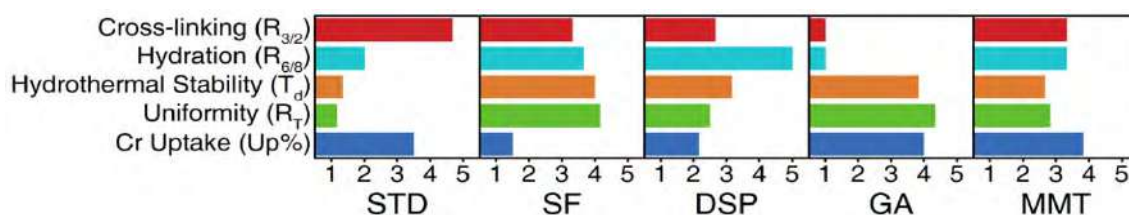


Fig. 2. Key aspects of the efficiency of chromium-collagen cross-linking through different pre-treating methods. © Int. J. Biol. Macromol. DOI: 10.1016/j.ijbiomac.2018.12.187.

The efficiency of chrome tanning can also be improved by using masking agents (Figure 2) such as monodentate complexing agent (sodium formate, SF), chelating agent (disodium phthalate, DSP), covalent cross-linker (glutaraldehyde, GA) and nanoclay (sodium montmorillonite, MMT).⁹ By using a combination of SAXS and DSC studies we introduced a strategy to improve the efficiency of the cross-linking reaction at different concentrations of chromium sulphate by evaluating the performance of four common types of pre-treatments. The results suggest that SF, DSP and MMT affect the performance by decreasing chromium-collagen cross-linking and increasing hydration of the collagen molecule, denaturation temperature and uniformity of chrome. GA was found to initiate a decrease in both chromium-collagen cross-linking and hydration by covalently cross-linking with the collagen. The chrome uptake was observed to increase when using GA and MMT due to covalent cross-linking and adsorption, respectively. However, the uptake decreased due to the masking of SF and DSP that reduce chrome fixation.⁹

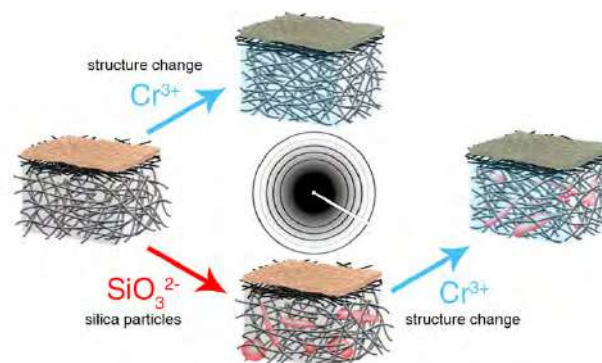


Fig. 3. Collagen structure changes during silicification with sodium silicate © RSC Adv. 10.1039/C7RA01160A

Benign inorganic materials can be used to fill the leather during the retanning process after cross-linking with low chrome offers.⁵ For example, the electrostatic interactions between the positively charged amino groups in collagen with negatively charged silicate species lead to precipitation, forming coatings and aggregates of silica particles on the surface of the collagen fibrils (Figure 3). The introduction of silica into the leather matrix did not affect the axial periodicities of the collagen molecules, however an increase in collagen fibril diameter was observed during the main tanning step. From DSC studies, it was found that sodium silicate treated samples (So-Si) impart no effect on collagen stabilization in the absence of chrome. However, a pseudo-stabilization effect is observed in the So-Si + chrome samples possibly due to the inability of the collagen molecules to undergo conformational changes due to the silica coating on the collagen fibrils.⁹

3 Conclusions

Synchrotron based small-angle X-ray scattering (SAXS) technique is a powerful technique that has helped us understand the molecular-level changes in collagen structure during leather processing. The technique provides valuable information about collagen structure changes that could lead to more efficient use of chrome (or other tanning agents) in the leather industry.

Acknowledgements

S.P, Y.Z & G.H would like to thank the Ministry of Business, Innovation and Employment (MBIE) for providing funding through grant LSRX-1801. The research was undertaken on the SAXS/WAXS beamlines at the National Synchrotron Radiation Research Centre (NSRRC) in Taiwan, the Diamond Light Source in UK and the Australian Synchrotron in Australia.

References

1. Covington, A. D.: *Tanning chemistry: the science of leather*, Royal Society of Chemistry: Cambridge, 2009.
2. Sreeram, K.; Ramasami, T.: 'Sustaining tanning process through conservation, recovery and better utilization of chromium', *Resources, conservation and recycling*, 38, 185-212, 2003.
3. UNIDO Future Trends in the World Leather and Leather Products Industry and Trade; UNIDO: Vienna, 2010; pp 1-120.
4. Sundar, V.; Rao, J. R.; Muralidharan, C.: 'Cleaner chrome tanning—emerging options', *Journal of cleaner production*, 10, 69-74, 2002
5. Zhang, Y.; Ingham, B.; Leveneur, J.; Cheong, S.; Yao, Y.; Clarke, D. J.; Holmes, G.; Kennedy, J.; Prabakar, S.: 'Can sodium silicates affect collagen structure during tanning? Insights from small angle X-ray scattering (SAXS) studies', *RSC Advances*, 7, 11665-11671, 2017.
6. Zhang, Y.; Ingham, B.; Cheong, S.; Ariotti, N.; Tilley, R. D.; Naffa, R.; Holmes, G.; Clarke, D. J.; Prabakar, S.: 'Real-Time Synchrotron Small-Angle X-ray Scattering Studies of Collagen Structure during Leather Processing', *Industrial & Engineering Chemistry Research*, 57, 63-69, 2018.
7. Zhang, Y.; Mansel, B. W.; Naffa, R.; Cheong, S.; Yao, Y.; Holmes, G.; Chen, H.-L.; Prabakar, S.: 'Revealing Molecular Level Indicators of Collagen Stability: Minimizing Chrome Usage in Leather Processing', *ACS Sustainable Chemistry & Engineering*, 6, 7096-7104, 2018.
8. Naffa, R.; Maidment, C.; Ahn, M.; Ingham, B.; Hinkley, S.; Norris, G.: 'Molecular and structural insights into skin collagen reveals several factors that influence its architecture', *International journal of biological macromolecules*, 128, 509-520, 2019
9. Zhang, Y.; Snow, T.; Smith, A. J.; Holmes, G.; Prabakar, S.: 'A guide to high-efficiency chromium (III)-collagen cross-linking: Synchrotron SAXS and DSC study', *International journal of biological macromolecules*, 126, 123-129, 2019.
10. Maxwell, C. A.; Smiechowski, K.; Zarlok, J.; Sionkowska, A.; Wess, T. J.: 'X-ray studies of a collagen material for leather production treated with chromium salt', *Journal of the American Leather Chemists Association*, 101, 9-17, 2006.
11. Pauw, B. R.; Smith, A.; Snow, T.; Terrill, N.; Thünemann, A. F.: 'The modular small-angle X-ray scattering data correction sequence', *Journal of applied crystallography*, 50, 1800-1811, 2017.
12. Ingham, B.; Li, H.; Allen, E. L.; Toney, M. F.: 'SAXSFit: A program for fitting small-angle X-ray and neutron scattering data', *arXiv:0901.4782*, 1-5, 2009.
13. Petruska, J. A.; Hodge, A. J.: 'A subunit model for the tropocollagen macromolecule', *Proceedings of the National Academy of Sciences*, 51, 871-876, 1964.
14. Hulmes, D. J.; Miller, A.; White, S. W.; Doyle, B. B.: 'Interpretation of the meridional X-ray diffraction pattern from collagen fibres in terms of the known amino acid sequence', *Journal of molecular biology*, 110, 643-666, 1977.
15. Prabakar, S.; Whitby, C. P.; Henning, A. M.; Holmes, G.: 'The Effect of Cloisite (R) Na plus Nanoclay Filler on the Morphology and Mechanical Properties of Loose Leather', *Journal of the American Leather Chemists Association*, 111, 178-184, 2016.
16. Drljaca, A.; Anderson, J.; Spiccia, L.; Turney, T.: 'Intercalation of montmorillonite with individual chromium (III) hydrolytic oligomers', *Inorganic Chemistry*, 31, 4894-4897, 1992.
17. Abollino, O.; Aceto, M.; Malandrino, M.; Sarzanini, C.; Mentasti, E.: 'Adsorption of heavy metals on Na-montmorillonite. Effect of pH and organic substances', *Water research*, 37, 1619-1627, 2003.
18. Fein, M.; Filachione, E.; Naghski, J.; Harris Jr, E.: 'Tanning with glutaraldehyde III. Combination tannages with chrome', *The Journal of the American Leather Chemists Association*, 58, 202-221, 1963.
19. Liu, Y.; Ma, L.; Gao, C.: 'Facile fabrication of the glutaraldehyde cross-linked collagen/chitosan porous scaffold for skin tissue engineering', *Materials science and engineering: c*, 32, 2361-2366, 2012.
20. Madhan, B.; Muralidharan, C.; Jayakumar, R.: 'Study on the stabilisation of collagen with vegetable tannins in the presence of acrylic polymer', *Biomaterials*, 23, 2841-2847, 2002

STUDY ON THE ANTIBACTERIAL PROPERTIES OF LEATHERS TANNED WITH NATURAL TANNINS AND THEIR INTERACTIONS WITH SHOES INHABITING BACTERIA

E. Poles^{1a}, A. Polissi^{2b}, A. Battaglia¹, S. Giovando¹, M. Gotti¹

¹ Silvateam S.p.a., Leather division - Via Torre, 7 - 12080 San Michele Mondovì (CN) Italy

² Department of Pharmaceutical and Biomolecular Sciences (DiSFeB), University of Milan - Via Balzaretti, 9 - 20133 Milan (MI) Italy

a)Email: epoles@silvateam.com

b)Email: alessandra.polissi@unimi.it

Abstract. Tannins are high molecular weight polyphenols, naturally synthesised by plants to defend themselves against biotic and abiotic stress factors. Their role as antioxidant, antibiotic and antibacterial agent has been known for many years among agriculture, animal nutrition, pharma and cosmetics industry. If tannins would perform an antibacterial activity in a vegetable tanned leather, this effect could be very interesting for all the applications in which the leather, being in contact with sweat and bacteria, becomes a solution to reduce more or less severe hyperhidrosis and bromhidrosis. The goal of the study was the assessment of the antibacterial activity of vegetable tanned leathers with natural tannins to produce articles in direct contact with human skin and, therefore, their effect on sweat, bacterial growth and metabolite production. Firstly, the antibacterial activity has been evaluated and compared between leathers tanned with Chestnut, Quebracho and Tara extracts, chrome tanned leathers and synthetic material. The trial was performed *in vitro* by inoculating Gram-positive (*Staphylococcus aureus*) and Gram-negative (*Escherichia coli*) bacterial strains. A later step defined the most suitable blend of tannins to obtain, after tanning and/or retanning, an antibacterial natural leather. Furthermore, the vegetable tanned leathers, made with this tannins blend, have been the target of an *in vivo* trial during which 15 panellists, have worn two differently made shoes. The lining and insole inside the right shoe have been made with vegetable tanned leathers with tannins, while the ones inside the left shoe contained only synthetic material. The shoes have been worn for 28 consecutive days, followed by a molecular and bioinformatic analysis of microbiota samples taken from the inner surface of the shoes by using a sterile swab. Lastly, a biochemical analysis of volatile short chain fatty acids has been carried out to investigate the by-products of the bacteria responsible for the unpleasant odour of shoes.

1 Feet Odour: A Common Problem

Feet odour is a very impacting and popular issue: the results of a 2012 US based survey carried out by Institute for Preventive Foot Health (IPFH) over 1,456 panellists showed that it affects 16% of the population over 21.

Most consumers do not know what happens to their feet while they are wearing shoes. High sweating and unpleasant odours are just part of their daily life. Something people usually take for granted but that makes them feel guilty, embarrassed and helpless.

Feet odour is a pretty common condition, especially among people who are very active and/or whose feet tend to sweat a lot because of emotions (e.g. anxiety, stress and embarrassment), use of particular drugs or hereditary predispositions.

Certain food, drinks, caffeine, and nicotine can also trigger sweating in a way that is anything but normal. While it is natural, for instance, to sweat when you eat especially hot or spicy food, people with gustatory hyperhidrosis may do so when they eat something cold. In some cases, even smelling or thinking of food can elicit a response.

1.1 Production of Unpleasant Odours in Feet

Thermoregulation is a process that allows the body to maintain its core internal temperature. Whenever the body temperature rises, the hypothalamus tries to lower it by producing sweat through eccrine glands. Sweat is an odourless solution that mainly consists of water (99%) and a mixture of inorganic salts, vitamins, glucose, lactic acid, urea and amino acids, such as leucine, isoleucine and valine. These organic molecules also originate from the keratin-rich thickened stratum corneum of plantar skin, called callus.

Bacteria inhabiting the foot skin flora feed on sweat, especially by biodegrading the branched-chain amino acids into volatile fatty acids (VFAs). VFAs are responsible for the production of unpleasant cheesy/acidic notes usually associated with foot. The key causative bacteria are *Staphylococcus* spp, *Corynebacterium*, *Brevibacterium*, *Micrococcus*, *Kytococcus* and *Propionibacterium*, mainly found on the plantar area and the toe clefts.

The microbiota, the totality of microorganisms that populate a certain ecologic niche, can vary depending on different environmental, topographical and biochemical conditions as well as within-person variability, without impacting the total amount of microorganisms. It is therefore important to increase the beneficial bacteria, essential for human well-being, while reducing the dangerous ones in the feet.

Humans were born to walk barefoot, the ideal situation for a perfect foot thermoregulation. Without shoes, the foot temperature barely rises and the eccrine glands do not have to produce much sweat to lower it. With less sweat, bacteria are not able to grow and the number of VFAs produced is very limited. Therefore, the result is a barely noticeable odour, without any offensive cheese-like/acidic notes.

1.2 What Happens Inside a Shoe with a Synthetic Insole and Lining?

The foot experiences an increase in temperature, pH and humidity together with a minor pitting of the stratum corneum every time a person puts his/her shoes on.

High levels of hydration, as a consequence of the use of occlusive footwear and/or high environmental temperatures, lead to an increase in microbial numbers, particularly *Staphylococcus*, that cause hyperhidrosis.

Hyperhidrosis is an excessive sweating, 4/5 times more than normal, usually caused by emotional factors, medical conditions, use of particular drugs and hereditary predispositions. This condition nurtures the secretion of high levels of peptides and amino acids in the sweat which are biodegraded by bacteria into volatile fatty acids, responsible of the unpleasant odour.

Distinct cheese-like/acidic notes are generated by the high microbial load fostering the biotransformation of amino acids and callus into volatile fatty acids, such as isovaleric acid, butyric acid and isobutyric acid. The chronic condition of human feet emanating excessive sweat with foul odour is called bromhidrosis.

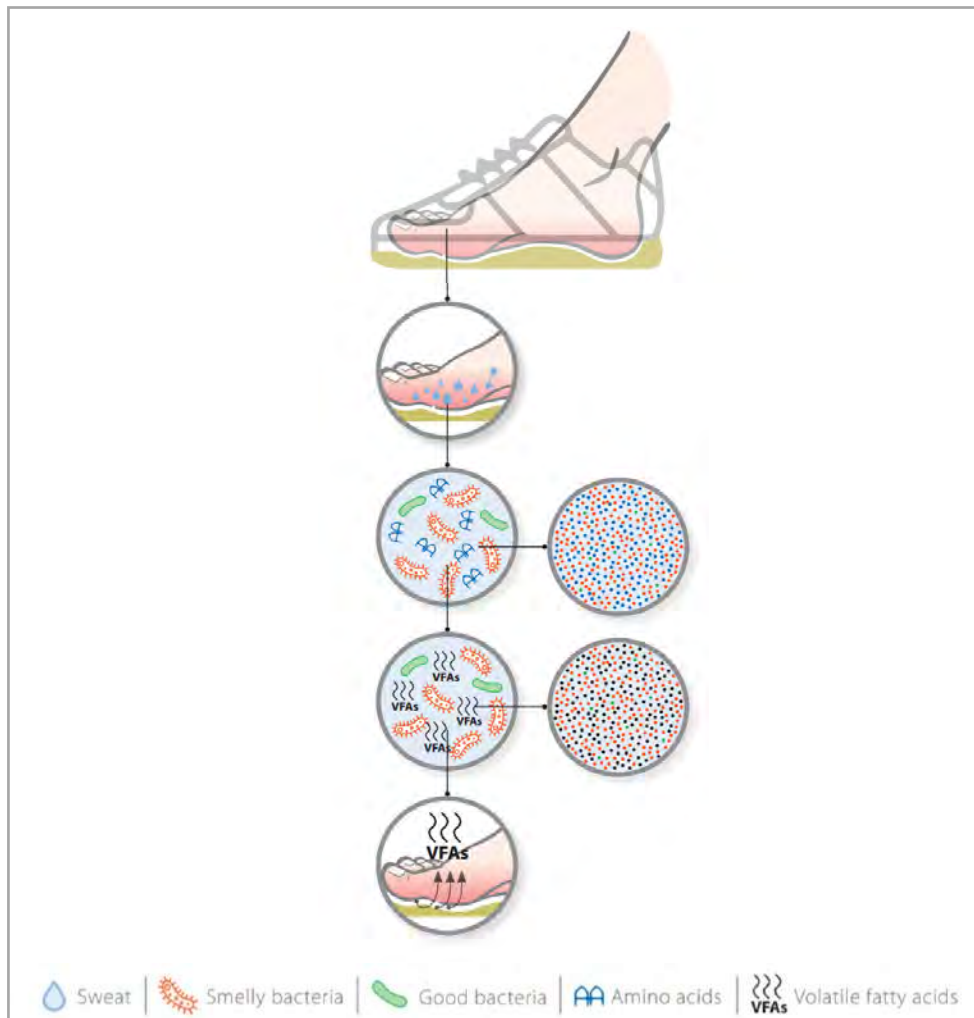


Fig. 1. Production of unpleasant odours in feet wearing shoes with inside made of synthetic material.

The internal part of the shoe (insole and lining) made of synthetic material is not able to counteract the overproduction of foot sweat. This leads to the unpleasant odours that cause social embarrassment and reduce self-confidence, especially among women. Moreover, shoes remain wet and humid even when a person is not wearing them, for example throughout the night. Therefore the shoe becomes the perfect habitat for bacteria proliferation (Fig. 1).

Usually worn shoes host up to 10 million of those “smelly” bacteria responsible for odour per cm^2 , especially in toe clefts. Every time a person puts shoes on, the clean feet will be contaminated by the bacterial population growing inside the shoes. So it is not important how many times somebody washes his/her feet. Washing one’s feet every day is necessary but it is not a sufficient condition to defeat feet odour. Day after day, the bacterial population inhabiting the shoe expands, more VFAs are produced and a strong cheesy/acidic odour sticks with the shoe.

Common disinfectants or Do-It-Yourself home remedies in the long run can cause rashes, allergies and other problems with direct impact on human well-being. The “odour” issue comes from the shoe, not from the foot.

All these solutions are fairly limited, not permanent and very expensive. In some cases, they are harmful since they irritate the skin or alter the body thermoregulation mechanism.

1.3 Tannins: Classification and their Role in Leather Making

Tannins are a complex family of water-soluble polyphenolic compounds, synthesised as secondary metabolites by many plants. Tannins are present in numerous types of trees and plants and they can be found in barks, leaves, wood and also in fruits and roots. From a chemical point of view, it is difficult to define tannins due to their heterogeneity in terms of chemical compositions and molecular weight (MW). Traditionally, tannins have been divided into two large groups: hydrolysable and condensed tannins. Hydrolysable tannins are composed of a carbohydrate core whose hydroxyl groups are esterified with phenolic acids with a MW ranging from 300 to 5,000 Dalton. Depending on the substances that are produced following hydrolysis (by acids, basis or certain enzymes), hydrolysable tannins can be classified in gallotannins (yielding gallic acid) or ellagitannins (yielding ellagic acid). Tara pod tannin and Chestnut wood tannin are representative of gallotannins and ellagitannins, respectively. Condensed tannins are oligomers of flavonoids units with a MW ranging from 1,000 to 20,000 Dalton. Quebracho extract is among the most industrially produced tannin that has been shown to be predominantly composed of oligomers of profisetinidins.

Natural tannins act by inhibiting the growth of many bacteria. In fact, tannins are the main protection agents against bacteria in the plant kingdom. Their antimicrobial properties have raised particular interest and have been exploited in several fields such as food science and animal nutrition. Indeed, tannins have been used in the food industry as additives, natural colourants and preservatives. More recently tannins are replacing the use of antibiotics in livestock production to enhance animal health and performance due to their ability to improve feed digestion and to protect from microbial caused intestinal disease.

The abundance of tannins in nature together with their chemical and biological properties and their ability to form complexes with proteins (mainly) and polysaccharides has led to their widespread use in the leather industry.

Tannins bind to the collagen proteins inside the hide and coat them, causing them to become less water-soluble and more resistant to bacterial attack.

This process also causes the hide to become more flexible. Only tannins are able to impart to tanned leather these unique characteristics that make them so special and distinguishable. The “smell of leather” is something typical and unique.

In today’s leather making processes, tanners use vegetable tannins in both liquid and powder form. The most famous and ancient extract is obtained from the chestnut wood and is mainly used for the production of sole leathers, with high yield in weight, which are compact, firm and flexible, and the retanning of chrome-free leathers. Another tannin comes from the quebracho wood, a tree that grows in the Chaco region in Argentina. In this case the extract imparts to the leathers an unmistakable reddish shade, a warm touch and a bright appearance, required characteristics to make leather goods. In addition to chestnut and quebracho, Tara tannin is mainly used within the car and upholstery industries. This extract provides to the leathers excellent properties, such as fullness, softness, good resistance to light and to heat.

Tannins can also be used in the retanning of chrome tanned leathers to improve their “cold, impersonal feel” characteristics, by imparting the typical warm and natural feeling of vegetable tanned leathers.

Today a retreat towards more sustainable lifestyle and a slowdown to the use of chemicals, favoured by various deep changes in research, make tannins an important natural component in the tanning industry.

The use of leather tanned with vegetable tannins may offer a solution to prevent or decrease the development of unpleasant odours caused by the microbial fermentation of body secretions in feet.

1.4 How Can Tannins Make the Difference Inside a Shoe Made with Vegetable Tanned Leather?

Unlike what happens inside a shoe made of synthetic material, leathers made of tannins favour the absorption of the excess perspiration produced by the eccrine glands, along with the bacteria inhabiting the foot skin.

Thanks to tannins, leather insole and lining become hydroscopic. Once in contact with tannins within the leather, bacteria are immediately killed and destroyed (Fig. 2). Science has just proven that the right formula of tannins kills 99% of bacteria in a very short time.

The moisture absorbed by the leather made with tannins evaporates every time a person takes his/her shoes off. So when he/she puts them back on, the foot encounters a fresh and dry environment, free from unpleasant bacteria that could otherwise contaminate them while respecting and protecting the skin of the feet.

Tannins act as skin flora mediators because they foster the development of “good bacteria” and prevent the foot microbiota from being attacked by the “smelly” bacteria population of the shoe.

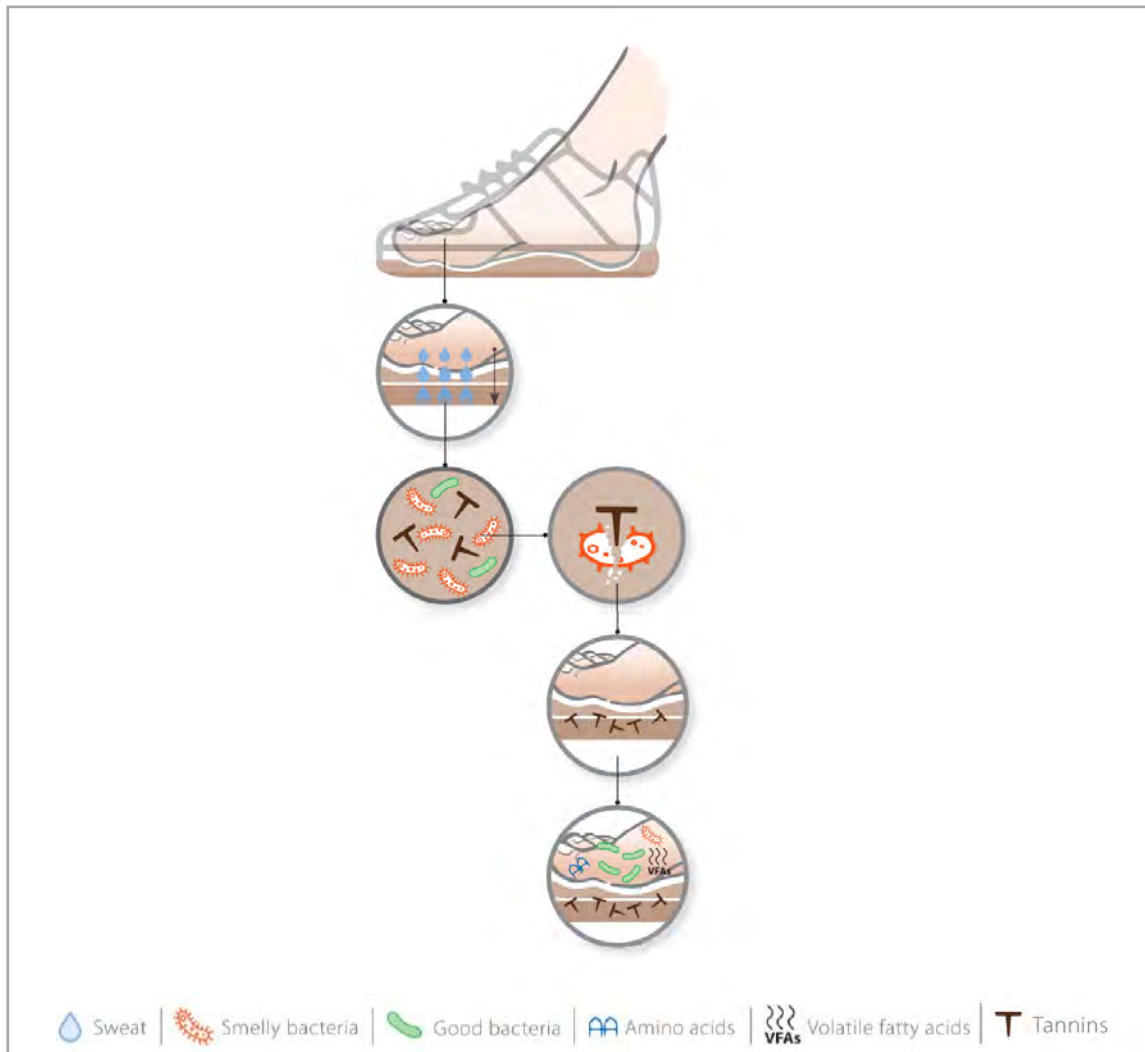


Fig. 2. The role of tannins in reducing the unpleasant odour of feet.

2 Assessment of the Antibacterial Activity of Tannins in Leathers

Recently, prestigious universities have assessed the antibacterial activity of natural tannins contained in vegetable tanned leather articles, especially shoes, that come in contact with human skin in comparison with chrome tanned leathers and synthetic materials. In particular the research was diverted in two different paths:

- *In vitro* assessment on the antibacterial activity of different types of tanned leathers and a synthetic material against a selection of Gram-negative and Gram-positive strains.
- *In vivo* research on the antibacterial activity of vegetable tanned leathers made with tannins within shoes (insole and lining) compared to using synthetic material.

2.1 *In Vitro* Research of the University of Milan

The antibacterial activity of vegetable tanned leathers made with natural tannins, such as chestnut, quebracho and tara extracts, was assessed in comparison with chrome tanned leathers and synthetic material.

The study was conducted by the Department of Pharmacological and Biomolecular Sciences of the University of Milan.

2.1.1 *Experimental conditions*

The trial was performed *in vitro* by inoculating *Staphylococcus aureus* and *Escherichia coli* strains, representing Gram-negative and Gram-positive bacteria, respectively. The antibacterial activity was tested at two different time points, time zero and after 6 hours, following contact with the bacterial cells (Fig. 3).

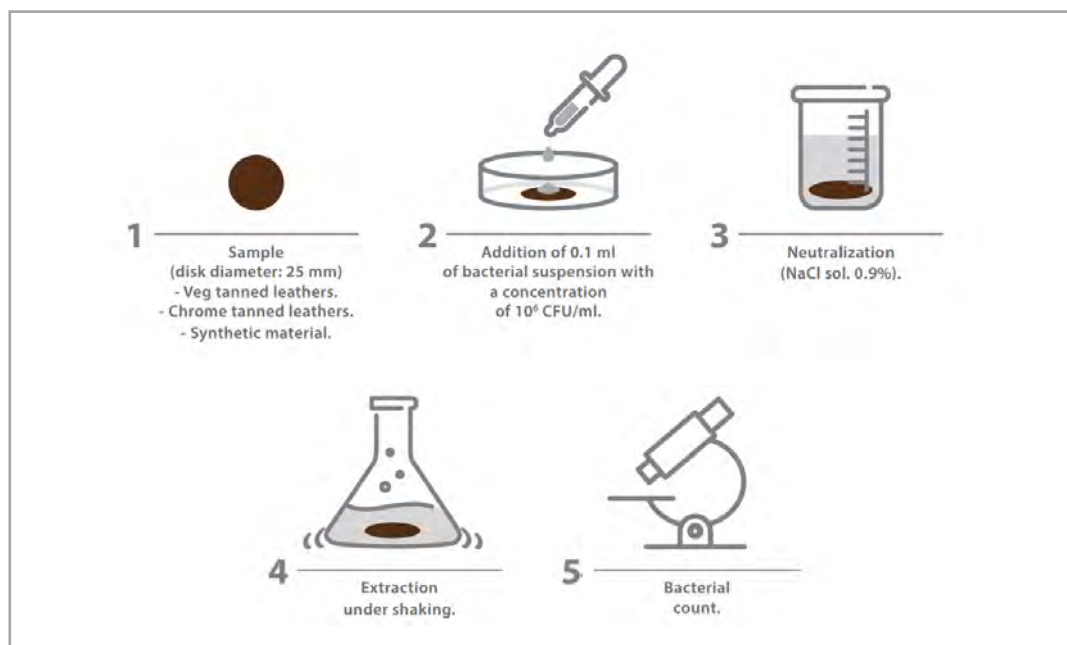


Fig. 3. Experimental conditions of the *in vitro* trial.

In order to be “antibacterial” a substance needs to be able to kill or inhibit the development of bacteria. The antibacterial power of a substance is the result of a quantitative assessment (*AATCC Test Method 100-2012*), evaluating the number of bacteria destroyed by the substance under evaluation, calculated in Colony Forming Unit (CFU).

The bacteria get counted using the following formula:

$$\%R = (A-B)/A \times 100 \text{ where } A = \text{CFU/ml at } t_0 \text{ and } B = \text{CFU/ml at } t_{6h}$$

The bigger the amount of killed bacteria, the stronger the antibacterial power of the substance under analysis. The antimicrobial activity was considered efficient when observing $\%R \geq 90\%$.

2.1.2 Results

Vegetable tanned leather samples made of tannins showed an excellent antibacterial activity against *Escherichia coli*, as witnessed by a 4 log reduction in bacterial viability following 6 hours contact. On the opposite, no antibacterial activity was observed for the synthetic lining nor for the chrome tanned leather sample (Fig. 4).

The same chrome tanned leather, if retanned with natural tannins, presented a good antibacterial activity, with more than 1 log reduction in bacterial viability following 6 hours contact. Similar results have been achieved against *Staphylococcus aureus*.

Therefore, the use of vegetable tanned leather made of tannins may offer a solution to prevent or decrease the development of unpleasant odours caused by the microbial biotransformation of body secretions in feet.

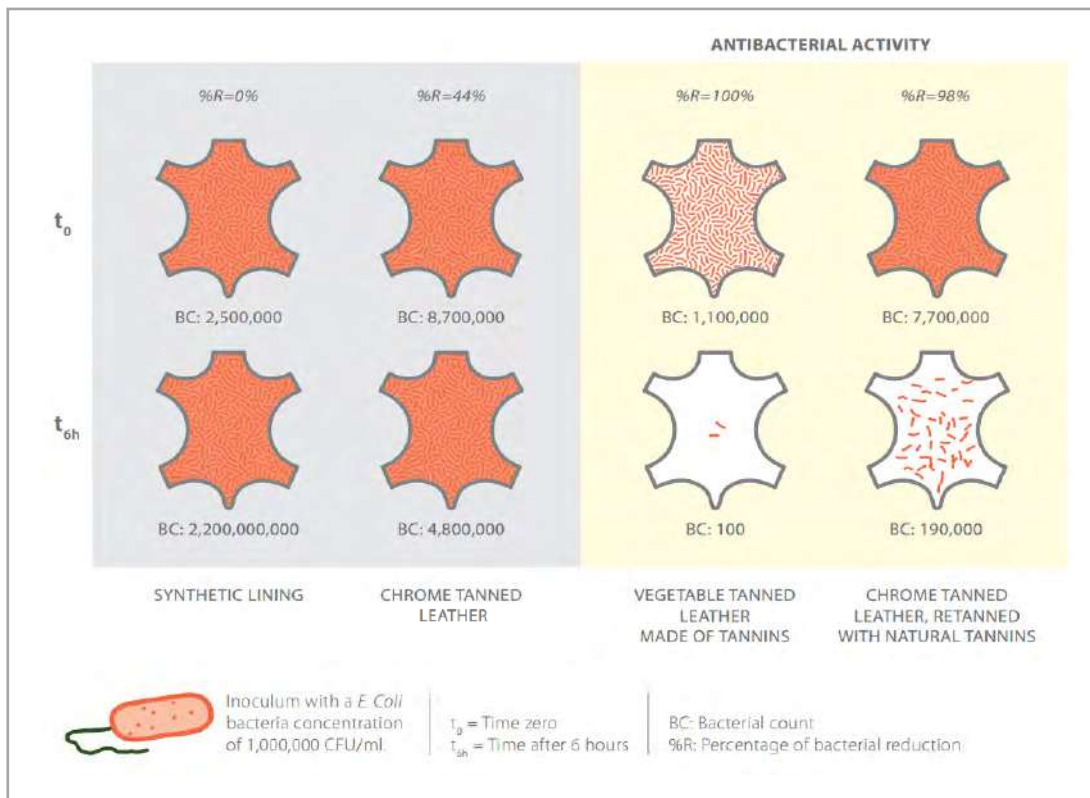


Fig. 4. Antibacterial activity of the materials under assessment against *E. coli*.

2.2 In Vivo Research of the Wellmicro

A molecular and bioinformatic analysis was performed to analyse the microbiota of the samples collected from the inside of a set of shoes worn by a selected panel.

The study was conducted by WellMicro, spin-off subsidiary of Alma Mater Studiorum - University of Bologna.

2.2.1 Experimental conditions

A group of 15 panellists worn for 28 consecutive days the same pair of shoes: one shoe showed a vegetable tanned insole and lining made of tannins; while the other one presented a synthetic insole and lining (Fig. 5).

Next Generation Sequencing (NGS) system was used to massively sequence DNA and RNA of bacteria inside the shoes. The parallel sequencing technology has revolutionised the biological sciences and it is less expensive and less time-consuming than a traditional sequencing.

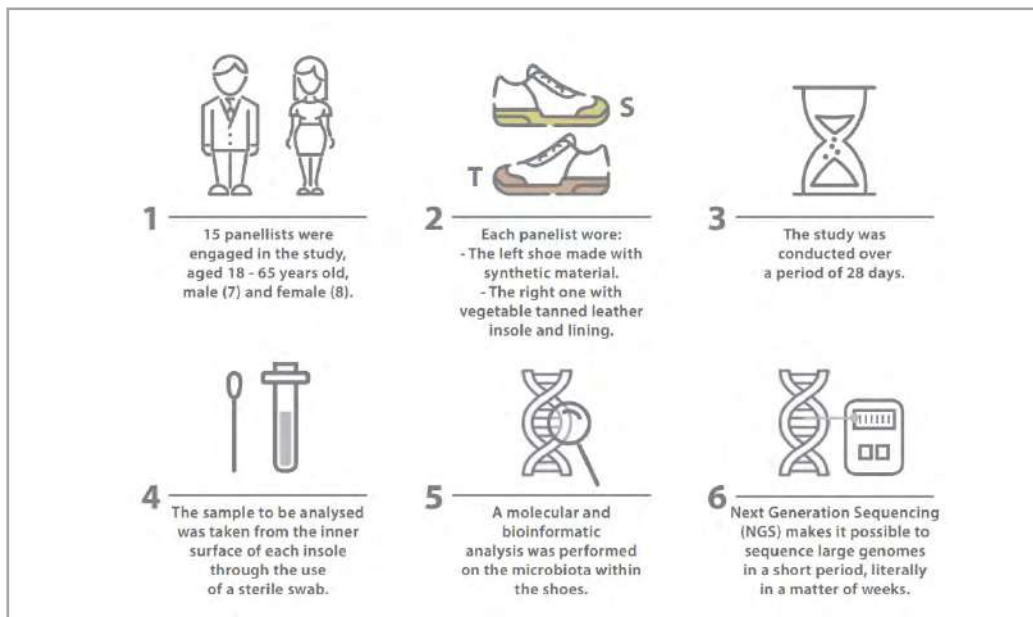


Fig. 5. Experimental conditions of the *in vivo* trial.

2.2.2 Results

The different type of material used to make the shoes brought to a significant difference in the selection of their bacterial population after the 28 days period (Fig. 6).

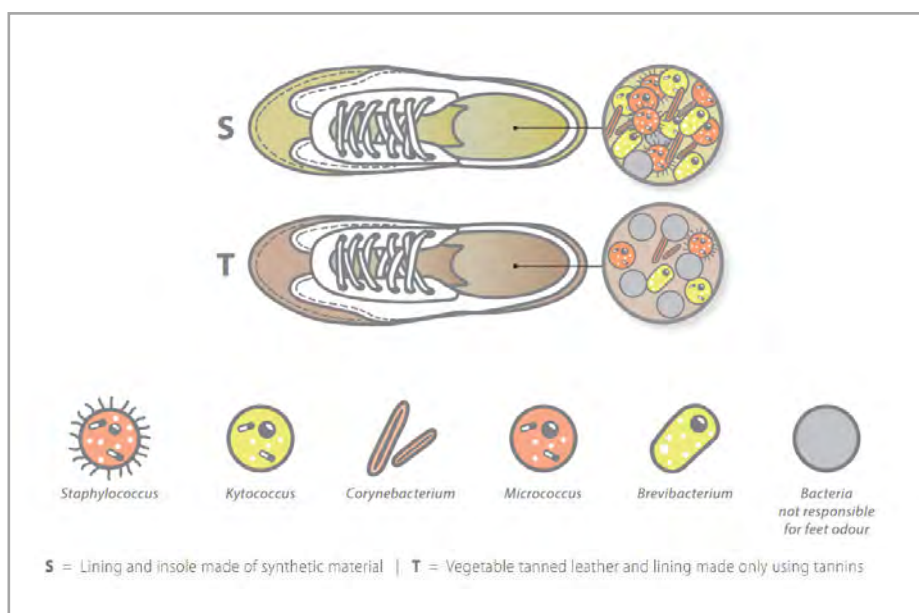


Fig. 6. Bacterial population difference between the shoes made with different materials.

The shoe with synthetic insole and lining fostered the development of the bacteria typical of sweat and responsible for feet odour, such as *Brevibacterium*, *Micrococcus* and *Kytococcus*. In fact, the shoe became an incubator of those bacteria biodegrading the amino acids present in the eccrine sweat and callus into volatile fatty acids, the cause of cheesy / acidic notes of foot.

The shoe with vegetable tanned leather insole and lining made with tannins created a dry and fresh environment, reducing the development of those bacteria responsible for foot odour and promoting the development of endogenous bacteria, the good ones for the foot microbiota. The foot is “safe” from bad bacteria.

3 Conclusion

The *in vitro* study, conducted by the University of Milan, shows that tanning of leather with chestnut, tara and quebracho tannins leads to materials with excellent antibacterial activity, especially against Gram-positives bacteria. All leathers tanned with the vegetable tannins act as non-leaching antimicrobial material, a property that makes these natural substances suitable for the contact with human skin. Therefore, the use of leather tanned with vegetable tannins may offer a solution to prevent or decrease the development of unpleasant odours caused by the microbial fermentation of body secretions in feet.

On the other hand, chrome tanned leather has a partial antibacterial property, only against *S. aureus* a representative of Gram-positive bacteria.

The same chrome tanned leather, if retanned with natural tannins, reaches a complete antibacterial activity against all tested bacteria.

The result of the *in vivo* study, conducted by Wellmicro, reports that the vegetable tanned leather made with tannins performs a selective antibacterial action, balancing the various element within the bacterial ecosystem of the inner part of a shoe. In fact it prevents the development of those bacteria responsible for shoe odour, such as *Brevibacterium*, *Micrococcus* and *Kytococcus* while fostering the growth of other bacteria that positively impact the feet skin flora.

References

1. Ara K., Hama M., Akiba S., Kenzo K.: 'Foot odor due to microbial metabolism and its control', *Can J Microbiol*, 52(4):357-64, 2006.
2. Bojar R. A., Holland K. T.: 'Review: the human cutaneous microflora and factors controlling colonisation', *World J Microb Biot*, 18:889-903, 2002.
3. Caroprese A., Gabbanini S., Beltramini C., Lucchi E., Valgimigli L.: 'HS-SPME-GC-MS analysis of body odor to test the efficacy of foot deodorant formulations', *Skin Res Technol*, 15(4):503-10, 2009.
4. Costello E. K., Lauber C. L., Hamady M.: 'Bacterial community variation in human body habitats across space and time', *Science*, 326(5960):1694-7, 2009.
5. Findley K., Oh J., Yang J.: 'Topographic diversity of fungal and bacterial communities in human skin', *Nature*, 498(7454):367-70, 2013.
6. Fogarty A. L., Barlett R., Ventenat V.: 'Regional foot sweat rates during a 65 minute uphill walk with a backpack', In: Mekjavic IB, Kounalakis SN, et al. (eds). *Environmental Ergonomics XII*, Ljubljana: Taylor NAS, 266-9, 2007.
7. Frutos P., Hervás G., Giráldez F. J., Mantecón A. R.: 'Review. Tannins and ruminant nutrition', *Spanish J of Agricultural Research* 2, 191-202, (2004).
8. Gotti M., Castagnetti A., Poles E., Battaglia A.: 'Caratterizzazione molecolare e analisi bioinformatica de lmicrobiota rilevato da campioni prelevati dalla superficie interna della scarpa e caratterizzazione biochimica diacidi grassi a corta catena', Wellmicro, Università degli Studi di Bologna, 2018.
9. Grice E. A., Segre J. A.: 'The skin microbiome', *Nat Rev Microbiol*, 9(4):244-53, 2011.
10. Grice E. A., Kong H. H., Conlan S.: 'Topographical and temporal diversity of the human skin microbiome', *Science*, 324:1190-2, 2009.
11. Hagerman A. E., Butler L. G.: 'The specificity of proanthocyanidin-protein interactions', *J Biol Chem* 256, 4494-4497, 1981.
12. Harker M., Harding C. R.: 'Amino acid composition, including key derivatives of eccrine sweat: potential biomarkers of certain atopic skin conditions', *Int J Cosmetic Sci*, 35:163-8, 2012.

-
13. Haslam E.: 'Natural polyphenols (vegetable tannins) as drugs: possible models of action', *J Nat Prod* 59, 205-215, 1996.
 14. James A. G., Cox D., Worrall K.: 'Microbiological and biochemical origins of human foot malodour', *Flavour and Fragrance Journal*, 28(4), 2013.
 15. Kanlayavattanakul M., Lourith N.: 'Body malodours and their topical treatment agents', *Int J Cosmet Sci*, 33(4):298-311, 2011.
 16. Landete J. M.: 'Ellagitannins, ellagic acid and their derived metabolites: a review about source, metabolism, functions and health', *Food Res Int* 44, 1150-1160, 2011.
 17. Marshall J., Holland K. T., Gribbon E. M.: 'A comparative study of the cutaneous microflora of normal feet with low and high-levels of odor', *J Appl Bacteriol*, 65:61-8, 1988.
 18. Mueller-Harvey I., McAllan A. B.: 'Tannins. Their biochemistry and nutritional properties', In: *Advances in plant cell biochemistry and biotechnology*, Vol. 1 (Morrison I.M., ed.), JAI Press Ltd., London (UK), 151-217, 1992.
 19. IPHF, National Foot Health Assessment Report, 2012.
 20. Panzella L., Napolitano A.: 'Natural phenol polymers: recent advances in food and health applications', *Antioxidants* 6(2), 2017.
 21. Poles E., Polissi A., Battaglia A., Giovando G., Gotti M.: 'Studio in vitro sul potere antibatterico dei pellami al vegetale conciati con tannini naturali'. Dipartimento di Scienze Farmacologiche e Biomolecolari (DiSFeB), Università degli Studi Milano, 2018.
 22. Quinton P. M., Elder H. Y., McEwan Jenkinson D.: 'Structure and function of human sweat glands', In: Laden K, Felger CB, et al. (eds). *Antiperspirants and Deodorants*. New York, NY: Marcell, Dekker Inc, 17-57, 1999.
 23. Smith C. J., Havenith G.: 'Body mapping of sweating patterns in male athletes in mild exercise-induced hyperthermia', *Euro J Appl Physiol*, 111:1391-404, 2011.
 24. Spencer C. M., Cai M.Y., Martin R., Gaffaney S.H., Goulding P.N., Mangolato D., Lilley T.H., Haslam E.: 'Phytophenol complexation - some thoughts and observations'. *Phytochemistry* 27, 2397-2409, 1988.
 25. Stevens D., Cornmell R., Taylor D., Grimshaw S. G., Riazanskaia S., Arnold D. S., Fernstad S. J., Smith A. M., Heaney L. M., Reynolds J. C., Thomas C. L., Harker M.: 'Spatial variations in the microbial community structure and diversity of the human foot is associated with the production of odorous volatiles', *FEMS Microbiol Ecol*, 91(1):1-11, 2015.
 26. Taylor D., Daulby A., Grimshaw S.: 'Characterization of the microflora of the human axilla', *Int J Cosmetic Sci*, 25(3):137-45, 2003

AGING PROCESSES AND CHARACTERIZATION METHODS FOR HISTORICAL BOOK BINDING LEATHER

Katarzyna Marcula¹, Katharina Schuhmann¹, Manfred Anders^{1, a}

¹ ZFB Zentrum für Bucherhaltung GmbH, Germany

a Corresponding author: anders@zfb.com

Abstract. The original substance of a book binding leather provides information about the place of origin, storage and user history of the book, which is why the preservation of this material in its original form is of crucial importance for research in the field of bookbinding. In a current research project in cooperation with FILK Freiberg, a newly sustainable treatment for historical leather book covers will be developed. The aim is to introduce a long-term mild care agent to increase leather flexibility and stability, which will remain in the structure and to stabilize the pH value at an optimal level with a buffer introduced in the form of deacidification agent. Preliminary research showed, that aging processes of vegetable tanned calf leather, which has been mainly used for leather book bindings in the past centuries, haven't been fully explored yet. Further, essential characterization methods like the determination of the acid content and methods for accelerated aging tests are not yet defined for leather. For a systematic development and evaluation of the newly treatment, the project had to be focused on accelerated aging and characterization methods first.

1 Introduction

Book binding leather not only has a decorative character in book bindings, but above all fulfills the protective and mechanical functions of the book. Therefore, it must have certain strength and flexibility. The original substance of a book binding provides information about the place of origin, storage and user history of the book which is of important scientific interest. For this reason, the preservation of this material in its original form is of fundamental importance for research in the field of bookbinding. The functionality of the leather book bindings is endangered because, like other organic materials, they undergo the continuous and unavoidable aging processes over the time. In recent decades in the various national libraries, special leather treatments have been developed, which, however, without exception, have been proven to be more destructive than stabilizing in long term. Components of these mixtures harden over the time and the leather becomes fragile and brittle. Partially they also migrate to the surface of the material, making it sticky. Looking at the issues of protection of leather book bindings, there are two main aspects to be dealt with: introducing long-term mild care agent to boost leather flexibility, which will remain in the structure and stabilize the pH value at the optimal level with the buffer introduced in the form of deacidification agent. One reason why there is still no solution to these problems is the inhomogeneity of the leather and difficult analysis of this material.

In a current research project in cooperation with the Forschungsinstitut für Leder und Kunststoffbahnen FILK, a newly sustainable treatment for the chemical stabilization and flexibilization for historical leather book covers will be developed.

Within the preliminary research, it turned out that the aging processes of vegetable tanned calf leather, which has been mainly used for leather book bindings in the past centuries, hasn't been fully explored yet. Therefore, the main degradation processes oxidation and acid-catalyzed hydrolysis have been investigated further to determine the most dominant process. Furthermore, standardized characterization methods and methods for accelerated aging tests are not defined yet and had to be developed, regarding the results of the degradation investigations. The analytical approach to leather aging processes was focused on chemical and mechanical collagen assessment.

The analysis of change of tannins has not been conducted, as it would have exceeded the limits and possibilities of the current project.

2 Materials and Methods

2.1 Production of homogeneous collagen and leather samples

Animal skin itself, and accordingly book binding leather as well, is a very inhomogeneous material. Depending on the specific animal, applied leather manufacturing technologies, the sampling point, the storage and usage history of a book, especially the mechanical properties of book binding leather varies a lot. This inhomogeneity is a very challenging aspect for comparative studies, investigating degradation processes or evaluating new developed care treatments. As there is no suitable completely non-destructive test method available yet, a novel approach for the use of possibly homogeneous samples for comparative experiments has been developed.

To determine the chemical effect of the developed treatments on collagen, “Freiberger Hautpulver”, a slightly chromium tanned collagen powder, has been used for analysis. For the current project, the powder did undergo a vegetable tanning, like it has been used extensively for the production of historic book binding leather. Experiments on the tanned collagen powder allow to investigate the effect of the care treatment without being limited by diffusion effects of the product into the leather matrix.

To investigate the diffusion processes into a physical collagen matrix and the effects of the developed treatment on the mechanical behaviour of leather, real leather samples had to be examined as well. To receive possibly comparative results in that case as well, defined and reproducible model leathers have been produced at FILK. According to historic book binding leather, a vegetable tanning has been applied to calf skins to produce a so-called restoration leather. For the treatment development, accelerated aging experiments have been performed on the model leathers to achieve a reproducible state of degradation. To compare different initial states, some of the model leathers have been produced with a specifically higher acid content.

2.2 Sampling

In initial experiments, selected mechanical and chemical parameters of the model leathers have been examined in defined reference spots of small distances over the total skin area of all produced model leathers. The results delivered a defined set of reference values for further tests on the one hand, as well as an overview of the comparability in between the model leathers on the other. For a further improvement of the comparability of results before and after a treatment, samples of the model leathers have been taken in a possibly small distance after a defined scheme (Fig. 1).

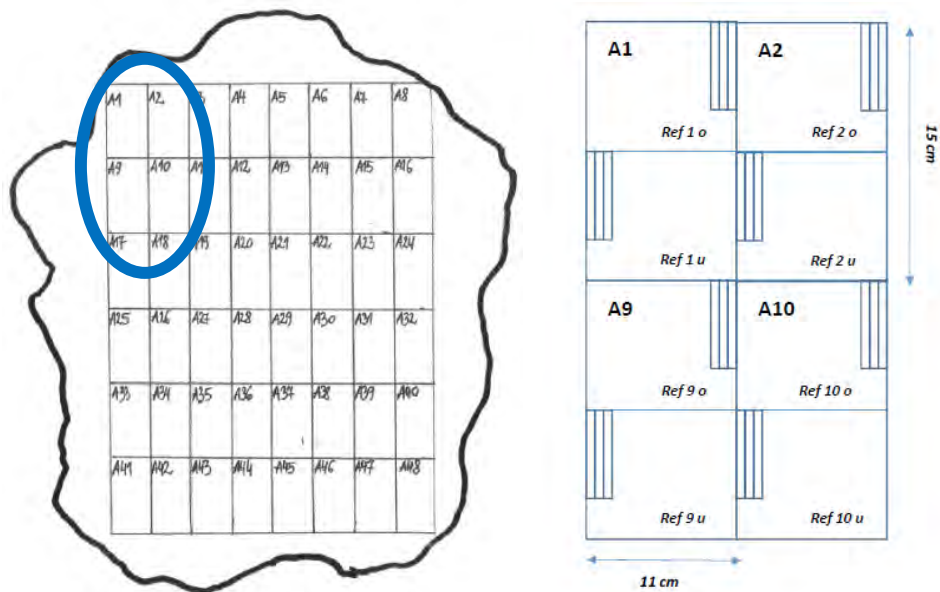


Fig. 1. Sampling on model leather skins

2.3 Accelerated Aging

The developed accelerated aging method is based on ISO 5630-5 for paper aging which provides a heating of the samples in a closed vessel of a defined volume at 100 °C for five days. For the model leather samples, a two-step aging procedure has been developed. Within a first step, a typical state of degradation like it can be found in historical book binding leathers, shall be simulated. This can be achieved by triggered acidic catalyzed hydrolysis reactions by the addition of acid(s) to the sample in the closed vessel. After the care treatment which has to be tested has been applied, its sustainability shall be proven in a second aging step.

With this objective, numerous versions of aging methods with varied aging time, temperatures and acid additives have been tested.

2.4 Analysis of Amino Acids

A qualitative and quantitative analysis of the included amino acids has been performed by FILK within the project. Therefore, acids have been dissolved out of the leather samples by acidic hydrolysis and separated by ion exchange chromatography. Subsequently, the single amino acids have been identified by a post-column derivatization with ninhydrin which enables a photometric detection and after calibration a quantitative analysis of α amino acids.

2.5 Warm water solubility

The warm water solubility of the samples has been determined by giving 1.00 g of a sample in 50.0 ml water of 60 °C for 120 minutes. The weight decrease of the dry sample allows information about the content of hydrolyzed or denatured collagen in the sample. The determination of this value is especially important for historical samples, which are characterized by high solubility in warm water (30-50%), due to a far-reaching hydrolysis. This value has become the main indicator for determining the degree of hydrolysis in the study of historical leathers, and serves as a guideline value for the development of methods of artificial aging.

2.6 Shrinkage temperature

The shrinkage temperature of collagen fibers is a well-known measure for the degree of denaturation. Within the project, it has been visually determined with the micro hot table (MHT) method, where the samples are heated in water at a constant rate of 2-4 °C/min and observed under a light microscope. Two states have been documented per sample:

T_1 – first motions of single fibers

T_s – majority of the fibers is shrinking

The shrinkage temperature allows qualitative information about the state of degradation of the collagen fibers – the further the degradation process, the lower T_s . The T_s of a single and complete hydrated triple helix is about 37-38 °C. With the natural arrangement of the triple helices to fibrils and collagen fibers and finally their physical intertwining, T_s increases to about 60°C. A vegetable tanning leads to a T_s of 75-80°C. If a triple helix is heated over its T_s , it will be irreversibly degraded. Another method to determine the shrinkage temperature of collagen is the differential scanning calorimetry (DSC) which has been carried out within the project for selected samples by FILK. An acceptable accordance between T_1 (MHT) and T_{onset} (DSC) as well as between T_s and T_{max} could be found which allows both measurements to be used in comparative studies. The DSC method delivers the denaturing enthalpy as a further interesting parameter.

2.7 pH value and differential number

The measurement of the pH value has been carried out following DIN EN ISO 4045 in an extract of 1.00 g sample in 20.0 ml water. Each sample has been measured in a three-fold determination. Further information on the acidity composition of the sample gives the measurement of the differential number (only for samples with pH below 3.5 or above 9.0). Therefore, the sample extract has to be diluted 1:10 after the initial pH measurement and measured again. The differential number corresponds to the difference between both pH values.

A differential number below 0.7 indicates the presence of either free strong acids in combination with a large amount of buffering salts or the presence of mainly weak acids. A differential number above 0.7 is a sign for mainly strong acids and the presence of buffering salts. [1]

With a pH below 4.0 and a differential number below 0.7, major acid-caused damages within the leather can be foreseen.

Both measurements have been made with a METTLER TOLEDO Five Easy pH meter and deionized water (< 10 µS/cm).

2.8 Acid-base titration

In addition to the determination of pH value and differential number, which deliver information about the acidity of the samples, an acid-base titration allows quantitative statements about the acid amounts. This information is decisive for the development of an accelerated aging method and in particular for the development of the sought pH adjustment. As the leather industry usually refers to the pH value and differential number, a standard method for the quantitative determination of the acid content surprisingly doesn't exist yet and had to be developed within the project first.

A titration method for the quantitative determination of the leather's acid content has been developed on the basis of ISO 10716, a back titration with NaOH after addition of HCl, developed for the alkalinity determination of paper. To adapt the method for the analysis of leather samples, several alkalimetry and acidimetry methods have been tested on extracts of leather samples with varied extraction and filtration parameters, different extraction media (H₂O, NaCl or KCl solution),

sample amounts and titration volumes. Furthermore, the influence of CO₂ presence has been investigated. A METROHM DMS Titrino 716 has been used for titration.

2.9 Ion chromatography

To gain more information about the contained acids in typical historical leather samples and the produced and accelerated aged model leathers, a semi-quantitative ion chromatography on selected leather samples has been performed at HTWK Leipzig. In three different test sets, inorganic anions (F⁻, Cl⁻, NO₃⁻, PO₄³⁻, SO₄²⁻), inorganic cations (Na⁺, NH₄⁺, K⁺, Mn²⁺, Ca²⁺, Mg²⁺) and organic anions (lactate, formate, acetate, oxalate) have been detected.

For the comparison of the total detected acid content with the results of the developed acid-base titration, the following equation 1 has been applied under consideration of the ions valence:

$$\text{Acid content} \left[\frac{\text{mmol}}{\text{g}} \right] = \sum \text{anions} - \sum \text{cations} \quad (1)$$

3 Results and discussion

3.1 Leather degradation

The aging of leather is a complex of related chemical reactions and physical processes. The chemical processes that destroy vegetable tanned leather are generally subdivided into reactions caused by oxidation and hydrolysis (mainly acid catalyzed hydrolysis). All major components of the tanned leather: collagen, tannins and fats are undergoing these degradation processes. Due to hydrolytic degradation, the cleavage of the peptide bond –CO-NH-, the protein chain separates into two parts as a result of binding of water molecule. Gradual breakdown of the collagen chain at different places simultaneously causes severe shortening of the collagen, which on the macroscopic scale is expressed as powdering and gelatinizing. As a consequence, the collagen becomes water soluble. For this reason, the determination of warm water solubility is a suitable indicator for the degree of hydrolysis degradation.

The oxidation of the fats, tanning agents and other substances contained in leather is favored by the presence of light. In the process of photo oxidation, the photon absorbed by the material reacts with an oxygen molecule to form a free radical, which after reaction with water produces hydrogen peroxide – a very powerful oxidant. However, the oxidation does not have to take place only with the contribution of light. The auto-oxidation of unsaturated fatty acids can also lead to damaging degradation processes [2].

According to Larsen, both oxidation and hydrolysis occur simultaneously, however hydrolysis seems to be more aggressive and faster than oxidation. Moreover it could be noticed that the less acidic the sample, the more important are oxidation processes. [3]

Oxidative damage is well detectable by a reduction of the methionine residues in the collagen. Methionine is easily oxidized by hydroxyl radicals, so the amount of methionine is a suitable marker for oxidation. From the amino acid analysis of collagen, the ration of basic and acidic acids (B/A) can be determined. The relationship between the two groups of amino acids has been used by Larsen to predict the denaturation temperature of historical leather samples and to describe the state of degradation processes. [4]

The methionine content of several historical leather samples was analyzed. The amount of methionine remains stable or only slightly reduced towards the newly tanned model leather. Especially natural aged samples with the typical powdering effect, known as “red rot”, showed no

change in the methionine content. The amino acid analysis results therefore support the hypothesis, that oxidation processes play only a subordinate role in leather degradation.

3.2 Accelerated aging method

In order to be able to work on samples that imitate the historical leather and to influence their properties in a controlled manner, the focus was initially placed on the development of the artificial aging method.

The aim of accelerated ageing was to reproduce as precisely as possible acid catalyzed hydrolysis as main degradation mechanism in the natural aged leather. To induce the hydrolysis and then to examine the efficacy of the newly developed care agent used to prevent it, a two-step aging process has been developed. The first stage is to introduce the acid into the material to initiate this type of degradation and thermal aging in closed vessel. The second thermal aging after treatment verifies its effectiveness by comparing treated and untreated leathers at this stage of aging.

Both stages of aging were carried out in closed 250 ml glass vessels, in which 9,01 – 9,05 g of leather were aged. Keeping the amount of leather constant in the defined volume of the glass vessels, allows to control the moisture content of equal level by all aging trials. Two methods of introducing acids into the skin structure have been tested: gas phase (in case of volatile acids) and impregnation (in case of strong inorganic not volatile acids). In case of aging in gas phase an intermediate/double bottom was used to avoid direct contact between the leather and the liquid volatile acid.

In estimating the amount of acid required for this aging method, it was assumed that the acid would be adsorbed by the leather in the vapor phase and thus removed from the gas phase. In order to achieve equilibrium, the acid has to change continuously from the liquid to the gaseous state. Therefore, it has been worked with excess of liquid phase to ensure the continuously exchange-dynamic balance between these two phases.

These aging tests by absorption of acids from the gas phase shows a significant dependence on the water content in the system. The use of 1 M formic acid resulted in the complete destruction of the leather, while the use of concentrated formic acid had a less destructive effect. Moreover, not pre-dried leather shrinks greatly and loses its shape already at about 70 °C when closed in the glass vessel without the addition of acid. Accordingly, the amount of water needs to be significantly reduced, to avoid denaturing reactions or the temperature must be maintained at a level at which no shrinkage under the given conditions occurs. It should be noted, however, that even pre-dried leather still contains water in the triple helix which should be sufficient to provide enough water for slow hydrolysis under acidic conditions. These artificial aging tests have shown that the acid amount of 1.8 mmol / 1 g of leather is sufficient to achieve the hydrolytic leather degradation when keeping the aging temperature below the denaturation temperature T_S . It was further confirmed that the denaturation temperature increases with decreasing moisture content. The water content in the closed vessel can be controlled by pre-drying the sample and then adding a defined amount of water or by using samples with a water content of between 9.5 and 11.0%. To determine the effectiveness of accelerated aging, the focus was placed on the analysis of the following skin properties: visual assessment, loss of mechanical properties, lowering the shrinkage temperature (but without reaching the state of denaturation), reducing the pH to about 2.5 - 3.5 and in a later stage determining the acid amount in the structure using titration methods. Among the tried-and-tested acids such as formic acid, acetic acid and mixtures of these acids with hydrochloric acid, which were tested at temperatures of 35 to 70 °C in different molar ratios, concentrations and for a different time, one method has been chosen which gave the best results. The selected method is based on 7 days aging in a closed vessel in a gas atmosphere of formic acid at a temperature of 60 °C. This way of aging allowed to obtain samples, which had reduced mechanical strength (loss of tensile strength of approx. 50 % compared to the reference sample), shrinkage temperature at about 55-60 °C, pH value of 3.0 and increased solubility in warm water by approx. 25 % compared

to the reference sample. In addition, the long-term observations were made to examine the stability of this method by testing the pH value over time. Multiple measurements of artificial aged samples revealed a time-dependence of the pH value, especially in the first weeks after aging (Fig. 2 and Fig. 3).

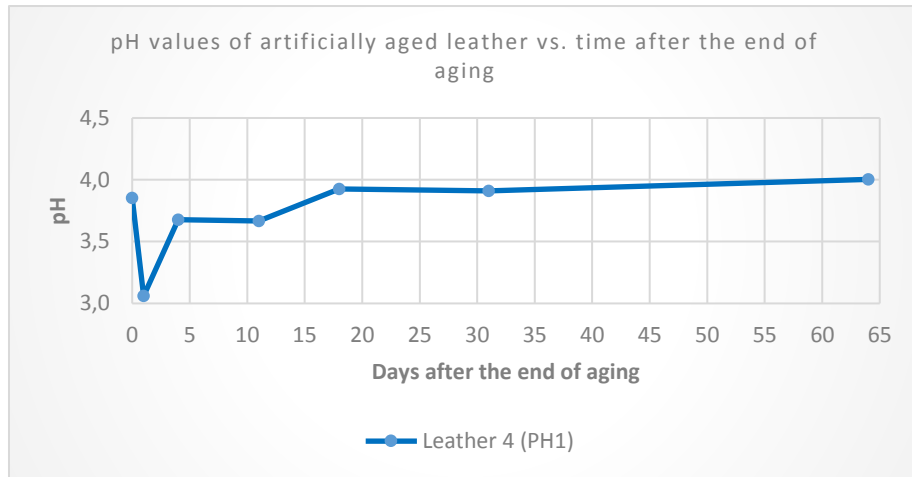


Fig. 2. pH values of artificially aged leather vs. time after the end of aging

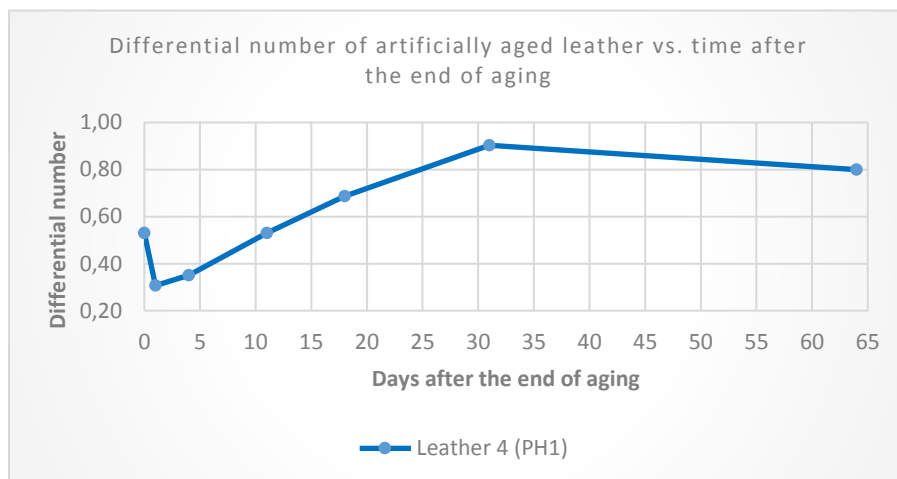


Fig. 3. Differential number of artificially aged leather vs. time after the end of aging

After artificial aging, the pH drops almost one unit to about 3.0. When samples have been stored under standard conditions, the pH values increase after 14-18 days and reach their original value after this time. The pH increases over time as the volatile formic acid desorbs from the collagen. Because the pH of these samples does not remain stable after aging and no further damage can be achieved in the second (thermal) stage of aging, this type of artificial aging had to be modified. Nevertheless, these experiments have proven that weak organic acids are able to lead to very significant leather damage.

A new aging method was developed based on the introduction by soaking in the leather structure mixture of two acids used in tanning: sulfuric acid and formic acid. The samples were soaked in a bath of acid solution in water for 10 minutes, air-dried and then aged for 7 days at 60 °C in a closed glass vessel. 0,1 M sulfuric acid was used with 1 M formic acid in a proportion 1:1. Conducted experiments for the first stage of aging yielded very satisfactory results and were subsequently subjected to second stage thermal aging at 60 °C for next 7 days. The results of pH values and

differential number after two aging stages remained stable and amounted 2.3 and 0.97 subsequently.

Table 1. pH and differential number values – reference and after two stages of artificial aging

Sample	pH value/ difference number- reference leather	Aging - I stage	pH value/ difference number- leather after I-st stage of aging	Aging - II stage	pH value/ difference number- leather after II-nd stage of
1	3,7/ 0,61		Aging - I stage		2,3/ 0,97
2					
3					
4					
5	3,7/ 0,70	Aging - I stage	2,3/ 0,98	Aging - II stage	2,4/ 0,99
6					
7					
8					

The shrinkage temperature for the reference samples was within 72-74 °C, dropped after the first stage of aging to 53-60 °C, and after the next stage to the value of 49-55 °C.

Table 2. Shrinkage temperatures (in °C) and color difference ΔE^*ab (2000) for reference leather and after two stages of artificial aging

Sample	Shrinkage temp.		ΔE^*ab (2000)	Aging - I stage	Shrinkage temp.		ΔE^*ab (2000)	Aging - II stage	Shrinkage temp.		ΔE^*ab (2000)
	(Ti) °C	(Ts) °C			(Ti) °C	(Ts) °C			(Ti) °C	(Ts) °C	
1	74,0	78,0	x	Aging - I stage	52,7	60,0	1,8	Aging - II stage	49,0	55,2	2,1
2	74,0	78,0	x		53,8	60,8	1,2		49,7	56,7	1,4
3	74,0	78,0	x		54,2	60,7	1,4		51,0	56,8	1,5
4	74,0	78,0	x		53,7	60,8	1,4		48,5	55,0	2,0
5	72,0	79,0	x		55,2	64,0	1,3		43,3	54,7	1,5
6	72,0	79,0	x		58,0	63,7	1,1		48,8	56,2	1,4
7	72,0	79,0	x		59,7	65,3	1,0		55,3	61,3	1,2

The difference between the tensile strength in relation to the reference sample after the first stage of aging was from 20 to 74 % and after the second stage it decreased by another 10-20 %.

This type of ageing made it possible to distribute acids in leather evenly. Moreover, sulfuric acid is not volatile and remains in the structure, which is necessary in order to realize the second stage of aging at all. Although, the amino acid analysis has shown that this aging does not alter the amino acid composition, indicating a pure hydrolytic damage, which is a main chain cleavage.

Table 3. Mechanical properties of leather – reference and after two stages of artificial aging

Sample	Tensile strength σ	Elongation at max. force D	Aging - I stage	Change of tensile strength $\Delta\sigma$	Change of elongation at max. F	Aging - II stage	Change of tensile strength $\Delta\sigma$	Change of elongation at max. F
	N/mm2	%		%	%		%	%
1	8,0	15,4	Aging - I stage	-36,7%	-9,1%	Aging - II stage	-46,1%	-27,7%
2	17,0	17,7		-43,7%	-23,2%		-50,7%	-32,4%
3	9,8	22,0		-46,8%	-9,7%		-49,0%	-18,1%
4	18,2	26,7		-19,9%	-14,1%		-45,8%	-27,1%
5	21,2	22,2		-46,5%	-18,7%		-52,9%	-28,7%
6	25,5	20,8		-26,7%	-5,9%		-89,8%	-69,0%
7	29,5	22,8		-73,4%	-43,9%		-85,4%	-62,1%

3.3 Acid content determination

The main objective of the experiment was to use titration to perform quantitative analyses of acids in modern as well as artificial or naturally aged leather. The determination of the exact amount of acids contained in the structure of the leather is of great importance in characterizing the modern skins for artificial aging and afterwards pH adjustment, as well as for determining the acidity level of historical samples. In order to get the most accurate picture of skin response to titration, all three possible titration options were used for the initial analysis: back-titration with 0.1M NaOH, back-titration with 0.1 M HCl and direct titration with 0.1 M NaOH. In the case of leather, several equivalence points (EP) were detected during the titration. The result (amount of acid) is the amount of acid / base used, which is consumed at the maximum value of the first derivative (dE/dV). At the same time, the pH value for each EP at the maximum of the first derivative is determined. As an additional result, the amount of acids at a constant pH of 5.5, which is considered to be the isoelectric point of the skin, has been listed as well. For the development of this method, several different modern leathers and artificially aged skins with a different amount of acids were used. The results that are discussed in this publication refer only to one type of modern leather, which during the tanning was intentionally (over)acidified with sulfuric acid.

Fig. 4 shows the titration curves during the titration for all tested methods listed above. These curves correspond to the titration of the same amount of leather sample (1.00 g) extracted in 20.0 ml of water, decanted/filtered and supplemented with 90.0 ml of distilled water. Titrations were carried out under nitrogen to minimize the influence of carbon dioxide. The Leather was extracted in pure distilled water, free from CO₂.

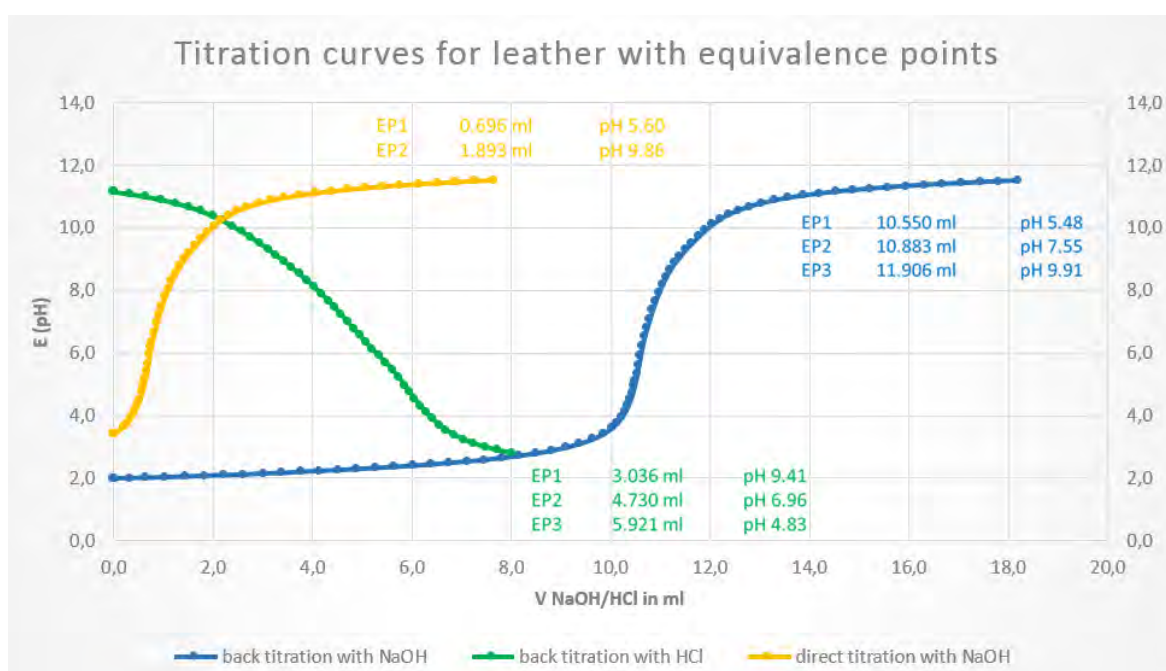


Fig. 4. Titration curves with equivalence points for three different types of titration

In case of each of these methods, modifications were made, which were aimed at selecting the best method for the objectives set in the project. Results of each of these modifications are collected in Table 4. The experiments in which extracts were boiled were excluded for further development, since the volatile organic acids evaporate during heating. In back titration with HCl, where NaOH was added to the extracts, higher amount of acids were obtained compared to other results, which

is probably related to swelling of the collagen by higher pH values. After careful analyses of these results two options were selected for further development of these methods – method no.4 and 7. It was found that filtration had no effect on the measured acid amount by modern leather compared to the values obtained from decanted extracts. The influence, however, can be seen in the measurements of the historical leather and for this reason filtering is recommended.

It was also attempted to investigate whether collagen acts as an ion exchanger. The acidic and basic side chains in collagen carry both negative and positive charges. In the acidic pH range, the corresponding amino groups are protonated and present in the solution as cations. In the basic pH range, the amino acids perform as an anion with an excess of negative charges. The electric charge depends on the pH of the surrounding eluent. The addition of acids or alkalis in the leather leads to a dissociation or charging of the collagen molecule and thereby also to a swelling. The collagen acts as an ion exchanger in this case, which can falsify the results, since the charge state is kept constant over a wide pH range. To minimize these undesirable effects extracts in aqueous NaCl and KCl solution were tested (variation: 0.3 M and 1.0 M). By presence of Na⁺/ K⁺ and Cl⁻ ions, a diffuse double layer should be introduced. These effects were tested using the direct titration with 0,1 M NaOH method.

Table 4. Titration: Method development 1

Method number	Modern leather - acidified with 0,8% H ₂ SO ₄	Acid content by max. EP in mmol/gDM	pH by max. EP	acid content by pH approx.= 5.5
1	Back titration with 0,1N NaOH - Mettler-Toledo (according ISO 10716 for determination of alkali reserve in paper)	0,10	5,7	0,09
2	Back titration with 0,1N NaOH +N ₂ - Metrohm - Water(-CO ₂) (A) (20ml extract+ 10ml 0,1N NaOH (10 min) + decanting + 90ml H ₂ O)	0,02	5,8	0,02
3	Back titration with 0,1N HCl +N ₂ - Metrohm (20ml extract+ 10ml 0,1N NaOH (10 min) + decanting + 90ml H ₂ O)	0,33	4,9	0,35
4	Back titration with 0,1N HCl +N ₂ - Metrohm - Water(-CO ₂) (C) (20ml extract+ 10ml 0,1N NaOH (10 min) + decanting + 90ml H ₂ O)	0,46	4,8	0,51
5	Back titration with 0,1N HCl +N ₂ - Metrohm- Water(-CO ₂)/ extracts boiled (F) (20ml extract+ decanting+ 90ml H ₂ O+ boiling+ 10ml 0,1N NaOH)	0,48	4,8	0,51
6	Back titration with 0,1N HCl +N ₂ - Metrohm- Water(-CO ₂)/ extracts in NaOH solution (D) (20ml extract in NaOH-solution + decanting+ 90ml H ₂ O)	0,88	5,0	0,96
7	Direct titration with 0,1N NaOH +N ₂ - Metrohm - Water(-CO ₂) (B) (20ml extract+ decanting + 90ml H ₂ O)	0,08	5,8	0,08
8	Directe titration with 0,1N NaOH +N ₂ - Metrohm - Water(-CO ₂)/ extract boiled (E) (20ml extract+ decanting+ 90ml H ₂ O+ boiling)	0,05	5,0	0,06

The evaluation of the results leads to the conclusion that the preparation of the extract in NaCl solution has a very low and from leather to leather different influence on the amount of acid, which in turn does not confirm the statement that collagen acts like an ion exchanger. However, it seems to have an influence on the pH at the equivalence point, which could confirm the ion exchange theory. A shift in the EP could also be due to the heterogeneity of the leather. After a thorough examination of the reasons for the lowering of the pH value it turned out that it is related to the disalibration of the electrode under the influence of the measurement in NaCl. In order to test the negative effects of the NaCl solution again, a similar series of measurements in KCl was carried out. It could be confirmed that collagen does not act as ion exchanger in this case. In addition, measurements in 1 M KCl solution were found not to interfere with the electrode – the calibration remained stable during the measurement time. Comparable amounts of acid were measured in extracts in H₂O, 1 M NaCl and 1 M KCl. It is worth emphasizing that the result of the measurement is influenced by the ratio of leather weight to the amount of extraction medium (compare Table 5). The less leather sample is subjected to an extraction in a given amount of solution, the larger amounts of acid will be measured. Therefore, it is extremely important to maintain a constant proportion between these two factors. For these studies, the proportions of 0.1 g of the sample per 10.0 ml of solvent will be the standard procedure for sample preparation.

Table 5. Comparable measurements of acid in H₂O, NaCl and KCl extract

Method number	Modern leather - acidified with 0,8% H ₂ SO ₄	Sample amount in 50 or 110 ml extract	Acid content by max. EP in mmol/gDM	pH by max. EP	acid content by pH approx.= 5.5
7.8A	Direct titration with 0,1M NaOH (110ml extract+ filtering)	1g	0,15	5,8	0,14
7.8G	Direct titration with 0,1M NaOH (50ml extract+ filtering+ 60ml H ₂ O)	0,5g	0,14	5,6	0,13
7.2(A)	Direct titration with 0,1M NaOH / 1M NaCl (110ml extract in 1M NaCl + filtering)	1g	0,13	2,5	0,29
7.2A repeated	Direct titration with 0,1M NaOH / 1M NaCl (110ml extract in 1M NaCl + filtering)	1g	0,11	3,9	0,17
7.2B	Direct titration with 0,1M NaOH / 1M NaCl (110ml extract in 1M NaCl + filtering)	0,5g	0,16	3,5	0,27
7.2C	Direct titration with 0,1M NaOH / 1M KCl (110ml extract in 1M KCl + filtering)	1g	0,13	5,2	0,14
7.2D	Direct titration with 0,1M NaOH / 1M KCl (110ml extract in 1M KCl + filtering)	0,5g	0,16	5,3	0,17
7.2E	Direct titration with 0,1M NaOH / 1M KCl (50ml extract in 1M KCl + filtering+ 60ml H ₂ O)	0,5g	0,13	5,4	0,13

To determine the amount of acid in the skin structure, aqueous extracts (0.1 g of skin per 10.0 ml of water) were used, which were directly titrated with 0.1 M NaOH. Using this method, the acid quantity was determined for reference leather, over acidified skins during the tanning, artificially aged leather and historical samples (Table 6).

Table 6. Acid content, pH value and differential number for some of measured samples – reference, over acidified reference, artificial aged samples and historical leather

Sample	Acid content by max. EP in mmol/gDM	pH by max. EP	acid content by pH approx.= 5.5	pH	differential number
Modern leather, artificial aged reference leather					
8 - reference leather	0,05	5,7	0,05	3,8	0,64
8 after 1st stage of aging	0,28	5,2	0,29	2,4	0,80
8 after 2nd stage of aging	0,28	6,1	0,27	2,5	0,74
Modern leather over acidified during the tannage					
overacidified with HCOOH	0,07	4,8	0,09	3,5	0,81
overacidified with H ₂ SO ₄ with rinsing	0,14	5,8	0,14	2,8	0,88
overacidified with H ₂ SO ₄ without rinsing	0,25	5,5	0,25	2,4	0,84
Historical leather from book covers					
HL1	0,55	6,7	0,48	3,0	0,48
HL2	0,38	6,8	0,30	3,3	0,45
HL3	0,45	6,7	0,39	3,0	0,54

Results obtained from titration were compared with the results of the acid content determined by the IC method. A very strong correlation between these two methods has been found for reference and artificial aged samples. The history of the samples was known and it could be predicted which acids should be found in the structure of leather.

Table 7. Comparison – acid content calculated from IC analysis/ acid content titrated for reference and artificially aged leather

Sample	Acid content calculated (anions-cations) in mmol/gDM	Acid content in mmol/gDM
	"H+" mmol/gDM	titrated
Ref 1.2	0,11	0,09
Ref 2.2	0,00	0,04
Ref 4	-0,01	0,03
artificial aged 119	0,21	0,23
artificial aged 123	0,33	0,38

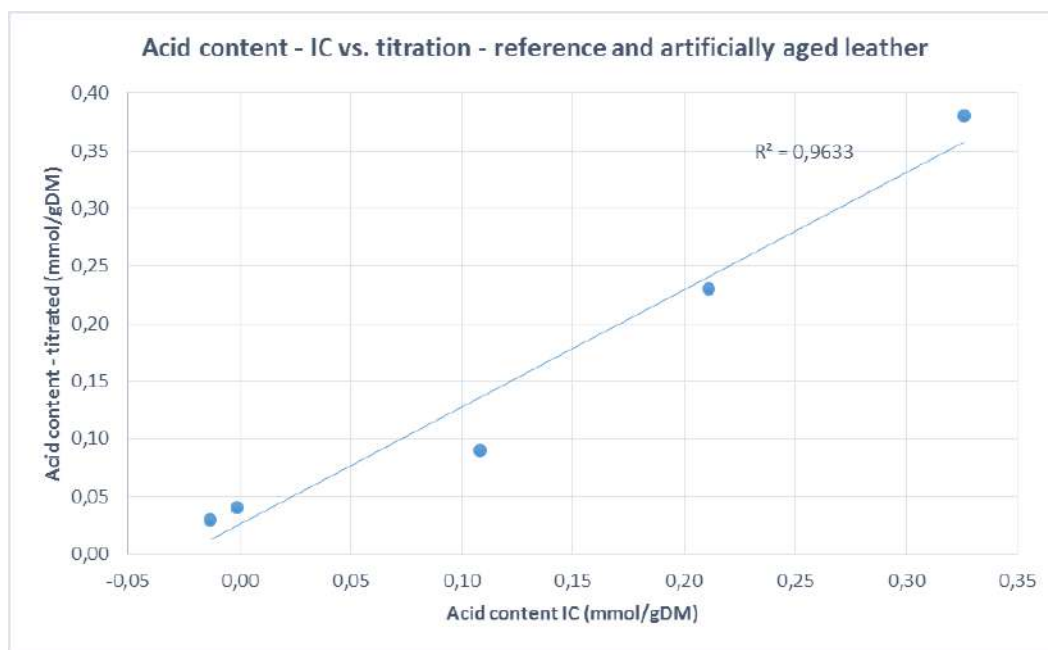


Fig. 5. Comparison – acid content calculated from IC analysis/ acid content titrated for reference and artificially aged leather

The comparison within the historical book cover leathers was also satisfactory with a coefficient of determination of 89 %. Differences between both analyzing methods can be traced here to further possible contained acids, which haven't been included in the IC analysis.

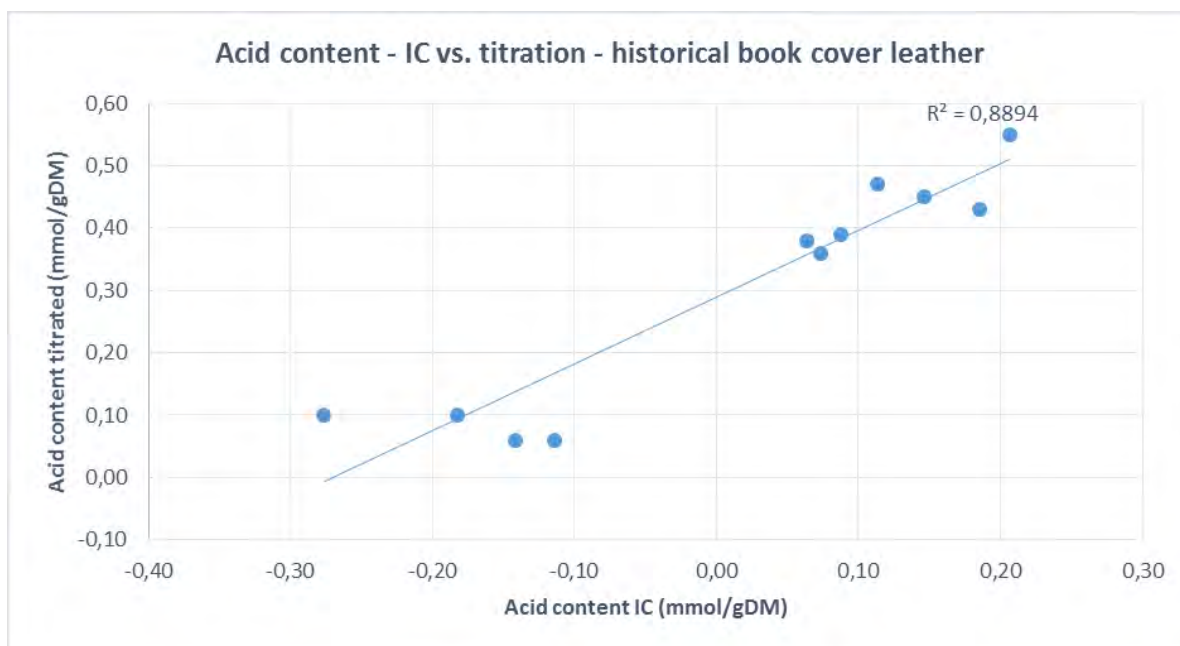


Fig. 6. Comparison – acid content calculated from IC analysis/ acid content titrated for historical samples

While comparing the acid contents obtained from these two methods for all types of examined leather together, it was not possible to find a significant correlation. But regarding the measurement of the reference and artificial aged samples with a known history, the IC results support the confirmation of the developed titration method.

4 Conclusion

Oxidation and acid-catalyzed hydrolysis have an enormous impact on the state of the leather. Both take place simultaneously and affect each other. The executed investigations have confirmed the hypothesis that the damage by acid hydrolysis is much more dominant than the damage by oxidation. Since oxidation plays only a minor role and can be slowed down only preventively by storage conditions, the project focused on the hydrolysis as the significant degradation mechanism. The aim of accelerated aging was to reproduce as precisely as possible observed and identified degradation mechanisms in the natural aged leather. Therefore, a two-step aging process has been developed. The first stage is to introduce the acid into the material that is to be used to simulate the acid catalyzed hydrolytic degradation. The second step is to verify the effectiveness of the newly developed care products by comparing treated and untreated leathers at this stage of aging. It has been proved that not only strong acids but weak organic acids also have a very destructive effect on the leather degradation. The aging was evaluated by optical/haptic tests, shrinking temperature, mechanical properties, hot water solubility, pH value and differential number. The influence of the alteration of the tanning agent has not been studied yet.

Regarding the leather characterization, the determination of the exact amount of acid introduced by the artificial aging is of great importance for the development of the aging method as well as for the pH adjustment of the leather for conservation purposes. For the method development, an acid-base titration was selected, which allows quantitative results of the acid content in the examined material. The developed method is easy to carry out and allows the measurements of different sample quantities (0,1 g - 1,0 g).

5 Acknowledgement

The authors want to thank for generously support of the project by EU funds (ESFR) and administration by Sächsische Aufbaubank – Förderbank (SAB).

Further, we acknowledge the Forschungsinstitut für Leder und Kunststoffbahnen, especially Dr. Anke Mondschein and Dr. Michael Meyer for the constructive project cooperation, the production of model leather, all conducted analysis and numerous discussions and consultings.

Large gratitude is offered to HTWK Leipzig, especially Dr. Jürgen Gebhardt for the further development and provision of the ion chromatography methods.

References

1. A. Küntzel (1943) *Gerbereichemisches Taschenbuch*, Verlag von Theodor Steinkopff, Dresden und Leipzig, p. 265
2. M. E. Florian (2006) *The mechanisms of deterioration in leather in: Conservation of Leather and Related Materials* (M. Kite, R. Thomson), Amsterdam, p.38- 40.
3. R. Larsen (14-15.06.2018) *Oral presentation during the interdisciplinary workshop in Freiberg/ Germany*
4. A. Mondschein (2017) *Interim report. Procorium: Nachhaltig wirkendes Pflegemittelsystem zur Behandlung von vegetabil gegerbtem Bucheinbandleder.*

SUSTAINABLE VALUE CREATION FROM LEATHER SOLID WASTES: PREPARATION OF SHOE SOLING MATERIAL USING NANO FILLERS

Sanjeev Gupta^{1a}, S. Ponsubbiah², S. K. Gupta³, Sujata Mandal^{1b}

1CSIR– Central Leather Research Institute, Chennai,India.

2 Institute of Leather Technology, Chennai, India

3 Shiv Nadar University, Uttar Pradesh,India

a)Corresponding author: sgupta1281@gmail.com

b)Corresponding author: sujata@clri.res.in

Abstract. This research aims at recycling of the leather industry solid waste, chrome shaving, into shoe components, such as outsole and insole material. Chrome shaving waste from the leather industry was used for making shoe soles by mixing with rubber and inorganic nanoparticles. Isoprene and Ethylene propylene monomer (EPDM) rubbers were used for this purpose. Various combinations of rubber, nanoparticle and chrome shaving waste were studied to get the desired characteristics of soling material. The prepared shoe soles were characterized for physico-mechanical behaviours like hardness, density, abrasion resistance and tensile strength, and compared with those of the rubber-based soling material available commercially. The shoe sole prepared using a combination of the isoprene and EPDM (1:1) rubber along with chrome shaving waste and kaolinite/silica nanoparticles showed physico-mechanical characteristics very close to the commercial soling material with higher value of percentage elongation. Hence, an efficient use of the fibrous chrome shaving and trimming wastes from leather industry in sole making would avoid the environmental problem, and could be a source of sustainable value-creation.

1 Introduction

Leather processing contains discharge of enormous amounts of liquid and solid wastes. Though there has been noticeable progress in recycling and in-plant controls of liquid effluent, methods or practices to manage solid waste in sustainable way still put the leather manufacturers in decision making dilemma. Wastes generated from the various unit operations are namely, desalting salts, raw trimmings, hairs, fleshing waste, shaving and buffing waste & finished leather trimmings. An easy choice to dispose solid wastes like chrome shavings and trimmings is land filling, which is subjected to strict environmental protocols due to the presence of chromium in these solid wastes. In India, more than 2.4 crores pieces of cattle hides, 2.2 crores of buffalo hides, 10.6 crores of goat skins and 3.7 crores of sheep skins are processed in about 1600 tanneries of leather industry. This generates around 0.2 million tons of solid wastes annually (CLRI, 2015). Chrome shavings are considered as a hazardous waste owing to the chrome present in it, also there is a certain risk that chromium may be washed off and it may contaminate the ground water if dumped carelessly. Hence, the safe disposal/application of chrome shavings should be addressed.

Considerable efforts have been made to recycle the chromium containing wastes by using recycling methods such as incineration, pyrolysis and alkaline or enzyme hydrolysis; these methods, however, are seldom complete without adding onto the environmental problems. Unfortunately, in such recycling processes, the inherent fibrous structure of these materials gets totally destroyed. Presently, chrome shavings are utilized as several low value applications such as –

- Preparation of regenerated leather using natural and synthetic blend polymer [1].
- Composite board made from chrome shavings and various binders [2].

- Using chrome shaving as a filler of Butadiene-acrylonitrile rubber [3].
- Production of parchment like materials [4].
- Value added composite from leather and non-leather fibers [5].
- Chemical sand [6].
- Bio Gas Production [7].

However, most of these applications have not been commercialized. Conventional leather boards have also been made that are used as insoles and packing materials etc.

Applications based on the fibrous nature of the shavings and trimmings are presently limited, but various possibilities are being explored even today. An efficient way of using these fibrous waste materials may be to combine them in a suitable form with synthetic polymers to give composite materials. Short fiber reinforcement of polymers is an important area in polymer composites, where both synthetic and natural fibers are effectively used.

The present communication describes the making of rubber soles using chrome shaving waste as the filler. Besides, three inorganic nanomaterials were also used as filler along with the chrome shaving waste. The influence of chrome shaving waste and inorganic nanomaterials on the physico-mechanical properties of the soles were studied and compared with those properties of a commercial rubber sole.

2 Materials and Methods

2.1 Materials

Isoprene rubber, EPDM rubber were used for preparation of soling materials, Zinc oxide and Stearic Acid as an activator & Pilcure CBS, Pilcure MBTS & Pilcure TMT as an accelerator and other chemicals like sulphur used is laboratory grade. Bentonite (BNT), Kaolinite (KLN) and silica (SI) nanoparticle were procured from Sigma Aldrich. Chrome shaving waste was collected from the leather industry.

2.2 Pre-treatment of the Chrome shavings

Normally chrome shavings are acidic in nature. To remove the acidity, the chrome shaving wastes collected from the leather industry were treated with aqueous ammonia, 1% solution of urea and sodium bicarbonate followed by washing with water and drying under sunlight for 24 hours. The dried chrome shaving fibers were turned into fine particles by using strap cutting machine and stored for further use.

2.3 Preparation of soles

Rubber soles of six different compositions were made using isoprene and/or EPDM rubber along with the treated chrome shaving as filler. The detail compositions are presented in Table 1 and Table 2. Table 1 presents the three different compositions of rubber soles, TA, TB and TC. Table 2 presents the sole compositions similar that of TC but the CaCO_3 has been replaced with bentonite (BNT) / kaolinite (KLN) / silica (SI) nanoparticles.

Table 1. Trial with Isoprene & EPDM Rubber and chrome shavings

Composition of the different Trials			Role of the material	Quantity (Phr)
Trial-A (TA)	Trial-B (TB)	Trial-C (TC)		
Isoprene rubber	EPDM Rubber	Isoprene + EPDM rubber	Base polymer	100
Chrome shaving	Chrome shaving	Chrome shaving	Solid waste / filler	50
Zinc oxide	Zinc oxide	Zinc oxide	Activator	10
Stearic acid	Stearic acid	Stearic acid	Activator	4
CBS	CBS	CBS	Accelerator	1
MBTS	MBTS	MBTS	Accelerator	1
TMT	TMT	TMT	Accelerator	0.5
Sulphur	Sulphur	Sulphur	Vulcanising Agent	5
CaCO ₃	CaCO ₃	CaCO ₃	Filler	50

Table 2. Trial with Isoprene & EPDM Rubber and chrome shavings

Composition of the different Trials			Role of the material	Quantity (Phr)
TC-BNT	TC-KLN	TC-SI		
Isoprene rubber	Isoprene rubber	Isoprene rubber	Base polymer	50
EPDM Rubber	EPDM Rubber	EPDM Rubber	Base polymer	50
Chrome shaving	Chrome shaving	Chrome shaving	Solid waste / filler	50
Zinc oxide	Zinc oxide	Zinc oxide	Activator	10
Stearic acid	Stearic acid	Stearic acid	Activator	4
CBS	CBS	CBS	Accelerator	1
MBTS	MBTS	MBTS	Accelerator	1
TMT	TMT	TMT	Accelerator	0.5
Sulphur	Sulphur	Sulphur	Vulcanising Agent	5
BNT	KLN	SI	Nano-Filler	10

To prepare the sole samples, accurately weighed quantities of the ingredients were fed to a two roll rubber mixing mill (with roller dimension D=220mm and L = 450 mm) maintained at a temperature of 47-67 °C and rolling at a speed of 15 rpm. Rubber soles of 6–8 mm thickness were made and stored at room temperature.

The above experiments were carried out in the curing temperature around 140–160 °C and curing time around 5 to 12 minutes in the compression moulding machine. Corresponding female and male mould halves were used in this process. A pre-weighed charge cut were placed inside the mould. To facilitate polymerization (or cross-linking) and consolidation of composite material an appropriate pressure force were maintained. During this compounding process proper nip cap and cuts were maintained in order to get the uniform compounding.

Soles of different compositions, TA, TB, TC, TC-BNT, TC-KLN and TC-SI were made following the above mentioned procedure.

2.3 Characterization techniques

The morphology of the prepared sole materials was characterized using scanning electron microscopy (SEM make: Phenom world, model: phenom Pro). Physico-mechanical properties of the sole materials were studied using Universal Test Machine (INSTRON, model: 3369/J7257), Bata Flexing Resistance (SATRA, Model: STM 612) and Leather Sole Abrasion Tester (SATRA, Model: STM 140).

3 Results and Discussions

3.1 Scanning Electron Microscopic (SEM) Study

The SEM Micrographs of the fractured surfaces of the tensile tested specimens of TA, TB and TC are presented in figure 1. Figure 1 also shows the SEM images of cross-sectional surfaces of the nano-filler incorporated soles, TC-BNT, TC-KLN and TC-SI.

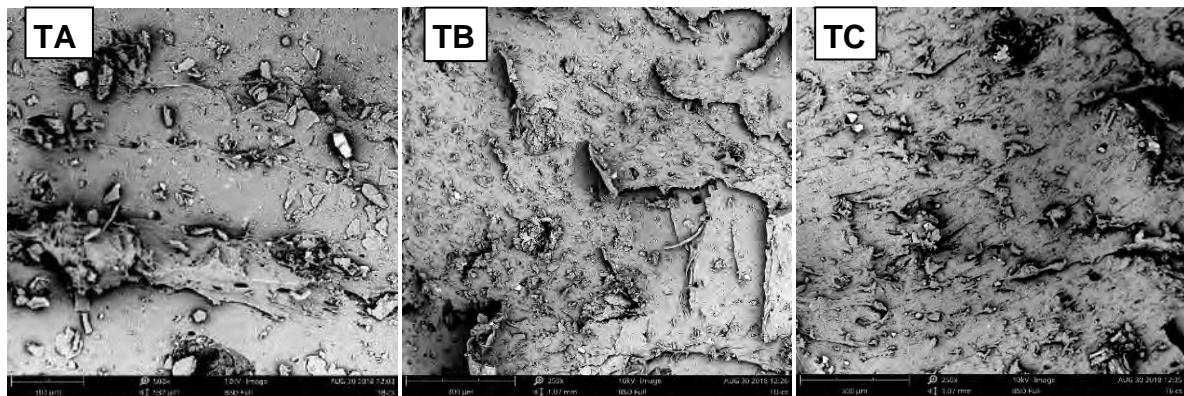


Figure 1. SEM images of the fractured surfaces of TA, TB, TC, and cross sectional view of TC-BNT, TC-KLN and TC-SI sole samples.

The SEM images of the experiment I and experiment II are shown in the above Fig. 5 to 8. The SEM images of sample TA, TB and TC show aggregation of fibre due to blending of Isoprene and EPDM with chrome shavings. The SEM image reveals that in all three samples chrome shavings are intermingled with polymers and also can be seen that in all the six samples chrome shavings are closely knitted.

3.2 Physico-mechanical properties

The prepared soling materials were subjected to physic-mechanical testing to study the properties like, abrasion resistance, tensile strength, percentage of elongation at break, hardness, density and flexing endurance. The values obtained for these properties were compared with those properties of the control sole sample. The control sole sample is a commercial rubber sole obtained from AGGU Soles Pvt Ltd, Ranipet, Tamilnadu, India. The physico-mechanical properties of the control sole material are tabulated below:

Table 3. Values of physico-mechanical parameters of the control sole sample.

S.No	Mechanical Properties	Values
1.	Tensile strength	8.0 MPa
2.	Percentage of Elongation	300 %
3.	Flexing endurance	150000 flexes
4.	Density	1.25 gm/cc
5.	Abrasion Resistance	150 mm ³
6.	Hardness	70 (Shore A)
7.	Thickness	0.8 mm

The physico-mechanical characteristics of the rubber soles made using isoprene and/or EPDM rubber along with chrome shaving waste (as per the composition listed in table 1) are presented in table 4. The same characteristics of the rubber soles made using mixture of isoprene and EPDM rubber along with chrome shaving waste and inorganic nanomaterials as filler (as per the compositions in table 2) are presented in table 5.

Table 4. Values of physico-mechanical parameters of the rubber sole samples prepared using chrome shaving waste as filler.

Sole Sample	Tensile Strength (MPa)	Elongation at Break (%)	Flexing endurance (flexes)	Density (gm/cc)	Abrasion Resistance (mm ³)	Hardness (Shore A)
Control	8.0	300	150000	1.25	150	70
TA	4.5	121	150000	1.161	297.98	73
TB	3.6	46.60	78000	1.102	293.97	70
TC	3.2	106.60	150000	1.184	335.25	84

The values presented in table 4 show that the properties like, sole flexing (except TB), density, and hardness, of the sole samples prepared by using chrome shaving waste as filler (TA, TB and TC) are comparable with those of the control sole sample. The abrasion resistance values of these soles are much higher than that of the control sample. However, the values of tensile strength are lower (almost half) than that of the control sample.

Based on the physico-mechanical properties of the sole samples TA, TB and TC, the sole composition of TC was selected for further study by incorporation of inorganic nanoparticles as filler in place of CaCO₃.

Table 5. Values of Physico-mechanical parameters of the rubber sole samples prepared using chrome shaving waste along with inorganic nanomaterials as filler.

Sole Sample	Tensile Strength (MPa)	Elongation at Break (%)	Flexing endurance (flexes)	Density (gm/cc)	Abrasion Resistance (mm ³)	Hardness (Shore A)
Control	8.0	300	150000	1.25	150	80
TC-BNT	5.6	450	150000	0.989	127	82
TC-KLN	11.1	350	150000	0.979	144	85
TC-SI	7.5	450	150000	0.984	145	83

The values of physic-mechanical characteristics presented in table 5 clearly show that incorporation of nanoparticle along with the chrome shaving waste improves all the sole characteristics (except

density). The marginal decrease in density of the soles might be due to the replacement of CaCO_3 . All the sole samples with nanoparticle showed either similar or higher tensile strength than that of the control sole. Among the three inorganic nanoparticles, kaolinite and silica showed excellent soling characteristics when compared with the control sole sample.

The physico-mechanical characteristics exhibited by the prepared sole samples from rubber and chrome shaving waste proves good mutual compatibility. Hence, the composition of TC-KLN and TC-SI can be considered for further development.

4. Practical Implications

Comparison between conventional and proposed method of leather solid waste management indicates that negative externalities caused by incineration, pyrolysis and alkaline or enzyme hydrolysis and land filling could be eliminated with the use of fibrous content of solid waste in shoe sole manufacturing.

5. Conclusion

Sole samples were successfully made using the chrome shaving waste with rubber and with/without inorganic nanoparticles. The SEM images showed that the chrome shaving waste showed good compatibility with both isoprene and EPDM rubber. The sole samples without the nanoparticles showed good physico-mechanical characteristics except the tensile strength. However, incorporation of kaolinite and silica nanoparticle along with the chrome shaving waste improved the tensile strength of the sole samples. Therefore, the isoprene + EPDM + chrome shaving + inorganic nanoparticles composite can be considered for further development, which in turn could be a sustainable way of making use of the hazardous solid waste generated by the leather industry. Hence, it may be concluded that efficient use of the fibrous nature of chrome shavings and trimmings would avoid the environmental problem, and could be a source of sustainable value-creation from these solid wastes.

References

1. Parrini, P.; Peroni, G.; Corrieri, G.; Righi, G.P.: 'Fibrous materials useful as leather substitutes and consisting essentially of leather fibers, fibrils or fibrils of synthetic polymers and cellulose fibers', US Patent No. 4162994, 1977.
2. Sekar, S.; Mohan, R.; Ramasastry, M.; Das, B.N.: 'Preparation and partial characterization of composite boards using chrome shavings and various binders', *Leather Age*, 86-92, May 2007.
3. Przepiorkowska, A.; Chronsha, K.; Zaborski, M.: 'Chrome tanned leather shaving as a filler of butadiene-acrylonitrile rubber', *J. Hazard. Mater.* 141, 252-257, 2007.
4. Ramamurthy, G.; Mohammed Farhan, K.; Sekar, S.; Mohan, R.; Das, B.N.; Sastry, T.P.: 'Preparation and characterization of modified parchment like materials using synthetic polymer', *Leather Age*, 45-50, Feb. 2009.
5. Sekar, S.; Mohan, R.; Das, B.N.; Sastry, T.P.: 'Preparation and characterization of composite board using chrome shavings and plant fibers', *J. Indian Leather Technologist Assoc.*, 765-769, Oct. 2009.
6. Dang, X.; Yuan, H.; Shan, Z.: 'An eco-friendly material based on graft copolymer of gelatine extracted from leather solid waste for potential application in chemical sand-fixation', *J. Clean. Product.* 188, 416-424, 2018.
7. Priebe, G.P.S.; Kipper, E.; Gusmão, A.L.; Marcilio, N.R.; Gutterres, M.: 'Anaerobic digestion of chrome-tanned leather waste for biogas production', *J. Clean. Product.* 129, 410-416, 2016.

STRONG SKIN, IS NOT ALWAYS THICK: COMPARATIVE STRUCTURAL AND MOLECULAR ANALYSIS OF DEER SKIN AND COW HIDE

R. Naffa^{1,a)}, C. Maidment¹, G. Holmes¹ and G. Norris²

1 NZ Leather & Shoe Research Association Inc. (LASRA), Palmerston North, New Zealand

2 Massey University, Institute of Fundamental Sciences, Palmerston North, New Zealand,

a) Corresponding author: rafea.naffa@lasra.co.nz

Abstract. A comprehensive analysis of the molecular and structural components of deer skin and cow hide was undertaken. These skins are known to be strong. However, they derive their strength from different combinations of molecular and structural properties. Firstly, the physical properties of deer skin and cow hide including tensile strength, tear strength, and denaturation temperature were measured. Secondly, the structure of the collagen fibrils and glycosaminoglycans was investigated using transmission electron microscopy (TEM) and small angle X-ray scattering (SAXS). Finally, the chemical composition of deer skin and cow hide, such as amino acids, crosslinks and glycosaminoglycans, were analyzed. Our results showed that the physical properties of deer skin and cow hide are derived from different combinations of several chemical components, resulting in a different architecture. It was found that the large and “wavy” collagen fibers in deer skin are made up of collagen fibrils with small diameters. Additionally, deer skin fibrils appeared to be linked by regular arrays of filaments of large glycosaminoglycans that are distributed uniformly. Deer skin contained a higher proportion of trivalent collagen crosslinks. In contrast, the collagen fibrils in cow hide were larger, contained a diverse glycosaminoglycan distribution and a higher proportion of tetravalent collagen crosslinks, resulting in straight collagen fibers. This study suggests that although deer skin and cow hide are both strong, they have different structural and molecular features.

1 Introduction

Every year billions of animals are slaughtered for meat, producing millions of tons of hides and skins. These are converted to leather which is considered the most significant economic co-product of the meat industry. New Zealand hides and skins contribute to the world’s leather industry by providing raw skins and hides for the tanning industry. Leather is used for many manufactured products because of its physical and aesthetic properties [1]. One of these properties is strength, which is critical for many leather products, especially footwear. Leather is manufactured by stabilizing the fibrous collagen networks of animal skins using chemical reagents, a process that is colloquially known as tanning [1]. The origin of the skins and the processing methods used in tanning play a crucial role in determining the properties of the final leather product. Different animal skins and hides, with different physical characteristics, are used to make leather. Strong leather is used for footwear and upholstery while weaker softer leather is used for clothing. Skins from cow, goat, and deer produce strong leather, while sheep skins from dual-purpose sheep produce relatively weak leather [1]. For this study, deer skin and cow hide were chosen, because they are commonly used in the New Zealand tanning industry. Deer skin is thin while cow hide is thick; however, both produce strong leather.

Skin has a complex structure composed mainly of collagen and elastin fibers that associate with proteoglycans [2]. Collagen is the major structural protein and the main component of skin. Collagen type I is the major collagen, making up 70% of dry skin weight, followed by collagen III which makes up 10% [3]. Structurally, skin is composed of three well-defined layers the epidermis, dermis, and flesh layer (hypodermis) [2]. The dermis layer accounts for 90 % of the weight of skin

and is named as the grain and corium layers in the leather industry [1]. The grain layer has a fine and loose collagen fibrous structure with a larger proportion of collagen III and is responsible for the distinctive appearance of leather [1]. The corium layer contains a thicker and more compact collagen fiber network running parallel to the skin surface that imparts strength to the skin [1].

Increasing demand for information about the quality of leather produced from different animal skins and hides has required a better understanding of the molecular differences of skins and hides. To address the structural and molecular factors that affect skin and hide properties, the amino-acid and cross-link composition and structure of deer skin (thin and strong) and cow hide (thick and strong) were analysed using analytical methods and confocal, transmission electron microscopy (TEM) and small angle X-ray scattering (SAXS) respectively. The results from this study will help inform the leather industry to enhance the physical properties of skins and hides by suggesting modifications to existing leather processes.

2 Experimental Procedure

2.1 Chemicals and materials

Chemicals were purchased from Sigma-Aldrich (St. Louis, MO, USA) except for the following: 6-aminoquinolyl-N-hydroxysuccinimidyl carbamate (AQC) which was purchased from SYNCHEM (Altenburg, Germany); the Blyscan glycosaminoglycan assay kit purchased from Biocolor Ltd. (Northern Ireland); mass spectrometry grade water, acetonitrile, methanol and formic acid (>99%) purchased from Fisher Chemical (Fair Lawn, NJ, USA); hydrochloric acid and acetic acid purchased from Panreac (Barcelona, Spain); n-butanol (97%) purchased from Ajax Finechem, Univar (TarenPoint, NSW, Australia); dihydroxylysinoonorleucine (DHLNL) purchased from Santa Cruz Biotechnology (Delaware Ave, CA, USA). HLNL, HHL, and HHMD were isolated and purified in our laboratory. Potassium permanganate, sodium tungstate, toluidine blue, and uranyl acetate were purchased from BDH (Poole, England); phosphomolybdic acid from Hopkins and Williams (Essex, England); Sirius red from F3B Spectrum (CA, USA); picric acid from VWR Chemicals (PA, USA); xylene from Labscan (Thailand); glutaraldehyde from Merck (NJ, USA); cuproline blue from Polysciences (PA, USA); deuterium oxide (99.9 atom%) (Cambridge Isotope Laboratories, catalog number: DLM-4-100); heparan sulfate (Celsus Laboratories, PN HO3105, Batch HS10697) Tert-butanol (t-BuOH, ACS reagent) (Sigma-Aldrich, catalog number: 360538).

2.2 Skin and hide samples

Deer skin and cow hide were obtained through the New Zealand Leather and Shoe Association Inc. (LASRA®). In summary, the skins and hides were removed from the carcass and immediately chilled to under 8 °C by washing with chilled water through a rotary screen. The skins and hides were then transported to LASRA before the hair was removed from each piece of skin/ hide (1.0 cm × 3.0 cm), cut from the official sampling position (OSP). The samples were then cut parallel to the animal backbone to obtain three technical replicates for each orientation. The thickness of each skin sample was measured using an instrument developed by Wodzicka (1958), which has an accuracy of 0.01 mm [4].

2.3 Tear and tensile strength

Both tear and tensile strength were carried out on fresh skins using a Texture Analyzer (Stable Micro Systems, model TA.XT Plus, Surrey, UK) and according to the international standards ISO 3377-2:2002 and ISO 3376:2011 respectively.

2.4 Small angle x-ray scattering (SAXS)

Scattering patterns of the fresh samples were recorded using the Australian Synchrotron SAXS/WAXS beamline [5-9]. The X-ray beam size was $50 \times 50 \mu\text{m}$, the wavelength 1.0332 \AA , and the instrument calibrated using a silver behenate standard. Diffraction patterns were recorded using a Pilatus 1 M detector with an exposure time of 2 s and a sample to detector distance of 3342 mm, giving a q-range of 0.002 to 0.25 \AA^{-1} . Data analysis was performed using in-house software to extract the scattering intensity from the raw data image [7].

2.5 Microscopy

Polariser light microscopy (PLM), laser scanning confocal microscopy (LSCM) and transmission electron microscopy (TEM) were carried out on fresh samples [7]. Sample sections were examined with a light microscope and photographed using a Nikon Eclipse E600WPOL polarising light microscope (Nikon Instruments, Melville, New York, USA) at magnifications from 1X to 10X to select the sections to be examined by laser scanning confocal microscopy. For LSCM, samples Skin samples were cut into small pieces ($20 \text{ mm} \times 20 \text{ mm}$) then stained with picosirius red [7, 10, 11]. Sample sections were sliced into a thickness of $40 \mu\text{m}$ then examined using a Leica SP5 DM6000B confocal microscope (Leica Microsystems Ltd, Knowlhill, Milton Keynes, UK) at different magnifications by capturing one image every $0.05\text{-}0.3 \mu\text{m}$ to generate 3D images [11]. Skin samples were cut into thin slices (1.0 mm) then fixed in a solution containing 2.5 % (v/v) glutaraldehyde and treated with 0.5 % sodium tungstate in acetate buffer for 1 hour then overnight in 0.5 % sodium tungstate in 30 % ethanol before being embedded with resin [12]. The embedded Samples were then examined with a FEI Technai G2 Spirit BioTWIN Transmission Electron Microscope (Czech Republic).

2.6 Lipid, carbohydrate, glycosaminoglycan, amino acid, and crosslink analysis

Lipids, including phospholipids, triglycerides, diglycerides, monoglycerides, sterols, sterol esters, free fatty acids, and others, were extracted from skin samples using the Folch method and analyzed on thin chromatography using three different stains [12, 13]. Glycosaminoglycans in skin samples were determined using the Blyscan Sulfated Glycosaminoglycan Assay Kit (Biocolor Ltd., Carrickfergus, Co Antrim, United Kingdom). Measurement of carbohydrate was carried out using the phenol-sulfuric acid method [14]. Amino acids and crosslinks in skin and hide were analyzed using our previously published method [15, 16].

3 Results and discussion

3.1 Thickness, tear and tensile strength of deer skin and cow hide

Thickness, tear and tensile strength of deer skin and cow hide are listed in table 1. There is a significant difference in the thickness of deer skin and cow hide with a thickness of 1.6 mm and 4.6 mm respectively (table 1). On the other hand, the tensile strength of deer skin and cow hide is statistically the same ($P = 0.05$). However, tear strength of deer skin of 130.1 N/mm is much lower than that of cow hide of 228.9 N/mm . We have previously reported that deer skin and cow hide showed typical stress-strain curves with the toe, heel and linear regions [7, 12]. However, we showed that deer skin had the longest toe region with the shallowest slope and cow hide had the shortest and steepest toe region.

Table 1. Thickness, tear and tensile strength of deer skin and cow hide.

Skin	Thickness (mm)	Tensile strength (N/mm ²)	Tear strength (N/mm)
Deer	1.6	28.3	130.1
Cow	4.6	29.2	228.9

3.2 SAXS of deer skin and cow hide

We have previously optimized the experimental conditions to obtain an x-ray scattering pattern which represents the true fibril diameters, d-banding, and orientations in the skin and hide [5-9, 12, 17]. The sum of the diffraction rings from 2 to 6 was chosen to determine the collagen fibril diameters and d-periodicity [7]. The fibril diameter of deer skin is smaller than that of cow hide; however, both d-banding of deer skin and cow hide is the same (Table 2).

Table 2. The fibril diameter and collagen d-banding of deer skin and cow hide as determined by SAXS experiment.

	Deer skin	Cow hide
Fibril diameters (Å)	1308 (± 2.0 %)	1438 (± 5.5 %)
d-banding (Å)	650 (0.02 %)	650 (0.16 %)

3.3 Polariser light microscopy (PLM), laser scanning confocal microscopy (LSCM) and transmission electron microscopy (TEM) of deer skin and cow hide

The polariser light microscope images show that the diameters of the collagen fibers in deer skin are much smaller than those seen in cow hide (Figure 1 & 2).

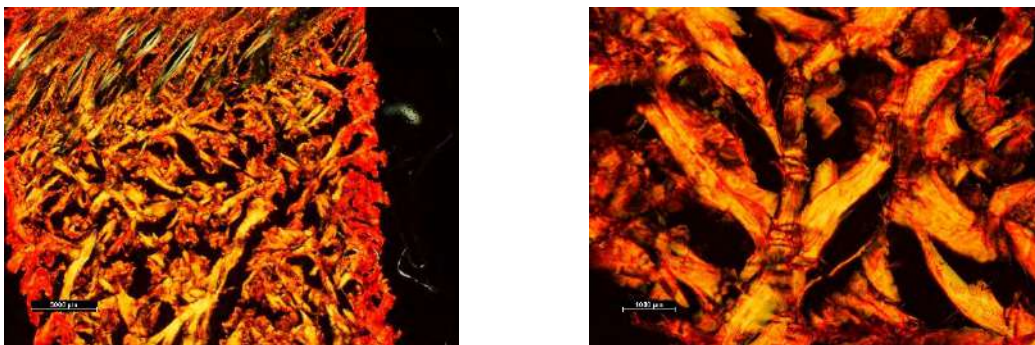


Figure 1. Polariser Light microscopy of the cow hide (scale bar 5000 µm and 1000 µm).

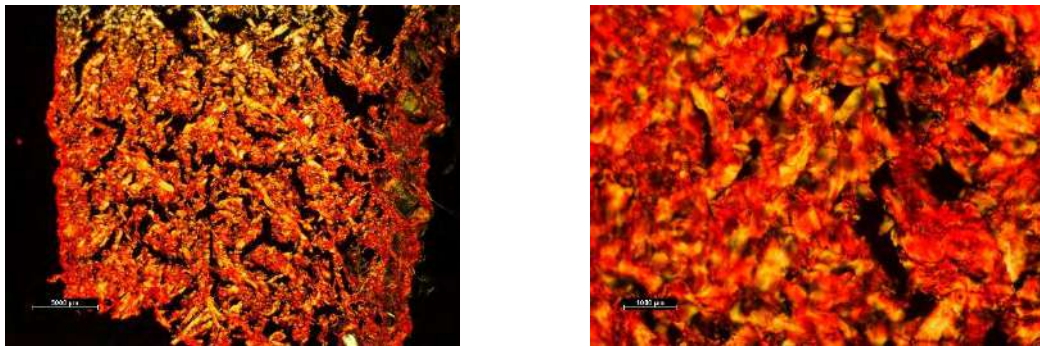


Figure 2. Polariser Light microscopy of the deer skin (scale bar 5000 µm and 1000 µm).

The images of deer skin and cow hide under the laser scanning confocal microscope show that the structural appearance of the grain layer including the organization and size of collagen fibers for both deer skin and cow hide is similar (Figure 3A & 3C). However, a significant difference is seen in the apparent collagen fiber structure in the corium layer (Figure 3B & 3D). It appears that deer skin contains collagen fibers that are smaller and wavier than those seen in cow hide.

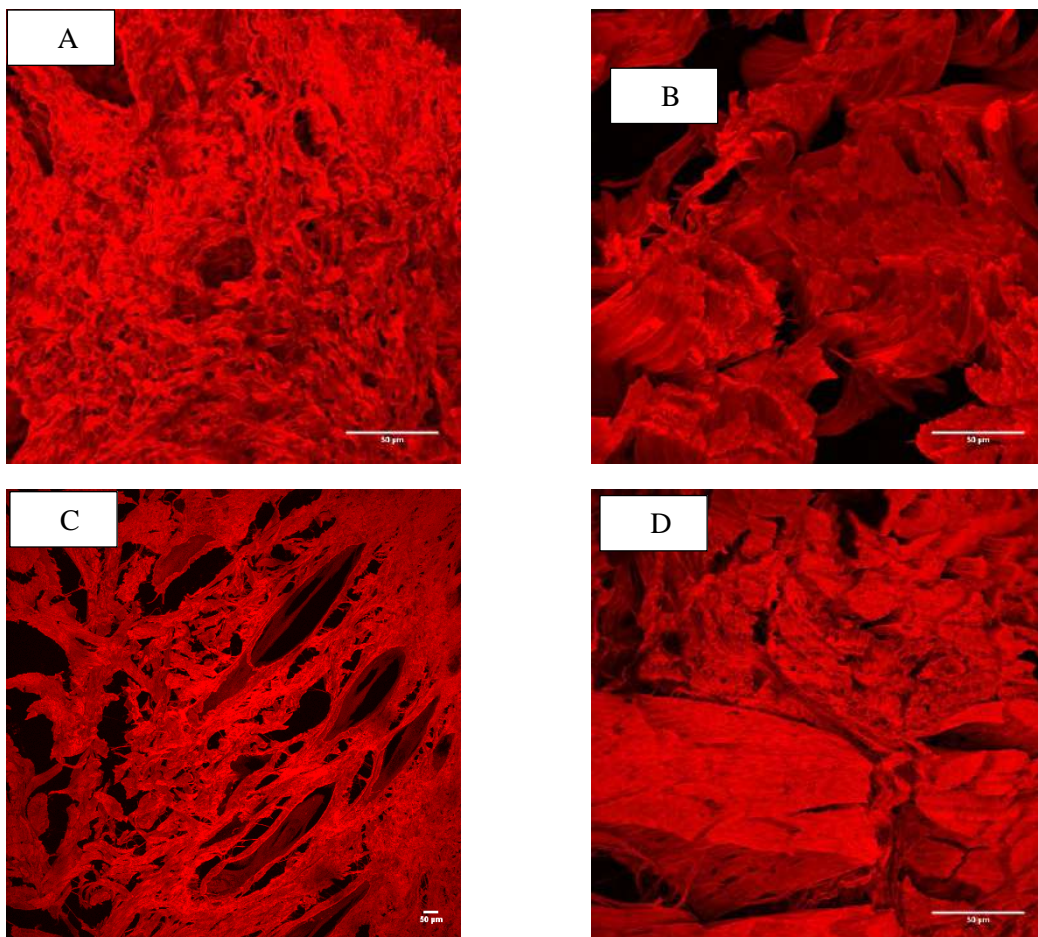


Figure 3. Laser scanning confocal microscopy (LSCM) of grain and corium layers of deer skin and cow hide. A) grain layer of deer skin, B) corium layer of deer skin, C) grain layer of cow hide and D) corium layer of cow hide.

The TEM images of deer skin and cow hides are shown in figure 4. The apparent size of the collagen fibrils of deer skin is smaller than those of cow hide. Also, the fibril bundle of collagen in deer skin appears to have fewer and smaller fibrils compared to cow hide.

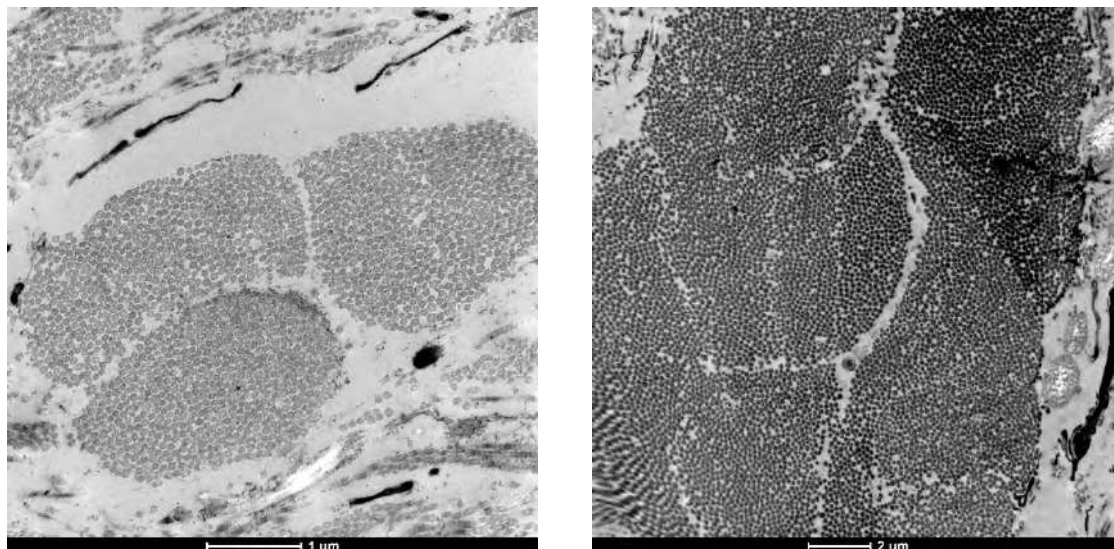


Figure 4. TEM of deer skin (Left) and cow hide (Right).

3.4 Lipid, carbohydrate, glycosaminoglycan, amino acid, and crosslink analysis

Table 3 summarises the molecular composition of deer skin and cow hide. The total protein in deer skin (88.7 %) is lower than that measured in cow hide (92.6 %), and this is associated with the lower collagen content in deer skin of (61.9 %) compared to cow hide (70.9 %). Similar to protein, the grease content in deer skin is lower than that of cow hide with 3.7 % and 5.8 % respectively. The collagen crosslinks are the same in both deer skin and cow hide which is in agreement with previous reports [7, 17]. The ratio between mature (HHL and HHMD) to immature crosslinks (HLNL and DHLNL) shows that deer skin contains a much higher ratio than cow hide

Table 3. Lipid, carbohydrate, glycosaminoglycan, amino acid; and crosslink analysis of deer skin and cow hide.

	Deer	Cow
Glycosaminoglycans % (mg/mg dry skin)	0.47 (±0.04)	0.48 (±0.05)
Total protein % in dry skin	88.7 (±8.5)	92.6 (±9.2)
Collagen % in dry skin	61.9 (±2.19)	70.9 (±1.57)
(mature crosslinks)/(immature crosslinks)	30.07	12.44
Grease content %	3.7 (7.0 %)	5.8 (5.5 %)

The analysis of the lipid profile of deer skin and cow hide using the thin layer chromatography (TLC) method shows differences (Figure 4). Deer skin appears to have a higher content of phospholipids, sterols and sterol esters than cow hide. Interestingly, deer skin does not show any spot for triglycerides, unlike cow hide which shows a clear spot (Figure 5).

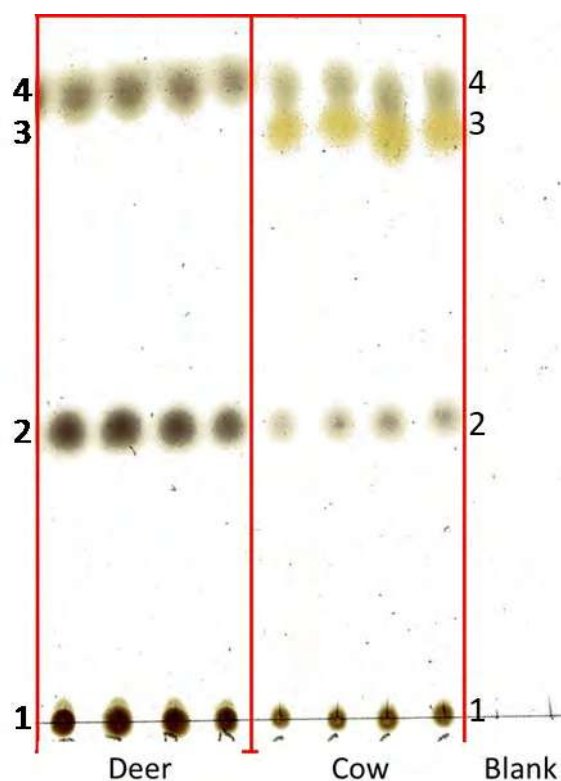


Figure 5. Cellulose TLC of total grease extracts of deer skin and cow hide. Spots 1, 2 and 3 indicate the increased application volumes of total lipid. (1) Phospholipids, (2) Sterols, (3) Triglycerides, (4) Sterol esters. The TLC plate was developed using chloroform then the plate was charred with 10 % H_2SO_4 . Spots 4 and 10 were pink before turning black. Blank is the extraction solvents without samples.

4 Conclusion

The molecular composition and collagen structure of deer skin and cow hide were measured including amino acids, collagen crosslinks, glycosaminoglycans and grease content and profile. The collagen structure was then studied using polariser light microscopy (PLM), laser scanning confocal microscopy (LSCM) and transmission electron microscopy (TEM). There was a relationship between the protein, grease and collagen content in deer skin and cow hide and their strength. The amount and profile of grease in deer skin and cow hide was different, where deer skin did not show any presence of triglycerides. Deer skin had a higher ratio of mature to immature crosslinks than cow hide. LSCM showed that collagen fibres in deer skin are smaller and wavier than those seen in cow hide. SAXS data of deer skin and cow hide indicated that both have the same d-banding however deer skin had smaller collagen fibrils while cow hide contained larger collagen fibrils. This study shows that the analysis of the molecular composition and collagen structure of the strong deer skin and strong cow hide helps us to gain a better understanding of the factors that affect physical properties, particularly strength.

5 Acknowledgement

This work was supported by the New Zealand Ministry of Business, Innovation and Employment (MBIE) through grant numbers LSRX1301 & LSRX1701. The SAXS/WAXS work was undertaken on the Australian Synchrotron beamline, part of ANSTO.

References

- [1] T. Covington, *Tanning Chemistry: The Science of Leather*, Royal Society of Chemistry, Cambridge, UK, 2009.
- [2] L.A. Goldsmith, *Biochemistry and physiology of the skin*, Oxford University Press, New York, USA, 1991.
- [3] P. Fratzl, in: P. Fratzl (Ed.) *Collagen: Structure and Mechanics*, Springer, Boston, MA, 1-13, 2008.
- [4] M. Wodzicka, *Studies on the thickness and chemical composition of the skin of sheep: I—Development techniques*, *New Zeal. J. Agr. Res.*, 1, 582-591, 1958.
- [5] Y. Zhang, B. Ingham, S. Cheong, N. Ariotti, R.D. Tilley, R. Naffa, G. Holmes, D.J. Clarke, S. Prabakar, *Real-time synchrotron SAXS studies of collagen structure during leather processing*, *Ind. Eng. Chem. Res.*, 57, 63-69, 2018.
- [6] Y. Zhang, B.W. Mansel, R. Naffa, S. Cheong, Y. Yao, G. Holmes, H.-L. Chen, S. Prabakar, *Revealing molecular level indicators of collagen stability: minimizing chrome usage in leather processing*, *ACS Sustain. Chem. Eng.*, 6, 7096-7104, 2018.
- [7] R. Naffa, C. Maidment, M. Ahn, B. Ingham, S. Hinkley, G. Norris, *Molecular and structural insights into skin collagen reveals several factors that influence its architecture*, *Int. J. Biol. Macromol.*, 128, 509-520, 2019.
- [8] Y. Zhang, T. Snow, A.J. Smith, G. Holmes, S. Prabakar, *A guide to high-efficiency chromium (III)-collagen cross-linking: Synchrotron SAXS and DSC study*, *Int. J. Biol. Macromol.*, 126, 123-129, 2019.
- [9] Y. Zhang, B. Ingham, J. Leveneur, S. Cheong, Y. Yao, D.J. Clarke, G. Holmes, J. Kennedy, S. Prabakar, *Can sodium silicates affect collagen structure during tanning? Insights from small angle X-ray scattering (SAXS) studies*, *RSC Advances*, 7, 11665-11671, 2017.
- [10] L.C.U. Junqueira, G. Bignolas, R. Brentani, *Picrosirius staining plus polarization microscopy, a specific method for collagen detection in tissue sections*, *Histochem. J.*, 11, 447-455, 1979.
- [11] B. Vogel, H. Siebert, U. Hofmann, S. Frantz, *Determination of collagen content within picrosirius red stained paraffin-embedded tissue sections using fluorescence microscopy*, *MethodsX*, 2, 124-134, 2015
- [12] R.M. Naffa, *Understanding the molecular basis of the strength differences in skins used in leather manufacture: a dissertation presented in partial fulfillment of the requirements for the degree of Doctor of Philosophy at Massey University, Palmerston North, New Zealand, Massey University, 2017.*
- [13] J. Folch, M. Lees, G. Sloane Stanley, *A simple method for the isolation and purification of total lipides from animal tissues*, *J. Biol. Chem.*, 226, 497-509, 1957.
- [14] T. Masuko, A. Minami, N. Iwasaki, T. Majima, S.-I. Nishimura, Y.C. Lee, *Carbohydrate analysis by a phenol-sulfuric acid method in microplate format*, *Analytical biochemistry*, 339, 69-72, 2005.
- [15] R. Naffa, G. Holmes, M. Ahn, D. Harding, G. Norris, *Liquid chromatography-electrospray ionization mass spectrometry for the simultaneous quantitation of collagen and elastin crosslinks*, *J. Chromatogr. A*, 1478, 60-67, 2016.
- [16] R. Naffa, S. Watanabe, W. Zhang, C. Maidment, P. Singh, P. Chamber, M.T. Matyska, J.J. Pesek, *Rapid analysis of pyridinoline and deoxypyridinoline in biological samples by liquid chromatography-mass spectrometry and silica hydride column*, *J. Sep. Sc.*, 42, 1482-1488, 2019.
- [17] R. Naffa, C. Maidment, G. Holmes, G. Norris, *Insights into the molecular composition of the skins and hides used in leather manufacture*, *J. Am. Leather Chem. As.*, 114, 29-37, 2019.

MODERN UNHAIRING TECHNOLOGIES FOR EFFECTIVE CONTROL OF H₂S RELEASE FROM BEAMHOUSE OPERATIONS

C.Gabagnou^{1a}, J. Fennen¹ and D. Herta²

1 TFL Ledertechnik AG, Rothausstrasse 61, CH-4132 Muttenz

a) catherine.gabagnou@tfl.com

b) Jens.fennen@tfl.com

c) Daniel.herta@tfl.com

Abstract. The toxicity and obnoxious smell of hydrogen sulphide (H₂S) gas is an issue for the leather industry that has been contained rather than eliminated in tannery practice. Completely eliminating H₂S from tanneries while maintaining practical and economically feasible processing is still a big challenge to be addressed. Significant progress has been made by introducing robust and reliable low sulphide unhairing systems based on selective soaking and specific enzymatic liming auxiliaries. These systems allow the reduction of sodium sulphide offers from the typical 2.5% to 1% of pelt weight. These lower levels reduce the amount of hydrogen sulphide gas released into the environment from the liming float, as well as the amount of sulphide that is carried over in the hide to subsequent processing steps. Overall, the H₂S problem is not eliminated, but significantly reduced with this technology. In a further evolution of the technology, organic thio compounds can be used to fully or partially replace the already low levels of sulphide required, and thus allow to operate with offers well below 1%, or even completely without inorganic sulphide. Alternatively to, or in combination with organic thio compounds, H₂S scavengers can be used to reduce or eliminate hydrogen sulphide released from liming floats. Different types of scavengers are available, but the selection is limited for technical and economic reasons.

1 Introduction

The tanning process aims to transform hides in stable and imputrescible products namely leather using a large amount of chemicals. The complete leather manufacturing process is divided into three fundamental stages: beamhouse, tanning and post tanning, involving each several steps.

The first step is the soaking, which in an optimal way prepares the hide for the liming-unhairing treatment, one of the most important operations in the leather making process. The purpose of liming-unhairing is not only to remove hair, but also interfibrillary components, fatty matter and epidermis and to open up fiber structure.

A conventional hair burn unhairing process uses sulphide to achieve the goal of a fairly complete hair removal. The down-side is a high effluent load caused by the high amounts of chemicals used and the complete liquefying of hair.

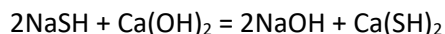
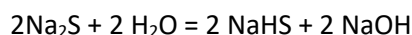
The use of sulphide for unhairing has always been problematic. It has made unhairing one of the most investigated areas over the past few decades, where the focus has been to reduce the amount of sulphur-based products, but due to a lack of a workable economic alternative, sodium sulphide and sodium hydrosulphide are still the preferred chemicals used for breaking-down the hair. It results in the effluent being highly loaded with sulphide, with the associated risk of hydrogen sulphide emission from the effluent when the pH drops below 9.5.

This paper on hand shows how the release of hydrogen sulphide from beamhouse operations can be effectively controlled by a combination of technologies involving more effective unhairing with lower amounts of reductive agents, replacement of inorganic sulphide by an organic thio compound and the use of an appropriate H₂S scavenger.

2 Background

2.1 Unhairing effect of sodium sulphide

The traditional reductive liming process employs sodium sulphide in alkaline medium. Sodium sulphide is an effective and economic unhairing agent. The unhairing effect of sodium sulphide is at its maximum when SH^- and OH^- ions in the solution are present in equal quantities:



Covington has calculated the theoretical required amount of sodium sulphide of industrial grade (60-70%) for a hair burn process to be just 0.6%, relative to hide weight. In practice, the typical amounts employed for a reliable process are much higher, namely 2-3%. The main reason for this is the fact that the rate of unhairing depends on the concentration of sulphide ions (S^{2-}) in the float. Short floats are commonly used to obtain a high concentration of sulphide allowing an easy access of active process chemicals (e.g. lime, sulphide, enzymes etc) to the points of attack of the hair.

In a traditional hair burn process the point of attack of the hair is the keratin in the hair cortex, which is degraded by sulphide due to the breaking-down of cysteine bridges.

In the state-of-the-art hair safe process, where the keratin is protected by an immunisation step, the point of attack is mainly the protein of the hair bulb which is hydrolysed either solely due to the alkaline conditions or by proteolytic enzymes, if present. A second and equally important point of attack is the pre-keratin that is above the hair bulb; it can be degraded by proteolytic hydrolysis combined with the keratolytic effect of sulphide. (**Fig. 1**)

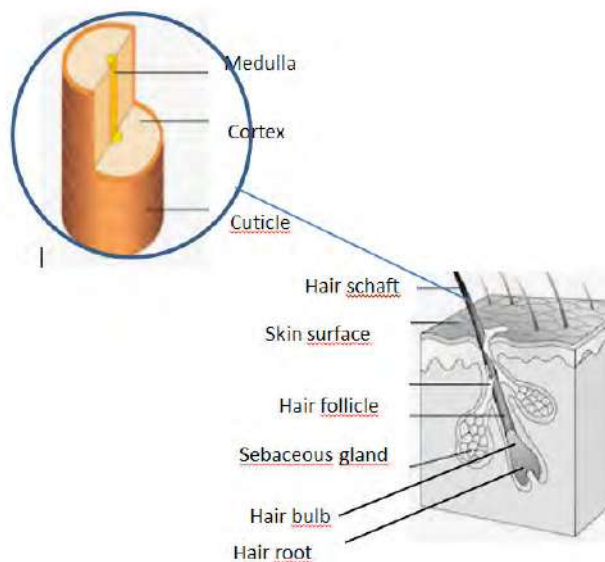


Fig. 1. Layers of the skin and hair structure.

Sodium sulphide used in the unhairing-liming step is one of the most dangerous materials applied in the leather making process. Upon acidification, solutions containing sulphide will release hydrogen sulphide gas into the working place.

Hydrogen sulphide is the reduced form of sulphur which can be formed by the reduction of sulfate (SO_4^{2-}) ions in contact with organic matter according to the following equation:



Depending on the pH of the solution, there is an equilibrium between ionic species HS^- and S^{2-} and the neutral H_2S gas as shown in the **Fig. 2** below.

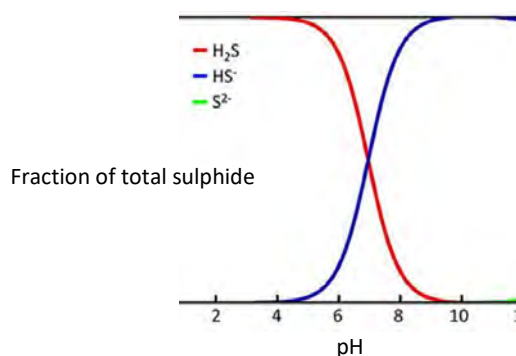
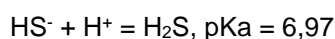


Fig. 2. Dissociation of H_2S with the pH.

2.2 Hydrogen sulphide

Hydrogen sulphide gas is an extremely hazardous gas, colourless, heavier than air, providing a strong and unpleasant odour already at low concentration.

In any tannery using sodium sulphide, the emission of low levels of hydrogen sulphide gas cannot be completely avoided, and the risk to release higher, potentially even lethal doses needs to be controlled very carefully.

Levels as low as 0.2 ppm of H_2S are already unpleasant. The effect on humans who absorb the gas through inhalation ranges from drowsiness to loss of consciousness to death, depending on how much the concentration exceeds the prescribed threshold exposure limits. At a concentration of 100 – 150 ppm the olfactory nerve is paralyzed after a few inhalations, and the sense of smell disappears, often together with the awareness of danger. At a concentration of 0.5% (5000ppm), the toxicity is so pronounced that a single breath is enough to cause immediate death within seconds.

There are legal limits for the concentration of H_2S gas at the workplace. A concentration of 15ppm over 15 minutes is internationally acknowledged as the Short Term Exposure Limit (STEL). Because sodium sulphide is such a highly toxic compound requiring safety precautions and extensive waste water treatment, the substitution of sodium sulphide by a non-hazardous alternative is a long held ambition.

The main challenge for the tanneries is to remove the hair completely with a sulphide offer of 1% or less.

The present work demonstrates the partial or total replacement of sodium sulphide by specific enzymes followed by an organic sulphur compound, matches the effectiveness of a traditional unhairing process.

Within a hair saving unhairing process, the removal of hair takes place by enzymatic hydrolysis of the soft proteins in the hair follicles, keeping the hair shaft intact. The thio compound has the capacity of cleaving the cystine molecule of the keratin protein, making it an excellent unhairing agent in its reduced form.

3 Materials and methods

3.1 Raw hide

Wet salted hides were used in the experiments. Liming experiments with thio compound were performed on a laboratory scale each with ca. 1000 g bovine hide. Formulations based on a thio compound and special additives were prepared in the lab and used as reductive agents. The concentration of the thio compound was varied over a range of 0.5 – 5.0% with 1% lime. All the chemical percentages were based on soaked weight. The unhairing efficiency for each trial was evaluated visually.

3.2 Measuring Hydrogen Sulphide

The measurement of the concentrations of hydrogen sulphide in the air were carried out with a portable hydrogen sulphide detector with a detection range of 0 - 100 ppm.

4 Results and discussion

4.1 Low sulphide enzymatic assisted unhairing

As outlined above, a hair save process requires first an immunisation step that protects the hair from degradation. This is affected by adding lime before any unhairing agents are introduced. Under the influence of the lime the cysteine of the hair is transformed into lanthionine, which can no longer be hydrolysed by reduction.

After the keratin of the hair is protected by immunization, the keratolytic effect of sulphide is directed solely at the pre-keratin above the hair bulb. This explains why, compared to a traditional hair burn process, the enzymatically assisted unhairing allows the reduction of the sulphide offer to levels of only 1% relative to hide weight on bigger bovine hides. The enzyme provides the strong proteolytic effect that is still also required, because the cells in Malpighi's layer and the basal cells of the hair bulb need to be attacked to achieve a good and consistent unhairing effect. In effect, the medulla, but not the cortex of the hair is being degraded. (Fig. 1)

The selection of specific proteolytic enzymes ensures that the collagen of the hide and particularly the grain remains undamaged throughout the process.

With the appropriate enzyme, a hair save process can be done without any compromise regarding the rate and effectiveness of unhairing or the cleanliness of the pelt as shown in the **Table 1**. The lower offer of sulphide also results in significantly reduced levels of S²⁻ in the liming float as well as in the hide. This means that later on in deliming and pickling, less H₂S will be released.

Table 1. Unhairing at different dosage of sodium sulphide.

Na ₂ S dosage (%on salted weight)	Condition of limed pelts	
	Unhairing degree	H ₂ S gas formation
2.6% in the lime float	excellent loosening of hair	pH12.6= 0ppm pH11 > 100ppm pH9 > 100ppm
1% in the lime float	excellent loosening of hair	pH12.6= 0ppm pH11= 60ppm pH9= 60ppm
0.6% in the lime float	moderate loosening of hair	pH12.6= 0ppm pH11= 25ppm pH9= 25ppm

The results from the low sulphide enzymatic assisted unhairing show a significant reduction of the main pollution parameters such as COD, TKN Nitrogen and total dissolved solids (TDS) when compared with a conventional unhairing system. However, the H₂S gas formation issue is still not completely eliminated.

4.2 Further evolution of the technology, the use of organic sulphur compounds

Organic thio compounds with high reductive potential are effective unhairing agents and can be used as replacements for inorganic sulphide. The expected advantage of the use of the thio compound is the avoidance of H₂S gas formation even at low pH. The selected thio compound was checked at different concentrations and pH values for H₂S formation, and as expected it was confirmed that no H₂S was released at any pH between 12.5 and 3 for concentrations up to 5%. The results are given in **Table 2**.

Table 2. H₂S gas formation with thio compound.

Thio compound dosage	H ₂ S gas formation (from pH 12,5 to 3,0)
5 g/l	not detectable
15g/l	not detectble
30g/l	not detectable
50g/l	not detectable

The same organic thio compound was then used in an enzymatically assisted hair save unhairing process. The soaked hides were pre-treated in the drum with lime and the thio compound. With a concentration of 3% of thio compound, very satisfactory unhairing results were obtained without any additional offer of inorganic sulphide.

The result of these unhairing trials can be found in **Table 3**. Apart from the convincing unhairing effect, it was however very surprisingly found that some low levels of H₂S were still released from the pelt when the pH was lowered during the deliming stage.

Table 3. Unhairing at different dosage of thio compound used in an enzymatically assisted hair save system.

Thio compound dosage (% base on salted weight)	Unhairing degree	scud presence	H ₂ S gas formation (from pH 12.5 to 3.0)
0.5%	no loosening of hair	present	not detectable
3.0%	very good loosening of hair	clean pelt with yellowish aspect	pH 12.5= 0ppm pH9 <15ppm pH3 < 10ppm

This apparently seems to contradict the results previously obtained with the organic thio compound alone.

To understand these results, we need to consider that the immunization of the hair against reductive hydrolyses is never complete under practical circumstances. Without a physical elimination of the hair by filtering already at the early stage of unhairing, some reductive degradation of keratin will always happen. It may be assumed that the sulphur containing degradation products are absorbed by the pelt, leading to the formation of H₂S at lower pH during deliming and pickling. The exact mechanism of this conversion still to be elucidated.

4.3 Use of H₂S scavenger

As the previously described work shows, not even the complete removal of sulphide from the unhairing steps will fully avoid the release of H₂S during subsequent operations at lower pH. An effective method to nevertheless completely suppress any release of H₂S is the use of oxidative auxiliaries during the relevant steps of the beamhouse process.

The effectiveness of the approach was demonstrated with a test performed in two steps, the first step consisting of an enzymatically assisted unhairing using an organic thio compound and the second consisting of a H₂S scavenging treatment using a formulation of oxidizing agents with additives. The unhairing results and detected H₂S gas formation are summarised in **Table 4**.

Table 4. Results of unhairing followed by H₂S scavenging.

Unhairing process	Results
hair save sulphide method	hide completely unhaird but H ₂ S gas formation
oxidative unhairing method with percarbonate	hide not completely unhaird but no H ₂ S gas formation
enzymatically assisted unhairing process with reduced sulphide and H ₂ S scavenger	hide completely unhaird with reduction of H ₂ S gas formation
enzymatically assisted unhairing process with thio compound and H ₂ S scavenger	hide completely unhaird without H ₂ S gas formation

The results indicate that the use of an enzymatically assisted unhairing process with organic thio compounds followed by an oxidative treatment step allows the full elimination of H₂S from beamhouse operations.

5 Conclusion

The objective of the study was to show that evolution of unhairing technologies allows reducing or eliminating hydrogen sulphide released from liming floats and pelts.

The suggested unhairing technology involving the use of an organic thio compound, in combination with oxidative agents with additives as H₂S scavengers in an enzymatically assisted unhairing provided the best available solution to eliminate sulphur in the liming process. The tests performed resulted in a great outcome in terms of cleanliness and complete removal of the hair without damaging the grain of the hide. The possible future studies combined with the obtained results make this process suitable for an industrial application.

The optimized low sulphide hair save liming process offers today the best possible compromise between leather quality, safety and significant reduction of the environmental impact.

References

1. Andrioli, E., Petry, L. and Gutterres, M., *Process Safety and Environmental Protection*, 2015, 93,9
2. *Tanning of Hides and Skins*, IPPC, (2013)
3. R. Spinosi, S. Zamponi, A. Bacardit and M. Berrettoni, *Oxidative Unhairing versus Sulphide Use – A critical comparison*, 2017, 102, 27
4. A.M.S, Kamal, Y. Nomura, Y. Ishii and K. Shirai, *Properties of Bovine hair Keratins solubilized with thioglycolate*, *J.Amer.Leather Chem.Ass.*, vol. 93, pp. 272-282, 1998
5. A. Masal, J.M. Morera, E. Bartoli and M. Borrás, *Study on an unhairing process with hydrogen peroxide and Amines*, *J.Amer. Leather Chem. Ass.*, 95: pp. 1-10, 200

6. A.D. Covington and T. Covington, *Tanning Chemistry: The science of leather*, Cambridge, UK, Royal Society of Chemistry, pp. 112-153, 2009
7. D.W. Nazer, RM. Al-Sa'ed and MA. Siebel, *Reducing the environmental impact of the unhairing-liming process in the leather tanning industry*, *J. of Cleaner Production* 14 (2006) 65-74
8. J. Fennen, D. Herta, JT. Pelckmans and J. Christner, *Improved Leather Quality using less Sulphide*, *J. Leather International*, January, 2014

INVESTIGATION ON VOC CONTENT FROM CAR INTERIOR FINISHING SYSTEMS AND ITS INFLUENCE ON LEATHER PERFORMANCES

R. Pasquale^{1b}, D. Cisco¹, T. Pellegrini^{1a}

¹ GSC GROUP SPA via dell'Industria 5 Montebello Vicentino (VI) 36054 ITAL

corresponding author: a) tomasopellegrini@gscspa.it, b) riccardopasquale@gscspa.it

Abstract. Car industry is highly demanding for low emission parameters and despite remarkable results have been achieved since the last decade, the requests are day by day more sophisticated. The focus on emission is a severe task and requires the investigation on emissions on a full-range perspective and involves the expertise of multi and inter disciplinary competences. This investigation demonstrated that silicon-based compounds were the most important part of the car-interior emissions, which were also responsible for remarkable leather physical performances. However, these compounds contribute to less sustainable emissions, due to the intrinsic hazardless (SVHC substances) and volatility. In this context, this research has focused on the study of novel finishing formulation aiming to overcome the impact of the high emission contribution from the silicon-based compounds and to maintain/improve the leather performances.

Keywords: automotive industry, air quality, VOC, leather performances, sustainability.

1 Introduction

The 2019 Car Industry is currently looking at of the most explosive change and developments in this area: automated driving, sharing economy/transportation, artificial intelligence, industry 4.0, connectivity, electric vehicles are some of the hot topics that this industrial sector is facing, and which are bringing innovation and new technological developments. In addition, the meaning of transportation is also changing, thus urging the re-evaluation of the construction/design of the vehicles: such amendments will pose attention on safety, seating and interior functionality and in a general way to all the vehicle architecture. Sustainability will then be taken as a principle for the architecture of the new vehicles. The new car-industry will also focus on environmental impact of the design, construction and development of the vehicle; which mean that all the materials involved in these actions must meet the same concerns/requirements (ADIANT, 2018).

The leather industry is a clear key ring for car interior suppliers and it is also focusing on more sustainable processes and reducing the emission of pollutants to the environment, prompting the commitment of leather suppliers, tanneries, and chemical auxiliaries' producers. From our perspective, in fact, one of the major problems that car interior producers are currently facing is the production of low-emitting leather, which requires special chemical auxiliaries to be achieved. At a glance, the concept of emission must be applied to any discharged substance from one to another environment: each substance has a vapour tension which tells how difficult is its release from the source to the external environment. The car-industry considers the emissions due to combustion engine (i.e. CO₂, NO_x etc), or other power sources, but also the emissions derived from the manufacture of the vehicle and all the material which are part of it. Thus, leather is definitely included as a source and contribution (Drive Sustainability, Responsible Minerals Initiative, The Dragonfly Initiative, 2018).

In this context, our research has focused on the study of volatile organic compounds VOC substances from car interiors, in particular on finishing systems, aiming at their reduction without losing the original performances of the finished leather articles. It is important to underline that the quality and quantity of such emissions influence the quality of the environment, especially if the emission is made of pollutants, or hazardless substances.

Previous study from Feduruk and Kergent showed that the pattern and magnitude of the emissions is influenced by temperature and air turnover, thus suggesting that the static determinations were higher in volatile content than the dynamic analyses (Feduruk & Brent, 2013). VOCs are organic chemicals that have a high vapor pressure at ordinary room temperature, which include large numbers of molecules that evaporate or sublime from the liquid or solid form of the compound and enter the surrounding air. VOC classification is therefore based on the boiling point of the substances, which are summarised in **Table 1**.

Table 1. VOC classification with respect to boiling point of the substances.

Boiling Point (Bp, °C)	Name	Example
< 50	VVOC Very Volatile Organic Compounds	Formaldehyde, Acetaldehyde
50 < Bp < 260	VOC Volatile Organic Compounds	BTEX (Toluene, xylene etc)
> 260	SVOC Semi-Volatile Organic Compounds	Phthalates
> 400	Particulate Organic Matter	PCB (Polychlorinated biphenyl)

Table 2. methods developed for VOC and FOG analyses.

Method	Name	Principle	Unit of Measure
ISO 17071	Fogging Test	Evaporation followed by condensation on cooled surface (R o G)	mg or %
VDA 275	Aldehydes/ketones Emission	Evaporation followed by water absorption; colorimetric analysis of water	mg/kg
ISO 17226-1	Chemical determination of formaldehyde content from leather	Evaporation followed by water absorption; HPLC analysis	mg/kg
VDA 276	BMW Summer test (GS 97014—3), Toyota Test	Active air sampling of specimen from thermostatic chamber	ug/m ³ or ug/m ³ per m ²
VDA 277	VOC Determination	Static headspace analysis	mg/kg
VDA 278	VOC FOG Determination	Dynamic headspace analysis	mg/kg
ISO 16000	Blue Angel	Active air sampling of specimen from thermostatic chamber	ug/m ³
ISO 12219	Interior air of road vehicles	Active air sampling of specimen from thermostatic chamber	ug/m ³

Faber (Faber, Brodzik, Gołda-Kopek, & Łomankiewicz, 2013) *et al.* identified VOCs from car-interior into three main group of compounds (aliphatic, aromatic, and cycloalkanes), along with other compounds which belonged to hydrocarbons family. Their investigation also showed that the observed differences in VOC content could directly be related to the equipment and the materials used to finish the interior. Since 2013, our R&D collected a series of analytical data with respect to the evaluation of the leather emissions: different methodologies were used, although most of them were based using heating to pull out from the sample the emitted substances, and gas chromatography as the analytical technique for the analysis of the emission. It is therefore necessary to underline that different substances can be extracted at different temperatures with the respect to the same sample (temperature and time), to produce different results in terms of

emission; for this reason, the methods developed in order to analyse the emissions from such samples took into account of the heating conditions, the vessel where the thermal conditioning was carried out and sampling of the volatiles (see **Table 2**). An outline of these results showed that four classes of substances contributed to these emissions: organic solvents, silane-based substances, small molecular weight substances (MW < 150) and fatty substances (see **Table 3**). The silicon based compounds were the most effective in terms of magnitude with respect to the emitted VOC, and their contribution was remarkable. In addition, the same silicon-based compounds were responsible for the finishing effect; thus, it was necessary to investigate on their role and impact on the emission and finishing performance since their application could affect the final leather properties. **Table 4** summarises the most representative results for the VOC determination from finished and intermediate leather with adaptation of ISO 12219-4; the tests were performed on car-interior leather.

Our investigation focused on full grain finished leathers, evaluating the contribution to the VOC emission from crust leather to the finished articles.

Table 3. List of most recurrent substances found from emission analysis throughout previous investigation.

SUBSTANCE	CAS NO	DESCRIPTION	NOTES
Acetaldehyde	75-07-0	Aldehyde/Ketone	
Acetone	67-67-1	Aldehyde/Ketone	
DIBK	108-83-8	Aldehyde/Ketone	
Formaldehyde	50-00-0	Aldehyde/Ketone	
Heptanal	111-71-7	Aldehyde/Ketone	
Hexanal	66-25-1	Aldehyde/Ketone	
Nonanal	124-19-6	Aldehyde/Ketone	Side product generated upon heating the leather.
NEP	2684-91-4	Distending agent/leveller	
NMP	872-50-4	Distending agent/leveller	
Butyl Digol		Glycol	
DPGME	34590-94-8	Glycol	Residue as solvent for PU dispersion; highly impacting towards the emission
PGMEA	108-65-6	Glycol	
Propyleneglycol Monomethyl Ether		Glycol	
C18-OMe Ester	84988-79-4	Hydrocarbon	
Decane	124-18-5	Hydrocarbon	
Dodecane-1-phenyl	120-01-3	Hydrocarbon	
Undecane	1120-21-4	Hydrocarbon	
CS ₂	75-10-0	N.D.	
Triethylamine	121-44-8	Organic Amine	Neutralising agent for PU dispersion.
2-Hexyl-1-Octanol	19780-79-1	Raw Material	Used in fatliquoring
Ethylhexanol	104-76-7	Raw Material	Used in fatliquoring
Bis(trimethylsilyl) Oxide	107-46-0	Silane Derivative	
D4-Silane		Silane Derivative	

D6-Silane		Silane Derivative	
Siloxane		Silane Derivative	
Trimethylsilanol	1066-40-6	Silane Derivative	1-5% of the emission, 200-500 ppm as a constant with respect to the sample
Isobutanol	78-83-1	Solvent	
Propylene Carbonate	108-32-7	Solvent	Residue and part of finishing auxiliaries.
Pyridine	110-86-1	Solvent	Side product generated upon heating the leather.
Ethyl Benzene	100-41-4	Solvent BTEX	
Toluene	108-88-3	Solvent BTEX	
Xylene	1330-20-7	Solvent BTEX	
Ethylhexyl Acetate	103-09-3	Solvent for finishing auxiliaries	

Table 4. Most relevant examples for VOC determination via adaptation of ISO 12219-4.

ENTRY	FORM-ALDEHYDE (ug/m3)	ACET-ALDEHYDE (ug/m3)	VOC (ug/m3)	BTEX	SILYL-ETHERS	SOL-VENTS	UN-KNOWN
Finished leather-01	N.D.	1.18	947.00	N	Y	Y	Y
Finished leather-02	N.D.	3.40	2960.00	N	Y	Y	Y
Finished leather-03	N.D.	4.83	25508.00	N	Y	Y	Y
Finished leather-04	0.78	22.06	7711.00	N	Y	Y	Y
Finished leather-05	N.D.	12.32	106791.00	Y	Y	Y	N
Finished leather-06	4.22	0.95	153319.00	N	Y	Y	Y
Finished leather-07	2.20	11.15	2887.00	N	Y	Y	Y
Finished leather-08	2.21	34.60					
Finished leather-09	1.91	38.75					
Intermediate-01	N.D.	N.D.	7.95	Y	Y	Y	Y
Intermediate-02	N.D.	23.29	14.76	Y	Y	Y	Y

2 Materials and Methods

Commercially available chemicals were purchased from *Aldrich*, *Fluka*, *Acros* and *Alfa Aesar* and used as received, unless stated.

Liquid chromatography was used for quantification of aldehydes and ketones if required prior derivatisation with dinitrophenyl hydrazine (DNPH) and was carried out on a *Perkin Elmer ALTUS A-*

10, equipped with a C18 COLUMN 5 (150 x 4.6 mm) from Perkin Elmer and using diode-array detector (DAD). Eventually, the quantification was carried out prior chemical desorption with acetonitrile from special designed cartridges DNPB TUBE JUMBO purchased from Aquaria for air-quality analysis.

Analytical gas chromatography was performed on a CLARUS 580 instrument from Perkin Elmer with a SQ8 S detector (EI) using an ELITE-624 MS capillary column (30 mt x 0.25 mm i.d.) and hydrogen as carrier gas. Static headspace analyses were carried out using a TURBOMATRIX HS 40 TRAP from Perkin Elmer, using hydrogen as carrier gas. Analytical gas chromatography was also carried out on a CLARUS 400 instrument from Perkin Elmer using a FID detector for the quantitative determination of the volatiles prior chemical desorption with carbon disulphide (CS₂) from special designed cartridges CARBON TUBE JUMBO purchased from Aquaria. The chromatography was carried out using nitrogen as carrier gas and an ELITE-624 (30 mt x 0.25 mm i.d.) as column.

The leather samples evaluated throughout this investigation were from different countries of origin and from different manufactures. It is noteworthy that this is a typical case scenario which occurs every day in most of the tanneries, and which is affected by strong differences from one to another sample within the same batch. Thus, to reduce such differences due to the raw material, it was decided to carry out the investigation on specially designed paper as substrate, which normalized any potential difference of matrixes; these papers were the BYKO-CHARTS DRAWDOWN CARDS purchased from BYK. However, investigation on leather was also carried out and has been considered of crucial importance. The application of the auxiliaries was carried out using a BYKO-DRIVE AUTO APPLICATOR 2122 from BYK and the appropriate spiral-bar coater, followed by drying *via* forced air oven at 105°C (UF 55 from Memmert).

The leather auxiliaries involved in the project implementation were provided and produced by GSC Group spa and used its facility; no commercial names and/or trademarks are reported in the description, but generic names adapted for the investigation. These products included PREGOUND, GROUND, INTERMEDIATE FOR EMBOSsing, BASECOAT, TOPCOAT and SILICONE auxiliaries; for our purposes, GSC Group spa produced also the corresponding LOW VOC versions of the abovementioned products.

2.1 General Procedure for the Preparation of the Novel Finished Samples

In order to verify the emission of the substrates treated with the novel finishing system, mixtures of finishing auxiliaries were prepared according to internal company procedures and specification. The matrix was then treated with a specific sequence of the chemicals to give the final article, followed by emission evaluation and physical-mechanical testing.

After the preparation of the auxiliaries, the application was carried out using the automatic film applicator and the appropriate spiral-bar coater (25, 50 or 100 µm), followed by 2 minutes drying *via* forced air over at 105°C. Herein, the composition and the sequence of the samples are reported; for this study, the sample was identified by the code 9384 followed by a suffix which identified the step of the application.

2.1.1 Sample 0 = standard chart

Sample 0 is the reference from the chart support.

2.1.2 Sample ODA

ODA	
Demineralized water	1 Application Film 100 µm
Forced Air Drying 2' at 105 °C	

2.1.3 Sample 9384/OA

9384/OA	
Preground STD	1 Application Film 100 µm
Forced Air Drying 2' at 105 °C	

Ground STD	1 Application Film 100 µm
Forced Air Drying 2' at 105 °C	
Ground STD	1 Application Film 100 µm
Forced Air Drying 2' at 105 °C	
Intermediate for Embossing STD	1 Application Film 25 µm
Forced Air Drying 2' at 105 °C	

2.1.4 Sample 9384/0B

9384/0B	
Preground LOW VOC	1 Application Film 100 µm
Forced Air Drying 2' at 105 °C	
Ground LOW VOC	1 Application Film 100 µm
Forced Air Drying 2' at 105 °C	
Ground LOW VOC	1 Application Film 100 µm
Forced Air Drying 2' at 105 °C	
Intermediate for Embossing LOW VOC	1 Application Film 25 µm
Forced Air Drying 2' at 105 °C	

2.1.5 Sample 9384/1

9384/1	
Preground STD	1 Application Film 100 µm
Forced Air Drying 2' at 105 °C	
Ground STD	1 Application Film 100 µm
Forced Air Drying 2' at 105 °C	
Ground STD	1 Application Film 100 µm
Forced Air Drying 2' at 105 °C	
Intermediate for Embossing STD	1 Application Film 25 µm
Forced Air Drying 2' at 105 °C	
Basecoat STD	1 Application Film 50 µm
Forced Air Drying 2' at 105 °C	
Topcoat STD 0% (9384/1)	1 Application Film 50 µm
Forced Air Drying 2' at 105 °C	
Topcoat STD 0% (9384/1)	1 Application Film 50 µm
Forced Air Drying 2' at 105 °C	

2.1.6 Sample 9384/2

9384/2	
Preground STD	1 Application Film 100 µm
Forced Air Drying 2' at 105 °C	
Ground STD	1 Application Film 100 µm
Forced Air Drying 2' at 105 °C	
Ground STD	1 Application Film 100 µm
Forced Air Drying 2' at 105 °C	
Intermediate for Embossing STD	1 Application Film 25 µm
Forced Air Drying 2' at 105 °C	
Basecoat STD	1 Application Film 50 µm
Forced Air Drying 2' at 105 °C	
Topcoat STD 1% Silicone STD (9384/2)	1 Application Film 50 µm
Forced Air Drying 2' at 105 °C	
Topcoat STD 1% Silicone STD (9384/2)	1 Application Film 50 µm
Forced Air Drying 2' at 105 °C	

2.1.7 Sample 9384/3

9384/3	
Preground STD	1 Application Film 100 µm
Forced Air Drying 2' at 105 °C	
Ground STD	1 Application Film 100 µm
Forced Air Drying 2' at 105 °C	
Ground STD	1 Application Film 100 µm
Forced Air Drying 2' at 105 °C	
Intermediate for Embossing STD	1 Application Film 25 µm
Forced Air Drying 2' at 105 °C	
Basecoat STD	1 Application Film 50 µm
Forced Air Drying 2' at 105 °C	
Topcoat STD 3% Silicone STD (9384/3)	1 Application Film 50 µm
Forced Air Drying 2' at 105 °C	
Topcoat STD 3% Silicone STD (9384/3)	1 Application Film 50 µm
Forced Air Drying 2' at 105 °C	

2.1.8 Sample 9384/4

9384/4	
Preground STD	1 Application Film 100 µm
Forced Air Drying 2' at 105 °C	
Ground STD	1 Application Film 100 µm
Forced Air Drying 2' at 105 °C	
Ground STD	1 Application Film 100 µm
Forced Air Drying 2' at 105 °C	
Intermediate for Embossing STD	1 Application Film 25 µm
Forced Air Drying 2' at 105 °C	
Basecoat STD	1 Application Film 50 µm
Forced Air Drying 2' at 105 °C	
Topcoat STD 6% Silicone STD (9384/4)	1 Application Film 50 µm
Forced Air Drying 2' at 105 °C	
Topcoat STD 6% Silicone STD (9384/4)	1 Application Film 50 µm
Forced Air Drying 2' at 105 °C	

2.1.9 Sample 9384/5

9384/5	
Preground STD	1 Application Film 100 µm
Forced Air Drying 2' at 105 °C	
Ground STD	1 Application Film 100 µm
Forced Air Drying 2' at 105 °C	
Ground STD	1 Application Film 100 µm
Forced Air Drying 2' at 105 °C	
Intermediate for Embossing STD	1 Application Film 25 µm
Forced Air Drying 2' at 105 °C	
Basecoat STD	1 Application Film 50 µm
Forced Air Drying 2' at 105 °C	
Topcoat STD 0% Silicone LOW VOC (9384/5)	1 Application Film 50 µm
Forced Air Drying 2' at 105 °C	
Topcoat STD 0% Silicone LOW VOC (9384/5)	1 Application Film 50 µm
Forced Air Drying 2' at 105 °C	

2.1.10 Sample 9384/6

9384/6	
Preground STD	1 Application Film 100 µm
Forced Air Drying 2' at 105 °C	
Ground STD	1 Application Film 100 µm
Forced Air Drying 2' at 105 °C	
Ground STD	1 Application Film 100 µm
Forced Air Drying 2' at 105 °C	
Intermediate for Embossing STD	1 Application Film 25 µm
Forced Air Drying 2' at 105 °C	
Basecoat STD	1 Application Film 50 µm
Forced Air Drying 2' at 105 °C	
Topcoat STD 1% Silicone LOW VOC (9384/6)	1 Application Film 50 µm
Forced Air Drying 2' at 105 °C	
Topcoat STD 1% Silicone LOW VOC (9384/6)	1 Application Film 50 µm
Forced Air Drying 2' at 105 °C	

2.1.11 Sample 9384/7

9384/7	
Preground STD	1 Application Film 100 µm
Forced Air Drying 2' at 105 °C	
Ground STD	1 Application Film 100 µm
Forced Air Drying 2' at 105 °C	
Ground STD	1 Application Film 100 µm
Forced Air Drying 2' at 105 °C	
Intermediate for Embossing STD	1 Application Film 25 µm
Forced Air Drying 2' at 105 °C	
Basecoat STD	1 Application Film 50 µm
Forced Air Drying 2' at 105 °C	
Topcoat STD 3% Silicone LOW VOC (9384/7)	1 Application Film 50 µm
Forced Air Drying 2' at 105 °C	
Topcoat STD 3% Silicone LOW VOC (9384/7)	1 Application Film 50 µm
Forced Air Drying 2' at 105 °C	

2.1.12 Sample 9384/8

9384/8	
Preground STD	1 Application Film 100 µm
Forced Air Drying 2' at 105 °C	
Ground STD	1 Application Film 100 µm
Forced Air Drying 2' at 105 °C	
Ground STD	1 Application Film 100 µm
Forced Air Drying 2' at 105 °C	
Intermediate for Embossing STD	1 Application Film 25 µm
Forced Air Drying 2' at 105 °C	
Basecoat STD	1 Application Film 50 µm
Forced Air Drying 2' at 105 °C	
Topcoat STD 6% Silicone LOW VOC (9384/8)	1 Application Film 50 µm
Forced Air Drying 2' at 105 °C	
Topcoat STD 6% Silicone LOW VOC (9384/8)	1 Application Film 50 µm
Forced Air Drying 2' at 105 °C	

2.1.13 Sample 9384/9

9384/9	
Preground STD	1 Application Film 100 µm
Forced Air Drying 2' at 105 °C	
Ground STD	1 Application Film 100 µm
Forced Air Drying 2' at 105 °C	
Ground STD	1 Application Film 100 µm
Forced Air Drying 2' at 105 °C	
Intermediate for Embossing STD	1 Application Film 25 µm
Forced Air Drying 2' at 105 °C	
Basecoat LOW VOC	1 Application Film 50 µm
Forced Air Drying 2' at 105 °C	
Topcoat Low VOC 6% Silicone LOW VOC (9384/9)	1 Application Film 50 µm
Forced Air Drying 2' at 105 °C	
Topcoat Low VOC 6% Silicone LOW VOC (9384/9)	1 Application Film 50 µm
Forced Air Drying 2' at 105 °C	

2.1.14 Sample 9384/10

9384/10	
Preground LOW VOC	1 Application Film 100 µm
Forced Air Drying 2' at 105 °C	
Ground LOW VOC	1 Application Film 100 µm
Forced Air Drying 2' at 105 °C	
Ground LOW VOC	1 Application Film 100 µm
Forced Air Drying 2' at 105 °C	
Intermediate for Embossing LOW VOC	1 Application Film 25 µm
Forced Air Drying 2' at 105 °C	
Basecoat LOW VOC	1 Application Film 50 µm
Forced Air Drying 2' at 105 °C	
Topcoat Low VOC 0% Silicone LOW VOC (9384/10)	1 Application Film 50 µm
Forced Air Drying 2' at 105 °C	
Topcoat Low VOC 0% Silicone LOW VOC (9384/10)	1 Application Film 50 µm
Forced Air Drying 2' at 105 °C	

2.1.15 Sample 9384/11

9384/11	
Preground LOW VOC	1 Application Film 100 µm
Forced Air Drying 2' at 105 °C	
Ground LOW VOC	1 Application Film 100 µm
Forced Air Drying 2' at 105 °C	
Ground LOW VOC	1 Application Film 100 µm
Forced Air Drying 2' at 105 °C	
Intermediate for Embossing LOW VOC	1 Application Film 25 µm
Forced Air Drying 2' at 105 °C	
Basecoat LOW VOC	1 Application Film 50 µm
Forced Air Drying 2' at 105 °C	
Topcoat LOW VOC 1% Silicone LOW VOC (9384/11)	1 Application Film 50 µm
Forced Air Drying 2' at 105 °C	
Topcoat LOW VOC 1% Silicone LOW VOC (9384/11)	1 Application Film 50 µm
Forced Air Drying 2' at 105 °C	

2.1.16 Sample 9384/12

9384/12	
Preground LOW VOC	1 Application Film 100 µm
Forced Air Drying 2' at 105 °C	
Ground LOW VOC	1 Application Film 100 µm
Forced Air Drying 2' at 105 °C	
Ground LOW VOC	1 Application Film 100 µm
Forced Air Drying 2' at 105 °C	
Intermediate for Embossing LOW VOC	1 Application Film 25 µm
Forced Air Drying 2' at 105 °C	
Basecoat LOW VOC	1 Application Film 50 µm
Forced Air Drying 2' at 105 °C	
Topcoat LOW VOC 3% Silicone LOW VOC (9384/12)	1 Application Film 50 µm
Forced Air Drying 2' at 105 °C	
Topcoat LOW VOC 3% Silicone LOW VOC (9384/12)	1 Application Film 50 µm
Forced Air Drying 2' at 105 °C	

2.1.17 Sample 9384/13

9384/13	
Preground LOW VOC	1 Application Film 100 µm
Forced Air Drying 2' at 105 °C	
Ground LOW VOC	1 Application Film 100 µm
Forced Air Drying 2' at 105 °C	
Ground LOW VOC	1 Application Film 100 µm
Forced Air Drying 2' at 105 °C	
Intermediate for Embossing LOW VOC	1 Application Film 25 µm
Forced Air Drying 2' at 105 °C	
Basecoat LOW VOC	1 Application Film 50 µm
Forced Air Drying 2' at 105 °C	
Topcoat LOW VOC 6% Silicone LOW VOC (9384/13)	1 Application Film 50 µm
Forced Air Drying 2' at 105 °C	
Topcoat LOW VOC 6% Silicone LOW VOC (9384/13)	1 Application Film 50 µm
Forced Air Drying 2' at 105 °C	

2.1.18 Sample 9384/14

9384/14	
Preground LOW VOC	1 Application Film 100 µm
Forced Air Drying 2' at 105 °C	
Ground LOW VOC	1 Application Film 100 µm
Forced Air Drying 2' at 105 °C	
Ground LOW VOC	1 Application Film 100 µm
Forced Air Drying 2' at 105 °C	
Intermediate for Embossing LOW VOC	1 Application Film 25 µm
Forced Air Drying 2' at 105 °C	
Basecoat LOW VOC	1 Application Film 50 µm
Forced Air Drying 2' at 105 °C	
Topcoat LOW VOC 6% Silicone STD (9384/14)	1 Application Film 50 µm
Forced Air Drying 2' at 105 °C	
Topcoat LOW VOC 6% Silicone STD (9384/14)	1 Application Film 50 µm
Forced Air Drying 2' at 105 °C	

Table 5. Application for 9384 samples.

	9384/1	9384/2	9384/3	9384/4	9384/5	9384/6	9384/7	9384/8	9384/9	9384/10	9384/11	9384/12	9384/13	9384/14
Preground	1X	-	-	-	-	-								
Preground stripped	-	-	-	-	-	-	-	-	-	1X	1X	1X	1X	1X
Ground	2X	-	-	-	-	-								
Ground Stripped	-	-	-	-	-	-	-	-	-	2X	2X	2X	2X	2X
Intermediate for Embossing	1X	-	-	-	-	-								
Intermediate for Embossing Stripped	-	-	-	-	-	-	-	-	-	1X	1X	1X	1X	1X
Embossed by Rotopress6 m/min; 150 atm; 90 °C; Sandblasted														
Basecoat	1X	1X	1X	1X	-	-	-	-	-	-	-	-	-	-
Basecoat Stripped	-	-	-	-	1X	1X	1X	1X	1X	1X	1X	1X	1X	1X
Topcoat 0	2X	-	-	-	2X	-	-	-	-	-	-	-	-	-
Basecoat Low VOC 0	-	-	-	-	-	-	-	-	-	2X	-	-	-	-
Topcoat 1 %	-	2X	-	-	-	-	-	-	-	-	-	-	-	-
Topcoat 1 % sil Stripped	-	-	-	-	-	2X	-	-	-	-	-	-	-	-
Basecoat Low VOC 1 % Stripped	-	-	-	-	-	-	-	-	-	-	2X	-	-	-
Topcoat 3 %	-	-	2X	-	-	-	-	-	-	-	-	-	-	-
Topcoat 3 % sil Stripped	-	-	-	-	-	-	2X	-	-	-	-	-	-	-
Basecoat Low VOC 3 % Stripped	-	-	-	-	-	-	-	-	-	-	-	2X	-	-
Topcoat 6 %	-	-	-	2X	-	-	-	-	-	-	-	-	-	-
Topcoat 6 % sil Stripped	-	-	-	-	-	-	-	2X	-	-	-	-	-	-
Basecoat Low VOC 6 % stripped	-	-	-	-	-	-	-	-	2X	-	-	-	2X	-
Basecoat Low VOC 6 % Silicone	-	-	-	-	-	-	-	-	-	-	-	-	-	2X
Basecoat Low VOC 8 % stripped	-	-	-	-	-	-	-	-	-	-	-	-	-	-

2.2 General Procedure for the Analysis of the Leather Emission

As a general rule, the sample (i.e. leather or paper) was placed into an appropriate sealed container and heated, in order to saturate the inner atmosphere with its volatiles. Then, at specific timing, an aliquot of the volatile part was analysed by chromatography in order to determine the nature and the amount of the volatiles (qualitative and quantitative analyses). The techniques and methods involved in air quality analyses for the samples are briefly herein described. VOCs can be therefore defined according to the method used for their determination according to **Table 6**
Verweisquelle konnte nicht gefunden werden..

Table 6. VOC classification according to analytical methods used throughout the investigation.

Method	VOC Quantification	Extraction Conditions
VDA 277	All peaks from GC trace	5h @ 120°C
ISO 12219	All peaks from GC trace	1h @ 65°C (variant #4 small chamber)

2.2.1 Emission Evaluations via VDA 277

This method provided information of the emission of organic compounds using static headspace analysis combined with GC-MS analysis using a 2 g sample placed into a glass vial prior heating at 120°C for 5 hours. In such way, the most volatile compounds saturated the inner atmosphere of the vial, establishing an equilibrium with the same compounds to be released from the sample; however, in this case, the presence of high volatile compounds influenced the composition of the volatiles, since they were enriched of the more volatile derivatives, whilst the less volatile would have been kept from the matrix. The results are converted to acetone carbon (used as external standard) and expressed as µg C/g sample.

Table 7. Results for VOC emission according to VDA 277 test method.

Entry	Description	VOC (µgC/g)
ZERO-01	Chart	-
ZERO-DA	Chart After Washing	-
9384/0A	Intermediate for Embossing STD	73.19
9384/1	Silicon STD	23.08
9384/2	Silicon STD 1%	3.25
9384/3	Silicon STD 3%	14.31
9384/4	Silicon STD 6%	25.42
9384/5	Topcoat STD	29.57
9384/6	Topcoat STD + Stripped Silicone 1%	24.03
9384/7	Topcoat STD + Stripped Silicone 3%	23.17
9384/8	Topcoat STD + Stripped Silicone 6%	44.88
9384/9	Basecoat + Stripped Silicone 6%	40.93
9384/10	Topcoat Low VOC	19.09
9384/11	Topcoat Low VOC + Stripped Silicone 1%	9.18
9384/12	Topcoat Low VOC + Stripped Silicone 3%	28.99
9384/13	Topcoat Low VOC + Stripped Silicone 6%	19.49
9384/14	Low VOC Auxiliaries + STD Silicone 6%	52.42

2.2.2 Emission Evaluation via ISO 12219-4 (Small Chamber Test)

This method allowed the qualitative and quantitative determination of the emission of volatile species from samples heated at 65°C for 5 hours, under a constant purified air stream and sampling at specific timing. The samples were conditioned for approximately 10 days at 25°C, 50% R.U. In this case, no static headspace analysis was performed, but the continuous air sampling from the sample placed into a stainless-steel chamber in which purified air was streamed continuously. The airstream was passed into special cartridges in order to concentrate the analytes emitted (the choice of the cartridges depended on the kind of species to be analysed), and was also force upon gentle vacuum which provided continuous and constant air flow. For this investigation, *CARBON TUBE JUMBO* cartridges were used for the volatile VOC analyses and *DNPH TUBE JUMBO* cartridges were used for the aldehydes and ketone analyse. This is a major difference compared to static headspace analysis, since it allows to continuously sample and analyse all the chemicals emitted from the sample at a certain temperature, and their emission is not influenced by the presence of the most volatile species since purified air is continuously purged into the chamber. It is noteworthy that due to the high dimensions of the stainless-steel chamber and the corresponding oven required for the constant heating, a reduced dimension chamber was used for the investigation, particularly for the preliminary study of the VOCs emission. The smaller chamber was built considering the correct ratio of sample area /chamber dimension/air reported in the method ISO 12219-4; for our purposes, the chamber was of approximately 192 litres volume.

2.2.3 Emission Evaluation via GS 97014-3 (BMW Summer Test)

This method is very close to the ISO 12219-4, although it required more stringent conditions; the testing conditions also refer to ISO the sample was heated at 65°C for 5 hours and at 105°C for additional 3 hours.

A component is placed into an approximately ideally intermixed 0.24 m³ or 0.98 m³ test room and stored there at the prescribed temperature, humidity and air exchange rate. Organic substances that escape from the component accumulate in the test room and are discharged by means of the exhaust flow. Due to the high dimensions of the stainless-steel chamber and the corresponding oven required for the constant heating, a reduced dimension chamber was used for the investigation.

2.3 Physical and Mechanical Testings

The quality of the leather was also assessed and characterised through standard automotive tests such as stick-slip, abrasion trials with Taber tester and Martindale machine, ball plate method, fogging test; rub fastness provided with Veslic tester (wet, dry, alcohol, gasoline), dry-rubbing trial with Gakushin tester. For this study, the physical and mechanical tests for stick-slip, abrasion and rub-fastness are reported.

2.3.1 Wet-Rubbing Test

Wet rubbing tests were performed with *Veslic Giuliani IG/10/MOD*, following the guidelines of ISO 11640. Before the specimen preparation, the materials were stored for at least 24 h under normal climate conditions (temperature 23 +/- 2°C, humidity: 50 +/- 5% relative humidity).

The sample size for the wet rubbing test was 100 mm x 50 mm.

2.3.2 Stick-slip test VDA 230-206

This test method is meant for determining the stick-slip tendency of material pairs. The measurements were carried out using a *STICK-SLIP TESTER* from Ziegler.

The sliding carriage with the material specimen A is moved relative to a spring element (short steel spring) against the material specimen B. The force with which the material specimens are pressed against each other as well as the speed of the sliding carriage are given.

The spring's movement behaviour which is created during the change between adhesion and slipping (stick-slip effect) is a measurement of the stick-slip tendency according to VDA 230-206. Before the specimen preparation, the materials were stored for at least 24 h under normal climate conditions (temperature 23 +/- 2°C, humidity: 50 +/- 5% relative humidity). The sample size for the spring was 50 mm x at least 20 mm; the sample size for the sliding carriage was 100 mm x 50mm, preferably using a punching process. Measurements are done during three periods with the results averaged to a total result. Each measurement must be done on two specimens in order to confirm the test results.

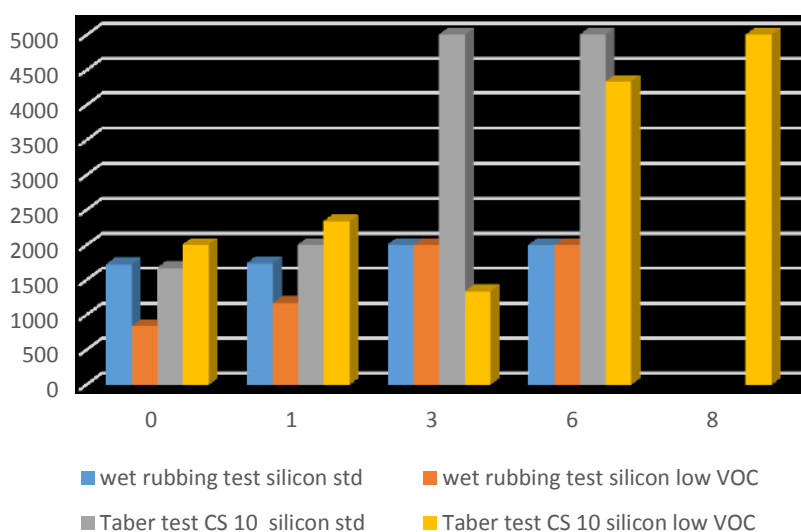


Figure 1. Physical performances comparison between standard silicon and low emitting derivative.

3 Results and Discussion

Our preliminary study showed that silicon compounds family brought an important contribution to the emission from a qualitative and quantitative perspective: these substances play a crucial role in terms of the final article performances (such as resistance), and quality.

From the preliminary results, it was therefore decided to compare two set of finishing auxiliaries: from one side the standard finishing chemicals, whilst from the other a novel series of auxiliaries designed for low VOC contribution. High performances leather with respect to abrasion resistance and wet rub-fastness require the utilisation of high quantities of silicone; as a consequence, the increase of such compounds is related to an increase VOC value.

So, our investigation focused on innovative low emitting silicones to give low contribution to the emissions the leather compared with the same performances of the original silicon containing finishing (see 2.1 and Table 5). The gradual increase in standard silicon content showed an increase in VOC emission, as expected (Table 7), whilst in the case of low-emitting silicones the VOC values are less than the respective counterparts. It is remarkable that the low-emitting derivatives showed equal wet rub-fastness performances (Figure 1), but they lacked in abrasion resistance; in order to obtain satisfactory results it was necessary to use 8% of low-emitting silicones in the formulation,

whilst only 6% was required for the standard derivative. It was also noted that the low VOC formulation with 3% of STD silicone showed higher VOC content than the 6% test, but also higher than the standard preparation entries (see **Table 7** entry 9384/13). This was not explicable and unexpected; several trials were carried out, although the VOC content from VDA 277 test method was confirmed throughout the investigation.

The set of result showed that standard leather containing silicon compounds on the finishing produced high VOC emission and high-performance articles, thus contributing to VOC emission. Conversely, the novel finishing auxiliaries had low VOC emission, less quantity of silicones, yet high performance leather and therefore should be chosen from a more environmental point of view as depicted in **Figure 2**.

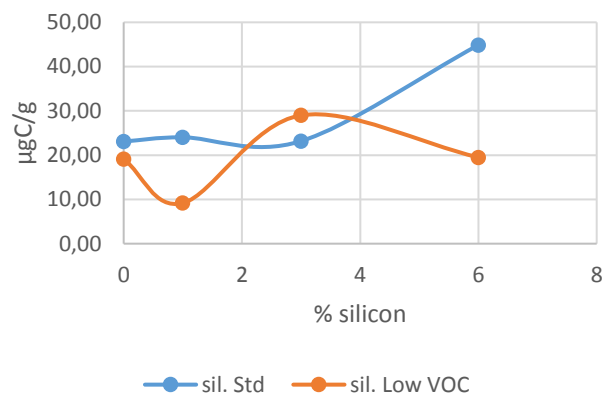


Figure 2. VOC emission according to VDA 277 for standard and low emitting silicone derivatives.

Furthermore, low emitting silicones promoted an unexpected positive effect towards the VDA 230-206 (Stick-slip test): an increase in concentration of the standard silicones usually raises the values of the VDA 230-206, which is therefore a negative effect. As depicted in **Figure 3**, in the case of the low emitting auxiliaries the effect is positive since the results did not increase.

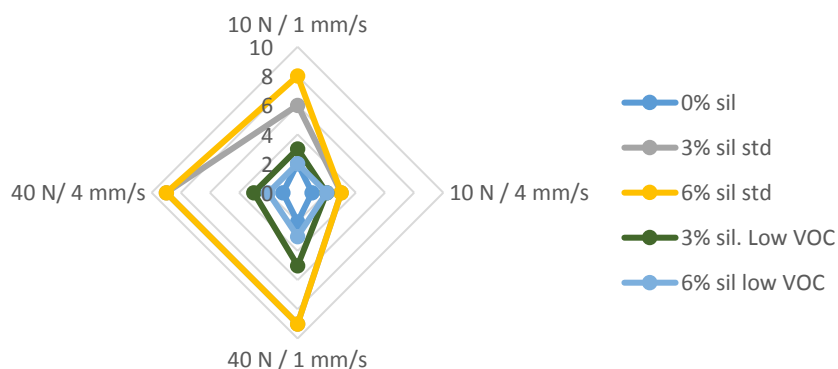


Figure 3. Stick-slip test VDA 230-206 comparison.

4 Conclusions

The major components found from the leather emissions were silane-based compounds, regardless the method used for the analysis. Taking into account the fact that some of the silanes and the organic volatiles are currently object of safety evaluation from authorities (EC), it is appropriate to make all efforts to minimize the presence of these species and their contribution to VOCs.

The silane compounds come from the finishing auxiliaries, although also from retanning; silicons can take part in fatliquor formulation as retanning agents, yet it is important to choose the correct species to ensure to provide chemicals which are in compliance with the regulations and the customers' requests. However, it was demonstrated that a free from silanes leather matrix, can be provided (LIFE GOAST), which also exhibited low to negligible emission compared to standard leather. It is therefore stressed the importance of prompting new research to alternative tanning systems to traditional chrome tanning substrates, which could lead to more sustainable and less impacting manufactures from the emission point of view.

This investigation is a proof that leather auxiliaries' producers are active part of the supply chain: if the presence of the silane-compounds from the emission could give problems in terms of emissions and safety concerns, the leather performances could not be met if they were not included in finishing auxiliaries. So, the chemical supplier is entitled of an important work, which will use inter-disciplinal competences to show that new finishing system could solve the safety issues and maintain the leather performance, without losing the final article.

5 Acknowledgments

This investigation was fully supported and sponsored by GSC Group spa, which carried out all the leather production, auxiliaries production and leather chemical and physical testing. It is therefore important to thank all the GSC Group R&D team, the analytical staff, the experimental centre and the production department. A special mention has to be given to Lorenzo Diddi, Annamaria Marangon, Elisa Zordan and Arturo Bortolati for the samples preparation and testing; this study was integrated with the analytical support of Francesco De Laurentiis, Giacomo Chiodarelli and Mariana Moretto. A special thank has to be given to all the customers and partners that since 2013 had contributed to screen and monitor the VOC emissions by using our expertise.

References

1. ADIENT. (2018, 02). *Adient - Taking automotive seating to the next level*.
2. *Drive Sustainability, Responsible Minerals Initiative, The Dragonfly Initiative*. (2018, July). MATERIAL CHANGE.
3. Faber, J., Brodzik, K., Gołda-Kopek, A., & Łomankiewicz, D. (2013). *Air Pollution in New Vehicles as a Result of VOC Emissions from Interior Materials*. *Pol. J. Environ. Stud.*, 22, 6, 1701-1709.
4. Fedoruk, M., & Brent, K. (2013). *Measurement of volatile organic compounds inside automobiles*. *Journal of Exposure Analysis and Environmental Epidemiology*, 13, 31-41.

DEVELOPMENT OF SUSTAINABLE RE-TANNING AGENTS FROM FUNGAL DEGRADATION OF LIGNOSULFONATES

Jochen Ammenn

Stahl, Benzstraße 11, 70771 Leinfelden-Echterdingen; Germany; +49 174 1878217

jochen.ammenn@stahl.com

Abstract. Lignosulfonates are abundantly available by-products of the paper industry. In the vast majority of applications on leather lignosulfonates are physically blended with other chemistries to augment filling properties of the resulting products. We targeted to decrease the molecular weight of lignosulfonates using fungi to achieve increased application possibilities and to improve tanning properties. We screened various basidiomycetes for their capability to modify the molecular weight of calcium lignosulfonates and identified five species that actually polymerized the chosen lignosulfonate further. Only *Irpex consors* was found to depolymerize calcium lignosulfonate in surface and later in liquid cultures in our hands. We achieved a six fold reduction of the molecular weight determined by size exclusion chromatography.

1 Introduction

Lignin is the second most available bio polymer in the world only exceeded in volume by cellulose. The role that this biopolymer plays in wood is to incorporate strength into the structure. In paper factories lignin is separated from water insoluble cellulose by chemical modification producing water soluble forms of lignin. A common reaction is the sulfonation of lignin with the salt of sulfurous acids to result in lignosulfonates. These by-products are dominantly burned in the paper factories to supply heat for the energy consuming process of converting cellulose into paper. Some quantities of lignosulfonates are marketed in the construction industry, in animal nutrition, as dispersers, and as fillers, also in the leather industry. There are only few chemical modifications of lignosulfonates known. Recently, Y. Ma and P. C. Berends published the incorporation of lignin into poly-condensates using phenol sulfonic acids and several aldehydes, among them glyoxal to form water soluble tanning agents (1). Biological modification of lignin or lignosulfonates are also rare. In 2005 O. Suprano, A. Covington, and C. Evans published the degradation of lignin with the enzyme heme into monomers and condensed these with formaldehyde to obtain tanning agents in lab scale quantities (2). We targeted to decrease the molecular weight of lignosulfonates using fungi to achieve increased application possibilities. As can be seen in figure 1, the structure of lignin is a rigid one due to extensive crosslinking. Most of the phenolic OH groups required for tanning are etherified within the crosslinked structure. We targeted to reduce the molecular weight of lignin to improve penetration into the interior parts of the leather on the one hand and aimed to release more phenolic OH groups to be available for interaction with collagen and improve tanning properties. While the biological details of the degradation have been published before (3), the results for the application on leathers will be presented here.

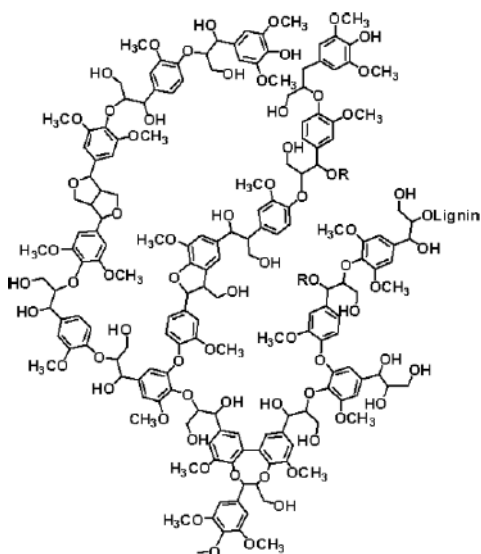


Fig. 1. Structure of lignin.

2 Materials and Methods

2.1 Screening of Fungi for the Degradation of Lignosulfonates

The biological part of the project was carried out in collaboration with the workgroup of H. Zorn at the institute of nutrition chemistry of the university of Giessen in Germany. There, various basidiomycetes were screened for their capability to modify the molecular weight of calcium lignosulfonates in two assays. The basidiomycetes used in this work were supplied from the Centraalbureau voor Schimmelcultures (CBS, Baarn, Netherlands), the Deutsche Sammlung für Mikroorganismen und Zellkulturen (DSMZ, Braunschweig, Germany), and the Friedrich Schiller University (FSU, Jena, Germany). Stock cultures of the fungi were maintained on standard nutrition solution agar plates containing agar, d-(+)-glucose, l-(-)-asparagine, yeast extract, and trace element solution. The fungi were grown in an incubator at 24°C under light exclusion. These stock culture could be stored at 4 °C. A piece of one square centimeter of the mycelium was transferred to an M200 plate for surface culture screening. For this first screening assay seventeen white-rot basidiomycetes were chosen assuring a wide spread of biodiversity. The calcium lignosulfonate served as the sole carbon and nitrogen source for the fungi to grow and was diluted to afford a 5% concentrated medium on agar plates in surface culture. During a cultivation period of four weeks thirteen fungi grew on M200 agar plates. Twelve fungi darkened the plates during growing, while only *Irpex consors* bleached the plates. In a subsequent second screening assay six fungi that had grown well in the surface culture assay were chosen and transferred to liquid cultivation including *Irpex consors*. Here a concentration of 0,5% of the lignosulfonate was applied and again only *Irpex consors* bleached the culture after a cultivation period of sixteen days. Size exclusion chromatography was employed using sulfonated polystyrene solutions ranging from 1.100 to 69.300 Dalton to determine the molecular weight distribution of the lignosulfonates. Only *Irpex consors* had decreased the molecular weight significantly while the other five basidiomycetes had increased the molecular weight. In a repeated trial with *Irpex consors* in a culture period of 56 days the molecular weight was reduced from initial 26.000 Dalton to 1.000 Dalton. Further experiments were focused on *Irpex consors*.

2.2 Upscaling of the fungal Degradation of Lignosulfonates

The upscaling procedure was a two step sequence in submerged cultures. The culture medium consisted again of agar, d-(+)-glucose, l-(-)-asparagine, yeast extract, and trace element solution and was adjusted to a pH of 6. For the pre-culture a piece of one square centimeter of the mycelium of *Irpex consors* from the stock culture was cultivated with 100 mL culture medium in a 250 mL Erlenmeyer flask after Ultra Turrax homogenization. The fungal growth proceeded for seven days under light exclusion in an incubation shaker at 24°C with 150 revolutions per minute and a deflection of 25 millimeter.

For the main culture 40 mL of the preculture was treated in 400 mL solution containing culture medium and the calcium lignosulfonate in a 1 L Erlenmeyer flask for 15 days at 24°C in an incubator with 150 revolutions per minute and a deflection of 25 millimeter. As can be seen in figure 2 the molecular weight of the calcium lignosulfonate was reduced from initial 33.000 Dalton to 5.000 Dalton. This corresponds to a six fold reduction in molecular weight. The fact that in the upscaling experiment a starting molecular weight of 33.000 Dalton was observed, while during the screening the starting weight of 26.000 Dalton was measured, might be explained with the change of samples. Nevertheless, the two calcium lignosulfonates samples came from the same paper factory.

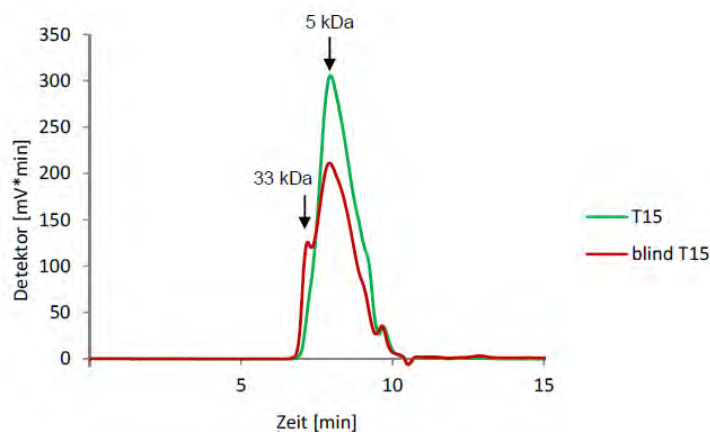


Fig. 2. Gel permeation chromatography of the degradation of calcium lignosulfonate with *Irpex consors* after 15 days (T15 = day 15)

2.3 Sole Tanning Method

The sole tanning was carried out with pickled bovine pelt with 150% pickle float and 25% tanning agent related to pelt weight at a pH of 3. The tanning agent was dosed in five portions over a period of one hour. After 24 hours the pH was raised with bicarbonate to afford leathers with a pH of 4 (4).

3 Results and Discussion

Vegetable tanning agents and synthetical tanning agents (syntans) on the basis of phenol both have phenolic OH groups that enable them to interact with collagen and expose a tanning effect that can be measured via shrinkage temperature of resulting leathers (4). Dispersing agents on the basis of naphthalene lack these phenolic OH groups and therefore have no tanning effect. In lignin most phenolic OH groups are etherified within the crosslinked rigid structure and are not available for tanning. Consequently, lignosulfonates have a weak tanning effect. Lignosulfonates have a rather large molecular weight of several thousand Daltons. A smaller molecular weight positively effects the penetration of tanning agent (5). Goal of treating lignosulfonates with fungi was twofold. Firstly, to degrade the molecular weight of lignosulfonates and hereby increase penetration performance of the resulting products. Secondly, to cleave some of the etherified phenolic OH group enabling formation of more free phenolic OH groups and enabling for an increased tanning effect. As can be seen in table 1 the degraded calcium lignosulfonate did not show any improved tanning effect compared to the starting material.

Table 1. Results of the sole tanning of bovine pelt with lignosulfonates and vegetable tanning agents

	Degraded Ca-Lignosulfonate (5 kDa)	Ca-Lignosulfonate (33 kDa)	Pelt (no tanning agent)	Tara (~ 0,6 kDa)	Mimosa (~ 0,3 kDa)
Shrinkage temperature	61°C	62°C	41°C	68°C	75°C
Leather quality	poor	poor	untanned	soft, round, full	softest, round, full

As a control the shrinkage temperature of pelt was determined to be 41°C. This reflects the stabilisation of collagen without any tanning agent. The two lignosulfonates increased the stabilization of collagen by about 20 degree Celsius, compared to untanned pelt. The leather quality of both pieces tanned with the lignosulfonates was insufficient. The leathers were hard and the tanning was in-homogenously throughout the thickness of the leathers, giving rise to superficial tanning effect on the flesh and grain side but not in the inner layers of the leather. The leather quality was especially insufficient compared to leathers tanned with widely used vegetable tanning agents like tara or mimosa, which were soft, round, full and evenly tanned, with mimosa achieving the softest leather. Major differences between the vegetable tanning agents and the two lignosulfonates are two fold. One difference is the molecular weight. Even the degraded lignosulfonate is still about fifteen times larger than mimosa. Another difference is the number of available OH groups which in lignosulfonates is lower than in vegetable tanning agents.

The degradation of the calcium lignosulfonate with Irpex consors did not change the number of OH groups significantly, as reflected in the basically unchanged shrinkage temperature of the degraded calcium lignosulfonate compared to the starting material. Another outcome of the work was the bleaching effect that Irpex consors exposed on the lignosulfonate. This could be a potential solution for the problem that lignosulfonates are rather dark in color and transfer this problem also to leather, giving rise to a brown shade. This could be overcome via bleaching of the lignosulfonate with Irpex consors and remains to be followed up.

References

1. Ma, Yujie; Behrends, Petra Conny; A method for manufacturing a Lignin-modified polyphenolic product, WO 2019 048480 A1, 24 p.
2. Suprano, O; Covington, A.; Evans, C; Kraft Lignin degradation products for tanning and dyeing of leather, J. Chem. Technol. Biotechnol., 80, 44-49, 2005.
3. Imami, Adrian; Riemer, Stefanie; Schulze, M.; Amelung, F.; Gorshkovb, V.; Rühl, M.; Ammenn, Jochen; Zorn, Holger; Depolymerization of lignosulfonates by submerged cultures of the basidiomycete Irpex consors and cloning of a putative versatile peroxidase, Enzyme and Microbio. Tech., 81, 8-15, 2015.
4. Tu, Shu-Tung; Lollar, Robert; A concept of the Mechanism of Tannage by Phenolic Substances, JALCA, 45, 324-348, 1950.
5. Ammenn, Jochen; Huebsch, Corinna; Schilling, Emil; Dannheim, Bernd; Chemistry of Syntans and their Influence on Leather Quality, JALCA, 110, 349-354, 2015.

Acknowledgements

I wish to express my gratefulness to my collaboration partner the workgroup of Holger Zorn (university of Giessen, Germany) for the screening and upscaling, to Corinna Hübsch (BASF, Ludwigshafen, Germany) and Marvin Mangler (Stahl, Leinfelden, Germany) for the application trials and to Frank Brouwer and Andre van der Ham (Stahl, Waalwijk, Netherlands) for fruitful discussions.

CHROME TANNING PROCESS AND THE LEATHER PROPERTIES UNDER MICROWAVE IRRADIATION

Jinwei Zhang^{1, 2, b}, Wuyong Chen^{1, 2, a} and Carmen Gaidau^{3, c}

1 Key Laboratory of Leather Chemistry and Engineering of Ministry of Education, SICHUAN UNIVERSITY, CHENGDU 610065, CHINA

2 National Engineering Laboratory for Clean Technology of Leather Manufacture, SICHUAN UNIVERSITY, CHENGDU 610065, CHINA

3 Leather Research Department, INCDEP-Leather and Footwear Research Institute Division, BUCHAREST 031215, ROMANIA

a) Corresponding author: wuyong.chen@163.com

b) scutanner@163.com

c) carmen_gaidau@hotmail.com

Abstract. Some studies clarified that microwave strengthened tanning effect and made the leather have better thermal stability, but influence of microwave on tanning process and leather properties have not been elaborated in detail. For illustrating the influence of microwave on chrome tanning process, pickled skin was tanned for 6h as penetration procedure and then basified for another 4h as fixation procedure. The tanning under microwave irradiation (MW) was experimental sample and under water bath heating (WB) was control. UV-Vis, pH and ICP-OES were used to measure the changes of tanning effluent and leather chrome content during tanning. Shrinkage temperature meter, DSC and TG were used to determine the differences between MW and WB on aspect of thermal stability and resistance. SEM was applied to character how microwave affected leather structure compared with conventional heating. The results indicated microwave accelerated chrome tanning agent penetration and brought about higher chrome exhaustion. The leather tanned with microwave assisting had better hydrothermal and thermal stability as well as thermal decomposition property. However, the leather structure of MW, including hierarchical structure, was same as WB. In sum, microwave had positive effect on accelerating tanning rate and resulting in better leather properties without any negative effect on leather structure. Therefore, microwave would be a potential choice for achieving clean and sustainable chrome tanning by making tanning much faster and more efficiency.

1 Introduction

Microwave is the electromagnetic wave with frequency between 300MHz and 300GHz, and the civil frequency of microwave in China is 2450MHz¹. Microwave could accelerate chemical reaction rate, promote reaction yield and make some reactions happen under milder condition rather than high temperature and high pressure. Just as the characters, microwave is widely used to assist huge amount of chemical reactions^{2,3}. The reason why microwave has positive effect on chemical reaction could be attributed to thermal effect and non-thermal effect. However, the kinetic⁴, mechanism⁵, activation energy⁶ and pre-exponential factor of reactions⁷ under microwave are changes, indicating non-thermal effect which is not relating to temperature increasing is unique effect of microwave to promote chemical reactions^{8,9}.

In leather industry, microwave is used in many procedures, such as unharing and bating¹⁰, dyeing¹¹, fatliquoring¹² and drying¹³, in which microwave promotes the chemicals penetration into leather and results in more even distribution, in addition, the combination between collagen and chemicals is strengthened by microwave also¹⁴. In tanning aspect, microwave has more significant influence on chrome tanning liquor hydrolysis and olation compared with heated by conventional method^{15,16}. For vegetable tanning liquor, microwave has positive effect on colloid stability and dispersibility¹⁷. Moreover, microwave could enhance tanning effect. When microwave was used to treat chrome well penetrated leather, the leather had higher Ts and better tear strength¹⁸. In vegetable tanning, microwave not only made leather have higher Ts but also resulted in better polyphenol exhaustion^{19,20}.

Furthermore, microwave made zirconium tanned leather have better thermal stability. These evidences suggest microwave has positive effect on tanning.

Chrome tanning contains relatively independent procedures, chrome tanning penetration and fixation, as hides or skins have certain thickness. The previous study demonstrated microwave could improve chrome tanning process and tanning effect by using hide powder²¹. However, the penetration and fixation procedures were not clear because of applying powdered tanning material. Hitherto, the influence of microwave on chrome tanning process, like tanning agent penetration rate and distribution during tanning, as well as how it affected leather properties had not been illustrated in detail. In this work, chrome tanning was undertaken with microwave heating (MW) and water bath heating (WB) respectively, and then the differences between the two samples on aspects of tanning liquor properties and chrome penetration were compared. Next, the thermal stability of leathers tanned under different heating was measured by Thermal Gravimetric Analyzer (TG) and Differential Scanning Calorimeter (DSC), and leather structure was characterized by Scanning Electron Microscope (SEM). The research would provide reference to apply microwave in chrome tanning process to achieve more effective tanning.

2 Experimental

2.1 Materials

Pickled goat skins were prepared according to conventional upper shoe leather process with thickness around 1.0mm. Chromium sulfate hexahydrate was from Shanghai Aladdin Reagents Company. Sodium bicarbonate and sodium chloride were purchased from Chengdu Kelong Chemical Ltd. Other chemicals were commercial grade for leather manufacturing and research grade for analysing.

2.2 Chrome tanning process stract

90.00±0.05 sodium chloride and 191.33±0.01g chromium sulfate hexahydrate were dissolved in 1400mL distilled water at first, then 10.714±0.002g sodium bicarbonate was dissolved in 1400mL distilled water and the solution was put in chrome solution within 30min under stirring, finally, the mixture was stirred for another 30min to obtain the chrome tanning liquor with 100g/L chromium sulfate and 33% basicity.

Pickled goat skin was cut into 2cm×6cm pieces. 140g skin pieces were tanned in a 1000mL beaker with 700mL chrome tanning liquor prepared above. The MW sample was heated by microwave at 40 °C with stirring and the WB sample was warmed by water bath heater at same condition. After 5h tanning, 1g sodium bicarbonate was added into the tanning system every one hour and repeated for 5 times. The total tanning time was 10 hours. The first 5 hours were regarded as penetration procedure and the last was fixation procedure.

The pH of both tanning liquors were measured every 1 hour by pH-3C pH meter (Shanghai Yidian Instruments Co., Ltd.), at the same time, 2mL tanning liquor was sampled for UV-Vis determination. Moreover, skins were taken out every 1hour for chrome content test and the shrinkage temperature measurements were carried out after 4h tanning and 10h tanning. The leathers were lyophilized when tanning was finished for other tests.

2.3 Testing methods

2.3.1 *Ts measurement*

The shrinkage temperature was tested by Shrinkage Temperature Tester (MSW-YD4, China) into the bath of 75% glycerine solution. Each value was an average of two tests.

2.3.2 Leather chrome content measurement

0.150±0.001g lyophilized leather was digested in a 100mL flask with 10mL nitric acid and 5mL hydrogen peroxide under boiling for 30min. After cooling down, the digested solution was dissolved in 100mL volumetric flask. The total chromium content in digestion solution was determined by Optima 8000DV Inductively Coupled Plasma Atomic Emission Spectroscopy (ICP-AES, PerkinElmer, America) following the manufacturer’s direction and then the content of Cr₂O₃ in hide powder was calculated.

2.3.3 UV-Vis determination

The tanning liquors were filtrated by using 0.22µm microporous membrane and then diluted ten times with distilled water. A UV1900 UV-Vis spectrometer (Beijing Puxi General Instruments Co., Ltd.) was used to scan the diluted solution from 350 to 650nm with the scanning rate of 120nm/min and wavelength (WL) interval of 1nm. The wavelength of the solution at about 420nm was named λ₁, and the corresponding absorbance (ABS) was named A₁. The wavelength of the solution at about 580nm was named λ₂, and the corresponding absorbance was named A₂. The R value was calculated as R=A₁/A₂.

2.3.4 DSC measurement

The dried leathers were put into Aluminium crucibles and heated by a DSC 200 PC differential scanning calorimeter (Germany) with heating rate 10 °C/min in a N₂ atmosphere (flow N₂: 100mL/min). The range of temperature was from 30 to 250 °C.

2.3.5 TG measurement

The dried samples were put into ceramic crucibles and heated by a NETZSCH TG 209 F1 thermal gravimetric analyzer (Germany) with heating rate 10 °C/min in a N₂ atmosphere (flow N₂: 100mL/min). The range of temperature was from 40 to 800 °C.

2.3.6 SEM observation

A JSM-7500F scanning electron microscope (Japan Electronic Co. Ltd., Japan) was used for observe leather cross section images by operating the SEM at low vacuum with 15kV accelerating voltage.

3 Results and discussion

3.1 Influence of microwave on chrome tanning process

Table 1. The influence of different heating method on chrome tanning process.

Time (h)	WB			MW		
	pH	R value	Cr ₂ O ₃ content (mg/kg)	pH	R value	Cr ₂ O ₃ content (mg/kg)
1	2.66	1.1856	7.96	2.64	1.1749	9.52
2	2.72	1.1970	12.16	2.70	1.1930	14.15
3	2.68	1.2015	15.84	2.65	1.1964	18.36
4	2.66	1.2038	18.26	2.62	1.2007	21.62
5	2.65	1.2044	20.02	2.62	1.2002	22.66
6	2.73	1.2119	21.62	2.70	1.2065	25.84
7	2.94	1.2392	29.79	2.89	1.2328	33.11
8	3.18	1.2595	35.23	3.16	1.2452	39.54
9	3.48	1.2981	39.56	3.44	1.2758	44.08
10	3.89	1.2942	41.88	3.83	1.2872	47.15

In Table 1, it could be found that the pH, R value of WB tanning liquors were always higher than MW under corresponding time in the whole chrome process. However, the leather Cr₂O₃ content of MW was larger than WB at same condition. Because microwave had more powerful effect on chrome complex hydrolysis and olation and resulted in lower pH, the lower pH of MW samples compared with WB indicated microwave also promoted chrome complex hydrolysis and olation¹⁶. In general, if there is bridge formed between chromium and ligands, the R value is larger than 1.19, and the more bridge the higher R value. The results of R value in Table 1 suggested that microwave might improve the combination between collagen large-size chrome complexes for causing lower R value, and the Cr₂O₃ content results also indicated same situation. Furthermore, the Cr₂O₃ content of MW always larger than WB indicated microwave promoted chrome penetration and combination during tanning. On the other hand, microwave-assisting could reduce tanning time but increase efficiency as less time was needed to achieve same chrome. In summarize, microwave had positive effect on chrome penetration and combination during tanning.

As chrome complexes and collagen were polar molecules, they were affected by microwave and generated additional movement style which had oscillation under electromagnetic field while the system under conventional heating only contained the movement caused by temperature. Therefore, molecule movement under microwave was more turbulent to benefit for chrome penetration, and higher possibility for the collision between collagen residue and chromium complex to produce better chrome exhaustion.

3.2 Influence of microwave on leather thermal stability

One of the most important tanning effects is strengthen the thermal stability of leather. In this part, the leather tanned under different heating methods was subjected DSC, TG and shrinkage temperature tests to clarify influence of microwave on chrome tanning effect. The DSC and TG results were listed in Table 2.

Table 2. The influence of different heating method on leather thermal stability.

Sample	T _d (°C)	ΔH (J/g)	T _{max} (°C)	Carbon residue (%)	T _s (°C)
WB	98.5	351.2	350.5	19.57	103.0
MW	104.8	374.9	354.7	29.58	109.3

In DSC results, higher denaturation temperature (T_d) and greater energy-consuming during denaturation (ΔH) of MW sample were obtained. They indicated the collagen conformation of leather tanned under microwave was much more stable. In TG results, the maximum decomposition temperature (T_{max}) but less weightlessness between 200 °C and 600 °C which attributed to peptide decomposition during heating and could be used to represent collagen structure stability of MW were observed; in addition, more carbon residue of MW indicated there were more unviolated substances, such as chrome, in leather and much less collagen decomposed during tanning. They illustrated microwave-assisting during tanning improved leather thermal resistance. In T_s results, the terminal T_s of MW was 6.3 °C higher than WB. Moreover, the T_s of MW after penetration (tanning 6h) was 85.6 °C while the WB at same condition was only 73.5 °C (the results were not showed in Table 2). They showed microwave not only improved cross-linking effect but also made the effect work under lower pH.

Since there were more high-positive charge and molecular-size chromium complexes, which have better affinity to collagen and contribute to cross-link mainly, in tanning liquor under microwave irradiation, the combination between collagen and chromium complexes were strengthened, in other word, the tanning effect was stronger. On the other hand, just as microwave promoted other chemical reactions obviously, the cross-linking reaction between collagen and chromium was easier to emerge and the efficiency might be higher under microwave compared with water bath heating. No matter higher chrome exhaustion or better cross-link, microwave promoted chrome tanning effect and resulted in better thermal stability of leather.

3.3 Influence of microwave on leather structure

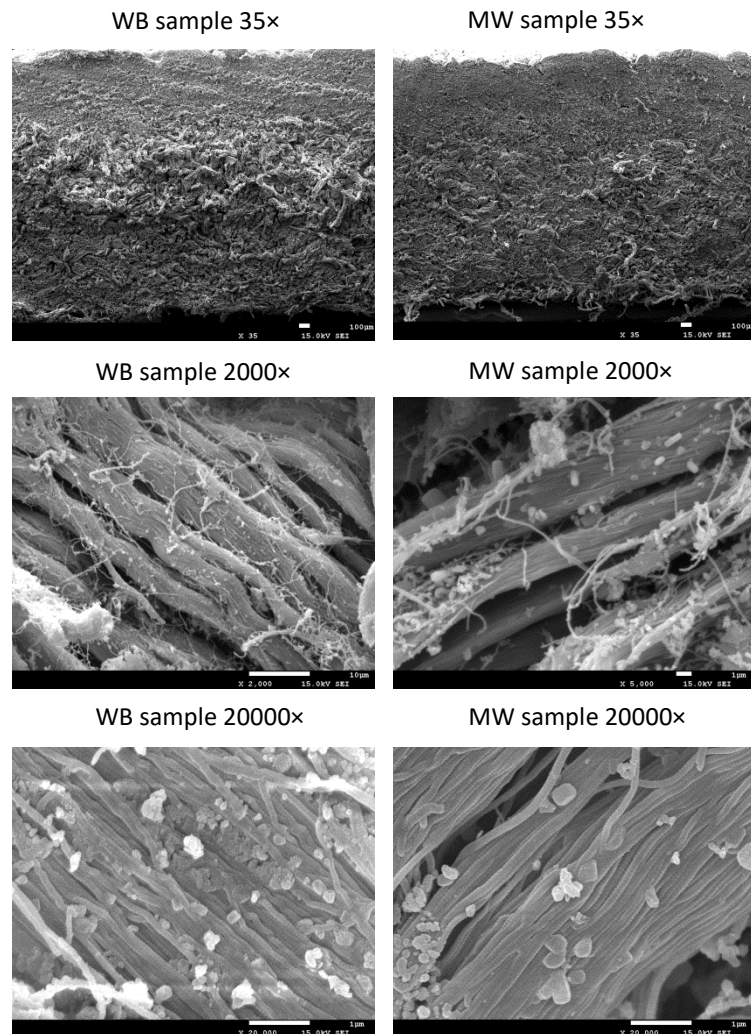


Fig. 3. SEM images of leather tanned under different heating method.

SEM was used to observe the morphologies of leather tanned under different heating method, and the images were shown in Fig. 3. When the magnification was 35, the cross section of two samples had clear interwoven flexuous fiber bundles network. With the increasing of magnification to 2000, the leather consisted of thin uniform fibers which packed together orderly and there was no significant difference between the two samples. Under magnification higher to 20000, collagen fibrils exhibited the alternative brightness and darkness, it attributed to the unique staggered by a quarter of collagen. Although microwave promoted chrome tanning process and effect, the hierarchical structure of leather remained as normal.

4 Conclusions

By comparing the differences on aspects of tanning process and leather performance between chrome tanning with microwave assisting and water bath heating, it could summarize as following: firstly, chrome tanning process under microwave irradiation was faster than traditional heating, so microwave would be an effective routine for accelerating chrome tanning process; secondly, the leather tanning with microwave assisting had better thermal stability, in other word, the tanning

effect was promoted by microwave, thus, microwave could be used to innovate chrome tanning process for excellent performance leather; thirdly, the tanning process and effect were affected by microwave but collagen structure remained. In short, microwave has positive effect on chrome tanning process and leather performance.

5 Acknowledgements

The authors wish to thank the financial support of National Natural Science Foundation of China (No. 21576171).

Reference

1. Smith, G. B.: *Low and high impact*, Academic Press, 2005
2. Surname, M.: 'The IULTCS Guidelines in Use', *App. Biol. Lett.*, 58, 173-175, 2019
3. Wang N., Wang P.: 'Study and application status of microwave in organic wastewater treatment – A review', *Chemical Engineering Journal*, 283, 193-214, 2016.
4. Díaz-Ortiz Á., Prieto P., de la Hoz A.: 'A Critical Overview on the Effect of Microwave Irradiation in Organic Synthesis', *The Chemical Record*, 19, 85-97, 2019.
5. Asomaning J, Haupt S, Chae M, et al.: 'Recent developments in microwave-assisted thermal conversion of biomass for fuels and chemicals', *Renewable & Sustainable Energy Reviews*, 92, 642-657, 2018.
6. Mudrov A N, Tishchenko A S, Ageeva T A, et al.: 'Kinetic features of radical polymerization of styrene under microwave irradiation conditions', *Russian Journal of General Chemistry*, 86, 1510-1514, 2016.
7. Pang Y, Lei H.: 'Degradation of p-nitrophenol through microwave-assisted heterogeneous activation of peroxymonosulfate by manganese ferrite', *Chemical Engineering Journal*, 287, 585-592, 2016.
8. Ahirwar R, Tanwar S, Bora U, et al.: 'Microwave non-thermal effect reduces ELISA timing to less than 5 minutes', *Rsc Advances*, 6, 20850-20857, 2016.
9. Nazari S, Ghandi K.: 'Solvent and microwave effects on oxidation of aromatic α -diketones', *Journal of Industrial & Engineering Chemistry*, 21, 198-205, 2014.
10. Nozariasbmarz A, Dsouza K, Vashae D.: 'Field induced decrystallization of silicon: Evidence of a microwave non-thermal effect', *Applied Physics Letters*, 112, 93-103, 2018.
11. Fukushima J, Kashimura K, Takayama S, et al.: 'In-situ kinetic study on non-thermal reduction reaction of CuO during microwave heating', *Materials Letters*, 91, 252-254, 2013.
12. Wu J., Sun T., Zhang J., et al.: 'Interaction of Enzymes and Hide/Leather Based on Microwave', *Journal of the Society of Leather Technologists and Chemists*, 102, 204-209, 2018.
13. Gong Y, Cheng K, Zhang T, et al.: 'Automated Clear Leather Dyeing Assisted by Wringing, Ultrasound and Microwave', *Journal- American Leather Chemists Association*, 106, 127-132, 2011.
14. Gong Y, Zhang T, Chen W.: 'Behavior of Fatliquored Leathers in a Microwave Field', *Journal of the American Leather Chemists Association*, 107(2): 60-67, 2012.
15. Zhang J, Zhang C, Wu J, et al.: 'The influence of microwave non-thermal effect on leather properties in drying', *Journal- American Leather Chemists Association*, 112, 135-139, 2017.
16. Zhang J, Wu J, Chen W.: 'Special review paper: Applications of microwave in leather field: Further research for leather chemists and technologists', *Journal- American Leather Chemists Association*, 112, 311-318, 2017.
17. Zhang J, Cao N, Zhou N, et al.: 'Hydrolysis and Olation of Chromium Sulphate Under Microwave Irradiation', *Journal of the Society of Leather Technologists and Chemists*, 101, 1-5, 2017.
18. Cao N., Zhang J.W., Wang S.J., et al.: 'Behaviors of chromium nitrate hydrolysis and olation under microwave irradiation', *Leather Science and Engineering*, 26, 5-9, 2016.
19. Wu J, Zhang L, Zhang J, et al.: 'Electrochemical Behavior of Tannin Solutions under Microwave Irradiation', *Leather & Footwear Journal*, 17(2):91-96, 2017.
20. Wang H, Chen W, Gong Y, et al.: 'Based on the Studies of Chrome Tanning Chemistry with Microwave', *Leather Science and Engineering*, 21(2):5-9, 2011.
21. Wu J, Liao W, Zhang J, et al. Thermal behavior of collagen crosslinked with tannic acid under microwave heating[J]. *Journal of Thermal Analysis & Calorimetry*, 2018(4):1-7.
22. Wu J, Fan Z, Zhang J, et al.: 'Impact of Microwave Irradiation on Vegetable Tanning', *Journal of Society of Leather Technologists and Chemists*, 120:7-11, 2017.
23. Chen J, Zhang J.W., Zhou N., et al.: 'Influence of microwave irradiation on the stability of chromium (III) complexes', *Leather Science and Engineering*, 27(4): 5-9, 2017.

STRUCTURE AND TANNING PROPERTIES OF DIALDEHYDE CARBOXYMETHYL CELLULOSE: EFFECT OF DEGREE OF SUBSTITUTION

Yudan Yi¹, Wei Ding¹, Zhicheng jiang¹, Ya-nan Wang^{1,2*}, Bi Shi^{1,2}

1 National Engineering Laboratory for Clean Technology of Leather Manufacture, Sichuan University, Chengdu 610065, China, Tel: +86-28-85405508,

Email: wangyanan@scu.edu.cn

2 Key Laboratory of Leather Chemistry and Engineering (Sichuan University), Ministry of Education, Chengdu 610065, China

Abstract. Developing novel tanning agents from renewable biomass is regarded as an effective strategy for sustainable leather industry. In this study, a series of dialdehyde carboxymethyl cellulose (DCMC) were prepared by periodate oxidation of carboxymethyl cellulose (CMC) with varying degree of substitution (DS: 0.7, 0.9 and 1.2). The structural properties of DCMC were characterized. Size Exclusive Chromatography measurements showed that CMC underwent severe degradation during periodate oxidation, resulting in the decline of weight-average molecular weight from 250,000 g/mol to around 13,000 g/mol. ¹H NMR and FT-IR analysis illustrated that aldehyde group was successfully introduced into DCMC. The aldehyde group content of DCMC decreased from 8.38 mmol/g to 2.95 mmol/g as the DS rose from 0.7 to 1.2. Interestingly, formaldehyde was found to be produced in DCMC, and its content was 3.45, 2.99 and 2.18mg/g, respectively when the DS of CMC was 0.7, 0.9 and 1.2, respectively. Further analysis by HPLC confirmed that glucose and fructose were formed during oxidative degradation, and were subsequently oxidized to generate formaldehyde. Higher DS resulted in lower formaldehyde content in DCMC. Tanning trials showed that the shrinkage temperature and thickening rate of DCMC tanned leather decreased as the DS increased. This should be due to the difference in aldehyde content of DCMC. Leather tanned by DCMC-0.7 (DS of CMC was 0.7) had the highest shrinkage temperature of 81°C and thickening rate of 76%. In general, we hope the work on dialdehyde tanning agent derived from CMC could provide some essential data for the development of sustainable tanning material and process.

1 Introduction

Carboxymethyl cellulose (CMC), an anionic linear polymer derived from cellulose, poses advantages of renewability, nontoxicity, excellent biocompatibility and biodegradability¹. CMC is widely used in various fields including paper, textile, food, pharmaceutical industries and mineral processing². It can be converted to its dialdehyde derivatives (DCMC) by periodate oxidization since sodium periodate can specifically oxidize the adjacent hydroxyl groups on C2 and C3 of the anhydroglucose unit (AGU) to form two aldehyde groups³. DCMC has been proved to be an ideal crosslinking agent for preparation of gelatin films and collagen cryogels since the Schiff's base is formed between aldehyde groups of DCMC and amino groups of gelatin or collagen^{4,5}. Hence, DCMC is supposed to be used as tanning agent since leather is actually a collagen fiber matrix. It is known that the use of existing aldehyde tanning agents would introduce free formaldehyde into leather, leading to potential risk to human health. We hope the use of DCMC whose aldehyde groups are located on the polysaccharide chains could solve this problem.

With respect to the degree of substitution (DS) of CMC, three hydroxyl groups at the 2, 3, and 6 positions in AGU of cellulose can be substituted by carboxymethyl group. Thus, the average number of substituted hydroxyl groups per AGU, viz. DS, ranges from 0 to 3 theoretically⁶. The substitution reactivities of hydroxyl groups on C2 and C6 were equal and significantly higher than that on C3 when CMC was prepared by traditional slurry process^{7,8}. Substitution on C2 may hinder the periodate oxidation of CMC and the formation of aldehyde group. This means that DS of CMC would probably affect the tanning performance of DCMC. Therefore, the aim of this study was to explore the effect of DS on the structure and tanning properties.

In the present work, CMC with DS of 0.7, 0.9 and 1.2 were oxidized to DCMC. The structural parameters of CMC and DCMC were characterized by gel permeation chromatography (GPC), Fourier transform infrared (FT-IR) spectroscopy and nuclear magnetic resonance (NMR) spectroscopy. Moreover, the aldehyde group content and formaldehyde content of DCMC were also determined. Then the tanning performance using DCMC with different DS was evaluated.

2 Materials and Methods

2.1 Materials

Sodium carboxymethyl cellulose (CMC) with DS of 0.7, 0.9 and 1.2 were of analytical grade and purchased from Sigma-Aldrich Co. LLC. (St. Louis, USA). Sodium periodate and hydroxylamine hydrochloride were of analytical grade and purchased from Chengdu Kelong Chemical Co., Ltd. (Chengdu, China). Pickled cattle pelt was supplied by a local tannery. The other chemicals used in tanning were of commercial grade.

2.2 Preparation of DCMC and H-DCMC

Sodium periodate was solubilized in 500 mL distilled water away from light, then 25.0 g CMC (DS: 0.7, 0.9 and 1.2) was added into the sodium periodate solution under stirring at 25°C. The mol ratio of sodium periodate to monomeric unit of CMC was 1:1. After the mixture was stirred in the dark for 24 h, the oxidized product, referred to DCMC (Figure 1) was obtained.

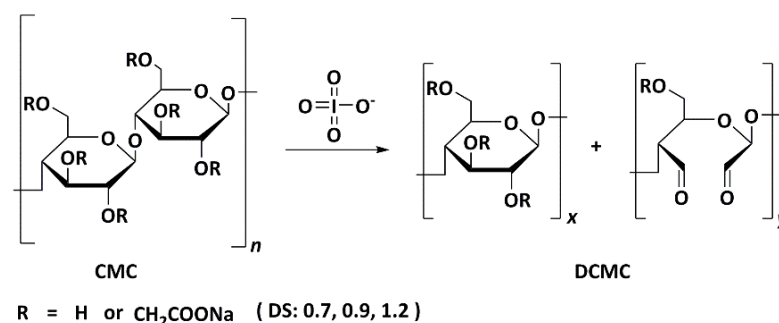


Figure 1. The illustration of periodate oxidization of CMC to DCMC.

25.0 g CMC (DS=0.7) was uniformly dispersed in 500 mL distilled water at 90°C. Then 5 mL concentrated hydrochloric acid was added into the blend under stirring with 1 h interval (totally 25mL). After hydrolysis for 6 h, the solution was cooled to room temperature and its pH was adjusted to 5.0 by the addition of a 50% (w/w) NaOH solution. This acid hydrolyzed CMC solution was labeled as H-CMC. Subsequently, sodium periodate with a mole ratio of 1:1 was added into H-CMC and stirred in the dark at 25°C for 24 h, then the oxidative product, labeled as H-DCMC, was acquired.

2.3 Determination of molecular weight

Weight-average molecular weight (Mw), number-average molecular weight (Mn) and polydispersity (Mw/Mn) of CMC and DCMC were determined by Size-exclusion chromatography (Malvern 270 max, Malvern Instruments, UK), equipped with a TSK-gel GMPWXL column (7.8 mm × 300 mm, Tosoh, Japan). Aqueous solution of CMC (2 mg/mL) and DCMC (5 mg/mL) were filtered through a 0.22 μm pore membrane to eliminate dust particles. The injection volume of sample was

100 μL . The eluent was 0.1 mol/L NaNO_3 at a flow rate of 0.6 mL/min under 30°C elution temperature. Molecular weight of samples was calculated using OmniSEC 4.7 software with a dn/dc value of 0.136 mL/g by the comparison to Shodex pullulan standard P-20 (2 mg/mL, $M_w = 34.4 \times 10^4$ for CMC and $M_w = 10.7 \times 10^4$ for DCMC, Showa Denko K.K., Japan)⁹.

2.4 Nuclear magnetic resonance (NMR) spectroscopy

The ^1H NMR spectra of CMC and DCMC were acquired on a Bruker Avance II-400 spectrometer (Bruker, Germany) using D_2O as solvent at a concentration of 50 mg/mL.

2.5 Fourier transform infrared (FT-IR) spectroscopy

CMC and DCMC samples were lyophilized using LGJ-30F freezer dryer (XinYi, China). Then their FT-IR spectra were recorded by a FT-IR spectrophotometer (Thermo Scientific Nicolet IS10, USA). The discs containing sample and potassium bromide (KBr) were measured in the wavenumber region 500-4000 cm^{-1} at room temperature, using 32 scans and a resolution of 4 cm^{-1} .

2.6 Determination of aldehyde group content

The aldehyde group content of DCMC was determined by hydroxylamine hydrochloride method¹⁰. 0.1 g dried DCMC was dissolved in 25 ml distilled water. The pH of the solution was adjusted to 5.0 with 0.1 mol/L NaOH solution. 20 ml of 0.25 mol/L hydroxylamine hydrochloride (pH = 5.0) was added into the DCMC solution and the mixture was stirred for 4 h in the thermostated water bath at 40°C. Then 0.05 mol/L NaOH standard solution was used to titrate with the hydrochloric acid produced in the mixture and the consumption of NaOH solution was obtained. Thus, the aldehyde group content of DCMC was calculated via equation (1):

$$\text{Aldehyde group content (mmol/g)} = \frac{V_{\text{NaOH}} \times M_{\text{NaOH}} \times 0.001}{m} \quad (1)$$

where V_{NaOH} is the consumption of NaOH solution, M_{NaOH} is 0.05 mol/L and m is the dry weight of DCMC sample. Measurements were made in triplicate.

2.7 Determination of formaldehyde content

The determination of the formaldehyde content in DCMC aqueous solution was performed following ISO 27587-2009¹¹ with some modifications. 0.2 mL of 50 g/L DCMC solution was put into the U-tube and was incubated at 90°C. The released free formaldehyde in the sample was continuously purged by nitrogen gas and was collected by DNPH absorption solution. After 30 min, the DNPH absorption solution was kept in dark for 30-150 min and then filtrated through a 0.45 μm membrane filter. High Performance Liquid Chromatography (HPLC, 1260 Infinity II, Agilent, USA) with a CAPCELL PAK C18 MG II column (4.6mm \times 150mm, Shiseido, Japan) was used to analyze the formaldehyde in DNPH absorption solution. The injection volume of sample was 20 μL . The eluent was the mixture of acetonitrile and distilled water (60%: 40%, v/v) at a flow rate of 1.0 mL/min under 30°C elution temperature. Then the target substance (formaldehyde phenylhydrazone) was detected by Diode Array Detector (DAD) at 360 nm. The formaldehyde content was calculated according to the standard calibration curves obtained by using formaldehyde standard solution with different concentrations.

2.8 DCMC tanning trials

Pickled cattle pelt was cut along the backbone into matched pieces. Then they were tanned with 4wt% DCMC of different DS (based on twice the weight of pickled pelt) at 25°C, respectively. The

initial tanning pH was 3.0. After penetration of DCMC for 4 h, the pH of tanning bath was increased to 7.8-8.0 by the controlled addition of sodium bicarbonate. Then the drum kept running for 4 h at 40°C and then left overnight. After running for 30 min next morning, the tanned leather was washed by water at 25°C for 10 min and then horsed up for 24 h.

Two small pieces of each group of leather were sampled for shrinkage temperature (T_s) test using a digital leather shrinkage temperature instrument (MSW-YD4, Shanxi University of Science and Technology, China).

Thickness of pickled pelt and leathers tanned by DCMC was measured using a digital display thickness gauge (MY-3130-A2, Ming Yu, China). The thickening rate was calculated by the equation (2):

$$\text{Thickening rate (\%)} = \frac{T_a - T_b}{T_a} \times 100 \quad (2)$$

where T_a represents the thickness of DCMC tanned leather and T_b is the thickness of pickled pelt.

2.9 Constituents analysis of DCMC

Constituents analysis of DCMC was performed by HPLC (1260 Infinity II, Agilent, USA) using an Aminex column (model HPX-87H, 300 mm × 7.8 mm, Bio-Rad) and a RI detector. 5 mmol/L H_2SO_4 solution was used as the mobile phase at a flow rate of 0.6 mL/min. The temperature of column and RI detector was maintained at 50°C¹². The components in DCMC were quantified by comparison with standard calibration curves obtained by using authentic chemicals with different concentrations. The yield of products was calculated following equation (3):

$$\text{Yield (wt\%)} = \frac{\text{Weight of products}}{\text{Weight of raw material}} \times 100\% \quad (3)$$

3 Results and discussion

3.1 Molecular weight

The molecular weights (M_w and M_n) and polydispersities (M_w/M_n) of CMC and DCMC (DS=0.7, 0.9, 1.2) are shown in Table 1. The molecular weight decreased remarkably after periodate oxidization owing to the concomitant degradation during oxidization of CMC. In addition, DS of CMC had little impact on molecular weight of DCMC for M_w of the three samples were all around 12000-16000.

Table 1. The molecular weights of CMC and DCMC

DS	Sample	M_w	M_n	M_w/M_n
0.7	CMC	419540	200257	2.095
	DCMC	12319	2931	4.202
0.9	CMC	225461	64346	3.504
	DCMC	15572	2594	6.003
1.2	CMC	255047	127352	2.003
	DCMC	13594	2878	4.722

3.2 ¹H NMR

The successful preparation of DCMC was confirmed by ¹H NMR as given in Fig 2. Three new chemical shifts were obtained in the ¹H NMR spectra of DCMC compared with that of CMC. The most

pronounced peak at $\delta=8.38$ ppm was considered as aldehyde group^{13,14}. The aldehyde group was also present as the hemiacetal form as judged by chemical shift at $\delta=4.8-5.5$ ppm^{15,16}. The intramolecular hemiacetal was formed between the dialdehyde groups and hydroxyl groups of neighboring unoxidized AGU¹⁷. Moreover, the assignment of $\delta=9.20$ ppm to aldehyde proton was consistent with a typical ¹H-chemical shift region of aldehydes¹⁸.

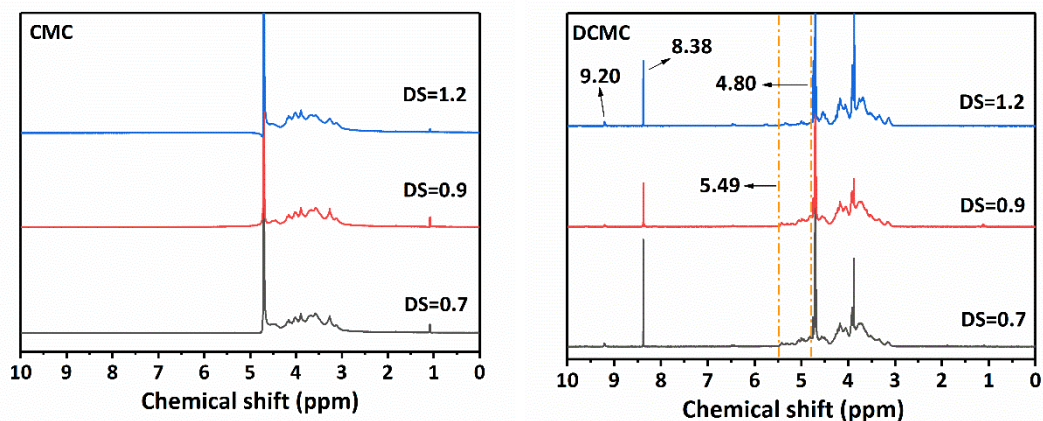


Figure 2. ¹H NMR spectra of CMC and DCMC.

3.3 FT-IR

FT-IR analysis was used to further support the formation of aldehyde groups in DCMC (Figure 3). A new IR band appeared at 1737 cm^{-1} region in DCMC, which was attributed to the stretching vibration of aldehyde group¹⁹. The absorption peaks at 1606 and 1424 cm^{-1} were assigned to the asymmetric and symmetric stretching vibration of carboxylate group, respectively²⁰. The absorption peak at 896 cm^{-1} indicated the presence of the hemiacetal bond between aldehyde group and neighbor hydroxyl group, which was in correspondence with the result of ¹H NMR²¹. A broad band occurred at 3434 cm^{-1} was assigned to the stretching vibrations of hydroxyl group²¹. The number of hydroxyl group in DCMC declined notably compared with those in CMC because the hydroxyl groups were mostly oxidized. In addition, the absorption bands at 2915 cm^{-1} and 1326 cm^{-1} were attributed to CH stretching, CH₂ stretching respectively^{21,22}.

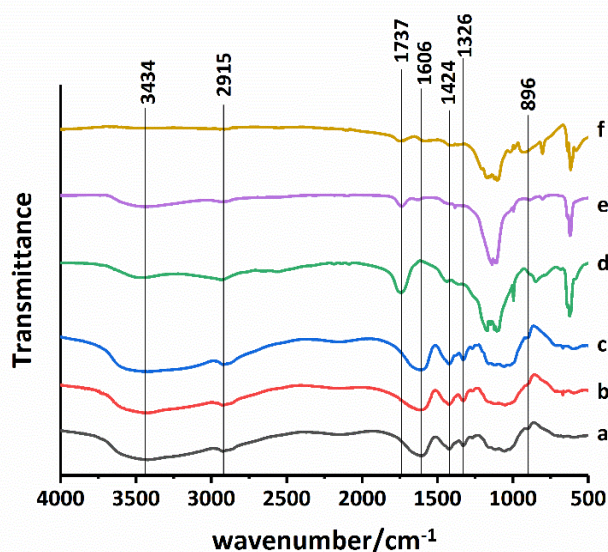


Figure 3. FT-IR spectra of CMC and DCMC. a) CMC (DS=0.7); b) CMC (DS=0.9); c) CMC (DS=1.2); d) DCMC (DS=0.7); e) DCMC (DS=0.9); f) DCMC (DS=1.2).

3.4 Aldehyde group and formaldehyde in DCMC

The aldehyde group content and formaldehyde content of DCMC are shown in Figure 4. The aldehyde group content declined along with the increased DS, which may result from the decreased number of adjacent hydroxyl group in CMC since the hydroxyl group in C2 tended to be substituted by carboxymethyl group. Surprisingly, formaldehyde was detected in DCMC. The formaldehyde content also decreased with the increased DS. The reason for formaldehyde formation will be explored in the following section.

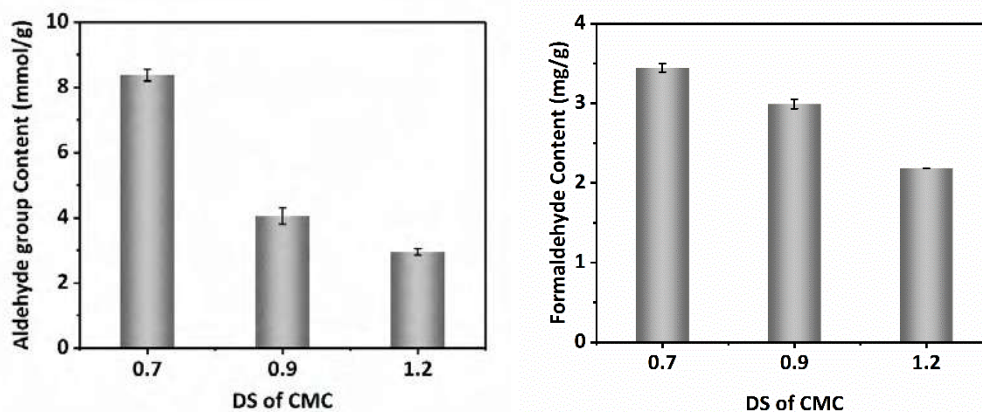


Figure 4. The content of aldehyde group and formaldehyde of DCMC.

3.5 Constituents analysis of DCMC

Figure 6 shows the HPLC spectra of DCMC and a mixed standard solution containing D-(+)-Glucose, D-(-)-Fructose, formic acid and other small-molecule acids. Formic acid (peak c at 13.7min in Figure 5) was detected in DCMC by HPLC with a RI detector. Additionally, formaldehyde was also detected in DCMC (Figure 4). Degradation of CMC with the cleavage of 1-4-glycosidic bond occurred during periodate oxidization²³. Accordingly, oligosaccharide or even monosaccharide would be generated. If further oxidation is allowed to proceed, the formaldehyde and formic acid which were already monitored in the periodate oxidation products of D-glucose (Table 2) are likely to be produced²⁴. Additionally, the content of formaldehyde and formic acid were negatively correlated with DS of CMC as shown in Table 2. The decreasing number of hydroxyl group with the increase of DS leads to the less yield of monosaccharide, which subsequently contributes to the fewer content of formic acid as well as formaldehyde. All in all, it was estimated that the small-molecule degradation products of CMC such as glucose yields formaldehyde since formic acid and formaldehyde are usually the oxidative products of monosaccharide. Nevertheless, glucose was undetected in DCMC by the means of HPLC, which may owe to the low content of glucose in DCMC and the rapid reaction between sodium periodate and monosaccharide so that the glucose was consumed thoroughly within a short time.

Herein, in order to achieve a more drastic degradation of CMC, hydrolysis using concentrated hydrochloric acid was performed on CMC (DS=0.7) before periodate oxidation. Glucose was found in the hydrolysate of CMC (H-CMC). Furthermore, one of the oxidative products of fructose (d at 9.27min in Figure 7), which was in correspondence with the oxidized fructose (B in Figure 7), existed in H-CMC too. Consequently, glucose and fructose were produced during the hydrolysis of CMC. It was found that glucose in H-CMC was entirely consumed after oxidization. At the same time, the substance d (Figure 7) was still remained in H-DCMC and the content of formic acid in H-DCMC was far more than that in H-CMC, as shown in Table 2. A great deal of formaldehyde was produced after oxidization of H-CMC while there was no formaldehyde in H-CMC. Hence, the conceivable sources

of formaldehyde in DCMC were as follows (Figure 8): 1. Glucose produced during oxidation of CMC was oxidized by sodium periodate to form formaldehyde; 2. Glucose was isomerized to fructose, then the periodate oxidation occurred on fructose and formaldehyde was generated²⁵.

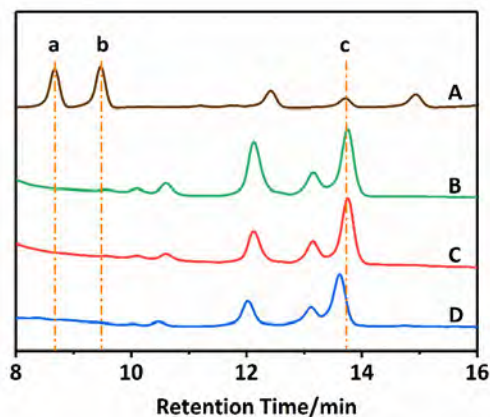


Figure 5. HPLC spectra of DCMC. A) The mixed standard solution; B) DCMC (DS=1.2); C) DCMC (DS=0.9); D) DCMC (DS=0.7); a) D-(+)-Glucose; b) D-(-)-Fructose; c) formic acid.

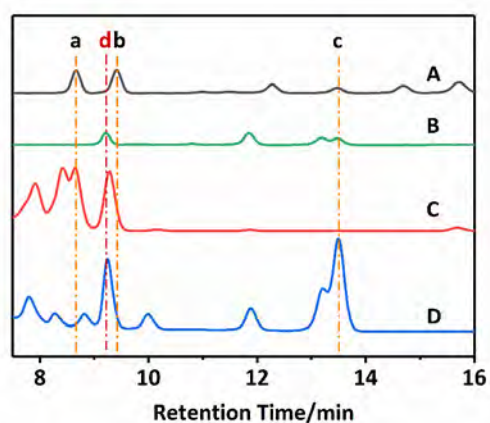


Figure 6. HPLC spectra of H-CMC and H-DCMC A) The mixed standard solution; B) Oxidized fructose (mole ratio of NaIO₄/fructose was 5:1); C) H-CMC (DS=0.7); D) H-DCMC (DS=0.7); a) D- (+) -Glucose; b) D- (-) - Fructose; c) formic acid; d) one of the oxidative products of fructose.

Table 2. Yield of formaldehyde and formic acid in oxidized fructose, DCMC and H-DCMC.

Sample	Yield (wt%)	
	Formaldehyde	Formic acid
oxidized fructose	11.37	46.81
DCMC-0.7	0.34	1.37
DCMC-0.9	0.30	1.33
DCMC-1.2	0.22	0.53
H-CMC-0.7	0	0.08
H-DCMC-0.7	0.70	15.01

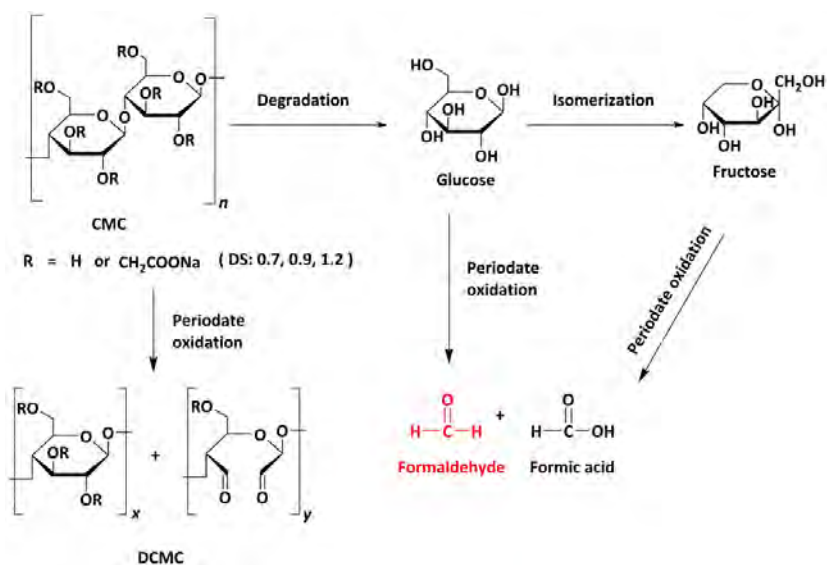


Figure 7. The illustration of the production of formaldehyde accompany with periodate oxidation of CMC.

3.6 DCMC tanning properties

DCMC were used in tanning of leather in order to investigate the effect of DS on tanning performance. Ts is often used to characterize the hydrothermal stability of leather²⁶. As shown in Figure 8, an increase in the DS from 0.7 to 1.2 brought about a decrease in the Ts of leathers, which may stem from the descensive aldehyde group content of DCMC. Leather tanned with DCMC-0.7 exhibited highest Ts of 81°C and thickening rate of 76%.

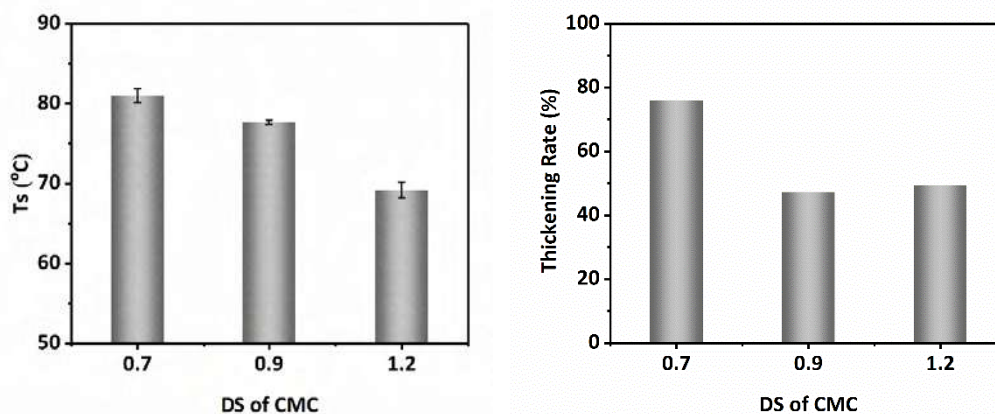


Figure 8. Shrinkage temperature and thickening rate of leathers tanned with DCMC (DS: 0.7, 0.9, 1.2).

4 Conclusion

CMC with DS of 0.7, 0.9 and 1.2 were successfully converted to DCMC. The tanning effect of DCMC was negatively correlated with DS of CMC due to the declined content of aldehyde group of DCMC. Interestingly, formaldehyde was found in DCMC. The mechanism of formaldehyde formation accompany with the periodate oxidation of CMC was investigated. The formaldehyde and formic acid, which are usually the products of periodate oxidation of monosaccharide, were detected in the DCMC. The components of H-CMC were proved containing formic acid, glucose and one of the oxidative products of fructose. After oxidation of H-CMC, formaldehyde was released and the

content of formic acid rose greatly. Simultaneously, the glucose which originally existed in H-CMC was absolutely consumed while one of oxidative products of fructose remained after oxidation. The results suggest that the glucose and its isomer, viz. fructose are the main sources of formaldehyde. The finding about formaldehyde formation is promising and should be validated by the further analysis of dialdehyde polysaccharide.

5 Acknowledgements

This work was financially supported by the National Key R&D Program (2017YFB0308500).

References

1. Arinaitwe, E., Pawlik, M.: Dilute solution properties of carboxymethyl celluloses of various molecular weights and degrees of substitution, *Carbohydr. Polym.*, 99, 423-431, 2014.
2. El-Hag Ali, Amr, Abd El-Rehim, Hassan, A., Kamal, H., et al.: Synthesis of Carboxymethyl Cellulose Based Drug Carrier Hydrogel Using Ionizing Radiation for Possible Use as Site Specific Delivery System, *J. Macromol. Sci. A.*, 45(8), 628-634, 2008.
3. Kim, U. J., Kuga S, Wada M, et al.: Periodate Oxidation of Crystalline Cellulose, *Biomacromolecules*, 1(3), 488-492, 2000.
4. Tan, H., Wu, B., Li, C. P., et al.: Collagen cryogel cross-linked by naturally derived dialdehyde carboxymethyl cellulose, *Carbohydr. Polym.*, 129, 17-24, 2015.
5. Mu, C., Guo, J., Li, X., et al.: Preparation and properties of dialdehyde carboxymethyl cellulose crosslinked gelatin edible films, *Food Hydrocolloids*, 27(1), 22-29, 2012.
6. Shakun, M., Heinze, T., Radke, W.: Determination of the DS distribution of non-degraded sodium carboxymethyl cellulose by gradient chromatography, *Carbohydr. Polym.*, 98(1), 943-950, 2013.
7. Heinze, T., Koschella, A.: Carboxymethyl Ethers of Cellulose and Starch – A Review, *Macromol. Symp.*, 223, 13-39, 2005.
8. Hiroyuki, Konoa., Kazuhiro, Oshimaa., Hisaho, Hashimotoa.: NMR characterization of sodium carboxymethyl cellulose 2: Chemicalshift assignment and conformation analysis of substituent groups, *Carbohydr. Polym.*, 150, 241-249, 2016.
9. Wang, B., Chen, K., Yang, R., et al.: Stimulus-responsive polymeric micelles for the light-triggered release of drugs, *Carbohydr. Polym.*, 103(Complete), 510-519, 2014.
10. Liu, B. H., Wei, Z., Wang, Y. N., et al.: Preparation of Oxidized Poly (2-hydroxyethyl acrylate) with Multiple Aldehyde Groups by TEMPO-mediated Oxidation for Gelatin Crosslinking, *J. Am. Leather Chem. Assoc.*, 114, 163-170, 2019.
11. ISO 27587-2009, *Leather. Chemical tests, Determination of the free formaldehyde in process auxiliaries*, 2009.
12. Fu, X., Dai, J. H., Guo, X. W., et al.: Suppression of oligomer formation in glucose dehydration by CO₂ and tetrahydrofuran, *Green. Chem.*, 19, 3334-3343, 2017.
13. Kholiya, F., Chaudhary, J. P., Vadodariya, N. G., et al.: Synthesis of bio-based aldehyde from seaweed polysaccharide and its interaction with bovine serum albumin, *Carbohydr. Polym.*, 150, 2778, 2016.
14. Balakrishnan, B., Joshi, N., Banerjee, R.: Borate aided Schiff's base formation yields in situ gelling hydrogels for cartilage regeneration, *J. Mater. Chem. B.*, 1(41):5564-5577, 2013.
15. Dahlmann, J., Krause, A., Lena Möller., et al.: Fully defined in situ cross-linkable alginate and hyaluronic acid hydrogels for myocardial tissue engineering, *Biomaterials*, 34(4), 940-951, 2013.
16. Hou, C., Qi, Z., Zhu, H.: Preparation of core-shell magnetic polydopamine/alginate biocomposite for *Candida rugosa* lipase immobilization, *Colloid. Surface. B.*, 128, 544-551, 2015.
17. Mikaela, B., Anette, L., Gunnar, W., et al.: Periodate oxidation of xylan-based hemicelluloses and its effect on their thermal properties, *Carbohydr. Polym.*, 202, 280-287, 2018.
18. Azevedo, E. P, Mariappan, S. V. S, Kumar V.: Preparation and characterization of chitosans carrying aldehyde functions generated by nitrogen oxides, *Carbohydr. Polym.*, 87(3), 1925-1932, 2012.
19. Colthup, N. B.: *Introduction to Infrared and Raman Spectroscopy*, ed. N. B. Colthup, L. H. Daly and S. E. Wiberley, Academic Press, Sydney, 3rd edn, 1990.
20. Ding, W., Yi, Y. D., Wang, Y. N., et al.: Preparation of a Highly Effective Organic Tanning Agent with Wide Molecular Weight Distribution from Bio-Renewable Sodium Alginate, *Chemistryselect*, 43, 12330-12335, 2018.
21. Wang, P., He, H. W., Cai, R., et al.: Cross-linking of dialdehyde carboxymethyl cellulose with silk sericin in force sericin film for potential biomedical application, *Carbohydr. Polym.*, 212, 403-411, 2019.
22. Aykara, T., Demirci, S., Mehmet, S. E., et al.: Poly(ethylene oxide) and its blends with sodium alginate, *Polymer*, 2005, 46(24):10750-10757.
23. Li, H., Wu, B., Mu, C., et al.: Concomitant degradation in periodate oxidation of carboxymethyl cellulose, *Carbohydr. Polym.*, 84(3), 881-886, 2011.

24. Perlin, A. S.: Glycol-cleavage oxidation, *Adv. Carbohydr. Chem. Bi.*, 60(60), 183-250, 2006.
25. Harris, D. W., Feather, M. S.: Evidence for a C-2→C-1 intramolecular hydrogen-transfer during the acid-catalyzed isomerization of D-glucose to D-fructose, *J. Carbohydr. Res.*, 30(2), 359-365, 1973.
26. Covington, A. D.: *Tanning chemistry: The science of leather*, Cambridge: Royal Society of Chemistry, 2009.

FINE HAIR ON AMERICAN BOVINE LEATHERS

Dr. Luis A. Zugno^{1a} and Andreas Rhein^{2b}

¹ Buckman, 1256 North Mclean Blvd, Memphis, TN, 38108, USA

² Tyson Foods, Inc., 800 Stevens Port Drive, Dakota Dunes, SD, 57049, USA

a) lazugno@buckman.com

b) andreas.rhein@tyson.com

Abstract. Fine hair is the biggest seasonal challenge for bovine leather production in the United States. The origin, timing and severity of the fine hair problem can be unpredictable and vary from year to year. Seasonal changes in the hair growth cycle are prompted by the lower temperature from fall to winter; the bovine hair increases in amount, length and thickness. This problem is very old and has increased in severity due to changes in the leather manufacturing process, cattle breeding conditions and breed diversity. The amount of fat and thickness of the hide also play important roles. The extent of the problem has not been documented and is not fully understood by the scientific community. The presence of fine hair (residual hair) on the wet blue and final leather is a cause of downgrading the leather. If the wet blue has fine hair, it cannot be removed in further processing in crust or finishing. Some leather types can tolerate more fine hair than others. In this paper we will conduct a scientific evaluation of the fine hair on American bovine hides, wet blue and finished leathers through cross sections and stains, and optical and electron microscope observations. We will include measurements of hair thickness and hair depth inside the hide. The work will compare sulfide and oxidative unhairing of winter hides, characterize and show the details of the fine hair through cross sections, and offer indicative measures to minimize the problem. Information from the largest wet blue manufacturer in the US with four tanneries will provide insight on the fine hair seasonality, types of breeds, and cattle displacement temperature ranges and will discuss adaptive changes needed in the “winter” to control the fine hair.

1 Introduction

The presence of fine hair on American hides is an old problem and has increased in the last decades due to changes in breed, feed, herd movement and climatic adaptations. The changes in the processing conditions in the tannery have also contributed to this problem. There is limited information on the topic, and the industry has accepted that fine hair is a seasonal problem and cannot be resolved; beamhouse leather producers and customers work to manage it the best way possible to minimize the problem. The limited processing time practiced in the US during soaking, and unhairing/liming of fresh hides aggravates the fine hair problem. In comparison, the salted or brine cured hides processed in the US or overseas have minimized this problem. For simplification purpose in the paper we will use the term wet blue to define both wet blue and wet white leathers.

Jean J. Tancous (1) in her book *Skin, Hide and Leather Defects* says: “The fine hair problem cannot be completely blamed on poor beamhouse techniques as it may arise from a ‘natural characteristic’ of the animal, i.e., the shedding of the hair root which occurs at seasonal intervals. As a hair grows older, the root atrophies and shrinks; it then falls out. A new papillary hair invaginates below the receding old hair; and thus, the old hair is replaced by a deeply rooted, new fine hair. It is unfortunate for the tanner that new short hair has firmly anchored roots, as they resist easier removal in the beamhouse and cause the fine hair difficulties.”

Merril (2) describes that papillary hairs, being more deeply set and more firmly anchored, are more difficult to remove, giving rise to the vexatious ‘fine hair’ problem.

Thorstensen (3) describes the use of sodium borohydride as an aid to fine hair removal. On the hair-root studies Kuntzel and Stirtz (4) answer the question whether the more deeply anchored papillary hairs are more difficult to remove in the tannery practice than the less-rooted club hairs:

No difference in ease of removal of these two hair types is to be found either in enzymatic or sulfide unhairing. According to the authors, leaving behind the pigmented parts of papillary hair roots and the pigmented young hairs found beneath the club hairs may well cause trouble.

2 Hair Growth Cycle

Most of the studies on hair growth cycle were made on human hairs. There are some similarities and differences with the bovine hair cycle. This is very complex even within the bovine hair due to the changes that can happen with the animals due to age, climatic conditions, breeds and feed.

One of the earliest reviews of the biological and chemical properties of animal hair was done by Stoves (5) in 1947. Stoves described the process of hair development: "After a period of time, dependent on the type of fibre, the papilla of the mature hair ceases to proliferate and hair growth terminates. Changes then occur in the basal portion of the follicle which, together with natural movement of the skin, result in the hair becoming detached from the papilla. The hair root shrinks and a growth of the cells of the root sheath takes place between the root and the papilla. The upward pressure of these growing cells forces the old hair towards the skin. Through this matrix of proliferating epithelial cells, the new fiber ultimately grows by a process analogous to that already described. Opinions have differed as to whether or not the cells of the old papilla completely disappear and are replaced by a new structure."

Schleger (6) studied the relationship between cyclic changes in the hair follicle and sweat gland size in cattle and used the classification of hair follicles based on Chase, Rauch and Smith (7). In his paper he describes the eleven phases of the follicle cycle. Butcher (8) described the papillary system and replacement of hair in mammals.

In *The Biology of Hair Follicles*, Paus and Cotsarelis (9) describe with details the development and cycling of human hair follicles (Fig. 1).

Here is the glossary of terms used:

- Anagen: growth stage of the hair-follicle cycle
- Bulb: lowermost portion of the hair follicle, containing rapidly proliferating matrix cells that produce hair
- Catagen: stage of the hair cycle characterized by regression and involution of the follicle
- Club hair: fully keratinized, dead hair - the final product of a follicle in the telogen stage
- Telogen: resting stage of the hair cycle; club hair is the final product and is eventually shed
- Terminal hair: large, usually pigmented hair on the scalp and body

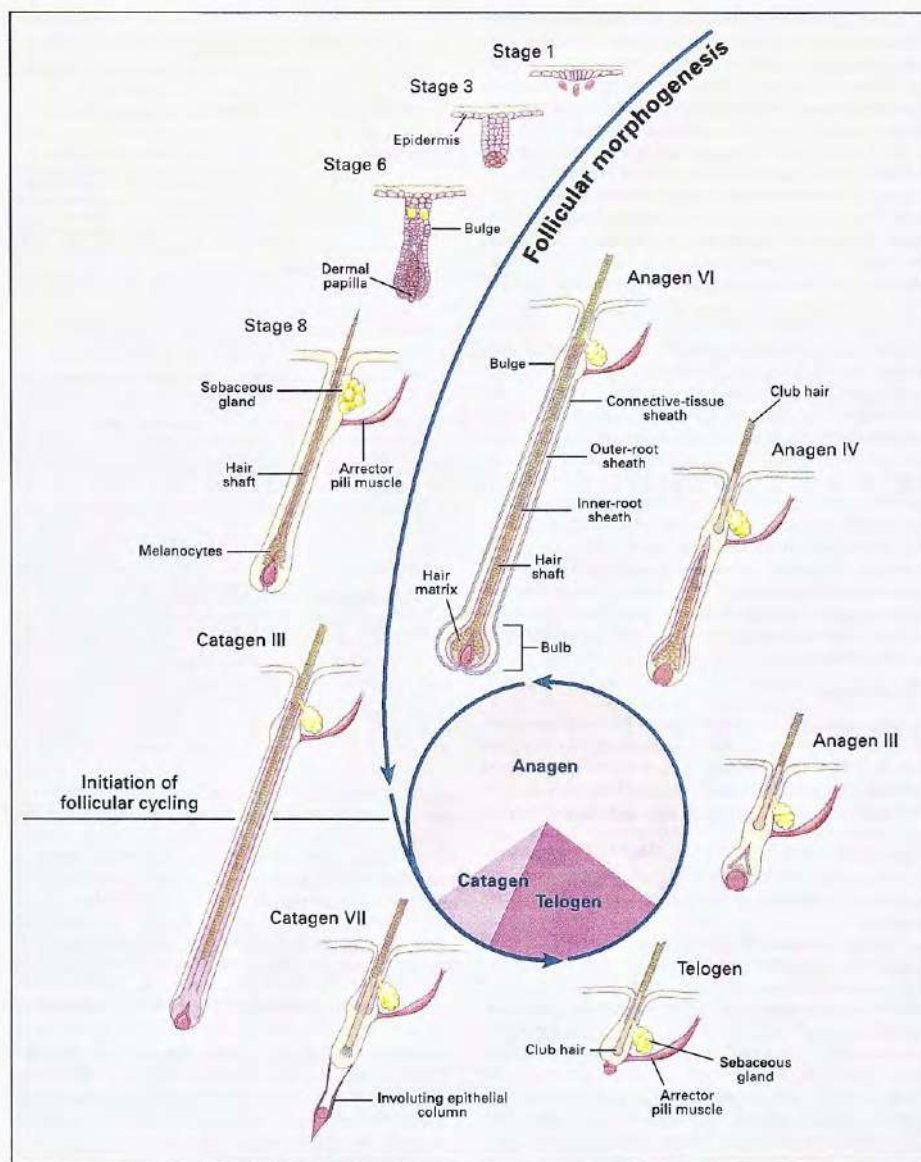


Fig. 1. Development and cycling of hair follicles. Selected stages of the morphogenesis of hair follicles and the three stages of follicular cycling (anagen, catagen, and telogen) are shown. The Roman numerals indicate morphologic sub-stages of anagen and catagen. The pie chart shows the proportion of time the hair follicle spends in each stage (9). Published with permission from *The New England Journal of Medicine*.

The human hair cycling is described by Paus and Cotsarelis (9): Each hair follicle perpetually goes through three stages: growth (anagen), involution (catagen) and rest (telogen). Numerous growth factors and growth factor receptors are critical for normal hair-follicle development and cycling, but no single growth factor appears to exert ultimate control over these processes. The onset of the anagen stage recapitulates hair-follicle development, since the formation of the new lower hair follicle begins with the proliferation of secondary germ cells in the bulge. During the catagen stage, hair follicles go through a highly controlled process of involution that largely reflects a burst of programmed cell deaths (apoptosis) in the majority of follicular keratinocytes. Toward the end of the catagen stage, the dermal papilla condenses and moves forward. During the telogen stage, the hair shaft matures into a club hair, which is eventually shed from the follicle, usually during combing or washing.

Stenn and Paus (10) made a complete review of *The Controls of Hair Follicle Cycling* fifty years after Chase (11). One of their conclusions is that we need to know more about the controls for inducing each of the phases of the cycle – anagen, catagen, telogen, and exogen – and the role of apoptosis in the cycle.

3 Seasonal Changes in Hair Growth

Most of the studies on seasonal changes and hair growth were made in the 1960s. Australia was a great contributor in this area; the studies made are still a reference today. Unfortunately, the detailed work done in many regions (and countries) do not have the extreme temperatures (hot and cold) or sun exposure that we have in the US areas of cattle growth.

Yeates (12) has shown that cattle go through a regular seasonal cycle of hair growth and shedding influenced by light. In his study, the daily photoperiod was altered to simulate the synchronous duration of daily lighting of the opposite (northern) hemisphere. The results show that the full range of coat changes may, irrespective of seasonal temperature, be reversed by artificially reversing the seasonal trend of daylight duration. This is presumptive evidence that the natural light environment is a major controlling factor in normal pattern of seasonal coat change with cattle of European origin. Dowling (13) had reason to believe that the process of shedding can also be influenced by other things such as the nature of food supply and the condition of the animal. The important thermal property for the prevention of heat loss from the body is the capacity of the winter hair covering to stabilize an insulating layer of air, whereas the summer coat must allow heat loss which is the site of the balance upon which regulation is usually affected under hot conditions. *Bos indicus* species of cattle and relatively heat tolerant breeds of *Bos taurus* species of cattle have more medulated hair fibers, denser, more compact coats and better developed skin glands than the less tolerant breeds of *Bos taurus*.

Schengler and Turner (14) used the coat score instead of the felting score to provide indication of the coat type. The superiority of the coat score probably lies in the fact that it takes account of features of coat structure which are lost in hair samples. It gives weight to the different coat characters, and to their expression over the whole body of the animal rather than in a very small sample area. The degree to which various coat characters are interrelated is notable. Length, diameter, medullation, curvature, and follicle angle are all quite different had measurements, and they all had correlated with skin temperature and gain.

Hayman and Nay (15) made observations on *Bos taurus* and *Bos indicus*. Two shedding periods were observed, spring and autumn. Approximately four months were required for the complete change from winter to summer coat, the change in appearance being dramatic. Less time was required for autumn shedding and there was a less dramatic change of the coat. That are two peak shedding periods, in spring and autumn, when almost the entire coat is changed. The pattern and rate of shedding in a temperate environment are similar on *Bos taurus* and *Bos indicus* and in crosses between them. Histological data showed that during shedding almost all mature hairs were lost from the skin follicles. All types of cattle had light summer coats and long, heavy winter coats. No difference in hair diameter was observed between summer and winter coats in *Bos taurus*, but in *Bos indicus* hair diameter was much greater in the summer coat.

They observed that approximately 6% of the follicles were found to be very much larger than the rest. They lay at a different angle to the surface, penetrated to a greater depth in the dermis, were of a greater diameter, and were associated with a multilobar sebaceous gland and a much larger sweat gland than the other follicles. Drawings are shown in Fig. 2. The new hair (A) is club hair, and mature hair (B) is the papillar (or terminal) hair.

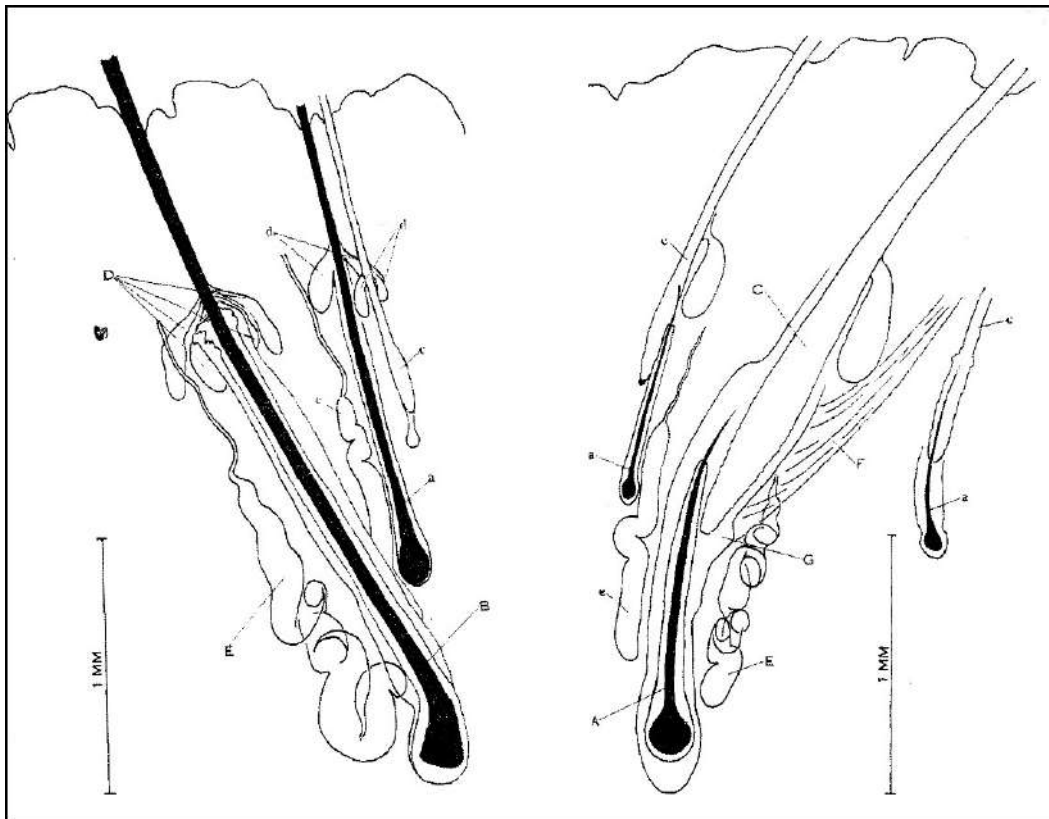


Fig. 2. Giant and average follicles in various stages of activity (drawn to scale). Capital letters, giant follicles; lowercase, average follicles. A, new hair; B, mature hair; C, shedding hair; D, multilobar sebaceous gland; d, bilobar sebaceous gland; E, large sweat gland; e, smaller sweat gland; F, large arrector pili muscle; G, ental swelling at attachment of large arrector pili muscle. (15)

Dowling (16) observed that the difference in heat tolerance of the same animal at different seasons can be attributed to corresponding changes in the hair coat. Animals in a long, woolly winter coat were not heat tolerant, whereas that same animals clipped were.

Dowling and Nay (17) have shown the complexity of studying the cycle of growth and shedding of hairs; the difficulty is to say whether an individual hair is growing, is resting, firmly held in the follicle, or is about to shed. Nor when the hair is shed can one say when the follicle will produce a successor. According to the authors there are two seasons of follicle activity and hair growth, one in spring and another in the autumn; except in these seasons most follicles are mature and hold a club hair whose growth is finished. Some follicle activity is going on in all seasons. They propose a probable sequence of events: "In spring, a short, thick, hard coat is grown, most of the winter hairs being shed from the growing follicle. In autumn, the short hairs are shed to make way for hairs growing in follicles which have again become active, and these now grow longer, thinner hairs. The changes in coat between winter and spring and between summer and autumn are due to a replacement of fibres at both times. The winter coat is a new coat, and not an elongation of the summer coat. The summer coat is mostly present as club hairs which cannot continue growth but will stay as they are until they are shed. Further, the winter coat is made of hairs with smaller diameter than those of the summer coat, and the summer coat has shorter hairs than the winter coat. Continued growth could account for hairs becoming longer, but not for hairs becoming shorter."

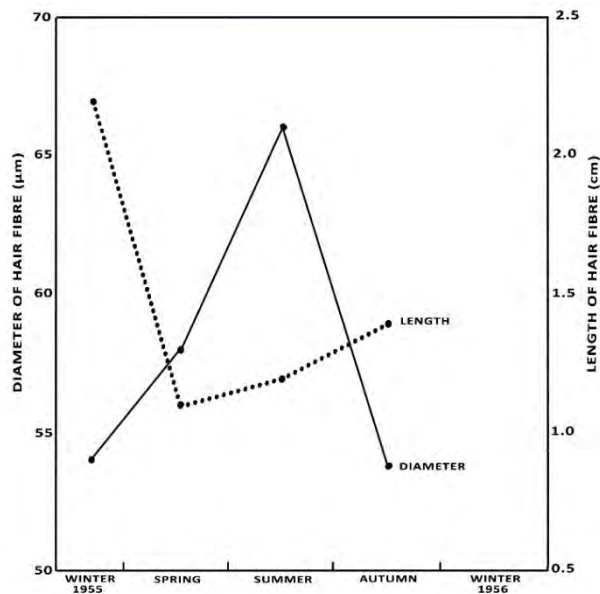


Fig. 3. The average diameter of the fibres of the coat compared with the average length. Each point represents the mean measurements of 10,000 hair fibres. (17)

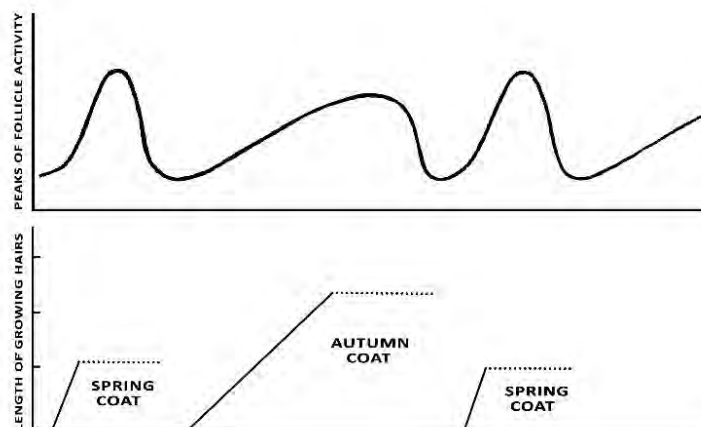


Fig. 4. Diagrammatic illustration of cyclic giant and average follicles in various stages in the follicle activity (above) and fibre length (below). (17)

Berman and Volcani (18) studied the annual cycle of coat growth and shedding rates in Holstein and Syrian x Holstein cattle in three different climatic regions of Israel. The results show that day length is not the only factor influencing the annual cycle of hair quantity and coat thickness but that the air temperatures are of influence too. In this experiment the hair diameter was influenced by variations in the day length.

Webster, Chlumecky and Young (19) raised heifers indoors in a room at 20°C or outdoors at -28°C with or without shelter. They found that the rate of hair growth ($\text{mg}/\text{cm}^2 \cdot 24\text{h}$) was the same, but the heifers raised outdoors had twice the total hair cover (mg/cm^2) of the heifers raised indoors because of the reduced shedding.

Schleger (6) studied the morphology of hair follicles in the 11 growth phases. He found that gland size was significantly influenced by follicle phase. Glands were largest in anagen VI and catagen c and were completely regressed in telogen. He concluded that there is an association between hair growth phase and sweat gland size and sweat gland activity. These three he found to vary together when comparisons are made with breeds or strains, between animals within breeds, between different body regions, and between seasons.

Nay and Hayman (20) found that Zebus have much larger and more numerous sweat glands than European animals. Within Zebus, sweat glands were slightly larger, and much more numerous, on the midside than on the dewlap. They are much closer to the skin surface in Zebu cattle than in European. Udo (21) evaluated the hair coat characteristics in Friesian heifers in the Netherlands in Kenya. He observed that heifers brought to Kenya had increased hair density initially, and then it decreased again to normal values. The seasonal changes in hair density in the Netherlands indicate that in spring and summer there are more empty follicles than in autumn and winter. This could be because several follicles producing non-medullated hairs in autumn shed their hair in spring and remain empty in the summer months. So, when there are fewer non-medullated hairs per unit area, there are probably more empty follicles per unit area. He also found large seasonal changes in melanin content: it was much higher in the winter than summer.

Most of the recent research on cattle adaptation, diet, and health is made with the objective of increased body weight and productivity. Here are some of the recent works. Psaros' (22) research has shown that cattle that are able to shed their winter hair coat in warmer summer months are more likely to tolerate heat stress and produce a heavier calf.

Gray et al. (23) evaluated the differences in hair coat shedding and effects on calf weaning weight and BCS (Body Condition Scoring) among Angus dams. They concluded that hair coat shedding is a heritable trait and could be altered by selection. Producers within the Southwestern or Southern United States who are concerned about heat stress may want to select cattle that shed their winter hair coat earlier in the season. Cows who shed their winter coat by June 1st will wean heavier calves on average. In another study Gray et al. (24) observed that cows that fail to shed in a timely manner tend to show more sign of heat stress when compared to slick-coated contemporaries.

Aiken et al. (25) conducted experiments to characterize and evaluate rough hair coats of cattle grazing endophyte (*Neotyphodium coenophialum*)-infected tall fescue (*Lolium arundinaceum*) during the summer, and the effect of this food source on body temperature. They observed that 80% of the hairs were emerged during long day lengths rather than short day lengths. They concluded that rough hair coats on cattle grazing endophyte-infected tall fescue composed predominantly of hair emerged during long day lengths in the late spring and summer. Growing to excessive hair lengths, these rough hair coats insulate elevated core body temperature to intensify hyperthermia triggered by ergot alkaloid-induced vasoconstriction.

Gilbert and Bailey (26) observed that Angus cattle tended to have shorter, less medullated coats, shorter, larger diameter undercoat hairs and guard hairs with less medullation than Herefords.

Williams (27) published the thesis "Hair Shedding Scores Relating to Maternal Traits and Productivity in Beef Cattle" with pictures illustrating the five Hair Shedding scores. Decker and Parish (28) made a publication on hair shedding scores as a tool for selecting heat tolerant cows.

4 Materials and Methods

Wet blue samples were collected from different suppliers in the United States. Crust and finished leathers were supplied from commercial samples from Asian tanneries using American wet blue. Black Angus hides were brine cured from Texas and north Texas.

Wet blue, crust and finished leather were analysed by SEM and optical microscope. For optical microscopy evaluations on the grain, cross sections were done using various standard laboratory stereoscopic light microscopes. Electron microscopy evaluation and pictures (SEM) were done with Jeol JSM-6480LV, at 15 to 20kV.

Hair thickness measurements were made by mounting the hairs in five minute setting epoxy and sanding the epoxy perpendicular to the hairs. The measurements were made on the electron microscope Jeol JSM-6480LV. Other measurements were made directly on the cross sections or on the grain side using the electron microscope.

Cross sections of the salted hides were prepared using a radial microtome with cryostat and stained using Haematoxylin and Eosin as described by Tancous (1). The Haematoxylin solution Harris modified (cat. HHS16) and Eosin (cat. HT 110116) were purchased from Sigma-Aldrich, St. Louis, MO, 63103, USA. Cross sections of the wet blue, crust and finished leather were prepared using a radial microtome with cryostat and photographed by optical microscope.

For the unhairing evaluations we have separated the club (average 60 µm thickness and 20 mm long) and papillary hairs (average 150 µm thickness and 60 mm long) after removal from salted winter Black Angus hide pieces. The hairs were mounted on a piece of plexiglass 6 mm x 8 mm x 80 mm. Ten club and ten papillary hairs were glued with epoxy to the plexiglass, see Fig. 5. Unhairing solutions were made with sulfide, sulfide plus calcium hydroxide or peroxide in alkaline medium. Sodium dodecyl sulphate was added as a surfactant to reduce the superficial tension. Sodium dodecyl sulphate, sodium sulfide, sodium hydroxide 50%, hydrogen peroxide 35% and calcium hydroxide were purchased from Alfa Aesar, 2 Radcliff Rd, Tewksbury, MA, USA. The unhairing tests were run in a 1 L glass beaker with 800 mL solutions that were placed in a magnetic stirrer with a magnetic bar; the testing was conducted at 23°C for up to 10 hours with very frequent observations. The plexiglass with hairs was mounted parallel to the beaker wall so the hairs were submerged parallel to the liquid surface. The following solutions were used for test (Table 1):

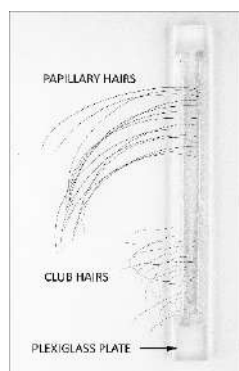


Fig. 5. Plexiglass plate with the papillary and club hairs glued with epoxy.

Table 1. Compositions of the solutions used for the unhairing tests.

	Sulfide (g)	Sulfide and calcium hydroxide (g)	Oxidative (g)
Sodium sulfide nonahydrate 98%	29.6	29.6	
Lime 95%		24	
Hydrogen peroxide 35%			100
Sodium hydroxide 50%			48
Water	770.4	746.4	652
Sodium dodecyl sulphate 10% solution	1 drop	1 drop	1 drop

5 Results and Discussion

Since our initial investigation of the fine hair (29) we have made an extensive literature review and obtained data from the tanneries. The fine hair problem is far more complex than initially expected. In this publication we will have some answers, but many more questions need to be answered. The diverse number of variables makes this problem very complex, and it probably cannot be solved fully.

The cross sections of black Angus salted hides in the wintertime show clearly the presence of club and papillary hairs. Fig. 6 shows the difference in diameter and length between the two types of hair; the papillary hairs are deeper inside the hide and much thicker than club hairs.

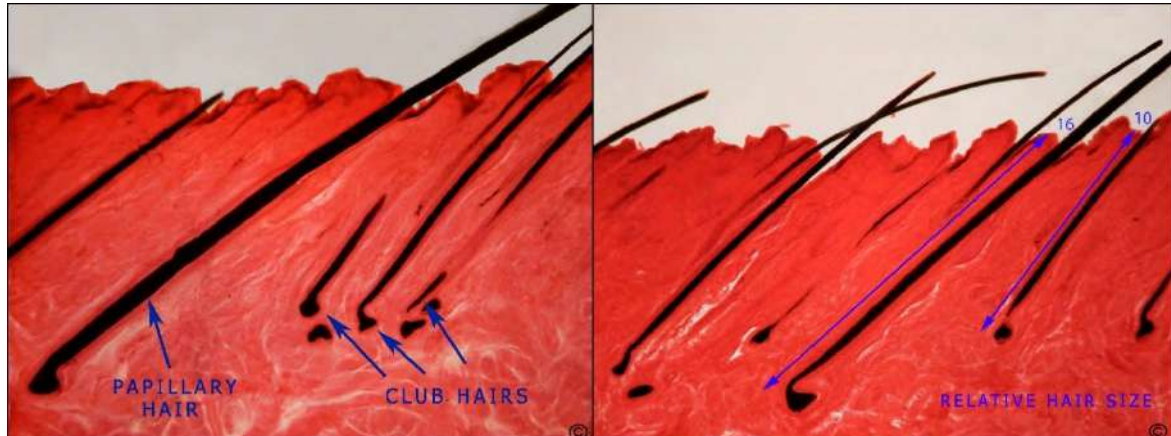


Fig. 6. Cross sections Haematoxylin-eosin stain. Left shows examples of papillary and club hairs. Right shows the relative size of the papillary and club hairs.

On the unhairing tests with sulfide, sulfide plus calcium hydroxide we have observed that club and papillary hairs are dissolved in almost the same ratio. With peroxide in alkaline medium we observed that both types of hairs start to bleach, and the club hairs are dissolved before the papillary hairs; this matches our previous observations made with hides. The test we designed had limited mechanical action in the hairs; this was made mostly with the purpose of observing the chemical effect on the dissolution of the hairs. On bovine hides processed in the tannery, the mechanical action will play a very important role in the removal of the hairs.

We have collected samples of wet blue with fine hair from different suppliers through the years, and all the samples have in common the defined and almost intact presence of the hair. The black hairs are predominant, but in some cases, we also have observed brown hairs. The white hairs either were not present or were not observed. It is sometimes suggested if we could just bleach the hairs with an oxidizer the problem would go away. The use of an oxidizer will bleach the hair and weaken the hair; this probably can work if the leathers are used full grain. In corrected grain leathers, the problem is only minimized and will magnify after buffing. Oxidation is not a viable option for wet blue due the danger of Chromium VI formation. The wet blues were observed under optical and electron microscope (SEM). Hair diameter and length were measured. We found a wide distribution of hair diameter and hair length. The wide diameter (60 μm to 100 and 160 μm) range suggests that papillary and club hairs are still present on the leathers. The fine hairs, club hairs, are present in most cases, but papillary hairs were also observed. See Fig. 7.



Fig. 7. Left optical photograph of wet blue with fine hairs. Right cross section of the wet blue showing intact hairs.

On full grain crust we could readily observe the fine hairs. Here in this commercial sample from Asia we have hairs from 60 to 155 microns. In this case we also have the presence of papillary and club hairs. The hairs have remained intact after retan and mechanical operations. See Fig. 8.

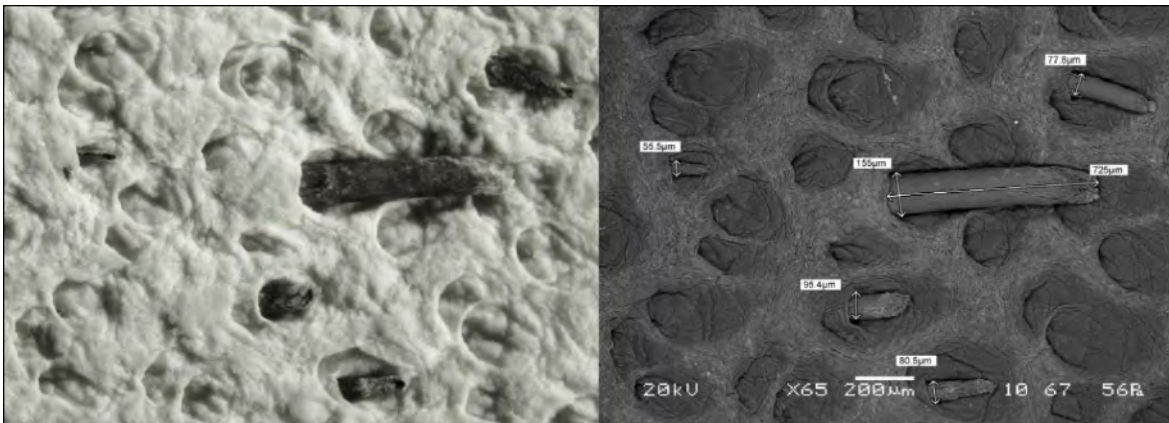


Fig. 8. Left, optical photograph of crust leather with fine hair. Right, SEM image with hair measurements (65X)

Our observations also have shown that hair remains intact, partially broken or removed on the surface of the nubuks. Many times, the hairs are only visible after coarse buffing to produce nubuk. Having fine hair on nubuk degrades the leather considerably. In Figure 9 below, we have an example of how a nubuk surface looks having fine hairs and a detail of a hair cut in half upon buffing; here the hair was intact after buffing and shows detail of the effect of the sanding paper on the hair.

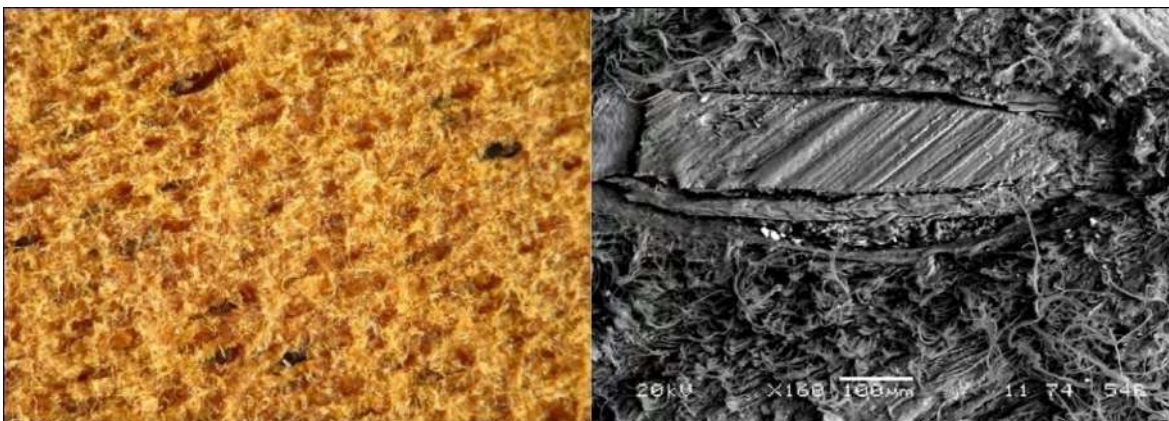


Fig. 9. Left, optical photograph of nubuk leather with fine hair. Right, SEM picture of a nubuk, where the hair was cut on the middle during buffing. (160X)

It remains a puzzle why we can have very few fine hairs on a few leathers in a drum. In many cases the hairs are very intact, as if they were immunized and cannot be removed. This happens with winter hairs.

In our opinion what is called “fine hairs” do not refer exclusively to the thin club hairs because both club and papillary hairs are responsible for the “fine hair” problem. Probably the problem could be better defined as “short winter hairs.”

6 Significance to the Tanning Industry

The US converts about 10 million hides per year to wet blue mostly for the export market. Most of the hides are processed fresh, coming straight from the abattoir, still hot and are cooled for proper fleshing before soaking. The hide weight after fleshing ranges from 25 to 50 kg. The beamhouse time is less than 24 hours, which includes loading the drum, soaking, unhairing, liming and unloading the drum. The typical drum loads are 16 tons with 300 to 500 hides/drum.

Every year the fine hair problem starts in the fall - in early to late November. The problem usually peaks from mid-December to mid-January. Most of the time it is completely gone by the end of March. The location of the hair on the wet blue is usually on the two front pockets (see Figure 10) and can be extended to the neck area if the problem is aggravated. In severe cases the hair is all over the hide including the butt area. It is unusual to have hair in the neck (or butt area) without having hair on the front pockets.

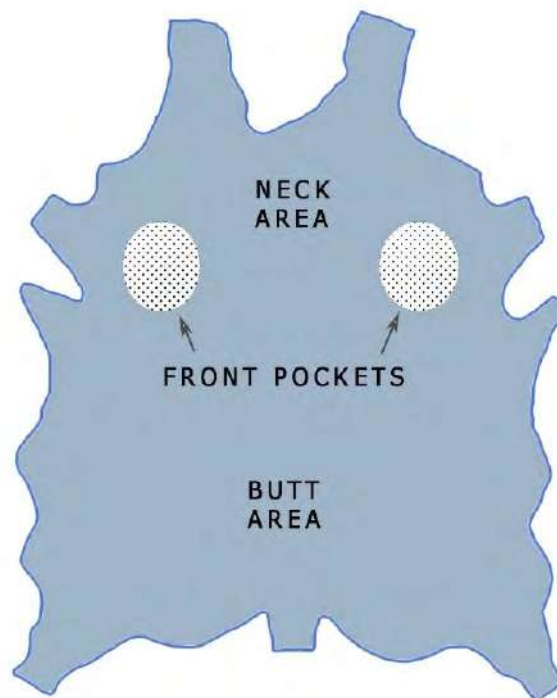


Fig. 10. Drawing of a bovine wet blue leather showing the three most common areas of fine hair. The front pocket is the most common, followed by the neck and butt areas.

The amount of hair in a drum is calculated as a percentage of wet blue with hair. A wet blue is considered to have hair if it is visible and bigger than a hand size after wringing; the inspection is one hundred percent on the wet blue. The size of the hair is usually not taken in account; in summer the hair is almost non-existent. During the fall and winter seasons the percentages can go from 0

to 20%. Wet blue with hair is separated and sold at a lower price. Unfortunately, not all the hair can be visible after wringing, and this can cause a very big problem to produce full grain, nubuks or corrected grain leathers.

Many times, the wet blue with fine hair is sold at a lower price and is downgraded. We estimate that downgrading reduces the wet blue selling price by 10 to 20%. Some types of leathers can accept some quantity of fine hairs like the automotive leathers that go to splitting and then have heavy mechanical action that can dislodge most of the fine hairs; the heavy finish with embossing also helps to make the residual fine hair not visible. Many automotive leathers are also snuffed. The biggest problem for the tannery is to process the wet blue for example to a nubuk, and then find out after buffing that the leather has residual fine hair, like as shown in Figure 9. This leather must be downgraded and sold as reject, reducing the value about 60% and sometimes resulting a discount claim against the wet blue supplier.

The severity of fine hair changes from year to year. Some years are better than others, but this is related only to the amount of fine hair. Every year wet blue will be produced with fine hair, the question is only how much.

Here are some historical and practical observations:

- Lighter hides and heifers usually have more hair than jumbo hides. The age difference between heifers and animals that have jumbo hides is usually three months. This is probably due to the increased surface area and amount of hair. The heavier hides also have more mechanical action that can dislodge the hair. In a drum most of the time the hides have the same weight, but it is frequently the case that a percentage of hides can be either lighter or heavier than the average of the load.
- Hides from large confinement areas like Amarillo and Finney County have a more uniform size of animal and breed. These areas have an irregular profile for fine hair.
- Hides from small farms have more diversified size of animal and breeds, and this brings an increased amount of fine hair.
- There is no pattern to when in the season the fine hair will be visible; sometimes one location may have hair in December, none in January and February and suddenly the percentage of hair increases in March and April.
- During late spring, summer and beginning of fall no fine hair is observed.
- On the drum by drum basis it is possible that in one day a few drums will have about 2% of leather with fine hair, and then the next 10 days no hair is observed.
- Black Angus is one of the most common breeds in north Texas; in the Texas area, Oklahoma and New Mexico, the Zebu and Brahma are predominant. These breeds are tropical breeds and will not withstand the harsh winter. Most probably these breeds suffer most with the winter in these locations and therefore produce a heavier and more stable coat in the winter. These hides also have a more intense problem of fine hair.
- Salted or brine cured hides have less problem with fine hair. During salting or brine curing the globular proteins are mostly removed. The hide permeability increases with the addition of salt. These hides require a longer soaking time and are properly soaked for further processing, much better than fresh hides that have a limited and improper soaking.
- Our observations do not clearly correlate the reduction of daylight hours to the increase of fine hair. In our opinion the temperature changes, breeds and nutrition play a more important role. What is surprising is that production can go many days without fine hair, and suddenly the problem appears for a few days and disappears again. Other times only a few drums have 5 to 10 hides with hair for a period, then the number of hides with hair can increase or simply not exist. Other times the fine hair appears at the end of October or late April, which are times that fine hair should not happen.

- In cattle raising in the United States, we have two important factors that severely affect hair cycling according to the literature: change of hours of sunlight and temperatures. In Figure 11 we have the US map with indication of cattle and calf population location. Also, we identified the average winter and summer temperatures for north and south which show the harsh winter in the north. The daylight hours at summer and winter solstice are also listed, In the north the difference can reach eight hours, and in the south, four hours.

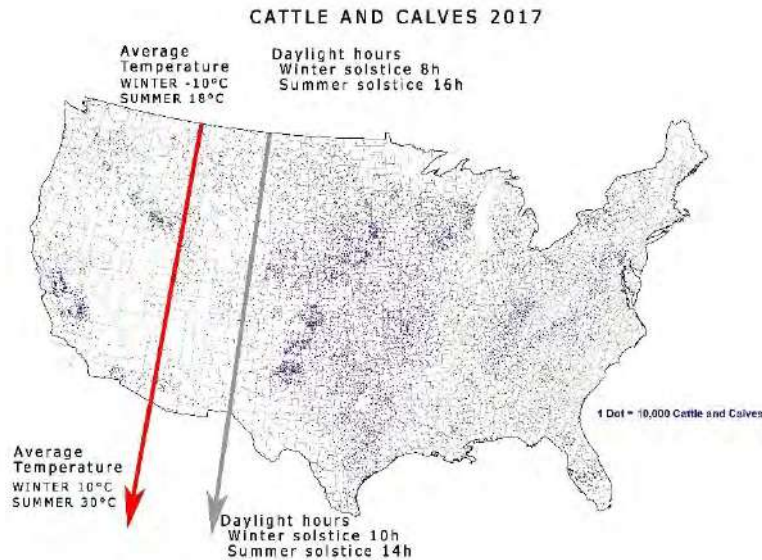


Fig. 11. Map of the US population of cattle and calves (30). We added information on average temperatures and daylight hours for the north and south. The numbers are estimated.

Factors that can minimize the fine hair problem:

- 1) Green fleshing. During wintertime the hides accumulate manure that makes it very difficult to properly flesh the hide without damaging it. Improper fleshing leaves the hide with a large amount of subcutaneous tissue and fat, which makes it more difficult to soak properly the hides.
- 2) Soaking. There is a need to extend the soaking times to counterbalance the improper fleshing. This is seldom possible because the tanneries run a very tight 24-hour processing time from soaking to liming. Proper soaking auxiliaries that remove the globular proteins and improve the permeability of the subcutaneous tissue can be used, as well as powerful wetting agents. Enzymes can play a very important role here.
- 3) Drum loads. Proper mechanical action is needed during soaking, unhairing, liming and deliming. Overloading in drums does not allow proper mechanical action needed to remove the hair. Not always it is possible to reduce the drum loadings.
- 4) Swelling control. When excessive swelling happens, the hair gets trapped inside the hair follicle and no chemical can further attack the hair. This is clearly visible Figure 6 where the hair seems to be almost intact. This can also be caused by insufficient reductive potential, where pH and reducing chemicals are not properly balanced.
- 5) Lime fleshing and lime splitting.
- 6) Uniform loads. There is a proper formulation for different weights of hides that also includes drum weight, alkalinity, reducing agents and auxiliaries. A mixed load can have improper balance and result in an increase on the amount of fine hair. Processing fresh hides makes it almost impossible to weight-break the loads for proper formula use.
- 7) Seasonal formulations. Formulations need to be adjusted for winter. Most tanneries have a summer and a winter formula. The formulas need to be used at the correct time.

- 8) Proper formulations. If formulations are not properly balanced for winter, having a security reserve of reducing agents, any variation associated with a process such as process time, improper drainage, float volume, mechanical action, drum load and mixed loads can have improper balance that will increase the amount of fine hair.

7 Acknowledgments

The authors thank Ms. Maureen Fitzer, Research Analyst, for the comprehensive work on literature search; Dr. Elton Hurlow and Ms. Debbie French for the review; and Dr. Thomas McNeel for the support on the unhairing tests.

References

1. Tancous, J.J., *Skin, Hide and Leather Defects*, Leather Industries of America, Lee Corporation, Cincinnati, OH, 45241, 1992
2. Merrill, H.B., *The Mechanism of Unhairing*, Chemistry and Technology of Leather, Krieger Publishing, Malabar, FL, USA, 1978
3. Thorstensen, T. C., *The use of sodium borohydride as an aid to Fine Hair removal*, JALCA 62, 181-190, 1967
4. Kuntzel, A. and Stirtz, T., *Hair Roots Studies*, JALCA, 53, 445, 1958
5. Stoves, J. L., *Some Biological and Chemical Properties of Animal Hair*, J. Soc. Dyers Colourists, 63,3, 1947
6. Scheger, A. V., *Relationship between cyclic changes in the hair follicle and sweat gland size in cattle*. Aust. J. Biol. Sci., Vol. 19, No. 4, pp. 607-617, 1966
7. Chase, H.B., Rauch, H. and Smith, V.W., *Physiol. Zool.* 24, 1, 1951
8. Butcher, E. O., *Development of the Papillary System and the Replacement of Hair in Mammals*, Ann. N.Y. Acad. Sci., 53, Art 3, 508, 1951
9. Paus, R. and Cotsarelis, G., *The biology of hair follicles*, New Eng. Jour. Med., V 341, 7, 491-497, 1999
10. Stenn, K. S. and Paus, R., *Controls of Hair Follicle Cycling*, Physiological Reviews, V.81, 1, 449-494, 2001
11. Yeates, N.T.M., *Photoperiodicity in Cattle*, Aust. J. Agric. Res. 6, 891-902, 1955
12. Dowling, D. F., *Seasonal Changes in Coat Characters in Cattle*, Proc. Aust. Soc. Anim. Prod. 2:69-80, 1958
13. Scheger, A.V. and Turner, H. G. *Analysis of coat characters of cattle*, Aust. J. Agric. Res. Vol. 11, No. 5, pp. 875-885, 1960
14. Hayman, R. H. and Nay, T., *Observations on hair growth and shedding in cattle* Aust. J. Agric. Res., Vol. 12, No. 3, pp. 513-527, 1961
15. Dowling, D.F., *The significance of the coat in heat tolerance of cattle*, Aust. J. Agric. Res., 10:5, pp. 744-748, 1959
16. Dowling, D.F. and Nay, T., *Cyclic changes in the follicles and hair coat in cattle*, Aust. J. Agric. Res. 11:1064, 1960
17. Berman, A. and Volcani, R., *Seasonal and Regional Variations in Coat Characteristics of Dairy Cattle*, Aust. J. Agric. Res., Vol. 12, No. 3, 528-538, 1961
18. Webster, A.J.F, Chlumecky, J. and Young, B. A., *Effect of cold environments on the energy exchanges of young beef cattle*, Can. J. Anim. Sci. 50:89, 1970
19. Nay, T. and Hayman, R. H., *Sweat glands in Zebu (Bos indicus L.) and European (B. taurus L) cattle*, Aust. J. Agric. Res., 7:5, 1956
20. Udo, H.M., *Hair Coat Characteristics in Friesian Heifers in the Netherlands and Kenya*, Wageningen, Netherlands, 78-6, 1978
21. Psaros, K.M., *Heritability of Hair Coat Shedding Scores in Angus Dams and the Relationship with Pre-Weaning Growth in their Calves*, M. Sc. Thesis in Animal Science, North Carolina State University, Raleigh, NC, 2013
22. Gray, K. A.; Smith, T.; Maltecca, C.; Overton, P.; Parish, J. A.; Cassady, *Differences in hair coat shedding, and effects on calf weaning weight and BCS among Angus dams*. J. P. Livestock Science, Vol. 140, No. 1-3, pp. 68-71, 2011
23. Gray, K.A., Cassady, J.P., Maltecca, C, Overton, P., Parish, J. A., Smith, T., *Hair Coat Shedding in Angus Cows*, BIF Annual Research Symposium, Bozeman, MT, June 1-4, 2011
24. Aiken, G.E., Pas, J.L., Looper, M.L., Taber, S.F. and Schrick, F. N., *Disrupted hair follicle activity in cattle grazing endophyte-infected tall fescue in the summer insulates core body temperatures*, The Professional Animal Scientist, 27, 336-343, 2011
25. Gilbert, R.P. and Bailey, D.R., *Hair coat characteristics and postweaning growth of Hereford and Angus cattle*, J. Anim. Sci., 69(2):498-506, 1991
26. Williams, A., *Hair Shedding Scores Relating to Maternal Traits and Productivity in Beef Cattle*, Undergraduate Honours Thesis, Animal Science Department, University of Arkansas, AK, 2013
27. Decker, J. and Parish, J., *Hair shedding scores: A tool to select heat tolerant cow*, e-Beef.org, 2017
28. Zugno, L.A., *Investigation of Fine Hair on American Cow Leathers Part I*, 114th ALCA Convention, Itasca, IL, USA, June 19-22, 2018
29. US Department of Agriculture. National Agricultural Statistics Service Document 17-M208 https://www.nass.usda.gov/Publications/AgCensus/2017/Online_Resources/Ag_Atlas_Maps/17-M208.php

SYNTHESIS AND APPLICATION OF DENDRITIC-LINEAR POLYMER PAMAM-Si FOR LEATHER FATLIQUORING PROCESS

Xuechuan. Wang^{1, a}, Siwei. Sun^{2, b}, Haijun. Wang¹ and Ji. Li¹

¹ College of Bioresources Chemical and Materials Engineering, Shaanxi University of Science & Technology, Weiyang District, Xi'an 710021, China.

² College of Chemistry and Chemical Engineering, Shaanxi University of Science & Technology, Weiyang District, Xi'an 710021, China.

a) Corresponding author: wxc-mail@163.com

b) susiesun16@163.com

Abstract. Environmental pollution caused by leather making is the primary concern in the development of leather industry. The use of safe, effective and multi-functional green chemical products has the advantages of reducing leather operations, increasing chemicals utilization, decreasing the environmental burden, improving leather quality. In this study, dendritic-linear polymers of PAMAM-Si 1G and PAMAM-Si 2G were applied to fatliquoring process, which were prepared by branching polysiloxane on the dendritic polyamide-amine (PAMAM). Then the emulsion properties, fatliquoring properties and fatliquoring mechanism were studied by EDS, SEM, XRD, TG and washing experiments. The conclusion was drawn that PAMAM-Si are weak alkali products with high emulsion stability. The particle size of PAMAM-Si 1G was 35.8 nm, and that of PAMAM-Si 2G was 26.7 nm. They can improve the softness, shrinkage temperature and physical and mechanical properties of leather. The softness of leather with PAMAM-Si 1G and PAMAM-Si 2G increased by 115.6% and 104.7% respectively. The shrinkage temperature of leather with PAMAM-Si 2G increased by 2.9 °C. The Breaking elongation of leather with PAMAM-Si 1G and PAMAM-Si 2G increased by 38.6% and 32.4% respectively. At the same time, PAMAM-Si not only increased the distance and disorder of fiber but combined with collagen fiber through hydrogen bond, electrovalent bond and a certain amount of physical adsorption and covalent bond.

1 Introduction

Environmental pollution caused by leather making is the primary concern in the development of leather industry ^[1]. Currently, the methods adopted to improve it are strengthening terminal treatment ^[2], promoting clean production technology ^[3] and developing new eco-friendly material ^[4-5]. The use of safe, effective and multi-functional green chemical products has the advantages of reducing leather operations, increasing chemicals utilization, lowering the cost of consumption, decreasing the environmental burden, improving leather quality and so on ^[6-7]. Therefore, it is considered the necessary product in reducing leather pollution.

Fatliquor agent is among the most important leather chemicals to decide the leather handle and applicability ^[8]. The earliest method is to put animal and plant oil in leather by soaking and painting. The oil is only effective on the surface but cannot penetrate into the leather sample, so the improvement on leather softness is not obvious. Later, a method of adding additional emulsifier was developed. But apart from the disadvantage of too many processes, the emulsion performance proved to be unstable, and the property of fatliquored leather was not uniform ^[9]. Therefore, some researchers developed a partial modifying method in which sulfate, sulfite oxidation, sulfonation and phosphorylation were employed to partly modify animal and plant oil for forming a self-emulsification system ^[10]. However, a large amount of abandoned fat and salt solutions will be produced in the modification process, thus, polluting the environment. In recent years, with the development of the petroleum products, synthetic oils based on petroleum products as fatliquoring agent gradually shows its unique performance, whose varieties and dosage are increasing ^[11]. The characteristic of this kind of product is the structure in accordance with the requirements of people, integrating various functions ^[12]. Bao et al. ^[13] synthesized polyurethane microemulsions (MC-PURs) by maleic anhydride modified castor oil (MCO),

PEG1000 (polyethylene glycol) and IPDI (isophorone diisocyanate) for leather to improve its softness. Nashy et al. [14] studied two different nano-emulsions based on methyl methacrylate/butyl acrylate copolymers as retanning and lubricating agents for chrome-tanned leather. But its linear molecular structure affects modification, resulting in poor leather quality, and failing to meet the various needs of fatliquoring.

Dendritic molecular, however, has three-dimensional molecular structure, making certain filling possible [15-16]. Moreover, its multiterminal reactive group can produce a large number of active site reaction to introduce functional groups and combine leather fiber closely. Qiang et al. [17] prepared a series of hyperbranched linear surfactants (HLS) by using oleic acid to modify the first generation hydroxyl-terminated hyperbranched polymer (HBP-1), which was obtained through a step synthesis method using trimethylolpropane and N,N-dihydroxyethyl dodecylamine-3-amine-methyl propionate (AB(2)-type monomer). Ibrahim et al [18] studied polyamidoamine hyperbranched polymer (HPAM), which significantly improves the shrinkage temperature, and the texture and softness of the leather. Li et al. [19] synthesized a novel leather chemical product from pentaerythritol, phosphorus oxychloride, melamine and tetrakis-hydroxymethyl phosphonium chloride (THPC) by three steps, which effectively inhibits leather burning and improve leather properties like fullness, softness, grain tightness.

In this study, dendritic-linear polymers of PAMAM-Si 1G and PAMAM-Si 2G were prepared respectively by branching polydimethylsiloxane which has excellent softness on the dendritic polyamide-amine (PAMAM). Then the emulsion properties of PAMAM-Si were studied. Finally, PAMAM-Si were applied to fatliquoring process. The properties of fatliquored leather were examined, and the interaction mechanism of PAMAM-Si and leather were discussed.

2 Experimental section

2.1 Materials

Hydrogen-terminated polydimethylsiloxane (H%=0.5, commercial product), allyl glycidyl ether and chloroplatinic acid (analytically pure) were obtained from Nanjing Chengong Silicon Co., Ltd., Jiangsu, China. Dendritic polyamide-amine (commercial product), which were purified by n-butyl alcohol, was purchased from Weihai Chenyuan Molecular New Materials Co., Ltd., Shandong, China. Synthetic fatliquor (DESOPON LQ-5, commercial product) was purchased from Decision Chemical Industrial Co. Ltd.

2.2 Synthesis

2.2.1 Synthesis of SEPDMS

First, HTPDMS (11.70 g, 27.68 mmol), AGE (3.00 g, 26.27 mmol) and toluene (20 g) were firstly charged into a 250 ml four-necked flask along with a low stream of nitrogen. When the temperature was heated to 75 °C, 0.15 wt% of Pt-catalyst was added to the flask. Then the mixture was heated to 90 °C and stirred for 6 h. The trace of platinum was removed by stirring with activated charcoal. The toluene of solvent was removed by rotary evaporator, and unreacted HPDMS was separated from the raw products in methanol. The prepared SEPDMS was colorless transparent oily liquid.^[20] IR (KBr, cm^{-1}): 2963, 2873 (aliphatic C-H stretching), 2129 (Si-H stretching), 1260 (Si-C-H bending), 1130~1000 (Si-O-Si stretching), 911 (Si-H bending), 798 (Si-C-H stretching); ¹H-NMR (300MHz, CDCl_3 , ppm): δ 4.72(s, 1H, -Si-H), 3.75 (d, 2H, -O-CH₂-CH-), 3.46 (t, 2H, -CH₂-O-), 3.18 (m, 1H, -CH-CH₂-), 2.61, 2.82 (d, 2H, -CH-CH₂-), 1.64 (m, 2H, -CH₂-CH₂-CH₂-), 0.6 (m, 2H, -CH₂-CH₂-), 0.20 (s, -Si-CH₃).

2.2.2 Synthesis of PAMAM-Si 1G

PAMAM 1G (8.33 g, 16.11 mmol) and isopropanol were mixed with constant stirring in a 250 ml four-necked flask. Then SEPDMS (10.00 g, 15.30 mmol) was dropwise added into the mixture for

30min. And the reaction of epoxy group and amino group was taken at a certain temperature and time. Then the product was redissolved in dichloromethane, and then precipitated and centrifugally separated several times to remove the excess PAMAM. The pale yellow viscous PAMAM-Si 1G was obtained by removing the solvent with rotary evaporator.^[16] IR (KBr, cm^{-1}): 3478, 3300 (primary amino N-H stretching), 2943, 2860 (aliphatic C-H stretching), 1648, 1550 (-NH-CO-), 2129 (Si-H stretching), 1260 (Si-C-H bending), 1130~1000 (Si-O-Si stretching), 911 (Si-H bending), 798 (Si-C-H stretching); ¹H-NMR (300MHz, D₂O, ppm): PAMAM 1G: δ 3.07 (m, 8H, -CO-NH-CH₂-), 2.61 (m, 8H, -CH₂-NH₂), 2.55 (m, 8H, -N-CH₂-), 2.44 (m, 4H, -CH₂-N-), 2.27 (m, 2H, -CH₂-CO-); PAMAM-Si 1G: δ 3.87 (d, 2H, -O-CH₂-CH-), 1.55 (m, 8H, -CH₂-CH₂-CH₂-), 0.52 (m, 2H, -CH₂-CH₂-), 0.08 (s, -Si-CH₃).

2.2.3 Synthesis of PAMAM-Si 2G

PAMAM 2G (11.91 g, 8.05 mmol) and isopropanol were mixed with constant stirring in a 250 ml four-necked flask. Then SEPDMMS (5.00 g, 7.65 mmol) was dropwise added into the mixture for 30 min. And the reaction of epoxy group and amino group was taken at a certain temperature and time. Then the product was redissolved in dichloromethane, and then precipitated and centrifugally separated several times to remove the excess PAMAM. The pale yellow viscous PAMAM-Si 2G was obtained by removing the solvent with rotary evaporator.^[16] IR (KBr, cm^{-1}): 3500~3300 (primary amino N-H stretching), 2958, 2860 (aliphatic C-H stretching), 1648, 1550 (-NH-CO-), 2129 (Si-H stretching), 1260 (Si-C-H bending), 1130~1000 (Si-O-Si stretching), 911 (Si-H bending), 798 (Si-C-H stretching); ¹H-NMR (300MHz, D₂O, ppm): PAMAM 2G: δ 3.29~3.20 (m, 24H, -CO-NH-CH₂-), 2.78 (m, 16H, -CH₂-NH₂), 2.75 (m, 24H, -N-CH₂-), 2.69 (m, 8H, -CH₂-N-), 2.55 (m, 4H, centre -CH₂-CH₂-), 2.38 (m, 24H, -CH₂-CO-); PAMAM-Si 2G: δ 3.87 (d, 2H, -O-CH₂-CH-), 1.56 (m, 8H, -CH₂-CH₂-CH₂-), 0.52 (m, 2H, -CH₂-CH₂-), 0.08 (s, -Si-CH₃).

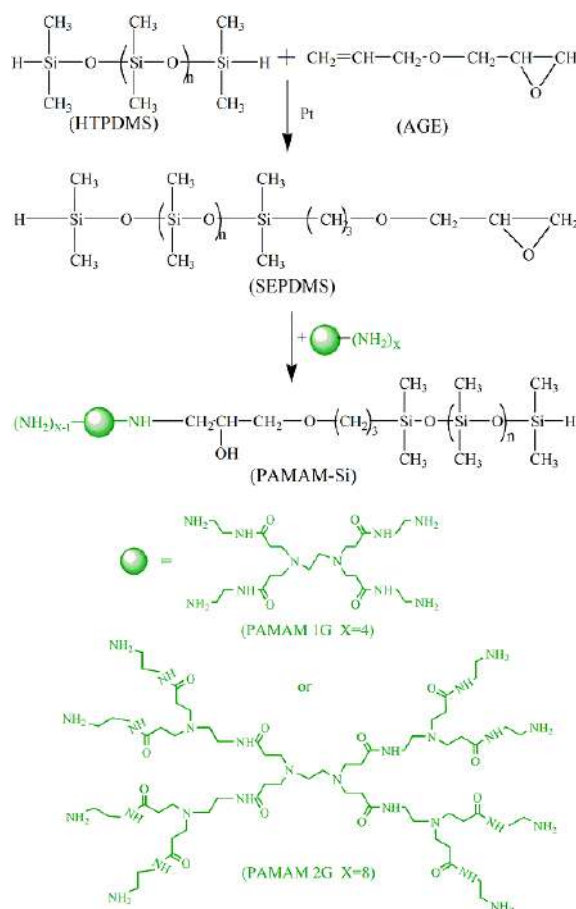


Fig. 1. Synthesis route of PAMAM-Si 1G and PAMAM-Si 2G.

2.3 Application in leather fatliquoring

For the fatliquoring research there were used sheepskin chrome tanned (wet-blue). The leather thickness was 0.8~1.1 mm. The leather was cut into 25 cm x 25 cm size samples. The shaved weight of the leather samples was recorded. Fatliquoring process with PAMAM-Si 1G, with PAMAM-Si 2G, with the commercial product (DESOPON LQ-5) and without any fatliquor was respectively carried out according to detailed methodology (Table 1) [21].

Table 1. The fatliquoring technology.

Process	Materials	Dosage (ω)/%	Temperature/°C	Time/min	PH	Remarks
Washing	water	300	30	10		
	water	100	30			
Neutralization	NaHCO ₃ (1:10)	1.5		120	5.5	
	fatliquor	10	55	60		
Fatliquoring	formic acid (1:10)	1.5		10+10+30	4.0	
Washing	water	200	30	10		Setting out

2.4 Analytical Methods

2.4.1 FT-IR and ¹H-NMR

The structure of PAMAM-Si obtained under optimal conditions was characterized using fourier infrared spectrometer (Vector-22, Bruker Daltronics Co., Ltd.), and proton nuclear magnetic resonance spectra (Avance-400MHz, Bruker Daltronics Co., Ltd.) [22].

2.4.2 Emulsion property

The stability of emulsion was measured by the particle size (Zetasizer NANO-ZS90, Malvern Instruments Co. Ltd.) and the property of that in acid, alkali or salt base fluid was conducted according to the reference [23].

2.4.3 Fatliquored leather property

Energy dispersive spectrometer (Octane Prime, EDAX Co. Ltd.) was used to observe the distribution of silicon in leather. The loose degree of collagen fiber was observed by scanning electron microscope (SEM Q45, FEI Company.). The distance of collagen fiber was obtained by X-ray diffraction instrument (D/Max2200PC, Rigaku Co. Ltd.), equipped with Cu-Ka radiation source to identify the d-spacing of MMT. The X-ray generator operated at 40 kV, 40 mV, with a scanning speed of 2°/min and $\theta=5^\circ \sim 60^\circ$. Thermogravimetry was used to determine the thermostability of leather, in which the heating rate was 10 °C/min and the range of temperature was from 25 °C to 600 °C.

2.4.4 Binding form

The combination rate of PAMAM-Si refers to the ratio of the changed weight of sample before and after processing and the combined PAMAM-Si total weight with sample. Samples without any fatliquor, with PAMAM-Si 1G, and PAMAM-Si 2G were washed by water, acetone solution ($m_{\text{acetone}}:m_{\text{water}}=1:1$) and dilute alkali solution ($\omega_{\text{Na}_2\text{CO}_3}=0.5\%$) in turn. Every treatment was repeated many

times until a constant weight (difference between parallel measurements < 1%) was obtained. It was kept washing until a constant weight (1% difference between parallel measurements)

3 Results and discussion

3.1 Emulsion property

Table 2. Emulsion properties of PAMAM-Si.

Parameters	PAMAM-Si 1G	PAMAM-Si 2G
Appearance	Pale yellow transparent oily dope	Pale yellow transparent oily dope
pH	8.5~9.0	8.5~9.0
Particle size ($\omega=10\%$)	35.8 nm	26.7nm
1:9 dilution emulsion (48 h)	uniformity	uniformity
Potassium chromium sulfate solution (1 mol/L)	uniformity	uniformity
Hydrochloric acid solution (1 mol/L)	uniformity	uniformity
Ammonia solution(1 mol/L)	uniformity	uniformity

Table 2 shows that PAMAM-Si 1G and PAMAM-Si 2G were weak alkali products with high stability against acids, alkalies and chromium salts. There was not a sedimentation in the PAMAM-Si dilution ($\omega=10\%$) for 48 h at 25 °C. It is worth noting that the particle size of PAMAM-Si 1G was 35.8 nm, and PAMAM-Si 2G was 26.7, far less than the collagen fiber distance of 50~300nm^[24], which was better to permeate into leather and distribute uniformly for PAMAM-Si.

3.2 Leather property

Table 3. Properties of the leather by Fatliquor.

Parameters of leather	Experiments			
	I Without	II Commercial	III PAMAM-Si 1G	IV PAMAM-Si 2G
Softness/mm	1.92	4.54	4.14	3.93
Thickness/%	-3.33	5.88	12.35	5.49
Shrinkage temperature /°C	99.40	98.10	100.50	102.30
Tensile strength/MPa	27.61	27.14	29.84	35.91
Breaking elongation/%	77.69	114.04	107.71	102.84
Tear strength/(N/mm)	67.73	68.56	68.72	73.03
Permeability of water /{mg/(10cm ² ·24h)}	0.50	0.52	0.54	0.54

Wet-blue leather was fatliquored using PAMAM-Si 1G and PAMAM-Si 2G, as well as commercial product (LQ-5) and anything with comparable aim. The properties of leather fatliquored were presented in Table 3. Compared with blank, the properties of leather fatliquored by PAMAM-Si

were improved in softness, thickness, shrinkage temperature, mechanical properties and permeability of water. To softness, leather fatliquored by PAMAM-Si 1G and PAMAM-Si 2G were similar with leather fatliquored by commercial product. The softness of leather with PAMAM-Si 1G and PAMAM-Si 2G increased by 115.6% and 104.7% respectively. The thickness of sample with PAMAM-Si 1G was the highest among these samples, which was due to that the spheric structure of PAMAM-Si has better filling effect than the line structure of commercial product. And it is important to note that the thickness changed rarely, because the more active groups (e.g. amine group) PAMAM-Si 2G contains, the stronger it's interconnection with leather. The results of shrinkage temperature and mechanical properties were as what described above. Especially, the shrinkage temperature of leather with PAMAM-Si 2G increased by 2.9°C. The Breaking elongation of leather with PAMAM-Si 1G and PAMAM-Si 2G increased by 38.6% and 32.4% respectively. That is to say, PAMAM-Si serves as a bridge between fiber-to-fiber, in which the active groups offer interconnecting site with fiber, and the spheric structure fills interfiber. In addition, the improvement of water permeability of leather fatliquored by PAMAM-Si indicated that hygienic property improved.

3.3 Distribution of PAMAM-Si in leather

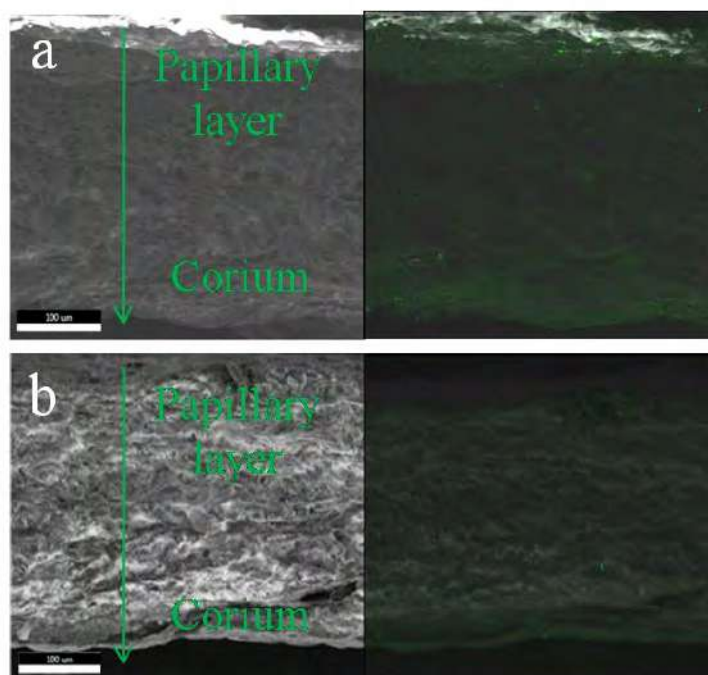


Fig. 2. EDS results of silicon by scanning of longitudinal section with PAMAM-Si 1G (a) and PAMAM-Si 2G (b).

Figure 2 shows the EDS results of silicon by scanning of longitudinal section of crust leather with PAMAM-Si. The green point stands for the silicon, which shows the distribution of PAMAM-Si in leather. Fatliquoring process is the balance between permeating and combining, rather than physical filling for fatliqur in leather. Since leather has papillary layer and corium, different fiber waving structures which leads to different degree of interaction between fatliqur and leather, the distribution of fatliqur in longitudinal section is not uniform. From the samples with PAMAM-Si 1G (Fig. 2a) and PAMAM-Si 2G (Fig. 2b), it can be noted that silicon was distributed in the whole section, but it can be also noted that the content of silicon decreased first, then increased, along with papillary layer to corium, revealing that the content is higher in papillary layer than that in corium, and lowest in the centre of the whole section. It also indicated that PAMAM-Si was distributed into

the whole leather, and enriched on both sides, which was attributed to the fact that the excess combined PAMAM-Si with leather took effect on further permeation. Moreover, the content of silicon in sample containing PAMAM-Si 1G was higher than that in sample containing PAMAM-Si 2G, consistent with that in molecule.

3.4 Loose degree of collagen fiber

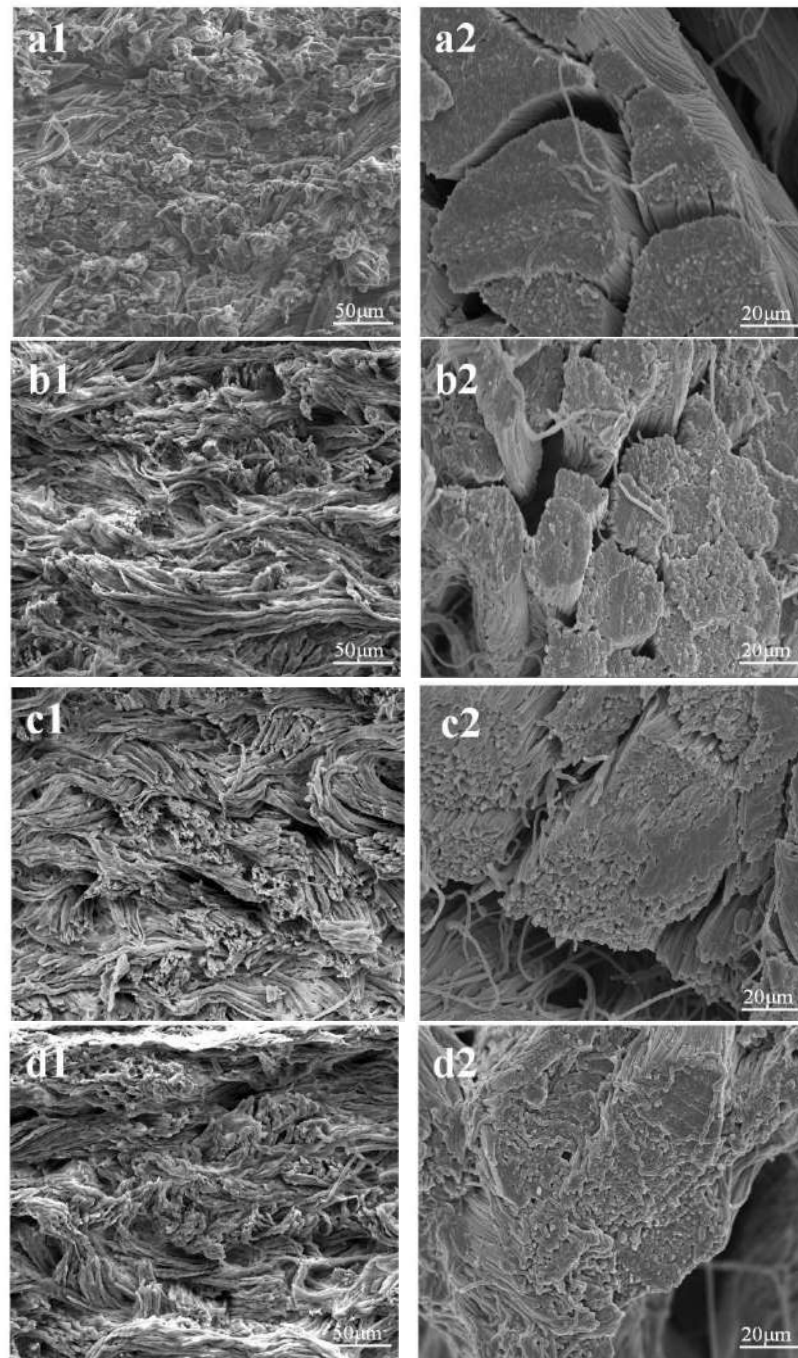


Fig. 3. SEM of leather fatliquored without anything (a), with commercial product (b), with PAMAM-Si 1G (c) and with PAMAM-Si 2G (d); 1:x1 k, 2:x10 k.

Fatliquoring agent is mainly used to reduce friction and increase space between fibers, so as to achieve soft leather. Therefore the fiber loose degree of fatliquored leather proves the soft performance. Fiber arrangement of longitudinal section under low multiple can be observed from Fig. 3(1). The sample without any fatliquror was arranged closely, and that with commercial product, PAMAM-Si 1G and PAMAM-Si 2G distributed loosely and random, indicating that the spheric structure of PAMAM-Si has filling effect on increasing interfiber space, meanwhile there was more flexible long chain in commercial fatliquror and PAMAM-Si 1G attached fiber surface to decrease resistance force for fibers movement than that in PAMAM-Si 2G. Under high multiple, the above phenomenon was more noticeable (Fig. 3(2)). Fibril packing without any fatliquror arranged neatly and closely, dividing clearly, but that with commercial product distributed to small clusters and increased the gap. It is worth noting that the disorder of arrangement and mutual crosslinking degree increased and some small random fibers appeared among fibril packing with PAMAM-Si 1G and PAMAM-Si 2G, on account of the increased combination of multi terminal active groups and fibers.

3.5 Fiber distance

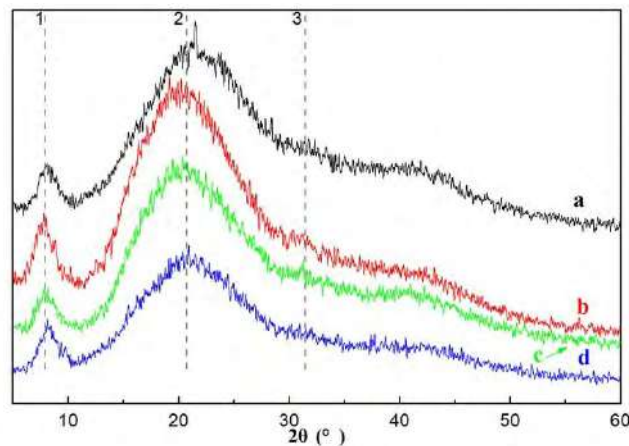


Fig. 4. XRD curves of leather samples without any fatliquror (a), with commercial product (b), with PAMAM-Si 1G (c) and with PAMAM-Si 2G (d).

Table 4. XRD results of leather samples without any fatliquror (a), with commercial product (b), PAMAM-Si 1G (c) and PAMAM-Si 2G (d).

Sample	$2\theta_1$	$2\theta_2$	$2\theta_3$	d1a	d2a	d3a
Without	7.967	21.522	31.425	1.108	0.412	0.284
Commercial	7.715	20.044	31.133	1.144	0.442	0.287
1GPAMAM-Si	7.847	19.501	31.080	1.125	0.455	0.287
2GPAMAM-Si	8.168	20.409	31.242	1.081	0.435	0.286

^a Bragg equation: $2d\sin\theta=\lambda$, $\lambda=0.154$, $d=\lambda/2\sin\theta=0.077/\sin(2\theta/2)$.

The loose degree of fatliquored leather fiber increased and the order degree of fatliquored collagen fibril packing with PAMAM-Si decreased significantly against the blank sample, (Fig. 3). The progress of fatliquror could not only change the external form of the leather fibril packing, to a certain extent, but change its internal structure as well. XRD curves of leather samples without any fatliquror (a) and with PAMAM-Si (b) are shown in Fig.4. Three main diffraction peaks appeared in the XRD curves of leather fiber: the first sharp peak at $7^\circ\sim 8^\circ$ indicates the distance between the molecular chains,

the broad peak at 20° is due to diffuse scattering and the third peak at 30° corresponding to the unit height, typical of the triple helical structure^[25-26]. According to Bragg equation to calculate the spacing of area corresponding to 2θ , the results were summarized in Table 4. $2\theta_1$ of leather fatliquored by PAMAM-Si 2G was in comparison with blank, but that by commercial product and PAMAM-Si 1G significantly reduced, indicating that the distance between the collagen fiber molecular chains increased. $2\theta_2$ of leather fatliquored is smaller than that of leather without any fatliquor, revealing that the disorder of arrangement increased. Meanwhile $2\theta_3$ of various samples were very close, in accordance with a single residue triplex pitch. Combined with the size of PAMAM-Si 1G and PAMAM-Si 2G emulsion, PAMAM-Si can permeate into fiber, increase fiber distance, combine with fiber active groups and enhance fiber arrangement disorder. In addition, PAMMA-Si 2G has larger molecule structure and more amino groups, which formed stronger bonds with fibers, resulting in that fiber distance changed insignificantly. Notably, the progress of various fatliquors did not destroy the molecular structure of collagen.

3.6 Leather thermal property

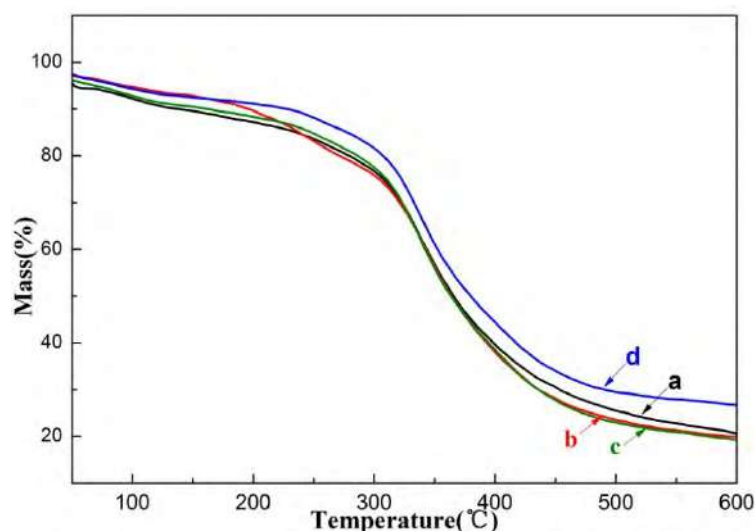


Fig. 5. TG curves of leather samples without any fatliquor (a), with commercial product (b), with PAMAM-Si 1G (c) and with PAMAM-Si 2G (d).

The thermal degradation curve of leather samples after fatliquoring was divided into two stage (Fig.5): When the temperature remained from 25°C to 230°C , the loss weight was mainly evaporable moisture and small molecules; At the second stage, the temperature was ranged from 230°C to 600°C , during which under the action of heat, the collagen intermolecular hydrogen bond, Vander Waals force and coordination bond ruptured, collagen structure destroyed and molecular chain distorted, then collagen was degraded to peptide and amino acid, finally amino acid residues were destroyed, deaminated and dehydrated^[27-28].

At the first stage, the sample with commercial fatliquor thermal weight loss was the highest. Commercial fatliquor contained small molecules volatile oil, which led to the increase of degradation rate and decrease of the weight.

The order of sample thermal degradation rate at the second stage is described as follows: with PAMAM-Si 2G < with PAMAM-Si 1G < without any fatliquor << with commercial Fatliquor. It was attributed to the fact that a large number of active groups of PAMAM-Si 2G enhanced the interaction with fibers, giving rise to the decrease of thermal degradation rate. On the contrary, commercial fatliquor increased the distance and reduced fiction, resulting in the increase of thermal degradation rate. The polysiloxane chain was filled among fibers to reduce their interaction. The

polysiloxane chain content of PAMAM-Si 1G was higher than that of PAMAM-Si 2G, and the active group number was lowered. Therefore, at the beginning of second stage, the increased fiber gap reduced fiction and enhanced degradation rate, but the combination reduced degradation rate later.

3.7 Binding form

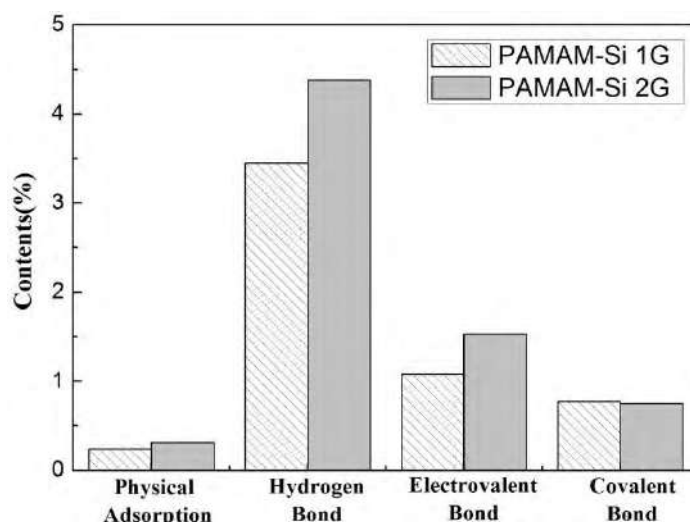


Fig. 6. Binding form of PAMAM-Si 1G and PAMAM-Si 2G with leather.

Water washing can remove the physical adsorption on the leather; acetone liquid washing can remove combination with collagen fiber by hydrogen bond; dilute alkali washing can remove substances by electrovalent bond; the remaining amount after dilute alkali washing can be considered to be material combined with collagen fiber base on the form of covalent bond. The bank is standard.

Sample after water washing, the combination of PAMAM-Si 1G fell by 0.24 %, the combination of PAMAM-Si 2G fell by 0.31 %; After acetone liquid washing, PAMAM-Si 1G fell by 3.45 % and PAMAM-Si 2G by 4.38 %; After dilute alkali washing, PAMAM-Si 1G fell by 1.08 % and PAMAM-Si 2G by 1.53 %; After the above treatment, PAMAM-Si 1G reduced to 0.77 %, PAMAM-Si 2G to 0.75 %, indicating that the binding form between PAMAM-Si and collagen fiber was mainly hydrogen bond, electrovalent bond and a certain amount of physical adsorption and covalent bond. Hydrogen bond was the combination among PAMAM-Si peripheral amino and hydroxyl, amino and carboxyl of leather. The electrovalent bond was generated by the partial amino with a positive charge (NH^{3+}) and ionized carboxyl with negative charge (COO^-) in experimental condition. And a few amino was reacted with hydroxyl group or carboxyl group of collagen fibers to make covalent bond. Fig. 6 shows that the amount of hydrogen bond and electrovalent bond between PAMAM-Si 2G and leather was significantly more than that of PAMAM-Si 1G. The combined group was mainly amino in PAMAM-Si. PAMAM-Si 2G has larger molecule structure and more amino groups than PAMAM-Si 1G, which was helpful to combine leather tightly and enhance interaction. The interaction mechanism of PAMAM-Si and collagen fiber was shown in Fig. 7.

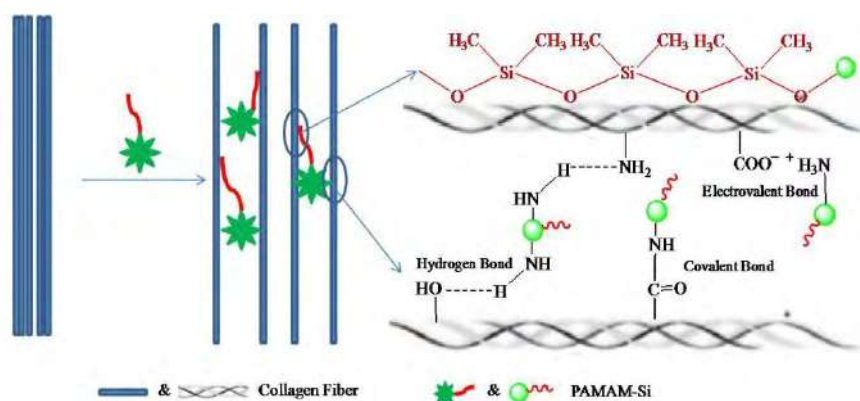


Fig. 7. Schematic illustration of PAMAM-Si in the collagen fiber.

4 Conclusions

The dendritic-linear polymer PAMAM-Si was prepared with 1G and 2G PAMAM and SEPDMs obtained by hydrosilylation reaction. The molecular structure of PAMAM-Si was characterized by FT-IR and ¹H-NMR. According to the investigation of emulsion properties, PAMAM-Si were weak alkali products, with high stability against acids, alkalies and chromium salts. The particle size of PAMAM-Si 1G was 35.8 nm, and PAMAM-Si 2G was 26.7 nm.

When PAMAM-Si was applied to fatliquoring process, the softness, fullness, physical and mechanical properties and healthiness of fatliquored leather were significantly improved. The silicon content of PAMAM-Si 1G was higher than that of PAMAM-Si 2G, so the softness of leather with PAMAM-Si 1G was superior to that of PAMAM-Si 2G. However, there are more active groups in PAMAM-Si 2G. Therefore, when it was combined with PAMAM-Si 2G, the interaction of fibers became stronger and shrinkage temperature and physical and mechanical properties of crust changed more obviously.

PAMAM-Si can permeate into the skin and distribute between the collagen fibers, increase the distance and disorder, but not destroy the molecular structure of collagen. There are interaction with PAMAM-Si and collagen fiber. It improved the thermal properties of the fiber. The binding form of PAMAM-Si and collagen fiber was mainly hydrogen bond, electrovalent bond as well as a certain amount of physical adsorption and covalent bond. Hydrogen bond was the combination among the peripheral amino of PAMAM-Si and hydroxyl, amino and carboxyl of leather. The electrovalent bond was generated by the partial amino with a positive charge (NH³⁺) and ionized carboxyl with negative charge (COO⁻) in experimental condition. And a few amino were reacted with hydroxyl group or carboxyl group of collagen fibers to make covalent bond.

References

1. Jayanthi, D.; Victor, J. S.; Chellan, R.; Chellappa, M.: (2019). Green processing: minimising harmful substances in leather making, *Environ Sci Pollut Res*, 26(7), 6782-6790, 2019
2. Rahman, M. S.; Islam, M. R.; Mondol, O.; Rahman, M. S.; Sabrin, F.; Zohora, U. Screening of Protease Producing Bacteria from Tannery Wastes of Leather Processing Industries at Hazaribag, Bangladesh. *JUJBS*, 7(1), 23-34, 2018
3. Rosu, L.; Varganici, C. D.; Crudu, A. M.; Rosu, D.; Bele, A.: Ecofriendly wet-white leather vs. conventional tanned wet-blue leather. a photochemical approach, *J Clean Prod*, 117(10), 708-720; 2017
4. Errasti, M.E.; Caffini, N.O.; López, L.M.I.: Proteolytic extracts of three Bromeliaceae species as eco-compatible tools for leather industry, *Environ Sci Pollut Res*, 25(22), 21459–21466, 2018
5. Ramalingam, S.; Sreeram, K. J.; Rao, J. R.: Hybrid composites: amalgamation of proteins with polymeric phenols as a multifunctional material for leather processing, *RSC Advances*, 5(42), 33221-33232, 2015

6. Abul, H. M.; Abdul, M. M.; Mehedi, H.: Leaf paste aided goat skin preservation: significant chloride reduction in tannery, *J. Environ. Chem. Eng.*, 6(4), 4423-4428, 2018
7. Sun, X.; Jin, Y.; Lai, S.; Pan, J.; Du, W.; Shi, L.: Desirable retanning system for aldehyde-tanned leather to reduce the formaldehyde content and improve the physical-mechanical properties, *J Clean Prod*, 175(20), 199-206, 2018
8. Jan, A.; Krzysztof, M.; Katarzyna, M.; Agnieszka, T.: Research on application of flax and soya oil for leather fatliquoring, *Journal of Cleaner Production*, 65(15), 583-589, 2014
9. Sivakumara, V.; Rao, P.G.; Ramabrahama, B.V.; Swaminathana, G.: Power ultrasound in fatliquor preparation based on vegetable oil for leather application, *Journal of Cleaner Production*, 16(4), 549-553, 2008
10. Leticia M. S.; Mariliz, G.: Reusing of a hide waste for leather fatliquoring, *J Clean Prod*, 15(1), 12-16, 2007
11. Du, J.; Shi, L.; Peng, B.: Amphiphilic acrylate copolymer fatliquor for ecological leather: influence of molecular weight on performances, *J Appl Polym Sci*, 133(20), 43440, 2016
12. Lv, B.; Gao, J. J.; Ma, J. Z.; Gao, D. G.; Wang, H. D.; Huang, X. W.: Nanocomposite based on erucic acid modified montmorillonite/sulfited rapeseed oil: Preparation and application in leather, *Appl Clay Sci*, 121, 36-45, 2016
13. Bao L.H.; Lan Y. J.; Zhang S. F.: Aliphatic anionic polyurethane microemulsion leather filling-retanning agent, *Journal of the Society of Leather technologists and Chemists*, 91(2), 73-80, 2007
14. Nashy, El-Shahat H. A.; Essa, Mohamed M.; Hussain, Ahmed I.: Synthesis and application of methyl methacrylate/butyl acrylate copolymer nanoemulsions as efficient retanning and lubricating agents for chrome-tanned leather, *Journal of applied polymer science*, 124(4), 3293-3301, 2012
15. Zhu, W. P.; Gao, J.; Sun, S. P.; Zhang, S.; Chung, T. S.: Poly (amidoamine) dendrimer (pamam) grafted on thin film composite (tfc) nanofiltration (nf) hollow fiber membranes for heavy metal removal, *J Membrane Sci*, 487, 117-126, 2015
16. Wang, X. C.; Sun, S. W.; Wang, H. J.; Guo, X. X.: Synthesis and characterization of polysiloxane grafted polyamide-amine surfactants, *J Surfactants Deterge*, 20(2), 1-8, 2017
17. Qiang, T. T.; Bu, Q. Q.; Huang, Z. F.; Wang, X. C.: Synthesis and characterization of hyperbranched linear surfactants, *J Surfact Deterg*, 17(2), 215-221, 2014
18. Ibrahim, A. A.; Youssef, M. S. A.; Nashy, E. H. A.: Using of hyperbranched poly (amidoamine) as pretanning agent for leather, *International Journal of Journal of Polymer Science*, (5), 690-695, 2013
19. Li, B.; Li, J. X.; Li, L. X.: Synthesis and application of a novel functional material as leather flame retardant, *J Am Leather Chem As*, 109(7), 239-245, 2014
20. Tang C, Liu W.: Syntheses of novel photosensitive polysiloxanes and their effects on properties of UV-cured epoxy methacrylate coatings, *J Coat Technol Res*, 7(5), 651-658, 2010
21. Jia, L.; Ma, J, Z.; Gao, D. G.; William R.T.; Sun, L. Y.: A star-shaped POSS-containing polymer for cleaner leather processing, *J Hazard Mater*, 361(5), 305-311, 2019
22. Shi, X. Y.; Lesniak, W.; Islam, M. T.: Comprehensive characterization of surface-functionalized poly (amidoamine) dendrimers with acetamide, hydroxyl, and carboxyl groups, *Colloid Surface A*, 272(1), 139-150, 2006
23. GB/T 6369-2008, Surface active agents-determination of emulsifying power-colorimetric method [S]. Beijing: China Standard Press, 2008.
24. Maxwell C A, Wess T J, Kennedy C J.: X-ray diffraction study into the effects of liming on the structure of collagen, *Biomacromolecules* 7(8):2321-6, 2006
25. Yang, Q.Y.; Qin, S.F.; Chen, J.F.; Ni, W.; Xu, Q.: Supercritical Carbon Dioxide-assisted Loosening Preparation of Dry Leather, *Applied polymer*, 113(6), 4015-4022, 2009
26. Gao, X.; Zhou, J. F.; Huang, X.: Facile synthesis of mesoporous sulfated Ce/TiO₂ nanofiber solid superacid with nanocrystalline frameworks by using collagen fibers as a biotemplate and its application in Esterification, *RSC Advances*, 4(8), 4010-4019, 2014
27. Zoltán, S.; Zsuzsanna, C.; Elena, B.; Cristina, C.; Claudiu, S.; Eszter B.; Rajnaia, J.; Lucretia, M.; Emma, J.: Thermal characterization of new, artificially aged and historical leather and parchment, *Journal of Analytical and Applied Pyrolysis*, 115, 419-427, 2015
28. Marcillaa, A.; Garcíaa, A. N.; Leóna, M.; Martínezb, P.; Bañónb, E.: Study of the influence of NaOH treatment on the pyrolysis of different leather tanned using thermogravimetric analysis and Py/GC-MS system, *Journal of Analytical and Applied Pyrolysis*, 92(1), 194-201, 2011

LIGNIN MODIFIED PHENOLIC SYNTAN - A CONTRIBUTOR TO OUR BIO-BASED SOLUTIONS

Yujie Ma^{1a}, Petra Berends¹, René Pauli¹, Mark Wijland¹, Roberto Rumnit¹ and Rob Meulenbroek¹

1 Smit & zoon, Nijverheidslaan 48, 1382LK Weesp, the Netherlands

a)Corresponding author: Yujie.Ma@smitzoon.com

Abstract. Bio-based chemicals are considered to play a central role in our transition towards a bio-based and circular economy and contribute to a more sustainable leather manufacturing process with reduced environmental impact. One of the logical steps in this direction is to increase the renewable contents of existing leather chemicals. Towards this end we've developed a patent-pending technology for the production of new types of polyphenolic syntan products, in which industrial lignins are used during the chemical conversion process to replace part of the phenol used in the production of otherwise 100% petro-based polyphenolic retanning chemicals. We have shown that our innovative technology is compatible with most of the industrial lignins (kraft, soda, organosolv, hydrolysis) from different origins (soft/hard wood, grass, straw). The obtained polyphenolic products have tanning power and are suitable to be used as retanning agents for various types of leather rendering good organoleptic properties with additional added value of increased bio-based content and improved biodegradability that can contribute to decrease the effluent treatment load. Moreover, these products can be tailor-made to meet low emission (low free phenol, low free formaldehyde) requirements.

1 Introduction

In order to contribute to a more sustainable leather manufacturing process and leather value chain, in 2016 Smit & zoon started its own designing process of new products through the Bio-Based innovation platform. As a logical first step, answers to several key questions have been looked for: What is Bio-Based? What is renewable? Which term and method do we use to define the Bio-Based content in the Bio-Based platform? What is biodegradable? How do our current products perform? What is our vision for future products? In the process of answering these questions and guided by the Cradle-to-Cradle (C2C) Certified™ program, Material Reutilization Score (MRS) was used to obtain deeper insights into the formulation and environmental performance of our leather chemicals and treated as the basis for the design of new generation bio-based chemicals. Three main focus areas are setting the tone of current activities in the Bio-based platform: 1. Increasing the renewable contents of the existing product groups; 2. Smart valorization of industrial side streams from biological origin and 3. Improving the general biodegradability of leather chemicals. While focusing on such topics, it is well-understood that a proper balance needs to be found between cost, sustainability and performance. In the mean time, leather's end of life scenario plays a role and needs to be revisited.

Many polyphenolic macromolecules are routinely used in the manufacturing of leather. These water soluble compounds are either of natural origin such as tannins and lignosulfonates or of largely petro-chemical nature such as phenolic syntans.^{1,2} The use of petro-chemical building blocks in the manufacturing of phenolic syntans not only contributes to their relatively high Carbon Footprint (CF)³ but also poses harmful emission risks. Improvements in syntan's petro-chemical nature are expected to eliminate these problems and contribute to a more sustainable leather value chain. In one study carried out following the C2C methodologies, Material Reutilization Scores (MRSs) of different groups of leather wet-end chemicals have been calculated and compared.⁴ MRS takes into account the combined effect of the renewability and biodegradability of chemical ingredients in a product. The preliminary results indicate that improvements in syntan's MRS is likely to generate bigger positive impacts compared to other wet-end chemicals e.g. natural oil-based fatliquors. To this end, a priority area in our bio-based

research platform is to improve the bio-based content of syntan products. Lignin, a natural polyphenol being the most abundant natural aromatic resource is well-known for its role in woody biomass to give resistance to biological and chemical degradation due to its hydrophobic nature and insolubility in aqueous systems. Derived from natural lignin, liginosulfonate presents sulfonate groups that make it water soluble is by far the only type of lignin used as such in leather making processes. As the most important source of bio-based aromatics, the valorization of lignin streams that are currently mostly used directly for producing process energy has become an increasingly important topic for the bio-based and circular economy. In this paper, the first examples of using water insoluble industrial lignins as phenol replacements for the manufacturing of phenolic syntan are discussed.

2 Materials and methods

2.1 Materials

Lignin contains three different structural components/monomers: p-coumaryl, coniferyl and sinapyl alcohol in p-hydroxylphenyl (H), guaïacyl (G) and syringul (S) units, respectively (see Figure 1).⁵ The cross-linked structure of lignin is very complex and can vary a lot depending on the specific species, the season, the geological region/climate and the age of the plant. Generally speaking the H/G/S composition strongly depends on the type of plant: hardwood mainly contains G and S, soft wood mainly G and grass species contains all three.

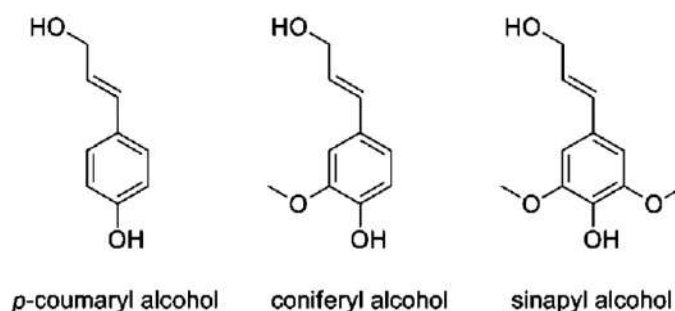


Fig. 1. Building blocks of lignin (adapted from Ref. 5).

Table 1 presents an overview of most of the different lignin types used in this study, they vary not only in their origin/biomass feedstock, but also in the type of pretreatment applied prior to lignin separation. It is worth noting that as a result of these variations, each specific type of lignin may present different composition of functional groups: namely varying contents of phenolic, aliphatic and carboxylic hydroxyl groups. In addition to those listed in the table, some lab-scale prototypes have also been tested. All lignins used in this study have similar physical form as a (dark) brown powder.

Table 1. Types of lignin used in this study, their origin and typical characteristics.

Type of lignin	Pretreatment Chemistry	purity	Ash	Mw (g/mol)	origin
Kraft	Alkaline	high	low	≤ 6000	soft & hard wood
Soda	Alkaline	high	low	≤ 6000	grass/straw
hydrolysis	Acid	moderate	low	n.a.	wood
organosolv	Acid	Very high	low	≤ 2000	wood

Depending on the type of applications either pickled calf pelt, chrome-tanned calf wet-blue (WB) or glutardialdehyde-tanned wet-white (WW) are used as starting materials for leather trials.

2.2 Methods

The synthesis of lignin modified syntan follows a modified procedure largely based on the traditional synthesis of phenol-aldehyde condensates or phenol-urea-aldehyde condensates.^{1,6} Depending on the type of lignin chosen, lignin is added in its original powder form after phenol sulfonation. Afterwards the condensation with different aldehydes or mixture of aldehydes took place with or without the addition of urea at elevated temperatures. After termination of the polymerization, the pH of the reaction mixture is adjusted to obtain a clear liquid product. The product can be further processed, for example by spray-drying, to obtain a powder product.

The molecular weight (Mw) of the lignin and lignin modified phenol-urea-formaldehyde polymer is measured by alkaline gel permeation chromatography (GPC) according to the procedure described by Gosselink et al.⁷

GPC analysis of representative samples based on different types of lignins following varying polymerization procedures are carried out at neutral pH using a PSS MCX column combination medium and the elution curve is recorded using a UV-detector at 280 nm. Standard used for calibration of the molar mass distribution are sodium polystyrene sulfonates with a molecular weight range of 891 to 976000 dalton.

Shrinkage temperature (Ts) tests are performed according to IUP 6. Ready biodegradability test of chemicals is done following an in-house Manometric Respirometry method based on OECD 301F. Free phenol is determined by an in-house method using Emerson's reagent and detected by UV-Vis spectroscopy.⁸

Free formaldehyde is determined by an in-house method using acetylacetone and ammonium acetate and detected by UV-Vis spectroscopy at 412 nm. Free glyoxylic acid is determined by an in-house titration method using hydroxylamine.

3 Results and Discussion

3.1 Incorporation of lignin to the product

All the lignins listed in the previous section can be used for the preparation of lignin-phenol based polycondensates. However, every lignin type requires (slight) modifications on the synthesis procedure and results in syntans with different product characteristics (e.g. Mw, viscosity) and different effects on leather. The maximum lignin:phenol ratio (w/w) also varies per lignin type.

There are strong indications that lignin is participating in the polycondensation reaction and not just incorporated in the final product in a sulfonated form: 1. The amount of sulfuric acid used in the reaction is either in very slight excess to even not enough to completely sulfonate the phenols used. In either case the sulfuric acid concentration seems to be too low⁹ to allow lignin sulfonation or phenolation under the applied experimental conditions. Only after the initiation of the polycondensation reaction with the addition of the aldehydes the slow dissolution of the insoluble lignins is observed when viscosity build-up becomes obvious eventually leading to almost total dissolution of all insolubles. 2. Even when the amount of sulfuric acid used is not even enough to sulfonate all the phenol the lignin dissolution at the end of the condensation procedure is still observed. 3. A somewhat higher Mw is obtained when products are made following similar procedures but replacing the 100% phenol with a combination of phenol and lignin. 4. Comparison of alkaline GPC results on the original lignin and the product with lignin incorporated in the chemical recipe clearly shows Mw build up after the synthesis with no exact overlap of any peak values. Theoretically there are probably several chemical reactions taking place at the same time. First of all, lignin does contain phenolic hydroxyl groups, which would be the most obvious possibility for lignin to act just as a phenol to participate in the polycondensation reaction. Secondly, lignin can also be

phenolated under acidic conditions and eventually resulting in its incorporation into the polymers. A third possibility is the self-condensation of the phenyl propane subunits of lignin under such conditions.⁹ In Fig.2 the most obvious possibility of lignin participating in the polycondensation reaction is illustrated.

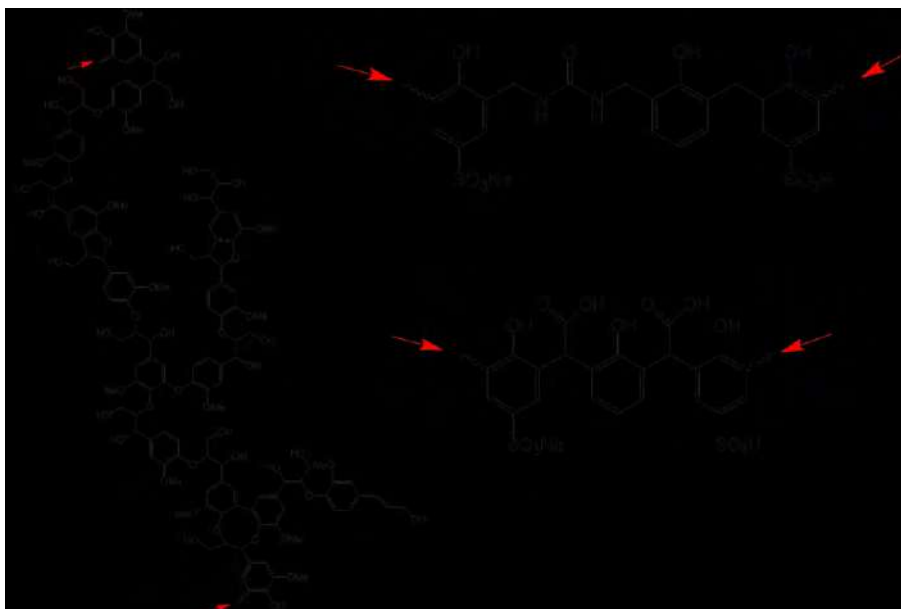


Fig. 2. Possible crosslinking sites on lignin and on the polymer (indicated by the red arrows).

For most of the prototypes the emission profile of the lignin modified polymers has been checked and can be controlled via optimized synthesis procedure to minimize the free monomer contents. The free phenol content is generally below the detection limit of 20 ppm. Depending on the type of aldehyde used in the reaction, the product can be made free from formaldehyde.

3.2 Tanning effect of the lignin modified prototypes

The obtained prototypes display tanning effect in stabilizing the fiber network, which was demonstrated by their ability to raise the shrinkage temperature (T_s) of hides. This has been tested in two ways: on pickled pelt following the traditional tanning procedure and on glutardialdehyde pre-tanned wet-white leather.

Following a typical tanning procedure starting from pickled pelt, one of the lignin-phenol-aldehyde condensates is applied with an amount of up to 70% (w/w) based on pelt weight in combination with a dispersing syntan as an auxiliary. The measured T_s of the obtained leather is 75°C.

When the same lignin-phenol-aldehyde condensate is applied on WW leather pre-tanned with glutardialdehyde that typically displays a shrinkage temperature of 68-70°C at up to 30% (w/w) based on shaved weight, a maximum increase of T_s of 12 °C has been recorded. It was also seen that the higher the amount applied, the higher the T_s of the obtained leather will be.

3.3 Retanning effects of the lignin modified prototypes

We have demonstrated that the obtained lignin-phenol-aldehyde prototypes are suitable to be used as retanning agents for both chrome-tanned and chrome-free leather rendering good organoleptic and physical properties. When a typical usage of up to 30% (w/w) based on shaved weight is applied in the retanning stage, pronounced effects in improvements in the grain tightness, grain smoothness and fullness of the crust can be expected.

In some cases when specific types of lignins are incorporated in the product, the treated leather may display very unique, nice and soft touch.

3.4 Biodegradability of the lignin modified prototypes

Biological degradation of lignocellulosic biomass is essential for the closure of the ecological carbon cycle.⁷ It is known that the biological degradation of wood results in lignin degradation by enzymes under the influence of environmental factors such as light, temperature and humidity.¹⁰ In our study the degradation of a lignin-phenol-urea-aldehyde syntan (with a lignin:phenol ratio of 3:4) has been compared with that of a similar, traditional urea containing but 100% petro-based phenolic syntan: an increase of the BOD₅/COD of 400% was obtained. Our most recent developments show that with higher lignin:phenol ratio there are still room for further improvements.

4 Conclusions

Various industrial, water insoluble lignins from different origins can be used to prepare polyphenolic (re)tanning agents with higher bio-based contents. Compared with otherwise 100% petro-based phenolic syntans, the lignin-modified syntans can be made with a mixture of lignin and phenol that contains a majority of lignin (w/w). The bio-based syntans display tanning effects in its capability of raising the shrinkage temperature of leather or hide. When used in the retanning stage, they render leather improved grain tightness, grain smoothness and fullness. Lignin modified syntans can be further tailor-made to meet low emission requirements and contribute to improvements in waste water quality due to its higher biodegradability. We hope to show you that our innovative technology not only facilitates a novel way of utilizing and upgrading bio-based industrial side-streams, but also offers truly added value in upgrading leather qualities and contributing to minimizing the environmental impact of leather making process.

In addition to the lignin-based polymers, the quickly developing project portfolio within the bio-based platform manifests that Smit & zoon is making steady steps towards a largely sustainable leather value chain by 2025.

References

1. Heidemann, E.: *Fundamentals of Leather Manufacturing*, 1993, Roether, Darmstadt, p397-411.
2. Ammenn, J.: *100 years of Syntans: How Chemistry Enabled Increasing Performance on Leather*, Proceedings of XXXII Congress of IULTCS 2013, Istanbul/Turkey.
3. Wegnar, B.: *Reducing the carbon footprint of leather*, *World Leather*, December 2014/January 2015, p34-35.
4. Smit & zoon internal data.
5. Zakzeski, J. Bruijninx, P. C. A. Jongorius, A. L. Weckhuysen, B. M. *The Catalytic Valorization of Lignin for the Production of Renewable Chemicals*, *Chemical Reviews* 2010, 110, p3552-3599.
6. Covington, A. D.: *Tanning Chemistry: The Science of Leather*, 2009, The Royal Society of Chemistry, Cambridge CB4 0WF, Chapter 14 p318-326.
7. Gosselink, R. J. A. *Lignin as a Renewable Resource for the Chemical Industry*, PhD thesis, Wageningen University (The Netherlands), 2011, Chapter 2.
8. Chitra V, G Tamilselvan, IVMV Enoch, Paulraj M S. *Phenol Sensing Studies by 4-Aminoantipyrine Method—A Review*. *Organic & Medicinal Chem IJ*. 2018; 5(2): 555657. DOI: 10.19080/OMCIJ.2018.05.555657.
9. Inwood, J. P. W. *Sulfonation of Kraft Lignin into Water Soluble Value Added Products*, MSc Thesis, Lakehead University (Canada), 2014.
10. Hammel, K. E. *Fungal degradation of lignin: In: Driven by Nature: Plant Litter Quality and Decomposition*, CAB International, p33-45.

EXTRACTION OF NEW VEGETABLE TANNING AGENT FROM CORIARIA NEPALENSIS BARK AND ITS APPLICATION IN TANNING

Linxin Guo^{1,2}, Taotao Qiang^{1*}, Yangmin Ma^{3*}, Xuechuan Wang¹

¹ College of Bioresources Chemical and Materials Engineering, Shaanxi University of Science & Technology, 710021, Xi'an, China

² College of Chemistry & Chemical Engineering, Ankang University, 725000, Ankang, China

³ College of Chemistry & Chemical Engineering, Shaanxi University of Science and Technology, 710021, Xi'an, China

a)glx9933@foxmail.com; b)qiangtt515@163.com; c)mym63@sina.com; d)wxc-mail@163.com

Abstract. Traditional chromium tanning agents cannot conform to the requirement of sustainable and green development under current leather producing. Compared with chromium tanning agents, vegetable tanning agents have been widely used in tanning process by the virtue of its non-toxicity, low pollution, biodegradability and regenerability. In this study, a novel vegetable tanning agent was extracted from the *Coriaria nepalensis* bark (CNB) by sodium hydroxide. The experimental results showed that under the conditions of 0.2% sodium hydroxide concentration, 20 mL g⁻¹ liquid to solid ratio, 80 °C extraction temperature and 60 min extraction time, the extraction yield of CNB tannin is 15.8%. Afterwards, the composition and molecular mass were evaluated, the CNB tannin belong to hydrolyzable tannin and its molecular mass ranged from 424 Da to 1464 Da. When the CNB tannin was used for sheepskin garment leather tanning, the shrinking temperature (Ts) is 76.40 °C, thickening percentage is 95.13%, tensile strength is 6.08 N mm⁻², tear strength is 38.23 N mm⁻¹, elongation at break is 75.80%. When the CNB tannin was used for wet-blue leather retanning, the Ts is 132.10 °C, thickening percentage is 7.72%, tensile strength is 5.01 N mm⁻², tear strength is 21.89 N mm⁻¹, elongation at break is 98.03%. Surprisingly, the tanning performances of CNB tannin are better than commercial BA tannin (*Acacia mangium* tannin) and the color of tanned leather coincide with the requirement of light leather.

1 Introduction

It is imperative to seek for a sustainable and cleaner biomass resource in the current rapid industrial development. As a polyphenolic substance, tannin can be obtained in the stems, leaves, flowers and fruits of plants (1). The special structure of tannin gives its unique chemical properties and functions, and has been widely used in food colorants (2), the elimination of free radicals (3), active materials (4), sewage purification (5), leather tanning (6) and other industries (7). In leather production process, tannin can be used as leather tanning agent considering that the phenolic hydroxyl group of tannin can form multi-point hydrogen bonded with the peptide chain, hydroxyl group, amino group and carboxyl group of collagen (8). Compared with chrome tanning agents, vegetable tanning agents have broad application prospects due to the advantages of sustainable and green. The resources of tannin are mainly from *Eucalyptus globulus* bark (9), *Acacia mangium* bark (10), *Acacia mearnsii* bark (11), valonea (12).

Coriaria nepalensis Wall, a non-economic plant, is belong to deciduous shrub of *Coriaria*, with strong environmental adaptability and wide distribution. It is distributed in various provinces and cities in the west of China, such as Tibet, Sichuan, Gansu, Shaanxi, etc., with an altitude of 400-3,200 meters. In the process of agricultural and forestry production, the rapid propagation of *Coriaria nepalensis* Wall will affect the growth of other crops, often being felled and discarded, resulting in the waste of resources.

In this study, single factor experiment was used to obtain the extraction conditions of CNB tannin, and the correlative factors including sodium hydroxide concentration, liquid to solid ratio, extraction time and extraction temperature. Furthermore, CNB tannin was used as a vegetable tanning agent in the tanning and retanning of sheep garment leather, and the performance was discussed.

2 Materials and methods

2.1 Experimental materials and reagents

Coriaria nepalensis bark (CNB) was collected in the Qinling Mountains (Shaanxi Province, China) in August 2018. Pickled sheepskin and Wet blue sheepskin were supplied by Hebei Dong Ming Leather Technol. Co., Ltd. China. Chromed hide powder (executive standard is LY/T 1639-2005) were supplied by Chinese Academy of Forestry, China. Commercial condensed tannin (BA tannin) were supplied by Sichuan Decision Chemical Co., Ltd., China. Potassium bromide (KBr) were supplied by Kermel Chemical Reagent Co., Ltd. China. Sodium hydroxide (NaOH) and methanol (MeOH) were supplied by Tianli Chemical Reagent Co., Ltd. China. Hydrochloric acid 37% (HCl) were supplied by Sinopharm group chemical reagent Co., Ltd. China. All these reagents were analytically graded.

The HC-3018 high-speed centrifuge was produced by Anhui USTC Zonkia scientific instruments Co., Ltd., China. The Bruker Vertex70 Fourier transform infrared spectrometer (FT-IR) was produced by Bruker Co., Germany. The Waters 2695 Gel permeation chromatography (GPC) was produced by Waters Co., U.S.A. The drum was made by Wuxi Rong Hao leather machinery manufacturing Co., Ltd., China. The MSW-YD4 digital leather T_s meter was produced by Shaanxi University of Science & Technology, China. The CH-10 thickness gauge was produced by Hefei Yuan Zhong measuring instrument Co., Ltd. The UTM2203 tension tester was produced by Shenzhen San Si Science and Technology Co., Ltd.

2.2 Tannin extraction experiment

2.2.1 Extraction of tannin from CNB

Different extraction conditions will significantly affect the extraction yield of active ingredients in plants (13). In this study, the effects of sodium hydroxide concentration, liquid to solid ratio, extraction temperature and extraction time on the extraction yield were investigated. The CNB powder was extracted with sodium hydroxide solution at the specified temperature for a desired time. Subsequently, the solids were separated from the liquid by high-speed centrifuge. The CNB tannin extract solutions were obtained after neutralized by 1 mol L⁻¹ HCl and diluted to 250 mL volumetric flask with deionized water (14). Tannin extraction yield (%) was calculated with the formula:

$$Y(\%) = \frac{M_1}{M_2} \times 100\% \quad (1)$$

M_1 represent the weight of tannin in extract solutions (g), M_2 represent the weight of dried CNB powder (g), respectively.

2.2.2 Analysis of tannin content

The content of tannin was determined by the previously reported (12). 100 mL of CNB tannin extract solution was added to 5.0 g of chromed hide powder, and the suspension was stirred for 60 min. It was separated by centrifugal separation after standing for 30 minutes. The obtained filtrate was dried at 100 °C to calculate the non-tannin. Another CNB tannin extract solution was dried to calculate the soluble solids. The tannin content (%) was calculated by the difference between soluble solids (%) and non-tannin (%).

2.3 Purification of tannin

Purification of the extracted tannin according to the reported method (15). The CNB tannin extraction solvent was removed by rotary evaporator, and the paste was dried under reduced pressure. About 200 mg of dried CNB tannin was collected and added to a Sephadex LH-20 column equilibrated with ethanol. The CNB tannin was thoroughly dissolved in ethanol, loaded on the Sephadex LH-20 column,

and eluted thoroughly with ethanol. Subsequently, the column was eluted with 50% aqueous acetone solution, and the eluate was collected for concentrated and freeze-dried to obtain purified CNB tannin.

2.4 Tannin structure determination by Fourier Transform Infrared Spectroscopy

Analysis of CNB tannin structure by Fourier transform infrared spectrometer (FT-IR). Potassium bromide (KBr) was dried and pressed into a thin wafer for calibration (16). The powder samples were diluted with KBr and compressed by tableting machine at a pressure of 10 MPa. Purified CNB tannin and BA tannin were scanned registering the spectrum with the wave number range between 4000 and 500 cm^{-1} . All spectra were studied after vector normalization and baseline correction (17).

2.5 Molecular weight determination by gel permeation chromatography

Molecular weight of purified CNB tannin was determined by gel permeation chromatography (GPC) with PLgel 7.8 \times 300 mm column (Waters company, Milford, USA) and Waters 2414 refractive index detector. Used 0.1 mol L^{-1} NaNO_3 as the mobile phase, the purified CNB tannin was configured with mobile phase to a concentration of 3 mg mL^{-1} . Injected 50 μL volumes and measured at a flow rate of 0.8 mL min^{-1} . Relative molecular weight was calculated after calibrated with polyethylene glycol (molecular weight standards) in the range of 106-21,300 Da. The relative molecular weight of CNB tannin was represented by weight-average molecular weight (M_w). polydispersity index (PDI) indicates that the distribution of individual molecular mass in a batch of polymers and as a measure of the molecular weight distribution in the polymer sample. PDI is calculated through the weight-average molecular weight (M_w) divided by the number average molecular weight (M_n): $\text{PDI} = M_w/M_n$ (18).

2.6 Tanning experiments

The dried CNB tannin extraction was used for leather tanning and retanning, the performance of tanned leather was compared with the commercially available BA tannin. The pickled sheepskin was used for leather tanning and its process parameters shown in Table 1. The wet blue sheepskin (chrome-tanned leather) was used for leather retanning and its process parameters is listed in Table 2. The main performance of tanned leather including shrinkage temperature, thickening percentage, tensile strength, tear strength and elongation at break was measured.

Table 1. Technological parameters in tanning process of sheepskin light leather.

Process	Material/g	Dosage/%	Temperature/ $^{\circ}\text{C}$	pH	Time/min
recover acid and wet	water	150	25		
	sulfuric acid	0.8		3.0	10
	sodium chloride	8			60
neutralizing	sodium	0.6	25	5.5	180
	bicarbonate				
pre-tanning tanning	CNB/BA	2	25		60
	sulfited fish oil	2			
	CNB/BA	5	25		60
	CNB/BA	5	25		120
basification	CNB/BA	8	25		180
	sodium	0.1		4.5	
	bicarbonate				
washing	water	100	25		10
fatliquoring	water	100			
	LQ-5	8	45		120
	formic acid	1		4.0	60
stopped drum, dry					

Table 2. Technological parameters in retanning process of sheepskin light leather.

Process	Material/g	Dosage/%	Temperature/°C	pH	Time/min
recover wet	water	200	35		30
washing	water	100	35		10
neutralizing	water	150	35		
	sodium bicarbonate	0.8			
	sodium formate	1	35	5.5	180
washing	water	100	35		10
tanning	CNB/BA	5	35		60
	CNB/BA	5			120
	CNB/BA	5			180
washing	water	100	35		10
fatliquoring	water	100			
	LQ-5	8	50		120
	formic acid	1	50	4.0	60
stopped drum, dry					

3 Results and discussion

3.1 Extraction experiments

3.1.1 Effect of sodium hydroxide concentration on the yield of tannin

The effect of sodium hydroxide concentration on tannin extraction yield is shown in Fig. 1 (a). sodium hydroxide concentration was set at 0, 0.1, 0.2, 0.3, 0.4 and 0.5% when other extraction conditions were as follows: liquid to solid ratio 15 mL g⁻¹, extraction temperature 60 °C and extraction time 60 min. It can be seen from the figure that the extraction yield of tannin increases when the concentration of sodium hydroxide were 0%-0.2%. When the concentration of sodium hydroxide was exceeded 0.2%, the extraction yield of tannin decreased sharply. This is because appropriate concentration of sodium hydroxide solution can promote the efficient extraction of tannin from the powder of CNB, while when the concentration of sodium hydroxide was overrich, it will inhibit the dissolution of the tannin in CNB, resulting in lower extraction efficiency (9).

3.1.2 Effect of liquid to solid ratio on the yield of tannin

The effect of liquid to solid ratio on tannin extraction yield is shown in Fig. 1 (b). liquid to solid ratio was set at 5, 10, 15, 20, 25 and 30 mL g⁻¹ when other extraction conditions were as follows: sodium hydroxide concentration 0.2%, extraction temperature 60 °C and extraction time 60 min. It can be seen from the figure that the liquid to solid ratio had a positive effect on the extraction yield of CNB tannin. When the liquid to solid ratio was less than 20 mL g⁻¹, the extraction yield was significantly increased. When liquid to solid ratio was more than 20 mL g⁻¹, the increased of extraction yield of CNB tannin becomes slower. This is due to the sufficient extraction solvent was beneficial to the extraction of tannin in the CNB. When the extraction solvent was excessive, the dissolution of CNB tannin reaches saturation, and the extraction yield was no longer significantly increased (19).

3.1.3 Effect of extraction temperature on the yield of tannin

The effect of extraction temperature on tannin extraction yield is shown in Fig. 1 (c). extraction temperature was set at 40, 50, 60, 70, 80 and 90 °C when other extraction conditions were as follows: sodium hydroxide concentration 0.2%, liquid to solid ratio 15 mL g⁻¹ and extraction time 60 min. It can be seen from the figure that with extraction temperature increment, the extraction yield

of CNB tannin increased gradually. When the extraction temperature was below 80 °C, the extraction yield increased obviously. While when the extraction temperature was above 80 °C, the extraction yield of the CNB tannin did not increase significantly. Because of the increase of extraction temperature was beneficial to the penetration of the solvent into the CNB powder. As a result, CNB tannin extraction yield increased (20).

3.1.4 Effect of extraction time on the yield of tannin

The effect of extraction time on tannin extraction yield is shown in Fig. 1 (d). extraction time was set at 20, 40, 60, 80, 100 and 120 min when other extraction conditions were as follows: sodium hydroxide concentration 0.2%, liquid to solid ratio 15 mL g⁻¹ and extraction temperature 60 °C. It can be seen from the figure that the extraction yield of tannin reached the maximum when the extraction time was 60 min, and it began to decrease when the extraction time was further increased. Tannin in the CNB will be destroyed when soaked in sodium hydroxide solution for a long time which will reduce the extraction yield (21).

According to the experimental results of single factor, the optimal extraction conditions of CNB tannin were as follows: sodium hydroxide concentration 0.2%, liquid to solid ratio 20 mL g⁻¹, extraction temperature 80 °C, extraction time 60 min. CNB tannin was extracted according to the optimal extraction conditions, and the extraction yield was 15.8%.

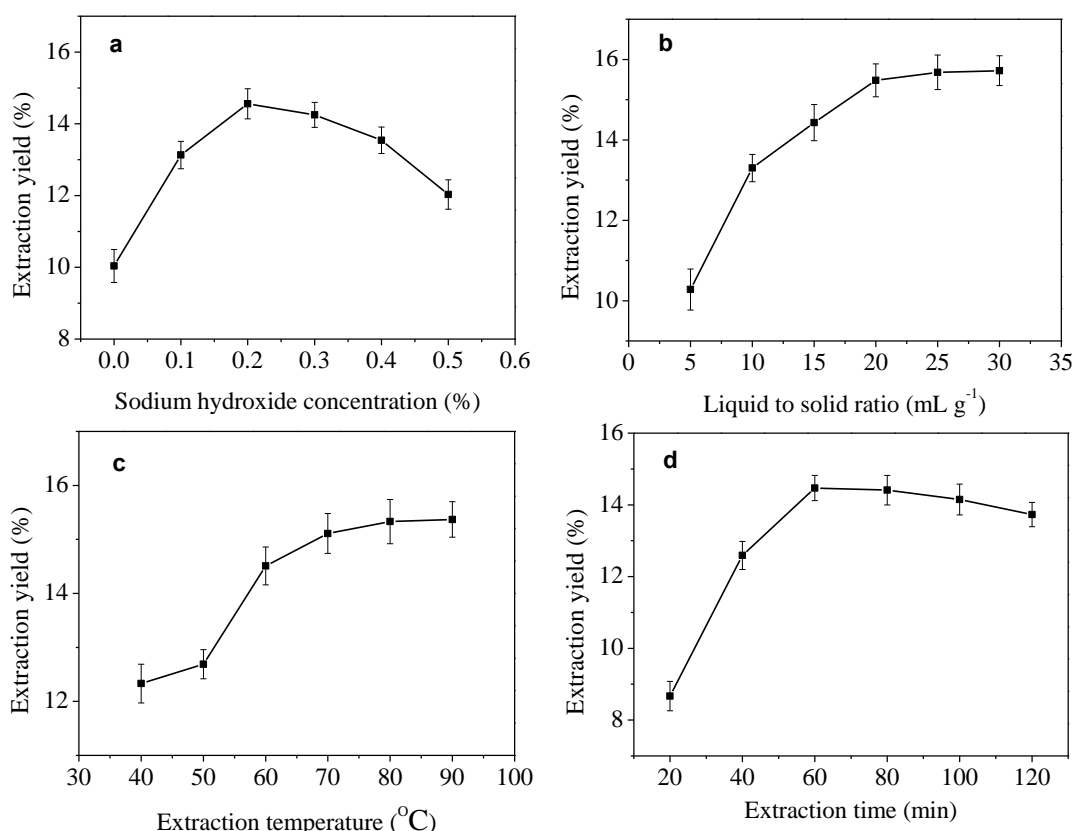


Fig. 1. Effect of different sodium hydroxide concentration (a), liquid to solid ratio (b), extraction temperature (c), and extraction time (d) on the yield of CNB tannin.

3.2 Tannin structure analysis

Fourier transform infrared spectrometer (FT-IR) is a technique that began in the early 20th century to study molecular motion, also known as molecular spectroscopy. It is widely used for chemical

analysis in the mid-infrared range of 4000 to 500 cm^{-1} . The spectral scanning of this range is extremely specific and can be used to analyze compound structure. The FT-IR scanning of purified CNB tannin and BA tannin in the range of 4000-500 cm^{-1} are shown in Figs. 2 (a) and 2 (b).

It can be obtained from the FT-IR scanning spectrum of CNB tannin in Fig. 2a. The significant absorption band at 3376 cm^{-1} is the -OH stretching vibrations. The absorption band around 1724 cm^{-1} corresponds to the C=O stretching vibrations. The regions from 1612 to 1451 cm^{-1} are the aromatic ring skeleton vibrations. The absorption band around 1344 cm^{-1} , which matched the -OH in-plane bending vibrations. The absorption bands at 1204 cm^{-1} and 1033 cm^{-1} could be attributed to C-O stretching vibrations. The peaks between 868 and 750 cm^{-1} are the aromatic ring out-plane bending vibrations (22), (23). Therefore, it can be indicated according to the absorption band at 1724 cm^{-1} , CNB tannin is hydrolyzable tannin with ester group (24). Fig. 2b is BA tannin FT-IR scanning spectrum. BA tannin is known as condensed tannin form *cacia mangium* Willd. There is no absorption band of C=O in BA tannin.

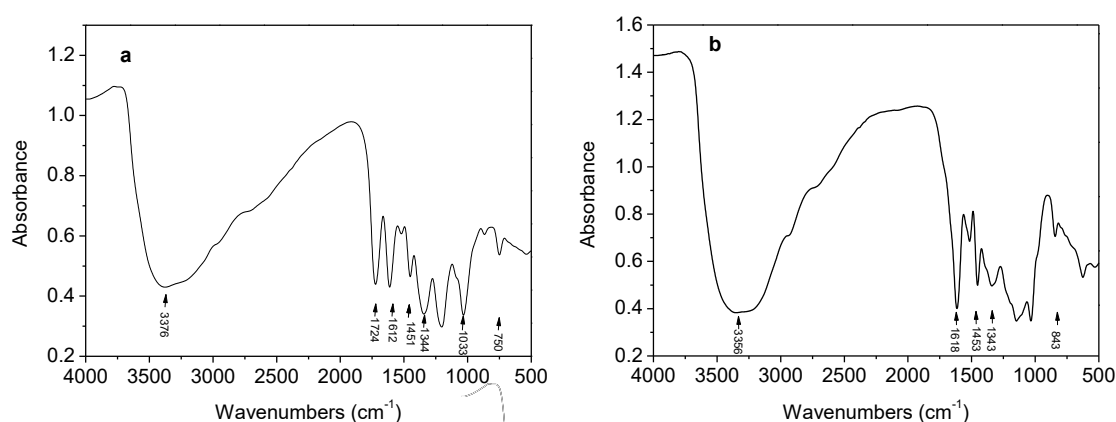


Fig. 2. FT-IR spectra (4000-500 cm^{-1}) of the CNB tannin (a) and BA tannin (b) after baseline correction and normalization scale.

3.3 Molecular weight distribution of CNB tannin

The molecular weight of tannin is the basis for its different roles in industrial production. In the light industry, tannin can be used as vegetable agents for the tanning of leather. The relative molecular weight of tannin is one of the important indicators for determining the performance of tanning. Tannins with a relative molecular weight of less than 500 Da can hardly produce effective cross-linking between the collagen fibers of the skin, and it is difficult to penetrate into the sheath fibers with respect to tannins having a molecular weight of more than 3,000 Da (25). The GPC of purified CNB tannin is shown in Fig. 3. The number average molecular weight (M_n) of purified CNB tannin is 422-1455 Da, the weight-average molecular weight (M_w) of purified CNB tannin is 424-1464 Da, and the polydispersity index (PDI) indicated a appropriate distribution with the value between 1.002 and 1.010. The results of the relative molecular weight distribution of purified CNB tannin were shown in Table 3. CNB tannin has a suitable molecular weight and can use for tanning of leather.

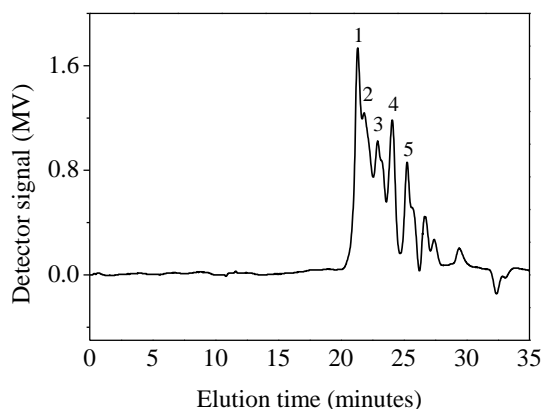


Fig. 3. The GPC determination of CNB tannin.

Table 3 Molecular weight distribution of the purified CNB tannin.

Peak	M_n^a	M_w^b	PDI ^c
1	1455	1464	1.006
2	940	949	1.010
3	564	568	1.007
4	434	435	1.002
5	422	424	1.005

^a M_n : number average molecular weight (Da).

^b M_w : weight average molecular weight (Da).

^c PDI: polydispersity index (M_w/M_n).

3.4 Leather tanning and retanning experiments

The CNB tannin extraction was used for leather tanning and retanning, the performance of tanned leather including shrinkage temperature, thickening percentage, tensile strength, tear strength and elongation at break was measured and shown in Table 4.

Table 4. Physical properties of different typological tanning agents tanned leather.

Tanning method	Tanning agents	Shrinkage temperature (°C)	Thickening percentage (%)	Tensile strength (N mm ⁻²)	Tear strength (N mm ⁻¹)	Elongation at break (%)
Tanning	CNB	76.40	95.13	6.08	38.23	75.80
	BA	78.70	113.46	1.07	18.38	61.45
Retanning	CNB	132.10	7.72	5.01	21.89	98.03
	BA	126.40	7.63	3.26	19.01	90.41

When CNB tannin is used in the tanning of sheep garment leather, the shrinkage temperature (T_s) of the leather is 76.40 °C, which is similar to the commercially available BA tannin (78.70 °C). Despite the thickening percentage (95.13%) is inferior to BA tannin (113.46%), the tensile strength (6.08 N mm⁻²), tear strength (38.23 N mm⁻¹), elongation at break (75.80%) are superior to the BA tannin. After CNB tannin was used in the retanning of wet blue sheepskin, the T_s of the leather can reach 132.10 °C, which is higher than the BA tannin (126.40 °C). The thickening percentage (7.72%) is equivalent to BA tannin (7.63%), and the tensile strength (5.01 N mm⁻²), tear strength (21.89 N mm⁻¹), elongation at break (98.03%) are superior to BA tannin.

The performance of leather after tanning and retanning are improved significantly compared to BA tannin. After tanning the sheep garment leather, the strength of the leather is increased. With the

retanning of wet blue sheepskin garment leather, the CNB tannin can produce a stronger bond with the collagen fibers of the leather. The photos of tanned leather are shown in Figs. 4, the color of leather coincides with the requirement of light leather.

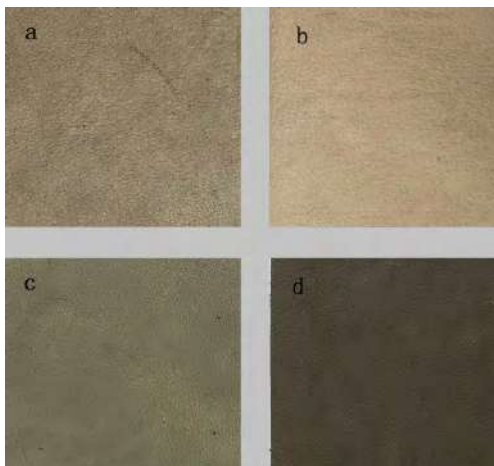


Fig. 4. The photos of CNB tannin leather tanning (a), BA tannin leather tanning (b), CNB tannin leather retanning (c), BA tannin leather retanning (d).

4 Conclusions

The present study reported a new tannin resource was extracted from CNB and sodium hydroxide concentration, liquid to solid ratio, extraction temperature and extraction time were explored in the extraction process. The CNB tannin was extracted according to the optimal extraction conditions, the extraction yield was 15.8%. FT-IR showed that CNB tannin is hydrolyzable tannin and the relative molecular weight are found to be between 424 Da and 1464 Da by GPC. When CNB tannin is used in the tanning of sheep garment leather, the T_s is 76.40 °C, which is similar to the commercially available BA tannin (78.70 °C). The tensile strength (6.08 N mm⁻²), tear strength (38.23 N mm⁻¹), elongation at break (75.80%) are superior to the BA tannin. After CNB tannin was used in the retanning of wet blue sheepskin, the T_s can reach 132.10 °C, which is higher than the BA tannin (126.40 °C), and the tensile strength (5.01 N mm⁻²), tear strength (21.89 N mm⁻¹), elongation at break (98.03%) are superior to BA tannin. The performance of leather after tanning and retanning are significantly improved compared to BA tannin.

Acknowledgments

This study was sponsored by the Key Research & Development Project of Shaanxi Province, the Youth Innovation Team of Shaanxi Universities and the New Style Think Tank of Shaanxi Universities, the National Science and Technology Major Project (2017YFB0308500). Authors thank the teachers and students of the Biomass Materials (<http://www.leather420.cn>) and SUST Natural Products Chemistry Group for their help during the experiment.

References

1. Haslam, E., *Natural Polyphenols (Vegetable Tannins) as Drugs: Possible Modes of Action*. *J. Nat. Prod.* 59, 205-15, 1996
2. Pinela, J.; Prieto, M. A.; Pereira, E.; Jabeur, I.; Barreiro, M. F.; Barros, L.; Ferreira, I. C. F. R., *Optimization of heat- and ultrasound-assisted extraction of anthocyanins from Hibiscus sabdariffa calyces for natural food colorants*. *Food Chem.* 275, 309-321, 2019
3. Dutra, R. P.; Abreu, B. V. d. B.; Cunha, M. S.; Batista, M. C. A.; Torres, L. M. B.; Nascimento, F. R. F.; Ribeiro, M. N. S.; Guerra, R. N. M., *Phenolic Acids, Hydrolyzable Tannins, and Antioxidant Activity of Geopropolis from the Stingless Bee Melipona fasciculata Smith*. *J. Agric. Food Chem.* 62, 2549-2557, 2014
4. Missio, A. L.; Mattos, B. D.; Ferreira, D. d. F.; Magalhaes, W. L. E.; Bertuol, D. A.; Gatto, D. A.; Petutschnigg, A.; Tondi, G., *Nanocellulose-tannin films: From trees to sustainable active packaging*. *J. Cleaner Prod.* 184, 143-151, 2018
5. Hameed, Y. T.; Idris, A.; Hussain, S. A.; Abdullah, N.; Man, H. C.; Suja, F., *A tannin-based agent for coagulation and flocculation of municipal wastewater as a pretreatment for biofilm process*. *J. Cleaner Prod.* 182, 198-205, 2018
6. Seabra, I. J.; Chim, R. B.; Salgueiro, P.; Braga, M. E. M.; de Sousa, H. C., *Influence of solvent additives on the aqueous extraction of tannins from pine bark: potential extracts for leather tanning*. *J. Chem. Technol. Biotechnol.* 93, 1169-1182, 2018
7. Bacelo, H.; Vieira, B. R. C.; Santos, S. C. R.; Boaventura, R. A. R.; Botelho, C. M. S., *Recovery and valorization of tannins from a forest waste as an adsorbent for antimony uptake*. *J. Cleaner Prod.* 198, 1324-1335, 2018
8. Sundar, V. J.; Muralidharan, C., *Salinity free high tannin fixation vegetable tanning: Commercial success through new approach*. *J. Cleaner Prod.* 142, 2556-2561, 2017
9. Pinto, P. C. R.; Sousa, G.; Crispim, F.; Silvestre, A. J. D.; Neto, C. P., *Eucalyptus globulus Bark as Source of Tannin Extracts for Application in Leather industry*. *ACS Sustain Chem Eng.* 1, 950-955, 2013
10. Teng, B.; Gong, Y.; Chen, W., *Molecular weights and tanning properties of tannin fractions from Acacia mangium bark*. *J. Soc. Leather Technol. Chem.* 97, 220-224, 2013
11. Timotheo, C. A.; Lauer, C. M., Jr., *Toxicity of vegetable tannin extract from Acacia mearnsii in Saccharomyces cerevisiae*. *Int. J. Environ. Sci. Technol.* 15, 659-664, 2018
12. Luo, X.; Bai, R.; Zhen, D.; Yang, Z.; Huang, D.; Mao, H.; Li, X.; Zou, H.; Xiang, Y.; Liu, K.; Wen, Z.; Fu, C., *Response surface optimization of the enzyme-based ultrasound-assisted extraction of acorn tannins and their corrosion inhibition properties*. *Ind Crop Prod.* 129, 405-413, 2019
13. de Hoyos-Martinez, P. L.; Merle, J.; Labidi, J.; Charrier- El Bouhtoury, F., *Tannins extraction: A key point for their valorization and cleaner production*. *J. Cleaner Prod.* 206, 1138-1155, 2019
14. Low, J. H.; Abdul Rahman, W. A. W.; Jamaluddin, J., *The influence of extraction parameters on spent coffee grounds as a renewable tannin resource*. *J. Cleaner Prod.* 101, 222-228, 2015
15. Melone, F.; Saladino, R.; Lange, H.; Crestini, C., *Tannin Structural Elucidation and Quantitative 31P NMR Analysis. 2. Hydrolyzable Tannins and Proanthocyanidins*. *J. Agric. Food Chem.* 61, 9316-9324, 2013
16. Tondi, G.; Petutschnigg, A., *Middle infrared (ATR FT-MIR) characterization of industrial tannin extracts*. *Ind Crop Prod.* 65, 422-428, 2015
17. Cozzolino, D.; Cynkar, W. U.; Damberg, R. G.; Mercurio, M. D.; Smith, P. A., *Measurement of Condensed Tannins and Dry Matter in Red Grape Homogenates Using Near Infrared Spectroscopy and Partial Least Squares*. *J. Agric. Food Chem.* 56, 7631-7636, 2008
18. Naumann, H. D.; Hagerman, A. E.; Lambert, B. D.; Muir, J. P.; Tedeschi, L. O.; Kothmann, M. M., *Molecular weight and protein-precipitating ability of condensed tannins from warm-season perennial legumes*. *J. Plant Interact.* 9, 212-219, 2013
19. Ouyang, H.; Hou, K.; Wang, L.; Peng, W., *Optimization protocol for the microwave-assisted extraction of antioxidant components from Pinus elliotii needles using response surface methodology*. *BioResources.* 12, 478-494, 2017
20. Wu, Z.; Li, H.; Ming, J.; Zhao, G., *Optimization of Adsorption of Tea Polyphenols into Oat β -Glucan Using Response Surface Methodology*. *J. Agric. Food Chem.* 59, 378-385, 2011
21. Liu, Y.; Gong, G.; Zhang, J.; Jia, S.; Li, F.; Wang, Y.; Wu, S., *Response surface optimization of ultrasound-assisted enzymatic extraction polysaccharides from Lycium barbarum*. *Carbohydr. Polym.* 110, 278-284, 2014
22. Fernandez, K.; Agosin, E., *Quantitative analysis of red wine tannins using Fourier-transform mid-infrared spectrometry*. *J. Agric. Food Chem.* 55, 7294-7300, 2007
23. Edelmann, A.; Lendl, B., *Toward the Optical Tongue: Flow-Through Sensing of Tannin-Protein Interactions Based on FTIR Spectroscopy*. *J. Am. Chem. Soc.* 124, 14741-14747, 2002
24. Gvazava, L. G.; Alaniya, M. D., *Hydrolyzed Tannin from Euphorbia glareosa Leaves*. *Chem. Nat. Compd.* 41, 308-310, 2005
25. Qiang, T.; Chen, L.; Zhang, Q.; Liu, X., *A sustainable and cleaner speedy tanning system based on condensed tannins catalyzed by laccase*. *J. Cleaner Prod.* 197, 1117-1123, 2018

ACRYLIC RESINS IN WET WHITE

O. Ballús¹, M. Guix¹, R. Micó¹ and R. Palop¹

¹Leather Department. Cromogenia Units S.A, Telf.: (+34) 93.264.34.64.

ojballus@cromogenia.com

Abstract. The purpose of this paper is to study the influence of acrylic resins on the properties of the hide when added at the pickling-tanning stage of a wet white process. In this study, 9 resins with different molecular weights and different monomer compositions were selected (Table 1). Resins were applied to pelt leathers of Spanish origin split at 3.5 mm. Hides were cut along the backbone. A standard process was applied to the left halves and the same process adding the resin was applied to the right halves. The resin was added at two points of the process: after adjusting the salt of the bath and after adding the pickling acids. The COD of both processes was assessed as compared to the resin-free process, and the shrinkage temperature and the degree of whiteness of the tanned hide were assessed. Hides were retanned and fatliquored with a standard process, and degree of whiteness, thickness and organoleptic properties (sponginess and leveling) were assessed. Hide shrinkage under temperature was also assessed, and images of hide sections were obtained by scanning electron microscopy (SEM). While acrylic resins did not increase shrinkage temperature, they did fix and/or deposit themselves on the interfibrillary spaces of the hide; indeed, highly reduced COD values were observed. This study showed that homopolymer acrylic resins provided fuller and fluffier hides, while the rest of resins practically did not improve the physical and organoleptic properties of the hides. Hide properties also improved more when resins were applied together with the salt, although at this point these products are less stable, particularly if working with semi-hard or hard waters.

Key words: tanning, retanning, wet white, acrylic resins.

Table 1. Products, monomers used, and molecular weights.

Product	Monomers	Molecular weight (Da)
AC 1	Acrylic acid	4,500
AC 2	Acrylic acid	4,400
AC 3	Acrylic acid	154,000
AC 4	Acrylic acid	500,000
ACN 1	Acrylic acid / Acrylonitrile	120,000
EST 1	Styrene / Maleic	10,000
EST 2	Acrylic acid / Styrene / Maleic anhydride	25,000
EST 3	Acrylic acid / Styrene / Maleic anhydride	450,000
MAL 1	Maleic anhydride	900

1 Introduction

Acrylic resins are very frequently used in wet blue tanning and retanning processes because they lend very good properties to the hide on account of their high affinity for chromium.

The acrylic resins used in tanning processes are usually polymers of high molecular weight, and the properties conferred to the hide depend basically on the type of monomer used during synthesis and on the molecular weight of the resins. The most frequently used monomers are acrylic acid, acrylonitrile, styrene, and maleic anhydride.

When applied at the wet blue retanning stage, many and varied properties are provided by these resins, from compactness or softness to a certain degree of water repellency. When applied during chrome tanning, these resins provide the hides with high fullness and high chrome salt exhaustion

on account of the strong interaction of the carboxylate groups of acrylic resins with chromium. These products also provide light fastness and lower leather degradation because they are chemically stable and do not supply phenol or formaldehyde to the hides.^(1,2)

While extensive bibliography is available on the application of acrylic resins in wet blue, less information is found when these products are applied in wet white tanning.

Heidemann, E.⁽³⁾ and A'mma, A.⁽⁴⁾ described acrylic resins and their reactivity in chrome tanned leather. They discussed how acrylic resins have no tanning capacity but are able to form covalent complexes with chromium and react as polycarboxylates.

Dequing, Wei et al.⁽⁵⁾ addressed wet white pretanning of a pig hide with a polymethacrylate resin. They concluded that the interactions between the acrylic polymer and collagen are electrostatic. Indeed, when the product is applied at pH=5.0 and then reduced to pH=3.0, a greater fiber separation is observed as compared to a product-free reference sample, which translates into higher fullness. Madhan, B. et al.⁽⁶⁾ studied the effect of a methacrylic resin in vegetable tanning on a collagen substrate and determined that acrylic resins are fixed on collagen through electrostatic forces and favor opening, thus improving the penetration of the products added afterwards.

This paper studied the influence of different resins applied in wet white tanned leathers. To this end, 9 resins with different molecular weights and different monomer compositions were selected and applied in wet white tanning at two different points of the process: together with the salt and after pickling acid addition.

2 Materials and methods

2.1 Materials

Nine resins from different monomers (acrylic acid, acrylonitrile, styrene and/or maleic anhydride) with different molecular weights were selected (Table 2).

Pelt leathers of Spanish origin split at 3.0-3.5 mm were used. Bating and deliming were performed according to a standard formula. The hides were then cut in half and divided into 40 x 100 cm pieces. The left halves were taken as (resin-free) references and the product was applied to the right halves. Resins were applied at pickling together with the salt (process I) and after adding pickling acids (process II). The application formula is shown in Table 3. Finally, the product without glutaraldehyde was applied to determine the tanning power of the resin (Table 4).

Table 2. Products, monomers used, and molecular weights.

Product	Monomers	Molecular weight (Da)
AC 1	Acrylic acid	4,500
AC 2	Acrylic acid	4,400
AC 3	Acrylic acid	154,000
AC 4	Acrylic acid	500,000
ACN 1	Acrylic acid / Acrylonitrile	120,000
EST 1	Styrene / Maleic anhydride	10,000
EST 2	Acrylic acid / Styrene / Maleic anhydride	25,000
EST 3	Acrylic acid / Styrene / Maleic anhydride	450,000
MAL 1	Maleic anhydride	900

Table 3. Process description.

Process I	Resin application together with the salt
	80% Water at 25 °C, 8% of salt. Run 10'. °Bé=7
	(Product-free) reference. Run 120' 0.5% Resin (active matter). Run 120'
Pickling-tanning	1% Formic acid. Run 60'
	1.2% Sulfuric acid. Run 120'. Control pH=3.0 and cross with vbc
	2% Glutaraldehyde at 50%. Run 120'
	1% Sodium formate. Run 30'
	0.5% Sodium bicarbonate. Run 120'. pH=5.0 – crossed. Night in bath
Process II	Resin application after pickling acids
	80% Water at 25 °C, 8% of salt. Run 10'. °Bé=7
	1% Formic acid. Run 60'
	1.2% Sulfuric acid. Run 120'. Control pH=3.0 and cross with vbc
Pickling-tanning	(Product-free) reference. Run 120' 0.5% Resin (active matter). Run 120'
	2% Glutaraldehyde at 50%. run 120'
	1% Sodium formate. Run 30'
	0.5% Sodium bicarbonate. Run 120'. pH=5.0 – crossed. Night in bath

Table 4. Application formula to determine resin tanning power.

Process	Resin tanning power before acidification
	80% Water at 25 °C, 8% of salt. Run 10'. °Bé=7
Pickling-tanning	(Product-free) reference. Run 120' 5.0% Resin (active matter). Run 120'
	1% Formic acid. Run 60'
	1.2% Sulfuric acid. Run 120'. Control pH=3.0 and cross with vbc
Process	Resin tanning power after acidification
	80% Water at 25 °C, 8% of salt. Run 10'. °Bé=7
Pickling-tanning	1% Formic acid. Run 60'
	1.2% Sulfuric acid. Run 120'. Control pH=3.0 and cross with vbc
	(Product-free) reference. Run 120' 5.0% Resin (active matter). Run 120'

2.2 Methods

2.2.1 Bath analysis

The chemical oxygen demand (COD) of the residual baths of processes I and II was determined at the following stages: in process I, 120 min after product application and after acidification; in process II, 120 min after resin application. The CODs of the products under the same bath conditions were also measured.

Analysis was performed with 1-1500 mg/l vials heated under reflux for 2 hours at 150 °C, and COD was measured with an Aqualytic AL100 spectrophotometer.

2.2.2 Hide analysis

In pretanned hides, the degree of whiteness was measured with a Color Data Spectraflash SF-30 colorimeter, the shrinkage temperature (Ts) was measured according to IUP 16, and photographs were taken with a scanning electron microscope (SEM) equipped with EDX detector (Phenom Pro-X).

Once hides were assessed at this stage, they were retanned, dyed and fatliquored according to a standard formula. Color intensity, resistance to dry heat, physical properties (degree of softness, thickness, tensile strength, tear load, grain burst) and organoleptic properties were determined.

The degree of softness was determined according to IUP 36, thickness according to IUP 4, tensile strength according to IUP 6, tear load according to IUP 8 by means of Zwick TM22.5/TN1S, and grain

bursting strength according to IUP 9 by means of Satra STM 463. Leather resistance to dry heat was analyzed under the following conditions: oven at 90°C for 48 h and 400 h. Finally, the organoleptic properties (sponginess and leveling) were evaluated by 5 technician specialists.

3 Results and discussion

3.1 Bath analysis

In general, a decreased COD was observed at the end of tanning in both processes, before and after acidification, although this decrease was more pronounced when the resin was applied before acidification (process I).

In alkaline medium, the carboxyl groups of collagen are mostly negatively charged and the amine groups are deprotonated. At this point, resins can penetrate without interaction with collagen. When the medium is acidified, amine groups are protonated and the carboxyl groups of the resins interact with collagen by means of electrostatic charges. On the other hand, acrylic resins are less soluble in acidic medium and therefore an acidic pH also favors resin fixation.

The percentage values of resin fixed on the hide are obtained from the relationship between the residual bath COD and the product COD (Fig. 1). While these results suggest acrylic resin fixation or deposition on the skin, this fixation is improved when the resin is applied in neutral medium together with the salt.

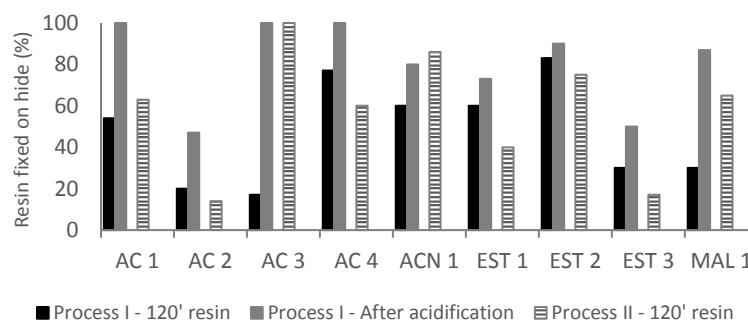


Fig. 1. Resin fixed on hide in processes I and II.

3.2 Hide assessment

3.2.1 Determination of tanning power, degree of whiteness and SEM images of the resins in pretanned hides

The Ts of the resin applied alone (application formula of Table 4) was assessed to determine the tanning power and was also assessed in the two processes (described in Table 3) to determine whether the resin had any influence on or synergy with the tanning product (glutaraldehyde). The results obtained are shown in Table 5. When the product was applied alone, none of the studied resins increased shrinkage temperature significantly. These results suggest that acrylic resins are not strong enough to bind two collagen chains and therefore provide no tanning or very little tanning, increasing Ts by 2-8°C as compared to the reference. Significant differences were also not observed between the Ts values obtained in the two processes, thus suggesting that Ts is determined by glutaraldehyde.

On the other hand, no significant differences were obtained in the degrees of whiteness of pretanned hide samples, that is, acrylic resins neither increase nor decrease the degree of whiteness. Finally, SEM was performed to deeply observe effects on skin fibers after tanning. SEM

imaging shows more structured fibers in the samples containing resin than in the respective references, in both processes I and II. The SEM imaging of the samples tanned in the two processes with products AC 3 and AC 4 are shown in Fig. 2. Fiber structuring is more prominent for the samples in process I as shown in Fig. 2 (A, B, E, F), fibril bundles are more structured and fibers are separated. This higher degree of opening up allows the fatliquoring agent to penetrate easily and leather becomes more flexible, soft and spongy. Regarding process II, it is observed that the fibers are also more structured but less separated than process I.

Table 5. Ts of the resin, process I and process II, and degree of whiteness.

Sample	Resin alone		Process I				Process II			
	Ts (°C)		Ts (°C)	Degree of whiteness			Ts (°C)	Degree of whiteness		
	I	II		L*	a*	b*		L*	a*	b*
Reference	57	56	78	88.28	0.02	10.15	80	82.57	5.82	29.91
AC 1	56	60	79	91.61	0.09	9.00	80	79.07	6.01	27.19
Reference	57	56	79	76.56	-0.60	10.25	80	84.88	4.41	27.51
AC 2	54	56	77	82.42	1.32	14.57	80	82.69	5.74	31.08
Reference	57	56	80	87.66	0.11	9.15	79	84.56	4.00	25.52
AC 3	63	62	78	89.13	0.16	8.90	79	85.13	3.97	23.06
Reference	57	56	80	89.38	-0.05	9.36	79	83.90	3.00	24.86
AC 4	62	64	79	83.32	1.01	10.85	80	88.11	3.80	21.62
Reference	57	56	80	82.84	-0.08	9.42	80	83.63	5.70	26.50
ACN 1	63	59	81	88.49	0.46	11.14	80	86.13	4.24	25.32
Reference	57	56	80	90.53	0.18	10.85	80	83.58	4.21	26.55
EST 1	60	61	82	72.86	0.72	11.33	82	82.21	5.14	29.27
Reference	57	56	80	87.60	-0.04	11.25	80	80.13	5.34	27.36
EST 2	60	58	83	87.38	-0.33	10.29	83	84.69	4.02	25.11
Reference	57	56	80	81.69	-0.21	9.32	79	85.16	3.54	21.94
EST 3	59	59	80	82.61	-0.01	10.08	83	77.64	3.62	25.26
Reference	57	56	80	87.71	0.45	11.76	80	80.69	7.21	30.89
MAL 1	56	57	80	91.52	0.51	10.62	80	85.16	3.54	21.94

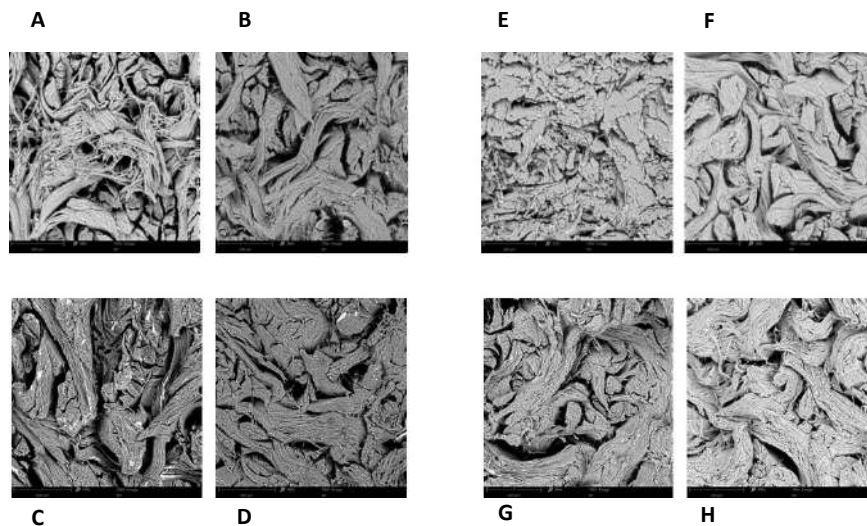


Fig. 2. SEM images of fiber cross section (x400), of resins AC 3 and AC 4 with their reference. **A:** AC 3 reference of process I. **B:** AC 3 of process I. **C:** AC 3 reference of process II. **D:** AC 3 of process II. **E:** AC 4 reference of process I. **F:** AC 4 of process I. **G:** AC 4 reference of process II. **H:** AC 4 of process II.

Table 6. Thickness and softness in crust hides.

Sample	Thickness (mm)		Softness (d=30)	
	I	II	I	II
Reference	2.8	2.2	3.4	2.6
AC 1	2.9	2.3	3.7	2.7
Variation	+3.6%	+4.5%	+8.8%	+3.8%
Reference	2.9	2.4	3.7	2.7
AC 2	2.9	2.4	3.8	2.5
Variation	0%	0%	+2.7%	-7.4%
Reference	3.0	2.3	3.9	3.1
AC 3	3.2	2.4	4.3	3.3
Variation	+6.7%	+4.3%	+10.3%	+6.5%
Reference	2.9	2.3	3.7	3.6
AC 4	3.0	2.4	4.0	3.8
Variation	+3.4%	+4.3%	+8.1	+5.6%
Reference	3.1	2.3	3.2	2.4
ACN 1	3.1	2.2	3.1	2.5
Variation	0%	-4.3%	-3.1%	+4.2%
Reference	2.9	2.5	3.1	2.8
EST 1	3.0	2.5	2.9	2.7
Variation	+3.4%	0%	-6.5%	-3.6%
Reference	3.1	2.5	3.1	2.9
EST 2	2.9	2.3	3.1	2.8
Variation	-6.5%	-8.0%	0%	-3.4%
Reference	3.1	2.4	3.8	2.7
EST 3	3.0	2.5	4.1	2.8
Variation	-3.2%	+4.2%	+7.9%	+3.7%
Reference	3.0	2.5	3.3	2.9
MAL 1	2.9	2.6	3.4	2.9
Variation	-3.3%	+4.0%	-3.0%	0%

3.2.2 Determination of resistance and other properties in crust hides

The thickness and degree of softness in crust hides are shown in Table 6. Homopolymer acrylic resins AC 1, AC 3 and AC 4 increased the degree of softness. While resin AC 2 is also a homopolymer acrylic resin, it is an acidic resin and therefore behaves differently. The degree of softness was not increased by the rest of resins. Homopolymer acrylic resins AC 1, AC 3 and AC 4 slightly but not significantly increased thickness. No significant changes in thickness values were observed with the rest of products. The values were slightly higher when the resin was applied in process I.

The results obtained in physical resistances (tensile strength, tear load and grain burst) are shown in Table 7. Although it was expected an improvement of strength in the final leather due to the positive correlation between softness and strength⁽⁷⁾, no significant differences were observed. The products applied had no influence on tensile strength, tear load and grain burst.

The resistances to dry heat assessed, measured as surface decrease, at 48 h and 400 h in processes I and II are shown in Fig. 3. The resistances are higher for AC 1, AC 3 and EST 2, which means that these products improve shrinkage surface vs. their references. The rest of the products did not change the leather surface.

Table 7. Physical resistances in crust hides.

Sample	Process I				Process II			
	Tensile (MPa)	Elong (%)	Tear (N)	Burst (mm)	Tensile (MPa)	Elong (%)	Tear (N)	Burst (mm)
Reference	28.02	45.67	535.8	10.76	34.66	15.88	202.2	7.21
AC 1	30.99	41.35	459.5	10.71	32.44	17.56	203.4	8.01
Variation	+11%	-9%	-14%	0%	-6%	+11%	+1%	+11%
Reference	28.45	31.12	401.2	11.28	25.65	16.78	271.2	6.54
AC 2	30.54	34.67	386.0	12.54	28.30	18.90	273.1	6.21
Variation	+7%	+11%	-4%	+11%	+10%	+13%	+1%	-5%
Reference	26.44	35.58	432.3	11.03	30.35	12.50	267.4	6.81
AC 3	26.64	29.81	368.5	10.32	29.05	15.38	218.6	6.68
Variation	+1%	-16%	-15%	-6%	-4%	+23%	-18%	-2%
Reference	27.22	35.10	448.2	10.52	30.94	12.02	267.3	6.71
AC 4	26.26	33.65	348.4	10.23	30.70	14.42	241.7	6.93
Variation	-4%	-4%	-22%	-3%	-1%	+20%	-10%	+3%
Reference	30.51	51.29	400.1	9.45	27.88	15.90	300.4	7.91
ACN 1	31.45	48.32	396.7	8.64	24.76	14.56	287.1	8.24
Variation	+3%	-6%	-1%	-9%	-11%	-8%	-4%	+4%
Reference	24.66	47.58	379.0	8.88	47.91	16.99	276.8	7.83
EST 1	25.88	44.25	376.5	7.43	45.83	15.64	305.4	7.42
Variation	+5%	-7%	-1%	-16%	-4%	-8%	+10%	-5%
Reference	25.53	36.71	450.4	10.66	29.66	18.55	300.5	8.14
EST 2	23.89	34.76	437.5	9.65	30.67	19.44	298.5	9.15
Variation	-6%	-5%	-3%	-9%	+3%	+5%	-1%	+12%
Reference	32.66	35.40	400.6	10.89	28.88	20.55	298.55	8.15
EST 3	31.78	31.78	387.1	10.54	31.90	21.67	279.43	8.39
Variation	-3%	-10%	-3%	-3%	+10%	+5%	-6%	+3%
Reference	34.66	42.80	476.51	8.67	29.54	16.88	215.1	9.77
MAL 1	39.65	40.79	481.90	9.66	31.76	19.52	210.5	8.32
Variation	+14%	-5%	+1%	+11%	+8%	+16%	-2%	-15%

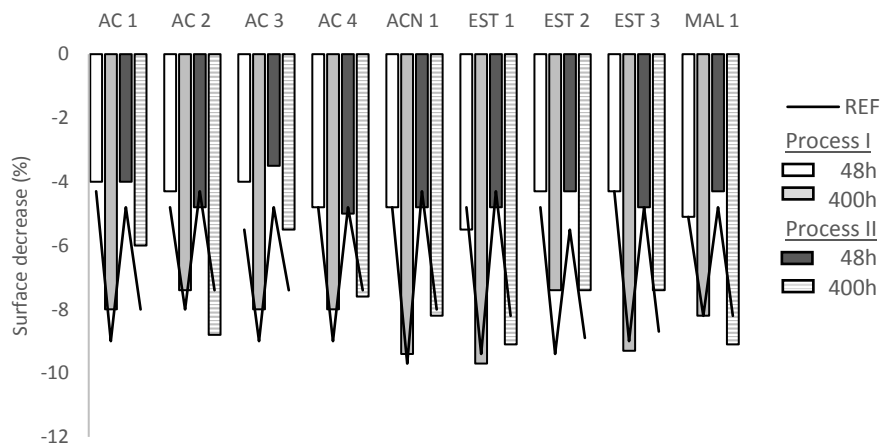


Fig. 3. Surface decrease in processes I and II.

Table 8. Sponginess and leveling in crust hides.

Sample	Sponginess		Leveling	
	I	II	I	II
Reference	2	2	1	1
AC 1	4	3	3	4
AC 2	3	2	2	2
AC 3	5	4	5	5
AC 4	3	5	3	4
ACN 1	3	2	4	3
EST 1	1	2	4	3
EST 2	2	3	3	3
EST 3	3	2	3	4
MAL 1	2	2	3	3

Finally, the organoleptic properties assessed in a 1-5 scale (in ascending order) are shown in Table 8. The values of the reference are an average of all references. The results suggest that the resin providing greater sponginess and leveling to the hides is homopolymer acrylic resin AC 3, followed by AC 4 and AC 1. Sponginess results are consistent with softness results, the better the softness the higher the sponginess.

Conclusions

The resins that provided the best properties to wet white tanned leather were homopolymer acrylic resins AC 1, AC 3 and AC 4, improving softness, surface decrease with temperature, sponginess and leveling. No significant changes in hide properties were observed with the rest of resins.

The results obtained suggest that acrylic resins interact with the amine groups of collagen by means of electrostatic charges because the COD decreases as pH is decreased. These results are consistent with the bibliography.

As shown in the SEM photographs, resin fixation increased fiber structuring and fiber separation, thus providing better sponginess and softness.

References

1. Danhong, S. et al. Evaluation of environmental impact of typical leather chemicals. Part II: Biodegradability of organic tanning agents by activated sludge. A: *Journal of the Society of Leather Technologists and Chemists*. 2008, Vol. 92, núm. 2, p. 59-64. ISSN 01440322.
2. Dix, J.P. The Characteristics and Mode of Action of Modern Polymers in Post-Tanning Treatment Processes. A: *Journal of the American Leather Chemists Association*. 1998, Vol. 93, p. 283-284.
3. Heidemann, E. *Fundamentals of leather manufacturing*. 1993. Roether, 1993.
4. A'mma, A. El. High Exhaust Acrylic Chemistry. A: *Journal of the American Leather Chemists Association*. 2003, Vol. 98, p. 1-5.
5. Deqing, Wei, Zhang Rong, and Zhang Xinming. n.d. "A study of pig hide tanned with polymethacrylic acid". *Journal of the Society of Leather Technologists and Chemists*. Vol. 79, p.110.
6. Madhan, B., C. Muralidharan, and R. Jayakumar. 2002. "Study on the Stabilisation of Collagen with Vegetable Tannins in the Presence of Acrylic Polymer." *Biomaterials* 23 (14): 2841-47.
7. Covington, A. *Tanning Chemistry: The science of leather*. 2016. RSC, 2011.

A MULTIFUNCTIONAL GELATIN-QUATERNARY AMMONIUM COPOLYMER EXHIBITING SUPERIOR ANIONIC DYE ADSORPTION FOR EFFICIENT EMISSION REDUCTION IN LEATHER TANNING PROCESS

S. L. Xu, J. Xu, J. M. Lu and T. D. Li

Shandong Provincial Key Laboratory of Molecular Engineering, School of Chemistry and Pharmaceutical Engineering, Qilu University of Technology (Shandong Academy of Sciences), Jinan 250353, P. R. China

3You would list an author's second affiliation here.

a)Corresponding author: xujing@qlu.edu.cn, ylp6296@vip.163.com

b) xushilin521314@qq.com, jianmei.lu@126.com

Abstract. Leather wastewater is one of the most polluting industrial emissions. An in-situ, green, and innovative strategy that limits dye emissions is required to replace subsequent waste management. A novel cationic protein with a high quaternary ammonium degree was designed and synthesized. The results show that at concentrations ranging from 3 to 15 wt%, this cationic protein rapidly and completely adsorbs Direct Purple N and Acid Black 24 within 5 min. A remarkable efficiency in removing Acid Red 73, Acid Golden G, Acid Lake Blue A, Acid Green, and Acid Orange II, with >96% removal rates, was achieved. The cationic protein was most accurately represented by the pseudo-second-order kinetic model. Acid Orange II (2000 mg L⁻¹) and 15 wt% cationic protein were used in an actual tanning process. The residual concentration of Acid Orange II in the wastewater was 23.1 mg L⁻¹. These results reflect that the emission reduction targets have been effectively achieved.

1 Introduction

The presence of pollutants in the environment can be attributed to both natural and anthropogenic sources^{1,2}. Dyeing wastewater has drawn great public concern owing to its strong colority, high toxicity, carcinogenicity, degradation resistance, and easy accumulation in living organisms^{2,3}, which has led to concerns about water pollution as a global challenge^{1,4}. To date, many technologies, including membrane technologies⁵, adsorption^{6,7}, biodegradation⁸, distillation⁹, photocatalysis^{10,11}, and other approaches, have been utilized for the purification and remediation of polluted water.

The leather industry is one of the most polluting industrial sectors and generates enormous amounts of dye wastewater via the tanning process^{3,12-15}. The volume wastewater of per kilogram of the tanned leather produced and the wastewater dye concentrations (>400 mg L⁻¹) in the different wet-finishing process steps are generally high¹⁶. Leather wastewater has a high pH value and strong color, and comprises complex components. The main pollutants include heavy metals such as chromium, soluble proteins, dandruff, suspended matter, tannins, lignins, inorganic salts, oils, surfactants, dyes, and resins¹⁷⁻¹⁹. Therefore, it is very difficult to deal with such complicated sewage in a simple way. A cleaner and green tanning process has become the focus of attention in the leather industry²⁰. Dye emissions can be minimized if the leather dyes in the tanning process are retained in the leather via sufficient adsorption; this will be an efficient and cleaner method to prevent water pollution. It will also be a green way to cater to the needs of the tanning industry. Therefore, the purpose of this study was to design and synthesize a new type of cationic protein that not only fully fills the leather but also quickly and firmly adsorbs dye molecules in large quantities, to prevent dye emissions.

In leather dyeing, direct and acid (anionic) dyes that contain functional groups such as benzene rings, and azo and sulfonate groups are mainly used^{21,22}. Cationic compounds effectively adsorb

these anionic dyes through ionic interactions. Quaternary ammonium compounds are widely recognized cationic compounds because of their non-toxicity and strong antibacterial efficiency²³. Moreover, it can be deduced that a high quaternary ammonium degree is beneficial for adsorption. In addition, copolymers are also suitable compounds to improve the performance of auxiliaries, particularly dyes, in the dyeing process²⁴⁻²⁷. These copolymers react with the substrates at multiple points to improve the uptake of chemicals; this has attracted the attention of researchers. Copolymers are very effective in adsorbing dyes because, unlike normal polymers, they contain mainly reactive groups in the backbone surrounded by linearly and randomly distributed side chains that can attract more adsorbents²⁸. For the above reasons, a cationic protein that contains gelatin and quaternary ammonium salt components was designed and synthesized in this study, for dye adsorption in the tanning process. Gelatin polymers can be prepared via the hydrolysis of leather collagen²⁹. Their homology effectively enhances their combination ability, which is very helpful to fill these cationic proteins into leather.

The objectives of this study were to synthesize a new type of cationic protein with a high quaternary ammonium degree, evaluate its adsorption kinetics and isotherm, demonstrate the feasibility of its use for dye adsorption, and realize trace dye emissions in an actual tanning process. A series of anionic dyes, including Acid Black 24, Acid Red 73, Acid Golden G, Acid Lake Blue A, Acid Green, Direct Purple N, and Acid Orange II, were used to investigate the adsorption capacity of the cationic protein. The residual concentrations of the dyes in the distillates indicated the dyes that were adsorbed efficiently; Direct Purple N and Acid Black 24 attained equilibrium rapidly (within 5 min). Acid Orange II (2000 mg L⁻¹) was used in a tanning process. The residual concentration of this dye in the wastewater was 23.1 mg L⁻¹. This result indicates that this dye is fully adsorbed by the cationic protein. Dye emission can therefore be prevented very effectively in the tanning process, which is beneficial to realize cleaner and green leather tanning.

2 Results and discussion

2.1 Synthesis of cationic proteins

The DEQAS was synthesized in 87% yield using epichlorohydrin and tetramethylethylenediamine at a molar ratio of 2.5:1. Then, it was used as the raw material to prepare the cationic protein. Chemical reactions occurred between the functional groups in gelatin and the DEQAS in a sodium hydroxide-water medium. During the cross-linking reactions, epoxy groups belonging to the DEQAS molecules reacted mainly with the free -NH₂ groups on the gelatin chains to form cross-linked products via a nucleophilic substitution pathway. Two possible structures of the cationic protein are described (Fig. 1a). The ¹H NMR spectra of epichlorohydrin, tetramethylethylenediamine, and the DEQAS are shown in Fig. 1b. The FTIR spectra of epichlorohydrin, tetramethylethylenediamine, the DEQAS, and the cationic protein (sample 2) are depicted in Fig. 1c. The bands in the 650-800 cm⁻¹ region can be assigned to the C-Cl groups in epichlorohydrin. The bands at 845, 957, and 1271 cm⁻¹ were attributable to the characteristic absorption bands of the epoxy ring in epichlorohydrin³⁰, and were assigned to the 12μ, 11μ, and 8μ peaks, respectively. The bands at both 1047 and 1104 cm⁻¹ were attributed to contributions from the symmetric stretching of the C-O-C and skeletal vibrations of the C-O stretching, respectively. The sharp peak at 1033 cm⁻¹ was attributed to the C-N stretching of the tertiary amine group in tetramethylethylenediamine³¹. An absorption band at 1473 cm⁻¹ appeared due to the C-H functional groups of the methyl substituent of tetramethylethylenediamine or the quaternary ammonium groups. After the formation of the DEQAS, characteristic absorption bands of epoxy groups, and bands at 1047 and 1104 cm⁻¹ also appeared; however, the sharp peaks at 1033 cm⁻¹ and in the 650-800 cm⁻¹ region disappeared. These results indicated that a DEQAS was

obtained. When the cationic protein was prepared, the bands at both 957 and 1104 cm^{-1} disappeared. This result indicated that the epoxy groups were nearly completely consumed.

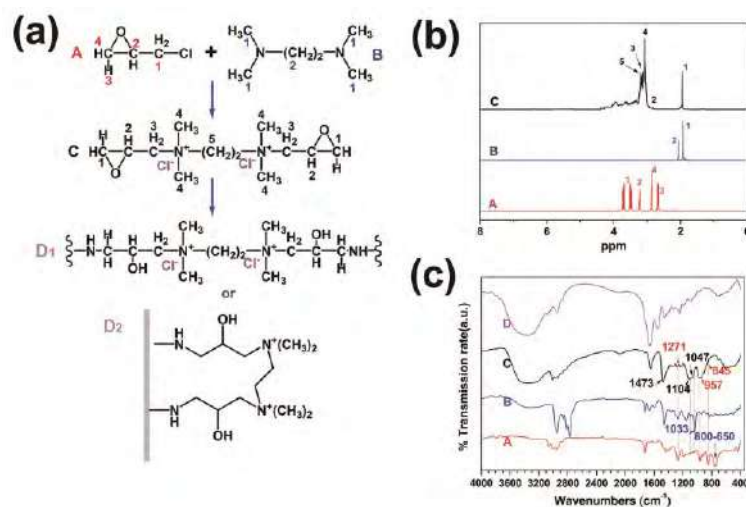


Fig. 1. (a) Synthesis of DEQAS and cationic protein (sample 2). (b) 400 MHz ^1H NMR spectra of epichlorohydrin (A), tetramethylethylenediamine (B), and DEQAS (C) in CDCl_3 at 25 °C. (c) IR spectra of epichlorohydrin, tetramethylethylenediamine, DEQAS, and cationic protein (sample 2, D₁ or D₂).

2.2 Adsorption behavior of cationic protein

Since the cationic protein was designed with cationic branched quaternary ammonium groups that could attract anionic dyes, it could be used to evaluate the removal of various anionic dyes. The initial concentration of the dyes was 2000 mg L^{-1} . The cationic protein (sample 2) showed a remarkable efficiency ($\sim 100\%$) for removing Direct Purple N (**Fig. 2a**) and Acid Black 24 (**Fig. 2b**) within 5 min. Direct Purple N and Acid Black 24 attained adsorption equilibriums within 5 min. It is notable that a favorable cationic protein adsorption efficiency was maintained at concentrations of cationic protein ranging from 3 to 15 wt%. The maximum efficiencies for removing Acid Orange II (**Fig. 2c**), Acid Red 73 (**Fig. 2d**), Acid Lake Blue A (**Fig. 2e**), Golden Orange G (**Fig. 2f**), and Acid Green (**Fig. 2g**) were 95%, 90%, 90%, 91%, and 93%, respectively, within 30 min; adsorption equilibrium was quickly attained when the concentration of the dye ranged from 3 to 7 wt%, whereas about 6 h was needed for a higher concentration. These results suggest that the operation time should be increased when these five dyes are used in real industrial processes. **Fig. 2** shows that the remarkable adsorption efficiency of sample 2 increased with an increase in the contact time under various concentration levels. The color variations after filtering the dye solutions through the cationic protein (sample 2) films are displayed in **Fig. 2**.

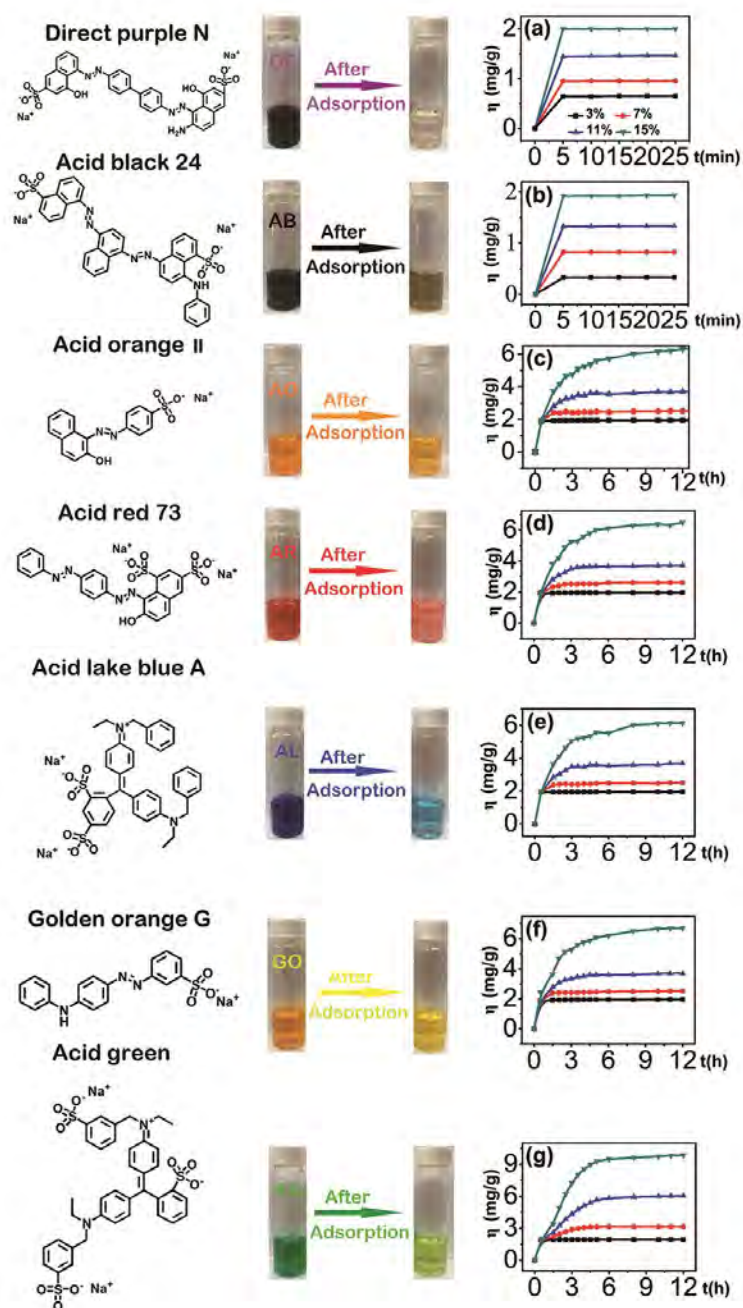
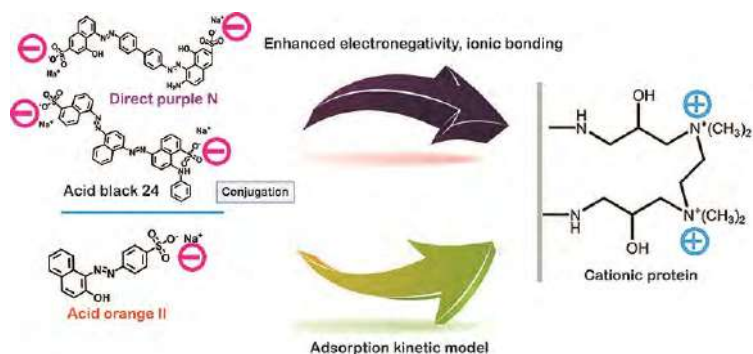


Fig. 2. Comparison of dye adsorption effects (the dye chemical formulae, standard solutions, and effluents are shown on the left, in the middle, and on the right, respectively). Adsorption equilibrium versus t curves for dyes: (a) Direct Purple N, (b) Acid Black 24, (c) Acid Orange II, (d) Acid Red 73, (e) Acid Lake Blue A, (f) Golden Orange G, and (g) Acid Green. The concentrations of the cationic protein (sample 2) were 3, 7, 11, and 15 wt%.

2.3 Re-tanning experiment in leather industry

π - π and p - π conjugates built by aromatic, azo, and sulfonic acid groups exist in Direct Purple N, Acid Black 24, and Acid Orange molecules. This strong conjugated interaction enhances the electronegativity of the dye molecules³². The ionic bonds with positive charge that existed in the quaternary ammonium group were obviously improved (**Scheme 1**). In the adsorption experiment, the removal efficiencies for Direct Purple N, Acid Black 24, and Acid Orange were better. The results

encouraged us to study the efficacy of the cationic proteins using real samples. Acid Orange II, which had a neutral adsorption capacity, was selected as the model dye to study the adsorption effect of the cationic proteins in a real tanning process. The cationic protein samples 1 and 2 were used in actual tanning experiments to compare their adsorption capabilities. The kinetic data suggested that a higher concentration of the cationic protein was beneficial for adsorption; considering the real needs of industrial conditions, the concentrations of samples 1 and 2 were set as 15 wt%, and the optimum adsorption period was identified as 2.5 h. The concentration of Acid Orange II was 2000 mg L⁻¹. Use style 'Abstract': 10 pt Calibri, justified, flush left, two line space between Abstract and Author address. Make the word Abstract bold followed by a point.



Scheme 1. Ionic interaction between cationic protein (sample 2) and Direct Purple N, Acid Black 24, and Acid Orange II.

After the tanning experiments, the three wastewaters were collected. They were from the cationic protein-free system, sample 1-containing system, and sample 2-containing system. The wastewaters were analyzed using fluorescence spectroscopy (**Fig. 3a**). The results show that the maximum absorption peak of Acid Orange II is at 542 nm. The peak strength at 542 nm was lowest for the sample 2-containing system. This result indicates that the residual concentration of Acid Orange II was lowest in this system. The relative concentrations were quantified using the standard curve (**Fig. 3b**). The results showed that the residual concentration of Acid Orange II was 23.1 mg L⁻¹ in this system. In comparison, the residual concentration of Acid Orange II was 1188.7 mg L⁻¹ in the sample 1-containing system. In the cationic protein-free system, the dye was barely adsorbed.

Gelatin, which was the main component of the cationic proteins, is a hydrolysis product of leather collagen. The homology of gelatin and leather collagen leads to a strong combination force between them. There are many polar functional groups such as amino groups, carboxyl groups, and hydroxyl groups in gelatin and leather collagen. The close combination of these components can promote intermolecular hydrogen bonds, and thus improve the anti-wiping ability of the leather surface. In addition, a higher quaternary ammonium degree of the cationic protein can improve the ionic interaction between these positive and negative ions. **Fig. 3c** shows that the anti-wiping ability of tanned leather containing sample 2 under dry, wet, and sweat conditions is obviously enhanced. Similarly, the filling effect and tearing strength of this leather are also the best among those of all the samples (**Fig. 3d**).

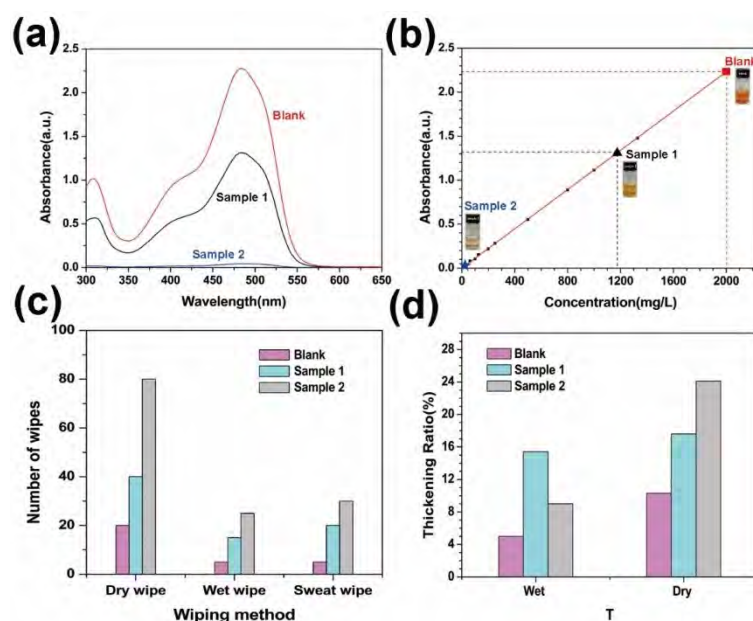


Fig. 3. (a) UV analysis of wastewater from tanning process for blank, sample 1-containing system, and sample 2-containing system. (b) Concentration analysis of Acid Orange II in wastewater from tanning process for blank, sample 1-containing system, and sample 2-containing system. (c) Wiping test for tanned leather, i.e., blank leather, sample 1-containing leather, and sample 2-containing leather. (d) Determination of thickening rate for tanned leather, i.e., blank leather, sample 1-containing leather, and sample 2-containing leather.

3 Conclusions

In this work, a cationic protein with a high quaternary ammonium degree was synthesized; it presented an excellent adsorption ability for direct and acid (anionic) dyes. The ^1H NMR, IR, DSC, and TGA results revealed the structure of the DEQAS and cationic protein. At concentrations of 3, 7, 11, and 15 wt%, the cationic protein rapidly and completely adsorbed Direct Purple N and Acid Black 24 within 5 min. A remarkable efficiency in removing Acid Red 73, Acid Golden G, Acid Lake Blue A, Acid Green, and Acid Orange II, with >96% removal rates, was achieved. Acid Orange II (2000 mg L^{-1}) was used in an actual tanning process. The residual concentration of this dye in the wastewater was 23.1 mg L^{-1} . This result indicated that the dye was almost entirely adsorbed by the cationic protein. This work can help realize an in-situ, green, and innovative strategy for limiting dye emissions, to replace subsequent waste management.

4 Acknowledgments

This work was supported by the National Natural Science Foundation of China (Grant No. 21776143, 21606138) and Program for Li Tianduo Taishan Scholar Team of Shandong Province.

References

1. Mafu, L.D., Msagati, T.M., Mamba, B.B.: Adsorption studies for the simultaneous removal of arsenic and selenium using naturally prepared adsorbent materials, *Int. J. Environ. Sci. Te.*, 11, 1723-1732, 2013
2. Akhtar, M.F., Ashraf, M., Javeed, A., Anjum, A.A., Sharif, A., Saleem, A., Akhtar, B., Khan, A.M., Altaf, I.: Toxicity appraisal of untreated dyeing industry wastewater based on chemical characterization and short term bioassays, *B. Environ. Contam. Tox.*, 96, 502, 2016.
3. Gupta, V.K., Suhas.: Application of low-cost adsorbents for dye removal—a review, *J. Environ. Manage.*, 90, 2313-2342, 2009
4. Mohan, D., Pittman, C.U.: Arsenic removal from water/wastewater using adsorbents—A critical review, *J. Hazard. Mater.*, 142, 1-53, 2007
5. Alventosa-Delara, E., Barredo-Damas, S., Alcaina-Miranda, M.I., Iborra-Clar, M.I.: Ultrafiltration technology with a ceramic membrane for reactive dye removal: Optimization of membrane performance, *J. Hazard. Mater.*, 209, 492-500, 2012
6. Garg, V.K., Gupta, R., Bala, Y.A., Kumar, R.: Dye removal from aqueous solution by adsorption on treated sawdust, *Bioresource Technol.*, 89, 121-124, 2003
7. Rafatullah, M., Sulaiman, O., Hashim, R., Ahmad, A.: Adsorption of methylene blue on low-cost adsorbents: a review, *J. Hazard. Mater.*, 177, 70-80, 2010
8. Kulkarni, A.N., Kadam, A.A., Kachole, M.S., Govindwar, S.P.: Lichen *Permelia perlata*: a novel system for biodegradation and detoxification of disperse dye Solvent Red 24, *J. Hazard. Mater.*, 276, 461, 2014
9. Criscuoli, A., Zhong, J., Figoli, A., Carnevale, M.C., Huang, R., Drioli, E.: Treatment of dye solutions by vacuum membrane distillation, *Water Res.*, 42, 5031-5037, 2008
10. Zhou, Y., Gu, X., Zhang, R., Lu, J.: Influences of various cyclodextrins on the photodegradation of phenol and bisphenol A under UV light, *Ind. Eng. Chem. Res.*, 54, 426-433, 2015
11. Ameen, S., Akhtar, M.S., Seo, H.K., Shin, H.S.: Solution-processed CeO₂/TiO₂ nanocomposite as potent visible light photocatalyst for the degradation of bromophenol dye, *Chem. Eng. J.*, 247, 193-198, 2014
12. Abdel-Shafy, H.I., Hegemann, W., Genschow, E.: Fate of heavy metals in the leather tanning industrial wastewater using an anaerobic process, *Environ. Manage. Health*, 6, 28-33, 1995
13. Gilpavas, E., Dobrosz-Gómez, I., Gómez-García, M.á.: The removal of the trivalent chromium from the leather tannery wastewater: the optimisation of the electro-coagulation process parameters, *Water Sci. Technol.*, 63, 385, 2011
14. Ahmed, E., Abdulla, H.M., Mohamed, A.H., El-Bassuony, A.D.: Remediation and recycling of chromium from tannery wastewater using combined chemical-biological treatment system, *Process Saf. Environ.*, 104(Part A), 1-10, 2016
15. Cao, S., Wang, K., Zhou, S.: Mechanism and effect of high-basicity chromium agent acting on Cr-wastewater-reuse system of leather industry, *ACS Sustain. Chem. Eng.*, 6, 3957-3963, 2018
16. Piccin, J.S., Gomes, C.S., Feris, L.A., Gutterres, M.: Kinetics and isotherms of leather dye adsorption by tannery solid waste, *Chem. Eng. J.*, 183, 30-38, 2012
17. Saxena, G., Chandra, R., Bharagava, R.N.: Environmental pollution, toxicity profile and treatment approaches for tannery wastewater and its chemical pollutants, *Rev. Environ. Contam. T.*, 240, 31-69, 2016
18. Mella, B., Barcellos, B.S.D.C., Costa, D.E.D.S., Gutterres, M.: Treatment of leather dyeing wastewater with associated process of coagulation-flocculation/adsorption/ozonation, *Ozone Sci. Eng.*, 3, 133-140, 2017
19. Grace-Pavithra, K., Senthil-Kumar, P., Carolin-Christopher, F., Saravanan, A.: Removal of toxic Cr(VI) ions from tannery industrial wastewater using a newly designed three-phase three-dimensional electrode reactor, *J. Phys. Chem. Solids*, 110, 379-385, 2017
20. Lu, J., Ma, J.Z., Gao, D.G., William Tait, R.T., Sun, L.Y.: A star-shaped POSS-containing polymer for cleaner leather processing, *J. Hazard. Mater.*, 361, 305-311, 2019
21. Jia, Z.G., Li, S.B., Liu, J.H., Zhu, R.S.: Synthesis of MgAl-LDH/CoFe₂O₄ and MgAl-CLDH/CoFe₂O₄ nanofibres for the removal of Congo Red from aqueous solution, *B. Mater. Sci.*, 38, 1757-1764, 2015
22. Cheng, R.M., Ou, S.J., Xiang, B., Li, Y.J., Liang, Q.Q.: Equilibrium and molecular mechanism of anionic dyes adsorption onto copper (II) complex of dithiocarbamate-modified starch, *Langmuir*, 26, 752-758, 2010
23. Wen, Y., Zhang, X.R., Chen, M., Wu, Z.C., Wang, Z.W.: Characterization of antibiofouling behaviors of PVDF membrane modified by quaternary ammonium compound-combined use of QCM-D, FCM, and CLSM, *J. Water Reuse Desal.*, 2018.
24. Kanagaraj, J., Panda, R.C., Senthilvelan, T., Gupta, S.: Cleaner approach in leather dyeing using graft copolymer as high performance auxiliary: related kinetics and mechanism, *J. Clean. Prod.*, 112, 4863-4878, 2015
25. Santos, V.C.G.D., Salvado, A.D.P.A., Dragunski, D.C., Peraro, D.N.C., Tarley, C.R.T., Caetano, J.: Highly improved chromium (III) uptake capacity in modified sugarcane bagasse using different chemical treatments, *Quim Nova*, 35, 1606-1611, 2012
26. Lagergren, S.: About the theory of so-called adsorption of solution substances, *K. Sven. Vetenskapsakad. Handl.*, 24, 1-39, 1898
27. Yang, Z., Chen, S., Fu, K.: Highly efficient adsorbent for organic dyes based on a temperature and pH responsive multiblock polymer, *J. Appl. Polym. Sci.*, 135, 46626, 2018
28. Wei, X., Sun, P., Yang, S.H., Zhao, L., Wu, J., Li, F.Y., Pu, Q.S.: Microchip electrophoresis with background electrolyte containing polyacrylic acid and high content organic solvent in cyclic olefin copolymer microchips for easily adsorbed dyes, *J. Chromatogr. A*, 1457, 144-150, 2016

29. Dang, X.G., Yuan, H.C., Shan, Z.H.: *An eco-friendly material based on graft copolymer of gelatin extracted from leather solid waste for potential application in chemical sand-fixation*, *J. Clean. Prod.*, 188, 416-424, 2018
30. Chalykh, A.E., Zhavoronok, E.S., Kolesnikova, E.F., Yu, V., Kostina, B., Bondarenko, G.N.: *Kinetics of curing of diene and aliphatic epoxy oligomer blends: IR-spectroscopy study*, *Polym. Sci. Ser. B+*, 53, 466–475, 2011
31. Jiang, Q.W., Xu, J., Li, T.D.: *Synthesis and antibacterial activities of quaternary ammonium salt of gelatin*, *J. Macromol. Sci. B*, 53, 133-141, 2014
32. Gautam, P., Wang, Y., Zhang, G.X., Sun, H.D., Chan, J.M.W.: *Using the negative hyperconjugation effect of pentafluorosulfanyl acceptors to enhance two-photon absorption in push-pull chromophores*, *Chem. Mater.*, 30, 7055-7066, 2018

BIOPOLYMERS FOR A MORE SUSTAINABLE LEATHER

L. Taddei¹, F. Ugolini¹, G. P. Bonino¹, G. Giacomelli¹, C. Franceschi², R. Sole³, M. Bertoldini³ and V. Beghetto³

¹ Codyeco S.p.a., Vicolo del Grano 8, 56029 S. Croce sull'Arno (PI), Italy, Tel. +39 057141671, L.taddei@codyeco.it

² ILSA S.p.a., Via Quinta Strada 28, 36071 Arzignano (VI), Italy, Tel. +39 0444 452020, cfranceschi@ilsagroup.com

³ Department of Molecular Sciences and Nanosystems, University Ca' Foscari of Venice, Via Torino 155, 30172 Venice, Italy, Tel. +39 0412348928, beghetto@unive.it

Corresponding author: L.taddei@codyeco.it

Abstract. A novel class of bio-based polymers have been developed within the LIFE BIOPOL European project aiming to replace traditional re-tanning and fat-liquoring products reducing environmental impacts and increasing the safety of leather. The purpose of the project is to enhance the recovery and reuse of different bio derived wastes and by-products from leather and agro-industrial sector to produce eco-friendly and renewable biopolymers with high re-tanning and fat-liquoring characteristics.

1 Introduction

Nowadays, there is a general environmental concern regarding the huge amount of petrochemical based chemicals commonly used in industrial processes. According to the European Directive 96/61EC,¹ the leather industry is highly environmental demanding and requires integrated prevention and pollution control. Moreover, there is a growing demand for eco-friendly alternatives to replace hazardous and petro-based chemicals. High amounts of sludge and wastewater are formed during the tanning process, which require expensive treatments in order to remove the pollution load^{4,5}. BREF (Best Available Techniques Reference document) and IPPC UE 2008, EU directives, push the leather industry to project safer and more sustainable processes.⁶

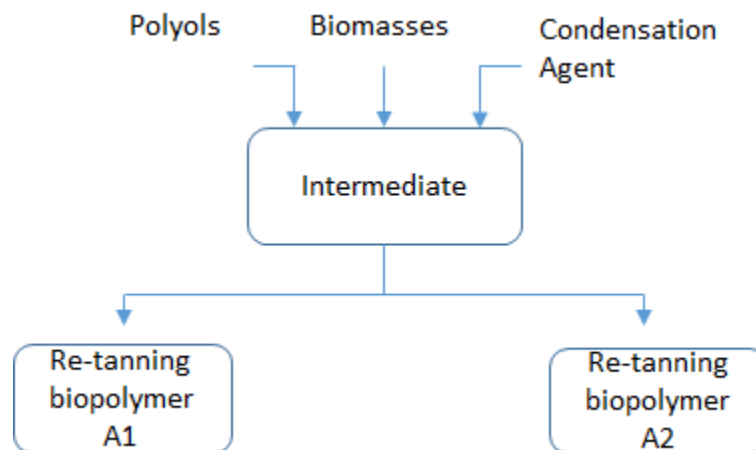
In this frame, LIFE BIOPOL is a project co-financed by European Union as part of the LIFE 2014-2020 programme, which aims to synthesize a new class of biomass-derived biopolymers as re-tanning and fat liquoring agents. The Biopolymers produced represent an innovative, eco-friendly and suitable alternative to traditional fossil fuel based products, which are still the main class of chemicals currently used in leather making process. With a view to enhance circular economies, biopolymers are produced using raw materials derived from industrial wastes and by-products. Animal and vegetable biomass have been used as starting materials for the synthesis of biopolymers. Both the raw materials have been enzymatically treated to achieve lower molecular weight reagents, which better perform once they react with polyols and a condensation agent to produce the modified biopolymers.

Optimization of reaction parameters led to efficient protocols for the synthesis of the biopolymers up to industrial scale, using a prototype plant specifically designed and built up.

LIFE BIOPOL intends to verify that:

- the environmental impact and the total water consumption of the leather making process by using the new biopolymers will be highly reduced compared to conventional processes.
- the Product Environmental Footprint (PEF) of the Biopolymers produced will be highly inferior compared to conventional leather making products.

The present work concerns the synthesis of re-tanning biopolymers starting from animal (A1) or vegetable (A2) biomasses, polyols and a condensation agent. Biopolymers performances have been tested in comparison with traditional chemicals in the leather making process (see Scheme 1)



Scheme 1. General scheme for the synthesis of biopolymers.

2 Results and discussion

2.1 Protein derived biopolymers (A1)

Animal biomasses, such as proteins, are complex organic matrixes which require the combination of several analytical techniques in order to provide detailed information about composition and reactivity. Proteins consist of peptide sequences, which lead to a heterogenous and variable mixture. When enzymatically hydrolysed, lower molecular weights chain are expected to be obtained. The presence of several amino and carboxyl terminal groups makes proteins a very reactive substrate which can be treated with various types of reagent. As expected for complex molecules the $^1\text{H-NMR}$ of the protein shows numerous unresolved multiplets. The signals between 0.7 and 4.7 ppm may be attributed of different CH_2 moieties due to the various amino acid present in the biomass. A relevant signal is the singlet at 8.5 ppm, which is zoomed in the upper left corner of Figure 1 and is supposed to correspond to $-\text{NH}$ amide protons of the protein from animal biomass. The intensity of the signal is relatively modest, which can be in accordance with the relatively low molecular weight of the protein. This signal is present also in the spectra of the intermediates (Figure 3), even if at different chemical shift. This signal is diagnostic for amide bonds which are present in animal biomass; it can be easily identified and usually is between 8.0 and 9.0 ppm; no superimposition with other signals is observed. A very weak unresolved multiplet is present between 7.0 and 8.0 ppm, characteristic of the aromatic part of the protein.

2.2 Soya derived biopolymer (A2)

Hydrolysed soya is a complex substrate. The hydrolysate does not present just a mixture of sugars (abt. 30%), but it also contains a large amount of proteins (abt. 40%), fibers (abt. 10%), fat (abt. 10%) and ash (abt. 10%).

This complex mixture of different organic matrixes is reflected by the corresponding spectroscopic data, which show a wide range of broad and overlapped signals, difficult to predict. Cadet *et al.*⁵ reported that fermentation of sugar cane juice could lead to the formation of lactic acid. Similarly, the same can be hypothesised for soya, which has a similar composition. Characteristic doublet rising from $-CH_3$ methyl terminal group of lactic acid at 1.24 ppm are spotted on, in the upper left window in Figure 2. Upon reaction with a condensation agent, in the presence of polyols, hydrolysed soya reacts to produce new olefinic and amide bonds (Figure 3).

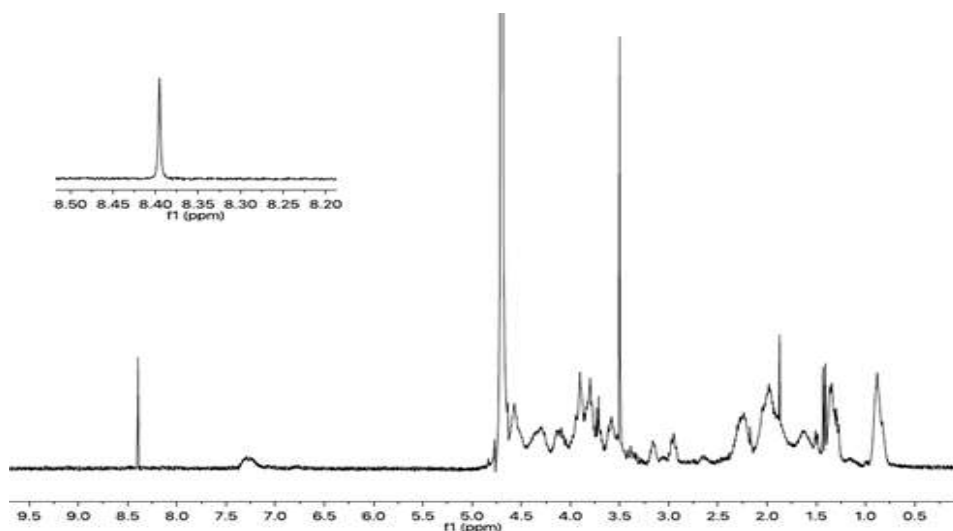


Fig. 1. 1H NMR spectrum of animal biomass in D_2O .

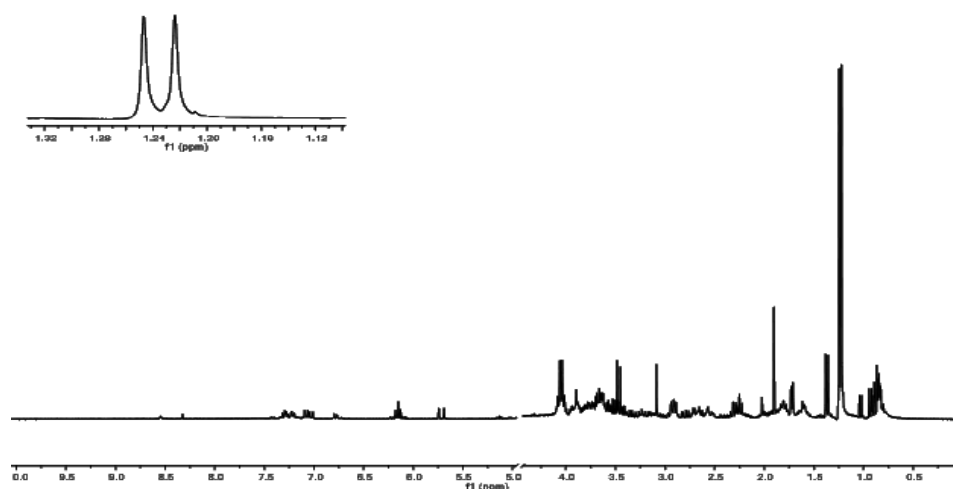


Fig. 2. 1H NMR spectrum hydrolysed soya biomass, in D_2O . Solvent peak has been removed for sake of clarity.

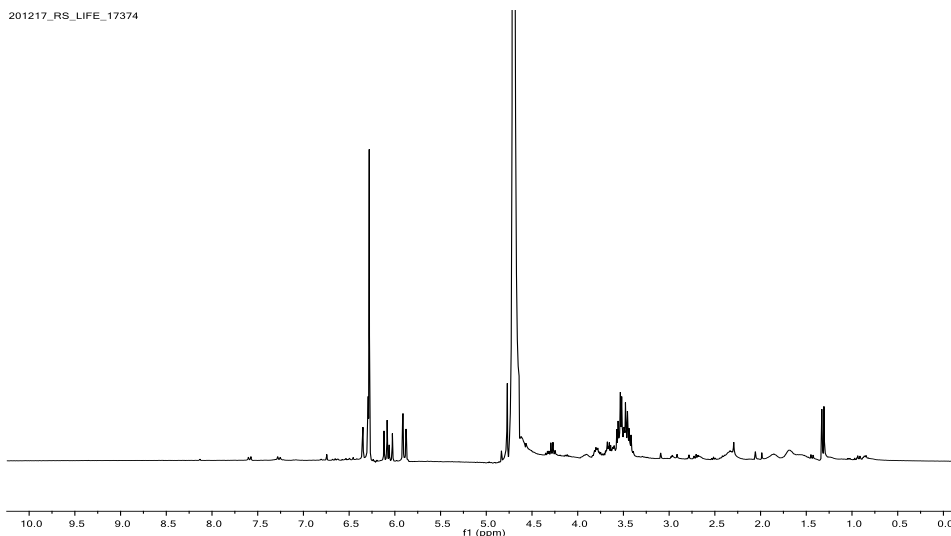


Fig. 3. ¹H NMR spectrum of intermediate, in D₂O.

2.3 Biopolymers application for leather making

Chrome tanned bovine hides of a thickness of 1,2-1,3 mm were used in order to carry out application trials. Biopolymers A1 and A2 were applied on leather following the re-tanning formulation reported below (Table 1):

Table 1. BIOPOL recipe

Wetting Back:	0.3% Ethoxylated surfactant
Retanning:	6 % Biopolymer A1 or A2;
Fatliquoring:	3 % of Sulphited oil
Dyeing :	4 % of Acid Brown 425

% Based on wet blue weight

Comparison trials were carried out using traditional petro-based chemicals such as Phenolic Syntan and Acrylic resin (Table 2).

Table 2. Standard recipe

Wetting Back:	0.3 % Ethoxylated surfactant
Retanning:	6 % Acrylic resin or Phenolic Syntan
Fatliquoring:	3 % of Sulphited oil
Dyeing:	4 % of Acid Brown 425

% Based on wet blue weight

2.4 Trial Results

The leathers treated with Biopolymers showed good performances in comparison with the standard treatment as well as environmental benefits. In particular, Biopolymer A1 led to a very tight and firm crust whereas Biopolymer A2 led to very full crust with a fine grain and pleasant feel. All the leather showed a good dyeability: more brilliant color and deeper shade than standard crusts. The physical tests were performed on the obtained crust, as reported in Table 3.

Table 3: Physical test on leather crust

ANALYSIS	Method	A1	A2	Std1	Std2
Light Fastness 72h/BST 50°C (Blue wool scale)	UNI EN IOS 105- B02	5	4.5	4	4
Fogging Refectometric 6h/75°C (%)	ISO 17071 A	99	98	96	94
Fogging gravimetric 6h/100°C (mg)	ISO 17071 B	0.8	1.1	2.3	3.5

A1: Biopolymer A1, A2: Biopolymer A2, Std1: Acrylic Resin, Std2: Phenolic Syntan

Table 4. wastewater pollution load

ANALYSIS	A1	A2	Std1	Std2
COD (mg O ₂ / L) ISO 6060	2700	3600	3900	4600

A1: Biopolymer A1, A2: Biopolymer A2, Std1: Acrylic Resin, Std2: Phenolic Syntan

3 Experimental

3.1 Materials

Materials used for the synthesis of biopolymers were obtained from CODYECO whereas the hydrolysed biomasses were supplied by ILSA.

3.2 General procedure for the synthesis of biopolymers

A glass reactor fitted with stirrer, heating mantle and condenser has been used in the synthesis of novel biopolymers. The reaction was carried out between 50 °C-100 °C. Initially polyols were heated into the reactor and the biomass was added upon dispersing. The condensation agent was added and the reaction was continued for several hours till the desired molecular weight was achieved.

4 Conclusions

The possibility to recycle wastes and by-products from the leather and agricultural industry has been reported.

Characterization data confirm that interaction among reagents lead to the desired biopolymers. The biopolymers produced, appear promising for automotive leather because of the good reflectometric/gravimetric fogging values. The resulting exhausted bath CODs for both biopolymers application was lower than reference chemicals, meaning that less environmental impacts can be achieved using the new products.

5 Acknowledgements

This study was carried out with the contribution of the LIFE PROGRAMME of the European Union.

References

1. *Official Journal of the European Communities*, L 257, 10 October 1996
2. Dixit, S.; Yadav, A.; Dwivedi, P.D.; Das, M.: *Toxic hazards of leather industry and technologies to combat threat: a review*, *J. Clean. Prod.*, 87, 39-49, 2015
3. Lofrano, G.; Meric, S.; Zengin, G.E., Orhon, D.: *Chemical and biological treatment technologies for leather tannery chemicals and wastewaters: A review*, *Science of the Total Environment*, 461-462, 265-281, 2013
4. Black, M.; Canova, M.; Rydin, S.; Scalet, B.M.; Roudier, S.; Sancho, L.D.; *Best Available Techniques (BAT) Reference Document for the Tanning of Hides and Skins*, Luxembourg: Publications Office of the European Union, 2013
5. A. Ramanjooloo, A. Bhaw-Luximon, D. Jhurry, F. Cadet, *¹H NMR Quantitative Assessment of Lactic Acid Produced by Biofermentation of Cane Sugar Juice*, *Spectroscopy Letters*, 42, 296-304, 2009

DENOISING AND SEGMENTATION OF MCT SLICE IMAGES OF LEATHER FIBERS

Hua Yuai^{1,b)}, Lu Jianmei^{2,c)}, Zhang Huayong^{3,d)}, Cheng Jinyong^{4,e)}, Liang Wei^{5,f)}, Li Tianduo^{3,a)}

1. Qilu University of Technology, School of Mathematics and Statistics, Jinan, China

2. Jiangnan University, School of chemical and material engineering, Wuxi, China

3. Qilu University of Technology(Shandong Academy of Sciences), Shandong Provincial Key Laboratory of Molecular Engineering, School of Chemistry and Pharmaceutical Engineering, Jinan, China

4. Qilu University of Technology, School of Computer Science and Technology, Jinan, China

5. Qilu University of Technology, School of Electrical Engineering and Automation, Jinan, China

a)Corresponding author: ylpt6296@vip.163.com

b) huayuai2015@163.com

c) jianmei.lu@126.com

d) sdzhy@qlu.edu.cn

e) cjy@qlu.edu.cn

f) dzhlw0918@126.com

Abstract. A series of image denoising algorithms, segmentation algorithms and reconstruction algorithms are designed for processing in-situ leather fiber MCT images and resin-embedded MCT slice images. Three-dimensional reconstruction images of fiber bundles were obtained.

1 Introduction

The braiding structure of leather fibers has not been understood clearly and it is very useful and interesting to study it, whether in theory or in application.

Microscopic X-ray tomography (MCT) technology can produce cross-sectional images of the leather fibers without destroying their structure. The three-dimensional structure of leather fibers can be reconstructed by using MCT slice images, so as to show the braiding structure and regularity of leather fibers. The denoising and segmentation of MCT slice images of leather fibers is the basic procedure for three-dimensional reconstruction. In order to study the braiding structure of leather fibers, the resin-embedded leather fiber MCT slice images and the in-situ leather fiber MCT slice images were analyzed and processed. It is showed that the resin-embedded leather fiber MCT images were quite different from the in-situ leather fiber MCT images. The in-situ leather fiber MCT images could be denoised relatively easily. But denoising of resin-embedded leather fiber MCT images is a challenge because of its strong noises. In addition, some fiber bundles that adhere to each other in the slice image are difficult to be segmented. Lots of image denoising and segmentation methods and algorithms have been proposed up to now. But each image processing method and algorithm may be effective only in some cases. There is no general method to deal with all types of images. In this paper, a series of computer-aided denoising and segmentation algorithms are designed for in-situ MCT slice images and resin-embedded MCT slice images of leather fibers. Each fiber bundle is reconstructed in three dimensional. The structure is fine that has never been seen before.

In this paper, there are two main image denoising methods introduced: one is threshold-denoising method based on grayscale value for the image with lower grayscale level, and the other is threshold-denoising method based on areas for the image with higher grayscale level. The MCT slice image of embedded leather sample has strong noises, which is much more difficult to denoise

than the in-situ MCT slice image. According to the distribution of the grayscale value of the fiber region, background region and the distribution of the block area, the Grayscale-threshold method based on pixel values or region areas are selected for image denoising.

The fiber bundles in wide field MCT images are distributed densely and adherent to each other. Many fiber bundles are separated in one of the images but tightly bound in the adjacent image. This leads to great difficulties for image segmentation. In the process, three main segmentation methods are used: The Grayscale-threshold segmentation method, the Region-growing segmentation method and the Three-dimensional Segmentation method.

2 Image acquisition

Oxygen resin embedding method was used to acquire MCT images. The concentration of epoxy resin is set to be 25% and the curing temperature is set to be 80°C.

2357 embedding section images and 2357 in-situ section images were acquired by MCT method, respectively.

The size of the raw MCT image is 4032×4032 pixels, and the size of each pixel is 0.31um×0.31um. After image acquisition, the images were resized by removing the redundant parts, producing smaller images, in order to perform denoising, segmentation and reconstruction algorithms on the computer automatically and effectively.

Fig.1(a) shows a small part of a raw in-situ leather fiber MCT image, with the size of 1250×1250 pixels; Fig.1(c) shows a small part of a raw resin-embedded leather fiber MCT image, with the size of 1250×1250 pixels.

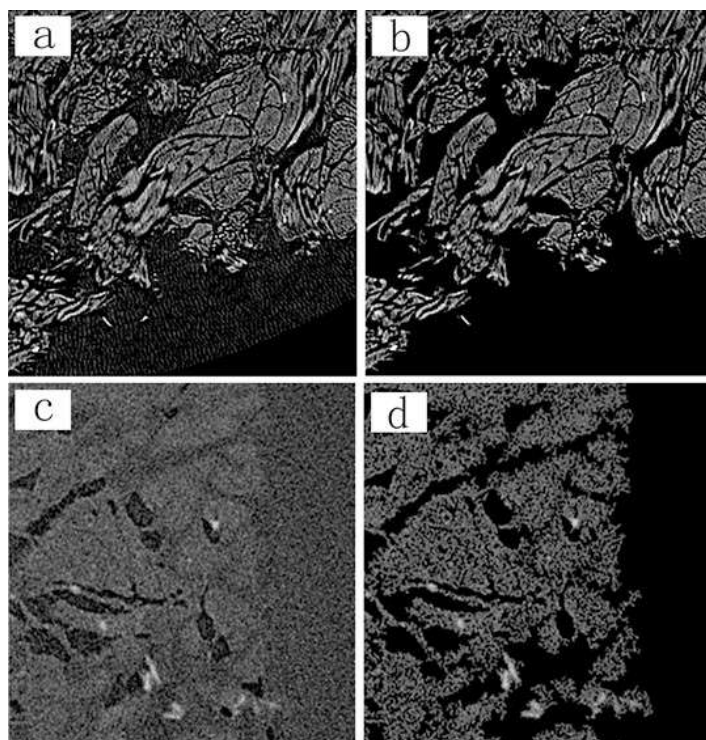


Fig. 1. a. A part of the raw in-situ leather fiber MCT image; b. A part of the denoised in-situ leather fiber MCT image; c. A part of the raw resin-embedded leather fiber MCT image; d. A part of the denoised resin-embedded leather fiber MCT image.

3 Denoising Algorithms

It is relatively easy to denoise in-situ MCT images with the help of two threshold algorithms. Firstly, remove pixels of lower grayscale value, and then remove isolated islands with small areas. In the process of denoising, the low-gray-value pixels inside the fiber bundle may be removed at the same time. The Region-filling Algorithm, the Region Expansion and the Region Contraction Algorithm can be used to compensate the 'erroneously deleted' pixels. Fig.1(b) shows a small part of the denoised in-situ MCT image.

For embedding images, a series of image processing algorithms were used to perform denoising procedure, including the Threshold Algorithm based on the grayscale value and based on the area of region, respectively, the Region-filling Algorithm, the Expansion Algorithm and the Corrosion Algorithm. Fig.1(d) shows a small part of the denoised embedding MCT image.

All the works mentioned above were performed with the help of the software Matlab automatically.

As shown in Fig.1.(c), the resin-embedded leather fiber MCT images have much more strong noises than the in-situ leather fiber MCT images.

4 Segmentation and Reconstruction Algorithms

The fiber bundles in wide field MCT images are distributed densely and adherent to each other. Many fiber bundles are separated in one image and tightly bound in another. This leads to great difficulties to image segmentation. In the process of segmenting fiber bundles, the following segmentation methods are used:

a. the Grayscale-threshold Segmentation method: Since the boundary of some adjacent fiber bundles has relatively lower grayscale values, so it can be removed by a grayscale threshold value. This makes different fiber bundles separated.

b. The Region-growing Segmentation method: A set of pixels from the fiber bundle was chosen and expanded by connecting their neighborhood to obtain the maximum connected region.

c. Three-dimensional Segmentation method: Because of the complexity of fiber structure, it was not effective to segment the fiber bundles slice by slice. The cross-sectional shape of the same fiber bundle may be quite different in two adjacent slices. It is difficult to determine whether it belongs to the same fiber bundle. The reconstruction procedure works well with the segmentation algorithm for segmenting some of this kind of bundles but not all.

On the basis of denoising and preliminary image segmentation as mentioned above, Three-dimensional Reconstruction algorithms is carried out. In this process, Forward-tracking method and Backward-tracking method are used. The Forward-tracking method is to select the cross-sectional area of a fiber bundle from the first slice image and connects the cross-sectional area of the bundle on the adjacent image in turn until reaching the last one. This algorithm may lead the loss of some of the backward branches of the fiber bundles. In order to remedy this defect, on the basis of the three-dimensional reconstruction of the fiber bundle obtained by the Forward-tracking method, the cross-section area of the fiber bundle in the front adjacent image is connected in turn from the last picture of the fiber bundle to the first one. This algorithm is called the Backward-tracking method.

The Three-dimensional Reconstruction Algorithm combined with the Forward-tracking method and the Backward-tracking method produces a three-dimensional reconstruction image, as shown in Fig.2.

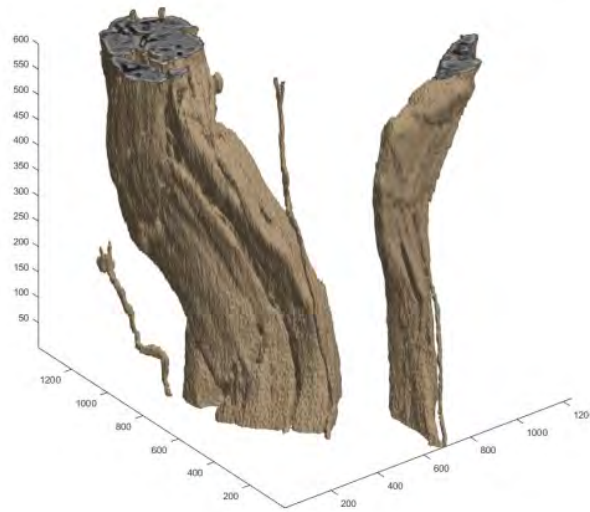


Fig. 2. 3-D reconstruction of the in-situ leather fiber MCT image in part. The scale unit is the pixel.

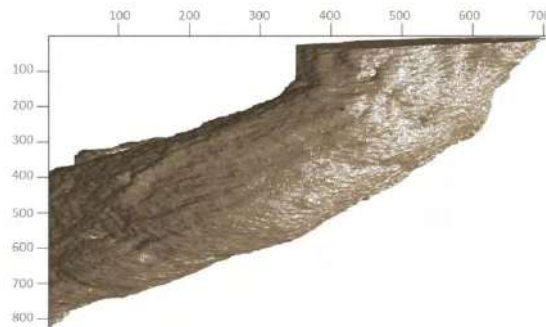


Fig. 3. 3-D reconstruction of the in-situ leather fiber MCT image in small part. The scale unit is the pixel.

Since the size of three-dimensional reconstruction image is usually too large to display with the software Matlab, it is necessary to reduce the size of the image to display panorama, or display some parts of the image in order to show details, as shown in Fig.3.

5 Conclusions

A series of image denoising algorithms, segmentation algorithms and reconstruction algorithms are designed for processing in-situ leather fiber MCT images and resin-embedded MCT slice images. These algorithms are automatically implemented by computer with software Matlab. For the in-situ leather fiber MCT images, two main algorithms were developed to do image denoising and segmentation. One is the Threshold-denoising Algorithm based on grayscale value for the image with lower grayscale level, another is the threshold-denoising method based on area for the image with higher grayscale level. For the embedded MCT images, the Grayscale Threshold Algorithm based on pixel values and the Grayscale Threshold Algorithm based on region areas were used to do image denoising according to the distribution of the grayscale value of the fiber region and background region and the distribution of the block area. At last three-dimensional reconstruction images of fiber bundles were obtained.

The image denoising, the image segmentation and the image reconstruction algorithms proposed in this paper have remarkable effect in processing the in-situ leather fiber MCT images. A series of three-dimensional images based on this work demonstrate the fine spatial braiding

structure of leather fibers, which would help us to understand the braiding structure of leather fibers better. Due to the complexity of the fiber structure, interlaced bundles of fibers are not yet well segmented. Further study is needed.

6 Acknowledgments

This work was supported by the National Natural Science Foundation of China (Grant No. 21776143, 21606138) and Program for Li Tianduo Taishan Scholar Team of Shandong Province.

References

1. D. Birk, E.I. Zycband, D.A. Winkelmann, R.L. Trelstad, *Collagen Fibrillogenesis in Situ: Fibril Segments are Intermediates in Matrix Assembly*, PNAS, USA, 1989, 86, 4549–4553.
2. I. Johanes, E. Mihelc, M. Sivasankar, A. Ivanisevic, *Morphological Properties of Collagen Fibers in Porcine Lamina Propria*, J. Voice, 2011, 25(2), 254–257.
3. J.A.M. Ramshaw, *Probing Collagen Structure and Function*, Heidemann Lecture, 2017.
4. S. Osher, J.A. Sethian, *Fronts Propagating with Curvature Dependent Speed : Algorithms Based on Hamilton-Jacobi Formulations*, J. Comput. Phys., 1988, 79, 12–49.
5. W. Denk, H. Horstmann, *Serial Block-face Scanning Electron Microscopy to Reconstruct Three-Dimensional Tissue Nanostructure*, Plos. Biol., 2004, 2, 1900–1910.
6. H.Y. Zhang, Y.M. Xia, J.Y. Cheng, L. Shi, T.D. Li, *A Novel Technique for Getting Leather Section Image Based on Metallographic Sample Preparation*, JALCA, 2013, 108 (5), 166–170.
7. H.Y. Zhang, Y.M. Xia, L. Shi, T.D. Li, *Characterization of Leather Structure via Metallographic Sample Preparation*, JALCA, 2014, 109 (1), 1–7.
8. H.Y. Zhang, H.W. Lu, Y.L. Zan, Y.M. Xia, T.D. Li, *Characterization of Goat Leather Structure Using A Metallographic Technique*, JALCA, 2015, 99(1), 23–29.
1. 9. Rafael C. Gonzalez, Richard E. Woods, *Digital Image Processing, Third Edition*, New Jersey :Pearson Education, Inc.
2. 10. Matlab-The Language of technical Computing, The Math Works, Inc.
3. 11. Rafael C. Gonzalez, Richard E. Woods, *Digital Image Processing, Third Edition*. Pearson Education. Inc., 2010.

FACTORS AFFECTING PENETRATION OF ACRYLIC RESIN IN CRUST LEATHER DURING RETANNING PROCESS

Y. Song¹, Y. H. Zeng¹, M. R. Cao² and B. Shi^{1,2}

¹National Engineering Laboratory for Clean Technology of Leather Manufacture, Sichuan University, Chengdu 610065, P. R. China

²Key Laboratory of Leather Chemistry and Engineering (Sichuan University), Ministry of Education, Chengdu 610065, P. R. China

a)Corresponding author: zengyunhang@scu.edu.cn

b)First author: sdngdong123@126.com

Abstract. Acrylic resin (AR) is a most popular retanning agent due to its selective filling property and advantage of formaldehyde-free. The retanning performance of acrylic resin mainly depends on its penetration depth and filling parts in leather. Therefore, to improve the retanning performance, it is necessary to fully understand the factors affecting the mass transfer and the distribution of acrylic resin in leather. We have found that the structure and the charge of leather and the dosage of acrylic resin rather than the molecular weight of acrylic resin are important factors affecting the penetration rate of acrylic resin in crust leather by using fluorescent tracer technique. In this study, from the view of electrostatic interaction, effects of neutralizing pH and retanning auxiliaries such as phenol sulfonic acid condensation (PSAC) and sodium carboxymethylcellulose (CMC) on the penetration and the distribution of acrylic resin in crust leather were investigated. Higher neutralizing pH led to a faster transfer of acrylic resin in leather because of the decrease in the positive charges of chrome-tanned leather (isoelectric point 7.1) and the increase in the negative charges of acrylic resin. Employing PSAC and CMC enhanced acrylic resin transfer in crust leather due to the dramatic increase in the negative charges of acrylic resin. These results indicated that decreasing the electrostatic binding force between acrylic resin and crust leather is beneficial to the penetration of acrylic resin in leather, which could be achieved by adjusting the neutralizing pH or using acrylic resin together with proper retanning auxiliaries.

1 Introduction

Retanning process plays a crucial role in leather manufacture since it can improve the aesthetic and physical properties such as the handle, the cutting value or some specific properties of leather¹⁻³. Acrylic resin (AR) is a most popular retanning agent due to its selective filling property and advantage of formaldehyde-free⁴⁻⁵. It is well known that the retanning performance of acrylic resin is closely related to its penetration depth and filling parts in leather⁶. Therefore, to improve the retanning performance, it is necessary to fully understand the factors affecting the penetration and the distribution of acrylic resin in leather. In our previous work, an accurate method for visualizing and semi-quantifying the penetration of acrylic resin in leather has been developed with a fluorescent tracer technique⁷. Using this technique, we have found that the structure⁸ and the charge of leather⁹⁻¹⁰ and the dosage of acrylic resin⁸⁻⁹ rather than the molecular weight of acrylic resin⁹ are important factors affecting the penetration rate of acrylic resin in the crust leather.

Since the electrostatic force between the acrylic resin surface and the leather surface is significant for controlling the penetration and the uptake of acrylic resin in leather¹¹⁻¹³, therefore, in this study, factors affecting the penetration of acrylic resin in crust leather were investigated from the view of electrostatic interaction between acrylic resin and leather. Because the float pH is of great importance to control the surface charge of leather¹³⁻¹⁴, tanners usually change the neutralizing pH to adjust the electrostatic force between the retanning agents and the leather. Phenol sulfonic acid condensation (PSAC), a main component of syntans, is a strong anionic substance with sulfonic acid group and phenolic hydroxyl. Moreover, sodium carboxymethylcellulose (CMC) is a kind of green and biodegradable polymer compounds¹⁵, which has lots of carboxymethyl groups¹⁶. The strong anionic properties of PSAC and CMC might decrease the surface charge of acrylic resin and leather and enhance the penetration of acrylic

resin in leather. Thus, effects of neutralizing pH, PSAC and CMC on the distribution of acrylic resin in the retanned leather were investigated using the fluorescent tracer technique. The results obtained would enlighten us on finding the key point to control the acrylic resin penetration and achieve a desired retanning performance.

2 Material and Methods

2.1 Materials

Two pieces of the chrome-tanned cow leather with a shaved thickness of 1.2 mm (200 g for each) were used for neutralizing and retanning trials. One piece of the shaved leather was neutralized to pH 4.5, and the other piece of the shaved leather was neutralized to pH 6.5, according to the typical leather processing procedures. Acrylic resin (AR, 35 wt.% in water), composed of the poly(acrylic acid), was synthesized in our laboratory. 5-aminofluorescein (AF) were purchased from Shanghai aladdin Biochemical Technology Co., Ltd.. The fluorescent labeled acrylic resin (AF-AR) was prepared according to the method described in our previous study^{7,9}. Phenol sulfonic acid condensation (PSAC, solid content \geq 95%) was provided by Sichuan Decision Chemical Co., Ltd. (China), and sodium carboxymethylcellulose (CMC) was purchased from Chengdu Jinshan Chemical Reagent Co., Ltd. (China). All the chemicals used for leather processing were of commercial grade, and the other chemicals were of analytical grade.

2.2 Effect of neutralizing pH on penetration of AR in leather

To investigate the pH effect on the penetration of AR in leather, two pieces of the neutralized leather (pH 4.5, 3g for each) were retanned with 3% AF-AR and 6% AF-AR (based on weight of neutralized leather) for 90 min, respectively. Another two pieces of the neutralized leather (pH 6.5, 3g for each) were also retanned with 3% AF-AR and 6% AF-AR for 90 min, respectively. The float ratio of retanning herein was 100%, and the temperature was 35°C.

After retanning for 90 min, the four retanned leathers were sampled and cut into vertical sections of 20 μ m thickness on a freezing microtome (CM1950, Leica, Germany). The distribution of AF-AR in the sections was observed using an inverted fluorescence microscope (Ti-U, Nikon, Japan), and the relative content and the penetration rate of AF-AR in the leathers were semi-quantified by processing the fluorescence micrographs with LAS X software.

2.3 Effect of PSAC on penetration of AR in leather

Three pieces of the neutralized leathers (pH 4.5) numbered 1-3 (3 g for each) were retanned as below. The leather No. 1 was retanned with 3% AF-AR and 100% water at 35°C for 90 min, and the leathers No. 2-3 were retanned in the same conditions except addition of 0.25% and 0.50% PSAC, respectively. Moreover, another three pieces of the neutralized leathers (pH 6.5) numbered 4-6 were treated in the same conditions as leathers No. 1-3. After retanning for 90 min, the six leather samples were analyzed as described in Section 2.2 for obtaining the distribution of AF-AR in leather.

2.4 Effect of CMC on penetration of AR in leather

To investigate the effect of CMC on the penetration of AR in leather, three pieces of the neutralized leathers of pH 4.5 and three pieces of pH 6.5 were retanned in the same conditions of Section 2.3 except replacing PASC with CMC. After retanning, the leather samples were also analyzed as described in Section 2.2 for obtaining the distribution of AF-AR in leather.

3 Results and Discussion

3.1 The Effect of neutralizing pH on Penetration of AR in Leather

The distributions of AR in the retanned leathers were as shown in Figures 1(a), 1(b) and 1(c). It can be seen that the penetration depth, relative content and penetration rate of AF-AR in leather were increased with increasing neutralizing pH and AF-AR dosage. After retanning with 3% AF-AR for 90 min, the penetration depths of AF-AR in the grain layer and flesh layer of the leather neutralized to pH 4.5 were 0.07 mm and 0.18 mm, respectively, while those in the grain layer and flesh layer of the leather neutralized to pH 6.5 were 0.32 mm and 0.35 mm, respectively (see Figure 1 (b1)). This is because compared with neutralizing to pH 4.5, neutralizing to pH 6.5 decreases the positive charges of chrome-tanned leather (isoelectric point 7.1) and increases the negative charges of acrylic resin, which is helpful in reducing the electrostatic attraction between the acrylic resin and the crust leather (Figure 2). When the AF-AR dosage was increased from 3% to 6%, the penetration rate of AF-AR in the leather (pH 4.5) was increased from 18% to 39%, but it still lower than that (48%) in the leather (pH 6.5) retanned with only 3% AF-AR. Moreover, AF-AR penetrated the whole leather neutralized to pH 6.5 when using 6% AF-AR. These results indicate that neutralizing pH has a greater effect than the acrylic resin dosage, meaning that the electrostatic attraction is a more important factor affecting the penetration rate of acrylic resin in leather than the concentration gradient.

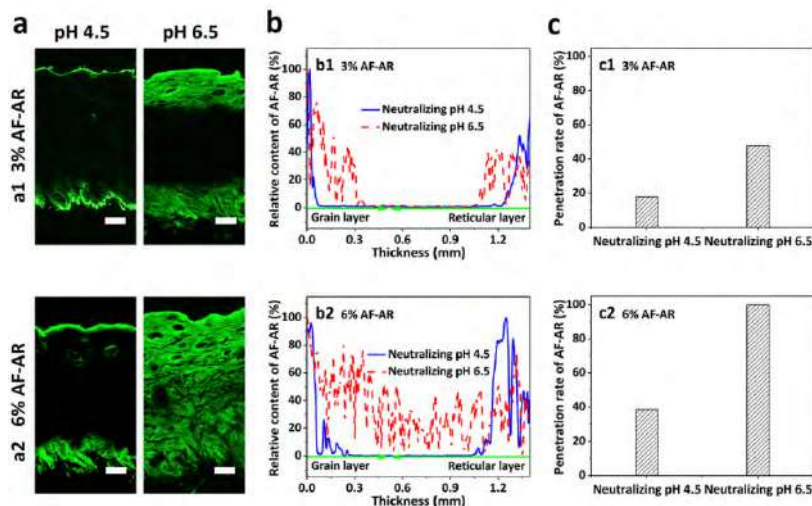


Fig. 1. (a) Fluorescence micrographs of vertical sections (bar 500 μ m) from the retanned leathers; (b) relative contents and (c) penetration rates of AF-AR in the leathers obtained by analysis of Figure 1 (a) using Image J software.

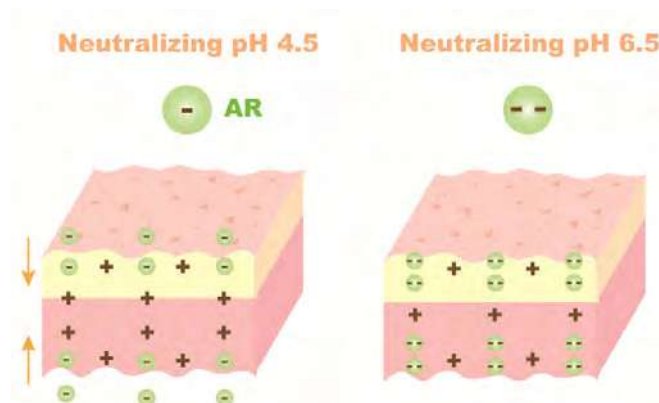


Fig. 2. Schematic diagram of penetration of acrylic resin in the leathers neutralized to pH 4.5 or 6.5.

3.2 The Effect of PSAC on Penetration of AR in Leather

In retanning process, tanners usually compound retanning agents with various auxiliaries to obtain an excellent retanning performance. In this part, PSAC, a strong anionic substance with sulfonic acid group and phenolic hydroxyl, was used to decrease the surface charge of acrylic resin and leather for enhancing the penetration of acrylic resin in leather.

From Figures 3(a), 3(b) and 3(c), it was obvious that the penetration depth of AF-AR in leather was increased with the dosage of PSAC. When the leather was neutralized to pH 4.5, the penetration rate of AF-AR in the leather retanned with 3% AF-AR was about 18%, and that in the leather retanned with 3% AF-AR and 0.5% PSAC was increased to 39%. When the leather was neutralized to pH 6.5, the penetration rate of AF-AR in the leather retanned with 3% AF-AR was about 48%, while the penetration rate of AF-AR in leather was higher than 84% even if using only 0.25% PSAC together with 3% AF-AR. Specifically, AF-AR almost fully penetrated the crust leather when retanning with 3% AF-AR together with 0.50% PSAC. This is because using PSAC could decrease the positive charges of leather due to the reaction between the phenolic hydroxyl of PSAC and leather and the incorporation of the sulfonic acid group of PSAC into leather. On the other hand, adding PSAC could also increase the negative charges of acrylic resin, which is helpful in reducing the electrostatic attraction between acrylic resin and leather (Figure 4). Adding 0.5% PSAC effectively increased the penetration rate of acrylic resin in leather (92%, Figure 3(c2)), which was close to that by using 6% AF-AR (100%, see Figure 1(c2)). These results also confirm that the electrostatic attraction between acrylic resin and leather plays an important role in the penetration of acrylic resin in leather.

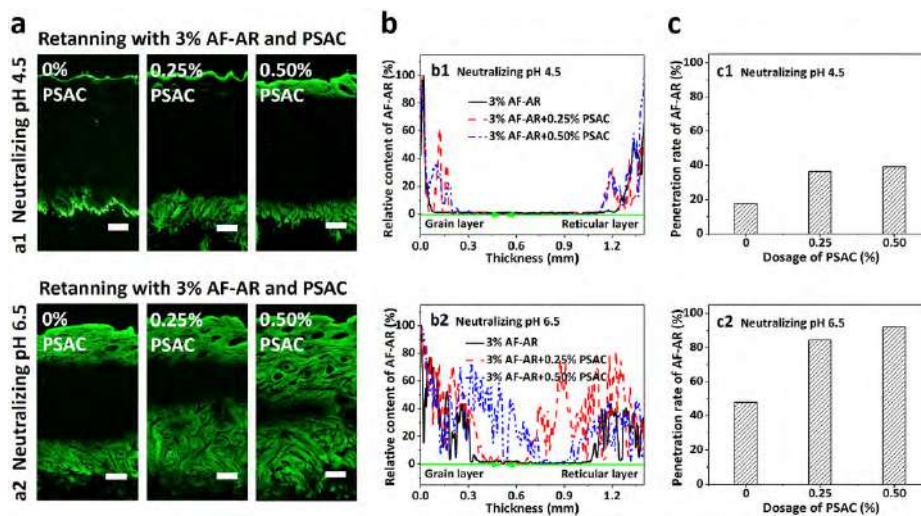


Fig. 3. (a) Fluorescence micrographs of vertical sections (bar 500 μ m) from the leathers retanned with 3% AF-AR and PSAC; (b) relative contents and (c) penetration rates of AF-AR in the leathers obtained by analysis of Figure 3 (a) using Image J software.

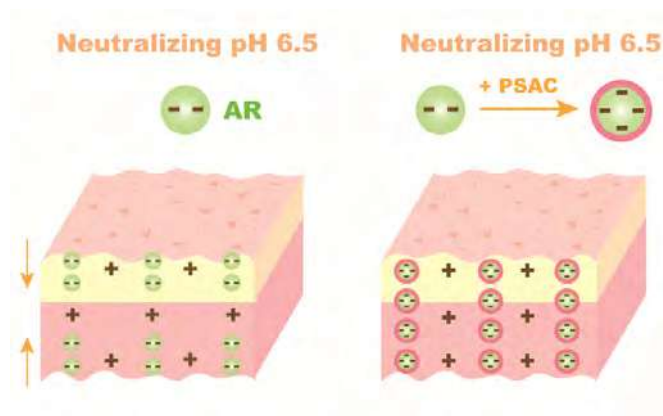


Fig. 4. Schematic diagram of penetration of acrylic resin in the leathers retanned with AF-AR or the mixture of AF-AR and PSAC.

3.3 The effect of CMC on penetration of AR in leather

In this part, anionic CMC with abundant carboxymethyl groups and good biodegradability was also chose to investigate the effect of electrostatic attraction between acrylic resin and leather on the penetration of acrylic resin in leather.

Figures 5(a), 5(b) and 5(c) showed that adding CMC obviously increased the penetration depth, the relative content and the penetration rate of AF-AR in leather. When the crust leather was neutralized to pH 4.5, after retanning with 3% AF-AR, the penetration rate of AF-AR in leather was about 18%. After retanning with 3% AF-AR and 0.5% CMC, the penetration rate of AF-AR in the leather was increase to 39%, where the penetration depths of AF-AR in the grain layer and flesh layer were 0.25 mm and 0.30 mm, respectively. When the crust leather was neutralized to pH 6.5, the penetration depths of AF-AR in the grain layer and flesh layer of the leather retanned with 3% AF-AR and 0.25% CMC were 0.43 mm and 0.55 mm, respectively, and those in the grain layer and flesh layer of the leather retanned with 3% AF-AR and 0.50% CMC were 0.44 mm and 0.78 mm, respectively. Moreover, the penetration rates of AF-AR in leather by adding 0.25% CMC and 0.50% CMC were 70% and 87%, respectively, which were significantly higher than that in the leather retanned with only 3% AF-AR (48%). These results show that using anionic CMC can obtain a similar effect to PSAC on promotion of acrylic resin penetration, which indicates that reducing the electrostatic attraction between acrylic resin and leather indeed increases the penetration rate of acrylic resin in leather (Figure 6). The fact that the penetration rate of acrylic resin by adding CMC was slightly lower than adding PSAC might be due to the thickening property and the higher molecular weight of CMC.

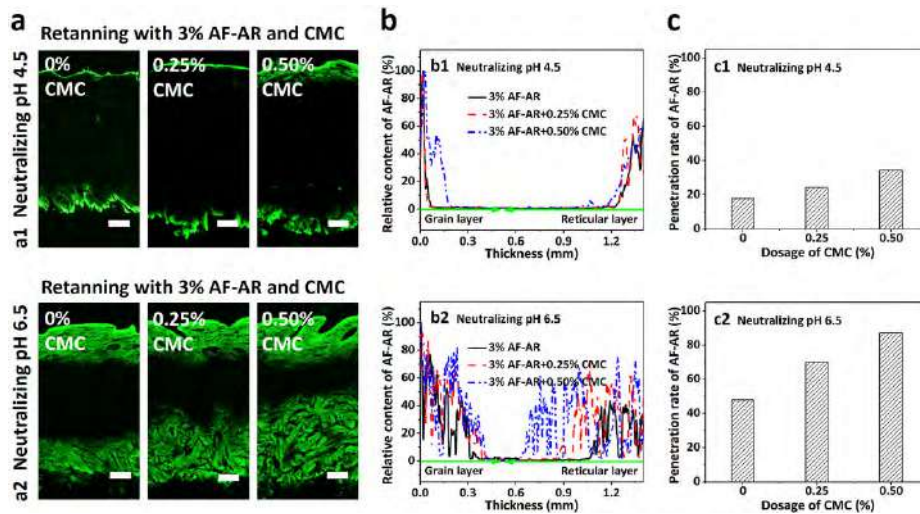


Fig. 5. (a) Fluorescence micrographs of vertical sections (bar 500 μm) from the leathers retanned with 3% AF-AR and CMC; (b) relative contents and (c) penetration rates of AF-AR in the leathers obtained by analysis of Figure 5 (a) using Image J software.

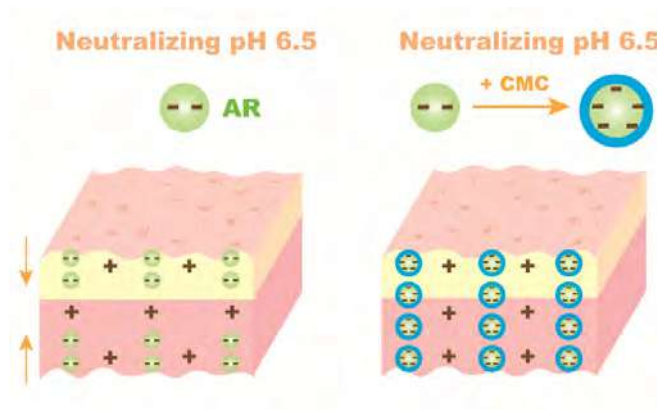


Fig. 6. Schematic diagram of penetration of acrylic resin in leathers retanned with AF-AR or the mixture of AF-AR and CMC.

4. Conclusion

Surface charge properties of acrylic resin and leather are important factors affecting the penetration of acrylic resin in retanning process. Neutralizing to higher pH and employing anionic materials, such as PSAC and CMC, can effectively improve the penetration rate of acrylic resin in leather due to the decrease in the positive charges of leather and the increase in the negative charges of acrylic resin. These results suggest that decreasing the electrostatic binding force between acrylic resin and leather is a promising approach to improve the penetration of acrylic resin in leather and obtain an intended retanning performance.

5. Acknowledgements

This work was supported by the National Natural Science Foundation of China (21878193) and the Graduate Student's Research and Innovation Fund of Sichuan University (2018YJSY086).

References

1. Taylor, M., Lee, J., Bumanlag, L. P., Balada, E. H.: *Treatments to enhance properties of chrome-free (wet white) leather*, *J. Am. Leather Chem. Assoc.*, 106, 35-43, 2011
2. Covington, A. D.: *Tanning chemistry: The science of leather*, Cambridge: Royal Society of Chemistry, pp. 352, 2011
3. Sun, X., Jin, Y., Lai, S., Pan, J., Du, W., Shi, L.: *Desirable retanning system for aldehyde-tanned leather to reduce the formaldehyde content and improve the physical-mechanical properties*, *J. Clean. Prod.*, 175, 199-206, 2018
4. Jin, L. Q., Wang, Y. L., Zhu, D. Y., Xu, Q. H.: *Effect of amphoteric acrylic retanning agent on the physical properties of the resultant leather*, *Adv. Mater. Res.*, 284-286, 1925-1928, 2011
5. Jankauskaite, V., Jiyembetova, I., Gulbiniene, A., Sirvaityte, J., Beleska, K., Urbelis, V.: *Comparable evaluation of leather waterproofing behaviour upon hide quality. I. Influence of retanning and fatliquoring agents on leather structure and properties*, *Mater. Sci.-Medzg.*, 18, 150-157, 2012
6. Sivakumar, V., Swaminathan, G., Rao, P. G. Ramasami, T.: *Influence of ultrasound on diffusion through skin/leather matrix*, *Chem. Eng. Process.*, 47, 2076-2083, 2008
7. Zeng, Y. H., Song, Y., Li, J., Zhang, W. H., Shi, B.: *Visualization and quantification of penetration/mass transfer of acrylic resin retanning agent in leather using fluorescent tracing technique*, *J. Am. Leather Chem. Assoc.*, 111, 398-405, 2016
8. Song, Y., Zeng, Y. H., Shi, B.: *Effect of histological feature of leather on acrylic resin retanning*, *J. Soc. Leather Technol. Chem*, 102, 149-154, 2018
9. Song, Y., Zeng, Y. H., Xiao, H. L., Wu, H. P., Shi, B.: *Effect of molecular weight of acrylic resin retanning agent on properties of leather*, *J. Am. Leather Chem. Assoc.*, 112, 128-134, 2017
10. Song, Y., Wang, Y. N., Zeng, Y. H., Wu, H. P., Shi, B.: *Quantitative determinations of isoelectric point of retanned leather and distribution of retanning agent*, *J. Am. Leather Chem. Assoc.*, 113, 232-238, 2018
11. Heidermann, E.: *Fundamentals of leather manufacture*, Darmstadt: Eduard Roether KG, 1993
12. Cantera, C., Martegani, J., Esterelles, G., Vergara, J.: *Collagen hydrolysate: 'soluble skin' applied in post-tanning processes Part 2: Interaction with acrylic retanning agents*, *J. Soc. Leather Technol. Chem*, 86, 195-202, 2002
13. Wang, Y. N., Huang, W. L., Zhang, H. S., Tian, L., Zhou, J. F., Shi, B.: *Surface charge and isoelectric point of leather: A novel determination method and its application in leather making*, *J. Am. Leather Chem. Assoc.*, 112, 224-231, 2017
14. Guthrie-Strachan, J., Flowers, K.: *Protein and leather charge*, *World Leather*, 18, 19-23, 2005
15. Khalil, H. P. S., Tye, Y. Y., Saurabh, C. K., Leh, C. P., Lai, T. K., Chong, E. W. N., Nurul Fazita, M. R., Mohd Hafidz, J., Banerjee, A., Syakir, M. I.: *Biodegradable polymer films from seaweed polysaccharides: A review on cellulose as a reinforcement material*, *Express Polym. Lett.*, 11, 244-265, 2017
16. Umoren, S. A., Eduok, U. M.: *Application of carbohydrate polymers as corrosion inhibitors for metal substrates in different media: A review*, *Carbohydr. Polym.*, 140, 314-341, 2016

MESOPOROUS HOLLOW SiO₂ SPHERES STABILIZED PICKERING EMULSION TO IMPROVE WATER VAPOR PERMEABILITY AND WATER RESISTANCE FOR LEATHER FINISHING AGENT

Yan Bao^{1,3*}, Yuanxia Zhang^{1,2*} and Jianzhong Ma^{1,3*}

¹ College of Bioresources Chemical and Materials Engineering, Shaanxi University of Science and Technology, Xi'an, 710021, PR, China.

² National Demonstration Center for Experimental Light Chemistry Engineering Education, Shaanxi University of Science and Technology, Xi'an, 710021, PR, China.

³ Shaanxi Research Institute of Agricultural Products Processing Technology, Xi'an, 710021, PR, China.

1) Corresponding author: Yan Bao, E-mail: baoyan@sust.edu.cn

2) Jianzhong Ma, E-mail: majz@sust.edu.cn

Abstract. In order to solve the negative impact of coating on water vapor permeability of leather and overcome the poor water resistance of polyacrylate leather finishing agent, it was proposed that the mesoporous SiO₂ spheres with hollow structure instead of traditional surfactant were introduced into polyacrylate by Pickering emulsion polymerization. It was expected to increase the water vapor permeability of polyacrylate membrane by increasing the path and shortening the route of water vapor molecules through the membrane, and improve the water resistance of membrane by avoiding the use of surfactant. Hence, stable Pickering emulsion stabilized by mesoporous hollow SiO₂ spheres was prepared and its stability was investigated by Turbiscan Lab in this paper. Water vapor permeability and water uptake of polyacrylate membrane were also studied. Compared with emulsion stabilized by surfactant, Pickering emulsion indicated excellent stability with lower TSI value of 0.5. Contrasted with polyacrylate membrane with SDS, the introduction of mesoporous hollow SiO₂ spheres can improve the water vapor permeability of polyacrylate membrane. Meanwhile, water absorption measurements showed that the water absorption ratio of the membrane with mesoporous hollow SiO₂ spheres reduction of down to 40.84%, possessing the ideal ability to water resistance of polyacrylate membrane. This study can provide a theoretical foundation for designing and synthesizing leather finishing agent with excellent stability, water vapor permeability and water resistance synchronously.

Keywords: Pickering emulsions; mesoporous hollow SiO₂ spheres; stability; water vapor permeability; water resistance

1 Introduction

Water vapor permeability of coating for leather is of great importance when the leather is used for the shoes and clothes [1]. In order to keep human bodies comfortable, shoes and clothes should have high water vapor permeability value, which allows perspiration to evaporate promptly, especially when people are in hot environments.

Up to date, many effects to improve the hygienic performance of leather have been done. In the study conducted by Zheng et al., high water vapor permeable porous materials were prepared by polyporous coating, blending of waterborne polyurethanes (WPU) and polyacrylate (AC) on fabrics [2]. It revealed that the introduction of hydrophilic groups can significantly improve the moisture permeability of the membrane, but the presence of hydrophilic groups of AC will lead to the poor water resistance. Wu et al. improve the water vapor permeability of polyurethane membranes by increasing the number of micropores in the membrane [3]. It can obviously enhance water vapor permeability of coating. Unfortunately, those ideals have only focus on polyurethane and polymer fiber. There are few studies on water vapor permeability using polyacrylate, although polyacrylate is commonly used in leather. Of particular note, polyacrylate emulsions by emulsion polymerization always show poor water resistance on account of the presence of surfactant.

Inspired by those results, physical blending of hollow SiO₂ spheres and polyacrylate has been proposed to provide pores for the water vapor molecules' passing in our work [4]. Most interestingly, compared with pure polyacrylate membrane, the water vapor permeability of polyacrylate membrane

containing mesoporous hollow SiO₂ spheres is improved greatly. Besides, in the latest study conducted by Yang et al., mesoporous SiO₂ microspheres stabilized Pickering emulsion was reported. It possessed outstanding stability against coalescence, suggesting that the internal pores of particles had positive impacts on the stability of Pickering emulsions [5]. To obtain Ideal polyacrylate leather finishing agent, which possesses excellent stability, water vapor permeability and water resistance synchronously, we aim to fabricate mesoporous hollow SiO₂ spheres stabilized Pickering emulsion. We will deduce the positive effect of the introduction of mesoporous hollow SiO₂ spheres for the stability of polyacrylate emulsion and the water vapor permeability and water resistance of polyacrylate coating for leather.

2 Results and Discussion

As is known, the stability is a key for the property of emulsion. Firstly, the stability of mesoporous hollow SiO₂ spheres stabilized Pickering emulsion has been investigated by Turbiscan Lab Expert. The turbiscan stability index (TSI) was further calculated from the experimental results (Program Turbiscan Easy Soft) using the following equation (1) [6]. Generally, a low value of TSI indicates the ideal stability of polyacrylate emulsion [7].

$$TSI = \sqrt{\frac{\sum_{i=1}^n (x_i - x_{BS})^2}{n-1}} \quad (1)$$

Where: x_i is the mean backscattering and transmission of each scan in experiment, x_{BS} is the mean x_i , and n is the number of scans.

It can be seen that the TSI value (Fig. 1b) of polyacrylate emulsion stabilized by SDS changes quicker within 5h. While mesoporous hollow SiO₂ spheres stabilized polyacrylate emulsion exhibits the smaller change and lower TSI value of in Fig. 1b (The maximum TSI value of 0.5). Compared with emulsion stabilized by surfactant, mesoporous hollow SiO₂ spheres stabilized Pickering emulsion indicates excellent stability. It further reveals that mesoporous hollow SiO₂ spheres possess higher adsorption energy at the oil-water interface so that they possess excellent ability to against droplets coalescence.

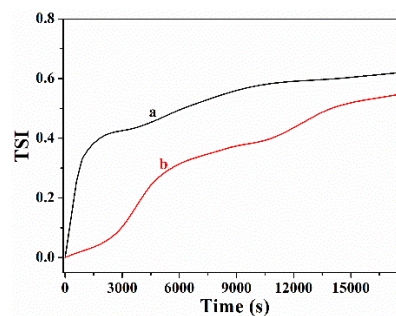


Fig. 1. Time dependence of the stability coefficient TSI of polyacrylate emulsion stabilized by different stabilizers: (a) stabilized by conventional surfactant SDS, (b) stabilized by mesoporous hollow SiO₂ spheres.

In order to clearly understand the effect of mesoporous hollow SiO₂ spheres on water vapor permeability of membrane, water vapor permeability of polyacrylate membrane with SDS as a comparison has been investigated. Of particular interest, the water vapour permeability of membrane with mesoporous hollow SiO₂ spheres is higher than that of membrane with SDS. It shows the introduction of mesoporous hollow SiO₂ spheres can enhance water vapour permeability of membrane. This is because mesoporous hollow SiO₂ spheres further introduce a lot of free volume in the membrane due to their hollow core, which provide many channels for water vapor. Meanwhile, a

small amount of water vapor from the hollow core of SiO₂ spheres can bring a water vapor pressure difference between inside and outside of SiO₂ spheres, enhancing water vapour permeability [8].

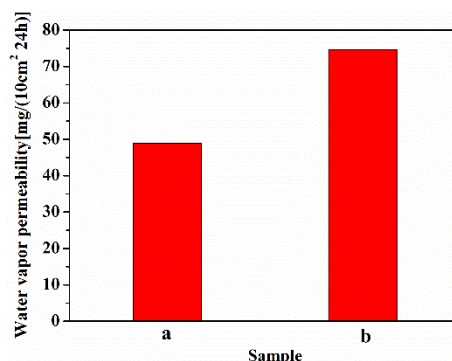


Fig. 2. Water vapor permeability of polyacrylate membranes (a) SDS stabilized polyacrylate emulsion; (b) mesoporous hollow SiO₂ spheres stabilized polyacrylate emulsion.

Further, it can be seen in Fig 3 that water resistance of polyacrylate membrane with SDS is the worst. It is because that surfactant containing hydrophilic group will migrate to the membrane surface in the process of membrane forming and make the water molecules are more likely to enter the membrane inside. However, polyacrylate membrane with mesoporous hollow SiO₂ spheres show water absorption of 40.84%, possessing the ideal ability to water resistance of polyacrylate membrane. Better water resistance also accounts for the strong interfacial adsorption interaction between mesoporous hollow SiO₂ spheres and polyacrylate latex particles.

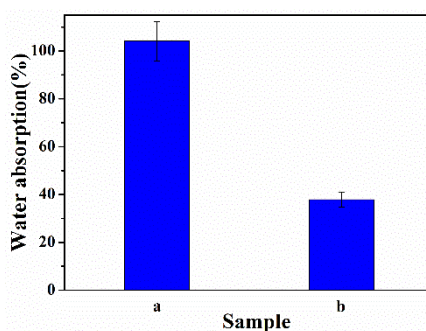


Fig. 3. The water uptake of polyacrylate membranes (a) SDS stabilized polyacrylate emulsion; (b) mesoporous hollow SiO₂ spheres stabilized polyacrylate emulsion.

In summary, mesoporous hollow SiO₂ spheres stabilized polyacrylate emulsion was successfully obtained. The results show that mesoporous hollow SiO₂ spheres stabilized polyacrylate emulsion has excellent stability. The effect of hollow SiO₂ spheres on water vapor permeability and water uptake of polyacrylate membrane were investigated. It indicates that hollow SiO₂ spheres can significantly improve water vapor permeability of polyacrylate membrane, and enhance its water resistance. Overall, this study not only provides a novel ideal stabilizer for the fabrication of polyacrylate emulsion, but also reveals that as-prepared polyacrylate/hollow SiO₂ membrane maybe found potential applications in coatings for leather.

References

1. Huang, J.: Comparison of test methods for measuring water vapor permeability of fabrics, *Text Res J.*, 78, 342–352, 2008
2. Zheng, G. K.: The effect of acrylate on structure and properties of waterborne polyurethane porous coated fabrics, *J Appl Polym Sci.*, 5, 45783, 2018
3. Wu, Y.: Laser-drilled micro-hole arrays on polyurethane synthetic leather for improvement of water vapour permeability, *Appl Surf Sci.*, 305, 1-8, 2014
4. Bao, Y.: Effect of hollow silica spheres on water vapor permeability of polyacrylate film, *RSC Advances*, 5, 11485-11493, 2015
5. Xue, F.: Tuning the interfacial activity of mesoporous silicas for biphasic interface catalysis reactions, *ACS Appl Mater & Inter.*, 9, 8403-8412, 2017
6. Wiśniewska M.: Stability of colloidal silica modified by macromolecular polyacrylic acid (PAA) â application of turbidymetry method, *J. Macromol. Sci., Part A: Pure Appl. Chem.*, 50, 639-643, 2013
7. Hu, J.: Ceria hollow spheres as an adsorbent for efficient removal of acid dye, *ACS Sustainable Chem. Eng.*, 5, 3570-3582, 2017
8. Bao Y.: Fabrication of monodisperse hollow silica spheres and effect on water vapor permeability of polyacrylate membrane, *J Colloid Interf Sci.*, 407, 155-163, 2013

TRACEABILITY OF HIDES AND SKINS: FROM FIELD TO LEATHER

T.B.Poncet¹, C.Vigier²

a)tponcet@ctcgroupe.com

b)cvigier@ctcgroupe.com

Abstract. Raw material – hides and skins – traceability is a major issue for the tanning industry. CTC has developed a simple, reliable and economically viable traceability system to ensure individual traceability (each hide is trace) from raw hide to wet blue (or wet white) and even finish leather.

1 Introduction

Raw material – hides and skins – traceability is a major issue for the tanning industry. Setting up a reliable, simple and economically viable traceability system provides the leather sector a necessary tool to improve the quality of leather and by the way, makes quality charters more credible.

As we can see, the traceability of leathers per se is not only a tool which, rather than creating value added directly, is a prerequisite for other actions to be meaningful.

There are two main goals in implementing traceability. The first, which drove this project's instigation, is to improve the quality of leather by being able to carry out corrective actions throughout the livestock farming chain, going back as far as the animal's birth. The second, which emerged from the work and results obtained by the global solution designed and implemented by CTC, is to provide reliable knowledge on the origin of leathers and therefore offer guarantees with regards to suppliers by monitoring animal welfare and environmental responsibility in farming practices and slaughterhouses.

2 Detailed description of developments

This is a 10 years project with the aim of tracing each hide or skin in a simple, reliable and economically viable way. The global solution that has been designed and developed is now being industrialized. The concept requires 4 different phases.

2.1 Making meat traceability reliably transfer to hides on the slaughter line

In ideal conditions, this solution relies on the meat traceability requirements in place in most industrialized countries. At worst, it makes hides traceable from the moment the animal is slaughtered.

The first phase of this solution is to be able to transfer a standardized and unique identification number, attributed to the animal, onto the hide (or the skin). This must take place on the slaughter line before the flaying so as to avoid breaking the traceability chain off. There are two options here: either a label is printed in real time, instantly and autonomously, when the slaughterer flashes the animal's earring, and an operator equipped with a simple knife punches the hide on the flank to seal this label there so that it stays on the hide until the second phase of the process; or the printer is connected directly to the slaughterhouse's computerized management system, which sends the order to print the label so that it is present with the number chosen by the slaughterhouse

(slaughter number or animal identification number) at the pre-skinning labelling station at the appropriate time.

The cost of this equipment is relatively low (< 5 k€) and the cost of consumables is very low (< 0.067 €HT/printed label). This first phase allows small slaughterhouses to transfer meat traceability onto hides so as to provide reliably traceable hides to their clients at an economically viable cost, and also allows large slaughterhouses to ensure the continuity of traceability between the slaughter lines and the salting workshop where hides can be marked at their core.

2.2 Securing the transfer of traceability from labels to the core of hides

We were quick to notice that no label or added matter on the hide could resist the beamhouse and tanning processes, which means the unit mark must be copied at the core of the material. After several trials, it was agreed that the best area for marking was on the shoulder, 15 cm to the left of the back line and 15 cm below the hide's edge. For this purpose, CTC has developed an approximately 150 Watts CO₂ laser marking system. The time required to transfer a 14-character code to the core of the hide by marking on the grain side is about one second. This duration makes it possible to fully automate the operation and complete it in a masked time, during the process of salting or sorting raw hides. The cost of the industrial system deployed in several French slaughterhouses and tanneries ranges from €100k to €150k depending on the level of automation and integration chosen. At this stage of the solution's development, the marking process has proved itself on bovine leather (ranging from calf to bull) and exotic skins (alligator, snake), and tests are underway on lamb skins. This operation can be carried out at all stages from the extraction of the hide on the slaughter line to tannery entry if the hide bears a label as previously described.

Another crucial point in the success of this solution is the marked code. This code must respect a strict typology defined in terms of size, type of marking font, marking power by animal species and code structure (number and length of each line and information carried by each line), all of which are prerequisites to obtain very high automatic reading rates in the next phase.

2.3 Automatic reading of the marks from the tanning stage onwards

During the development of the previous phase, tanners received tanned hides bearing unit numbers that they had to read visually and enter in an Excel file along with mentions of any defects the hide might present. As volume increased, this operation became very tedious because the mark was affixed to the shoulder, whereas operators sort hides at the culata. CTC was therefore commissioned to set up automatic mark reading stations, initially located where hides are sorted at the tanned stage (Wet Blue, Wet White), and then at later stages of the process, up to the finished leather. For this purpose, various leather image acquisition stations were developed to suit the different configurations of sorting stations at each tannery.

Algorithms based on artificial intelligence (specifically neural networks) for these stations. We could have used more common OCR-type image processing algorithms but the results would not have met expectations. The merit of the algorithms developed is that they lie on the fact that they work like humans, i.e. with a very large database of marks arriving at their station. The wet work / tanning process is unique to each tannery, as is the provenance of leathers and, therefore, so is the acquisition station. Tannery entry processes result in distorted, masked, contrasted or hidden marks. Building a database that contains all these eventualities and artifacts makes it possible to obtain perfectly decoded automated reading rates that exceed 90% of production. To illustrate these algorithms' power, it should be mentioned that they can decode a number 3 of which a part has been cut off because it was printed too close to a bell's edge if there were 3s close to bell edges in their training set. Provided it was built on a sound base, this method yields better results than human operators for deciphering marked codes.

To date, 3 acquisition station configurations (to capture images of the marked area) have been developed.

- The first acquisition station, which is the only one that is not fully automated (a human operator is required to manually scan the collar mark), allowed us to carry out the feasibility study and algorithmic modeling. This station is composed of an area scan camera and a portable grazing light; the operator places this station on the mark and presses a button to trigger the image capture. The system then automatically locates and rotates the mark, decodes all the characters, and stores the code in a database.
- The second acquisition station, which is fully automated, is designed for tanners equipped with a conveyor and an automatic stacker unit for sorting. Each hide passes under a linear camera and a grazing light, allowing for an image of the whole hide to be reconstructed, and the algorithms then automatically search for the mark, rotate it and decode it to store the code in a database. The algorithmic processing time is about 0.5 sec, which is considerably shorter than the time it takes to determine the potential a Wet Blue leather and sort it.
- Our latest acquisition station, which is also fully automated, is intended for tanneries that sort hides piled on a pallet placed on a lifting table in front of the sorter. This station consists of a simple very high resolution area scan camera and a specific light, it scans the shoulder and the entire decoding operation is carried out by artificial intelligence algorithms that adapt to changes in image capture conditions over the course of the sorting operation. This station is currently undergoing a feasibility study.

This part of the solution is CTC patented.

2.4 A centralized management system for material quality and traceability data

The last phase of the global solution we are putting forth is to set up a data management system. To this end, a common hide quality reference system has been defined in collaboration with a group of tanners and slaughterers. The aim is to collect critical information on defects occurring on tanned hides that should be passed on to the slaughterer for corrective action to be taken. This standard describes defect categories and grades, their severity according to their number and location. This data is fed into a touch screen software by the sorter during the hide check, while the hide's tracking number is automatically entered next to it in the database by the aforementioned scanning device.

Next step is the definition of a database at the output of the automatic reading to associate the tracking number with the presence of defects noted by the sorter via a touch screen application. All this information will be forwarded to the slaughterhouse for corrective actions to be carried out in the relevant farms. It is easy to conceive of a database organized by tanner/slaughterer relation. In this case, each tanner has any n number of databases working in parallel, each of which is linked to a slaughterer/supplier. This allows tanners to centralize all this data internally on a single database aggregating these n databases and therefore to capitalize on it by extracting and analysing it. Each slaughterer can also have a centralized internal database aggregating the data coming from its tanners. Separating the system's data into secure external databases containing only one tanner or slaughterer's data maximizes confidentiality.

Building on this architecture of quality data on the raw material associated with a unitary and complete traceability going back to each animal's birth. The implementation of a quality charters that can ensure the origin of the raw materials and guarantee animal welfare.

3. Conclusion and prospects

This project conducted by CTC at the request of the French leather industry has provided the trade with various industrial tools to ensure reliable, simple and economically viable traceability. These tools are undeniably a necessary support for the implementation of corrective actions aimed at improving hide quality and of quality charters allowing hide supply sources to be guaranteed and secured.

The implement of this solution outside France is now possible in order to provide all players with a reliable and secure technology for the traceability of raw materials, which is a crucial issue for our industries.

This technology can also be applied to exotic hides in order to be able to transfer the CITES ring code to the core material, which will make it possible to remove this ring and work on the whole hide in through-feed machines.

EXTENDED SURFACTANTS FOR LEATHER

I. Reetz^{1,a} and A. Kilikli¹

¹ Pulcra Chemicals GmbH, Isardamm 79-83, D-82538 Geretsried, Germany

^aCorresponding author: Ivo.Reetz@pulcrachem.com

Abstract. Surfactants of different ionic nature are used in virtually all steps of leather production. In processes like soaking, degreasing and wool washing, tremendous amounts of surfactants are applied and to a great extent discharged into the tannery effluent. In order to improve the sustainability of leather processing, there is a constant search for more efficient, environmentally friendly emulsifiers, which give superior results already in smaller usage amounts. By introduction of propylene oxide based lipophilic linkers between the hydrophilic head and hydrophobic tail, the wetting and emulsion capability of a surfactant can be increased significantly. The resulting surfactants, so called extended surfactants have an extended tail, which reaches further into the oil phase without scarifying the water solubility, what would be the results when increasing the alkyl chain. Thus, the use of lipophilic linker changes the emulsion on a structural level. Extended surfactants have been found to be superior in various applications, including textile laundry or tertiary oil recovery. In the present work, the efficiency of various types of non-ionic and anionic extended surfactants is demonstrated in various stages of leather processing. Model surfactants with lipophilic extensions are compared to their analogues without extension. In many processes, significantly improved surfactant efficiencies are found making this group of molecules an interesting topic for further exploitation.

1. Introduction

Surfactants are widely used in different stages of leather manufacturing. Notably, especially high quantities are used during the production of small skins, for degreasing and in wool washing. In bovine leather, relatively high quantities are used in soaking, but also in other process steps. In Fig. 1, the relative usage of emulsifiers in different leather processes is depicted.¹

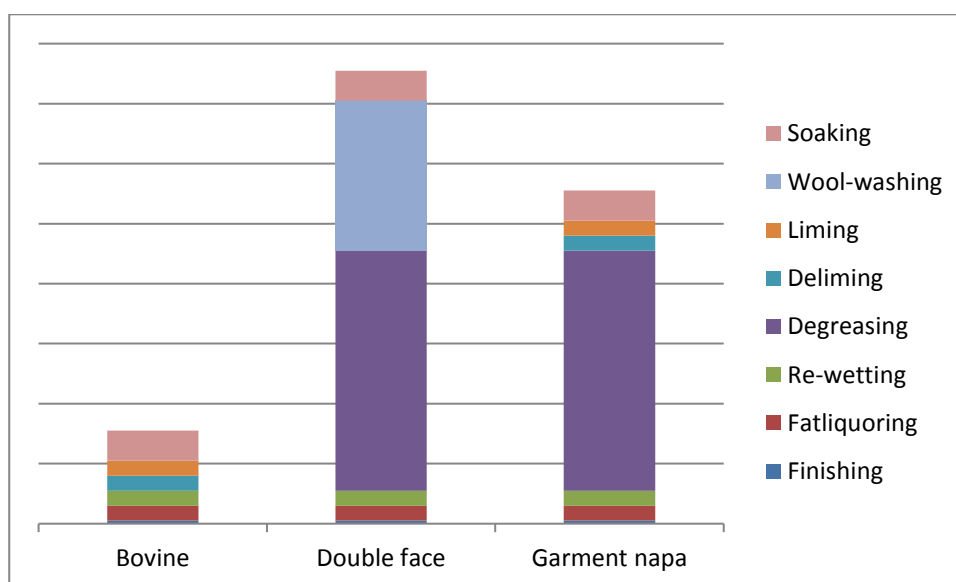


Fig. 1. Usage of surfactants for leather processing, relative amount

In Tab. 1., an overview over the chemical nature of the surfactants commonly used in leather production is given.

Table 1. Chemical structure used as surfactants for leather.

Anionics	Non-ionics	Cationics
Sulfonates/Sulfates (sulfated alcohols or alkylethers, sulfosuccinates, ABN, sulfonated esters, secondary alkane sulfonates)	Polyethers (fatty alcohol ethoxylates (FAEO) ² , propoxylates, mixed alkoxyates)	Alkyl quaternary compounds
Phosphates (alkyl or alkylether phosphates)	Alkylpolyglycosides (APG) ³	Esterified alkyl quaternary compounds (esterquats)
Carboxylates (polymers or soaps)	Aminoxides ⁴ , Betains ⁵	Imidazoline derivatives

Non-ionic surfactants are normally used for the emulsion of natural fat or of fatty components in fatliquoring. Thus, this class of emulsifiers is especially important in soaking, degreasing, fatliquoring, or for improving the penetration in finishing formulations. Anionic surfactants, on the other hand, play an important role for thorough cleaning of dirt, dung or other non-desired, not purely oily substances. Consequently, anionic surfactants play an important role in formulations for wool-washing or soaking. Cationic emulsifiers, on the other hand, are limited to special applications, such as acid degreasing or as component in top fatliquoring.

Extended surfactants contain a lipophilic linker unit in the surfactant molecule, which is positioned between the polar head and the non-polar tail group⁶. As a linker, propylene-oxide blocks are used. By many researchers and in different applications it was found that extended surfactants perform extremely well in the preparation of microemulsions, being the most successful surfactants for achieving ultralow interfacial tensions^{7,8,9}. This fact is explained by their unique chemical structure. On one hand, the intermediate PO block gives a gradual change of polarity, what changes or smoothens the structure of the micelles¹⁰. On the other hand, the hydrophobic tail is made longer what increases the interaction of the surfactant tail with the oil phase and subsequently the structure in the latter. The use of PO blocks as lipophilic extension has a big additional advantage – the introduction of PO units renders the long hydrophobic chain, which is normally based on a long-chain alcohol, more liquid. Normally, emulsifiers based on alcohols with chains longer than C18-20 are not accessible since they are solid, have lower solubility and detergency. By propoxylation longer carbon chains can be made liquid, and the propoxylated block itself further increases the length of the surfactant molecule.

The use of extended surfactants, which can be of any charge, has never been described in applications for leather. In this work, extended surfactants are compared with their analogues without extension, adjusting the chain length of the hydrophobic tail in order to have similar HLB values. This gives a more direct information on the effect of the lipophilic extension in application.

2. Experimental

The surfactant samples used in this work have been synthesized starting from the respective iso-alcohols of ExxonMobil Chemical (Exxal 10, Exxal 11 and Exxal 13). Three types of surfactants with no (0), short (X) and long (XX) extensions have been synthesized and tested:

1. Nonionic surfactant based on ethoxylation: E0, EX and EXX

2. Anionic surfactant based on sulfation: A0, AX, AXX
 3. Mixed non-ionic / anionic surfactant based on sulfosuccinate: M0, MX, MXX.
- Details of the surfactants used depicted in the table below

Table 2. Samples of surfactants tested.

(*) Calculated molecular weight of surfactant (w/o) cation (**) HLB according to Davies¹¹

Sample name	Chemical Structure	n	x	M _w (*)	HLB(**)	Basic Parameters
E0		13	0	460	2.8	OHV=128mgKOH/g, conc. 95%, pH(10%)7.4
EX		11	4	668	3.2	OHV=98mgKOH/g, conc. 95%, pH(10%)7.5
EXX		10	6	770	3.3	OHV= 88mgKOH/g, conc. 95%, pH(10%)7.5
A0		13	0	277	39.5	%SO3=6.0, conc. 32%, pH(10%)7.7
AX		11	4	484	39.9	%SO3=4.0, conc. 32.6%, pH(10%)7.8
AXX		10	6	586	40.1	%SO3=3.6, conc. 31.8%, pH(10%)8.2
M0		13	0	638	n.a.	%SO3=3.0, conc. 30.8%, pH(10%) 6.2
MX		11	4	846	n.a.	%SO3=2.0, conc. 30.7%, pH(10%) 5.6
MXX		10	6	948	n.a.	%SO3=2.0, conc. 30.9%, pH(10%) 5.7

Alkoxylation was done following the general alkoxylation procedure. Sulfation was carried out by reaction with amidosulfonic acid with further neutralization by NaOH 50%. In the case of the sulfosuccinate, reaction conditions of the reaction with maleic anhydride were chosen in order to give the hemiester (typical conversion 70-80%). Sulfitation was done with sodium disulfite solution 33%.

The wetting power of the samples was determined by EN 1772:2000, using solutions of 0.1% a.m. and standard cotton pieces. For a wetting test on leather, a drop test was used on standard hydrophobic leather, with 0.1% of a.m. solutions, monitoring the time to the full disappearance of the drop. Surface tension was measured according to DIN 53914:1997 using KRÜSS Tensiometer K11. Critical micelle concentration (CMC) was determined by plotting the results of surface tension = log(concentration), with the critical micelle concentration being the point of intersection of the two linear graphs.

Emulsion testing was done using 1g of animal triglyceride pre-emulsified with a given amount of surfactant. The mixture was placed in a cowles stirring unit adding 2ml of water during 2 min. Then, while stirring, 100ml of water were added slowly. The emulsions were checked after certain period of time. As an additional characterization, the particle size of the emulsions was measured using a Mastersizer Hydro

2000SM of Malvern Instruments. For this measurement, the emulsions were diluted in order to obtain results within the accessible zone for the intensity measurement of the scattered light, with all samples of one group being adjusted to exactly the same concentration. For degreasing trials, the following recipe was used: Raw material: pickled English domestic sheep skin, % based on pickled weight + 30%

	%		°C	min	comment	
De-pickling	100	water	30			
	10	salt		10	Bé >6	
	2.0	sodium formate		20		
	2.0	surfactant				
	1.0	sodium bicarbonate		90	pH 4.6	
		drain			take sample (#1)	
Degreasing	100	water	35			
	2.0	surfactant		45		
	100	water	35	60	pH 5.0	
		drain			take sample (#2)	
Degreasing	100	water	30			
	0.2	surfactant		15		
		drain, repeat (2x)				take sample (#3 and 4)
		wash, pickle, Cr-tanning				

The degreasing trials were repeated totally 3 times and average values have been used for the calculation. Fat content was determined according to EN ISO 4048:2008. Soaking was tested using a dry salted Turkish bovine hide with the following general recipe (% based on salted weight).

	g/l		°C	min	comment
Pre-soak	200	water	27		
	0.2	bactericide		60	
		drain			
Main soak	100	water	27		
	1	surfactant			
	0.3	bactericide		480	overnight turn 5min/h
		drain			

Wool washing trials were done using the following recipe: Raw material: pickled Australian sheep skin, % based on pickled weight

	g/l		°C	min	comment
1st washing	1:10	water	30		
	1.0	surfactant			
		bactericide		60	60min rest
		drain, wash, centrifuge			evaluation #1
2nd washing	1:10	water	25		
	2.0	surfactant		30	overnight turn 5min/h
		drain, wash, fleshing			evaluation #2
3rd washing	1:10	water	37		
	3.0	surfactant		30	rest 30min, run 30min
		drain			evaluation #3

The sheep skins were assessed after each washing step. Also, the hair was cut and the fat content was determined. For the fatliquoring trials, the following recipe was used: Raw material: South German bull wet-blue, 1.4mm.

	%		°C	min	comment
Washing	200	water	35	10	
		drain			
Rechroming	100	water	45		
	3.0	chrome sulfate 33% basic.		60	
	0.5	CORATYL® G			
		drain, wash			
Neutralization	100	water	35		
	2.0	sodium formate			
	0.5	sodium bicarbonate		60	pH 5.0
		drain, wash			
Fatliquoring	150	water	50		
	8	fatliquor		60	
	2	formic acid 75%		30	
	2	formic acid 75%		30	pH 3.4
		drain, wash, horse-up, vacuum			

The organoleptic properties were assessed in a scale 1(poor)-5(excellent). Furthermore, yellowness index was measured according to ASTM E313 after aging. Tear resistance of the leathers was determined according to DIN53.328 (IUP6).

3. Results and discussion

3.1 Simulation trials

Results of simulation trials carried out with the surfactant samples are displayed below.

Table 3. Results of determinations of surfactant properties.

	Surface tension 0.1% a.m.	CMC	Wetting power	Drop test
substrate	solution	solution	cotton	hydrophobic crust
conc. a.m.	0.1%		0.1%	0.1%
unit	mN/m	mg/l	sec	min
E0	28	40	17	5
EX	29	100	13	3
EXX	30	200	14	4
A0	33	100	31	77
AX	32	~180	16	23
AXX	31	~200	14	30
M0	28	200	82	51
MX	30	~500	68	37
MXX	31	700	64	39

Regarding surface tension, there is a general trend for a slightly increased surface tension with introducing the extension. Since the concentration used, 1g active matter/l, is in all cases above CMC, it is believed that this is simply due to the higher molecular weight by introduction of the extension. The critical micelle concentration itself is increasing, both when calculated on weight and molar base. This is normally explained by the fact that the extension is occupying some space on the interphase of the micelles, and for that reason the surfactant molecules are not packed as dense as without a spacer group.

As far as wetting power is concerned, the trend is very clear that the extension is helping to have a faster wetting of the standard cotton cloth, i.e., surfactant properties in the practical test are actually improved when introducing an extension. Also in the drop test on hydrophobic leather a much faster wetting was found. In fact, in both the wetting trials on cotton and the hydrophobic leather it was found that the difference in introduction of the lipophilic extension is much more significant than the fact whether it was a short or longer extension.

Furthermore, as an additional simulation, emulsion tests were run with different triglycerides from animal sources, using the nonionic surfactants E0, EX and EXX. The idea of these tests was that the stability of emulsions with the very fat of a skin may give conclusions on the performance of the very emulsifier in degreasing of this particular skin (Candar et al., 2005).

In many emulsion trials which had been done with freshly extracted sheep skin fat, it was found that the stability of the emulsions with the three surfactants tested is in fact not very different. In many trials, it was found that the longer extension EXX works better than the shorter extension EX. However, in many cases, the product without extension gives even more stable emulsions.



Fig. 2. Emulsion test with 0.5g surfactant /100ml

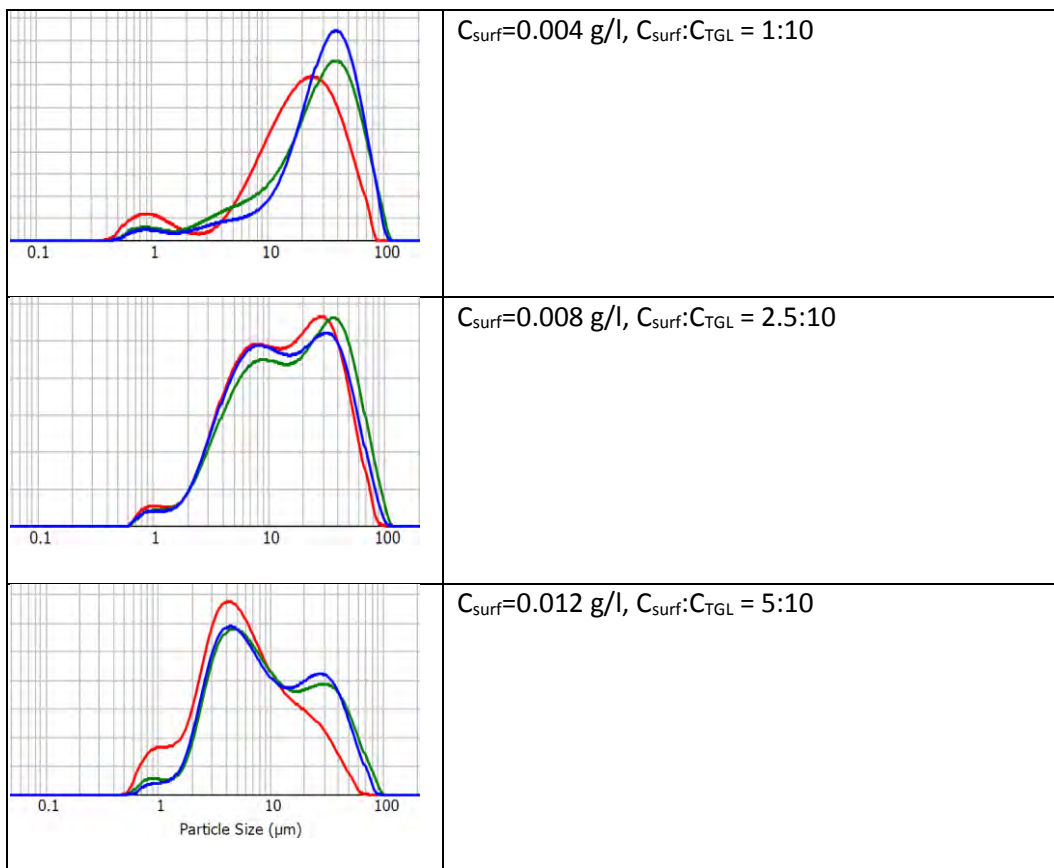


Fig. 3. Particle size measurement with system surfactant-triglyceride using **E0**, **EX** and **EXX**.

A similar behavior was also found when measuring the particle size of the emulsions. With the surfactant without extension, E0, the emulsion was found to be of smaller particle size. In this case, the concentrations used were far below the respective CMC of the surfactants. It can clearly be seen that with the Emulsifier E0, at the highest concentration a close to unimodal distribution is achieved at about $4\mu\text{m}$ average particle size. For the emulsion with the extended surfactant, there is still a pronounced portion of higher particle size of $30\mu\text{m}$. Again, the surfactant with the longer extension, EXX, gives better emulsions than the emulsifier EX with shorter extension, the maximum of the respective particle size curve being shifted slightly towards lower particle size.

Thus, in the different simulation trials in fact a very complex picture is found. General surfactant properties, like CMC or the stability and particle size of emulsions are not improved with the extension. On the other hand, in wetting trials on different substrates, cloth and leather, the extended surfactants behave better than the not-extended analogues.

3.2 Trials in Degreasing

Degreasing trials were performed using the three ethoxylated samples E0, EX and EXX. Notably, nonionic surfactants are the state of the art in degreasing, especially when degreasing is done on raw or pickled hides. In the trial, always halves of pickled skins were compared with each other. The efficiency was calculated as $\eta = \% \text{ residual fat} / \% \text{ initial fat}$, with at least three different results per sample. In all comparisons, the efficiency for the extended surfactant was found to be superior to the conventional surfactant. Furthermore, with the increase of extension, the efficiency improves.

Table 4. Result of degreasing efficiency, in %, and standard deviation.

Surfactant	η_{AVG}	DEV
E0	76	9
EX	82	6
EXX	86	8

3.3 Trials in soaking

Soaking was tried on a relatively dry and dirty salted bovine hide using the mixed nonionic/anionic emulsifiers M0, MX and MXX. Sulfosuccinates are a type of surfactants which are successfully used in many commercial soaking agents. It turned out that with the extended surfactant better cleanness of the skins on hair and flesh side was achieved with both types of extensions, in comparison with the skin, which was soaked using the surfactant without extension, M0. In fact, it was evaluated that the difference between the results with the two extended surfactants is minor in comparison with the difference to M0. This is demonstrated in the pictures below:

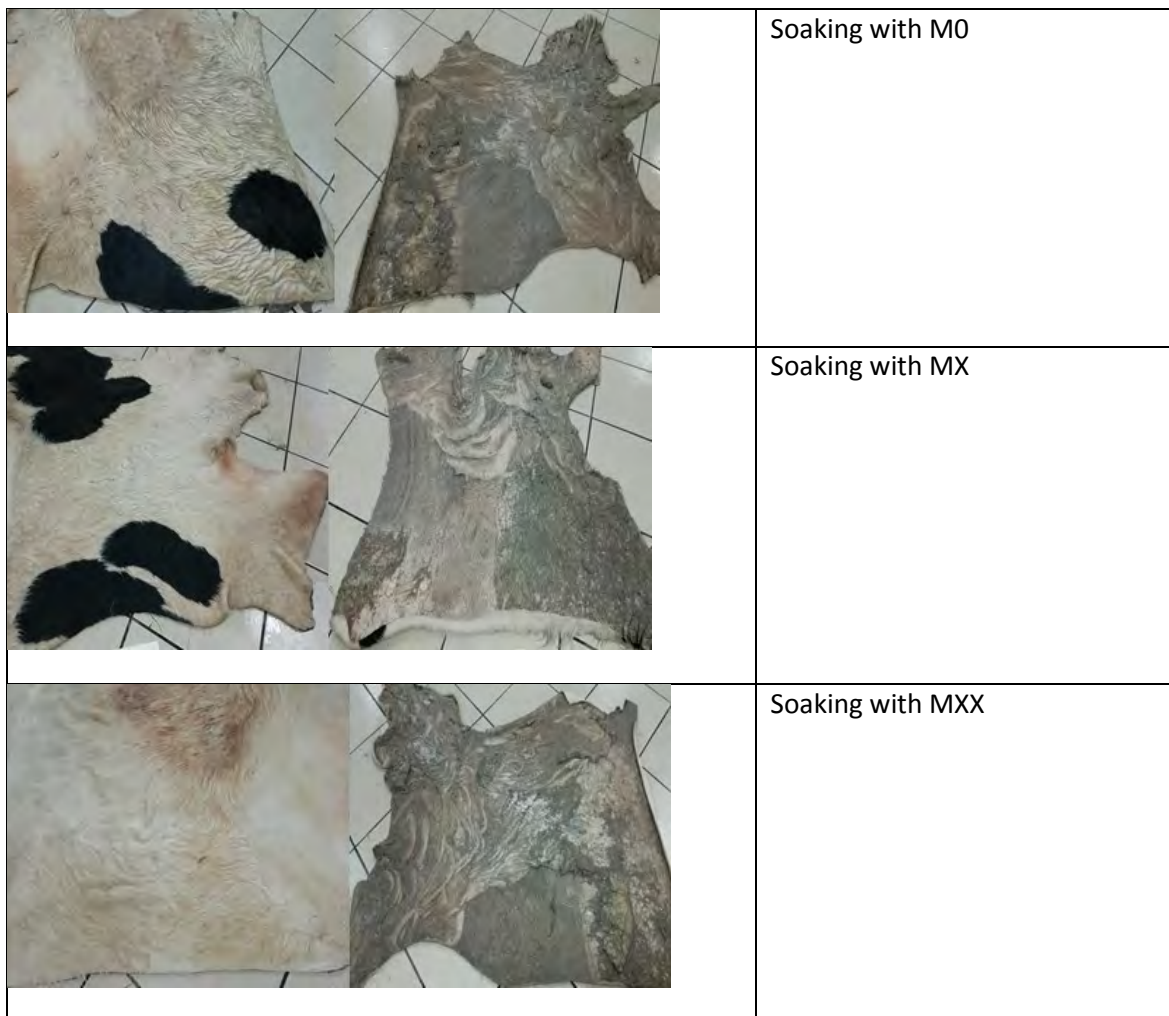


Fig. 4. Results of soaking with extended surfactants

3.4 Trials in wool-washing

Wool washing was tested with the sulfated samples A0, AX and AXX. For washing, often anionic surfactants are used, sometimes also in combination with non-ionic emulsifiers. In order to see the direct influence of the extension we decided to test the purely anionic types. As a reference, a commercially very successful wool washing agent of our portfolio was used. Chemically, this reference product is also based on an anionic surfactant, and further contains environmentally friendly alkyl polyglycosides, which, apart from improving the eco-balance of the product are known to act synergistically in cleaning and degreasing operations (Segura et al., 1997).

As seen in the tables and Fig. underneath, the efficiency in wool washing is significantly improved with the introduction of the lipophilic extension, as compared with the same chain type without lipophilic extension. With the longer extension, the results are even better than with the commercial wool washing agent.

Table 5. Evaluation of results wool washing after washing steps #1-3

#	Parameter	Reference	A0	AX	AXX
1	Whiteness	3	2	2,5	4
	Cleanness	3	3	3	3
	Openness	3	2	3	4
	Touch	3	2	3,5	4
2	Whiteness	3	2,5	2,5	4
	Cleanness	3	3	3	3
	Openness	3	2	2	4
	Touch	3	2	2	4
3	Whiteness	3	3	2,5	3,5
	Cleanness	3	3	3	3
	Openness	3	2	2,5	3,5
	Touch	3	2	2,5	4
Total score		100	79	89	122

Tab. 6. Results of Determination of fat content of hair after step #3

	Reference	A0	AX	AXX
Fat content hair (#3)	3,9%	6,0%	1,8%	1,5%

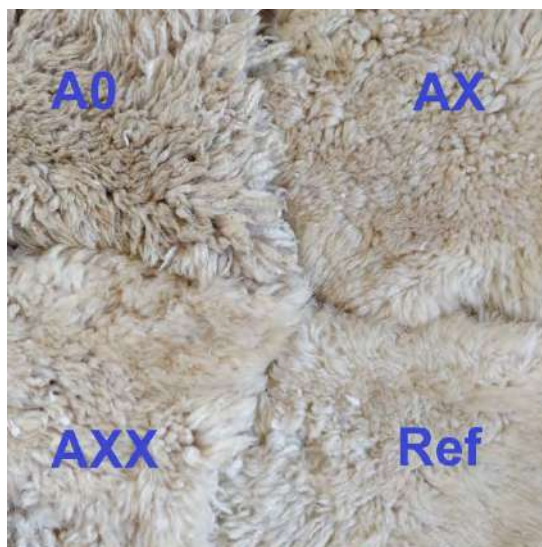


Fig. 5. Result wool washing after step #3

3.5 Trials in Fatliquoring

For fatliquoring, a very simple trial scheme was applied. To a sulfited fish oil of 90% a.m., 10% of a.m. of surfactant was added and the mixture was adjusted to a product concentration of 80%. The trial was done with the anionic/nonionic surfactants M0, MX and MXX, since this type of surfactants would be the most likely to be used in product formulations of state-of-the-art fatliquors. As a result, softness and tear resistance were found to be improved, when an extension was introduced, with the optimum being the shorter extension. The better softness is seen as an indicator for a better penetration of the fatliquor. Also, the improvement in tear resistance is interpreted in terms of a more homogeneous distribution of the fatliquor within the cross-section of the leather. The yellowing after thermal aging was measured as an additional simple means to follow the penetration of the fatliquor – the part of the fatliquor which is penetrated does not give yellowing on the surface. In this trial, too, it turned out that yellowing is reduced by the extension, i.e., the sulfited oil presumably penetrates better with the extended surfactants. Notably, the fish oil did not contain added antioxidants in order not to interfere with the results.

Table7. Results in fatliquoring with the use of extended surfactant.

Surfactant	Softness, score	YI (144h/100°C)	Tear resistance N/mm
M0	3.0	29.5	55
MX	4.5	26.8	59
MXX	4.0	27.1	57

4. Conclusion

The virtue of extended surfactants was demonstrated using model substances with similar HLB's. In basic trials of surfactant properties, the extension did in many cases give similar or even slightly inferior results: emulsions were generally less stable and of higher particle size and the CMC values

measured where higher. On the other hand, when used in different applications for leather, all model substances with the extension actually behaved better than the homologues without extension. In degreasing and wool-washing, the longer extension was clearly found to work better than the short extension. In the trial regarding fatliquoring, the shorter extension was found to work better. Also in soaking the extended surfactants worked very well. Thus, the use of extensions in different types of surfactants gives an important improvement in efficiency in leather application, making it possible to test lower usage amounts and to improve the quality of the finished leather article.

An interesting further advantage of extended surfactants is the possibility to make use of longer carbon chain molecules creating surfactants which are otherwise not accessible due to their low solubility.

References

1. Canicio, R., Reetz, I.: *Technical Meeting Aqueic 'Substancias químicas reguladas en el sector de la pie'*, 2003
2. Candar, V., Eryasa, Y.: *A new approach to the degreasing process, IULTCS Congress, Florence, 2005*
3. Segura, R., Candar, V., Zorluoglu Y.: *Alkyl polyglycosides (APG): A new generation of surfactants for leather processing, IULTCS Congress, London, 1997*
4. Kilikli, A, Sudemen, M., Reetz I.: *New emulsifiers for the Leather Industry, Freiburger Ledertage, Freiberg, 2014*
5. Senturk, F., Sarac, H. Candar, A.V. Reetz, I.: *'New Generation Emulsifiers for the Leather Industry', Journal of Aqueic, 64, 31-39, 2014*
6. Miñana-Perez, M., Garciaa, A., Lachaise, J., Salager, J.-L.: *'Solubilization of polar oils with extended surfactants', Colloids and Surfaces: Physicochem. Eng. Aspects, 100, 217-224, 1995*
7. Miñana-Perez, M., Garciaa, A., Lachaise, J., Salager, J.-L.: *'Systems containing mixtures of extended surfactants and conventional nonionics. Phase behavior and solubilization in microemulsion', 4th World Surfactant Congress, Barcelona, Proceedings, Vol. 2, 226-23, 1996*
8. Do, L.D., Withayapayanon, Harwell, J.H., Sabatini, D.A.: *'Environmentally friendly vegetable oil microemulsions using extended surfactants and linkers', J. Surfact. Detergent. 12, 91-999.2009*
9. Phan, T.T., Attaphong, C., Sabatini, D.A.: *'Effect of extended surfactant structure on interfacial tension and microemulsion formation with triglycerides', J. Am. Oil Chem. Soc., 88, 1223-1228, 2006*
10. He, Z.-Q., Zhang, M.-J., Fang, Y., Jin, G.-Y., Chen, J.: *'Extended surfactants: a well-designed spacer to improve interfacial performance through a gradual polarity transition', Colloids and Surfaces A: Physicochem. Eng. Aspects, 450, 83-9, 2014*
11. Griffin, W.C.: *Classification of Surface-Active Agents by "HLB", Journal of Cosmetic Science, 1, 311-326, 1949*

UNHAIRING AND FIBER BUNDLE-OPENING OF COWHIDES USING KCl AND LiBr/[AMIm]Cl ASSISTED NEUTRAL PROTEASE FOR LEATHER MAKING

Hui Liu, Qian Zhang, Yafei Zhang, Xiumin Li, Keyong Tang*, Jie Liu, Xuejing Zheng, Ying Pei

(School of Materials Science and Engineering, Zhengzhou University, Zhengzhou 450001, P. R. China)

Corresponding author: kytangzsu@hotmail.com

Abstract. Nowadays, tannery pollution is of great concern worldwide. The unhairing and fiber bundle-opening processes produce the majority of the pollution by the use of sodium sulfide and calcium hydroxide, which were proposed to be replaced by neutral protease combined with KCl, LiBr/[AMIm]Cl in the present work. Proper amount of KCl can speed up the unhairing with the grain not destroyed by the neutral protease. Four methods for unhairing and fiber bundle-opening were used as follows: 1#. Two steps in different float as KCl/neutral protease unhairing, followed by LiBr/[AMIm]Cl for fiber bundle-opening; 2#. Two steps in different float as neutral protease unhairing, followed by LiBr/[AMIm]Cl for fiber bundle-opening; 3#. One step in the same float as neutral protease for unhairing firstly and then LiBr/[AMIm]Cl for fiber bundle-opening. 4#. One step in the same float as neutral protease/KCl for unhairing firstly and then LiBr/[AMIm]Cl for fiber bundle-opening. It was found that using neutral protease/KCl solution for unhairing and LiBr/[AMIm]Cl solution for fiber bundle-opening is the best in fiber bundle-opening at the liming process. Besides, all the methods used here are better than the conventional liming processes (C) from the viewpoints of unhairing and fiber bundle-opening.

Keyword: Ionic liquid/LiBr, KCl, unhairing, fiber bundle opening, leather, neutral protease

1 Introduction

The beamhouse processing of leather production involves soaking, unhairing, liming, reliming, deliming, bating, picking and more water solution unit operations¹, involving many biochemical reagents. Its objective is to remove dirt, hairs, epidermis layer, non-collagenous proteins (proteoglycan) and grease from rawhide, and open up collagen fiber bundles so as to favor the subsequent tanning process. During this processing, the conventional unhairing and fiber-opening processes involve the use of calcium hydroxide and sodium sulfide. And the low solubility of calcium hydroxide leads to the formation of lime sludge and the liberation of toxic hydrogen sulfide through the use of sodium sulfide². What's more, the mechanism of unhairing using calcium hydroxide and sodium sulfide is the way of damaging hair, which brings suspended solids, carbon and nitrogen pollution. To address these problems, various approaches have been tried to reduce or avoid the use of calcium hydroxide and sodium sulfide in leather processing³.

Nowadays, enzyme and enzyme technology are widely applied to unhairing and liming of leather manufacturing, which have specificity, efficiency, selectivity and environmental friendly such as alkaline protease, neutral protease, cellulase, α -amylase⁴, β -glucanase, α -galactosidase, etc.. Many researcher and leather industries have obtained the leather manufacturing technology with enzymes and made great progress, but many problems were found with a lot of reports read. For instance, while proteolytic enzymes attack the proteoglycan of the hair root, the collagen of the grain layer may be partly destroyed, resulting in poor quality and inferior appearance of final leather. Besides, although many studies were focused on the development of enzymatic unhairing technology, very few techniques have been applied at industrial level, due to various obstacles such as damage of collagen⁵ and grain surface, incomplete removal of fine hair⁶ and epidermis⁷, and inefficient manual operation⁸, which will lead to low yield of leather. Hence, how to unhairing quickly, reduces the destruction of the pelt grain layer and accelerate the hydrolysis and dissolution

of glycosaminoglycan (proteoglycan and mucopolysaccharide) for collagen fiber bundle-opening are the key points to leather researcher. Similarly, neutral protease is widely employed in unhairing and fiber bundle-opening with above same problems. Therefore, it is necessary to improve the efficiency of the neutral protease for unhairing and liming.

The enzyme is a macromolecule protein with highly specific and catalytic, which the molecular weight is more than 10 kDa. And, in unhairing/liming processing, the cowhide is a huge blocky tissue with dense orientation structure, which increase the difficulty of the active center of enzyme to contact and catalyze the proteoglycan of the hair root. However, the catalytic rate of enzyme is depended on the type of binding such as hydrogen bond and metal ionic bond. And the binding ability of metal ionic bond with enzyme/ proteoglycan is stronger than the hydrogen bond in the water solution. Hence, adding metal ions can improve the binding ability of the enzyme with proteoglycan, which named salt bridge. Neutral protease usually is used for unhairing, which is very easy coagulation in water solution lead to a decline in catalytic rate. Therefore, adding metal ions can increase the stability of neutral protease solution and the binding ability of the enzyme and zymolyte, which improving the catalytic rate of neutral protease.

Up to now, most of researcher has reported about using salt to improve the catalytic activity⁹ and the stability of enzyme solution¹⁰⁻¹³. For instance, the correlation of the effect of ions on the stability of protein/enzyme conforms to the typical ordering of the anion/cation series (Hofmeister series). The metal cation usually as an activator and adjuvant to build a salt bridge between the enzyme and zymolyte for improving the catalytic efficiency of the enzyme. In this study, potassium chloride was chosen as a salt bridge to improve the catalytic efficiency of neutral protease owing to the same function with sodium chloride for leather manufacture. Besides, the wastewater containing potassium chloride can be discharged into the soil to provide potassium ions for plant growth, and will directly absorbed by crops. In liming processing, LiBr and [AMIm]Cl have good function of opening up hydrogen bond owing to strong ionic bonds, especially [AMIm]Cl. [AMIm]Cl is a low temperature molten salt and can easily bond with the hydrogen bonds. In this work, the effect of potassium chloride on neutral protease activity and unhairing rate, the stability and permeation rate of the neutral protease solution was studied. The results of fiber bundle-opening through one step, two steps and traditional methods were analyzed by Verhoeff's Van Gieson (EVG) staining technique. The contents of protein, carbohydrate, hydroxyproline and COD_{Cr} in wastewater were also investigated. Potassium chloride as a salt bridge to improve unhairing rate and further reduce enzyme hydrolysis of collagen is expected to improve the yield of leather.

2. Materials and methods

2.1 Materials

Salt cowhides were kindly provided by Xinxiang Huixian Leather co., LTD. (Henan, China). Neutral protease (Dispase) (BR, 50u/mg), sodium sulfide nonahydrate (ACS), calcium hydroxide (ACS, ≥ 95.0%) , lithium bromide solution(LiBr, 99%) and silver nitrate (AR, 99.8%) were purchased from Aladdin reagent co., LTD. Potassium chloride(KCl, AR) was purchased from Tianjin hengxing chemical reagent manufacturing co., LTD. 1-allyl-3-methylimidazolium chloride([AMIM]Cl, ≥99%) was supplied by Lanzhou Institute of Chemical Physics, Chinese Academy of Sciences. An enhanced BCA protein assay reagent kit was purchased from the Beyotime Institute of Biotechnology, China. Distilled water.

2.2 The treatment of cow hides

Dried salt cowhide with a uniform thickness from the same body part were immersed in quintuple distilled water in volume, and then transited and rolled in the rollers of leather tanning machine (DJDØ350, Xishan, Beitang mine Leather Machinery Factory, Jiangsu, China). The soaking liquid was substituted every hour until no white precipitation when the liquid was instilled silver nitrate solution. Thereafter, the hairs and cuticle of obtaining cow hides were scraped by scraper, while the subcutaneous tissue of cow hides was excised by fillet knife. The hides were washed with distilled water. Next, the bovine hides were cut into square pieces with 2 g and stored in 4 °C.

Table 1. Unhairing and Fiber-Opening Processes.

Process	Materials	Percentages (%)				Temperature (°C)	Time (h)	Remarks	
		Two steps		One step					
		1	2	3	4				C
Unhairing	Cowhides ^a	100	100	100	100	100			
	Distilled water ^b	1000	1000	1000	1000	1000			
	Neutral protease	8	8	8	8	-	30	13	Magnetic stirring (about 200r/min)
	Potassium chloride	8	-	-	8	-			
	Sodium sulfide nonahydrate	-	-	-	-	8			
Fiber opening	Distilled water	1000	1000	-	-	-			Magnetic stirring (about 200r/min)
	Lithium bromide	8	8	8	8	-	30	19	
	[AMIm]Cl	8	8	8	8	-			
	Calcium hydroxide	-	-	-	-	50			

^a The weight of hides is 2 g in each method.

Unhairing and fiber opening of cowhides using KCl and LiBr/[AMIM]Cl assisted neutral protease for leather making are denoted as 1#, 2#, 3#, 4#, and C. Unhairing of method 1# was carried out using the solution of KCl/neutral protease and was followed by the solution of LiBr/[AMIM]Cl for the fiber-opening process. For 2#, unhairing was accomplished using the solution of the neutral protease without KCl and was followed by fiber-opening using the solution of LiBr/[AMIM]Cl. Unhairing of method 3# was carried out using the solution of the neutral protease without KCl, then adding LiBr/[AMIM]Cl for the fiber-opening process into the same solution. For 4#, unhairing was accomplished using the solution of KCl/neutral protease, and adding LiBr/[AMIM]Cl for the fiber-opening process directly into the same solution. The conventional unhairing and fiber-opening method was C. The sodium sulfide solution was used to unhairing for 13h and then calcium hydroxide was added into the same solution for 19h. As detailed a description of the unhairing and fiber-opening processes is provided in **Table 1**. The percentages reported in the table are based on cowhide weight.

2.3 Neutral protease activity

For the measurement of the activity of the neutral protease, the universal protease activity assay with casein as the substrate and tyrosine was used as the standard. 0.8 g of the neutral protease was dissolved in 100 mL of phosphate buffer solution (pH 7.2), and this enzyme solution 1 mL was diluted 10 times to be measured. Next, measured 1mL and added casein solution 1 mL, and kept 10 min in the 40 °C. After that, the reaction was inhibited using trichloroacetic acid, the solution was then filtered and used for colorimetric analysis. The optical density was measured at 680 nm after the addition of sodium carbonate and Folin's phenol reagent. Detailed experimental steps referred to the national standard of China SB/T10317-1999.

In addition, the activity of the neutral protease was analyzed in the presence of the KCl at different concentrations and temperature was the central composite design (CCD) of response surface methodology (RSM). The selection of CCD was made based on preliminary experiments in order to identify the minimum number of experimental runs and fitting surface model based on the second order polynomial equation^{14, 15}. At last, achieved the regularization of the neutral protease activity at different KCl concentration and temperature. The independent variables of KCl concentration (x_1) and temperature (x_2), which were varied at the real levels and coded levels presented in **Table 2**. The activity of neutral protease (y) was selected as dependent variables. And the data was analyzed with RSM based on the CCD of experiments via Design Expert Software 8.0.6. Experiments were conducted up to 13 trial runs involving the analysis of variance (ANOVA) applied to analyze the results and the following second order polynomial model was used for the observations:

$$y = \alpha_0 + \sum_{i=1}^2 \alpha_i x_i + \sum_{i=1}^2 \alpha_{ii} x_i^2 + \sum_{i=0}^1 \sum_{j=i+1}^2 \alpha_{ij} x_i x_j \quad (1)$$

Where y is the predicted response i.e. the activity of the neutral protease, α_0 is the constant coefficient, α_i is the i th linear coefficient of the input factor x_i , α_{ii} is the i th quadratic coefficient of the input factor of x_{ii} , and α_{ij} is the different interaction coefficient between the input factors x_i and x_j .

The interactions between the process variables and response were obtained from ANOVA. The correlation coefficient (R^2) demonstrated the goodness-of-fit of the second-order polynomial model and an F-test was performed to determine the statistical significance of the model. The ANOVA of the model was analyzed using the 95% confidence level ($P < 0.05$).

Table 2. Real and coded levels of variables ($\alpha=1.5$).

Variable	Symbol	Coded levels				
		$-\alpha$	-1	0	+1	$+\alpha$
KCl content (%)	x_1	0.00	0.20	0.60	1.00	1.20
Temperature (°C)	x_2	20.00	26.00	38.00	50.00	56.00

2.4 Turbidity, transmittance, zeta potential and the contact angle of neutral protease solution

The turbidity, transmittance and zeta potential of the neutral protease solution were determined through turbidity meter (HACH, 2100Q, USA), ultraviolet spectrograph (UVS) (PERSEE, TU-1950, China) and zeta potentiometer (Malvern Panalytical, UK) respectively. The contact angle of neutral protease solution on the cowhide surface via the contact angle and interfacial tension tester (KINO, C60, USA)

2.5 Protein and carbohydrate analysis

Bicinchoninic acid (BCA) was used to determine the protein content of the solution after unhairing and fiber-opening processes. The concentration of carbohydrate was measured by anthrone colorimetry and glucose was used as the standard. 2mL of solution after unhairing and fiber-opening processes and added to the solution of anthrone (2g/L), concentrated sulfuric acid as solvent) 4 mL. Cool to room temperature after boiling water for 10 minutes and measured at 652 nm.

2.6 Verhoeff's Van Gieson (EVG) staining techniques

Samples were embedded using paraffin and then cut into thin slices (about 4 μ m). Slices were dewaxed using dimethylbenzene and ethanol absolute, and then cleaned up with distilled water. Next, slices were stained using Verhoeff's solution for 15-30min until they became dark black. These slices were differentiated using ferric trichloride solution for 10-20s until elastic fibers were

becoming black and background was becoming gray using upright optical microscope (NIKON ECLIPSE CI-L, Japan). Excess iodine of slices was removed by sodium thiosulfate, then counterstained by Van Gieson's for 3-5min and finally cleaned by ethanol absolute. Then it was dehydrated by ethanol absolute and dimethylbenzene, and sealed with neutral balsam. Finally, the surface morphologies were observed by digital slice scanning system (Pannoramic 250/MIDI, Hungary). Elastic fibers are black blue, collagen fibers are red, and other tissues are yellow.

2.7 Wastewater characteristics

To understand the environmental implications of neutral protease-based leather processing, wastewaters from the unhairing and fiber bundle-opening processes (1#, 2#, 3#, 4#, and C) were collected and analyzed for chemical oxygen demand (COD).

3. Results and discussion

3.1 KCl and LiBr/[AMIM]Cl assisted neutral protease for unhairing and fiber-opening processes

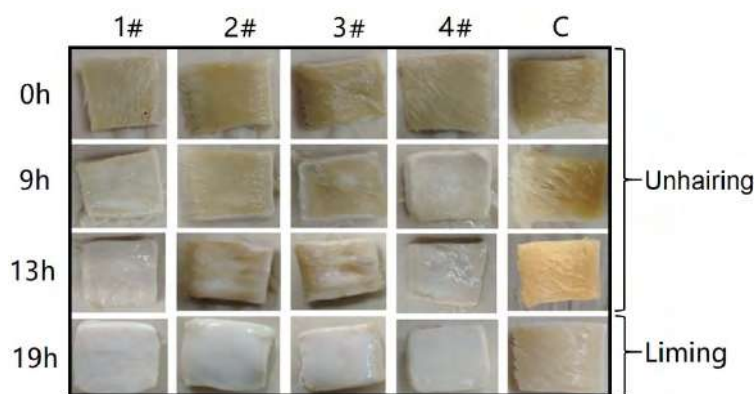


Fig. 1. The digital images of samples of cowhides during unhairing and fiber-opening processes.

In unhairing processing, the method 1# and 4# used potassium chloride to assist neutral protease for unhairing. The method 2# and 4# used neutral protease for unhairing. The method of C used conventional calcium hydroxide/sulfide for unhairing. And the results are shown in Fig. 1. The samples were not processed by mechanical or manual unhairing in order to maintain the appearance of cowhides surface at different time in whole unhairing process. It is found that the method 1# and 4# unfair completely after 13h, the method 2# and 3# were not. And the method C still has many hairs. Therefore, it is suggested that potassium chloride as salt bridge can successfully realize the goals of accelerating unhairing and loosening hair root. In liming processing, the method 1# and 2# used LiBr/[AMIm]Cl for liming, the methods 3# and 4# used LiBr/[AMIm]Cl together with unhairing solution for liming. In method C, calcium hydroxide was added in the solution of unhairing for liming processing. The method C still has many hairs, but the method 1#, 2#, 3# and 4# are not, which are white color on their surface.

3.2 Effect of potassium chloride concentration and temperature on neutral protease activity

Suitable potassium chloride can speed up the unhairing rate. Therefore, the effect of potassium chloride and temperature on neutral protease activity using CCD was studied. The results of the CCD experiments to investigate the effects of the two independent variables together with the

predicted and actual responses are shown in **Table 3**. In this study, the experimental data fit well with the empirical second-order polynomial models. Final equation in terms of actual factors:

$$y = -17.72701 - 25.61260x_1 + 2.16475x_2 + 0.14709x_1x_2 + 16.13318x_1^2 + (2.3239E - 003)x_2^2 \quad (2)$$

Analysis of variance (ANOVA) was conducted to test the significance of fit of the second order polynomial equation for the experimental data as shown in **Table 4**. ANOVA for neutral protease activity indicated that model terms were significant because of the values of 'Prob>F' less than 0.05. Therefore, the variables x_2 and x_1^2 are significant in neutral protease activity, but x_1 , x_1x_2 , x_1x_2 and x_2^2 are not significant.

Furthermore, the correlation coefficient R^2 (**Table 5**) of 0.9962 indicated that only 0.38% of the total variation could not be explained by the empirical model. The value of Adeq. Precision higher than 4 was desirable¹⁶. Adeq. Precision measures the signal to noise ratio, which in this case the value of 64.980 was obtained, indicating an adequate ratio. Besides, low coefficient of variation (C.V. % is 3.12 less than 10%) and the standard deviation (Std. Dev. is 1.98) values proved that this model is efficient for navigating the design space¹⁷, implying that this model is good.

Table 3. Experimental results of CCD central composite design and predicted responses.

Run	Variable				Actual value(U/mg)	Predicted value(U/mg)
	x_1	Coded	x_2	Coded		
1	0.60	0	56.00	1.5	103.88	102.24
2	1.20	1.5	38.00	0	66.66	65.31
3	1.00	1	26.00	-1	32.89	34.47
4	0.20	-1	26.00	-1	33.93	40.65
5	0.20	-1	50.00	1	94.52	90.86
6	0.60	0	38.00	0	61.70	61.68
7	0.60	0	38.00	0	61.70	64.14
8	1.00	1	50.00	1	96.30	91.74
9	0.60	0	38.00	0	61.70	59.26
10	0.60	0	20.00	-1.5	21.33	21.13
11	0.60	0	38.00	0	61.70	61.68
12	0.60	0	38.00	0	61.70	61.68
13	0.00	-1.5	38.00	0	68.66	64.53

Table 4. ANOVA results for response surface quadratic model for neutral protease activities.

Source	Sum of Squares	df	Mean Square	F Value	p-value Prob > F	Status
Model	7283.27	5	1456.65	371.06	< 0.0001	significant
x_1	0.60	1	0.60	0.15	0.7078	Not significant
x_2	7225.32	1	7225.32	1840.54	< 0.0001	significant
x_1x_2	1.99	1	1.99	0.51	0.4991	Not significant
x_1^2	55.20	1	55.20	14.06	0.0072	significant
x_2^2	0.93	1	0.93	0.24	0.6417	Not significant
Residual	27.48	7	3.93			
Lack of Fit	27.48	3	9.16			
Pure Error	0.000	4	0.000			
Cor Total	7310.75	12				

Table 5. Statistical parameters of ANOVA of the neutral protease activities predicted model

Statistics	Value	Statistics	Value
Std. Dev.	1.98	R-Squared	0.9962
Mean	63.59	Adj R-Squared	0.9936
C.V. %	3.12	Pred R-Squared	0.9729
PRESS	197.91	Adeq Precision	64.980

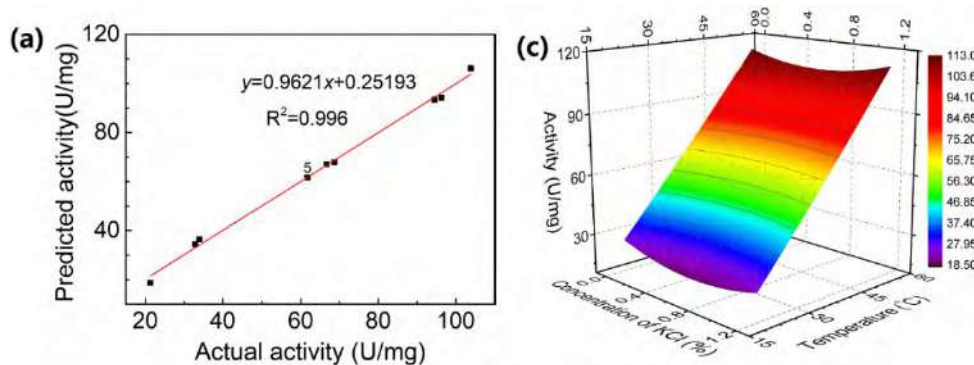


Fig 2. (a) Comparison of predicted and experimental responses; (b) three-dimensional response plots of neutral protease activities at different potassium chloride concentrations and temperature.

Fig. 2 shows the relationship between potassium chloride content (insignificant, independent variables) and temperature (significant, independent variables) and the activity of neutral protease (dependent variable). The activity of neutral protease shows a slightly concave trend with the potassium chloride concentration (0-1.2%) raise. But potassium chloride concentration was not significant on the activity of neutral protease, which has been demonstrated in (Table 4). At a suitable temperature, it does not affect the depilatory activity of the neutral protease. In contrast, the variable of temperature is a very significant factor influencing neutral protease activity. As is shown in the Fig. 2, the activity of neutral protease raised with the increasing temperature (20-56°C) and has linear relationship between the activity of neutral and temperature in same content of potassium chloride.

3.3 Turbidity, transmittance, zeta potentials and the contact angle of neutral protease solution

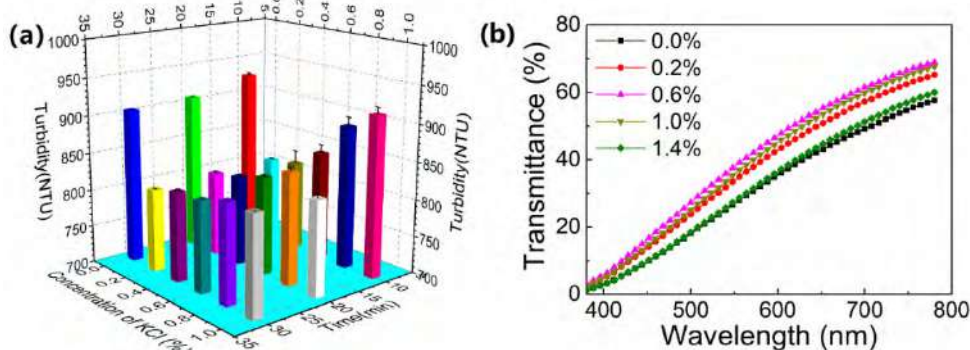


Fig. 3. (a) Effect of KCl concentration on turbidity of neutral protease solution; (b) Effect of KCl content on visible light transmittance of neutral protease solution.

The turbidity of neutral protease decreases after adding suitable KCl, and it can be seen in Fig. 3(a). In the beginning, the turbidity increases with the increasing concentration of KCl (0-1%), but it is lower

compared with the solution of the neutral protease without KCl. The turbidity of the neutral protease solution tends to be stable after 30min. However, the turbidity is still very high. Therefore, it is beneficial to improve the solubility and dispersibility of water solution after adding suitable KCl for neutral protease.

It was investigated that the transmittance of neutral protease solution when adding different concentration of KCl by ultraviolet spectrograph (UVS). The transmittance of the neutral protease solution increased with the KCl concentration raised and then decreased over 1% as Fig. 3(b) showed. This also indicated that KCl can adjust the solubility and dispersibility of water solution.

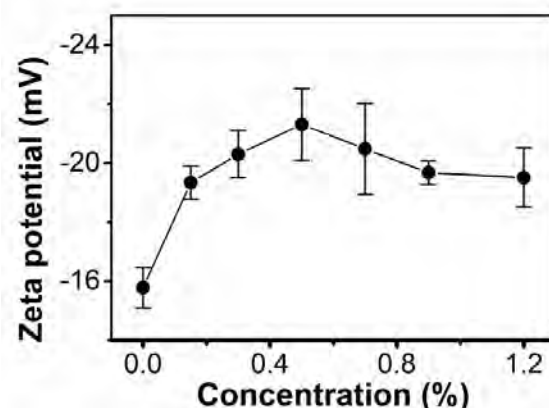


Fig. 4. Effect of KCl on zeta potential of the neutral protease solution.

The zeta potential of KCl/neutral protease solution was investigated, which is shown in Fig. 4. Increasing the concentration of KCl is beneficial to improve the stability of neutral protease solution owing to the increased zeta potential of the neutral protease solution (Fig. 4). However, the stability of neutral protease solution decreased when the concentration of KCl is greater than 0.5%.

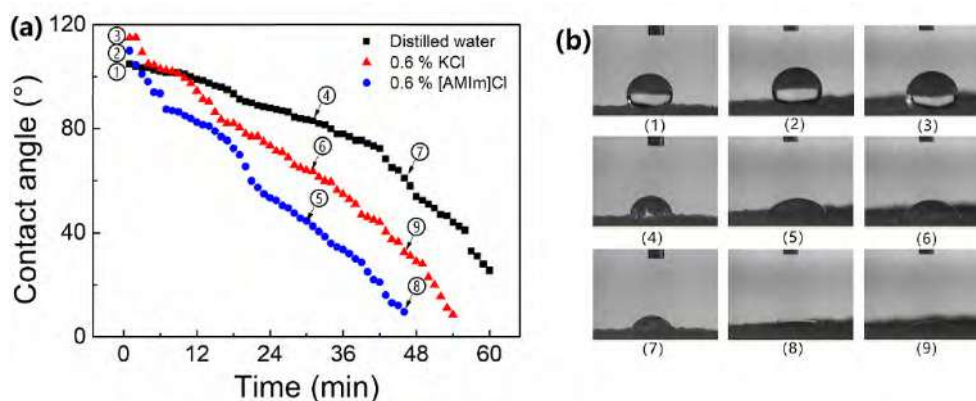
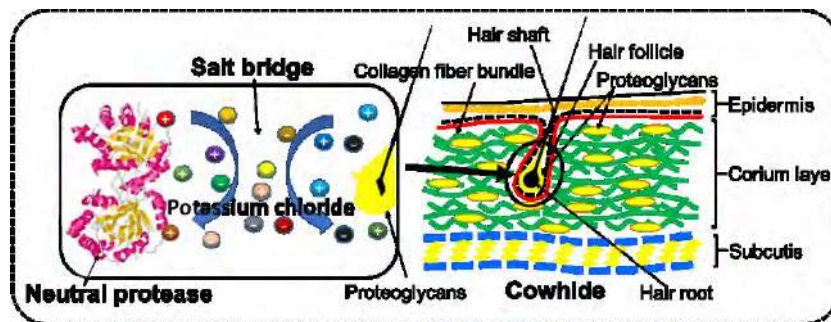


Fig. 5. (a) Effect of potassium chloride and [AMIm]Cl on the contact angle of water on the surface of cowhide; (b) the images of contact angle corresponding to the number in the left figure.

The penetration of water solution was improved when adding KCl and [AMIm]Cl, and the results are shown in Fig. 5(b). Both of them can accelerate the penetration rate of the neutral protease solution and shorten the time of binding between neutral protease and zymolyte (proteoglycan/mucopolysaccharide), improving the catalytic efficiency of neutral protease.

Therefore, KCl was introduced into the neutral protease solution. On the one hand, it can improve the dispersibility of the water solution and the stability of the neutral protease solution. On the other hand, the penetration of the neutral protease solution is improved, and further increasing the catalytic efficiency of neutral protease.



Scheme 1. Potassium chloride as a salt bridge between neutral protease and proteoglycans in cowhide for unhairing.

The catalytic mechanism diagram of the neutral protease on polysaccharide was preliminarily obtained, according to the above results analysis of improving the stability and subcutaneous penetrating quality of neutral protease solution and the dispersibility of the water solution after adding KCl, as well as result of improving the unhairing rate of the neutral protease (**Scheme 1**). However, the catalytic mechanism of protease activity center on polysaccharides needs further study.

3.4 The protein, carbohydrate, hydroxyproline and COD_{Cr} of wastewater analysis

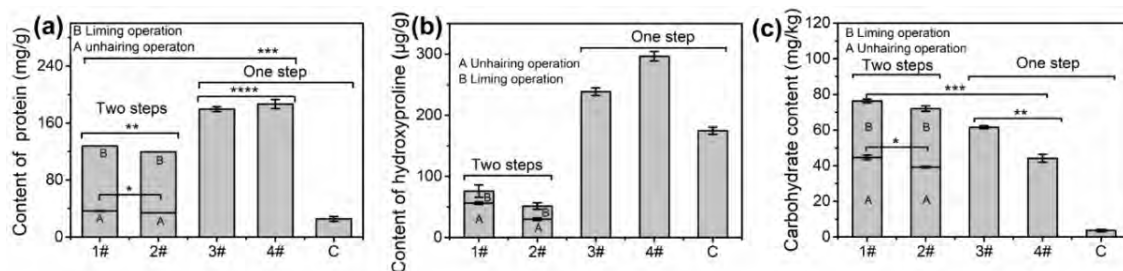


Fig. 6. Comparison of protein (a), hydroxyproline content (b) and carbohydrate content (c) in wastewater of method 1#, 2#, 3#, 4# and C. (*, ** and *** significance (P) less than 0.05; ****P > 0.05)

The contents of protein, carbohydrate and hydroxyproline of wastewater after unhairing and liming processing can be used to evaluate the degree of collagen and neutral protease to polysaccharides/mucopolysaccharide hydrolysis, which the results are shown in **Fig. 6**. The content of protein in wastewater of method 1# is higher than method 2# when adding KCl in method 1#. The addition of KCl increases the catalytic efficiency of the neutral protease to polysaccharides (**Fig. 6(b)**) and collagen (**Fig. 6(c)**) especially polysaccharides. The protein of method 3# and 4# is higher than method 1# and 2# owing to neutral protease in whole operation of unhairing and liming. Compared with method 2# and 3#, the contents of hydroxyproline in the wastewater of method 1# and 4# are higher. The results indicated that KCl can expedite hydrolysis of cowhide collagen (**Fig. 6(b)**). The contents of hydroxyproline in wastewater of method 3# and method 4# are much higher than method 1# and 2# because neutral protease always exists in the unhairing and the liming solution of method 3# and 4#. The content of carbohydrate in wastewater of method C is lower than others (**Fig. 6(c)**). It is suggested that calcium hydroxide/sodium sulfide system is bad for the dissolution of polysaccharides/mucopolysaccharide. The content of carbohydrate in wastewater of method 1# is higher than method 2# and the method 3# is higher than method 4#, indicating that adding KCl is good for the dissolution of polysaccharides/mucopolysaccharide.

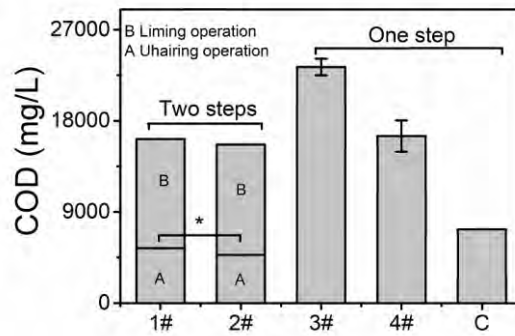


Fig. 7. Comparison of COD_{Cr} content in wastewater of method 1#, method 2#, method 3#, method 4# and method C. (* significance (P) less than 0.05)

COD_{Cr} is an indicator to measure the amount of reducing substances in wastewater. The reducing substances mainly are organic matter (protein and polysaccharides/mucopolysaccharide) in wastewater of the unhairing and liming solution. The COD_{Cr} content in wastewater of method 1#, method 2#, method 3#, method 4# and method C are shown in **Fig. 7**. It is found that COD_{Cr} content in wastewater of method 3# is higher than other methods since the summation contents of protein and carbohydrate is the highest (**Fig. 6** (a) and (c)).

3.5 Verhoeff's Van Gieson (EVG) staining analyses

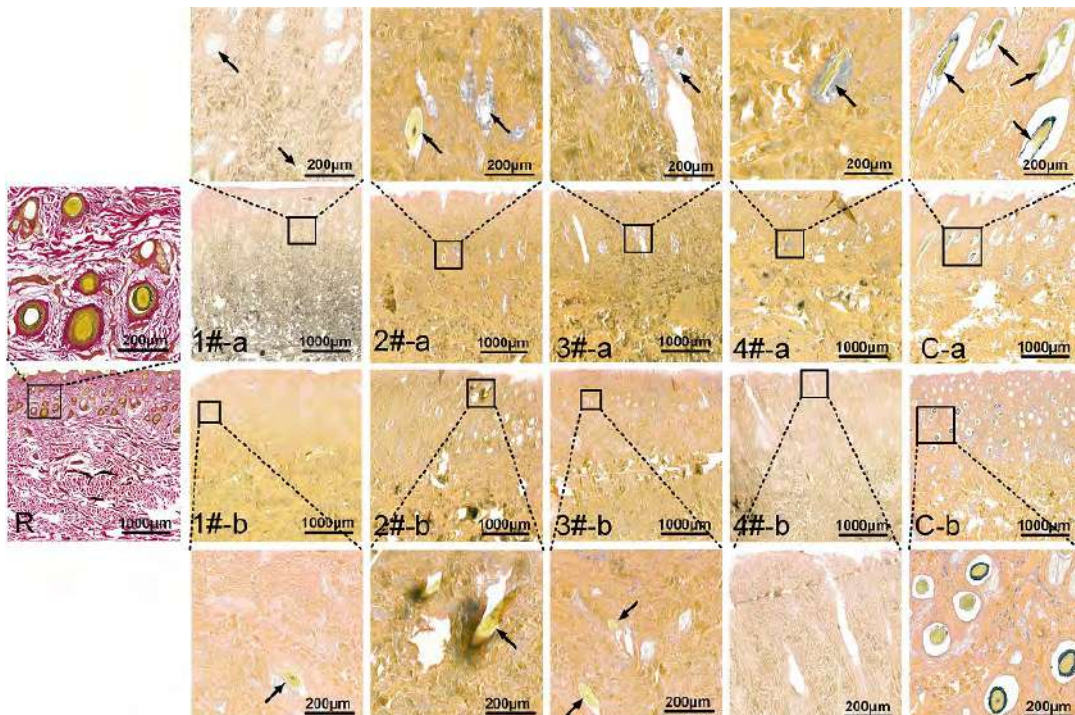


Fig. 8. The cross-section images of cowhides by the EVG staining slice after (a) unhairing and (b) liming through method 1#, 2#, 3#, 4# and C; (R) Raw cowhide.

The cross-section images of cowhides by the EVG staining slice after unhairing and liming processing are shown in **Fig. 8**. Red is cowhide collagen fiber bundles. Brownish yellow is polysaccharides/mucopolysaccharide. The content of polysaccharides/mucopolysaccharide in hair follicle using method C is higher than others, the fiber bundles swelling and their gaps increase after

unhairing and liming (**Fig. 8(C)**). It is concluded that the dissolved ability of calcium hydroxide/sodium sulfide solution system to polysaccharides/mucopolysaccharide was not excellent for unhairing and liming operation. Adding KCl (**Fig. 8(2# and 3#)**) is good for dissolution of polysaccharides/mucopolysaccharide owing to the effect of salt bridge. Strong ability of the ions will open hydrogen bonds to promote the hydrolysis of polysaccharides/mucopolysaccharide.

The open degree, mechanical and thermal properties of collagen fibers will be further analyzed by SEM, texture analyzer (TA) and thermogravimetry (TG) after tanning operation in our future work, as well as recycling technology of wastewater after unhairing and liming.

4 Conclusions

In this study, KCl as a salt bridge assist neutral protease to accelerate unhairing rate and reduce the hydrolysis of cowhides collagen. Neutral protease can increase the hydrolysis of collagen and decrease leather yield, if it is continue to be used in liming processing. Choosing KCl, neutral protease and LiBr/[AMIm]Cl to open collagen fiber bundles for leather making can reduce the pollution of the environment. This novel technology exhibits great potential in commercial exploitation of cleaner unhairing/liming process in leather industry for eco-friendly production of leather.

Acknowledgement

The financial supports from the National Natural Science Foundation Commission of China (No. 51673177).

References

1. Santos, L. M.; Gutterres, M., Reusing of a hide waste for leather fatliquoring. *Journal of Cleaner Production*, 15(1), 12-16, 2007.
2. Alla, J. P.; Rao, J. R.; Fathima, N. N., Integrated Depilation and Fiber Opening Using Aqueous Solution of Ionic Liquid for Leather Processing. *ACS Sustainable Chemistry & Engineering*, 5(10), 8610-8618, 2017.
3. Durga, J.; Ranjithkumar, A.; Ramesh, R.; Girivasan, K. T. P. V.; Rose, C.; Muralidharan, C., Replacement of lime with carbohydrases – a successful cleaner process for leather making. *Journal of Cleaner Production*, 112, 1122-1127, 2016.
4. Pandi, A.; Ramalingam, S.; Rao, J. R.; Kamini, N. R.; Gowthaman, M. K., Inexpensive α -amylase production and application for fiber splitting in leather processing. *RSC Advances*, 6(39), 33170-33176, 2016.
5. Najafi, M. F.; Deobagkar, D.; Deobagkar, D., Potential application of protease isolated from *Pseudomonas aeruginosa* PD100. *Electronic Journal of Biotechnology*, 8(2), 197-203, 2005.
6. Dettmer, A.; Cavalli, E.; Ayub, M. A. Z.; Gutterres, M., Environmentally friendly hide unhairing: enzymatic hide processing for the replacement of sodium sulfide and delimiting. *Journal of Cleaner Production*, 47, 11-18, 2013.
7. Li, S.; Li, J.; Yi, J.; Shan, Z., Cleaner beam house processes trial on cattle sofa leather. *Journal of Cleaner Production*, 18(5), 471-477, 2010.
8. Saran, S.; Mahajan, R. V.; Kaushik, R.; Isar, J.; Saxena, R. K., Enzyme mediated beam house operations of leather industry: a needed step towards greener technology. *Journal of Cleaner Production*, 54, 315-322, 2013.
9. Lu, P.; Zhao, Z.-P.; Wang, X.-Y.; Lan, G.-J.; Wang, X.-L., Understanding effect of molecular structure of imidazole-based ionic liquids on catalytic performance for biomass inulin hydrolysis. *Molecular Catalysis*, 435, 24-32, 2017.
10. Zhang, Y.; Cremer, P. S., Interactions between macromolecules and ions: The Hofmeister series. *Current opinion in chemical biology*, 10(6), 658-63, 2006.
11. Kumar, A.; Bisht, M.; Venkatesu, P., Biocompatibility of ionic liquids towards protein stability: A comprehensive overview on the current understanding and their implications. *International journal of biological macromolecules*, 96, 611-651, 2017.
12. Bastos-González, D.; Pérez-Fuentes, L.; Drummond, C.; Farauo, J., Ions at interfaces: the central role of hydration and hydrophobicity. *Current Opinion in Colloid & Interface Science*, 23, 19-28, 2016.
13. Zhao, H.; Olubajo, O.; Song, Z.; Sims, A. L.; Person, T. E.; Lawal, R. A.; Holley, L. A., Effect of kosmotropicity of ionic liquids on the enzyme stability in aqueous solutions. *Bioorg Chem*, 34(1), 15-25, 2006.
14. Cheng, S.-W.; Wu, C., Factor screening and response surface exploration. *Statistica Sinica*, 11(3), 553-579, 2001.

15. Khwanmuang, P.; Naparswad, C.; Archakunakorn, S.; Waicharoen, C.; Chitichotpanya, C., Optimization of in situ synthesis of Ag/PU nanocomposites using response surface methodology for self-disinfecting coatings. *Progress in Organic Coatings*, 110, 104-113, 2017.
16. A. Talib, N. A.; Salam, F.; Yusof, N. A.; Alang Ahmad, S. A.; Sulaiman, Y., Optimization of peak current of poly(3,4-ethylenedioxythiophene)/multi-walled carbon nanotube using response surface methodology/central composite design. *RSC Advances*, 7(18), 11101-11110, 2017.
17. Zaviska, F.; Drogui, P.; Blais, J.-F.; Mercier, G.; Lafrance, P., Experimental design methodology applied to electrochemical oxidation of the herbicide atrazine using Ti/IrO₂ and Ti/SnO₂ circular anode electrodes. *Journal of hazardous materials*, 185(2-3), 1499-1507, 2011.

3D IMAGE BASED STRUCTURAL ANALYSIS OF LEATHER FOR MACROSCOPIC STRUCTURE-PROPERTY SIMULATION

S. Dietrich¹, H. Schulz¹, K. Hauch², K. Schladitz³, M. Godehardt³, J. Orlik³ and D. Neusius³

1 Forschungsinstitut für Leder und Kunststoffbahnen (FILK) gGmbH

2 University Kaiserslautern, Department of Mathematics

3 Fraunhofer-Institut für Techno- und Wirtschaftsmathematik ITWM, Kaiserslautern

a) Corresponding author: sascha.dietrich@filkfreiberg.de

b) Additional author: katja.schladitz@itwm.fraunhofer.de

Abstract. The intrinsic structure significantly influences the mechanical properties of leather. Deeper insight into the leather's hierarchical structure is therefore essential for optimising choice and processing of the leather for the intended application. 3D imaging, quantitative image analysis combined with stochastic micro-structure modelling and numerical simulation of macroscopic properties is a promising approach to gain a deeper understanding of the complex relations between the leather's micro-structure geometry and its material properties. For leather, both imaging and image analysis are particularly challenging, due to the multi-scale nature of the leather's micro-structure. Segmentation of typical structural elements at varying scales has been achieved by sophisticated morphological image processing based on local orientations. This approach lacks, however, of robustness. Here, recent results for morphology on the space of directions in 3D are used to improve the segmentation method.

1 Introduction

Leather material is well established for applications in upholstery and automotive interiors. Knowledge regarding leather properties is as old as humankind as the material is highly variable, not the least due to structural variations depending on species, race, gender, age, husbandry conditions as well as individual body parts and tanning processes. However, quantification e.g. of the impact of the collagen-based leather structure's anisotropy on the leather's physical properties is both, of great interest and still challenging.

The mechanical properties of leather are significantly influenced by leather's intrinsic structure. In consequence, knowledge of the leather's hierarchical structure is essential in order to find the most suited leather for a specific application. Leather structure based parameters are of major importance for both manufacturing and leather processing industries. Therefore, the leather structure has been investigated intensively in continuous research work. 2D microscopic studies of the structure of leather revealed significant structural differences. The 3D microstructure of leather has been studied, however, only recently. Non-destructive testing methods like ultrasound imaging, small angle X-ray scattering, and computed tomography (CT) have been applied to capture structural features of the collagen fiber bundles.

Quantitative image analysis combined with stochastic micro-structure modelling and numerical simulation of macroscopic properties is a promising approach to gain a deeper understanding of the complex relations between a material's micro-structure geometry and its macroscopic properties. A key ingredient for this is a reliable geometric description provided by the quantitative analysis of 3D images of the materials micro-structures. For leather, both imaging and image analysis are particularly challenging, due to the multi-scale nature of the leather's micro-structure (**Fig. 1**).

2 Robust segmentation based on local orientations

2.1 Waterfall on orientations

Neither absolute gray values nor local shape information can be exploited to segment the leather micro-structure. Moreover, the dense and interwoven structure even of soft leather prohibits simple object separation methods.

The local orientation, however, is the suitable feature for defining an object structure as it both fits the known hierarchical build of the leather from collagen fibers as well as the visual impression. There are well-established methods for estimating the local fiber orientation from 3D image data. Out of them, the two based on partial gray value derivatives, e.g. the structure tensor [4] and the Hessian matrix perform best [5]. The result is in both cases a discrete orientation field. That is, the result is another 3D image holding in each voxel the locally preferred orientation. This orientation image is however noisy and contains outliers due to the multiscale structure with components near and below the CT scan resolution, due to noise, and due to CT imaging artefacts caused by the collagen's overall low X-ray absorption contrast. The latter is even worsened by spurious heavy-metal particle inclusions. Local orientation information is therefore usually averaged in order to smoothen the result. For instance, the structure tensor result is usually finally smoothed by a Gaussian. MAVI [6] averages the derived 2nd order orientation tensor in small cubic sub-volumes. Both approaches lack, however, robustness against outliers.

2.2 Median on orientation space

The median is a robust method for determining a preferred orientation in the presence of outliers. Applying the median to the gray value data, however, would erase exactly the local gray value gradient information being essential for local orientation estimation. Thus the median has to be applied to the orientational data.

A mathematical model for the representation of orientations (for example of fibers) in 3D are facing points on the unit sphere [7]. **Fig. 3** shows an orientation as a line through the origin.



Fig. 3. An orientation in 3D as a line through the origin. The line intersects the unit sphere in the two facing red points.

A set of orientations can be uniquely represented as a set of points $\{x_i; i = 1, \dots, N\}$ on the upper half of the unit sphere S_+^2 , which are called orientation points. A geodesic is the shortest path between two points on the surface of the unit sphere. It is a segment of a great circle. A point on the sphere that minimizes the sum of the lengths of the geodesics to all other orientation points x_i is not susceptible to outliers, since points closer to outliers have longer geodesics to all other points. Finding this point can be formulated as a minimization problem:

$$\min_{x \in S_+^2} \sum_{i=1}^N \arccos(x_i \cdot x)$$

The problem of computation of the minimization problem can be solved using a gradient descent algorithm [8]. The point on the sphere that minimizes the sum of all geodesics to all other orientation points x_i is a median on the orientation space and corresponds to a robust preferred orientation of the considered orientations. It should be noted that points close to the equator require special treatment due to the periodicity requirements. **Fig. 4** shows the effect for a toy example.

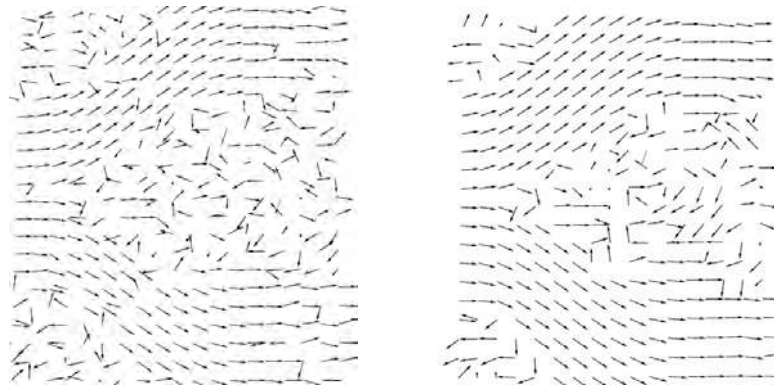


Fig. 4. 2D slice of a 3D vector field of a branching fibers with outliers (left) and same vector field after applying the described method only to the nearest neighbours (right). The resulting vector field is much smoother.

2.3 Smoothing the leather micro-structure

Application of the median filtering to the leather structure (Fig. 5) allows for structure adapted smoothing and thus has the potential to significantly improve the segmentation of individual structural elements.

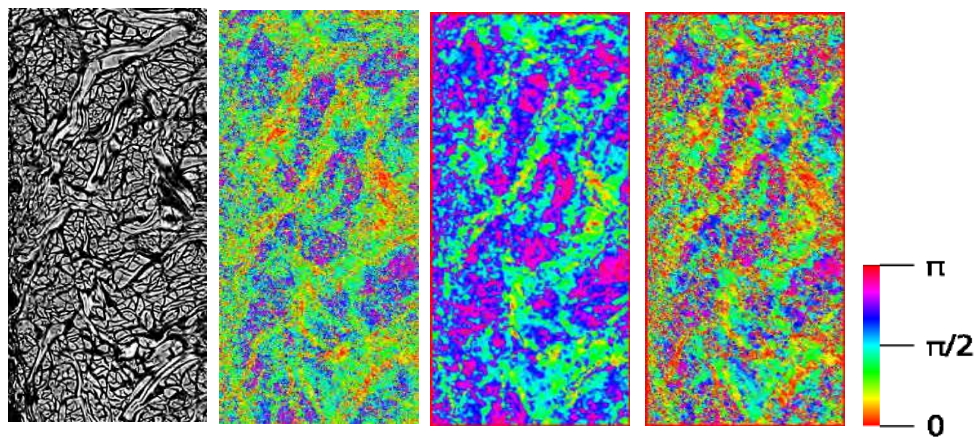


Fig. 5. Virtual 2D xy-slices through the 3D image of the leather sample visualized in **Fig. 1**; Left: Original gray value image; Center left: Colour coded angle to the z-axis (out of the shown plane); Center right: Smoothed by a mean filter on the orientations with 7 x 7 pixel filter mask, structure information is clearly reduced; Right: Smoothed by the new method, same filter mask size, much better following the structure.

2.4 Structural analysis on the collagen fiber bundle scale

The separation of the leather micro-structure into individual bundles as shown in **Fig. 6** can be used along with local, voxel-wise analysis of the gray values, to analyze and compare the structure of leather samples, e. g. from different body parts or different species. Size and shape of the structural elements as well as their sub-structure yield information, e. g. on undulation, branching, thickness, cross-sectional shape, and preferred directions [2].

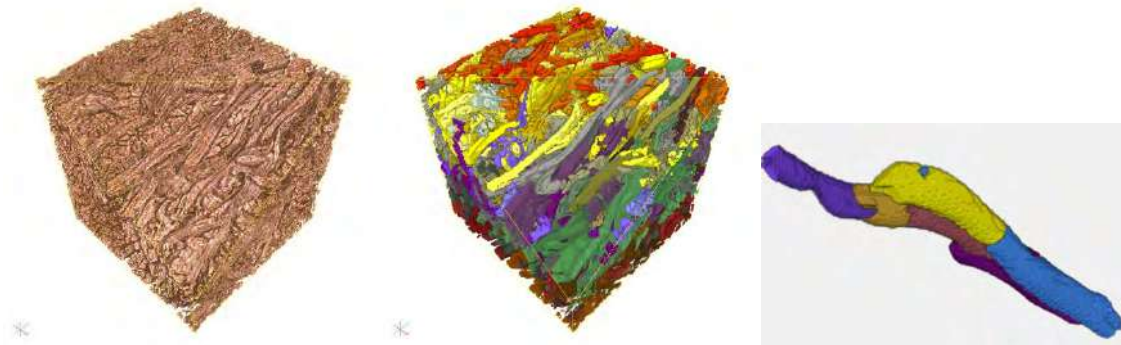


Fig. 6. Left: Volume rendering of a leather sample, 500^3 voxels of edge length $3.3 \mu\text{m}$; Center: coarse scale segmentation as achieved in [2], colours indicate the individual bundles. Right: Typical smoothed structural element with substructure.

3 Micromechanical modelling on the collagen fiber bundle scale

Realistic finite element simulation of the behaviour of the leather under mechanical load is demanding as it has to incorporate the stretching of bundles as well as all relevant contact and friction mechanisms. Significant contributions towards this goal have been made in [9, 10].

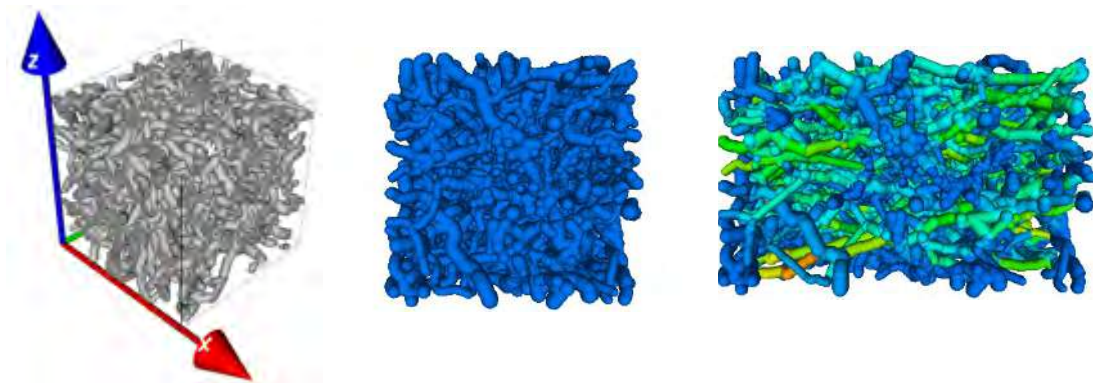


Fig. 7. Left: Virtuell leather structure; Center and Right: Virtual tensile experiment. Center: No load. Right: Loaded, colours indicate local strains – blue low, red high.

Acknowledgements

This work is supported by the IGF-projects 16378 BG, 18102 BG and 19719 BG of the Research Association Leather (FGL) that was funded via the AiF on behalf of the Bundesministerium für Wirtschaft und Technologie (Federal Ministry of Economics and Technology) based on a resolution of Deutscher Bundestag. We are thankful for the support granted.

References

1. Bittrich, E., Schladitz, K., Meyndt, R., Schulz, H., Godehardt, M., *Micro-computed tomography studies for three-dimensional leather structure analysis*, *Journal of the American Leather Chemists Association*, 109(11), 2014, 367-371.
2. Godehardt, M., Schladitz, K., Dietrich, S., Meyndt, R., Schulz, H., *Segmentation of collagen fiber bundles in 3D by waterfall on orientations*, In *Proceedings of Mathematical morphology and its applications to signal and image processing, ISMM 2017, Fontainebleau, France, LNCS 10225*.
3. Frontera-Pons, Joana & Angulo, Jesús, 2012, *Morphological operators for images valued on the sphere*, *Proceedings International Conference on Image Processing*, 113-116, 10.1109/ICIP.2012.6466808.
4. Krause M., Hausherr J., Burgeth B., Herrmann C., Krenkel W., 2010, *Determination of the fibre orientation in composites using the structure tensor and local X-ray transform*, *J. Mater. Sci.* 45, 888-896.
5. Wirjadi, O., Schladitz, K., Easwaran, P., Ohser, J., *Estimating fibre direction distributions of reinforced composites from tomographic images*, *Image Analysis and Stereology* 35(3), 2016, 167-179.
6. MAVI – *Modular Algorithms for Volume Images*. Fraunhofer ITWM, 2005.
7. Fisher, N., Lewis, T., Embleton, B. (1987), *Statistical Analysis of Spherical Data*, Cambridge, Cambridge University Press, doi:10.1017/CBO9780511623059.
8. Drezner, Z., Wesolowsky, G. (1978), *Facility Location on a Sphere*, *The Journal of the Operational Research Society*, 29(10), 997-1004, doi:10.2307/3009474.
9. Shiryayev, V., Orlik, J., *A one-dimensional computational model for hyperelastic string structures with Coulomb friction*, *Mathematical Methods in the Applied Sciences*, 40, 2017, 3, 741-756, ISSN: 0170-4214, DOI: 10.1002/mma.4005.
10. Shiryayev, V., Neusius, D., Orlik, J., *Extension of One-Dimensional Models for Hyperelastic String Structures under Coulomb Friction with Adhesion*, *Lubricants* 2018, 6(2), 33, <https://doi.org/10.3390/lubricants6020033>.

HIGH EXHAUSTION SYSTEM (HES) FOR LEATHER PROCESS: ROLE OF BIOCATALYST AS AN EXHAUSTIVE AID FOR WET-END

G. C. Jayakumar , V. Karthik, A. D. AsanFathima, A. Tamil Selvi, C. Muralidharan, S. V Kanth

G. C. Jayakumar , V. Karthik, A. D. AsanFathima, A. Tamil Selvi, C. Muralidharan, S. V Kanth

CSIR - Central Leather Research Institute, Chennai, India

Department of Leather Technology, Anna University, Chennai, India

Corresponding authors: karthik.vijayarangan@gmail.com&jayakumarclri@gmail.com

Abstract. Application of biocatalyst becomes an imperative due to their eco-friendly advantages. Enzymes in pre-tanning for unhairing, fibre opening, defleshing and bating are well reported and practiced. However, the role of enzymes as a chemical aid is less explored and consider as secondary applications. Leather enzymes are known for their hydrolytic behavior which makes it more suitable for pretanning operations. However, typical chemical exhaustive aids acts as a vehicle for the diffusion of chemicals, whereas enzymes aids in the splitting of fibres which facilitate the diffusion of chemicals and create more functional sites for the tanning and post tanning chemicals to interact. In this research, pickled pelts are treated with acid protease and subsequently tanned using chrome tanning agent. Enzymatic treated pelts resulted in better uptake of chromium as compared to conventionally processed leathers. Similarly, after neutralization, chrome tanned leathers are pretreated before post tanning process. Enzymatic treated wet blue leathers showed higher uptake of post tanning chemical, uniform dyeing and reduction in the pollution load. From the preliminary research, an interesting finding has augmented that application of enzymes at an optimized concentration would lead to better uptake of chrome which reduces the pollution and minimization pollution load in post tanning. This study, emphasize on the application of enzymes in tanning and post tanning for higher diffusion of chemicals.

1 Introduction

Application of enzymes in leather processing finds an inevitable role due to eco-benign aspects. Conventionally, protease is commonly used in bating process for the opening up of fibres and removal of short hairs which are left after liming process. Recently, many attempts have been made to use enzymes in different stages of leather processing. Enzymes such as protease, amylase and lipase are commonly used in the tannery for various functions. Protease aids in scissoring proteoglycans and non-collagenous proteins from the skin. Amylase split the inter-fibrillar proteins and proteoglycans whereas fats and triglycerides are removed using lipase. Though, enzymes are eco-friendly and replace the conventional chemicals like lime and sodium sulfide. It also limits the practical application due to several factors, such as concentration, pH, temperature and time. Overexposure of enzymes to skins would lead to complete depletion of the materials. Application of enzymes during tanning and post tanning is less explored owing to its limited activity on leather. Recently, novozymes have introduced enzymes to treat tanned leathers which relax the fibres that enhance the area yield. Similarly, acid protease has been used as an auxiliary agent for better uptake of dyes. In the present study, a novel attempt has been made to maximize the utilization of enzymes in tanning and post tanning process for better area yield and uptake of chemicals.

2 Material and Methods

2.1 Materials

Wet salted goat skins were chosen as raw materials for the study. All chemicals used for leather processing were of commercial grade while the chemicals used for the analysis of spent liquors were of analytical grade. Chemicals used for analysis were of analytical grade.

2.2 Combination tanning trials

Conventional chrome tanning was followed as given in Table 1. Control trial was processed without protease treatment and experimental trials were done with protease treatment before chrome tanning.

Table 1. Application of enzyme during chrome tanning.

Process	Chemicals	% offered	Time (minutes)	Remarks
Pickling	Water	100		
	Salt	10	10'	pH-2.8 to 3
	Formic acid	1	3x10'+20'	
	Sulfuric acid	0.5	3x10'+20'	
Tanning	Pickle bath	50		
	Protease	X	60'	Check penetration
	BCS	6	Y	
Basification	Water	100		
	Sodium formate	1	3x10'+20'	pH-3.8 to 4
	Sodium bicarbonate	1	3x10'+20'	
Drain/Wash/Drain				

After neutralization, chrome tanned leathers were treated with protease as given in Table 2 and conventional post tanning process was followed. Control trial was carried out without protease treatment.

Table 2. Application of enzyme during post tanning.

Process	Chemicals	% offered	Time (minutes)	Remarks
Wetback	Water	100	15'	Drain out
	Wetting agent	0.5		
Neutralization	Water	100		pH 5.3-5.5 D/W/D
	Sodium formate	1	45'	
	Sodium bicarbonate	0.5		
Enzyme Treatment	Protease	X	30'	
Washing	Water	100	10'	D/W/Pile
Retanning	Protease	1.0	30'	Check penetration
	Acrylic resin	2	20'	
	Veg fatliquor Replacement	2	15'	
	Syntan	3		
	Melamine	5	120'	
Fatliquoring	Wattle	3		60'
	Dye	2		
	Synthetic	6		
	Semi synthetic	2	60'	
Fixing	Vegetable	2		D/W/Pile
	Formic acid	3	3x15'	

2.3 Determination of hydrothermal stability of leather

The hydrothermal stability of leather was determined by Theis shrinkage tester. The shrinkage temperature test was carried out as per SATRA STD 114 method. A strip of about 2 by 3 leather and a thermometer were suspended in the sight glass filled with water, the upper end of the leather was fixed and the position of the lower end was indicated by an adjustable marker outside the tube to help judge when shrinkage occurs. The system was heated and the temperature at which leather shrinks to one third of its original length was recorded as a shrinkage temperature, which connotes hydrothermal stability.

2.4 Physical testing

Leather samples were subjected to physical testing to determine the influence of enzyme on physical properties of leather. Tear strength water vapour permeability tests were carried out using SATRA TM 162:1992. All test samples were conditioned at 20°C and 65% relative humidity. Control samples were tested in the same way. All analyses were done in duplicate.

2.5 Scanning Electron Microscopic Analysis of Leather Samples

Samples from control and experimental pelts/tanned leathers were cut from the official sampling position. Samples were then dehydrated gradually using acetone as per standard procedures. The micrographs for the grain surface and cross section were obtained by operating the SEM at an accelerating voltage of 10 KV.

3 Results and discussion

In the present study, biocatalyst, protease enzyme is used as an exhaustive aid during tanning and post tanning (schematic representation is shown in Fig.1). Pickled pelt has been treated with different concentration of protease before chrome tanning as given in Table.1. Chrome content and hydrothermal temperature of wet blue leathers are estimated and results are shown in Fig.2.

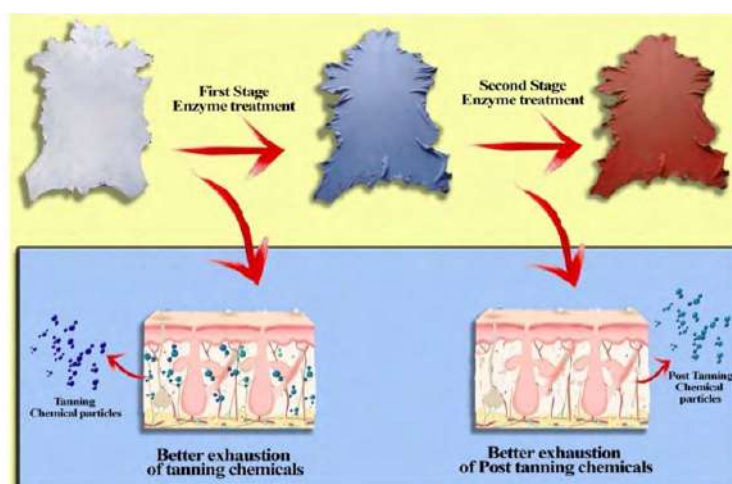


Fig. 1. Schematic representation of enzyme treatment at tanning and post tanning.

From the results, it can be inferred that chrome content in wet blue at 1% protease treated leathers showed better uptake of tanning chemicals. Similarly the shrinkage temperature of wet blue is found to be higher for protease treated leathers.

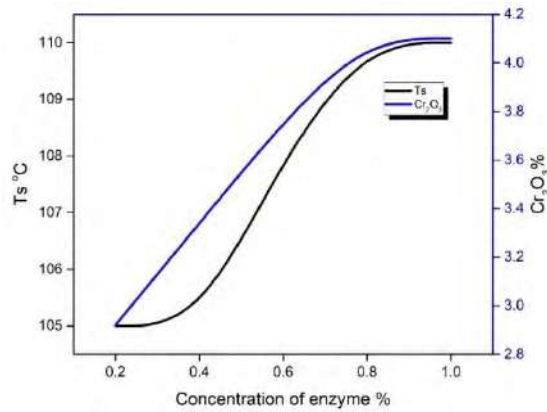


Fig. 2. Chrome content and hydrothermal stability of wet blue leathers.

Though, enzyme treatment might lead to relaxation of fibres which in turn could lead to better exhaustion of tanning chemicals. From the results, it can be ascertained that enzymatic treatment has not affected the quality of leathers in terms of wet resistance which is a primary quality measurement of wet blue leathers. Microscopic images of wet blue leathers provide topographical information on surface and compactness of fibres. Enzymatic treatment has not deteriorated the surface and makes it more compact.

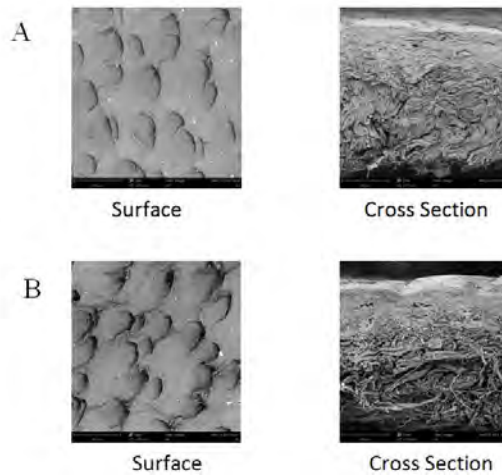


Fig. 3. Scanning electron micrograph of wet blue leathers A-Control wet blue leather and B-Experimental leather (1% protease treated).

The study further extended for treating wet blue leather using protease during neutralization process as given in Table 2 and subsequently processed into crust leathers.

Table 3. Physical strength characteristics.

Sample	Tensile strength (Kg/cm ²)	Elongation @ break (%)	Load @ grain crack (Kg)	Distension @ grain crack (mm)
Control	116.52	48.77	6.19	7.06
Experimental	162.77	56.27	6.65	7.14

Though, enzymatic activity on the leather is minimal, however, the relaxation of fibres would lead to better uptake of post tanning chemicals. After neutralization the wet blue leather is treated with 1% protease and thoroughly washed and post tanning process has been carried out. Crust leathers are evaluated for physical strength characteristics and microscopic images have been obtained to understand the influence of protease on post tanning process.

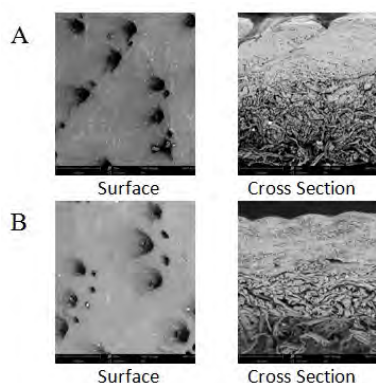


Fig. 4. Scanning electron micrograph: A-Control crust leather and B-Experimental leather (1% enzyme treatment).

From the physical strength results, it can be inferred that that strength has significantly enhanced for the enzyme treated crust leather. This might be due to better uptake of post tanning chemicals and uniform distribution. The data is in-line with microscopic image of crust leather as shown in Fig.4.

4 Conclusion

The present study provides a new insight on application of enzyme during tanning and post tanning processes. Interesting result has been obtained from the enzymatic treatment process. Enzyme treated wet blue leathers shows higher uptake of chrome tanning agent and slight increment in the hydrothermal resistance. Similarly, enzyme treatment during neutralization, the leather has shown better physical strength characteristics and compact fibres due to better uptake of post tanning chemicals. The study can be extended further to understand the kinetics of enzyme on leather substrate during pickling and neutralization.

5 Acknowledgements

Authors acknowledge the financial support from Department of Leather Technology, Anna University, India.

Reference

1. Jayakumar GC, Sathish M, Aravindhan R, Raghava Rao J.: 'Studies on the use of bi-functional enzyme for leather making', *J. Am. Leather Chem. As.*, 111, 455-460, 2016
2. Jayakumar GC, Sivaraman G, Mohan R, Saravanan P, Raghava Rao J.: 'Cohesive system for enzymatic unhairing and fibre opening: Architecture towards Eco-benign pretanning operation', *J. Clean. Prod.*, 83(8), 428-436, 2014
3. Usharani N, Jayakumar GC, Swarna VK, Raghava Rao J.: 'Stabilization of Collagen through Bioconversion: An Insight in Protein-Protein Interaction', *Biopolymers*, 101(8), 903-911, 2014
4. Swarna VK, Venba R, Jayakumar GC, Chandrababu NK.: 'Kinetics of leather dyeing pretreated with enzymes: Role of acid protease', *Bioresour. Technol.*, 100(8), 2430-2435, 2009

5. *NovoCor AX - So much to gain and nothing to lose, Leather International, 15 July 2003*
6. *BioTimes Leather Special Editio, Novozyme, September 2007*
7. *Swarna VK, Ramesh Kannan P, Usharani N, Jayakumar GC, Yasothai A, Chandrasekaran B.: 'Studies on the use of enzymes in tanning process: Part I. High exhaust vegetable tanning', J. Am. Leather Chem. As., 104(12), 405-415, 2009*
8. *Swarna VK, Ramesh Kannan P, Usharani N, Jayakumar GC, Deepa S, Chandrasekaran B.: 'Studies on the use of enzymes in tanning process: Part II. kinetics of vegetable tanning', J. Am. Leather Chem. As., 105(1), 16-24, 2010*
9. *Gunavathi M, Jamal ZM, Jayakumar GC, Yasmin K, Sreeram, KJ, Raghava Rao, J.: 'A novel approach to enzymatic unhairing and fibre opening of skin using enzymes immobilized on magnetite nanoparticles', ACS Sustainable Chem. Eng., 4 (3), 828-834, 2016*
10. *Bin Lyu , Kun Cheng , Jian zhong Ma , Xueyan Hou , Dangge Gao , He Gao , Jing Zhang , Yuliang Qi.: 'A cleaning and efficient approach to improve wet-blue sheep leather quality by enzymatic degreasing', J. Clean. Prod., 148, 701-708, 2017*

FALSE POSITIVES II – CHLOROPHENOLS IDENTIFICATION TOWARDS HPLC-DAD-MS ANALYSIS COMPARED TO ISO 17070:2015 TECHNIQUE

Gustavo Adrián Defeo F.S.L.T.C., Miria Borgheresi PhD., Dr. Manila De Cicco, Dr. Bianca Carpignani

Ars Tinctoria SRL – Analytical laboratory

Via del Bosco 125 (IT-56029) Santa Croce sull'Arno (PI) Italy +39 0571 35110

info@arstinctoria.it.

Abstract. The restriction of certain dangerous substances according to REACH (Registration, Evaluation, Authorisation of Chemicals as well as the Restricted Substances Lists (RSL) requirements promoted by various renowned brands obliges tanneries to everyday more numerous analysis with undesired conflictual situations on false positive tests results. This situation is worsened by the voluntary reduction of requested detection limits far below the levels recommended by the accepted ISO methods. On this context, ISO 17070:2015 was extended in its current version from the determination of pentachlorophenol to tetrachlorophenol, trichlorophenol, dichlorophenol and monochlorophenol isomers. Some brands also included under this technique the ortho phenyl phenol (OPP) analysis, requesting a quantification limit below 1 mg/kg for all analytes. The present paper proposes a new HPLC-DAD-MS direct method for the verification of chlorophenols positive cases, and its extension to leather chemicals analysis, as well as the discrimination among false positive cases and real positive ones. The paper also illustrates case studies reporting differences in the quantification of the said analytes and the chlorophenol scission in different analytical conditions

1 Introduction

Chlorophenols is a family of substances traditionally used as pesticides, herbicides and fungicides, but also as intermediates for dyes production. Following the limitation of use in many countries of Pentachlorophenol (PCP), different norms were developed for its determination on different materials.

For Pentachlorophenol determination on Leather, ISO 17070 (IULTCS/IUC 25)¹ norm “*Leather - Chemical tests - Determination of pentachlorophenol content*” was developed as reference method. The normalised test of just PCP remained so until the 2006 version included. This norm intended originally to validate the compliance of Leather to a European limitation of 1000 mg/kg of Pentachlorophenol. In the following different countries and brands requested lower limits for PCP, and thus the method was stressed in its quantification limit (some brands imposed voluntary limitations down to 0,01 mg/kg), but also in its extension to the complete chlorophenols five basic types, including positional isomers (19 analytes in total). From the 2015 version on, ISO 17070 norm was extended in scope to the different chlorophenol types (ISO 17070:2015 (IULTCS/IUC 25))².

In some voluntary analytical protocols, ISO 17070 method was also extended in scope to the quantification of orthophenylphenol (OPP) and 4-chloro-3-methylphenol (PCMC) known as chlorometacresol (CMK). Both additional analytes have a more accurate dedicated method (ISO 13365:2011 (IULTCS/IUC 29))³ developed for HPLC, and with a demonstrated higher accuracy than the said adaptation.

¹ ISO 17070:2006 (IULTCS/IUC 25) *Leather -- Chemical tests -- Determination of pentachlorophenol content*

² ISO 17070:2015 (IULTCS/IUC 25) *Leather -- Chemical tests -- Determination of tetrachlorophenol-, trichlorophenol-, dichlorophenol-, monochlorophenol-isomers and pentachlorophenol content*

³ ISO 13365:2011 (IULTCS/IUC 29) *Leather -- Chemical tests -- Determination of the preservative (TCMTB, PCMC,*

2 Chlorophenols

Chlorophenols include five basic types, depending the number of chlorine substituents, namely mono-chlorophenols (MonoCP), dichlorophenols (DiCP), trichlorophenols (TriCP), tetrachlorophenols (TeCP) and pentachlorophenol (PCP). Including their positional isomers in total sum 19 analytes (Fig. 1).

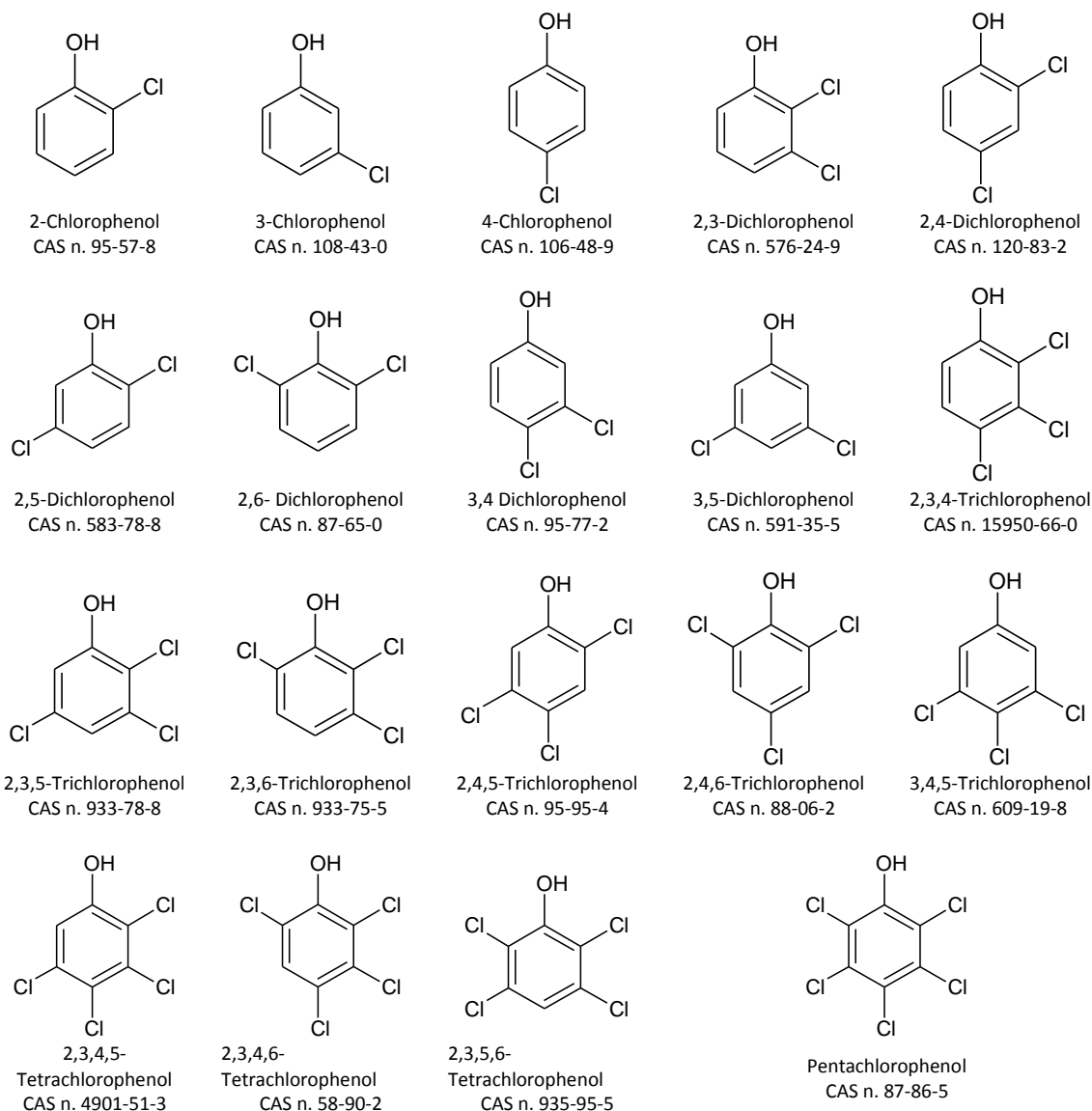


Fig. 1. Chlorophenols basic types and their isomers.

3 ISO 17070:2015 brief description

The grinded sample is dispersed in a 1M solution of H_2SO_4 and steam distilled. Acidic media is needed for the correct solvent separation of this analyte. At least 450 ml of distillate are collected in a K_2CO_3 solution. This solution is brought to a final volume of 500 ml, from where 100 ml are taken to undergo acetylation. This reaction is achieved by adding acetic anhydride

OPP, OIT) content in leather by liquid chromatography

and Triethylamine catalyst in a separating funnel where the carbonate solution is in contact with hexane. For quantification, the hexane phase containing acetylated chlorophenol is then injected in GC-MS, comparing with a similarly prepared internal standard.

Considering that this method includes a relatively long preparation technique uncertainty becomes relatively high below 5 mg/kg leading to frequent false positive results specially if quantification limits are requested below 1 mg/kg. Because of these critical points, we have studied a simpler direct method to confirm the effective presence of chlorophenols in suspected false positive analysis, or in cases where the requested quantification limit enters within the rumor levels of the GC-MS detector.

4 Chlorophenols determination in HPLC-MS direct method

4.1 Preparation

The HPLC-MS direct method for chlorophenols determination, was developed both for Leather and Leather chemicals.

For Leather: a sample was grinded, weighed and extracted in ultrasound bath during 20 minutes with an aliquot of terbutylmethylether, taking the supernatant solvent and repeating the operation other 2 times collecting together all three extractions. The extract is dried with a rotary evaporator and dissolved in 2 ml. methanol. Filtered with a 0,22 µm nylon filter, into e 2 ml vial and analysed in HPLC-DAD-MS.

For dyes and chemicals: In this case we adapted different extraction methods for mono and dichlorophenols respect tri, tetra and pentaclorophenol: For mono and dichlorophenols, a sample is weighed into an Erlenmeyer flask, adding an aliquot of distilled water, dissolving in ultrasound bath at room temperature.

Extraction of Tri-, Tetra- and Pentachlorophenol: a sample is weighed into an Erlenmeyer flask, adding an aliquot of methanol, dissolving in ultrasound bath at room temperature. In both cases, filtered with a 0,22 µm nylon filter, into e 2 ml vial and analysed in HPLC-DAD-MS.

4.2 Chromatographic HPLC-DAD-MS conditions

Chromatographic column: GEMINI C18 - 250 mm x 4,6 mm, 5 µm, 110 Å.

Mobile phase: Sodium bicarbonate 0.01 mmol/L: Methanol

Gradient: time program

Time	Methanol concentration
0 min to 20min	40% to 80% Methanol
20 min to 25 min	80% Methanol
25 min to 30min	40% Methanol

Flow: 800 µL/min

Injection volume: 20µL

Column oven temperature: 40°C

Mass-Spectrometer parameters

Nebulizing gas flow: 1,5 L/min

DL temperature: 250°C

Heat block temperature: 400°C

Drying gas flow: 10 L/min

Measurements were recorded in SIM mode.

In Tab. 1 we have reported the m/z ratios used for the identification of the different chlorophenols basic types.

Table 1. m/z signals for Chlorophenols identification.

	Target m/z	m/z	m/z	m/z
Pentachlorophenol	262.7	264.7	266.7	268.7
Tetrachlorophenols	228.7	230.7	232.7	
Trichlorophenols	194.9	196.9	198.9	
Dichlorophenols	160.9	162.9	164.9	
Monochlorophenols	127.0	128.0		

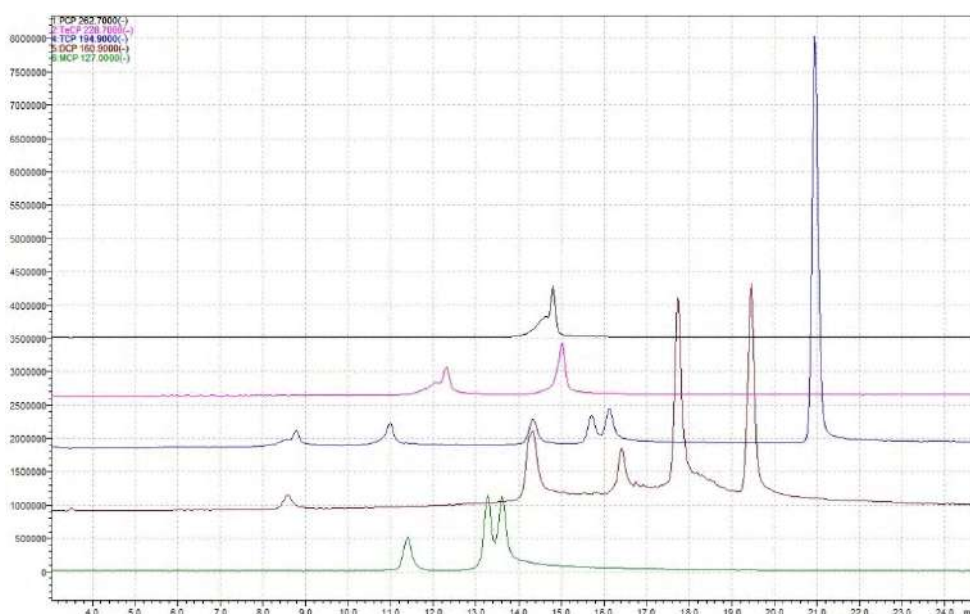


Fig. 2. Chromatogram shifted in the five registered SIM events.

5 Chlorine isotopic masses as identification evidence

The recorded mass signals for each chlorophenol showed the typical behaviour originated in the typical isotopic abundance of the chlorine atom. Each chromatographic peak, shows a signal where the target mass is associated to one or more mass peaks which differs of 2 mass units related to the number of chlorine substituents present on the phenolic ring. This effect, due to the natural abundance of the two stable chlorine isotopes ^{35}Cl and ^{37}Cl respectively in ratio 76%: 24 %. We consider this effect a very clear evidence for chlorophenols identification (Fig. 3).

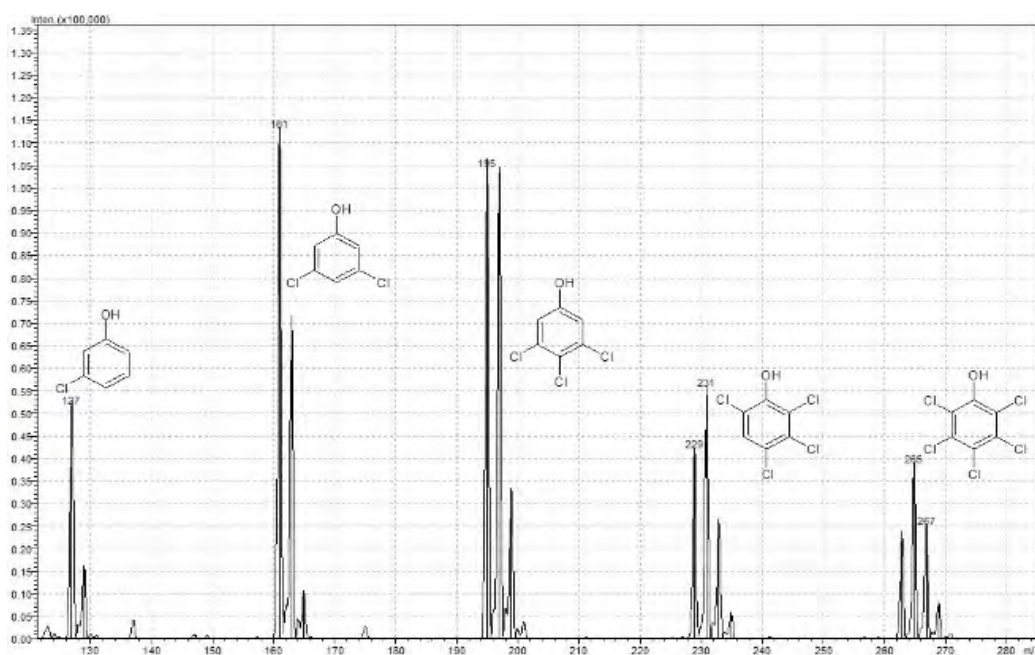


Fig. 3. m/z peaks to identifying the different Chlorophenols.

6 Comparison between ISO 17070:2015 and direct HPLC-DAD-MS methods.

Results obtained by means of ISO 17070:2015 and HPLC-DADMS direct method, were aligned within a reliable quantification limit of ca. 1 mg/kg of tetrachlorophenol and considering a workable uncertainty. Many retests done on samples reported positive with ISO 17070:2015 below 1 mg/kg and demonstrated in many cases the absence of the typical isotopic masses pattern, thus showing the false positive result. In some cases, the method allowed to determine the presence of pentachlorophenol and tetrachlorophenols within the 0,1 mg/kg // 1 mg/kg range, where the said effect was very evident. The HPLC-DAD-MS direct method helped for a quick quantification of chlorophenols traces on dyestuffs, and dyes intermediates.

7 A suspect case of 4-chlorophenol development from a halogenated dyestuff

Most tests carried out for the validation of this test method gave reasonable results on Leather samples and chemicals, considering a reasonable uncertainty level.

In the positive cases found it was demonstrated the use of the detected chlorophenol as precursor of related dyes intermediates. A peculiar case was observed with a monoazo dye, which gave positive results in the order of 100 mg/kg with the indirect method, but negative results with the direct method.

In this case we suspect break of the C-N bond of the monoazo dye during distillation or acetylation.

An analogous case of C-azo coupling reversibility was published in 1998 by V.S. Mokrushkin and M.A. Bezmaternikh⁴. One possible interpretation of 4-chlorophenol generation is described in Fig. 4. Further tests are being performed to demonstrate this eventual radical degradation.

⁴ V.S. Mokrushkin, and M.A. Bezmaternikh: 'The first example of reversible C-azo coupling in a series of aromatic and heteroaromatic compounds', *Mendeleev Commun.*, 1998, 8(5), 197–198

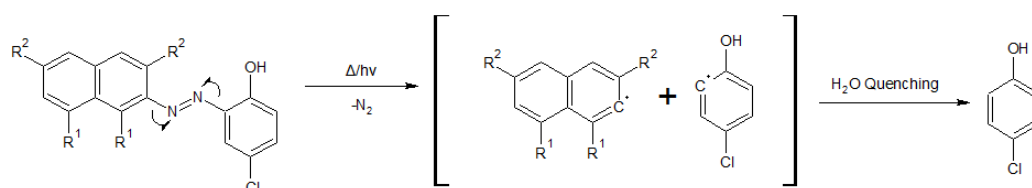


Fig. 4. Proposed radical degradation mechanism.

Conclusions

The proposed direct HPLC-DAD-MS method shown quick and reliable results, demonstrating eventual false positive results on the lower detection limits. Further tests are being performed to detect the possible generation of chlorophenols during distillation and acetylation when applying ISO 17070:2015 on halogenated substances.

Acknowledgement

Special thanks to Dr. Angelo Cascino for his intellectual support during our research.

ADSORPTIVE REMOVAL OF SULFATE, PHOSPHATE AND CHLORIDE BY MG-AL AND ZN-AL LAYERED DOUBLE HYDROXIDES FROM AQUEOUS SOLUTIONS

M. A. Maia^{1,2}, O.W. Perez-Lopez¹ and M. Gutterres²

Federal University of Rio Grande do Sul, Porto Alegre, Brazil

1 PROCAT – Catalytic Processes Laboratory, Department of Chemical Engineering

2 Laboratory for Leather and Environmental Studies – LACOURO, Department of Chemical Engineering

a) avenamarina@gmail.com

b) perez@enq.ufrgs.br

c) mariliz@enq.ufrgs.br

Abstract. The wastewater of leather industry contains pollution loads which includes anionic contaminants such as chloride, sulfate and phosphate. Different treatment technologies for tannery wastewater have been investigated. Adsorption is a promising technique due to its greater selectivity, simple operation, faster regeneration kinetics and high uptake capacity even at trace levels. In the present study, Mg-Al and Zn-Al Layered Double Hydroxides were synthesized by the co-precipitation method at variable pH through a semi-batch system. The prepared material was characterized by XRD, BET surface area determination, TG-DTA and FTIR. The chloride, sulfate and phosphate adsorption properties onto Mg-Al and Zn-Al Layered Double Hydroxides from aqueous solutions were evaluated. The adsorption experiments of chloride, sulfate and phosphate were investigated through batch studies at initial concentrations of 100 mg/L of these anions as NaCl, K₂SO₄ and KH₂PO₄, respectively. The experiments were carried out separately for each anionic specie by mixing 10 ml of solution with 1 g/L of adsorbent for 5 h. Mixing was performed on a thermostatic shaker at 200 rpm and at room temperature (25 °C). The effect of co-existing anions on the adsorption capacity was also analyzed. After ion adsorption, chloride, sulfate and phosphate concentrations were measured by ion chromatography. The results showed a removal ratio for Mg-Al Layered Double Hydroxide of 24.4% and 51% for sulfate and phosphate, respectively, while chloride was not removed from the solution. For the adsorbent Zn-Al Layered Double Hydroxide, the removal ratio of sulfate, phosphate and chloride reached 12.8 %, 69.1 % and 6.3%, respectively.

1 Introduction

Leather tanning is a common industry all over the world and represents an important economic field in Mediterranean countries and in developing nations, such as Turkey, China, India, Pakistan, Brazil, and Ethiopia [1-5]. The transformation of raw or wet-blue hides into commercial products for various purposes requires high water consumption and the use of several chemical products. However, these chemicals are not completely fixed by the hides and remain in the effluent [6]. Therefore, leather tanning industry wastewater is characterized by dark brown color, objectionable odour, variable pH, chemical oxygen demand (COD), biochemical oxygen demand (BOD), total dissolved solids (TDS), chromium (Cr), sulfate, phosphate, nitrate, and a variety of highly toxic organic chemicals and heavy metals [7, 8].

The high concentrations of pollutants in tannery wastewater represent an environmental and technological challenge [9-11]. If not properly removed in prior treatment plants, anionic contaminants, such as chloride, sulfate and phosphate, can have a significant impact on aquatic environments. High concentrations of chloride in wastewaters cause corrosion of waste pipes or agricultural wreck of crops [12]. Concentrations of sulfate above 250 ppm imparts bitter taste in water and cause corrosion in water pipes which can have a laxative effect, dehydration and gastrointestinal irritation on humans and young livestock. Besides that, high concentrations of sulfate can cause the release of toxic sulfide to water bodies, due to sulfate reduction in sulfide, and damage the environment [13, 14]. Furthermore, the over-abundance of phosphate in water

can result in algal bloom and eutrophication of water sources. The latter causes the degradation of water quality, decreases biological diversity and, consequently, increases the cost of water treatment [15-17]. For these reasons, the adequate wastewater treatment is necessary prior to its discharge in aquatic environments.

A variety of techniques have been investigated regarding tannery wastewater treatment, such as biological treatment [18, 19], chemical processes including coagulation-flocculation [8, 20, 21], ion exchange [22], adsorption [23, 24], electrochemical [25], and combined chemical/biological processes [26-29]. Among these techniques, the main technologies adopted to treat industrial tannery wastewater are chemical and biological methods [5]. The employment of the conventional biological method, which utilizes activated sludge, presents some challenges due to the presence of heavy metals in tannery wastewater that inhibits this technique [30, 31]. However, these challenges can be overcome by combining the aforementioned methods. Adsorption is a promising technique that could be used as a tertiary treatment due to its greater selectivity, simple operation and high uptake capacity even at trace levels [32, 33].

Layered Double Hydroxides (LDH), also known as hydrotalcite-like materials or anionic clays, have attracted attention as effective adsorbents [34]. The structure of LDH is based on positive charged brucite-like sheets, where the positive charges are balanced by the intercalation of anions and water molecules in the interlayer regions [35]. LDH are represented by the general formula: $[M^{+2}_{1-x}M^{+3}_x(OH)_2]^{x+}A^{m-}_{x/m} \cdot nH_2O$ where M^{+2} and M^{+3} are divalent and trivalent cations, respectively. A^{m-} represents the incorporated anions in the interlayer space and the value of x is equal to the molar ratio of $M^{+3}/(M^{+2} + M^{+3})$. The identities of M^{+2} , M^{+3} , A^{m-} and the value of x may vary in a wide range giving rise to a large class of isostructural LDH with varied physicochemical properties [36]. Due to their large surface area and high anion exchange capacity, LDH have been successfully employed in several studies for removing different anions from aqueous solutions [12-17, 37, 38].

In the present work, Mg-Al and Zn-Al LDH were studied as adsorbents to individually remove chloride, sulfate, and phosphate from aqueous solutions. In addition, the effects of co-existing anions on the removal of chloride, sulfate, and phosphate were investigated. Mg-Al and Zn-Al LDH were prepared containing carbonate anions in the interlayer space. The morphological structure of the materials was examined with X-ray diffractometry (XRD), BET surface area, thermogravimetry coupled with differential thermal analysis (TG-DTA), and Fourier-transform infrared spectra (FTIR).

2 Materials and Methods

2.1 Synthesis of Layered Double Hydroxides

The LDH were synthesized by the co-precipitation method at variable pH through a semi-batch system. Aqueous solutions of the following metal nitrates were used: $Mg(NO_3)_2$ and $Al(NO_3)_3$ for Mg-Al LDH, $Zn(NO_3)_2$ and $Al(NO_3)_3$ for Zn-Al LDH. The atomic ratio of cations M^{2+}/M^{3+} was fixed at 3 and $[M^{2+}] + [M^{3+}] = 1 \text{ mol L}^{-1}$. A solution of Na_2CO_3 was used as the precipitant agent.

The solutions containing the mixture of bivalents and trivalent metal nitrates were added dropwise, with constant flow rate into the Na_2CO_3 solution. The co-precipitation was conducted in a glass stirred vessel at room temperature (25 °C). The resulting slurry was kept under stirring for crystallization at room temperature for 24 h, filtered and washed several times with deionized water. The wet solid was dried at 80 °C for 12 h and milled to pass through an 80 mesh sieve.

2.2 Characterization of Layered Double Hydroxides

The materials were characterized by X-ray diffractometry (XRD), surface area measurements, thermogravimetry coupled with differential thermal analysis (TG-DTA) and Fourier-transform infrared spectra (FTIR).

The X-ray diffraction patterns were collected through the powder method in a Shimadzu XRD7000 diffractometer, between 2° and 90° 2θ using Cu-Kα radiation.

The specific surface area measurements were determined by N₂ adsorption/desorption at liquid nitrogen temperature (77 K) on a Quantachrome Nova 1200 surface area analyzer. The samples were pretreated at 250 °C under a He flow rate of 30 mL min⁻¹ for 24 h before measurements. The specific surface area (*S*_{BET}) was calculated according to the multipoint Brunauer–Emmett–Teller (BET) method.

Thermal analysis of the prepared solids was performed by thermogravimetry coupled with differential thermal analysis using a thermobalance (Model SDT600). The samples were heated in the temperature range of 20–900 °C with a heating rate of 10 °C min⁻¹, under a synthetic air flow rate of 100 mL min⁻¹.

FTIR spectra were collected on a Frontier spectrophotometer (PerkinElmer) using the attenuated total reflection (ATR) method. Infrared spectra over the 4000–650 cm⁻¹ range were obtained by averaging 32 scans with a resolution of 4 cm⁻¹ at room temperature.

2.3 Adsorption studies

For the adsorption experiments, individual stock solutions (100 mg L⁻¹) of sulfate, phosphate and chloride were prepared with ultrapure water (Gehaka) and K₂SO₄, KH₂PO₄, NaCl, respectively. The adsorption experiments were performed in 15 mL centrifuge tubes by mixing 10 mL of each anion aqueous solution with 1 g L⁻¹ of Mg–Al or Zn–Al LDH under constant stirring for 5 h. Mixing was performed on a thermostatic shaker (Marconi 832) at 200 rpm and at room temperature (25 °C). The batch studies were conducted without any pH adjustment made to the solutions to avoid the influence of complementary anions.

After adsorption, the samples were filtered through a 0.45 μm cellulose nitrate membrane filter. The effect of competitive anions on sulfate, phosphate and chloride adsorption was also evaluated. 1 g L⁻¹ of each adsorbent was introduced in a multi anion solution, containing 100 mg L⁻¹ of each of the following anions: chloride, bromide, nitrate, sulfate and phosphate. The mixtures were shaken for 5 h.

The residual sulfate, phosphate and chloride concentrations were analyzed by ion chromatography (IC) (Metrohm Professional IC 850–AnCat). The IC separation was performed on a Metrosep A Supp 5 analytical column (250 × 4.0 mm) using a standard carbonate eluent (sodium hydrogen carbonate: 1.0 mmol L⁻¹ and sodium carbonate: 3.2 mmol L⁻¹) at a flow rate of 0.7 mL min⁻¹. Each run was carried out in duplicate.

The removal ratio *R*(%) of sulfate, phosphate and chloride (Eq. 1) was obtained from the following relation:

$$R(\%) = \frac{(C_0 - C_e)}{C_0} 100 \quad (1)$$

Where *C*₀ and *C*_{*e*} are the initial and equilibrium concentration of each anionic specie in solution (mg L⁻¹).

3 Results and Discussion

3.1 Characterization

The XRD patterns of the synthesized materials are illustrated in Figure 1. Mg–Al and Zn–Al LDH exhibited the characteristic reflections of the layered structures. Both samples presented reflections at angles 11.8° , 23° , 34.7° , 60.5° and 61.8° corresponding to the crystalline planes of (003), (006), (012), (110) and (113), respectively, which are related to the hydrotalcite structure [39, 40].

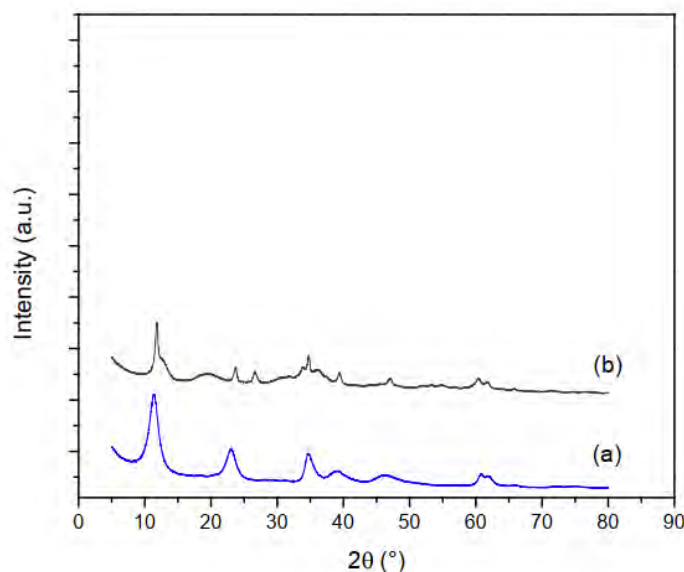


Fig. 1. XRD patterns of Mg–Al (a) and Zn–Al (b) LDH.

The BET surface area of Mg–Al and Zn–Al LDH were 93.7 and $133.2 \text{ m}^2 \text{ g}^{-1}$, respectively. For adsorbents, a large surface area can offer more available adsorption sites. Furthermore, The TG–DTA profiles are depicted in Figure 2. It was observed that Mg–Al and Zn–Al LDH showed endothermic decomposition in two stages, in agreement with typical results for hydrotalcites [41, 42]. The first step in the range of $25\text{--}200^\circ\text{C}$ had a weight loss of approximately 23% and 12% for Mg–Al and Zn–Al samples, respectively, which can be attributed to the elimination of the surface and interlayer water. The second thermal decomposition occurred at a temperature range between 200 and 400°C . The weight loss in this stage is due to the loss of OH groups and anion carbonate decomposition. At higher temperatures, the weight loss corresponds to the formation of the mixed oxide and the collapse of the LDH structure [43].

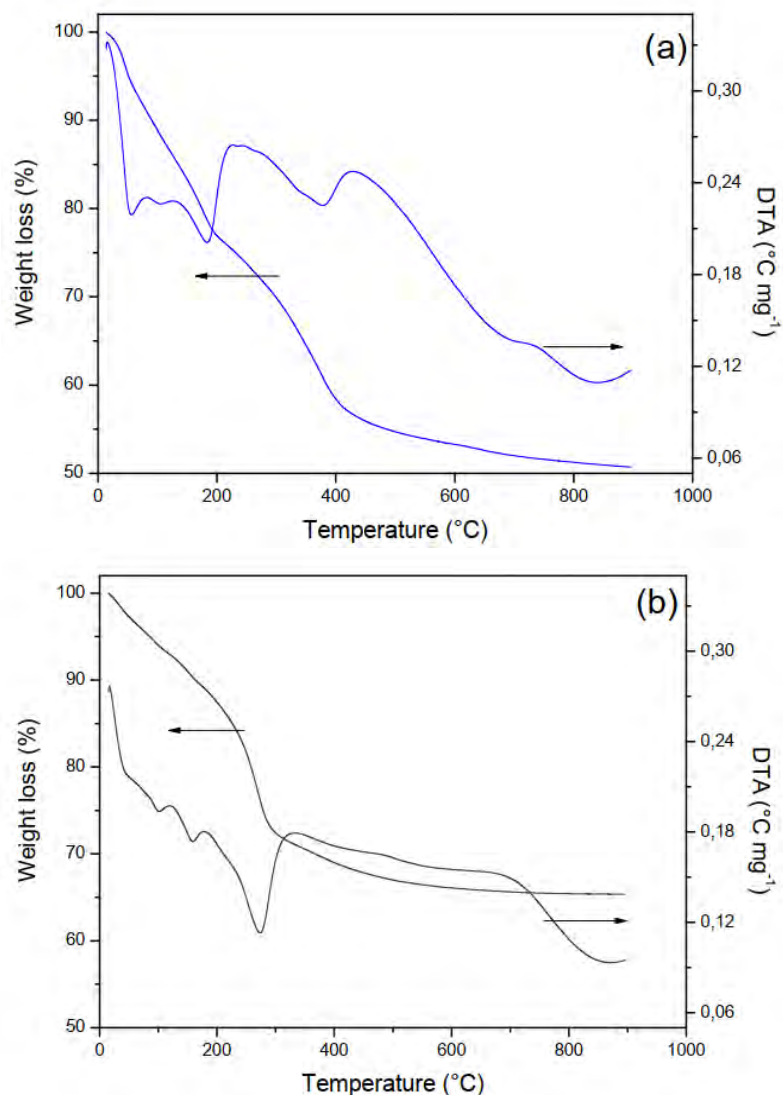


Fig. 2. Thermogravimetric profile (TG–DTA) of Mg–Al (a) and Zn–Al (b) LDH.

Based on the vibrational bands and its respective assignments (FTIR) for Mg–Al and Zn–Al LDH, as presented in Table 1, it can be inferred the presence of O–H stretching vibrations from structural hydroxyl groups and interlayer water molecules; O–H bending mode of water molecules and the indication of the existence of CO_3^{2-} species in the interlayer space [32, 44].

Table 1. FTIR bands and respective assignments for Mg–Al and Zn–Al LDH.

Bands (cm^{-1})		Assignment
Mg–Al LDH	Zn–Al LDH	
3350.6	3308.7	O–H stretching
1634.9	1427.9	O–H bending
1359.2	834.1	CO_3^{2-}

3.2 Adsorption studies

Adsorption experiments were performed to verify the removal potential of chloride, sulfate and phosphate by Mg-Al and Zn-Al LDH. Chloride, sulfate and phosphate removal were individually evaluated at initial concentration of 100 mg L^{-1} and contact time of 5 h. The obtained results are illustrated in Figure 3. It was observed that the anion phosphate achieved highest removal values of 51% and 69.1% for Mg-Al and Zn-Al LDH, respectively. Chloride was not adsorbed by Mg-Al LDH and reached a removal value of only 6.3% for Zn-Al LDH. Moreover, the polyvalent anion sulfate had removal values of 24.4% and 12.8% for Mg-Al and Zn-Al LDH, respectively. Previous studies by Novillo et al. (2014) and Lv et al. (2008) showed that LDH have a significant selectivity towards multivalent inorganic anions when compared with monovalent inorganic anions [45, 46].

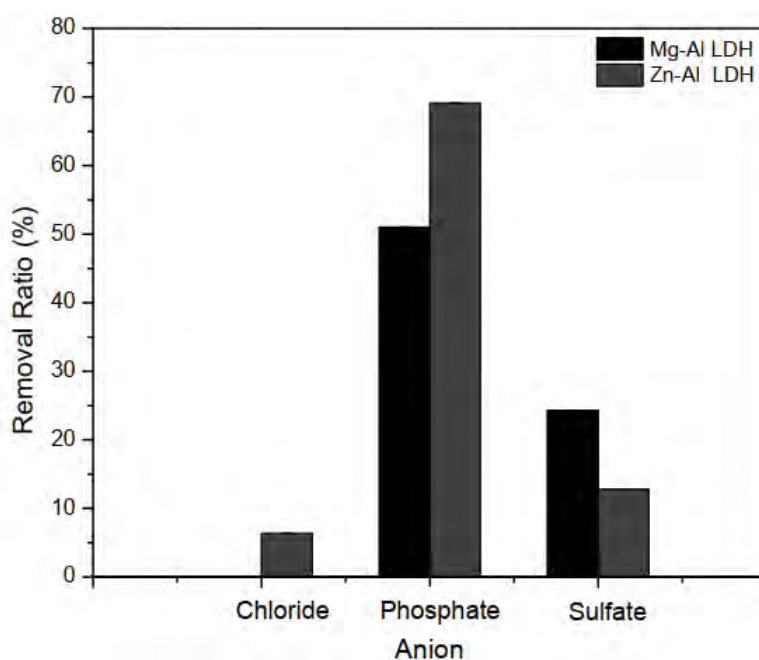


Fig. 3. Chloride, phosphate and sulfate removal from aqueous solutions utilizing Mg-Al and Zn-Al LDH.

3.2.1 Effect of competitive anions

Wastewater usually contains many anionic species such as nitrate, sulfate, bromide, phosphate and chloride. These anions are expected to interfere in the adsorption process of desired anions. The effects of co-existing anions on the removal of chloride, sulfate and phosphate were studied by using a multi-anion solution containing equal concentrations of chloride, bromide, nitrate, phosphate and sulfate of 100 mg.L^{-1} .

The results presented in Table 2 showed a selective adsorption for the phosphate anion also in the multi-anion experiment. It demonstrates that the active adsorption sites preferred the higher effective charge anion. The World Health Organization (WHO) has set a maximum discharge limit of phosphorus of $0.5 - 1 \text{ mg L}^{-1}$ as a guideline. Since biological and chemical processes display fluctuating and unsteady results for phosphate removal, the adsorption technique could be incorporated as a complementary treatment based on the results obtained in this current work [47].

There was a decrease in the removal of chloride, sulfate and phosphate when compared with their individual removal values. Phosphate adsorption by Mg-Al LDH is practically unaffected by the presence of other anions in solution. For the adsorption experiment with Zn-Al LDH, phosphate removal is decreased by almost 15% due to interfering anions. In addition, sulfate adsorption efficiency onto Mg-Al LDH is strongly reduced in the presence of other anionic species. Chloride was

not removed by neither Mg-Al nor Zn-Al LDH. This fact showed that Mg-Al and Zn-Al LDH had in fact greater affinities for multivalent anions. Similar results were obtained by Das et al. (2006) who showed that phosphate removal ratio decreased approximately 25% in the presence of sulfate but only 15% in the presence of monovalent anions [48].

Table 2. Effects of competitive anions on the adsorption of chloride, sulfate and phosphate by Mg-Al and Zn-Al LDH.

Anion	Mg-Al LDH		Zn-Al LDH	
	Individual solution Removal (%)	Co-existing anions Removal (%)	Individual solution Removal (%)	Co-existing anions Removal (%)
Chloride	0.0	0.0	6.3	0.0
Phosphate	51.0	50.8	69.1	54.6
Sulfate	24.3	6.8	12.8	8.4

4 Conclusions

In this study, Mg-Al and Zn-Al LDH were prepared and used to remove chloride, phosphate, and sulfate from aqueous solutions. Characterization analysis showed that both adsorbents formed the structure of hydrotalcite-like materials. The BET surface area of Zn-Al LDH was larger than Mg-Al LDH. Both LDH did not show remarkable selectivity towards the monovalent anion chloride and it was not effectively removed from the solution. Although sulfate achieved a removal of 24.3% when utilizing Mg-Al LDH, the presence of several competitive anions decreased its removal value. In the individual and multi-anion adsorption studies, Mg-Al and Zn-Al LDH exhibited high selectivity for phosphate ions, achieving removal values higher than 50%. Due to the significantly higher removal values, Mg-Al and Zn-Al could be used as effective adsorbents in a tertiary treatment for phosphate removal.

Acknowledgements

This study was financed in part by the Coordenação de Aperfeiçoamento de Pessoal de Nível Superior – Brasil (CAPES) – Finance Code 001 and supported by FINEP (Edital MCTI/FINEP CT-HIDRO 01/2013).

References

1. MANNUCCI, Alberto et al. *Anaerobic treatment of vegetable tannery wastewaters: a review. Desalination*, v. 264, n. 1-2, p. 1-8, 2010.
2. LETA, Seyoum et al. *Biological nitrogen and organic matter removal from tannery wastewater in pilot plant operations in Ethiopia. Applied microbiology and biotechnology*, v. 66, n. 3, p. 333-339, 2004.
3. LEFEBVRE, O. et al. *Anaerobic digestion of tannery soak liquor with an aerobic post-treatment. Water research*, v. 40, n. 7, p. 1492-1500, 2006.
4. RAJESH BANU, J.; KALIAPPAN, S. *Treatment of tannery wastewater using hybrid upflow anaerobic sludge blanket reactor. Journal of Environmental Engineering and Science*, v. 6, n. 4, p. 415-421, 2007.
5. LOFRANO, Giusy et al. *Chemical and biological treatment technologies for leather tannery chemicals and wastewaters: a review. Science of the Total Environment*, v. 461, p. 265-281, 2013.
6. AICH, Anulipi et al. *Ecotoxicological assessment of tannery effluent using guppy fish (Poecilia reticulata) as an experimental model: a biomarker study. Journal of Toxicology and Environmental Health, Part A*, v. 78, n. 4, p. 278-286, 2015.
7. GOUTAM, Surya Pratap et al. *Green synthesis of TiO2 nanoparticles using leaf extract of Jatropha curcas L. for photocatalytic degradation of tannery wastewater. Chemical Engineering Journal*, v. 336, p. 386-396, 2018.

8. LOFRANO, G. et al. Toxicity reduction in leather tanning wastewater by improved coagulation flocculation process. *Global NEST journal*, v. 8, n. 2, p. 151-158, 2006.
9. SCHRANK, S. G. et al. Generation of endocrine disruptor compounds during ozone treatment of tannery wastewater confirmed by biological effect analysis and substance specific analysis. *Water Science and Technology*, v. 59, n. 1, p. 31-38, 2009
10. JAHAN, M. A. A. et al. Characterization of tannery wastewater and its treatment by aquatic macrophytes and algae. *Bangladesh Journal of Scientific and Industrial Research*, v. 49, n. 4, p. 233-242, 2014.
11. TAMMARO, Marco et al. A comparative evaluation of biological activated carbon and activated sludge processes for the treatment of tannery wastewater. *Journal of Environmental Chemical Engineering*, v. 2, n. 3, p. 1445-1455, 2014.
12. LV, Liang et al. Removal of chloride ion from aqueous solution by ZnAl-NO₃ layered double hydroxides as anion-exchanger. *Journal of Hazardous Materials*, v. 161, n. 2-3, p. 1444-1449, 2009.
13. IFTEKHAR, Sidra et al. Application of zinc-aluminium layered double hydroxides for adsorptive removal of phosphate and sulfate: Equilibrium, kinetic and thermodynamic. *Chemosphere*, v. 209, p. 470-479, 2018.
14. TAIT, Stephan et al. Removal of sulfate from high-strength wastewater by crystallisation. *Water Research*, v. 43, n. 3, p. 762-772, 2009.
15. JOHIR, M. A. H. et al. Phosphate adsorption from wastewater using zirconium (IV) hydroxide : Kinetics, thermodynamics and membrane filtration adsorption hybrid system studies. *Journal of Environmental Management*, v. 167, n. 3, p. 167-174, 2016
16. YADAV, Deepak et al. Adsorptive removal of phosphate from aqueous solution using rice husk and fruit juice residue. *Process Safety and Environmental Protection*, v. 94, p. 402-409, 2015.
17. CUI, Xiaoqiang et al. Removal of nitrate and phosphate by chitosan composited beads derived from crude oil refinery waste: Sorption and cost-benefit analysis. *Journal of Cleaner Production*, v. 207, p. 846-856, 2019.
18. EL-SHEIKH, Mahmoud A. et al. Biological tannery wastewater treatment using two stage UASB reactors. *Desalination*, v. 276, n. 1-3, p. 253-259, 2011.
19. DURAI, G. et al. Biological Treatment of Tannery Wastewater- A Review. *Journal of Environmental science and Technology*, v. 4, n. 1, p. 1-17, 2011.
20. HAYDAR, Sajjad; AZIZ, Javed Anwar. Coagulation-flocculation studies of tannery wastewater using combination of alum with cationic and anionic polymers. *Journal of Hazardous Materials*, v. 168, n. 2-3, p. 1035-1040, 2009.
21. HAYDAR, Sajjad; AZIZ, Javed Anwar. Characterization and treatability studies of tannery wastewater using chemically enhanced primary treatment (CEPT)—a case study of Saddiq Leather Works. *Journal of Hazardous Materials*, v. 163, n. 2-3, p. 1076-1083, 2009.
22. SAHU, S. K. et al. Removal of chromium (III) by cation exchange resin, Indion 790 for tannery waste treatment. *Hydrometallurgy*, v. 99, n. 3-4, p. 170-174, 2009.
23. TAHIR, S. S.; NASEEM, R. Removal of Cr (III) from tannery wastewater by adsorption onto bentonite clay. *Separation and purification Technology*, v. 53, n. 3, p. 312-321, 2007.
24. ANANDKUMAR, J.; MANDAL, B. Adsorption of chromium (VI) and Rhodamine B by surface modified tannery waste: Kinetic, mechanistic and thermodynamic studies. *Journal of Hazardous Materials*, v. 186, n. 2-3, p. 1088-1096, 2011.
25. PANIZZA, Marco; CERISOLA, Giacomo. Electrochemical oxidation as a final treatment of synthetic tannery wastewater. *Environmental science & technology*, v. 38, n. 20, p. 5470-5475, 2004.
26. RAMESHRAJA, D.; SURESH, S. Treatment of tannery wastewater by various oxidation and combined processes. *International Journal of Environmental Research*, v. 5, n. 2, p. 349-360, 2011.
27. AYOUB, G. M.; HAMZEH, A.; SEMERJIAN, L. Post treatment of tannery wastewater using lime/bittern coagulation and activated carbon adsorption. *Desalination*, v. 273, n. 2-3, p. 359-365, 2011.
28. RYU, Hong-Duck; LEE, Sang-Il; CHUNG, Keun-Yook. Chemical oxygen demand removal efficiency of biological treatment process treating tannery wastewater following seawater flocculation. *Environmental engineering science*, v. 24, n. 3, p. 394-399, 2007.
29. SONG, Z.; WILLIAMS, C. J.; EDYVEAN, R. G. J. Treatment of tannery wastewater by chemical coagulation. *Desalination*, v. 164, n. 3, p. 249-259, 2004.
30. FARABEGOLI, G. et al. Biological treatment of tannery wastewater in the presence of chromium. *Journal of Environmental Management*, v. 71, n. 4, p. 345-349, 2004.
31. BARTH, E. F. et al. Summary report on the effects of heavy metals on the biological treatment processes. *Journal (Water Pollution Control Federation)*, p. 86-96, 1965.
32. YANG, Kun et al. Adsorptive removal of phosphate by Mg-Al and Zn-Al layered double hydroxides: kinetics, isotherms and mechanisms. *Separation and Purification Technology*, v. 124, p. 36-42, 2014.
33. PICCIN, Jeferson S. et al. Mass transfer models for the adsorption of Acid Red 357 and Acid Black 210 by tannery solid wastes. *Adsorption Science & Technology*, v. 35, n. 3-4, p. 300-316, 2017.
34. GOH, Kok-Hui; LIM, Teik-Thye; DONG, Zhili. Application of layered double hydroxides for removal of oxyanions: a review. *Water research*, v. 42, n. 6-7, p. 1343-1368, 2008.
35. FORANO, C. et al. Layered double hydroxides. *Handbook of Clay Science*. Elsevier Ltd, p. 1021-1095, 2006.
36. DELGADO, R. Rojas et al. Influence of MII/MIII ratio in surface-charging behavior of Zn-Al layered double hydroxides. *Applied Clay Science*, v. 40, n. 1-4, p. 27-37, 2008.
37. JIA, Zhiqian; HAO, Shuang; LU, Xiaoyu. Exfoliated Mg-Al-Fe layered double hydroxides/polyether sulfone mixed matrix membranes for adsorption of phosphate and fluoride from aqueous solutions. *Journal of Environmental Sciences*, p. 1-11, 2017

-
38. THEISS, Frederick L. et al. A review of the removal of anions and oxyanions of the halogen elements from aqueous solution by layered double hydroxides. *Journal of colloid and interface science*, v. 417, p. 356–368, 2014.
 39. THOUCHPRASITCHAI, Nutthavich; LUENGNARUEMITCHAI, Apanee; PONGSTABODEE, Sangobtip. The activities of Cu-based Mg–Al layered double oxide catalysts in the water gas shift reaction. *international journal of hydrogen energy*, v. 41, n. 32, p. 14147-14159, 2016.
 40. TRIANTAFYLIDIS, Kostas S. et al. Iron-modified hydrotalcite-like materials as highly efficient phosphate sorbents. *Journal of colloid and interface science*, v. 342, n. 2, p. 427-436, 2010.
 41. ROJAS, Ricardo et al. Intercalation of metal–EDTA complexes in Ni–Zn layered hydroxysalts and study of their thermal stability. *Microporous and Mesoporous Materials*, v. 112, n. 1–3, p. 262–272, 2008.
 42. LOPEZ, T. et al. DTA–TGA and FTIR spectroscopies of sol–gel hydrotalcites: aluminum source effect on physicochemical properties. *Materials Letters*, v. 31, n. 3–6, p. 311–316, 1997.
 43. ROSSET, Morgana; PEREZ–LOPEZ, Oscar W. Catalytic properties of Cu–Mg–Al hydrotalcites, their oxides and reduced phases for ethanol dehydrogenation. *Reaction Kinetics, Mechanisms and Catalysis*, v. 123, n. 2, p. 689–705, 2018.
 44. LUENGO, Carina V.; VOLPE, María A.; AVENA, Marcelo J. High sorption of phosphate on Mg–Al layered double hydroxides: Kinetics and equilibrium. *Journal of Environmental Chemical Engineering*, v. 5, n. 5, p. 4656–4662, 2017.
 45. NOVILLO, Corina et al. Evaluation of phosphate removal capacity of Mg/Al layered double hydroxides from aqueous solutions. *Fuel*, v. 138, p. 72-79, 2014
 46. LV, Liang et al. Bromide ion removal from contaminated water by calcined and uncalcined MgAl–CO₃ layered double hydroxides. *Journal of hazardous materials*, v. 152, n. 3, p. 1130-1137, 2008.
 47. BARNARD, James L. Biological nutrient removal: where we have been, where we are going?. *Proceedings of the Water Environment Federation*, v. 2006, n. 13, p. 1-25, 2006.
 48. DAS, J. et al. Adsorption of phosphate by layered double hydroxides in aqueous solutions. *Applied Clay Science*, v. 32, n. 3-4, p. 252-260, 2006.

LEATHER SHAVING – A NEW APPROACH FOR UNDERSTANDING THE SHAVING PROCESS

T. Witt¹, E. Klüver², A. Nikowski¹ and M. Meyer²

1 Technische Universität Dresden, Institut für Naturstofftechnik, 01062 Dresden

2 FILK gGmbH, Meißner Ring 1-5, 09599 Freiberg

a) Corresponding author: tilman.witt@tu-dresden.de

b) Corresponding author: enno.kluever@filkfreiberg.de

Abstract. The shaving process is one of the most important steps in the production of leather, in which an even thickness of the semi-finished product (wet-blue or wet-white) is adjusted by material removal on the rear side. This process is carried out by means of a razor roller in a shaving machine. The success of the shaving process as well as the quality of the resulting surface significantly depend on the long-time experience of the operators. The principles and mechanisms of the underlying cutting process are still insufficiently understood. A current research project deals with the investigation of the cutting process and the interactions between the shaving blade and the material to be processed. The aim is to gain a competent knowledge of the physical processes involved in shaving, which will serve as a basis for the development of new and more effective blades. For this purpose, the theoretical courses of the cutting edge, which describe the expected cut, are to be determined experimentally with the aid of a test setup. The complex cutting behaviour of a knife roller with helical blades will be reduced to a simple model with an exemplary blade. The expected forces can be applied to the cutting edge progressions and their individual determination can be systematized by measurement evaluation. The present study describes the fundamentals of the experimental setup in addition to that the derivation of a material model for computer simulations.

1 Introduction

The process step of leather shaving involves the removal of material from the rear surface of the flat semi-finished leather product (wet-blue or wet-white) in order to produce a homogeneous thickness. Shaving is performed with the aid of cutting blades arranged helically on a knife roller so the material is removed in the shape of small chips (“leather shavings”). The quality of the shaved leather surface is evaluated, among other things, by the dimensional accuracy of the thickness and the absence of optical artefacts. In general, the shaving process of leather is influenced by the characteristics of the leather, the geometry of the cutting tool and the relative movement of the leather towards the cutting tool. The mechanical properties of the semi-finished leather product are strongly influenced by the preceding manufacturing steps, e.g. liming and tanning. Leather shows viscoelastic properties [1] as well as a highly anisotropic material structure due to its fibrous texture and the locally different orientation and density of the leather fibers [2] [3] [4] [5]. Leather thus differs significantly from metallic or polymeric materials, whose anisotropy is much lower. The geometry of the cutting tools and the guidance of the cut are determined by the given construction of the commercial shaving machines and are limited in their variation possibilities. A key property of cutting processes is a defined cutting edge, which is described in the literature by several approaches concerning natural products. SCHULDT associates the defined cutting edge at the beginning of the cut with an early cut initiation [6], which in turn is affected by the Blade Sharpness Index [7]. A geometric model for material removal can be created under the prerequisite of a defined cutting behaviour. This geometric model is used to apply forces that allow the energy input to be modeled and serves as a fundament for experimental investigations. A test setup based on this model must be able to reduce the cutting behaviour of a knife roll to the cut of a single blade.

Furthermore forces and effects occurring during the interaction between blade and leather have to be determined. From these experimental data, a model for computer simulations will be derived which includes the anisotropy and viscoelasticity of leather and represents a realistic description of the shaving process.

1.1 Approaches on the description of the cutting process

For the separation of materials by cutting, the cutting force can be determined for any point in time. A first distinction in friction and deformation is made according to equation (1) [8] [9].

$$F_C = F_{adhesion} + F_{deformation} \quad (1)$$

Since 1900 there has been a large number of investigations on the cutting of metallic, polymeric and wooden materials. Compared to leather, these materials have a high bending stiffness. In the field of natural materials, the deformation content of the elastic, plastic and viscous area is considered. These properties are also very pronounced in leather, so that a strong similarity is assumed. The term for the deformation is divided into elastic, plastic and viscous [10] contributions, while the adhesion consists of breaking force and friction force [11]. This results in equation (2).

$$F_C = F_E + F_{D,v} + F_{D,f} + F_{fract} + F_{frict} \quad (2)$$

F_E , $F_{D,v}$ and $F_{D,f}$ are the forces that deform the chip, F_{fract} describe the force that separates the material and F_{frict} identifies the friction between the cutting tool and the material. Regarding metallic materials, the plastic deformation of the chip is dominant over the elastic deformation. Based on the work of MERCHANT [8], models were developed to describe and predict the forces occurring during orthogonal cutting [12]. Other models were developed and investigated for the more complex oblique cutting [13] [14] [15]. The cutting of composite materials is even more complex due to the existing anisotropy. In his experiments, KOPLEV [16] showed that the fiber orientation of carbon fibers in an epoxy matrix is decisive for the forces occurring and the progress of the cut. Fig. 1 shows that in orthogonal fiber orientation no premature cut can be seen, which significantly distinguishes the mechanical processing of composite materials and metals.

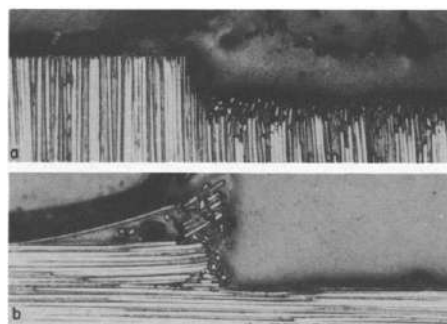


Fig. 1. Cross section of 'quick-stop' specimen showing the notch formed by the tool: (a) machined perpendicular the fibers. (b) machined parallel to the fibers [16]

Further experiments and modelling with different approaches allow better predictions [17] [18]. This shows that the mechanical machining of composite materials poses different challenges than the machining of metals. The approach used so far for these materials is inadequate. The orientation of the fibers in relation to the relative direction of movement of the cutting tool is of particular importance. The investigations with fiber-reinforced plastic from SREEJITH [19] showed that the surface quality is dependent on the fiber orientation and must be taken into account during processing. Fig. 2 shows the

problem of fiber orientation for the shaving process of leather. An undesirable effect when shaving leather is the formation of a staircase-shaped texture, which can probably be explained with similar relationships.

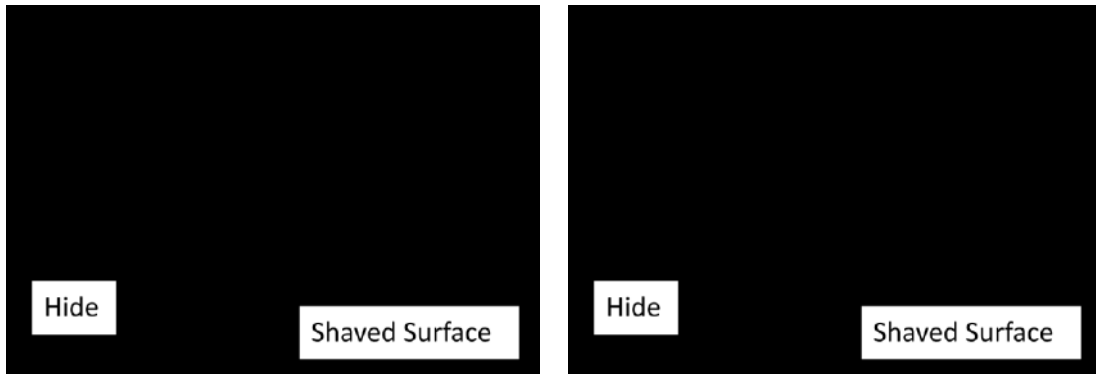


Fig. 2. Shaving under consideration of the fiber alignment

In addition, SREEJITH's study found that with increasing cutting speed, both cutting force and cutting temperature do not increase uniformly and there is a local minimum. Increasing the feed rate, on the other hand, leads to a lower feed force and a higher temperature. CALZADA [20] presented a fracture model for fibers in which different types of fracture could be detected depending on the fiber orientation. The modelling of composite materials with fibers is still part of current research [21] [22] [23]. The approach functions for modelling refer to geometric predictions for chip formation. The work of BUSHLYA [24] provides a summary of the geometric determination of cutting volumes and cutting lengths for milling work.

1.2 Shaving Process

Leather shaving machines are an integral part of a tannery and have been used in their basic design since the end of the 19th century [25]. Their function is to produce a certain thickness of a flexible surface material by chip removal. For this purpose, the flexible semi-finished leather product is guided over a chrome-plated roller. On a second roller, the helix-shaped blades are arranged symmetrically with reference to the center. The gap between the rollers determines the thickness of the product after the process. The principle arrangement of the rollers and the directions of movement are shown in Fig. 3.

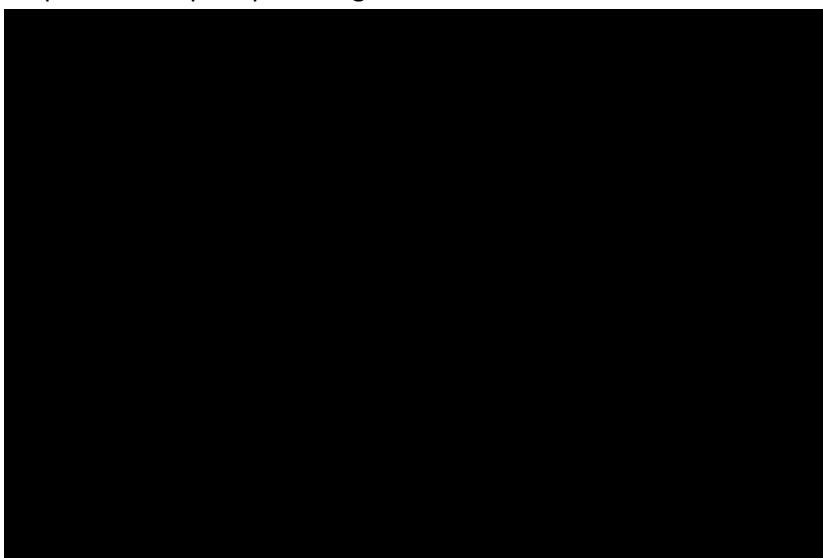


Fig. 3. Active unit for the shaving of leather with moving direction indicators. (a) Knife roller. (b) Chrome-plated roller. (c) Leather.

The blades are continuously sharpened with a grinding wheel in order to achieve a constantly high sharpness. Due to the different sizes of different animals, machines are available in various working widths. In addition, there are differences in the cylinder diameter of the chrome and knife roller as well as different pitches of the blades. The pitch angle of the knife roller λ_{kr} plays an important role in this investigation and is calculated according to equation (3) from the pitch of the spiral per revolution P_{kr} and the diameter of the blade shaft d_{kr} .

$$\lambda_{kr} = \arctan\left(\frac{P_{kr}}{\pi \cdot d_{kr}}\right) \cdot \frac{180^\circ}{\pi} \quad (3)$$

Fig. 4 is derived on the basis of collected machine data. It shows the pitch of the blades in respect to different core diameters of the knife roller. The data set includes the blades from two different manufacturers.

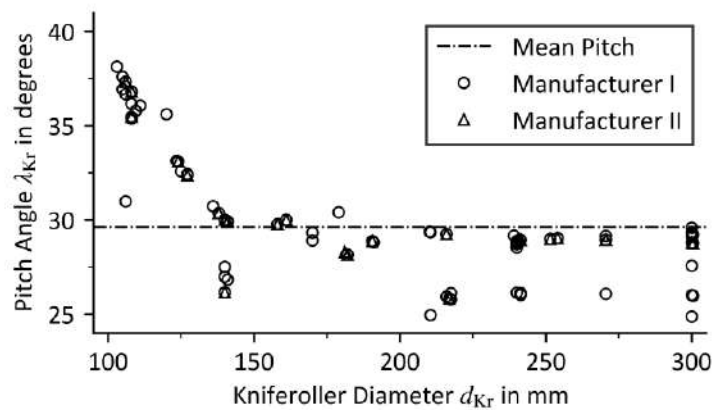


Fig. 4. Pitch angle of the knife roller in respect to different core diameters of the knife roller from two different manufacturers and the mean value of the pitch.

The pitch angle of the knife roller λ_{kr} of slightly less than 30° is dominant and corresponds approximately to the mean value of the data set. Due to the pitch of the helix, the orientation of the cutting edge is not orthogonal to the current feed direction. This results in an oblique cut. The feed rate is set or indicated on the machine in meters per minute and the speed of the measuring cylinder is specified in revolutions per minute (rpm).

2 Material and Methods

2.1 Exemplary machine data

For the analysis of the shaving process the machine Arenco-BMD type FM 1800 is used as an example. The machine has a working width of 1800 mm. The cutting tool rotates at a speed of 1500 rpm and has a knife roller diameter of 252 mm, which is reduced by grinding. The lower limit of the blade length is assumed to be 10 mm. The pitch of the knife helix is 330 mm per revolution and thus has a pitch angle of about 30 degrees. The chrome-plated roller has a measured radius of 92 mm. A feed rate of 6 m/min to 21 m/min can be set. The number of blades varies depending on the machine version with 9, 12, 15 or 18 pieces. A number of blades of 15 is assumed for further consideration.

2.2 Calculation of characteristic geometric quantities

To determine the basic geometric properties of a cut, the length of the cutting edge, the theoretical maximum thickness of the chip and the displaced area per cutting operation are used. The calculation of these values from metal processing is adapted for the feed movement on a circular path to represent the process of leather shaving. The variables relevant for the calculation are shown in the schematic sketch (Fig. 5).

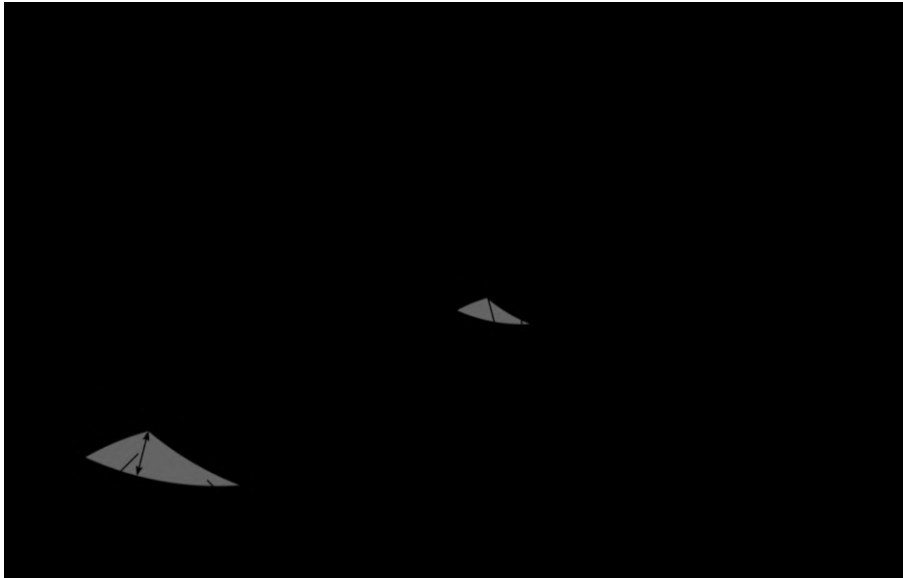


Fig. 5. Schematic sketch of the geometric structure with the relevant variables.

The radius of the surface of the leather is determined by the diameter of the chrome roller d_{Cr} and the thickness of the leather t_H .

$$r_{Surf} = \frac{d_{Cr}}{2} + t_H. \quad (4)$$

The initial contact of the cutting tool with the leather surface is described by the angle β_{Init} , which is calculated according to the cosine theorem from the triangle of the surface radius r_{Surf} , the distance of the pivot points of the knife roller and chromium roller r_{Dist} and the radius of the knife roller r_{Kr} .

$$\beta_{Init} = \frac{3 \cdot \pi}{2} - \arccos\left(\frac{r_{Dist}^2 + r_{Kr}^2 - r_{Surf}^2}{2 \cdot r_{Dist} \cdot r_{Kr}}\right). \quad (5)$$

The feed angle α_{Feed} is required to calculate the exit angle β_{Exit} . For reasons of clarity, the last section of a spiral is also shown as a circle in Fig. 5. The feed angle can be calculated from the feed speed of the leather v_{Feed} , the rotation speed of the knife roller n_{Kr} , the number of blades on the knife roller i_K and the radius of the surface r_{Surf} .

$$\alpha_{Feed} = \frac{v_{Feed}}{n_{Kr} \cdot i_K \cdot r_{Surf}}. \quad (6)$$

The exit angle β_{Exit} at the point of exit of the helix is to be determined by the intersection of the circles of the current cut and the previous cut. Two mathematical angles result from the solution of the equation. Due to the given arrangement, the smaller angle is to be used.

$$\beta_{Exit} = \frac{3 \cdot \pi}{2} + \arcsin\left(\frac{r_{Dist}}{r_{Kr}} \cdot \sin\left(\frac{\alpha_{Feed}}{2}\right)\right) - \frac{\alpha_{Feed}}{2}. \quad (7)$$

The upper and lower limits of the polar index variable φ are thus present. With the knife radius r_{Kr} and the limits of the angle φ the curve $\gamma(\varphi)$ for the cutting edge is set up. The pitch in axial direction per revolution p_{Kr} is added in the third spatial direction and set depending on φ .

$$\gamma_{\text{Edge}}(\varphi) = \begin{pmatrix} r_{Kr} \cdot \cos \varphi \\ r_{Kr} \cdot \sin \varphi \\ \frac{p_{Kr}}{2 \cdot \pi} \cdot \varphi \end{pmatrix}, \beta_{\text{Init}} \leq \varphi \leq \beta_{\text{Exit}}. \quad (8)$$

The derivation of the curve according to the index variable φ is necessary for the application in the curve integral.

$$\gamma'_{\text{Edge}}(\varphi) = \begin{pmatrix} -r_{Kr} \cdot \sin \varphi \\ r_{Kr} \cdot \cos \varphi \\ \frac{p_{Kr}}{2 \cdot \pi} \end{pmatrix}, \beta_{\text{Init}} \leq \varphi \leq \beta_{\text{Exit}}. \quad (9)$$

The length of the cutting edge is formulated with a curve integral, which is formed according to the rule in equation (10).

$$l_{\text{Chip}} = \int_{\beta_{\text{Init}}}^{\beta_{\text{Exit}}} \|\gamma'_{\text{Edge}}(\varphi)\| d\varphi. \quad (10)$$

The radii of the edges of the knife roller and leather upper edge must be determined as a function of the index variable φ in order to determine the thickness of the chips and the displaced area. This requires a further integration limit. The upper edge of the chip is partly determined by the surface of the uncut leather and partly by the previous cut. In a first step, the angle of the preceding cut α_{Prev} is determined in relation to the axis of rotation of the chrome roller.

$$\alpha_{\text{Prev}} = \arccos\left(\frac{r_{\text{Surf}}^2 + r_{\text{Dist}}^2 - r_{\text{Kr}}^2}{2 \cdot r_{\text{Surf}} \cdot r_{\text{Dist}}}\right) \quad (11)$$

The angle α_{Prev} determines the angle β_{Prev} for the coordinate system of the current cutter roller.

$$\beta_{\text{Prev}} = \frac{3 \cdot \pi}{2} + \arctan\left(\frac{\sin(\alpha_{\text{Prev}} - \alpha_{\text{Feed}}) \cdot r_{\text{Surf}}}{r_{\text{Dist}} - \cos(\alpha_{\text{Prev}} - \alpha_{\text{Feed}}) \cdot r_{\text{Surf}}}\right). \quad (12)$$

The first part of the surface has not yet been cut. There are two solutions, whereby in the given arrangement the radius with the smaller amount must be used.

$$r_{\text{redSurf}}(\varphi) = \sin(-\varphi) \cdot r_{\text{Dist}} \pm \sqrt{(\sin^2(-\varphi) - 1) \cdot r_{\text{Dist}}^2 + r_{\text{Surf}}^2}, \quad \beta_{\text{Init}} \leq \varphi \leq \beta_{\text{Prev}}. \quad (13)$$

The maximum thickness of the chip t_{Cut} is determined using the reduced radius $r_{\text{redSurf}}(\varphi)$ at the location of the β_{Prev} angle.

$$t_{\text{Chip}} = r_{\text{Kr}} - r_{\text{redSurf}}(\beta_{\text{Prev}}). \quad (14)$$

The second part of the upper edge is determined by the previous cut. The variable radius $r_{\text{redPrev}}(\varphi)$ describes the upper edge within the limits β_{Prev} to β_{Exit} . The solution of the square equation gives two results. The root term must be added for the given arrangement.

$$r_{\text{redPrev}}(\varphi) = \pm \sqrt{\frac{2r_{\text{Dist}} \sin \frac{\alpha_{\text{Feed}}}{2} \cdot \cos \left(\varphi + \frac{\alpha_{\text{Feed}}}{2} \right)}{4 \cdot r_{\text{Dist}}^2 \cdot \sin^2 \left(\frac{\alpha_{\text{Feed}}}{2} \right) \cdot \cos^2 \left(\varphi + \frac{\alpha_{\text{Feed}}}{2} \right) + r_{\text{Kr}}^2}}, \quad (15)$$

$$\beta_{\text{Prev}} \leq \varphi \leq \beta_{\text{Exit}}$$

In a final step, the formulation of the area integral for the displaced area A_{Chip} is given in the form of a double integral.

$$A_{\text{Chip}} = - \int_{\beta_{\text{Init}}}^{\beta_{\text{Exit}}} \int_0^{r_{\text{Kr}}} \sqrt{\left(\frac{p_{\text{Kr}}}{2 \cdot \pi} \right)^2 + r^2} dr d\varphi \cdot$$

$$- \int_{\beta_{\text{Prev}}}^{\beta_{\text{Exit}}} \int_0^{r_{\text{redSurr}}(\varphi)} \sqrt{\left(\frac{p_{\text{Kr}}}{2 \cdot \pi} \right)^2 + r^2} dr d\varphi \cdot$$

$$- \int_{\beta_{\text{Prev}}}^{\beta_{\text{Exit}}} \int_0^{r_{\text{redPrev}}(\varphi)} \sqrt{\left(\frac{p_{\text{Kr}}}{2 \cdot \pi} \right)^2 + r^2} dr d\varphi$$
(16)

With equations (10), (14) and (16), the three characteristic quantities of the cutting process can be calculated and used for sensitivity analyses.

2.3 Determination of the torque based on the rotational speed for an electric motor

The determination of the prevailing load in a processing operation can be determined on the basis of the load acting on the driving motor. In the FM 1800 shaving machine, the knife roller and the scraper roller are driven by a 225M three-phase motor with 45 kW and 1500 rpm. A motor of the same design was procured and tested on a test stand to determine the torque as a function of the speed of rotation of the motor. The test stand is presented in detail in the dissertation by WINDISCH [26]. The test arrangement is shown in Fig. 6.

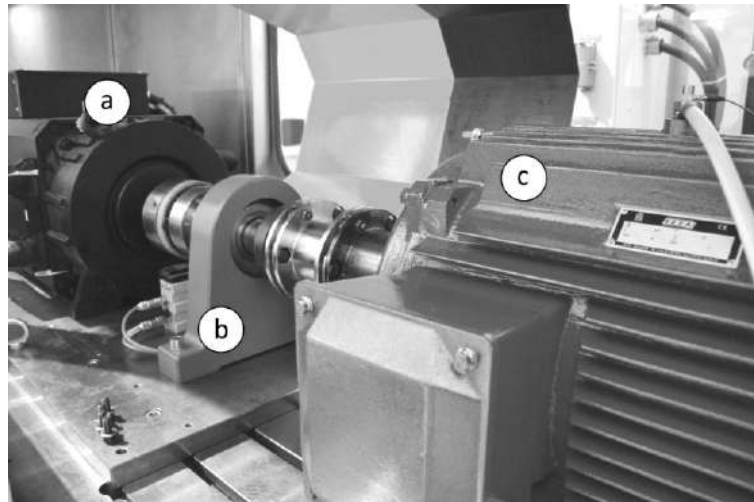


Fig. 6. Test arrangement for torque determination. (a) Brake motor. (b) Torque sensor. (c) Engine under test.

On the bench, the brake motor (a) is connected to the torque sensor (b) by a coupling and the latter is connected to the motor (c) to be tested by another coupling. The motor runs under rated load for 20 minutes to allow the motor to reach operating temperature. The test series is operated with a software which sets a speed at the dominant brake motor and holds it for 10 seconds. The measured torque values are recorded over the period for the rotational speed. Finally, the torque curve is approximated by a linear regression in respect to the rotational speed.

3 Results

3.1 Sensitivity analysis for a type FM 1800 machine

The sensitivity analysis is performed for a machine Arenco-BMD type FM 1800 with different parameter variations. On the machine, settings can be realised with regard to the feed speed, the shaving gap and the speed of the blade roller by means of a frequency converter added subsequently. On the material side, the process is influenced by the initial thickness of the leather and the target thickness. For the calculation, it is assumed that the thickness after shaving corresponds exactly to the width of the gap. The calculation always assumes a thickness of 4 mm to be manufactured, whereby the initial thickness of the leather is varied from 4.1 to 4.8 mm, which consequently corresponds to a removed height of 0.1 to 0.8 mm. The influence of the removal and the machine parameters (motor turning speed n_{Motor} , diameter of the cutting cylinder r_{Kr} and feed rate v_{Feed}) are graphically shown in Fig. 7, Fig. 8 and Fig. 9. The cutting depth is plotted on the x-axis, while the y-axis represents one of the three machine parameters. The change in the diameter of the cutting cylinder is a consequence of the grinding of the knives. The range of variation of the parameters is shown in Table. 1. All other parameters are considered constant.

Table. 1. Parameter variations.

Graph	t_{Cut} in mm	n_{Motor} in 1/min	r_{Kr} in mm	v_{Feed} in m/min
I	0.1 - 0.8	1200 - 1800	115	12
II	0.1 - 0.8	1500	105 - 125	12
III	0.1 - 0.8	1500	115	8 - 16

The results of the sensitivity analysis are displayed graphically as a surface plot. First of all, the influence of the engine speed and the removal height are examined in Fig. 7.

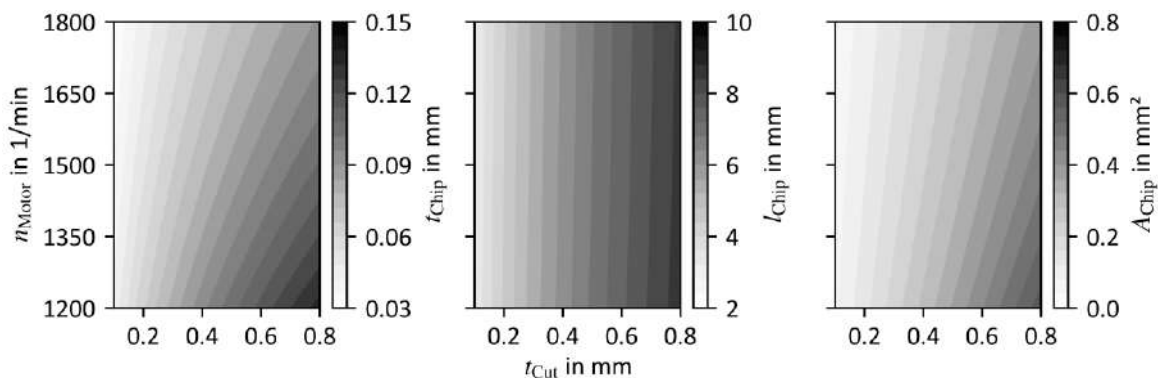


Fig. 7. Response variables as a function of cutting depth and engine speed

The change in the rotational speed of the motor (Fig. 7) has a minor influence on the cutting edge length. Both the maximum thickness of the chip and the cross-sectional area of the chip decrease with increasing speed of the motor.

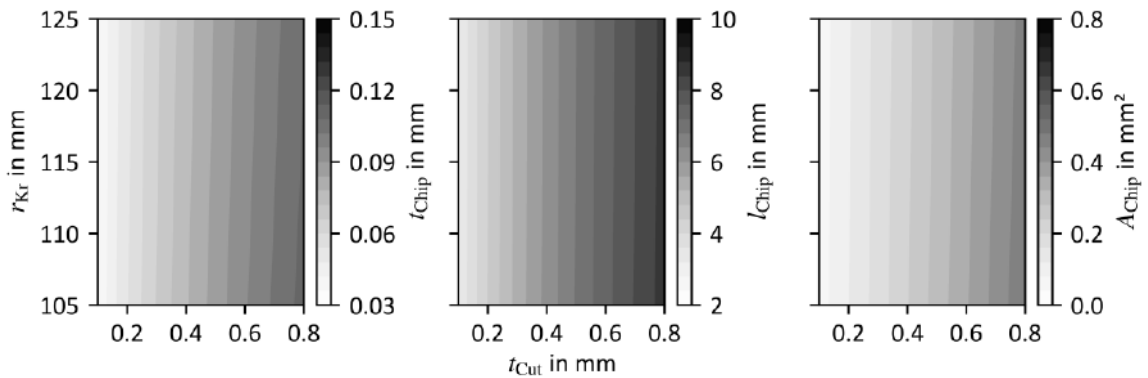


Fig. 8. Response variables as a function of cutting depth and knife roll diameter.

The change in the diameter of the knife roller (Fig. 8) has very little effect on the quality criteria for the area investigated. A tendency can be seen, but this is hardly noticeable with a knife roller diameter of 200 mm or more.

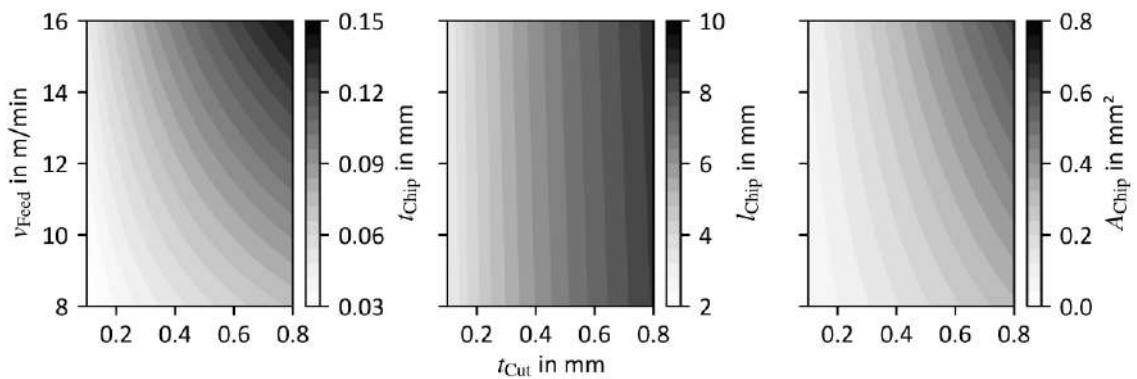


Fig. 9. Response variables depending on cutting depth and feed rate.

An increase in the feed rate (Fig. 9) results in an increase in the thickness of the chip. The increase is reinforced nonlinearly by an increase in the cutting depth. As in the previous cases, the length of the cutting edge is only slightly influenced by the feed rate. The displaced area increases in a similar way due to the increase in chip thickness.

3.2 Torque characteristics for the main drive of a machine of type FM 1800

The tests to determine the torque curve as a function of the rotational speed were carried out with a new motor of size 225M with an output of 45 kW and 1500 rpm. The results of the tests are shown in Fig. 10.

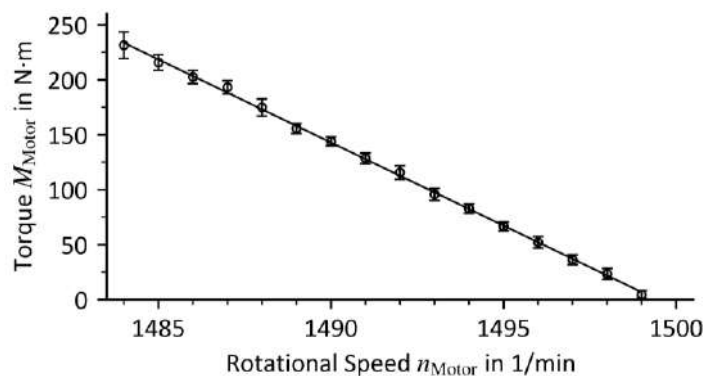


Fig. 10. Motor torque in respect to rotational speed. The linear regression applies to the test points with standard deviation.

The equation (17) for linear regression does not lead through the idle speed of 1500. This is due to fluctuations in the electrical grid.

$$M_{\text{Motor}}(n_{\text{Motor}}) = -15.121 \cdot n_{\text{Motor}} + 22673 . \quad (17)$$

This enables to determine the mechanical load in the process by specifying the torque for the turning frequency in the range of 1485 to 1500 rpm.

3.3 Torque during shaving of cattle hides

The tests were carried out on a machine Arenco-BMD type FM 1800 with half hides of cattle. The machine was additionally equipped with a rotary position sensor. The process load is determined from the encoder data and the determined relationship between torque and rotational speed. The machine has 15 helical blades on both sides and was operated with a feed speed of 9 m/min. The skins were tanned with glutaraldehyde and the thickness was measured before and after shaving. The gap between chrome roller and knife roller was set to 0.8 mm. The shaved hides had a thickness of 1.1 ± 0.2 mm. Each individual leather was first shaved from the tail two thirds. Then the leather was removed from the machine, turned and the remaining third of the skin was treated. The experiments were carried out with hides. Fig. 11 shows the motor torque M_{Motor} curves for the first side on the left and the 6 torque curves for the second side for the shaving process on the right.

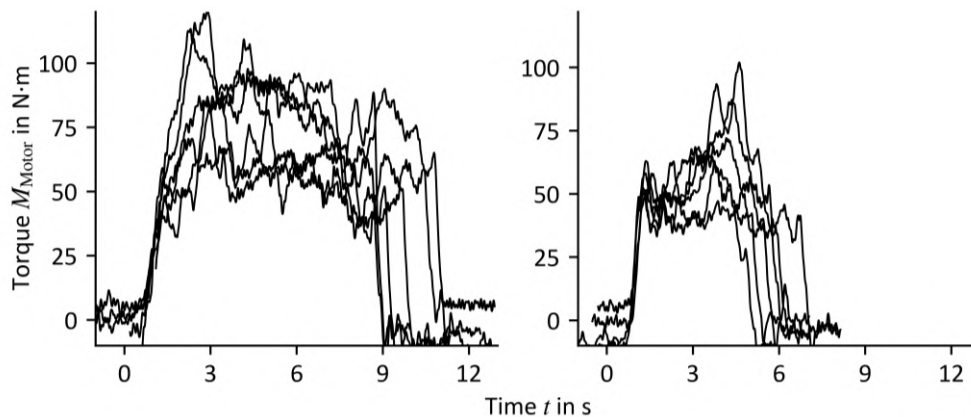


Fig. 11. Motor torque in respect to time during shaving. Process starting from the tail (left). Process starting from the neck (right).

The curves are post-synchronized in Fig. 11 to obtain a comparable representation. The mean value from the torque curve is determined for shaving on the tail side M_{Tail} and on the head side M_{Head} for the time range $t = 1.5$ s to $t = 4.5$ s for each curve. The torques as well as the maximum and minimum thickness t_{min} and t_{max} for the hides are documented in

Table 2.

Table 2. Thickness of cattle hides before shaving.

Hide	I	II	III	VI	V	VI
t_{Min} in mm	1.5	1.3	1.6	1.6	1.4	1.4
t_{Max} in mm	1.7	1.5	1.8	1.8	1.6	1.6
M_{Tail} in N · m	93.7	59.7	76.8	59.8	66.3	87.6
M_{Neck} in N · m	53.4	40.7	59.2	59.8	43.8	54.0

Although the initial thicknesses are relatively similar, a strong divergence of the measured values can be observed. This is due, among other things, to the different widths of the hides and the

general inhomogeneity of the natural material. The mean value of all torques is 62.9 N with a standard deviation of 16.0 N. No further statistical evaluation is carried out due to the small number of hides examined and the low variance of the setting parameters.

4 Discussion

Based on the results, it can be assumed that the length of the active cutting edge cannot be influenced to any relevant extent by variations in the machine settings. All investigated parameters, on the other hand, show a very strong influence on the thickness of the removed chip. MERCHANT already held that the mechanical work caused by forming accounts for a large proportion of the cutting work. On the other hand, the investigations by SREEJITH and CALZADA show that the fiber orientation is of great importance for the proportion of deformation work to cutting work. The material to be processed is markedly viscoelastic. With a constant chip thickness and a higher processing speed it is expected that a considerably higher deformation work is to be performed. This is in line with practical experience, according to which the rotational speed of the motors decreases more as the thickness of the leather to be shaved increases. The measurements of the torque when shaving cattle hides give a first indication of the forces to be expected during the shaving process. However, the number of tests must be increased considerably in order to be able to make reliable statements. In particular, the differences due to moisture and the tanning process must be investigated more extensively in order to provide a stable data basis for the simulation. Nevertheless, the created data are sufficient to serve as a reference for the comparison with first simulations.

5 Conclusions

The shaving of leather is comparable to the cutting of composite materials and therefore the findings in this field can serve as a basic principle for the onward development of the shaving process. The settings on the leather shaving machines plus the modification options of the cutting geometry provide the basis for an experimental investigation on the shaving process. The execution of designed tests combined with the developed geometric correlations will determine the most important parameters influencing the shaving process. Initial tests have been used to determine the essential values that will allow simulation results to be checked. An optimized geometry of the cutting tools has to be determined by using a computer simulation of the cutting process.

Acknowledgements

We gratefully acknowledge the German Federal Ministry for Economic Affairs and Energy for financial support within the Central Innovation Program for small and medium-sized enterprises (ZIM). We are grateful to Heusch GmbH for their participation in the project and to SÜDLEDER GmbH for their support in large-scale experiments. Stefan Gütling is acknowledged for the preparation of leather samples and the performance of shaving experiments.

References

1. Ward, A. G.: *The mechanical properties of leather*, *Rheologica Acta*, 12, pp. 103-112, 1974
2. Haines, B.M.: *Review. The Anatomy of Leather*, *Journal of Materials Science*, 10, pp. 528-538, 1975
3. Michel, A.: *Variations within hides and skins. Part 1: The Influence of the Fibre Structure*, *World Leather*, Nr. October/November, pp. 18-19, 2009
4. Basil-Jones, M. M.: *Collagen Fibril Orientation in Ovine and Bovine Leather Affects Strength: A Small Angle X-ray Scattering (SAXS) Study*, *Journal of Agricultural and Food Chemistry*, 59, pp. 9972-9979, 2011
5. Basil-Jones, M. M.: *Collagen Fibril Orientation and Tear Strength across Ovine Skins*, *Journal of Agricultural and Food Chemistry*, 61, pp. 12327-12332, 2013
6. Schuldt, S.: *High-speed cutting of foods: Cutting behavior and initial cutting forces*, 230, pp. 55-62, 2018
7. McCarthy, C. T.: *On the sharpness of straight edge blades in cutting soft solids: Part II—Analysis of blade geometry*, *Engineering Fracture Mechanics*, 77, pp. 437-451, 2010
8. Merchant, M.: *Mechanics of the metal cutting process. I. Orthogonal cutting and a type 2 chip*, *Journal of applied physics*, 16, pp. 267-275, 1945
8. Bowden, F.: *Friction, lubrication and wear: a survey of work during the last decade*, *British Journal of Applied Physics*, 12, p. 1521, 1966
9. Van Vliet, T.: *Large deformation and fracture behaviour of gels*, *Current Opinion in Colloid & Interface Science*, 1, pp. 740-745
10. Atkins, A. G.: *Fracture toughness and cutting*, *International Journal of Production Research*, 12, 263-274, 1974
11. Budak, E.: *Prediction of milling force coefficients from orthogonal cutting data*, *Journal of Manufacturing Science and Engineering*, 118, pp. 216-224, 1996
12. Moufki, A.: *Thermoviscoplastic modelling of oblique cutting: forces and chip flow predictions*, *International Journal of Mechanical Sciences*, 6, pp. 1205-1232, 2000
13. Li, S. J.: *Dynamic force modelling for a ball-end milling cutter based on the merchant oblique cutting theory*, *The International Journal of Advanced Manufacturing Technology*, 7, pp.477-483,2001
14. Moufki, A.: *Thermomechanical modelling of oblique cutting and experimental validation*, *International Journal of Machine Tools and Manufacture*, 9, pp.971-989, 2004
15. Koplev, A.: *The cutting process, chips, and cutting forces in machining CFRP*, *Composites*, 14, pp. 371-376, 1983
16. Dandekar, C. R.: *Modeling of machining of composite materials: A review*, *International Journal of Machine tools and manufacture*, 57, pp. 102-121, 2012
17. Che, D.: *Machining of carbon fiber reinforced plastics/polymers: a literature review*, *Journal of Manufacturing Science and Engineering*, 136, pp. 034001, 2014
18. Sreejith, P. S.: *Evaluation of PCD tool performance during machining of carbon/phenolic ablative composites*, *Journal of Materials Processing Technology*, 104, pp. 53-58, 2000
19. Calzada, K.: *Modeling and interpretation of fiber orientation-based failure mechanisms in machining of carbon fiber-reinforced polymer composites*, *Journal of Manufacturing Processes*, 14, pp. 141.149, 2012
20. Wan, M.: *Cutting force modelling in machining of fiber-reinforced polymer matrix composites (PMCs): a review*, *Composites Part A: Applied Science and Manufacturing*, 2018
21. Wang, H.: *Modeling and analysis of force prediction in milling process of unidirectional fiber reinforced polymer composites*, *The International Journal of Advanced Manufacturing Technology*, pp. 1-8, 2018
22. Shang, S.: *A bond-based peridynamic modeling of machining of unidirectional carbon fiber reinforced polymer material*, *The International Journal of Advanced Manufacturing Technology*, pp. 1-8, 2018
23. Bushlya, V.: *On the Analytical Representation of Chip Area and Tool Geometry when Oblique Turning with Round Tools. Part 1: Chip Area Parameters under Variation of Side and Back Rake Angle*, *Procedia CIRP*, 31, pp. 417-422, 2015
24. Landmann, W.: *The Machines in the Tannery*, Dewsbury: World Trades Publishing, 2003
25. Windiwisch, T.: *Energieeffiziente Antriebsregelung für hochausgenutzte Drehstrommotoren in elektrisch angetriebenen Fahrzeugen*, Shaker Verlag, 2018

COMPARATIVE STUDIES ON EFFECT OF CATIONIC AND ANIONIC FINISHING AGENTS ON SURFACE PROPERTY OF FINISHED LEATHER

M. W. Wajino¹, A. D. Dhathathreyan², S. V. K. V. Kanth³

1 Leather Industry development institute of Ethiopia, leather technology, Addis Ababa, Ethiopia

2 central leather research institute of India, CLRI, Chemical laboratory, Chennai, India

3 central leather research institute of India, CLRI, Centre for human resource development, Chennai, India

Abstract. The present work attempts to analyse the surface and physical properties of leathers finished with cationic and anionic finishing chemicals. The contact angles of liquid drops resting on the leather surface have been used to evaluate surface energy, acidity, basicity components of the surface energy, polarity and work of adhesion. Contact angle values have been measured for chrome tanned and conventionally re-tanned crust and finished leather made by varying pigment and binder combinations. The wettability of finished leather has been correlated with the contact angle values: the higher the contact angle value the lesser is the wetting observed. Complete wetting can be obtained when the contact angle value is zero i.e. the drop of liquid spreads spontaneously on the surface and partial wetting is obtained when the contact angle value is in between 0 and 90°. Acrylic binders with different film forming properties, protein, polyurethane and butadiene binders have been combined to prepare different finish formulations. The results have been correlated with wet and dry rub fastness, finish adhesion, vamp flexing value, water vapour permeability and water proofness. It has been observed that when the surface of leather is coated with acrylic binder the contact angle value due to polar solvents (water), non-polar solvents (hexadecane) and moderately polar (DMSO) and methyl iodide show that as the thickness of coating increases, the contact angle value decreases for the base coat and sharply increases when top coat is applied. Top coats have the ability to increase the contact angle and they improve the performance properties of leather such as water resistance, fastness, finish adhesion etc. Cationic and anionic finishing formulations have been compared to study their effect in modifying the surface of finished leather based on contact angle values, wet and dry fastness to circular rubbing and water resistance. It has been observed that leathers finished using anionic finishing technique shows better wet rub fastness and water resistance effect compared to cationic finishing technique.

1 Introduction

The object of finishing is to give a treatment of coatings to the grain surface to protect it against dirt, staining, wetting, mechanical stresses like rubbing, scuffing, flexing etc., levelling or evening out the colour of the grain surface, hiding grain blemishes and upgrading its quality, improving the aesthetic appeal and the sales value of the product. By the finishing process, the grain surface of the leather is coated with various substances and is then submitted to different mechanical operations, depending upon the purpose intended whereby the appearance of leather can be highly influenced to make it more useful, attractive and appealing to users. Finishing may be employed to impart colours, a uniform shade, special patterns, a smooth or grained or printed/embossed surface, lustre (Matt or glossy) as well as opaque (covered) or transparent (aniline/semi-aniline) appearance to the leather surface. Finishing operation is the most vital part of the processing of leather as the final product is judged by its appearance, evenness of colour and surface, feel, handle, break, gloss etc. Hence it is usually the finishers who have to face the complaints or blames, if anything goes wrong. They are also expected to correct whatever faults that have occurred during the earlier operations [1]. Finishing was once considered as an art and was kept a secret but today with the introduction and availability of a wide variety of leather finishing chemicals and mechanisation, finishing is no longer that secret. However, in spite of the innumerable finishing auxiliaries available and marketed by the firms providing details like general composition and properties of the products, mode of application with formulation for different types of finishing of leather, finishing is still dependent upon the finisher's ability of judging and blending of different auxiliaries to make his own combination to give the best finishing effect. Also, he keeps in mind the high qualities required from finishing, like

adhesion, flexibility, durability against weathering and aging, durability against dry and wet rubbing, resistant to peeling, cracking on flexing, light fastness, resistant to the various mechanical operations involved in finishing and permeability to water vapour thus ensuring the hygienic conditions.

The absorption of surface and anchorage and adhesion of finish film can be affected by the surface charge and presence of fatty substances. In the case of chrome tanned crust leathers, the final PH is around 3.5 and this means the surface has cationic residual charge. Most of finishes used in leather finishing are anionic in nature and too much of residual cationic charge may not allow the finish film to anchor well. This combined with the presence of fatty matter will result in poor adhesion of the finish film. The absorptive nature can be assessed by putting a drop of water on the surface and measuring the time taken for absorption. In case, the leather is absorbing less water that means the leather surface may have materials which are hydrophobic. In this case the water contact angle will be more so that the water molecules will form spherical beads rather than spreading on the surface. In which case, traditionally clearing coats are applied to improve the absorptive nature. Clearing coats contain a water miscible solvent like isopropyl alcohol or diacetone alcohol along with a mild alkali like ammonia. The solvent clears the surface fat and ammonia reduces the surface cationic charge on the surface. Sometimes the surface non- uniformity is reduced and made more level by using a dye solution along in which case the coat is called stain coat [2].

When a leather technician wants to make soft leather excessive anchorage is not required because it causes hardening of the surface of leather hence too much clearing coat is counterproductive. In such cases traditionally people use cationic oil ground to seal the surface of the leather so as to avoid excessive sinking of finishing chemicals. This is called sealing coat. In this case we are blocking the absorption of excess chemicals by incorporating the cationic charge on the surface of the leather. Care should be taken to avoid excessive use of the cationic oil ground. Usually 100-150 gram per liter is used to get the optimum effect. When the cationic oil ground is used in excess amount the season coat cannot be adhered properly to the surface of leather, in such case ammonia can be used to reduce the cationic charge. In conventional pigmented leather finishing technique, the natural look and feel of leather is usually lost because of heavy loading of pigments and binders which in turn affect the profitability of a given company. Even though the leather chemical industries are developing different finishing chemicals for up gradation of the surface defects and blemishes, the understanding of effect of each finishing chemicals and auxiliaries on surface and optical property of leather is still limited among leather technicians and researchers. A buyer's first consideration when faced with the leather is probably its feel. "Plastic" finishes with a cold, synthetic feel, or finishes which are too rigid and do not show good levelling and integration with the leather, should be avoided by means of suitable selection from the first phases of making the leather. Efforts to improve the situation on leather already finished are difficult and largely ineffective, even if the wide range of feel modifiers can help.

In this work, the overall objective has been to understand the surface energy parameters of different finishing of leather and relate these properties to the quality of finishing. Further, the work has attempted to optimize the quantity, nature and the combination of different finishing chemicals to obtain optimal finishing properties for different types of leathers.

Thus to quantify the amount of finishing chemicals especially binders and pigment in finishing of shoe upper leather goat crust having similar grain quality were selected and finished by varying the concentration of different binders. Contact angle values were measured for leathers finished with different finish formulations. From contact angle value polar and non-polar component of surface energy, the degree of wetting, work of adhesion were calculated. In addition to this, effects of other finishing chemicals and top coats on the surface and physical properties were also determined. The amount of surface coating applied to the leather influences whether or not the item can be described as genuine leather. If the leather has a surface coating, the mean thickness of this surface layer, however applied, has to be 0.15mm or less, and does not exceed 30% of the total thickness of the leather. The results of this study are especially helpful to develop finishing technology for special type of leathers like water resistance, self-care, light weight and high water vapour permeability and etc.

2 Materials And Methods

The required materials and methods to study the effect of different binder and pigment in surface properties of finished leather were described. The chapter proceeds with the description of characteristics of different commercially available finishing chemicals used for the study. Several finish formulations were prepared to study the surface property of finished leather by varying binders and pigments alternatively and keeping other auxiliaries constant. Contact angle value for different solvents such as water, methyl iodide, DMSO and hexadecane were determined for the respective finish formulations by the help of optical microscope having digital camera mounted perpendicular to the test sample where the drop of solvents going to be applied. The detail procedure for preparation of sample in order to determine contact angle, and the design of the whole experiments were described. The experiments were also conducted to study the advantage and disadvantage of anionic and cationic finishing technique, the effect of pigment to binder ratio on the surface and physical properties of finished leather, film forming properties of different binders, effect of commonly used top coats on the surface of the leather and etc. In addition to this the procedure and methodology to conduct the entire physical tests were also explained.

2.1 Materials

Wet blue leather from goat skin and cow hides were made to be ready for post tanning operation by using conventional post tanning process techniques in order to produce dyed crust leather for finishing process. The leathers which have similar grades were selected for experimental work.

Different finishing chemicals, which are described in the Table 1 and laboratory equipments and instruments (universal testing machine, contact angle measuring instrument, vamp flexing machine, water proofness machine, rub fastness testing machine, water vapour permeability tester, optical microscope, Lastometer, oven, glass wares and glass plates (for film formation) were used.

Table 1. The nature of finishing chemicals used in the experiment.

s/no	Chemical name	Nature	Remarks
1	B1 27047	Medium soft aqueous waxy protein binder	
2	B1 507	Soft protein binder	
3	BM 388-FO	Beauty maker	
4	LW 65416	Clear CAB lacquer water born, hard	
5	HM 51760	Handel modifier, aqueous modified silicon emulsion	
6	HM 51251	Water dilutable silicon emulsion	
7	RA 1216	Very hard acrylic binder	Tg = 53°C
8	B1 27154	Aqueous protein binder	
9	LS 65258	Clear NC lacquer solvent borne	
10	RA 17	Very soft acrylic binder	
11	RA 2354	Medium soft acrylic binder	Tg = -29°C
12	RA 27006	soft acrylic binder	

13	FI 50	Filler wax	
14	PP25824	pigment, brown	
15	PP25884	Pigment, red	
16	WT2586/13886	Water based pu top coat	
17	B1 1370	Aqueous protein binder	
18	XR79053	Water dilutable imine ester crosslinking agent	
19	HM183	Hand modifier, water dilutable silicon emulsion	
20	WT25853/13892	Dull waterborne aliphatic PU dispersion for producing high performance finishes	
21	WT13400	Clear high gloss waterborne acrylic copolymer emulsion	
22	WR 22409	Water repellent, modified polyfluorocarbon emulsion	
23	Lepton aqua top TG	Water based top coat	

2.2 Methods

The methods used to reach at each specific objectives of this study are described in the following sub-titles.

2.2.1 Crust preparation

Thirty pieces of goat wet blue having similar size and grades were purchased from the market. The materials were sammed to remove the excess moisture content and to flatten the surface for subsequent mechanical and chemical operations. Since the materials were designed for production of dyed crust for shoe upper leather, it was shaved with a thickness of 1-1.2mm with strict control to maintain thickness uniformity. After thickness was adjusted, the re-tanning fat-liquoring and dyeing were conducted by conventional post tanning process for shoe upper production.

2.2.2 Finished upper leather preparation

Different finish formulations were prepared by varying concentration and type of pigment and binders alternatively fixing other ingredients constant. Types of Acrylic binders like very soft, soft and medium soft and polyurethane binders have been employed for a given pigment by varying binder concentration. In addition to this different formulation were prepared by using PU binders with or without cross linkers and using some performance chemicals. Finish formulation by using cationic chemicals were also prepared. The formulations were sprayed by using hand spraying machine on crust leather maximum of three coats. As described in the tables below, all the formulations were prepared at the same time and equal volume of the season was sprayed on crust leather having the same area. In all cases three coats were applied in between each coats, the leathers were allowed to be dried to avoid the quality inconsistency.

For anionic finishing technique, different commercially available acrylic resin binders, different PU top coats and cationic finishing chemicals were selected from stahl chemical company for whole experiments and one litre finish formulation were prepared at different p/b ratios by using each a single binder as well as combining the three binders at different p/b ratios. The three resin binders were chosen for experimental work based on their 'Tg' values and universal applicability.

Table 2. Finish formulation by using combination of acrylic binders.

Types of chemicals	Finish formulations (gm)					
	F19	F20	F21	F22	F23	F24
Pigment	100	100	100	100	100	100
Vs- resin binder	25	25	25	50	50	50
S- resin binder	25	25	25	50	50	50
Ms- resin binder	50	75	100	150	200	250
Filler Wax	30	30	30	30	30	30
Protein	30	30	30	30	30	30
Water	740	615	660	640	590	540
Total	1000	1000	1000	1000	1000	1000

Note :VS- very soft, S- soft, MS- medium soft

Table 3. Cationic finish formulations.

Chemicals	Finish formulations(quantity in grams)							
	Cat-1a		Cat-1b		Cat-2a		Cat-2b	
	SC	TC	SC	TC	SC	TC	SC	TC
PP 17732	25	-	25	-	50	-	50	-
BI17737	100	-	100	-	100	-	100	-
RU 17702	50	-	50	-	50	-	50	-
FI 1292	25	-	25	-	-	-	-	-
FI 17701	25	-	25	-	75	-	75	-
LW65377	-	100	-	-	-	100	-	-
FI 77055	-	-	-	-	50	-	50	-
MA 27108	-	-	-	100	-	-	-	100
Water	500	100	500	100	650	100	650	100

2.3 Finish film formation

Finish films were formed by combining soft and hard acrylic binders with and without protein binder, filler wax and pigments and the tensile strength were measured.

Finish films were formed by using the appropriate substrate for casting the formulations described in Table 3. In this experiment glass plates having 25*15cm dimension were prepared and the calculated amount of formulations were poured on the required area and allowed to dry at 60°C. After the

film were dried the film forming nature of acrylic and protein binders were studied. The dried films were used to determine, young's modulus, elongation, tensile strength and contact angle.

2.3.1 Finish film tensile strength determination

Glass plates having dimensions 25cm by 15cm have prepared and different binder combinations with known volume were poured uniformly and film forming nature of different binders and binder combinations were studied. The samples have allowed drying at room temperature for tensile strength measurement. After the films have dried the samples were prepared by cutting with 10mm width in the direction along the glass plate and across the glass plate. The thickness of the film sample is measured at five different points and the average value has taken for calculation. The tensile strength and percentage elongation have been tested by using Instron universal testing machine by setting the clip pressure of 3 bars and testing speed of 100mm/min for all samples.

$$\text{tensile strength} = \text{load}/\text{area where, Area} = \text{width} \times \text{thickness}$$

2.4 Adhesion of finish test /SATRA TM 411 sole bond test

This test is intended to determine the strength of finish adhesion to the leather surface. Force required pulling the leather away from its surface finish layer, the force being applied steadily at an angle of about 90° to a rigid adherent plate to which the finished side of the leather has been bonded. The finished side of a strip of leather is bonded to a PVC plate by means of heat activated adhesive film. Force was applied to the free end of the strip to peel the leather from the finish over a distance and measured by using universal testing machine.

2.5 Flexing endurance of finished leathers: SATRA 25:1992/BALLY TM 55

Flexing endurance is one of the wear properties of leather. If leather surface coating (finish) is not properly applied with correct proportions and following all technical procedures, the finish surface upon bending repeatedly develops cracks, flaking, brittle and delamination.

For all the finish formulations prepared by varying the concentration and type of resin binder, both wet and dry flexing endurance test were conducted. The tests were performed by the machine called vamp flexing machine. In performing the test first the test specimens were folded along the longer sides so that the finish side facing inward and one end of the folded specimen were clamped in upper clamp and the other end was clamped on lower clamp. The tests were conducted based on the above standard. For dry flexing test, the test specimens were flexed for 10,000 and 500,000 flexes and the finish damage were observed by magnifying glass and the type of damage were recorded. For wet flexing endurance test, first the test specimen was gently immersed in to water for approximately 30 seconds prior to clamping it on to the machine. The test specimen was clamped on to the machine in similar way to that of dry flexing but the number of flexing was adjusted for 10000 and 100000 flexes based on the above standard and the finish damage observed were assessed experienced expert with help of magnifying glass and the type of damage were recorded.

2.6 Color fastness to circular rubbing - SATRA TM 8:1992

2.6.1 Dry Rub Test

The test specimen was cut about 75mm square from the finished leather. And the specimen was placed on the horizontal platform and a felt pad was secured on the spindle and brought in contact with the test specimen. The weight was adjusted to 24.5±0.5N and the machine was operated for 512 revolutions. After the required revolutions were completed, the leather and the felt pad were removed from the machine. To assess the colour change and transfer of colour (degree of staining)

standard grey scales were used. The number of cycles and the colour change and colour transfer depend up on the type of leather and customer's requirement.

2.6.2 Wet Rub Test

Clean white felt pad was immersed in cold water and boiled until all the felts are completely wetted. After complete wetting, the felts were allowed to be cooled. The felts were removed one by one and excess water was slightly squeezed out prior to attaching it to spindle. The loads were adjusted to 7.1N forces. The spindle was brought into contact with leather specimen for 60 seconds and the machine was allowed to operate for 256 cycles and the colour change and colour transfer from test piece to felt pad was assessed based on the grey scale.

2.7 Water vapour permeability – ISO 14268/IUP15/EN 20344

Water vapour permeability is the unique property of leather. Under normal conditions about 5 grams/hour sweat is produced by a human when the atmospheric condition is between 30-35°C. Under industrial working condition, the sweat produced by a human foot is around 10 gram/hour. This sweat has to be sent out to the outside of the shoe for comfort wear. Leather footwear has the ability to absorb the sweat produced and transmit to the upper part of the leather through wicking process. Once it reaches the upper surface, the sweat evaporates into atmosphere. This process is known as Water vapour permeability or water vapour transmission. This is possible by the porosity characteristic of leather. Filling, finishing and fat liquoring processes in leather making reduces this water vapour transmission property to a greater extent.

Based on the above standards

Water vapour permeability (wvp), mg/cm²/hr is equal to:

$$Wvp = \frac{7.640XW}{d \times dt}$$

Where, w is the mass difference in mg W= w1-w0

- W0 is initial mass of the leather and the dried silica jells.
- W1 is the final masses after the moisture from the leather is transmitted to silica jell within 8 hrs.
- d is the diameter of the leather sample in mm
- t is the time in taken for moisture transmission form water to silica jell

2.8 Determination of water resistant property, SATRA/ STM 606D

A test piece were formed into the shape of a trough and flexed whilst partially immersed in water. The time taken for water to penetrate through the test piece is measured. The method also allows the percentage mass of water absorbed and the mass of water transmitted through the test piece to be determined. In addition to this the time taken for penetration of water through the cross-section was determined. In this experiment percentage water absorption and the time taken for water to penetrate to the cross-section were determined for shoe upper leather finished with different PU based binder combinations and cationic binders.

2.9 Determination of contact angle

Contact angle is very important technique to understand wettability of polymeric surface up on different polar solvents and non polar solvents. Three solvents are usually used for contact angle measurements

which are water (highly polar), DMSO (moderately polar) and hexadecane (non polar).The contact angle values will vary based on the type of coating when a drop of these solvents are applied on the surface of finished leather by using micropipette, the drop position were adjusted, and the contact angle picture were taken by using the camera which is mounted on the microscope. For all the contact angle measurement, the following instruments were used.



Figure 1. Contact angle instrument.

2.9.1 Contact angle for the crust leather

The crust sample was cut into appropriate rectangular shape with size similar to microscopic slide with dimension of 3cm by 1cm. The contact angle for the dyed crust leather was measured with the help of contact angle measuring instrument described in Fig. 1. By using three different solvents highly polar (water), medium polar (methyl iodide) and completely non-polar (hexadecane) contact angle value were measured and recorded

2.9.2 Determination of contact angle for binders

Different binders were coated on microscopic slid and allowed to dry completely in the desiccators. After the coating has dried, the contact angle was determined by the help of the instrument described above similarly three different solvents were used i.e. water, hexadecane and methyl iodide and the values were recorded.

2.9.3 Determination of contact angle for finish formulations

Different finish formulations were prepared and applied on crust leather by using hand spray technique and the samples have prepared similarly and the contact angle have been determined similarly with the above solvents and the values have noted.

2.10 Surface energy calculation

By using young’s equation, the surface energy of any solids can be calculated from the contact angle value.

Surface energy of chrome crust leather can be calculated as follows

$$\gamma_{lv}(1 + \cos\theta) = 2 [\gamma_{sv}^d \gamma_{lv}^d + \gamma_{sv}^p \gamma_{lv}^p] \text{-----(1)}$$

Where θ = contact angle γ_{fp} =liquid- vapour surface energy

γ_{sv}^d =solid- vapour interfacial energy of non polar component γ_{lv}^d =liquid- vapour interfacial tension of non polar solvent γ_{sv}^p =solid- vapour interfacial energy of polar component γ_{lv}^p =Liquid- vapour interfacial energy of polar component

In this experiment, two liquids were used to calculate the polar and non-polar component of surface energy, water and hexadecane respectively.

In order to calculate Non polar component of surface energy, the polar component in equation [1] will vanished and the equation will be reduced to the form:

$$\gamma_{lv}(1 + \cos\theta) = 2 \gamma_{sv}^d \gamma_{lv}^d \quad (2)$$

By rearranging terms, the non polar component of surface energy, γ_{sv}^d can be expressed as

$$\gamma_{sv}^d = \frac{H \cos\theta}{2 \gamma_{lv}^d} \quad (3)$$

Where, θ is contact angle For hexadecane, $\gamma_{lv} = 27.47 \text{ mN/m}$ Hence, equation [3] reduced to

$$\gamma_{sv}^d = \frac{H \cos\theta}{2 \gamma_{lv}^d} \quad (4)$$

By combining equations [3] and [4], the polar component of surface energy, γ_{sv}^p can be calculated as follows:

$$\gamma_{sv}^p = \frac{[\gamma_{lv}(1 + \cos\theta) - \gamma_{sv}^d \gamma_{lv}^d]^2}{2 \gamma_{lv}^d} \quad (5)$$

Where, θ = contact angle

γ_{lv} = total surface tension of liquid

γ_{lv}^d = non polar component of surface tension Value for a given liquid γ_{lv}^p = polar component of surface tension for a given liquid

For water, the total, polar and non-polar surface tension values are given in literature these are:

$$\gamma_{lv} = 72.8 \text{ mN/m} \quad \gamma_{lv}^d = 21.8 \text{ mN/m} \quad \gamma_{lv}^p = 51 \text{ mN/m}$$

By substituting the above surface tension values for water and non-polar component of surface energy value, γ_{sv}^d obtained by using equation [4], the polar component of surface energy for the given solid material i.e. leather can be calculated and equation [5] can be reduced to:

$$\gamma_{sv}^p = \frac{72.8(1 + \cos\theta) - 21.8 \gamma_{sv}^d}{2} \quad (6)$$

Here, $\cos\theta$ value will vary based on the water contact angle, θ and γ_{sv}^d depend on the hexadecane contact angle value, θ

Therefore it is possible to calculate the polar and non-polar component of surface energy values by using equation [6] and [4] respectively.

And the total surface energy, γ_{sv} will be the sum of polar and non-polar components, i.e.

$$\gamma_{sv} = \gamma_{sv}^d + \gamma_{sv}^p \quad (7)$$

Van Oss- Chaudhury- Good (OCG) thermodynamic approach can also be used to determine the surface free energy components of solids.

A similar comparison can be made by considering the Van Oss, Chaudhury and Good (OCG) model [13] in which the solid/liquid work of adhesion is expressed as a sum of three terms:

In these approach, the polar component of surface energy, γ_{sv}^p is expressed in the form of two components i.e. Lewis acid and Lewis base (γ_{s+} and γ_{s-}) parameters respectively. To calculate these values in these experiments, three liquids such as water, hexadecane and di-methyl sulfoxide (DMSO) were used.

$$\gamma_{sv}^p(1 + \cos\theta) = 2 \gamma_{sv}^{LW} \gamma_{sv}^{LW} + 2 \gamma_{s+} \gamma_{sv}^p + 2 \gamma_{s-} \gamma_{sv}^p \quad (8)$$

Where θ = contact angle γ_{sv} = liquid- vapour surface energy

γ_{sv}^{LW} = the Lifshitz-van der Waals (non-polar) component of the surface free energy γ_{s+} and γ_{s-} = the Lewis acid parameter and the Lewis base parameter, respectively.

From the contact angles of at least three liquids of known surface tension parameters ($\gamma_{lv}, \gamma_{sv}^{LW}, \gamma_{sv}^d, \gamma_{lv}^d$ and γ_{lv}^p) equation (8) can be used to determine the van Oss, Chaudhury and Good parameters for the surface free energy of the solid.

Thus, by considering three polar liquids, it is theoretically possible to determine the Lifshitz-Van Der Waals (non-polar) component, γ_s^{LW} of the surface free energy of polymers. This result can be compared to the value obtained with the equation (2)

$$\gamma_L(1 + \cos\theta) = 2\gamma_s^{LW}\gamma_L^{LW} \quad (9)$$

Equation 2) can be used for determination of non-polar component of surface energy by using the contact angle of non-polar liquids such as hexadecane, di-iodomethane, a-bromonaphthalene and etc. In this paper contact angle and surface tension values of water and DMSO were used as polar liquids. By using these values it is possible to determine the Lewis acid and Lewis base parameters of surface energy of the given liquid this in turn help to know the charge characteristics of the surface of the given finished leather [13].and it can be expressed as a square root of geometric mean of the Lewis acid(γ_s^+ and Lewis base (γ_s^-) parameters [1]. Mathematically:

$$\gamma_s^p = 2\sqrt{\gamma_s^+\gamma_s^-} \quad (10)$$

3 Results And Discussion

3.1 Contact angle and surface energy value for dyed crust and different finish formulations.

The crust sample was cut into appropriate rectangular shape with size similar to microscopic slide i.e. 3cm by 1cm. The contact angle for the dyed crust was measured with the help of contact angle measuring instrument which is microscope where digital camera is mounted on it to take the droplet pictures on the test specimen. Three different solvents highly polar (water), less polar (methyl iodide) and completely non-polar (hexadecane) have chosen and the values were described as follows:

Table 4. Contact angle values for crust leather for shoe upper (black)

Sample no.	Contact angle values			Remarks
	WCA	MICA	HDCA	
B1	69.01	ND	ND	In each cases one drop of the solvents (approximately 5µl) were applied
B2	80.69	ND	ND	
B3	80.66	ND	ND	
B4	66.02	ND	ND	
B5	85.61	ND	ND	
B6	73.47	ND	ND	
B7	78.12	ND	ND	
B8	83.59	ND	ND	
B9	62.43	ND	ND	
Average	75.51	-	-	

ND=not detectable

From table II one can conclude that the surface contact angle with less polar solvent (methyl-iodide) and non polar solvent (hexadecane) for the crust leather is negligible i.e. the drop of the liquid was spontaneously dispersed on the surface of the leather this might be due to the imbalance between

the solid - liquid interfacial energy and the cohesive force of the molecules of the solvents. But in the case of water the contact angle is approximately more than 75° which is indication of hydrophobic nature of the given leather. The cohesive force which is due to the interaction of the molecules of water/surface tension of water is more than the solid- liquid (leather surface/water) interaction. Therefore the molecule of water tends to form droplets rather than spontaneously spreading as it was observed in the case of methyl iodide and hexadecane. The higher value of the contact angle indicates the slower wettability of the surface by respective liquids in contact with the surface.

By using equation [1], it is possible to determine the surface energy of crust leather and finished leather finished with different finish formulations as follows. As it has described in table-II above, the average value of contact angle for the crust leather is 75.51 in degrees. By using equation [1], it is possible to calculate polar and non polar components of surface energy and hence total surface energy. For the surface energy calculation, contact angle for water and hexadecane were used.

3.2 Surface energy calculation for two liquid systems

Consider the contact angle for hexadecane to be zero and for water to be 75.51°

$$\theta \text{ of water} = 75.51^\circ$$

$$\theta \text{ of hexadecane} = 0^\circ$$

$$\gamma_{lv} \text{ for water} = 72.8 \text{ mN/m}$$

$$\gamma_{lv} \text{ for hexadecane} = 27.47 \text{ mN/m}$$

It is possible to calculate the total surface energy by using equation (3.1) as follows:

$$\gamma_{lv}(1 + \cos\theta) = 2 [\gamma_{sv}^d \gamma_{lv}^d + \gamma_{sv}^p \gamma_{lv}^p]$$

In the case of hexadecane, the polar component will be vanished because it is highly nonpolar substance, therefore; The above equation becomes:

$$\gamma_{lv}(1 + \cos\theta) = 2 [\gamma_{sv}^d \gamma_{lv}^d]$$

$$27.47 \text{ mN/m} (1 + \cos 0) = 2 [\gamma_{sv}^d * 27.47 \text{ mN/m}] \text{ By rearranging the values}$$

$$\gamma_{sv}^d = 27.47 \text{ mN/m}$$

In similar way, the polar component of surface energy (γ_{sv}^p) can be calculated, by considering the contact angle value of water and its polar and non polar component of surface tension values as follows:

$$\gamma_{lv}(1 + \cos\theta) = 2 [\gamma_{sv}^d \gamma_{lv}^d + \gamma_{sv}^p \gamma_{lv}^p]$$

By substituting the values

$$72.8 \text{ mN/m} (1 + \cos 75.51^\circ) = 2 [\gamma_{sv}^d * 27.47 \text{ mN/m} + \gamma_{sv}^p * 51 \text{ mN/m}]$$

By rearranging terms, the polar component of surface energy will be:

$$\gamma_{sv}^p = 8.53 \text{ mN/m}$$

From the polar (γ_{sv}^p) and non polar (γ_{sv}^d) component of surface energy values one can see that there is inverse relationship between surface energy and contact angle i.e. the higher contact angle the smaller the surface energy and vice versa.

The total surface energy of the solid material (crust leather) is the sum of polar and non polar components.

$$\gamma_{sv} = \gamma_{sv}^p + \gamma_{sv}^d = 8.53 \text{ mN/m} + 27.47 \text{ mN/m} = 36 \text{ mN/m}$$

The above surface energy value is the specific for the particular crust leather taken for the control. The magnitude will vary based on the type of re-tanning and fat-liquoring chemicals used. Any surface treatments like coating and different mechanical operations have significant influence on the surface energy.



Figure 2. Water contact angle values on crust leather.

Effect of different leather finishing chemicals like binders, pigments, fillers, waxes, top coats and feel modifiers have significant influence on the magnitude of surface energy values. It has been observed that the surface energy parameter value was reduced by finishing the given crust leather by the help of different pigments and binder combinations and other leather finishing ingredients. By using the contact angle value of hexadecane and water with the finished leather the surface energy for each binder pigment combinations applied on the surface of leather, individual binders coated and dried on the microscopic slide and different finish films have been calculated.

Table 5. Effect of cationic oil ground on contact angle value.

Specimen	Type of solvents			surface energy		
	0 of Water	0 of methyl iodide	0 of Hexadecane	<i>ySpd</i>	<i>ySpP</i>	<i>ysv</i>
1	98.51	46.95	63.15	14.48	3.46	17.94
2	98.48	55.43	63.16	14.48	3.47	17.95
3	104.48	55.69	70.62	12.19	2.38	14.58
Average	100.51	52.69	65.64	3.71	3.06	16.75

From Table 5 it is evident that the contact angle value is increased because of the oil ground used at the very beginning of the finishing operation. This hinders the excessive sinking of finishing season whenever the absorptive nature of leather is very high this in turn reduces the wettability of the surface. This technique is applicable whenever there is excessive sinking of finishing chemicals if the crust leather is too absorptive which can affect the natural look of the leather to be finished. The amount of oil ground used has to be optimum i.e. 100-150gram per 1000ml of Sealing coat mixture. If it is beyond this range there might be poor adhesion of the season since the water contact angle will be much far from 90°. Therefore the finishing technician has to control excessive use of oil ground.

Table 6. Determination of water resistance of flexible leather.

S.No	Formulation name Water resistance of flexible leather	% Water absorption	Penetration time(min)
1	PUT1A	64.4	13.7
2	PUT2A	42.3	54.3
3	PUT3A	91.7	3.5
4	PUT4A	87.7	4.6
5	PUT5A	69.0	53.4

6	PUT6A	61.2	4.4
7	PUT1	111.1	24.5
8	PUT2	87.7	23.0
9	PUT3	116.1	15.7
10	PUT4	100.7	10.1
11	PUT5	81.4	23.2
12	PUT6	95.0	9.4
13	Cat-1a	129.2	1.2
14	Cat-2a	128.9	0.4
15	Cat-1b	158.5	0
16	Cat-2b	109.0	0.4
17	ccat	161.6	0

Note: ccat is control dyed crust

From the table one can deduce that percentage water absorption is more in the case of cationic finishing technique. In addition to this water was penetrated immediately to the cross section of the leather finished with formulations cat-1a, cat-2a cat-3a and cat-4a and hence the water resistance effect is poor. As it has explained in determination of contact angle value, the value is lower as compared with all other anionic finishing techniques. Almost no difference in percentage water absorption was observed as compared with the control crust. From this result one can conclude that cationic finishing technique is not suitable to improve the water resistance effect and other performance properties but the main advantage of cationic finishing is to get good covering effect without affecting the natural look, flexibility and softness.

3.3 Rub fastness result for cationic finish

Poor colour fastness to circular rubbing was observed in the table below in the case of cationic finishing this is because of the cationic nature of chrome tanned crust. Since the charge of the substrate/crust and the charge of cationic finishing chemicals have similar nature, the chemicals are loosely bound to the surface of the leather.

Table 7. Rub fastness result for leather finished with cationic finishing technique.

Specimen	Formulation name	Colour fastness to circular rubbing	
		Dry at 512 cycles Felt pad	Wet at 256 cycles Felt pad
1	Cat-1a	3	1
2	Cat-2a	3	1/2
3	Cat-1b	3	1/2
4	Cat-2b	3	1

4 Conclusion

Contact angle was used as a parameter to study the effect of each finish formulations on the surface property of the leather. Water, methyl iodide, hexadecane and DMSO were used to measure the liquid-solid contact angle. The experimental result from contact angle value showed that coating with pigments and binders have increased the contact angle value compared to the control crust. And the corresponding value of surface energy were calculated by using Thomas young equation and the results showed that there is decrease in surface energy when the contact angle increases. It was observed that when the contact angle increases the degree of adhesion and the wettability of the surface of the leather were decreased. In addition to this the effect of top coats and other finishing auxiliaries other than pigments and binders on contact angle value were investigated. Fillers have the ability to increase the contact angle. CAB top coated leather showed more contact angle than PU and acrylic top coats. This value clearly showed that wettability is more in the case of PU and acrylic top coated leathers than CAB top coated leathers.

The effect of number of top coats on water contact angle value were determined ,and the experiment showed that the value were decreased gradually at the beginning of the coat because the top coats are water based so during the coating process the hydrophobic nature of the surface of chrome tanned leather have decreased. And finally the contact angle value were increased and the corresponding surface energy were reduced when CAB top coat were sprayed. In general when the coating chemicals have more polar groups the contact angle values were observed to be increased.

Physical tests like rub fastness, finish adhesion, water vapour permeability and flexing endurance were conducted for leather samples finished with different acrylic binder pigment combination, cationic finish formulations and PU binders with and without incorporation of performance chemicals. The physical test results showed that pigment binder ratio and the property of the given binder have significantly affected the above mentioned physical test parameters. In the case of acrylic binder-pigment combination better result were obtained when we use combination of soft, medium soft and very soft binders at 1 to 3 p/b ratios but very soft binder has to be used in smaller proportion to minimize the tackiness effect. And better wet rub fastness and water resistance effects were observed in the case of acrylic resin finish and PU based finishing technique compared to cationic finishing technique.

Film forming property of different acrylic binders and protein binders were studied and the result showed that soft, medium soft and very soft acrylic binders form flexible, softer films and hard acrylic binders do not form film at room temperature whereas protein binders form discontinuous and brittle film.

The wettability of the surface of leather has to be good before applying the top coat otherwise the top coat cannot adhere to the surface of the leather whenever such hard binder is used at the base coat in larger proportion. Resin binders having lower water contact angle are ideal for base coat since they can easily spread on the surface of the leather this in turn facilitates degree of adhesion.

Compared to anionic finishing, cationic finishing chemicals are shows less contact angle with water and hence more wettable and poor fastness properties. Improving the performance properties such as fastness, water absorption and etc. of cationic finishing technique is open for further research and development.

5 Acknowledgements

My praise goes to the lord Jesus Christ for the strength He bestows on me throughout the development of this thesis work.

- My special thanks go to my advisors Dr. Aruna Dhathathreyan (Chief Scientist, CSIR-CLRI, India) and Dr. Swarna V. Kanth (Principal Scientist, CSIR-CLRI, India) for rendering their invaluable supervision, support and guidance for the accomplishment of this work.
- My appreciation and gratitude also goes to Dr. N.K. Chandrababu, (Chief Scientist, CSIR-CLRI, India) for his technical support at the very beginning of my thesis work.
- I am also very grateful to Dr. B. Madhan (Principal Scientist, CSIR-CLRI, and India) for his advice during the experimental work.
- I would like to express my special thanks to Ms. D. Madhumitha, Research Assistant at CSIR-CLRI, and Mr. Maheshkumar Jaganathan research scholar, Biophysics lab for their help in measuring contact angle.
- I am also glad to thank my beloved sisters Aberesh Wakaso and Amerech Teketel for their encouragement until the accomplishment of this thesis work.
- Finally, I would like to thank Ato Wondu Legesse, Director General of LIDI and management staff for giving this chance to me in order to pursue my study.

References

1. S.S.DUTTA *In introduction to the principle of leather manufacture (Fourth edition)*,
2. N.K.Dr. Chandrababu. *Manual on principle of leather finishing (unpublished)*, CLRI, India
3. *Synthetic Resins & Leather Finish*. www.aagt.org.ar/congresos/china2009/download/2-4/2-152.pdf
4. J.H Sharpouse, *Leather Technician's Hand book*.
5. S.V.Kanth, , B.Madhan, R.Venba and A.Dhathathreyan. *Effect of different re-tanning systems on surface properties of leather*. JALCA, VOL, 102, 2007.
6. D.Y. Kwok, A.W. Neumann, *Contact angle measurement and contact angle interpretation*, *Advances in Colloid and Interface Science*81 (1999) 167-249.
7. *Journal of achievements in materials and manufacturing engineering. Methods for calculation of surface free energy of solids*.Vol.24, Sep. 2007
8. K. B. GilleoSheldahl, Inc. *Rheology and Surface Chemistry*
9. Van OSS, C.J. and R.F. Giese, *colloid and surface properties of clay materials and related minerals*. New York, 2002. Marcel Dekker.
10. Norris, J.G. *surface free energy of smectite clay materials*, in SUNY, 1993: Buffalo
11. P. F. Rios 1, H. Dodiuk1, S. Kenig1, S. Mccarthy2 and A. Dotan1.*The effect of polymer surface on the wetting and adhesion of liquid systems*. Vol. 21, No. 3-4, pp.227 - 241 (2007)
12. A. W. Adamson, *Physical Chemistry of Surfaces*, 5th edn. Wiley, New York, NY (1990).
13. ALAIN CARRE, *Polar interactions at liquid/polymer interfaces*, *J. Adhesion Sci. Technology.*, Vol. 21, No. 10, pp. 961-981 (2007)
14. Henry Fleming Payne, "Organic Coating Technology", Vol. 1, John Wiley & Sons, Inc., USA, 1954
15. *Colour quantification based on CIE guideline*, European association of flat glass manufacturers, January 2005.
16. Kryszt of Bienkiewicz, "Physical Chemistry of Leather Making", Robert E. Krieger Publishing Company, Florida, 1983.
17. Kinloch, A.J., "Adhesion and Adhesives - Science and Technology", Chapman and Hall, 1987
18. Heidemann, E., "Fundamentals of Leather Manufacture", Edward Roether Ed., Darmstadt
19. Sthal chemical company, *Leather International.*, Cationic finishing technology: October 2002.
20. Saimani Sundara, NarasimanVijayalakshmia, Sanjeev Gupta b, R. Rajaramc, Ganga Radhakrishnan. *Aqueous dispersions of polyurethane-polyvinyl pyridine cationomers and their application as binder in base coat for leather finishing*. *Progress in Organic Coatings*. Vol.56, page 178-184, July.2006.

A NOVEL PRESERVATION-CUM-UNHAIRING PROCESS FOR SUSTAINABLE LEATHER MANUFACTURING: AN UNCONVENTIONAL APPROACH IN LEATHER MAKING

J. Raghava Rao^{1a}, M. Sathish^{2a}, R. Aravindhan^{2b} and P. Thanikaivelan^{2c}

1a) Corresponding author: jrrao@clri.res.in, Inorganic and Physical Chemistry Laboratory, CSIR-CLRI, Chennai, India

2a) Co-author: leathersathish@gmail.com, Leather Process Technology Division, CSIR-CLRI, Chennai, India

2b) Co-author: aravindhan78@gmail.com, Leather Process Technology Division, CSIR-CLRI, Chennai, India

2c) Co-author: thanik8@gmail.com, Advanced Material Laboratory, CSIR-CLRI, Chennai, India

Abstract. Preservation (or) curing is an important unit process for transportation and storage of raw hides/skins without any deterioration. Popular preservation process is mostly achieved by reducing the moisture content of hides/skins using common salt (NaCl). Usage of salt in preservation process leads to generation of large amount of contaminated salt, total dissolved solids (TDS) and consume huge amount of water for subsequent rehydration step. On the other hand, lime-sodium sulphide based reductive process is commonly employed for the removal of hair from hides/skins. This process leads to generation of lime sludge and possible evolution of toxic hydrogen sulphide gas thereby making the working atmosphere more unpleasant. Several alternative techniques for preservation as well as unhairing process have been developed individually to replace salt and sulfide, respectively. However, a single compound performing dual functions such as preservation and unhairing action in neutral pH conditions has not explored so far. In the present work, a novel formulation has been developed, which possess the both preservation and unhairing potential, and applied on the hides/skins for storage up to 6 months at ambient conditions without dehydration. Low level of sulphide was used during alkaline fiber opening for removal of traces of hair. The strength and organoleptic properties are on par with salted skins/hides. The developed process completely eliminates the use of salt and 75% sulphide and also reduces the time and water required for soaking process. The developed system reduces 85% of pollution load discharged from soaking and unhairing processes.

1 Introduction

The hides/skins are susceptible for bacterial attack once flayed from animal. The normal time lapse between skinning and tanning process of green hides/skins demands for temporary preservation technique. Conventionally, salt (30-40% w/w) based preservation technique is widely practiced where the salt acts as dehydrant (Cooper & Galloway 1965). The conventional salt based dehydration technique demands for additional step such as rehydration in subsequent leather processing which consumes huge amount of water. Therefore, the conventional dehydration-rehydration model results in generation of a huge amount of wastewater with increased TDS load (Kannan et al. 2010). On the other hand, removal of TDS from wastewater requires sophisticated techniques like membrane filtration or reverse osmosis, which increase the cost of wastewater treatment process. This limitation can be capitalized by way of providing a suitable alternative for elimination of rehydration step in leather processing. Several attempts have been made to develop less salt and salt free preservation techniques to reduce the TDS load in wastewater (Money 1974; Bailey & Hopskins 1977; Bailey 1995). However, significant reduction in TDS has not been achieved. Polymeric compound based preservation technique has been developed using various molecular weight of polyethylene glycol (PEG). However, the cost of PEG is higher than the conventional salting technique (Kannan et al. 2010). Some attempts have been made to develop new preservation techniques which avoid the rehydration step (soaking) in leather manufacturing. Chandrababu et al. (2012a, 2012b, 2012c) provided a method for direct transportation of flayed

hides/skins to tanneries by employing mobile chiller (4°C), which eliminates the rehydration step, but the process is energy intensive.

Addition of ice to the raw stock would preserve the hides/skins (Hausam 1939) and this method is being followed on larger-scale in Switzerland, Germany and Austria, however, the process is applicable only for short duration. In order to increase the process efficiency, preservative containing ice has been employed in preservation process (Hausam 1951). But, the major limitation of the process is that draining of liquor containing high concentration of preservative. Short-term preservation can also be achieved by spraying bactericides and employing various plant extracts. Bailey & Hass (1988) and Bailey (1999) have provided an irradiation technique where gamma rays or electron beam applied on the hides/skins followed by packing in separate air tight bags for effective preservation. However, the process suffers from the requirement of skilled labor, high cost of investment and sophisticated instrumentation system.

Unhairing is a sequential process after soaking where the combination of lime and sodium sulfide is used conventionally as unhairing agents. But, the major limitations are generation of lime sludge and the possible release of toxic hydrogen sulfide gas during subsequent leather processing or from effluent treatment plant. Heidemann's Darmstadt process deals with spraying 10% sodium sulfide solution on the hair side of hides/skins and hung for 10-20 min. The degradation of epidermis layer enables easy removal of hair and the residual sulfide present in the skin matrix is further oxidized with 10% sodium peroxide solution (Heidemann 1993). Though the process is effective, the toxic sodium sulfide has not been replaced. Some attempt have been made to use hydrogen peroxide (Marmer 2004; Bronco et al. 2005; Morera et al. 2006), calcium peroxide (Gehring et al. 2003) and sodium percarbonate (Marmer & Dudley 2005) as sulfide free sharpening agents (oxidative unhairing), but it required higher quantity than sulfide, which in turn increases the process cost. Replacement of sulfide with thioglycolate (Frendrup 2000), sirolime (Cranston et al. 1986, 1986a) and dimethylamine (Somerville et al. 1963; Hetzel et al. 1965, 1966) is less effective and its odor makes the working atmosphere unpleasant. In acidic unhairing, concentrated acetic acid and salt is applied on the flesh side of fresh skins and stored overnight. Due to the combined actions of lyotropic effect induced by acetic acid and autolytic enzymes present in the skin matrix on basement membrane enables selective removal of epidermis from the grain surface (Heidemann 1993). Though the process eliminates the lime and sulfide, it is not suitable for dried and salted skins. Schlosser et al. (1985) utilized the lactobacillus culture, which selectively destroy the epidermis layer of the skin matrix thus enables the hair loosening. However, addition of salt is required to prevent acid swelling due to the formation of lactic acid during fermentation process, which increases the TDS load.

Several attempts have been made to use enzymes for the development of chemical free unhairing process (Green 1952; Bose 1955; Dhar 1974; Bradly et al. 1990; Feigel 1998), but the process cost is higher than the conventional lime/sulfide based system. Therefore, the development of a preservation technique without dehydrating the hides/skins matrix simultaneously enabling lime-free and low-sulfide unhairing process is essential in order to reduce the water consumption profile and pollution generation of pre-tanning process.

2 Materials and Methods

2.1 Preservation Efficiency of Salted and Preservation-Cum-Unhairing (PCU) Process

Raw sheep skins were procured from Permabur slaughter house, Chennai, Tamil Nadu, India and transported to CLRI pilot tannery within 2 h under cold condition and cut along the back bone. All the left halves were subjected to conventional salt based preservation and right halves were treated with developed PCU formulation. The preservation efficiency was monitored based on the

hydroxyproline release from preserved skin. After the preservation period of 30 days, the salted skins were soaked, unhaired and chrome tanned as per the conventional process. The PCU processed skins were subjected to manual unhairing followed by lime based fiber opening and converted into wet-blue leather in a conventional way. The wet-blue leathers obtained from both salted and PCU process were converted into crust leathers.

2.2 Analysis of Physical Strength Characteristics and Organoleptic Properties

The physical properties such as tensile strength, % elongation at break (IUP 6 2000), tear strength (IUP 8 2000), grain crack load and distension at grain crack of crust leathers obtained from conventional and PCU processes were analyzed. The specimens for physical testing as mentioned above were obtained as per IULTCS standard method and conditioned for 24 h at $25\pm 1^\circ\text{C}$ and $65\pm 2\%$ RH (IUP 2 2000). The crust leathers were also evaluated for various organoleptic properties such as softness, grain smoothness, fullness, grain flatness and overall appearance by hand and visual examination. Each property was rated on a scale of 1-10, where higher point indicates better properties.

2.3 Analysis of Wastewater

Wastewater discharged from conventional and PCU based preservation system was subjected to COD, TS, TDS, TSS, TKN and Cl- analysis as per the standard method (Clesceri et al. 2005).

3 Results and Discussion

3.1 Preservation Efficiency of Salted and PCU Process

Preservation efficiency of the developed PCU process has been monitored over a period of 30 It is evident from Figure 1 that the hydroxyproline release increases with increasing time and reaches a maximum of 320 mg/kg for conventional process and 356 mg/kg for PCU process. It is clear that there is no significant increase in hydroxyproline for the PCU process over the salted technique. Therefore, it can be perceived that the preservation efficiency of the developed PCU process is on par with the conventional process.

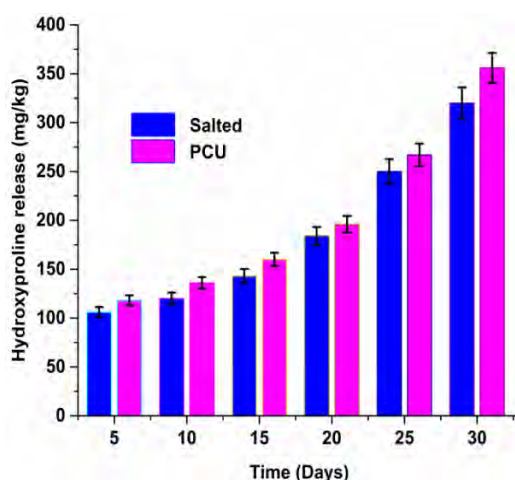


Figure 1. Effectiveness of the salted and PCU process against skin degradation

3.2 Analysis of Physical Strength Characteristics and Organoleptic Properties

The crust leathers obtained from conventional (salt) and experimental (PCU) processes have been subjected to various physical strength characteristics measurement and the results are given in Table 1. It has been observed from Table I that the physical strength characteristics of PCU treated leathers are on par with the conventionally processed leathers.

Table 1. Physical strength characteristics of crust leathers processed from salt and PCU processes

Characteristics	Salt	PCU
Tensile strength (N/mm ²)	13.5±1	15.2±1
Elongation at break (%)	78.1±3	70.5±3
Tear strength (N)	26.5±4	25.1±3
Load at grain crack (kg)	16.6±1	19.4±1
Distension at grain crack (mm)	12.5±0.5	14±0.5

The organoleptic properties of crust leathers have been rated on a scale of 1-10. Higher points indicate better properties of final leather. The results indicate that the PCU leather exhibits better softness (9/10) and grain smoothness (9/10) than the conventionally processed leather (softness 8/10, smoothness 8/10). But, the fullness and grain flatness of conventional leather (8/10) is slightly higher than PCU leather (7.5/10).

3.3 Analysis of Wastewater

The wastewater characteristics of soak liquor discharged from salt and PCU preservation system have been analyzed and the results are given in Table 2.

Table 2. Pollution/emission load from salted and PCU system

Pollution Parameters	Emission Load (kg/ton)	
	Salt Preservation	PCU
pH	7.2±0.2	6.9±.2
Cl ⁻	123± 8	3±0.2
TS	268±14	41±4
TDS	235±20	36±2
TSS	34±3	6±0.4
TKN	3.7±0.4	2.7±0.1

It is evident from Table II that the pH of soak liquor from PCU and salted system is almost similar. Total solids discharged from conventional process is about 268 kg/ton, whereas for PCU system is only about 41 kg/ton. The other parameters like TDS/TSS have also been significantly reduced in PCU process due to the complete elimination of salt.

4 Conclusions

In this work, the preservation and unhairing process have been successfully interconnected through the development of preservation-cum-unhairing process. And the developed system reduces 85% of pollution load discharged from soaking process in addition to eliminating the lime and reducing the toxic sodium sulfide required for the hair removal process. Therefore, the developed preservation-cum-unhairing process would be a promising technology lead for sustainable leather manufacturing.

References

1. Cooper, DR & Galloway, AC: 'Curing methods for wet salted hides. Part II. The reuse of salt for the curing of hides', *Journal of American Leather Chemists Association*, vol. 61, pp. 162–170, 1966.
2. Kannan, KC, Pradeep Kumar, M Rao, JR & Nair, BU: 'A Novel approach towards preservation of skin', *Journal of American Leather Chemists Association*, vol. 105, pp. 361-369, 2010.
3. Money, CA: 'Short term preservation of hides. II The use of zinc chloride or calcium hypochlorite as alternatives to sodium chlorite', *Journal of American Leather Chemists Association*, vol. 69, pp.112–120, 1974.
4. Bailey, DG & Hopskins, WJ: 'Cattle hide preservation with sodium sulfite and acetic acid', *Journal of American Leather Chemists Association* vol. 72, pp. 334–339, 1977.
5. Chandrababu, NK, Karthikeyan, R, Kumari, BS, Ramesh, R, Shanthi, C & Sadulla, S: 'A systematic study on the role of chilling temperatures on the curing efficacy of hides and skins', *Journal of the American Leather Chemists Association*, vol. 107, pp. 362-374, 2012.
6. Chandrababu, NK, Kumari, BS, Vimalarani, SH, Shanthi, C, Karuthapandian, S & Sadulla, S: 'Microbiological aspects of hide and skin preservation by chilling' *Journal of the Society of Leather Technologists and Chemists*, vol. 96, pp. 71-76, 2012.
7. Chandrababu, NK, Thiagu, R, Karthikeyan, R, Kumari, BS, Ramesh, R & Sadulla, S: 'Using a mobile chiller for hides: a green method to resolve the TDS problem' *Journal of the Society of Leather Technologists and Chemists*, vol. 96, pp. 200-209, 2012.
8. Hausam: 'Preservation by cooling', *Journal of American Leather Chemists Association*, vol. 36, pp. 44-48, 1939.
9. Hausam: 'Behaviour of hide during salting and the action on the hide protein', *Journal of American leather Chemists Association*, vol. 12, pp. 1-6, 1951.
10. Bailey, DG: 'Gamma radiation preservation on cattle hides: A new twist on an old story', *Journal of American Leather Chemists Association*, vol. 94, pp. 259–266, 1999.
11. Bailey, DG & Haas, MJ: 'Electron beam irradiation of fresh hides, salted hides and leather, Microbial control and effect of physical properties', *Journal of American Leather Chemists Association*, vol. 83, pp. 46–55, 1988.

MODELLING THE CHARGE ACROSS pH AND ISO-ELECTRIC POINT OF BOVINE COLLAGEN DURING LEATHER MANUFACTURE

A.D. Ballantyne^a and S. J. Davis^b

Institute of Creative Leather Technology (ICLT), University of Northampton, University Drive, Northampton NN1 5PH

a) Corresponding author: andrew.ballantyne@northampton.ac.uk

b) stefan.davis@northampton.ac.uk

Abstract. Many areas of leather production rely heavily on the manipulation of acidic and basic residues within the primary collagen structure to vary the overall charge of the substrate. For example, it is the basis which enables swelling during liming, deswelling during deliming, penetration of chromium after addition of chrome tanning salts and the fixing of chrome to carboxylate residues during basification. Manipulation of the charge on collagen is readily achieved through the addition of acids or bases into the float which may react with these residues to alter the charge. Often, the increase in anionic charge and reduction in cationic charge with increasing pH are shown to happen concurrently and linearly with the iso-electric point (IEP) given as the point at which the positive and negative charges present on the collagen are equal. However, the pH at which carboxylate/acid groups undergo protonation/deprotonation is significantly lower than that at which an amine/ammonium is protonated/deprotonated, meaning the linear model described above is not a true representation of charge of collagen at varying pH. Here we model the charge of a collagen substrate based off the amino acid profile of bovine skin, considering their relative levels within the collagen and concentrations within a water/collagen matrix, representative for collagen saturated with water. Models are presented for raw and limed bovine hides. This broader approach enables greater understanding of the influence of charge on the collagen substrate compared to IEP on its own, revealing contrasting charge profiles in acidic and alkaline regions of raw collagen, providing greater understanding of their differing behaviour during alkali swelling.

1 Introduction

Collagen is of critical importance in leather due to its unique hierarchical structure based on the triple helix of tropocollagen. However, in the context of leather manufacture the manipulation of charge on the collagen substrate is of equal importance as manipulation of charge is prevalent throughout almost all stages of wet processing. It is primarily responsible for swelling during liming, deswelling during deliming, determination of suitable pickling pH for the appropriate tannage and control of penetration and fixing of tanning, retanning, dyeing and fatliquoring agents. [1]

The charge on collagen originates from the presence of acidic and basic amino acid residues which, depending on the amino acid and pH may be positively charged, negatively charged or neutral. **Fig. 1** shows a peptide composed of the most common amino acids present in collagen that may hold charge. Aspartic acid (Asp) and glutamic acid (Glu) have side chains that have a carboxylic acid group present which, depending on the pH may either be in its neutral protonated form at lower pH or its negative deprotonated carboxylate form at higher pH. Histidine (His), lysine (Lys) and arginine (Arg) each contain side chains that may be in a protonated in positively charged form at lower pH or a deprotonated neutral form at higher pH. Tyrosine (Tyr), an amino acid containing a phenolic ring is also acidic, being in either its neutral phenolic form at low pH or as an anionic phenoxide at high pH. [2]

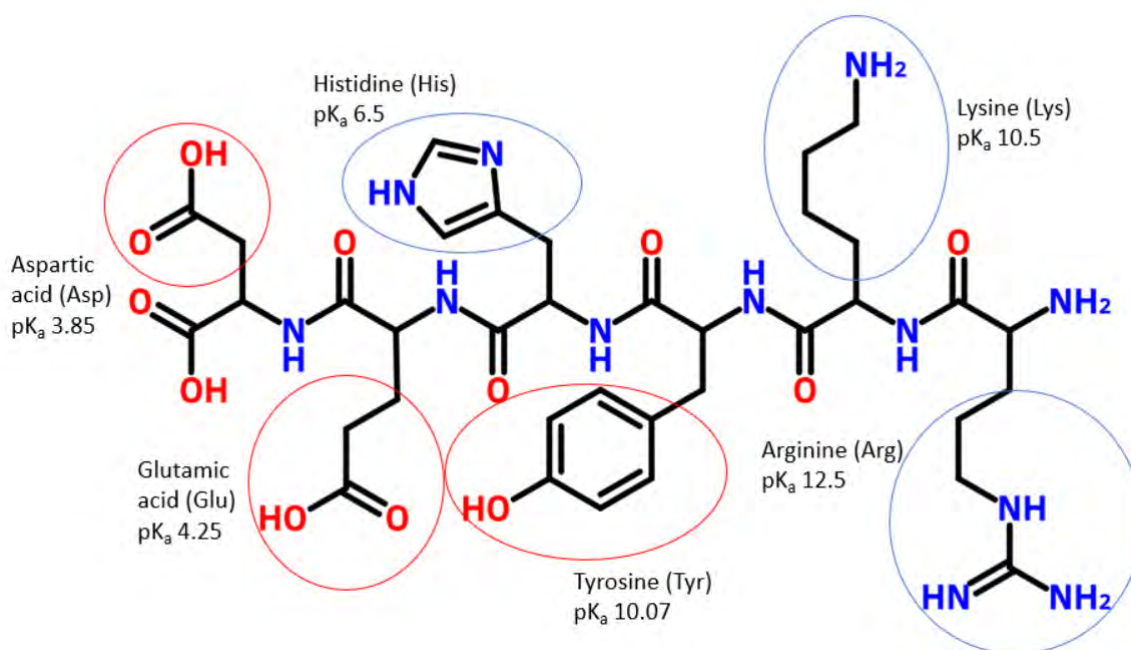
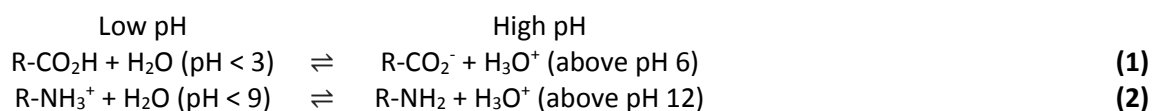


Fig. 1. Common amino acid residues of collagen that can hold charge and respective pK_as of the side chain functional groups. Residues represented in their neutral form.

It is commonly stated that below a pH of 3 all acid groups are protonated and below a pH of 9 all amine groups are protonated. Above a pH of 6 all acid groups are deprotonated and above a pH of 12 all amine groups are deprotonated, **eqns 1 & 2**, however there are notable, important exceptions to this as will be discussed later. [3]



There is a pH range between pH 6 and 9 where predominantly carboxylate and ammonium groups are present. It is within this region that is generally accepted as “full neutralisation” in leather manufacture. [3] The isoelectric point of collagen can be found within this region at approximately pH 7.4. [4] The IEP is a fixed pH where the sum of positive and negative charges of a substrate, in this case collagen, are equal and thus there is no overall charge. At pHs below the IEP the overall charge will be positive as progressively more carboxylate are protonated, reducing the negative charge component. At pHs above this the charge will be negative as progressively more ammonium groups are deprotonated, reducing the positive charge component. IEP is often discussed in isolation with the implication on charge of collagen at a given pH often only inferred from the IEP value. A more holistic approach is to consider the charge on the collagen substrate across a broad pH range, providing not only information about the pH where there is neutral overall charge (IEP) but also all other pHs as well.

Here we have prepared a model for predicting the overall charge of bovine collagen at differing pHs. Molar concentrations of each individual amino acid residues, the charge of each of the residues at differing pHs, and overall charge on the collagen substrate were calculated. This model was then extended to study changes in charge and IEP during the liming process.

2 Description of model and calculations

2.1 Determination of concentration of acidic and basic amino acid residues per kg hydrated collagen

2.1.1 Molar mass of collagen molecule containing 1000 residues

Bovine skin collagen is predominantly composed of Type I, the composition of which is well understood. The amino acid profile of bovine hides used in the generation of this model is detailed in table 1. [1]

Table 1: Amino acid profile of type I bovine collagen.

Amino acid	Residues per 1000	Amino acid	Residues per 1000	Amino acid	Residues per 1000
Glycing (Gly)	330	Proline (Pro)	126	Glutamic acid (Glu)	73 in total
Alanine (Ala)	110	Hydroxyproline (Hyp)	93	Glutamine (Gln)	
Valine (Val)	22	Methionine (Met)	4	Arginine (Arg)	48
Leucine (Leu)	26	Phenylalanine (Phe)	14	Lysine (Lys)	38
Iso-leucine (Ile)	12	Tyrosine (Tyr)	5	Hydroxylysine (Hyl)	6
Serine (Ser)	34	Aspartic acid (Asp)	47 in total	Histidine (His)	4
Threonine (Thr)	18	Asparagine (Asn)			

Initially an overall mass of a collagen molecule containing an arbitrary 1000 amino acid residues was calculated from the above amino acid profile according to **eqn. 3.** below, where the total mass is obtained from the sum of the molecular weights of each amino acid multiplied by the number of their residues. Collagen is a protein formed from the condensation reaction of amino acids, with the elimination of water. To compensate for water elimination the molecular mass of 999 moles of water was then subtracted. This produced a mass of **111 425 g/1000 mol** amino acid residues of collagen.

Total mass 1000 amino acid residues =

$$\sum (\text{mwt amino acid} * \text{no residues per 1000}) - 999 * \text{mwt H}_2\text{O} \quad (3)$$

One limitation of the above calculation is the measurement of acidic amino acids and those containing an amide group but otherwise indistinguishable structures (i.e. Asp/Asn and Glu/Gln) are difficult to measure independently as the amides are converted into acid residues during the protein digestion process necessary for the measurement of concentration. This has limited implication in this case as their respective molecular weights are close. For example, aspartic acid has a mwt of 133.11 whereas asparagine has a mwt of 132.12. At extreme ratios of acid to amide residue this would result in a total mass error of 0.1% and as such is incorporated here as an acceptable error.

2.1.2 Determination of concentration of individual amino acids per 1 kg raw hydrated collagen

Knowing the mass of a theoretical collagen molecule containing 1000 amino acid residues, the concentration of amino acids per unit mass (in this case 100 g) can be calculated as shown in **eqn. 4.**

Conc. individual amino acid per 100 g collagen =

$$(100 \text{ g} / \text{Total 1000 amino acid residues}) * \text{no. residues of individual amino acid} \quad (4)$$

For example, the concentration of glycine per 100 g collagen can be given as follows

$$\begin{aligned} \text{Glycine concentration} &= (100 / 111425) * 330 \\ &= 0.296 \text{ moles} / 100\text{g dry collagen} \end{aligned}$$

If hydrated collagen contains 30% collagen and 70% water, the concentration of individual amino acids per kg can be calculated by multiplying the concentration per 100 g dry collagen by 3. The calculated concentrations are detailed in **Table 2**. Concentrations are calculated in mol kg⁻¹ hydrated leather.

2.2 Prediction of charge on raw collagen at variable pH

The dissociation behaviour of acids is described by **eqn. 5** where [H₃O⁺] can be quantified directly from the pH and the K_a from the pK_a of a given residue of an amino acid. [A⁻] and [HA] are the amounts of a functional group, such as a carboxylic acid, that are in deprotonated or protonated forms respectively. Assuming no other additions of chemicals, the sum of [A⁻] and [HA] must equal the initial concentration of an acid added [HA]_i.

$$K_a = \frac{[H_3O^+][A^-]}{[HA]} = \frac{[H_3O^+]^2}{[HA]} \quad (5)$$

The concentrations of [A⁻] and [HA] are linked to the initial concentration of acid added, **eqns 6 & 7**.

$$[HA] = (1-x)[HA]_i \quad (6)$$

$$[A^-] = x[HA]_i \quad (7)$$

[A⁻] and [HA] can be substituted with x[HA]_i and (1-x)[HA]_i respectively to give **eqn. 8** where x represents the proportion of the acid which is dissociated.

$$K_a = \frac{[H_3O^+] x[HA]_i}{(1-x)[HA]_i} \quad (8)$$

Eqn. 8 can then be rearranged to **Eqn. 9** to find an expression for x.

$$x = \frac{1}{\frac{[H_3O^+]}{K_a} + 1} = \frac{K_a}{[H_3O^+] + K_a} \quad (9)$$

With a known concentration of acid added the associated and dissociated fractions can then be calculated as in **eqns. 8 & 9** respectively.

In the case an organic acid, [HA] represents the protonated form R-CO₂H and [A⁻] represents the deprotonated form R-CO₂⁻. In the case of an organic base such as an amine [HA] represents the ammonium form R-NH₄⁺ and [A⁻] represents the amine.

Consequently, the relative fractions of [A⁻] and [HA] can be calculated for each individual amino acid from their respective pK_a values and the amino acid concentrations in 1 kg hydrated collagen calculated in **section 2.1**. The overall charge of the collagen can be obtained through subtracting the total sum concentration of anionic residues from the total sum of cationic residues at a given pH **eqn. 10**.

$$\begin{aligned} \text{Total charge on collagen} &= \\ &= \Sigma \text{ conc. cationic functional groups} - \Sigma \text{ conc. anionic functional groups} \quad (10) \end{aligned}$$

The isoelectric point is measured as the point at which the overall charge is equal to zero. At this stage the total concentration of acidic and amide residues are known but their relative ratios are not. The IEP of collagen is believed to be at a pH of ca. 7.4. The ratio of acid: amide residues for aspartic acid/asparagine and for glutamic acid/glutamine were manipulated to provide concentrations that would result in an overall IEP of 7.4. The calculated concentrations of all amino acid residues contributing to the overall charge of collagen are provided in **Table 2**.

2.3 Modelling influence of liming on collagen charge at variable pH

During the liming process asparagine, glutamine and arginine are known to undergo hydrolysis to aspartic acid, glutamic acid and ornithine respectively. It is predicted that Glu and Arg have a half-life of approximately 18 – 20 hours, similar to that of the duration of the liming process. The concentrations of Glu and Arg during the liming process were calculated through the addition of the initial concentration of Gla and Asp with 20, 40, 50, 60, 80 and 100% of the concentrations of Gln and Arg added to these respectively. The overall charge of collagen at a given pH was then calculated following the same method as described in **section 2.2** from the revised amino acid concentrations. **Table 2** details the calculated concentration of the respective amino acid residues present in limed collagen where 50% of the Gln and Arg have been converted into their acid analogues. There is evidence that Arginine may also undergo hydrolysis during the liming process to produce ornithine, however this process is slow and as such was not incorporated into this calculation.

3 Results and Discussion

3.1 Quantification of amino acid profile of collagen per unit weight

The amino acid residues present in collagen capable of sustaining charge are responsible, along with pH, for the overall charge of collagen. It is necessary to quantify the concentration of these amino acid residues to calculate their contribution to overall charge. The method used to quantify the concentrations is described in section 2 and can be reduced to the following steps:

1. Defining relative amounts of amino acids present in collagen
2. Calculation of the mass of collagen containing 1000 moles of amino acid in the relative quantities defined in **1** above
3. Calculation of the concentration of a given amino acid per unit mass of dry collagen
4. Conversion of concentration of a given amino acid per unit mass of dry collagen to a concentration per hydrated unit mass

As with any model there are unavoidable assumptions that must be made in the absence of specific experimental data which can be used in its place. The amino acid profile for Type 1 Bovine collagen has been extensively studied and as such there is a good understanding of its composition. However, while the combined concentrations of Asp/Asn and Glu/Gln are known the specific concentrations of each can only be estimated. It is understood that the acid residues contribute to the charge of the collagen at pHs where some of the residues are in carboxylate form and the IEP point of collagen is at pH 7.4. Assuming that Asp: Glu and Asn: Gln ratios remain consistent with those overall, described in **Table 1**, then their relative concentrations can be quantified by manipulating their ratios so that the IEP is at pH 7.4. The concentrations of Asp and Glu were calculated as 61.3% of the sum of Asp + Asn or Glu + Gln concentrations, resulting in the values provided in **Table 2**. It is unlikely that there will be an equal ratio of Asp: Asn and Glu: Gln, however, in the absence of other values an assumption such as this must be made. Importantly, the calculated overall concentrations of acid and amide residue amino acids match those calculated for collagen with an IEP of 7.4 and the pK_a values of Asp and Glu are close enough that it is unlikely this assumption will introduce large errors into the model.

Table 2: Concentrations of acidic and basic amino acids in 1 kg hydrated raw and limed collagen

Amino acid	Concentration in hydrated raw collagen (mmol kg ⁻¹)	Concentration in hydrated limed collagen (mmol kg ⁻¹)	pK _a
Aspartic acid	77.4	102.0	3.85
Asparagine	49.1	24.6	
Glutamic acid	119.7	159.1	4.25
Glutamine	76.9	38.4	
Arginine	129.2	129.2	12.48
Lysine	102.3	102.3	10.5
Hydroxylysine	16.15	16.1	10.5
Histidine	10.8	10.8	6.2
Tyrosine	37.7	37.7	10.07

The amino acids present in collagen that can be ionised at certain pH ranges are provided in **Table 2**. Both Asp and Glu are the acidic amino acids of highest concentration of 77.4 and 119.7 mmol kg⁻¹ respectively, however appreciable amounts of tyrosine (Tyr) are also present at 37.7 mmol l⁻¹. Importantly, Tyr has a significantly different pK_a of 10.07.

The basic amino acids present in highest concentrations are Arg and Lys at concentrations of 129.2 and 102.3 mmol kg⁻¹ respectively. In contrast with the acid amino acid residues Asp and Glu, Arg and Lys have substantially different pK_a values from each other of 12.48 and 10.5 respectively, as such they will have significantly different ionisation behaviour. This feature arises due to the differing basic functional group of each of these amino acids (guanidine for Arg and an amine for Lys) and is seldom discussed in the leather literature. Also present are low levels of His, which also has a substantially different pK_a value of 6.2 and hydroxylysine, which has been assumed to have an identical pK_a value to lysine.

3.2 Modelling charge profile on raw, hydrated collagen

The degree of protonation of an acid or amine group on a protein can be described in terms of the concentration of the amino acid residue and a protonation factor, x , as defined in **eqn. 9**. As the value of x is dependent on the pK_a value (K_a) and the pH (H₃O⁺), the degree of protonation of the residues of amino acid residues can be easily predicted for the amino acids described in **Table 2**, assuming the pK_a of the residue within the protein is the same as that of the free amino acid.

Fig. 2 (a) plots the value of x across a pH range of 0 to 14 for the amino acids present in collagen capable of being either positively or negatively charged. In each case at low pHs, x has a value of 0 corresponding to a residue that is protonated, as a neutral carboxylic acid for Asp and Glu, neutral phenol for Tyr and protonated cationic basic groups for Arg, Lys and His. At higher pHs, x has a value of 1 for all amino acids corresponding to the residue being fully deprotonated, as an anionic carboxylate for Asp and Glu, anionic phenoxide for Tyr and deprotonated neutral basic groups for Arg, Lys and His. Where x does not equal either 0 or 1, a mixture of the protonated and deprotonated forms will be present, the levels of which are defined by the value of x . The values of these are calculated from **eqns 8 & 9** respectively.

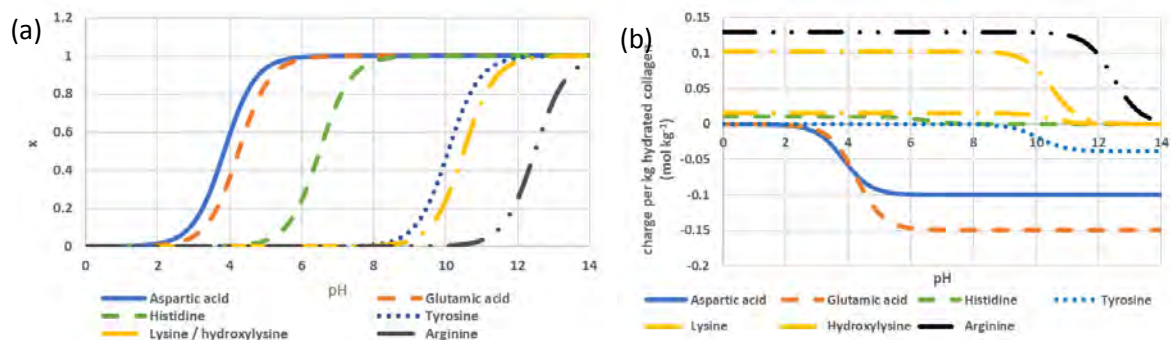


Fig. 2. (a) Theoretical deprotonation ratio of amino acids side chains and (b) calculated molar charge of different amino acid residues per kg of raw hydrated collagen at differing pHs

While all the functional groups on the amino acid side chains follow the same trend from $x = 0$ at low pH to $x = 1$ at high pH, the range of pH over which these changes occur is specific to each amino acid. For Asp and Glu, the acid containing residues, this occurs within a pH range of *ca.* 3 and 6 as is consistent with the current understanding. Interestingly, the pHs over which the two basic residues of highest concentration, Arg and Lys, are significantly separated. At pH 12 Arg is 24% deprotonated but Lys is 96% deprotonated. These differences between the acid and basic residues at high concentration indicate that the charge response at high and low pH are likely to be different. Additionally, despite containing an acidic proton, Tyr has a similar response to that of Lys, meaning that it will undergo a conversion from neutral to negative charge across a similar pH range as Lys. His undergoes its transition from protonated to deprotonated from pH 5 to pH 8, a pH region that is independent of any other transitions.

Fig. 2(b) shows the calculated charge on collagen contributed by individual amino acid residues at differing pHs as a molar concentration per kg of hydrated collagen. This does not take into consideration deviations arising due to swelling, assuming identical hydration throughout the pH range. The transitions from positive to neutral (for basic residues) and from neutral to negative correspond to the pH ranges observed in **Fig. 2(a)**. The total contribution of each can then be compared. The significant contributors to positive charge are Arg, which is fully cationic below pH 11 and Lys/Hyl which are fully cationic below pH 9. Present at comparatively low concentration His has a small influence on the overall cationic charge. Asp and Gla are the significant contributors to negative charge, present fully as carboxylates at pHs above 6 and neutral below pH 3. Tyr also has a comparatively small contribution of negative charge at pHs above 9.

The total charge on the collagen substrate can be calculated through the sum of the charge of the individual amino acid residues, with the resulting dependence on pH given in **Fig. 3 (a)**. At $< \text{pH } 3$ the collagen structure is close to fully cationic as almost all the amino acid residues are protonated at this point. Within pH 6 and 9 is the “neutralised” region where substantial change of the pH has little influence on the overall charge. In contrast to the acid region, where the protonation of the acidic amino acids occurs within a pH range of 3 – 6, the deprotonation of the basic residues at high pH shows a consistent change from pH 9 through to 14, double the pH range of the acidic region. The origin of this difference arises from the respective pK_a values of the amino acid residues. Asp and Glu have similar pK_a s so their values of x at a given pH are close, whereas Arg and Lys have substantially different pK_a values, leading to an extended response across a broader range of pH.

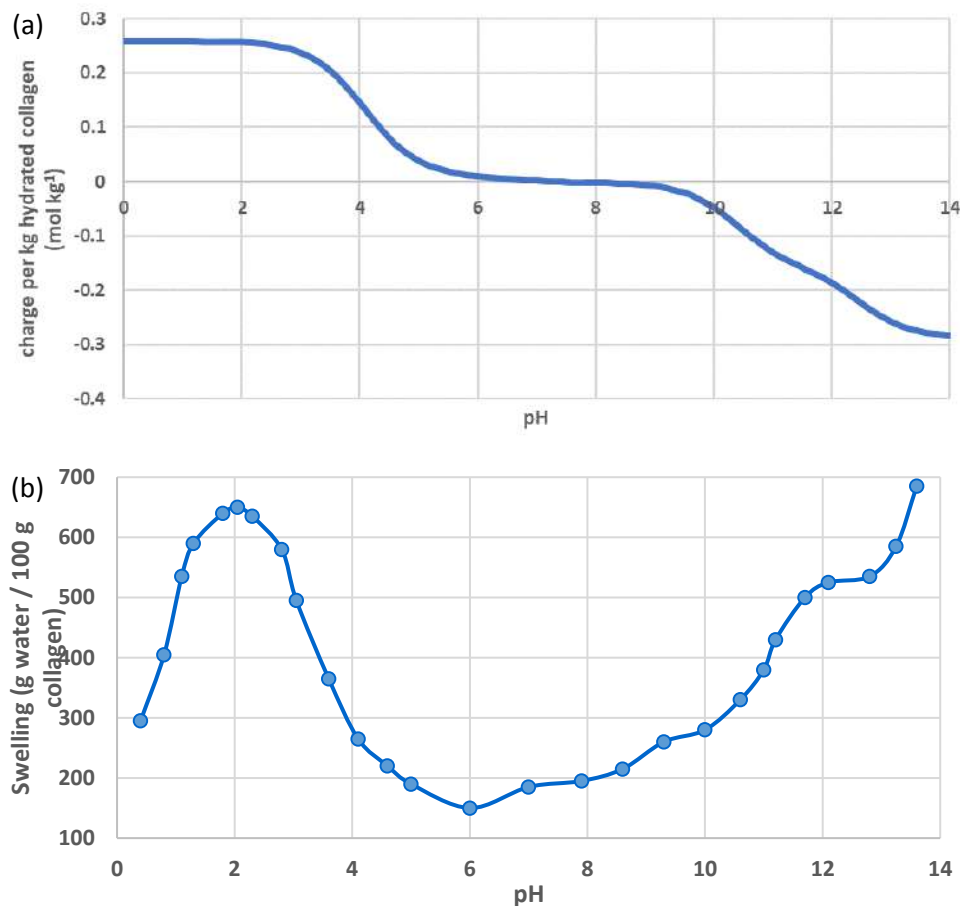


Fig. 3. (a) Total molar charge per kg hydrated collagen at different pHs and (b) swelling curve of alkali treated sheepskin reproduced from Bowes, *Biochem J.* 1950, 46 (1), 1 – 8. [4]

The difference in behaviour at acid and alkaline pHs has important implications for the processes that occur within these regions. Due to its limited solubility, lime has a self-limiting pH of 12.6. In this region 99% of Lys residues are deprotonated, whereas, Arg residues vary considerably within a small pH range: 25% deprotonated at pH 12 and 77% deprotonated at pH 13. Consequently, during liming a small increase in the pH above 12.6 can contribute significantly to the overall charge in this region.

The swelling curve of collagen at variable pH has been reproduced from the original publication by Bowes in **Fig. 3 (b)**. [5] The results plotted on this graph originate from experiments on alkali treated sheepskin so the substrate may be substantially different from the raw bovine collagen modelled here. However, with care some useful comparisons can be made. At progressively lower pH the pelt will swell until a maximum at pH 2. At this pH almost all the carboxylic acid groups are protonated, at pH 2 the total overall charge is 99.2% of the value at pH 0. The swelling is understood to occur due to a combination of electrostatic repulsion from the positively charged sites on the collagen and osmotic swelling. Below pH 2 swelling decreases as, once all acid groups are protonated, additional acid required to reduce the pH acts as an electrolyte, screening charge on the collagen.

At high pH the swelling response does not mirror that observed in acid swelling. There is a gradual increase in the swelling at increased pH, as with acid swelling. However, there is a plateau in the swelling at pH 12 followed by a further rapid increase. This different behaviour has previously been rationalised as a difference in the swelling mechanisms between acidic and alkali conditions, with electrostatic and lyotropic swelling dominant at increased pH. However, this does not consider the comparatively high pK_a of arginine, which leads to the sustained increase in the charge of collagen at high pH. As with swelling under acidic conditions, increase in the charge imbalance on collagen,

breaking salt links, causing electrostatic repulsion of the protonated basic residues leads to progressively larger swelling values up to pH 14. These results suggest that the type of swelling, osmotic or lyotropic, may have less of an implication on swelling behaviour than is currently accepted, with the differing pK_a values of Arg and Lys playing a stronger contribution through their influence on the overall charge, and therefore electrostatic repulsion.

3.3 Modelling charge profile on limed collagen

The process of alkali treatment (liming) is understood to influence the IEP and charge profile of collagen. [4] Partial deamidation occurs, converting some of the Asn and Gln residues to their carboxylic acid analogues. The increasing the concentrations of Asp and Glu, provide a consequent shift in the IEP to values of 5 or lower. [5] This effect has been modelled here, plotted in **Fig. 4** where the charge across pH has been calculated for systems where 20, 40, 60, 80 and 100% of the Asn and Gln residues have been converted into their acid analogues. There is a consequent increase in the negative charge present from the formation of carboxylate from pH 3 and above. Because of the increased carboxylate concentration, the overall charge of the deamidated samples in the region of full neutralisation, pH 6 to 9, is progressively more negative. As a result, the IEP is shifted to progressively lower values from pH 7.4 for raw collagen to 4.7 where there is 50% deamidation and 4.4 where there is 100% deamidation. Notably, the trend in IEP with degree of deamidation is not linear, with large changes in the IEP initially trending to much smaller changes at large % deamidation, again suggesting that IEP alone is not sufficient to predict the behaviour of proteins at variable pH.

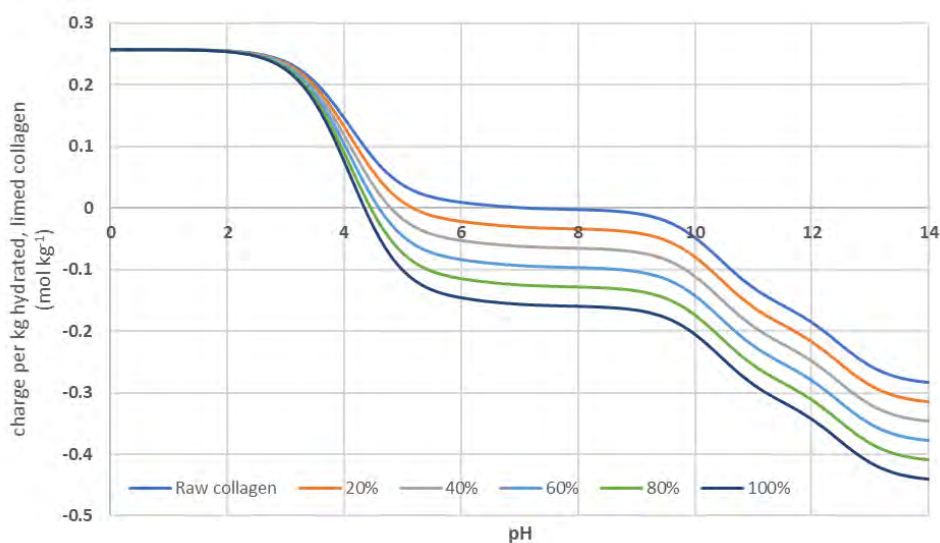


Fig. 4. Molar charge per kg of limed collagen where 20, 40, 60, 80 and 100% of asparagine and glutamine are hydrolysed to their acid analogues

There are suggestions that alkaline hydrolysis of arginine is an important process during alkali treatment. [1] However, measurements by Luck *et. al.* state that, while hydrolysis may occur, there was no conversion at pH 12 after heating at 37 °C for 24 hrs. Elevated temperatures and higher pHs were required to obtain significant hydrolysis. [6] Consequently, hydrolysis of Arg has not been studied here.

4 Conclusions

The importance of the substrate IEP on leather processing is considerable. However, quoting the IEP on its own removes a large quantity of valuable information regarding the collagen charge. For example, it provides little information about the total overall charge at extremes of pH or the rate at which the charge increases with changes in pH. A more holistic approach is to consider the charge on collagen across pHs, providing greater detail regarding its behaviour. For example, the influence of IEP on the charge of collagen at a given pH is non-linear, showing wide variations depending on the amino acid makeup. Additionally, discussions of IEP of raw collagen do not provide evidence for the difference in the charge behaviour at acidic and basic conditions.

References

1. A. D. Covington, *Tanning Chemistry: The Science of Leather*, Cambridge: RSC Publishing, 2011.
2. G. C. Barrett and D. T. Elmore, *Amino Acids and Peptides*, Cambridge: Cambridge University Press, 1998.
3. R. Daniels and W. Landmann, *The Framework for Leather Manufacture*, Liverpool: World Trades Publishing, 2013.
4. M. Meyer, "Processing of Collagen Based Biomaterials and the Resulting Materials Properties," *Biomedical Engineering Online*, vol. 18, no. 24, pp. 1 - 74, 2019.
5. R. H. K. J. H. Bowes, "The swelling of collagen in alkaline solutions. 1 Swelling in solutions of sodium hydroxide," *Biochem Journal*, vol. 46, no. 1, pp. 1 - 8, 1950.
6. J. H. Bowes and R. Kenten, "The effect of demination and esterification on the reactivity of collagen," *Biochem Journal*, vol. 44, p. 142, 1949.
7. K. Murray, P. Stroier Rasmussen, J. Neustaedter and J. Murray Luck, "The Hydrolysis of Arginine," *The Journal of Biological Chemistry*, vol. 240, p. 705, 1965.

AUTOMATION IN LEATHER MAKING – A CLEANER PRODUCTION APPROACH

Rames C. Panda¹ and James Kanagaraj²

1 Sr Principal Scientist, Department of Chemical Engineering, CSIR-CLRI, Adyar, Chennai - 600020, India.

2 Sr Principal Scientist, Department of Leather Process Technology, CSIR-CLRI, Adyar, Chennai - 600020, India

a) Corresponding author: panda@clri.res.in (b) jkraj68@gmail.com

Abstract. Leather auxiliaries, chemicals and raw materials are being handled manually in most of the tanneries. The practice give-rises to spilling over of costly chemicals and utilities causing increase in pollution load, financial loss and health hazards. In order to solve this, a computerized programmable logic controller based dosing system is designed and is installed to automate the unit operations in tanning drum. There are five modules which follow the sequences of operation to improve the working atmosphere and reduce the loss. The material handling through engineering inputs results in improved quality control and provides cleaner production.

1 Introduction

Tanning stabilizes putrescible skins/hides of animals to non-putrescible leather by establishing links between functional groups of collagen and chemicals. Almost 90% of the leather products are produced via chrome tanning. The raw hides and skins have their active binding sites which get bonded with these auxiliaries to avoid spoilage. In the process of leather making, there exist many unit operations where pH of float/hides is adjusted manually. Monitoring pH, hide to float ratio, rate of diffusion of chemicals, time of dosing, temperature and rpm of drums are few factors which need to be monitored continuously through-out the operations. Introduction of process controls at different sequences of operation yields a better consistency in leather quality. The prime important area becomes volume of water and temperature. The next priority comes to correct measurement/ weighing of chemicals followed by pH monitoring (Purushotam et al, 1990). Number of researchers (Huang & Liu, 1996; Hitchingham and Thomas, 2007; Li and Shitao, 2009) has proposed different automatic dosing systems, where the application is other than leather. There are many patents based on which commercial dosing systems are available for leather applications. Tailor made systems have also been reported. However, an integrated facility which takes care of minimizing waste (to avoid use of excess chemicals & water) through its control logic by minimizing cost function is not available. Hence the objective of this work is to develop process control techniques to implement through PLC to minimize rejects and batch-to-batch variation of wet blue quality. This will provide cleaner technology and abate pollution load

In order to achieve this, the rest of the paper is organized as follows: Section 1 gives an introduction to general unit operations in wet tanning of leather processing. Section 2 describes limitations to existing micro-processor based systems. The feature of present computer aided dosing (CAD) system is explained in section 3. Techno-economic study is presented in section 4. At the end, conclusion is drawn.

2 Leather Manufacturing: Unit operations

Leather making is an art where the layers are separated or split across the cross sections into two layers: top layer (hair side) and under layer (flesh side). The top layer is named as full grain which provides durability and malleability while the bottom layer provides stiffness. A coating is applied on it for practical use. The sequences of common operating steps are as follow.

2.1 Presoaking

Hides are soaked to remove salts (which was used for preservation) in revolving drums.

2.2 Liming

Hair and epidermis are removed by adding lime and sodium sulphide. This makes the hides softer, flexible and palpable necessary for upholstery leather. Hides are then delimed, and send for batting and pickling.

2.3 Splitting

The hides are separated into two layers: grain (smooth grains) layer and bottom (flesh side) layer.

2.4 Tanning

The hides are tanned using some leather chemicals which slowly diffuse into leather matrix through its pores. The chrome tanned hides get properties of leather.

2.5 Neutralization

After performing chroming and rechroming in acidic pH, the hides are subjected to neutralization using light alkaline media. Hides are then processed for retanning, dyeing and fatliquoring for making wet blue leather. For producing crust and finished leathers, some more steps like, piling, setting, drying, staking, toggling, trimming, buffing and de-dusting etc. may be necessary.

Most of the above operations are performed in tanning drums where water, chemical addition and pH verification of hides are done manually. This crude method of handling of raw materials give rises to waste and spill over of chemicals. These losses can be minimized by commissioning automatic dosing systems and automatic aqua systems.

3 Features of CAD System

The objective of this work is to produce consistent quality of leathers and to provide a healthy environment through automatic dosing and pollution abatement system. Therefore the entire process control operation is integrated to operate through PLCs with following five modules:

- i) Water addition module
- ii) Chemical preparation and dosing system
- iii) pH monitoring and float recycle system
- iv) Drum rotation module
- v) pollution reduction module.

In the integrated system, critical and bulk chemicals are stored in bulk storage tanks and are drawn into the load cell (LC) as per process sequence or recipe for feeding into the drums through auxiliary tanks. The float-recycle system helps to remix & heat the float where a pH electrode is housed to monitor pH online. The pH monitoring system adjusts addition of critical chemicals that indicates automatic end point. 10% NaOH is dosed to remove pollution. The control parameters monitored are: hide/float ratio, pH, moisture in the pollution abatement system and uniformity of media (contaminated process liquor). The humidity and temperature of inlet air is controlled and contact time with counter-current media is 10-30 secs. Flow rate of alkali solution is controlled to maintain pollution.

4 Techno Economic Study

Cleaner production is provided through automation of dosing & pH monitoring using PLC in indogeneous way. It has been found that for a 6 drum tannery, the cost of the system comes to be about INR 80 Lakhs. Raw to wet blue process have been experimented using this module. Six batches (each 100 pcs) of hides are processed under 3 batches with conventional and other 3 batches with modified. Wet blue & crust quality assessment have been made on the product. Effluent streams are also analyzed for composition. The gross savings (amount saved through chemicals, power, time saving and reduced wastage of water) play important role in these calculations. By working 300 days per year, the gross profit is calculated to be Rs. 8.63 lakhs per one shift basis or Rs. 17.25 lakhs per two shifts basis. Based on the 4 drums connected to automation system, percent of net return on additional investment comes to be 34%. The pay back period becomes 4 years. Following benefits were achieved:

- (1) Quality consistency was improved to a minimum of 3%
- (2) Existing capacities can be significantly enhanced by changing over to 3 shift schedules. This is mainly due to saving in process time and hence manpower and power consumptions are reduced.
- (3) Strong economic incentives exist for accepting a higher level of investment of automation system. More attractive returns can be realized on investment than hitherto possible with the conventional systems.
- (4) The work culture in a tannery wet section with automation system can be changed for the better occupational health and safety. Production teams can be kept well informed of the operation sequences and drudgery can be reduced in various repetitive operations. Work procedures can be systematized to a great extent. Due to reduction in chemical loads, the waste streams from the wet processing area are carrying less chemical loads.

5 Conclusion

Tannery wet operations are automated by implementing various process control measures that will help to yield more throughput, uniform quality product and build awareness on occupational safety. Comparison of products from processes & economic benefit analysis between conventional and PAS (partially automated system with CADS) reveals that the present technique can be implemented in more tanning units throughout the country.

References

1. Hitchingham L and Thomas H, 2007, *Development of a semiautomated chemical stability system to analyze solution based formulations in support in support of discovery candidate selection*, *J. Pharma & Biomedical Anal.*, 43 (2), 522-26
2. Huang C and Liu C B, 1996, *Automatic control for chemical dosing in laboratory-scale coagulation process by using an optical monitor*, *Water Research*, 30 (8), 1924-29
3. Li C Zhao and Shitao F Y, 2009, *Design of PLC based compound control system for coagulant dosing process*, *Process Automation Instrumentation, CNKI Journal*, 11, 19-23
4. Purushotham, H., Raghavan, K.V., Mitra, R.B. and T.K. Rao, 1990, "Tradition Accomodates Modernisation – An Indian Experience in Tannery Wet Processing", *Proceedings of 25th LERIG, CLRI, Chennai, India, Jan (1990)*.

Author's bibliography

Rames C. Panda: Received the M.Tech. and Ph.D. degrees in chemical engineering in 1989 and 1994, respectively, from the Indian Institute of Technology, Madras. In 1993, he joined Chemical Engg. Dept. of CLRI, Council of Scientific & Industrial Research, as a scientist. He looks after industrial instrumentation and process control related works. He has carried out research works at University of Karlsruhe (TH), Germany in 1997–8., at PSE, Chem Engg Dept, NTU, Taiwan (2002-3) and Chem Engg Dept, Curtin Univ of Tech, Australia (2006-7). Presently, he is working as a Principal scientist & faculty at Chem Engg Dept., CLRI. His research area includes autotuning, PID controllers and analysis of control systems, process modeling, and simulation

James Kanagaraj: Received his BTech, MTech & PhD degrees from Anna University, Chennai. He joined CSIR-CLRI as scientist in 1993 and presently he is working as a Sr Principal Scientist. He obtained three prestigious fellowships to pursue his higher research in abroad through academic bilateral exchanges. He has many research publications in reputed journals and his field of work is BioTechnology.

BIOPOLYMER-LIPOSOME COMPOSITE FOR FATLIQUOR APPLICATIONS – A ‘GREEN’ APPROACH TO OPTIMAL TRANSPORT AND DELIVERY OF NATURAL OILS

Narayana Reddy Gari Bhargavi¹, Kalarical Janardhanan Sreeram¹, Aruna Dhathathreyan²

1 CATER'S, Central Leather Research Institute, Adyar, Chennai-600020, India, kjsreeram@clri.res.in, 044-244302677168

2 Advanced Materials Laboratory, Central Leather Research Institute, Adyar, Chennai-600020, India, aruna@clri.res.in

Abstract. Combining 2 or 3 steps in leather processing to optimize chemicals usage, time for process and lower pollution load has been the prime objective of this work. The wastewater after fatliquoring process in post tanning/finishing of leathers contains surfactants, neutral salts and unspent or unbound oil. This is mainly due to the manner in which fatliquors are prepared. Normally the oil in water emulsions (fatliquors) are prepared through chemical modification of oils along with surface active agents that would enhance the dispersion of oil in water. In the processing of leather, the discharged chemical compounds from the fat liquors post tanning process are likely to exist as persistent organics in soil. In this paper, an ambitious effort to take forward the successful lessons from other sectors such as healthcare to leather processing is presented. Here, the use of liposomes as oil carriers in design of fat liquors has been envisaged. Here, the lacunae associated with liposomal carriers such as stability, encapsulation efficiency, the release of payload under desired conditions, etc. have been addressed. The study focuses on stabilizing the liposomes and the triggered delivery under the drum pH conditions during leather processing. A liposome -biopolymer composite based on Egg Phosphatidyl Choline and Pectin encapsulating oil (EPCPEC-O), has been prepared. Pectin influences the stability and oil encapsulation efficiency of the composite vesicles. Results show that the particle size of the oil encapsulated liposomes was 1.8 μm for EPC-O (oil encapsulated liposomes) system and for the EPCPEC-O 2.6 μm is observed. These systems have been applied on the leather as a lubricating agent. The release profile of the liposome composite was modeled using a dye instead of oil and its release under a narrow pH range was observed, suggesting that the oil could be released to fibres by modulating the pH. Preliminary studies indicate the potential of this product as a possible fatliquor is encouraging.

1 Introduction

The conventional practices for making fatliquor formulations are chemical modification of oils including sulfation and sulfitation; adding emulsifiers to solubilize the oil component inside the aggregated structures and using synthetic fatliquors. Synthetic fatliquors include sulphochlorinated products of C10-C20 long chain hydrocarbons. The step of Solubilization of the oils in water is associated with usage of large amount of emulsifiers which are hazardous and also energy intensive preparatory methods. The conventional fatliquoring with commercial fatliquors offers 85-90% of exhaustion leaving 10-15% of unexhausted matter in effluent that are made up of emulsifiers, metallic soaps, alkyl phenyl ethoxylates, chlorinated paraffin oils and non-volatile hydrocarbons which are known to be toxic.¹ This makes the process not eco-friendly. In this regard, The leather chemical manufacturing industry has been attempting to produce chemicals which are safe to use and result in zero discharge pollutants from the process. Replacing such systems with environment benign materials is important to make the process sustainable.² The present paper describes design of vegetable oil encapsulated liposomes, stabilized by biopolymers as a lubrication agent. It is expected that these alternative systems may overcome the disadvantages associated with conventional fatliquors while retaining the leather properties as with conventional method.

The unique properties of liposomes favor the encapsulation of a variety of materials. The renowned biocompatibility of these materials has already acquired much significance in food and pharmaceutical industrial applications.³ Besides being active delivery vehicles they protect the cargos, their functional properties and bioactivity. The drawbacks associated with these systems are from their physico-chemical instability towards various factors and subsequent leakage of the

contents at undesired site.⁴In leather processing, Stability of the fatliquor product out of the drum and in the drum conditions is imperative as it affects the penetration of the active material and does its job. Pectin is a bio-polymer contain homogalacturonan backbone, and involves hydrophobic interactions through ester methyl groups and hydrophilic interactions through hydroxyl groups. It is being used in many industrial applications because of its biocompatibility and gelling property.⁵ In the present study, pectin has been used to stabilize the lipid bilayers and to promote oil encapsulation in hydrophobic bilayer region of liposomes.

2 Materials and Methods

Egg phosphatidylcholine (EPC) 65% TLC, pectin from apple, chloroform (HPLC grade) were obtained from Sigma chemicals. Conventionally processed wet blue goat skins, Commercial synthetic, semi-synthetic vegetable based tanning materials have been used for the present study. Different syntans like naphthalene sulphonic acid, acrylic, phenol based, melamine based (commercial grade) obtained from local companies have been used.

Preparation of oil encapsulated liposomes

In a round bottom flask, 1:4 (vol.ratio)ratio of EPC and Castor oil was dissolved in Chloroform and Methanol mixture (9:1). This mixture was shaken well to get homogenous solution and placed on a Rota evaporator to remove the solvent, that results in the solubilization of EPC by the oil. This mixture was further kept in a desiccator overnight in order to remove solvent traces if any. Milli Q water(in the case of EPC-O) and Pectin solution (0.5%W/V) (in the case EPCPEC-O) has been added to this mixture to get a final 20%W/V oil. This solution was fixed to rota evaporator under 50 °C bath conditions. The resulting solution transferred to a separating funnel to remove free oil and pectin.

Determination of particle size and charge

The products EPCPEC-O and EPC-O were diluted 100 times by using Milli-Q water. These dispersions have been analyzed for their particle size by Dynamic Light Scattering technique. A high performance particle sizer (Zetasizer Nano series, Malvern), operating at 4 mW He-Ne laser power, scattering angle of 175° and wavelength of 633 nm was used to determine the particle size.

Optical microscopy

The products (EPC-O, EPCPEC-O) were analyzed for their droplet size and distribution by using an Optical microscope, Trinocular microscope with camera, Carl Zeiss(AxioscopeA2/Axiocam 105). All images were collected at 63X magnification.

Oil encapsulation efficiency

Both EPC-O and EPCPEC-O have been analyzed for oil encapsulation efficiency. These samples were centrifuged at 10000 RPM in a mini-centrifuge for 30 Minutes. The supernatant or the top layer was collected with the help of a syringe and placed in a pre-weighed crucible. This crucible was heated in hot air oven and change in mass readings was collected periodically, this was repeated till no further mass change of the residue was noticed. This final value was expressed as free oil or unbound oil.

Use of the oil encapsulated liposomes for leather lubrication

The efficacy of encapsulated composite products (EPC-O, EPCPEC-O) in leather lubrication was tested and compared with the conventional fatliquors. A Conventional leather processing for automotive upholstery leathers has been adopted for the control leather. Commercially available fatliquors of different class were offered as a total of 18% to the weight of the leather. In case of experimental leather trials, commercial fatliquors were replaced with the products designed in this study(EPC-O, EPCPEC-O).

3 Results and Discussion

The oil encapsulated liposomes (EPC-O) and oil encapsulated liposome-biopolymer composite (EPCPEC-O) have been analyzed for their physico-chemical characteristics by DLS and Optical microscopy.



Figure 1. Visual images of the EPC-O (Left) and EPCPEC-O (Right).

The visual images of the oil encapsulated liposomes are represented Figure1. From the image, it can be observed that free oil gets phase separated from the oil encapsulated liposomes in EPC-O system(Left). Whereas, in the case of EPCPEC-O system, phase separation is observed as oil encapsulated liposomes (organic layer) and aqueous layer containing unbound pectin. The organic layer of the EPCPEC-O system seems to be uniform and viscous. The visual stability of these products was observed over 6 months, and no further layer separation was observed. From Figure.1. it is clear that EPC-O system contains more amount of free oil compared to the EPCPEC-O. The oil encapsulation efficiency of EPC-O system found to be 20% and 95% for the EPCPEC-O system. The DSC results from our studies indicated pectin stabilizes the lipid bilayers (Through its hydrophobic interaction in the bilayer region) associated with an increase in the Enthalpy of the system(Data not shown here). These results suggest that pectin in the EPCPEC-O system stabilizes the lipid bilayers as well as encourages efficient oil encapsulation. The observed Zeta potential values for EPC-O system was -12mV and for the EPCPEC-O, -16mV.

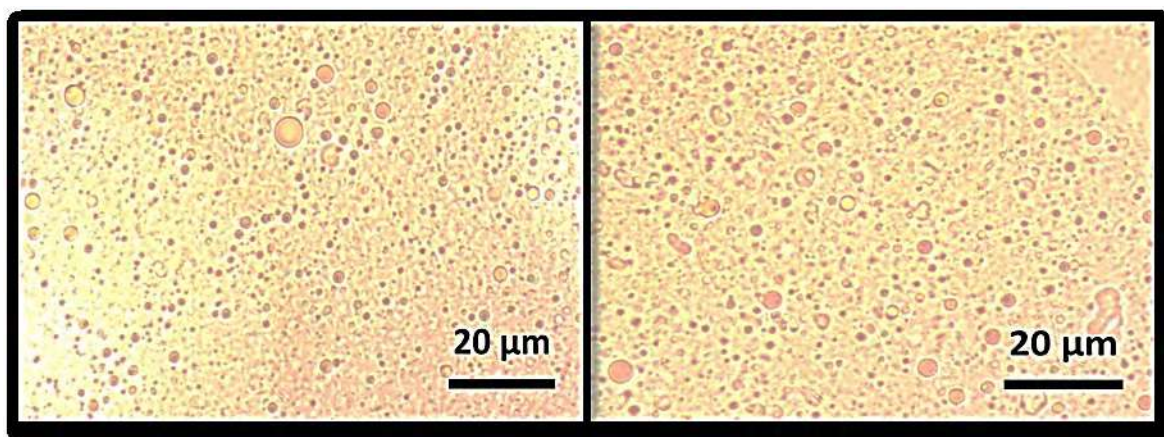


Figure 2. Optical Microscopic images of the EPC-O(Left) and EPCPEC-O(Right), Scale bar represents 63X magnification.

The optical microscopic images of the EPC-O and EPCPEC-O, Figure.2. the average droplet size was found to be around 2.2-2.5 μm for both systems. From the DLS results it is confirmed that particle size of the EPC-O system found to be 1804nm and for the EPCPEC-O 2623nm which is in line agreement with the result observed from the optical microscopy. Stability of the leather auxiliaries and subsequent diffusion into the leather matrix is crucial in manufacturing of leather. Both of these systems was found to form stable droplets in the water medium. In order to understand the triggering factors for the release of the encapsulated materials, a model dye Carboxy Fluorescence was encapsulated and its release pattern on change in the pH and temperature was studied. The results suggest that a rapid release of dye at pH 3 and a temperature above 55 $^{\circ}\text{C}$ was observed. It is well known that the beating action during the leather processing increases the bath temperature, at this conditions the release of the contents were anticipated. The EPC-O and EPCPEC-O systems applied on the leather to evaluate their performance in the leather lubrication. Visual assessment of the leathers carried out independently by 3 experts in a scale of 1-10, indicated that leathers had good roundness and softness. The EPC-O system has surface deposition of oil, possibly due to presence of large unbound oil in it. With the current understanding for softy uppers, the EPCPEC-O system provides good lubrication

4 Conclusion

A stabilized liposomal systems encapsulating oil as a delivery vehicle to deliver its contents under the triggered pH conditions and temperature is described. Biopolymer induced stability and ensures the oil encapsulation in the bilayer region for the composite vesicles. The oil encapsulation efficiency was high for the EPCPEC-O system when compared to EPC-O system. The leathers treated with EPCPEC-O system are soft and round in nature and are comparable with control leather. The leather treated with EPC-O system found to show surface deposition of the oil. The work demonstrates a process towards developing fatliquors based on biodegradable materials, avoiding the emulsifiers and conventional route to make oil in water emulsions, thus helping in optimal use of chemicals, better diffusion and lower pollution load. It is expected that this design and improvement in the process would help in cost and time effective leather process.

References

1. S. Saravanabhavan, J. Raghava Rao, B. Unni Nair and T. Ramasami: *An eco-efficient rationalized leather process*; *J. Chem. Technol. Biotechnol.*, 82, 971-984, 2007
2. N. Bhargavi, M. Venkatesh, K.J. Sreeram, B. Geetha, J. Raghava Rao, B. Unni Nair, A. Baran Mandal: *Emulsifiers-free lubrication process using natural oils dispersions in non-aqueous solvents for leather*; *RSC adv.*, 5, 68981-68990, 2015.
3. M. L. Immordino, F. Dosio and L. Cattel: *Stealth liposomes: review of the basic science, rationale, and clinical applications, existing and potential*; *International journal of nanomedicine*, 1, 297-315, 2006
4. M.-L. Briuglia, C. Rotella, A. McFarlane and D. A. Lamprou: *Influence of cholesterol on liposome stability and on in vitro drug release*; *Drug Delivery and Translational Research*, 5, 231-242, 2015.
1. S.C. D. May: *Industrial pectins: Sources, production and applications*; *Carbohydrate polymers*, 12, 79-99, 1990.

INVESTIGATION ON REDUCING CHROMIUM QUANTITY IN CHROMIUM CONTAINING WASTES OF LEATHER INDUSTRY USING OYSTER MUSHROOM (PLEUROTUS OSTREATUS)

Eser Eke Bayramoğlu^{1*}, Anıl Özçelik², Mehmet Çetin³, Erkan Eren⁴

1,2 Department of Leather Engineering, Faculty of Engineering, Ege University, 35100 Bornova-Izmir, Turkey

3,4 Bergama Technical and Business Collage, Mushroom Programme, Ege University, Bergama-Izmir, Turkey

Abstract. In the leather industry, the shaved wastes after the wet blue phase, which are exposed by the shaving process, are one of the substances that cause environmental pollution for the leather industry. Most of the time, these wastes can be buried and may cause serious environmental pollution. In this study, wet blue shaved wastes to be mineralized to chromium and so prevented oxidise to Cr (VI) by using oyster mushrooms (*Pleurotus ostreatus*). Wet blue shaved wastes were mixed with 0,5%, 1%, 1,5% and 2% doses into the growth medium. After the oyster mushroom growth, the consuming of chromium from the growth media and chromium content that uptaken by the mushroom were investigated with in House Method/ICP-MS.

1 Introduction

Nowadays, pollution in different steps of production in many industrial branches causes serious irremediable problems. [Yılmaz and Özgün, 2016]. Industrial production can be considered as the main reason of global warming, water pollution, air pollution and soil pollution [Ünal and Yılmaz, 2015].

There are many chemicals used in leather industry that cause pollution. Chromium is one of them and it is the most preferred tanning agent in leather industry. 80-90% of leather tanning is performed by Cr (III) salt [European Commission, 2013]. At the end of the chromium tanning, leathers are waited for the chemical reaction to continue. The leathers that become wet blue are shaved for the thickness adjustment. Wet blue shaved waste is one of the biggest factors that cause pollution in leather industry. Commercially, their biological and chemical treatments are endeavored; however, they are not fully succeeded. High amount of chromium is present in shavings. In many countries, these shavings are buried to the ground and ignored but they might cause severe health issues in the future. Due to toxic Cr (IV) and toxic gas outlet, removal of the shavings by burning is not recommended (http://www.mneproje.com/public/website/news/deri-sanayinde-krom-geri-kazanimi_20180924031547.pdf).

Chromate and chromate compounds can be used by plants and they can infiltrate through the deep soil layers causing the pollution in water resources. Chromates can be absorbed to the positively charged soil particles in less amount and they are prevented from convection to the atmosphere. However, unregulated storage of solid wastes containing chromium cause increment of the chromium concentration in soil and cause pollution in water resources [Environmental and Water Resources Institute (U.S.), 2004].

When the waste produced during production or after production in leather industry which contains chromium is buried and if the burying area is not insulated enough, the filtration, transportation or mixing of these wastes to the soil is inevitable. Cr (III) present in the leather is oxidized to Cr (VI) in the nature and creates great problems for being carcinogenic.

Table 1. Evaluation of Cr(III) and Cr(IV) from the point of human health. (IULTCS, IUR-1, August 2013)

Cr (III)	Sensitivity	Does not create sensitivity (no sensitization)
	Acute Toxicity	No harmful or toxic related to impact amount and compound
	Carcinogen	Is not included on CMR list
Cr (VI)	Sensitivity	Does create sensitivity
	Acute Toxicity	Toxic
	Carcinogen	Carcinogen and Mutagen

It has been reported that Cr (III) is generally not including any risk [REACH report Annex XV, Chapter B.5.8 (ECHA 2011)]. Cr (VI) salt is not used in leather processing however Cr (VI) can be observed on finished leathers and this is not an intended feature [Bayramoğlu et al., 2012]. For instance, pH increase during neutralization causes the oxidation of Cr (III) to Cr (VI) or the drying the leather provides a backdrop for the formation of Cr (VI) [European Commission, 2013].

Discharge of heavy metals to the earth and water without disintegration is very important. It cannot be divided to non-toxic forms and leaves therefore a lasting effect on the ecosystem. Most of them are toxic even in very low concentrations. Arsenic, cadmium, chromium, copper, lead, mercury, selenium, silver, zinc, etc. are not only cytotoxic but also carcinogenic and mutagenic in the nature. This fact is clearly observed on several reports which show harmful effects of heavy metals on human health [Shukla et al., 2017].

We have to find effective, cheap and practical solution proposals for the removal of waste chromium without harming the environment if we want to use chromium as tanning material in leather production. It is required that chromium should be disintegrated before turning out to Chromium (IV) at that the quantity of chromium in the environment should be decreased. Bioremediation, in this context, is an innovative and promising methodology for the removal of heavy metal. Micro-organisms, since they have developed new strategies to remain alive in environments including heavy metals, have adapted themselves to various detoxification mechanisms such as biosorption, bio-accumulation, biotransformation and biomineralization. They can thus make ex situ or in situ bioremediation.

Organisms which are mostly used on biological treatments in the scope of waste and environment technology are white rot fungi [Yeşilada, 1995]. Disintegration feature of white rot fungi is determined through various researches. They occupy an important and privileged place due to their characteristics. It is known that white rot fungi included in Basidiomycetes group, play a role in the elimination of environmental pollution shown up due to dense industrial activity, and the oxidation of organic compounds possessing very different molecular structures, together with various enzymes they synthesize, ie: lignin peroxidase (LIP), peroxidase related to manganese (MnP), to begin with laccase (lak) enzyme [Kunamneni et al., 2008; Pease et al., 1991].

Wood destroying *Pleurotus ostreatus* are saprophytic fungi. Easy development and yield on organic materials including lignin and cellulose without requiring any fermentation due to their strong mycelium structure allow the use of different industrial and agricultural wastes in the cultivation of *Pleurotus ostreatus* [Kurt, 2008]. *Pleurotus ostreatus* is resistant to toxic chemicals existing in the nature. It possesses a very strong oxidative biodecomposition potential.

We have tried in this research to show that white rot fungus will mineralize chromium wastes within its body and make them harmless and that the chromium can be decomposed without being oxidized to Cr (VI). Chromium on elementary level does not have any risk for human health is shown on Table 1 [IULTCS, 2013]. Leather wastes with chromium are mixed to the specially prepared compost in the research and chromium quantity existing in the compost before fungus inoculating and after fungus development and chromium quantity transferred to the fungus fruiting body are observed. Besides, impacts of chromium on the development and yield of fungus are also examined.

2 Material and Method

2.1 Material

Wheat straw and wheat bran to be utilized in the research are provided from local suppliers and chromium added leather shaving wastes from “Lider Leather Tannery” located in Menemen Leather Free Zone (Figure 1).



Figure 1. Shaving wastes containing chromium.

Sypra PL 28 (*Pleurotus ostreatus*) type mycelium is used in the test and is provided from the importer company “OPE Agriculture”.

2.2 Method

Nitrogen content of shaving wastes containing chromium is determined through Kjeldhal Method [Standard Methods, 1995].

2.2.1 Assembly of Tests

2.2.1.1. Preparation of Growing Environments

Wheat straw (WS) is used as basic material in the research, and wheat bran (WB) and leather shaving wastes containing chromium (Cr) are used as additives. Mixture rates and codes of growing environments used in the research are given on Table 2.



Figure 2. Preparation of Compost used on Tests.

Substrate prepared from the mixture of wheat straw and wheat bran (WS80+WB20) is used as the admixture (C) in the research. Leather shaving wastes containing chromium mixed in 4 different rates (0,5%, 1%, 1,5% and 2%) with wheat straw and wheat bran are used as control compost.

Table 2. Mixture substrate contents.

Compost Mixture Rates	Code
Wheat Straw (80%) + Wheat Bran (20%) (Mixture)	Control (WS80+WB20)
0,5% Cr + 99,5% Mixture (80% wheat straw + 20% wheat bran)	0,5% Cr
1% Cr + 99% Mixture (80% wheat straw + 20% wheat bran)	1% Cr
1.5% Cr + 98.5% Mixture (80% wheat straw + 20% wheat bran)	1,5% Cr
2% Cr + 98% Mixture (80% wheat straw + 20% wheat bran)	2% Cr

Shaving wastes containing chromium are grinded and sterilized. Every substrate mixture having different chromium dosage is separated into 4 groups and study is conducted with 4 repetitions. Convenient substrate mixture for the growing of *Pleurotus ostreatus* is prepared in Bergama Technical and Business Collage, Ege University. Materials are weighed with predetermined weights by taking percentage of dry substance if their mixture substrate as basis, for the preparation of substrate. Then, mixtures are damped and humidity rate is accessed to 70%.

2.2.1.2. Sterilization and Mycelium Grafting

Mixture substrate are pasteurized, after damping, by boiling in water (70°C) for 2 hours. Substrate are left for cooling after pasteurization and 1% plaster over the basis of weight is added to all mixtures to adjust pH level. Temperature is rapidly decreased to nearly 25°C, by draining excess water on the table possessing perforated grill with ventilation from the bottom. Growing mixtures with decreased temperatures are put into bags of 40x50 cm dimensions, 2 kg of mixtures substrate being in each bag and inoculation is done, by homogenously mixing 2% of the weight of spawn suitable for inoculation. Bags which are inoculated with spawn are compressed and their openings are covered by fastening.



Figure 3. Fungus Growing Room and Pre-tests.

2.2.1.3 Incubation and Harvest

Inoculated bags were incubated at 25°C±2°C temperature and 70-80% humidity during incubation period (15 days) until mycelium colonized. Bags are perforated after full colonization, for the induce fructification. Temperature is adjusted to 15°C±2°C in the production room to promote fungus formation, and the humidity is increased up to 85-90%.



Figure 4. Monitoring system of fungus production room which adjusts required parameters for fungus development.

12 hours of illumination with fluorescent lamps of 200 lux intensity is provided per day [Delmas and Mamoun, 1983]. Fresh air is supplied to the production room to promote primordium formation, and CO₂ level is gradually decreased. Mushrooms are harvested by cutting with a knife after having reached a giving size. Chromium contents existing in the substrate and mushroom fruiting body are determined in “Argefar Lab., Ege University” through ICP-MS In House Method.

2.2.2 Statistical Evaluation

Tests related to mushroom development and yields are structured with 4 repetitions, 4 bags existing on each repetition, according to random plots test design [Düzgüneş et al., 1983]. Variance analyses of data obtained are done through SPSS (ver. 17.0 for Windows) statistical program and Duncan Test of Multiple Comparisons is used for groupings.

Wilcoxon Signed Ranks Test is applied to prove whether there is any difference or not on statistical meaning in chromium quantity within the mushroom and compost samples collected before the spawning of *Pleurotus ostreatus* and after the harvest [Özdamar, 2011].

Kruskal-Wallis Test is applied to prove whether there is any meaningful difference or not on determined Cr rates (0,5%, 1%, 1,5% and 2%)[Özdamar, 2011].

3 Results and Discussion

Nitrogen content in shaving wastes containing chromium is determined as 14,18% . Fungi of *Pleurotus* genus are cellulosic [Silva et al., 2012]. Even if nitrogen content may show a development on substrates which have a nitrogen content from 0,03% to 1,0% [Machado et al., 2015], the best development is observed on 1,0% rate.

Addition to growing media of leather waste with chromium content is kept on rather low level due high N content. Correspondingly, N percentage content obtained from admixture substrate is given on Table 3.

Table 3. Composts possessing different chromium dosages.

Substrate	N (%)
Control (C)	0,84
0,5 % (Cr)	1,02
1,0 % (Cr)	1,17
1,5 % (Cr)	1,27
2,0 % (Cr)	1,44

Mushroom development is determined during the research, on tests conducted on 5 different groups. It is observed that the mushroom has incorporated the chromium to its body and that chromium quantity is decreased in the environment when chromium quantity is examined before spawning after the preparation of compost and after the harvest. Arithmetic means of these values are seen on Table 4 whereas arithmetic means of chromium left in the compost before and after spawning are seen on Figure 5. Chromium quantity existing in shaving waste containing chromium

is also examined during tests and 42330 mg/kg Cr content is determined in shaving waste through ICP-MS In House Method.

Table 4. Arithmetic means of Cr quantity left in the compost before and after mycelium inoculation and the one incorporated into the fungus fruiting body.

Compost (wet blue shaving dust)	Before <i>Pleurotus ostreatus</i> spawn inoculation (mean) (media) (Cr)	After <i>Pleurotus ostreatus</i> harvest (mean) (media) (Cr)	(Cr) within <i>Pleurotus ostreatus</i> fruiting body
0% (Control)	4,33 mg/kg	-	0,122 mg/kg
0,5% (Cr)	530 mg/kg	177,8 mg/kg	0,372 mg/kg
1% (Cr)	724 mg/kg	205,6 mg/kg	0,361 mg/kg
1,5% (Cr)	6374 mg/kg	482,8 mg/kg	0,568 mg/kg
2% (Cr)	11690 mg/kg	951,1 mg/kg	0,422 mg/kg

Kruskal-Wallis test is applied to examine whether Cr rate affects or not the capacity of *Pleurotus ostreatus* to incorporate into its body the Cr existing in the compost. H_0 is rejected according to test result obtained (Asymp. Sig. < 0.05). This fact proves that Cr rates create an important difference from the statistical point of view, on the capacity of *Pleurotus ostreatus* to incorporate Cr into its body.

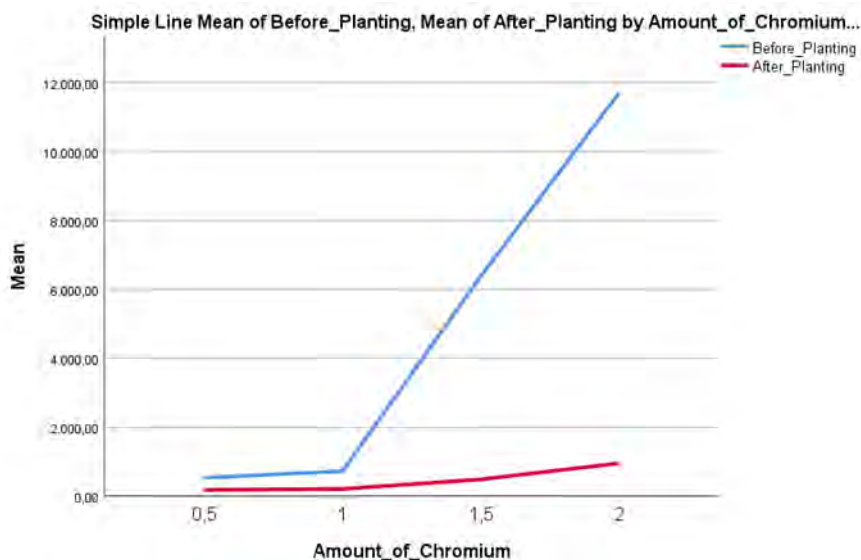


Figure 5. Statistical diagram graph of the chromium content in the media- before mycelium inoculation and after the harvest.

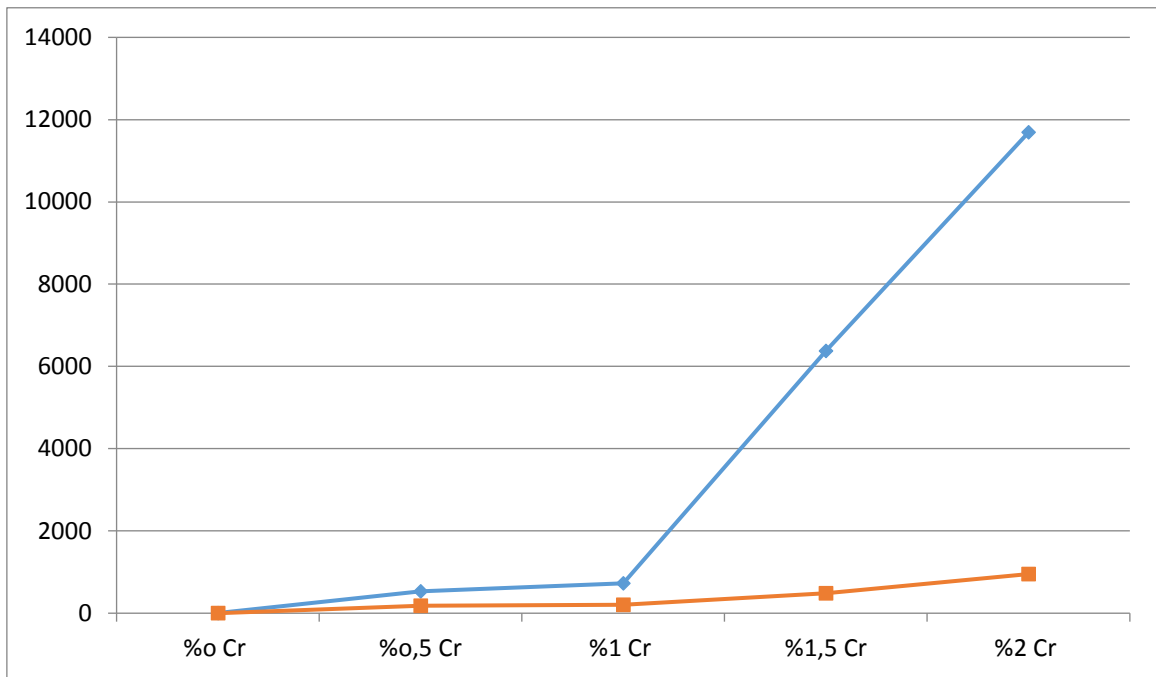


Figure 6. Arithmetic means diagram of Cr quantity left in the compost before mycelium inoculation and after the harvest.

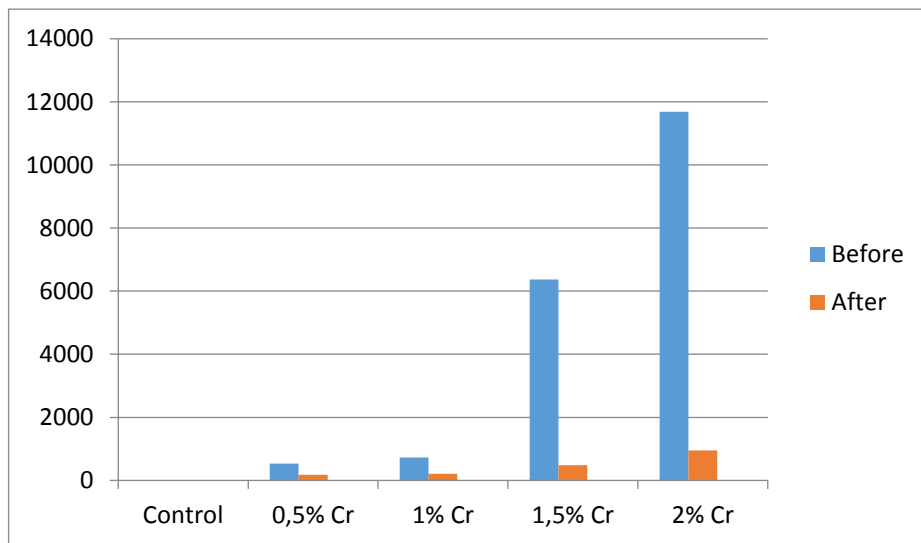


Figure 7. Chromium quantity left in the compost before the mycelium inoculation and after the harvest.

Under analyses done, it has been determined that *Pleurotus ostreatus*, while uptake into its body the chromium from convenient growing media containing shaving waste with different chromium rates, achieves the highest rate when 1,5 % is added to the compost (Figure 8).

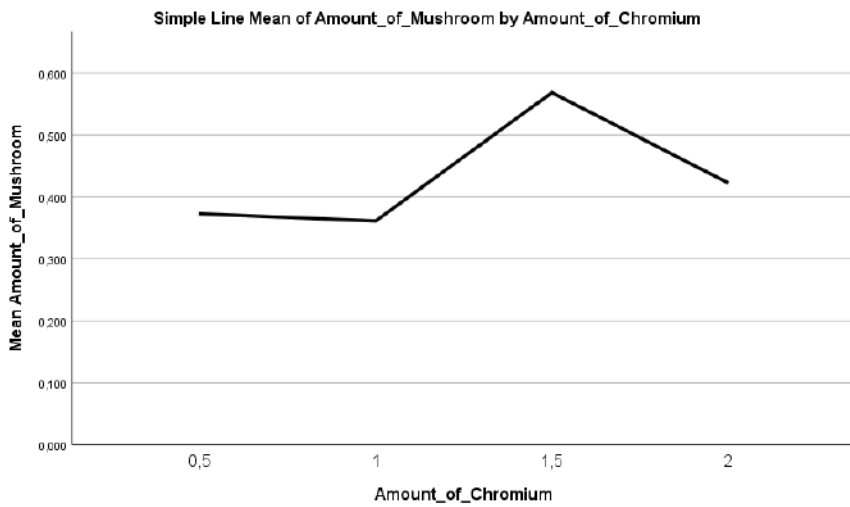


Figure 8. Uptake rate of chromium into the mushroom fruiting body.

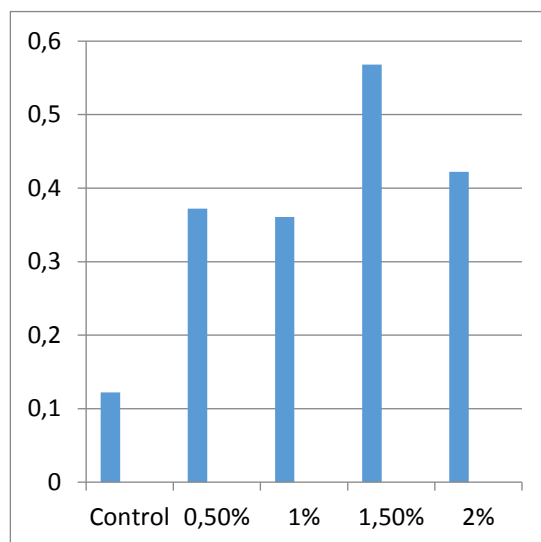


Figure 9. Chromium quantity the mushroom uptakes into its body in different compost contents.

The difference between compost mixed with shaving waste containing chromium with different rates and mushroom yield values obtained in the test conducted with the admixture substrate is determined as important statistically speaking. According to results of the study seen on Table 6, whereas the highest yield is obtained from the compost to which 1,5% shaving waste containing chromium is added (214,81 g/kg), 35% yield increase is observed when compared to the mixture (WS80+WB20) environment (159,00 g/kg). The lowest yield is obtained from control application. Substrate where 0,5%, 1,0% and 2,0% shaving waste containing chromium are included in the same group and yield increase of 14-26% is obtained when compared to the control [Yang et al., 2013]. Indicated that he obtained a yield of 214,6 g/kg from the substrate he prepared with WS80 (wheat straw) + WB20 (wheat bran). In another study, the yield of *P. ostreatus* in wheat straw growing media is indicated as 175 g/kg compost [Yıldız et al., 1998] and 246,5 g/kg compost [Küçükomuzlu and Pekşen, 2005]. [Kurt and Büyükalaca, 2008] indicated through the study conducted, the highest yield obtained from 2 WS (wheat straw) + WB (wheat bran) media (300,24 g/kg). It can be observed that yield values obtained in this study are coherent with data of these researchers.

Table 5. Physical measurements of mushroom grown in different compost contents.

Substrate	Yield (g/kg)	Quantity of mushroom (pcs/kg)	Cap Diameter (mm)	Stalk Diameter (mm)	Stalk Length (mm)
Control (Mixture) (WS80+WB20) (0%)	*159 ^b	*20,69 ^b	69,43 ^{ns}	9,71 ^{ns}	24,08 ^{ns}
0,5%Cr+99,5% Mixture	195,69 ^b	30,25 ^a	68,26	9,54	21,13
1,0% Cr+99% Mixture	200,06 ^{ab}	33,20 ^a	75,06	10,00	19,38
1,5% Cr+98,5% Mixture	214,81 ^a	33,44 ^a	74,17	9,92	24,29
2,0% Cr+98% Mixture	180,81 ^{ab}	30,50 ^a	69,12	10,46	24,42

Asterisks indicate significance at * $P < 0.05$, ^{ns} not significant; values within the same column followed by the same letter are not significantly different according to Duncan test.

In another study, it is indicated that high N quantity caused yield decrease on *Pleurotus* types [Desrumeaux et al., 2003]. Concordantly, yield value obtained in the study from 2.0 shaving containing chromium, where N content is higher indicated a decrease when compared to yield values obtained from substrates prepared with other shavings containing chromium.

The difference between the quantity of caps obtained from compost media mixed with different rates of shaving waste containing chromium and the test conducted with the control media is determined as important statistically speaking. When Table 5 is examined and concerning the quantity of caps obtained during the test from different compost media, the highest quantity of caps (33,44 pieces) is obtained from the substrate where 1,5% shaving containing chromium is added (Figure 8). Then we have substrates where 1% (33,20 pieces), 2% (30,50 pieces) and 0,5% (30,25 pieces) shaving containing chromium is added respectively. All substrates where shaving containing chromium is added are included in the same group. The lowest quantity of caps is obtained from the control media with 20,69 pieces.



Figure 8. Mushroom which are grown in mushroom production room, developed in compost media with 1,5% chromium dose and which are available for harvest.

Differences among values concerning cap diameter, stalk diameter and stalk length are not considered as important.

4 Conclusion

It has been understood through the study that *Pleurotus ostreatus* can easily develop and grow on leather shaving waste containing chromium and mineralize the chromium element by incorporating it in a certain extent into its body, when optimum conditions are provided. An important difference is determined in the quantity of chromium in the compost concerning composts prepared by adding different doses shaving waste containing chromium. The existence of chromium in the compost did not create any question in *Pleurotus ostreatus* growing from the stand point of mushroom development. On the contrary, a yield increase is observed due nitrogen existing in leather shaving waste containing chromium. However, though nitrogen rate is the highest in the compost having 2% rate of shaving waste containing chromium, the yield and chromium absorption are not at the maximum rate. As a reason we may say that high rate of nitrogen creates a negative impact for the development of *Pleurotus ostreatus*, and this point is coherent with the study of Desrumeaux et al., 2003.

When we compare both from the stand point of uptake of chromium to the body and high yield, most successful results are observed on fungi developed on the compost where 1,5% shaving containing chromium is added.

It has clearly been determined as the result of our study that chromium does not have any negative impact for the development of *Pleurotus ostreatus*. Moreover, *Pleurotus ostreatus*, mineralizes the chromium by uptaking it to its body and decomposes it from the environment. We showed with this study that *Pleurotus ostreatus* can be used as mycoremediation in leather wastes containing chromium. Edibility of fungi obtained is the subject of another research. On the other hand, whether these mushroom can be used as fertilizer or animal feed should also be searched. The mushroom obtained can also be used for several different purposes as chromium source. This study conducted is a basic research which can light the way for many scientists.

Acknowledgement

The authors would like to thank to Ege University Scientific Research Project Department Directorate for the financial support they provided (Project No: 16-MUH-102). The authors also acknowledge the project of "Industrial Doctorate Program of Textile and Leather-2007 DPT 001" supported by T.R. Ministry of Development.

References

1. Argefar: Ege University, ICP-MS In House Method, EPA Methods 3051 Feb. 2007 and NMKL No:186, 2007
2. Bayramoğlu E.E., Önem E., Yorgancıoğlu A., Reduction of Hexavalent Chromium Formation in Leather with Various Natural Products (*Coridothymus capitatus*, *Olea europaea*, *Corylus avellana* and *Juglans regia*), *Ekoloji*, 114-120, 2012
3. Delmas, J. Mamoun, M.: *Le Pleurote en Corne D'abondance un Champignon Aujourd'hui Cultivable en France*, P.H.M.-Revue Horticóule, 240, 39-46, 1983
4. Desrumeaux B., Sedeyn P., Desmedt H., Lannoy, P., Leenneght, L.: Addition of Intact Corn Grain Before Pasteurization to Oyster Mushroom Substrate (*Pleurotus spp.*), *Horticultural Abstracts*, 73(5):47-61, 2003
5. Düzgüneş, O., Kesici, T. ve Gürbüz, F.,: İstatistik metotları I, Ankara Üniversitesi Ziraat Fakültesi yayınları, no: 861, Ders Kitabı, Ankara, 1983
6. Environmental Agency (EA). *Reporting the Evidence: Dealing with Contaminated Land in England and Wales. A Review of Progress from 2000-2007 with Part 2A of the Environmental Protection Act*. Available online: https://www.gov.uk/government/uploads/system/uploads/attachment_data/file/313964/geho0109bpha-e-e.pdf (accessed on 1 January 2015)
8. Environmental and Water Resources Institute (U.S.): *Natural Attenuation Task Committee, Natural attenuation of hazardous wastes*, American Society of Civil Engineers, USA, 2004
9. European Commission, *JRC Reference Reports: BAT Reference Document for the Tanning of Hides and Skins*. İspanya: Lüksemburg Avrupa Birliği Ofisi, 2013

10. International Union of Leather Technologists and Chemists Societies, IUR – 1, 2013
11. Kunamneni, A., Ghazi I., Camarero, S., Ballesteros, A., Plou, F.J., Alcalde, M.: Decolorization of Synthetic Dyes by Laccase Immobilized on Epoxyactivated carriers, *Process Biochemistry*, 43(2), 169-178, 2008
12. Kurt, Ş and Büyükalaca, S.: Değişik Tarımsal Atıkların *Pleurotus ostreatus* Yetiştiriciliğinde Kullanım Olanaklarının Araştırılması, *Türkiye VIII. Yemeklik Mantar Kongresi*, 2008
13. Kurt, Ş.: Değişik Tarımsal Artıkların Kayın Mantarı (*Pleurotus Ostreatus*, *Pleurotus Sajor-Caju*) Yetiştiriciliğinde Kullanım Olanakları, *Çukurova Üniversitesi Fen Bilimleri Enstitüsü*, 2008
14. Küçüközlü, B., Pekşen, A.: Yetiştirme Ortamı Ağırıklarının *Pleurotus* mantar Türlerinin Verim ve Kalitesi Üzerine Etkileri, *OMÜ Zir. Fak. Dergisi*, 20(3):64-71, 2005
15. Machado, A.R.G., Teixeira, M.F.S., Kirsch, L.S., Campelo, M.C.L., Oliveira, I.M.A.: Nutritional Value and Proteases of *Lentinus Citrinus* Produced by Solid State Fermentation of Lignocellulosic Waste from Yropical Region. *Saudi J. Biol. Sci.*, 2015
16. Nitrogen 4500-Norg-C Semi micro Kjeldahl "Standard Methods" for the Examination of Water and Wastewater, APHA 19th Edition, Washington 1995
17. Özdamar, K.: Paket Programlar ile İstatistiksel Veri Analizi-1, MINITAB 15- PASW 18, 8.Baskı, 2011
18. Pease, E.A., Aust, S.D., Tien, M.: Heterologous Expression of Active Manganese Peroxidase From *Phanerochaete Chrysosporium* Using The Baculovirus Expression System. *Biochemical and Biophysical Research Communications*, 179, 897-903, 1991
19. Shukla, D.P., Mishra A.Y., Vaghela K.B., Jain, N.K.: Eco-Friendly Approach for Environment Pollution: A Review on Bioremeditaion, 6956-6961, 2017
20. Silva, M.C.S, Naozuka, J., da Luz, J.M.R., de Assunção, L.S., Oliveria, P.V., Vanetti, M.C.D., et al.: Enrichment of *Pleurotus ostreatus* Mushrooms with Selenium in Coffe Husks. *Food Chem.* 131, 558-563, 2012
21. Ünal Z.B, and Yılmaz S.: Environmental Damages Of Textile Industry And Its Role in the Global Climate Change XII th International Izmir Textile And Apparel Symposium, 2015
22. Yang, W.J., Guo, F.L., Wan, Z.J.: Yield and Size of Oyster Mushroom Grown on Rice/Wheat Straw Basal Substrate Supplemented with Cotton Seed Hull. *Saudi Journal of Biological Sciences*, 20, 333-338, 2013
23. Yeşilada, Ö.: Decolorization of Crystal Violet by Fungi, *World Journal of Microbiology and Biotechnology*, 11, 601-602, 1995
24. Yıldız, A., Karakaplan, M., Aydın, F.: Studies on *Pleurotus ostreatus* (Jacq. ex Fr.) Kum Var. *Salignus* (Pers ex. Fr.) Konr. Et Maubl.: Cultivation, Proximate Composition, Organic and Mineral Composition of Carpophores. *Food Chemistry*, 61 (1/2):127-130, 1998
25. (http://www.mneproje.com/public/website/news/deri-sanayinde-krom-geri-kazanimi_20180924031547.pdf)-22.05.2019
26. Yılmaz S. and Özgün S.: Recycling Possibility Of Buildings Destroyed In The Last 5 Years Due To Terror In Turkey And The WarIn Syria. *European Scientific Journal*, 47-55, 2016

BIOTECHNOLOGY FOR ENVIRONMENT-FRIENDLY LEATHER PRODUCTION

J. Y. Liu^{1,a} and G. Holmes¹

¹ New Zealand Leather and Shoe Research Association

Fitzherbert Science Centre Dairy Farm Road, Palmerston North 4414, New Zealand

a) Corresponding author: john.liu@lasra.co.nz

Abstract. LASRA research is guiding the application of biotechnology to help the New Zealand leather industry develop environmentally sustainable leather processes. Using 16S rRNA gene sequencing, we have isolated and identified a number of indigenous bacteria from the leather industry environment which are being adopted to develop benign leather processing technologies. We isolated and identified several *Bacillus* strains from a biofilter used in a leather manufacturing plant which exhibited sulphide oxidation activity, which are being applied in bioremediation of volatile organosulphur compounds emitted by leather products. We also discovered a strain of *Stenotrophomonas* spp. with significant and beneficial proteolytic activity in a tannery sludge. The identified strain not only displays collagenase activity but also the ability to reduce hexavalent chromium to trivalent chromium, making it an ideal candidate for biodegradation of tanned waste. Recently we revisited the natural autolytic processes of degradation of untreated pelts to guide a natural depilation method without any need for additional chemical treatment. In controlled experiments the wool could be removed completely from follicle after 2 days, without obvious damage and leathers could be processed with mechanical properties comparable to conventionally processed counterparts. The alkaline protease activity of the isolated bacteria is responsible for the observed natural unhairing.

1 Introduction

Leather production not only serves social needs by utilising a meat by-product such as hide and skin, but also contributes significantly to the global economy through trade and employment. But the social image of the leather industry has become negative with increasing awareness of environmental protection and the demand among consumers for products made in a sustainable way with less environmental impact. In line with New Zealand's global reputation of being an eco-friendly country, the New Zealand leather industry has committed to improving its environmental performance and image by adopting sustainable practice throughout the production process and providing high quality leather products with reduced environmental impact during their life cycle (Collins, Roper & Lawrence, 2010; Zhang, et al., 2018). Chemicals extensively used during leather production have also been regarded as a source of unpleasant odour sometimes emitted from leather products, especially in cabin upholstery (Wang, Ma, Chen, Sun & Fan, 2018). In certain regional markets, such as Asia, consumer concerns about the indoor or in-cabin air quality relate odour emission with health threats, which impacts their purchase decisions on leather products (Pan, Walsh, Dearth & Zhang, 2017). Besides consumers' preference, the odour has been proved to be caused mainly by volatile organic compounds (VOCs) which are indeed harmful at high concentrations (Dai, et al., 2017). Concerns for indoor air quality and consumers' health have driven the implementation of legal regulations applicable to the emission limits of VOCs from products, including leathers, which are becoming increasingly strict (Xu, Chen & Xiong, 2018). Therefore, the development of leathers with low VOC emissions will not only ensure improved market acceptance, but also contribute to a healthier indoor environment.

Biotechnology such as enzymatic processing has been considered a realistic substitute for current leather production practice (Thanikaivelan, Rao, Nair & Ramasami, 2004). Proteolytic enzymes including alkaline protease and keratinase have been investigated for their potential to replace the large quantities of chemicals used in the unhairing step, which is the most polluting operation (Rao,

et al., 2017; Giongo, Lucas, Casarin, Heeb & Brandelli, 2007). Since the raw materials used and waste generated during leather production are generally proteinous, the leather industry environment could serve as an ideal resource for the discovery of microbes producing useful proteolytic enzymes. Guiding the application of sustainable biotechnologies to assist the transition of the New Zealand leather industry (Naffa, Edwards & Norris, 2019; Naffa, et al., 2019), LASRA has developed the capability to identify potentially valuable microorganisms from the local industrial environment including storage, sludge, compost, etc. The identification of bacterial species is carried out routinely at LASRA by 16S rRNA gene sequencing, which has been widely applied to study bacterial phylogeny and taxonomy, as this conservative gene is believed to be the most common housekeeping genetic marker in almost all bacteria (Langille, et al., 2013). LASRA is also establishing platforms to characterise and produce useful microbial enzymes, which could be applied in alternative leather processes. While cleaner enzymatic processes are still being developed, issues related to VOCs emitted from leather products can be addressed by deploying VOC consuming bacteria during conventional leather production. As the oldest biological method for removal of undesirable gaseous compounds from air, biofiltration uses microorganisms as the engine of the biotreatment process (Delhoméie & Heitz, 2005). Because biofilters operate as fixed-bed bioreactors with immobilised active microorganisms, it is reasonable to hypothesize that VOC metabolising-bacteria can be isolated from biofilters dealing constantly with such pollutants, such as those used by tanneries.

In the present study, bacteria with the potential to benefit sustainable leather production were isolated from the New Zealand leather industry environment. Isolated strains were identified using 16S rRNA gene sequencing. A preliminary investigation of the impact of bacterial activity on leather performance was also carried out. Detailed characterisation of the properties of the identified bacterial strains, such as VOC metabolism, hexavalent chromium reduction, enzymatic activity and substrate specificity, etc. will be reported elsewhere separately.

2 Materials and Methods

2.1 Bacteria isolation

Bacteria with odour mitigation potential were isolated from the soil bed of a biofilter used by a New Zealand tannery. A sample of the soil was mixed with phosphate-buffered saline (PBS) solution to prepare a 10% (w/v) suspension. Serial dilutions of the soil suspension were plated onto LB agar plates, which were then incubated at 37 °C. Colonies with visually distinguishable morphology were selected for further studies.

Bacteria with proteolytic potential were isolated from sludge and sheepskins. Sludge samples collected from LASRA's tannery waste treatment plant were suspended in PBS to prepare 10% (w/v) suspensions. Sheepskins were freshly provided by a local slaughterhouse and cut into halves along the backbone. The right halves were depilated conventionally as a control, and the left halves were kept at ambient temperature until the wool could be manually removed. A piece of skin sample was then taken from each left half and a bacterial suspension was prepared by placing each skin sample in a 50 mL centrifuge tube containing 20 mL PBS solution shaken at room temperature for 4 hours at 200 rpm. Serial dilutions of the bacterial suspensions were plated onto LB agar plates with 2.5% (w/v) skimmed milk at 37 °C. The proteolytic activity was detected by the formation of translucent halos around the individual colonies, which was a result of the hydrolysis of casein in the milk.

2.2 Bacterial identification

Identification of the isolated bacterial strains was carried out by 16S rRNA gene sequencing. The candidate colonies were picked up and cultured in 5 mL LB broth medium for 24 h at 37 °C. Genome

DNA from each culture was extracted and 16S rRNA genes were amplified by PCR using primer pair 27F and 1427R. DNA electrophoresis with 2% agarose gel was employed to verify the successful amplification of the 16S rRNA genes from all the candidate colonies. The PCR products were purified before being submitted to Massey Genome Service for sequencing. The sequencing results were analysed using the Targeted Loci Nucleotide BLAST and the phylogenetic trees were constructed using the Neighbour-Joining method with p-distance.

2.3 Physical Properties of Crust Leathers

Sheepskins were processed into crust leathers following LASRA's standard protocol. Physical properties examined included tear strength, tensile strength and percentage elongation at break, and grain crack resistance. Comparison was made using 4 samples from each half of skin and each group consisted of 3 skins.

3 Results and Discussions

3.1 Bacteria with odour mitigating potential

The biofilter facility used by a New Zealand leather manufacturer was found to be supportive of the growth of plants within it. The air emitted from the production hall after filtration through the soil bed did not provoke any noticeable perception of unpleasant odour. From the soil sample collected in the biofilter 4 *Bacillus* species were identified as potential candidates responsible for the removal of odorous compounds during filtration of the gaseous waste emitted by the leather manufacturer.

These bacteria have been reported to promote plant growth mainly through nitrogen fixation (Yousuf et al., 2017), which was consistent with the overall observation of the biofilter facility where healthy plants were thriving across the entire soil bed of the biofilter. These species have previously been characterised as being interactive with sulfur and ash from coal (Abdel-Khalek & El-Midany, 2013), indicating their potential application in the bioremediation of leather odour by metabolising the sulfur-containing volatile compounds emitted from leather products. In other research at LASRA, the volatile compounds emitted by New Zealand leather products have been profiled to identify the odorous molecules, serving as targets to be mitigated by bioremediation (data not shown). The metabolism of the identified compounds by the *Bacillus* species isolated in this study has been examined to reveal the responsible bioremediation mechanisms and the results of this will be reported separately soon. Comparison between the volatile profile of leather products before and after bacterial treatment will demonstrate the efficacy of the proposed strategy for leather odour mitigation. Additionally, the identified species strongly inhibit the growth of pathogenic fungi across a wide range of host plants (Liu, Wei, Zhu, Du & Feng, 2008). Therefore, in addition to reducing unpleasant leather odours, the identified strains might be applied to develop novel biocontrol methods, to prevent damage to leather caused by fungi.

3.2 Proteolytic Bacteria in Tannery Sludge

Consistent with LASRA's previous finding on the proteolytic potential of tannery sludge, the present study isolated and identified the responsible bacterial strain from the sludge treatment. From 16S rRNA gene sequencing and phylogenetic analysis, the dominant strain in the tannery sludge exhibited 99% sequence identity with a *Stenotrophomonas* strain.

Members of the genus *Stenotrophomonas* have been reported to have keratinase activity (Fang, Zhang, Liu, Du & Chen, 2015) and also to reduce hexavalent chromium to benign trivalent chromium (Raman, Asokan, Sundari & Ramasamy, 2018). Our preliminary experiments have revealed that the

identified strain exhibits collagenase activity as well as tolerance to hexavalent chromium (data not shown). These results suggest that this strain might usefully contribute to the biodegradation of tanned leather waste. Currently we are optimising the enzyme production conditions and the bioremediation of hexavalent chromium. The activity of enzymes produced by the identified strain, including collagenase, keratinase, lipase, neutral protease, and alkaline protease are currently being characterised. The application in beamhouse operations of proteases produced by the identified strain is also being investigated with promising progress and the results will be reported soon.

3.3 Bacteria Responsible for Natural Wool Loosening

The natural wool loosening induced by microbial protease has attracted interest for a long time (Green, 1955). In the present study, it was found that after storage for 48 hours, the wool throughout the skin could be removed by pulling effortlessly, leaving empty follicles and a slightly damaged grain. Proteolytic bacteria on the skins which might be responsible for the observed natural wool loosening were identified as *Aeromonas* spp, *Proteus* spp, and *Wohlfahrtiimonas* spp.

Aeromonas spp has long been known to produce extracellular proteolytic enzymes (O'Reilly & Day, 1983). *Proteus* species secrete protease as one of the virulence factors associated with the infection process and disease (Yu et al., 2017). Among strains of *Proteus* spp., one identified in this study has previously been found to be present as one of the bacterial strains causing wool loosening (Maxwell & Lennox, 1944). *Wohlfahrtiimonas* spp has been demonstrated to be associated with myiasis, infection with the larvae of parasitic flies (Campisi, Mahobia, & Clayton, 2015). The strong chitinase activity of *Wohlfahrtiimonas* spp may play a role in the metamorphosis of the fly (Schröttner et al., 2017). *Lucilia sericata* larvae linked to the infection of *Wohlfahrtiimonas* spp are used as an alternative treatment for recalcitrant and chronic wounds, which could be attributed to the various peptidases within the excretions secretions (Franta et al., 2016). While the effect of chitinases on the depilation of sheepskin is still inconclusive, the proteolytic enzymes from maggots might contribute to the natural unhairing process.

In a subsequent study, the protease activity and the substrate specificity of the enzymes secreted by the identified strains has been determined and will be published soon. The potential enzyme candidate can be produced by fermentation and applied, experimentally, replace lime and sodium sulphide in the depilation process. The methods developed using sheepskin as a model can also be adopted on other materials such as cow hides. The noteworthy bacteria-associated maggots' activities will be investigated to enhance biodegradation of leather waste.

3.4 Physical properties

The crust leathers obtained from conventional chemical depilation and natural wool loosening were examined for their physical properties. As shown in Table 1, leathers produced from natural processing presented comparable strength properties to their chemically processed counterparts, such as tear strength, tensile strength, elongation. It is noteworthy that the grain crack resistance of the leathers processed with natural wool loosening is significantly high than that of the leathers processed traditionally. The improvement in the physical characteristics of leather processed from skins with natural wool loosening might be attributed to improved uptake of tanning chemicals which has been observed in enzymatically processed leather (Ranjithkumar, Durga, Ramesh, Rose, & Muralidharan, 2017).

Table 1. Physical properties crust leathers.

Group	Tear strength (N/mm)		Tensile strength (N/mm ²)		% Elongation at break		Grain load (N)	Grain extension (mm)
	Parallel	Perpendicular	Parallel	Perpendicular	Parallel	Perpendicular		
Chemical	31.0 ± 3.8	24.6 ± 8.6	11.7 ± 0.77	5.9 ± 0.7	50.3 ± 17.8	175.3 ± 11.5	6.1 ± 3.2	6.0 ± 0.4
Natural	27.0 ± 6.4	17.5 ± 6.2	14.2 ± 3.27	5.0 ± 2.3	47.1 ± 8.2	140.1 ± 67.9	39.8 ± 5.4*	11.1 ± 0.9*

* indicates statistically significant differences ($p < 0.05$).

4 Conclusions

Our research is aimed at enabling the New Zealand leather industry to produce high quality leather products with a much-reduced environmental footprint. The application of biotechnology helps the leather industry adopt a more sustainable practice. Our results demonstrate that the VOC profile of leather products can be improved by treatment with bacteria isolated from a biofilter. The bacteria isolated from sludge treatment presented protease activity, which is being investigated for biodegradation of leather waste as well as enzymatic depilation of hide and skin. Extracellular protease producing bacteria were isolated from locally-sourced sheepskins. The crust leathers processed from skins influenced by those bacteria presented comparable or even improved physical properties, compared with their conventionally-processed counterparts.

References

1. Abdel-Khalek, M. A., & El-Midany, A. A. (2013). Application of *Bacillus subtilis* for reducing ash and sulfur in coal. *Environmental earth sciences*, 70(2), 753-760.
2. Campisi, L., Mahobia, N., & Clayton, J. J. (2015). *Wohlfahrtiimonas chitiniclastica* bacteremia associated with myiasis, United Kingdom. *Emerging Infectious Diseases*, 21(6), 1068.
3. Collins, E., Roper, J., & Lawrence, S. (2010). Sustainability practices: trends in New Zealand businesses. *Business Strategy and the Environment*, 19(8), 479-494.
4. Dai, H., Jing, S., Wang, H., Ma, Y., Li, L., Song, W., & Kan, H. (2017). VOC characteristics and inhalation health risks in newly renovated residences in Shanghai, China. *Science of The Total Environment*, 577, 73-83.
5. Delhoménie, M. C., & Heitz, M. (2005). Biofiltration of air: a review. *Critical reviews in biotechnology*, 25(1-2), 53-72.
6. Fang, Z., Zhang, J., Liu, B., Du, G., & Chen, J. (2015). Insight into the substrate specificity of keratinase KerSMD from *Stenotrophomonas maltophilia* by site-directed mutagenesis studies in the S1 pocket. *RSC Advances*, 5(91), 74953-74960.
7. Franta, Z., Vogel, H., Lehmann, R., Rupp, O., Goesmann, A., & Vilcinskas, A. (2016). Next generation sequencing identifies five major classes of potentially therapeutic enzymes secreted by *Lucilia sericata* medical maggots. *BioMed research international*, 2016.
8. Giongo, J. L., Lucas, F. S., Casarin, F., Heeb, P., & Brandelli, A. (2007). Keratinolytic proteases of *Bacillus* species isolated from the Amazon basin showing remarkable de-hairing activity. *World Journal of Microbiology and Biotechnology*, 23(3), 375-382.
9. Green, G. H. (1955). The recovery of wool from sheepskin pieces. *Journal of Applied Chemistry*, 5(7), 296-313.
10. Langille, M. G., Zaneveld, J., Caporaso, J. G., McDonald, D., Knights, D., Reyes, J. A., ... & Beiko, R. G. (2013). Predictive functional profiling of microbial communities using 16S rRNA marker gene sequences. *Nature biotechnology*, 31(9), 814.
11. Liu, W. W., Wei, M. U., Zhu, B. Y., Du, Y. C., & Feng, L. I. U. (2008). Antagonistic activities of volatiles from four strains of *Bacillus* spp. and *Paenibacillus* spp. against soil-borne plant pathogens. *Agricultural Sciences in China*, 7(9), 1104-1114.
12. Maxwell, M. E., & Lennox, F. G. (1944). Bacteria responsible for the loosening of wool on sheepskins. *Nature*, 154(3899), 118.
13. Naffa, R., Edwards, P. J., & Norris, G. (2019). Isolation and characterization of collagen type I crosslink from skin: high-resolution NMR reveals diastereomers of hydroxylysine norleucine crosslink. *Amino acids*, 1-11.
14. Naffa, R., Maidment, C., Ahn, M., Ingham, B., Hinkley, S., & Norris, G. (2019). Molecular and structural insights into skin collagen reveals several factors that influence its architecture. *International journal of biological macromolecules*, 128, 509-520
15. O'reilly, T., & Day, D. F. (1983). Effects of cultural conditions on protease production by *Aeromonas hydrophila*. *Appl. Environ. Microbiol.*, 45(3), 1132-1135.
16. Pan, A., Walsh, A., Dearth, M., & Zhang, X. Q. (2017). Validating Target Compounds to Vehicle Interior Odor Complaints by Reconstituting Their Concentrations in Vehicles (No. 2017-01-0324). SAE Technical Paper.
17. Raman, N. M., Asokan, S., Sundari, N. S., & Ramasamy, S. (2018). Bioremediation of chromium (VI) by *Stenotrophomonas maltophilia* isolated from tannery effluent. *International journal of environmental science and technology*, 15(1), 207-216.
18. Ranjithkumar, A., Durga, J., Ramesh, R., Rose, C., & Muralidharan, C. (2017). Cleaner processing: a sulphide-free approach for depilation of skins. *Environmental Science and Pollution Research*, 24(1), 180-188.
19. Rao, R. R., Vimudha, M., Kamini, N. R., Gowthaman, M. K., Chandrasekran, B., & Saravanan, P. (2017). Alkaline protease production from *Brevibacterium luteolum* (MTCC 5982) under solid-state fermentation and its application for sulfide-free unhairing of cowhides. *Applied biochemistry and biotechnology*, 182(2), 511-528.
20. Schröttner, P., Rudolph, W. W., Damme, U., Lotz, C., Jacobs, E., & Gunzer, F. (2017). *Wohlfahrtiimonas chitiniclastica*: current insights into an emerging human pathogen. *Epidemiology & Infection*, 145(7), 1292-1303.
21. Thanikaivelan, P., Rao, J. R., Nair, B. U., & Ramasami, T. (2004). Progress and recent trends in biotechnological methods for leather processing. *TRENDS in Biotechnology*, 22(4), 181-188.

22. Wang, J., Ma, Z. Z., Chen, L., Sun, H. J., & Fan, W. K. (2018). *Determination of the Emission of Volatile Organic Compounds from Leather Seats in Environmental Test Chamber*. In *Key Engineering Materials* (Vol. 768, pp. 31-35). Trans Tech Publications.
23. Xu, B., Chen, X., & Xiong, J. (2018). *Air quality inside motor vehicles' cabins: A review*. *Indoor and Built Environment*, 27(4), 452-465.
24. Yousuf, J., Thajudeen, J., Rahiman, M., Krishnankutty, S., P. Alikunj, A., & A. Abdulla, M. H. (2017). *Nitrogen fixing potential of various heterotrophic Bacillus strains from a tropical estuary and adjacent coastal regions*. *Journal of basic microbiology*, 57(11), 922-932.
25. Yu, X., Torzewska, A., Zhang, X., Yin, Z., Drzewiecka, D., Cao, H., ... & Wang, L. (2017). *Genetic diversity of the O antigens of Proteus species and the development of a suspension array for molecular serotyping*. *PloS one*, 12(8), e0183267.
26. Zhang, Y., Mansel, B. W., Naffa, R., Cheong, S., Yao, Y., Holmes, G., ... & Prabakar, S. (2018). *Revealing molecular level indicators of collagen stability: minimizing chrome usage in leather processing*. *ACS Sustainable Chemistry & Engineering*, 6(5), 7096-7104.

THE HUNT FOR RED 'MICROBA': IDENTIFICATION OF MICROORGANISMS INVOLVED IN 'RED HEAT' CONTAMINATION OF SALT-CURED HIDES

S. M. Grace¹, M. L. Patchett¹ and G. E. Norris¹

¹ School of Fundamental Sciences, Massey University, Palmerston North 4410, New Zealand

a) Corresponding author: s.m.grace@massey.ac.nz

Abstract. 'Red heat' describes a specific and undesirable microbial contamination of salt-cured products, and is attributed to the occurrence of halophilic microorganisms in the curing salt. For this study, traditional microorganism cultivation is complemented by a cultivation-independent method to determine the taxonomic composition and diversity of microbial populations. Being compared are samples of untreated unaffected salt-cured, and red heat-affected salt-cured bovine hide, along with the curing salt products used. Marker gene sequencing is the primary method of identification for cultured isolates, with metagenomic amplicon sequencing or 'metabarcoding', planned to determine the bacterial, archaeal and fungal components of mixed microbial populations in these samples. This approach is predicted to reveal taxa that have escaped cultivation so far, which may be key to the onset of red heat contamination. This knowledge is expected to assist the leather industry by informing the design of a rapid screening method based on molecular techniques, to detect the occurrence of such taxa in curing salt.

1 Introduction

'Red heat' is an industry term that describes the appearance of brightly coloured patches, streaks or spots on salt-cured products, and is attributed to the occurrence of halophilic ('salt-loving'¹) microorganisms in the curing salt.²⁻⁵ Red heat contamination is associated with damage and spoilage of cured hides and skins, understood to be the result of degradative, hydrolytic enzymes secreted by such organisms²⁻⁷ often resulting in defective leather products⁸⁻¹¹ causing wastage and economic loss to industry participants.

Much of the historical work on the microorganisms of red heat has necessitated careful and laborious cultivation, limited to phenotypic analyses. Whilst such methods remain the gold standard of microbial diagnostics,¹² characterisation of slow-growing and difficult-to-culture microorganisms remains challenging.¹³ Cultivation-independent, molecular techniques such as marker gene sequencing and metagenomic analysis can circumvent some of these difficulties.¹⁴⁻¹⁵ Additionally, such techniques can directly sample a particular environment and begin to describe the *in situ* population of microorganisms.¹⁶⁻¹⁷

For this study, traditional cultivation was complemented by a cultivation-independent method to identify the composition and diversity of microorganism populations.¹⁸ To control for between-animal variation, a single biological sample of cattle hide was treated with two different salt products. This was carried out to compare the effect of these treatments on the composition and diversity of the microorganism population within that hide. One of the curing salts is a minimally processed, unsterilised product, shown to produce discolouration characteristic of red heat; while the other has been subjected to a heat sterilisation (stoving) step during processing.

The cultivation-independent approach is predicted to show greater microbial diversity by uncovering taxa that are difficult to culture under conventional laboratory conditions. Such microorganisms may be key to the onset of red heat contamination in salt-cured hides and skins. To this end, both approaches primarily employ marker gene sequencing: the phylogenetically-informative 16S ribosomal

RNA gene is targeted to identify organisms of bacterial and archaeal origin,¹⁹ while the ITS2 region of the eukaryotic ribosomal gene group is targeted for the identification of fungal organisms.²⁰

In cultivation, marker gene sequencing represents a single genome per isolate. In contrast, cultivation-independent methods attempts to capture the microbial metagenome; that is, all of the microbial genomes of a mixed population. As a relatively cost-effective and less computationally-demanding alternative to whole-genome metagenomics, only the phylogenetic marker genes are targeted, as a proxy for the metagenome of a given sample. This is known as metagenomic amplicon sequencing, or 'metabarcoding'.²¹⁻²² A metabarcoding approach planned for this study, using the Illumina MiSeq high-throughput sequencing platform.

This paper describes the progress made thus far with the identification of cultured isolates and the preparation for the metabarcoding experiment. Once completed, it is anticipated that these results may provoke further investigation into whole-genome, functional metagenomics of salt-cured products, to better understand the microbial genes that influence contaminations such as red heat. For the leather and tanning industry, this knowledge may be useful by identifying new microbial targets for both prevention and control. On the basis of the methods used in this study, a PCR-based test could be developed, to allow rapid screening curing salts for microorganisms that either influence or cause red heat in salt-cured products, thus preventing the potential for red heat to occur.

2 Methods

2.1 Curing Salts Used

Two commercially solar-evaporated salt products, graded for agricultural use, were selected for comparison. Both were sourced from a New Zealand salt works. The salt referred to as 'unsterilised' is a raw, coarse-grained (10 mm) product with a typical moisture content of 1.8%. The salt referred to as 'sterilised' is a crushed (grain size <2.0 mm), washed, kiln-dried (stoved) product with a typical moisture content of 0.05%. Microorganisms were easily cultured from the unsterilised salt and produced discolouration characteristic of red heat when applied to pieces of bovine hide. Such contamination was not replicated when the sterilised salt was used. The same batch of each salt product was used to cure both of the cattle hides used in this study.

2.2 Hide Treatment & Sampling

Unshaved cattle hide from the OSP (official sampling position) was divided into two equal-sized pieces, in order to compare the effect of the different salt treatments on the microorganism populations within the same biological sample. Each piece had either sterilised or unsterilised salt applied to the flesh/hypodermal surface at a rate of 50 % w/w of the hide sample. Each salted piece was sealed separately inside a clear plastic container with salted side facing up/outwards, and left to cure at room temperature, in ambient light, on the laboratory bench. Hide from two different cattle animals were salt-cured independently in this manner; one hide was used for the cultivation of microorganisms, which was sampled at 90 days of cure. The other hide was used for the metabarcoding experiment, with samples of between 3-5 grams cut from the hide piece prior to being treated with salt (day 0), then at 24 hours after application of curing salt (day 1), then at 10, 20, 40, 50 and 60 days post-salt application (Table 1). Because of the potentially huge disparity in microbial populations between the hides of different animals, no biological replicates were used. However, to account for differences in extraction and processing, each sampling was done on three different areas of each hide at each time point.

Table 1. Sampling scheme for culture-independent, metabarcoding experiment.

	Number of Samples Taken From:					
	Controls: (no hide)	Salt: Sterilised	Salt: Unsterilised	Hide: Untreated	Treated Hide: Sterilised Salt	Treated Hide: Unsterilised Salt
Day 0	3	2	2	6	-	-
Day 1	1	-	-	-	3	3
Day 10	1	-	-	-	3	3
Day 20	1	-	-	-	3	3
Day 40	1	-	-	-	3	3
Day 50	1	-	-	-	3	3
Day 60	1	-	-	-	3	3

2.3 Enrichment, Culture and Isolation Media

2.3.1 Media for enrichment from hide samples

Three different media were used: for enrichment of fungal organisms ('Malt'; malt extract 30.0 g/L, glucose 10.0 g/L, peptone 5.0 g/L, yeast extract 1.25 g/L, pH 5.6-5.8); Modified Seghal & Gibbons for enrichment of fastidious organisms ('MSG': acid-hydrolysed casein 5.0 g/L, peptone 5.0 g/L, yeast extract 5.0 g/L, trisodium citrate 3.0 g/L, glucose 1.0 g/L, pH 7.2-7.5;) and lysogeny broth for enrichment of mesophilic bacteria ('LB'; tryptone 10.0 g/L, yeast extract 5.0 g/L, pH 7.0). Each of these media types was prepared with three different concentrations of salt, by diluting a concentrated salt water SW30 stock solution²³ with sterilised, ultrapure water to produce media with a final sodium chloride content of either 20%, 8% or 0.5% (w/v). These amounts were selected as salt concentration optima for enrichment of (extremely) halophilic, moderately halophilic and halotolerant, and non-halophilic microorganisms respectively,²⁴ resulting in nine different formulations altogether. Solid media was supplemented with 1.5% (w/v) bacteriological agar. All plates were sealed with paraffin film and incubated at 37 °C under a fluorescent bulb, while all liquid cultures were incubated at 37 °C in a table-top shaker in ambient light. Uninoculated controls were incubated to check for presence of environmental contaminants.

2.3.2 Media for enrichment from salt samples

A modified salt-rice-broth formulation was used² where SW30 stock solution was diluted to a final sodium chloride content of 12% (w/v) with sterilised ultrapure water, to which 10 g/L tryptic soy broth and 5 g/L acid-hydrolysed casein was added. Two parts of this solution was combined with one part of uncooked, short-grain white rice in a glass tube, then autoclaved to produce a solid, white-coloured growth medium that filled most of the tube.

2.3.3 Media for culture and isolation

Colonies selected from enrichment media were transferred to MSG media containing a similar sodium chloride component of either 16%, 8% or 0.5% (w/v) for isolation by streak plate technique. The sodium chloride content was reduced from 20% to 16% (w/v) to ease the preparation of solid media for cultivation of halophilic microorganisms. Aliquots of liquid culture from discrete colonies were frozen -80 °C in glycerol solution with a final concentration of 15% (w/v)

2.4 Collection of Microorganisms from Hides and Salts

2.4.1 Collection from hides for isolation and culture

Samples of approximately 1.5 cm² were cut and sterilised tweezers used to press each of the flesh and the hair sides of the sample onto the surface of solid media. The sample was then halved with a sterile blade, with each piece immediately transferred to a flask of sterile brine to wash out microorganisms from within the hide tissue. One flask was prepared with undiluted SW-30 solution (pH 9.0) with a final sodium chloride content of 24% (w/v) and resultant pH of 9.0, to select for extremely halophilic and halotolerant microorganisms. The other flask was prepared by diluting SW-30 solution to achieve a final sodium chloride concentration of approximately 9.6% (w/v), with resultant pH of 8.0, to promote cultivation of halotolerant and slightly-halophilic microorganisms.²⁴ Flasks were incubated for 3 days at 37 °C with shaking and 120 µL of this liquid spread onto the surface of solid media.

2.4.2 Collection from salt for isolation and culture

To freshly-prepared rice-broth tubes, 2.5 g of salt sample was added, followed by 3 mL of sterilised water, to give an approximate sodium chloride concentration of 14.5% (w/v). Tubes, including uninoculated controls, were loosely capped and incubated at 37 °C under a fluorescent bulb. After ten weeks of incubation,²⁵ sterile loops were used to streak samples onto solid media for isolation.

2.4.3 Collection from hides for culture-independent, metabarcoding experiment

Approximately 3-5 g of hide sample was washed in 9.0 mL of 50 mM filter-sterilised ammonium bicarbonate solution (pH 8.0) for two hours at 37 °C on rotating arms. To remove particulate matter, the liquid mixture was passed through a nylon membrane (pre-soaked in 0.1% Tween-20) with 80 µm pore size, into a sterile collection tube.²⁶ The membrane was washed with a further 10.0 mL of the ammonium bicarbonate solution, with collected liquid lyophilised to powder. A 'reagents-only' (i.e. no hide sample) extraction was performed at each hide collection time point, as a control for environmental contaminants.

2.4.4 Collection from salt samples for culture-independent, metabarcoding experiment

Following the modified method of Henriët (2014),²⁷ brines of 25% (w/v) were made from 100 mL of sterilised, ultrapure water and 25 grams of salt sample and incubated in conical flasks at 37 °C with gentle shaking for 20-30 minutes. Brines were passed through 10 µm pore size nylon membranes to collect cells. A 'reagents-only' (i.e. no salt) collection was performed as a control for environmental contamination.

2.5 Genomic DNA Extraction

2.5.1 DNA extraction from pure cultures and from cell colonies.

Cell pellets from liquid cultures were subjected to mechanical homogenisation by bead-beating, using 106 µm glass beads (Sigma). Homogenisation was carried out in a RiboLyser scientific chemical mixer (model FP120HY-230, Hybaid Ltd, UK) at 4 °C with the following procedure: 4.5 m/s for three cycles of 25 seconds, with 2-min rest interval in between each cycle. After removal of cell debris by centrifugation for 1 minute at 12,000 g, cell lysates were treated with RNase A (Sigma) for 20 minutes at 37 °C to break down contaminating RNA, and Promega Protein Precipitation Solution to remove contaminating protein. DNA was purified using ethanol precipitation²⁸ and resuspended in autoclaved, ultrapure water. Picked colonies were boiled for 8 minutes at 95 °C in buffer (10 mM Tris HCl pH 8.0, 0.1 mM EDTA, 0.1% Triton X-100). Tubes were centrifuged at 12,000 g for 1 minute to pellet cell debris. The supernatant containing the DNA was carefully removed and used immediately for PCR.

2.5.3 DNA extraction from powdered hide extracts & salt extracts

Including for reagents-only controls, the DNeasy Powersoil Kit (Qiagen) was used with the following changes to the manufacturer's protocol: PowerBead tubes were subjected to mechanical homogenisation with a RiboLyser using the aforementioned procedure, and DNA was eluted from MB Spin Columns using sterile, ultrapure water. All other steps were carried out according to the manufacturer's protocol.

2.6 Marker Gene Amplification using Polymerase Chain Reaction (PCR)

For DNA extracted from culture isolates and cell colonies, MyTaq Red Polymerase (BioLine) was used under thermocycling conditions recommended by the manufacturer. For metagenomic amplicon sequencing/metabarcoding sample preparation, Phusion HF Polymerase (New England Biolabs) was used as recommended by the manufacturer. Sequences for oligonucleotide primers are listed in Table 2. Primers used for metabarcoding included Illumina overhang-adapter sequences incorporated at the 5'-end of the marker gene-specific sequence (in 5'-3' direction: TCGTCGGCAGCGTCAGATGTGTATAAGAGACAG for forward primers; for reverse GTCTCGTGGGCTCGGAGATGTGTATAAGAGACAG). All PCR was carried out in 20 µL reaction volumes and included water-only controls for detection of contaminant DNA. Amplification products were visualised using agarose gel electrophoresis and ethidium bromide staining.

2.7 Sequencing & Analysis

Sequencing reactions were carried out by Massey Genome Service (Palmerston North, New Zealand) using dye-labelled, terminator cycle sequencing method.³⁵ Data was analysed using Geneious® v9.1.2 (Biomatters Ltd.).

Table 2. Oligonucleotide primers used for marker gene amplification and sequencing.

Application	Primer Name	Sequence (5'-3')	Target	Reference
Marker gene sequencing of culture isolates	344-F	ACGGGGYGCAGCAGGCGCGA	Archaeal 16S rRNA gene	[29]
	915-R	GTGCTCCCCGCCAATTCCT		
	27-F	AGAGTTTGATCTGGCTCAG	Bacterial 16S rRNA gene	[30]
	1492-R	GGTTACCTTGTACGACTT		
	ITS86F	GTGAATCATCGAATCTTTGAA	Fungal ITS2 region	[31]
	ITS4-R	TCCTCCGCTTATTGATATGC		[32]
Metabarcoding/metagenomic amplicon sequencing ¹	Arc344-F	ACGGGGYGCAGCAGGCGCGA	Archaeal 16S rRNA gene	[29]
	Arc806-R	GGACTACVSGGGTATCTAAT		
	Bact-0341-F	CCTACGGGNGGCWGCAG	Bacterial 16S rRNA gene	[34]
	Bact-0785-R	GACTACHVGGGTATCTAATCC		
	5.8S-Fun	AACTTYRRAAYGGATCWCT	Fungal ITS2 region gene	[20]
ITS4-Fun	AGCCTCCGCTTATTGATATGCTTAART			

1. Illumina overhang adapter sequences were added to the 5'- end of each of the locus-specific sequences: 5' TCGTCGGCAGCGTCAGATGTGTATAAGAGACAG for forward primers and 5' GTCTCGTGGGCTCGGAGATGTGTATAAGAGACAG for reverse primers.

The primary database queried was the '16S ribosomal RNA sequence (Bacteria and Archaea)' database from NCBI, using the BLASTn tool optimised for megablast with default settings (word size = 28).³⁶ Descriptions were assigned on the basis of fulfilling both the highest total alignment score and >97% similarity with reference sequences.³⁷

3 Results & Discussion

3.1 Production of Red Heat

Both of the hide pieces cured with unsterilised salt developed discolouration characteristic of red heat, which first appeared as small, pale pink spots <1.0 mm diameter on the flesh surface, along with a faint pink colouration of the salt grains. This appeared at day 23 of cure on the hide used for microorganism cultivation. By day 46 of cure, the colour had deepened to a vivid, fuchsia-like pink and spots were distributed across the entire flesh surface (Fig. 1). At time of cultivation at day 90 of cure, the pink colouration had deepened and appeared quite dry.

Pink spots first appeared on the 40th day of cure on the hide piece sampled for metabarcoding. By day 60 of cure, about a quarter of the flesh surface displayed bright pink-coloured spots and small patches. Furthermore, most of the salt grains displayed a faint pink colouration. Interestingly, after being left for a total of 270 days, patches developed over the majority of the flesh surface and the most of the colour had changed from bright pink to a vivid pink-orange, with a glistening, semi-transparent appearance. Both of the discoloured pieces had a slight smell of rotting meat and urine, however it was not overpowering, nor reminiscent of ammonia.

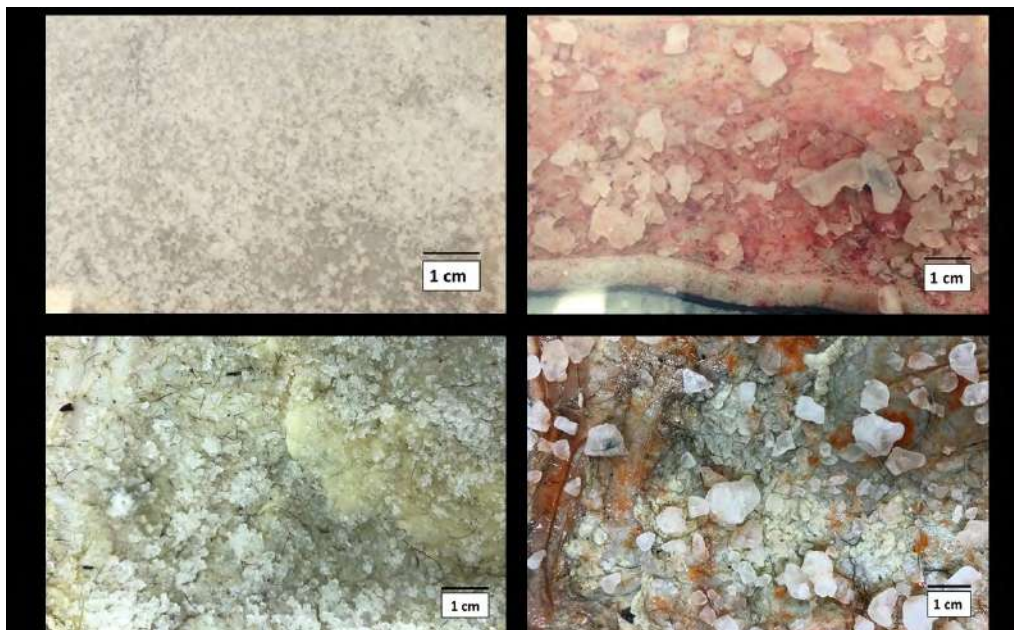


Fig. 1. 'Red heat' contamination of salt-cured products. Bovine hide pieces were dry-salted 50% (w/w) on the flesh side with either sterilised or unsterilised salt, sealed in clear plastic boxes and cured at ambient temperature and light. (A) Bovine hide treated with sterilised salt product and (B) unsterilised salt product at day 46 of cure, with both pieces sourced from the same animal. The hide of a different animal was used to provide both (C) hide treated with sterilised salt product and (D) hide treated with unsterilised salt product, both pictured at day 270 of cure. Hide pieces (B) and (D) show patchy blemishes of a bright pink and a pink-orange colour respectively, characteristic of red heat contamination.

Neither piece showed obvious liquefaction, though the pink-orange coloured piece had a slightly slippery, slimy feel when handling. Some hair was able to be pulled from both hides using tweezers.

The two hide pieces cured with sterilised salt did not develop any discolouration. Both had a very faint smell of rotten meat and urine. Neither piece showed any sign of liquefaction, appearing to be dry and relatively inflexible when handled, in comparison to the orange-pink contaminated piece. Hair slip was not apparent, but some hair was able to be pulled from the epidermal surface.

3.2 Isolation & Culture

A number of colony types were cultivated from the unsterilised-salted hide, with many successfully cultured, however, very few were captured on media containing 0.5% w/v sodium chloride (table 3). Coloured colonies were mostly of various shades of pink with some showing pink-orange pigmentation. All were glistening and semi-transparent. Shapes were either round or a 'fried egg' appearance; having an opaque, raised centre in an otherwise glistening, semi-transparent, irregular margin. These pink colony types occurred exclusively on the 20% and 8% sodium chloride containing plates. Some opaque, pale yellow colonies were evident on the plates with 8% sodium chloride or less. Many off white or beige types were isolated, mostly >3mm, with round to irregular margins, occurring most densely on plates containing 8% sodium chloride.

From the sterile-salted hide, a few large (20 mm) beige-pink, rugose growths with irregular margins growths were observed, as well as off-white colonies, and many yellow-pigmented colonies, mostly opaque with a glistening appearance. From this hide piece, a total of nine isolates were cultured (Table 3).

Many pale pink, glistening colonies were obtained from the unsterilised salt, along with one plate that developed deep red-pink, glossy, round colonies. However, efforts to culture the red colonies were largely unsuccessful, with only one isolate being cultured. No organisms were isolated from the sterilised salt using the rice-broth enrichment medium.

Table 3. Number of cultured isolates obtained in this study.

Sample	Enrichment Media	Total number of isolates	Total number of isolates cultured from enrichment media containing:		
			20% NaCl	8% NaCl	0.5% NaCl
Hide cured with unsterilised salt (red heat)	Malt	12	8	4	-
	MSG	13	10	3	-
	LB	11	3	5	3
Hide cured with sterilised salt (unaffected)	Malt	4	-	2	2
	MSG	3	-	2	1
	LB	2	-	1	1
Unsterilised salt	Malt	-	-	-	-
	MSG	1	1	-	-
	LB	-	-	-	-
Sterilised salt	Malt	-	-	-	-
	MSG	-	-	-	-
	LB	-	-	-	-

Additionally, to test the effectiveness of the rice-broth enrichment media, a variety of salt products were screened to detect the presence of coloured organisms (table 4). The aspect and onset of discolouration was markedly different between each of these salt samples, with sample 2547-2 producing a bright pink colour within 5 days of inoculation. The tube inoculated with unsterilised salt product developed colour more slowly, first appearing after 10 days, with others first showing obvious discolouration after 10-21 days of incubation. Most of those that produced discolouration of the enrichment media also produced slow-growing, pigmented, glossy, round to irregular shaped colonies on isolation media. However, non-pigmented colonies were also isolated, which were numerous but much smaller in size compared to the coloured isolates. No isolates were cultured from those tubes that remained white/uncoloured after the incubation period.

3.3 Marker Gene Amplification, Sequencing & Analysis

3.3.1 Marker gene sequencing analysis of cultivated microorganisms

A greater taxonomic diversity was cultivated from the hide samples cured with unsterilised salt, with 5 different bacterial and 3 archaeal genera identified by partial 16S rRNA marker gene sequencing (Table 5). In contrast, samples of hide cured with sterilised salt revealed only three different bacterial species across two genera. Only one species, *Staphylococcus equorum*, appears to be common to both hide samples, and has been identified in other cultivation studies of salted hides and skins that employ marker gene or partial 16S rRNA sequencing.⁵

Several colonies cultivated from the unsterilised salt were picked for colony PCR followed by marker gene sequencing, however, the required threshold of 97% reference similarity was not met (table 4). In all instances, one of several possible species of the genus *Haloarcula* was suggested as the closest phylogenetic relative. Additionally, the same followed for sequences obtained from a number of isolates cultivated from the unsterilised salted hide. In all but once instance, these sequences were unable to meet the similarity threshold due to a number mismatches arising from base-call ambiguities (more than one kind of nucleotide occupying the same sequence position), and all were suggested to be most closely related to *Haloarcula*. Intragenomic heterogeneity of the 16S rRNA gene is suggested as a possible reason for this observation. This is a particular feature of *Haloarcula*, which reportedly shows up to 5% sequence dissimilarity between the three copies of its 16S rRNA gene (designated as *rrsA*, *rrsB* and *rrsC*).³⁸ This was supported by multiple alignments of available *rrsA*, *rrsB* and *rrsC* reference sequences obtained from a number *Haloarcula* strains.

The resultant consensus data showed nucleotide ambiguities that aligned with those present in sequence data obtained from the isolates cultivated from unsterilised salt and hide (data not shown). Alternatively, these sequences could represent as yet uncharacterised strains of *Haloarcula*.

Table 4. Comparison of the microorganisms cultivated from different salt products.

Salt Sample Name	Enrichment Result	Colony Description	Sequence Description	Sequence Identity
Himalayan Rock Salt		Pale pink	<i>Halobacterium noricense</i>	99 %
Cornish Sea Salt		None	-	-
Tannery salt 2547-1		Bright pink Translucent white	<i>Halorubrum persicum</i> <i>Natrinema pellirubrum</i>	99 % 100 %
Tannery Salt 3387-9		Pink Off-white	<i>Halococcus</i> sp. <i>Chromohalobacter</i> sp.	99%
Unsterilised salt		Pink Red-pink	<i>Haloarcula</i> sp. (?)	92-93%
Sterilised Salt		None	-	-
AR-grade sodium chloride		None	-	-

Cultivated isolates were identified using phylogenetic marker gene sequencing. Sequence data was used to query the NCBI 16S ribosomal RNA sequence (Bacteria and Archaea) database using the BLASTn tool. Descriptions were assigned on the basis of the query sequence fulfilling both the highest total alignment score and >97% similarity with reference sequences.

Table 5. Phylogenetic identification of organisms cultivated from salt-cured bovine hide.

Sample	Organism domain	Description	Reference sequence accession	Number isolated from media containing:		
				20% NaCl	8% NaCl	0.5% NaCl
Cured with unsterilised salt	Bacteria	<i>Halomonas utahensis</i>	NR_117120.1	12	3	-
		<i>Salicola marasensis</i>	NR_043480.1	1	2	-
		<i>Staphylococcus equorum</i>	NR_027520.1	-	2	-
		<i>Halobacillus locisalis</i>	NR_025715.1	-	1	-
		<i>Halobacillus sediminis</i>	NR_145863.1	-	1	-
		<i>Thalassobacillus cyri</i>	NR_116915.1	-	1	-
	Archaea	<i>Halorubrum terrestre</i>	NR_113487.1	1	-	-
		<i>Haloarcula argentinensis</i>	NR_028218.1	1	-	-
		<i>Haloarcula marismortui</i>	NR_074201.1	1	-	-
		<i>Halorubrum californiense</i>	NR_113471.1	-	1	-
		<i>Halovivax asiaticus</i>	NR_042407.1	-	1	-
Cured with sterilised salt	Bacteria	<i>Staphylococcus equorum</i>	NR_027520.1	-	6	-
		<i>Bacillus licheniformis</i>	NR_118996.1	-	-	3
		<i>Bacillus paralicheniformis</i>	NR_137421.1	-	-	1

Bacterial and archaeal marker gene sequence data were used to query the NCBI 16S ribosomal RNA sequence (Bacteria and Archaea) database using the BLASTn tool. Descriptions were assigned on the basis of the query sequence fulfilling both the highest total alignment score and >97% similarity with reference sequences.

Three of the additionally-sampled salt products produced either colonies or cultured isolates that were able to be phylogenetically classified (Table 4). However, the small, transparent white/colourless colonies isolated from salt sample 2547-2 appears to be at-odds with the 100 % sequence similarity to 16S rRNA gene reference sequences (accession numbers NR_113528.1, NR_102444.1, NR_118137.1 & NR_112856.1) designated as *Natrinema pellirubrum*. The description of this microorganism includes formation of mostly orange-pigmented colonies due to the accumulation of carotenoid pigments and has been isolated from similarly-coloured patches appearing on salt-cured hides.^{5, 39} This demonstrates the need for phenotypic analyses to complement genotypic methods, in order to properly classify these cultivates.

So far in this study, fungal organisms have not yet been identified by marker gene sequencing.

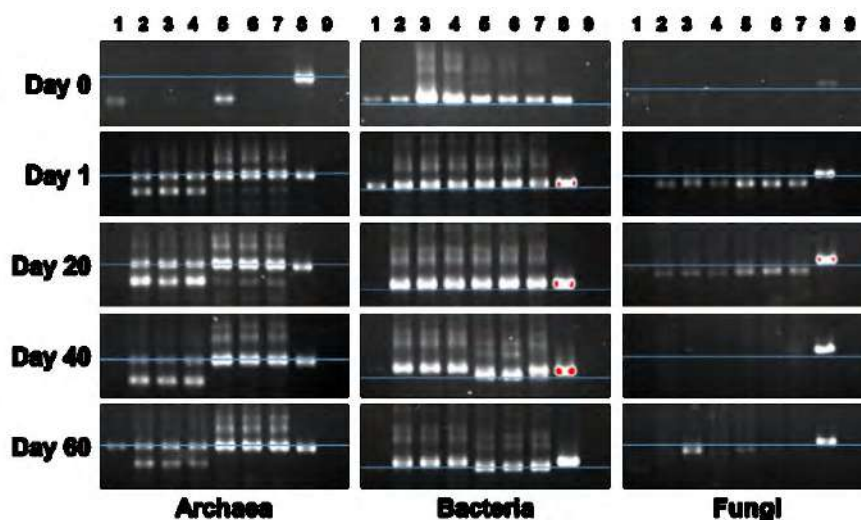


Fig. 2. Detection of microbial phylogenetic marker genes in salt-cured hide samples.

Genomic DNA was extracted from samples of salt-cured bovine hide and subjected to polymerase chain reaction (PCR) amplification targeting the following three marker genes: archaeal 16S rRNA; bacterial 16S rRNA and ITS2 region of fungal ribosome gene locus; with expected product sizes of 400-550 base pairs. Samples were taken prior to application of salt treatment (Day 0), at 24 hours after salt application (Day 1), then at 20, 40 and 60 days after salt application. Discolouration characteristic of 'red heat' contamination appeared on unsterilised salted hide samples at Day 40 onwards. PCR products were electrophoresed in 2% agarose gels and visualised using ethidium bromide stain. Blue lines show the position of the concurrently-run 500 base-pair size standard (not pictured). Red spots are artefacts of the gel imaging software used. Lane 1: Reagents-only (no hide) control extraction; Lanes 2-4: sterile-salted hide samples; Lanes 5-7: unsterilised salt-cured hide samples; Lane 8: known microbial strain (positive control for PCR); Lane 9: water-only reaction (negative control for PCR).

3.3.2 Visualisation of marker gene amplification from samples of cured hide using agarose gel electrophoresis and ethidium bromide staining

For the six samples taken from the hide pieces prior to being salted (day 0), bacterial marker gene amplification products were clearly detected in the untreated hide. However, amplification of archaeal marker genes across these six samples of untreated hide appeared inconsistent, and fungal marker gene amplification products were largely indistinguishable (Fig. 2).

Amplification of archaeal and bacterial marker genes was detected in all samples of cured hide taken from between day 1 and day 60 of cure, with clear differences in the DNA band profiles between the sterilised-salted hide and unsterilised-salted hide (Fig. 2).

In samples of hide cured with sterilised salt, the DNA band profile of archaeal marker gene amplification products shows one band approximately 500 base pairs (bp) in length, and another approximately 450 bp in length, and of similar staining intensity. This appears consistently within the three samples taken at each time point, and between each of the sampling time points. This contrasts with that shown for the unsterilised salted hide samples, where the staining intensity of the 500 bp band is greater compared to the faint, almost indistinguishable 450 bp band directly below it. The appearance of red heat discolouration on unsterilised salted hide from day 40 of cure did not appear to cause any change to the migration distances of these archaeal marker gene bands in agarose gel electrophoresis.

Interestingly, the appearance of red heat discolouration does coincide with a slight increase to the migration distance of the DNA band corresponding to bacterial marker gene amplification products, which is not seen in those obtained from samples of hide cured with the sterilised salt. In this case, the migration distance of this DNA band remains the same.

The 16S rRNA gene is reported to be approximately 1,500 base pairs in length for most bacterial and archaeal organisms.¹⁹ Therefore, marker gene amplification is expected to produce DNA fragments of a mostly uniform length. Species-specific size variations in the 16S rRNA gene have been reported, due to accumulation of nucleotide substitutions and deletions, as well as gene truncations and intervening sequences.⁴⁰ Thus, variability of amplification product length for this marker gene can be indicative of distinct taxa in these samples.

The appearance of fungal marker gene amplification products showed as faint but clearly visible bands estimated at 480 bp in size, in all of the day 1 and day 10 hide samples. However, their visibility was inconsistent between all of the sampling time points. The appearance of red heat discolouration on the hide with unsterilised salt from day 40 of cure did not appear to cause any change to the migration distances of these DNA bands in agarose gel electrophoresis.

3.3.3 Visualisation of marker gene amplification from samples of salt using agarose gel electrophoresis and ethidium bromide staining

Amplification of archaeal phylogenetic marker genes was detected in both the unsterilised and sterilised curing salt, meeting the expected fragment size of around 500 bp (figure 3). The resultant DNA band profiles of the two different salts appear very similar to each other. Surprisingly, bacterial

marker genes were not amplified from either of these salt samples. This is in contrast to the work of Yilmaz & Birbir (2019),⁴¹ who cultivated several *Bacillus* species directly from salt products from different leather factories, with 16S rRNA marker gene sequencing included in their method to characterise these isolates. Additional replicates will be screened in order to explain this result.

It is interesting to note that although archaeal organisms were (so far) unable to be cultured from the sterilised salt product, their presence (perhaps in a dormant form, or possibly non-viable) has been detected by marker-gene amplification.

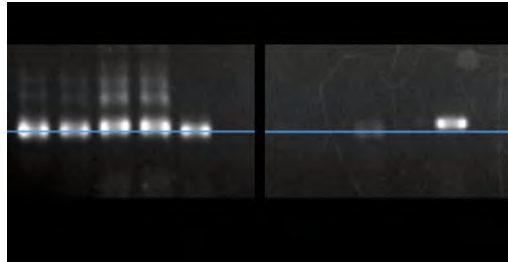


Fig. 3. Detection of microbial phylogenetic marker genes in curing salt products. Genomic DNA was extracted from salt samples and subjected to PCR amplification targeting the archaeal 16S rRNA and bacterial 16S rRNA marker genes, with expected product sizes of 400-550 base pairs. PCR products were electrophoresed in 2% agarose gels and visualised using ethidium bromide stain. Blue lines show the position of the concurrently-run 500 base-pair size standard (not pictured). Lanes 1-2: Sterilised salt; Lanes 3-4: unsterilised salt; Lane 5: known microbial strain (positive control for PCR); Lane 6: water-only reaction (negative control for PCR).

4 Conclusions

We have managed to induce red heat contamination in salt-cured cattle hide and cultivate microorganisms from samples of this hide and also from the salt product used to produce the contamination. We have also cultivated microorganisms from and unaffected hide samples. Further, in a cultivation-independent approach, red heat contamination was successfully reproduced in order to directly sample the *in situ* microorganism population of these hides, in preparation for analysis by high-throughput sequencing of marker gene amplification products. This work has produced a number of interesting results so far:

1. When treated with different salt products, the diversity and composition of both the cultivated and apparent *in situ* microorganism population differs markedly within single biological samples of bovine hide,
2. A number of different salt products harboured cultivable microorganisms that were phylogenetically distinct.
3. The marker gene sequences of cultivable microorganisms in the unsterilised salt product are so far quite dissimilar to known reference sequences, suggestive of an as-yet uncharacterised organisms. Analysis of high-throughput sequencing data is expected to clarify this observation.
4. A change in the composition of the bacterial population coincided with the appearance of red heat contamination, as detected by marker gene amplification, with no such changes apparent in the archaeal and fungal populations. We expect this to be explained by analysis of high-throughput sequencing data generated by these amplification products.
5. The salt product that was treated by heat-sterilisation did not yield cultivable organisms in this study. While microbial phylogenetic marker genes were detected, the viability of these organisms is not clear, indicating the importance of such treatments for the prevention of red heat.

5 Acknowledgements

The authors would like to thank the New Zealand Leather and Shoe Research Association (LASRA) for their financial and technical support. The kind contribution of a whole cattle hide to this study by M. Ahn and D. Allan is gratefully acknowledged.

6 References

- Oren, A.; *Halophilic microorganisms and their environments*, Springer, Dordrecht, 2002
- Stuart, L. S., Frey, R. W., & James, L. H.: 'Microbiological studies of salt in relation to the reddening of salted hides', *U.S. Dept Agric Tech Bull*, 383, 1-23, 1933
- Anderson, H.: 'The reddening of salted hides and fish', *Appl Microbiol*, 2(2), 64-69, 1954
- Birbir, M., Kallenberger, W., Igaz, A., & Bailey, D. G.: 'Halophilic bacteria isolated from brine cured cattle hides', *J Soc Leath Tech Ch*, 80(3), 87-90, 1996
- Akpolat, C., Ventosa, A., Birbir, M., Sanchez-Porro, C., & Caglayan, P.: 'Molecular identification of moderately halophilic bacteria and extremely halophilic archaea isolated from salted sheep skins containing red and yellow discolorations', *J Am Leath Chem As*, 110(7), 211-220, 2015
- Lochhead, A. G.: 'Bacteriological studies on the red discoloration of salted hides', *Can J Res*, 10(3), 275-286, 1934
- Bilgi, S. T., Yapici, B. M., & Karaboz, S.: 'Determination of hydrolytic enzyme capabilities of halophilic archaea isolated from hides and skins and their phenotypic and phylogenetic identification', *J Am Leath Chem As*, 110(2), 33-42, 2015
- Birbir, M., & Igaz, A.: 'Isolation and identification of bacteria adversely affecting hide and leather quality', *J Soc Leath Tech Ch*, 80(5), 147-153, 1996
- Bailey, D. & Birbir, M.: 'The impact of halophilic organisms on the grain quality of brine cured hides', *J Am Leath Chem. As*, 91, 47-51, 1996
- Vreeland, R. H., Angelini, S., & Bailey, D. G.: 'Anatomy of halophile induced damage to brine-cured cattle hides', *J Am Leath Chem As*, 93, 121-131, 1998
- Bitlisli, B.O., Karavana, H. A., Basaran, B., Sari, O., Yasa, I., & Birbir, M.: 'The effect of conservation defects on the suede quality of double-face', *J Am Leath Chem As*, 99(12), 494-501, 2004
- Overmann, J., Abt, B., & Sikorski, J.: 'Present and Future of Culturing Bacteria', *Annu Rev Microbiol*, 71, 711-730, 2017
- Burns, D. G., Camakarlis, H. M., Janssen, P. H., & Dyll-Smith, M. L.: 'Combined use of cultivation-dependent and cultivation-independent methods indicates that members of most haloarchaeal groups in an Australian crystallizer pond are cultivable', *Appl Environ Microbiol*, 70(9), 5258-5265, 2004
- Benlloch, S., Acinas, G., López-López, J. A., Luz, S. P., & Rodríguez-Valera, F.: 'Archaeal Biodiversity in Crystallizer Ponds from a Solar Saltern: Culture versus PCR', *Microb Ecol*, 41(1), 12-19, 2001
- Quigley, L., O'Sullivan, D. J., Daly, D., O'Sullivan, O., Burdikova, Z., Vana, R., Beresford, T. P., Ross, R. P., Fitzgerald, G. F., McSweeney, P. L. H., Giblin, L., Sheehan, J. J., & Cotter, P.D.: 'Thermus and the pink discoloration defect in cheese', *mSystems*, 1, e00023-16, 2016
- Fernández, A. B., Blanca Vera-Gargallo, B., Sánchez-Porro, C., Ghai, R., Papke, R. T., Rodríguez-Valera, F., & Ventosa, A.: 'Comparison of prokaryotic community structure from Mediterranean and Atlantic saltern concentrator ponds by a metagenomic approach', *Front Microbiol*, 5, 196, 2014
- Gibtan, A., Park, K., Woo, M., Shin, J. K., Lee, D. W., Sohn Jae Hak, Song, M., Roh, S. W., Lee, S. J., & Lee, H. S.: 'Diversity of Extremely Halophilic Archaeal and Bacterial Communities from Commercial Salts', *Front Microbiol*, 8, 799, 2017
- Oren, A.: 'Halophilic microbial communities and their environments', *Curr Opin Biotechnol*, 33, 119-124, 2015
- Clarridge J. E. III: (2004). 'Impact of 16S rRNA gene sequence analysis for identification of bacteria on clinical microbiology and infectious diseases', *Clin Microbiol Rev*, 17(4), 840-862, 2004
- Taylor, D. L., Walters, W. A., Lennon, N.J., Bochicchio, J., Krohn, A., Caporaso, J. G., & Pennanen, T.: 'Accurate estimation of fungal diversity and abundance through improved lineage-specific primers optimized for Illumina amplicon sequencing', *Appl Environ Microbiol*, 82, 7217-7226, 2016
- Sharpton, T. J.: 'An introduction to the analysis of shotgun metagenomic data', *Front Plant Sci*, 5, 209, 2014
- Walsh, A. M., Crispie, F., Claesson, M. J., & Cotter, P. D.: 'Translating Omics to Food Microbiology', *Annu Rev Food Sci Technol*, 28(8), 113-134, 2017
- Dyll-Smith, M.: *The Halo handbook: protocols for haloarchaeal genetics*, 2009, Retrieved from http://www.haloarchaea.com/resources/halohandbook/Halohandbook_2009_v7.2mids.pdf
- Kushner D. J.: *Microbial life in extreme environments*, Academic Press, 1978
- Cooper, S. & Crawford, E.: 'How long do salt samples need to be incubated for?' Paper presented at the Leather and Shoe Research Association Industry Technical Advisory Group meeting, Queenstown, New Zealand, 2015
- García-Garcerà, M., García-Etxebarria, K., Coscollà, M., Latorre, A., Calafell, F.: 'A New Method for Extracting Skin Microbes Allows Metagenomic Analysis of Whole-Deep Skin', *PLoS ONE* 8(9), e74914, 2013

27. Henriot, O., Fourmentin, J., Delincé, B., & Mahillon, J., 'Exploring the diversity of extremely halophilic archaea in food-grade salts', *Int J Food Microbiol*, 191, 36-44, 2014
28. Green, M. R., & Sambrook, J.: *Precipitation of DNA with ethanol*, *Cold Spring Harbour Protocols*, 2016(12), pdb.prot093377, 2016
29. Raskin, L., Stromley, J. M., Rittmann, B. E., & Stahl, D. A.: 'Group-specific 16S rRNA hybridization probes to describe natural communities of methanogens' *Appl Environ Microbiol*, 60(4), 1232-1240, 1994
30. Weisburg, W. G., Barns, S. M., Pelletier, D. A. & Lane, D. J.: '16S ribosomal DNA amplification for phylogenetic study', *J Bacteriol*, 173, 697-703, 1991
31. Turenne, C. Y., Sanche, S. E., Hoban, D. J., Karlowsky, J. A., & Kabani, A. M.: 'Rapid Identification of Fungi by Using the ITS2 Genetic Region and an Automated Fluorescent Capillary Electrophoresis System' *J Clin Microbiol*, 37(6), 1846-1851, 1999
32. White, T., Bruns, T., Lee, S. & Taylor, J.: *PCR protocols: a guide to methods and applications*, Academic Press, 1990
33. Takai, K., & Horikoshi, K., 'Rapid Detection and Quantification of Members of the Archaeal Community by Quantitative PCR Using Fluorogenic Probes'. *Appl Environ Microbiol*, 66(11), 5066-5072, 2000
34. Herlemann, D. P. R., Labrenz, M., Jurgens, K., Bertilsson, S., Waniek, J. J., & Andersson, A. F.: 'Transitions in bacterial communities along the 2000km salinity gradient of the Baltic Sea', *ISME J*, 5, 1571-1579, 2011
35. Smith, L. M., Sanders, J. Z., Kaiser, R. J., Hughes, P., Dodd, C., Connell, C. R., Heiner, C., Kent, S. & Hood, L. E.: 'Fluorescence detection in automated DNA sequence analysis', *Nature*, 321, 674-679, 1986
36. Morgulis, A., Coulouris, G., Raytselis, Y., Madden, T. L., Agarwala, R., & Schäffer, A. A.: 'Database indexing for production MegaBLAST searches', *Bioinformatics*, 24(16), 1757-1764, 2008
37. Stackebrandt, E., & Goebel, B.: 'Taxonomic Note: A Place for DNA-DNA Reassociation and 16S rRNA Sequence Analysis in the Present Species Definition in Bacteriology', *Int J Syst Evol Microbiol*, 44(4), 846-849, 1994
38. Baliga, N. S., Bonneau, R., Facciotti, M. T., Pan, M., Glusman, G., Deutsch, E. W., ... Ng, W. V.: 'Genome sequence of *Haloarcula marismortui*: a halophilic archaeon from the Dead Sea'. *Genome Res*, 14(11), 2221-2234, 2004
39. McGenity, T., Gemmell, R., & Grant, W.: 'Proposal of a new halobacterial genus *Natrinema* gen. nov., with two species *Natrinema pellirubrum* nom. nov. and *Natrinema pallidum* nom. Nov', *Int J Syst Evol Microbiol*, 48(4), 1187-1196, 1998
40. Pei, A. Y., Oberdorf, W. E., Nossa, C. W., Agarwal, A., Chokshi, P., Gerz, E. A., ... Pei, Z.: 'Diversity of 16S rRNA genes within individual prokaryotic genomes', *Appl Environ Microbiol*, 76(12), 3886-3897, 2010
41. Yilmaz, E. & Birbir, M.: 'Characterization of Halotolerant *Bacillus* Species Isolated from Salt Samples Collected from Leather Factories in Turkey', *J Am Leather Chem As*, 114(4), 118-130, 2019



POSTER
PRESENTATIONS +
SPEED SPEECH

ANALYSIS OF THE FUNCTIONAL COMPONENTS OF ACID PROTEASE AND INVESTIGATION OF BATING MECHANISM OF WET-BLUE

Hao Li¹, Deyi Zhu¹, Yanchun Li^{1a}, Shan Cao^{1b}, Changhua Jiang², Tianping Yu²

1School of Light Industry and Engineering, Qilu University of Technology(Shandong Academy of Sciences), Jinan. 250353, China,;

2Shandong Leather Industry Research Institute, Jinan, 250021, China

a)Corresponding author: qlulyc@126.com

b) anotherauthor: cs1988@foxmail.com.

Abstract. In recent years, acid protease is widely used in bating process of wet-blue by tanneries. Therefore, it is necessary to study the mechanism between acid protease and wet-blue for better practical application in bating process. In this study, one acid protease from *Aspergillus* was used to study the mechanism between protease and wet-blue. Firstly, the SDS-PAGE analysis revealed that the molecular weight of it was 48KD, the Zeta potential analysis showed that its pI was consistent with its optimum pH value, which was at 3.0. According to its enzymatic properties, the activated ingredients were separated from it by Tangential Flow Filtration (TFF) and used to treat wet-blue, then the enzymatic hydrolysate were obtained. On the one hand, the contents of Hydroxyproline(Hyp) and Desmosine(Des) in the hydrolysate were determined by HPLC and ELISA method, respectively, then, the biodegradation rates of collagen and elastin were calculated, the results showed collagen and elastin degraded 0.006‰ and 0.5‰ respectively. On the other hand, the changes of Elastic fibers in wet-blue before and after treated by the activated ingredients were characterized by Super Depth of Field Microscope. The results showed that the Elastic fibres are clearly dispersed by acid protease. And this paper would provide the basis and researches for the development of mechanism about acid protease in bating process.

1 Introduction

Protease is an irreplaceable biomaterial for improving leather quality and realizing cleaner production and sustainable development of leather industry, and the protease is widely used in many leather manufactures process, such as soaking¹, dehairng² and bating³. In leather industry, the processing of hides or skins to leathers involves three important stages: beam-house operations, tanning process, and finishing process.

At present, chrome-tanned leather has excellent physical and chemical properties such as high shrinkage temperature, softness, fullness and good hygienic properties, thus chrome tanning is the most popular tanning method. The beam-house operations are known to contribute more than 90% of the total pollution load from leather processing⁴. In order to reduce the cost of pollution control, most tanneries directly use wet-blue as raw material to produce finished leather with different types and styles. With a long-time transportation and preservation, the fibres of wet-blue may be further cross-linked by residual chrome. The tightly arranged fibres bundles bring a negative influence on the penetration of chemicals in subsequent process, which may result in defect of finished leather. In order to reduce grain defects and improve the quality of finished leather, a pre-treatment should be performed to homogenize wet-blue from different regions and disperse the fibres of wet-blue. Because pH of wet-blue was approximately 4.0, acid protease has potential to be applied in the bating process.

Most of currently used industrial enzymes are derived from microbial fermentation process, and the proteases remain the dominant enzyme type, so the composition of enzymes is very complex, and the enzymes were not used in any pure or well-characterized form⁵. So, in order to better explore the mechanism between acid protease and wet-blue, it is necessary to separate the active components of acid protease.

In this paper, the reaction mechanism between acid protease and wet-blue in bating process was investigated by exploring the biodegradability rate of the collagen and elastin in wet-blue. The changes of elastic fibres before and after acid protease treatment were observed. This study has a great significance for protease application in wet-blue bating.

2 Experimental

2.1 Materials

The wet-blue were purchased from Shandong Dexin Leather Industry. Hydroxyproline (Hyp) were purchased from Shanghai yuanye Bio-Technology Co.,Ltd. Desmosine (DES) ELISA Kit were purchased from Jiangsu Kete Biological Technology Co.,Ltd. Acid protease were purchased from Longda Biotechnology (Shandong,China). Rainbow predyed wide molecular weight protein marker (10-260 KD) purchased from HeFei BoMei Biotechnology Co.Ltd. The chemicals used for analytical techniques were of analytical grade.

2.2 Determination the Enzymatic Properties of Acid protease

2.2.1 The optimum pH value and isoelectric point(pI)

The acid protease was dissolved in buffers with different pH values(pH=2-11).The activity was determined with casein solution as the substrate, from the standard curve the activity of protease samples can be determined in terms of Units, which is the amount in micromoles of tyrosine equivalents released from casein per minute⁶⁻⁸. The pI was determined by Zeta Potential and Nanoparticle Size Measuring analysers(Malvern,UK).

2.2.2 The molecular weight by SDS-PAGE method

At the same time, the molecular weight of the acid protease was analyzed by Polyacrylamide Gel Electrophoresis methods(SDS-PAGE)⁹⁻¹², the standard curve was established with relative mobility of standard protein marker and the relative mobility of acid protease were substituted for the standard curve equation to calculate its molecular mass. 12% separation gel and 5% stacking gel were separately prepared, the loading quantity of marker and acid protease are all 20 μ L. The stacking gel voltage was 80 V and the separation gel voltage was 120 V and the thickness of the gel was 1mm.

2.3 Preparation of the Enzymatic Separation Hydrolysate of Acid protease

2.0 g enzyme powder was weighed accurately and dissolved in sodium lactate buffer (pH=3), filtered and fixed volume in 1 L volumetric bottle to prepare 2 g/L enzyme solution. According to the results of SDS-PAGE, the effective components of acid protease was separated by Tangential Flow Filtration (TFF) system (MinimateTM TFF Capsule with OmegaTM 50K Membrane, Pall Corporation, the USA).

A several circular samples with diameter of 5 cm were taken and divide into two groups with equal mass, A and B. Group A served as control group and the group B as experimental group. According to the conventional bating process, the group B was placed in the effective components and the group A was placed in the sodium lactate buffer(pH=3) at 40°C treated for 4 h. The volume of the solution used in the control group and the experimental group was 100 mL. After the process, the waste liquid of the two group was taken, filtered and stored at 4 °C for reserve.

2.4 Analysis of Enzymatic Hydrolysate

2.4.1 Determination of Hyp by HPLC method

The Hydrolysate was mixed with 6M HCl in equal volume (v:v=1:1) and digested at 150 °C for 15 min by Microwave Digestion machine(Ethos. UP, Milestone, Italin). The Hyp content were determined by HPLC method¹³⁻¹⁵ with pre-column derivation with 2,4-dinitrofluorobenzene. The mobile phase was A: ammonium acetate(30 mmol/L), B: acetonitrile. Gradient elution(0-7 min,80%A;7-10 min,60%A;10-30 min,60%A) with a flow rate of 1 mL/min. Aiglent TC-C18(5 um, 4.6×250 mm), the detection wavelength is 360 nm, loading quantity of sample was 20 uL and the temperature of chromatographic column is 27 °C.

2.4.2 Determination of Des by ELISA method

This experiment was carried out by using the double antibody sandwich ELISA method to detect the Des content in the Hydrolysate¹⁶⁻¹⁸. A solid-phase antibody was prepared by coating the microporous plate with purified anti-desin antibody. Des was added to the micropore of the coated monoclonal antibody in turn, and then combined with HRP-labeled antides antibody to form an antibody-antigen-enzyme labeled antibody complex. After thorough washing, TMB was added to the substrate to develop the antibody. TMB is converted to blue catalyzed by HRP enzymes and finally yellow by acid. The OD value was measured at 450 nm by Enzyme Labeling Instrument (Labsystems,Multiskan,MS-352,Finland).The concentration of Des in the samples was calculated by standard curve. The specific test method is carried out according to the requirements of the instructions of the Des Element Kit.

2.5 Determination of the Biodegradation Rate of Structural Protein by Protease

Collagen accounts for three-quarters of the dry weight of skin¹⁹,and Hyp is the unique amino acid of collagen and each 100 g of collagen contains 12.8 g of hydroxyproline²⁰. Thus the constant for calculating collagen degradation rate is designed as 96. Elastin content in the skin is low, only constituted 2%-5% of the dry weight of skin²¹,and the Des constant is $(2 \times 10^4)/17$ because 1 g elastin contains 17 μmol Des ($M_{Des}=526.6031$ g/mol) of Des²².The wet-blue samples used for bating process were dried to constant weight in an oven at 50 °C and the total dry weight of the samples was determined, that is m_0 . According to the concentration of Hyp and Des in enzymatic hydrolysate, that is C_{Hyp} and C_{Des} , respectively, and

according to the above relationship, then the biodegradation rates(Represent it with the letter D) of collagen and elastin during bating process were calculated according to the following formulas (1) and (2),respectively:

$$D_{collagen} = \frac{C_{Hyp} \times V}{96m_0} \times 1000\% \quad (1)$$

$$D_{Elastin} = \frac{20000V \times C_{Des}}{17M_{Des} \times m_0} \times 1000\% \quad (2)$$

2.6 Observation of the Change of Elastin Fibre by Acid Protease

The wet-blue samples were sectioned horizontal at 25 μm by the freezing microtome (CM1950 type, Leica Company, Germany). The slices were oxidized with potassium permanganate solution (5 g/L), then, the slices were bleached with oxalic acid solution (10 g/L), then, the slices were stained with aldehyde-fuchsin, and followed by separating, dehydrating, clearing, and sealing. The method of acid protease treatment for the slices is the same as the above. Then, the condition of elastic fiber treated or untreated by acid protease in wet-blue was observed by Super Depth of Field Microscope (Leica DVM6, Leica Company, Germany) with 1000 times magnification.

3 Results and Discussion

3.1 Analysing the Enzymatic Properties of Acid protease

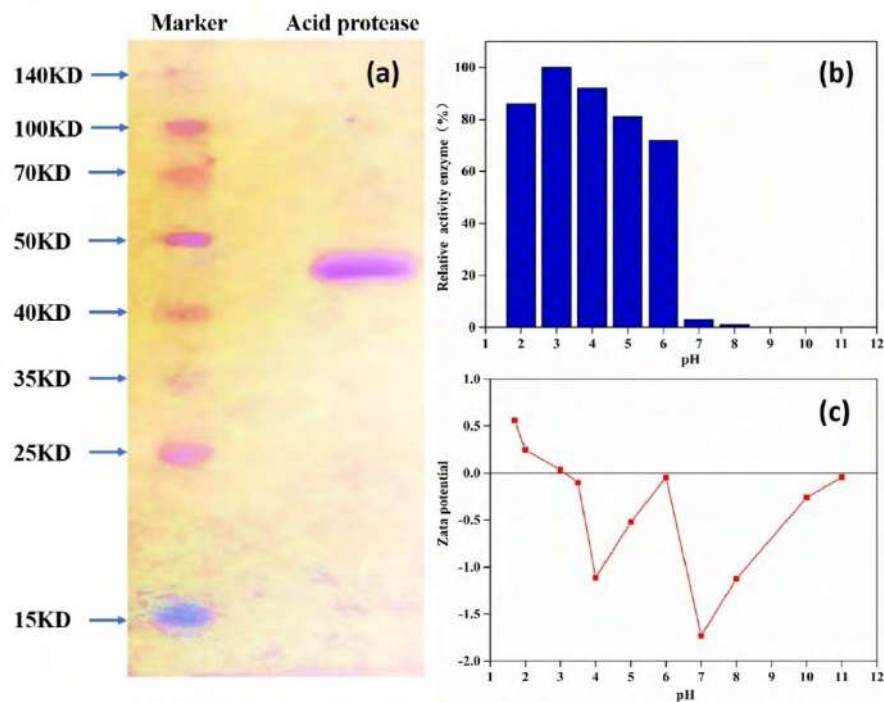


Fig. 1. The Enzymatic properties of Acid Protease. (a) the SDS-PAGE picture of acid protease;(b) the relative Enzyme activity of acid protease; (c) the isoelectric point(pI) of the acid protease.

From Fig. 1 (a), there is only one electrophoretic band, the map illustrate that the acid protease is highly expressed and the other enzymes are relatively few. According to the relative mobility standard curve equation of maker was $\lg M = -1.2316x + 2.1471$, $r = 0.9913$. and the molecular weight of acid protease was about 48 KD. Fig.1(b) and Fig.1(c) shows that the protease has stable catalytic activity under acid conditions, and the pI and the optimum pH are all around 3.0.

3.2 Analysing the Biodegradation Rate of Acid Protease

3.2.1 The content of Hyp and Des in hydrolysate

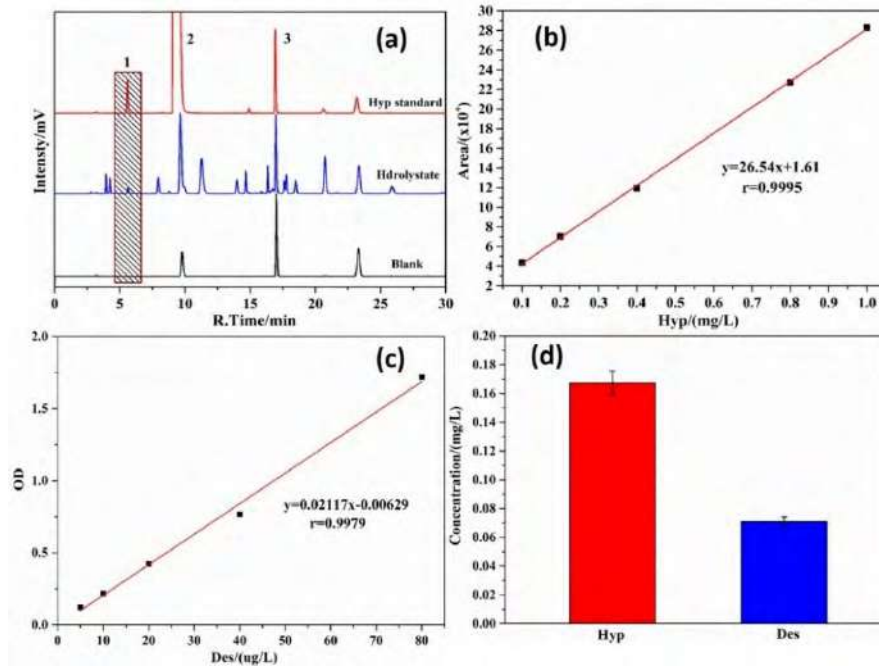


Fig 2. (a) The HPLC chromatograms. 1: Hyp; 2: 2, 4-Dinitrophenol; 3: 2, 4-Dinitrofluorobenzene (b) the standard regression curve of Hyp standard by HPLC; (c) the standard regression curve of Des by ELISA; (d) the concentration of Hyp and Des in Hydrolysate.

As shown in Fig. 2 (a), we can see that when elution time approached 6 minutes, the elution peak of Hyp appeared. Fig. 2 (b) shows that the standard curve equation of Hyp was $y = -26.54x + 1.61$, $y = A / 10000$, $r = 0.9995$. From Fig.2(d), the concentration of Hyp in enzymatic hydrolysate calculated by standard curve equation was 0.17 mg/L. In Fig. 2 (c), the standard curve equation of Des was $y = 0.02117x + 0.00629$, $r = 0.9979$. and from Fig. 2 (d), the concentration of Des in enzymatic hydrolysate calculated by standard curve equation was 0.071 mg/L.

3.2.2 The biodegradation rate of acid protease to structural protein

Table 1. The Biodegradation Rate of collagen and elastin in bating process.

Project	Structural Proteins in wet-blue	
	Collagen	Elastin
Biodegradation Rate (%)	0.006	0.5

Table 1 shows that the biodegradation rates of collagen and elastin was 0.006‰ and 0.5‰, respectively. The result illustrated that the degradation rate of elastin is about 100 times that of collagen in bating process of wet-blue. Therefore, the degradation ratio of elastin is much larger than that of collagen, and the major reason for the results was elastin has fewer amino acids containing carboxyl group than collagen. Therefore, the cross-linking reaction of elastin with chromium is weaker than that of collagen in tanning process, so acid protease is more likely to act on elastin. Based on the above results, we can conclude that the degradation of elastin in wet-blue by acid protease is the main reason for improving the properties of crust leather.

3.3 Analysing the Change of Elastic Fibres by Acid Protease

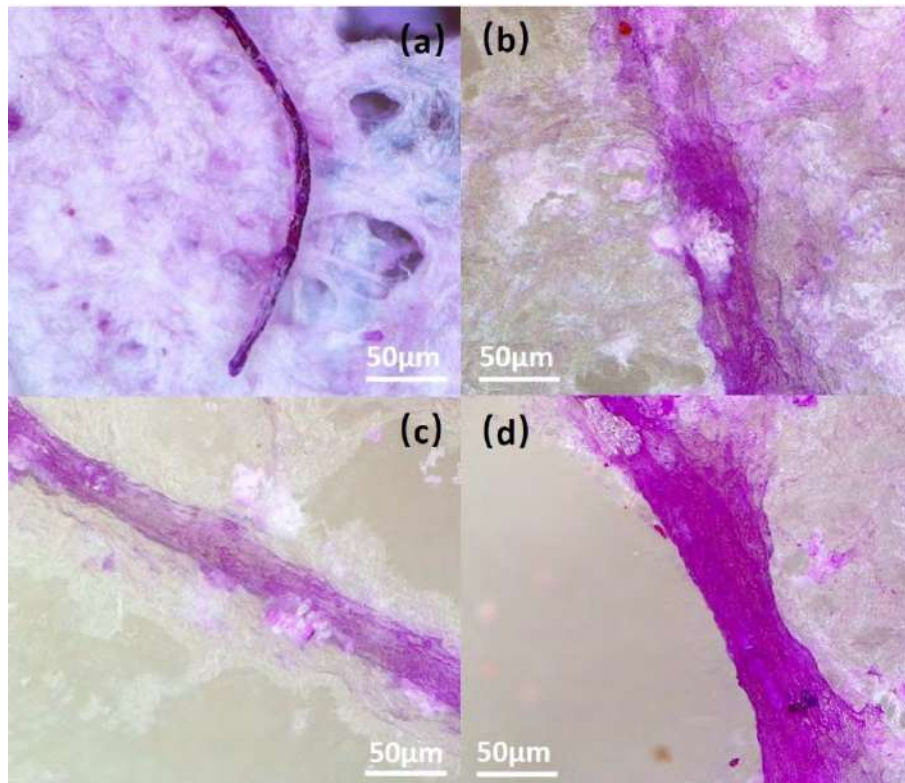


Fig. 3. The image of Elastic Fibres. (a) the Elastic Fibres untreated. (b), (c) and (d) the Elastic Fibres treated by acid protease.

Fig.3(a) shows that the elastic fibres in the wet-blue are dyed dark purple by aldehyde-fuchsin. Comparing the Fig.3(a) and (b), (c), (d), we can see the distribution range of the purple area is obviously enlarged, this indicates that elastic fibres are dispersed after treated with acid protease. Besides, the distribution of tissues (collagen, etc.) outside the elastin has also become uniform. This will make the flatness of grain surface and the softness of the crust leather be improved.

Conclusions

In the bating process, acid protease can degrade the two main structural proteins (collagen and elastin) in wet-blue and improve the performance of crust leather. However, in this process, the biodegradation rate of elastin is about 100 times that of collagen. Therefore, the conclusion that we come to is that the degradation of elastin in wet-blue by acid protease is the main factor affecting the improvement of performance of crust leather. This paper clears the degradation mechanism of wet blue to some extent which have great significance for the development of mechanism of acid protease to the bating process of wet-blue.

Acknowledgements

This study was financially supported by the National Key Research and Development Program of China under contract No. 2017YFB0308402.

References

1. Zambare, V. P.; Nilegaonkar, S. S.; Kanekar, P. P., *Protease production and enzymatic soaking of salt-preserved buffalo hides for leather processing. IIOAB Letters* 2014, 3 (1), 1-7.
2. Nilegaonkar, S. S.; Zambare, V. P.; Kanekar, P. P.; Dhakephalkar, P. K.; Sarnaik, S. S., *Production and partial characterization of dehairing protease from Bacillus cereus MCM B-326. Bioresour Technol* 2007, 98 (6), 1238-45.
3. Vasudeo Zambare, S. N. P. K., *Application of protease from Bacillus cereus MCM B-326 as a bating agent in leather processing. The IIOAB Journal* 2010, 1 (4), 18-21.
4. Saravanabhavan, S.; Aravindhan, R.; Thanikaivelan, P.; Rao, J. R.; Nair, B. U.; Ramasami, T., *A source reduction approach: Integrated bio-based tanning methods and the role of enzymes in dehairing and fibre opening. Clean Technologies and Environmental Policy* 2004, 7 (1), 3-14.
5. Kirk, O.; Borchert, T. V.; Fuglsang, C. C., *Industrial enzyme applications. Current Opinion in Biotechnology* 2002, 13 (4), 345-351.
6. Ji, H.; Sun, H. T.; Xiong, D. M., *Studies on activity, distribution, and zymogram of protease, alpha-amylase, and lipase in the paddlefish Polyodon spathula. Fish Physiol Biochem* 2012, 38 (3), 603-613.
7. Piechowiak, T.; Józefczyk, R.; Balawejder, M., *Impact of ozonation process of wheat flour on the activity of selected enzymes. Journal of Cereal Science* 2018, 84, 30-37.
8. Cupp-Enyard, C., *Sigma's Non-specific Protease Activity Assay - Casein as a Substrate. J Vis Exp* 2008, (19).
9. Hamsten, F. K. A., *Determination of apolipoproteins B-48 and B-100 in triglyceride-rich lipoproteins by analytical SDS-PAGE. Journal of Lipid Research* 1994, 35, 1311-1317.
10. Inoue, M. I. Y., *A New 4.8-kDa Polypeptide Intrinsic to the PS II Reaction Center, as Revealed by Modified SDS-PAGE with Improved Resolution of Low-Molecular-Weight Protein. Plant Cell Physiol.* 1988, 29 (7), 1233-1239.
11. NATALUCCI, M. F. P. C. L., *Electrophoretic Analysis (Tricine-SDS-PAGE). Acta Farm. Bonaerense* 2002, 21 (1), 57-60.
12. Qiu, J.; Sheedlo, M. J.; Yu, K.; Tan, Y.; Nakayasu, E. S.; Das, C.; Liu, X.; Luo, Z. Q., *Ubiquitination independent of E1 and E2 enzymes by bacterial effectors. Nature* 2016, 533 (7601), 120-4.
13. Hutson, P. R.; Crawford, M. E.; Sorkness, R. L., *Liquid chromatographic determination of hydroxyproline in tissue samples. Journal of Chromatography B* 2003, 791 (1-2), 427-430.
14. Tojo, Y.; Hamase, K.; Nakata, M.; Morikawa, A.; Mita, M.; Ashida, Y.; Lindner, W.; Zaitso, K., *Automated and simultaneous two-dimensional micro-high-performance liquid chromatographic determination of proline and hydroxyproline enantiomers in mammals. J Chromatogr B Analyt Technol Biomed Life Sci* 2008, 875 (1), 174-9.
15. Vázquez-Ortiz, F. A.; Morón-Fuenmayor, O. E.; González-Méndez, N. F., *Hydroxyproline Measurement by HPLC: Improved Method of Total Collagen Determination in Meat Samples. Journal of Liquid Chromatography & Related Technologies* 2009, 27 (17), 2771-2780.
16. GUNJA-SMITH, Z., *An Enzyme-Linked Immunosorbent Assay to Quantitate the Elastin Crosslink Desmosine in Tissue and Urine Samples. ANALYTICAL BIOCHEMISTRY* 1985, 147, 258-264.
17. Philippe Laurent, L. M., Jeanine De Palmas, Jean Bignon a and Marie-Claude Jaurand, *Quantitation of elastin in human urine and rat pleural mesothelial cell matrix by a sensitive avidin-biotin ELISA for desmosine. Journal of Immunological Methods* 1988, 107, 1-11.
18. Stoilov, I.; Starcher, B. C.; Mecham, R. P.; Broekelmann, T. J., *Measurement of elastin, collagen, and total protein levels in tissues. Methods Cell Biol* 2018, 143, 133-146.
19. Shoulders, M. D.; Raines, R. T., *Collagen structure and stability. Annu Rev Biochem* 2009, 78, 929-58.
20. ANA MARIA DE GUZZI PLEPIS, G. G., and DILIP K. DAS-GUPTA, *Dielectric and Pyroelectric Characterization of Anionic and Native Collagen. POLYMER ENGINEERING AND SCIENCE* 1996, 36 (24).
21. Mithieux, S. M., ; Weiss, A. S., *Elastin. Advances in Protein Chemistry* 2005, 70, 437-461.
22. M, M. S. E. K. M., *Influence of elastin degradation on the mechanical properties of leather. JALCA* 2014, 109, 306-313.

A NOVEL MICROSPHERES COMPOSITE HYDROGELS CROSS-LINKED BY METHACRYLATED GELATIN NANOPARTICLES, ENHANCED MECHANICAL PROPERTY AND BIOCOMPATIBILITY

C. H. Wang¹, C. D. Mu² and W. Lin¹

¹ Department of Biomass and Leather Engineering, Key Laboratory of Leather Chemistry and Engineering of Ministry of Education, Sichuan University, Chengdu, Sichuan, China .610065.

² Department of Pharmaceutics and Bioengineering, School of Chemical Engineering, Sichuan University, Chengdu, China, 610065.

a) Corresponding author, wlin@scu.edu.cn

b) wangchunhua@scu.edu.cn

Abstract. We report a novel macromolecular microsphere composites (MMC) hydrogel based on polyacrylamide with enhanced mechanical property and biocompatibility. The key feature of our approach is the use of prepared methacrylated gelatin nanoparticles (MA-GNP) as the cross-linker, which have the ability of chemical crosslinking by the polymerization of C=C bonds, such that the composite hydrogels can be formed by radical polymerization of acrylamide (AAm) on the surface of MA-GNP. The smooth spherical particles with an average size of ~100 nm have been synthesized through a modified two-step desolvation method as proved by atomic force microscopy (AFM). The results of nuclear magnetic resonance and dynamic light scattering further confirm the presence of reactive groups (C=C bonds) in the particles and its narrow sizes distribution. The resulting composite hydrogels (MA-GNP/PAAm) are porous materials with tunable pore sizes and exhibit enhanced compressive resistance and elasticity as well. Increasing appropriately the dosage of MA-GNP reduces the equilibrium swelling ratio and improves thermal stability of the gels. Moreover, all the hydrogels exhibit prolonged blood-clotting time, nonhemolytic nature and strong suitability for cell proliferation, indicating the improved antithrombogenicity and excellent cyto-compatibility. It suggests that the novel MA-GNP/PAAm hydrogels have potential application as tissue engineer scaffold materials, and the MA-GNP can be a promising macromolecular microsphere cross-linker for application in biomedical materials.

1 Introduction

Polymer hydrogels are non-water soluble materials with a hydrophilic three-dimensional crosslinking network structure and exhibit unique properties such as excellent permeability, high water absorptivity, good elasticity and biocompatibility. To date, hydrogels have been widely used in biomedical applications including contact lenses¹, wound dressings², tissue engineering materials³ and drug delivery⁴. Nevertheless, the non-uniform cross-linking structures in the conventional hydrogels lead to poor mechanical property, which greatly limits their practical applications.

To toughen the gels, great efforts have been made to fabricate new kinds of polymer hydrogels^{5,6,7}. One of the novel and important developments is macromolecular microsphere composite (MMC) hydrogels with well-defined structures, first proposed by Wang and coworkers in 2007⁸. In this hydrogel, the macromolecular microspheres act as crosslinking points and the uniform polymer chains are chemically grafted onto the microspheres. This unique microstructure can endow the MMC hydrogels with high mechanical strength and excellent resilience because the applied force can be evenly distributed by all polymer chains⁹. In contrast to the preparation of nanocomposite (NC) hydrogel made from specific polymers with a kind of water swellable clay, the synthesis of MMC hydrogels is a general and facile strategy. It only requires organic components and the compositions and properties of the hydrogels can be tailored by changing the microspheres and monomers. Moreover, the surface structure of organic microspheres can be more easily designed as required, compared with the inorganic particles used in NC systems.

So far, MMC gels have received considerable interest^{10,11}, and the formation mechanism^{12,13}, the relationship between network structure and property¹⁴⁻¹⁶ have also been explored. However, most of microspheres used in the MMC hydrogels are mainly synthetic polymer such as polystyrene (PS) or poly(styrene-cobutylacrylate) particles. Only a few reports have used the biodegradable starch-based microspheres for synthesis of MMC hydrogels¹⁰, but without any evaluation of the hydrogels for bio-related applications. Biocompatibility is one of the essential characteristics of hydrogels used in biomedical applications. Therefore, the fabrication of MMC hydrogels with good biocompatibility and mechanical properties is highly desirable.

Gelatin has exhibited significance in biomedicine and food field as it offers the advantages of excellent biocompatibility, biodegradability and low immunogenicity. In our previous works, the introduction of gelatin and methacrylamide-modified gelatin (MA-gelatin) into clay-polyacrylamide (PAAm) NC gels could substantially improve the biocompatibility of gels^{17,18}. However, the incompatibility of gelatin polyelectrolyte and clay limit the improvement both in mechanical property and biocompatibility of the gels. Inspired by the MMC hydrogels, it is believed that sole introduction of the gelatin-based microspheres into the PAAm is expected to strengthen the AAm hydrogels while simultaneously keeping the enhanced biocompatibility.

Hence, in this work a novel microsphere composite hydrogel with both good biocompatibility and enhanced mechanical properties has been prepared by using acrylamide (AAm) as the monomer and MA-gelatin nanoparticles (MA-GNP) as cross-linker. Herein, MA-gelatin is chosen instead of gelatin for the fabrication of the described nanoparticles because it not only can retain the good biocompatibility and hydrophilicity of gelatin^{19,20} but also has the possibility of chemical crosslinking due to the presence of reactive C=C bonds, in contrast to unmodified gelatin²¹. Therefore, the obtained biocompatible particles containing C=C bonds can be expected to be as an effective cross-linker and modifier due to the combined processes of polymerization and crosslinking during the synthesis of MMC hydrogels. Our aim is to prepare a novel microsphere composite hydrogel with the potential for wound dressings and tissue engineer scaffold materials.

2 Experimental Section

2.1 Materials

Acrylamide, gelatin (type B, ~240 Bloom), glutaraldehyde (50% aqueous solution), methacrylic anhydride (MA), 2,4,6-trinitro-Benzenesulfonic acid (TNBS) and glycine (AR) were purchased from Aladdin Inc. Ammonium persulfate (APS), acetone and N,N,N',N'-tetramethylethylenediamine (TEMED) were obtained from Sigma-Aldrich. The concentrations of the stock solutions of TEMED and APS were fixed at 10% v/v and 3% w/v, respectively. L929 cells were obtained from Chinese Academy of Science Cell Bank for Type Culture Collection (Shanghai, China). Dulbecco's modified Eagle's medium (DMEM) were purchased from Hyclone (USA), penicillin and streptomycin were purchased from Gibco (USA). Cell counting kit-8 (CCK8) was purchased from Kumamoto (Japan).

For the present study, the free amino groups of gelatin B were quantitatively measured by the Habeeb method²² with glycine solutions (the phosphate buffer as a solvent, pH 7.4) in various concentrations as standard. According to the calibration curve ($R^2=0.9998$), the amount of free amino groups of the gelatin was $0.355 \text{ mmol g}^{-1}$, this value is consistent with previous study²³.

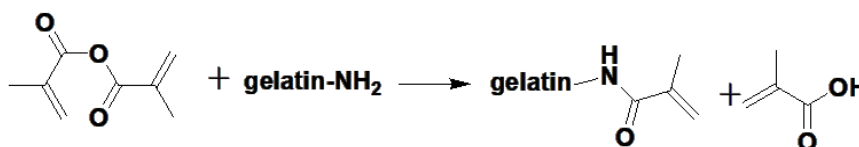
2.2 Sample preparation

2.2.1 Preparation of Methacrylated gelatin (MA-gelatin)

Methacrylated gelatin (MA-gelatin) was prepared by the reaction between gelatin and methacrylic anhydride, as previously reported²³. Detailedly, 5 g gelatin (~1.775 mmol free amino groups) was dissolved in 50 mL phosphate buffer (PBS, pH 7.4, 0.2M) at 50 °C for 1.5 h. Then 0.2~0.6 mL MA (1.30~3.90 mmol) was added dropwise under vigorously stirring at 2500 rpm, respectively and the reaction was allowed to proceed for 3 h. Subsequently the mixture was diluted with 100 mL PBS and dialyzed against deionized water at 40 °C for 24 h to remove the excess MA and other impurities. The resulting MA-gelatin was obtained as a white solid after lyophilization. The degree of substitution (DS) of MA-gelatin is defined as the percentage of ε-amino groups of gelatin that are modified and determined by Habeeb method²². Briefly, the reaction of TNBS and free amino groups at 40 °C led to a trinitrobenzene compound, and the optical absorbance of the solution was recorded with UV-Vis spectrophotometer at 415 nm. The DS of MA-gelatin was calculated using the following equation:

$$OD (\%) = \frac{OD_g - OD_m}{OD_g} \times 100 \quad (1)$$

where OD_g and OD_m are the optical density (OD) values of gelatin and MA-gelatin, respectively.



Scheme 1. Schematic representation of methacrylamide modification reactions yielding MA-gelatin.

2.2.2 Preparation of methacrylated gelatin nanoparticles (MA-GNP).

The MA-GNP was prepared from DS50% MA-gelatin crosslinked with glutaraldehyde by a modified two-step desolvation method, previously described by the group of Coester²⁴. Typically, 1.25 g MA-gelatin was dissolved in 25 mL distilled water under constant heating (T=40 °C) and stirring. Then 25 mL of a desolvating agent (acetone) was added to the solution to obtain the high-molecular-weight (HMW) gelatin. After that, the HMW-gelatin was redissolved in 25 mL distilled water and the pH of the solution was adjusted to 12.0. The gelatin was then desolvated again by dropwise addition of acetone under constant heating until the mixture becomes milky white. After stirring for 10 min, glutaraldehyde solution (100 μL) was added to cross-link the particle. The reaction was conducted at 50 °C for 16h under constant stirring. Finally, the dispersion was filtered and centrifuged at 10000g (Sigma, 3-18 K) for 20 min. After the last centrifugation, the particles were dispersed in supernatant distilled water and the residual acetone was removed by slow vaporization. The resulting MA-GNP was obtained as pale-yellow particles after lyophilization.

2.2.3 Preparation of polyacrylamide based composite hydrogels (MA-GNP/PAAm) crosslinked by MA-GNP

The composite hydrogels were synthesized through in-situ free radical polymerization. The initial reaction solution consists of monomer (AAm), cross-linker (MA-GNP), initiator (KPS), and accelerator (TEMED). The molar ratio of MMA/TEMED/APS was 7/0.132/0.2/0.2. In all cases, the concentration of AAm were set at 10% w/v, and the mass ratio of MA-GNP to AAm was varied from 0 to 25% w/w. AAm (0.5 g) and MA-GNP (0~0.125g) were added into a glass bottle, respectively, and the total volume was fixed to 4.87 mL with deionized water. After magnetic stirring at room temperature for 2 h, the mixture solution was bubbled with nitrogen gas for 10 min, and then APS (100 μL) and TEMED (30 μL) were added. The reaction was conducted at room temperature for 24 h. The resulting gels in this study are denoted as x% MA-GNP/PAAm, where x stands for 100×MA-GNP/AAm (w/w).

2.3 Characterizations

2.3.1 Nuclear Magnetic Resonance Spectroscopy (1H-NMR)

The MA-gelatin and MA-GNP were proved by 1H-NMR spectroscopy (AV II, Bruker, Germany)²⁵. 5~10 mg Samples of were dissolved in 550 μL of deuterium oxide (D_2O) before measurement. 1H-NMR spectra were collected at 35 °C and at a frequency of 600 MHz by using a Bruker AV II spectrometer.

2.3.2 Atomic force microscopy (AFM)

The particles dispersion (10 μL) at a concentration of 0.05 mg mL^{-1} was dropped onto a freshly cleaved mica substrate and dried at room temperature in a desiccator with silica gel for 24 h. The samples were scanned in air by a Dimension 3100 Nanoscope IV equipped with UrtalveerB probes (SPM-9600, Shimadzu, Japan) in a tapping mode.

2.3.2 Particle Size measurement

The particle sizes of MA-GNP samples was measured by a Malvern Nano-ZS ZEN3600 instrument using a Zetasizer at a detection angle of 90° at 25 °C in the dust-free circumstance. The concentration of MA-GNP dispersions was 0.04 mg mL^{-1} . The mean particle size and polydispersity index were recorded in the cumulant mode employing the built-in Malvern software.

2.3.3 Fluorescence spectrum and confocal laser scanning microscopy (CLSM)

Measurement of the fluorescence spectrum of the MA-GNP particles was performed by a fluorescence spectrophotometer (F-7000, Hitachi, Japan) at 25 °C. The excitation slit was set at 10 nm and scanning speed was 30000 nm/min. The excitation wavelength was 336 nm, 488 nm and 543 nm respectively. And the range of emission spectra was 355 ~ 700 nm, 500 ~ 700 nm, 520 ~ 700 nm respectively. The concentration of MA-GNP was 0.5 mg/mL . The Fluorescence properties and distribution of particles in as-prepared hydrogels were imaged by CLSM (Nikon Eclipse TI, Nikon, Japan), and an oil mirror 40 \times (numerical aperture, NA = 0.85) was used. The hydrogels were directly placed on the cover slides and a series of x/y layers were scanned. The laser wavelength was 543 nm and filter wavelength was 605 nm. Three different sets of experiments were performed for each sample.

2.3.4 Scanning electron microscopy (SEM)

The morphology of the hydrogels was obtained by a scanning electron microscope (Quanta 400 FEG, FEI, USA) with operating voltage of 20 kV. The samples were first freeze-dried in lyophilizer (ALPHA 1-2 LD, Christ, Germany) for 30 h at -50 °C before observation.

2.3.5 Measurements of mechanical properties

Compressive tests of the as-prepared hydrogel samples were carried out on a MTS Universal Testing Machine (CMT6202, MTS systems Co., Ltd., China) at room temperature. The highest compressive strain was set at reach a level of 90%. At least three measurements were performed for each sample.

2.3.6 Swelling Experiments

Swelling experiments were carried out at room temperature by immersing the as-prepared hydrogels in pure deionized water and also in buffer solutions to reach swelling equilibrium, respectively. The corresponding swollen weight of the gels was recorded (Ws). After that, the swollen gels were then freeze-dried and weighted again to measure the weight of the dry gel (Wd). The effect of ionic strength on the equilibrium swelling ratio (ESR) was also investigated. The ionic strength was changed from 0 to 0.1 M at room temperature. The equilibrium swelling ratio was calculated as

$$S = \frac{W_s - W_d}{W_d} \quad (2)$$

2.3.7 Measurements of Thermal Properties.

Thermal properties were performed on a thermogravimetric analyzer (NETZSCH TG 209F1, Selb, Germany) from 60 to 600 °C at a heating rate of 10 °C/min under a nitrogen atmosphere. All samples were freeze-dried before measurement and the mass of each sample was 4 mg.

2.3.8 Blood clotting test

The anticoagulant properties of the composite hydrogels were evaluated by the contact method and the fresh rabbit blood was extracted according to ASTM standards²⁶. 0.2 mL of diluted anticoagulant acid citrate dextrose (ACD) blood was dropped on the surface of the gel samples (the diameter of gels is 30 mm and thickness is 10 mm) or glass coverslips²⁷ and 25 mL of CaCl₂ solution (0.2 mol L⁻¹) was then added to the ACD blood to activate the clotting reaction. After incubation at 37 °C for 5 min, 50 mL deionized water was added and the incubation was continued for another 10 min to lyse the red blood cells that had not been trapped in the thrombus. The absorbance of the supernatant at 545 nm is measured by UV-vis spectrometer (Perkin-Elmer Lambda 25, Germany) to determine the concentration of free hemoglobin in the water. 0.2 mL of diluted ACD blood in 50 mL of deionized water was used as a control. The blood clotting index (BCI) was calculated according to the following equation:

$$BCI (\%) = \frac{OD_t \times 100}{OD_c} \quad (3)$$

where OD_t and OD_c denote the OD values of test and control samples, respectively.

2.3.9 Hemolysis assay

The hemolytic potential of the MA-GNP composite hydrogels was evaluated following the reported procedure²⁸. Briefly, the sterilized swollen hydrogel pieces were immersed into a glass tube with 10 mL physiological saline and the incubation was kept for 30 min at 37 °C. 0.2 mL of diluted ACD blood was then added and the mixture was incubated in a rocking shaker at 37°C for 1 h, followed by centrifugation at 2000 rpm for 5 min. The optical density of the supernatant was determined at 545 nm by a UV-vis spectrometer. Positive and negative controls were prepared by adding 0.2 mL diluted ACD blood into 10 mL deionized water or physiological saline, respectively. The percentage hemolysis was calculated as follows:

$$Hemolysis (\%) = \frac{(OD_t - OD_n) \times 100}{OD_p - OD_n} \quad (4)$$

where OD_t, OD_n, and OD_p denote the OD values of test, negative, and positive samples, respectively. The hemolysis results were average of six measurements.

2.3.10 In vitro cytotoxicity

These measurements were carried out using an indirect method in which the extracts were used to culture cells, similar as the previous report^{29,30}. The stock extracts (C = 100%) of MA-GNP/PAAm gels were obtained by immersing gels (thickness >0.05 mm) of each material (3 cm²/ mL) in Dulbecco's modified Eagle's medium (DMEM) at 37 °C for 3 days without agitation. Before cell culturing, the extract solutions were filter sterilized through a 0.22 μm microporous membrane. The extract with a concentration of 50% (C = 50%) was also prepared by diluting the stock extract with equal volumes of culture medium.

(1) Activation of L929 Cells and preparation of MA-GNP/PAAm gels materials. L929 cells were cultured in petri dishes (Thermo Nunclon™, USA, 100*20 mm) using Dulbecco's modified Eagle's medium with high glucose supplemented with penicillin and streptomycin. They were maintained in a 5% CO₂ atmosphere at 37 °C (Carbon dioxide incubator, Thermo, USA) and subcultured. Cells were passaged approximately 2 times per week and the medium was exchanged every 2 days.

(2) Exposure of cells to extracts. The cells were seeded into three 96-well plates at a density of 1×10^4 cell /well per well (Corning, USA) in 0.1 ml medium. After 24 h of incubation as described above to allow cell attachment, the medium was replaced with the corresponding solutions, respectively, (a) DMEM without cells, used as a blank control; (b) DMEM with cells, used as negative control; (c) 100% stock extracts (C=100%) and 50% extracts (C=50%). In order to determine the cells relative proliferation rate (RGR) at different incubation interval, the cells were cultured for 6, 24 and 48h in a humidified atmosphere with 5% CO₂ at 37 °C, respectively. After incubation, the medium was removed and replaced with 90 μL fresh DMEM and 10 μL CCK-8 assay stock solution (5 mg/mL). The cells were incubated for 80 min to allow the formation of formazan crystals, which was determined at 450 nm by a Microplate reader (550 BIO-RAD, USA). The cell relative proliferation rate (RGR) was calculated according to the following equation:

$$RGR(\%) = \frac{(OD_t - OD_b)}{(OD_n - OD_b)} \times 100 \quad (5)$$

where OD_t, OD_n, and OD_b the OD values of test, negative, and blank samples, respectively. The RGR results were average of three measurements. And qualitative grading of cytotoxicity of the extracts are referred to ISO 10993-5 standard³¹ and United States Pharmacopeia (USP)³².

3 Results and discussion

3.1 Synthesis of MA-gelatin and MA-GNP

The presence of the methacrylate groups in the molecular structure of MA-gelatin makes it polymerizable (Figure 1a)¹⁹. The percentage of 3-amino groups of gelatin that are modified (namely, DS) can be adjusted by varying the amount of MA present in the initial reaction mixture (table 1). DS50% MA-gelatin is chosen for the preparation of MA-GNP as it retains amino groups for the particle synthesis and simultaneously contains carbon-carbon double bond, which can participate in subsequent radical polymerization reactions to achieve the crosslinking of PAAm gels. The modification of gelatin and synthesis of MA-GNP were verified by ¹H-NMR spectroscopy (Figure 1b). The signal at δ=2.8 ppm (attributed to lysine methylene groups) in the spectrum of MA-gelatin decreases with the increasing DS, indicating that the amino groups of the lysine have partially been substituted by methacrylamide groups. As for the MA-GNP, the absence of signal δ=2.8 ppm suggests that the rest of the amino groups of the lysine of MA-gelatin have almost entirely reacted with aldehyde groups of glutaraldehyde, leading to the MA-GNP. In addition, compared with unmodified gelatin, new signals observed at 5.2 ppm < δ < 5.6 ppm and at δ = 1.7 ppm both in the spectra of MA-gelatin and MA-GNP are ascribed to the acrylic protons and the methyl function of the introduced methacrylic groups, respectively²⁵. It confirms the presence of C=C bonds both in MA-gelatin and MA-GNP.

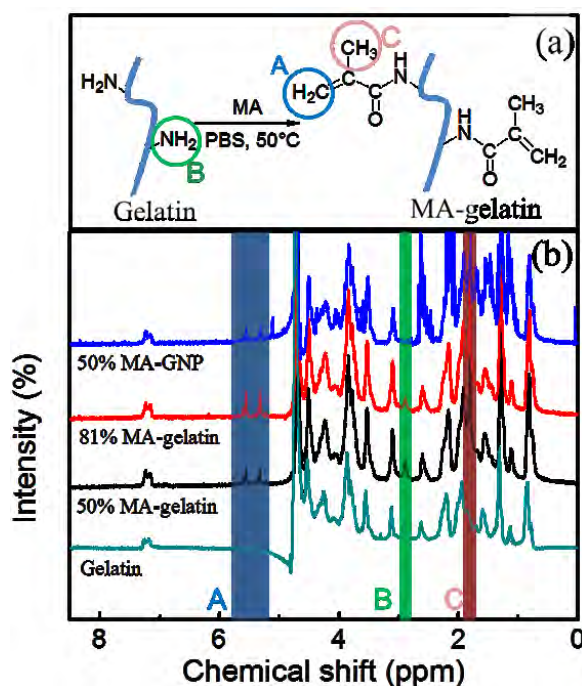


Fig. 1. (a) Schematic illustration showing the synthesis of MA-gelatin;(b) 1H NMR spectra of gelatin, MA-gelatin (DS50%, DS81%) and MA-GNP (DS50%). The signals of the acrylic protons and the methyl function of the introduced methacrylic groups are denoted as A and C, while lysine methylene signal of gelatin is denoted as B.

Table 1. Effect of the amount of MA on DS of MA-gelatin.

Dosage of MA (mL)	DS of MA-gelatin (%)
0.2	50.8±3.8
0.3	66.7±2.5
0.4	80.2±4.3
0.5	89.7±2.5
0.6	94.7±1.5

3.2 The characteristic of MA-GNP

Figure 2 shows the AFM morphology and size analysis of the synthesized particles. The nanoparticles is found to be spherical in shape with a smooth surface in a size range of 50~200 nm, fairly mono-dispersed on the mica. Studies have shown that the phase images can be used to visualize the local surface property of heterogeneous regions because the phase shift of the cantilever oscillation is very sensitive to the viscoelasticity like rigidity of the surfaces during tapping³³. The phase graph of the particles (Figure 2b) reflects the variation of the surface property of the MA-GNP by the contrast of cores (dark) and edges (light). It reveals that the density of the MA-GNP is not homogeneous whose edge parts are looser than the cores, which agrees well with our previous results³⁴. Moreover, the size distribution of the synthesized particles (Figure 2c) as measured by dynamic light scattering (DLS) further confirm that the average size of the particle is ~100 nm in diameter with a unimodal size

distribution (PDI = 0.17). The above-mentioned NMR analysis and AFM results indicate that the MA-GNP is suitable to be introduced into the microspheres hydrogel system as a cross-linking agent.

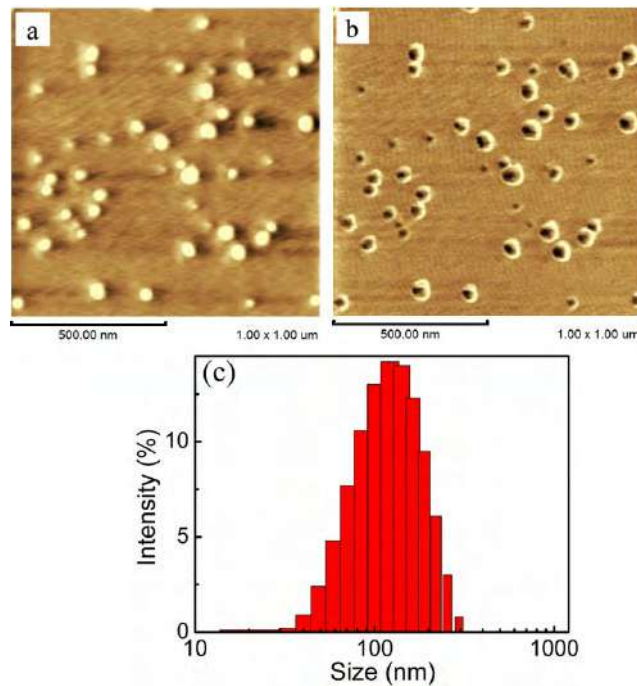


Fig. 2. (a) AFM height images of the MA-GNP, 1 $\mu\text{m} \times 1 \mu\text{m}$; (b) Phase graph of the MA-GNP; (c) Size distributions of the MA-GNP.

3.3 Copolymerization and structure of MA-GNP composite hydrogels

Figure 3a shows the schematic illustration of the preparation process of MA-GNP/PAAm hydrogels and proposed synthesis mechanism. The crosslinking at intra- or inter-molecular chains of MA-gelatin is due to the establishment of aldimine linkages (CH=N) between the free amino groups of MA-gelatin and glutaraldehyde, which leads to the formation of MA-GNP³⁵. Also, the C=C bonds of MA-GNP endow the particles with chemical crosslinking activity. Thus the microsphere composite hydrogels is formed by radical polymerization of AAm on the surface of MA-GNP (Figure 3a). The introduction of MA-GNP will change the nature of the gel network and improve various performances of the gels. When adding the pale yellow MA-GNP to the AAm solution, all of the suspensions were transparent and stable, which is favorable for the in situ polymerization (Figure 3b). The resulting composite hydrogels exhibit high transparency with yellow color. And the color of gels gradually deepen with increasing MA-GNP content.

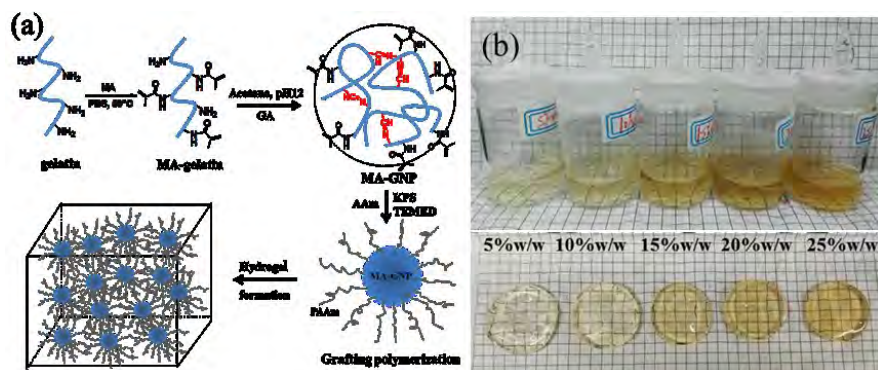


Fig. 3. (a) Proposed mechanism for the formation of an MMC hydrogel and an MMC hydrogel microstructure. (b) Mixtures solution before polymerization and resulting hydrogels composite hydrogels with different amounts of MA-GNP.

Figure 4a shows the fluorescence spectra of MA-GNP at different excitation wavelengths. For MA-GNP, the strongest emission band is observed between 420 and 480 nm (band I) upon excitation at 365 nm. And the emissions are centred at 560 nm (band II) upon excitation at 488 nm and 543 nm. The observed variations in autofluorescence relate to the different chemical structures of the MA-GNP particles. MA-GNP have two kinds of unsaturated double bonds including C=N bonds from the Schiff's base reaction and C=C bonds from MA-gelatin. Herein, the high-energy absorption (band I) is attributed to the π - π^* transition of C=C double bonds and the bands II is associated with the n - π^* transitions of C=N bonds in the Schiff's base³⁶. The autofluorescent characteristic of MA-GNP is beneficial to see how the particles are distributed in the cross-linked hydrogel networks. Note that the strongest emission intensity of microspheres is observed upon excitation at 543 nm. Therefore, the following CLSM image of the gels (Figure 4b and 4c) is given upon excitation at 543 nm, in which the red part represents the microspheres in composite hydrogels. It demonstrates that with increasing amounts of microspheres from 5% to 20%, the crosslinking density of the composite hydrogel is increased and the distribution MA-GNP is relatively uniform in the hydrogel even at the higher content of 20%.

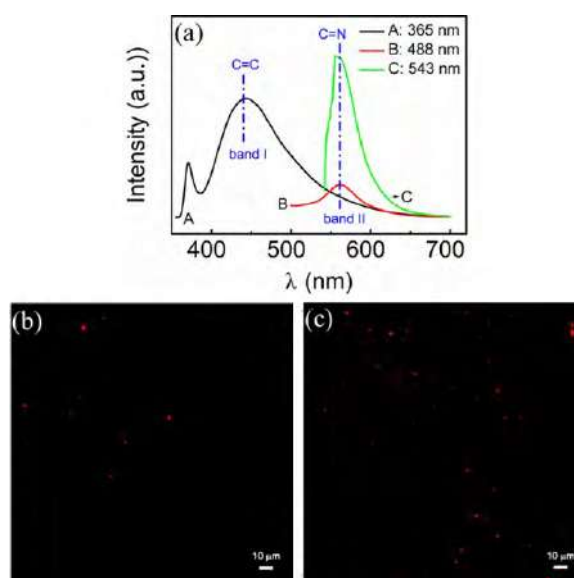


Fig. 4. (a) Fluorescence spectra of the MA-GNP at different excitation wavelengths. (b) CLSM image of 5% MA-GNP composite hydrogels. (c) CLSM image of 20% MA-GNP composite hydrogels.

The cross-sectional morphologies of the MMC hydrogels with different amounts of MA-GNP are given in Figure 5. It can be seen that, after drying and the removal of frozen water, all the gels are honeycomb-like with uniform interconnected pores due to the uniform dispersion of nanoparticles, the size of which decrease with the increasing amounts of MA-GNP. Considering the same initial gel compositions, subsequent preparation process and freeze-drying conditions, the reason for the difference in the porous structure can only be the varied amounts of cross-linkers MA-GNP and resulting crosslink density. Clearly, the lower the MA-GNP content (Figure 5b-f), the larger the pore size in the hydrogel, indicating that the porosity can be adjusted by controlling the content of the macromolecular microsphere cross-linker MA-GNP. Moreover, the pore sizes of the gels are distributed in the range of 20~200 μ m, which is the ideal pore size distribution for promoting cell adhesion and proliferation such as fibroblasts³⁷, suggesting that the gels can be potentially used as cell scaffold materials.

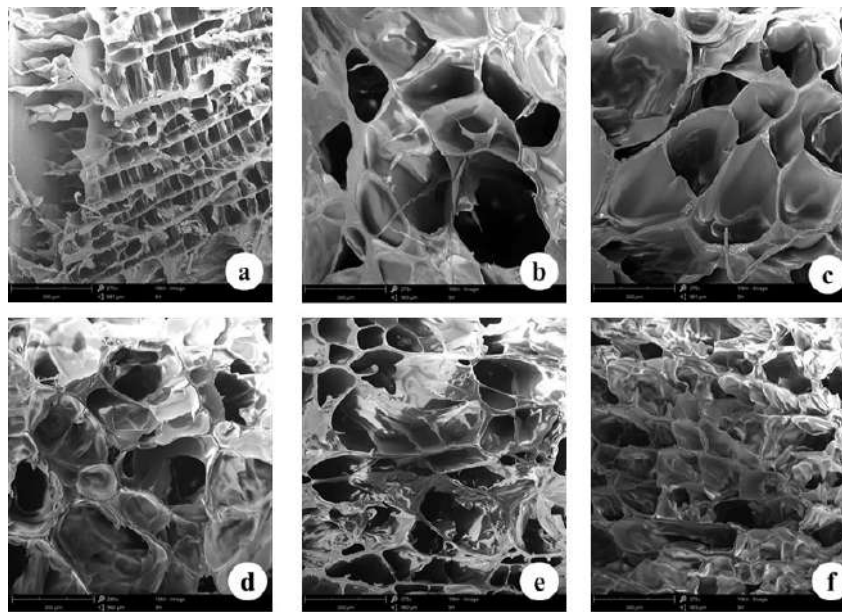


Fig. 5. SEM micrographs of composite hydrogels with different amounts of MA-GNP : (a) 0%; (b) 5%; (c) 10%; (d) 15%; (e) 20%; (g) 25%.

3.4 Mechanical properties

The compressed and stretched mechanical properties of the as-prepared MA-GNP/PAAm gels were evaluated as given in table 2 and Figure 6. Note that 5% MA-GNP/PAAm gels is viscous and its shape is destroyed after compression due to its low cross-linking degree. With the increase of cross-linker dosage ($\leq 20\%$), the compressive stress and elasticity shaping ability of MA-GNP gels is enhanced and they can be compressed and recover to their original length without visible permanent deformation. Even when compressed to the strain of 90%, the gels with 10%~20% content of MA-GNP can quickly recover to more than 90% of the initial thickness without breakage, and the compression strength can reach up to 160 kPa. However, when the MA-GNP content is further increased to 25%, the mechanical property of the gels is decreased, with some broken part after compression. This is due to the fact that mechanical properties of polymer gel are relevant to the number of effective chains that sustain the force³⁸. Hydrogels with appropriate dosage of cross-linker have more effective chains, and each effective chain can be loaded evenly before fracture, thus having higher mechanical properties. Compared with typical MA-gelatin crosslinked hydrogels¹⁸ with enhanced mechanical property but at the sacrifice of elasticity, the MA-gelatin nanoparticles crosslinked gels can sustain higher compressive strain while simultaneously exhibiting better deformation restorability. It is possibly attributed to the uniform chemical crosslinking and the long flexible chains between crosslinks MA-gelatin particles⁸. The compressive stress-strain test reveals that the macromolecular microsphere cross-linker, MA-GNP, can improve the rigidity of the hydrogel network while keeping the good elasticity. In addition, the 10% MA-GNP gels can sustain bending stretching and knotting, as shown in Figure 7. The gels can be stretched at least 500% in length without breakage. The results indicate that the MA-GNP/PAAm gels are a flexible and elastic material.

Table 2. Photographs of an MMC hydrogel during the compression test.

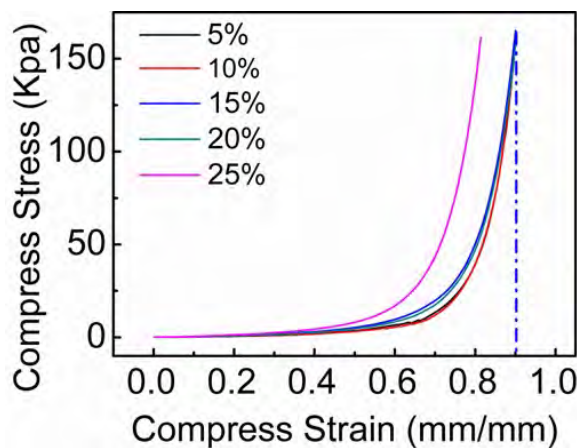
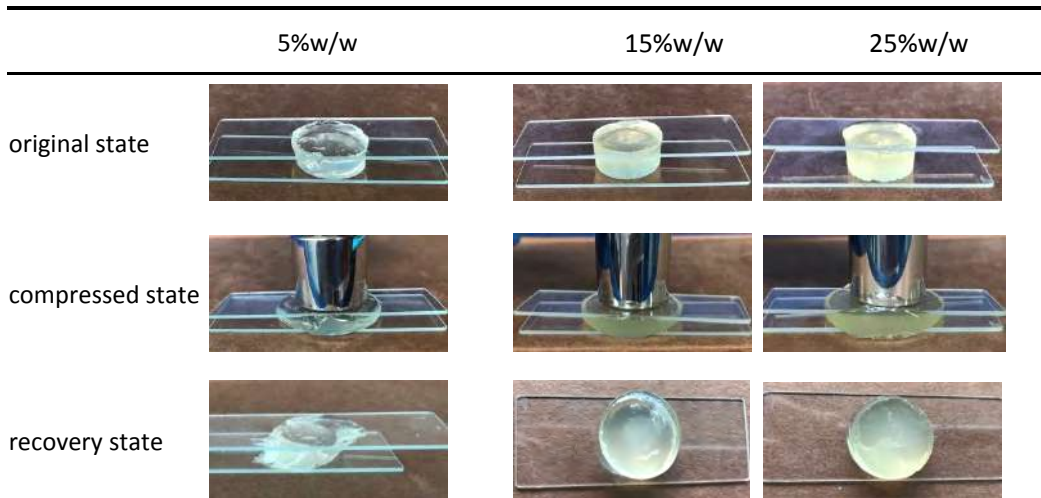


Fig. 6. Compression stress-strain curves of composite hydrogels with different amounts of MA-GNP.

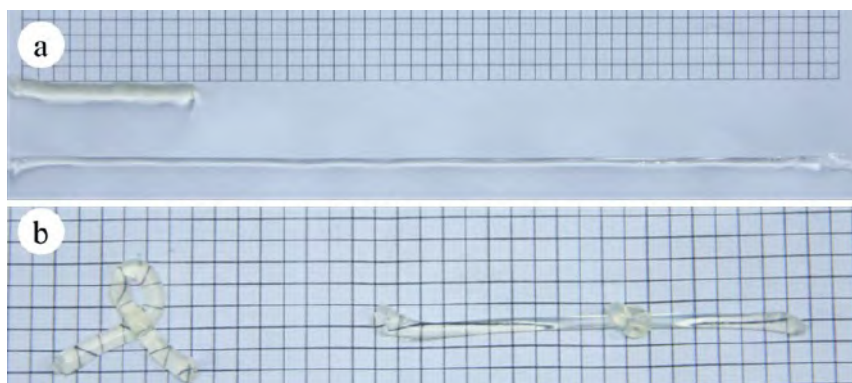


Fig. 7. Optical images showing the process of the 10% MA-GNP composite hydrogels, (a) being stretched; (b) bending and knotting state.

3.5 Swelling Behaviors

The swelling behavior of the hydrogels are investigated at room temperature in solutions of various ionic strength ranging from 0 to 0.1 M. Figure 8 shows that the equilibrium swelling ratio of the gels decreases with increasing ionic strength of the solution. It can be ascribed to the reduction in the osmotic pressure difference between the hydrogels and the external solution with increasing ionic

strength³⁹. Note that the MMC gels with lower MA-GNP contents have higher water absorption, which owes to the fact that a lower MA-GNP content means a less cross-linked network structure and thus more free space available for shrinking in the resulting MMC gels. However, when the MA-GNP content is further increased from 20% to 25%, the ESR is instead increased, which possibly relate to the hydrophilicity of the excessive MA-GNP inhomogeneously distributed in the gels.

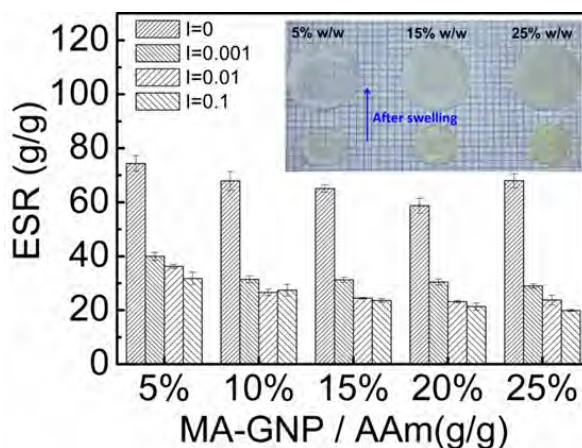


Fig. 8. Effects of ionic strength on the equilibrium swelling ratio of composite hydrogels with different amounts of MA-GNP.

3.6 Thermal properties

Figure 9 shows the thermal properties of the MMC gels as measured by thermogravimetric analysis (TGA). For all prepared MMC gels, there were three decomposition stages, ranging from 60 to 600 °C. The first stage (stage I) occurring between 50 and 150 °C is attributed to the removal of bound water¹⁷. The second degradation stage from 200 to 320 °C (stage II) is mainly associated with loss of ammonia with formation of imide groups through cyclization⁴⁰. The third decomposition stage in the range of 320 to 500 °C (stage III) mainly corresponds to the decomposition of the polymer chains⁴¹. The position of maximum decomposition temperature corresponding to stage I, stage II and Stage III for hydrogel samples (Table 3) all shift to higher temperature with increasing the content of MA-GNPs, indicating the enhanced thermal property. This is reasonable because MA-GNPs nanoparticles act as a cross-linker in MMC gels and can effectively enhance the cross-link density of the hydrogel network.

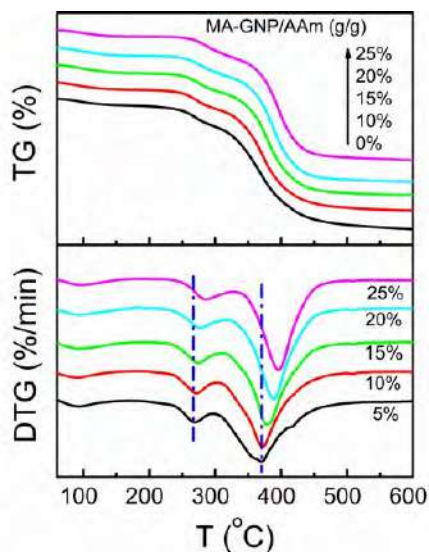


Fig. 9. The TG-DTG curves of composite hydrogels with different amounts of MA-GNP.

Table 3. The maximum decomposition temperature corresponding to stage I, stage II and Stage III of the Hydrogel Samples.

$m_{\text{MA-GNP}}/m_{\text{AAm}}$ (g/g)	Stage I / °C	Stage II / °C	Stage III / °C
5%	92.3	268.3	371.1
10%	92.4	270.8	371.1
15%	92.4	273.4	378.5
20%	92.3	278.4	388.6
25%	97.7	285.9	396.5

3.7 In vitro blood compatibility

The blood compatibility of materials is very important as it plays a key role in determining their utility for bio-medical applications. A thrombosis or hemolytic reaction is undesirable but frequently occurs when foreign materials come into contact with blood^{18,42}. Therefore, the in vitro blood compatibility of MA-GNP gels is evaluated in terms of the blood clotting index (BCI) and degree of hemolysis. The BCI of hydrogels with different amounts of MA-GNP are shown in Figure 10a. It is recognized that a higher value of blood clotting index indicates a better antithrombogenicity⁴³. The results show that BCI of all the MA-GNP gels can reach up to 70%, significantly higher than glass surface (45%). This is quite expected because of the well-known biocompatible nature of gelatin, which can effectively inhibit the platelet adhesion and thrombus formation^{44,45}. And our results confirm that MA-GNP can also retain this feature. Note that increasing MA-GNP can improve the BCI, but the 15% MA-GNP/PAAm hydrogel has the highest BCI. This result is possibly related to the combined consequence of the increase in the crosslink density of the network and the decreased water uptake capacity of gels, caused by increasing the content of cross-linker (MA-GNP). The surface with enhanced stiffness and smoothness and higher hydrophilicity may offer less interaction between the materials and the blood components⁴⁶, thus enhancing the blood compatibility of the polymeric hydrogels. Figure 10b shows the degree of erythrolysis and hemoglobin dissociation in contact with MA-GNP gels at 37 °C for 60 min. The hemolytic ratios for all the MA-GNP gels are below the international permissible level of 5%, indicating they are nonhemolytic²⁸.

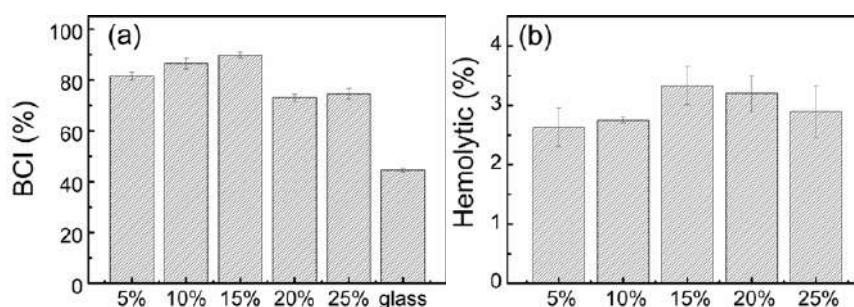


Fig. 10. (a) The BCI of composite hydrogels with different amounts of MA-GNP. (b) The haemolysis of composite hydrogels with different amounts of MA-GNP.

3.8 In vitro cytotoxicity

L929 cells are mouse fibroblasts with fusiform or flat stellate and protuberant, as shown in Figure 11a, and this kind of cell can be sub-cultured with the advantage of stability and repeatability. L929 cells after digestion with trypsin are wrinkled and rounded, as shown in Figure 11b. The results of the cell viability test of hydrogels are shown in Figure 11c and Figure 11d. And RGR of the L929 cells in the diluted extract and stock extract of hydrogels of all the samples for different incubation time (6-48h) are more than 85%, which achieve a numerical grade lower than 100%, indicating that all the MA-GNP/PAAm hydrogels exhibit good cytocompatibility^{31,32}.

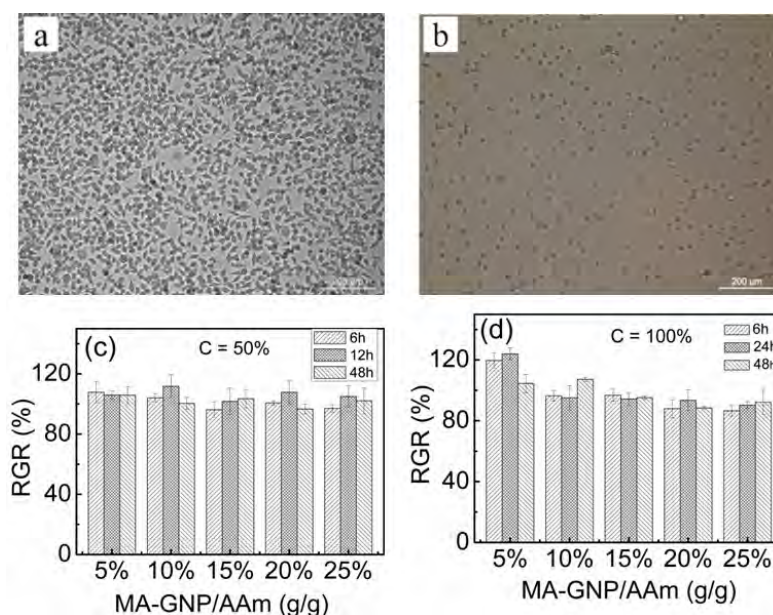


Fig. 11. (a) Images of adherent covered L929 cell, (b) images of digested L929 cell, (c) RGR in the 50% extracts of the gels, (d) RGR in 100% extracts of the gels.

4 Conclusions

In conclusion, this study introduces a general and facile route to fabricate novel microsphere composite hydrogel with good mechanical properties and biocompatibility. The smooth and spherical MA-GNP with an average size of 100 nm was obtained by the modified two-step desolvation process. It can be readily introduced into the PAAm hydrogels system as a cross-linker to prepare MMC hydrogels via a free radical polymerization reaction with acrylamide monomers. The results show the MA-GNP/PAAm gels are materials with uniform interconnected pores and the pore size can be adjusted by the dosage of gelatin. Compared with the MA-gelatin crosslinked systems, the crosslinking action of MA-GNP nanoparticles can improve both the compressive resistance and the elasticity of PAAm hydrogels. The hydrogels exhibit good water absorption and the swelling property is influenced by cross-linker dosage and ionic strength. Moreover, with increasing cross-linker dosage, the thermal stability of the composite hydrogel is improved distinctly. Most importantly, all the MA-GNP gels have enhanced blood compatibility endowed by MA-GNP and the extracts of MA-GNP hydrogels have no toxic side effect on cells. The present work not only exploits new strategies to fabricate MMC hydrogels but also advance the potential application of biodegradable gelatin-based nanoparticles in biomedical fields.

References

1. Maulvi, F. A., Lakdawala, D. H., Shaikh, A. A., Desai, A. R., Choksi, H. H., Vaidya, R. J. *In vitro and in vivo evaluation of novel implantation technology in hydrogel contact lenses for controlled drug delivery.* *J. Control. Release*, 226, 47-56, 2016
2. Singh, B., Sharma, S., Dhiman, A. *Acacia gum polysaccharide based hydrogel wound dressings, Synthesis, characterization, drug delivery and biomedical properties.* *Carbohydr. Polym.*, 165, 294-303, 2017
3. Lam, J., Clark, E. C., Fong, E. L., Lee, E. J., Lu, S., Tabata, Y. *Evaluation of cell-laden polyelectrolyte hydrogels incorporating poly (L-Lysine) for applications in cartilage tissue engineering.* *Biomaterials* 2016, 83, 332-346, 2016
4. Seeli, D. S., Prabakaran, M. *Guar gum oleate-graft-poly (methacrylic acid) hydrogel as a colon-specific controlled drug delivery carrier.* *Carbohydr. Polym.*, 158, 51-57, 2017
5. Okumura, Y., Ito, K. *The Polyrotaxane Gel, A Topological Gel by Figure-of-Eight Cross-links.* *Adv. Mater.*, 13(7), 485-487, 2001
6. Gong, J. P. *Why are double network hydrogels so tough?* *Soft Matter*, 6(12), 2583-2590, 2010
7. Gaharwar A K, Peppas N A, Khademhosseini A. *Nanocomposite hydrogels for biomedical applications.* *Biotechnol. Bioeng.*, 111(3), 441-453, 2014
8. Huang, T., Xu, H., Jiao, K., Zhu, L., Brown, H., Wang, H. *A novel hydrogel with high mechanical strength, a macromolecular microsphere composite hydrogels.* *Adv. Mater.*, 19(12), 1622-1626, 2007
9. Jiang, F., Huang, T., He, C., Brown, H. R., Wang, H. *Interactions Affecting the Mechanical Properties of Macromolecular Microsphere Composite Hydrogels.* *J. Phys. Chem. B*, 2013, 117(43), 13679-13687.
10. Tan Y, Xu, Wang P, Li, W. Sun, S., Dong, L. S. *High mechanical strength and rapid response rate of poly(n-isopropyl acrylamide) hydrogel crosslinked by starch-based nanospheres.* *Soft Matter*, 6(7), 1467-1471, 2010
11. Liu, C., Tan, Y., Xu, K., Li, Y., Lu, C., Wang, P. *Synthesis of poly(2-(2-methoxyethoxy)ethyl methacrylate) hydrogel using starch-based nanosphere cross-linkers.* *Carbohydr. Polym.* 105(6), 270-275, 2014
12. Zhai, D., Zhang, H. *Investigation on the application of the TDGL equation in macromolecular microsphere composite hydrogel.* *Soft Matter*, 9(3), 820-825, 2012
13. Li, X., Ji, G., Zhang, H. *Phase transitions of macromolecular microsphere composite hydrogels based on the stochastic Cahn–Hilliard equation.* *J. Comput. Phys.* 283, 81-97, 2015
14. Jiang, F., Huang, T., He, C., Brown, H. R., Wang, H. *Interactions Affecting the Mechanical Properties of Macromolecular Microsphere Composite Hydrogels.* *J. Phys. Chem. B*, 117(43), 13679-13687, 2013
15. Wu, Y., Zhou, Z., Fan, Q., Chen, L., Zhu, M. *Facile in-situ fabrication of novel organic nanoparticle hydrogels with excellent mechanical properties.* *J. Mater. Chem.*, 19(39), 7340-7346, 2009
16. Zhang, H. *Strain-stress relation in macromolecular microsphere composite hydrogel.* *Appl. Math. Mech-Eng.*, 37(11), 1539-1550, 2016
17. Li, C., Mu, C., Lin, W., Ngai, T. *Gelatin Effects on the Physicochemical and Hemocompatible Properties of Gelatin/PAAm/Laponite Nanocomposite Hydrogels.* *ACS Appl. Mater. Inter.*, 7(33), 18732-18741, 2015
18. Li, C., Mu, C., Lin, W. *Novel Hemocompatible Nanocomposite Hydrogels Crosslinked with Methacrylated Gelatin.* *RSC Adv.*, 6(49), 43663-43671, 2016
19. Nichol, J. W., Koshy, S., Bae, H., Chang, M. H., Yamanlar, S., Khademhosseini, A. *Cell-laden microengineered gelatin methacrylate hydrogels.* *Biomaterials*, 31(21), 5536-5544, 2010
20. Benton, J. A., Deforest, C. A., Vivekanandan, V., Anseth, K. S. *Photocrosslinking of gelatin macromers to synthesize porous hydrogels that promote valvular interstitial cell function.* *Tissue Eng. Part A.*, 15(11), 3221-3230, 2009
21. Dragusin, D. M., Van Vlierberghe, S., Dubrue, P., Dierick, M., Van Hoorebeke, L., Declercq, H. A. *Novel gelatin–PHEMA porous scaffolds for tissue engineering applications.* *Soft Matter*, 8(37), 9589-9602, 2012.
22. Habeeb, A. F. S. A. *Determination of free amino groups in proteins by trinitrobenzenesulfonic acid.* *Anal. Biochem.*, 14(3), 328-336, 1966
23. Bulcke A. V. D, Bogdanov, B., Rooze, N. D., Schacht, E. H., Cornelissen, M., Berghmans, H. *Structural and rheological properties of methacrylamide modified gelatin hydrogels.* *Biomacromolecules*, 1(1), 31-38, 2000
24. Coester, C. J., Langer, K., Van, B. H., Kreuter, J. *Gelatin nanoparticles by two step desolvation a new preparation method, surface modifications and cell uptake.* *J. microencapsul.*, 17(2), 187-193, 2000
25. Hoch, E. Hirth, T., Tovar, G. E. M., Borchers, K. *Chemical tailoring of gelatin to adjust its chemical and physical properties for functional bioprinting.* *J. Mater. Chem. B.*, 1(41), 5675-5685, 2013
26. *Standard test methods for haemolysis of materials.* ASTM-F90; ASTM international, West Conshohocken, United states, 1990.
27. Cui, L., Tang, C., Yin, C. *Effects of quaternization and PEGylation on the biocompatibility, enzymatic degradability and antioxidant activity of chitosan derivatives.* *Carbohydr. Polym.*, 87(4), 2505-2511, 2012
28. Meng, Z. X., Zheng, W., Li, L., Zheng, Y. F. *Fabrication and characterization of three-dimensional nanofiber membrane of PCL–MWCNTs by electrospinning.* *Mater. Sci. Eng. C*, 30(7), 1014-1021, 2010
29. ISO 10993-12, 2007–*Biological evaluation of medical devices—Part 12, Sample preparation and reference materials.*
30. Ciapetti G, Granchi D, Stea S, Savarino, L. Verri, E. Gori, A. Savioli, F. Montanaro, L. *Cytotoxicity testing of materials with limited in vivo exposure is affected by the duration of cell-material contact.* *J. Biomed. Mater. Res.*, 1998, 42(4), 485-490, 1998
31. *Cytotoxicity Biological Evaluation of Medical Devices – Part 5, Tests for In Vitro Cytotoxicity.* Australian Standard™, AS ISO 10993.5–2002, 2002

-
32. Anon. *Biological reactivity tests in vitro*, In *United States Pharmacopeia. 24th revision. United States Pharmacopeial Convention, Inc., Rockville, Maryland, 2014, pp 1813–1831*
 33. Ishida, N., Inoue, T., Minoru Miyahara, A., Higashitani, K. *Nano bubbles on a hydrophobic surface in water observed by tapping-mode atomic force microscopy. Langmuir.*, 16(16), 6377-6380, 2000.
 34. Tan, H., Sun, G., Lin, W., Mu, C. Ngai, T. *Gelatin particle-stabilized high internal phase emulsions as nutraceutical containers. Acs Appl. Mater. Inter.*, 2014, 6(16),13977-13982.
 35. Kesavan, S., Bai. S. A. *Effect of surfactant on the release of ciprofloxacin from gelatin microspheres. Ars pharm*, 51(1), 1-16, 2010
 36. Wei, W., Wang, L. Y., Yuan, L., Wei, Q., Yang, X. D., Su, Z. G. *Preparation and application of novel microspheres possessing auto-fluorescent properties. Adv. Funct. Mater.*, 17(16), 3153-3158, 2007
 37. Ma, L., Gao, C., Mao, Z., Zhou, J., Shen, J., Hu, X. *Collagen/chitosan porous scaffolds with improved biostability for skin tissue engineering. Biomaterials*, 24(26), 4833-4841, 2003
 38. Itagaki, H., Kurokawa, T., Furukawa, H., Nakajima, T. Katsumoto, Y. Gong, J. P. *Water-induced brittle-ductile transition of double network hydrogels. Macromolecules*, 43(22), 9495-9500, 2010
 39. Raafat, A. I. *Gelatin based pH-sensitive hydrogels for colon-specific oral drug delivery, Synthesis, characterization, and in vitro release study. J. Appl. Polym. Sci.*, 118(5), 2642–2649, 2010
 40. Nayak, B. R., Singh, R. P. *Development of graft copolymer flocculating agents based on hydroxypropyl guar gum and acrylamide. J. Appl. Polym. Sci.*, 81(7), 1776-1785, 2001
 41. Zhou, C., Wu, Q. *A novel polyacrylamide nanocomposite hydrogels reinforced with natural chitosan nanofibers. Colloid. Surface. B.* 84(1), 155-162, 2011.
 42. Menzies, K. L., Jones, L. *The impact of contact angle on the biocompatibility of biomaterials. Optometry Vision Sci.* 87(6), 387-399, 2010.
 43. Shankaraman, V., Davis-Gorman, G., Copeland, J. G., Caplan, M. R., Mcdonagh, P. F. *Standardized methods to quantify thrombogenicity of blood-contacting materials via thromboelastography. J. Biom. Mater. Res. B*, 100(1), 230-238, 2012
 44. Tabuchi N, De, H. J., Gallandat, H. R. C., Boonstra, P. W., Van, O. W. *Gelatin use impairs platelet adhesion during cardiac surgery. Thrombosis and haemostasis*, 74(6), 1447-1451, 1995
 45. Ren, J., Jin, W., Hong, S., Nan, H. *Surface modification of polyethylene terephthalate with albumin and gelatin for improvement of anticoagulation and endothelialization. Appl. Surface Sci.*, 255(2), 263-266, 2008
 46. Bajpai, A. K., Sharma, M. *Preparation and characterization of novel pH-sensitive binary grafted polymeric blends of gelatin and poly(vinyl alcohol), Water sorption and blood compatibility study. J. Appl. Polym. Sci.*, 100(1), 599-617, 2010.

CLOSED-LOOP LIMING AND TANNING SYSTEMS LARGE AND COTTAGE SCALE MANUFACTURE

Richard Daniels*⁽¹⁾, Jiasheng Su⁽²⁾, Falei Zhang⁽²⁾, Zhuangdou Zhang⁽²⁾

(1)Greentech + Associates, Northampton, UK, (2)BIOSK, Shangqiu City, Henan Prov, China

E-mail support@biosk.cn

Abstract. Residual floats from liming and chrome tanning processes are being recovered as chemical solutions for re-use within many tanneries in China, presently producing approximately 120,000 wet salted hides/week from USA, Europe and Australia in eight major tanneries. The closed-loop approach in these two major processing stages can now be considered as an established alternative to conventional processing of wet salted hides to the wet blue state. Advantages include chemical savings, reduced water use, simplification of effluent treatment and solid waste disposal with associated cost savings. Being the outcome from carefully controlled processing, these filtered solutions are consistent in composition. The techniques used provide good quality and uniform wet blue though-out the year. Soaking and deliming/bating processes are managed conventionally, with all washings and discharges delivered to the effluent treatment plant. However, the hair saving/liming and tanning stages omit the washing sequences. This results in concentrated solutions for reuse, with no discharges from for effluent treatment. This means an absence of both sulfide and residual chromium salts for treatment/recovery in subsequent effluent treatment. This approach to manufacture is found in established tanneries, but also in a new generation of wet blue units that by November 2018 were at advanced stages of construction. Moreover, the technology has made the technological transition from bovine hides to the manufacture of full grain wet blue sheepskins to the scale of 10,000 skins per day. And for small scale operations – bovine hides, bovine bellies, sheep and goat skins – chrome tannage is taking place in many tanneries too, the process having been adapted to the various conditions and tanners requirements.

Key Words: Closed-loop liming and tanning

1 Introduction

Closed loop processing for manufacturing hides and skins to the wet blue state is now firmly established in full scale manufacture. This comprises two closed-loops for the full recovery and reuse of processing floats at the end of liming and chromium tanning in the eight large scale tanneries who allowed site inspections to provide the information for this report. The technology was initiated and developed by BIOSK Chemicals over a five year period before introduction commercially in 2011. Now approximately 120,000/week of wet salted hides from USA, Australia and Europe are being processed to the wet blue state for their own use, sales and contract tanning.



Fig. 1. High quality bovine wet blue manufacture: High volume manufacture using closed-loop technology.

2 Development of a Technology

There are two key issues that BIOSK addressed when developing this technology:

- Traditional high uptake processes for wet blue manufacture always left residual chemicals for effluent treatment and this waste should be eliminated.
- The leather produced should be consistent and of high quality.

Central to the technology are two self-contained processing loops. The first is a hair save liming process, the second a combined pickle and pre-chroming followed by chromium tannage. Three auxiliary products developed by BIOSK are available to support the processing, and the technology is being used by tanneries of all sizes where their previous procedures have been modified to the new procedures.

2.1 The Hair Recovery and Liming Closed-Loop

The processing is managed as follows:

- All of the processing floats and drainings at the end of the liming stage are recovered for use in subsequent hair saving liming systems.
- There is a total absence of washes at the end of the liming stage. The recovered floats remain a resource of concentrated chemicals for reuse.

The recovered floats from all of the liming drums are delivered to a single holding tank. This is fitted with heat exchange, with the temperature raised or lowered to 20-220C.

- Before re-use this solution is mixed using compressed air to ensure the dispersion of any fine residual solids in suspension.
- Only the recovered solutions, and lime and sulfide/hydrosulfide (at reduced offer) is used within the hair loosening stage
- After hair loosening, the float is filtered for conventional hair recovery and compression, with the float returned to the drum.
- As the hair is compressed on recovery it acts as a filter for the residual fine solids. This keeps the suspended solids at a low level equilibrium within the ongoing process.
- The float for the main swelling phase is often increased in several offers using recovered solutions to carefully manage the swelling.
- At this stage some fresh water added too. In practice, this volume matches the water taken up by hide swelling.

2.2 Handling Operations

On discharge from liming the hides are tipped into a container set beneath the liming vessel, and delivered directly to the area by the lime fleshing machines. Here they are hooked onto a line-conveyor for feed to the fleshing operation. On offer to lime fleshing the hides are well drained and clean.

Scud, grease and residual surface water are squeezed from the grain by the action of the grip rollers at the time of fleshing. At the time of offer to splitting, the hides are clean and dry, and handle as usual.

In the deliming stage the swelling water, together with salts, residual protein and grease contained within the hides are released from the structure. At the end of this process these unwanted products are discharged, followed by fresh water washes as conventional practice.

2.3 The Chrome Tanning Closed-Loop

In general, the process is managed as follows:

- All of the floats and drainings at the end of the chrome tanning stage are recovered from the drums and stacking areas for use in subsequent pickling tanning systems.

- There is a total absence of washes at the end of tannage. The recovered solutions remains a resource of concentrated chemicals for reuse.
- These recovered floats are filtered using a filter press to remove fibres and other solids from solution, and become a resource of concentrated chemicals for reuse.
- These solutions are delivered to two containment tanks. One tank is temperature adjusted using heat exchange to 20-22°C, the second tank adjusted to between 55°C and 75°C - as required by the individual tannery.
- Salt at reduced offer is added to delimed and bated hides. The float level is the minimum possible to enable distribution of the salt.
- A small addition of pre-diluted formic acid is added for a light surface acidification.
- This is followed by a simultaneous main pickle and pre-chroming stage. Sulfuric acid is diluted as normal but using recovered chrome solution at 20-22°C. This is pumped into
- the drum, but recovered chrome solution at the same temperature is pumped in too over the same time period. This increases the float as required to 50%.
- These simultaneous additions onto the lightly acidified hides prevent chrome staining and provide a moderate float for the chrome tanning stage.
- After 90 to 120 minutes (according to split/unsplit substance), the chrome tanning agent is offered but at a reduced offer, followed by basification as conventional processing.
- A third offer of chromium is made as recovered solution from the containment tank at elevated temperature. This offer may be as high as 100% float as suits the tannery needs, to raise the processing temperature and improve chrome fixation.
- There are no washings with fresh water at the end of the process.

3 Water exchange and process equilibrium

In the liming stage fresh water is introduced as contained within the fully soaked hides, and as a fresh water addition within the swelling stage. As the process develops, an equilibrium is established by diffusion between the water/solubles in float and within the hide structure.

On hide discharge, the large volume of water held within the swollen collagen structure – together with solubles – is removed from the otherwise fully closed system. In practice, this continuous shift of hide-contained water through in this otherwise self-contained system allows a build-up of solubles that stabilises over five cycles.

In the tanning closed-loop there are no washing stages. Nevertheless, there are additions of water as contained in the delimed and bated hides, as a low float for the light surface acidification and from dilution of the formic acid, with hide-contained water removal at the end of process. In a similar manner to the liming closed-loop, as the process develops, an equilibrium is established by diffusion between the processing solutions and water within the hide structure. In this case, the level of solubles building up over twenty cycles and then stabilising.

4 Large and small scale manufacture

The technology is now being used in three quite different situations and for different leather types:

4.1 Large-Scale Bovine Manufacture

The process has been successfully introduced by BIOSK into many large scale manufacturers of bovine wet blue leather. Most of these tanneries have accommodated the technology by careful segregation of pipework and drainage. Essentially, the collection and recovery systems from both

liming and tanning are isolated from the rest of the tannery drainage systems. Holding-tanks are employed – either within or adjacent the work areas – for collection and temperature adjustment of the recovered solutions.

In some situations, the tanners have made a fresh start. These tanneries have been completely rebuilt from the foundations up around individual processing zones, each with their own systems for used-float management.

Here, both the liming and tanning departments are completely isolated, all floats being recovered, stored and reused with no provision for discharge to the effluent treatment plant.



Floats and drainings are kept in complete isolation and free from contamination.



Shows an isolated liming zone in a new-build tannery complete with holding tank.

Fig. 2. Existing and new-build tanneries.

The soaking departments are kept apart from the liming and tanning zones, with their drainage arrangements directly feeding the effluent treatment plant. In addition, these tanneries are performing the deliming and bating processes in isolated areas too. Here, the hides as unloaded and drained at the end of washings are delivered to the tanning zone for pickling, tanning and stacking. These separated zones and their management are illustrated as Figure 3:

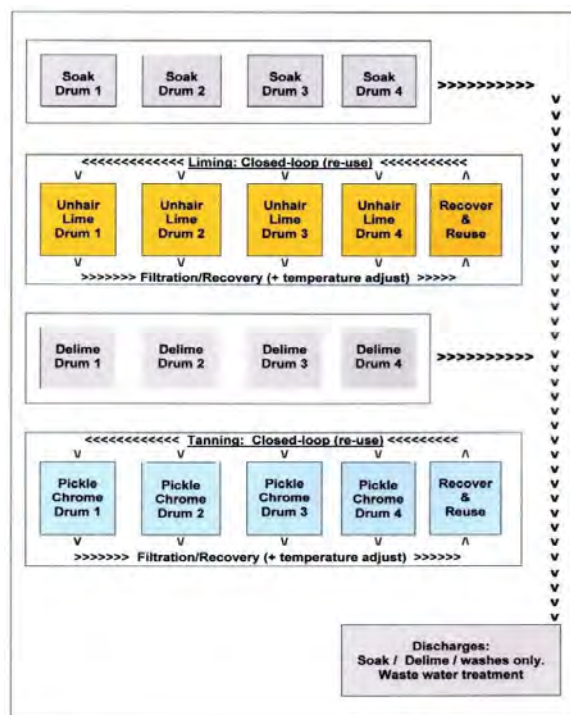


Fig. 3. Segregation: Management of closed-loop recovery and waste water discharges.

4.2 Large-Scale Sheep Skin Manufacture

In 2018 the technology was adopted for full grain sheepskin manufacture on scale up to 10,000 skins per day. After painting, wool removal and liming, the liming floats are recovered and reused in a closed-loop liming suited to sheep skin production. In a similar way to bovine manufacture, the closed-loop approach is used for sheep skin tannage. There are differences in float levels, somewhat higher pH levels during tanning, and slightly lower temperatures in pickling/pre-chroming and the final tanning stage.



Samples showing wet blue sheep skin leathers. Float recovery at the rear of the drum row before filtration and storage.



In this situation, the two chrome holding tanks are set in a sealed enclosure adjacent the tanning department.

Fig. 4. Closed-loop applications in large-scale sheep skin tanneries Samples showing.

4.3 Small-Scale (Cottage) Manufacture

The technology is not restricted to large scale manufacture, and is now being used for a variety of leathers. In November 2018, six small scale tanneries processing wet salted bovine hide butts (small scale fleshing machines limits the piece size), bovine bellies, nappa sheepskins and goat skins had adopted the technology for chrome tanning. There were many variations with the techniques used, according to the different plant and equipment and leather types, end-uses being footwear, bags, clothing and various leather goods. These tanneries are in a group of 30 tanning units and 30 retan/finishing units. Here, the waste waters are being processes in a CETP where they intend to achieve a discharge limit of 0.5 mg/l Cr. The remaining 24 tanneries have undertaken to the group management to convert their tanning departments under licence by BIOSK by June 2019.



Tanks used for holding recovered chrome solutions with temperature adjustment via heat exchange. These are new to specification as shown, but are often adopted from other uses.



Full hide manufacture is limited by the width of the fleshing machine, hence specialist belly leather processing. Air dried/tension free, these leathers are ideal for bags and leather goods.

Fig. 5. Closed-loop applications for small scale enterprise.

5 Advantages

There are significant advantages offered by this technology:

5.1 The Quality Of Leather

This is not a typical high chemical uptake approach to manufacture. The processing does not rely on low floats and sensitive pH conditions to drive a high chemical uptake. Consequently, issues such as tangling and poor chemical distribution are avoided, together with abrasion damage to the sensitive grain, or too much surface fixation of chromium. The processing is more relaxed to suit an expensive and delicate structure.

Also, the chemical composition of the recovered solutions is very uniform. They are a blend from the previous processing batches, the recovered solutions the outcome of carefully managed production.

5.2 Savings In Water And Chemicals

The savings in water and chemicals are considerable. The first three tanneries to adopt this processing found savings ranging between:

- 18 – 50% Sodium sulfide/hydrosulfide combined
- 17 – 43% Calcium hydroxide (slaked lime)
- 57 – 71% Sodium chloride (common salt)
- 29% Chrome tanning Powder (1 given value)
- A water reduction of 50% (1 given value)

5.3 Environmental Advantage

- No unused active chemicals discharged for waste water treatment from liming and tanning
- No sulfide containing waste waters to separate and then oxidise.
- No neutral sulfites/sulfates arising from oxidation of unused sulfides.
- No chromium salts discharged, hence no chrome precipitation/dewatering/regeneration plant needed.
- A lowering of neutral salts, Total Dissolved Solids, chemical oxygen demand and nitrogen for effluent treatment.
- Reduced water requirement. Provides advantage for longer retention times in existing effluent treatment to further raise standards, or for smaller and more compact effluent treatment plant.
- Energy saving from reduced air requirements for oxidation and for aerobic biological treatment.
- Reduced volume of solids generated within effluent treatment and can be chrome free.
- Uncontaminated compressed recovered hair.

6 Conclusions

This is a significantly different approach to leather making that avoids many of the issues associated with traditional manufacture. The technology is proven by many years production of high quality bovine wet blue leather, and is spreading to other leather types at all manufacturing stages and levels of sophistication

Major saving in chemical use are offered. A simplification of effluent treatment and higher standards for discharge, minimisation of solid waste, a reduction in volume of water use, and a relaxed high quality product.

7 Acknowledgements

- Special thanks to BIOSK Chemicals for developing this technology
- Auxiliaries developed by BIOSK to support the technology:
 - ELIPO-L (liming), ELIPO-D (tanning), DO-PRO (Liming Assist)
- Thanks to the 15 tanneries of various size who opened their doors for site inspection. Without their generosity this report on technology suited for the 21st century would not have been possible.

References

1. *For greater detail on this technology, see the paper "Closed-loop liming and chrome tanning systems in full-scale wet blue manufacture: Operational management, technical and environmental advantage". JALCA, Vol.113, 2018.*

ADVANCED DIAGNOSTICS AND INNOVATIVE SOLUTIONS FOR LEATHER DEFECTS: THE PROBLEM OF YELLOWING

Florio C.¹, Aveta R.¹, Calvanese, G.¹, Naviglio B.¹.

1 Stazione Sperimentale Industria Pelli e Materie Concianti, Via Campi Flegrei, 34, 80078 - Pozzuoli - NA

Phone: 39-081-5979100, Fax: 39-081-265574

Corresponding author: c.florio@ssip.it

Abstract. Providing peculiar enhanced features to leather items is a factor of primary importance for the marketing of high-end articles; although the tanning production is oriented to satisfy a wide market range, it is mainly in the "high end" and "premium luxury" categories that the quality properties of the material are more expressed, indeed. And it is particularly on this market segment that the main current challenges have been focalized, according to the growing requirement of technological innovation, sustainability and product quality. The light-coloured leathers, with particular reference to the white items, belongs to the category of materials designed especially for the luxury market. For this type of articles, the uniformity of the colour and the agreeableness of the overall surface appearance are crucial requirements for the most of international fashion and luxury brands. One of the most common and undesirable defects of this type of article is the alteration of the colour, with particular reference to the localized or diffused effects of yellowing of the surface of the material. There are several causes able to contribute to the production of this type of defects, due to the complexity of the matrix and to the variability of traditional or innovative production processes used: from the intrinsic fragility, photosensitivity and thermo-sensitivity of the finishing polymers, to the chemical instability of some components of the finishing pigments, further than the presence of photosensitive chemical additives, the migration of skin components or assembly components of the manufactured articles (fats, fillers, plasticizers, glues, etc.), up to the indirect contribution of environmental and thermo-climatic factors able to affect negatively the performance of the material. SSIP, which has always been involved in research and consulting activities for the leather industry with regards to defect monitoring, through this work, would offer an overview of all the main tools for advanced diagnostics (with particular reference to Scanning Electronic Microscopy and to chromatographic and spectroscopic methods) aimed to the identification of the causes of yellowing, beside to explore innovative solutions for the development of strategies for the resolution and/or minimization of the problem of yellowing. The technical solutions will include innovative tanning processes, innovative finishing methods, and leather surface treatments carried out in order to provide a sensible attenuation of surface absorption of IR and UV-visible radiation.

1 Introduction

The progress achieved in the field of tanning technology, have largely reduced the risk of the formation of many defects on the manufactured leather articles. However, there are some persistent issues affecting the tanning industry. More in detail, in many of the leather articles, particularly in those destined for a high-end market, frequently characterized by a light colour, the problematic of yellowing, where present, is particularly evident.

The most common causes of yellowing are known in literature^{6,7,8,9}, however the phenomenon generally appears to be rather complex, for the following main reasons:

- In addition to the common components inside the leather and the finishing, other substances used as additives can cause the defect;
- In some cases, the substances derive from assembly materials used for the production of the finished articles;
- More than one chemical component may be involved in the problem;
- Some chemical agents are of environmental origin;
- Other environmental/external factors can be involved in causing the problem (such as exposure to light or heat of the samples);

- The defect may originate from a set of previous direct and indirect factors that combine to cause the problem;
- The problem may arise after the article is marketed, as it does not appear immediately, thus falling within the hidden defects.

An overview of the main causes able to determine the problem is shown in Figure 1 below.

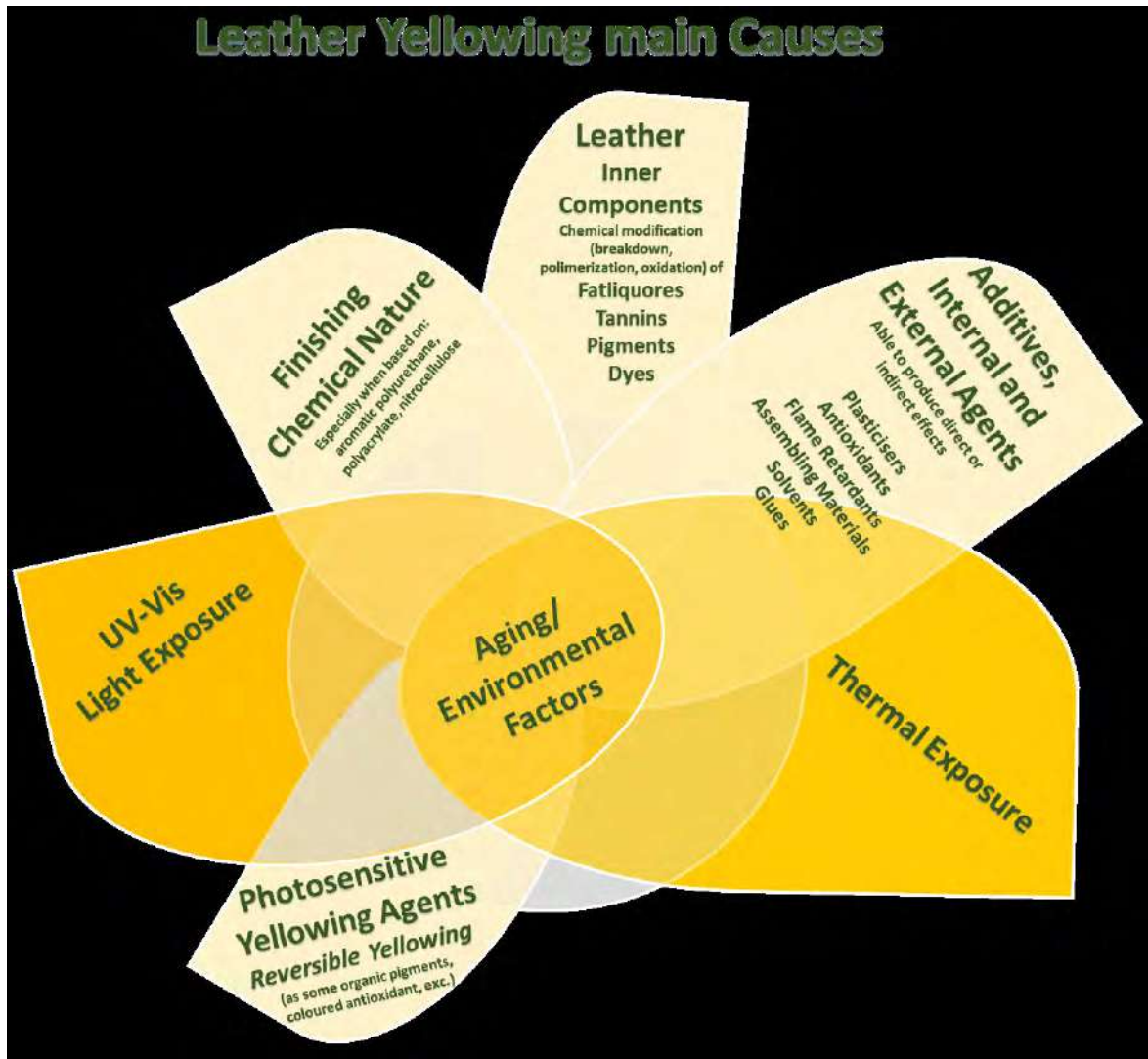


Fig. 1. The different main factors able to promote leather yellowing.

As shown in the figure, among the most common causes of yellowing, there may be the chemical nature of the finishing⁵: particularly, due to the presence of photo and/or thermosensitive polymers, as well as to chemically labile polymers which, in the presence of certain environmental conditions or atmospheric agents, may be possible of oxidative or hydrolytic degradations. Examples are constituted by nitrocellulose-based finishes, some polyacrylates and aromatic polyurethanes.

Other "physiological" causes of yellowing are related to degradation phenomena affecting fatty substances, due to the animal's natural fats or to fatliquors used during the production process; it is known, in fact, that many oils and fats, particularly rich in unsaturations, following to aging, or exposure to thermo-oxidative or photo-oxidative degradation factors, can produce degradation products characterized by a yellow-brown colour.

Further components physiologically passable of yellowing are some dyes and pigments; generally the leathers are dyed using a mix of these components, some of which may have a different resistance

to light; for example, some yellow azo-dyes exhibit better resistance to light, compared to those of red or blue colour, and therefore, following exposure to light, the yellow colour may be prevalent⁶.

Natural and synthetic tannins can also be involved in the problem, mainly due to photo-oxidative mechanisms.

Also the possible interaction between chemical agents used in the tanning process (retanning, fatliquors, dyes, etc.) can play a crucial role in the problem. Furthermore, other chemical agents used as additives, or deriving from the assembly materials (plasticizers, fillers, and some same antioxidants, and phenolic-based components, sometimes used to stabilize some of tanning chemicals, solvents, adhesives), can determine the problematic, directly (if they themselves or their products of degradation or reaction with atmospheric agents are yellow), or indirectly, by promoting the passage of coloured components to the surface.

In any case, the environmental exposure factors can determine the conditions to foster the problem, either by promoting the degradation of the yellowing agents, or by promoting the migration of coloured components on the leather surface. Also, some atmospheric agents, such as nitrogen oxides, can contribute by reacting with active components of the leather, determining the problem (as in the case of some reactive dyes).

To increase the complexity of the scene, some yellowing phenomena are reversible: this is the case, for example, of some coloured substances, mainly organic, rising to the surface, following migratory phenomena, in the presence of particular thermo-climatic conditions, where they are photosensitive, and therefore degraded by exposure of the articles to light (UV-Vis).

Other types of yellowing are reversible depending on the pH (like some phenolic products, which give yellow adducts in an alkaline environment and colourless in an acid environment).

In this work, 32 cases of yellowing were considered, as a result of research and consultancy activities, carried out for leather producers and users, for different destination uses of the material. The investigations carried out offered a widely comprehensive overview of the problem where the causes were identified in a very targeted way, sometimes only thanks to the use of advanced diagnostic tools.

In the following sessions, a framework of technical-analytical approaches and strategies to identify the cause or causes of the problem will be offered. The issue of resolution and prevention of defects will also be addressed, where necessary, also through innovative approaches, which will be explored and developed to respond in a targeted manner to this type of problem.

2 Materials and methods

32 cases of yellowing were investigated, by analysis of leather and leather articles of different origin (bovine, ovine, caprine) for different uses (furniture, automotive, footwear, leather goods). Where deemed necessary, chemical products used in the production process were also analysed, as well as products and materials other than leather used to assemble the finished articles (adhesives, fabrics, synthetic linings). The samples were analyzed with the following instruments:

- *Heraeus Industrietechnik Alpha LM Xenotest*
- *Binder FD 115 Heating Chamber*
- *Pegasil – Zipor EL-83 Veslic Machine.*
- *Atlas/SFTS B.V. Martindale Abrasion Machine.*
- *HP GC System/6890 - HP/5973 Mass Selective Chromatograph equipped with a Purge & Trap O.I.Analytical 4660 Sampler.*
- *DANI GC1000 Gas-Chromatograph - Flame Ionization Detyector.*
- *Spectrum One ATR-IR Spectrometer.*
- *Zeiss EVO MA10 Scanning Electron Microscope equipped with a INCA X-act detector.*

3 Results and Discussion

3.1 Technical and diagnostic approach

The approach used to identify the possible causes of the problem involved the use of adequate investigation strategies, starting from the simplest methods for merceological analysis, to pass to the execution of leather performance evaluation tests, to finally arrive at more sophisticated instrumental analytical techniques, where the cause of the defect was found to be more difficult to identify.

The initial product analysis of the samples started from a careful observation of the defect and was based on the following general considerations:

- the presence of yellowing both on the flesh side and on the grain side of the articles, in general, suggests that internal leather components can be migrated, such as fatty substances, and also suggests that the problem is not solely attributable to finishing; on the other side, if the yellowing, or the tendency to yellowing, even after specific aging tests, is observed only on the finished grain side surface, it would be advisable to focus the subsequent investigations mainly on the finishing;
- the particular location of the defect in a finished article also suggests other important elements for the investigation: if the yellowing is present only in the areas exposed to the environment, and not in the hidden ones (for example, below the seams, in assembled artifacts), this data suggests that the problem may have arisen following phenomena affected by the presence of light or atmospheric agents (such as in cases of photo-oxidative yellowing); if the problem is found, in the finished articles, in correspondence of gluing areas, it is possible to assume the involvement of the glues or other assembly materials; if, within a sample assembled with leather cuttings of different animal origin, the yellowing or the tendency to yellowing, even after specific aging tests, is observed only for some clippings, this finding suggests that the defect may be related to the nature of the leather used.

During the merceological analysis, the visual examination was sometimes supported by optical microscopy techniques, both through stereomicroscope analysis and through the phase contrast optical microscope, where it was necessary to observe the cross section of defective leather samples. For further details on the morphological features of the samples, the Scanning Electron Microscopy (SEM) was also used.

The product analysis of defective and non-defective samples was also repeated after performing tests to evaluate the performance of the material and to simulate aging after exposition to light, to heat and to the action of external agents. The mainly performed tests were:

- Artificial light exposure test (Xenotest method, according to UNI EN ISO 105-B02), from 24 to 72 hours;
- Artificial aging to heat and artificial aging to heat and humidity, according to the UNI EN ISO 17228 - 6C and 7B method (72 hours aging at 60 °C - 96 hours aging at 50 °C and 90% R.H);
- Colour fastness to rubbing, according to the UNI EN ISO 11640 method (before and after aging tests);
- Colour fastness to migration into plasticized PVC, according to the UNI EN ISO 15701 method (before and after aging tests);
- Exposure to solvent vapors and buffering with solvent soaked pad (internal method SSIP MI-PF 001 - 2008).

As chemical tests the determination of matter soluble in dichloromethane was performed, according to the UNI EN ISO 4048 method.

The merceological analysis of the samples surface was also supported by infrared spectroscopy, particularly by ATR-IR spectroscopy, a technique that allows to analyse the surface of solid state samples; this technique resulted particularly useful for identifying the chemical nature of the finishing and for assessing whether the problem was related to this. In general, the technique was also used to advance hypothesis on the possible chemical nature of surface organic substances (other than finishing, such as plasticizers, fats, phenols, adhesives, etc.).

Where the first investigations led to the hypothesis that the problem could depend on fats (high content of matter soluble in dichloromethane, yellowing also present on the flesh side, easy removal of the color by solvent), we proceeded with an in-depth study of their chemical nature: the degree of unsaturation was estimated using the determination of the Iodine Value; sometimes in-depth instrumental chromatographic analysis was necessary, through the use of GC-MS (Gas Chromatography - Mass Spectrometry) techniques, also used for the identification of other organic agents potentially involved in the defect and GC-FID (Gas Chromatography - Flame Ionization Detector).

More in detail, the second of the aforementioned techniques proved to be particularly useful for the speciation of all the fatty substances contained in the organic extracts of the leather, in the colored patinas taken by buffering the surface with dichloromethane or other organic solvents, as well as in the organic fraction of fatliquoring chemicals subjected to liquid-liquid separation; the overlap of the chromatograms allowed us to attribute the possible cause of the problem to chemicals rather than to the natural fats of the skin.

For further details on the chemical nature of substances with a predominantly inorganic base, the surface microanalysis of the samples was carried out using SEM-EDX (Scanning Electron Microscopy - Energy Dispersive X-ray Analysis).

Finally, to identify possible volatile substances involved in the defect (directly or indirectly, such as solvents, as agents capable of solubilizing and foster the migration of colored substances), the GC-MS technique (Gas-Chromatography - Mass Spectroscopy Detector/Purge & Trap sampler) was used; this last technique was also used to identify substances correlated to the degradation of the organic components of the leather, with particular reference to the degradation of fats (such as aldehydes, ketones, furans), as a consequence of a possible state of aging of the sample in correspondence with the defect.

3.2 Technical results

The survey on the 32 cases of yellowing was carried out on leather samples, leather goods and chemical products analyzed during the technical consultancy on the problem, about 44% of which related to defects in upholstery leather (14 cases out of 32), in reason for the greater use of white/light colors for the production of furniture items, and the remaining cases concerning defects in leather for footwear, automotive and leather goods. The overall survey has produced interesting results, the most relevant of which will be discussed in this section.

First, regardless of the intended use of the leathers, the main cause of yellowing was found to be correlated to the nature of the finishing (14 cases); in particular, a significant frequency has been found in the use of aromatic polyurethanes in the external finishing layer for defective samples (Figure 2). In all these samples analysed, an increase in the defect due to exposure to heat was found (especially to dry heat) and/or to light.

The second factor resulted involved in the onset of the defect was correlated with the presence of substances inside the matrix of the material (8 cases), with particular reference to fats; in the majority of the cases examined, the quantity of fats was found to be greater for the defective samples, which also presented a type of fats with a high degree of unsaturation. Regarding the origin of the fats, the instrumental tests carried out, as described in the previous paragraph, have shown that a crucial role was determined by the nature of the fatliquoring products used. However, in one case, the possible correlation of the defect to the natural fats of the skin was found; the case

concerned an article for furniture, consisting of assembled leathers of different origin (Figure 3): the non-defective parts, of calf, were characterized by a content of soluble matter in dichloromethane of 2.7%, while the defective parts, made of buffalo (processed by the same tannery), were characterized by a content of soluble matter in dichloromethane of 10.5%. Therefore, in this case, the particularly fatty nature of buffalo skins has been related to the onset of the defect.

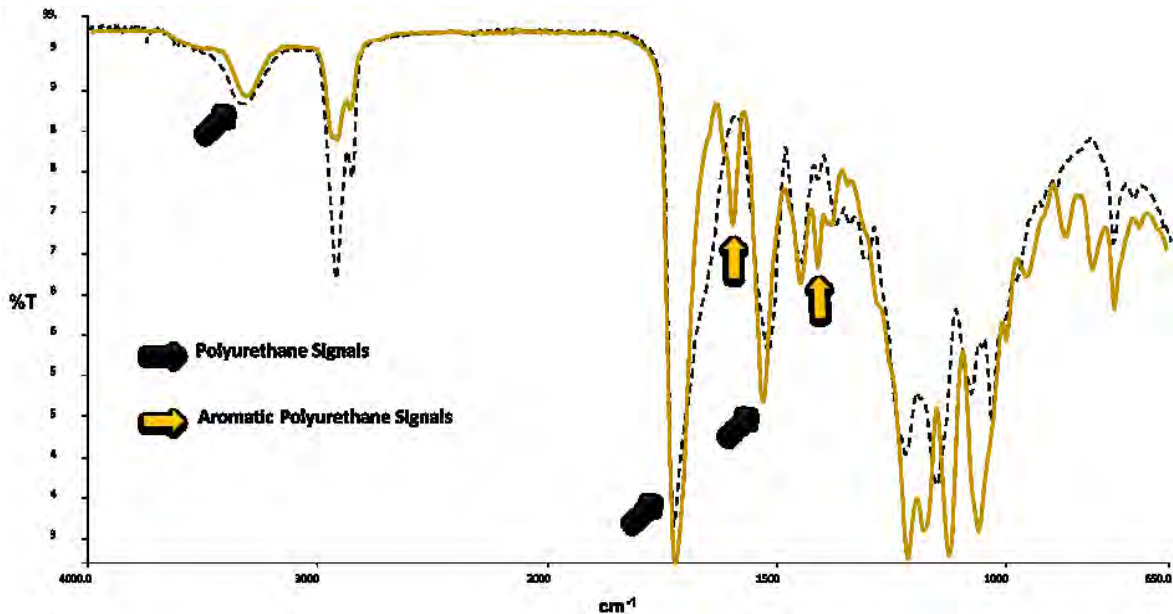


Fig. 2. IR spectra overlap of the topcoat of defective (yellow) and not defective (black) samples.

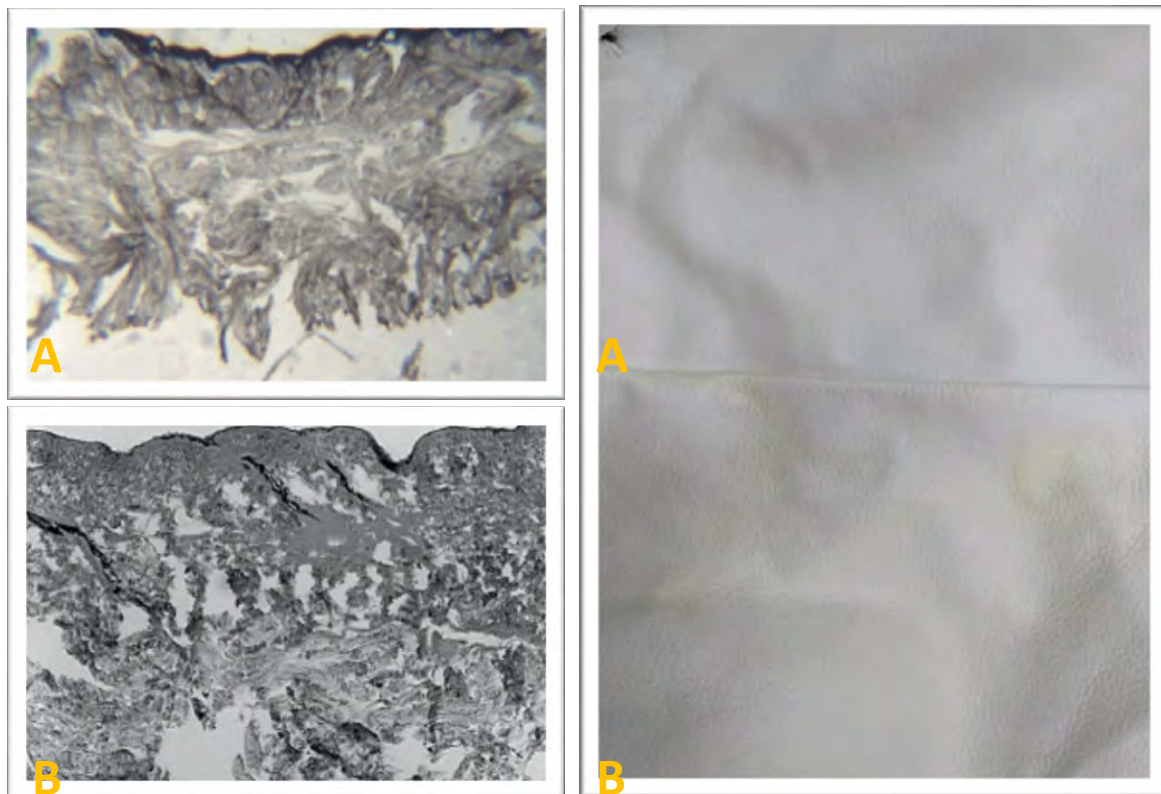


Fig. 3. A: cross section and surface of a not defective calf leather; B: cross section and surface of a defective buffalo leather.

In the remaining 10 cases, the problem was related to additives used in the production process (plasticizers, antioxidants), as well as with external agents deriving from the assembly materials (adhesives, solvents, coloured fabrics).

Particularly interesting, in this sense, was the survey on the yellowing of an article for leather goods, due to the association of the problem with more than one external agent. In this item the defective parts were affected by the presence of acrylic glues on the surface (Figure 4).

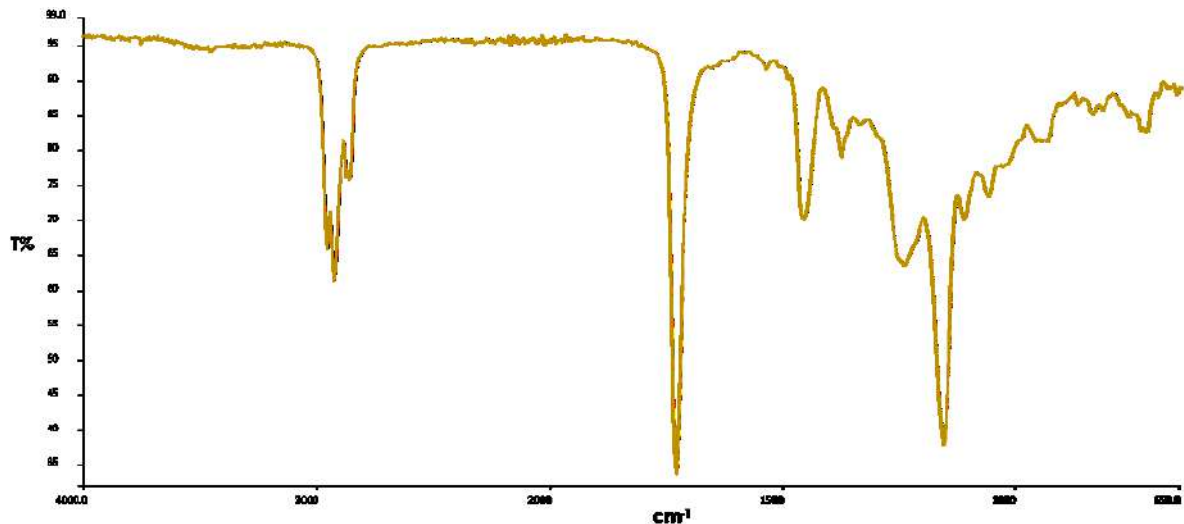


Fig. 4. IR Spectrum of the glue found on the sample: spectroscopic profile compatible with a polyacrylate

These substances, due to their own nature, are potentially able to produce the complained yellowish colour. However, in the specific case, the glue was also present in non-defective areas of the assembled product. Therefore, the mere presence of the glue did not justify the onset of the problem. On the other hand, an in-depth visive analysis of the sample provided more clues, highlighting that, in correspondence with the defect, there was also a regenerated leather reinforcement lining (absent in the areas without defects). The artificial aging tests (60 °C for 72 hours), as well as the ironing test, led to the onset of a yellowish colouring in not defective areas and to an increase in the yellowing in the defective ones. We then proceeded with the determination of the volatile substances of two specimens, using the Purge & Trap - GC-MS technique (Gas-Chromatography - Mass Spectroscopy Detector/Purge & Trap sampler):

- A. defective/yellowed specimen containing all the materials (leather, glue and lining);
- B. non-yellowed specimen in which the reinforcing lining was absent.

The result of this investigation is reported in Tables 1 and 2, and shows that:

- in both specimens the presence of volatile substances with solvent action was identified, as well as substances of other nature, such as hydrocarbons, fatty substances and respective degradation products;
- a higher percentage of hydrocarbons and chlorinated hydrocarbons was found in the defected area (substances whose migration tendency is known).

The investigations carried out and the results obtained led in this case to hypothesize that the problem was connected to a combined action of substances with a tendency to yellowing (glues) and substances able to foster the passage of the glue from the flesh side to the grain side of the item. The use of any high temperatures to assemble the artefact was considered, according to the experimental results, a factor potentially capable of contributing to the onset of the problem.

Tab. 1. Gas-chromatographic determination of the volatile substances in the not defective sample (A)

SUBSTANCE	T _R (MIN)	CAS N.	QUALITY%	AREA%
Acetone	12,3	000067-64-1	90	12,86
Hexane	14,5	000110-54-3	91	3,33
Pentanal	21,2	000110-62-3	78	1,84
Tetrachloroethylene	25,2	000127-18-4	52	0,87
4-Pentenal	29,9	002100-17-6	56	1,77
Oxirane, (bromomethyl)-	30,3	003132-64-7	50	1,91
Benzene, 1,3,5-trimethyl-	33,1	000108-67-8	27	0,97
1H-Pyrrole, 2,5-dihydro-1-nitroso-	33,7	010552-94-0	50	2,66
1-Hexanol, 2-ethyl-	34,6	000104-76-7	59	27,00
3'-Amino-6-methoxyaurone	36,0	077764-95-5	49	1,07
2-Nonenal, (Z)-	37,2	060784-31-8	90	6,22
3-Methylheptyl acetate	37,9	072218-58-7	58	12,36
Butane, 1-chloro-2-methyl-	38,3	000616-13-7	59	3,47
2-Nonynoic acid	39,5	001846-70-4	72	2,14
2-Octenal, (E)-	40,2	002548-87-0	59	3,41
1-Pentene, 5-chloro-	41,0	000928-50-7	43	3,73
1,2-Hydrazinedicarboxylic acid, di	42,5	004114-28-7	52	1,60
2-Pentenal, 2-ethyl-	42,6	003491-57-4	43	2,83
1-Pentanol, 2-methyl-	43,2	000105-30-6	91	7,10
Nonane, 2-methyl-	44,0	000871-83-0	92	2,86

Tab. 2. Gas-chromatographic determination of the volatile substances in the defective sample (B)

SUBSTANCE	T _R (MIN)	CAS N.	QUALITY%	AREA%
Acetone	12,3	000067-64-1	9	1,63
2-Butene, (E)-	14,6	000624-64-6	64	4,68
Ethane, 1,1-diethoxy-	20,3	000105-57-7	64	6,26
Propane	21,2	000074-98-6	40	1,38
Benzaldehyde, 2-methyl-	23,8	000529-20-4	78	1,97
Tetrachloroethylene	25,2	000127-18-4	99	4,79
1H-Pyrrole, 2,5-dihydro-1-nitroso-	25,8	010552-94-0	90	9,03
Benzene, 1,2-dimethyl-	28,2	000095-47-6	50	2,24
Propene	29,9	000115-07-1	53	3,40
Carbonic acid, diethyl ester	30,3	000105-58-8	53	4,99
2,4-Nonadienal	32,3	006750-03-4	53	1,52
Benzene, 1,2,4-trimethyl-	33,1	000095-63-6	50	3,48
4-Pentenal	33,7	002100-17-6	64	3,29
Cyclopropane, 1,1'-ethenylidenebis	33,8	000822-93-5	59	2,30
Butane, 1-chloro-2-methyl-	34,6	000616-13-7	91	16,51
Butane, 1-(ethenyloxy)-	37,2	000111-34-2	47	5,29
3-Methylheptyl acetate	37,9	072218-58-7	93	10,29
2-Penten-1-ol, (Z)-	38,3	001576-95-0	94	1,62
3-Hexenal, (Z)-	39,5	006789-80-6	64	0,97
3-Hepten-1-ol	40,2	010606-47-0	38	3,32
1-Pentene, 5-chloro-	41,0	000928-50-7	47	3,04
Hexanoic acid, butyl ester	41,7	000626-82-4	95	1,00
6-Oxabicyclo[3,1,0]hexane	42,5	000285-67-6	96	1,89
Nonane	43,2	000111-84-2	50	3,72
Cyclopentaneundecanoic acid	44,0	006053-49-2	20	1,39

With regard to the possible involvement of plasticizers, we report the case of a leather sample for footwear where, as in the previous case, the execution of the first tests described in paragraph 3.1 had not provided sufficient elements to advance hypothesis on the origin of the problem and therefore an in-depth investigation was necessary through specific instrumental techniques; in particular, considering that the yellowing agent resulted to be soluble in ethanol, the gas-

chromatographic analysis was performed of an extract in ethanol from the sample, using the GC-MS technique (Gas-Chromatography - Mass Spectroscopy Detector). The gas-chromatographic profile obtained for the extract is reported in Figure 5, showing that the most intense signal is the one characterized by a t_R (retention time) of 33.37 min, identified as "2-Ethylhexyl diphenyl phosphate", CAS: 1241-94-7. This substance is used as a plasticizer-flame retardant, insoluble in water which, as commercialized substance, is characterized by a pale yellow color (as reported in the technical sheets). Therefore, a possible involvement of this substance in the onset of the problem has been hypothesized, both for the coloration of the identified substance itself, and for the tendency to migration/transport of other substances, notoriously exhibited by plasticizers.

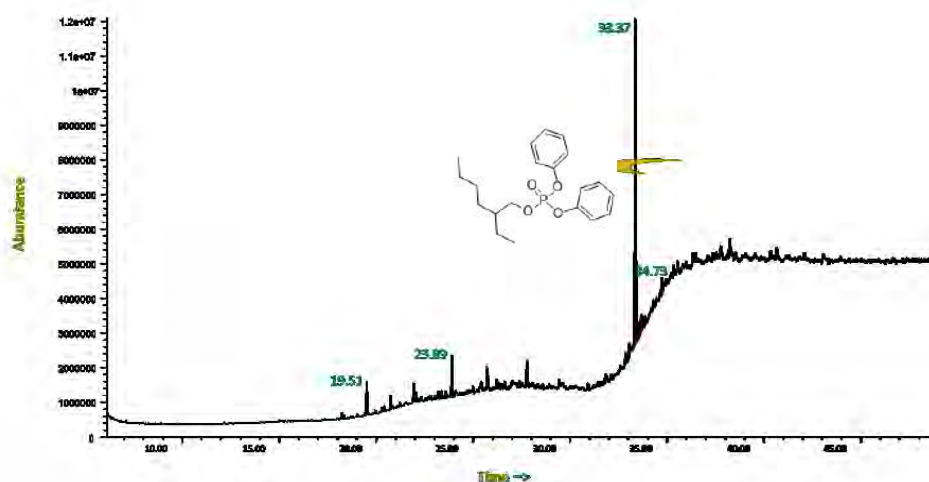


Fig. 5. Gas-chromatographic profile of the organic extract of the defective sample (leather for footwear)

Similarly, in-depth analysis was required, with the same technique, for the characterization of organic extracts (in 1: 1 acetone/dichloromethane mixture) of a leather sample for automotive with reversible defect following the exposure to light. The results obtained, for both its yellowed and not yellowed parts, are reported in Figure 6, and show that for the yellowed parts of the sample only, the presence of "2,2'-Methylenebis (6-tert-butyl-4-methylphenol)" was found at a t_R of 14.885 min", CAS: 119-47-1.

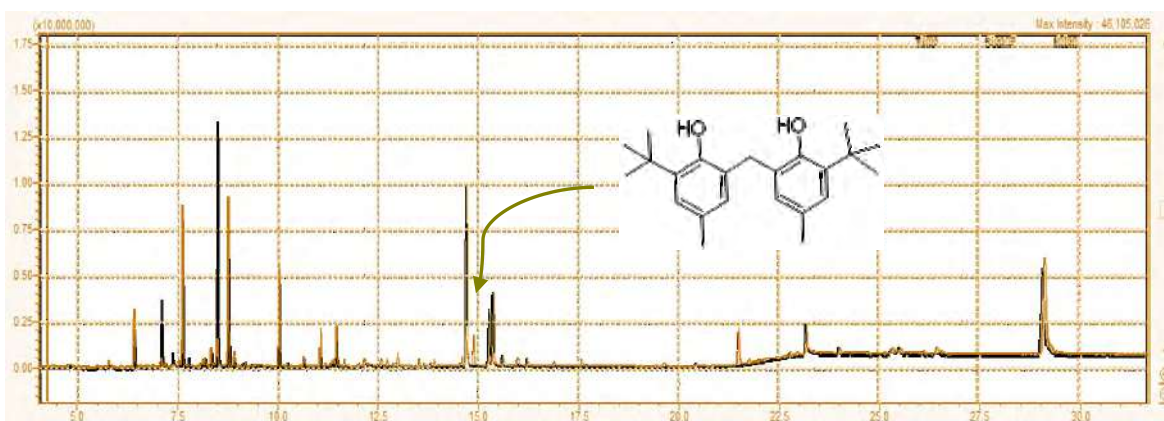


Fig. 6. Overlap of the gas-chromatographic profiles of the organic extract of the defective (yellow) and not defective parts (black) of the sample (leather for automotive)

This substance is used as an antioxidant and the technical data sheets report that the pure product is a white powder, which is slightly yellowish when exposed to air for a long time.

The sometimes controversial role of antioxidants, normally used just as stabilizers, but resulted instead potentially to be involved in the problems of alteration of the colouring, has already been discussed in previous works ^{3,2}; in the specific case, it has been hypothesized that the air reactivity of the antioxidant, migrated due to particular thermo-climatic conditions, may have contributed to the onset of the defect.

Finally, the in-depth investigation with the GC-MS technique was necessary to characterize the organic extracts (in a 1: 1 mixture acetone/dichloromethane) of a leather sample for furniture, where the other tests did not provide exhaustive and clarifying results on the possible origin of the defect. The results obtained in this case have shown the presence, in correspondence of the only defective parts, of 2-Octyl-2H-isothiazol-3-one, CAS: 26530-20-1, t_R of 10.535 min, whose structure is reported in Figure 7.



Fig. 7. 2-Octyl-2H-isothiazol-3-one

This substance is known to be used as a fungicide for the preservation of leather and has a yellow coloration (Light Yellow Oil, Yellow solid or clear dark amber liquid). The reactivity of this agent corresponds to that of an isothiocyanate, reacting particularly with amines, aldehydes, alcohols, alkaline metals, ketones, mercaptans, strong oxidants, hydrides, phenols and peroxides.

Also in this case, the problem was related to the migration of this agent to the surface, where the substance may have caused the problem, either directly (because of the colour exhibited) or indirectly (due to its reactivity).

3.3 Possible technical solutions

Since the most frequent cause of yellowing was found to be correlated to the chemical, intrinsic nature of the finishing, devices in this sense by the producers, can contribute to minimizing the problem. It would be particularly advisable, specifically, to avoid the use of aromatic polyurethanes in the outermost layer of the finishing of articles with light colours: although polyurethane polymers are known for their excellent mechanical and technological properties, presenting, overall, a high mechanical strength, on the other hand, it is known in fact that polyurethanes with aromatic components have a low resistance to light; alternatives can be constituted by aliphatic polyurethanes, for example starting from hexamethylenediisocyanate (HDI) or from trimethylmethylenediisocyanate (TMDI), or alternatively using mixed isocyanurates. In general, it may be appropriate to use adequate crosslinkers to increase the durability of the finishing polymers to hydrolysis ¹¹.

For problems of yellowing due to fats, the results obtained suggest, first of all, that it would be advisable to avoid using as raw materials skins characterized by a high fat content for the production of light coloured leather articles, while other measures concern the moderate use of fatliquors, where synthetic products should preferably be used, even if more environmentally friendly alternatives currently appear on the market, which include the use of fatliquors based on specially modified vegetable oils, able to provide high performance in heat and light fastness, which is comparable to synthetic products ¹⁰.

In general, and for all other cases, sector studies have shown that the use of stabilizers (such as UV absorbers, radical scavengers and an appropriate use of antioxidants) can significantly improve the light resistance of dyed and crust leathers ⁹.

However, in consideration of some limitations that traditional stabilizing agents can exhibit, SSIP is evaluating, together with some partners, the use of nanostructured TiO₂, appropriately doped or associated with SiO₂, to foster the shift of absorption towards the region of visible and improve its self-cleaning functions ^{1,4}.

4 Conclusion

The investigations carried out showed that the problem of yellowing can be caused by disparate factors, revealing a significant complexity of the phenomena potentially involved, and therefore requiring advanced diagnostic tools to identify some yellowing agents. However, some traditionally known causes of yellowing have been confirmed to be those that have the greatest impact on the problem: the most frequent cause of yellowing has in fact been found to be related to the chemical nature of the finishing. The use of aromatic polyurethanes in defected samples has been particularly frequent. The presence of fatty substances with a high level of unsaturation also proved to be a crucial factor in the onset of the problem.

In all the other cases, a more complex dynamic was found of the phenomena underlying the defect, instead, where the simultaneous responsibility for several factors was hypothesized, with particular reference to the factors of thermal and thermo-oxidative aging, associated to phenomena of migration and reactivity of potentially yellowing agents, used as auxiliaries or present in assembly materials. Examples in this sense refer to adhesives, plasticizers, antioxidants and fungicides, whose presence was found transversally in the defective samples, regardless of the nature of the skin of origin and of the intended use of the material.

Problem minimization strategies were also explored, which will be further developed later, including the possible use of applied nanotechnologies.

References

1. Anderson, C., Bard, A.J., 1997. Improved photocatalytic activity and characterization of mixed $\text{TiO}_2/\text{SiO}_2$ and $\text{TiO}_2/\text{Al}_2\text{O}_3$ materials. *J. Phys. Chem. B* 101, 2611–2616.
2. Florio C., Calvanese G., Naviglio B. - The dark side of leather. Finishing issues and light-dependent properties of pigments - XXXIII IULTCS CONGRESS, Novo Hamburgo, (BRASILE), 24-27 Nov. 2015, PDF 191; CPMC, 2016, 92(2/3), 87-94.
3. Florio C., Calvanese G., Naviglio B., Mascolo R., Grasso G. - Finishing defects. A special case concerning pigmented finishing based on TiO_2 - CPMC, 2009, 85(3), 131-143.
4. Fujishima, A., Zhang, X., 2006. Titanium dioxide photocatalysis: present situation and future approaches. *C.R. Chimie* 9, 750–760.
5. Krings L., Jimenez M., Oliveras M., Pont Pi J.M., Acrylic-urethan e hybrid polymers: materials with high potential in leather finishing, *JALCA*, 105(12), 388-394(2010)
6. Michel A., The many causes of yellowing, *Leather International*, 207(4756-april), 64(2005)
7. Michel P.B., Yellowing on footwear and leathergoods, *CTC Entreprise*, 21(10), 6-9(2005)
8. Mummenhoff P., Tegewa method for the determination of the yellowing of fatliquors on leather, *Das Leder*, 48(2), 40-1(1997)
9. Puntener A., The influence of fatliquors on the lightfastness of dyed leather, *Jalca*, 91(5), 126-35(1996)
10. Strijbos L., Saumweber R., Hess M., Gabagnou C., Page C., Fen J., high-fastness fatliquors from renewable resources, *World Leather*, 25(2), XIX-XXI (2012)
11. Yongyi Tsao, Yongbiao Liang, Xingyugong, Preparation of aqueous anti-yellowing polyurethane dispersion used as surface layer for transfer-film leather, XXX CV IULTCS, 385, Beijing (Cina), 11-14 october (2009)

INVESTIGATION ON THE RELEASE KINETICS OF CHROME FROM FINISHED CHROME TANNED LEATHER

L. Q. Peng^{§2}, W. J. Long^{§1,2}, R. Wang¹, W. H. Zhang^{*1} and B. Shi²

1 The Key Laboratory of Leather Chemistry and Engineering of Ministry of Education, Sichuan University, Chengdu 610065, Sichuan, China

2 National Engineering Laboratory for Clean Technology of Leather Manufacture, Sichuan University, Chengdu 610065, Sichuan, China

§These authors contributed equally to this work and should be considered co-first authors.

a)Corresponding Author : zhangwh@scu.edu.cn

b)First author:995097453@qq.com: 2893359970@qq.com

Abstract: Chrome tanning is the commonest tannage in leather manufacture, and the discard of chrome tanned leather goods inevitably leads to chrome release that might have potential environmental risks. In this study, the kinetic behaviors of the release of chrome were investigated by ICP-OES. Deionized water was used as medium and the parameters such as liquid/solid ratio, pH, contact time, temperature and rotational speed affected leaching behavior of chromium in the finished chrome-tanned leather shavings were studied. Then, the leaching tests were proceed at solid liquid ratio 1:20 as well as rotational speed 60 r/min to simulate the release of chrome tanned leather under natural conditions. The effect of temperature on the kinetics behavior was further explored. The results showed that the release of chrome could be well fitted by weber–morris model and the second-order kinetic equation, and two type of process controlled the rate of the release of chrome. Though the release of chrome is lasting, more than 85% leachable chrome in leather could be released in 24 h. The results could provide the theoretical parameters for the assessment of risks of chrome-tanned leather.

1 Introduction

Tanning is a important process procedure to converts animal hides or skins into leather[1, 2]. It's a resource utilization for recycling an organic waste from the meat industry and creates valuable products, such as footwear, that meet consumer's requirements in terms of comfort and fashion[3, 4]. There are many kinds of tanning methods, including metal salts, aldehyde derivatives, syntans, vegetable tannins and their combination tannages[5-7]. Because of the uniqueness properties that Cr-tanning leather confers to the resulting products[8], it accounts for more than 80% of the tannages in the past 20 years[9].

During the production of chrome-tanned leather, the chromium incorporated into the collagen fiber with at least three types of interactions, including that chromium is complexed with collagen, non-productive binding of chromium to collagen(chromium be bound to the collagen, but no crosslinked) and adsorption of chromium by the collagen matrix. The different interactions lead to different binding ability for chromium to collagen. Not more than 1.5% of the total chromium been adsorbed by the collagen matrix that could be removed easily. Nearly 58.5% of the total chromium is complexed with collagen, it has great effect on the thermal stability of chromium-collagen complex, and it is harder to removed. Nearly 40% of the total chromium is tightly bound to the collagen, but no crosslinked, that has no effect on thermal stability, and it is also harder to removed[10]. When the leather goods become waste at the end of their life span, the chemicals in leather especial chromium can be leached out to pollute surface water, soil or even underground water by surface rain's leaching procedure. The migration rule may be related to the interactions of chromium to collagen.

In this study, the deionized water was used as the leaching agent to simulate the leaching behavior of leather in surface water. Some parameters such as liquid/solid ratio, pH, contact time, temperature and rotational speed affected leaching behavior of chromium in the finished chrome-tanned leather shavings were studied and the leaching kinetics of chrome tanned leather was further studied.

2 Materials and Methods

2.1 Materials and Analysis

The finished chrome tanned leathers obtained from different tannery were used in the present study. The sample was shredded to ≤ 4 mm (using a Retsch mill with rotating knives and a 4 mm sieve), and thoroughly homogenized and conditioned in standard laboratory atmosphere (293.15 ± 2 K and $65 \pm 5\%$ relative humidity) for 48h. Deionized water was used as extractor fluid to evaluate the leaching behaviors of leather waste. All chemicals such as hydrochloric acid, nitric acid, sodium hydroxide and hydrogen peroxide were of analytical grade provided by Chengdu Jinshan Chemical Reagent Co Ltd. The standard solution of chrome was obtained from National Nonferrous Metals and Electronic Materials Analysis and Testing Center (Beijing, China), and inductively coupled plasma atomic emission spectrometry (ICP-AES, OPTIMA 8000) is used to detect the total chromium content in leaching solution.

2.2 Experimental Procedure

2.2.1 Determination of chrome content in finished chrome tanned leather

A weight of 1.0 g Cr-tanning powder was digested by microwave method. The procedure of microwave digestion[11] (Anton Paar Multiwave PRO, Austria) consisted of a 10-min gradual increase to 1400W, a 20-min digestion step at 1400W and then a cooling stage. The digestion solution was mixed thoroughly after adjusting to a constant total volume. The total chrome in leather was analyzed directly by inductively coupled plasma optical emission spectrometer (ICP-OES, PerkinElmer Optima 8000, USA).

2.2.2 Leaching experiments

Leaching experiments were conducted with air constant temperature shaker (ZWY-2102C, Shanghai China) with temperature precision of $\pm 0.1^\circ\text{C}$. The leachates passing through $0.45\mu\text{m}$ membrane filters were digested by wet digestion method that using concentrated nitric acid and hydrogen peroxide (3:1, v/v). The digestion liquor was filtered and adjusting to a constant total volume with deionized water, and the concentration of chrome was analyzed by inductively coupled plasma optical emission spectrometer (ICP-OES, PerkinElmer Optima 8000, USA). The calibration standard ($0.20\text{--}5.00\text{mgL}^{-1}$) was prepared by diluting the chrome standard stock solutions (100mg L^{-1}). All the tests were done in duplicate.

The leaching experiments in this paper are mainly divided into two parts. First, the leaching conditions such as temperature varying from 20°C to 35°C , the shaker speed from 30rpm to 210rpm, liquid-solid ratio from 70:1 to 10:1, and pH of extractor from 2 to 11 are optimized continuously. The pH of extractor was adjusted by addition of 0.1mol.L^{-1} HCl or NaOH appropriately, and measured using FE20-Five Easy Plus™ pH meter, Mettler-Toledo.

Second, the leaching kinetics of chromium from Cr-tanned leather powder in aqueous solution was investigated in detail. This part of the leather is thinner than those used in previous experiments. The kinetic researches were conducted for four different temperature 20°C , 25°C , 30°C and 35°C respectively. A weight of 4.0g Cr-tanning powder was taken in 250 ml conical flask, fully soaked using 80ml ultrapure water (resistivity $\geq 18.2\text{M}\Omega\text{-cm}$) to simulate surface water. Then the 18 flasks were kept in a shaker at fixed temperature with rotational speed of 60rpm. Take two flasks at 1h, 2h, 4h, 8h, 24h, 48h, 96h, 168h, and 240h respectively to analyze the total chrome of the leachates as the above.

3 Results and Discussion

3.1 The Total Chromium in Leather

After the chrome tanned leather was digested by the microwave digestion instrument, the total chromium content measured by ICP-OES were 21445.83mg/kg and 20672.50 mg/kg respectively for two kinds of Cr-tanned leather.

3.2 Leaching Behavior of the Chromium

The leaching experiments of finished chrome-tanned leather shavings (FCTLs) were carried out with various experimental parameters, including liquid-solid ratio(LSR), pH, contact time (CT), temperature(T), and rotational speed(RS). The extractive chrome content was calculated by the following equation.

$$C=C_0 \times A$$

Where C represents the extractive chrome content, C_0 represents the concentrations of leachate, A represents the liquid/solid ratio. The effects of these leaching parameters on chromium leaching efficiency were investigated, as illustrated in Fig. 1(a)–(e).

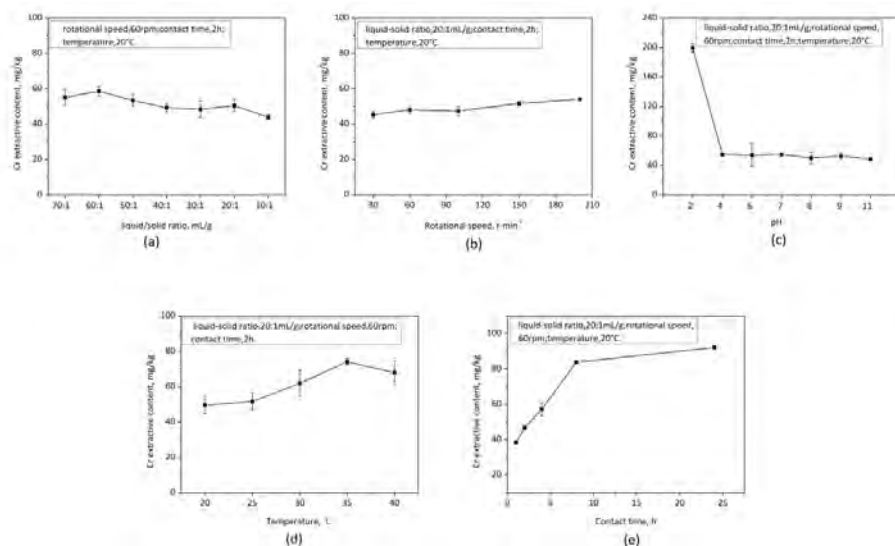


Fig. 1. The relation between Cr removal and leaching parameters:(a) liquid-solid ratio, (b) rotational speed (c)pH, , (d) temperature and (e) contact time.

The effect of liquid-solid ratio on chromium leach from the FCTLs was shown in Fig. 1(a). As presented, the leaching amount slightly decreased as the liquid-solid ratio decrease. However, considering the water absorption and swelling of leather powder, the liquid-solid ratio of 10:1 is not appropriate. The concentration of chromium released was in the range of 45.32-54.14mg/kg when changing the rotational speed of the shaker (Fig.1b), showing slight effect of rotational speed. In Fig. 1(c), the leachates of FCTLs contain a higher concentration of chromium, suggesting that the release of chromium from the FCTLs could be increased in an overly acidic environment. Whereas in the pH range of 4-11, the chromium concentration released was not significantly changed by the increase of pH value.

The contact time and temperature have greater influence on the extractive chrome content compared with liquid-solid ratio, rotational speed and pH of the fluid, as shown in Fig. 1d-e. The extractive content of Cr increases significantly with temperature. At 35°C, the extractive content of

Cr gets to the highest concentration. It indicated that the release of Cr was sensitive to the leaching temperature, the extractive content of Cr increased steadily as the contact time increased from 0 to 24 hours. At the first phase (1- 8 hours), the content of Cr increased rapidly with time. At the second phase (8-24hours), the change of Cr content was comparatively small. Then the effect of temperature and contact time were further investigated, whereas liquid-solid ratio and rotational speed were kept at 20:1 and 60rpm respectively, and deionized water was used as the fluid.

3.3 Kinetics Analysis for the Release of Cr

The release of chromium with respect to time was plotted in a graph shown as Fig. 1. From the figure, it is clear that the chromium release was temperature dependent. The chromium concentration was 0.21 mmol/L at 20°C and 25°C, and 0.25 mmol/L at 30°C and 35°C for the shaking time 1 h respectively. However, appreciable change in the chromium concentrations at different temperature was achieved for the shaking times beyond 1 h especially at 35°C. With the increase of temperature, the total leached chromium increase. In the meantime, the leaching process becomes slower with time, and the leaching equilibrium didn't reached even after shaking 24h with replenished leaching solvent. In order to more fully understand the leaching mechanism, the kinetics on Cr release with different times at various temperatures were analyzed by using the shrinking core model, diffusion-based model and the homogeneous model, respectively.

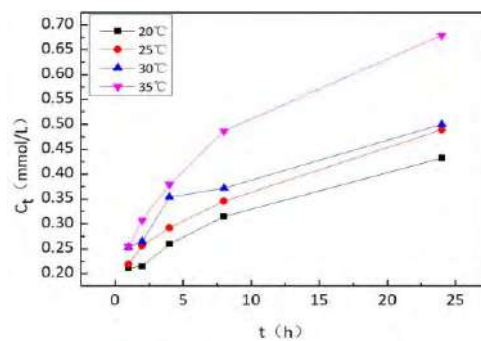


Fig. 2. Cr release at different temperature.

3.3.1 Shrinking core model (SCM)

This model was frequently used to describe the leaching reaction of the solid reactant with spherical particles. According to the model, the leaching reaction occurs first at the outer skin of the particle (ie. core) and moves into the solid, leaving behind completely converted material and inert solid (ie. shell). The model assumes the solid-liquid leaching reaction involves generally a chemical reaction on the surface of the core of unreacted reactants, accompanied by both fluid and solid phase (pore fluid) diffusion steps. Under the assumption of rate-control step, the shrinking core model could be simplified as the following equations[12-14].

For fluid film diffusion control:

$$x = k_1 t \quad (1)$$

For pore diffusion control:

$$1 - 3(1 - x)^{\frac{2}{3}} + 2(1 - x) = k_2 t \quad (2)$$

For chemical reaction control:

$$1 - (1 - x)^{\frac{1}{3}} = k_3 t \quad (3)$$

where, k_i is the apparent constant for different control steps, x is the ratio of chromium content in liquid phase to total chromium content in dry leather powder (dimensionless), and t is the leaching time (h). Then the three equations were applied to test the control step of the Cr extracted by water. The plots were shown in Fig. 3 and the correlation coefficients were listed in Table 1.

Table 1. Correlation coefficients (R^2) of various rate-control steps with the experimental data.

T/°C	Correlation coefficients(R^2) of three kinetic models		
	$x=k_1 t$	$1-3(1-x)^{2/3} + 2(1-x)=k_2 t$	$1-(1-x)^{1/3} =k_3 t$
20	0.9516	0.9542	0.9543
25	0.9546	0.9579	0.9580
30	0.8687	0.8739	0.8741
35	0.9121	0.9193	0.9196

Just as shown in table 1, the correlation coefficient (R^2) values for these fitted curves are below 0.96. Taking into consideration of the geometrical factor of the powder of waste leather, which is a strip flake material with a loose and porous structure surface[15, 16], these three kinetic equations (1-3) were not suitable to demonstrate the leaching process of the scraps.

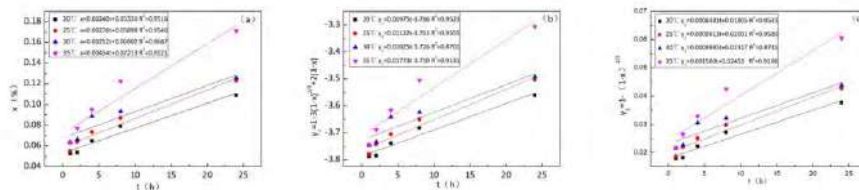


Fig. 3. Fitting of experimental data with fluid film diffusion control (a) and pore diffusion control (b) and chemical reaction control (c) of SCM.

3.3.2 Diffusion-controlled models

Weber–Morris model assumes that the mass transfer is the fast process, and only intraparticle diffusion is considered as rate-determining step. The kinetics equation is given as[17, 18]

$$C_t = k_w t^{0.5} + C \quad (4)$$

where k_w denotes the rate constant of intraparticle diffusion determined by the slope of plot of C_t vs. $t^{0.5}$, and C represents the intercept. The graph of intraparticle diffusion model (Fig.4) showed linearity at all temperatures. The high values of R^2 suggested the applicability of intraparticle diffusion of Cr from the interstitial spaces and pores of the leather matrix to the fluid.

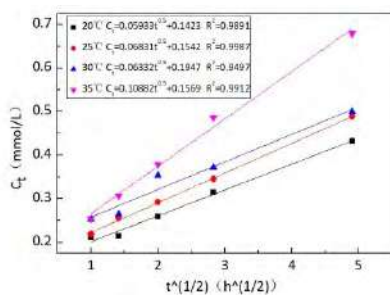


Fig. 4. Fitting of experimental data with Webber-Morris equation.

The deviation from the origin can be accounted by the fact that there is two type of process controlling the rate of the release of Cr.

3.3.3 Chemical kinetics-based model

Most of the reaction kinetics-based models consider the leaching process assuming that mass transfer is fast enough to be neglected. When the solid reactant is porous, the fluid reactant could freely diffuse into the interior of the solid. Then leaching could be considered as homogeneous reaction throughout the solid, and a gradual variation in the solid reactant concentration within the particle would appear during leaching process. Therefore, the experimental data were also applied to the pseudo-first-order kinetics and pseudo-second-order kinetics.

The equation for the pseudo-first-order kinetics can be expressed as[17, 18]:

$$\ln c_t = k_1 t + \ln C_s \quad (5)$$

The general form of the pseudo-second-order kinetic model is written as[17, 18]:

$$\frac{t}{c_t} = \frac{1}{k_2 C_s^2} + \frac{t}{C_s} \quad (6)$$

where c_t is the concentration of Cr in leachate in the time of t , and C_s is the concentration of chromium in leachate at the equilibrium state. while k_1 (h^{-1}) and k_2 ($L \text{ mmol}^{-1} h^{-1}$) are the rate constant of reaction respectively. The slope k_1 and $1/C_s$, as well as the intercept $\ln C_s$ and $1/k_2 C_s^2$ can be calculated by the linear fitting between the $\ln c_t$, t/c_t and t , respectively.

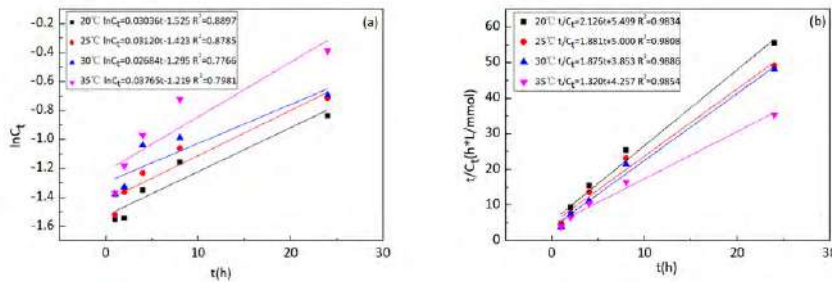


Fig. 5. Fitting of experimental data with pseudo-first-order (a) and pseudo-second-order kinetics (b).

From Fig. 5a, the plots of pseudo-first-order kinetics model at all the four temperatures have significantly deviated from the linearity with the value of R^2 lower than 0.9, indicating the non-suitability of this kinetic model. However, the fitting correlation coefficient R^2 of pseudo-second-order kinetics model are all above 0.98 (Fig. 5b), suggesting reaction order related to the concentration of the solid reactant could be affirmed as a second order reaction.

Based on Arrhenius equation[19]

$$\ln k = \ln A - \frac{E_a}{RT} \quad (7)$$

where k is the rate constant, A denotes frequency factor, which corresponds to the intercept of the straight line plotted by $\ln T$ against $1/T$ at $1/T=0$. E_a is apparent activation energy, which could be obtained from the slope of the line.

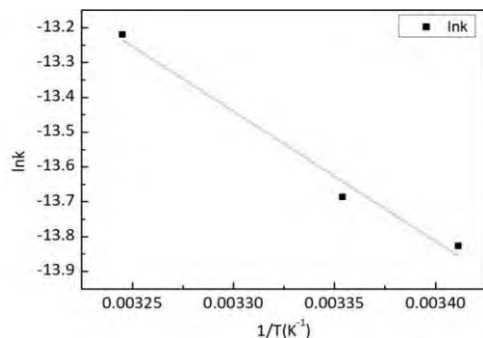


Fig. 6. Fitting of $\ln k$ with $1/T$.

The Arrhenius plot was obtained based on weber–morris model, and correlation coefficient was 0.9703. Then the apparent activation energy was estimated as 31.05kJ/mol on the basis of Fig.6, indicating higher energy barrier of chromium diffusion in leather matrix.

4 Conclusions

The releasing behavior of chromium from leather was tested to simulate the surface water in this study. Our results showed that the main factors affecting Cr release from leather were temperature and contact time. The optimal leaching condition was determined as liquid-solid ratio at 20:1mL/g , rotational speed at 60rpm and deionized water was used as the fluid. However, the leachable Cr by water was low, about 0.18%-0.43% of the total chromium on the leather.

The kinetics indicated that the release rate of Cr is two type of process controlling. Weber–Morris model and pseudo-second-order kinetics model were applicable in the release of chromium from leather by water. Though the release of Cr is lasting, more than 85% leachable chromium in leather could be released in 24 h.

5 Author Contributions

§Liangqiong Peng and Wenjun Long contributed equally.

6 Conflict of interest

The authors of this study declare no conflict of interest.

7 Acknowledgements

This work was supported by the National Key Research and Development Program of China [2017YFB0308503] 、 [2018YFC1802201].

References

1. Peng, L., et al.: 'Investigation into the Hazards of Finished Cr-tanned Leather as both Product and Waste', *J. Soc. Leather Technol. Chem.*, 103, 43-48, 2019.
2. Thanikaivelan, P., et al.: 'Recent trends in leather making: Processes, problems, and pathways', *Crit. Rev. Environ. Sci. Technol.*, 35, 37-79, 2005.
3. Maria J, F.: 'Finished leather waste chromium acid extraction and anaerobic biodegradation of the product', *Waste management (New York, N.Y.)*, 30, 2010.
4. Covington, A.D.: 'Modern tanning chemistry', *Chem. Soc. Rev.*, 26, 111-126, 1997.
5. Zhang, C., et al.: 'A salt-free and chromium discharge minimizing tanning technology: the novel cleaner integrated chrome tanning process', *J. Cleaner Prod.*, 112, 1055-1063, 2016.
6. Zengin, A.C.A., et al.: 'Eco-leather: Chromium-free Leather Production Using Titanium, Oligomeric Melamine-Formaldehyde Resin, and Resorcinol Tanning Agents and the Properties of the Resulting Leather', *Ekoloji*, 21, 17-25, 2012.
7. Mutlu, M.M., et al.: 'Eco-Leather: Properties of Chromium-Free Leathers Produced with Titanium Tanning Materials Obtained from the Wastes of the Metal Industry', *Ekoloji*, 23, 83-90, 2014.
8. Covington, T., *Tanning chemistry*, 2009.
9. Gong, Y., et al.: 'Stabilization of chromium: An alternative to make safe leathers', *J. Hazard. Mater.*, 179, 540-544, 2010.
10. Brown, E.M. and M.M. Taylor: 'Essential chromium?', *J. Am. Leather Chem. Assoc.*, 98, 408-414, 2003.
11. Ahmed, M., et al.: 'Microwave assisted digestion followed by ICP-MS for determination of trace metals in atmospheric and lake ecosystem', *J. Environ. Sci.*, 55, 1-10, 2017.
12. Yang, C.F., H.P. Hsu, and C.W. Lan: 'A rapid thermal process for silicon recycle and refining from cutting kerf-loss slurry waste', *Sep. Purif. Technol.*, 149, 38-46, 2015.
13. Boutouchent-Guerfi, N., et al.: 'Disposal of metal fragments released during polycrystalline slicing by multi-wire saw', *J. Cryst. Growth.*, 447, 27-30, 2016.
14. Chen, W., et al.: 'On the nature and removal of saw marks on diamond wire sawn multicrystalline silicon wafers', *Mater. Sci. Semicond. Process.*, 27, 220-227, 2014.
15. Yang, C., et al.: 'Effect of Chrome Content in the Chrome Tanning Liquid of the Leather Tanning Machine on the Properties of Leather', *J. Soc. Leather Technol. Chem.*, 99, 33-38, 2015.
16. He, X., et al.: 'Suitability of Pore Measurement Methods for Characterizing the Hierarchical Pore Structure of Leather', *J. Am. Leather Chem. Assoc.*, 114, 41-47, 2019.
17. Sathish, M., A. Dhathathreyan, and J.R. Rao: 'Ultraefficient Tanning Process: Role of Mass Transfer Efficiency and Sorption Kinetics of Cr(III) in Leather Processing', *ACS Sustainable Chem. Eng.*, 7, 3875-3882, 2019.
18. Hai Nguyen, T., et al.: 'Mistakes and inconsistencies regarding adsorption of contaminants from aqueous solutions: A critical review', *Water Res.*, 120, 88-116, 2017.
19. Liu, Y. and X. Yu: 'Carbon dioxide adsorption properties and adsorption/desorption kinetics of amine-functionalized KIT-6', *Applied Energy*, 211, 1080-1088, 2018.

CLEANER CHROME TANNING-TECHNOLOGY OF LOW-CHROME TANNING WITHOUT SALT, PICKLING AND SHORT PROCEDURE

LUO JIAN-XUN¹, FENG YAN-JUAN², MA HE-WEI¹

1 Department of Light Chemistry Engineering, College of Material & Textile Engineering, Jiaxing University, Jiaxing 314001, China

2 Research Centre of Spirit of Red Boat, Jiaxing University, Jiaxing 314001, China

Corresponding author: jianxunluo986@126.com

Abstract. Tannery effluent with high salinity and chromium have a serious environmental impact. The traditional chrome tannage that involved the use of sodium chloride, acid and chromium is one of the main origins of salt and chromium pollution. In this study, a non-pickling, chrome-less tanning technology was developed. The novel Chrome-free agent SL can be directly employed to tan bated bovine hide and the wet white was obtained. Then the shaved wet white was pre-treated by Poly-carboxylate auxiliary agent PAA and tanned by chrome powder. It was tested that the shrinkage temperature of the wet white, the initial pH of chrome tanning, the consumption of chrome powder, the shrinkage temperature of the chrome-tanned leather, the content of Cr₂O₃ in effluent, the absorption of chromium and the other properties of the chrome-tanned leather. It was found that the shrinkage temperature of the wet white tanned by SL reached over 80°C, the optimal consumption of Poly-carboxylate auxiliary agent was 2wt% based on the weight of the shaved wet white, the better chrome-less tanning conditions were that the wet white was tanned by 3-4wt% chromium powder for 150~180min at room temperature when the initial pH value was 3.0-3.5. The next processes were same as traditional chrome tannage. Meanwhile, the shrinkage temperature of the leather tanned by the chrome-less tannage reached more than 95°C, the absorption of chromium was 96%, the content of Cr₂O₃ in the effluent was under 200mg/L. For the chrome-less tanned leather, the absorption of dyestuff, fat-liquor reached 99.5%, 82.5% respectively. Compared with the traditional chrome tanned process, not only the conventional pickling process was eliminated, the process was been shorten and reduce the pollution of sodium chloride, but it can reduce 50% of the consumption of Chrome powder, improve the absorption of chromium and can reduce content of Cr₂O₃ in effluent.

1 Introduction

As we know, Chrome-tanned & finished leathers have good comprehensive properties such as high hydrothermal stability, softness, etc, so the Chrome tanning agents is considered as the best mineral tanning agent among the tanning agents used in the leather industry. Therefore most of all the tanneries in the world have now adopted chrome tanning. But the absorption level of chromium is only 60-80% during the traditional chrome tanning so that the tannery effluent contains chromium and waste containing chromium is produced¹. How to reduce or abolish the disadvantage of the Chromium tanning agent is always one of important topics in the leather industry. The key problem is to improve the absorption level in order to overcome the valid absorption and reaction between collagen and Chrome tanning agent. So many technologists have many research and obtain some results in the field of high absorptive chrome tannage, chrome-less tannage and non-chrome tannage. Based on the needs and trends of leather products of markets, Chrome-tanned leather and non-chrome tanned leather will be co-existed for a long time². Therefore in order to meet the demands of markets and environmental protection, the best way is to reduce the dosage of Chrome tanning agent and improve the absorption level of chromium in the tanning process. So chrome-less tannage is one of cleaner chrome tanning technologies.

Of existing chrome-less tannage, one way is that some organic tanning agent or other mineral tanning agent was adopted to achieve the combination tanning with Chrome tanning agent^{3,4,5}. The other way is that pelt was tanned by new chrome tanning agent modified by other mineral tanning agents⁵. In recent years, in order to improve the effect of less chrome tanning, the chrome-less

tannage based on wet white is studied, that is, the pelt is pre-tanned by Alumium tanning agent or aldehyde tanning agent to obtain the wet white, then the shaving wet white is tanned by Chrome tanning agent^{6,7}. But the appearance, softness and other properties of the chrome-less tanned leather less than that of traditional chrome tannage, the chrome-less tannage need be further studied.

Based on the new technology of non-chrome tanning agents in recent years, the purpose of our research is to develop new chrome-less tannage without salt, Pickling and short procedure which can remove the pickle, achieve the chrome-less tannage and match the quality of the leather tanned by traditional chrome tanning.

2 Experimental procedures

2.1 Materials

Bovine pickled hide (pH 2.6-3.0) and bated bovine hide (pH 7.5-8.0) were used as raw materials. The novel chrome-free agent SL prepared on laboratory scale is an amphoteric organic compound (approximately a 45% solution w/v; pH 2.5-4.0). The novel chrome-free agent SL prepared on laboratory scale is an amphoteric organic compound (approximately a 45% solution w/v; pH 2.5-4.0). The poly-carboxylate auxiliary agent PAA prepared on laboratory scale is an compound with more carboxyl groups (approximately a 35% solution w/v; pH 5.0-5.5; M_n 24344). TRUPON SWS, TRUPON DB were obtained from TRUMPLER Chemicals s.p.a, Germany. All chemicals used for leather processing were of commercial grade.

2.2 Tanning properties of the novel chrome-free agent SL

As we know, the novel chrome-free agent SL was synthesized by the radical co-polymerisation reaction with acrolein and diallyl dimethyl ammonium chloride, whose structure is shown in Fig. 1⁸. The tanning process of SL is shown in Table 1. The Six pieces of bated bovine hide (30cm×20cm, pH 7.0-7.5) were put in the stainless steel drums (50cm diameter) and the float was 100%. The offer of SL is 2%, 4%,5%, 6%,8%,10% (based on 150% times of the weight of bated pelt) respectively The time of penetration is 4 hours. Then the pH was adjusted to 7.0~7.5. Then the temperature of the float was raised to 40°C, the float ratio was adjusted to 2.0 and running continued for 5hours. The pH of the tanning float and the shrinkage temperature of the leather were measured the next day.

2.3 The properties of wet white tanned by the novel chrome-free agent SL

The five pieces of the wet white tanned by the novel chrome-free agent SL(2cm×10cm, pH 7.0-7.5) were put in the 250mL cone bottle and the water was 100mL. Then the cone bottles were put in the Water bath oscillator (25°C, 140rpm) and were operated for 2, 4, 6, 8, 10 hours. The shrinkage temperature of the leathers were measured. In addition, The seven pieces of the wet white tanned by the novel chrome-free agent SL (2cm×10cm, pH 7.0-7.5) were put in the 250mL cone bottle and the water was 100mL whose pH was adjusted to 2.5, 3.0, 3.5, 4.0, 4.5, 5.0, 5.5 respectively. Then the cone bottles were put in the Water bath oscillator (25°C, 140rpm) and were operated for 2 hours. The shrinkage temperature of the leather were measured.

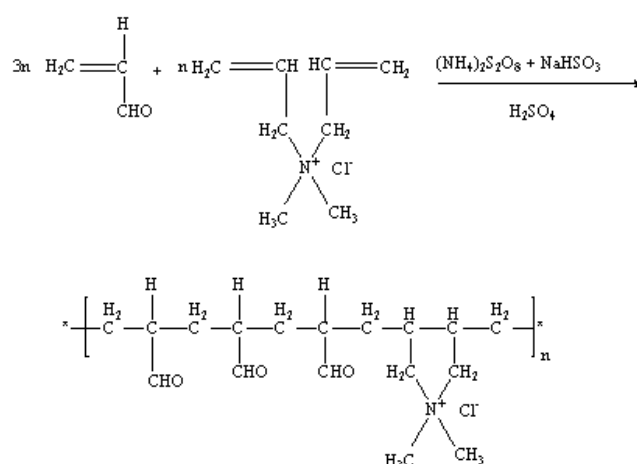


Fig. 1. The synthesis of the novel chrome-free agent SL.

Table 1. The procedures of tanning with SL based on the bated bovine hide.

Process	chemicals	Offer/%	T/°C	t/min	pH	Remarks
Wash	Water	200	25	15	7.0-7.5	3times, drain
Tanning	Water	100	18-22			
	SL	X*		240		
Basification	NaHCO ₃	0.6		30		
	NaHCO ₃	0.6		30	7.5-8.0	
	Water	100	50	300	7.0-7.5	

*X=2, 4, 5, 6, 8, 10

2.4 Optimization of the initial pH in tanning process

The six pieces of the shaved wet white tanned by the novel chrome-free agent SL (30cm×20cm, pH 7.0-7.5, 0.9-1.0mm) were put in the stainless steel drums (50cm diameter) and the float was 60%. The offer of Chrome tanning agent is 5% (based on the weight of the shaved wet white). The initial pH of the tanning float is adjusted to 2.5, 3.0, 3.5, 4.0, 4.5, 5.0 respectively. The tanning process was shown in Table 2. The time of penetration, the shrinkage temperature and the state of leather, the content of Cr₂O₃ in the effluent and the absorption of Chrome tanning agent were measured respectively.

Table 2. The chrome tanning process of the shaved wet white tanned by SL.

Process	Chemicals	Offer/%	T/°C	t/min	pH	Remarks
Re-wetting	Water	200	35			
	BCN 60	0.3		30	7.0	
Wash	Water	200	18-22	15		Twice, drain
Tanning	Water	60	18-22			
	Formic acid	0.5-2.5		20	Y*	
	Chrome powder	5		120		Check the penetration
Basification	Sodium formate	1				
	Sodium bicarbonate	0.8		30		
	Sodium bicarbonate	0.6		60	3.8-4.0	
	Water	150	50	300	3.8	Horse up

*Y=2.5, 3.0, 3.5, 4.0, 4.5, 5.0

Table 4. Chrome-less tanning process of the shaved wet white tanned by SL under the poly-carboxylate auxiliary agent (PAA).

Process	Chemicals	Offer/%	T/°C	t/min	pH	Remarks
Re-wetting	Water	200	35			
	BCN 60	0.3		30	7.0	
Wash	Water	200	18-22	15		Twice, drain
Pre-treatment	Water	100	35			
	PAA	M*		40		
Wash	Water	200	18-22	15		drain
Tanning	Water	60	18-22			
	Formic acid	1.0-1.2		20	3.5	
Basification	Chrome powder	4		120		Check the penetration
	Sodium formate	1				
	Sodium bicarbonate	0.8		30		
	Sodium bicarbonate	0.6		60	3.8-4.0	
	Water	150	50	300	3.8	Horse up

*M=0, 0.5, 1.0, 1.5, 2.0, 2.5

In order to increase the absorption of chromium, the poly-carboxylate auxiliary agent PAA was used to pre-treat the shaved wet white. The six pieces of the shaved wet white tanned by the novel chrome-free agent SL(30cm×20cm, pH 7.0-7.5,0.9-1.0mm) were put in the stainless steel drums (50cm diameter) and the float was 100%. The wet white was pre-treated by the poly-carboxylate auxiliary agent PAA, whose offer is 0%, 0.5%, 1.0%, 1.5%, 2.0%, 2.5% (based on the weight of the shaved wet white) respectively. The tanning process was showed in Table 4. The time of penetration, the shrinkage temperature and the state of leather, the content of Cr₂O₃ in the effluent and the absorption of Chrome tanning agent were measured respectively.

2.7 Contrast experiment between less-chrome tanning and traditional chrome tanning

A piece of bated bovine pelt (approximately 50 square foot, pH 7.0-7.5) was cut into two pieces along the backbone line. The left half was directly tanned by SL, then was shaved, pre-treated by the poly-carboxylate auxiliary agent PAA and less-chrome tanning. The right half (control) was pickled, chrome tanning according to traditional process. They were separately put in the stainless steel drums (100cm diameter). The recipes of tanning the subsequent processes are given in Table 5, 6.

The shrinkage temperature, the content of Cr₂O₃ in the effluent, the absorption of Chrome tanning agent softness and state of the leathers were measured. At the same time, samplers of the leathers were cut from the official sampling position¹¹. The cross sections of the samples were observed by Scanning Electron Microscope (JSM-5900LV, JEOL Ltd., Japan). The micrographs at a magnification of 100 were obtained with an accelerating voltage of 20KV.

2.8 Piolt production of Leather tanned by chrome-less tannage

Sixty pieces of bated bovine pelt (approximately 50 square foot, pH 7.0-7.5) were directly tanned by SL, then were shaved, pre-treated by the poly-carboxylate auxiliary agent PAA, less-chrome tanning. The recipes of tanning the subsequent processes are given in TABLE V, VI. The shrinkage temperature, the content of Cr₂O₃ in the effluent, the absorption of Chrome tanning agent softness and state of the leathers were measured.

Table 5. The procedures of tanning with novel Chrome-less tannage and traditional chrome tanning.

Process	Chrome-less tannage		Traditional chrome tanning		t/min	Remarks
	Chemicals	%	Chemicals	%		
Wash	Water, 25°C	200	Water, 25°C	200	15	3 times, drain
Pickling	/	/	Sodium Chloride	8	20	
	/	/	formic acid	0.6	15	
	/	/	Sulfuric acid	1.1-1.2	120	pH 2.8-3.0
De-acidification	/	/	HCOONa	1.5		
	/	/	NaHCO ₃	2.5	150	pH 6.0-7.0
	/	/	Water, 25°C	200	15	2 times, drain
Wash	SL	5	Chrome tanning agent	8	300	
Basification	NaHCO ₃	1.2	NaHCO ₃	1.2	60	pH 7.0-8.0
	Water, 55°C	100	Water, 55°C	100	300	pH 7.0-7.5

Out of drum and piled down. Wring, shaving to 1.0mm, weight

The chrome-less tannage based on the shaved wet white is done according to Table 4.

Table 6. The procedures of dyeing or fat-liquoring of the leathers tanned by Chrome-less tannage and traditional chrome tanning.

Process	Chemicals	%	Time(min)	Remarks
Re-wetting	Water, 35°C	200		
	BCN 60	0.3		
	Formic acid	0.8	30	pH 5.8
Wash	Water, 25°C	200	15	drain
	Water, 50°C	200		
Dyeing/Fat-liquoring	dyestuff	2	30	
	TRUPON SWS	12		
	TRUPON DB	5	90	
	Formic acid	0.6		
	Formic acid	0.6		pH 3.8
Wash	Water, 25°C	200	15	

Out of drum and horsed overnight, Vacuum and hang dry, vibration staking & milling

3 Results and Discussion

3.1 Analysis of Tanning properties of the novel chrome-free agent SL and its leather

Relation between the shrinkage temperature of the leather tanned by SL and its offer is shown in Fig 3. The shrinkage temperature of the leathers rise as the offer increases when the offer of SL is 2%-5%, when the level of tanning agent reacting with the collage increases as the offer increases and the shrinkage temperature of the leather rises greatly. The change of the shrinkage temperature of the leather is less when the offer of SL is 6%-10%, which show that the amino groups of the fiber collage almost entirely react with SL. Therefore the optimal offer of SL is 5% based on the weight of bated pelt. The shrinkage temperature of the leather is 85.7°C, whose color is white and has fine grain.

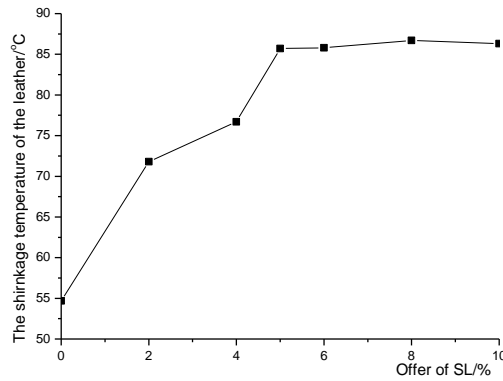


Fig. 3. Relation between the shrinkage temperature of the leather tanned by SL and its offer.

The properties of de-tanning resistance of SL-tanned wet white leather during washing with water and acid solution are shown in Fig 4. The shrinkage temperature of the SL-tanned leather has no change after it is washed with water, which show that the SL-tanned leather has good de-tanning resistance in the water. In addition, the shrinkage temperature of the SL-tanned leather is affected to a certain extent by acid solution with different pH. The change of the shrinkage temperature of the SL-tanned leather low when the pH of acid solution is changed from 5.5 to 2.5. But the range of the change of the shrinkage temperature of the SL-tanned leather less, which shown that the SL-tanned leather has good de-tanning resistance in the acid solution.

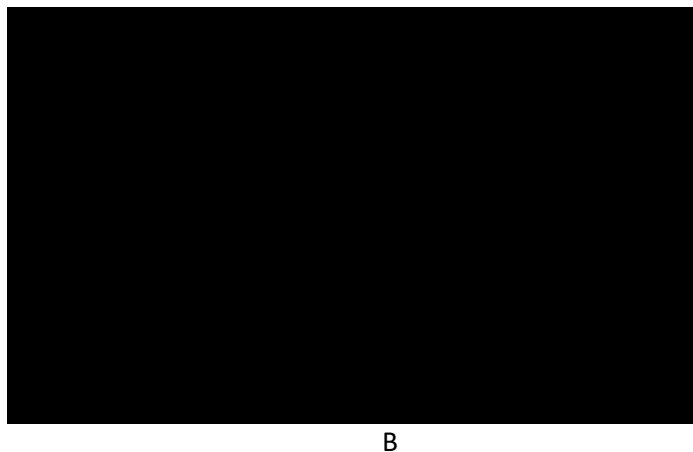
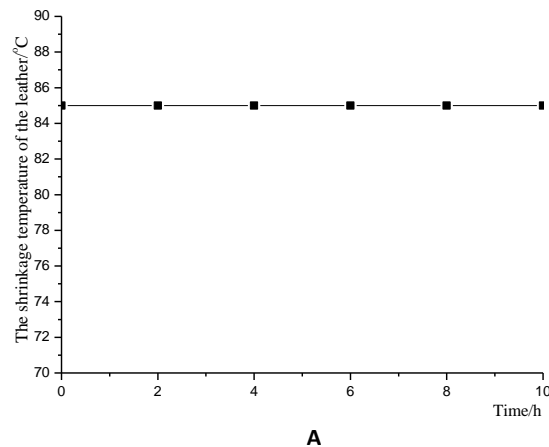


Fig. 4. The properties of de-tanning resistance of SL-tanned wet white leather during washing with water and acid solution (A: washing with water for different time B: washing with acid solution of different pH).

3.2 Optimum the initial pH of Chrome tanning agent in shaved wet white

The chrome-tanned effect of the shaved SL-tanned wet white under the different initial pH is shown in Table 7. The initial pH of float and wet white can affect the time of penetration of Chrome tanning agent, the shrinkage temperature and the state of Leather. The time of penetration of Chrome tanning agent increases along with the rise of pH of float. The reason is maybe that the more carboxyl group is transformed to ionic state and fixed with Chrome tanning agent under the condition of higher pH so as to penetrate slowly in the wet white. In addition the shrinkage temperature of Leather increases along with the rise of pH of float, which higher than 95°C. The color and the grain of Leather are from light blue to dark blue, from fine to coarse. So the initial pH of float is 3.5 based on the effect of tanning.

Table 7. The chrome-tanned effect of the shaved SL-tanned wet white under the different initial pH.

Initial pH	Time of penetration/h	Ts/°C	Color of Leather	State of Grain
2.5	2	100	Light blue	fine
3.0	2	103	Light blue	fine
3.5	2.5	105.5	Blue	fine
4.0	2.5	106	Dark blue	Coarse
4.5	3	108.5	Dark blue	Coarse
5.5	3	109.6	Dark blue	Coarse

3.3 Optimum the offer of Chrome tanning agent in shaved wet white

The chrome-tanned effect of the shaved SL-tanned wet white under the different offer of Chrome tanning agent is shown in Table 8. The offer of Chrome tanning agent can affect the time of penetration of Chrome tanning agent, the shrinkage temperature and the state of Leather. The time of penetration of Chrome tanning agent decreases along with the offer of Chrome tanning agent. The shrinkage temperature of Leather increases along with the rise of the offer of Chrome tanning agent, which higher than 95°C. But the color of Leather are from light blue to dark blue, which maybe that more Chrome tanning agent is fixed on the surface of Leather so as to darker than before. In addition, the absorption level of Chromium decreases along with the rise of the offer of Chrome tanning agent so as to the rise of the content of Cr₂O₃ of the effluent. So the offer of Chrome tanning agent is 3-4% based on the effect of tanning including the shrinkage temperature and the state of Leather, the content of Cr₂O₃ of the effluent and Absorption level.

Table 8. The chrome-tanned effect of the shaved SL-tanned wet white under the different offer of Chrome tanning agent.

Offer of the Chrome tanning agent/wt%	Time of penetration/h	Ts/°C	Color of Leather	Content of Cr ₂ O ₃ in the effluent/mg/L	Absorption Level/%
2	2.5	96	Light blue	48	98
3	2	100	Light blue	145	96
4	2	103	Blue	225	95.3
5	1.5	104.8	Dark blue	384	93.6
6	1.5	108	Dark blue	554	92.3

3.4 Optimum the offer of the poly-carboxylate auxiliary agent PAA in less-chrome tanning of shaved wet white

Effect of different offer of the poly-carboxylate auxiliary agent PAA on less-chrome tanning was shown in Table 9. The trends of the absorption level of Chromium is from increase to decrease along with the

rise of the offer of the poly-carboxylate auxiliary agent PAA, that is, the absorption level of Chromium increase in the range of 0 and 2%, but the absorption level of Chromium decrease when the offer of the poly-carboxylate auxiliary agent PAA is bigger than 2%. In addition, the time of penetration of Chrome tanning agent and the state of Leather are also affected based on the offer of the poly-carboxylate auxiliary agent PAA. Therefore the optimal offer of the poly-carboxylate auxiliary agent PAA is 1.5-2%.

Table 9. Effect of different offer of the poly-carboxylate auxiliary agent PAA on less-chrome tanning.

Offer of PAA/wt%	Time of penetration/h	Color of Leather	Content of Cr ₂ O ₃ in the effluent/mg/L	Absorption Level/%	State of Grain
0	2	blue	225	95.3	fine
0.5	2	blue	190	96	fine
1.0	2	blue	134.5	97.2	fine
1.5	2	blue	67.0	98.6	fine
2.0	2.0	Dark blue	96	98	Coarse
2.5	2.5	Dark blue	182.2	96.2	Coarse

3.5 Comparison chrome-less tannage and traditional chrome tanning

The status of the leathers tanned by chrome-less tannage and traditional chrome tanning is shown in Table 10. Both of the shrinkage temperature of Leathers are above 95°C. The leather has a fine grain, good softness and fullness. The offer of Chrome tanning agent in chrome-less tannage less than that of traditional chrome tanning. In addition, the absorption level of Chromium is up to 98% so that the content of Cr₂O₃ in the effluent also less than that of traditional chrome tanning. Furthermore the content of Cl⁻ is zero in the effluent so as to reduce the pollution of the content of chloride ion.

The scanning electron micrographs of sections of the leather samples are presented in Figure 8. The fiber bundles of the leather tanned by less-chrome tannage are well dispersed, which is on a par with the one of the leather tanned by traditional chrome tanning.

3.6 The properties of Leather tanned by less-chrome tannage from Piolt production

Sixty pieces of bated bovine pelt were tanned by the less-chrome tannage in the tannery. The properties of Leathers are shown in Table 11. The shrinkage temperature, the content of Cr₂O₃ in the effluent, the absorption of Chrome tanning agent softness and state of the leathers are satisfied and equal to that of traditional chrome tanning.

Table 10. The properties of Leathers tanned by less-chrome tannage and traditional chrome tanning.

Item	Leather tanned by less-chrome tannage	Leather tanned by traditional chrome tanning
T _s /°C	103	105
Color of Leather	Blue	Blue
Content of Cr ₂ O ₃ in the effluent/mg/L	67	1200
Absorption level/%	98.6	75
State of Grain	Fine	Fine
Offer of Chrome tanning agent/%	4 (based on the weight of Shaved wet white)	6 (based on the weight of limed split)
Content of Cl ⁻ in the effluent /mg/L	0	4000
Fullness	Full	Full
Softness	6.0	6.0
absorption of dyestuff/%	99.5	96
absorption of fat-liquor/%	82.5	85

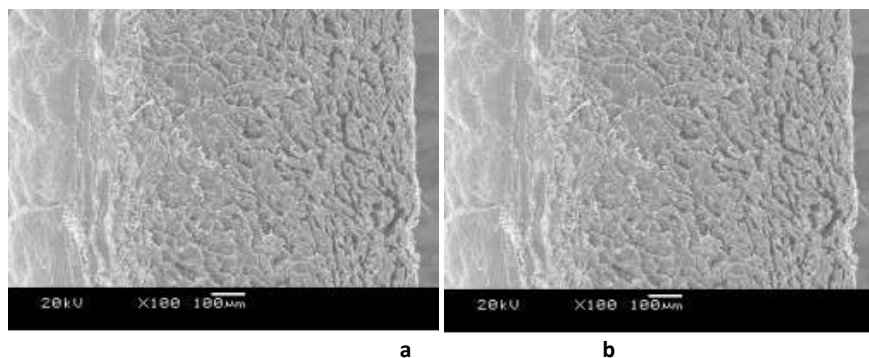


Fig. 8. Scanning Electron Microscopic photograph ($\times 100$ magnification) of the leathers tanned by less-chrome tannage and traditional chrome tanning (a: The leathers tanned by less-chrome tannage ; b: the leathers tanned by traditional chrome tanning).

Table 11. The properties of Leathers tanned by less-chrome tannage from Pilot production.

Item	Leather tanned by less-chrome tannage
Offer of Chrome tanning agent/%	4 (based on the weight of Shaved wet white)
T _s /°C	105
Color of Leather	Light blue
Fullness	Full
Softness	6.2
State of Grain	Fine
Content of Cr ₂ O ₃ in the effluent/mg/L	65
Absorption level/%	98.8
Content of Cl ⁻ in the effluent /mg/L	0

4 Conclusions

A non-pickling, chrome-less tanning technology was developed. The novel Chrome-free agent SL can be directly employed to tan bated bovine hide and the wet white was obtained. The shrinkage temperature of the wet white tanned by SL reached over 80°C and has good de-tanning resistance in water and the acid solution.

The shaved wet white was pre-treated by 1.5-2wt% Poly-carboxylate auxiliary agent and tanned by chrome powder. The better chrome-less tanning conditions were that the wet white was tanned by 3-4wt% chromium powder for 150~180min at room temperature when the initial pH value was 3.0-3.5. The next processes were same as traditional chrome tannage. Meanwhile, the shrinkage temperature of the leather tanned by the chrome-less tannage reached more than 95°C, the absorption of chromium was 98%, the content of Cr₂O₃ in the effluent was under 200mg/L. For the chrome-less tanned leather, the absorption of dyestuff, fat-liquor reached 99.5%, 82.5% respectively. Compared with the traditional chrome tanned process, not only the conventional pickling process was eliminated, the process was been shorten and reduce the pollution of sodium chloride, but it can reduce 50% of the consumption of Chrome powder, improve the absorption of chromium and can reduce content of Cr₂O₃ in effluent.

Acknowledgment

The authors would like to acknowledge the financial support of Key Laboratory of Textile Material Manufacturing and Processing of Zhejiang Province (Project number: MTC2014-005), and the help of Zhejiang Ruixing Leather, Co., Ltd.

References

1. Covington A D. *Theory and mechanism of tanning: present thinking and future implications for industry*, J. Soc. Leather. Technol. Chem. 2001, 85, 24.
2. Luo Jianxun, Lan Zhenchuan, Li Shuqing, et al. *The Current Situation and Difficult of the Clean Production of Leather-making*. *Leather Science and Engineering*, 2007, 17(3):50-55.
3. Qiang Xihuai, Shen Yiding , Yuan Jingxia. *The study about amine resin-aldehyde-chrome combination tannage*. *China Leather*, 2002, 31(13):1-3.
4. Luan Shifang, Shi Bi, Fan Haojun, et al. *Influence of poly-functional groups in the polymer auxiliary for chrome tanning on exhaustion of chrome and leather performance*. *China Leather*, 2003, 32 (21):24-28.
5. LIANG Yong-xian, WEN Hui-tao, YANG Yi-qing, et al. *Discussion on Production Technology of Less-chrome Tanning Cattle Shoe Upper Leather*. *West Leather*, 2018, 40(3): 50-55.
6. Sreeram K J, Aravindhan R, Rao JR, et al. *Mixed metal complexes of zirconium: A step towards reducing usage of chromium in tanning*, *Journal of the American Leather Chemists Association*, 2004, 99(3):110-118.
7. Zeng Shaoyu, Shi Bi, He Youjie, et al. *The Production of Goat Garment Leather by Chrome-free or Chrome Reduced Tannage*. *China Leather*, 1997, 26(5):3-5.
8. Luo Jianxun, Feng Yanjuan. *Cleaner processing of bovine wet white: synthesis and application of a novel chrome-free tanning agent based on an amphoteric organic compound*. *J.Soc. Leather. Technol. Chem*, 2015, 99(4):190-196.
9. Covington, A.D., *Modern tanning chemistry*. *Chem. Soc. Rev.*, 1997, 26, 111.
10. Xu Jiali, Luo Jianxun. *Synthesis and application of a polycarboxylate auxiliary agent*. *China Leather*, 2017, 46(3):35-41.
11. IUP 2, Sampling, *J.Soc. Leather Technol. Chem.*, 2000, 84, 303.

REVIEW OF THE SCIENTIFIC AND TECHNOLOGICAL LITERATURE OF FUNGICIDES IN TANNERY INDUSTRY: REDUCING THE USE AND INCREASING THE EFFICIENCY OF FUNGICIDES IN THE LEATHER INDUSTRY

Zulfe Urbano Biehl ¹

¹(1 ATC S/A Tannery Chemicals - Research and Development Department.

Av. Brasil, 3040 ,Bela Vista Zip Code 93600-000, Estância Velha - RS - BRAZIL

a)Corresponding author: zulfe@atcdobrasil.com.br

Abstract. One of the main challenges of the tannery industry chain is to reduce the use of biocides and restricted substances and at the same time increase efficiency with the available products. Such conduct must permeate suppliers and the tanneries in order to obtain better results, diminish the biocide resistance dissemination, optimize costs and be ecologically friendly. In this sense, we present herein an updated review and discussion of the scientific and technological literature on the aspects involving the action of fungicides in tannery industry and how the application of this knowledge can reduce application of biocides and restricted substances in the tanning process. We have organized a review by consulting the databases PUBMED, Web of Science, Science direct, and all literature with excellence scientific support available. The review focused on: (i) Fungal diversity involved in wet-blue biodeterioration; (ii) Mechanisms of action of fungicides; (iii) Fungicide combinations to enhance activity; (iv) Fungal mechanisms of resistance and the known causes of resistance emergence. As a result of this study we are able to track the fungal phylogenetics (and relationship) responsible for leather biodeterioration enabling a guiding strategy for fungal biocide application. Moreover, understanding of the mechanisms of action and interaction between molecules can determines the extent of the biocides inhibitory effect in different fungal species. Fungicide effect could vary, and such information corroborates with the idea that even in the same species the interaction of the different molecules may vary, possibly due to variation in cytochrome protein. For example, the most accepted mechanism of action of *azoles* is the inhibition of synthesis of or direct interaction with ergosterol (present in all fungi). Considering that the target is always the same, a question arise, how do the distinct *azoles* present different activities upon fungal strains? As result of this study we show that structural differences will influence the higher or lower interaction of the azole functional group and consequently the activity. The appropriated knowledge of the mechanisms by which microbial cells might develop resistance, highlights the need for an improved understanding of the reasons for their emergence and greater attention to methods that can be used to prevent and control them. In this sense, a successful combination of biocide molecules enhances a synergetic effect, avoiding fungal mechanisms of resistance and reduces dosage of each compound, being effective against a variety of fungi.

1 Introduction

Leather is a biological product suitable to microbial growth due to the presence of proteins and lipids. Additionally, tanneries provide an interesting environment for microbiological development, since there are sources of nutrients and water along the complete process (**Fig. 1**). Particularly pickled pelts, wet-blues and vegetable tanned moist leathers are prone to microbial attack, even when stored or shipped^{1,2}.

After chrome or vegetable tanning, leathers and finished leathers contain several compounds, such as ammonium salts, phosphates, surfactants, fat liquoring agents and other organic agents enabling microbial - especially fungal growth causing damages on leather matter.

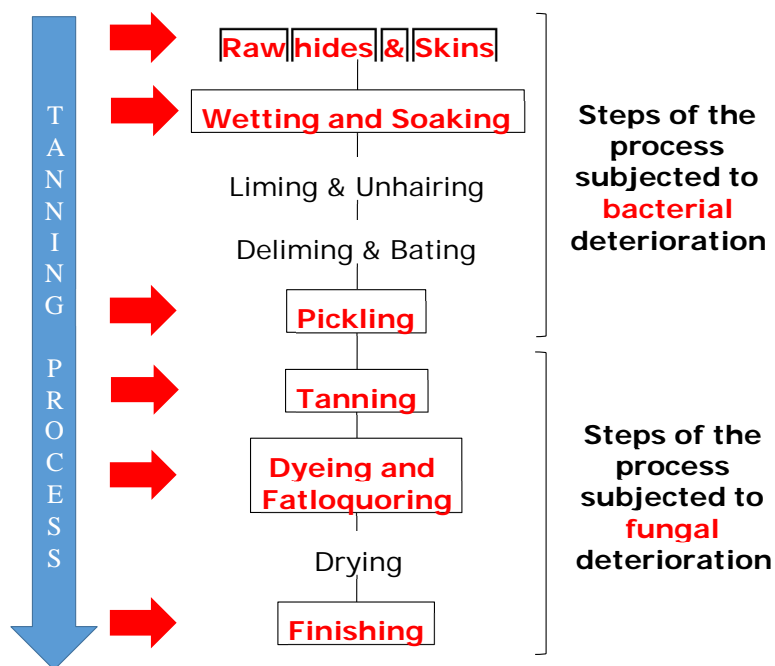


Fig. 1. General tanning process fluxogram. In red all steps in which is possible to use biocides.

2 Methods

The review presented herein was organized by consulting the databases PUBMED (PubMed comprises more than 29 million citations for biomedical literature from MEDLINE, life science journals, and online books), Web of Science, (a platform with more than 9,200 titles journals) and ScienceDirect (the world's leading source for scientific, technical, and medical research), and all literature with excellence scientific support available in books and internet.

3 Results

3.1 Environmental Conditions for Fungal Proliferation in Tanneries and Fungal Diversity Involved in Wet-blue Biodeterioration

Besides the fact that hides and leather are suitable substrates for microbial proliferation, other variables may directly influence the growth of fungi as well as bacteria. In this sense, some steps of the process could be cited as major problems which favor fungal growth:

- Tanning processes with quality deviations mainly related to insufficient degreasing and the presence of reducers compounds;
- Longer storage time than the half live of most of the fungicides;
- Poor storage conditions, with non-appropriated cleaning disinfection routines;
- Poorly controlled drying operations, where the humidity remains high or the drying process takes too long;
- Poor airflow;
- High temperatures inside the drying rooms.

Environmental conditions also have an influence on fungal diversity in leather contamination. Temperature, for example, directly impacts fungal growth. As we can observe in **Fig. 2** *Penicillium* sp. and *Scopulariopsis* sp. hardly grow in temperatures above 28 °C and most of fungi are not able to grow appropriately in temperatures around 45 °C². In this sense, it is important to highlight that at 45 °C fungi are not necessarily dead, even though there is no colony growth. In this case (and on other stressful conditions) most fungi are able to generate spores, which are the most resistant form of fungi in nature. Then, when environmental conditions are favorable again, they can grow as usual.

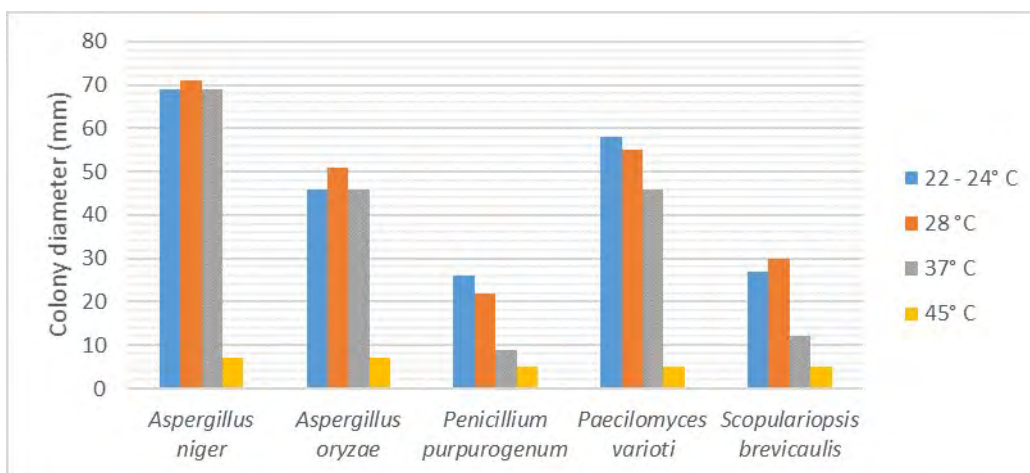


Fig. 2. Temperature influence in fungal growth. Adapted from 2.

Regarding the prejudices caused by fungal contamination diversity, the literature converges always to the same genera: *Alternaria*, *Aspergillus*, *Mucor*, *Rhizopus*, *Paecilomyces*, *Penicillium* and *Trichoderma*. Among them, many distinct species may appear, as indicated by different authors in the **Table 1**. On the other hand, no convergence is found on which is the most common fungi in general leather contamination. Some authors point out *Trichoderma* spp. as the most frequent³ while others indicate *Aspergillus niger* as well as various species of *Penicillium*⁴. Other genera also are cited, such as *Cephalosporium*, *Cladosporium*, *Curvularia*, *Fusarium*, *Scopulariopsis* and *Verticillium*, but they are not commonly found on all types of leather samples^{1,5,6}.

Table 1. List of fungi reported by distinct authors as source of damage in wet-blue leathers.

Most common fungi reported as agents of leather damage		Reference
<i>Aspergillus</i> sp.	<i>Penicillium</i> sp.	3
<i>Mucor</i> sp.	<i>Rhizopus nigricans</i>	
<i>Paecilomyces variotii</i>	<i>Trichoderma viride</i>	
<i>Aspergillus niger</i>	<i>Penicillium</i> sp.	7
<i>Aspergillus terreus</i>	<i>Trichoderma atroviride</i>	
<i>Paecilomyces nivea</i>	<i>Trichoderma harzianum</i>	
<i>Alternaria alternata</i>	<i>Paecilomyces variotii</i>	2
<i>Aspergillus niger</i>	<i>Penicillium commune</i>	
<i>Aspergillus oryzae</i>	<i>Penicillium duclauxii</i>	
<i>Aspergillus wentii</i>	<i>Penicillium glabrum</i>	
<i>Aspergillus versicolor</i>	<i>Penicillium ochrochloron</i>	
<i>Aureobasidium pullulans</i>	<i>Penicillium purpurogenum</i>	
<i>Chaetomium globosum</i>	<i>Penicillium rubrum</i>	
<i>Cladosporium herbarum</i>	<i>Penicillium verrucosum</i>	
<i>Cladosporium sphaerospermum</i>	<i>Scopulariopsis brevicaulis</i>	

<i>Fusarium chlamydosporum</i> <i>Myrothecium verrucaria</i>	<i>Trichoderma viride</i> <i>Verticillium tenerum</i>	
<i>Alternaria geophila</i> <i>Aspergillus niger</i> <i>Aspergillus chevalieri</i> <i>Aspergillus fumigatus</i> <i>Aspergillus conicus</i> <i>Aspergillus flavus</i> <i>Aspergillus terreus</i> <i>Aspergillus repens</i> <i>Aspergillus sulphureus</i> <i>Aspergillus tamari</i> <i>Aspergillus luchuensis</i> <i>Aspergillus amstelodami</i> <i>Aspergillus sydowii</i> <i>Botrytis cinerea</i> <i>Cladosporium herbarum</i> <i>Chaetomium globosum</i>	<i>Curvularia luneta</i> <i>Drechslera papendorfii</i> <i>Fusarium</i> sp. <i>Helminthosporium</i> sp. <i>Mucor ambiguus</i> <i>Paecilomyces varioti</i> <i>Penicillium asperum</i> <i>Penicillium camemberti</i> <i>Penicillium citrinum</i> <i>Penicillium funiculosum</i> <i>Penicillium oxalicum</i> <i>Penicillium purpurogenum</i> <i>Penicillium stipitatum</i> <i>Rhizopus nigricans</i> <i>Rhizopus oryzae</i> <i>Trichoderma lignorum</i>	4
<i>Aspergillus niger</i> <i>Aureobasidium pullulans</i> <i>Chaetomium globosum</i> <i>Cladosporium</i> sp. <i>Fusarium</i> sp. <i>Mucor</i> sp.	<i>Paecilomyces</i> sp. <i>Penicillium funiculosum</i> <i>Rhizopus stolonifer</i> <i>Trichoderma viride</i>	8
<i>Aspergillus</i> sp. <i>Mucor</i> sp. <i>Paecilomyces variotii</i> <i>Penicillium</i> sp.	<i>Rhizopus nigricans</i> <i>Trichoderma viride</i>	9

3.2 Mechanisms of Action of Fungicides

The tannery industry applies biocides along its production process chain in order to avoid leather damage due to fungal contamination. In summary, **Fig. 3** schematically represents the mechanisms of action of the fungicides most commonly used in this industry sector.

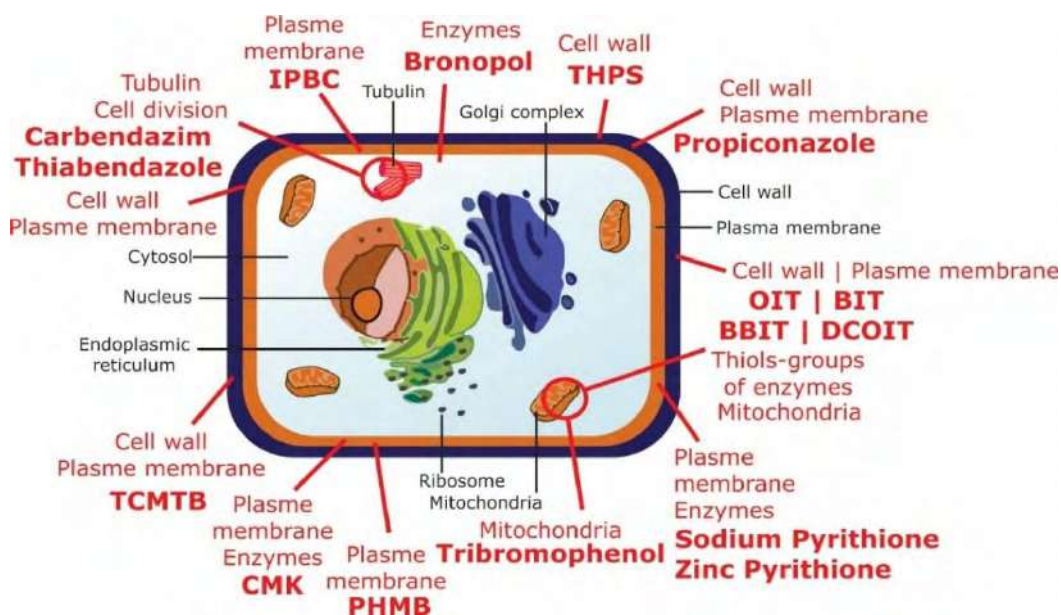


Fig. 3. Summary of the mechanisms of action of the main fungicides used in tannery industry.

In order to clarify the mechanisms of action of fungicides mentioned in **Fig. 03**, we present below an overview of the known fungal growth inhibition pathways may responsible for the biological activity of these biocides.

3.2.1 Azole compounds – mechanism of action

The use of AZOLE compounds as fungicides appeared as an important alternative to the use of amphotericin B, in the 1980's. Azoles, as well as polyenes and allylamine/thiocarbamates, are nowadays the three major groups of antifungal agents in use.

The most accepted mechanism of action of AZOLES, (including TCMTB, propiconazole, carbendazim, OIT, BIT, BBIT, DCOIT and also thiabendazole) is based on the inhibition of ergosterol biosynthesis or on the direct interaction of azole compounds with it. Ergosterol is a key molecule in fungi, since it serves as a bioregulator of membrane fluidity and integrity. (**Fig. 04**). Importantly, even though cell wall components may drastically vary among species, ergosterol is a molecule found on all fungi cell membranes, despite fungal genus (**Fig. 05**). That is why azole compounds usually have a broad spectrum of activity.

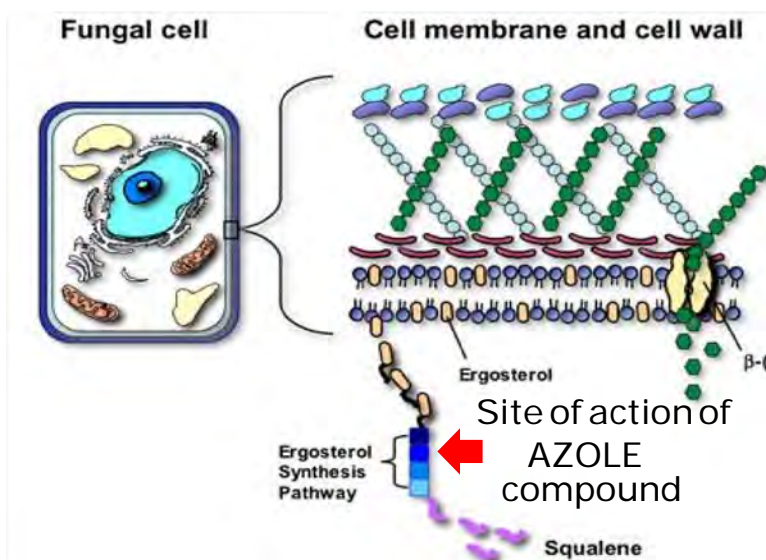


Fig. 4. Schematic representation of the mechanism of action of azole compounds. Red arrow indicates the target of azole compounds (adapted from 10).

However, considering that the target is always the same, a question may arise: *how do the distinct AZOLES exert different activities upon fungal strains?*

The primary target of azoles is the *heme* protein, which cocatalyzes cytochrome P-450dependent 14 α -demethylation of lanosterol (**Fig. 06**). Inhibition of 14 α -demethylase leads to depletion of ergosterol and accumulation of sterol precursors, including 14 α -methylated sterols (lanosterol, 4,14-dimethylzymosterol, and 24-methylenedihydrolanosterol), resulting in the formation of a membrane with altered structure and function.

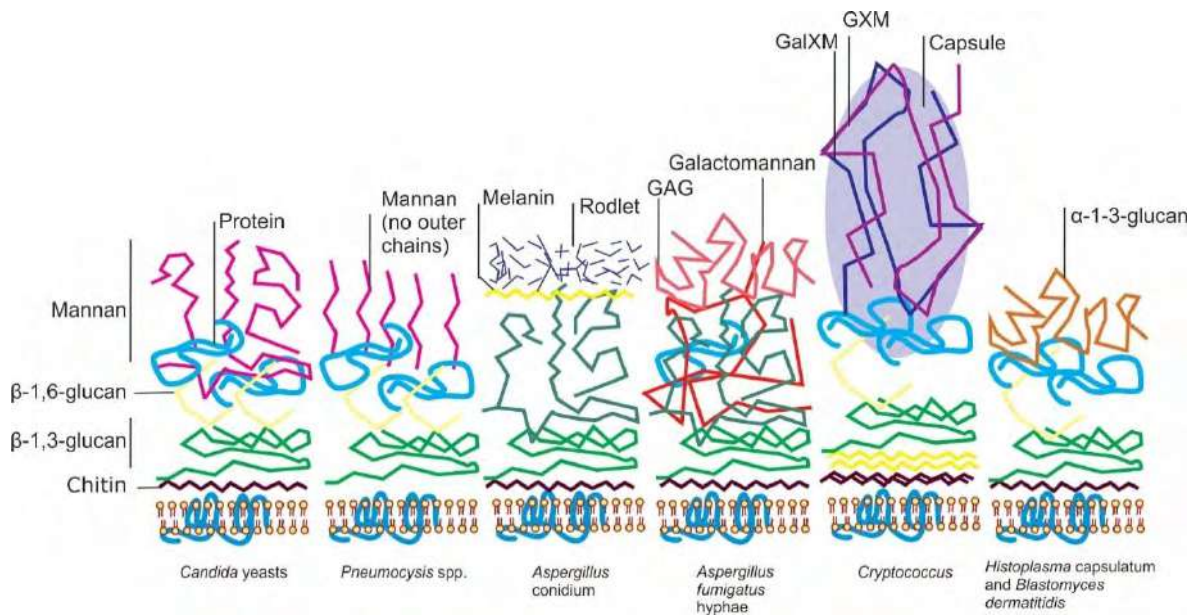


Fig. 5. Representation of the possible variation of the fungal cell wall in distinct genera (adapted from 11).

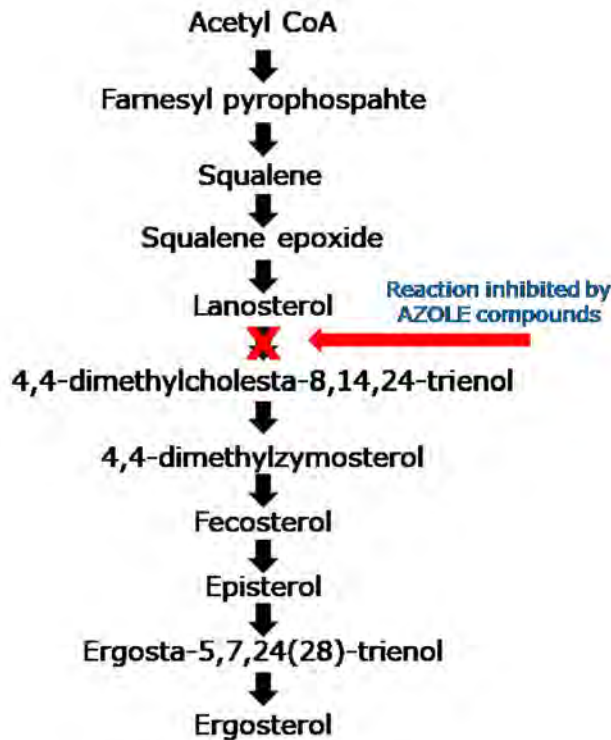


Fig. 6. Synthesis of ergosterol. Red arrow indicates the step which azole compounds are capable to inhibit.

Although contemporary azole antifungals are 14 α -demethylase inhibitors, there is a heterogeneity of action among them. The main azole target, *cytochrome P450*, catalyses the oxidative removal of the 14 α -methyl group of lanosterol and/or eburicol in fungi by a typical P450 mono-oxygenase activity. This protein contains an iron protoporphyrin moiety located at the active site, and the antifungal azoles bind to the iron atom via a nitrogen atom. Therefore, the azole molecule binds to the protein in a manner dependent on the individual azole's structure (Fig. 07).

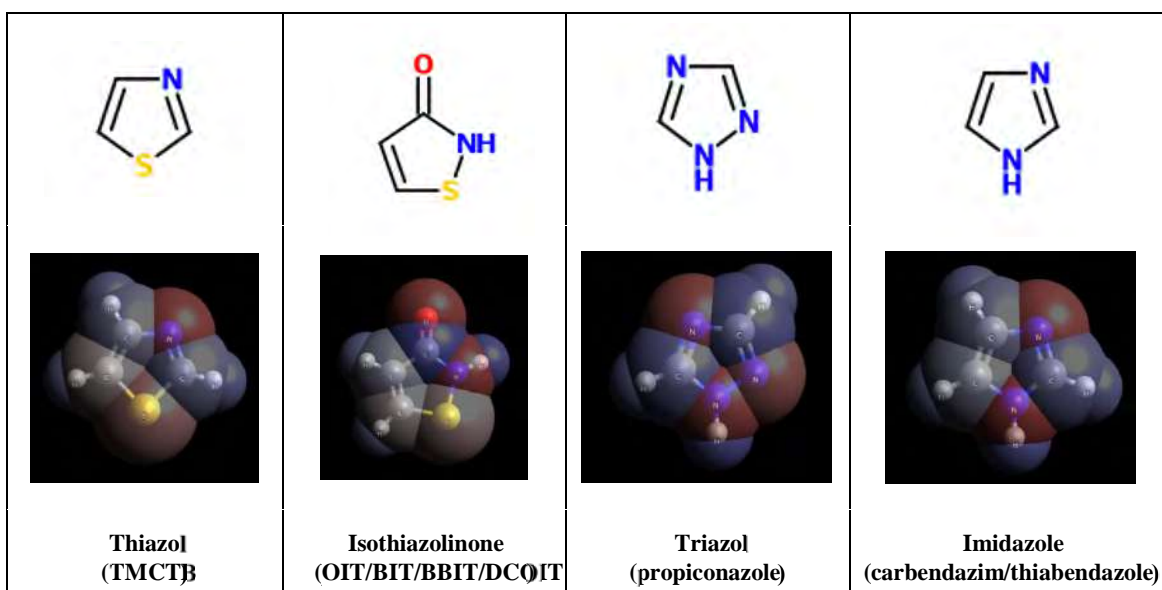


Fig. 7. Synthesis of ergosterol. Red arrow indicates the step which azole compounds are capable to inhibit.

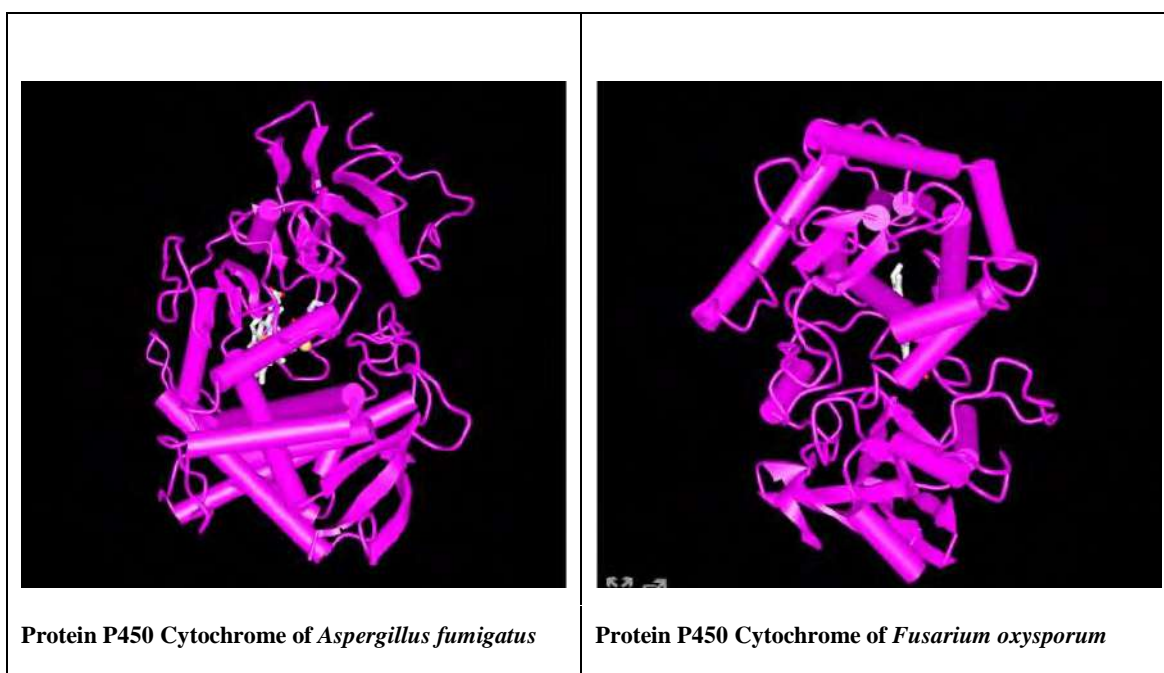


Fig. 8. Representation of the P450 Cytochrome protein of two fungal species, possessing remarkable differences which directs interferes in the fungicide activity¹².

The exact conformation of the active site differs between fungal species and among the many mammalian P450 mono-oxygenases. Above, it is possible to observe the structural differences between the two fungal P450 cytochrome protein (Fig. 08). These differences will influence the higher or lower interaction of the azole functional group and consequently its activity. In conclusion, the precise nature of the interaction between each azole molecule and each kind of P450 determines the extent of the azole's inhibitory effect in different fungal species.

3.2.2 Isothiazolinone compounds – mechanism of action

The ISOTHIAZOLINONE chemical group comprises OIT, BIT, BBIT, DCOIT and correlated compounds that exhibit the capacity to bind thiol-groups of fungal proteins, besides the previously described ability to inhibit ergosterol biosynthesis. Most of the scientific reports mention that isothiazolinone chemical group acts on distinct proteins related to crucial Krebs cycle pathways. The Krebs cycle (or citric acid cycle) is a part of cellular respiration (**Fig. 09**). All these reactions occur inside mitochondria of all aerobic organisms.

Isothiazolone biocides inhibit specifically sulfur-containing dehydrogenase enzymes related to crucial Krebs cycle pathways, including pyruvate dehydrogenase, alpha-ketoglutarate dehydrogenase, succinate dehydrogenase, NADH dehydrogenase, lactate dehydrogenase, and alcohol dehydrogenase. The disablement of these important enzymes can result in complete inhibition of critical metabolic functions concerned with energy generation and cell growth. Moreover, isothiazolone biocides are known to react with nucleophilic materials and proteins thiols, inactivating them. Thiol-active sites are common to dehydrogenase enzymes and other proteins^{13,16}.

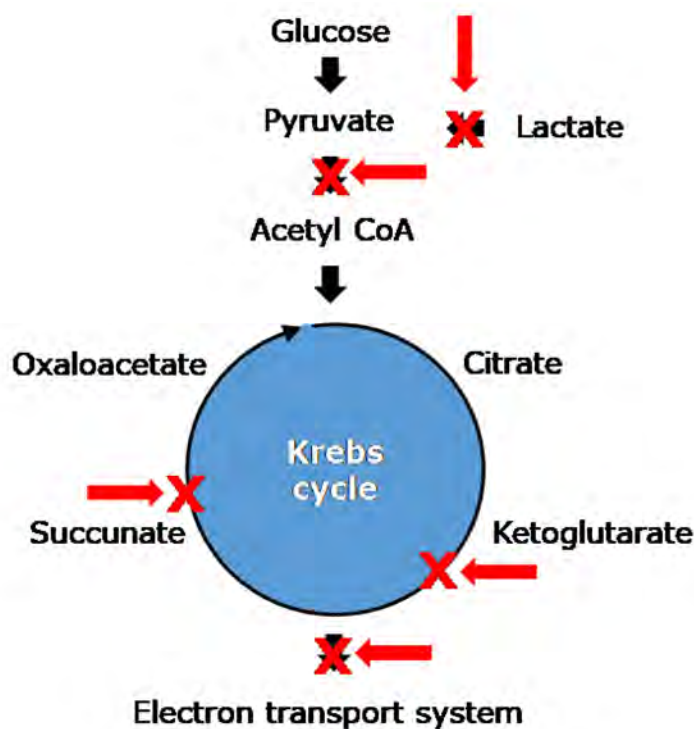


Fig. 9. Representative scheme of action of OIT upon Krebs cycle pathways.

3.2.3 Imidazole compounds – mechanism of action

Carbendazim and thiabendazole exert their biological activity by binding to tubulin proteins. Tubulin is a major component of the eukaryotic cytoskeleton which is involved in structural support, intracellular transport and DNA segregation. The action of imidazole compounds disrupts microtubule assembly, preventing appropriated cell division, and thus resulting in the malsegregation of chromosomes during cell division (**Fig. 10**).

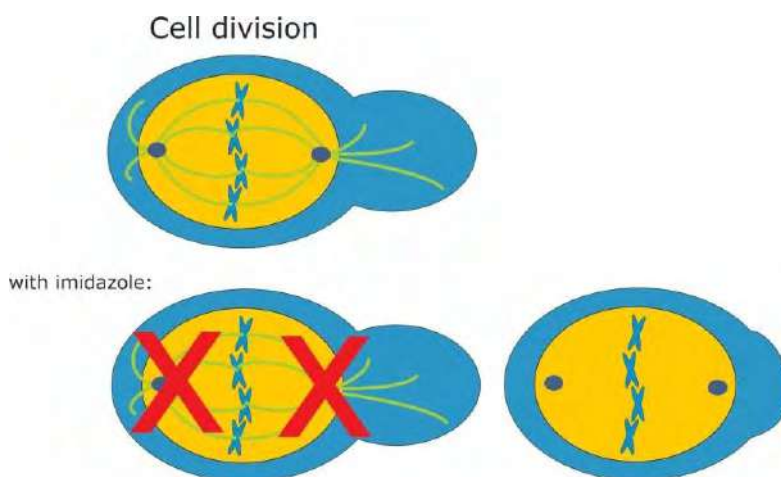


Fig. 10. Fungal cell division process. Up is the normal process and bottom the process being interfered by the fungicide carbendazim.

3.2.4 CMK – mechanism of action

CMK (4-chloro-3-cresol) acts specifically on the cell membrane and inactivates intracytoplasm enzymes by forming unstable complexes. The lipophilic molecules are trapped by the membrane phospholipids. The following processes are involved (**Fig. 11**):

- If CMK concentration is low, the cell constituents (nucleic acids, glutamic acid) are liberated in the external media.
- If CMK concentration is high, the disinfectants inhibit permeases, thus causing denaturation of the proteins and lysis of the cell membrane¹⁴.

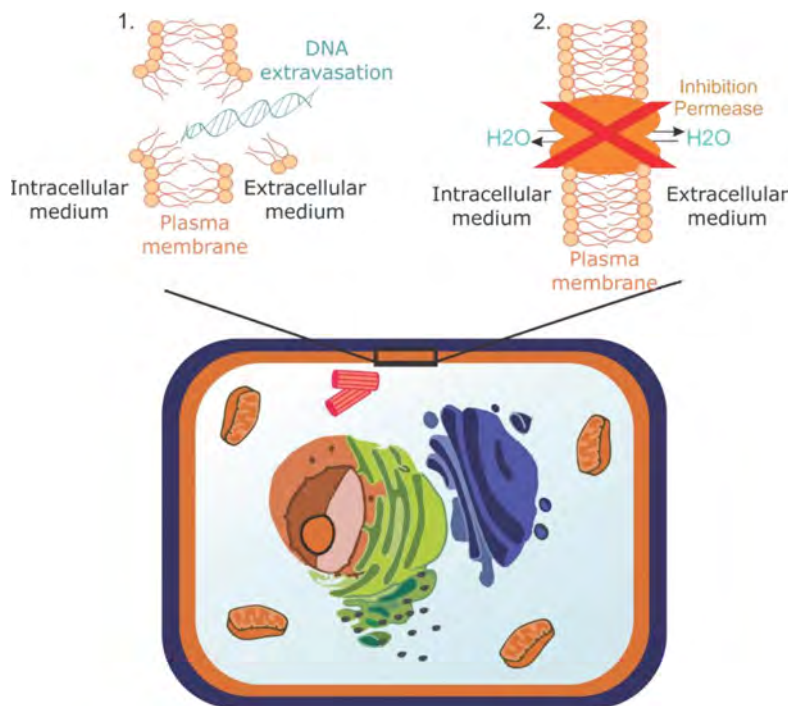


Fig. 11. Representation of the mechanism of action of CMK fungicide.

3.2.5 IPBC – mechanism of action

Carbamate fungicides, such as 3-iodo-2-propynyl butylcarbamate (IPBC), disrupt the formation of fungal cell walls by interfering with synthesis of phospholipids and fatty acids, as demonstrated in Fig. 12. They also affect mycelial growth, spore production and germination. Also, IPBC is considered an iodophore, since it is composed of iodine complexed with solubilizer, acting as "free" iodine. Therefore, this compound is corrosive to exposed membranes.

3.2.6 Pyrithione compounds – mechanism of action

Sodium Pyrithione and Zinc Pyrithione are inhibitors of fungal membrane transporters. Incubation of these compounds with Penicillium sp. resulted in decreased activity of transport systems, including those for inorganic sulfate, inorganic phosphate, glucose, L-methionine, among others. It has also been reported that pyrithione biocides are able to reduce ATP levels in fungi along with membrane depolarization (Fig. 13).

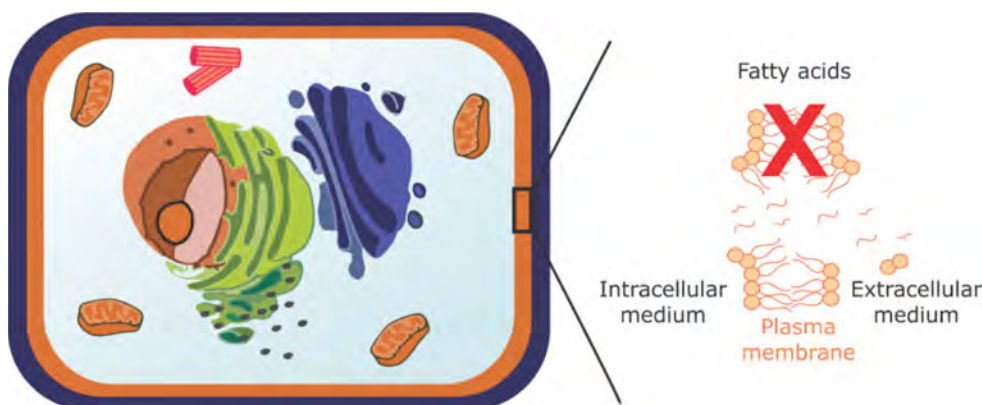


Fig. 12. Representation of the mechanism of action of IPBC fungicide.

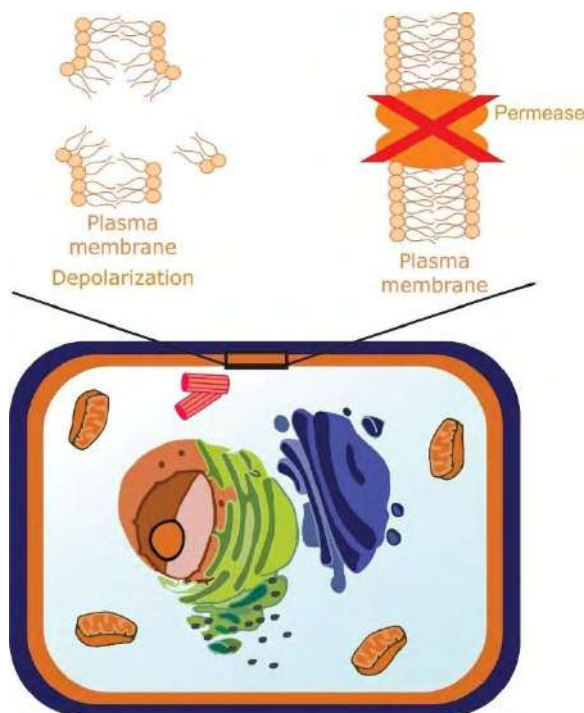


Fig. 13. Representation of Pyrithione compounds mechanism of action on fungal plasma membrane.

3.2.7 Tribromophenol – mechanism of action

Tribromophenol is the most produced brominated phenol in the world. This compound, as well as its water-soluble sodium tribromofenate salt, began to be used in Brazil approximately in 1985 as an alternative product to other oil-soluble products, such as pentachlorophenol and sodium pentachlorophenate.

The mechanism of action of pentachlorophenol and similar oleosoluble products is based on mitochondrial oxidative phosphorylation, causing acceleration in metabolism and heat production, thus resulting in loss of the membrane electrical resistance (Fig. 14).

3.2.8 THPS – mechanism of action

Tetrakis hydroxymethyl phosphonium sulfate (THPS) is a quaternary phosphonium compound. The molecule has a relatively fast mode of action and works well against various organisms, including fungi. The phosphine, THP, is responsible for its biocidal properties as it interferes with disulfide linkages in proteins, causing them to lose catalytic capacity due to the breakdown of tertiary structure. Besides, THP causes the loss of free thiol groups, leading to cell destabilization¹⁵. In addition, the sulfate reduction process within the sulfate reducing bacteria (SRB) is inhibited¹⁶. (Fig. 15).



Fig. 14. Schematic representation of Tribromophenol mechanism of action on fungal cells.

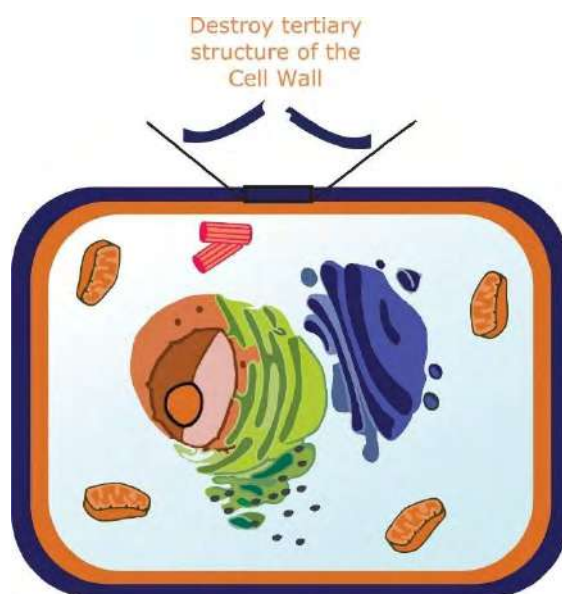


Fig. 15. Schematic representation of THPS mechanism of action on fungal cells.

3.2.9. Bronopol - mechanism of action

Bronopol has a broad spectrum of activity against all groups of bacteria, including the anaerobic sulphate reducing bacteria (SBR). On the other hand, its activity against fungi is more variable and generally higher doses are required to inhibit growth.

Anyway, under aerobic conditions, bronopol catalytically oxidizes intracellular molecules with thiol grouping, such as cysteine, using atmospheric oxygen as the oxidizing agent (**Fig. 16**). As a result, reactive oxygen species (ROS), such as superoxide and peroxide, are generated. These ROS are directly responsible for the bactericidal activity of the compound and for reduced growth rate after the bacteriostatic period.

3.2.10. PHMB – mechanism of action

Polyhexamethylene biguanide (PHMB) is a linear polymer comprised of a hydrophobic backbone with multiple cationic groupings separated by methylene chains. It is widely reported in literature that the lethal action of PHMB is due to membrane disruption and irreversible loss of essential cellular components. The molecule binds to the surface of the bacterial cell membrane and causes reorganization of the membrane in a way that prevents removal of the antimicrobial agent (**Fig. 17**)^{17,18,19}. This mode of action makes the development of microbiological resistance very unlikely. However, it has been observed that a range of bacterial species, when treated with PHMB, displayed cell division arrest and chromosome condensation, suggesting DNA binding as an alternative antimicrobial mechanism. A DNA-level mechanism was confirmed by observations that PHMB formed nanoparticles when mixed with isolated bacterial chromosomal DNA²⁰.

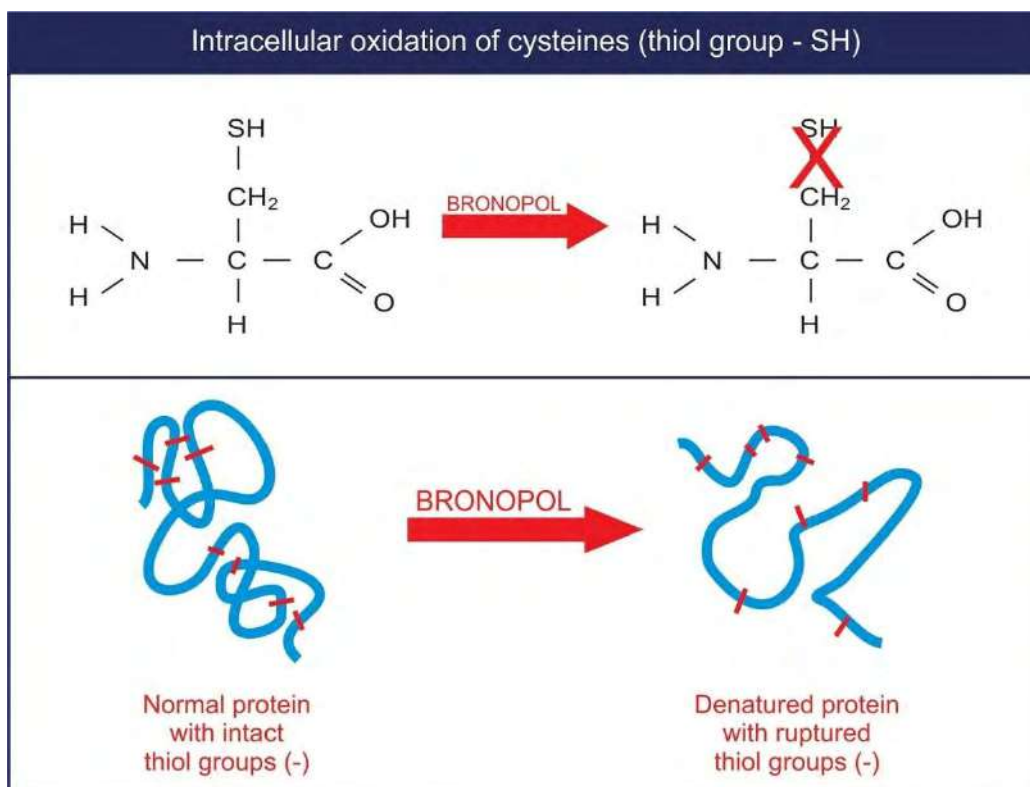


Fig. 16. Representation of Bronopol mechanism of action on intracellular molecules containing thiol grouping.

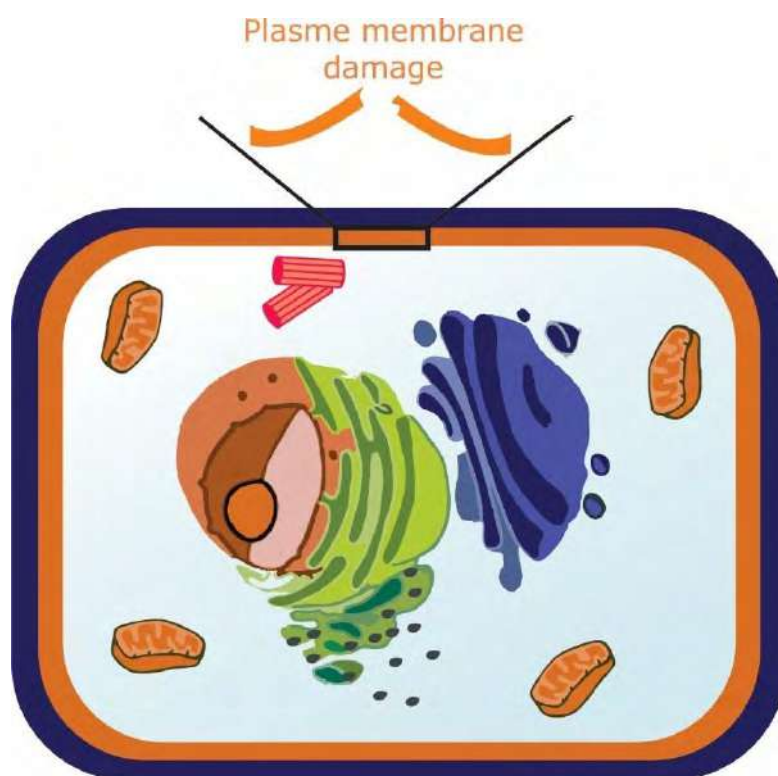


Fig. 17. Representation of PHMB mechanism of action on cellular components.

3.3 Fungal Mechanisms of Resistance and the Known Causes of Resistance Emergence

Fungicide resistance refers to change in the sensitivity of a fungi population to a fungicide. Such phenomenon provokes the failure of biocides in general. Typically, resistance can be developed in situations where the same compounds (or similar) with the same mechanism of action are used uninterruptedly. Resistance might be detected in populations or in single fungi isolates. TCMTB for example is not effective against *Trichoderma viride*, which can be brought into the tannery on the wooden pallets, and *Amorphotheca resiniae* are resistant to phenolics (CMK)⁹.

In the same way that antibiotics inhibit bacterial growth, antifungal compounds prevent fungal growth. The fact that bacterial antibiotics are no longer effective is well known; however, the antifungal resistance is an emerging phenomenon (Fig. 18). This highlights the need for an improved understanding regarding fungal resistance as well as a greater attention to methods that can be used to prevent and control them.

Some species of fungi are naturally resistant to certain types of antifungal agents. Other species may be normally susceptible to a particular type of agent, but develop resistance over time as a result of improper antifungal use - for example, dosages that are too low or treatment courses that are not long enough²².

As presented in Fig. 18, there are two possible ways to induce resistance. In this sense, it is important to highlight that sub-lethal fungicide regimen leads to further induction of genes that help resisting subsequent drug treatments. As a consequence, the population is shifted to increasing resistance, and increasing numbers of individuals with higher degrees of resistance are found. In practice, it is very important to apply right dosage indication, specially by teaching technical staff in order to avoid resistance induction.

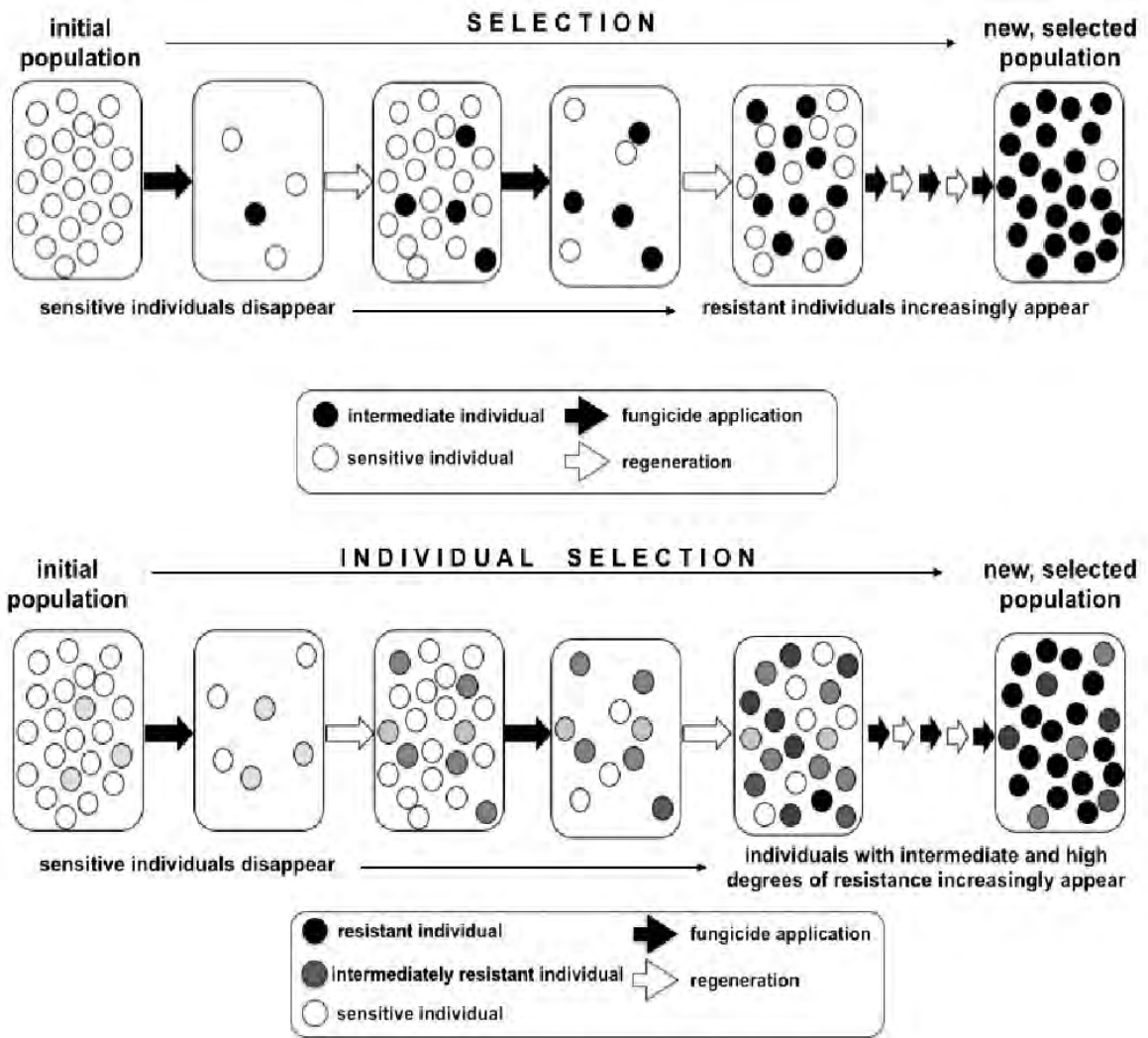


Fig. 18. Development of fungicide resistance is a selection process, with the fungicide as the selecting agent. In qualitative resistance (indicated as “selection”), mutation-based insensitive mutants are selected, and strains are either sensitive or resistant to the drug. In quantitative resistance (indicated as “individual selection”) individuals that express genes leading to reduced fungicide sensitivity, are more likely to survive a drug treatment. Adapted from 21.

Fig. 19, below, presents the seven known mechanisms of fungal resistance:

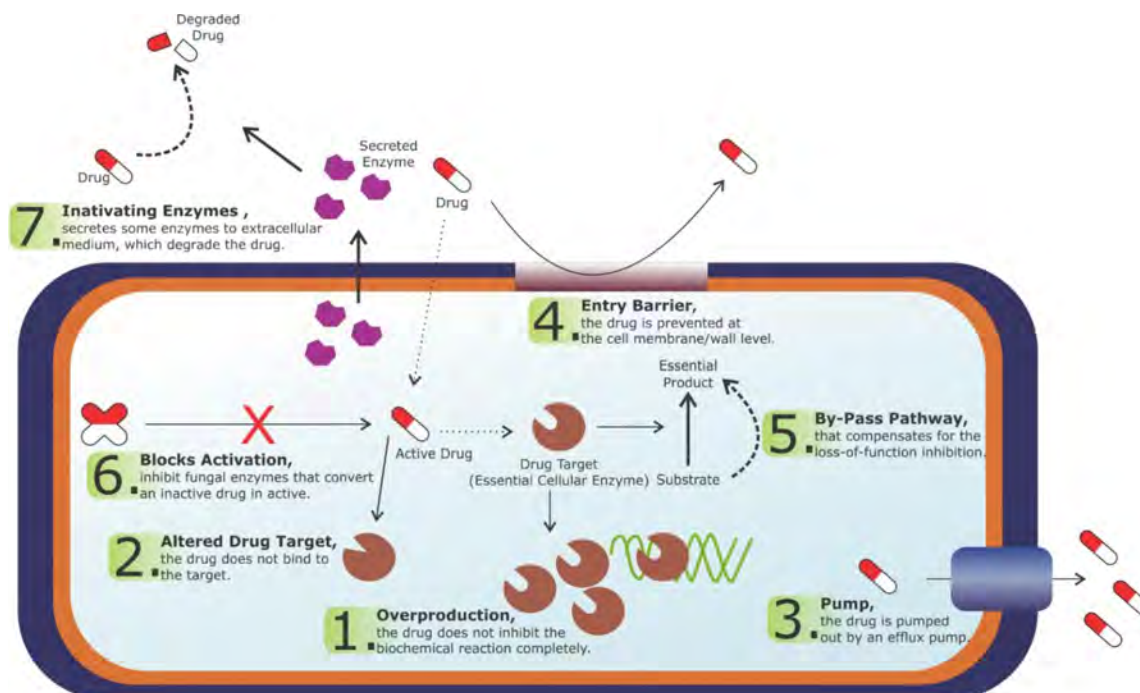


Fig. 19. Mechanisms by which microbial cells might develop resistance. 1: The target enzyme is overproduced, so that the drug does not inhibit the biochemical reaction completely; 2: The drug target is altered so that the drug cannot bind to the target; 3: The drug is pumped out by an efflux pump; 4: The entry of the drug is prevented at the cell membrane/cell wall level; 5: The cell has a bypass pathway that compensates for the loss-of-function inhibition due to the drug activity; 6: Some fungal “enzymes” that convert an inactive drug to its active form are inhibited; 7: The cell secretes some enzymes to the extracellular medium, which degrade the drug (adapted from 23).

3.4 Fungicide Combinations to Enhance Activity

Fungi can develop resistance to biocides, making commercially available fungicides less effective, as mentioned above. Assuming this growing crisis, the need of alternatives to not only diminish such emerging resistance scenario by proper use and regulations, but also new application strategies and search for new molecules is urgent.

In this sense, one of the most used strategy is the combination of distinct biocides – possessing different mechanism of action – in order to overcome resistance. The combination of bioactive compounds is meant to observe a synergetic effect – preferably in lower doses compared to single application – in so called congruous strategy. Additionally, two other strategies might be suitable: (i) syncretic, in which one of the molecules does not act on a essential target for microbe survival and (ii) coalistic, when none of the molecules combined act upon a specific essential target, but together can promote a bioactivity, as presented in **Fig. 20**, below ²⁴.

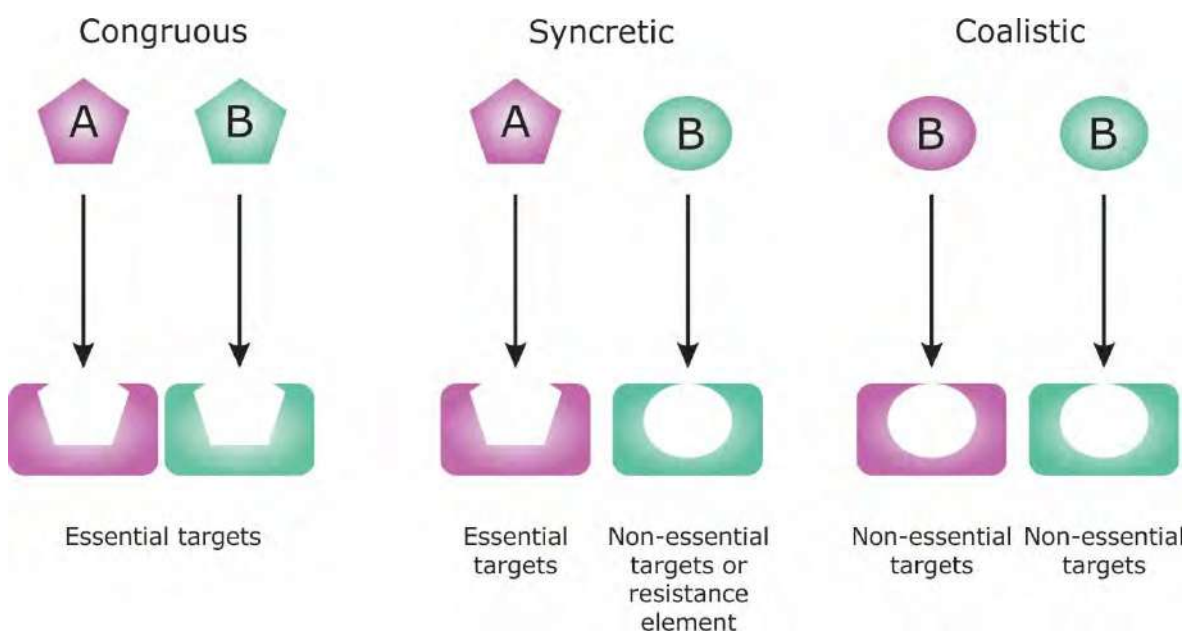


Fig. 20. Possible molecules synergic combinations in order to improve efficacy against fungal resistance.

The synergic effect and non-synergic effect (antagonism) might be calculated, in a so called fractional inhibitory concentration index (FICI). In this sense, combinations of distinct molecules that act (or not) upon a target is the new road to overcome the fungal biocide resistance. Companies are now worried in present solutions to suppress resistance by increasing efficacy. Moreover, investigations on the search for suitable fixed-dose combinations accurately formulated has to be done. Nowadays these frontiers of molecules combinations are only partially explored and it is expected that combinations of three or more molecules will be needed in order to achieve the right doses and duration.

References

1. Orlita, A.: *Biodeterioration in leather industry*, Elsevier publishing co., 1968
2. Orlita, A.: *Microbial biodeterioration of leather and its control: a review*, *International Biodeterioration & Biodegradation*, 53(3):157-163, 2004
3. Lindner & Neuber: *Preservation in the Tannery*, *International Biodeterioration*, 26, 195-203, 1990
4. Rathore et al.: *Isolation, Screening and relative capacity of fungi which causes infestation of finished leather*, *Int.J.Curr.Microbiol.App.Sci*, 2013
5. Sharma & Sharma: *Succession of mycoflora on finished leathers during storage*, *Defence science journal*, 1979
6. Stakishatite & Lugauskas: *Microscopic fungi that damage synthetic leathers and polyvinyl chloride films*, 1981
7. Zugno et al.: *Fungal Growth on Wetblue: Methods to Measure Impact on Leather Quality*, *Buckman Laboratories International*, 2011. Available at: www.aaqtc.org.ar/congresos/china2009/oralPresentation/1-2.pdf [Accessed: May 2019]
8. Paulus W.: *Directory Of Microbicides For The Protection Of Materials: A Handbook*, Kluwer Academic Publishers, 2004
9. *Journal Leather Technology Centre*. Nov/Dec, 2007.
10. *Doctor Fungus*.: Available at: <http://powersite3.com/drffungus/antifungalpharmacology/> [Accessed 8 Nov 2016]
11. Erwig & Neil: *Interactions of fungal pathogens with phagocytes*, *Nat Rev Microbiol*, 2016
12. NCBI Databank. Available at: <https://www.ncbi.nlm.nih.gov/>
13. Williams, T.M.: *The Mechanism of Action of Isothiazolone Biocides*, *NACE International*, 2007
14. Maris, P., *Modes of action of disinfectants*, *Rev Sci Tech.*, 1995.
15. Torben, L.S, Enning, D., Lee J. S.: *Microbiologically Influenced Corrosion in the Upstream Oil and Gas Industry*, p. 240, CRC Press, Taylor & Francis Group, 2017
16. Health Canada's Pest Management Regulatory Agency (PMRA): *Evaluation Report - ERC2010-02 - Tetrakis (Hydroxymethyl) Phosphonium Sulfate*, 2017. Available at: http://publications.gc.ca/collections/collection_2010/arlappmra/H113-26-2010-2-eng.pdf [Accessed: 13th May 2019]
17. Ascenzi, J.M.: *Handbook of Disinfectants and Antiseptics*. Marcel Dekker, Inc., 1996

17. Huai, W., Deng, Z., Lin, W., & Chen, Q.: Enhanced killing of *Escherichia coli* using a combination of polyhexamethylene biguanide hydrochloride and 1-bromo-3-chloro-5,5- dimethylimidazolidine-2,4-dione, *FEMS Microbiology Letters*, 2017
18. Rembe et al.: Comparing two polymeric biguanides: chemical distinction, antiseptic efficacy and cytotoxicity of polyaminopropyl biguanide and polyhexamethylene biguanide, *Journal of Medical Microbiology*, 2016
19. Chindera et al.: The antimicrobial polymer PHMB enters cells and selectively condenses bacterial chromosomes, *Scientific Reports*, 2016
20. Deising et al.: Mechanisms and Significance of Fungicide Resistance, *Braz. J. Microbiol.*, 2008
21. Chiller, T.: The Rise in Antifungal Resistance, Centers of Disease Control and Prevention. Available at: <<http://www.cdc.gov/fungal/antifungal-resistance.html>> [Accessed 05 Nov 2016]
22. Ghannoum et al.: Antifungal agents: mode of action, mechanisms of resistance, and correlation of these mechanisms with bacterial resistance, *Clin Microbiol Rev*, 1999
23. Tyers M. & Wright G.D.: Drug combinations: a strategy to extend the life of antibiotics in the 21st century, *Nat Rev Microbiol.* 2019. Smith, G. B.: Low and high impact, Academic Press, 2005

A PRAGMATIC APPROACH TOWARDS THE MANUFACTURE OF WET-WHITE LEATHERS USING A BIO-POLYMERIC TANNING SYSTEM

P. N. Kariuki^{1, 2, 3, b}, A. Yasothai^{3, 4}, G. C. Jayakumar^{2, 3} and S. V. Kanth^{2, 3, a}

¹Department of Chemistry, School of Science, Dedan Kimathi University of Technology, P.O. Box 657-10100, Nyeri, Kenya.

²Department of Leather Technology, Alagappa College of Technology, Anna University, Chennai 600 025, India.

³CSIR-Central Leather Research Institute, Adyar, Chennai 600 020, India.

⁴Department of Chemistry, College of Engineering, Anna University, Chennai 600 025, India

a)Corresponding author: swarna@clri.res.in

b)kpeterngugi@gmail.com

Abstract. Different tanning materials endow leather with varying colors observable in undyed leathers. Periodate-oxidized starch tanned leathers have a yellow tinge or light brown color and get darker with age. The color change in situ is ascribable to iodate ions that are products of the periodate oxidation reaction. Iodate ions undergo reduction to form iodine molecules that are yellow or brown in low or at higher concentrations. This study focuses on the removal of iodate ions from Dialdehyde Tapioca Starch (DTS) using a simple precipitation method. Preparation of DTS is by periodate oxidation and precipitation of iodate ions using an inorganic salt as a precipitant. The experiments for manufacturing wet-white leathers used delimed pelt and DTS (unmodified and modified) tanning agents at various percentages based on pelt weight. The percentage removal of iodate ions in modified DTS was 98%. Both unmodified and modified DTS had an aldehyde content of 70%. FT-IR analysis confirmed the aldehyde groups. Delimed pelt, DTS (Unmodified), and MDTS (modified) tanned leathers had shrinkage temperatures of 62, 80, and 82°C, respectively. The physico-mechanical properties of the leathers are comparable with the UNIDO specifications. The 'b' color value of DTS tanned leather was high at 36.6, confirming yellowing and subsequent browning of the leather. Wet-white leather tanned with MDTS had no discernible color change and affirms the effective removal of iodate ions. This study has overcome the drawback associated with periodate-oxidized starch tanning agents, viz. leather yellowing and darkening over time, considering the chemical and physico-mechanical properties of the resultant leathers.

1 Introduction

Animal skins/hides have been the predominant leather making material for centuries owing to leather's exceptional natural properties (Ockerman and Basu, 2004). Close to 90% of the 25-30% protein in the skin/hide is collagen (Kanagaraj et al., 2006). Collagen is the raw material for leather manufacture (Sizeland et al., 2015). It is thus necessary to preserve and protect the delicate protein matrix against microbial attack, chemical hydrolyzes, and thermo-mechanical stress (Krishnamoorthy et al., 2012). Plant polyphenols, metal ions, and aldehydes permanently preserve skins during tanning. Tanning is, therefore, the focal point and the basis of leather making (Kanth et al., 2009).

There is a wide range of tanning materials and techniques. Conventional chrome tanning accounts for 90% of the leather produced worldwide. Chrome tanned leather has by far the highest hydrothermal (shrinkage temperature = 110-115°C) and enzymatic stability (Covington, 2005; Liu et al., 2016). Pickled pelts use 60% of basic chromium(III) sulfate (BCS) during tanning. The remaining 40% BCS contributes to environmental pollution on release as part of the effluent (Sundar, Rao and Muralidharan, 2002; Liu et al., 2016). Chromium (whether Cr(+3) or Cr(+6)) has the distinct disadvantage of being environmentally persistent. The global leather industry discharges around 40,000 tons of BCS (Liu et al., 2016) and 548 billion liters of wastewater each year (Sathish et al., 2015). Tannery wastewater treatment is complex, as it consists of various chemical substances used in leather processing.

Attention has, therefore, shifted to the possibility of finding an alternative tanning agent with properties that most closely match those of trivalent chromium (Musa et al., 2009; Pati and

Chaudhary, 2014). Aldehyde tanning is a critical alternative that has gained prominence in the global leather industry over the years. Aldehydes, viz. aliphatic aldehydes, aldehydic agents, and dialdehydes starches are suitable for various practical applications of leather making, including tanning, retanning, and finishing. Aldehyde tanning produces high performance and thermally stable 'chrome-free' (wet white) leather with the thermal stability of around 85°C (Bowes, J. H. and Cater, 1965; Langmaier *et al.*, 2002; Sarkar, K.T. and Sorcar, 2005; Covington, 2009). Besides, aldehyde tanned leather possesses excellent properties - in particular, resistance to perspiration, a weak acid/base, and moderate washing. White tanned leather becomes whiter under sunlight and is well-suited to produce pastel shade leather. Unlike chrome tanned leather, wet-white leather is incinerable without the hazard of chromium (+6) formation and, therefore, eco-friendly. Wet-white leathers find extensive use in a wide variety of applications - such as in the manufacture of automobile seats and interiors, furniture, apparel, footwear, bags, and accessories (Alderman, 1975; Sarkar, K.T. and Sorcar, 2005).

Dialdehyde starches (polysaccharides) are bio-polymeric tanning agents synthesized by periodate oxidation of carbohydrates (Alderman, 1975). Periodate-oxidized starch tanned leathers yellow and darken with time. The color change is attributable to iodate ions that are products of the periodate oxidation reaction between starch and sodium or potassium (meta)periodate. Iodate ions undergo reduction to form iodine molecules that are yellow or brown in low or at higher concentrations.

This study focuses on two primary objectives: one, the removal of iodate ions from Dialdehyde Tapioca Starch (DTS) using an inorganic salt as a precipitant; and secondly, the use of DTS as a tanning agent to make wet white leather.

2 Materials and methods

2.1 Preparation of dialdehyde tapioca starches

Preparation of DTS (unmodified) is by periodate oxidation of tapioca starch (TS) using 0.35M sodium (meta)periodate (NaIO_4), at pH 3.75, and 35°C for 48 h. Fourier-transform infrared (FT-IR) spectrophotometer (FT/IR-4700 type A) was used to confirm the presences of aldehyde groups on oxidation. The aldehyde group content was determined using the method of quantitative alkali consumption as previously reported by Wongsagon, Shobsngob and Varavinit (2005).

Iodate ions removal from the sample solution was by precipitation with a calculated amount of inorganic salt (precipitant). Iodate content of MDTS (modified) was determined by the redox titration method by first reacting the iodate with added iodide under acidic conditions to produce iodine, which was titrated with thiosulfate.

2.2 DTS Tanning

The experiments for manufacturing wet-white leathers used delimed goatskins (pH = 8.0) and DTS (unmodified and modified) as tanning agents at various percentages based on delimed pelt weight and a 48 h tanning time at pH 8.0. The ratio of liquor to delimed pelt was 5:1.

2.3 Analysis of Leather

2.3.1 Shrinkage temperature (T_s)

The T_s was determined using a Theis shrinkage tester and standard procedures. All tests were carried out in triplicate, and the results expressed as the means with standard deviations of ± 1 .

2.3.2 Color evaluation

Reflectance measurements were made on DTS and MDTS tanned leather samples using a Milton Roy Color mate HDS instrument. The L, a, b, and c values were calculated, and means reported.

2.3.3 Physical tests

The sampling of test samples was carried out in line with the International Union of Leather Technologists and Chemists Societies (IULTCS) - Standard Method (IUP/2 2000). The test samples were conditioned at $80\pm 4^\circ\text{C}$ and $65\pm 4\%$ R.H. for 48 h. Tensile strength, % elongation at break, tear strength, and grain crack strength were tested following the Society of Leather Technologist and Chemists (SLTC) standard methods; IUP/6 2000, IUP/6 2000, IUP/8 2000, and IUP/9 1996, respectively. Each value reported is an average of four (2 along the backbone, 2 across the backbone) measurements.

2.3.4 Softness

The softness of the leather samples was measured using ST 300D leather softness tester, in conformity with IUP/36/EN ISO 17235 method.

3 Results and discussion

Both unmodified and modified DTS had a percentage aldehyde group content of 70%. Fourier-transform infrared (FT-IR) spectra confirmed the formation of aldehyde groups (Fig. 1). Compared with the TS curve, peaks of 1764 and 1741 cm^{-1} appear in the curves of DTS and MDTS, respectively. The two peaks are attributed to characteristic absorption of carbonyl groups; C=O stretching vibrations in aldehyde groups.

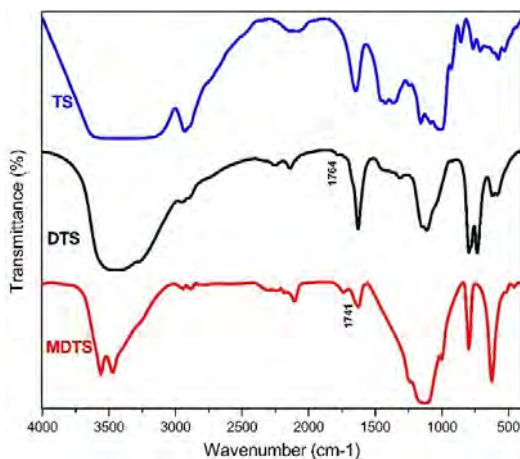


Fig. 1. FT-IR spectra of TS, DTS, and MDTS.

The percentage removal of iodate ions in MDTS was 98%. The effective removal of iodate ions guarantees that the ions are not present to undergo a reduction reaction subsequently generating iodine molecules that cause yellowing (at low concentration) and darkening (at high concentration) of materials over time.

Shrinkage temperature is a measure of the hydrothermal stability of leather and is characteristic of the effectiveness of a tannage (Ding, Taylor and Brown, 2008). The expected T_s of aldehyde-tanned leather is 70°C . The T_s of the delimed pelt, DTS and MDTS tanned leathers was 62 , 80 , and 82°C , respectively. Aldehydes combine with basic amino groups of skin/hide protein (collagen) and

cross-react with adjacent basic groups in the collagen to form an interwoven matrix of intra- and intermolecular cross-links (Paul and Bailey, 2003; Covington, 2009). The formed covalent cross-links improve the hydrothermal stability of the protein and thus raise the Ts of DTS and MDTS tanned leathers.

The 'L' value for DTS tanned leather is 72.2 and 93.9 for MDTS tanned leather (Table. 1). Accordingly, MDTS tanned leather has a lighter shade. The 'a' values for both pieces of leather are greater than 0, indicating the presence of a red shade with DTS tanned leather having a higher value (9.0) than that of MDTS tanned leather (0.5). The 'b' values of DTS and MDTS tanned leathers are greater than 0, that is, 36.6 and 2.6, respectively, signifying the color has a yellow shade. The high 'b' value confirms the yellowing of DTS tanned leather caused by iodine molecules from the iodate ions reduction reaction. The low 'b' values of MDTS tanned leather corroborate the fact that there was effective iodate ion removal. The 'c' value of DTS tanned leather (37.6) was high compared to that of MDTS tanned leather (2.7) denoting high and low intensities of the respective colors (Fathima *et al.*, 2004).

The tensile strength, elongation at break, tear strength, and grain crack resistance (load and distension) values of both DTS and MDTS tanned leathers are comparable to United Nations Industrial Development Organization (UNIDO) specifications (Table.2.). Besides, the values are comparatively lower than those of chrome-tanned leather.

The respective softness values of DTS and MDTS tanned leathers are 7.0±1 and 6.5±1. Softness is a measure of the deformation response of a material to external forces and, thus, depicts the handle (feel) of the leather. On a scale of 0-10, the higher the softness value, the better the feel of leather. The leathers were relatively soft, indicating the fiber structures were not affected.

Table. 1. 'L', 'a', 'b' and 'c' values of DTS and MDTS tanned leathers.

Test sample	L	a	b	c
DTS tanned leather	72.2	9.0	36.6	37.6
MDTS tanned leather	93.9	0.5	2.6	2.7

*Values are mean ± standard deviations, n = 3

Table. 2. Physical strength characteristics of DTS and MDTS tanned leathers.

Test sample	Tensile Strength (N/mm ²)	Elongation at break (%)	Tear Strength (N/mm)	Grain Crack Resistance	
				Load (N)	Distension (mm)
DTS tanned leather	22.86±1	52±2	51.94±2	280.40±14	8.4±1
MDTS tanned leather	23.11±2	54±2	52.23±3	283.90±16	10.1±1

*Values are mean ± standard deviations, n = 4

4 Conclusion

This study set out to remove iodate ions from Dialdehyde Tapioca Starch (DTS). The second object was to use DTS as a tanning agent to make wet white leather. A 98% iodate ions removal was achieved. The color values of MDTS tanned leather substantiate the effective removal of iodate ions. There is no observable yellowing or darkening of the leather. The shrinkage temperatures of the leathers tanned using DTS and MDTS are 80 and 82°C, respectively. The strength properties of the leathers are comparable to the UNIDO specifications. Taken together, these findings suggest that the novel iodate free MDTS can be scaled-up for commercial availability.

Acknowledgments

The authors acknowledge CSIR-Central Leather Research Institute (CLRI) for providing the equipment and the technical staff in carrying out this research work. Thank you for your incredible support.

References

1. Alderman, G. H. R. and M. L. (1975) 'Bleaching of aldehydes-Tanned Leather with Sodium Borohydride'. USA: United States Patent (19).
2. Bowes, J. H. and Cater, C. W. (1965) 'Crosslinking of collagen', *Journal of Applied Chemistry banner*, 15(7), pp. 296-304.
3. Covington, A. D. (2005) 'The Chemistry of Tanning Materials', in *Conservation of Leather and Related Materials*, M. K. and R. T. (ed.). London: Butterworth-Heinemann, pp. 22-35.
4. Covington, A. D. (2009) *Tanning chemistry: the science of leather*. Cambridge: The Royal Society of Chemistry.
5. Ding, K., Taylor, M. M. and Brown, E. M. (2008) 'Tanning effects of aluminum -genipin or -vegetable tannin combinations', *Journal of the American Leather Chemists Association*, 103, pp. 377-382.
6. Fathima N. N., Saravanabhavan S., Rao, J. R. and Nair, B. U. (2004) 'An eco-benign tanning system using aluminium, tannic acid, and silica combination', *Journal of the American Leather Chemists Association*, 99, pp. 73-81.
7. Kanagaraj, J., Velappan, K. C., Chandra Babu, N. K. and Sadulla, S. (2006) 'Solid wastes generation in the leather industry and its utilization for cleaner environment: A review', *J. Sci. Ind. Res. (India)* 65, pp. 541-548.
8. Kanth, S. V., Ramaraj, A., Rao, J. R. and Nair, B. U. (2009) 'Stabilization of type I collagen using dialdehyde cellulose', *Process Biochemistry*, 44, pp. 869-874.
9. Krishnamoorthy, G., Sadulla, S., Sehgal, P. K. and Mandal, A. B. (2012) 'Green chemistry approaches to leather tanning process for making chrome-free leather by unnatural amino acids', *Journal of Hazardous Materials*, 215-216, pp. 173-182.
10. Langmaier, F., Mladek, M., Kolomaznik, K., Sivarova, J. and Sukop, S. (2002) 'Calorimetry of the reactions of hydrolysates of chromed shavings with aldehydes', *Journal of Thermal Analysis and Calorimetry* 67(3), pp. 659-666.
11. Liu, M., Ma, J., Lyu, B., Gao, D. and Zhang, J. (2016) 'Enhancement of chromium uptake in tanning process of goat garment leather using nanocomposite', *Journal of Cleaner Production*, 133, pp. 487-494.
12. Musa, A. E., Madhan, B., Aravindhan, R., Rao, J. R., Chandrasekaran, B. and Gasmelseed, G. A. (2009) 'Studies on Combination Tanning Based on Henna and Oxazolidine', *Journal of the American Leather Chemists Association*, 104, pp. 335-343.
13. Ockerman, H. W. and Basu, L. (2004) 'BY-PRODUCTS | Hides and Skins', in *Encyclopedia of Meat Sciences*. Elsevier Science Ltd, pp. 125-138.
14. Pati, A. and Chaudhary, R. (2014) 'A review on management of chrome-tanned leather shavings : a holistic paradigm to combat the environmental issues', *Environmental Science and Pollution Research*, 21, pp. 11266-11284.
15. Paul, R. G. and Bailey, A. J. (2003) 'Chemical Stabilisation of Collagen as a Biomimetic', *Scientific World Journal*, 24(3), pp. 138-55.
16. Sarkar, K. T. and Sorcar, A. (2005) *Theory and Practice of Leather Manufacture*. 8th edn. Kolkata, India: The Author.
17. Sathish M., Madhan B., Sreeram K. J., Rao J. R., Nair B. U. (2015) 'Alternative carrier medium for sustainable leather manufacturing - a review and perspective', *Journal of Cleaner Production*, doi: 10.1016/j.jclepro.2015.06.118.
18. Sizeland, K. H., Edmonds, R. L., Basil-jones, M. M., Nigel, K, Hawley, A., Mudie, S. and Haverkamp, R. G. (2015) 'Changes to Collagen Structure During Leather Processing', *Journal of Agricultural and Food Chemistry*, 63(9), 2499-2505.
19. Sundar, V. J., Rao, J. R. and Muralidharan, C. (2002) 'Cleaner chrome tanning - emerging options', *Journal of Cleaner Production*, 10(1), pp. 69-74.
20. Wongsagon, R., Shobsngob, S. and Varavinit, S. (2005) 'Preparation and Physicochemical Properties of Dialdehyde Tapioca Starch', *Starch/Stärke*, 57, 166-172.

USE OF DIFFERENT PRE-TREATED CHROMIUM LEATHER SHAVINGS TO PRODUCE BIOGAS IN CONTINUOUS SCALE

C. S. Gomes¹, J-U. Repke² and M. Meyer¹

1 Forschungsinstitut für Leder und Kunststoffbahnen (FILK) gGmbH, Meißner Ring 1-5, 09599 Freiberg, Germany.

2 Dynamik und Betrieb technischer Anlagen, TU Berlin, Straße des 17. Juni 135, 10623 Berlin, Germany.

a) carolina.scaraffunigomes@filkfreiberg.de

Abstract. Leather goods are noble and sustainable but leather production may bear a potential for pollution. During leather manufacture, high amounts of chromium shavings, wet by-products of the leather industry, are produced worldwide. They are disposed of at landfill sites which results in long-term environmental problems. They are stable towards temperatures of up to 110 °C and enzymatic degradation, preventing anaerobic digestion in a biogas plant. This stability is due to the three-dimensional native structure, typical for collagen, and additional chemical cross-links between the collagen fibres achieved by Cr³⁺ salts in the tanning step in tanneries. Hitherto, chromium shavings are not utilized industrially to produce biogas. In order to ease enzymatic degradation, necessary to produce biogas, a previous denaturation of the native structure has to be carried out. Otherwise, the generation of biogas is hindered. In our projects, chromium shavings were pre-treated thermally and mechanically by extrusion and hydrothermal methods. In previous works, we intensively studied the use of these shavings to produce biogas in batch scale and significant improvement was reached when using pre-treated shavings. In this work, a scale-up of the process was performed in a continuous reactor using pre-treated and untreated shavings to examine the feasibility of the considered method. Measuring different parameters along the anaerobic digestion, namely organic matter, collagen content, and volatile fatty acids content, it was possible to show that a higher methane production can be reached and a higher loading rate can be used when feeding the reactor with pre-treated shavings instead of untreated shavings, which means a more economical and efficient process in an industrial scenario.

1 Introduction

The disposal of chromium leather waste is one of the most important ecological challenges in the leather industry. Due to their structure composed mainly of collagen and chromium cross-links, this solid waste is considered to be too stable for anaerobic degradation. However, Dhayalan et al. (2007) studied the anaerobic digestion of chromium leather and concluded that degradation of the waste is possible using anaerobic sludge. The problem is that using this substrate leads to a very slow process and low biogas production.

Currently, there are no biogas plants in the industry using chromium leather waste as a main substrate. However, the tannery SÜDLEDER (Rehau, Germany) already has a biogas plant in operation using their own organic waste (hair, protein, fat, and chromium loaded sludge) to produce energy (Schuberth-Roth, 2013). This kind of initiative illustrates the interest of the industry in biogas production. Nevertheless, using a complex substrate as chromium leather waste needs to be further developed.

Collagen molecules are endowed with mechanical and thermal stability of the fibrous network and high stability to enzymatic degradation (Reich, 2007). Additionally, the chromium tanning process makes the material even more stable (Usha and Ramasami, 2000). Hence, it is necessary to denature the collagen fibres present in chromium leather waste to enable the anaerobic microorganism to degrade this solid waste (Kanagaraj et al., 2006). A pre-treatment can be used to denature the collagen and enable degradation in order to reduce the digestion time and increase the biogas yield.

While some studies treated chromium leather waste under batch conditions (Dhayalan et al., 2007; Ferreira et al., 2010; Agustini et al., 2015 and 2018; Priebe et al., 2016; Gomes et al. 2017 and 2019), there is no published work on continuous reactors for this material. Continuous tests simulate long-term process conditions and are essential for adapting the method in the industry

since most large-scale industrial digesters work in continuous mode as this allows the digester to continually produce biogas (Gamble et al., 2015). These tests enable to investigate capabilities and loading limits of the process, mean residence time as well as formation and accumulation of metabolic intermediates and their influence on process stability (VDI 4630, 2006).

1.1 Objectives

The aim of this study is to investigate the biogas production with untreated and pre-treated chromium leather wastes in a continuous biogas reactor. Pre-treatment was performed by different heating and mechanical technologies.

2 Materials and Methods

2.1 Materials

The chromium leather waste tested were chromium shavings shaved from wet chromium tanned leather. The materials were obtained from a local tannery (HEWA Leder, Freiberg, Saxony, Germany). The chromium shavings used in this work have already been air-dried to some extent and present a water content of almost 20%.

For the biogas trials, mesophilic anaerobic sludge from the tannery SÜDLEDER was used as inoculum. Since the sludge was produced in a tannery, this inoculum was already adapted to chromium residues and collagen as substrate.

2.2 Pre-treatment of the chromium shavings

In order to denature the materials and promote the waste degradation and biogas production, different heat and mechanical pre-treatment techniques were tested. Extrusion, a classical technique from the polymer industry, and a continuous hydrothermal treatment, which is commonly used to plastify wood for the manufacture of wood composites, were used to pre-treat and denature the chromium shavings. While extrusion affects the material by heat, mechanical shear, and pressure, the hydrothermal treatment is based on heat and steam pressure only. During the process, temperatures higher than the denaturation temperature were achieved in order to enable enzymatic degradation to produce biogas.

2.2.1 Extrusion

Extrusion was performed on chromium shavings with a co-rotating twin screw-extruder Werner & Pfleiderer ZSK 25 at 100 °C in a continuous process. This extrusion process starts by feeding the sample from a hopper into the barrel of the extruder. The material is gradually degraded by the mechanical energy generated by turning screws and by heaters arranged along the barrel. The conversion of mechanical energy into heat makes it possible to use this process even under the denaturation temperature of chromium shavings (105 °C to 110 °C). The extrusion of chromium shavings resulted in a powdered material (Figure 1) with a water content of about 15%. The process takes approximately 3 minutes.

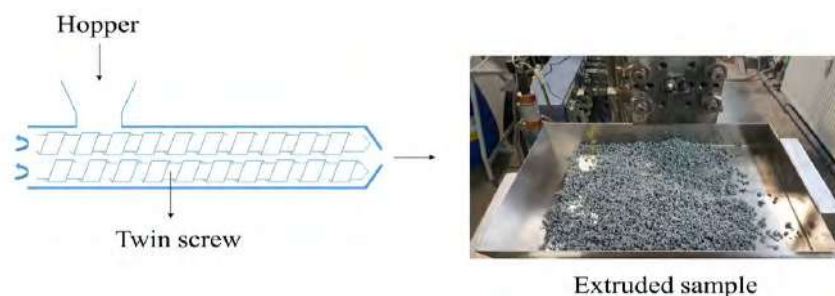


Fig. 1. Operation of the extruder machine.

2.2.2 Hydrothermal treatment

The chromium shavings were subjected to hydrothermal treatment through a continuous autoclave system attached to a refiner (Andritz CPH 12-1) at the Institut für Holztechnologie (Dresden, Germany). Usually, this equipment is used to plastify wood chips but it is also adequate to process a variety of organic materials. The process was carried out at 140 °C and 150 °C in saturated steam. The material was dosed into a digester in which it was denatured with steam under pressure. The pre-treatment time was around 45 seconds.

The pre-treated samples appeared like a dough with a high water content of about 80%. The direct use of these samples in the biogas trials was not possible due to their high water content. Therefore, drying and manual grinding of the material was necessary.

2.3 Characterization of the pre-treated shavings

The pre-treated materials were characterized regarding their inorganic matter (DIN EN ISO 4047, 1998), chromic oxide content (DIN EN ISO 5398-1, 2007), and collagen content by determination of the hydroxyproline content (Stegemann, 1958). Thermal profiles in fully hydrated state of the materials were taken using differential scanning calorimetry (DSC 1 STARe System Mettler Toledo) to verify that the pre-treated materials were completely denatured. The enthalpy calculated from this method represents the necessary energy to break down the hydrogen bonds that stabilize the triple helix. If no enthalpy was observed, there is no triple-helical collagen present in the sample. Results were compared with the values found for the untreated chromium shavings.

2.4 Biogas production trials

Continuous fermentation tests were performed according to the guideline VDI 4630 (2006). The continuous reactors consisted of a 20 L gastight stirred tank with infeed and outlet, and a gas offtake connection to collect the formed biogas (Figure 2). Temperature was kept under mesophilic conditions (37 °C ± 2 °C) using a circulation thermostat (Huber CC-202C), and the biomass was constantly mixed at 50 rpm using a paddle stirrer (Heidolph RZR 2041). The biogas formation in norm litres per kg of sludge (L kg⁻¹ d⁻¹) was measured daily using a drum-type gas meter (Ritter TG05/5), and the quality of the gas and the hydrogen sulphide concentration was measured using an electronic analyser (OPTIMA 7 BIOGAS) once every two days excluding weekends. The hydrogen sulfide concentration was controlled by the addition of iron (III) chloride hexahydrate (Merck), which works as an H₂S scavenger, when necessary. Mesophilic anaerobic sludge from the SÜDLEDER tannery was used as inoculum.



Fig. 2. Continuous fermentation test apparatus (source: MyFerm I manual – Landgraf Laborsysteme HLL GmbH).

At the beginning of the test, the reactor was filled with approximately 20 kg of inoculum (wet basis). Substrate was added once every two days excluding weekends via a dip tube located at the head end of the reactor, starting at a loading rate of substrate per kg of sludge of $0.5 \text{ g kg}^{-1} \text{ d}^{-1}$ (substrate mass in organic dry matter). After the daily methane production was constant, the loading rate was raised by 0.5 units and the process was repeated until the gas production no longer increased.

Once a week a sample of biomass was taken for characterization regarding its pH, inorganic matter (DIN EN ISO 4047, 1998), chromic oxide content (DIN EN ISO 5398-1, 2007), and collagen content (Stegemann, 1958). The biomass was also analysed chromatographically by HPLC (Shimadzu prominence Serie 20, equipped with a refractive index detector RID-10A and a photodiode array detector SPD-M20A) to determine its volatile fatty acids content.

3 Results and Discussion

3.1 Characterization of the pre-treated shavings

The characterization of the pre-treated samples gives important information for the biogas trials. Only organics are capable of producing biogas and, therefore, it is important to quantify the organic and inorganic content. The characterization of the samples is presented in Table 1.

Table 1. Characterization of the untreated and pre-treated chromium shavings.

	Organic matter (%) [*]	Chromium (%) ^{*,**}	Collagen (%) [*]	Denaturation enthalpy (J g ⁻¹)
Chromium shavings	88.8 ± 0.1	4.6 ± 0.0	77.0 ± 0.6	61.8 ± 0.6
Extruded shavings	88.9 ± 0.0	4.6 ± 0.0	74.2 ± 0.9	0
Shavings treat. hydrothermally	89.5 ± 0.4	4.4 ± 0.0	74.2 ± 0.8	0

^{*}Dry basis; mean ± standard deviation, n = 3

^{**}Measured as chromium oxide

The organic matter in the samples remains the same after pre-treatment. This is important because the organics must be preserved for producing biogas in the anaerobic digestion. The collagen content is also barely unchanged after pre-treatment. This protein is the main component of the chromium shavings, only about 12% of the samples are different types of organics, for instance fats. Therefore, collagen is the most important parameter to calculate the substrate degradation after anaerobic digestion. DSC results show that the collagen in the chromium shavings was completely denatured by pre-treatment. Consequently, chromium shavings are more easily accessible to enzymatic degradation. This is explored in more detail in a previous work (Gomes et al., 2017).

Almost half of the inorganic part of the samples is chromium oxide. Chromium also remains the same after pre-treatment. Other inorganics in the samples come from the chemicals used in tanneries.

3.2 Biogas production trials

3.2.1 Productivity of the reactors

The pre-treated samples were tested as substrates for biogas production in a continuous reactor and the results were compared with the performance of the untreated shavings. Figure 3 shows the time plot of digestion for the studied substrates.

Two of the biogas trials showed a drop in the daily methane production along digestion, indicating technical problems. The methane production drops can be seen on the 7th day of digestion for the reactor fed with extruded shavings (Figure 3b) and on the 21st for the reactor fed with shavings treated hydrothermally (Figure 3c). The former was caused by an oxygen infiltration on day 5 due to the rupture of the dip tube used to feed the reactor; the latter by an agitation failure, which resulted in the uneven heating of the reactor. Even though there is a drop in the methane production, the system recovered its former stability and appeared to function normally after a few days. The reactor fed with shavings treated hydrothermally needed only 2 days to recover, and the reactor fed with extruded shavings needed 5 days, that is more time to recover probably because the ingress of oxygen occurred very early in the digestion process. The daily methane production became very unstable for the extruded shavings when using loading rates higher than 1.4 g kg⁻¹ d⁻¹ and for the shavings treated hydrothermally for loading rates of 2.0 g kg⁻¹ d⁻¹.

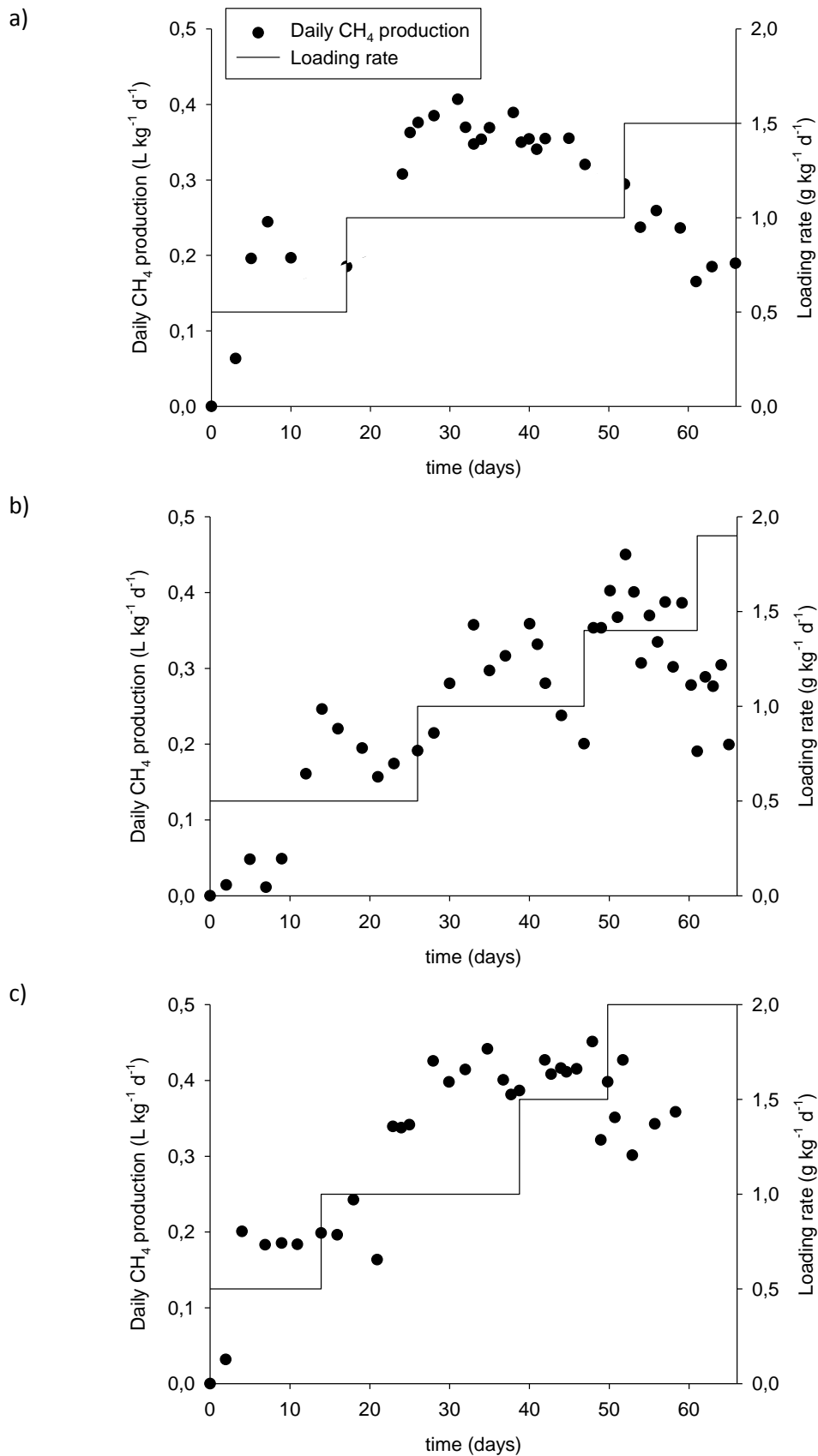


Fig. 3. Time plot of continuous fermentation of the untreated chromium shavings (a), extruded shavings (b), and shavings treated hydrothermally (c).

The production of a second batch of extruded shavings was necessary to feed the reactor starting on the 42nd day. This second batch of the substrate was not completely denatured because the use of the same extruder was not possible. DSC results still showed a denaturation enthalpy of 12.6 J g⁻¹ compared to 61.8 J g⁻¹ for untreated chromium shavings (Table 1).

Pre-treatment allowed the use of a higher loading rate and increased the maximum daily methane production. The trial with untreated chromium shavings (Figure 3a) had to be stopped at a loading rate of 1.5 g kg⁻¹ d⁻¹ but the extruded shavings (Figure 3b) could be tested up to a loading rate of 1.9 g kg⁻¹ d⁻¹ and the shavings treated hydrothermally (Figure 3c) up to 2.0 g kg⁻¹ d⁻¹. The chromium shavings reached the maximum daily methane production, 0.41 L kg⁻¹ d⁻¹, on day 31 of digestion with a loading rate of 1.0 g kg⁻¹ d⁻¹. The extruded shavings reached a higher value, 0.45 L kg⁻¹ d⁻¹, on day 52 of digestion but with a loading rate of 1.4 g kg⁻¹ d⁻¹.

Similarly, for the shavings treated hydrothermally, the maximum daily methane production was 0.45 L kg⁻¹ d⁻¹, on day 48 of digestion with a loading rate of 1.5 g kg⁻¹ d⁻¹.

No studies covering the anaerobic digestion of chromium leather waste in continuous trials could be found for comparison. Some authors studied the digestion of tannery waste in continuous (López et al., 2015a and 2015b) or semi-continuous mode (Berhe and Leta, 2018; Kameswari et al., 2015; Zupančič and Jemec, 2010) but the material was always collected from tanneries prior to the tanning step and this is known to be already in use industrially (Schuberth-Roth, 2013). These studies mainly used fleshings as substrate, which are also not suitable for comparison due to a high fat content.

3.2.2 Inhibition of digestion

In order to monitor the reactor stability and possible inhibitions, biomass samples were collected weekly and analysed regarding their concentration of volatile fatty acids. Figure 4 shows the results for the three anaerobic reactors.

Volatile fatty acids are intermediate products resulting from anaerobic digestion. However, they could inhibit the methane production at high concentrations (Gomes et al., 2019). To avoid failure of a fermenter, the total concentration of volatile fatty acids should be lower than 4 g L⁻¹. The acetic acid concentration should be lower than 3 g L⁻¹, the isobutyric acid concentration lower than 0.5 g L⁻¹, and the propionic acid concentration lower than 1 g L⁻¹ (Kaiser et al., 2008) but a concentration of propionic acid higher than 0.3 g L⁻¹ is enough to disturb the anaerobic digestion (Deublein and Steinhauser, 2008).

The reactor fed with untreated shavings (Figure 4a) showed a stable total volatile fatty acid concentration for a loading rate up to 1.0 g kg⁻¹ d⁻¹ but the concentration increased at a loading rate of 1.5 g kg⁻¹ d⁻¹ to more than 4 g L⁻¹, corresponding to the drop in daily methane production. For the final collected sample, the acetic acid concentration was 3.5 g L⁻¹ and the propionic acid concentration reached 0.6 g L⁻¹ indicating a complete failure of the reactor at this loading rate.

Similarly, for the extruded shavings (Figure 4b) as substrate, the total volatile fatty acid concentration was low for a loading rate up to 1.0 g kg⁻¹ d⁻¹. There was a small increase of acid concentration at the first loading rate, corresponding to the ingress of oxygen registered for this reactor but the system recovers its former stability and the acid concentration drops again. The acid concentration started increasing at a loading rate of 1.4 g kg⁻¹ d⁻¹ without reaching an inhibitory concentration, which could explain the unstable daily methane production values at this loading rate. Finally, at the last loading rate, the total acid concentration reached 5.4 g L⁻¹ and the propionic acid concentration reached a value of 1 g L⁻¹ indicating the failure of the reactor. The acetic acid and isobutyric acid concentrations were also high in this last sample but without reaching an inhibitory concentration.

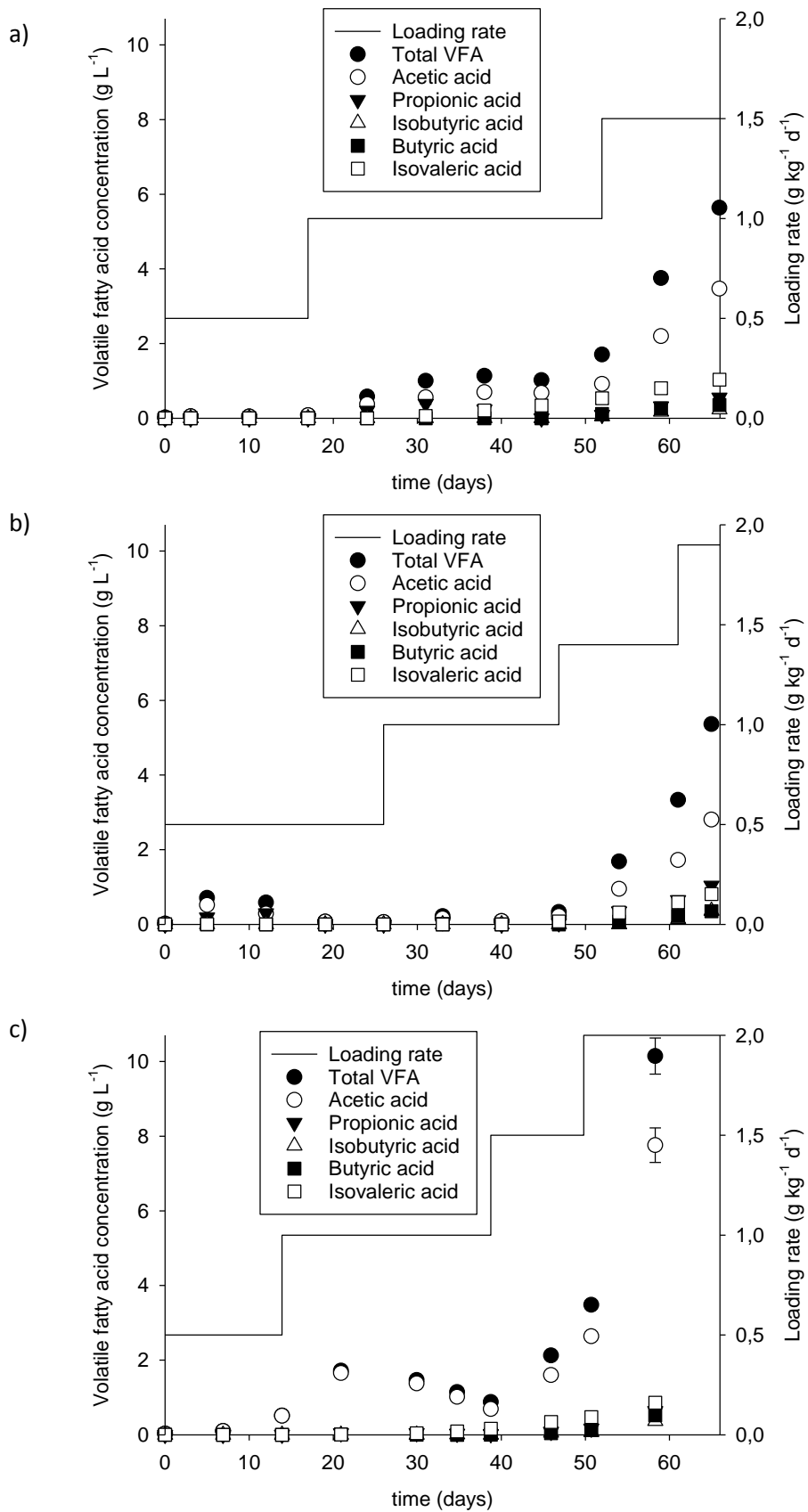


Fig. 4. Volatile fatty acid concentrations along the anaerobic digestion of untreated chromium shavings (a), extruded shavings (b), and shavings treated hydrothermally (c).

Table 2. pH and chromium content of the samples collected along the continuous digestion.

Chromium shavings			
Time (days)	Loading rate (g kg ⁻¹ d ⁻¹)	pH	Chromium (%) [*]
0		8.1	1.1
3	0.5		1.0 ± 0.0
10		7.9	1.4 ± 0.1
17		7.9	1.6 ± 0.1
24		7.9	1.9 ± 0.0
31		8.0	2.4 ± 0.1
38	1.0	8.1	2.7 ± 0.0
45		8.1	3.5 ± 0.0
52		8.1	3.3 ± 0.1
59	1.5	8.1	3.9 ± 0.1
66		8.0	4.3 ± 0.1
Extruded shavings			
Time (days)	Loading rate (g kg ⁻¹ d ⁻¹)	pH	Chromium (%) [*]
0		8.3	1.0 ± 0.0
5	0.5	7.8	1.3 ± 0.1
12		7.9	1.6 ± 0.0
19		8.0	2.0 ± 0.1
26		7.9	2.5 ± 0.0
33		8.0	3.1 ± 0.1
40	1.0	8.1	3.5 ± 0.1
47		8.0	3.8 ± 0.1
54		8.0	4.7 ± 0.1
61	1.4	8.1	4.9 ± 0.4
65	1.9	8.0	4.5 ± 0.0
Shavings treated hydrothermally			
Time (days)	Loading rate (g kg ⁻¹ d ⁻¹)	pH	Chromium (%) [*]
0		8.1	1.2 ± 0.0
7	0.5	8.0	1.6 ± 0.0
14		8.0	1.7 ± 0.0
21		7.8	2.3 ± 0.0
30	1.0	8.1	2.8 ± 0.1
35		8.1	3.1 ± 0.0
39		8.1	3.1 ± 0.0
46		8.1	3.5 ± 0.1
51	1.5	8.1	4.7 ± 0.0
58	2.0	8.0	4.7 ± 0.0

^{*}Dry basis; mean ± standard deviation, n = 2; measured as chromium oxide

The reactor fed with shavings treated hydrothermally (Figure 4c) also showed a small increase of the volatile fatty acid concentration due to the agitation failure at a loading rate of 1.0 g kg⁻¹ d⁻¹. Again, the reactor recovers stability and the acid concentration drops. Otherwise, the reactor showed stable volatile fatty acid concentrations. The concentration only increased in the last collected biomass sample at a loading rate of 1.5 g kg⁻¹ d⁻¹. Inhibition began at the last loading rate and daily methane production dropped. The total volatile fatty acid concentration increased to up to 10.1 g L⁻¹,

the acetic acid concentration to up to 7.8 g L⁻¹, propionic acid to up to 0.6 g L⁻¹, and isobutyric acid to up to 0.4 g L⁻¹.

The chromium content could also cause inhibition of the methane production in the reactors. Cr³⁺ ions could inhibit the methanogenic archaea without affecting the acidogenic bacteria, resulting in the accumulation of volatile fatty acids. Chromium could also have other negative effects on the anaerobic digestion such as a decrease in the total gas production rate, a fall in pH, a decrease in the percentage of methane in the gas produced, and an accumulation of organic matter (Alkan et al., 1996). The pH and chromium content of the collected biomass samples was analysed and results are shown in Table 2.

The pH of the biomass during digestion was very stable, between 7.8 and 8.3, causing no disturbance in the system. At the end of the trials, a total chromium content of almost 5% was achieved in all reactors, which appears not to affect digestion. The inoculum for the reactor fed with chromium shavings had a chromium content of 324 mg L⁻¹, the extruded shavings reactor had a chromium content of 233 mg L⁻¹, and the reactor fed with shavings treated hydrothermally had a content of 369 g L⁻¹. The bacteria present in the initial sludge were already adapted to high quantities of chromium prior to digestion. The determination of a limit would only be possible with a long-term trial at an appropriate loading rate, without other inhibitions.

3.2.3 Degradation of the substrate

The degradation of the substrate was evaluated analysing the biomass samples collected weekly along the anaerobic digestion. Table 3 shows the characterization of the collected biomass samples. The samples were analysed regarding their collagen, organic matter, and chromium content.

An increase in the organic matter content in the collected sludge would indicate the accumulation of unprocessed substrate and, therefore, inefficiency of the process. As seen in Table 3, the reactor fed with untreated chromium shavings showed a constant value of organic matter content (around 40%) for most of the time. An increase to 45% was detected at the end of the trial at a loading rate of 1.5 g kg⁻¹ d⁻¹, indicating that the reactor was overloaded. The methane production is very low and the added substrate accumulates.

The reactor fed with the extruded shavings had an organic matter content of around 39% at a loading rate of 0.5 g kg⁻¹ d⁻¹. At a loading rate of 1.0 g kg⁻¹ d⁻¹ the organic matter content remained constant at 40% and showed a slight increase to 42% at the end of this rate. In a next step, an increase in organic matter to around 44% was observed at a loading rate of 1.4 g kg⁻¹ d⁻¹. Finally, in the last step, the organic matter content increased to 47% at a loading rate of 1.9 g kg⁻¹ d⁻¹. With regard to the shavings treated hydrothermally, the reactor started with around 38% of organic matter at the first loading rate. Progression to the next step increased the organic matter content of the reactor to about 40%. The loading rate of 1.5 g kg⁻¹ d⁻¹ resulted in an increase to 45% and the last loading rate led to 48%. The increase of organic matter at the last loading rate when methane production slows indicates accumulation.

At the end of digestion, the collagen content was almost as low as it was prior to adding substrate at the beginning of the process for all reactors, showing that collagen was degraded and that there is no accumulation of collagen in the reactor. Therefore, the collagen of the added substrate was metabolized. However, the inorganic part of the samples accumulated, and the chromium content in the reactor increased.

Although a second batch of extruded shavings was used, which were not completely denatured, the reactor accomplished degradation of the substrate. When the reactor was shut down, it contained 33.7 g of collagen (dry basis), which represents a final degradation of 96.5% of all of the added collagen (953.8 g of added collagen). The reactor fed with untreated shavings contained 45.6 g of collagen (dry basis) at shutdown, equating to 95.5% of degradation (1014.4 g of added collagen) and the reactor fed with shavings treated hydrothermally showed a final amount of collagen of 58.3 g (dry

basis) meaning that 95.3% of the added collagen were degraded (1233.4 g of added collagen). That leads to the conclusion that there is efficient degradation of collagen notwithstanding the observed accumulation of organic matter (Table 3).

Table 3. Biomass characterization of the samples collected along the continuous digestion.

Chromium shavings			
Time (days)	Loading rate (g kg⁻¹ d⁻¹)	Collagen (%)*	Organic matter (%)*
0		2.9 ± 0.3	39.5 ± 1.4
3	0.5	4.3 ± 0.9	41.4 ± 1.2
10		4.4 ± 0.4	41.2 ± 1.8
17		5.8 ± 0.6	38.7 ± 0.2
24		6.3 ± 0.7	41.1 ± 0.3
31	1.0	5.1 ± 0.4	40.8 ± 0.0
38		3.6 ± 0.4	40.2 ± 0.3
45		2.5 ± 0.1	40.3 ± 0.2
52		2.3 ± 0.1	41.3 ± 0.2
59	1.5	2.6 ± 0.2	44.6 ± 0.3
66		3.3 ± 0.0	45.4 ± 0.1
Extruded shavings			
Time (days)	Loading rate (g kg⁻¹ d⁻¹)	Collagen (%)*	Organic matter (%)*
0		2.7 ± 0.3	38.3 ± 0.3
5	0.5	3.2 ± 0.1	38.4 ± 1.2
12		3.3 ± 0.1	38.5 ± 0.3
19		3.6 ± 0.1	39.6 ± 1.4
26		3.4 ± 0.1	37.9 ± 0.1
33	1.0	3.4 ± 0.3	40.2 ± 0.5
40		4.5 ± 0.2	40.3 ± 0.2
47		6.5 ± 0.3	42.0 ± 0.1
54		3.4 ± 0.1	43.7 ± 0.2
61	1.4	3.1 ± 0.1	44.4 ± 0.1
65		2.8 ± 0.0	46.9 ± 0.1
Shavings treated hydrothermally			
Time (days)	Loading rate (g kg⁻¹ d⁻¹)	Collagen (%)*	Organic matter (%)*
0		3.3 ± 0.0	37.4 ± 0.2
7	0.5	3.7 ± 0.0	39.1 ± 0.3
14		4.0 ± 0.1	37.9 ± 0.1
21		5.6 ± 0.0	40.7 ± 0.3
30	1.0	4.8 ± 0.3	39.8 ± 0.6
35		5.1 ± 0.1	39.8 ± 0.4
39		5.2 ± 0.1	40.6 ± 0.5
46		4.9 ± 0.1	42.3 ± 0.3
51	1.5	5.0 ± 0.0	45.3 ± 0.4
58		2.0	4.0 ± 0.1

*Dry basis; mean ± standard deviation, n = 3

The organic matter present in the final biomass is formed from organics from the inoculum and intermediate products from the hydrolysed substrate, such as volatile fatty acids, amino acids, and peptides. In a previous work (Gomes et al., 2017), it was shown that the anaerobic digestion of

inoculum without adding substrate leads to a final biomass of about 40% of organic content from which the conclusion can be drawn that part of the initial organic matter will remain unprocessed. The increase in organic matter content along the digestion is a consequence of the accumulation of unprocessed substrate in the form of intermediate products, which are not transformed into biogas probably due to inhibition of the anaerobic bacteria.

Considering that the highest daily methane production for the untreated shavings was reached at a loading rate of $1.0 \text{ g kg}^{-1} \text{ d}^{-1}$, the conclusion can be drawn that this is the most appropriate loading rate for this material. The reactor fed with extruded shavings showed the highest daily methane production at a loading rate of $1.4 \text{ g kg}^{-1} \text{ d}^{-1}$ proving to be the most suitable loading rate for the extruded sample among the studied rates. Finally, the reactor fed with shavings treated hydrothermally reached its highest daily methane production at a loading rate of $1.5 \text{ g kg}^{-1} \text{ d}^{-1}$ showing that this rate should be aimed at. Accumulation of organic matter and the increasing concentrations of volatile fatty acids verified in the collected biomass samples for the last tested loading rates lead to the same conclusion. Nevertheless, long-term trials of one year or more should prove this observation.

Pre-treatment of the chromium shavings allows for a higher loading rate of substrate in the reactor and a higher daily methane production. This increases the capability of reducing solid waste and the generation of energy. Consequently, the feasibility of chromium shavings to be digested for producing biogas in tanneries increases. It is also possible to digest untreated chromium shavings in continuous systems to produce methane but using a low loading rate. However, an explanation for this observation is still missing and this conflicts with the common doctrine that untreated shaving cannot be digested in biogas reactors. An economical evaluation to verify if the pre-treatment costs are compensated by the energy gains should be done. However, reduction of the disposal of final waste, which would otherwise generate costs, makes this method very attractive for industry purposes.

4 Conclusions

The production of biogas in continuous reactors was tested for two different pre-treated chromium shavings and untreated chromium shavings. Pre-treatment was carried out to denature the stable collagen structure of chromium shavings in order to enhance anaerobic digestion when using this waste as substrate to produce biogas. The reactors fed with pre-treated shavings showed a higher methane production than those using chromium shavings as substrate. For pre-treated shavings a loading rate could be used which was 40 to 50% higher than that for untreated chromium shavings, and the maximum daily methane production could be increased by almost 10%. A higher loading rate leads to a more economical process, and it can be expected that, on an industrial scale, the loading rate could be increased by 40 to 50% through pre-treatment of the chromium shavings or, in contrast, the reactor volume for a given loading rate could be decreased.

5 Acknowledgements

The authors would like to thank DAAD (German Academic Exchange Service) for the financial support of this work.

References

1. Agustini, C., Costa, M., Gutterres, M.: 'Biogas production from tannery solid wastes - Scale-up and cost saving analysis', *J. Clean. Prod.*, 187, 158–164, 2018
2. Agustini, C., Neto, W., Costa, M., Gutterres, M.: 'Biodegradation and biogas production from solid waste of tanneries', XXXIII IULTCS Congress, Novo Hamburgo, Brazil, 2015
3. Alkan, U., Anderson, G. K., Ince, O.: 'Toxicity of trivalent chromium in the anaerobic digestion process', *Water Res.*, 30, 3, 731 – 741, 1996
4. Berhe, S., Leta, S.: 'Anaerobic co-digestion of tannery waste water and tannery solid waste using two-stage anaerobic sequencing batch reactor: focus on performances of methanogenic step', *J. Mater. Cycles Waste Manag.*, 20, 1468–1482, 2018
5. Deublein, D., Steinhauser, A.: *Biogas from Waste and renewable Resources An Introduction*, Wiley-VCH, Weinheim, 2008
6. Dhayalan, K., Fathima, N. N., Gnanamani A., Rao J. R., Nair B. U., Ramasami T.: 'Biodegradability of leathers through anaerobic pathway', *Waste Manage.*, 27, 760–767, 2007
7. DIN EN ISO 4047: 'Leather - Determination of sulphated total ash and sulphated water-insoluble ash', German Institute for Standardization, Berlin, Germany, 1998
8. DIN EN ISO 5398-1: 'Leather - Chemical determination of chromic oxide content', German Institute for Standardization, Berlin, Germany, 2007
9. Ferreira, M. J., Almeida, M. F., Pinho, S. C, Santos, I. C.: 'Finished leather waste chromium acid extraction and anaerobic biodegradation of the products', *Waste Manage.*, 30, 1091–1100, 2010
10. Gamble, K. J., Houser, J. B., Hambourger, M. S., Hoepfl, M. C.: *Anaerobic Digestion from the Laboratory to the Field: An Experimental Study into the Scalability of Anaerobic Digestion*, ASEE Southeast Section Conference, Gainesville, USA, 2015
11. Gomes, C. S., Repke, J-U., Meyer, M.: 'Different pre-treatments of chrome tanned leather waste and their use in the biogas production', XXXIV IULTCS Congress, Chennai, India, 2017
12. Gomes, C. S., Repke, J-U., Meyer, M.: 'Diauxie during biogas production from collagen-based substrates'. *Renew. Energ.*, 141, 20-27, 2019
13. Kaiser, F., Metzner, T., Effenberger, M., Gronauer, A.: *Sicherung der Prozessstabilität in landwirtschaftlichen Biogasanlagen*, Bayerische Landesanstalt für Landwirtschaft (LfL), Freising-Weihenstephan, 2008
14. Kanagaraj, J., Velappan, K. C., Babu, N. K. C., Sadulla, S.: 'Solid wastes generation in the leather industry and its utilization for cleaner environment - A review'. *J. Sci. Ind. Res.*, 65, 541 -548, 2006
15. Kameswari, K. S. B., Kalyanaraman, C., Thanasekaran, K.: 'Optimization of organic load for co-digestion of tannery solid waste in semi-continuous mode of operation', *Clean Technol. Envir.*, 17, 693–706, 2015
16. López, I., Passeggi, M., Borzacconi, L.: 'Validation of a simple kinetic modelling approach for agro-industrial waste anaerobic digesters', *Chem. Eng. J.*, 262, 509-516, 2015 (a)
17. López, I., Passeggi, M., Borzacconi, L.: 'Variable kinetic approach to modelling an industrial waste anaerobic digester', *Biochem. Eng. J.*, 96, 7–13, 2015 (b)
18. Priebe, G. P. S., Kipper, E., Gusmão, A. L., Marcilio, N. R., Gutterres, M.: 'Anaerobic digestion of chrome-tanned leather waste for biogas production', *J. Clean. Prod.*, 129, 410–416, 2016
19. Reich, G.: *From collagen to leather – the theoretical background*, BASF Service center Media and Communications, Ludwigshafen, 2007
20. Schuberth-Roth, V. T.: 'Erster Schritt in neue Energie-Ära', *Frankenpost, Rehauer Tagblatt*, [<https://www.frankenpost.de/lokal/hofrehau/rehau/Erster-Schritt-in-neue-Energie-Aera;art2452,2627816>], 2013
21. Stegemann, H.: 'Microdetermination of hydroxyproline with chloramine-T and p-dimethylaminobenzaldehyde', *Hoppe-Seyler's Zeitschrift für physiologische Chemie*, 311, 41, 1958
22. Usha, R., Ramasami, T.: 'Effect of crosslinking agents (basic chromium sulfate and formaldehyde) on the thermal and thermomechanical stability of rat tail tendon collagen fibre', *Thermochim. Acta*, 356, 59-66, 2000
23. VDI 4630: 'Fermentation of organic materials, Characterization of the substrate, sampling, collection of material data, fermentation tests', The Association of German Engineers, Düsseldorf, Germany, 2006
24. Zupančič, G. D., Jemec, A.: 'Anaerobic digestion of tannery waste: Semi-continuous and anaerobic sequencing batch reactor processes', *Bioresour. Technol.*, 101, 26–33, 2010

STUDY ON THE APPLICATION OF A NEW MULTI-EPOXY REINFORCEMENT AGENT FOR SHEEP LEATHER

X. Y. Pang^{1,2,3}, N. Liu^{1,3}, W. Ding^{1,2}, X. P. Liao^{2*} and Z. W. Ding^{1,3*}

1 China Leather and Footwear Research Institute Co. Ltd., Beijing 100015, China

2 National Engineering Laboratory for Clean Technology of Leather Manufacture, Sichuan University, Chengdu 610065, China

3 Hebei Green Leather Industry Technology Research Institute

a)pang_xiaoyan@126.com; b)xpliao@scu.edu.cn; c) ding-zhiwen@163.com

Abstract. Leather is a kind of natural biomass composite material using animal skin as raw material. Its main structure is collagen fibre with three-dimensional network structure. Sheep leather is one of the important leathers except cattle and pig leather. However, it always exhibits weak mechanical strengths. Through the past decades, many methods have been tried to improve the strength of sheep leather, but the strength enhancement of sheep leather is extremely limited, although the fullness and softness may be improved. In this work, a new type of multi-epoxy reinforcement agent (IGE) and polyamine synergistic IGE (IGE-PA) were used to enhance the strength of sheep leather in tanning and fatliquoring process. Compared with chrome tanned leather, the tearing strength of tanned leather increased 56.8% when IGE was used as a reinforcement agent in tanning process. In addition, the tearing strength was significantly increased 97.9% when IGE-PA2000 was used. Furthermore, when IGE and IGE-PA were used in fatliquoring process, it has significant reinforcement effect for tetrakis hydroxymethyl phosphonium (THPS) salt tanned leather. Under the optimized conditions with IGE in fatliquoring process, the tear strength increased 50.2%, while when the IGE-PA400 was used, the tear strength increased 64.3% compared with blank experiment. In addition, the optimized conditions of IGE-PA2000 used in tanning process was obtained by orthogonal experiment: the dosage of PA-2000 and IGE were 0.5% and 10%, respectively, pH was 8, temperature was 35°C for penetration and 45°C for fixation, and tanning time was 10 h. The optimized conditions of IGE-PA400 in fatliquoring process was also obtained by orthogonal experiment: the dosage of IGE and PA-400 were 3% and 1%, respectively, meanwhile the treated temperature was 55°C, pH was 7.5 and time was 2h. Furthermore, TG and DTG results showed that the decomposition temperatures of IGE-PA enhanced leather were all higher than IGE. In addition, SEM results showed that IGE and IGE-PA enhanced leather obtained better opened-up fibre structure.

1 Introduction

Sheep leather has the properties of soft, large extension, smooth hand feeling, clear and beautiful leather grain. However, it has low strength owing to not only the large number of hair bunches, fat glands, sweat glands and erector hairs but also the finer collagen fibre bundle of reticular layer, loose braid, and parallel weave horn. Until now, the strength problem of sheep skin has not been effectively solved.¹

The characterization methods for leather strength mainly include tensile strength and tear strength. Tensile strength refers to the number of loads per unit cross-sectional area when the leather is stretched and broken, represented by N/mm². Tear strength refers to the number of loads per unit thickness of the leather crack when the leather is stretched, expressed as N/mm. The strength of the leather is closely related to the direction of the fibre bundle. The more parallel fibre bundle, the greater the strength will be. And when the bent fibre bundle has greater bending degree, it has bigger total stress and is easier to be destroyed, and then it has lower strength.

To date, weakening the mechanical force in processing has been proved to be an effective approach to reinforce the network structure of sheep leather, such as choosing sharp cutting equipment to reduce the damage of mechanical force on collagen fibre network, large liquid ratio and run combined stop processing mode, etc. On the other hand, the application of retanning or fatliquoring agent was common method to improve the strength for sheep leather, such as using

2.3 Reinforcement experiments for IGE

Leather was treated with IGE and IGE-PA in the tanning process and fatting process respectively, and the physical strength were tested. Meanwhile, the strength was compared with F90, THPS and chrome tanned leather when IGE was used in tanning process, while it was contrasted with commercial product of reinforcement agent U in the fatting process. The reinforcement process using IGE in tanning and fatliquoring process are shown in Tab. 1 and Tab. 2.

Table 1. IGE reinforcement in tanning process.

	Chemicals	Dosage (%)	Time (min)	Tem. (°C)	pH
	The bated skin as the raw materials				
Tanning process	Ethanol-50*	80	20	35	6.0~6.5
	Polyamine**	0~1.5	60	35	
	IGE	10%	120	30	
	NaHCO ₃		30	30	
			600	45	8.0
washing	water	200%	10 ×2	25	

* Ethanol-50 represents 50 wt. % of ethanol in water; **polyamine refers to MEL, PA-400 and PA-2000.

Table 2. IGE reinforcement in fatliquoring process.

	Chemicals	Dosage (%)	Tem. (°C)	Time (min)	pH
	the THPS tanned leather as the raw materials				
	water	150			
fatliquoring	Mixture				
	Fatliquoring agent	14	55		
	IGE or U	x		60	
	Formic acid	1		20×2	3.6
washing	Water	300	25	10×2	

Table 3. Orthogonal experiment for IGE reinforcement in tanning process.

No.	A	B	C	D
	Dosage of PA-2000 (%)	Dosage of IGE (%)	Penetrating time (h)	Tanning time (h)
1	0.5	6	0.5	10
2	0.5	8	1	12
3	0.5	10	2	14
4	1.0	6	1	14
5	1.0	8	2	10
6	1.0	10	0.5	12
7	1.5	6	2	12
8	1.5	8	0.5	14
9	1.5	10	1	10

Orthogonal tests of three levels and four factors were designed respectively, choosing the strength of leather as the evaluation index, the reinforcement effect of IGE at different conditions in tanning and fatting processes were determined. The orthogonal experiments are shown in Tab. 3 and Tab. 4. At the same time, the effect of IGE dosage on sheep skin was investigated by single factor experiment.

Table 4. Orthogonal experiment for IGE reinforcement in fatliquoring process.

No.	A	B	C	D
	Dosage of PA-400 (%)	Tem. (°C)	pH	Time (h)
1	0.5	50	5.5	1
2	0.5	55	6.5	2
3	0.5	60	7.5	3
4	1	50	6.5	3
5	1	55	7.5	1
6	1	60	5.5	2
7	1.5	50	7.5	2
8	1.5	55	5.5	3
9	1.5	60	6.5	1

2.4 Evaluation of reinforcement performances

2.4.1 Physical properties

All the sheep leathers samples were fatliquored according to the conventional process. Then, the fatliquored leathers were dried and softened to obtain crust leathers. The crust leather samples were conditioned at 20 °C with a relative humidity of 65% for 48 h according to the official sampling demand,¹² and tensile strength and tear strength were measured.¹³

2.4.2 TGA determination

The sample of 6~8 mg was put into a standard pan and the thermal decomposition behaviour of sample was measured using TGA (Netzsch 209 F1, Germany) in dynamic mode from 30 °C to 500 °C at a heating rate of 10 °C/min under N₂ atmosphere.

2.4.3 Scanning electron microscope (SEM) observation

The dried crust leathers were cut into 2 mm × 5 mm pieces. Then, the cross section of leather sample was coated with gold in vacuum. The SEM observation was carried out by using a scanning electron microscope (JSM-7500F, JEOL Ltd.) with a magnification of 500 times, acceleration voltage of 15 kV and resolution ratio of 1.0 nm.

3 Results and discussions

3.1 Evaluation of the reinforcement performance

3.1.1 Orthogonal experiment results for IGE reinforcement in tanning process

Tab. 5 and Tab.6 are the orthogonal experiment results for IGE reinforcement and range analysis for IGE reinforcement in tanning process. As shown in Tab. 5 and Tab. 6, the optimum process combination is A1B2C3D2 when the tensile strength was performance indicator, while the optimum process combination is A1B2C3D1 when the tear strength was performance indicator. From the range analysis, it can be concluded that the influence order of various factors on tensile strength was PA-2000 dosage, tanning time, osmotic time, IGE dosage in sequence and the influence order of various factors on tearing strength was penetrating time, IGE dosage, PA-2000 dosage, tanning time in turn.

Table 5. Orthogonal experiment results for IGE reinforcement in tanning process.

No.	Dosage of PA-2000 (%)	Dosage of IGE (%)	Penetrating time (h)	Tanning time (h)	Tensile strength (N/mm ²)	Tear strength (N/mm)
1	1	1	1	1	11.95	79.36
2	1	2	2	2	13.21	74.76
3	1	3	3	3	11.71	76.47
4	2	1	2	3	10.75	65.06
5	2	2	3	1	13.44	84.92
6	2	3	1	2	11.95	56.81
7	3	1	3	2	11.9	80.82
8	3	2	1	3	8.62	73.52
9	3	3	2	1	9.01	53.9

Table 6. Range analysis for IGE reinforcement in tanning process.

	Tensile strength				Tear strength			
Mean value 1	12.297	11.533	10.840	11.467	76.863	75.080	69.897	72.727
Mean value 2	12.047	11.757	10.990	12.353	68.930	77.733	64.573	70.797
Mean value 3	9.843	10.897	12.457	10.367	63.413	62.393	80.737	71.683
Range	2.454	0.860	1.517	1.986	7.933	15.340	16.164	1.930

Table 7. Results of optimum conditions.

No.	Dosage of PA-2000 (%)	Dosage of IGE (%)	Penetrating time (h)	Tanning time (h)	Tensile strength (N/mm ²)	Tear strength (N/mm)
10	1	2	3	2	13.95	84.36
11	1	2	3	1	13.21	89.76

Tab. 7 is the results of optimum conditions for the orthogonal experiments. As shown in Tab. 7, in the optimal conditions, the better tensile strength and tear strength were obtained. Therefore, for the optimum condition on tensile strength for reinforcement in tanning process, the dosage of PA-2000 and IGE was 0.5% and 10%, respectively, the penetrating time was 2h, tanning time was 10h. In case of the optimum condition on tear strength, the process combination was same except that the tanning time was 8h.

3.1.2 Orthogonal experiment results for IGE reinforcement in fatliquoring process

Tab. 8 is the orthogonal experiment results and Tab. 9 is the range analysis for IGE reinforcement in tanning process. It can be found that the optimum process combination is A2B2C3D2 when the tensile strength was set as indicator, while the optimum process combination is A2B3C2D1 when the tear strength was performance indicator. From the range analysis, it can be concluded that the influence order of various factors on tensile strength is the dosage of PA-400, dosage of IGE, penetrating time, tanning time in sequence and the influence order of various factors on tearing strength is the tanning time, penetrating time, dosage of IGE and dosage of PA-400 in turn.

Tab. 10 is the results of optimum conditions for the orthogonal experiments. In the optimal conditions, better tensile strength and tear strength were obtained. Therefore, for the optimum condition on tensile strength for reinforcement in tanning process, the dosage of PA-400 was 1.0%, temperature was 55°C, pH was 7.5 and time was 2h. In case of the optimum condition on tear strength, the dosage of PA-400 was 1.0%, temperature was 60°C, pH was 6.5 and time was 1h.

Table 8. Orthogonal experiment results for IGE reinforcement in fatliquoring process.

NO.	Dosage of PA-400 (%)	Tem.(°C)	pH	Time (h)	Tensile strength (N/mm ²)	Tear strength (N/mm)
1	1	1	1	1	11.4	65.32
2	1	2	2	2	15.39	56.29
3	1	3	3	3	15.28	59.78
4	2	1	2	3	13.02	68.92
5	2	2	3	1	16.43	60.78
6	2	3	1	2	13.77	62.32
7	3	1	3	2	10.49	46.89
8	3	2	1	3	11.51	64.83
9	3	3	2	1	9.69	71.65

Table 9. Range analysis for IGE reinforcement in fatliquoring process.

	Tensile strength					Tear strength		
Mean value 1	14.023	11.637	12.227	12.507	60.463	60.377	64.157	65.917
Mean value 2	14.407	14.443	12.700	13.217	64.007	60.633	66.620	56.168
Mean value 3	10.563	12.913	14.067	13.270	61.123	64.583	55.817	64.510
Range	3.844	2.806	1.840	0.763	3.544	4.206	9.803	10.750

Table 10. Experimental results of optimal combination in fatliquoring process.

No.	Dosage of PA-400 (%)	Dosage of IGE (%)	Penetrating time (h)	Tanning time (h)	Tensile strength (N/mm ²)	Tear strength (N/mm)
10	2	2	3	2	17.57	69.66
11	2	3	2	1	16.31	71.76

3.1.3 Effect of Dosage of IGE on physical property in fatliquoring process

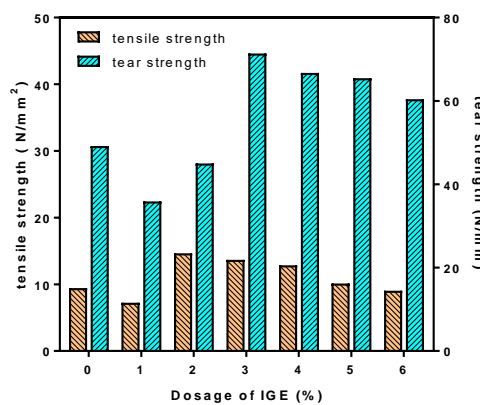


Fig. 2. Effect of IGE dosage on physical property in fatliquoring process.

As shown in Fig. 2, IGE exhibited obvious reinforcement effect on sheep skin in the fatliquoring process. The tensile strength and tear strength were enhanced with the increase of dosage of IGE, but they did not further increase when the dosage of IGE exceeded 2%, which may be attributed to the increasing of single-point combination between the epoxy group and collagen fibre when excess amount of IGE was used.¹⁴

3.1.4 Physical properties of different chemicals in tanning and fatliquoring process

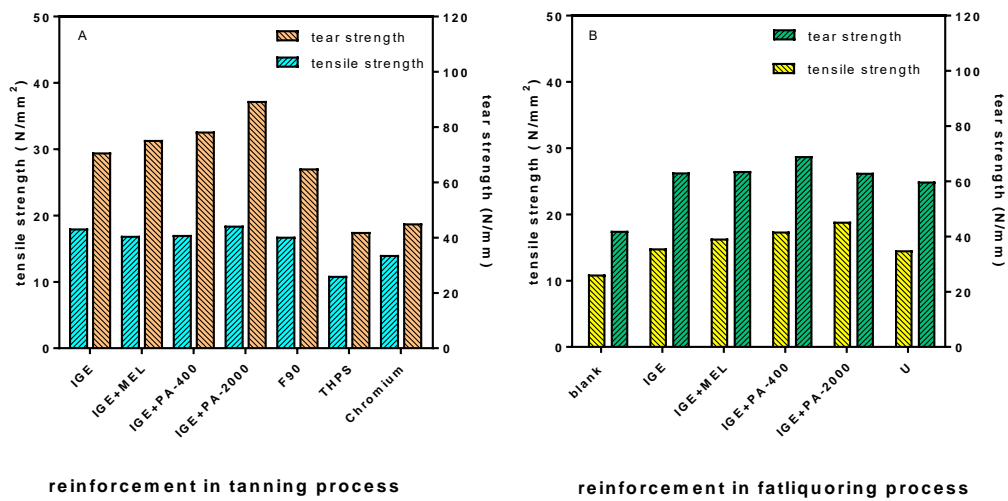


Fig. 3. Physical properties of sheep leather treated by different chemicals in tanning and fatliquoring process.

Fig. 3-A and Fig. 3-B illustrate the physical properties of sheep leather treated by different chemicals in tanning process and fatting process. Fig. 3-A shows that IGE and PA-2000 had the most obvious improvement on the tensile strength and tearing strength of sheep leather. Compared with chrome tanned leather, the tearing strength of tanned leather increased 56.8% when IGE was used as a reinforcement agent in tanning process. In addition, the tearing strength was significantly increased 97.9% when IGE-PA2000 was used. It can be seen from Fig. 3-B that the enhancement effect of IGE was similar to that of controlled chemical U, but the tensile strength and tearing strength of IGE treated sheep leather were significantly improved when polyamine was applied. When IGE and IGE-PA were used in fatliquoring process, it was found that the tear strength of leather increased 50.2%, while when the IGE-PA400 was used, the tear strength increased 64.3% compared with blank experiment. It could be suggested that PA-2000 or PA-400 first penetrated into the collagen fibre, and then the cross-linking should be mainly conducted among the epoxy groups of IGE, and amino groups of collagens and PA-2000 or PA-400, resulting the formation of interpenetrating network structure "rigid module" inside the collagen fibres (see Fig. 4).^{15,16} However, as compared with reinforcement in fatliquoring process, the improvement was higher for IGE-PA in tanning process, due to more amine group of collagen fibre exposed for IGE. But the interpenetrating network structure was difficult to form in fatliquoring process owing to more tanning and retanning agent have combined with the amine group of collagen fibre. Thus, IGE-PA exhibited more satisfactory reinforcement properties and was a competitive reinforcement candidate for sheep leather. It could be concluded the "rigid module" can increase the rigidity of the collagen fibres and improve the physical and mechanical strength of the leather.

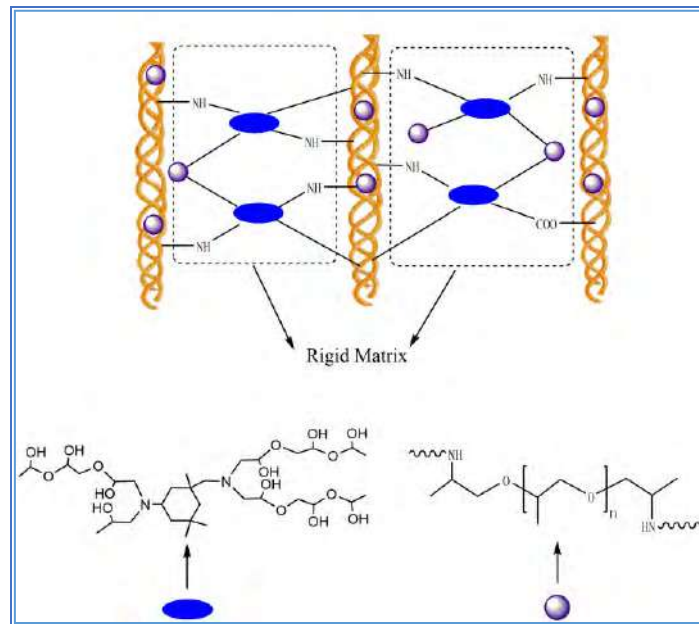


Fig. 4. Diagram of “rigid matrix” between IGE, PA and collagen fibre.

3.2 TGA analysis

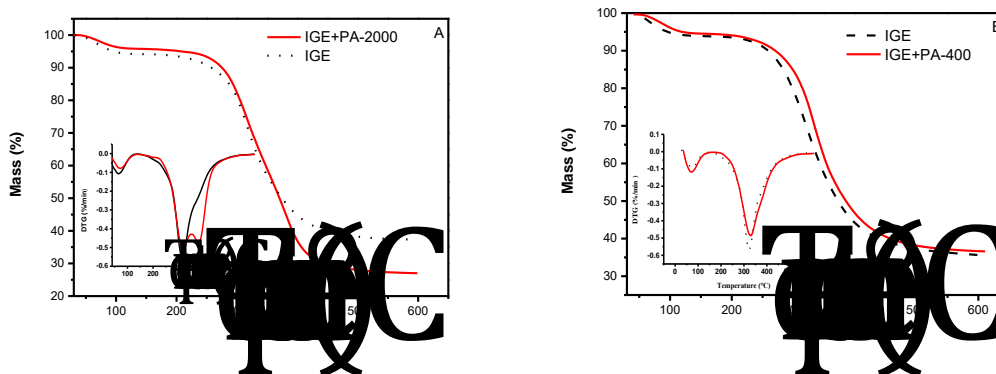


Fig. 5. TG and DTG thermograms of leather reinforced in tanning process (A) and fatliquoring process (B).

Fig. 5 is TG and DTG diagrams of leather reinforced in tanning and fatliquoring process. The decomposition temperature of samples was the second weightless peak of DTG. As shown in Fig. 5A, the decomposition temperature IGE treated leather was 315.2°C, while PA-2000+IGE treated leather appeared two decomposition peak temperature, the highest was 377.1°C. In combination with Fig. 3-A, the strength of IGE+ PA-2000 strengthened leather was the highest, indicating that IGE and polyether amine 2000 formed cross-linking among the collagen fibres and increased the decomposition temperature of the leather. It can be seen from Fig. 5B that the addition of PA-400 in the fatliquoring process can increase the thermal decomposition temperature of leather to a certain extent, but it was not as higher as that in the tanning process. It can be inferred that the covalent crosslinks between IGE, PA2000 and collagen fibres had formed to improve the thermal stability for sheep leather.

3.3 SEM analysis

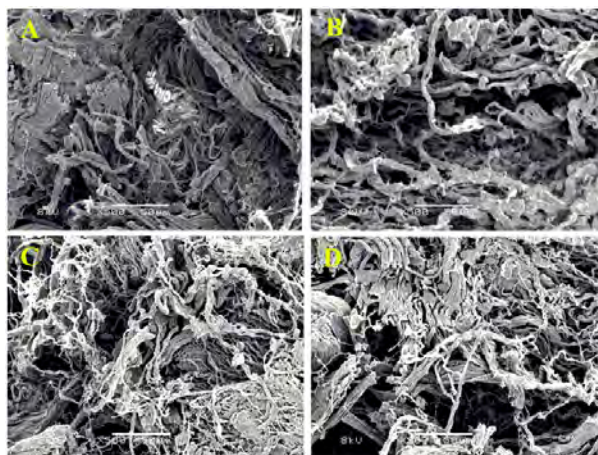


Fig. 6 SEM of leather (A: reinforced by IGE in tanning process, B: reinforced by IGE+PA-2000 in tanning process, C: reinforced by IGE in fatliquoring process, D: reinforced by IGE+PA-400 in fatliquoring process)

It can be seen from Fig. 6 that the dispersion of leather fibres with polyether amine participating in synergistic tanning and fatliquoring is significantly better than that of leather reinforced by IGE tanning alone. Generally, better fibre dispersion is in favour of the penetration of chemical materials into the collagen fibre network and react with the active groups on the collagen fibre, thus leading to increasing the mechanical strength of leather. As a result, IGE-PA exhibited more satisfactory fibre dispersion and therefore its outstanding reinforcement performance can be expected.

4 Conclusions

A new type of multi-epoxy tanning agent (IGE) was prepared and it proved that IGE had reinforcement effect on the strengths of sheep leather especially on tear strength. IGE and polyether amine can be used in tanning process with ethanol medium, and IGE-PA could show synergistic effect, resulting in a significant enhancement for sheep leather. IGE and IGE-PA can be also used in fatliquoring process to enhance the strength of sheep leather in water medium owing to the emulsification effect of fatliquoring agent. As a result, IGE-PA could be recognized as an effective reinforcement agent candidate for sheep leather.

Acknowledgement

This study was financial supported by the National Key R & D Program of China (2017YFB0308600).

References

1. Shan, Z. H., Guo, W. Y., Zhang, Y. C.: *Effect of application of leather chemicals on the strength of sheepskin leather*, *China Leather*, 31, 22-24, 2002
2. Ma, J.C., Li, Z. S., Li, J.: *Selecting chemicals to improve the tear strength of cattle split leather*, *Leather Science and Engineering*, 25, 39-43, 2015
3. Zhu, Z. J. : *Methods for increasing the tear strength of leather*, CN103103296A. 2013.
4. Hong, X. Q., Ma, H. W., Xu, J. N. et al.: *Influence of retanning agents on physical and pyrolysis of leather*, 43, 20-22, 2014

-
5. Mallikarjun, G., Saravanan, P.: *Microemulsion solutions of acrylic copolymers for retanning applications on chrome tanned goat skins*, *J. Am. Leather. Chem. Asso.*, 97, 215-224, 2002
 6. Wang, X. C., An, H. R., Sun, M., et al.: *Synthesis of acrylic resin retanning agent with a reinforcing effect by high solids content microemulsion copolymerization*, *J. Soc. Leather Technol. Chem.*, 89, 164-168, 2005
 7. Wang, X. C., An, H. R., Sun, M., et al. *Preparation of acrylic resin nanosized latex and its reinforced function to leather*, *Fine chemicals*, 22, 464-467, 2005
 8. Li, G. P.: *Leather chemical material chemistry and application*, Beijing: Light industry press, 1997
 9. Xu, W.; Zeng, H.; Zhou, J. et al. *Modification of fatliquored split by in-situ polymerization of n-butyl-methacrylate*. *J. Soc. Leather Technol. Chem.* 101,72-77,2017
 10. Xu, W.; Zeng, H.; Zhou, J. et al. *The reinforcement of leather split by constructing an interpenetrating network via in-situ recombination of PVA*, *J. Amer. Leather. Chem. Ass.* 113, 255-263, 2018
 11. Pang, X. Y., Ding, Z. W., Ding, W., et al.: *Investigation of the synthesis of a novel glycidyl ether-amine epoxy tanning agents and their tanning performance*, 114, 228-239, 2019
 12. QB/T 2710-2005, *Leather - physical and mechanical tests - determination of tensile strength and elongation*
 13. QB/T 2711-2005, *Leather - determination of tearing force by physical and mechanical tests: bilateral tearing*
 14. Di, Y. and Heath, R. J.; *Collagen stabilization and modification using a polyepoxide, triglycidyl isocyanurate*. *Polym. Degrad. Stab.*94, 1684-1692, 2009
 15. Chen, H., Shan, Z. H. *The being of metal-organic rigid matrix and synergistic effect of combination tannage*. *Leather chemicals*. 23,1-6,2006
 16. Covington A. D., Lampard G. S., Hancock R. A., et al. *Studies on the origin of hydrothermal stability: a new theory of tanning*. *J. Amer. Leather. Chem. Ass.* 93,107-120,1998

PRESERVATION OF BOVINE HIDE USING LESS SALT WITH LOW CONCENTRATION OF ANTISEPTIC

Majher I. Sarker¹, Wilbert Long III¹, Cheng-Kung Liu¹, Nicholas P. Latona¹ and George J. Piazza¹

1U. S. Department of Agriculture, Agricultural Research Service, Eastern Regional Research Centre, 600 East Mermaid Lane, Wyndmoor, PA 19038-8598, Phone: 215-233-6678. Fax: 215-233-6795. email: majher.sarker@ars.usda.gov

Abstract. A Conventional technique of bovine hide preservation requires approximately 40-50% sodium chloride or table salt on raw hide weight or 95% saturated brine in case of wet salting. This salt resides in wastewater after the soaking process and generates a huge environmental pollution in the form of total dissolved solids (TDS) and chloride (Cl⁻) during leather processing. The current research has developed an antiseptic based hide curing formulation using 45% saturated brine solution which reduces 50% salt usage in compare to the traditional method. For hide preservation, it is essential to arrest microbial attack on hide as the main constituent of raw hide is protein which is very susceptible for bacterial degradation. The newly developed formulations have been found more effective in limiting microbial growth on cured hide than the conventional method preserving the bovine hide for more than 30 days. In-process analysis of cured hides during storage period reveals the compatibility of the alternative curing process. Post-leather analysis e.g. grain pattern, scanning electron microscopic images, mechanical properties and organoleptic evaluation reveal that the crust leather produced from alternatively cured hides are comparable to the control obtained from traditionally preserved hide. The efficacy of the alternative system is also assessed by monitoring the environmental impacts caused by the leather processing effluents on the basis of TDS and chloride content, total solids (TS), total aerobic bacterial counts in soaking liquor, Bio-Chemical oxygen demand (BOD) and Chemical oxygen demand (COD). The environmental advantages of the alternative hide curing method are determined particularly by 50% reduction of TDS and chloride content. Therefore, this new development will not only preserve hide through better protection from microorganisms but also offer improved conservation of the environment.

1 Introduction

Animal hides and skins are valuable byproducts of meat industry because they are used to produce leather. Preservation of raw hide has always been a challenge for leather manufacturing companies as they are putrefied rapidly. The integrity of raw hide is the key to produce good quality leather. Animal hide contains a great variety of microorganisms, which are derived from air, water, soil, manure and extraneous filth.¹ In a living animal, bacteria and microorganism on its skins are held in control by the metabolic defences of the animal, but the flayed skins become vulnerable for bacterial attack within 5-6 h of removal.^{2,3} Skin microorganisms produce proteolytic and collagenolytic enzymes resulting in putrefaction of hide. The leather quality depends on the presence of necessary protein levels in raw hide. Therefore, it is extremely important to conserve protein from degradation in skin during the process of preservation.

Prevention of putrefaction is the main objective of hide curing process which can be accomplished by limiting or controlling microbial attacks on hides, either by killing the microorganism which is called bactericidal method or creating unfavourable conditions for the microorganisms to thrive, known as bacteriostatic method. The bactericidal method employs chemicals that are usually harmful for humans or living species and costly. On the other hand the bacteriostatic method utilizes dehydrating agents in bulk such as sodium chloride which generates pollution problems in terms of total dissolve solid (TDS) and chloride content in the resulting effluent from the soaking operation of leather production.

In traditional hide preservation process, 95% saturated brine solution or 40%-50% w/w sodium chloride on the raw hide's weight is used.⁴ Almost 75% of the salt ends up in the effluent stream

during soaking, which contributes to 40% of total solid content in the tannery effluent⁵ creating major salt pollution in the environment. Concentrated tannery effluent severely affects the germination of seeds and hampers the growth of seedlings and other floras when used for irrigation purpose or simply discharged to the field⁶. When the soils are irrigated with saline effluent, salts accumulate, unless they are leached out. Furthermore, saline irrigation water along with low-soil permeability, inadequate drainage, low rainfall and poor irrigation management, all cause salts to accumulate in soil, which has deleterious effects on crop production. Degradation of soils by salinity and sodicity profoundly affects environmental quality.⁷ The salts also affect release and solubility of heavy metals in solution, with potential adverse effects on water quality and plant growth.⁸ High concentration of sodium (Na^+) and chloride (Cl^-) affect plants directly by causing excessive uptake of these ions or indirectly by increasing soil pH. Therefore, it is very important to pursue new and more environmentally friendly methods of hide preservation.

Many researchers have investigated and proposed alternative hide curing methods which can be divided in to two categories: physical and chemical methods of hide preservation. As physical methods can be mentioned cooling⁹, cooling wit addition of ice¹⁰, cooling in vacuum¹¹, drying chamber¹² and irradiation based curing either by using gamma rays (photon emission from radioactive materials) or electron beams¹³. Although these physical methods are very convenient, as there is no chemical used, but have been found expensive and difficult to adopt in a hide processing facility. Therefore, chemical methods of hide preservation are more welcome due to simplicity of use and needless of expensive special equipment. The possibilities of using potassium chloride¹⁴, soda ash¹⁵, preservatives such as benzalkonium chloride¹⁶, antibiotics such as auromycin and terramycin¹⁷, neem oil¹⁸ and boric acid¹⁹ for preserving the hide have been explored. Higher cost, sub-optimal preservation efficiency, toxicity, poor quality of leather and adverse environmental impact are the main factors that explain why these methods have not been adopted commercially. Therefore, an alternative approach needs to be developed that eliminates/mitigates the problems associated with the existing hide preservation techniques.

In first part of this current research, a lower salt curing method was developed where, 45% saturated brine solution with low concentration of environmentally benign antiseptic was used to preserve bovine hide for more than 30 days.²⁰ This method reduced salt usage by more than 50% compared to the conventional method where 95% saturated brine solution is used. The efficacy of hide preserving formulations was assessed and reported²⁰ by monitoring a variety of parameters (i.e. microbial growth, water activity, moisture content, texture analysis, hair slip, odor, microscopic analysis and rehydration) of alternatively cured hides throughout the preservation period. The alternative method provided better resistance to microbial growth on skin than the conventional method during a 30 days storage period. This paper reports the 2nd part of low salt curing research which deals with the characteristics of leather produced from the alternatively cured hides and the environmental impacts caused by the method in compare to that generated by the traditional method of hide preservation.

2 Materials and Methods

Freshly flayed and de-fleshed bovine hides were acquired from a local meat packing facility, courtesy of JBS Packerland (Souderton, PA). Each hide was split down the back into left and right segments. The sides were then cut into pieces that weighed approximately 800 – 1000 g, with dimensions of 12 in x 12 in. All chemicals used for hide preservation listed in **Table 1** were of commercial grade. alkyltrimethylammonium bromide (ATMAB), chlorhexidine di-gluconate (CDG), lactic acid solution $\geq 85\%$, peracetic acid solution, hydrogen peroxide were purchased from Sigma Aldrich Chemical company (Milwaukee, WI). All other reagents used for the formulations were of the highest purity available from commercial suppliers. Brine solutions were prepared by dissolving

specific amount of common salt (sodium chloride) in water and a salometer was used to measure their saturation level. The preparation of all curing formulations was carried out as detailed in Table 1, where mixed or dissolved in tap water at room temperature (~21 °C). All formulations were prepared ~12 h prior to the experiments.

Table 1. Composition of the developed curing formulations for hide preservation

Formulations	Composition
F-A (control)	95% saturated brine soln. + 0.043% NaOCl (v/v)
F-B	45% saturated brine soln. + 0.6% ATMAB (wt./v) + 0.06% CDG (v/v)
F-C	45% saturated brine soln. + 0.6% ATMAB (wt./v) + 0.06% CDG (v/v) + 0.043% NaOCl (v/v)
F-D	45% saturated brine soln. + 0.6% ATMAB (wt./v) + 0.06% CDG (v/v) + H ₂ O ₂ (135 ppm) + Peracetic Acid (80 ppm)
F-E	45% saturated brine soln. + 0.6% ATMAB (wt./v) + 0.06% CDG (v/v) + 0.043% NaOCl (v/v) + 2% Lactic Acid (v/v)
F-F	45% saturated brine soln. + 0.6% ATMAB (wt./v) + 0.06% CDG (v/v) + H ₂ O ₂ (135 ppm) + Peracetic Acid (80 ppm) + 2% Lactic Acid (v/v)

2.1 Laboratory Scale Protocol for the Alternative Hide Preservation

A 150 % float (volume of sol/w of hide or v/w) was used for preservation treatment. Hide pieces were soaked individually in the 6-in-1 Dose drums (Dose Maschinenbau GmbH, Lichtenau, Germany) with in respective solutions for 18 h. During the treatment, the 6-in-1 Dose drums controls were set to 6 rpm for tumbling. A 95% saturated brine solution with 0.043 % (v/v) bleach (NaOCl) was utilized for the control (F-A, **Table 1**). This formulation is being used commercially for conventional hide preservation. For alternative methods (F-B to F-F, **Table 1**), a 45 % saturated brine solution was used along with other additives which cut the salt usages by more than 50 %. After 18 h of treatment, the hide samples were hung to dry, folded and stored in a humidity chamber at the temperature of 38-40 °C, and were monitored periodically for physical changes such as smell and hair slip which are the indications of putrefaction.²¹ The effectiveness of the developed curing formulations was assessed by determining different parameters of cured hides during storage period and the results were recorded and published.²⁰

2.2 Analysis of Soaking Liquid Generated in Leather Processing

After preservation for 35 days, the hide samples were subjected to soaking with 200% float of water for 4 hours. Then, the spent liquors from the soaking operation were collected and analyzed for different pollution parameters such as, total dissolved solid (TDS), chlorides (Cl⁻) content, total solid (TS) using standard analytical procedures.^{22,23,24} Aerobic bacterial colony count, total carbon (TC), total organic carbon (TOC), chemical oxygen demand (COD), biochemical oxygen demand (BOD) of soaking liquid were also determined to assess the overall pollution load from soaking operation in preparation of leather from the alternatively cured hides.

2.2.1 Total aerobic bacterial colony count of soaking liquor

The samples were collected independently in sterile containers to analyze residual aerobic bacterial concentrations in the soaking liquors, 1 ml of sample solution was serially diluted in sterile water. Diluted sample was then plated on Tryptic Soy Agar and incubated at 37 °C for ~24 hours and bacterial counts were reported in log CFU/ml. with the lowest detection level of 1 log/CFU ml. All samples were conducted in triplicate.

2.2.2 Analysis of TOC and COD in soaking liquor

To determine TOC and COD of the soaking liquids, a Quick COD/TOC ultra single-stream analyzer purchased from Liquid Analytical Resources LLC (LAR), West Bend, WI was used. LAR's high temperature TOC analyzers provide a summary measurement of organic contaminants by oxidizing a sample's carbon compounds (Total Carbon, TC) in a high temperature furnace (1200 °C). A Near Infrared Detector then measures the resulting CO₂. Total Inorganic carbon (TIC) is measured separately, then subtracted from the total carbon, thus providing Total Organic Carbon (TC-TIC=TOC). This method is derived from EPA Standard Method 415.1.

LAR's COD analyzer's operating method is formalized as ASTM D6238-98. This method also combusts the sample at 1200 °C, but uses a nitrogen carrier gas and measures oxygen consumption using a zirconium dioxide O₂ gas detector. LAR's high temperature method provides accurate, repeatable results in three minutes, uses no reagents and achieves far greater accuracy and repeatability of 3% coefficient variation (CV), compared to ±20% which follows US EPA Method 410.4.

2.2.3 BOD analysis of soaking liquor

The biochemical oxygen demand (BOD) in soaking liquor is the amount of oxygen that is consumed during the degradation of organic substances through biochemical processes. For BOD measurement, each sample was analyzed for 5 days using a Lovibond BOD-System BD 600 (Tintometer Inc. Sarasota, FL). BOD measurement was carried out by means of pressure differential in a closed system (respirometric BOD measurement). The BOD measuring unit comprising test bottle and BOD sensor, is a closed system. There is a gas compartment with a defined quantity of air in the test bottle. The bacteria in the soaking water filled in the bottle consume the oxygen dissolved in the sample over the course of BOD measurement. It is replaced by air oxygen from the gas compartment of the test bottle. The simultaneously developing carbon dioxide is chemically bound by the potassium hydroxide in the seal cap of the test bottle. As a result a pressure drop occurs in the system, which is measured by the BOD sensor and shown directly in the display as a BOD value in mg/l O₂. The system records a measurement every hour on the first day, every other hour on the second day, and once every 24 hours starting on the third day up to 5th day.

2.3 Tanning of Cured Hides

After soaking operation, the alternatively cured hide samples were placed in one dehairing drum and the control sample panel was placed in another dehairing drum and de-haired per the USDA tanning protocol.^{25,26,27} All the hide panels were combined into one drum for the pickle, tanning, re-tanning, coloring, and fat liquoring steps. The samples were tanned into crust upper shoe leather and kept in a temperature (21 °C) and humidity (50% relative humidity) controlled environmental chamber (Caron Environmental Chamber, Marietta, OH) until subjective, mechanical, and microscopic analyses were performed.

2.4 Evaluation of Leather Quality

To assess the effects of the hide preserving formulations on leather quality produced from alternatively cured hides, the mechanical properties of the produced crust leather were measured. The mechanical properties included tensile strength, Young's Modulus ("stiffness"), elongation ("stretchability"), and fracture energy ("energy required to open unit area of crack surface") were conditioned and tested as per the ASTM methods D1610 and D2209 to verify the effect of the newly developed hide preservation formulas on the quality of leather. Five dumbbell shaped leather samples were cut from each leather piece following the protocol in ASTM D2209 parallel to the backbone. The average thickness range of the leather samples were observed from 2.13 to 2.82 mm. An Insight-5 test frame and Testworks-4 data acquisition software (MTS Systems Corp., Minneapolis, MN) were used to evaluate the mechanical properties of the leather samples. The strain rate and the grip distance for this study were set to 24.5 cm/min and 10.16 cm respectively. Samples were tested in a room set at 23 ± 3 °C and 50 ± 5 % relative humidity. Tannery subjective tests (break, handle, fullness, and color) were conducted by an expert in-house USDA tanner.

2.5 Microscopic Imaging

Representative crust leather samples produced from the hides which were cured by individual hide preserving formulation (F-A to F-F, Table 1) were inspected under a stereo microscope (Nikon Digital Microscope SMZ-2T, Melville, NY) to determine any detectible changes in the hide grain structure from curing. Additionally, scanning electron microscope (SEM) images were taken to identify potential finer structural changes in the surface of the leather. For SEM images, samples were mounted on stubs and sputter gold coated for 1 minute (EMS 150R ES, EM Sciences, Hatfield, PA). Samples were viewed with a FEI Quanta 200 F Scanning Electron Microscope (SEM), (Hillsboro, OR, USA) with an accelerating voltage of 10KV in high vacuum mode.

3 Results and Discussion

Five novel formulations have been developed and tested to preserve bovine hide where, a 45% saturated brine solution in combination with bactericidal antiseptics is used. This new development reduces salt consumption by 50% from the conventional curing process, where 95% saturated brine solution is being used. The effectiveness of the newly developed formulas in hide preservation has been reported in previously published article.²⁰ This technology is adopted principally to address the pollution problem created from conventional curing methods either by the soaking liquor discharged to the environment during leather making process or/and tannery effluents. To develop the reported five formulations, a surfactant (ATMB) and an antimicrobial agents (CDG) have been used in common. ATMB is a quaternary ammonium compound which in addition to possess antibacterial properties.^{28,29} ATMB is able to damage cell membranes and destroy the cellular structure of various microorganisms including fungi, bacteria and other single cell organisms. ATMB is non-toxic when applied directly to the skin. Chlorohexidine salt (CDG) dissociates in water and releases positively charged chlorhexidine cation which results bactericidal effect through the binding of this cationic molecule to negatively charged bacterial cell walls.³⁰ CDG is active against Gram-positive and Gram-negative organisms, facultative anaerobes, aerobes, and yeasts.³⁰ Among the additives, lactic acid (a alpha-hydroxy acid) is a well-known antimicrobial³¹ and also acts as humectant³² which attracts water and improve hydration of the stratum corneum of the skin. Alpha-hydroxy acid such as lactic acid also increases cohesion of the stratum corneum cells and thus reduces roughness and scaling. Also two combinations of spore killing agents, hydrogen peroxide with peracetic acid³³ (F-D and F-F, Table 1) and sodium hypochlorite³⁴ (F-C and F-E, Table 1) have

been added to enhance the antimicrobial properties of the particular formulations. In this paper, the environmental impacts of leather making from the alternatively versus traditionally cured hides have been evaluated and also the impact of the developed curing formulations on leather are reported.

3.1 Soaking Liquor Analysis

3.1.1 Aerobic bacterial colony count determination

Aerobic bacterial colony counts were conducted to determine the bacterial concentration per mL of soaking liquor up to 5 log CFU/mL. Figure 1 shows all the formulations control bacterial growth significantly better than the control even in spent liquor. A 10 fold dilution of soaking liquor from traditionally preserved sample (F-A) were TNTC (Too Numerous to Count) thus they had counts in excess of 5 log CFU/mL. However, colony counts for F-B and F-E were 2.96 and 2.30 log CFU/mL respectively. No microbial growth was observed from the other soaking liquors in a 24 hours incubation period at 37 °C. This results demonstrate the effectiveness of these formulations in limiting microbial growth compare to the control which consisted of the industry standard of 95% brine solution.

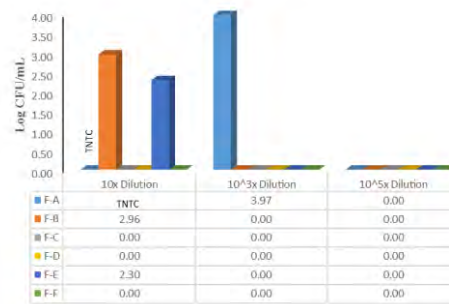


Fig. 1. Bacterial colony count per milliliter of soaking liquors of hide samples preserved by the different formulations

3.1.2 Chloride content determination

The determination of chloride content in spent soak liquor directly correlates to the salinity in tannery waste water.

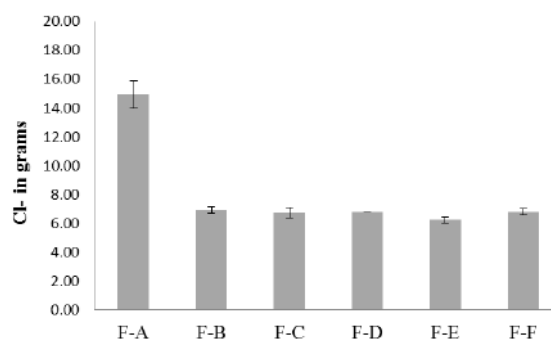


Fig. 2. Chloride content of spent liquors generated by soaking of 1 kg of preserved hide

The results in Figure 2 clearly shows that, comparing to conventional treatment (F-A), chloride content in spent soaking liquor can be reduced by 50% or more if any of the developed formulation is used for hide preservation. This significant reduction in salinity and chloride loads will help in achieving cleaner and greener leather processing.

3.1.3 Determination of TOC and COD in soaking liquor

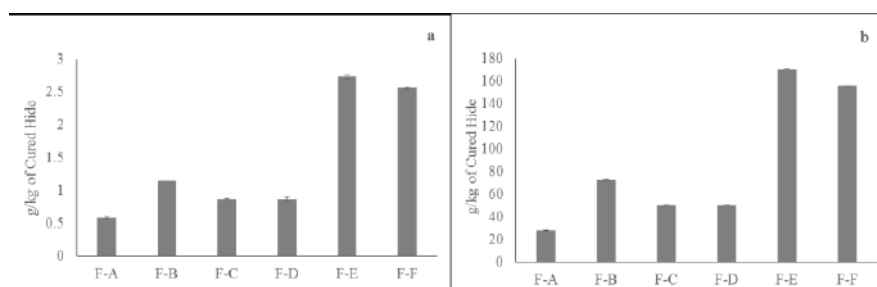


Fig. 3. a) Total Organic Carbon (TOC) and b) Chemical Oxygen Demand (COD) values (in gram) of soaking liquors processing 1 Kg of cured hide.

The results of COD and TOC analysis are consistent to each other. Higher carbon content present in the soaking liquor will presumably result higher COD. Compared to the control (F-A), both TOC and COD loads are increased for the alternative treatments (F-B through F-F). This is due to the addition of antimicrobials in newly developed hide preserving formulas. However, the significant increase in TOC and COD loads for F-E and F-F could be accounted for the use of 2% lactic acid in the formulations.

3.1.4 Determination of BOD

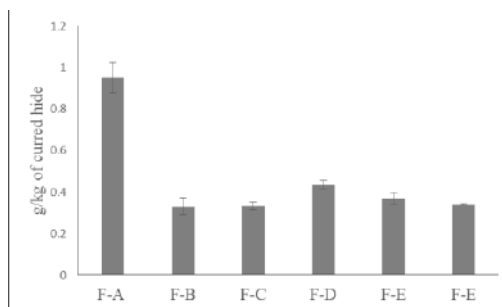


Fig. 4. Biochemical Oxygen Demand (BOD) values (in gram) of soaking liquors processing 1 Kg of cured hide.

Five day analyses was carried out for the BOD determination of the soaking solutions of differently cured hides. Results show a significant decrease of 54 to 65% in BOD load for the soaking liquors of alternatively cured hides in compare to traditionally preserved hide. The higher BOD value for the control is due to the presence of high concentrations of bacteria in the soaking liquor which is consistent with the bacterial colony count analyses as shown in Figure 1. Beside the availability of other biochemical substances, the dead cells of microorganism also provide with the source of nutrients for the living cells present in the soaking effluents.

3.1.5 Determination of Solid Pollutants

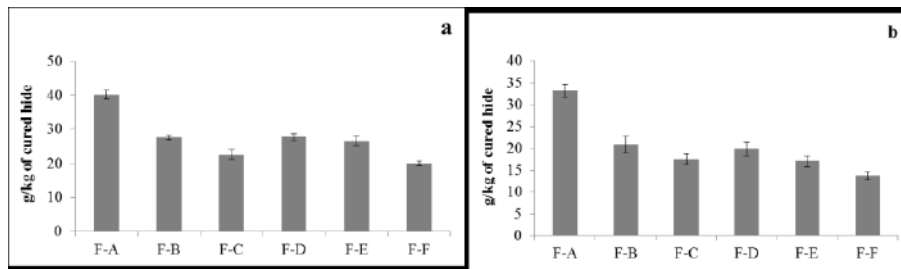


Fig. 5. Pollution load generated in the soaking process of hides cured by the different formulations: a) Total Solid (TS) and b) Total Dissolved Solid (TDS)

The data in Figure 5 represent the amount of solid pollutants in the soaking liquors contributed by the different curing chemicals. The results clearly show that there is substantial reduction in the values of the pollution parameters, Total solid (TS) and Total dissolved solid (TDS) for the alternative methods compared to the conventional treatment. These changes are caused mainly due to the reduction of salt in the preservation step.

3.2 Quality Determination of Crust Leather

After the preservation period of 35 days, the cured hides were processed into crust upper shoe leather following the standard tanning protocol.

3.2.1 Grain surface pattern study

In-order to study the surface finesse or coarseness of the crust leather, the grain pattern was studied. The grain structure of the leathers made from the traditionally (F-A) and alternatively cure hides (F-B, F-C, F-D, F-E and F-F) were analyzed under a stereo microscope. There was no discernable difference between the grain structure of leather made from conventionally treated hide and leathers made from the experimentally treated hides (Figure 6). Additionally, the leather panels were folded, and a stereo microscopic image was taken at the crease to assist with analysis of the surface features (Figure 7). Again, there was no discernable difference between the leathers made from the hides treated with the control and developed formulas. No sueding (fraying) was observed from any of the samples. This indicates that none of the developed formulation for hide preservation damage the hide grain.

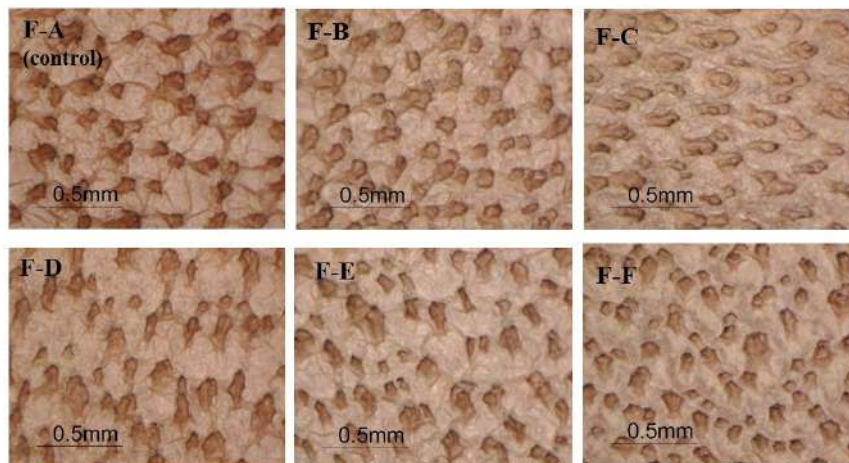


Fig. 6. Stereo microscopic images of the leather made from the differently preserved hides. Bars represent 0.5mm.

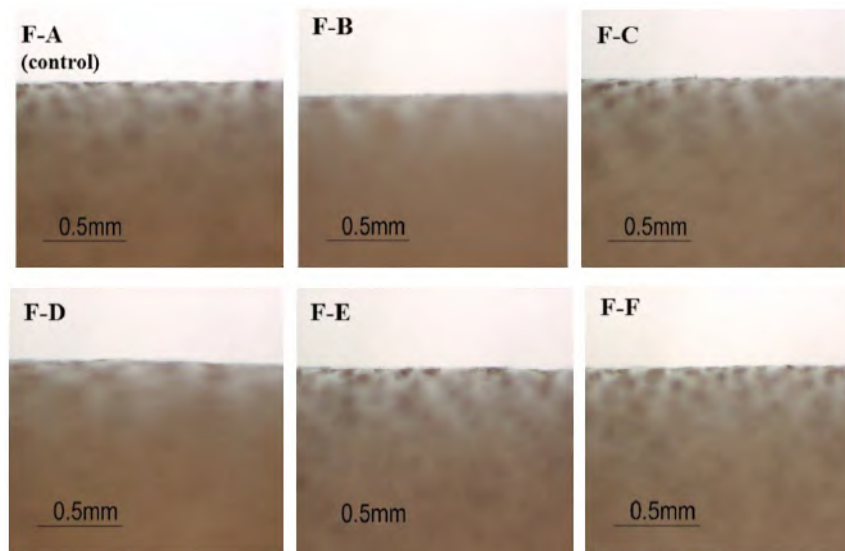


Fig. 7. Stereo microscopic images of the leather at the crease made from the differently preserved hides. Bars represent 0.5mm.

3.2.2 Surface image of crust leather using scanning electron microscope

Surface images of crust leathers from individually cured hides were observed using scanning Electron microscope at 100 x magnifications. The images (Figure 8) of the crust reveal uneven or rough surface of the leather made from traditionally preserved hide (F-A), whereas the leather from alternatively cured hides appears to have smoother and homogeneous surfaces.

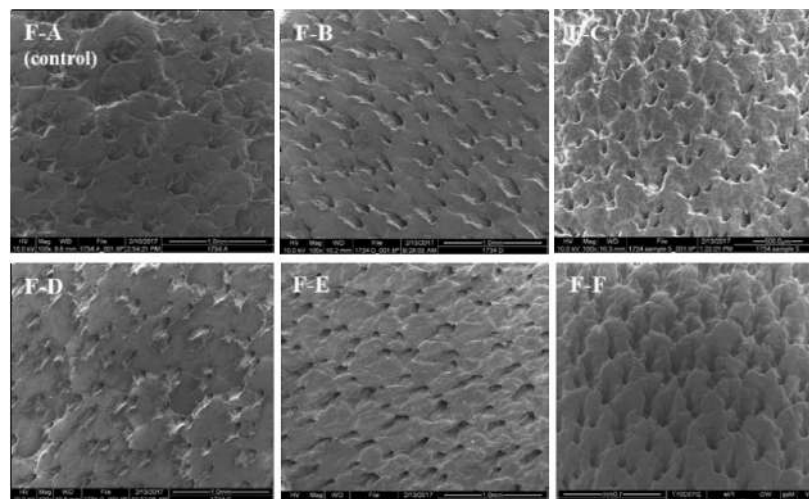


Fig. 8. SEM surface images at 100 x (as shown in bar length) of crust leathers from individually preserved hides.

3.2.3 Determination of mechanical properties of leather

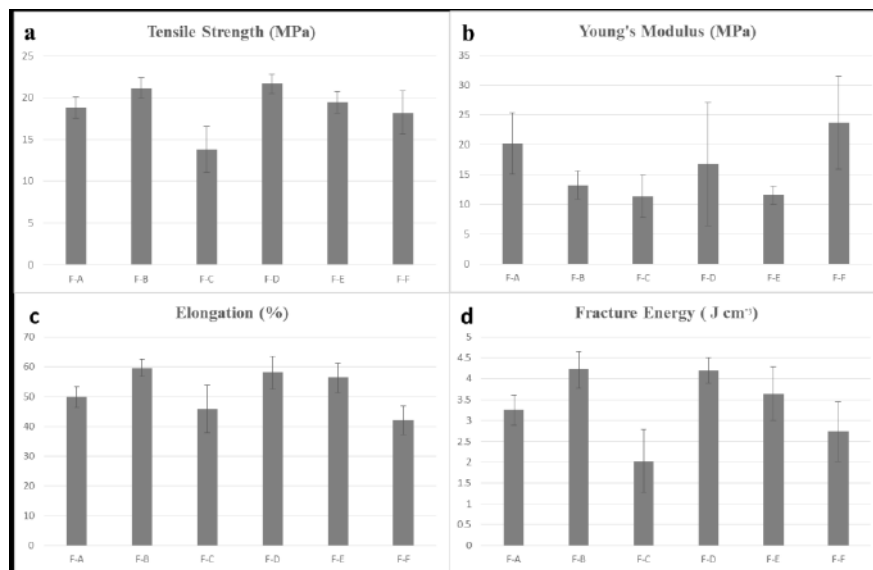


Fig. 9. Mechanical properties of the crust upper shoe leather from differently cured bovine hides

The overall mechanical properties of the resulting leather products from the alternatively cured hides were comparable to that produced from the traditionally preserved hide (F-A). In some cases alternatively cured hides produce better quality of leather. For example, leather yielded from F-B and F-D treated hides showed improved quality in every property shown in Figure 9 in comparison to quality of leather produced from control treatment (F-A). More flexible leathers resulted from alternatively preserved hides in compare to conventionally treated hide (Figure 9b) and this is potentially because of the using of low salt.

3.2.4 Subjective Evaluation of Leather

Crust leathers from preserved hides were assessed for softness, fullness, grain tightness (break), color and general appearance by hand and visual examination (Figure 10). The leathers were rated on a scale of 0-5 points for each functional property where higher points indicate better property.

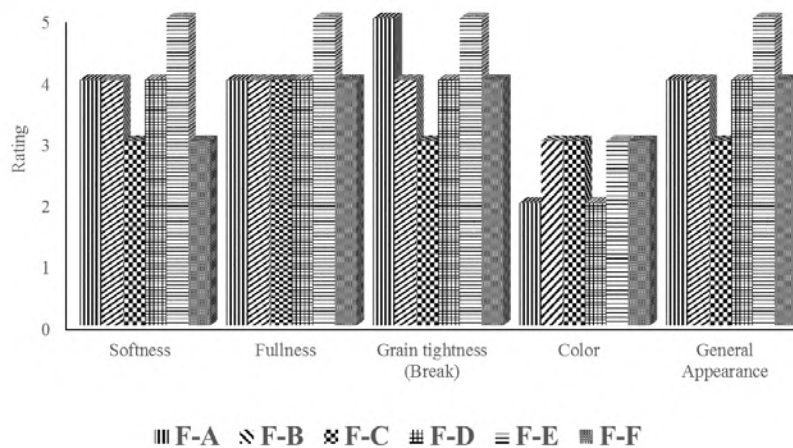


Fig. 10. Organoleptic evaluation of crust leathers from differently cured hides

The leathers from alternatively cured hides by every formulation exhibit better or similar fullness and color in comparison to the leather from a traditionally cured hide. Especially, the leather from the F-E treated hide which has superior rating in almost every property of the subjective test. Other formulated hides produced leathers of comparable quality to the conventionally processed leather (F-A).

4 Conclusions

The developed curing formulas are proven to be effective in preserving bovine hide for more than 35 days limiting microbial growth on hide better than the traditional curing process. The new process utilizes 45% saturated brine solution in general, which offers more than 50% reduction of salt usage in conventional method. The dehydrating brine solution helps to keep the moisture level of cured hides low creating an inhospitable environment for the bacteria to survive and a low concentration of antiseptic kill the bacteria at the same time. The evaluation of environmental impacts from process discharge reveals that the alternative hide curing methods reduce pollution loads significantly in comparison with the traditional method in terms of Chloride content, TDS, TS, BOD and solid pollutants. From grain pattern analysis, surface images, mechanical properties and organoleptic evaluation, no detrimental impact has been identified on crust leather made from the experimentally treated hides. Rather, in many cases, alternatively treated hides appear to produce better quality of leather than the control. The results obtained in this study suggest that this technology can be potentially used as an alternative to traditional salt curing to preserve raw bovine hide.

References

1. Birbir, M., Ilgaz, A.; *Isolation and identification of bacteria adversely affecting hide and leather quality. J. Soc Leath Tech Ch.* **80**, 147-153, 1995.
2. Edward, H.B., William, N.M., Karl, K.P., Cooke, H.R., Dudley, L.; *Mathematical model of raw hide curing with brine. JALCA* **103**, 167-173, 2008.
3. Thorstensen, T.C.; *Practical leather technology. Krieger Publishing Company, Malabar, Florida, USA*, pp. 30, 1993.
4. Hausam, W.; *Behaviour of hide during salting and the action on the hide protein. JALCA*, 35-44, 1951.
5. Ramasami, T., Rao, J.R., Chandrababu, N.K., Parthasarathi, K., Rao, P.G., Sarvanan, P., Gayathri, R., Sreeram, K.J.; *Beamhouse and tanning operation: Process chemistry revisited. J. Soc. Leather Technol. Chem.* **83**, 39-45, 1999.
6. Sharma, P.K.; Varma, S.K.; Datta, K.S.; Kumar, B.; Angrish, R., *Differential response of wheat to chloride and sulfate, salinities at germination and early seedling growth. Haryana Agricultural University. Journal of Research.* **26**, 1-7, 1996
7. Erdei, L., Kuiper, P.C.J.; *The effect of salinity on growth, cation content, Na⁺-uptake and translocation in salt-sensitive and salt-tolerant Plantago Species. Physiol. Plant.* **47**(2), 95-99, 1979.
8. Kahlown, M.A., Azam, M.; *Effect of saline drainage effluent on soil health and crop yield. Agric. Water Manage.* **62**, 127-138, 2003.
9. Vijayalakshmi, K.; Judith, R.; Rajakumar, S., *Novel plant based formulation for short term preservation of animal skins. Journal of Scientific and Industrial Research.* **68**, 699-707, 2009.
10. Kanagaraj, J.; Chandra, N.K., *Alternatives to salt curing techniques-A review. Journal of Scientific and Industrial Research.* **61**, 339-348, 2002.
11. Gudro, I.; Valeika, V.; Sirvaityte, J., *Short term preservation of hide using vacuum influence on properties of hide and of processed leather. PLOS ONE.* **9**(11), 1-9, 2014.
12. Waters, J.J., Stephen, L.J., Sunridge, S.; *Controlled drying. J. Soc. Leather Tech. Chem.* **65**, 32, 1997.
13. Bailey, D.G.; *Evergreen hide market ready. The Leather Manufacturer* **115**, 22-26, 1997.
14. Bailey, D.G., Gosselin, J.A.; *The preservation of animal hides and skins with potassium chloride. JALCA* **91**, 317-333, 1996.
15. Rao, B.R., Henrickson, R.L.; *Preservation of hides with soda ash. JALCA* **78**, 48-53, 1983.

16. Cordon, T.C., Jones, H.W., Naghski, J., Jiffee, J.W.; Benzalkonium chloride as a preservative for hide and skin. *J. Soc. Leather Trade Chem.* **59**, 317-26, 1964.
17. Berwick, P.G., Gerbi, S.A., Russel, A.E.; Use of antibiotics for short term preservation. *J. Soc. Leather Trade Chem.* **74**, 142-50, 1996.
18. Venkatachalam, P.S., Sadulla, B., Duraisamy, V.S., Krishnamurthi; Short-term preservation of hide with neem oil, *J. Soc. Leather Tech. Chem.*, **61**, 24, 1977.
19. Hughes, I.R.; Temporary preservation of hides using boric acid. *J. Soc. Leather Trade Chem.* **58**, 100-103, 1974.
20. Sarker, M.; Long, W.; Liu, C-K., Preservation of bovine hide using less salt with low concentration of antiseptic, part I: effectiveness of developed formulations. *JALCA*, **113**(1), 12-18, 2018.
21. Sivaparvathi, M., Nandy, S.C.; Evaluation of preservatives for skin preservation. *JALCA*, **69**, 349-62, 1974.
22. Eston, A.D.; Clesceri, L.S.; Greember, A. E. Standard method of the examination of water and wastewater. American Public Health Association, 19th ed. Washington, DC, 1995.
23. ASTM D4458-94 Standard test method for chloride ions in brackish water, seawater, and brines. ASTM International, West Conshohocken, PA, 1994.
24. Taylor, M.M.; Diefendorf, E.J.; Phillips, J.G.; Fearheller, S.H.; Bailey, D.G. Wet process technology 1. Determination of precision for various analytical procedures. *JALCA*, **81**, 4-18, 1986.
25. Cabeza, L.F, Taylor, M. M., DiMaio, G. L., Brown, E. M., Marmer, W. N., Carrio, R., Celma, P. J., Cot, J. Processing of Leather Waste: Pilot Scale Studies on Chrome Shavings. Part II. Purification of Chrome Cake and Tanning Trials. *JALCA* **93**(3), 83-98, 1998.
26. Long, W.; Sarker, M.; Marsico, R.; Ulbrich, L.; Latona, N.; Muir, Z.; Liu, C-K.; Efficacy of citrilow and ceure spray wash on prevalence of aerobic and enterobacteriaceae bacteria/gram-negative enteric bacilli and cattle hide quality. *J. Food Safety*, **e12441**, 1-7, 2018.
27. Long, W.; Sarker, M., Liu, C-K; Evaluation of novel decontamination wash formulations on bovine hides for meat safety and leather quality assurance. *Advance Journal of Food Science and Technology*, **14**(2), 33-41, 2018.
28. Laemmli, U. K.; Cleavage of structural proteins during the assembly of the head of bacteriophage T4. *Nature*, 680-685, 1970.
29. Ito, E., Yip, K. W., Fonseca, S. B., Hedley, D. W., Chow, S., Xu, G. W., Liu, F. F.; Potential use of cetrimonium bromide as an apoptosis-promoting anticancer agent for head and neck cancer. *Mol. Pharmacol.* 969-983, 2009.
30. Leikin, J. B., Paloucek, F. P.; Chlorhexidine Gluconate", *Poisoning and Toxicology Handbook* (4th ed.). Informa, 2008.
31. Mies, P. D., Covington, B. R., Harris, K. B., Lucia, L. M., Acuff, G. R., Savell, J. W.; Decontamination of cattle hides prior to slaughter using washes with and without antimicrobial agents. *J. Food Prot.* 579-582, 2004.
32. Lynde, CW.; Moisturizers: what they are and how they work. *Skin Therapy Lett.* **6**(13), 3-5, 2001.
33. Leggett, M.J.; Schwarz, J.S.; Burke, P.A.; McDonnell, G.; Denyer, S.P.; Maillarda, J.; Mechanism of sporicidal activity for the synergistic combination of peracetic acid and hydrogen peroxide. *App. and Env. Micro.* **82**(4), 1035-1039, 2016.
34. Sandle, T. Risk of microbial spores to cleanrooms: Part 2: Selection of sporicidal disinfectants. *Clean Air and Containment Rev.* **29**, 14-16, 2017.

Acknowledgments

The authors would like to thank Vincent Hui, an undergraduate student at Drexel University for his help in soaking liquor analysis. We would also like to thank Joe Uknalis for preparing and taking SEM micrographs of our samples. This research was supported in part by an appointment to the Agricultural Research Service (ARS) Research Participation Program administered by the Oak Ridge Institute for Science and Education (ORISE) through an interagency agreement between the U.S. Department of Energy (DOE) and the U.S. Department of Agriculture (USDA). ORISE is managed by ORAU under DOE contract number DE-AC05-06OR23100. All opinions expressed in this paper are the author's and do not necessarily reflect the policies and views of USDA, ARS, DOE, or ORAU/ORISE.



ENGINEERING SESSION

COLD MILLING: INNOVATIVE TEMPERATURE/HUMIDITY CONTROL ON MILLING OPERATION

A. Galiotto and A. Peruzzi

1 Erretre spa - Italy

a)Corresponding author: adriano@erretre.com

Abstract. Air temperature and humidity are fundamental in the milling operation. There is a complicated correlation between air conditions and leather moisture that is practically impossible to predict in industrial process. Many important characteristics like softness, grain, pebble, yield depend on leather moisture. This patented system is the latest improvement in milling drums technology that keeps the leather cooler and allows a precise and optimal humidity control. Designed for soft, tight-grained leathers, especially from organic tannages and opened to a wide range of new operating conditions impossible with traditional machinery. The original new design makes the milling drum completely independent from the outside environment with many advantages: consistency over seasons, shorter transition time, energy savings.

1 Introduction

In the leather industry “milling” is meant a mechanical processing in which leathers are subjected to mechanical action due to its rolling/falling inside the cylindrical body which constitutes the main part of the milling drum.

Simultaneously with the mechanical action, it is possibile to have a conditioning of the material present inside the cylindrical drum by means of air subjected to predetermined temperature and humidity. Temperature and humidity controls and dust filtration are demanded to external unit identified with name “deduster”.

The application of a dedusting unit on wood milling drum starts between 1920-1930 [2], stainless steal milling drum starts mid-seventy. This new generation of drums were improved for dust removal and air conditions control [3]. New heating and humidifying unit were designed and milling became a key operation in many articles to enhance leathers’ features. Thanks to the success of this first generation of controlled milling drums a large number of innovations were introduced in the period 1990-2010 like filter performance and air quality control [4], chemicals injection [6]. As result of those innovations consistent mass production and an automatic and easy to use machine is what the market know nowadays.

2 Result and discussion

Physics behind milling drums can be briefly summarized as follow: leather are treated by centrifugal force in a rotating drum; the amount of energy generated inside the drum by this movement depend on many variables: hides' number and size, thickness, drum size and construction, outside temperature, leather moisture, finishing/tanning chemicals.

This energy (potential and friction) raise internal temperature but the increasing rate is not predictable. Part of this energy will be absorbed by the structure, part lost, part remain on hides. The result of this energy, continuously generated during the whole process, impact on the

temperature and humidity control. Production data show this energy is able to increase inside air temperature from 5 to 15°C.

This temperature growth could affect milling operation in some critical situation and caused undesired results. This can be analyzed on a batch process, like milling, only through a production data registration and comparison with quality inspection.

Some different design were tried [1] in order to improve temperature control but no one of this consider this “self generated” energy before the Erretre Cold Milling patent [5]. Standard milling drum exchanges air with outside to keep the temperature down, this air is normally dryer than inside air and as a results of that there are two negative impacts. Leathers dry out and drum sprays water inside to counteract this effect but never reach an equilibrium. Static energy is generated reducing de-dusting efficiency.

Work experience of those conditions is leathers' shrinkage with yield and grain quality loss. Temperature is the key parameter, air humidity and moisture depend on it.

The tannage and retan/fatliquor determines the drying out rate, all organic tannages loose water faster than chromium leathers so are very susceptible to low RH and high temperatures condition. Water is coming into the drum from the humidity control or from hides, changes on initial moisture cause variable milling results if perfect control is not realised.

The original Cold Milling design, recognized by international patent, is a new temperature control based on two separated circuits. Milling drum became a completely closed system, independent from the external ambient. No air exchange is needed during the process finding a solution of all limitations described previously.

Moreover, VOC contaminations are prevented, hides are always in contact with their own air and the emissions generated inside the drum during the process.

From the original idea tests started in 2018, several batches of different articles for a total of more than ten thousand hides from different customers and articles (mainly automotive seat and nappa shoes upper) were analyzed. Quality and appearance were checked by independent technician, a quality improvement and a reduced grain loss were detected as a results of this new technology.

For all batch tested initial temperature is constant thanks to energy absorbed by Cold Milling circuit.

3 Conclusion

Air temperature and humidity are fundamental in the milling operation. There is a complicated correlation between air conditions and leather moisture that is practically impossible to predict in industrial process.

Many important characteristics like softness, grain, pebble, yield depend on leather moisture. Cold Milling is the latest improvement in milling drums technology that keeps the leather cooler and allows a precise and optimal humidity control.

Production data show this original designed made for soft, tight-grained leathers, especially from organic-tannages can be opened to a wide range of new unattainable operating conditions with traditional machinery.

Cold Milling makes the milling drum completely independent from the outside environment with many advantages: consistency over seasons and locations, leather quality, energy savings. Comparison with the standard productions show the process can be extended without risk of looseness or yield lost.

References

1. *CN 203 247 270 U 23 october 2013*
2. *US 1 623 943 A 5 April 1927*
3. *EO 0 960 948 A1 1 December 1999*
4. *EP 1 690 950 A2 15 August 2006*
5. *WO 2018/172837 A1*
6. *EP 0 990 707 B1 11 February 2004*

STEEL MEETS LEATHER – THE INFLUENCE OF CUTTING PARAMETERS IN THE LEATHER SPLITTING PROCESS

G.E.Hank

Rudolf Alber GmbH & Co. KG, Sales director 73061 Ebersbach, Germany,

g.hank@alber-tools.de

Abstract. This article wants to combine two perspectives: First, Leather production with its diverse quality requirements and second, the new evolutions in the field of bandknife properties. In a short introduction the splitting process as such will be described, its different use in several stages and leather types, also in the field of leather conversion (in shoe, leathergoods and automotive parts production). Influencing factors of the possible goals like quality and cost efficiency will be discussed. In the second part some main requirements and problem fields of leather splitting are analyzed in more detail. Requirements such as thickness tolerance, tensile strength or fibre-free smooth cutting surface. Difficulties in practice like chrome nests, hard water, poor raw material, feeding speed, influence of abrasivity of leather. In a third part the physics of the cutting process as such are described. Explanation of basic terms as “cutting ability”, “edge retention”, “pull vs. press cut”. Resulting from this we get important parameters that refer to the bandknife blade: e.g. steel characteristics (hardness, flexibility, grindability, microstructure at cutting point, geometry of knife bevels, weldability etc.). The possibilities in modern bandknife production will be shown as for example: CNC-sensor-based tolerance measurements, pre-sharpening, surface roughness variations. This is completed with a short view on the other components of the process like splitting machine (points like sharpness measuring), grinding stones (roughness-exactness controversy diagram). The fourth and last part puts the two perspectives together: Optimized bandknife characteristics for specific leather material. Alternative steel types that due to new properties allow to meet also new requirements.

1 Introduction

The author of this article works at Rudolf Alber GmbH & Co. KG Germany, a manufacturer of splitting bandknives for the leather industry. This article wants to combine two perspectives: First, the splitting process in leather production with its diverse quality requirements and second, the new evolutions in the field of bandknife properties. Through thorough analysis of the parameters that affect the performance of a splitting blade, optimum blade selection can be achieved. Issues like splitting machine set-up, grinding stones, etc. are peripheral to this essay and are, despite their importance for the whole process, not in focus this time.

2 Splitting leather

Splitting is often described as the “most complex” or “key process” for achieving a maximum utilization of the hide area in even thickness. Animal hides consist of a structure of three-dimensional fibers building a derma and a flesh layer of varying thickness, while for the final product (shoe, leathergoods, automotive component etc.) a constant thickness of leather is required.

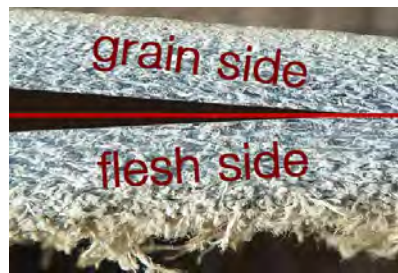


Fig. 1. Splitting leather.

Splitting can be done in different stages: Lime, tanned (Wet-Blue etc.) and dry leather. Additionally, for the production of shoes, leathersgoods, automotive seat covers and components the converting industry splits the finished leather again into various thinner layers for its final use.

The physical separation of the grain and the flesh side happens by the process of feeding the hide through the splitting machine.



Fig. 2. Front-view of a splitting machine used in tanneries.

Splitting machines are complex systems of high-precision components that require for an optimum performance a bandknife with the following minimum characteristics:

- Thickness tolerance below 0,02mm as blade guides settings can be adjusted in practice with only a 0,03mm gap.
- Tracking, i.e. parallelity of blade with tolerances below 0,02mm.
- Possibility to work on different bevel lengths according to hide type.

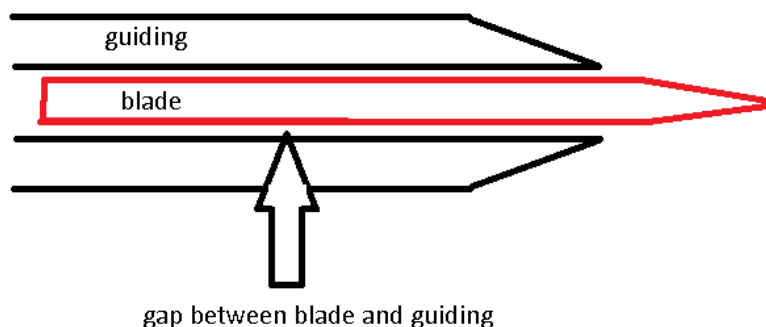


Fig. 3. Sketch of bandknife and machine guidings, also called jaw plates.

There are specific requirements and considerations according to the stage of splitting.

2.1 Lime splitting

The weight of the hide is basis for the needed volume of tanning agents. This means that splitting should remove as much of the flesh side as possible and leave as much of the grain side as needed. Splitting reduces the tensile strength of the hide, values for grain and flesh material depend on their

remaining thickness. Volume of chrome waste resulting from further steps in Wet-Blue tanning is reduced. As swelling has increased the thickness of hides, an exact splitting, and therefore a high precise bandknife, becomes even more important to achieve the intended final thickness range. Lime splitting allows the use of the split flesh side for products where untanned material is needed. Untanned material can be sold e.g. to the collagen industry, meat casing, cosmetics. Considering these points it is clear that the splitting process plays an important role for the overall economical view.

Hides in lime stage are softer than in wet-blue or dry stage, therefore easier to split, but dirt or lime nests built up from hard water might damage the fine edge. A steel with a higher shock-load-capacity keeps the edge longer. Up to 50.000 bovine hides can be split per blade in lime stage.

2.2 Wet-Blue

After tanning hides are having a stiffer fiber structure, swelling effect as in Lime is far less. Higher precision in splitting in this stage reduces efforts and cost done in the following shaving process. In case wet-blue split is sold, an optimization in surface outcome is reached by better splitting.

Humidity of hides has influence on hardness, abrasiveness of freshly tanned hides is lower than for transported and stored material. The edge of the blade needs more sharpening in the second case, life-time of blade is lower. The number of hides split per blade ranges between 5.000 – 40.000, depending also on the type of hides and tanning method. Often splitting is done by contractors outside the , for them the possible feeding speed directly influences the daily production potential. The impact of other tanning agents than chrome, like e.g. aluminium, on the bandknife is in many cases negative, as higher abrasiveness requires more intense resharpenering.

2.3 Wet-White

Wet-White covers a wide field of chrome-free tanned or pre-tanned hides. Effects on splitting depend on whether synthetic contents leaves a more or less abrasive fibre structure. In the cases studied for this analysis the Wet-white material had a softer structure compared to similar hides in Wet-Blue. But splitting of this material is more difficult, especially when its humidity is low. In practice Wet-White finds often application in high quality end products, the need to reach necessary precision often leads to a higher grinding intensity for the blade, in order to even more clearly minimize rejections due to over or under thickness.

2.4 Dry leather

Dry leather is split in tanneries to reduce thickness further for Crust or finished leather. In some cases it is done to clean inner side from fibers and to reach a smooth surface. In the production of shoes, leathergoods, automotive leather etc., finished leather is split again according to the thickness needs of final products. This is done on smaller component splitting machines with working width of 300-800mm. Dry leather is a quite abrasive material, edge robustness becomes a decisive factor for the right steel selection for the bandknife. Errors in splitting can't be cured by following processes.

3 Theory of splitting

„Splitting“ is a sub-category of „Cutting“ that divides one layer in two by moving a knife edge through hides horizontally. In comparison to a „Sawing“ process that is used to cut rigid material, the flexible hide opens its structures and therefore the knife does not need to destroy material (sawdust) but leaves both layers intact.

3.1 Cutting ability

In the following we want to have a deeper view of what happens at the cutting edge. While the knife enters the material two cutting forces work physically

- Draw cut
- Press cut

To better define the „cutting ability“ of a bandknife we have to see the following parameters

- Edge angle β
- Edge thickness d
- Sharpness b
- Theoretical sharpness b'

Forces that work are

- Pressure
- Friction F_r

A wide edge angle increases the stiction, friction caused by material sticking on the surface.

- Speed i.e. Velocity V_z of bandknife turning on machine

Elements of cutting ability

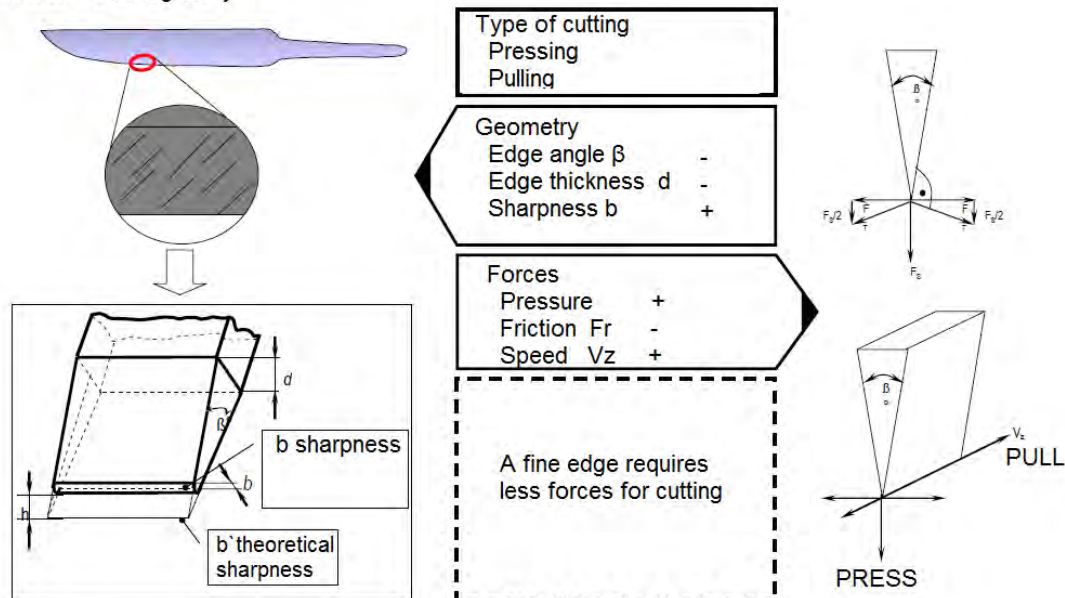


Fig. 4. Elements of cutting ability¹.

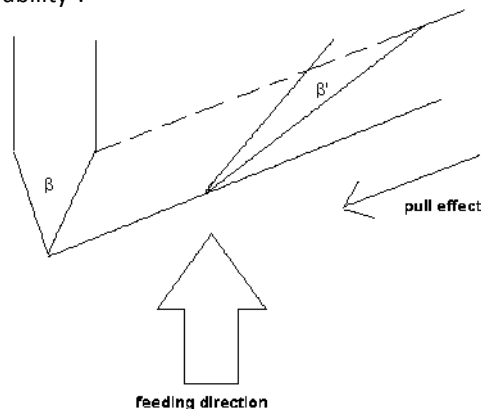


Fig. 5. Edge angle with pull-effect.

¹ Adapted from Landes (2003)

With the movement of the blade the edge angle β turns into thinner cutting angle β' . A thin edge angle with high sharpness has the best cutting ability, for leather splitting this means a precise cut, fibres are cut and not torn, result is smooth fibre-free cutting surface.

3.2 Edge robustness

Before coming back to the cutting ability, we have to take a look at the „Edge Robustness“. A thin razor blade has a high cutting ability, but is weak, a wood axe is robust but due to its thick edge only able to cut with heavy forces. For leather splitting we need to combine both characteristics - ability and robustness - as cutting precision is important and volume to be cut is quite high. e.g. up to 50.000 hides with one blade. The edge robustness depends on Edge angle, Material (steel type), Hardening of steel, Infrastructure (machine, grinding system etc.).

3.2.1 Edge robustness und edge angle

Steel has carbide grains that differ with the content of alloy elements. We can distinguish fine and rough grains. With a fine carbide structure a narrow edge is possible. This narrow edge at the same time has a higher edge robustness.

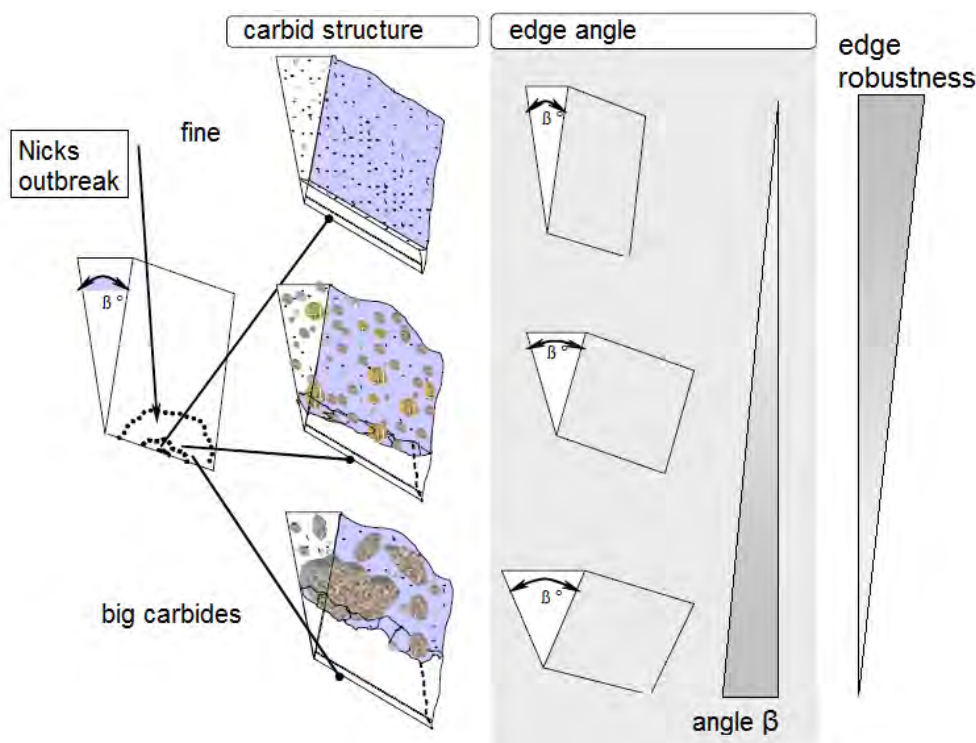


Fig. 6. Bevel robustness².

The bevel robustness decreases by increasing the edge angle β . Steel particles break out of the edge due to the friction against the hides to be split. This means the harder the material to be cut, the shorter should be the bevels. In tanneries splitting machines usually use inner bevels (flesh side) shorter than the outer bevels (grain side), this is reached by different size of grinding wheels or same size of grinding wheels but different position. In tanneries the following bevels in mm are in use.

² Adapted from Landes (2003)

Table 1. edge geometry according to process step in tanneries.

	inner bevel	outer bevel
Lime	3,7-4,0	5,5-6,0
Wet-Blue	3,2-3,7	5,0-5,5
Crust/Dry	2,5-3,5	4,0-5,0

3.2.2 Sharpening

On modern splitting machines ceramic disc grinding stones are used. The harder the steel, the softer the grinding stone should be. Hardness for grinding stones used in leather splitters ranges from soft to medium, described in alphabet letters like H, I, J. The grain of the stones break during use, resharpen themselves and finally get lost.

Porosity is needed to avoid overheating. Softer steels tend to paste the porosity of the grinding stones that have to be dressed then more often. Besides the parameters hardness and material of grinding stones, the main variable is the grain level. Stones which are used for leather range from rough grain at 36, middle is 46, fine 60 or 80.

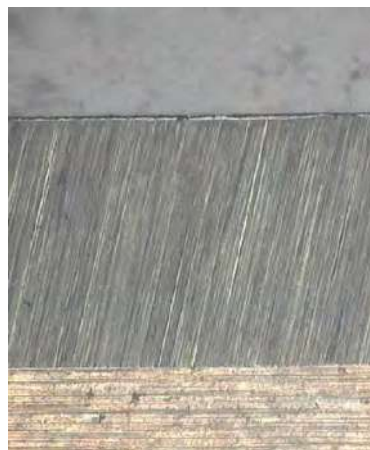


Fig. 7. Picture of a bevel profile sharpened with grain 46, edge not yet 100% sharpened.

A fine grain creates a finer blade edge, notches are avoided. This increases life-time of the bandknife. Working in an environment where the edge gets easily blunt, due to harder material to be split, in practice a more aggressive grinding stone with rough grain can be the better choice when focus is on speed of production and resharpening time means unused production time. ³

³ The author knows the discussion about alleged advantages of a micro-toothing caused by rough grinding wheels. However, this micro-toothing has the disadvantage of a minor theoretical sharpness.

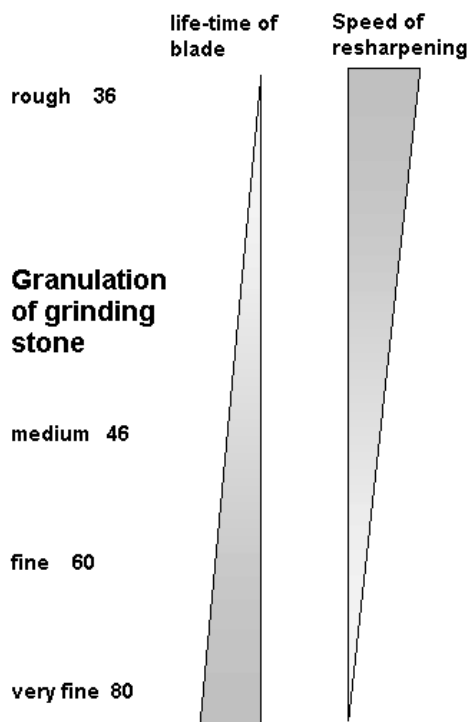


Fig. 8. Trade-off between speed of sharpening and life-time of blade.

The intensity of sharpening defines the life-time of the bandknife. In modern splitting machines an automatic level of sharpening can be programmed. Measuring the degree of sharpness as input signal for this automatism is a prerequisite for further optimization.

4 Steel type

Steel is an alloy of iron and carbon, by including other elements like chromium, manganese, nickel, etc. the characteristics can be influenced.

Due to the special machine set-up for splitting with two wheels, a turning bandknife is used. (compared to other types, e.g. fix static knives, cylindrical shaving knives, oscillating knives etc.) The steel has to comply additionally with characteristics such as

- Flexibility : machine wheels have diameter of 30-100cm , means band has to bend and then come back to a linear cutting line. The bending gives an upper limit to the hardness of steel.
- Weldability: Bandknives are „endlessly welded“, to avoid irregular cutting, welding joint has to be homogeneous with rest of the band.
- Availability and cost efficiency: Steel for splitting bandknives has to be available in constant quality and reasonable cost. By Intense sharpening the blade is “consumed” and needs to be substituted after its life-time.

4.1 Flexibility vs. Hardness - tensile strength of steel

While flexibility is a minimum requirement defined by the bending angle of the fly-wheels of the machine, Hardness is a maximum aim to be reached. A C75 steel, used for splitter blades has a yield point at around $R_p = 1300N/mm^2$. Elasticity-modul at 210 Gigapascal. Important that also the welding joint has a similar level. The needed elasticity is in conflict with the aim to increase tensile

strength for better edge resistance. In other words: For bandknives the need to stay flexible puts a limit to positive influence of higher steel hardness. As maximum hardness drops out as the sole variable, the steel composition becomes the decisive factor for edge resistance and optimum cutting ability.

4.2 Cutting quality

The combination of cutting ability and edge robustness over the time give the total result as „Cutting quality“.

The „edge robustness“ might be better for blades made out of materials like ceramic or hard-metal coated edges.

4.3 Carbon content

In the production of steel, Carbon content is the main parameter. A content of 0,8%C is the line where below there is still α -Ferrite included, above not. For higher carbon content the free carbon allows higher hardening of steel as in molecular scaffold interruptions to the Fe-structure are possible. At the same time, more grain boundary cementite builds up at the grain limits, this leads to a possibly harder but more brittle structure.

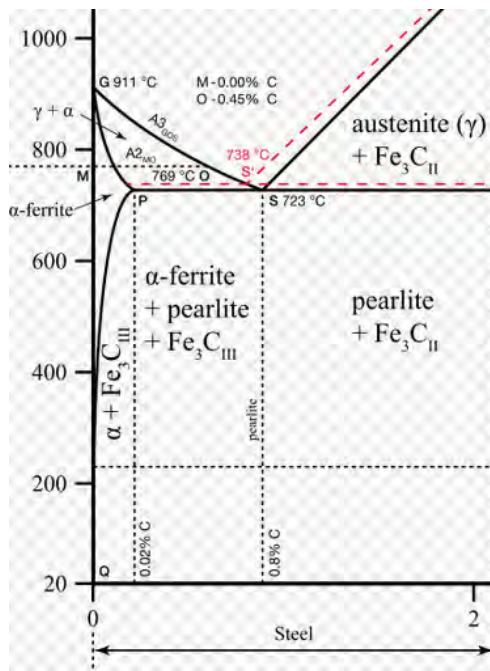


Fig. 9. Detail of the Fe-C equilibrium phase diagram.

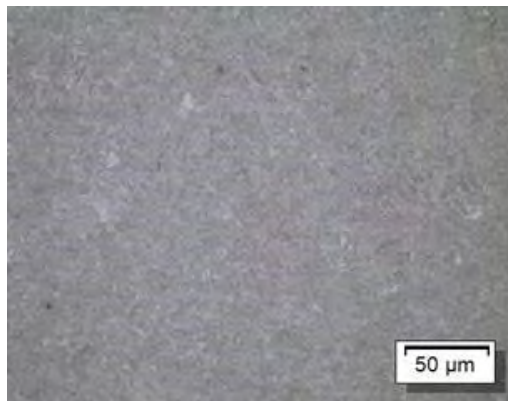
The building up of a different grain structure needed for higher hardness also can be achieved with other elements than Carbon, avoiding this effect of higher brittleness, like e.g. Chrome 4. The steel options for splitting bandknives are limited by the above mentioned requirements. Most manufacturers use a simple C75 spring steel, available as a side-product from the much bigger market for bandsaws. We will compare in the following four steel types C75, C75CR1, C100, and SY5.

⁴ It is by coincidence that Chrome plays already an important role in the tanning industry.

⁵ (SY is a non official norm description, used for reasons of protection against competitors by the author).

Microscopic structure

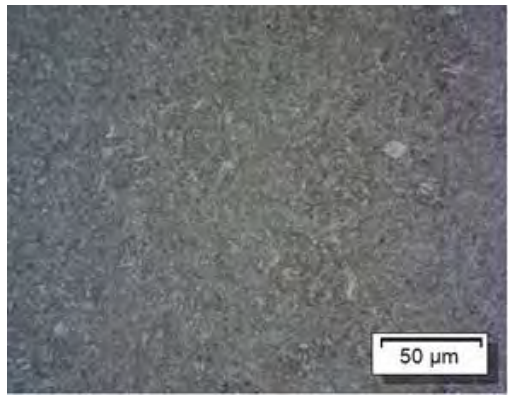
C75



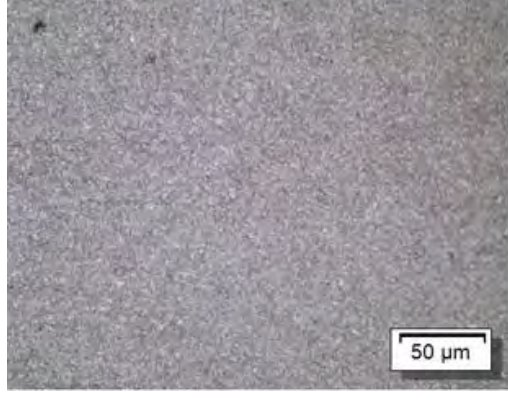
C75CR1



C100



Alber SY



C75 and Alber SY show a fine homogeneous structure, for the C75CR1 and C100 the expected grains are visible.⁶ The following diagram illustrates edge-resistance vs. ability for hardening as regards the four steel types:

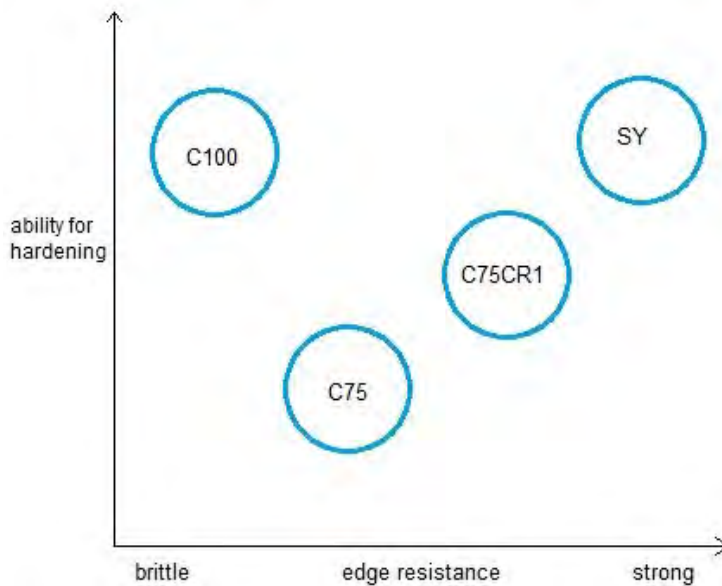


Fig. 10. Edge-resistance vs. ability for hardening.

5 Modern bandknife production

Having chosen the optimum steel, the manufacturer of bandknives has to source this steel and convert it to a perfect tool.

Steel production is a two-step process. In the steel mill the composition of the final steel is defined by preparing the melt. In a second step the cold-rolling defines dimension and hardness of the coil that is the base for further processes. In bandknife production the steps are then

- Initial quality control
- Cutting to length
- Welding
- Rectification of surface – correct thickness
- Bevelling and back preparation – correct tracking
- Final quality control and packing

5.1 Cutting to length

The length of a bandknife is determined by the splitting machine. As for other machines in leather production working width range of 1500mm, 2300mm, 2700mm, 3000mm, 3200mm and 3400mm are standard. The blade is kept on the machine by a system tensioning the blade with the two wheels. The tensioning of the splitting machine compensates the possible expansion of thermal expansion, with a coefficient for steel of 0,0115 and a blade length of for example 10meters, the expansion for a 20 degree temperature increase comes to 2,3mm. These parameters determine the length value and the allowed tolerance range.

⁶ The structure visible in the microscopic structure of the steel is not only a result of the steel composition, but also of the different processes like hardening and rolling.

5.2 Welding

Welding is done with butt-welding machines. No additional weld elements are added. Pressure, electrical impulse and temperature curve are programmable for each different steel type. The target is to reach same level of tensile strength in welding zone as in the rest of the band. Optimum glowing temperature can vary for different steel types.



Fig. 11. Welding machine.

5.3 Rectification – correct thickness

As said in the beginning, a bandknife is an endlessly welded band, that should be homogeneous and constant in order to guarantee a smooth surface. Before rectification a welded raw steel band has a thickness tolerance of approx. 0,5mm, mainly caused by the welding point. This high irregularity would leave grooves and marks on the hides. The aim is to minimize the thickness tolerance of the blade. Tolerances of less than 0,02mm in thickness and tracking have to be guaranteed by CNC-machines with its non-touching sensors. This is necessary to allow the band to run between the blade guiding which gap is set down to 0,03mm.

One of the main reasons for poor performance of the splitting process is the wrong adjustment of machine components or a use of a bandknife that is not fulfilling the required tolerances.⁷ Surface roughness of the blade is the result of the rectification process. Standard value for roughness is between 0,8 and 0,95. A blade surface that is too rough may damage the blade guidings and leads to a reduced overall performance in medium term.



Fig. 12. Rectification grinding stone and manual final thickness control after rectification.

5.4 Beveling and blade back preparation – correct tracking

After having prepared the exact thickness, bandknives are pre-bevelled. Parallel tracking of blades with tolerance below 0,02mm has to be guaranteed in order to avoid side-movement of blade inside machine.

⁷ Brochure of problem solving for wrong splitting performance available with the author

Arriving at the tannery, the bandknife is already pre-bevelled – the final 100% sharpening is done on the splitting machine. A well-done pre-bevelling saves time when mounting the blade. Asymmetrical bevels can be done for pre-bevelling to save even further minutes and reduce down-time of machine. For quality control systems at end-user, blades can be identified with serial number and protocol of precision values.



Fig. 13. Tracking sensors able to measure tightest tolerances.

6 Final conclusion and optimum steel selection

The bandknife is a small but important component in the whole production process of leather products. For the steel selection several parameters have to be considered that limit in practice the available choices. To our comparison we add parameters:

- sharpening ability
- welding ability
- shock load capacity

We come to the following more complete comparison:

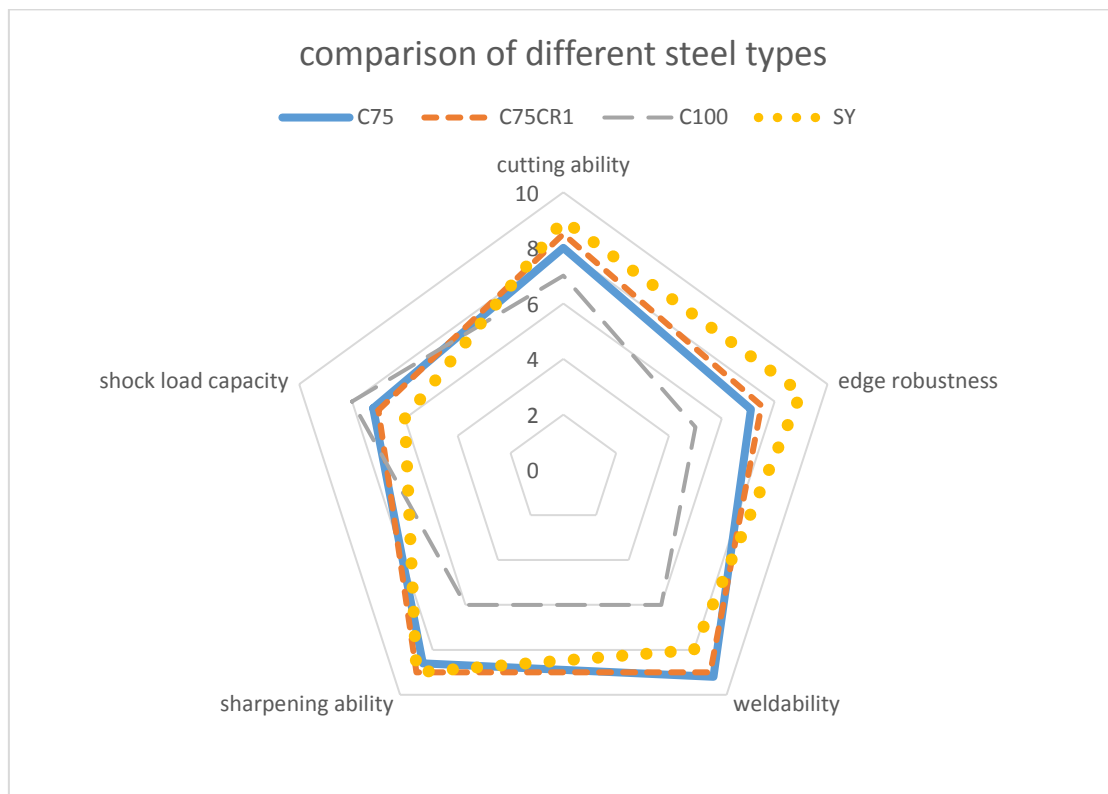


Fig. 14 Steel evaluation of different characteristics

An optimum steel selection, based on the above-discussed arguments looks as follows:

Table 2. Steel recommendation.

sector	Leather type	Steel Recommendation	
		Standard	increased performance
Tannery	Lime	C75, 48 HRC	C75CR1, 48 HRC
	Wet-Blue	C75, 48 HRC	C75CR1, 48 HRC, SY 49HRC
	Wet-White	C75CR1, 48HRC	SY, 49 HRC
	Crust	C75CR1, 48HRC	SY, 49 HRC
	Dry	C75CR1, 48HRC	SY, 49 HRC
	Dry automotive	C75CR1, 48HRC	SY, 49 HRC
Converting industry	finished leather	C75, 52 HRC	SY, 53 HRC
	finished leather automotive	C75, 52 HRC	SY, 53 HRC

Whether the technical benefits of better performance can be realized in practice depend on further conditions as described under topics 2 and 3. Commercial aspects, steel cost and availability, contribute to the overall result. Material science is a wide field evolving further, this is valid both for leather as for steel. We invite you to accompany us in the search for optimization of the splitting process.

References

1. *Burmester, Jürgen et.al. (2017), Fachkunde Metall, Josef Dillinger, Walter Escherich, Eckhard Ignatowitz, Stefan Oesterle, Ludwig Reißler, Andreas Stephan, Reinhard Vetter, Falko Wieneke, Europa-Lehrmittel, Haan, Germany*
2. *Chambon, Romain, Sales director at MERCIER TURNER Annonay, France*
3. *La spaccatrice, Quaderni di ingegneria conciaria, Quaderno 5, Assomac, Vigevano, Italy, w/o year*
4. *Landes, Roman (2003): Messerklingen und Stahl, Wieland Verlag, Bad Aibling, Germany*
5. *Moog, Gerhard E. (2005): Der Gerber, Eugen Ulmer KG, Stuttgart Germany*

AUTOMATIC LEATHER SPECIES IDENTIFICATION USING MACHINE LEARNING TECHNIQUES

M. Jawahar^{1a}, S. V. Kanth¹, V. Rajangam¹ and T. Selvi¹

¹ Central Leather Research Institute, Leather Process Technology, Chennai, India

a)Corresponding author: malathy.jawahar@gmail.com

Abstract. Identification and classification of leather species becomes valuable and necessary due to concerns regarding consumer protection, product counterfeiting, and dispute settlement in the leather industry. Identification and classification of leather into species is carried out by histological examination or molecular analysis based on DNA. Manual method requires expertise, training and experience, and due to involvement of human judgment disputes are inevitable thus a need to automate the leather species identification. In the present investigation, an attempt has been made to automate leather species identification using machine learning techniques. A novel non-destructive leather species identification algorithm is proposed for the identification of cow, buffalo, goat and sheep leathers. Hair pore pattern was segmented efficiently using k-means clustering algorithm. Significant features representing the unique characteristics of each species such as no. of hair pores, pore density, percent porosity, shape of the pores etc., were extracted. The generated features were used for training the Random forest classifier. Experimental results on the leather species image library database achieved an accuracy of 87 % using random forest as classifier, confirming the potentials of using the proposed system for automatic leather species classification.

1 Introduction

Identifying the species of leather is of paramount importance due to concerns regarding authenticity issues, protecting endangered species, product counterfeiting, consumer protection, etc., Leather industry is fragmented and lacks information exchange systems, neither does it have a provenance system thus information regarding origin of leather is often lost. Labelling of leather is often not done clearly and many a time's disputes arise based on doubts over the origin of the leather. Often disputes between two parties regarding species of leather is brought to expert leather authority to be settled so standardizing the system and removing the human judgment and bias is required to promote free and fair trade thereby enabling the growth of the leather industry.

Each species of the animal has a unique hair pore pattern and this information can be used to detect the species of an unknown leather by examining under a microscope. This method is most efficient while using full grain leathers. It is fast and cost-effective when it comes to identifying leather compared to other methods such as DNA finger printing techniques [1,2] and other histological studies of species identification[3,4].

In this current investigation, image analysis technique has been used to segment hair pores from the leather background and measurement of hair pore properties by extracting image features.

2 MATERIALS AND METHODS

Representative goat, sheep, buffalo and cow leather samples of each species (20 each) as shown in Fig. 1 were selected from the official butt portion for microscopic imaging. Image analysis and machine learning algorithms were implemented in Scilab. The computational workflow for the identification of leather species is shown in Figure 2.

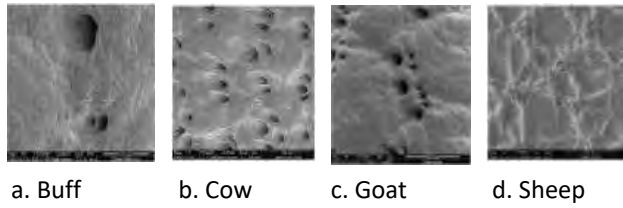


Fig. 1. Microscopic leather species image.

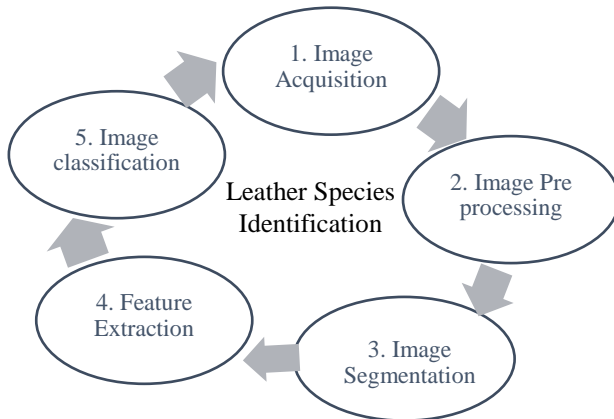


Fig. 2. Work flow diagram of leather species identification.

2.1 Image Preprocessing

Microscopic leather images were preprocessed to highlight the difference between the pores and the surrounding background using adaptive histogram equalization (Fig.3).

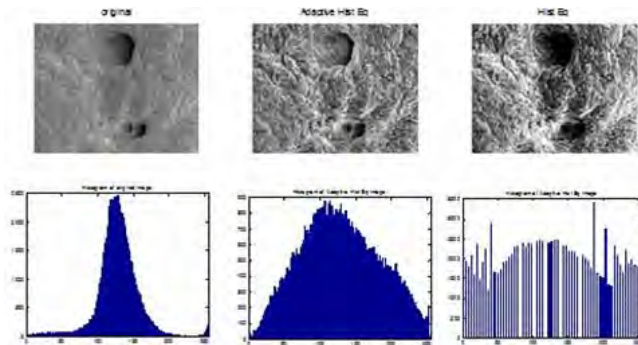


Fig. 3. Preprocessing using Adaptive histogram equalization.

2.2 Image Segmentation

In this study, k-means clustering algorithm is used for segmenting the hair pores from the background leather image. This is an unsupervised learning mechanism where in pixels are clustered or grouped into k clusters based on similarity in intensity and grey values. This algorithm requires k seed points or starting points which dictates the way in which the region will grow along with the membership function which defines the criteria according to which pixels are put into clusters.

Assume the data set is given by (x_1, x_2, \dots, x_n) , where each observation is a d -dimensional real vector, k -means clustering aims to partition the n observations into k sets where $(k \leq n)$, $S = \{S_1, S_2, \dots, S_k\}$ in such a way that it minimizes the within-cluster sum of squares.

$$\arg \min_{\mathbf{S}} \sum_{i=1}^k \sum_{x_j \in S_i} \|x_j - \mu_i\|^2 \quad [1]$$

Where μ_i is the mean of points in S_i .

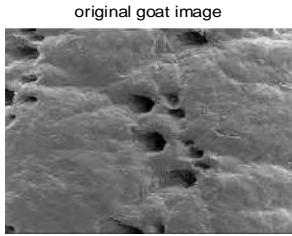
Assignment :

$$S_i^{(t)} = \{x_p : \|x_p - m_i^{(t)}\|^2 \leq \|x_p - m_j^{(t)}\|^2 \forall 1 \leq j \leq k\}, \quad [2]$$

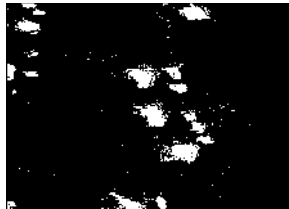
Further updating:

$$m_i^{(t+1)} = \frac{1}{|S_i^{(t)}|} \sum_{x_j \in S_i^{(t)}} x_j \quad [3]$$

original goat image



manual threshold image

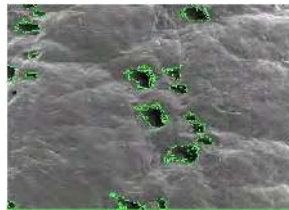


manual threshold image

binary img after areaopen



overlay image ss1



overlay image ss1

Fig. 4. Segmentation using K-means clustering.

The segmented image (Fig. 4) had many spots which were undesirable and lead to false data. These unwanted data points were effectively removed using erosion of the image followed by dilation. These morphological operations were performed using various structuring elements or masks of which a circular or disk element was found to be most effective.

2.3 Feature Extraction

Segmented image was described using features. In this work, features such as average pore-size distribution, least inter-pore distance, porosity, hair pore density and shape attributes like circularity, aspect ratio, solidity of the pores were computed. The area of the hair pores was estimated by computing the total number of pixels occupied by each pore i.e. region of interest (ROI). Mean, standard deviation, minimum and the maximum intensity value within the ROI were also computed. The Feret's diameter was computed as the longest distance between two parallel lines tangent to the pore. Inter-pore distance was obtained by measuring the distance between the adjacent centroids that ideally represents the centre of the pores. Hair pore density represents the number of pores in a unit area of the image. Porous area fraction or porosity was calculated as the total area occupied by the pores divided by the total area of the investigated image region. Shape of the hair pore was examined in terms of circularity, aspect ratio (AR), solidity.

2.4 Random Forest Classifier

Random Forest (RF) classifier proposed by Breiman[5] is a multiple combination of decision tree. Each tree casts a unit vote for the final classification of the input feature set. Random Forest splits each node using randomly chosen best subset of features. Feature variable importance measure, prediction error on the out-of-bag portion for each tree was computed. The same computation was carried out after permuting each feature variable. Mean and normalized standard deviation was computed. Splitting of tree stops when standard deviation of the difference in feature variable equal to 0.

Random forest uses the gini index to measure the node impurity. It is the measure most commonly chosen for classification-type problems. Gini(T) is defined as

$$Gini(T) = 1 - \sum_{j=1}^n P_j^2 \quad [4]$$

Where P_j represents relative frequency of dataset T with n classes.

Validation was done with unseen dataset (test samples) to evaluate the ability of the classifier to discriminate the four leather species. The performance of the classification in leather images using random forest was measured in terms of Accuracy, Sensitivity, Specificity, and Precision/Positive Predictive Value (PPV), Recall/Negative Predictive Value (NPV) and F score as given in equations 5 to 10.

$$Accuracy = \frac{TP + TN}{TP + FP + FN + TN} \quad [5]$$

$$Precision \text{ or } PPV = \frac{TP}{TP + FP} \quad [6]$$

$$Recall \text{ or } NPV = \frac{TN}{TN + FN} \quad [7]$$

$$F1 \text{ Score} = 2 * (Recall * Precision) / (Recall + Precision) \quad [8]$$

3 Results and Discussion

In this study, leather grain surface images were obtained using optical microscope. Leather hair pore arrangement and distinctive features for the buffalo, cow, goat and sheep leather species were investigated. Representative sample images of buffalo, cow, goat and sheep leathers are shown in Figure1. 80 leather samples (each species 20) were chosen for image analysis. K-means clustering algorithm was used to segment the hair pore pattern from the leather images which were preprocessed using adaptive histogram equalization algorithm. Features describing the hair pore pattern were extracted. Classification was carried out using random forest to identify the leather species. The work flow diagram is described in Fig 2.

Qualitative analysis of the preprocessed buffalo image using adaptive histogram equalization technique (Fig.3) was found to have a low MSE and a high PSNR value. Segmentation using K-means clustering technique for goat leather shown in Fig. 4. It can be observed that the intensity distributions of the pores and the background often overlapped, thus complicating the separation of information

relating to pores alone. Since the hair pores were basically of circular shape, disk structuring element was selected for morphological operation. The basic morphological operators such as dilation and erosion were used to eliminate the unwanted spots thus segmenting the hair pores alone. Performance analysis on segmented image was validated using quality measures Area Error Rate (AER), Overlap Error (OE) and Zijdenbos Similarity index(ZSI) and the results are set out in Table 1.

Table 1. Performance analysis of the segmented image.

Sample	ZSI	AER	OE
Cow	0.8323	0.1967	0.2201
Goat	0.8034	0.2212	0.1898
Sheep	0.7945	0.2215	0.2101
Buffalo	0.8143	0.2123	0.2154

The error between the K-means segmentation algorithm and manually segmented region was represented in terms of AER and OE. AER and OE values were closer to 0. This shows that segmentation error is negligible. Zijdenbos Similarity Index (ZSI) quantifies the accuracy of the segmentation [6]. From Fig.1 it can be observed that the cow and buffalo species can be easily segmented and there were no overlapping regions. Hence, ZSI score nearing to 1 was observed for cow (0.83) and buffalo (0.81). Goat and sheep had overlapping regions, therefore ZSI values were 0.80 and 0.79 respectively. The results of the segmentation performance measures show that the K-means clustering algorithm followed by morphological operations could be used for segmentation of leather species. After segmentation of the hair pores, centroid of the hair pores were identified by repeated application of morphological erosion operation and labelled so that feature extraction can be carried out for each label.

Table 2. Hair Pores Distribution based on pore density.

Species	Pore Density (per sq cm)				Percent Porosity
	Overall	Small	Medium	Large	
Goat	2185	1248	936	0	0.027
Cow	2263	0	2263	0	0.046
Sheep	1099	1099	0	0	0.005
Buffalo	304	152	76	76	0.021

All the features extracted from the microscopic image were multiplied with the calibration factor calculated by measuring the length of the known distance in pixels. Hair pores were counted and classified as small (≤ 1000 sq μm), medium (1000 – 4000 sq μm) and large (> 4000 sq μm). In this study, hair pore density was calculated from the number of pores present per sq cm (Table 2). Buffalo hair pore density was found to be the least among the four species. Overall hair pore density for cow and goat leathers were found to be almost similar but there are differences in the size and distribution of the pores. Cow leathers have uniform pores which are in medium size range whereas. goat hair pores are in both small and medium ranges The pore density of sheep leathers was found to be half the pore density for goat leathers. Porosity defines the ratio of the cumulative surface area occupied by pores to the total surface area of the leather. Goat and cow differ quite considerably in terms of percent porosity. Due to the presence of larger pores buffalo leathers was found to have higher percent porosity than that for sheep leathers. Thus the above extracted features were found to effectively describe the unique characteristics of each of the leather types investigated in this study.

Random forest classifier was trained with extracted features. Performance of the classifier was validated using 5-fold cross validation. The samples were divided into 5 subsets and for every fold one subset was randomly selected as validation set and the remaining 4 subsets were combined together to form as a training set. Average validation scores obtained from the five folds (Table 3) were calculated.

Table 3. Average Classification report for leather species classification.

S.no	Accuracy	Error	Recall	Precision	F-score
Fold 1	83.33	16.67	1.00	0.79	0.88
Fold 2	86.11	13.89	0.92	0.88	0.90
Fold 3	88.89	11.11	0.93	0.93	0.93
Fold 4	80.56	19.44	0.92	0.82	0.87
Fold 5	91.67	8.33	0.96	0.93	0.94
Average	86.11	13.88	0.95	0.87	0.90

It can also be observed from Table 3 that the average recall and precision were found to be 95% and 87% respectively. The F-score was 90%. The overall classification accuracy for the proposed method was 86.11%.

4 Conclusion

This study develops automatic leather species recognition system. In the system, a novel non-destructive leather species identification algorithm is proposed for the identification of cow, buffalo, goat and sheep leathers. Hair pore pattern was segmented efficiently using k-means clustering algorithm. Significant features representing the unique characteristics of each species such as no. of hair pores, pore density, percent porosity, shape of the pores etc., were extracted. The generated features were used for training the Random forest classifier. Experimental results show that the proposed system can recognize all the four types of leathers with high efficiency and accuracy. In conclusion, it is possible to apply computer vision system to the automatic leather species identification and potential to replace the leather experts.

References

1. Long, A.L. Addy, V. L., Booth, S., Dwyer, R.O., Loftus, R.; *Extraction of DNA from Leather and applications to the supply chain. JALCA, 102(1), 22-26, 2007*
2. Stenzel, S., Bohrisch, J., Pach, M., Meyer, M.; *A New Marking System for Leather Based on Encapsulated DNA. JALCA, 110(9), 277-287, 2015.*
3. Saheb Baha, S.S., Satya Prasad, K., "Automatic detection of Hard Exudates in Diabetic Retinopathy using Morphological segmentation and Fuzzy Logic" *International Journal of Computer Science and Network Security, 8 (12), 2008.*
4. Ziel, A., Haus, R., Tulke, A., *Quantification of the pore size distribution (porosity profiles) in microfiltration membranes by SEM, TEM and computer image analysis. J.Mem.Sci, 323(2); 241-246, 10/2008.*
5. Breiman, L. (2001). *Random Forests. Machine Learning, 45, 5–32.*
6. Alkan, A., Tuncer, S.A., Gunay, A. (2014). *Comparative MR image analysis for thyroid nodule detection and quantification. Measurement, 47, 861–868.*



POSTER PRESENTATIONS

APPLICATION OF VEGETABLE BARK EXTRACT AS ALTERNATIVE RETANNING AGENT FOR LEATHER PROCESSING

A.E Musa^{1*}, G.A. Gasmelseed², E.F. Faki³, H.E Ibrahim², O.A Haythem⁴, M.A Manal¹, S.B Haythem¹

¹Department of Leather Technology, College of Applied and Industrial Sciences, University of Bahri, Khartoum – Sudan, P.O.Box 1660

*²University of Science and Technology, Faculty of Engineering, Department of chemical engineering
Khartoum – Sudan*

³Department of Leather Engineering, School of Industrial Engineering and Technology, Sudan University of Science and Technology, Khartoum – Sudan,

⁴National Leather Technology Centre, , Khartoum – Sudan

** Corresponding author: A.E Musa – musaalileather@gmail.com*

Abstract. The retanning process is considered as one of the most important processes in leather making, and it plays an important role in the modern leather industry. The fibre structure of hide or skin is not uniform and the retanning agent improves the properties of leather by filling the empty part of wet-blue leather. It could contribute to further stabilization of collagen fibres and give better handle properties to leather such as fullness and elasticity. In a conventional leather retanning process, retanning materials used include both inorganic salt like basic chromium salt, zirconium salt and aluminum salt and organic materials such as vegetable tanning agent, synthetic tanning agent, resin retanning and aldehyde tanning agent. Extract from the barks of *Acacia seyal* (Talh bark), widely distributed in Sudan, has been evaluated for its utilization in the retanning of the leather and presented in this paper. Barks of talh have been extracted for 1 hour with distilled water (1:10 w/v) at temperature above 80°C. The talh extract prepared has been used for the retanning of wet blue leathers. The effectiveness of talh extract in retanning of wet blue leathers has been compared with mimosa retanning. The organoleptic properties of the leathers viz. softness, fullness, grain smoothness, grain tightness (break), general appearance, uniformity of dyeing of talh retanned leather have been evaluated in comparison with mimosa retanned leathers. Talh retanning resulted in leathers with good grain tightness. Dyeing characteristics of talh retanned leathers have been found to be better than mimosa retanned leathers. Also physical strength characteristic and shrinkage temperature and economic viability were noted. The effluent arising from this retanning system has been analyzed for its environmental impact.

1. Introduction

Retanning process plays an important role in leather making because it can improve the cutting value, the handle and some specific properties of leathers (like buffing property, embossing property, perspiration resistance, fastness to washing, flammability, etc.) by using various types of retanning agents and modifying their application processes¹⁻⁴. The retanning performance depends on the penetration and the uptake of retanning agents in leather, which are mainly controlled by the electrostatic force between the retanning agent and the surface of the leather collagen fiber⁵⁻⁷. Therefore, in order to improve the retanning performance scientifically, it is essential to fully understand the surface charges of both retanning agents and leathers and their effect on the penetration and the uptake of retanning agents in leather during retanning process.

In order to meet customers' requirements, a wide variety of retanning agents is used in retanning process, such as mineral retanning agents⁸, vegetable tannins⁹, Syntans¹⁰⁻¹², resins^{8,13}, polymers^{14,15} which could bring about a difference in adsorption capacity of leather to water and may influence the thermal stability closely related to the moisture content of leather¹⁶.

Bio-active ingredients in the form of tannins are present in some of the plant materials capable of imparting tanning effect. The vegetable tannins are water-soluble polyphenolic compounds having molecular weight in the range of 500 –3000 Daltons^{17, 18}. They occur in bark, wood, fruits,

fruit pods, leaves, roots, and plant galls^{19,20}. Based on their chemical structure, the vegetable tannins are classified as Hydrolysable type (e.g. Myrobalan) and Condensed type (e.g. Wattle).

Hydrolysable type tannins are based on esters of phenol carboxylic acid and glucose such as 1,2,3,4,6-pentagalloyl glucose (**Fig. 1**) along with several other compounds²¹. Condensed or flavonoid tannins being structurally related to flavonoid group of compounds, form insoluble “phlobaphenes” or tannins reds on the treatment on mineral acids in aqueous media²². The typical structure of flavanoid is shown in **Fig.2**. The condensed tannins, also called proanthocyanidins are oligomers and polymers formed in the flavan-3-ol basic structure ie . epicatechin and catechin (**Fig. 3**)²³.

The manufacture of the vegetable tanning extract is based on extraction of tannin using a suitable solvent, usually water, followed by concentration and spray drying (to get powder) or vacuum dried (to get solid)¹⁸.

Sudan has various indigenous tanning materials. Some of these, such as Garad pods (*Acacia nilotica sub. sp. nilotica*) and Talh bark (*Acacia seyal*) are used extensively in the Sudan by rural tanners²⁴.

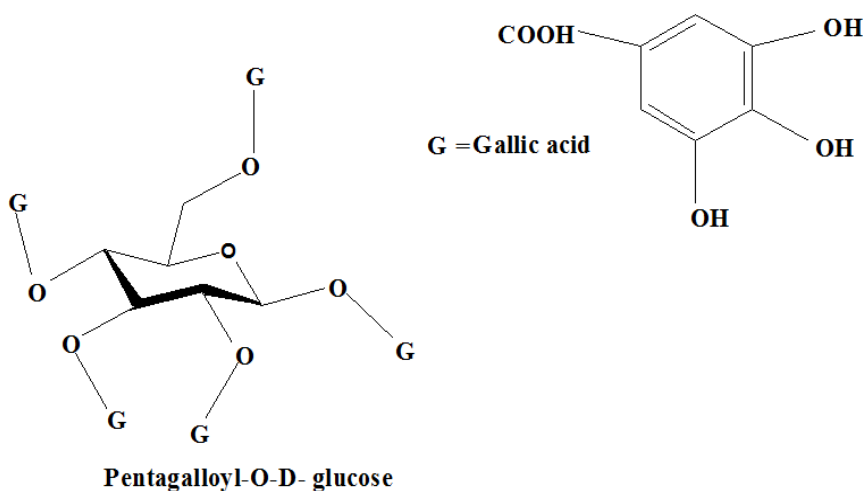


Fig. 1. 1,2,3,4,6-pentagalloyl glucose.

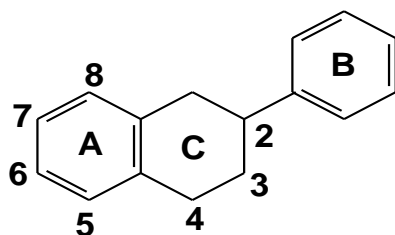


Fig. 2. Structure of flavonoids.

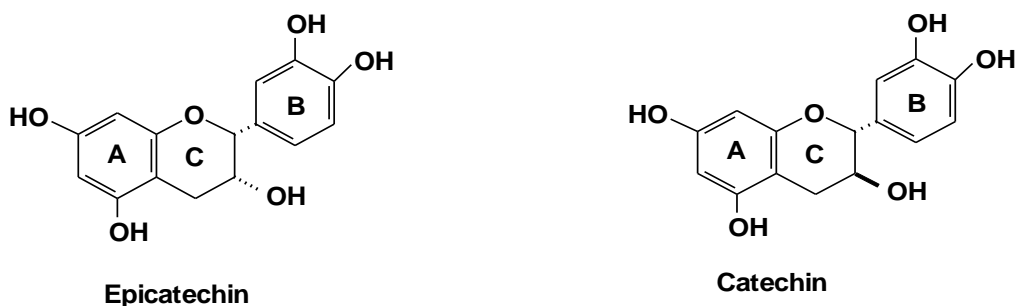


Fig. 3. Structure of epicatechin and catechin (Flavan-3-ols).

Acacia seyal pods and bark contain 20% tannin. The acacia seyal bark contains 18-30 % tannins and is a source of red dye. The bark, leaves and gums are used for colds, diarrhoea, hemorrhage, jaundice, headache and burns. A bark decoction is used against leprosy and dysentery, is a stimulant and acts as a purgative for humans and animals. Exposure to smoke is believed to relieve rheumatic pains²⁵. Since the *acacia seyal* bark (Talh bark) extract contains polyphenolic compounds with varied molecular weight, an attempt has been made in this study to utilize them for the retanning of wet blue leathers to produce upper leathers.

2. Materials and Methods

2.1 Materials

Conventionally processed wet blue goat skins were taken for the tanning trials. Talh (*acacia seyal*) barks were sourced from Sudan. Chemicals used for post tanning were of commercial grade. Chemicals used for the analysis of spent liquor were of analytical reagent.

2.2 Aqueous Extraction of Talh Barks

The required amount of ground talh (*Acacia seyal*) barks were soaked in water (1:10 w/v) at temperature above 80°C in water bath for an hour, filtered through a piece of cotton cloth and the volume of the talh extract is noted. Part of the talh extract was filtered through Whatman no.1 filter paper and 10 ml of filtrate were used for the determination of percentage total solubles.

2.3 Retanning Trials

The retanning experiments were carried out on conventionally processed wet blue goat skins using talh barks extract. The retanning trials were carried out using mimosa as a matched pair control as a comparison for the experimental leathers. The post tanning process mentioned in Table 1 and Table 2 followed for both experimental and control leathers.

Table 1. Experimental Formulation of Post-tanning process for making upper crusts, Raw material: Shaved wet blue goat skins of thickness ~1.2 mm, % chemicals for post tanning process is based on shaved weight.

Process	%	Product	Duration (min)	Remarks
Washing	200	Water	10	Drain
Neutralization	100	water		
	1	Sodium formate		
	0.75	Sodium bicarbonate	3 × 15	pH 5-5.5
Retanning	20	Talh barks extract	1 hour	
Fatliquoring	10	Synthetic fatliquor	90 min	
Dyeing	3	Acid brown dye	45 min	Penetration of dye was checked
Fixing	1.5	Formic acid	3 × 10 +30 min	pH 3.5
Washing	200	Water	10 min	Leathers were piled over night; Next day set, hooked to dry, staked, trimmed and buffed

2.4 Determination of Shrinkage Temperature

The shrinkage temperature of both control and experimental leathers were determined using the Theis shrinkage tester²⁶. A 2cm sample, cut out from the leather was clamped between the jaws of the clamp, which in turn was immersed in a solution of glycerol: water mixture (3:1). The solution was stirred using mechanical stirrer attached with the shrinkage tester. The temperature of the solution was gradually increased and the temperature at which the sample shrinks was noted. Triplicates were carried out for each sample and the average values are reported.

Table 2. Control Formulation of Post-tanning process for making upper crusts, Raw material: Shaved wet blue goat skins of thickness ~1.2 mm, % chemicals for post tanning process is based on shaved weight.

Process	%	Product	Duration (min)	Remarks
Washing	200	Water	10	Drain
Neutralization	100	water		
	1	Sodium formate		
	0.75	Sodium bicarbonate	3 × 15	pH 5-5.5
Retanning	20	Mimosa	1 hour	
Fatliquoring	10	Synthetic fatliquor	90 min	
Dyeing	3	Acid brown dye	45 min	Penetration of dye was checked
Fixing	1.5	Formic acid	3 x 10 +30 min	pH 3.5
Washing	200	Water	10 min	Leathers were piled over night; Next day set, hooked to dry, staked, trimmed and buffed

2.5 Evaluation of Organoleptic Properties

Experimental and control crust leathers were assessed for softness, fullness, grain smoothness, grain tightness (break), general appearance and dye uniformity by hand and visual examination. Three experienced tanners rated the leathers on a scale of 0-10 points for each functional property, where higher points indicate better property. The tanners have also evaluated the dyeing characteristics viz., uniformity of dye, shade intensity and differential dyeing for both experimental and control crust leathers.

2.6 Mechanical Properties Test of Leather Samples

Samples for various physical tests from experimental and control crust leathers were obtained as per IULTCS methods²⁷. Specimens were conditioned at 20 ± 2 °C and 65 ± 2 % R.H over a period of 48 hrs. Mechanical properties such as tensile strength, percentage elongation at break²⁸, grain crack strength²⁹ and tear strength³⁰ were measured as per standard procedures. Each value reported is an average of four (2 along the backbone, 2 across the back bone) samples.

2.7 Analysis of Composite Waste Liquor

The spent liquor from control and experimental post tanning processing were collected, filtered and analyzed for chemical oxygen demand (COD), Biochemical oxygen demand (BOD₅), and total solids (TS) as per standard procedures³¹.

2.8 Chemical Analysis

The chemical analysis of the leathers viz. for % moisture, total ash content, % oils and fats, % water soluble, % insoluble ash % hide substance, and degree of tannage were carried out for control and experimental leathers as per standard procedures³² Triplicates were carried out for each sample and the average values are reported.

3. Results and Discussion

3.1 Shrinkage Temperature

The way to determine that the tanning process has been carried correctly is to measure the 'hydrothermal stability' – its resistance to wet heat – more commonly referred to as the 'shrinkage temperature'. A characteristic of hides, skins and leathers is that if they are gradually heated in water, they reach a temperature at which they are subject to sudden, irreversible shrinkage. The shrinkage temperature of wet blue leathers retanned using talh and wattle is given in Table 3. The wet blue leathers resulted in shrinkage temperature of 109°C; however the retanning with wattle and talh resulted in increase of shrinkage temperature to 117°C and 113°C respectively. It is clear that the treatment of talh enhances the shrinkage temperature significantly similar to the case of wattle; hence retanning with talh bark extract improved the hydrothermal stability.

Table 3. Shrinkage temperature of crust leathers retanned with talh and wattle.

Sample	Shrinkage temperature, Ts (°C)
Wattle (Control)	117±3
Talh (Experimental)	113±2

Note- Shrinkage temperature of wet blue leathers were 109±2°C

3.2 Organoleptic Properties Assessed by Tactile Evaluation

The organoleptic properties of leathers retanned using talh and control wattle is given in **Fig. 4**. Higher numbers indicate better property. From the figure it is observed that retanning with talh resulted in leathers with good grain tightness and roundness compared to wattle retanned leathers. The fullness of the leathers with talh retanning had been found to be comparable to that of wattle. However, the softness of leathers with wattle retanning is found to be better than that of talh. To be an effective agent for retanning, the retanning material should improve the fullness, grain tightness and roundness of the leather, as they are the important parameters especially for making upper leathers. The grain smoothness of talh retanned leathers has been found to be similar to that of wattle retanning. On the whole the leathers retanned with talh had been found to be better than wattle retanning. Hence using talh bark extract appears to be a good alternative for the retanning processes for making leathers with good organoleptic properties.

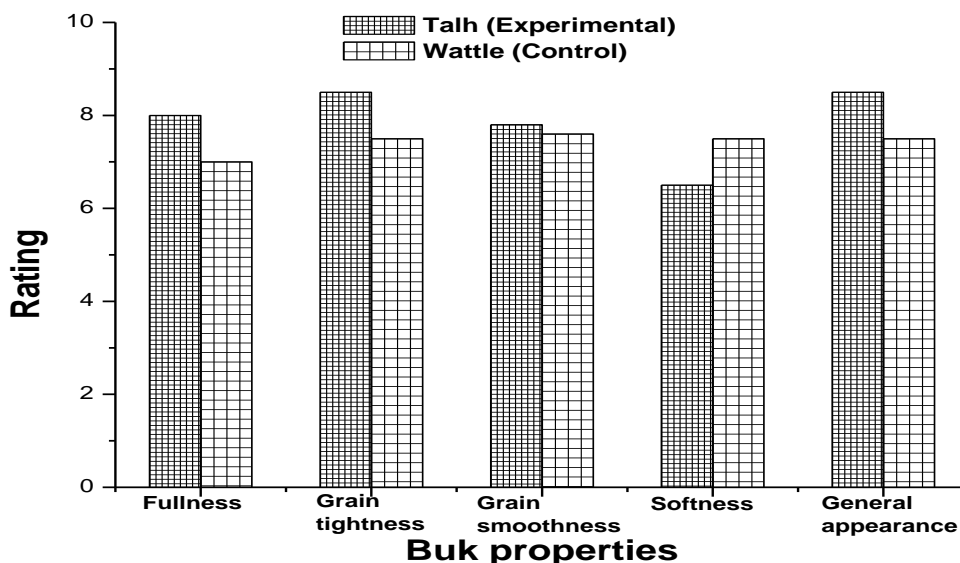


Fig. 4. Graphical representation of organoleptic properties of the experimental and control crust leathers.

3.3 Dyeing Characteristics of Talh Retained Leathers

The dyeing characteristics of talh and wattle retained leathers have been evaluated by experienced tanners and the results are given in Table 4. The uniformity of dye of the talh retained leathers has been found to be similar to wattle retained leathers. The shade intensity of the talh retained leathers has been found to be better than the wattle retained leathers. No differential dyeing (between grain and flesh) has been observed for both talh and wattle retained leathers. The overall performance of both control and experimental leathers are comparable.

Table 4. Visual evaluation of the dyeing characteristics of crust leathers retained with talh a and wattle.

Property	Talh (Experimental)	Wattle (Control)
Uniformity of dye	Good	Good
Shade intensity	V.good	Good
Differential Dyeing	Nil	Nil

3.4 Mechanical Properties of Talh Retained Leathers

The physical strength measurements of matched pair talh retained experimental and wattle retained control leathers are given in Table 5. The physical strength measurements viz., tensile strength, elongation, tear strength, load at grain crack and distension at grain has been found to be comparable. The strength values of talh retained leathers have been found to meet the BIS standards³³ for chrome retained leathers.

Table 5. Physical strength characteristics of crust leather retanned using talh (Exp) and wattle (Con.).

Property	Talh	Wattle	BIS norms*
Tensile strength (Kg/cm ²)	255± 5	252±5	250
Elongation at break (%)	67± 2	65±2	60-70
Tear strength (Kg/cm thickness)	48±2	46±2	30
Load at grain crack (kg)	26±3	24±5	20
Distention at grain crack (mm)	10.5±0.5	9.4±0.2	Min 7

* Bureau of Indian standards (BIS) specification for chrome retanned upper leathers

3.5 Environmental benefits

Oxygen demand, biological oxygen demand and total solids are main parameters in assessing the quality of wastewater. The COD, BOD₅ and TS of the spent liquor for both experimental and control trials were determined and are given in Table 6. From the table it is observed that the COD and BOD of the spent liquor processed using talh retanning is lesser than the spent liquor from wattle retanning. However the environmental impact of talh retan liquor has been observed to be lesser than the wattle retan liquor.

Table 6. Characteristic of spent liquor for control and experimental post tanning trials.

Parameter	Talh (Experimental)	Wattle (Control)
COD (mg/l)	81600±1200	93500±2550
BOD ₅ (mg/l)	32800±900	34500±800
Total solid (mg/l)	23560±740	32650±750

3.6 Chemical Analysis of the crust leather

The chemical measurements of matched pair experimental crust leather (talh) and control (Wattle) are given in Table 7. The chemical analysis data for the experimental leathers is comparable to the control leathers. However, the water soluble matter for the control (wattle) leathers is more than the experimental leathers (talh).

Table 7. Chemical Analysis of crust leather of experimental and control.

Parameter	Talh (experimental)	Wattle (control)
Moisture (%)	13.10	12.30
Total ash content (%)	3.00	2.70
Fats and oils (%)	3.60	3.30
Water soluble matter (%)	5.40	4.70
Insoluble ash (%)	1.30	1.10
Hide substance (%)	50	51
Degree of tannage (%)	53	54.12

4. Conclusions

Retanning plays an important role in the leather industry. It can not only further supplement tanning, improve the fullness and softness of leather, tighten the grain of leather, but also can enhance the hydrothermal stability, level-dyeing property and wear resistance of leather. Meanwhile, the retanning process is helpful to subsequent finishing operations. Therefore, the quality of the retanning materials is a significant factor to determine the effect of retanning. Most organoleptic properties of the experimental leathers produced from talh bark extract are better than control leathers produced from wattle. However softness property is better in the case of wattle retanned leather and the mechanical properties are comparable with the matched pair control leathers. Retanning with talh also enhances in intense dyeing. Hence using talh bark extract appears to be a good alternative for the retanning processes viz., it can complement the tanning effect, improving fullness and softness of the leather plus, having a certain of filling performance especially in the looser parts such as the belly, and make a firmer grain and fuller leather. In addition, there is a certain enhancement for the hydrothermal stability and dyeing uniformity.

References

1. Leafe, M. K.: *Leather technologist's pocket book*. West Yorkshire: The Society of Leather Technologists and Chemists, pp. 85, 1999.
2. Taylor, M., Lee, J., Bumanlag, L. P., Balada, E. H.: *Treatments to enhance properties of chrome-free (wet white) leather*. JALCA 106, 35-43, 2011.
3. Covington, A. D.: *Tanning chemistry: The science of leather*. Cambridge: Royal Society of Chemistry, pp. 352, 2011.
4. Zhang, J. W., Cheng, F., Ai, Z. W., Chen, W. Y.: *The synthesis and application of phosphorus-nitrogen flame retardant retanning agent*. *Leather Footwear J.* 15, 179-188, 2015.
5. Song, Y., Zeng, Y. H., Xiao, H. L., Wu, H. P., Shi, B.: *Effect of molecular weight of acrylic resin retanning agent on properties of leather*. JALCA 112, 128-134, 2017.
6. Heidermann, E.: *Fundamentals of leather manufacture*. Darmstadt: Eduard Roether KG, 1993.
7. Cantera, C., Martegani, J., Esterelles, G., Vergara, J.: *Collagen hydrolysate: 'soluble skin' applied in post-tanning processes. Part 2: Interaction with acrylic retanning agents*. *J. Soc. Leather Technol. Chem.* 86, 195-202, 2002.
8. Jankauskaite, V., Jiyembetova, I., Gulbinienė, A., Sirvaityte, J., Beleska, K. and Urbelis, V.: *Comparable evaluation of leather waterproofing behaviour upon hide quality. I. Influence of retanning and fatliquoring agents on leather structure and properties*. *Mater. Sci.-Medzg.* 18, 150-157, 2012.
9. Cassano, A., Adzet, J., Molinari, R., Buonomenna, M. G., Roig, J. and Drioli, E.: *Membrane treatment by nanofiltration of exhausted vegetable tannin liquors from the leather industry*. *Water Res.* 37, 2426-2434, 2003.
10. Munz, G., De Angelis, D., Gori, R., Mori, G., Casarci, M. and Lubello, C.: *The role of tannins in conventional and membrane treatment of tannery wastewater*. *J. Hazard. Mater.* 164, 733-739, 2009.

11. Lofrano, G., Meric, S., Belgiorno, V. and Napoli, R. M. A.: Fenton's oxidation of various-based tanning materials. *Desalination* 211, 10-21, 2007.
12. De Nicola, E., Meric, S., Gallo, M., Iaccarino, M., Della Rocca, C., Lofrano, G., Russo, T. and Pagano, G.: Vegetable and synthetic tannins induce hormesis/toxicity in sea urchin early development and in algal growth. *Environ. Pollut.* 146, 46-54, 2007.
13. Jaisankar, S. N., Gupta, S., Lakshminarayana, Y., Kanakaraj, J. and Mandal, A. B.: Water-based anionic sulfonated melamine formaldehyde condensate oligomer as retanning agent for leather processing. *JALCA* 105, 289-296, 2010.
14. Nashy, E. H. A., Essa, M. M. and Hussain, A. I.: Synthesis and application of methyl methacrylate/butyl acrylate copolymer nanoemulsions as efficient retanning and lubricating agents for chrome-tanned leather. *J. Appl. Polym. Sci.* 124, 3293-3301, 2012.
15. Zou, X. L., Lan, Y. J., Zhang, Q. H., Li, Z. Y. and Zhan, X. L.: Effects of polyacrylic acid on the structure of collagen fibre. *J. Soc. Leather Technol. Chem.* 98, 172-176, 2014.
16. Tang, K. Y., Zheng, X. J., Yang, M., Shelly, D. C. and Casadonte, D. J.: Influence of Retanning on the Adsorption Capacity of Water on Cattlehide Collagen Fibers. *JALCA* 104, 367-374, 2009.
17. Balfe, M.P.: *Progress in leather science*. British Leather Manufacturer Association, 1948.
18. Sundara Rao, V.S., Santappa, M.: Vegetable Tannins – A Review. *J. Sci. Ind. Res.* 41, 705-718, 1982.
19. Mané, C., Sommerer, N., Yalcin, T., Cheynier, V., Cole, R.B., Fulcrand, H.: Assessment of the molecular weight distribution of tannin fractions through MALDI-TOF MS analysis of protein-tannin complexes. *Anal. Chem.* 79, 2239-2248, 2007.
20. Ricci, A., Olejar, K.J., Parpinello, G.P., Kilmartin, P.A., Versari, A.: Application of fourier transform infrared (FTIR) spectroscopy in the characterization of tannins. *Appl. Spectrosc. Rev.* 50, 407-442, 2015.
21. Dutta, S.S.: *An Introduction to the Principles of Leather Manufacture*, ILTA, Calcutta, 1985.
22. Hemingway R.W. and Karchesy J.J.: 'Chemistry and significance of condensed tannins', Plenum Press, New York, 1989.
23. Falcão, L., Araújo, M.E.M.: Tannins characterization in historic leathers by complementary analytical techniques ATR-FTIR, UV-vis and chemical tests. *J.Cult. Herit.* 14, 499-508, 2013.
24. Gasmelseed, G. A. and Mulla, T. H. A. : *Simulation of Continuous Counter-current Leaching of Garad Pods.*, *J. Chem. Biotech., Britain*, 1976.
25. El Amin HM.: *Sudan acacias*. Forest Research Institute Publishing Section Information Department, 1973.
26. McLaughlin, G.D. and Thesis, E.R.: *The chemistry of leather manufacture*, Reinhold Publishing Corp., New York, p. 133, 1945.
27. IUP 2. : Sampling. *J. Soc. Leather Technol. Chem.* 84, 303, 2000.
28. IUP 6. : Measurement of tensile strength and percentage elongation. *J. Soc. Leather Technol. Chem.* 84, 317, 2000.
29. SLP 9 (IUP 9) . : Measurement of distension and strength of grain by the ball burst, *Official methods of analysis*. The Society of Leather Technologist and Chemists, Northampton, 1996.
30. IUP 8. : Measurement of tear load – double edge tear. *J. Soc. Leather Technol. Chem.* 84, 327-329, 2000.
31. Clesceri.L.S.: Greenberg, A.E., Trussel, R.R, Eds. *In standard methods for the examination of water and wastewater*, 17th ed, American public health association Washington DC, 1989.
32. *Official Methods of Analysis: The Society of Leather Technologist and Chemists*, Northampton, 1965.
33. Bureau of Indian Standards: *Specification for chrome retan upper leather*; IS 2961: New Delhi, India, 1964.

INFLUENCE OF PHOTOPERIOD ON BIOMASS PRODUCTION AND REMOVAL OF NUTRIENTS FROM TANNERY EFFLUENTS WITH MICROALGAE CONSORTIUM

Aline C. Campos Pena^{1, a}, Luciane F. Trierweiler² and Mariliz Gutterres¹

1 Laboratory for Leather and Environmental Studies (LACOURO)

2 Group of Intensification, Modeling, Simulation, Control, and Optimization of Process,

Federal University of Rio Grande do Sul, Chemical Engineering Department.

a campos@enq.ufrgs.br

Abstract. Wastewater from tanneries besides having toxic compounds also contain nutrients such as carbon, phosphorus, and nitrogen, which facilitate the rapid multiplication of microalgae. Currently, several researches search microalgae capable of growing in industrial effluents, exploiting the advantages of removing the nutrients present in these waters and producing biomass with high value added. The liquid effluents produced in tanneries for finished leather have essential nutrients for the growth of microalgae, but also some compounds that may restrict or hinder the growth of microalgae in this medium. Therefore, the present work has the objective to evaluate the growth of a microalgae consortium for the removal of phosphorus and ammonia from wastewater streams of a tannery processing wet-blue to finished leather with different photoperiods. Microalgae consortium was cultivated at two different compositions of mixtures of raw wastewater (R) and wastewater after secondary biological treatment (B): 50% of R + 50% of B, (50R50B) and 75% of R + 25% of B, (75R25B), in photoperiod of 24 hours and 12 hours of light, temperature of 25 °C and constant aeration. The growth of microalgae in the effluent and the removal of phosphorus, nitrogen and ammonia were monitored throughout the cultivation. The highest growth was achieved in the 24-hours condition with maximum biomass concentrations in the 75R25B effluent (1.40 g L⁻¹) and phosphorus removal (97.94% for the 50R50B), nitrogen removal (71.53% for the 50R50B) and ammonia removal (100% for both effluent).

1 Introduction

In most stages of leather production, clean water is utilised as transport liquid to diffuse the chemicals and for the extraction of undesirable materials from the hide. In this way, the liquid effluents generated in the beamhouse stage, as well in the tanning and finishing stages, have high impact potential to the environment due to high concentrations of nitrogen, phosphorus, toxic metals, sulphides, biological oxygen demand (BOD), oxygen chemical demand (COD) and suspended solids. Thus, because of the large volumes generated with high chemical and organic loads, the effluents need adequate treatments before being discarded in the water bodies GUTTERRES et al., 2015; SHARMA & MALAVIYA, 2016, DE AQUIM; HANSEN; GUTTERRES, 2019). The characteristics of tannery wastewater vary widely, depending on the nature and preservation of the hide, the tanning and leather processing technology, the amount of water used, and the procedure adopted by the industry to reduce pollution.

In the finishing stage, wet-blue leather receives the desired final characteristics, such as physical-mechanical strength, softness, color, durability, stamping and surface coating. The leather finishing consists of wet end (deacidulation, retanning, dyeing and fatliquoring), drying, pre-finishing and finishing. In these steps various chemical is used in the processing, such as deacidulants, dyes, oils, surfactants, polymers, pigments, solvents, resins and other chemical products, as well as remainings of organic matter inherent to the process, result in contamination of the effluents that require treatment (PICCIN et al., 2016).

Several researches have investigated in the last years treatment techniques of effluents generated in the leather industry, involving biotechnology, as it is a sustainable and economical way to treat pollutants. These studies have used biological agents as microalgae, bacteria, fungi and

their bioproducts to treat effluents (FONTOURA *et al.*, 2017, ORTIZ-MONSALVE *et al.*, 2017; SINGH, VYAS & MALAVIYA 2016;).

Microalgae represent a versatile possibility for treatment of effluents since they have high capacity of fixation of carbon dioxide of the air and phosphorus and nitrogen dissolved in the water, adapt easily to the changes in the environment (temperature, pH, salinity, and availability of nutrients) making possible their cultivation in effluents (WHITTON, 2012). These microorganisms can also be used for the removal of metals that are present in the effluents since their surfaces contain negative charges and adsorb the metal ions of the liquid effluent (SUNDARAMOORTHY *et al.*, 2016). In addition, they can achieve high rates of cell growth in these media and present cleaner solutions when compared to other alternatives of effluent treatment (ANGELIS *et al.*, 2012; HU *et al.*, 2017). However, raw effluents from the leather industry, that is, without previous treatment, are a challenge for the growth of microalgae due to the high chemical load and turbidity, which can often be toxic to these microorganisms, inhibiting their growth (AJAYAN *et al.*, 2015). Fontoura *et al.* (2017) used raw wastewater from the beamhouse stage in different concentrations to grow the *Scenedesmus* sp. microalgae. Results were obtained with 88.4% effluent concentration, reaching a maximum biomass concentration of 0.90 g L⁻¹, maximum removal of ammoniacal nitrogen, phosphorus and COD of 85.63%, 96.78% and 80.33%, respectively.

Pena *et al.* (2018) carried studies with the microalgae *Tetraselmis* sp. in the effluent from the finishing phase with continuous light regime. Removal of 96.59% and 99.81% for phosphorus, 99.90% and 89.2% for ammoniacal nitrogen, 89.06% and 54.78% for total nitrogen, 40, 46% and 43.54% for COD, 59.24% and 57.90% for total organic carbon, 32.70% and 44.73% for biological oxygen dissolved, were achieved at the 50R50T concentrations (50% raw/50% treated effluent), and 75R25T (75% raw/25% treated effluent), respectively.

Microalgae become an attractive alternative for wastewater treatment, since these microorganisms present many benefits, as they also remove unwanted substances from the effluent, they have high storage capacity of reserve substances in their biomass, which can be transformed into bioproducts (JAHAN *et al.*, 2014). Some studies have reported higher efficiency when using a microalgae consortium in the removal of pollutants and nutrients, such as nitrogen, phosphorus and ammonium from wastewater, when compared to individual microorganisms (KOREIVIENĖ *et al.*, 2014; HENA *et al.*, 2015).

In this way, the present study was carried out with the purpose of analysing the growth of microalgae consortium and the efficiency for removal of total Nitrogen, phosphorus, and ammonia from effluent of wet end to leather finishing processing at different effluent concentrations and photoperiods.

2 Material and methods

2.1 Cultivation of microalgae

A sample of microalgae was collected in a deactivated effluent treatment pond from a tannery located in Montenegro / RS, Brazil and throughout microscopic analysis, it was possible to see that there was a consortium of microalgae (Fig. 1). When analysing the microalgae present in this consortium Pena *et al.*, (2018) identified the predominance of the microalgae *Tetraselmis* sp.. The culture of microalgae consortium was cultured under constant aeration with 1 L min⁻¹ of compressed air at room temperature under continuous light. 20 mL of the microalgae consortium was maintained using 180 mL of the Tris-Acetate-Phosphate (TAP) in 250 mL Erlenmeyer every 10 days. All culture inoculation and maintenance procedures were performed with glassware and sterile culture medium inside a vertical laminar flow hood with air filtration system and ultraviolet (UV) lamps.

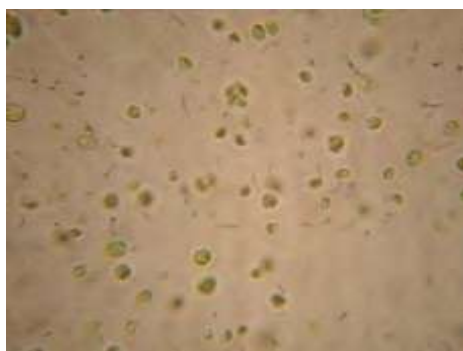


Fig. 1. Optical microscopy of the microalgae consortium (10x) (PENA *et al.*, 2018).

2.2 Tannery Wastewater

The wastewater was collected from a tannery that processes leather from wet-blue to finished leather, located in the city of Novo Hamburgo/RS, Brazil. Two kinds of effluents were collected in the treatment effluent plant: raw effluent without treatment (R) and effluent after primary physicochemical treatment (coagulation-flocculation-sedimentation) followed by biological secondary treatment with sludge-sedimentation (B). Nevertheless, this treated effluent does not meet environment standards for discharge to water bodies, requiring advanced treatment realized in the wastewater treatment plant (WWTP).

The microalgae consortium was cultivated with continuous light and at room temperature in 5000 mL bottles for 19 days, in the two following compositions:

- 50% raw/50% wastewater after secondary biological treatment (50R50B): (i) 1800 mL of raw effluent; (ii) 1800 mL of treated effluent; and (iii) 400mL of the microalgae consortium pre inoculum, totalling 4000mL.
- 75% raw/ 25% wastewater after secondary biological treatment (75R25B): (i) 2700 mL of the raw effluent; (ii) 900 mL of treated effluent; and (iii) 400 mL of the microalgae consortium pre inoculum, totalling 4000 mL.

The culture of microalgae consortium was cultured under constant aeration with 1 L min^{-1} of compressed air at room temperature, under two photoperiod conditions: continuous fluorescent light (24-hours) and fluorescent light in 12 h light/12 h dark cycles (12-hours).

2.3 Analytical methodology

The quantification of ammonia (N-NH_3) present in the culture was analysed on the Ion Chromatograph (Metrohm) using the Metrosep C4-150 column, eluent HNO_3 2.5 g L^{-1} and dipicolinic acid 1.5 g L^{-1} with a flow of 0.9 ml min^{-1} .

Phosphorus (P-PO_4) was analysed according to Standard Methods for the Examination of Water and Wastewater (APHA, 2005). The effluent analysis followed the colourimetric method with quantification using UV / VIS spectrophotometer (880 nm).

Total nitrogen (TN) analyse was performed on the Shimadzu TOC-L analyzer equipped with a total nitrogen measurement unit (TNM-L Shimadzu) and 8-port sampler (OCT-L Shimadzu).

3 Results and Discussion

The maximum biomass concentrations of the cultures of 24-hours light and 12-hours light for composition 50B50S and 75B25S are presented in Table 1. The highest biomass concentration of the microalgae consortium was 1.40 g L^{-1} on day 11, for 75B25S in 24-hours light. The condition

75B25S favored the growth of the microalgae consortium explained by the higher concentrations of nutrients in this effluent mixture.

However, 12-hours did not favor the growth of the microalgae consortium, mainly in the 75R25B, which has a lower incidence of light because it is a more concentrated and turbid effluent, making the passage of light difficult. It is necessary a balance between the luminosity and the absence of light, since under low illumination the available energy is insufficient, whereas the opposite, that is, the excess of light causes photoinhibition (YAN *et al.*, 2011). The light in the cultures varies both in space (depth and latitude) and in time (daily), making it a determinant factor for microalgae growth. This explains the lower growth of the consortium in the 12-hours culture when compared to the 24-hours cultivation since there was no light every 12 hours and as it is a turbid effluent the entry of light is hindered into the culture medium due to the time reduction.

Table 1. Maximum biomass concentration of the microalgae consortium during of cultivation 24-hours light and 12-hours light in tannery wastewater.

	24-hours light	12-hours light
50R50B (g L ⁻¹)	1.04±0.03	1.26±0.005
75R25B (g L ⁻¹)	1.40±0.02	0.79±0.01

Removal of TN, N-NH₃ and P-PO₄ over the 19 days of culture for 50R50B and 75R25B concentrations is shown in **Fig. 2** for 24-hours. The removals were 100% of ammoniacal nitrogen for both, 71.54% and 58.84% total nitrogen and 97.94% and 95.54% phosphorus for 50R50B and 75R25B, respectively.

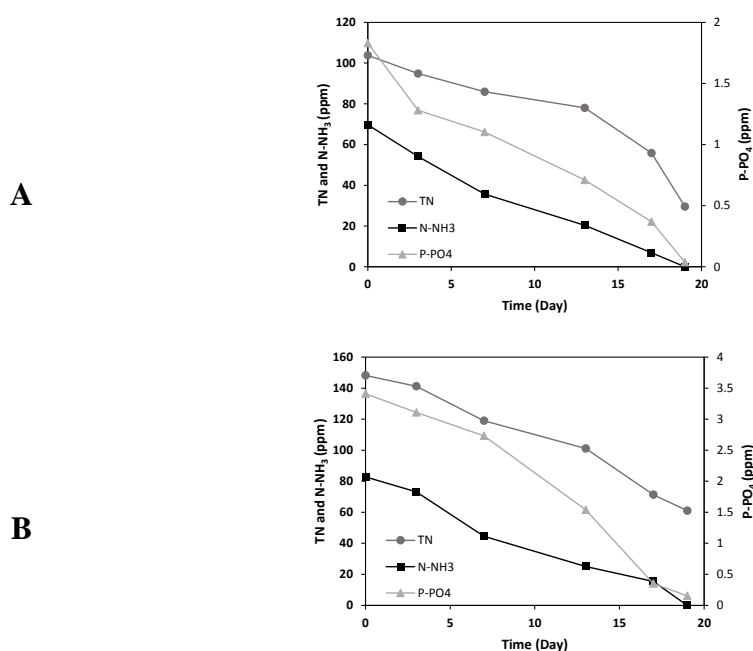


Fig. 2. Removal of TN, N-NH₃ and P-PO₄ in composition 50R50B (A) and 75R25B (B) in 24-hour culture with light.

Removal of TN, N-NH₃ and P-PO₄ over the 19 days of culture at 50R50B and 75R25B concentrations are shown in **Fig. 3** in 12-hours. The removal of 70.16% and 56.36% for ammoniacal nitrogen, 53.28% and 41.67% for total nitrogen and 97.37% and 97.39% for phosphorus were observed in assays with tannery wastewater concentration 50R50B and 75R25B, respectively.

The metabolism of phosphorus and nitrogen present in wastewater is directly linked to the production of biomass and metabolic activities. Ammonia is a form of nitrogen that is more easily assimilated by microalgae, and usually, nitrite and nitrate are assimilated after the complete removal of ammonia (Maestrini et al., 1986). Phosphorus is an essential element for the growth of microalgae and plays many roles in the cells. The initial amounts of phosphorus are low and decay rapidly in the cultivation, it becomes a growth-limiting factor since it is directly linked to some functions of the cell.

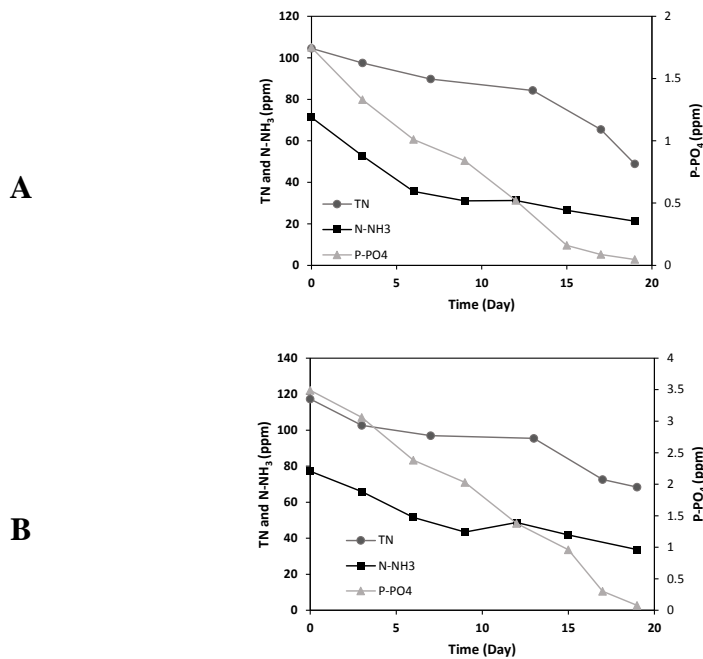


Fig. 3. Removal of TN, N-NH₃ and P-PO₄ in composition 50R50B (A) and 75R25B (B) in 12-hour culture with light.

Conclusion

This study showed that the microalgae consortium grown in raw tannery wastewater being efficient in the removal of nitrogen, ammonia and phosphorus. The highest growth was achieved in the 24-hours condition with maximum biomass concentrations in the 75R25B effluent (1.40 g L⁻¹) and phosphorus removal (97.94% for the 50R50B), nitrogen removal (71.53% for the 50R50B) and ammonia removal (100% for both effluent). Thus, the study showed that tannery wastewater can be used as an alternative source of nutrients for the production of biomass microalgae.

Acknowledgements

We would like to thank the scholarships provided by Coordination for the Improvement of Higher Education Personnel (CAPES), and Agency Financier of Studies and Projects (FINEP) for the financial support by the public MCTI/FINEP CT-HIDRO 01/2013.

References

1. Ajayan, K. V., Selvaraju, M., Unnikannan, P., & Sruthi, P. Phycoremediation of Tannery Wastewater Using Microalgae *Scenedesmus* Species. *International Journal of Phytoremediation*, 2015.
2. Angelis, S., Novak, A. C., Sydney, E. B., Soccol, V. T., Carvalho, J. C., Pandey, A., Soccol, C. R. Co-Culture of Microalgae, Cyanobacteria, and Macromycetes for Exopolysaccharides Production: Process Preliminary Optimization and Partial Characterization. *Applied Biochemistry and Biotechnology*, 2012.
3. de Aquim, P. M., Hansen, É., & Gutterres, M. Water reuse: An alternative to minimize the environmental impact on the leather industry. *Journal of Environmental Management*, 2019.
4. Fontoura, J. T. da, Sebastião Rolim, G., Farenzena, M., & Gutterres, M. Influence of light intensity and tannery wastewater concentration on biomass production and nutrient removal by microalgae *Scenedesmus* sp. *Process Safety and Environmental Protection*, 2017.
5. Gutterres, M., Ortiz-Monsalve, S., Fontoura, J., & Benvenuti, J. Characterization of Raw Wastewater from Tanneries. *Journal of the Society of Leather Technologists and Chemists*, 2015.
6. Hena, S., Fatimah, S., & Tabassum, S. Cultivation of algae consortium in a dairy farm wastewater for biodiesel production. *Water Resources and Industry*, 2015.
7. Hu, Y., Hao, X., Loosdrecht, M. Van, & Chen, H. Enrichment of highly settleable microalgal consortia in mixed cultures for effluent polishing and low-cost biomass production, 2017
8. Jahan, M. A., Akhtar, N., Khan, N. M. S., Roy, C. K., Islam, R., & Nurunnabi. Characterization of tannery wastewater and its treatment by aquatic macrophytes and algae. *Bangladesh Journal of Scientific and Industrial Research*, 2014.
9. Koreivienė, J., Valčiukas, R., Karosienė, J., & Baltrėnas, P. Testing of *Chlorella*/*Scenedesmus* microalgae consortia for remediation of wastewater, CO₂ mitigation and algae biomass feasibility for lipid production. *Journal of Environmental Engineering and Landscape Management*, 2014.
10. Maestrini, S.Y., Collos, Y., Leftley, J.W. Ammonium thresholds for simultaneous uptake of ammonium and nitrate by oyster-pond algae. *J. Exp. Mar. Biol. Ecol.*, 1986.
11. Ortiz-Monsalve, S., Dornelles, J., Poll, E., Ramirez-Castrillón, M., Valente, P., & Gutterres, M. Biodecolourisation and biodegradation of leather dyes by a native isolate of *Trametes villosa*. *Process Safety and Environmental Protection*, 2017.
12. Pena, A. D. C. C., Schaumlöffel, L. D. E. S., Trierweiler, L. F., & Gutterres, M. *Tetraselmis* sp. Isolated from a Microalgae Consortium for Tannery Wastewater Treatment, 2018
13. Piccin, J. S., Guterres, M., Salau, N. P. G., & Dotto, G. L. Mass transfer models for the adsorption of Acid Red 357 and Acid Black 210 by tannery solid wastes. *Adsorption Science & Technology* *Adsorption Science & Technology*.
14. Sharma, S., & Malaviya, P. (2016). Bioremediation of tannery wastewater by chromium resistant novel fungal consortium. *Ecological Engineering*, 2016.
15. Singh, A., Vyas, D., & Malaviya, P. Two-stage phyto-microremediation of tannery effluent by *Spirodela polyrrhiza* (L.) Schleid. and chromium resistant bacteria, 2016.
16. *Standard methods for the examination of water and wastewater*, 21thed. Washington, D. C.: American Public Health Association, 2005.
17. Sundaramoorthy, B., Thiagarajan, K., Mohan, S., Mohan, S., Rajendra Rao, P., Ramamoorthy, S., & Chandrasekaran, R. Biomass characterisation and phylogenetic analysis of microalgae isolated from estuaries: Role in phycoremediation of tannery effluent. *Algal Research*, 2016.
18. Whitton, B. A. *Ecology of Cyanobacteria II*. Springer, New York, 2012
19. Yan, C., Zhao, Y., Zheng, Z., Luo, X., 2013. Effects of various LED light wavelengths and light intensity supply strategies on synthetic high-strength wastewater purification by *Chlorella vulgaris*. *Biodegradation*, 2013

MODIFIED POLYACRYLATES AS A NEW LEATHER RETANNING AGENTS

M. Canudas^{1,2}, N. Menna¹, A. Torrelles¹, J. de Pablo², and J. M. Morera³

1R&D Department, Cromogenia Units S.A., c/ 42 Polígon Industrial Zona Franca, 2-10, 08040 – Barcelona (Spain)

2Chemical Engineering Departmen, Universitat Politècnica de Catalunya (UPC), Av. d'Eduard Maristany, 10-14, 08930 – Barcelona (Spain)

3Department of Computer Science and Industrial Engineering, Universitat de Lleida (UdL), Av. Pla de la Massa, 8, 08700 – Igualada (Spain)

a)Corresponding author: mcanudas@cromogenia.com

Abstract. Acrylic resins have affinity for chrome tanned leather, for this reason, they are widely used as a retanning products. Its main use as a retanning agents is to produce full leathers. However, the leathers retanned with them have lower colour intensity and poorer structural properties because of their high anionicity which change the cationic surface of the leather causing a lower interaction of dyeing and fatliquoring agents with leather. This study proposes the use of modified polyacrylates as a new retanning agents. They were applied in leather versus traditional acrylic resins. The properties of the retanned leathers were evaluated concluding that this type of resins improve some leather properties avoiding the dyeing and fatliquoring problems of the traditional acrylic resins. The structure and the molecular weight of the modified polyacrylates play an interesting role in the improvement of the fixation of dyes and fatliquors, but also its lower anionic charge in comparison to the traditional acrylic resins. It has been observed that final leathers have a better colour intensity and softness. Moreover, its use as retanning agents favours the absorption of dyes and fatliquors which means an environmental improvement for the wet end process.

1 Introduction

Retanning process is one of the important steps in the manufacture of leather. It influences directly in the final steps (dyeing, fatliquoring and finishing) and, at the same time, defines the final properties of the leather. It is based in the treatment of the tanned leather with one or more chemical products to complete the tanning process and to give the end properties to the leather like fullness, softness, elasticity, colour levelness, etc.¹⁻³

The products used as retanning agents can be based on different chemical natures: mineral agents (chromium, aluminium and zirconium salts); vegetable tannins (mimosa, tara, chestnut, etc.); synthetic tannins (based on naphthalenics, phenolics and sulfones); resins (based on urea, melamine, dicyandiamide, acrylic) and others (aldehydes, polyphosphates, etc.). Each product provides different properties to the end leather.¹

Nowadays, the acrylic resins are extensively used because of its high affinity for chrome tanned leathers.⁴⁻⁷ The acrylic resins used as a retanning agents in the wet end process are homopolymers or copolymers of acrylic acid and its derivatives synthesized by free radical polymerization.⁹ They are linear chains with a number of carboxyl side groups that give resins an anionic charge.⁵ This negative charge density allows them to react by ionic ligands with chrome tanned leather which has a cationic charge.^{8,10,11} The resulting leather shows better properties such as fullness, flexibility and tensile strength.^{4,12} However, this reaction with chrome reduces the cationic charge on the surface of the leather which is an inconvenience for dyeing and fatliquoring steps. In these stages anionic chemical products are mostly used, so, they can't react with the surface of the leather and the result is a leather with rigid grain (low fatliquoring) and lower colour intensity (low dyeing).^{1,13}

In other fields, polyalcoholic branched polyacrylates are being used because of the presence of a backbone chain with one chemical nature and a multiple side chains with another chemical nature.¹⁴⁻¹⁹ This structure suggests that maybe these products can work as retanning agents acting similar to the acrylic resins because of their backbone chain and introducing some advantages for their side chains.¹⁵

In this work, a new modified polyacrylate is tested as a retanning agent to analyse if the fixation of the fatliquors and dyes is better than that obtained using acrylic resins.

2 Experimental

2.1 Material and Chemicals

To make the retanning tests, two Cromogenia's products were chosen. On one hand, an experimental modified polyacrylate that is composed of a polyacrylic acid with polyalcohol branches with a molecular weight (Mw) of 35000g/mol. On the other hand, and because of the good performance as a retanning agent in comparison to other commercial acrylic resins, a standard acrylic resin produced by Cromogenia that is composed of a polyacrylic acid with a molecular weight (Mw) of 615000g/mol.

The other chemicals used for the retanning tests apart from those of common use in the tanning industry were: chrome sulfate with a basicity of 33% and a richness of 25% in Cr₂O₃; anionic dyestuff (colour index Acid Brown 83); sulphated neatsfoot oil (75% of active matter); sulfochlorinated paraffin (67% of active matter).

The retanning tests were performed with split wet blue sheepskins from France shaved at 1.1mm.

2.2 Equipment

Simplex DF-2 Inoxvic drums with a dimension of 50cm in width and 100cm in diameter were used to carry out the retanning tests. All of them were equipped with velocity and temperature regulators.

2.3 Retanning tests

To avoid the anisotropic effect and to be able to make the comparison between the hides retanned with the two products, retanning tests were carried out splitting the sheepskins through the backbone. The right side was retanned with the experimental modified polyacrylate meanwhile the left side was retanned with the acrylic resin (both products were applied at 5% of active matter). The retanning procedure applied is listed below in Table 1.

Table 1. Retanning tests formula

Process	Chemical	%	time (min)	T (°C)	pH
Washing	Water	200		35	
	Non-ionic surfactant	0.2	30		
	Formic acid	0.2			
Drain					
Rechroming	Water	100		35	
	Chrome sulfate	5	30		
	Sodium formate	1.5	30		4.1
Overnight. Drain and rinse					
Neutralization	Water	150		30	
	Sodium formate	2	15		
	Sodium bicarbonate	0.5	60		5.0
Drain and rinse					
Retanning	Water	50		35	
	Retanning Agent (5% of active matter)	5	60		
Dyeing	Dispersing agent	2			
	Dyestuff	2	45		
Fatliquoring	Water	50		50	
	Sulphated neatsfoot oil	5	60		
	Sulfochlorinated paraffin	5			
	Formic acid	2	60		3.7
Drain and rinse					

2.4 Leather Characterization

To evaluate the leather physical properties, it was used the IUP (physical test methods) standard leather rules defined by the International Union of Leather Technologist and Chemists Society (IULTCS). These rules have an equivalence with the International Organization for Standardization rules (ISO).²⁰

Before the analyses of the physical properties, leather samples were cut and conditioned during 48h at $20\pm 2^{\circ}\text{C}$ with a 65% of relative humidity following rules IUP 1 & IUP 3 (ISO 2419:2012) and IUP 2 (ISO 2418:2017).

The physical properties evaluated were:

- Softness degree according to IUP 36 (ISO 17235:2015) using a Softness Tester. Seven measures are done in belly, backbone and middle doing an average of the 21 values.
- Thickness value according to IUP 4 (ISO 2589:2016) using a thickness gauge. Seven measures are done in belly, backbone and middle doing an average of the 21 values.
- Colour intensity using a colorimeter Color Data Spectraflash SF-30 based on chromatic model CIELAB for colour measures. Three measures in three leather different points are done obtaining an average value from the colorimeter.

All the leathers obtained in the retanning tests were checked by organoleptic tests carried out by experts in the field. The properties evaluated were fullness, visual colour levelness and colour intensity, grain tightness and superficial touch.

3 Results

The performed retanning tests were done following the methodology explained in the Experimental part to obtain comparative results between the leather retanned with the acrylic resin and those retanned with the modified polyacrylate.

In table 2 are described the values obtained for the physical retanned leather properties for three of the retanning tests done.

The physical property to be highlighted is the colour intensity. Acrylic resins are characterized by decreasing the colour intensity of the leathers because of their high anionicity. In this case, all the leathers retanned with the modify polyacrylate have a better colour intensity as it can be seen in the lightness (L^*) values of table 2 (highest values mean more lightness and, consequently, less colour intensity). These values are logical because the modified polyacrylate is less anionic than the acrylic resin, basically because of their side chains. Therefore, the retanned leather with the modified polyacrylate is more cationic and favours the fixation of the dyes on its surface.

Regarding the other two properties, practically no difference is appreciated in thickness, but it does concerning softness. Leathers retanned with the modified polyacrylate are softer than the other ones. Apart from the influence of charge, the modified polyacrylate is less anionic which means more fatliquors fixation, it seems that the polyalcoholic side chains play an important role too. On one hand, the chemistry nature of these lateral chains can lubricate the collagen fibrils and, on the other hand, these lateral chains can produce a different distribution or packaging of the modified polyacrylate resin inside the leather which favours an increase of softness in leather.

Table 2. Physical properties values for retanned leathers of PCE A vs AR

		Colour intensity (L*)	Thickness [cm]	Softness [mm]
Test 1	AR	65.03 ± 1.30	1.1 ± 0.1	5.3 ± 0.2
	PCE A	54.22 ± 1.09	1.1 ± 0.1	5.6 ± 0.2
	Variation	19.9%	0.0%	5.7%
Test 2	AR	61.09 ± 1.22	1.1 ± 0.1	4.3 ± 0.2
	PCE A	52.99 ± 1.06	1.0 ± 0.1	5.0 ± 0.2
	Variation	15.3%	10.0%	16.3%
Test 3	AR	57.54 ± 1.15	2.1 ± 0.1	2.3 ± 0.1
	PCE A	50.58 ± 1.01	2.1 ± 0.1	3.0 ± 0.1
	Variation	13.8%	0.0%	30.4%

These laboratory results were confirmed by experts in the leather field who analysed the organoleptic properties. Leathers retanned with the modified polyacrylate have a silky and soft touch while those retanned with the acrylic resin have a rough and hard touch. Fullness has similar values, but the visual colour intensity and the colour levelness are greater for those retanned with the modified polyacrylate. Both of the retanned leathers are similar in that they have low grain tightness (typical for acrylic resins or derivatives).



Figure 1. Colour intensity for leather retanned with acrylic resin and leather retanned with the modified polyacrylate.

After all the wet end process (retanning, dyeing and fatliquoring), it could be observed that the drums float of the modified polyacrylate test was more exhausted than the acrylic resin. It means that the products used in the retanning, dyeing and fatliquoring processes, are better absorbed using as a retanning agent the modified polyacrylate. This better absorption, which is traduced to an environmental improvement of the process, is probably linked to the structure, conformation and the charge of the modified polyacrylates.

4 Conclusions

Modified polyacrylates were evaluated as new retanning agents. They improve the fixation of dyes and fatliquors avoiding the principal problem of the acrylic resins used as retanning agents. The use of these new products as retanning agents will provide leathers with increased softness and colour intensity. Moreover, their use favours the absorption of the retanning, dyeing and fatliquoring agents which means the use of less quantities of these products and the presence of less quantities of them in the drum's float. Therefore, the use of modified polyacrylates means an environmental improvement for the retanning, dyeing and fatliquoring processes.

New studies will be done to complete the explanation of the positive effects of the modified polyacrylates on the physical retanned leathers properties.

References

1. Covington, A. D.; *Tanning chemistry: The science of leather*. RSC Publishing. UK, 2011.
2. Black, M., Canova, M., Rydin, S., Scalet, B. M., Roudier, S., Delgado, L.; *Best Available Techniques (BAT) Reference Document for the Tanning of Hides and Skins*. JRC Reference Reports (Joint Research Centre - European Commission). 2013.
3. Xianglong, Z., Yunjun, L., Qinghua, Z., Zhongyu, L., Xiaoli, Z.; *Effects of polyacrylic acid on the structure of collagen fibre*. *J. Soc. Leather Technol. Chem.* 98(4), 172-176, 2014.
4. Ugbaja, M. I., Ejila, A., Mamza, P. A. P., Uzochukwu, M. I., Opara, H.; *Evaluation and application of acrylic based binder for leather finishing*. *Int. J. Innov. Res. Sci. Eng. Technol.* 5(4), 4635-4644, 2016.
5. Xuebin, D., Qiang, X., Yuanhua, P.; *CN Patent 103255243 A, China, CN Patent & Trademark Office, 2013.*
6. Jian, L., Wang, Y., Zhu, D., Xu, Q.; *Effect of an amphoteric acrylic retanning agent on the physical properties of the resultant leather*. *Adv. Mat. Res.* 284-286, 1925-1928, 2011.
7. Xianglong, Z., Yunjun, L., Qinghua, Z., Xiaoli, Z.; *Synthesis and mechanical properties of polyacrylic acid resin retanning agent*. *J. Soc. Leather Tech. Chem.* 98, 127-130, 2014.
8. Dix, J. P.; *The characteristics and mode of action of modern polymers in post-tanning treatment processes*. *J. Am. Leather Chem. As.* 93(9), 283-294, 1998.
9. Naviglio, B., Calvanese, G., Tortora, G., Cipollaro, L., Pierrri, G.; *Characterization of tannery chemicals: Retanning agents*. *Stazione Sperimentale per l'industria delle pelli e delle materie concianti*. Italia, 1996.
10. Armstrong, R. W., Strauss, U. P.; *Encyclopedia of polymer science and Technology*. Wiley, New York, 1969.
11. El A'mma, A.; *Structure-property relationships of polyacrylate retanning agents*. *J. Am. Leather Chem. As.*, 93(1), 1-
12. Sheng, L., Dequing, W., Zonghui, L., Shuying, Z., Xinming, Z.; *Investigations of the mechanism of the reactions of acrylic resin tannage with Chrome leather*. *J. Am. Leather Chem. As.* 84, 79-85, 1989.
13. Morera, J.M.; *Tanning Technical Chemistry (in spanish)*. first ed. Igualada Engineering School, Spain, 2000.
14. Sakai, E., Yamada, K., Ohta, A.; *Molecular structure and dispersion-adsorption mechanisms of comb-type superplasticizers used in Japan*. *J. Adv. Concr. Technol.* 1(1), 16-25, 2003.
15. Marchon, D., Sulser, U., Eberhardt, A., Flatt, R.J.; *Molecular design of comb-shaped polycarboxylate dispersants for environmentally friendly concrete*. *Soft Matter.* 9(45), 10719-10728, 2013.
16. Yamada, K., Takahashi, T., Hanehara, S., Matsuhisa, M.; *Effects of the chemical structure on the properties of polycarboxylate-type superplasticizer*. *Cem. Concr. Res.* 30, 197-207, 2000.
17. Winnefeld, F., Becker, S., Pakusch, J., Götz, T.; *Effects of the molecular architecture of comb-shaped superplasticizers on their performance in cementitious systems*. *Cem. Concr. Comp.* 29, 251-62, 2007.
18. Toledano, M., Lorenzo, M., González, B., Seara, S.; *Effect of polycarboxylate superplasticizers on large amounts of fly ash*. *Constr. Build. Mater.* 48, 628-635, 2013.
19. Yuye, C., Xiangxiang, W., Yunjun, L., Shufen, Z.; *Synthesis and Application of Highly Branched Polymers as Filling-Retanning Agents*. *J. Soc. Leather Technol. Chem.* 94(5), 200-204, 2010.
20. The IULTCS official methods of analysis for leather: http://www.iultcs.org/pdf/IULTCS-ISO-EN_Leather_test_methods.pdf (accessed April 2019).

DEVELOPMENT AND INVESTIGATION OF LOW COLLAGEN DEGRADABILITY UNHAIRING ENZYME BY GENE MODIFICATION

S. Cao^{1,2*}, J. Song¹, Y. Shen¹, Q. Xin², Y.C. Li^{1*}, Y. Li^{2*}

¹School of Light Industry Science and Engineering, Qilu University of Technology (Shandong Academy of Sciences), Shandong, China

²Key Laboratory of Industrial Fermentation Microbiology, College of Biotechnology, Tianjin University of Science and Technology, Tianjin, 300457, P. R. China.

a)Corresponding author: cs1988@foxmail.com

b)llyu@tust.edu.cn

Abstract. Unhairing process brought serious pollution, and enzyme application for replacing polluting chemicals in unhairing process attracted much attention in recent years. However, the unhairing enzymes haven't been accepted widely in actual production due to low purity, complex composition and poor stability. To solve these problems, unhairing enzyme is suggested to be improved by genetic modification in this research. The High-keratinase-producing gene (KerT), which was extracted from *B. amyloliquefaciens* TCCC11319, was introduced into the *B.subtilis* WB600 by heterologous expression. Because *Bacillus subtilis* WB600 is deficient in six extracellular proteases, this process successfully reduced the collagenolytic protease content in crude broth as well as improved the keratinase content. Meantime, the recombinant KerT produced by *B.subtilis* WB600 had the obviously unhairing effect to remove hairs. The results showed that the collagen degradability of recombinant KerT was slightly and it did not cause any adverse effects on the hide quality. This research will contribute to the development of unhairing enzyme, and the novel unhairing enzyme might be applied as the key factor for the advanced cleaning biotechnology in leather production process.

Keywords: KerT gene; *B.subtilis* WB600; Enzyme unhairing; Low collagen degradability; Heterologous expression.

1 Introduction

In leather production, sulfur pollution mainly is produced in unhairing process. Besides, It's known that every ton of hides processed into hair-free leather will generate 150- 250 kg of unhairing-liming solid waste and 30 m³ wastewater, which lead to environmental pollution and toxic effect on human health.¹ Thus there is an urgent demand for reducing pollution in unhairing process. It is considered that the enzyme can be used to replace the sodium sulfur for many years. However, traditional unhairing enzyme application needs strict control, otherwise it may lead to the collagen fiber degradation thereby the quality of finished leather will reduce.² Until now, complete replacement of sulfide by enzyme unhairing cannot be achieved. It should be attributed to the high content of collagenolytic protease existed in traditional unhairing enzyme.

In unhairing, keratins compose the bulk of the horny layer of the epidermis, the epidermal appendages and hairs, which are typically durable and tough.³ All of them should be removed in leather production. Though hydrogen bonding and hydrophobic interaction in keratin molecules create a fine filament-matrix structure by tightly bonded polypeptide that withstands degradation by common protease,⁴ keratinase can degrade the insoluble structure by hydrolyzing disulfide bond of keratin.⁵ The purified keratinase can effectively remove hair without damaging hide collagen. However, taking into account industrial costs, the unhairing enzymes used for production are usually of low purity. In order to obtain an ideal unhairing enzyme, the substrate specificity to keratin of unhairing enzyme should be highly improved, while its collagen degradation ability must be inhibited.

The traditional methods to avoid collagen degradation are usually by addition of some chemicals. But the keratinase activity will be inhibited simultaneously. With the development of genetic engineering, heterologous expression provides a means for characterizing the biosynthetic

pathways in a genetically amenable host, whilst allowing the modification of such pathways for the generation of required products.⁶ Therefore, by construction of a producing strain of keratinase and adjusting the fermentation conditions, the keratinase activity in fermentation broth can be improved and the collagenolytic protease activity can be controlled to low level. The fermentation broth can be used as unhairing enzyme, which has a acceptable industrial cost.

In this paper, it investigates the unhairing enzyme characteristics which are produced by transferring keratinase gene KerT into *Bacillus subtilis* WB600. Because *B.subtilis* WB600 is deficient in six extracellular proteases,⁷ it is suitable for the extracellular production of the recombinant proteins and is helpful to reduce collagenolytic protease productivity. Furthermore, the application conditions and effects are explored and evaluated.

2 Experimental

2.1 KerT Gene Clone and Express

2.1.1 Cloning of Keratinase KerT gene

DNA fragments encoding for keratinase (KerT) from *B. amyloliquefaciens* TCCC11319 were amplified with the reaction primers following Liu's methods.⁸ The primer pair kerT-F and kerT-R were designed as Primer kerT-F: '- GCGGATCCATGAGAGGCCAAAAAGGTATGGA -3' and Primer kerT-R: 5'- CGGAATTCTTACTGAGCTGCCGCCTGT -3'. The PCR cycling condition comprised an initial step of 5 min at 95 °C, a second step of 30 cycles including 10 s at 95 °C, 30 s at 56 °C and 90 s at 72 °C, and a final extension step of 10 min at 72 °C. The PCR product was purified and cloned into the pMD19-T simple vector using standard procedures,(Hu et al., 2013) and transformed into E.coli JM109. In addition, the plasmids were extracted from E.coli JM109 using Plasmid Mini kit (Omega, USA) according to the manual, and the restriction enzymes were purchased from Takara. The recombinant E.coli JM109/pMD19-T-kerT was confirmed by DNA sequencing.

2.1.2 Construction Plasmids and Expression

The kerT fragments were amplified by PCR using kerT primer, and the original plasmid carrying the kerT gene were digested with relevant restriction enzyme including EcoRI and BamHI,⁹ then objective DNA fragments were inserted into pLY plasmid digested with EcoRI and BamHI, resulting in pLY- kerT (Fig.1). The recombinant plasmids were then transformed into *B. subtilis* WB600. The recombinant cell of *Bacillus* WB600-kerT was inoculated into 5 mL of LB medium and incubated at 37 °C in a 220 r/min shaker overnight. 5 mL overnight culture was inoculated into SPI medium for about 4 h at 37 °C until the cells grew to OD_{600nm}=1.1-1.3. And then 200 µL of the culture suspension was further inoculated into 2 ml SPII medium and incubated at 37 °C in a 100 r/min shaker for 1.5 h. DNA samples and 10 µL competent cell were mixed and incubated at 37 °C for 30 min. After a centrifugation at 1377 xg for 5 min, 200 µL of supernatant was plated on the LB medium and further incubated at 37 °C overnight.

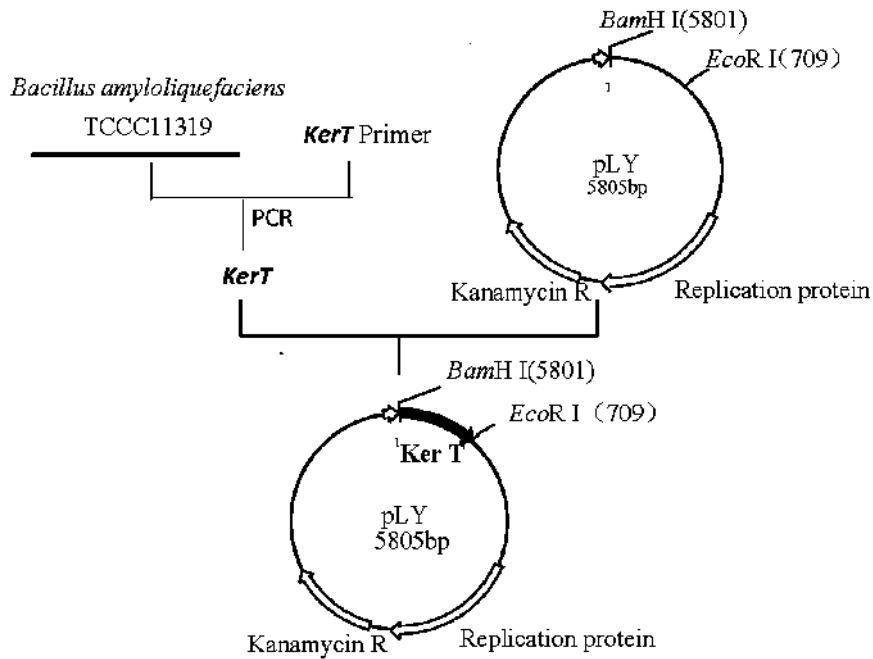


Fig. 1. Construction of the recombinant plasmid pLY-kerT.

2.2 KerT/Wb600 Characterization and Application Evaluation

2.2.1 Keratinolytic Activity and Protein Analysis

After purification,¹⁰ the keratinolytic activity was determined by using keratin as substrates by A280 method.¹¹ One unit (U) of keratinolytic activity was defined as the amount of enzyme that resulted in an increase in absorbance at 280 nm of 0.01 under the above conditions. The characteristics of purified *KerT/WB600* were evaluated and the suitable conditions of fermentation broth were optimized.

2.2.2 Enzyme Unhairing Process and Evaluation

In unhairing process, the control group was carried out with 150% (w/w) water, 2.5% (w/w) sodium sulfide and 0.5% (w/w) calcium hydroxide as the normal unhairing process. The *KerT/Wb600* was used under different conditions. The hide samples were collected after delimiting and analyzed by Emission Scanning Electron Microscopy (FESEM, Hitachi, S4800, Japan). Meantime, the liquids before and after unhairing process were collected and analyzed using HPLC analysis (AFS-8220, Beijing Titan Instruments, China). Besides, the hydroxyproline measurement was performed with Stoilov's methods.¹²

3 Results and Discussion

3.1 Expression of recombinant KerT in *B.subtilis* WB600 and Purification

As illustrated in Fig.2A, it revealed that the inserted DNA fragment in the *kerT* gene with the expected size. In order to confirm the correct insertion of the *kerT* gene, the recombinant plasmid pLY-*kerT* was extracted and digested by *Eco*RI and *Bam*HI. The molecular mass of double-digested DNA fragment was the same as the PCT product (Fig.2B), which indicating the *kerT* gene was successfully cloned into pLY plasmid. Furthermore, the expressed product was analyzed by SDS-Page, and the molecular weight of the purified enzyme was found to be 28 kDa (Fig.2C).

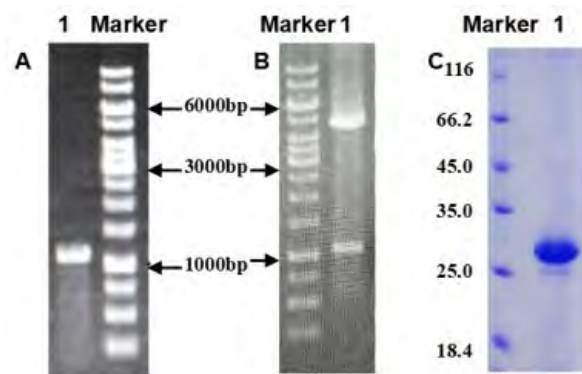


Fig. 2. (A) kerT gene amplified by PCR; (B) Double digestion of recombinant plasmid pLY-kerT. (C) Purified recombinant KerT. Lane M, Markers.

3.2 Characterization of KerT/WB600 and the Novel Unhairing Enzyme

From Fig.3, when temperature was 60 °C and pH was approximately 10, the pure KerT displayed its optimum activity. After incubating for 2 h, little loss of activity was observed when temperature was below 50 °C (Fig.2A). Meantime, it showed that more than 60% of the keratinase activity was detectable where pH ranged from 6.0 to 10.0 with the temperature of 70 °C for 2 h. In addition, the unhairing enzyme without purification displayed the optimal keratinase activity when temperature was 40 °C as well as pH was 10.5. Thus this enzyme is suitable for unhairing process. Besides, in order to study the influence of different chemicals, Na⁺, K⁺, Ca²⁺, Mg²⁺, Cu²⁺, Fe³⁺, Mn²⁺, Co²⁺, EDTA and PMSF at 5 mmol/L was incubated with pure KerT. From Fig.2E, it was seen that KerT had a well activity with the addition of Na⁺, K⁺, Ca²⁺, EDTA and PMSF. Meanwhile, Cu²⁺ completely inhibited keratinase activity at 5 mmol/L, and Mg²⁺, Fe³⁺, Mn²⁺ and Co²⁺ showed high inhibition to KerT activity.

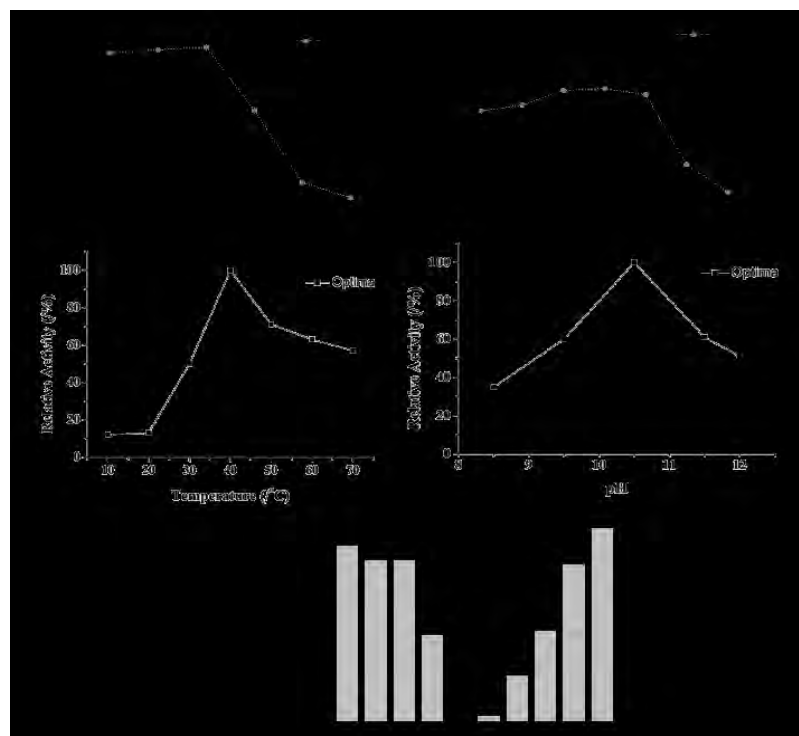


Fig. 3. (A) Relative keratinase activities of pure KerT at different temperatures; (B) Relative keratinase activities of pure KerT at different pH; (C) Optimal temperature of unhairing enzyme. (D) Optimal pH of unhairing enzyme. (E) Relative keratinase activities influenced with different chemicals; *Optima enzyme activities were assayed by incubating for 5 min; The stability enzyme activities were incubated for 120 min while the optima enzyme activities were used as a control.*

3.3 Analysis of hydroxyproline

Hydroxyproline is considered as the signature amino acid for fibrillary collagens. It stabilized the collagen triple helix structure by forming hydrogen bonds with neighboring collagen α -chains.¹³ Therefore, Hyp can be measured to evaluate the degradation degree of hide collagen fibers. From Fig.4A, it was seen that the Hyp and Gly contents in *WB600/KerT* unhairing liquid were both lower than that of before gene modification. It represented the collagen degradation activity of the designed unhairing enzyme was successfully reduced by heterologous expression of its producer. In order to observe applicability of *WB600/KerT*, the Hyp concentration changes influenced by time were analysis in Fig.4B. The Hyp concentration in *TCCC11319/KerT* unhairing liquid continued to grow in 24 h. Meantime, the Hyp contents in *WB600/KerT* unhairing liquid increased obviously in the first 8 h, and it only showed a slightly increase in the range of 8 h to 24 h. Thus the *WB600/KerT* would be more safety and easier to apply in unhairing-liming steps. Even overnight, the hide isn't damaged.

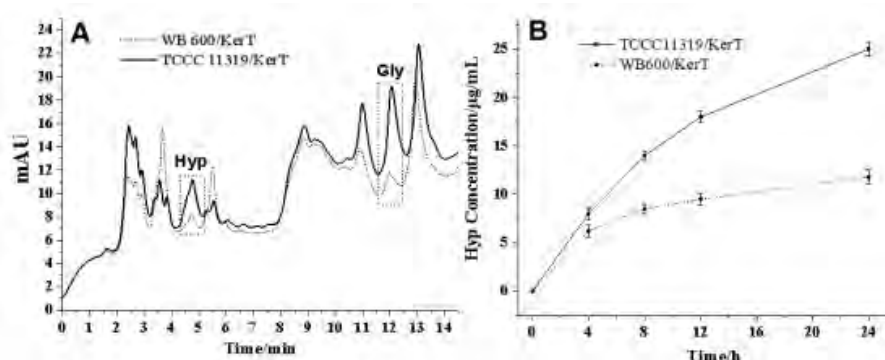


Fig. 4. Changes of hydroxyproline concentration. (A) HPLC analysis; (B) Hyp concentration influenced by time.

3.4 Unhairing Effect Evaluation

The Unhairing process was performed with different conditions, and the results was shown in Table I. The unhairing time was observed continuously and recorded until the hair were remove completely. In fig.1, the sensory properties of hide were evaluated by traditional evaluation method. The hides were evaluated by three experienced tanners and classified into different grades according to their appearance and touch sense. Higher points indicate better properties of the hide. The results showed the optimal temperature was 30 °C and the enzyme activity was 200 U/ml. When the enzyme activity was under 800 U/ml, the hide wouldn't be damaged. As known, the activity of industrial enzyme is usually under 300 U/ml. Therefore, the KerT/WB600 is remarkably safe when it is used in unhairing process.

Table 1. The unhairing effect evaluation for selecting suitable conditions.

Different Ts	20 °C	30 °C	40 °C	50 °C
Unhairing Time /h	12	10	6	4
Sensory Evaluation	A+	A++	A+	A
Different Dosage	200 U/ml	400 U/ml	800 U/ml	1200 U/ml
Unhairing Time /h	15	10	6	4
Sensory Evaluation	A++	A+	A	B

3.5 Observation of Unhairing Effect

From Fig.5, it was seen that the hairs could be fully removed when time was over 9 h. Some fine hairs still existed when the time was 8 h. After unhairing, it was observed that the hide surface

wasn't be damaged, and it possessed an excellent grain surface. By comparing the unhairing effect of KerT/Wb600 unhairing and traditional sodium sulfur unhairing, the appearances of their surfaces were looked similar. Afterwards, their microstructures were analyzed by SEM. The results showed that the hair pores remained intact by KerT/Wb600 Unhairing. It indicated this enzyme didn't degrade collagen fibers in unhairing process.

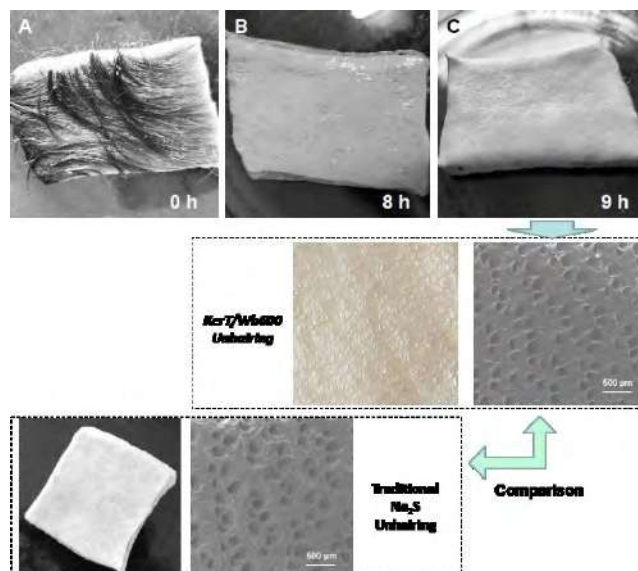


Fig. 5. Observation of unhairing process with KerT/Wb600.

4 Conclusion

In this research, the keratinase gene KerT from *B. amyloliquefaciens* TCCC11319 was introduced into the recombinant *B.subtilis* WB600 expression system. It is positive to improve the substrate specificity to keratin while reducing collagenolytic protease activity in unhairing enzyme. The fermentation broth is directly used as unhairing enzyme, which can save cost effectively. The hide structure wouldn't be destroyed when unhairing time is 15 h and enzyme activity is 200 U/mL. Therefore, it ensures the economic value of leather. The KerT/Wb600 unhairing effect is similar with traditional sodium sulphide method.

References

1. E. Ravindranath, K. Chitra, S. Porselvam, S. Srinivasan and R. Suthanthararajan, *Energy & Fuels*, 2015, **29**, 1892-1898.
2. P. Sujitha, S. Kavitha, S. Shakilanishi, N. K. C. Babu and C. Shanthi, *Int.J.Biol.Macromol.*, 2018.
3. B. Wang, W. Yang, J. McKittrick and M. A. Meyers, *Prog. Mater. Sci.*, 2016, **76**, 229-318.
4. B. Herzog, D. P. Overy, B. Haltli and R. G. Kerr, *Systematic and applied microbiology*, 2016, **39**, 49-57.
5. Z. Fang, Y.-C. Yong, J. Zhang, G. Du and J. Chen, *Appl. Microbiol. Biot.*, 2017, **101**, 7771-7779.
6. S. E. Ongley, X. Bian, B. A. Neilan and R. Müller, *Nat.Prod.Rep.*, 2013, **30**, 1121-1138.
7. J. Zhang, B. Li, X. Liao, G. Du and J. Chen, *World J. Microb. Biot.*, 2013, **29**, 825-832.
8. Y.-h. Liu, F.-p. Lu, Y. Li, X.-b. Yin, Y. Wang and C. Gao, *Appl. Microbiol. Biot.*, 2008, **78**, 85-94.
9. Y. Deng, Y. Nie, Y. Zhang, Y. Wang and Y. Xu, *Protein Expres. Purif.*, 2018, **148**, 9-15.
10. A. Deng, G. Zhang, N. Shi, J. Wu, F. Lu and T. Wen, *J. Microbiol. Biotechnol*, 2014, **24**, 197-208.
11. D. Shrinivas and G. Naik, *Int. Biodeter. Biodegr.*, 2011, **65**, 29-35.
12. I. Stoilov, B. C. Starcher, R. P. Mecham and T. J. Broekelmann, in *Methods in cell biology*, Elsevier, 2018, vol. 143, pp. 133-146.
13. W. Y. Chow, D. Bihan, C. J. Forman, D. A. Slatter, D. G. Reid, D. J. Wales, R. W. Farndale and M. J. Duer, *Sci. Rep.*, 2015, **5**, 12556.

ENHANCING PERFORMANCE PROPERTIES OF CONVENTIONAL LEATHER FINISHING TOPCOAT BY INCORPORATING METAL OXIDE BASED FORMULATIONS

S. Gupta², RamKumar Kothandam ², S. K. Gupta¹

1 Shiv Nadar University, Greater Noida, India 2 CLRI, Chennai, India

Abstract. ZnO nanoparticles were developed by 1:2 ratios of Zinc sulphate heptahydrate and Sodium hydroxide by using precipitation method. The structure, morphology of ZnO nanoparticles were investigated by using X-Ray Diffraction and Scanning Electron Microscopy. X-Ray Diffraction confirms the formation and average crystallite size of ZnO nanoparticles. Scanning Electron Microscopy studies shows the ZnO nanoparticles were in spherical in structure. ZnO nanoparticles were used in different ratios along with conventional finishing formulations and coated on the leather surface. The performance properties such as flexing resistance were evaluated. Application of ZnO nanoparticles in leather finishing showed significant improvement in overall performance properties than conventional finishing formulations. XRD confirms the formation of ZnO nanoparticles (wurtzite structure) at 36.31° (101) plane and the particles size was in the range of 34 nm. SEM image shows that the particles are in the spherical structure whereas EDAX investigate the stoichiometry and chemical purity of the samples to confirm the presence of zinc and oxygen. Optimum quantity up to 2-5 g/L of the solution of ZnO nanoparticle is desirable for upgrading the value of leathers by improving the flexing resistance (wet & dry) properties significantly in PU top coat dispersions in finishing formulations.

1 Introduction

Leather finishing refers to the process of coating on leather surface to protect and beautify the leather i.e prolonging the lifetime of the leather, and considerably improving the quality and the commercial value of the leather products.(1,2) Conventional leather products lacks the appearance and performance properties required by the customer demands. Therefore, it is necessary to redesign and modify the conventional leather finishing formulations in order to achieve the improved organoleptic properties in leather finishing applications. Hence, much research work has been focussed on developing nanofinishing formulations to enhance the performance properties of the leather. Zinc oxide (ZnO) nanoparticles has gained more attention because of its application in numerous fields such as in electronics (3), optics (4), photonics (5), varistors (6), photocatalysis (7), gas sensors (8), solar cells (9), pigments (10) etc. In this present study, ZnO nanoparticles have been synthesized by precipitation technique

2 Experimental

2.1. Materials

Zinc sulfate heptahydrate ($\text{ZnSO}_4 \cdot 7\text{H}_2\text{O}$) and Sodium hydroxide (NaOH) in analytical reagent grade were procured from Merck (India), and deionized water was used for the preparation of solutions. The cow crust leather was collected from Tannery Division, CLRI, India. All the leather finishing chemicals were procured from Stahl, Nagalkeni, Chennai, India.

2.2 Synthesis of ZnO nanoparticles

The aqueous solution of $\text{ZnSO}_4 \cdot 7\text{H}_2\text{O}$ and NaOH solution was prepared separately and added dropwise in a molar ratio of 1:2 under vigorous stirring, and the stirring was allowed to continue for 12 hrs.

The obtained precipitate was filtered and washed thoroughly with deionized water and followed by air drying at 100°C and ground to a fine powder. The obtained powder was calcined at 800°C for 4 hrs.

3 Results and Discussion

3.1. XRD

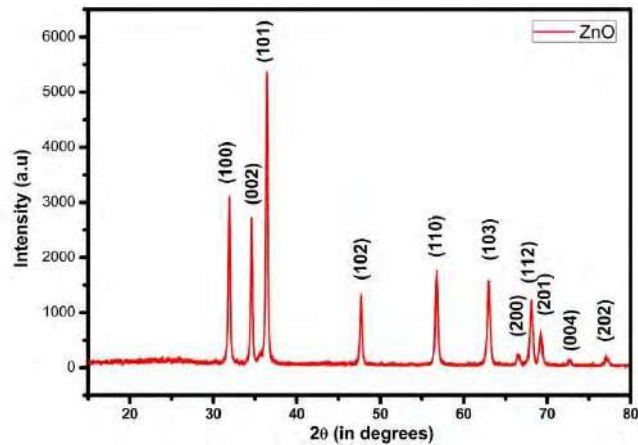


Fig. 1. shows the XRD image of ZnO nanoparticles.

Figure 1 shows the XRD diffraction peaks of ZnO nanoparticles. The peaks indicating that the synthesized ZnO nanoparticles were crystalline in nature and the peak intensity is sharp and narrow which confirms the ZnO nanoparticles are in high quality with good crystallinity and fine grain size. The XRD pattern confirms the hexagonal ZnO wurtzite structure in the synthesized ZnO nanoparticles and in good agreement with the crystallographic structure (11) according to the (JPCDS card number: 36-1451). Typical XRD pattern of hexagonal structure of znO nanoparticles shows three strongest lines at 2θ values equal to 31.82° , 34.48° , and 36.31° due to reflection from the crystallographic (100), (002), and (101) planes, respectively.

3.2 SEM

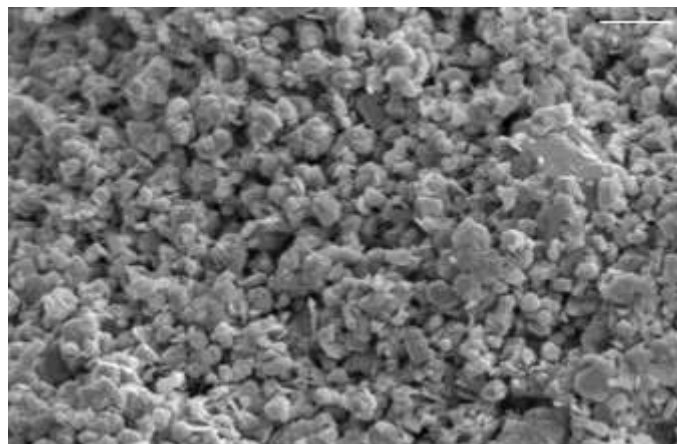


Fig. 2. shows the SEM image of ZnO nanoparticles.

The morphology of the synthesized ZnO nanoparticles was investigated by using scanning electron microscopy (SEM). Figure 2 shows that the surface morphology and shape of the ZnO nanoparticles are nearly spherical and agglomerated. The aggregation occurred probably during the process of drying [12,13].

4. Preparation of ZnO nanoformulations for leather finishing applications

Standard cow upper crust leather from Indian origin was selected for the evaluation. ZnO nanoformulations prepared for leather finishing applications carried out by leather PU top coat formulations and their performance properties were evaluated. A clearing coat (a mixture of ammonia, isopropyl alcohol (IPA) and water) were applied to increase the season adhesion with leather (Table 1). The cow upper base coat (Table 2) leather finishing formulation prepared with water, acrylic binder, PU resin binder, casein, filler, and the pigment was sprayed on the standard cow upper leather crust by HVLP gun at 30 psi. The formulation of 8g/sqft was deposited on leather by two cross coat spray with intermediate drying. The synthesized ZnO nanoparticles were sonicated for 10 min and then they were incorporated in the PU top coat dispersions (Table 3) in finishing formulation with various concentrations for optimum results. The above formulation was sprayed on by HVLP spray gun bullows 630 at 30 psi. The formulation was deposited on the leather 4g/sqft by one cross coat. Then the leather was subjected to 80oC/80 kg/cm2 pressure in a hydraulic press.

Table 1. shows the standard clear coat formulation.

Sl. No	Ingredients	Mass (g)
1	Water	470
2	Ammonia	5
3	Isopropyl alcohol	25

(All the values were expressed as g)

Table 2. shows the standard cow upper leather base coat formulation.

Sl.No	Ingredients	Parts
1	Water	550
2	Acrylic resin	150
3	PU binder	100
4	Casein binder	50
5	Filler Wax	50
6	Pigment	100

(All the values were expressed as g)

Table 3. shows the standard cow upper leather top coat formulation with ZnO Nanoparticles

Sl.No	Ingredients	Control	Trial I	Trial II	Trial III	Trial IV
1	Water	500	498.75	497.50	496.25	495
2	PU top coat	500	500	500	500	500
3	ZnO nanoparticles	0	1.25	2.50	3.75	5

(All the values were expressed as g)

4.1 Determination of applied physical properties of ZnO nanoparticles coated leather

4.1.1. Vamp Fluxing

Measurement of fluxing is carried out by SATRA STM 601/12 12 and the values are given in (Table 4).

Table 4. Performance properties of ZnO nanoparticles coated leather with PU top coat finishing formulations.

Sl.No	Performance properties	Control	Trial I	Trial II	Trial III	Trial IV
1	Flexing resistance (wet)					
	No. of cycle	A	A	A	A	A
	10000	↓	↓	↓	↓	↓
	30000	↓	↓	↓	↓	↓
	50000	B	↓	↓	↓	↓
	80000	↓	↓	↓	↓	↓
	100000	C	B	B	B	B
	Flexing resistance (dry)					
	No. of cycle	A	A	A	A	A
	10000	↓	↓	↓	↓	↓
	30000	↓	↓	↓	↓	↓
	50000	B	↓	↓	↓	↓
80000	↓	↓	↓	↓	↓	
100000	C	↓	↓	↓	↓	
250000	↓	↓	↓	↓	↓	
300000	↓	↓	↓	↓	↓	
500000	D	B	B	B	B	

*Finished coat slight crack; A- No effect; B- Slight creasing; C-Slightly pipiness; D-Marked creasing; E-Severe creasing; F-Severe pipiness; H-Marked crack; I-Severe crack; J-Complete Failure.

5 Conclusion

ZnO nanoformulations were successfully prepared and its performance properties were evaluated. XRD confirms the formation of ZnO nanoparticles at 36.31° at (101) plane and using XRD data crystallite size is calculated as 30-70 nm. SEM image reveals that the particles are in nearly spherical structure and agglomerated. ZnO nanoparticles enhanced the flexing resistance properties along with conventional finishing formulations. Optimum quantity (upto 2-5 g/L in the season) of ZnO nanoparticle is desirable for upgrading the value of leathers.

References

1. Li, Z. J. *The comprehensive description about leather marking chemicals part IV. finishing agent. Leather Sci. Eng.* 1995, 5, 4–10.
2. Fan, Y.; Du, Z. P.; Chen, W. C.; Wang, X. J. *The development and prospect of leather finishing. Leather Chem.* 2009, 26, 19–21.
3. Xu, C.X., Sun, X.W., Chen, B.J., Shum, P., Li, S., Hu, X.,; *Nanostructural zinc oxide and its electrical and optical properties. Appl. Phys.* 95, 661, 2004.
4. F.Q. He, Y.P. Zhao; *Growth of ZnO nanotetrapods with hexagonal crown. Appl. Phys. Lett.* 88, 193113, 2006.
5. C.C.M. Ma, Y.J. Chen, H.C. Kuan; *Polystyrene nanocomposite materials - preparation, mechanical, electrical and thermal properties, and morphology. J. Appl. Polym. Sci.* 100, 508-515, 2006.

6. Bai, S.N.; Tseng, T.Y; Influence of sintering temperature on electrical properties of ZnO varistors, *J.Appl. Phys.* 74 (1), 695–703, 1993.
7. Li, D, Haneda, H; Morphologies of zinc oxide particles and their effects on photocatalysis. *Chemosphere* 51, 129–137, 2003.
8. Aslam, M.; Chaudhary, V.A.; Mulla, I.S.; Sainkar, S.R.; Mandale, A.B.; Belhekar, A.A.; Vijayamohan, K. A highly selective ammonia gas sensor using surface ruthenated zinc oxide. *Sens. Actuat. B* 75, 162-167, 1999.
9. Kluth, O.; Recha, B.; Houbena, L.; Wiedera, S.; Schöpea, G.; Benekinga, C.; Wagnera, H.; Löfflb, A.; Schockb, H.W. Texture etched ZnO:Al coated glass substrates for silicon based thin film solar cells. *Thin Solid Films* 351, 247–253, 1999.
10. Zayer, N.K.; Greef, R.; Roger, K.; Grellier, A.J.C.; Pannell, C.N: In situ monitoring of sputtered zinc oxide films for piezoelectric transducers. *Thin solid films* 352(1-2), 179-184, 1999.
11. Sukhpreet Singh, Tushar Mahajan and Kiratbir Kaur, Synthesis, Characterization and Effect of Increasing Nitrogen Concentration on the Growth of ZnO Nanoparticles, *RRJOMS*, Volume 7, Issue 1, June-July, 2018, pp-141-151.
12. R.Y. Hong, J.Z. Qian, J.X. Cao, Synthesis and characterization of PMMA grafted ZnO nanoparticles, *Powder Technol.* 163 (2006) 160.
13. R.Y. Hong, J.H. Li, L.L. Chen, D.Q. Liu, H.Z. Li, Y. Zheng, J. Ding, Synthesis, surface modification and photocatalytic property of ZnO nanoparticles, *Powder Technol.* 189 (2009) 426.

MINUS SALT GOAT SKIN PRESERVATION: EXTREME CHLORIDE REDUCTION IN TANNERY WASTEWATER

M. A. Hashem^a, M. Hasan, M. A. Momen, S. Payel

Department of Leather Engineering, Khulna University of Engineering & Technology, Khulna-9203, Bangladesh

a) Corresponding author: mahashem96@yahoo.com, mahashem@kuet.ac.bd

Abstract. In the tannery, soaking is the first operation which emits a huge amount of chlorides in the water body during the processing of wet salted hide and skins. The increasing concern the chlorides encourage salt-free or less-salt methods for preservation of hides and skins. In this study, an alternative preservation 'minus salt' method has been developed. The *Sphagneticola trilobata* leaf was applied on the flesh side of the goat skin and observed for 28 days. The comparison of the present minus salt method with the conventional method using common salt (NaCl) revealed that the method could be approached without any deterioration to the fibres and the physical properties of the produced leather. Moreover, the suggested method reduces the pollution load of chlorides, total dissolved solids, BOD and COD by 98.04%, 92.9%, 90.2% and 85.5% respectively. The overall assessment indicates that the salt-free method using *Sphagneticola trilobata* leaf could be an attractive preservation system over the conventional wet salting method.

Keywords. *Sphagneticola trilobata*, salt diminution, pollution load, soaking

1 Introduction

In spite of originating as a by-product industry, the leather industry has aspired with its growing demand of consumers worldwide. The existence of this industry starts with the raw hides and skins, coming from the meat industry. Being natural organic material, hides and skins tend to deteriorate with time after flaying which contradicts with the purpose of leather processing.

The term preservation or curing has been introduced as a solution to this degradation with the purpose of storing and safe transportation. The ideal preservation method, whether physical, chemical or other, is expected to be reversible to the original raw condition of the hides and skins in an environmental-friendly process. Common salt, sodium chloride (NaCl) is the most popularly used curing agent due to its dual effect of dehydration and bacteriostatic effect on hides and skins at a very convenient price and availability. It is reported that approximately 6.5 million tons of hides and skins on the wet salted basis are processed globally per annum discharging 2.6 million tons of salt are in the soaking process alone (Kanagaraj et al. 2001; Kanagaraj et al. 2006). With the growing concerns of available fresh water, the chloride (Cl⁻), total dissolved solids (TDS) and salinity added to fresh water from preservation and soaking of the leather industry are raising question and concern about the outcome in the near future.

Alternative several preservation techniques have been adopted by controlling moisture content like in sun drying (Roddy and Hermoso, 1943), controlled drying (Waters et al. 1981) or by controlling the action of microorganisms like using powder biocide or irradiation. Salt-free chemical preservation techniques have also been tried including boric acid (Hughes, 1974), sulphites (Vankar et al. 2009), bacteriocin compounds (Kanagaraj et al. 2014), sodium silicofluoride (Haines, 1973) in low salt skin preservation trials.

Some salt-less preservation system like cooling and chilling (Babu et al. 2012), vacuum (Gudro, 2014), dry ice (Sathis et al. 2013), aryl alcohols (Venkatachalam et al. 1982), potassium chloride (Aloy, 1998) has been adapted for laboratory and pilot scale. The limitations with these methods are that the preserving agents are hazardous itself or expensive to carry out or not practically

adaptable. Organic plant extract like *Moringa oleifera* (Hashem et al. 2018) has been applied as an alternative organic preservative. *Rumex abyssinicus* with salt have also been tried for preservation but it affects the strength and other properties of the final leather (Shegaw et al. 2016). Therefore, it has become a challenge to find out a suitable preserving agent that can preserve the skin in an environmentally safe condition, is available and inexpensive to use.

In this study, *Sphagneticola trilobata* plant, locally known as “bhringraj”, leaf paste has been tried without any salt as an attempt to meet the challenge of preserving the goat skin for 28 days. *Sphagneticola trilobata* plant extract has been found to have antibacterial and antifungal activity (Toppo et al. 2013). The preservation process was evaluated by various parameters: moisture content, odour, hair slip, bacterial count, extractable nitrogen, and thermal stability in comparison to the conventional preservation method.

2 Materials and Methods

2.1 Materials

2.1.1 Skin and plant extract

Freshly flayed goat skins of average weight 1 kg per skin were purchased from a nearby local slaughterhouse, Khulna, Bangladesh. The *Sphagneticola trilobata* leaf was collected from the university campus of Khulna University of Engineering & Technology, Khulna, Bangladesh and pasted using laboratory mortar for the experiment.

2.1.2 Salt and chemicals

Commercial NaCl and auxiliaries were used for preservation and pre-tanning and post-tanning processes for shoe upper leather and analytical grade chemicals were used for other experiments.

2.2 Experimental modelling and application

A preliminary experiment was conducted to define the minimal amount of leaf paste required for the preservation. Four (04) samples of size 30 cm × 30 cm was cut from the freshly flayed goat skin. The different combinations of curing materials were offered based on the raw skin weight and assessed periodically (fresh, 1st, 2nd, 4th, 7th, and 14th day) to observe the changes like odour, hair slip, and moisture content, physical feel etc. Based on the preliminary result, the experimental sample was selected and compared with conventionally preserved skin by 50% NaCl, for further experiments.

2.3 Monitoring and evaluation

2.3.1 Moisture content

The Dean and Stark method (BIS, 1971) was followed to determine the moisture content based on the initial and final weight of the preserved skins.

2.3.2 Bacterial count

A 5 g preserved skin per piece was taken and shaken in 50 ml sterile water at 200 rpm for 30 min. After 10 times dilution, a volume of 0.1 ml of the respective diluted solution was taken in sterile Petri plates and molten nutrient agar at 40°C was poured and uniformly distributed by gentle

motion. After 48 h incubation at 37°C, the number of colonies on the agar medium was counted using a bacterial colony counter (Colony Counter, CC- 1, BOECO, Germany).

2.3.3 Extractable nitrogen content

The preserved skin samples of known weight (5 g) were treated with ten times (w/v) its weight of distilled water, shaken well in a bottle for 3 h at 30-35 rpm. The liquor was then filtered through a filter paper, digested and the amount of nitrogen was determined using the Kjeldahl method of extraction.

2.3.4 Hydrothermal stability

A shrinkage tester (SATRA STD 114, UK) was used to measure shrinkage temperature following ISO 3380 standard (SATRA, ISO 3380, 2015) as a scale of determining hydrothermal stability where the temperature at which the specimen starts shrinking was noted as shrinkage temperature of the particular skin.

2.4 Characterization of leather

2.4.1 Physical strength and organoleptic properties

Both experimental and control sample were processed to produce shoe upper leather following conventional process and physical properties of the leather were assessed following ISO 3379 (SATRA, ISO 3379, 2015).

2.4.2 Scanning electron microscope (SEM)

Crust leathers both from the control and experimental goat skins were subjected to assess the effect of the proposed preservation method on the fibre structure of the leather. Firstly, leather samples from the same area have placed on conducting carbon tape. After preparing, the samples were analyzed to an SEM (JEOL JSM-7600F, USA). The photographs were obtained by operating the SEM at an accelerating voltage 1.0 kV with magnification 300X.

2.5 Pollution load

Different pollution load parameters, e.g., chlorides (Cl⁻), biochemical oxygen demand (BOD), chemical oxygen demand (COD), total dissolved solids (TDS), and total suspended solids (TSS) of the soaking liquor from experimental and control sample were measured following APHA standard methods (APHA, 2012).

3 Results and Discussion

3.1 Preliminary experiment

The preliminary experimental data, as shown in Table 1, indicates that only sample 01 showed little fungal growth but no hair slip. It indicates that the leaf paste acts as an antibacterial agent but due to lower pH or humidity fungal growth was visible. The other samples showed no fungal growth and only sample 04 and 05 were softer than the rest.

3.2 Optimizing percentage of plant leaf

Table 1 shows the four samples preserved in the preliminary experiment by various % (w/w) of leaf paste. Based on the physical feel and visual examination, 20% leaf paste (w/w) was found soft with no hair slip, odour and fungal growth. Therefore, 20% of leaf paste was considered as optimum and termed as the experimental sample.

Table 1. Leaf paste optimization in this study (14 days)

No.	% of curing agents (w/w)	Hair slip	Odour	Physical feel	Fungal growth
01	10% leaf paste	No	No	Hard	Little growth
02	15% leaf paste	No	No	Moderately soft	No growth
03	20% leaf paste	No	No	Soft	No growth
04	25% leaf paste	No	No	Soft	No growth
05	30% leaf paste	No	No	Soft	No growth

3.3 Assessment of preservation method

3.3.1 Moisture content and total extractable nitrogen vs. time

Fig. 1 expresses the change in moisture content (a) and total extractable nitrogen (b) in the control and experimental sample with respect to the preservation period. It is clear that the moisture content decreased with time and on the 14th day the percentage of moisture content in both techniques was nearly the same. The moisture content was nearly constant from the 14th in both cases respectively. On the 28th day, the moisture content found in experimental and control sample was 45.9% and 44.8%, respectively. It ensures no skin degradation which is confirmed by the changes in nitrogen content.

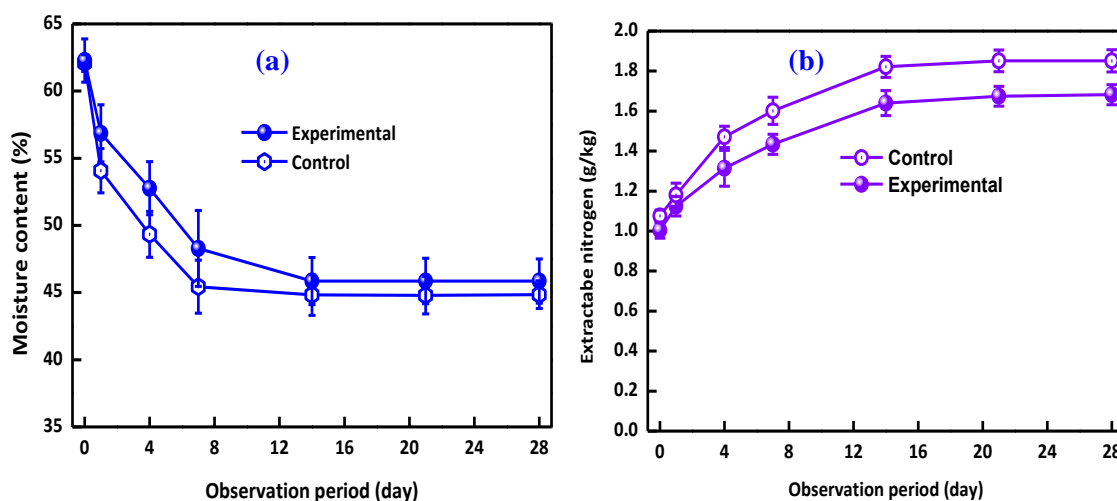


Fig. 1. Changes in moisture content (a) and total extractable nitrogen (b) with respect to the preservation period

With the reduction of moisture content, the bacterial action within the skin is restricted prohibiting the breakdown of protein. As a result, on the 21st day, the nitrogen content remains constant as the moisture content is unchanged. In comparison with the control sample, it can be seen that there are slight changes between the control and experimental sample. Since in control sample, NaCl initiates osmosis for moisture reduction, the reduction rate is faster. Whereas, the control sample cannot resist the bacterial attack as well as the experimental sample shows.

The extractable nitrogen data is also consistent with moisture content. On the 14th day, both moisture content and nitrogen content reaches an equilibrium point. On the 28th day, the extractable nitrogen content for both in the experimental and control sample was 1.7 and 1.9 g/kg, respectively which indicates higher total extractable nitrogen in the control sample. It ensures the antibacterial action of the leaf paste as well as the preservation of the goat skin.

3.3.2 Hydrothermal stability and total extractable nitrogen vs. time

Fig. 2 shows the relation of hydrothermal stability with changes in preservation time. The shrinkage temperature is the measurement of the breakdown of stabilizing linkages and the bases for the type of interactions existing in the collagen matrix (Babu et al. 2012).

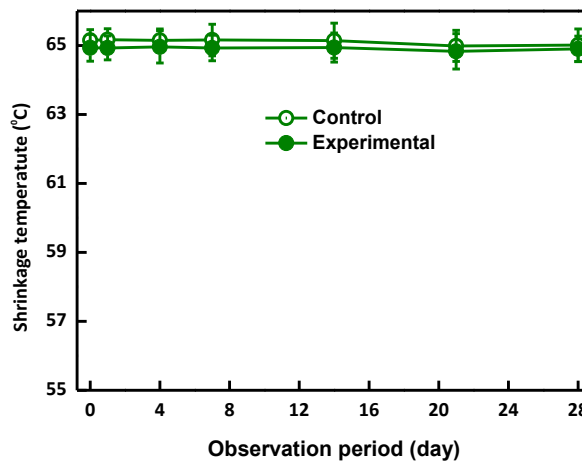


Fig. 2. Changes in hydrothermal stability with respect to preservation period

It indicates that during the preservation period the shrinkage temperatures were almost the same for both the experimental and control methods although the nitrogen content increases up to 14th day as shown in Fig. 1 (b). The reason might be because the increase of nitrogen content is due to the breakdown of non-structural protein but not collagen protein. Therefore, it can be said that *Sphagneticola trilobata* leaf paste based preserving does not modify the stability of the collagen protein matrix in the goat skin.

3.3.3 Bacterial count

The bacterial count of the control and experiment preservation of the goat skins is shown in Table 2. Till on the 1st day, the bacterial count for control and experimental was 1×10^6 /g and 1×10^6 /g, respectively.

Table 2. Bacterial count (CFU/g) in preserved goat skins

Preservation period	Experimental	Control
Fresh	1×10^6	1×10^6
1 st	1×10^6	1×10^6
4 th	1×10^6	2×10^6
7 th	9×10^6	8×10^6
14 th	6×10^6	5×10^6
21 st	3×10^6	5×10^6
28 th	3×10^6	5×10^6

The bacterial count in the experimental and control sample increased until on the 7th day and then slowly decreased. It became constant for both experimental and control on 21st and 14th day, respectively. It might be due to the reason is that the preservation method in the present approach (20% *Sphagneticola trilobata* leaf paste) have antibacterial effects, which inhibit the bacterial population. As a result, the experimental showed less bacterial growth than the control sample. There was also no hair slip, odour in the present approach preservation method by using 20% *Sphagneticola trilobata* leaf paste.

3.3.4 Pollution load comparison

Table 3 depicts the pollution parameters in soaking operation for both the control and experimental sample. It seems that the Cl⁻ and TDS load were greatly reduced by 98.04% and 92.9%, respectively with the present preservation method (20% leaf paste) in place of the conventional wet salting method. The BOD and COD were also reduced at the levels of 90.2% and 85.5%, respectively in the experimental soaking wastewater compared to the control. The reduction in pollution makes the present preservation approach more attractive with its effectiveness.

Table 3. Pollution load generated in soaking operation

Parameters	Control Sample	Experimental Sample	Removal (%)
Cl ⁻ (mg/L)	24942.3	488.9	98.04
TDS (mg/L)	4115	291	92.9
BOD ₅ (mg/L)	1240	122	90.2
COD (mg/L)	4480	650	85.5

3.4 Inspection of leather quality

3.4.1 Determining the physical properties of leather

The crust leathers were assessed for softness, grain tightness, fullness, and smoothness and the physical properties are tabulated in Table 4 and compared with the required value for shoe upper leather.

Table 4. Physical properties of processed experimental and control leather

Parameters	Experimental	Control	Requirements (Kanagaraj et al. 2001)
Tensile strength (kg/cm ²)	213.4	226.3	200
Elongation at break (%)	51.08	59.02	40-65
Bursting strength:			
Distension at grain crack(mm)	7.2	8.3	7
Load at grain crack (kg)	27.3	25.1	20

The tensile strength (kg/cm²), elongation at break (%), distension at grain crack (mm) and load at grain crack (kg) values fulfilled the required values for the experimental and control sample. It could be concluded that the present approach for preservation of the goat skin in 20% leaf paste is suitable for shoe upper leather.

3.4.2 SEM analysis of fibre structure

SEM photographs of the crust leather processed from the controlled and experimental salt preserved goat skin are illustrated in Fig. 3.

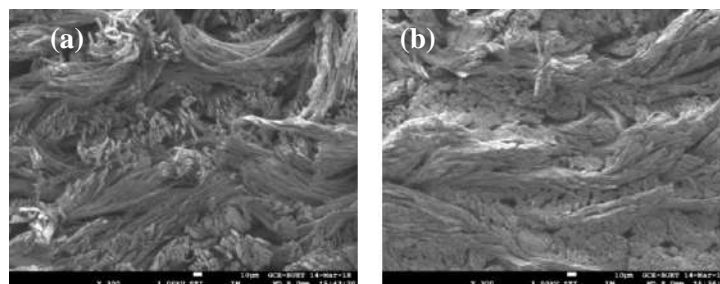


Fig. 3. SEM photographs of prepared crust leathers a) control (50% salt) and b) experimental (20% leaf paste) of the preserved skins

The fibre structure of the experimental goat skin is almost the same compared with the controlled goat skin. The texture and quality of the goat skin of the proposed leather and controlled preservation method also nearly similar to each other at crust condition. This supports that the proposed preservation method could be safely approached for goat skin preservation.

5 Conclusion

The present study concedes that *Sphagneticola trilobata* leaf paste could preserve the skin for a period of 28 days in an environmentally sound way without the addition of common salt. The comparison and assessment with the conventional wet salting method reveal the effectiveness of the method. This preservation ‘minus salt’ method reduces major pollution load parameters, Cl^- , TDS, BOD and COD in soaking operation by 98.04%, 92.9%, 90.2% and 85.5%, respectively. The physical properties of the produced leather fulfilled the requirement of shoe upper leather. The SEM analysis confirmed no deterioration in the fibre structure of the goat skin. Thus, the recommended preservation method could be a sustainable option to preserve goat skin, which would reduce the pollution load at a great extent during leather processing especially in soaking operation.

References

1. Aloy M.: ‘Cleaner tanning technologies in the beam house operation’, *Symp. Cleaner Tanning Technology.*, 6, 1998
2. APHA, American Public Health Association. *Standard Methods for the Examination of Water and Wastewater*, 2012
3. Babu N. K. C., Karthikeyan R., Swarna B., Ramesh R., Shanthi C., Sadulla S.: ‘A systematic study on the role of chilling temperatures on the curing efficacy of hides and skins’, *J Am Leather Chem As.*, 107(11), 362–370, 2012
4. BIS, Bureau of Indian Standards, *Chemical Testing of Leather*, 2-80, 1971
5. Gudro I., Valeika V., Sirvaityte J.: ‘Short Term Preservation of Hide Using Vacuum’, *PLOS ONE.*, 9(11), 1-9, 2014
6. Haines.: ‘Short term preservation with various preservatives’, *J. Soc. Leather Tech. Chem.*, 57, 356, 1973
7. Hashem M. A., Momen M. A., Hasan M.: ‘Leaf paste aided goat skin preservation: Significant chloride reduction in tannery’, *J. Environ. Chem. Eng*, 6(4), 4423–4428, 2018
8. Hughes I. R.: ‘Temporary preservation of hides using boric acid’, *J Soc Leather Trade Chem*, 58, 100–3, 1974
9. ISO 3379, *Leather-Determination of distension and strength of surface (Ball burst method)*, 2015
10. ISO 3380, *Leather-Physical and mechanical tests-Determination of shrinkage temperature up to 100°C*, 2015
11. Kanagaraj J., Babu N. K. C., Sadulla S.: ‘Cleaner techniques for the preservation of raw goat skins’, *J. Clean. Prod.*, 9, 261-268, 2001
12. Kanagaraj J., Tamil Selvi A., Senthilvelan T., Chandra Babu, N. K., Chandrasekar, B.: ‘Evaluation of New Bacteriocin as a Potential Short-Term Preservative for Goat Skin’, *Am. J. Microbiol. Res.*, 2(3), 86–93, 2014
13. Kanagaraj J., Velappan K. C., Babu N. K. C., Sadulla S.: ‘Solid wastes generation in the leather industry and its utilization for cleaner environment-A review’, *J Sci Ind Res.*, 65, 541-548, 2006
14. Roddy W. T., Hermoso R. P.: ‘The coagulable protein of animal skin’, *J. Amer. Leather Chem. Assoc.*, 38, 96, 1943
15. Sathish M., Madhan B., Saravanan P., Rao J. R., Nair B. U.: ‘Dry ice - an eco-friendly alternative for ammonium

- reduction in leather manufacturing*, *J. Clean. Prod.*, 54, 289-295, 2013
16. Shegaw M. A., Balaraman M., Berhanu D. A. Brindha V., Alagumuthu T. S.: ' *Rumex Abyssinicus (mekmeko) Ethiopian plant material for preservation of goat skins: Approach for cleaner leather manufacture*', *J. Clean. Prod.* 133, 1043-1052, 2016
 17. Toppo K. I., Gupta S., Karkun D., Agrwal S., Kumar A.: 'Antimicrobial activity of *sphagneticola trilobata (L.) Pruski*, against some human pathogenic bacteria and fungi', *The Bisocan*, 8(2), 695-700, 2013
 18. Vankar P. S., Dwivedi A. K.: ' *Sulphates for skin preservation-A novel approach to reduce tannery effluent salinity hazards*', *J Hazard Mater*, 163(1): 207-212, 2009
 19. Venkatachalam P., Sadulla S., Duraiswamy B.: ' *Further experiments in salt-less curing*', *Leather Science*, 29, 217-221, 1982
 20. Waters P. J., Stephen L. J., Sunridge: ' *Controlled drying*', *J. Soc. Leather Tech. Chem.*, 65, 41, 1981

CHARACTERISTICS ANALYSIS OF HIGH MECHANICAL STRENGTH GYMNASTIC LEATHER AND ITS PRODUCING PROCESS OPTIMIZATION

Jinzhi Song¹, Wenhui Lu¹, Ke Wang², Baozhen Cheng², Shan Cao^{1*}, Yanchun Li^{1*}

¹ School of Light Industry and Engineering, Qilu University of Technology (Shandong Academy of Sciences), Shandong, 250353, P. R. China

² College of Material Science and Chemical Engineering, Tianjin University of Science and Technology, Tianjin, 300457, P. R. China

a) Corresponding author: cs1988@foxmail.com, qlulyc@126.com

Abstract. With the development of China sports, researches related to sports leather should be paid attention because they usually required higher strength than commonly used leather. In this paper, we focus on the production of gymnastics leather. In gymnastics, the athlete's hand will contact with the balance bar in a long time, so the gymnastics leather is required to have high intensity performance. At the same time, in order to comply with the ornamental function, gymnastics leather is required to be light color. In this research, in order to obtain high strength, environmentally friendly white gym leather, glutaraldehyde was used as the main tanning agent, while acrylic polymer and synthetic were used for retanning. The shrinkage temperature and mechanical properties of tanned leather were determined and analyzed for selecting the suitable tanning agent. Besides, other properties including softness, gas permeability, water permeability, flexing resistance and yellowing-resistance were also measured for selecting proper production process. The results show that the leather prepared by GTA has good yellowing resistance, and its air permeability has been up to 867.46 mL/(cm²·h). Therefore, gymnastics leather with ideal performance can be prepared by this method, and the leather conforms to the practical application standard. In addition, the research has guiding significance and application prospect for high strength chrome-free tanned leather.

1 Introduction

Gymnastics is a kind of physical exercise which need to be carried out by hand or with equipment. Gymnastics requires explosive sprinting, jumping, pushing and pulling skills, together with balance and artistry.¹ This complex movements may cause violent friction between the hand and the lever. At the same time, gymnasts need to practice giant circles without the fear of losing their grip.² Therefore, gymnastics leather plays an important role in protecting athletes' arms and reducing the impact of sports. This puts forward very high request to the performance of gymnastics leather. Based on the importance of protecting human body, gymnastics leather is required to have better mechanical strength and hygienic performance. Above all, the requirement of physical properties of gymnastic leather must possess high strength and low elongation. Thus the handguards can make the passive wrist joint carry the greater loads. Due to long-term contact between skin and handguards, the gymnastic leather should be produced environmental friendly with low toxic leather-making chemicals. Besides, the color of handguards should be similar with skin color which can bring better ornamental effect, thus the light color of gymnastics leather is necessary.³

So far, chrome tanning is the most commonly used and effective tanning method in leather production field, and chrome tanning leather accounts for more than 80% of the world's tanning leather output.⁴ However, the safety of chrome tanning leather is also a problem, this is because the Cr(III) may be converted to Cr(VI) with the existence of oxidants, and the Cr(VI) is certainly harmful to human health with long-term contact.⁵ Among other chrome-free tanning agents, aldehyde tanning agent is a kind of environmental friendly tanning agent with better tanning effect and lower price, therefore, this tanning agent can be considered for the production of gymnastic leather.⁶ In addition, in order to further improve the physical and mechanical properties of gymnastics leather, it is necessary to research and develop the process of retanning gymnastics leather to meet the requirements.⁷

In this paper, the production technology of gymnastic leather was explored and optimized. Aldehyde tanning agents and retanning agents, which can be used for gymnastics leather making, were evaluated and selected. Then the suitable agents can be selected to achieve ideal effect of finish leather. Meantime, the mechanism relating to how to improve physical mechanical properties was investigated and explained. Meanwhile, the hygienic properties of leather prepared with different tanning agents were studied. The suitable tanning agent for gymnastic leather was studied, and the preparation technology and optimum dosage of the tanning agent were discussed. This research is meaningful to produce not only gymnastics leather but also other sporty leather which require high strength.

2 MATERIALS AND METHODS

2.1 Materials

The cattle pelts were purchased from Hebei Kanghuida Leather Co., Ltd. The agents used for leather production in CL system operation were all of industrial grade (Lanxess Chemical, Chengdu, China), and chemicals used for mechanism analysis were of analytical grade (Jiangtian Chem. Co., Ltd, Tianjin, China). Other chemicals used in this research were all of chemical grade and also purchased from Jiangtian Chem. Co., Ltd.

2.2 Simulated tanning process with different aldehyde agents

After soaking, liming, deliming, bating and pickling process conventionally used,⁸ the pickled pelts were tanned with leather drums (GSD-401, Xinda Machinery, China) for 4 hours with different aldehyde agents at 30 °C including formaldehyde agent (FA), oxazolidine (OX), glutaraldehyde agent (GTA) and modified glutaraldehyde agent (GTW). The pH was then raised to 5.0 by using sodium carbonate aqueous solution (1:20, w/w). After basifying, the reaction was continued for another 12 h. Subsequently, these leather were stocked with constant temperature and humidity, and they were used to prepare collagen fibers for mechanism analysis.⁹

2.3 FTIR analysis

The discrepancy caused by different aldehyde tanning agents is related to the differences of the combination between hide and aldehyde agents. Thus these leather samples tanned with different aldehyde agents were investigated by FT-IR analysis20 (FTIR, Nicolet iS10, Thermo Scientific, USA). They were performed in a region of 500-4000 cm^{-1} .

2.4 SEM analysis

The leather samples were collected and observed. The typical surface changes and collagen fiber morphology of these samples were analyzed by Emission Scanning Electron Microscopy (FESEM, Hitachi, S4800, Japan). Experiments were repeated three times to validate the results.

2.5 Physical mechanical properties and organoleptic properties analysis

The physical measurements of tensile strength and elongation of leather were performed using a tensile tester (SERVO, GOTECH, Taiwan). The air permeability of leather prepared by different tanning agents is measured by a leather air permeability tester (GOTECH). The water vapor permeability of leather was tested by low temperature penetration test (SERIES, GT-7005, GOTECH). Leather aging resistance is tested by leather aging machine and electronic universal testing machine (GT-7017, GOTECH; XWN-20, Changchun). The yellow resistance of leather is tested by the yellow resistance

test box (GT-7035-UA, GOTECH). Organoleptic properties of hide were evaluated by traditional evaluation method. They were evaluated by three experienced tanners and classified into 5 grades according to their appearance and touch sense. Higher points indicate better properties of the hide.

3 Results and Discussion

3.1 FTIR analysis

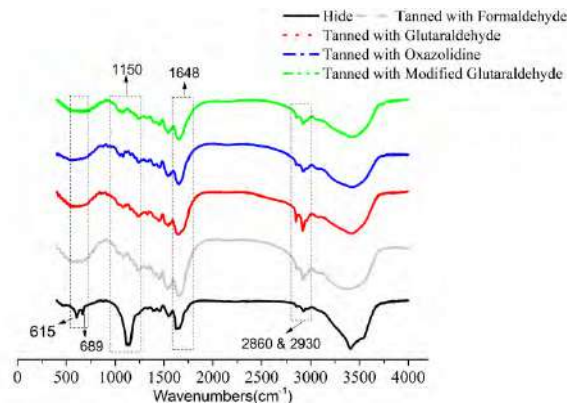


Fig. 1. FTIR spectra.

The FTIR spectra of hide tanned with different aldehyde tanning agents was observed in Fig.1 including formaldehyde, glutaraldehyde, oxazolidine and modified glutaraldehyde. As shown, two peaks appeared at 2860 cm^{-1} and 2930 cm^{-1} , which were attributed to C-H of aldehyde. Meanwhile, the single peak at 1648 cm^{-1} was contributed by C=O of aldehyde. It was seen that peaks intensity at 615 cm^{-1} , 689 cm^{-1} and 1150 cm^{-1} decreased after tanning, which demonstrates that these aldehyde agents reacted with both carboxyl groups and amino groups of collagen fibers which mainly composed hide.

3.2 SEM analysis

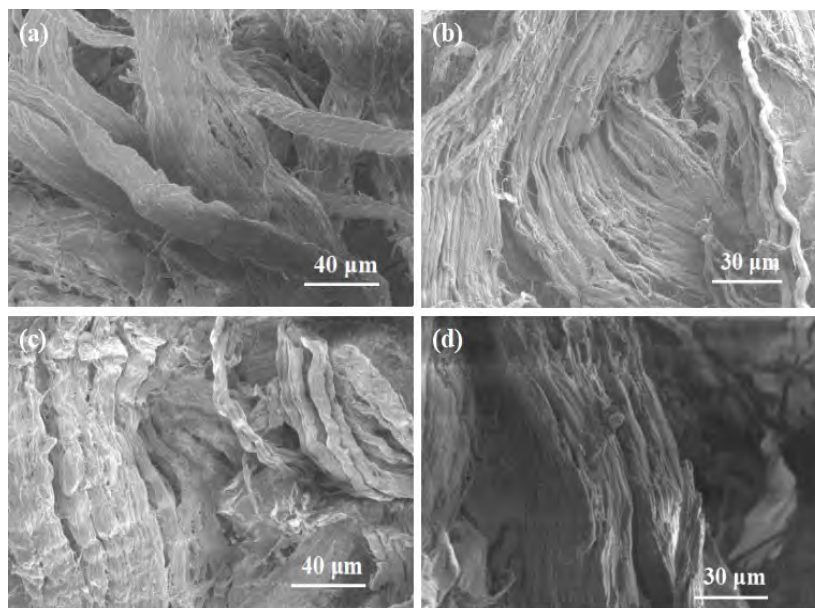


Fig. 2. SEM analysis of wet-white tanned by different aldehyde agents. (a) FA tanning; (b) OX tanning; (c) GTA tanning; (d) GTW tanning.

The micro structures of collagen fibers tanned with different aldehyde agents were shown in Fig.2. The FA agent wasn't considered to be used in gymnastics leather production due to the irregular structures (Fig.2a) and the carcinogenicity.¹⁰ The OX and GTW weren't selected because the tanned collagen fibers were finer, which would result in low strength properties. Besides, the crosslink reaction between OX and collagen fibers wasn't viewed clearly (Fig.2b) thereby it couldn't be used alone in tanning. Furthermore, considering the costs, effectiveness and availability of tanning agents, GTA was more suitable for producing gymnastics leather and the collagen fibers which tanned by GTA displayed highly order structure.

3.3 Analysis of wet-white properties

Table 1. Physical measurements of Wet-whites tanned with different aldehyde tanning agents.

	FA	OX	GTA	GTW
Shrinkage Temperature(°C)	88.3	78.55	86.9	86.45
Tensile Strength (Mpa)	14.8	11.01	20.3	19.63
Elongation rate(%)	74.4	57.	42.5	41.62
Softness	8	35	4	4
Graininess	4	3.3	5	5
air permeability [mL/(cm ² ·h)]	4	4	5	4.7
moisture permeability [mg/(cm ² ·h)]	514.	218	867.	392.5
yellowing resistance	29	.18	46	8
	0.06	0.0	0.06	0.057
	1	28	9	
	2.5	1	2	1.5

The physical mechanical properties of Wet-whites, which were tanned with different aldehyde agents, were measured including shrinkage temperature, tensile strength and elongation rate. Meantime, the organoleptic properties were also evaluated. The results were shown in Table I. From Table I, it was seen that the shrinkage temperatures of Wet-whites of FA, GTA and GTW were 88.3, 86.9 and 86.45 °C respectively. Furthermore, the tensile strength of GTA and GTW were 20.34 and 19.63 Mpa respectively, thus the wet-white produced by GTA possessed the highest tensile strength. Meantime, the elongation rates of wet-white tanned with GTA and GTW were similar, which was resulted by the crosslink reaction style of glutaraldehyde and collagen. Besides, it showed that the elongation rate of FA wet-white was the highest owing to the irregular structures of collagen fibers. In order to analysis the organoleptic properties, softness and graininess were evaluated by experienced tanners. When added glutaraldehyde in tanning process, the organoleptic properties were obviously improved. The wet-white tanned with GTA has the highest air permeability, and it's up to 867.46 mL/(cm²·h). The wet-white tanned with GTA also has the best moisture Permeability. Among the four kinds of leather, FA and GTA had better resistance to yellowing.

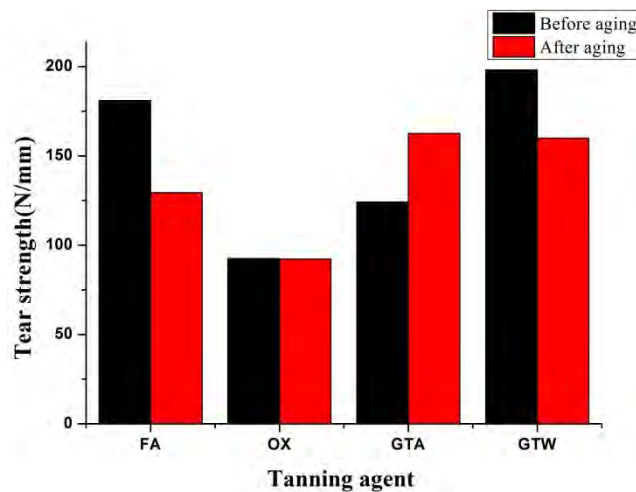


Fig. 3. The aging resistance analysis of wet-white tanned by different aldehyde agents.

The change of leather tearing strength before and after the aging test was tested by simulating the sunshine irradiation in 3-4 months. The results indicate that the leather prepared by OX has a stable aging resistance. Meantime, the tear strength increasing of GTA leather may be resulted by the further crosslinking reaction between tanning agent and collagen fibers in aging resistance measurement. Based on these results, GTA can be selected for gymnastics leather production, and the production process should be designed to further improve the tensile strength and reduce elongation rate.

3.4 Redesign of gymnastics leather processes

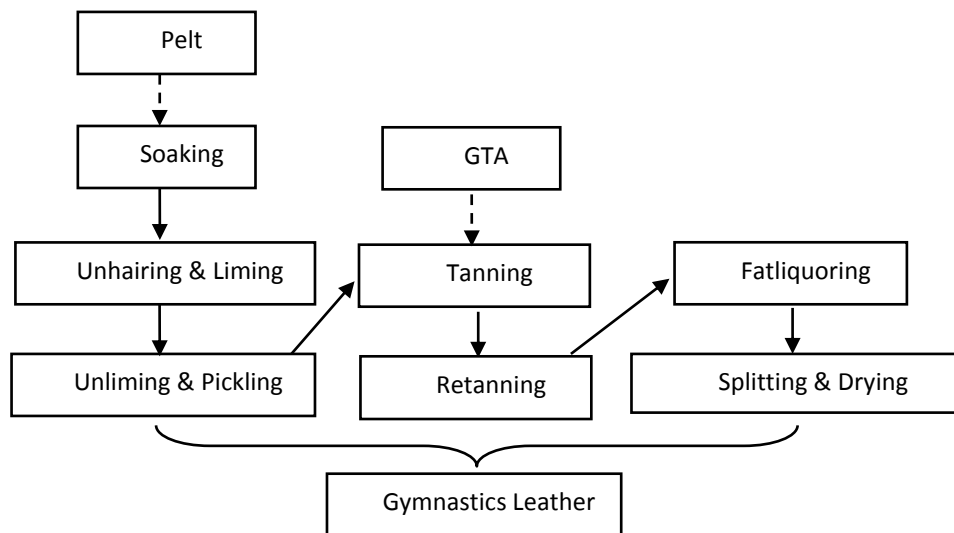


Fig. 4. Gymnastics Leather Production Process.

By conventionally production methods, the tensile strength of wet-white was only 20.34 Mpa. It couldn't meet the requirements of gymnastics leather. Therefore, the production process must be redesigned. The preliminary steps should be adjusted to improve the strength of collagen fibers, and the usages of tanning agent and retanning agent were further optimized. The production process was seen in Fig.4. It showed that the traditional bating step was removed, and the pelts wasn't dyed due to long-term contact with human skin. The properties of finish gymnastics leather would be further investigated.

3.5 Optimization of GTA usage

Table 2. Properties analysis of finished gymnastics leather tanned with different GTA dosage.

	4%	6%	8%	10%
Shrinkage	79.1	83.	82.	84.
Temperature(°C)		2	6	1
Tensile	34.1	41.	40.	42.
Strength (Mpa)	7	03	02	67
Elongation	49.3	45.	48.	46.
rate(%)	5	45	75	02

The finished gymnastics leather were produced by the redesigned production processes. From Table II, it was seen that 6% GTA should be selected while considering the cost and effectiveness. Through the redesigned processes, the tensile strength reached 41.03 Mpa, which could successfully match the demands.

Conclusion

In this paper, a novel method for producing gymnastics leather was presented by aldehyde tanning. Tanning effects of different tanning agents were compared and evaluated including formaldehyde agent (FA), oxazolidine (OX), glutaraldehyde agent (GTA) and modified glutaraldehyde agent (GTW). The results showed that 6% GTA was the most suitable in gymnastics leather tanning process. It has high air permeability and good yellowing resistance. In order to improve the physical mechanical properties, the traditional production processes were redesigned, and bating step was removed which resulted the tensile strength decrease. The final tensile strength reached 41.03 by this method while the elongation rate was 45.45%, which could successfully meet the requirements of gymnastics leather.

References

1. Bradshaw, E. J., and Hume, P. A. (2012) Biomechanical approaches to identify and quantify injury mechanisms and risk factors in women's artistic gymnastics, *Sports biomechanics* 11, 324-341.
2. Neal, R. J., Kippers, V., Plooy, D., and Forwood, M. R. (1995) The influence of hand guards on forces and muscle activity during giant swings on the high bar, *Medicine and science in sports and exercise* 27, 1550-1556.
3. Forster-Scott, L. (2011) Understanding colorism and how it relates to sport and physical education, *Journal of Physical Education, Recreation & Dance* 82, 48-52.
4. Zhang, C., Lin, J., Jia, X., and Peng, B. (2016) A salt-free and chromium discharge minimizing tanning technology: the novel cleaner integrated chrome tanning process, *J. Clean. Prod.* 112, 1055-1063.
5. Qiang, T., Gao, X., Ren, J., Chen, X., and Wang, X. (2015) A chrome-free and chrome-less tanning system based on the hyperbranched polymer, *ACS Sustain. Chem. Eng.* 4, 701-707.
6. Sun, X., Jin, Y., Lai, S., Pan, J., Du, W., and Shi, L. (2018) Desirable retanning system for aldehyde-tanned leather to reduce the formaldehyde content and improve the physical-mechanical properties, *J. Clean. Prod.* 175, 199-206.
7. Jankauskaitė, V., Jiyembetova, I., Gulbinienė, A., Širvaitytė, J., Beleška, K., and Urbelis, V. (2012) Comparable evaluation of leather waterproofing behaviour upon hide quality. I. Influence of retanning and fatliquoring agents on leather structure and properties, *Materials Science* 18, 150-157.
8. Liao, X., Zhang, M., and Shi, B. (2004) Collagen-fiber-immobilized tannins and their adsorption of Au (III), *Ind.Eng.Chem.Res.* 43, 2222-2227.
9. Wang, X., Li, J., Chen, Z., Lei, L., Liao, X., Huang, X., and Shi, B. (2016) Hierarchically structured C@SnO₂@C nanofiber bundles with high stability and effective ambipolar diffusion kinetics for high-performance Li-ion batteries, *J. Mater.Chem.A.* 4, 18783-18791
10. Salthammer, T., Mentese, S., and Marutzky, R. (2010) Formaldehyde in the indoor environment, *Chemical reviews* 110, 2536-2572.

THE QUALITY OF LEATHER PRODUCTS AS SEEN FROM THE USER'S VIEWPOINT

Daisuke Murai

CONSUMER PRODUCT END-USE RESEARCH INSTITUTE CO., LTD.

csyh499@dent.daimaru.co.jp

Abstract. We are a group company of a major department store in Japan and are in charge of quality control and customer service of items we sold. We constantly monitoring the customer's voices, and we have the records of correspondence with customers since 1996, and we hold over 100,000 cases for all items of food, clothing, living and services. The record includes not only the customer's request but also the test result of each item before sales and the reproduction test result of based on the customer's offer. We use the database to build our quality standards of sales items and education of salespersons, but each records of correspondence are of course private. However, quality improvement of sales items is not simply a problem of self-solving within our supply chain. Therefore, using aggregated results, we want to clarify the type and level of problem of users of leather goods and want to lead to the overall quality improvement of supply items of scale that we can not alone. As a survey method, it is based on grouping all 7,000 records of leather goods in past decade by our original 'product-code' and 'consultation-code'. By using grouped results, we will clarify what kinds of items and what kind of complaints is more often in major sales items. Additionally, by using text extraction from the content of the customer's offer and grouping by manual operation, and totalization will be performed for each use period and for each product color. For example, it compares with the test result such as colour fastness. Referring to required performance items specified by ISO standards, the gap between customer's request and quality standard will be clarified. With the internationalization of the purchasing network of sales items, quality control based on setting various safety standards and quality standards is becoming increasingly important. In terms of the characteristics of leather, I think that there is probably a level that is impossible to realize, but not only the problems of regulations and safety but also the quality of the customer's viewpoint must be discussed.

1 Material and Method

Our customer's complaint received at the customer service center is collected to our exclusive database. From the database, we extract statistical analyzes.

The scope is 10 department stores in Japan, and it is a product complaint received in recent 11 years from 2008 to 2018. Furthermore, the total 13,652 cases including textiles, leather goods, living goods are analyzed. Of these, 4,864 cases are leather products.

2 Result and Discussion

2.1 Trend of Leather Items

We show an overview of the product complaints targeted by this survey. First, it is shown what kind of items (Leather Products) there are many product complaints in Table 1. You can see that there are many complaints about women's shoes and bags. These are also the main selling items of our department store.

Table 1. Items composition of Product Complaints

	Composition
Women's shoes	44%
Bags	31%
Men's shoes	9%
Wallet	6%
Belts	4%
Watch band	3%
Leather wear	2%
Furniture	1%
Gloves	<1%

Next, it is shown what kind of product complaints are common in major 2 items, women’s shoes and bags in Table 2. In women’s shoes, the problem of scratches and breaks (tears) is most frequent. And in bags, the problem of color and appearance change and scratches and breaks are frequent.

Table 2. Content of Complaints about Major Items

	Women's shoes	Bags
Color and Appearance Change	18%	38%
Scratches and Breaks	44%	36%
Health and Safety	18%	9%
Performance, Feeling of use	15%	6%
Other	5%	11%
Total	100%	100%

And, it is shown when product complaints are the most frequent in Table 3. Most of product complaints are in the initial purchase stage. If you look at the range that contains 80% of the whole, you can see the required durability length for each item. For example, women's shoes are more than three years and bags are more than five years. These are considered to be closely related to the usage period of the consumer.

Table 3. Complaints of the Offer Period from Purchase

	1 Mo	6 Mos	1 Yr.	3 Yrs.	5 Yrs.	10 Yrs.	Unknown	Total
Women's shoes	43%	19%	12%	11%	5%	3%	7%	100%
Bags	27%	21%	13%	16%	8%	7%	8%	100%
Men's shoes	29%	21%	10%	12%	9%	10%	9%	100%
Wallet	25%	31%	18%	10%	2%	4%	10%	100%
Belts	25%	20%	6%	16%	10%	11%	12%	100%
Watch band	17%	22%	11%	27%	8%	8%	7%	100%
Leather wear	17%	19%	19%	21%	15%	5%	5%	100%
Furniture	15%	16%	12%	16%	8%	26%	5%	100%
Gloves	57%	23%	9%	11%	0%	0%	0%	100%

Finally, we show the composition of the production country of the items in Table 4. Although many databases do not have records, domestic (made in Japan), made in China, and made in Italy are most frequent. While many Japanese fashion brands are domestic or made in China, imported ones are popular in Italy.

Table 4. Production Country of Offered Products

	Japan	China	Italy	Southeast Asia	Other	Unrecorded	Total
Women's shoes	27%	16%	6%	4%	6%	41%	100%
Bags	8%	19%	11%	2%	6%	53%	100%
Men's shoes	18%	8%	14%	6%	10%	43%	100%
Wallet	16%	13%	9%	1%	5%	56%	100%
Belts	13%	7%	20%	1%	4%	55%	100%
Watch band	5%	6%	2%	1%	30%	56%	100%
Leather wear	12%	31%	12%	0%	17%	29%	100%
Furniture	18%	4%	7%	0%	5%	66%	100%
Gloves	9%	11%	20%	3%	11%	46%	100%

2.2 Details of Leather Parts

We show that what kind of complaints are frequent and when they are frequent about women's shoes and bags in Table 5 and 6. Compared with women's shoes, the color and appearance change of the bag has many complaints over a long period of time.

Table 5. Content of Complaints about Women's Shoes

	1 Mo	6 Mos	1 Yr.	3 yrs.	5 yes	10 rest	Unknown
Color and Appearance Change	15%	4%	3%	2%	1%	0%	2%
Scratches and Breaks	13%	8%	6%	5%	1%	1%	2%
Health and Safety	10%	3%	1%	2%	0%	0%	1%
Performance, Feeling of use	8%	3%	2%	1%	0%	0%	1%
Other	1%	1%	1%	0%	0%	0%	0%
Total				100%			

Table 6. Content of Complaints about Bags

	1 Mo	6 Mos	1 Yr.	3 yrs.	5 yes	10 yrs.	Unknown
Color and Appearance Change	16%	14%	8%	10%	3%	4%	2%
Scratches and Breaks	4%	6%	6%	4%	2%	1%	2%
Health and Safety	3%	1%	1%	1%	0%	0%	1%
Performance, Feeling of use	3%	1%	0%	0%	0%	0%	1%
Other	2%	2%	1%	1%	0%	0%	0%
Total				100%			

2.3 Analysis of Typical Problem

2.3.1 Color and Appearance Change

The details of color and appearance change are shown in Table 7 and 8. In women's shoes and bags, color stain is the most common. Next to that, there are many discolorations.

Table 7. Content of Color and Appearance Change in Women’s Shoes

Women's shoes	1 Mo	6 Mos	1 Yr.	3 Yrs.	5 Yrs.	10 Yrs.	Unknown
Color Stain	28%	8%	4%	3%	0%	0%	5%
Discoloration	12%	5%	3%	4%	1%	0%	2%
Stickies and Cracks	1%	0%	1%	0%	1%	0%	0%
Stain from Outside	4%	2%	1%	0%	0%	0%	1%
Other	8%	1%	2%	1%	0%	0%	1%
Total				100%			

Table 8. Content of Color and Appearance Change in Bags

Bags	1 Mo	6 Mos	1 Yr.	3 Yrs.	5 Yrs.	10 Yrs.	Unknown
Color Stain	15%	11%	4%	5%	0%	0%	2%
Discoloration	7%	8%	7%	8%	4%	2%	1%
Stickies and Cracks	0%	0%	2%	1%	1%	5%	0%
Rough Break and Water Spots	3%	1%	1%	1%	1%	0%	0%
Stain from Outside	2%	3%	1%	2%	0%	0%	1%
Other	1%	1%	0%	1%	0%	0%	0%
Total				100%			

Next, it is shown that the test results of color fastness that have become a product complaint. Interestingly, consumers are more sensitive to color stain under dry conditions than wet conditions. It seems to be a problem for consumers that the dirt does not go down even after washing.

Table 9. Test Results of Color Fastness in Women’s Shoes

	1 or 1-2	2 or 2-3	3 or 3-4	4 or 4-5	5	Total
Dry Rubbing	3%	39%	28%	28%	3%	100%
Wet Rubbing	28%	45%	24%	3%	0%	100%

And it is shown in Table 10, what kind of colors are frequent in color stain. There were more problems with darker products than lighter colors. We think that dark stains are noticeable.

Table 10. Frequent color of Color Stain in Women’s Shoes

Color	Black	Red	Dark Brown	Dark Blue	Total
	70%	10%	15%	5%	100%

Finally, it is shown which part of the shoe is frequent in color stain. There were more lining problems than the upper.

Table 11. Offered Parts of Color Stain in Women’s Shoes

Parts	Boots Lining	Quarter lining	Upper	Linings	Total
	33%	24%	24%	19%	100%

2.3.2 Scratches and Breaks

It is shown a breakdown of Scratches and Breaks in Table 12 and 13. In both women's shoes and bags, there are many problems such as cracking of the leather surface and tearing around the seams.

Table 12. Content of Scratches and Breaks in Women’s Shoes

	1 Mo	6 Mos	1 Yr.	3 Yrs.	5 Yrs.	10 Yrs.	Unknown
Upper / Scratches and Cracks	7%	4%	1%	1%	0%	0%	1%
Upper / Breaks and Worn out	11%	9%	7%	4%	1%	0%	2%
Upper / Deformations	5%	1%	1%	2%	0%	0%	1%
Sole / Cracks and Breaks	1%	1%	0%	1%	0%	1%	0%
Sole / Worn out	1%	1%	0%	0%	0%	0%	0%
Sole / Others	0%	1%	0%	1%	0%	0%	0%
Heel / Detach and Deformation	6%	4%	3%	1%	1%	0%	1%
Adhesive Peeling Off	5%	2%	3%	3%	1%	0%	0%
Others /	3%	2%	1%	1%	0%	0%	1%
Total				100%			

Table 13. Content of Scratches and Breaks in Bags

Bags	1 Mo	6 Mos	1 Yr.	3 Yrs.	5 Yrs.	10 Yrs.	Unknown
Surface / Scratches and Cracks	3%	5%	10%	4%	1%	1%	1%
Body / Breaks and Worn out	5%	7%	6%	4%	2%	1%	3%
Lining / Breaks and Worn out	0%	0%	1%	0%	2%	1%	1%
Parts / Detach and Deformation	5%	4%	2%	3%	0%	2%	0%
Adhesive Peeling Off	0%	2%	4%	4%	1%	1%	1%
Others	3%	4%	1%	2%	1%	0%	1%
Total				100%			

2.3.3 Health and Safety

It is shown a breakdown of health and safety in Table 14 and 15. In women's shoes, there are many problems that cause shoe rubbing at the beginning of purchase.

Table 14. Content of Health and Safety in Women’s Shoes

	1 Mo	6 Mos	1 Yr.	3 Yrs.	5 Yrs.	10 Yrs.	Unknown
Sharps	6%	1%	2%	3%	1%	0%	1%
Unstable and slip	5%	3%	2%	1%	1%	0%	1%
Shoe sore	36%	10%	3%	4%	1%	0%	2%
Human damaged	4%	2%	1%	1%	1%	0%	0%
Bad Smell and Mildewed	4%	3%	0%	1%	0%	0%	0%
Others	1%	1%	0%	1%	0%	0%	0%
Total				100%			

In bags, sharp points are an issue at the beginning of purchase. A sharp point is the end of sewing, and if the finish is bad, it will damage the clothes.

Table 15. Content of Health and Safety in Bags

	1 Mo	6 Mos	1 Yr.	3 Yrs.	5 Yrs.	10 Yrs.	Unknown
Sharps	14%	11%	8%	3%	0%	3%	3%
Bad Smell and Mildewed	22%	8%	14%	3%	0%	0%	6%
Other	3%	0%	0%	3%	0%	0%	0%
Total				100%			

3 Conclusion

By the analysis of the product complaints, it revealed the major problem on the quality of leather products.

- 1) Depending on items, differences were found in the durability required by consumers. As a result of analyzing how long complaints are submitted after purchase, for example, I think that it is about 3 years for women's shoes, 5 years for bags, and nearly 10 years for furniture.
- 2) There were a lot of problems with color stain and appearance change, and problems with tear in any item. Consumers are also very strict about color fastness in the dry condition.
- 3) The leather products should be very strong, but there were a lot of tearing problems. Leather is thinner and more delicate than before. There are also many individual differences in intensity.
- 4) Most problems are purchased within one year, and quality control in a new condition is required.
- 5) This time we analyzed it in detail, we hope that the data can be used to further improve the quality of leather products, promote sales, and develop the leather industry.

4 Acknowledgement

We gratefully acknowledge the work of past and present member of our company, and Daimaru Matsuzakaya Department Stores Corp., Japan Association of Leather Technology (JALT).

References

1. *JALT : Development and Practical Application Report for Japanese eco-leather (2008-2018)*

SORPTION COMPARISON OF TRIVALENT CHROMIUM ON VARIOUS *FICUS CARICA* CHARCOAL FROM TANNERY WASTEWATER

M. A. Hashem^a, S. Mim, M. Z. R. Shaikh, S. Payel and M. S. Nur-A-Tomal

Department of Leather Engineering, Khulna University of Engineering & Technology Khulna-9203, Bangladesh

a) Corresponding author: mahashem96@yahoo.com, mahashem@le.kuet.ac.bd

Abstract. In this study, equipped charcoal of *Ficus carica* without being impregnated impregnated with potassium hydroxide (KOH), zinc chloride (ZnCl₂) and phosphoric acid (H₃PO₄) was used for sorption comparison of trivalent chromium, Cr (III) from tannery wastewater. The equipped charcoals are characterized by Fourier transforms infrared spectroscopy (FT-IR) before and after sorption of Cr(III). The quantitative elemental analysis of the charcoal is performed using PGT Energy dispersive X-ray spectrometry (EDX). The Cr(III) sorption efficacy of charcoal was examined investigating charcoal dose, contact time, and relative pH. Batch sorption test revealed that *Ficus carica* charcoal without impregnation had the maximum sorption capacity of Cr(III). At the same conditions, Cr(III) sorption efficiency on the *Ficus carica* charcoal without impregnation, impregnated with potassium hydroxide, zinc chloride, and phosphoric acid was 98.9%, 98.8%, 8.9% and 2.5%, respectively. The study could be helpful to design the sorption of trivalent chromium from the tannery wastewater in-house prior to discharge.

Keywords: Sorption, Cr (III) extraction, Impregnation, Environment

1 Introduction

The leather industry has a significant position in Bangladesh economy considering its importance in production, employment and export. In the absence of effluent treatment plant (ETP), about 113 tanneries in Bangladesh generate approximately 20,000 m³ tannery effluent per day (Paul et al. 2013). Usually, leather processing operations are conducted with a huge amount of chemicals. But a majority of these chemicals are not up-taken by the pelt. Mostly, chemicals remaining in wastewater are discharged as waste without being treated causing serious pollutions. Chrome tanning is mostly used to obtain an extraordinary dyeing, hydrothermal stability, and excellent mechanical resistance in leather. More than 90% of the global leather production of 18 billion sq. ft is conducted through the chrome-tanning process (Sundar et al. 2002). Only 60-70% of chromium (Cr) applied in the tanning process are consumed by leather where untreated wastewater holds 1500-3000 mg/L of Cr (Aravindhan et al. 2004). Every day approximately 1.25 tons of chromium is discharged into the Bangladeshi river (UNIDO, 2000). Usually, trivalent chromium, Cr (III) discharging through the wastewater is further oxidized to hexavalent chromium, Cr (VI) that is acutely and chronically toxic to humans even in low concentrations. Therefore, it is essential to remove Cr from chrome tanning effluent before it is released.

By using biological treatment, dissolved solids like Cr removal are not possible. Remediation of Cr from tannery waste effluent can be performed by ion exchange (Rengaraj et al. 2003), chemical precipitation (Zhou et al. 1995), membrane separations (Kozłowski et al. 2002), electrochemical precipitation (Kongsricharoern et al. 1996) but high capital and operational costs limit these methods to use commercially. Moreover, a separate pre-treatment or a set of treatments are required for most of the treatment processes. But in the case of the adsorption process, no pre-treatment is required with cheap, simple and easy application.

For having the availability of extensive surface area, microporous structure and high adsorption capacity; the production of charcoal from cheaper materials has gained significant attention for wastewater treatment (Anirudhan and Sreekumari, 2011). All carbonaceous materials are possible

to be converted into charcoal, though the properties of the final product will be different, depending on the nature of the raw material, activating agent and activation processes (Bansal and Goyal, 2005). A large number of products, such as coffee husks (Oliveira et al. 2009), mahogany sawdust (Santra et al. 2008), cocoa shell (Ahmad et al. 2012), waste tea (Auta and Hameed, 2011), coffee grounds (Reffas et al. 2010), pomegranate shell (Ghaedi et al. 2012), mahogany sawdust (Malik, 2003), rice husk (Malik, 2003; Santra et al. 2008), coconut shell (Santra et al. 2008), etc. have been successfully converted into low-cost charcoal. The major use of activated carbon is for removing taste, colour, odours, and impurities from liquids/wastewaters and also in solution purification. Besides, in recent times it has been increasingly used for the prevention of environmental pollution (Onyeji and Aboje, 2011).

Ficus carica, a plant is the source of fruit known as fig. It is widely grown throughout the world without any special caring for being dispersed by birds and mammals. In some countries, *Ficus carica* has been used for medicinal benefits (Duke et al. 2002) and a supplement food for diabetics (Mawa et al. 2013) but in Bangladesh, it has no conventional utilization. *Ficus carica* charcoal can be effectively used for removal of Cr from tannery effluent. It has been found that after chemical or thermal modifications, carbonaceous material exhibited tremendous Cr removal capability. Thermal modification is easy and inexpensive but in chemical activation, chemical reagents like zinc chloride ($ZnCl_2$), phosphoric acid (H_3PO_4), potassium hydroxide (KOH) are used (Buczek, 2016). The drawback of activation with $ZnCl_2$ is the occurrence of pollution with zinc salts which are difficult to remove (Owabor and Iyaomolere, 2013). Others the price of $ZnCl_2$ is higher and extra treatment like washing and pH maintenance are required after activation. From washing, chloride (Cl^-) is usually released that inhibits the growth of plants, bacteria, and fish in surface waters with occurring surface salinity. Activation with H_3PO_4 results in a pitch like sticky charcoal inhibiting the application with additional chemical costs. But natural *Ficus carica* charcoal preparation is possible without any chemical treatment and additional costs. Only thermal modification using pyrolysis is enough to make this type of charcoal. The main advantages of using this charcoal are cheap, accessible and available in abundant quantity.

The aim of this study was using *Ficus carica* to produce charcoal adsorbent to remove Cr (III) from the wastewater. The investigation could fulfil the purpose of Cr (III) removal from tannery wastewater using a low-cost adsorbent prepared from *Ficus carica* which is not generally used profitably in Bangladesh.

2 Materials and Methods

2.1 Sample Collection

Chrome containing wastewater was collected from the SAF Leather Limited, Khulna, Bangladesh. The chrome liquor was collected in a high-density polyethylene container. Before collecting the chrome liquor the container was washed with diluted nitric acid according to the standardized laboratory method. The industrial wastewater was primarily filtered to remove unexpected suspended solids and the filtered liquor was used for treatment. *Ficus carica* was collected from university campus of Khulna University of Engineering & Technology, Khulna, Bangladesh.

2.2 Charcoal Preparation

The collected *Ficus carica* were chopped into small pieces and sun-dried. Afterwards, it was burnt at 600 °C in a furnace and crushed with mortar to produce a charcoal powder. Lastly, the required size of the charcoal adsorbent was obtained by sieving on 80-mesh. Fig. 1(a) shows the prepared *Ficus carica* charcoal.

2.2.1 Preparation of KOH impregnated charcoal

Dried *Ficus carica* was mixed with ground KOH in a ratio (1:3). Treatment carried out at 600°C in a furnace. Then, the solution was neutralized with 5% HCl at pH 6.5. After filtration, it was dried at 120 °C in the oven (Buczek, 2016). Lastly, the required charcoal adsorbent was obtained by crushing with mortar. Fig. 1(b) shows the KOH impregnated *Ficus carica* charcoal.

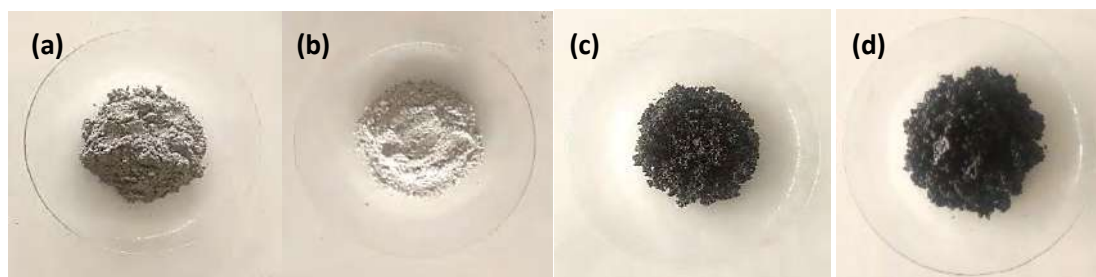


Fig.1. *Ficus carica* (a), KOH impregnated (b), ZnCl₂ impregnated (c) and H₃PO₄ impregnated (d) charcoal

2.2.2 Preparation of ZnCl₂ impregnated charcoal

To prepare ZnCl₂ impregnated charcoal, dried *Ficus carica* was impregnated in an aqueous solution of 0.05M ZnCl₂ for 72 h with occasional stirring. It was then dried and carbonized at 600°C. Then, the solution was neutralized with 5% HCl solution. Finally washed with distilled water to remove (Cl⁻) and dried in an oven (El-Maghraby et al. 2014). Then the charcoal adsorbent was obtained by crushing with mortar. Fig. 1(c) shows the ZnCl₂ impregnated *Ficus carica* charcoal.

2.2.3 Preparation of H₃PO₄ impregnated charcoal

The dried *Ficus carica* was soaked in a boiling solution of 40 % H₃PO₄ for 1 h and then kept at room temperature for 24 h (El-Maghraby et al. 2014). After that, the *Ficus carica* was separated, air dried and carbonized in the furnace at 600°C. Then the material was washed with water to remove residual acid, dried and stored in an airtight plastic container for adsorption studies. Fig. 1(d) shows the H₃PO₄ impregnated *Ficus carica* charcoal.

2.3 Reagents

The reagents that were used in this experiment were potassium hydroxide (Merck, India), zinc chloride (Merck, India), hydrochloric acid (Merck Specialties Private Limited, Mumbai), phosphoric acid (Merck Specialties Private Limited, Mumbai), pure concentrated nitric acid (Merck Specialties Private Limited, Mumbai), sulfuric acid (Merck Specialties Private Limited, Mumbai), perchloric acid (Merck, India), ammonium iron (Merck, India), sulfate hexahydrate (Merck Specialties Private Limited, Mumbai) and *N*-phenyl anthranilic acid (Loba Chemie, India), filter paper (Whatman No. 1), anti-bumping agent glass beads (Loba Chemie, India). All of the reagents were collected from local scientific store, Khulna, Bangladesh.

2.4 Effect of Impregnated Charcoal

To know the effect of KOH, ZnCl₂ and H₃PO₄ impregnated adsorbent dosage on the uptake of Cr(III), 50 mL of filtered solution was taken in three different conical flasks incubated with 2 g of natural *Ficus carica* charcoal, KOH impregnated, ZnCl₂ impregnated and H₃PO₄ *Ficus carica* charcoal, respectively.

The flasks were agitated in a shaker at 120 rpm for 10 minutes at room temperature. After 10 minutes of settling, filtration was performed. Then, the Cr (III) content in the supernatant with different types of adsorbent was determined.

2.5 Studies of Non-impregnated Charcoal Dose

To know the effect of adsorbent dosage on the uptake of Cr (III), 50 mL of filtered Cr (III) solution at pH 4 was taken in five different conical flasks incubated with 0.5, 1, 1.5, 2 and 2.5 g of natural *Ficus carica* charcoal. The flasks were agitated in a shaker at 120 rpm for 10 min at room temperature. After 10 min of settling, filtration was performed. Then, the Cr (III) content in the supernatant with different dosage of adsorbent was determined.

2.6 Characterization of Wastewater and Treated Effluent

2.6.1 Chromium and pH determination

Quantitative analysis of Cr (III) in the waste liquor and treated liquor was ascertained by the titrimetric method according to the Society of Leather Technologist and Chemists (1996) official method of analysis SLC 208 (SLT6/4) (SLTC, 1996). At first, 25 mL sample was taken in a 500 mL conical flask and 20 mL nitric acid and 20 mL of perchloric acid and the sulfuric acid mixture was added into it. Then the heat was applied gently to boil the mixture until it became a pure orange-red colour and the boiling was continued for one minute after the point had been reached. Later, the flask was taken aside from the heating source before exhilaration. Afterwards, the flask was inserted into a cold bath for rapid cooling and then 100 mL distilled water was carefully poured into the flask with glass beads. The heat was applied for 10 minutes to make the mixture chlorine free and after that 10 mL of 30% (v/v) sulphuric acid was carefully added. Finally, when the mixture was cooled, titration was performed with freshly prepared 0.1N ammonium iron (II) sulfate solution with six drops of *N*-phenyl anthranilic acid as an indicator and the end colour was pointed out as a colour change from violet to green. The pH of the raw chrome tanning wastewater and treated effluent was measured using calibrated pH meter (UPH-314, UNILAB, USA).

2.7 Characterization of Charcoal

The charcoal (pure and Cr (III) loaded) samples were analyzed using Fourier transform infrared spectrometer (FTIR, Spectrum 100, PerkinElmer, USA) where data recorded at (4000–400 cm^{-1}) on potassium bromide (KBr) discs and Energy dispersive X-ray spectroscopy (EDX) analysis using PGT Energy dispersive X-ray spectroscopy (Sigma HV, Carl Zeiss Microscopy Ltd.).

3 Results and Discussion

3.1 Comparison of Impregnated and Non-impregnated Charcoal

The effect of natural *Ficus carica* charcoal and impregnated charcoal on the adsorption of Cr (III) was investigated. The removal efficiencies for *Ficus carica* charcoal, KOH impregnated, ZnCl_2 impregnated and H_3PO_4 impregnated *Ficus carica* charcoal were calculated 98.86%, 98.77%, 8.86%, and 2.5% respectively shown in Fig. 2. Removal efficiency for ZnCl_2 and H_3PO_4 impregnated *Ficus carica* charcoal being 8.86% and 2.46% respectively indicate that removal of Cr (III) from wastewater by using these charcoal was ineffective. In the case of activation with ZnCl_2 , pollution with zinc salts occurs which are difficult to remove (Owabor and Iyaomolere, 2013). With costly

ZnCl₂ salt, washing requires too much water consumption. Moreover, pH maintenance requiring after activation with ZnCl₂ poses additional time-consuming step. Usually from washing, released Cl⁻ may inhibit the growth of plants, bacteria, and fish in surface waters with occurring surface salinity. Again, H₃PO₄ activated charcoals are not easy to apply because of its gummy nature. Also, the cost of H₃PO₄ used for activation is not negligible. Whereas, thermal modification using pyrolysis at 600°C was enough to prepare natural *Ficus carica* charcoal.

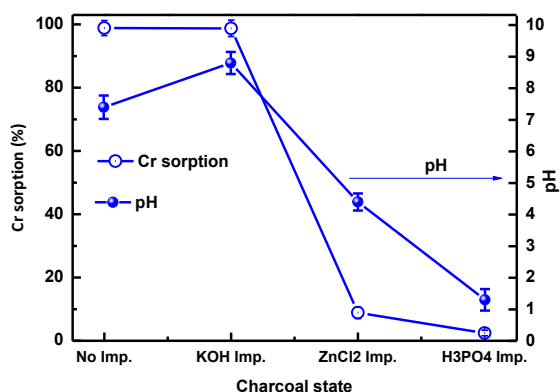


Fig. 2. Batch sorption of trivalent chromium: 2 g charcoal/75 mL tannery wastewater with contact time 10 min.

3.2 Effect of Adsorbent Dose on Chromium Uptake and pH

The effect of adsorbent dose on the adsorption of Cr (III) into natural *Ficus carica* charcoal was investigated. The maximum removal efficiency was calculated 98.26% with dose 2 g of the adsorbent with 50 mL of chromium solution.

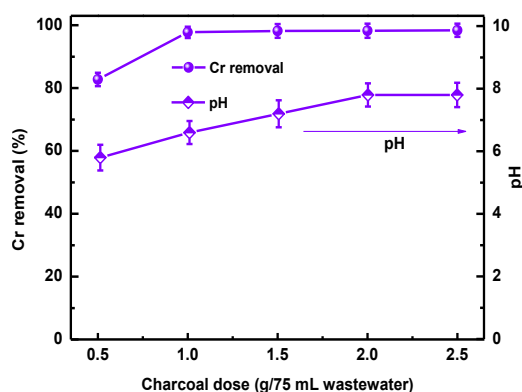


Fig. 3. Changes in chromium removal (%) and pH with *Ficus carica* charcoal dose

Fig. 3 shows the removal efficiency with respect to the adsorbent dose. As the adsorbent dose increases from 0.5 to 2 g the removal efficiency was found to increase. The removal efficiency with 2 g and 2.5 g dose was 98.26% and 98.39%, respectively. Removal efficiency slightly increases with 2.5 g dose which is negotiable. Thus considering the amount and removal efficiency 2 g was chosen as the best one. The effect of adsorbent dose on pH was also investigated (Fig. 3) where the pH was 5.8, 6.6, 7.2, 7.8, 7.8 for a dose of 0.5, 1.0, 1.5, 2.0, 2.5 g, respectively. In this case, pH was also found to increase with increasing adsorbent dose.

3.3 Characterization of Charcoal

3.3.1 FT-IR analysis

The sorption capacity of different charcoal depends upon porosity as well as the chemical reactivity of functional groups on the surface. The FT-IR spectrum of pure charcoal and Cr (III) loaded charcoal were compared and given in Fig. 4, Fig. 5 and Fig. 6.

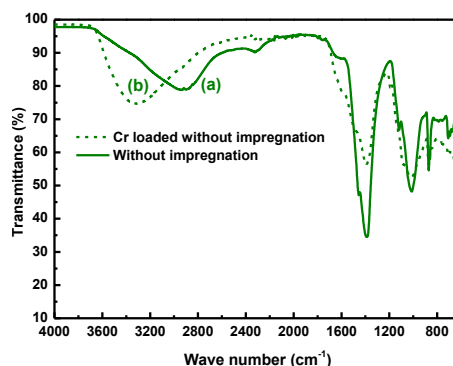


Fig. 4. FT-IR analysis of pure (a) and Cr (III) loaded (b) *Ficus carica* charcoal

In case of charcoal without impregnation, a broad region around 2918.2-2954 cm^{-1} wavelength is the indications of the presence C-H group, C-N at 2322.8-2138.1 cm^{-1} , alkane at 1405-1445 cm^{-1} , C=O, C-H, C=C groups at 1382- 1036 cm^{-1} (Kalaivani et al. 2014) as shown in Fig. 4(a). Again, a broad region around 3373-3422 cm^{-1} is the indications of the presence of O-H, N-H, C-H group, 1550-1560 cm^{-1} of secondary amine in case of Cr loaded charcoal without impregnation (Kalaivani et al. 2014) shown in Fig. 4(b).

In case of KOH impregnated charcoal, 3000 cm^{-1} wavelength is the indications of the presence C-H group, 2322.8-2138.1 cm^{-1} of C-N, 1654-1646 cm^{-1} of C=O, C=O, C-H, C=C groups at 1382- 1036 cm^{-1} (Kalaivani et al. 2014) shown in Fig. 5(c). Again, 1550-1560 cm^{-1} is the indications of the presence of secondary amine in case of Cr loaded KOH impregnated charcoal (Kalaivani et al. 2014) shown in Fig. 5(d).

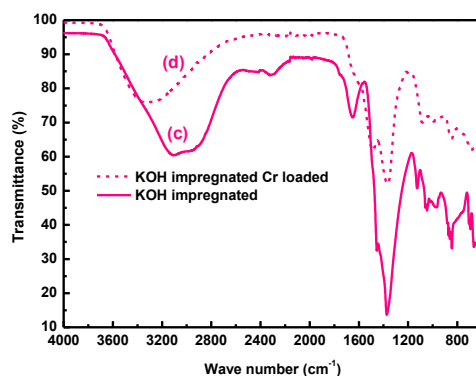


Fig. 5. FT-IR analysis of pure KOH impregnated (c) and Cr loaded KOH impregnated (d) *Ficus carica* charcoal

In the case of ZnCl_2 impregnated charcoal, 2918.2-2954 cm^{-1} wavelength is the indications of the presence C-H group (Kalaivani et al. 2014) shown in Fig. 6(e) and 1550-1560 cm^{-1} are the indications of the presence of secondary amine, 1050-1030 cm^{-1} of C-N (Kalaivani et al. 2014) for Cr loaded ZnCl_2 impregnated charcoal shown in Fig. 6(f). The functional groups in the ZnCl_2 impregnated *Ficus carica* charcoal were relatively less than two others which were the cause of less Cr removal by this charcoal. It ensures the involvement of different functional groups like carbonyl and carboxylic groups of pure charcoal in the sorption process. From FT-IR analysis it is found that after Cr sorption the functional groups in charcoal changed their positions as Cr was up-taken.

It is noticeable that without impregnated charcoal has a higher sorption capacity. Conversely, impregnation with chemical requires cost involvement, time-consuming, long process time, and not safe. Fig. 4, Fig. 5 and Fig. 6 depict a shift in the peak intensity which indicates the change of frequency in the functional groups of the charcoal due to chromium sorption. It indicates various responsible functional groups for the removal of Cr(III) through *Ficus carica* charcoal.

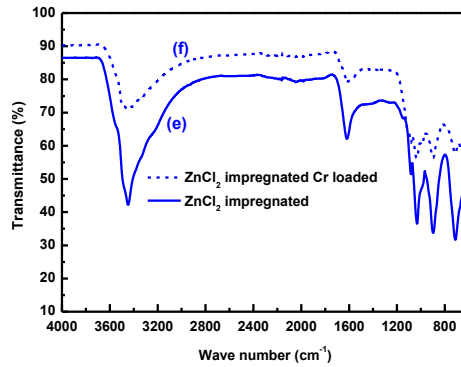


Fig. 6. FT-IR analysis of pure ZnCl₂ impregnated (e) and Cr loaded ZnCl₂ impregnated (f) *Ficus carica* charcoal

3.3.2 EDX analysis

Fig. 7(a) and Fig. 7(b) represent the EDX analysis of pure *Ficus carica* charcoal and Cr loaded *Ficus carica* charcoal, respectively. The presence of Cr is clear that non-impregnated *Ficus carica* charcoal has the sorption capacity. The impregnated charcoal analysis for before and after treatment is shown in Fig. 8 (a), (b), (c) and (d) representing KOH impregnated *Ficus carica* charcoal, Cr loaded KOH impregnated *Ficus carica* charcoal, ZnCl₂ impregnated *Ficus carica* charcoal, Cr loaded ZnCl₂ impregnated *Ficus carica* charcoal respectively. The comparison between before and after treatment showed the presence of Cr-after treatment confirming sorption of Cr(III).

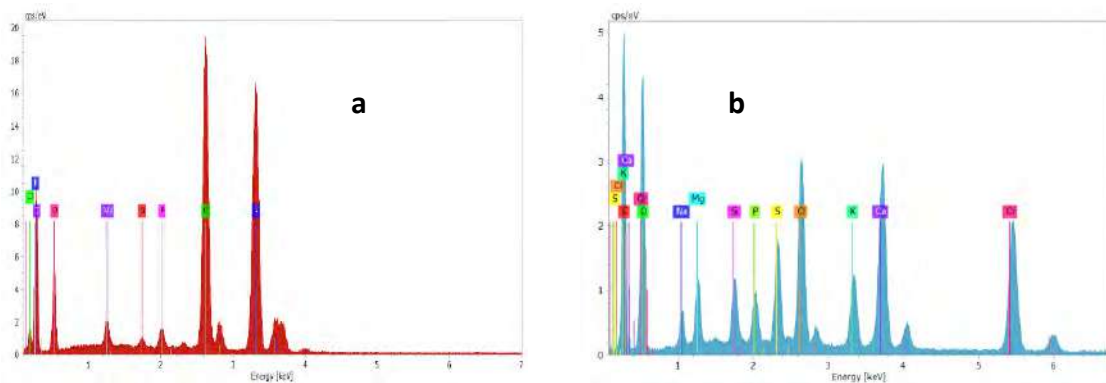


Fig. 7. EDX analysis of (a) *Ficus carica* Charcoal (b) Cr loaded *Ficus carica* Charcoal

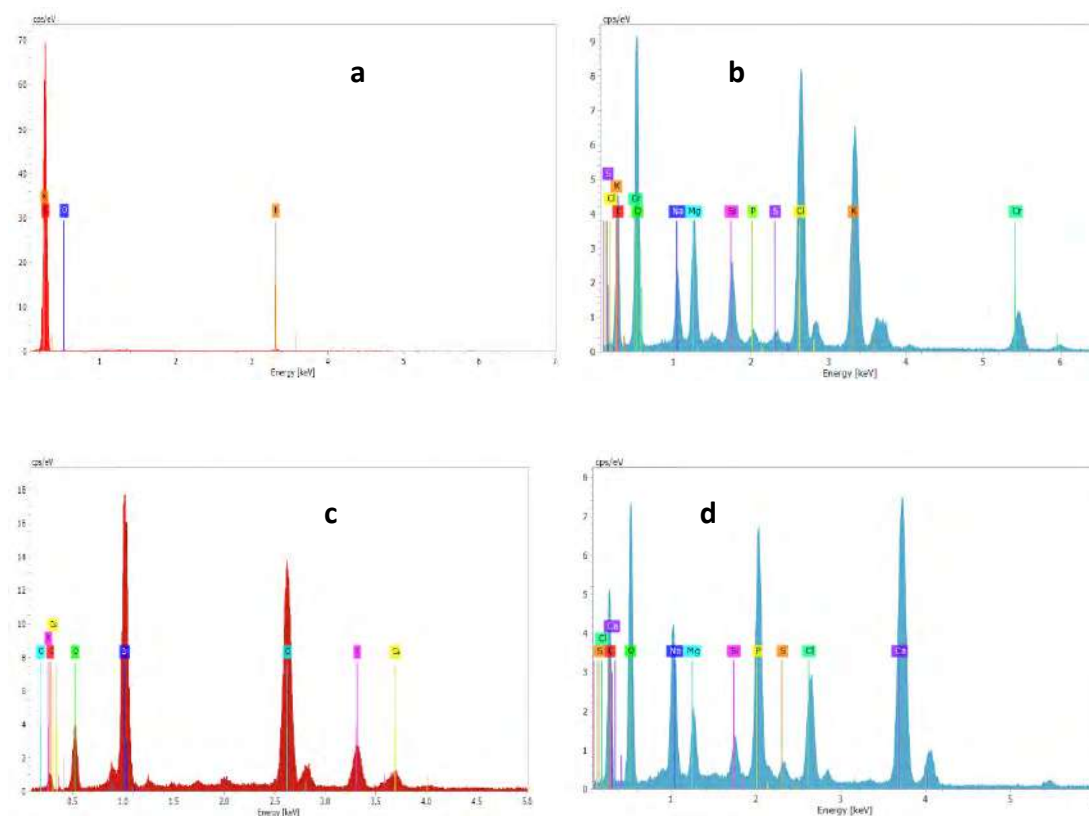


Fig. 8. EDX analysis of (a) KOH impregnated *Ficus carica* charcoal (b) Cr loaded KOH impregnated *Ficus carica* charcoal (c) ZnCl₂ impregnated *Ficus carica* charcoal (d) Cr loaded ZnCl₂ impregnated *Ficus carica* charcoal

From Fig. 7(b), 8 (b) and 8 (d) it is clearly evident that the non-impregnated *Ficus carica* charcoal showed the presence of higher Cr content than the impregnated samples. It indicates a higher sorption capacity of *Ficus carica* charcoal in natural condition without any impregnation. Between impregnated samples, Fig. 8 (b) showed some presence of Cr but in Fig. 8 (d) it was untraceable.

4 Conclusion

This study shows that without chemical impregnation *Ficus carica* charcoal has better trivalent chromium removal efficiency (98.9%). Although potassium hydroxide impregnated charcoal provided upright efficiency (98.8%), the higher chemical cost reduces its potentiality. The examination indicates that it was an effective method to reduce pollution load especially trivalent chromium from the spent chrome liquor. Preparation of natural *Ficus carica* charcoal is easy and inexpensive. It could be simply applied industrially for chromium removal from wastewater with some further investigation on cost analysis and input-output ratio.

References

1. Ahmad F., Daud W.M.A.W., Ahmad M.A., Radzi R.: 'Cocoa (*Theobroma cacao*) shell-based activated carbon by CO₂ activation in removing of cationic dye from aqueous solution: kinetics and equilibrium studies', *Chem. Eng. Res. Des.*, 90 (10), 1480-1490, 2012
2. Anirudhan T. S., Sreekumari S. S.: 'Adsorptive removal of heavy metal ions from industrial effluents using activated carbon derived from waste coconut buttons'. *J. Environ. Sci.*, 23(12), 1989–1998, 2011

3. Aravindhan R., Madhan B., Rao J.R., Nair B.U., Ramasami T.: 'Bioaccumulation of chromium from tannery wastewater: an approach for chrome recovery and reuse', *Environ. Sci. Technol.*, 38(1), 300-306, 2004
4. Auta M., Hameed B.H.: 'Optimized waste tea activated carbon for adsorption of Methylene Blue and Acid Blue 29 dyes using response surface methodology', *Chem. Eng. J.*, 175, 233-243, 2011
5. Bansal R. C., Goyal M.: *Activated carbon adsorption*, CRC Press, 5, 2005
6. Buczek B.: 'Preparation of active carbon by additional activation with potassium hydroxide and characterization of their properties', *Advances in Materials Science and Engineering*, 2016, 1-4, 2016
7. Duke J. A., Bugenschutz-Godwin M. J., Du Collier J., Duke P. K.: *Hand Book of Medicinal Herbs*. 2nd edition, Boca Raton, Fla, USA: CRC Press, 2002
8. El-Maghraby A., Taha N. A., Mahmoud A., El- Aziz A.: 'Preparation of activated carbon (chemically and physically) from banana pith for heavy metal removal from wastewater', *Sci-Afric Journal of Scientific Issues, Research and Essays*, 2 (9), 399-403, 2014
9. Ghaedi M., Tavallali H., Sharifi M., Kokhdan S.N., Asghari A.: 'Preparation of low cost activated carbon from *Myrtus communis* and pomegranate and their efficient application for removal of Congo red from aqueous solution', *Spectrochim., Acta A* 86, 107-114, 2012
10. Kalaivani S. S., Vidhyadevi T., Murugesan A., Thiruvengadaravi K. V., Anuradha D., Sivanesan S., Ravikumar L.: 'The use of new modified poly (acrylamide) chelating resin with pendent benzothiazole groups containing donor atoms in the removal of heavy metal ions from aqueous solutions', *Water Res. Ind.*, 5, 21-35, 2014
11. Kongsricharoern N., Polprasert C.: 'Chromium removal by a bipolar electrochemical precipitation process', *Water Sci. Technol.*, 34(9), 109-116, 1996.
12. Kozłowski C. A., Walkowiak W.: 'Removal of chromium (VI) from aqueous solutions by polymer inclusion membranes', *Water Res.*, 36(19), 4870-4876, 2002
13. Malik P.K.: 'Use of activated carbons prepared from sawdust and rice-husk for adsorption of acid dyes: a case study of Acid Yellow 36', *Dyes Pigments*, 56 (3), 239-249, 2003
14. Mawa S., Husain K., Jantan I.: '*Ficus carica* L. (Moraceae): Phytochemistry, Traditional Uses and Biological Activities', *Evid. Based Complement Alternat. Med.*, 2013, 2013.
15. Oliveira L.C., Pereira E., Guimaraes I.R., Vallone A., Pereira M., Mesquita J.P., Sapag K.: 'Preparation of activated carbons from coffee husks utilizing FeCl₃ and ZnCl₂ as activating agents', *J. Hazard. Mater.*, 165 (1-3), 87-94, 2009
16. Onyeji L. I., Aboje A. A.: 'Removal of Heavy Metals from Dye Effluent Using Activated Carbon Produced from Coconut Shell', *Int. J. Eng. Sci. Technol.*, 3(12), 8238-8246, 2011
17. Owabor C. N., Iyaomolere A. I.: 'Evaluation of the influence of salt treatment on the structure of pyrolyzed periwinkle shell', *J. Appl. Sci. Environ. Manage.*, 17 (2), 321-327, 2013
18. Paul H. L., Antunes A. P. M., Covington A. D., Evans P., Phillips P. S.: 'Bangladeshi Leather Industry: An Overview of Recent Sustainable Developments', *J. Society Leather Technol. Chem.*, 97 (1), 25-32, 2013
19. Reffas A., Bernardet V., David B., Reinert L., Lehocine M.B., Dubois M., Batisse N., Duclaux L.: 'Carbons prepared from coffee grounds by H₃PO₄ activation: characterization and adsorption of methylene blue and Nylosan red N-2RBL', *J. Hazard. Mater.*, 175 (1-3), 779-788, 2010
20. Rengaraj S., Joo C. K., Kim Y., Yi J.: 'Kinetics of removal of chromium from water and electronic process wastewater by ion exchange resins: 1200H, 1500H and IRN97H', *J. Hazard Mater.*, 102, 257-275, 2003
21. Santra A.K., Pal T.K., Datta S.: 'Removal of metanil yellow from its aqueous solution by fly ash and activated carbon produced from different sources', *Separ. Sci. Technol*, 43 (6), 1434-1458, 2008
22. Society of Leather Technologist and Chemists, *Official Methods of Analysis*. Northampton, UK, 1996
23. Sundar V. J., Rao J. R., Muralidharan C.: 'Cleaner chrome tanning—emerging options', *J. cleaner production*, 10, 69-74, 2002
24. UNIDO, *Environmental impact assessment (EIA) on the industrial activities at Hazaribagh area, Dhaka Project-US/RAS/97/137-EIA, Final Report*, Government of Bangladesh and United Nations Industrial Development Organization, Vienna, Austria, 2000
25. Zhou X., Korenaga T., Takahashi T., Moriwake T., Shinoda S.: 'A process monitoring/controlling system for the treatment of wastewater containing chromium (VI)', *Water Res.*, 27, 1049-1054, 1995

SUSTAINABLE TANNERY EFFLUENT TREATMENT SYSTEM WITH TDS MANAGEMENT

Dr. S. Rajamani¹

*Chairman-Asian International Union of Environment (AIUE) Commission,
Old No. 18, New No. 45, First Street, South Beach Avenue, MRC Nagar, Chennai-600028, India,
Mobile : +91 9840063210*

Corresponding author: dr.s.rajamani@gmail.com

Abstract. Sustainable tannery effluent treatment system in achieving required discharge standards including Total Dissolved Solids (TDS) is one of the major challenges faced by the World Leather Industry. Conventional treatment system reduces Biochemical Oxygen Demand (BOD), Chemical Oxygen Demand (COD), Suspended Solids (SS), heavy metals etc. and not the TDS and salinity. To achieve the TDS level, the tanneries in South India were forced to adopt Zero Liquid Discharge (ZLD) system by incorporating Reverse Osmosis (RO) system and Multiple Effect Evaporator (MEE). Though recovery of water is beneficial to certain extent in adopting ZLD system, the major challenges are high energy consumption, huge operation & maintenance cost and no safe disposal method for large quantity of mixed/contaminated salt generated from MEE. In view of the challenges faced in adoption of ZLD system, sustainable major technological developments have been made to control more than 50% of TDS in the effluent by adopting cleaner tanning process, segregation of saline streams, treatment and recovery of chromium and salt for reuse by the member units. The balance composited waste stream with low TDS is further treated and taken for mixing/dilution with treated domestic sewage to achieve all discharge standards including TDS. This development is being implemented in many tannery clusters in India such as Pallavaram in South India and Jajmau, Unnao, Banthar, etc. in North India. The Common Effluent Treatment Plants (CETPs) are being upgraded with financial support from Govt. of India and respective State Governments.

Key words: Tannery effluent, Chromium, ZLD, CETPs, Water recovery

1 Introduction

Conventional treatment system reduces Biochemical Oxygen Demand (BOD), Chemical Oxygen Demand (COD), Suspended Solids (SS), heavy metals etc. and not the Total Dissolved Solids (TDS) and salinity. The TDS limit in the discharge standard is being enforced in India and other parts of the world depending upon the final mode of disposal.

There are limitations for mixing/dilution of the treated industrial effluent with domestic sewage to achieve all discharge standards where required quantity of treated domestic sewage is not available. Hence the tanneries in land locked locations such as North Arcot in Tamilnadu were forced to adopt Zero Liquid Discharge (ZLD) system. For achieving ZLD system incorporation of energy intensive membrane system for water recovery and thermal evaporation for the management of saline reject generated from the Reverse Osmosis (RO) system is required. Though the recovery of water is beneficial to certain extent in adopting ZLD system, the major challenges are high energy consumption, huge operation & maintenance cost and no safe disposal method for large quantity of mixed/contaminated salt generated from the Multiple Effect Evaporators (MEE). The life of the membrane system, MEE and other monitoring systems are less than 3 to 5 years and require frequent replacements with huge investment.

In view of the challenges faced in adoption of ZLD system, sustainable major technological developments have been made to control more than 50% of TDS in the effluent by adopting cleaner process, segregation of saline streams, treatment and recovery of chromium and salt for reuse by the member units. The balance composited waste stream with low TDS is further treated and taken for mixing/dilution with treated domestic sewage in a feasible level to achieve all discharge standards including TDS. This development is being implemented in many tannery clusters in India. The upgradation of Common Effluent Treatment Plants (CETPs) is being implemented with a financial outlay of more than 200 million US Dollar. The Govt. of India, Department of Industry Policy and Promotion (DIPP), National Mission for Clean Ganga (NMCG) and respective State Governments provide major contributions to the tune of more than 150 million US Dollars.

2 Sustainable option for TDS Management and Salinity

In general, the treated tannery effluent is mixed/diluted with treated domestic sewage or discharged into backwaters/Sea, wherever feasible for managing the TDS aspects. The Pollution Control authorities in South India insisted upon ZLD scheme incorporating membrane system for water recovery and evaporation for saline reject from RO system. Accordingly, nearly 10 CETPs in Leather Sector implemented the ZLD projects incorporating membrane system and MEE with huge investment of more than Rs.600.00 crores (i.e. about 100 million USD) with financial support from DIPP, Govt. of India and respective State Government during the period 2008-2015. The major challenges in adopting ZLD system are high energy consumption, huge operation & maintenance cost which is in the range of Indian Rupees 400 to 500 per m³ (i.e. 6 to 8 US Dollars per m³) without the depreciation cost. There is no viable solution for safe disposal of the mixed / contaminated salt generated and accumulated in the CETPs. In addition to this within 5-6 years of the ZLD implementation, the CETPs are faced with replacement of membranes and MEE. For this purpose, the CETPs are seeking once again financial support from Govt. of India and State Govts. In technological angle, the performance of membrane system and MEE are not matching the design parameters in the field conditions. The ZLD system especially the MEE installed was not suitable in some of the CETPs where the member tanneries adopt semi-finish to finishing operations.

To overcome the technical challenges in ZLD system, disposal of large amount of hazardous category sludge from the treatment system and to achieve sustainable option for TDS management the following technological upgradations have been designed and are being implemented in the CETPs located in Pallavaram (South India), Jajmau, Banthar & Unnao (North India).

- Adoption of cleaner production, integrated chrome tanning process, etc. to reduce the TDS and pollutional load at source
- Two stage biological treatment with improved aeration using jet aspirators
- Minimize the chemical usage by 60-70% which results in reduction of sludge generation
- Tertiary treatment including low pressure membrane system (Ultrafiltration/MBR) for removal of residual suspended solids and turbidity.

3 Segregation of Streams and Cleaner Production

For sustainable TDS management, adoption of cleaner productions practices such as desalting, segregation of spent chrome liquor for chrome recovery, etc. are being practiced in tanneries. The balance composited stream with low TDS is collected separately for treatment in the CETP and discharged the treated effluent in to public sewer or mix with treated sewage for managing the TDS are proposed to be followed in some of the locations such as Dindigul, Pallavaram & Uttarpradesh in India similar to the practices adopted in other international locations such as Italy, Spain, etc. Alternatively, the treated effluent can be discharged into sea or back water wherever feasible (i.e. Kolkata Leather Complex and Nellore Leather Complex in India, Istanbul and Izmir in Turkey, Italy etc.) for TDS management.

The limitations in the technologies to adopt ZLD concept has been taken in to account in designing and adopting future systems for TDS management in the upgradation plan of CETPs.

The following technological developments are being implemented in tanneries connected to the CETPs:

- Collection of segregated saline soak liquor as per the directions of pollution control authorities to control TDS and conveyance through separate line to CETP.
- Adoption of Cleaner production technologies such as desalting of hides and skins at individual tannery or by providing common facility with special equipments for the use of all the units.
- Improved chrome recovery system and recovery of chromium in the form of cake for reuse.

The segregated spent chrome liquor from tanneries is collected through special tankers fitted with Global Positioning System (GPS) to the Common Chrome Recovery System (CCRS) established as a central facility for the cluster of tanneries. The spent chromium is pass through screens and pH level is increased to more than 8 by adding sodium hydroxide solution in the main reactor. The chromium is precipitated in the reactor and settled as sludge in the bottom of the reactor. The supernatant with high TDS (i.e. 30000-40000mg/l) which is free from chromium is separated and further treated by using Dual Media Filter (DMF) and membrane system for reuse in the pickling process.

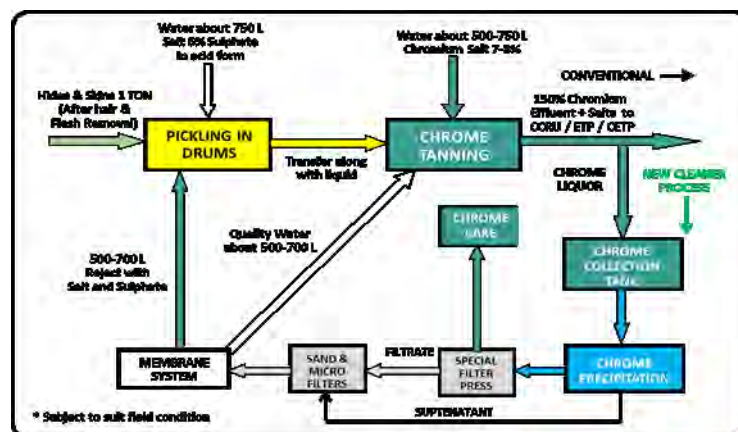


Fig. 1. Improved Common Chrome Recovery System (CCRS)

The chrome slurry is collected in the bottom of the reactor and passes through chamber filter press. The chromium is recovered in the form of cake and disposed to the authorized vendors for further process and distributed in the form Basic Chromium Sulphate (BCS) to the tanneries. The CCRS is becoming popular and is being implemented in many tannery clusters in India.

4 Upgradation and Modified Treatment Systems

4.1 Treatment of saline soak stream and recovery of water and reusable salt

The segregation of saline soak stream, separate physiochemical and biological treatment and further adoption of membrane system, partial reuse of saline stream for pickling and separation of salt using MEE for obtaining quality salt has been successfully developed in pilot scale. The following sustainable upgradations are being implemented in many tannery clusters in India.

A separate wastewater collection line has been being provided for saline soak stream from individual tanneries to the CETP. The composited streams excluding soak and chrome are continued to be collected in the existing conveyance system.

A separate centralized treatment system is established with two stage biological treatment, membrane system and TDS management including recovery of quality salt. The quality water is recovered using RO system and reused in the tanning process. The concentrated saline stream is used partly for pickling process and the balance stream is passed through MEE to recover quality salt. The salt with 99% purity is sold for industrial uses. The process flow diagram of saline stream treatment for sustainable TDS management is shown below:

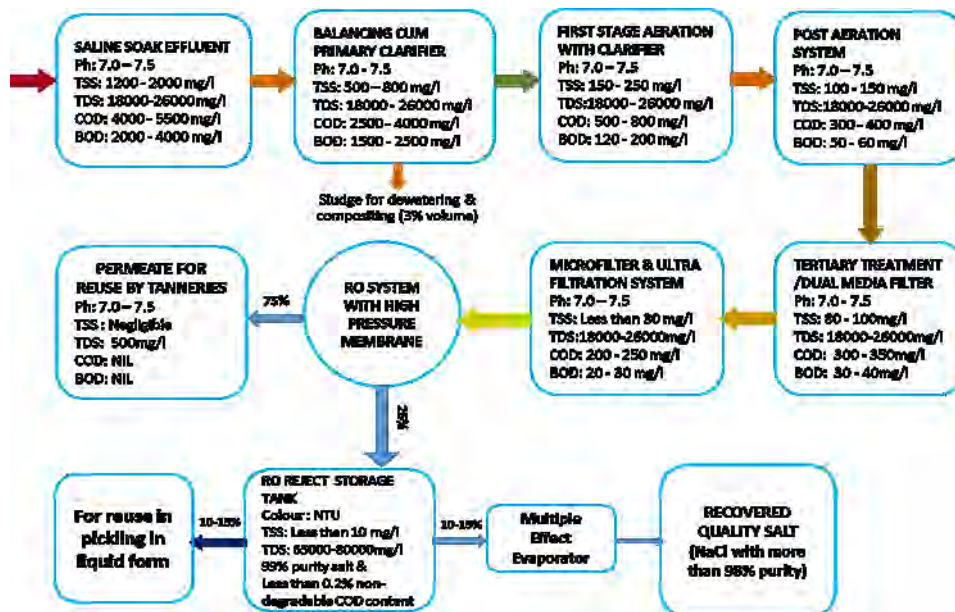


Fig. 2. Treatment flow chart – Saline Soak Stream

The separate treatment of saline soak stream and successful recovery of water and quality salt which is being implemented in tannery clusters of India would become a sustainable ZLD system and first of its kind in the world.

4.2 Sustainable TDS management of composite stream excluding soak and chrome liquor

The TDS of the combined streams is reduced from about 15000mg/l to less than 8000mg/l by segregation and separate treatment of soak and chrome liquor. The upgradation of biological and tertiary treatment units for the combined stream with low TDS at the CETP is done by utilizing the existing treatment units.

The tertiary treatment systems including microfilters, UF units etc. have been incorporated for achieving the prescribed parameters except TDS. The treated effluent is being conveyed and mixed/diluted with treated effluent from slaughter houses and treated domestic wastewater generated from the nearby area to achieve the TDS level within 2100mg/l and meeting all discharge parameters.

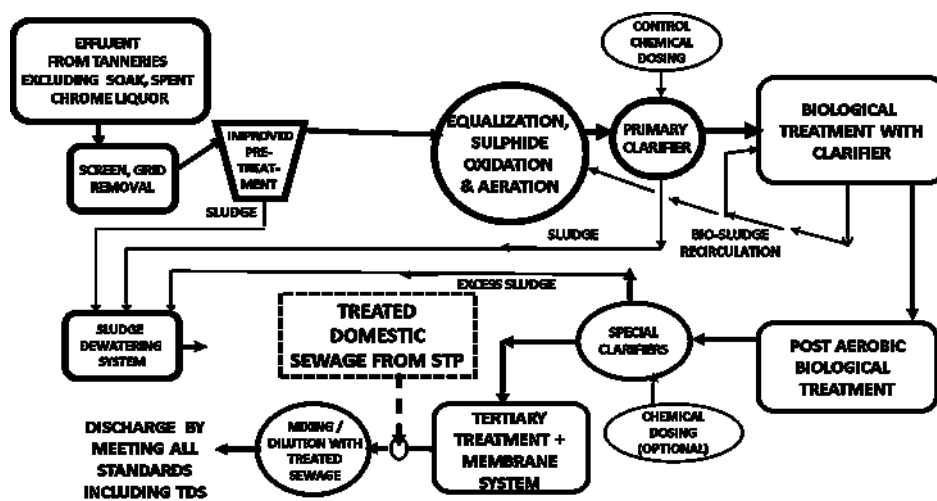


Fig. 3. Process flow diagram for upgradation of CETP – Dilution/Mixing with treated domestic sewage for TDS management and disposal

The upgradation projects are under implementation in many tannery clusters with financial support from Govt. of India and respective State Governments.

5 Improved Marine Disposal of Treated Saline Effluent

A novel technological development has been made for the drawl of Seawater of 30,000m³/day from nearby Sea for the desalination plant integrated with a major leather complex in South India. Out of the total water quantity, freshwater of about 10,000m³/day will be generated and the remaining 20,000m³/day will be discharged into sea with special bio-control and dispersion system to safe guard the aquatic life. The leather complex will be using the quality water generated by desalination plant for its process requirements. About 9,000m³/day wastewater generated from the tannery units will be collected and treated in the centralized treatment plant. The treated effluent is mixed with saline reject of the desalination plant, stored in a water tight pond for a capacity of about 10 days and discharged into the Sea by laying 5 km pipeline using high pressure HDPE pipe and special sprinkling system. The combined treated saline stream with a quantity of about 29,000m³/day will be discharged once in a week under the overall control of environmental protection authorities.



Fig. 4. Treated effluent discharge – Improved mode of disposal into Sea

With the support of many National Institutes and other organizations, model studies were carried out in finalizing the novel marine outfall. The spreading of an effluent cloud released in a marine environment is governed by advection caused by large scale water movements and diffusion caused by comparatively small scale random and irregular movements without causing any net transport of water. Hence, the important physical properties governing the rate of dilution of an effluent cloud in coastal waters are bathymetry, tides, currents, circulation and stratification.

A five port diffuser systems with 0.18 m diameter is planned with a jet velocity of 2.5 m/sec, for the release of treated effluents and reject water from the proposed desalination plant. The Environmental Clearance (EC) has been accorded to this unique integrated project with water recovery using desalination process, industrial wastewater treatment, novel and safe saline reject disposal into Sea without affecting the marine life which is first of its kind in India.

6 Acknowledgement

- The contributions of Asian International Union of Environment (AIUE) Commission with 30 representatives from 20 countries, UNIDO, European Union are acknowledged.
- Acknowledgment is made for technical assistance by UNIDO, Vienna and RePO, Chennai. The contributions of CSIR-CLRI Environmental Technology Dept., KPILC, IL&FS Cluster are greatly acknowledged.
- Acknowledgement is made for DIPP, NMCG for rendering assistance for implementation and upgradation of tannery sector CETPs. The contributions of Government of India, Govt. of Tamilnadu, UP, West Bengal, Punjab, CLE, CII and Industry Associations are acknowledged.

7 References

1. Alemu, T., Lemma, E., Mekonnen, A., Leta, S., 2016, *Environ. Process*, 3, 815–827.
2. S. Rajamani, IULTCS Congress, Novo Humbargo, Brazil - 2015.
3. Zhang, C., Xia, F., Long, J., Peng, B., 2017, *Journal of Cleaner Production*, 154, 276-283.
4. S. Rajamani, IAFLI 2017, Ismir, Turkey – 2017.
5. S. Rajamani, ZLD Concept, *Leather Age* – 2016.
6. Zhang, C., Lina, J., Jia, X., Peng, B., 2016, *Journal of Cleaner Production*, 1055-1063.
7. S. Rajamani, AICLST 2018, Xian, China – 2018.
8. S. Rajamani, TDS Management, *Indian Leather-2018*.

LIFE GOAST GREEN ORGANIC AGENTS FOR SUSTAINABLE TANNERIES (LIFE16 ENV/IT/000416)

R. Pasquale¹, C. Bortolati^{1a}, F. Serafini¹, M. Signoretto³, S. Tieuli³, M. Silvestri², L. Frighetto,² L. Culpo⁴, E. Mistrorigo⁴, E. Pivetti⁴

1 GSC GROUP SPA, Montebello Vic.no, Italy, 2 PASUBIO SPA, Arzignano, Italy, 3 Università Ca' Foscari- Venezia, Dipartimento di Scienze Molecolari e Nanosistemi, Venezia, Italy, 4 MEDIO CHIAMPO S.P.A., Montebello Vic.no, Italy; a) Corresponding author: claudiobortolati@gscspa.it .

Abstract. LIFE GOAST Green Organic Agents for Sustainable Tanneries (LIFE ENV/IT/000416) belongs to European LIFE programme which supports and promotes the research and innovation on environmental and sustainability topics. The project started on July 2017 and is an ongoing investigation, and involves the competences of three direct actors in the leather industry such as GSC Group spa as chemical supplier, Conceria Pasubio as tannery and Mediochiampo as waste-water treatment agency, in conjunction with the expertise of Università 'Ca Foscari di Venezia. It aims at demonstrating the benefits of a new tanning technology on a semi-industrial scale, particularly focusing at the tanning stage of the leather manufacture, and put itself as a more sustainable alternative to Traditional Chrome Tanning Process (TCTP). The technical feasibility of LIFE GOAST implementation, as well as its social and economic impact, have been monitored and compared with the TCTP in order to demonstrate the reduced environmental impacts of the new process, while producing comparable or better quality leather. It was then demonstrated that it was possible to treat collagen with the GOAST technology to give stabilised collagen to be used in the leather industry. A series of leather swatches were realised according to the new protocol in order to obtain preliminary information on chemical oxygen demand COD of the effluents and technical feasibility of the process. The results were remarkable: the collected waste-water generated from tanning and retanning showed COD values in line with TCTP and it was possible to obtain soft and firm grain leather despite a shrinkage temperature lower than chromium process.

Keywords: Clean technology, water quality, hazardous substance, tanning, sustainability.

1 Introduction

Leather manufacturing is classified as water, energy and waste intensive by the Industrial Emissions Directive (2010/75/EU); it requires the combination of different physical and mechanical actions and the utilisation of various chemical substances, which range from simple inorganic salts to more complex organic substances and polymers. As a consequence, both such elements and tannery effluents generated, could cause significant damage to soil and water bodies, and therefore could lead to safety and environmental concerns, if not properly used and/or treated respectively.

The European IPPC Bureau report 2013 states that at present over 85 % (w/w) of the world leather production is chrome tanned and only a minor part is manufactured with alternative processes. Worldwide, shoe leathers (uppers and linings) are the dominant leather types, although upholstery leather, especially automotive leather, is winning an increasing market share (see the Distretto Vicentino della Pelle in the Arzignano area of Veneto, Italy). An estimated 7×10^6 t of hides and skins containing about 2.8×10^6 t of collagen are used yearly worldwide for leather production, although, unfortunately, due to technical reasons only 50 % of the hide collagen is converted into leather (Buljan, Reich, & Ludvík, 1998). The loss of water by samming, loss of collagen due the shaving processes influence the overall low yield of the leather manufacture; the focus of the tanning is clearly to stabilise and preserve the collagen, but also to reduce the thickness of the leather article, which is in relationship with the remarkable mass loss. (Reich, Die Nutzung von Kollagen außerhalb der Lederindustrie, Teil I: Allgemeines und Einsatzgebiete mit hoher, 1995). Therefore, there is an important waste of material which needs to be recovered within the process.

Furthermore, the current use of chrome poses serious environmental and health problems due to the potential formation of carcinogenic Cr (VI) in finished articles, prompting users to find innovative solutions. Table 1 summarises the chemicals and water balance required for the production of approximately 1000 m² of chrome-tanned shoe upper leather, (Buljan, Reich, & Ludvík, 1998) whilst Table 2 provides the quantities of the most important chemicals (as general class) used for the leather production per annum. (Taeger, 2003) Table 1 is a dated insight and could not perfectly fit with the present parameters, especially with respect to the inorganic and organic acids and the sodium sulphide quantities, which should be increased to 60 and 275 kg respectively. It is noteworthy that the most used chemicals in the leather tanning are water, chromium salts and inorganic salts, and therefore their utilisation should be revised and/or improved in order to give a more sustainable industrial process.

LIFE GOAST implementation aims:

1. to produce *free of chrome* (FOC) high quality leather articles achieved by unprecedented pilot scale implementation of LIFE GOAST.
2. to improve the quality of tannery effluents by total reduction of chromium salts, acids/bases sodium chloride in tanning and retanning steps, since no chrome, nor pickling (acid treatment) or basification, typically foreseen when chromium is used;
3. to demonstrate lower environmental impact of LIFE GOAST technology in terms of reduction of hazardous substances, environmental risks (human and ecological), primary resource consumption (water) due to simplification/reduction of industrial steps to process hides, according with the 7th Environment Action Programme, and environmental releases in water and soil;
4. to eliminate/reduce the chrome containing sludge.

The project started on July 2017 and is an ongoing investigation: at present, the entire team is working with respect of the optimisation of the leather production through the LIFE GOAST technology and the re-utilisation/recycle of the aqueous waste generated throughout the consequently tanning and retanning steps. Herein, it will be summarized and described the achievements obtained during the implementation.

Table 1. Approximate demand for water and chemicals to produce 1000 m² of chrome-tanned grain leather (ca. 7.1 t of wet salted hide) and as by-product 430 m² of split leather from cattle hide

Substance	Quantity (kg unless otherwise stated)
Water	215.000
Inorganic salts (NaCl)	570
Inorganic and organic acids	30
Sodium sulphide	175
Calcium hydroxide	285
Enzymes	20
Bactericides	20
Tensides	20
Chrome extracts (Cr ₂ O ₃)	700 (175)
Vegetable tannins	50
Synthetic tannins	50
Polymers	50
Resins	10
Fatliquors	150
Dyestuffs	35
Polymer binders (finishing)	30

Table 2. Quantities of the most important leather chemicals used for world leather production in 2000.

Substance	Quantity, 10 ³ t/y (unless otherwise stated)
Water	320 x 10 ⁶ m ³
Tensides	120
Lime hydrate	300
Sodium sulphide	200
Sodium chloride	270
Chrome extracts (Cr ₂ O ₃)	1.600
Vegetable tannins	300
Aromatic syntans	150
Glutaraldehyde	30
Resins	30
Polymers	150
Lubricating agents	400
Dyestuffs	90
Polymer binder	200

2 Materials and Methods

The leather auxiliaries involved in the project implementation were provided and produced by *GSC Group spa* and used either at *GSC Group spa* or *Conceria Pasubio* facilities.

The leather used for the trials and the entire project implementation was purchased from *Conceria Pasubio* and used either by *GSC Groups spa* or *Conceria Pasubio* at their facilities.

Leather tests were carried out by *Conceria Pasubio*; thickness measurements were carried according to ISO 2589 using IG/MS (CD-6'') from *Giuliani Technologie*. Tear strength (traction), elongation at break of leather (%), elongation at specified load (100 N) were performed according to ISO 3376 using a dynamometer LR 5K from *Lloyd Instrument*. Single edge tear was carried out according to ISO 3377-1 using the previous described dynamometer. Leather softness was performed following ISO 17235 with a softness tester /ST300D from *MSA Engineering*. Gravimetric fogging was carried out according to ISO 17071 with a PC201-FTS (heating) combined with ACCEL250 (cooling) system from *Thermo Scientific*. Reflectometric fogging was carried out with the same devices, although the measurement was performed with a glossmeter MICROTRIGLOSS from *BYK*. Heat resistance was performed in a heating over FD115 from *Binder*.

Soluble chemical oxygen demand (COD) was monitored and assessed to obtain information on the fixation grade of the chemicals applied in the tanning and retanning tests. COD was determined by LCK 014 and LCK 914 kit analysis in combination with HT 200S as digesting system and DR3800 as spectrometer from *Hach Lange*. The COD values were calculated after filtration of the aqueous solution using filtering paper grade *IF5H*.

Shrinkage temperature was assessed either *via* SHRINKAGE TG TESTER by *Giuliani*.

Analytical gas chromatography for VDA 277 was performed on a GC7820A instrument from *Agilent Technologies* with a FID detector using a DB-WAX UI capillary column (30 m x 0.25 mm i.d.) and helium as carrier gas. Static headspace analyses were carried out using a 7687 headspace sampler from *Agilent Technologies*. Alternatively, analytical gas chromatography was performed on a CLARUS 580 instrument from Perkin Elmer with a SQ8 S detector (EI) using an ELITE-624 MS capillary column (30 mt x 0.25 mm i.d.) and hydrogen as carrier gas. Static headspace analyses were carried out using a TURBOMATRIX HS 40 TRAP from Perkin Elmer, using hydrogen as carrier gas.

Leather shavings were analysed by *Università 'Ca Foscari di Venezia* within the LIFE GOAST implementation and were generated after the leather tanning of at least one entire bovine hide.

Waste-water was analysed by *Medio Chiampo* and *Università 'Ca Foscari di Venezia* in the event of leather tanning and retanning of at least one entire bovine hide.

Metals screening was carried out using MP-AES 4210 by *Agilent Technologies* after microwave-assisted dissolution of waste-water samples by *CEM Discover SP-D*. In the digestion procedure, 2 mL of each samples were mixed with 4 mL concentrated nitric acid and 1 mL oxygen peroxide in the system specific quartz reactor. The digestion lasted for a total of 15 min at 170°C under stirring. After cooling the sample solutions were transferred to 25 mL flask and diluted with *Milli-Q water*. Then, the metals analysis was performed on the samples diluted to 100 times. The viewing position and nebulizer flow for the MP-AES were optimized before each run. The selected elements and the corresponding wavelengths are given in **Table 3**.

Table 3. Elements and the corresponding wavelengths.

Element	Wavelengths (nm)
Ag	328.068
Al	396.152
Cd	228.802
Co	345.351
Cr	425.433
Cu	324.754
Fe	371.993
Mn	403.076
Ni	361.939
Pb	405.781
Tl	535.046

3 Results and Discussion

3.1 Production of the tanning agents

The tanning agents were developed and produced by the R&D of GSC Group spa and are based on polymeric functionalised acrylic polymers in combinations with synthetic tannins, and are part of an unprecedented research. LIFE GOAST tanning agents belong to acrylic polymers category that could be obtained either via aqueous and/or in-solvent radical polymerization of the appropriate allyl, acrylic, vinyl, methacrylic monomers. Furthermore, chemical functionalization of these species improved the polymer interaction with the collagen in a covalent fashion, to produce a pelt with remarkable physical and chemical properties. An appropriate laboratory protocol for the production was elaborated, and consistent results within the trials were obtained. The scaling-up process from lab-scale to semi-industrial scale is currently in progress; despite our implementation produced different species of polymers, it was decided to focus on a single version of the polymer, since it produced remarkable results in terms of tanning properties. So, this summary will concentrate on the utilisation of the **GOAST TANNING AGENT 8555/1**, which was produced and characterised between 2017-18; the tanning agent is a white dispersion of resin in water with 50% dry residue and approximately pH 4.00.

3.2 Production and characterization of leather articles

Before the actual tannage, the hides and skins were prepared following the standard procedure for the TCTP. LIFE GOAST technology aims at substitute the chrome tannage, and therefore it inserts perfectly within the standard procedure. The LIFE GOAST tanning protocols consist on a series of

mechanical and chemical actions performed on the raw hide to give tanned leather (see **Table 4**, **Table 5**, **Table 6** and **Table 7** as examples).

The mechanical action performed consisted in rotation of the tanning drum and the heating of the vessel, whilst, the chemical actions consisted of the addition of the chemicals (tanning agents), pH adjustment via addition of bases (sodium bicarbonate) or weak acids (formic acids).

After the tanning step, the hides were sammed to get rid of the excess of water and shaved, followed by retannage. It is important to underline that the leather shavings constitute an important by-product of the tannage process, and also of the LIFE GOAST technology; however, our team is currently investigating at the revaluation of the shavings to give novel and less environmental impacting products (see 3.4). Finally, the hides were retanned with a specially developed procedure. Herein, specifications and data related to several experiments carried out during the investigation are reported; the given examples focus on car-interior leather production. **Table 4**, **Table 5** and **Table 6** depict typical procedures for the LIFE GOAST tanning technology; water is still unfortunately the most abundant chemical used in the process, as it is found in TCTP, although preliminary calculations showed that water is slightly less impacting for LIFE GOAST than in TCTP (this investigation is still in progress) Such examples led to a white-brownish leather which exhibited a shrinkage temperature between 70°C to 75°C right after the tannage; the tanning floats showed COD between 20000 mg O₂/l to 60000 mg O₂/l, depending on the combination of tanning and the GOAST TANNING AGENT 8555/1 concentration. It is important to underline that the processed hides were easily shaved to 1.0 to 1.2 mm thickness, to get the intermediate to be retanned as reported in **Table 7**.

Table 4. LIFE GOAST tanning procedure example #1

Articolo/Article:		LIFE GOAST TANNING EXAMPLE 1				
Tipo pelle/Type of Leather:		Bovine Hide		Spessore/Thyckness:		
				Peso/Weight [g]:		20.000
Operatore/Operator:						
%	Prodotti Products	Quantità Q.ty [g]	Temp. [°C]	Tempo Time	pH	Operazione Operation
100,00%	WATER		30°C			
9,00%	NaCl			20'		6/7 Bè
2,50%	GOAST TANNING AGENT 8555/1			120'		
6,00%	SYNTAN 01					
12,00%	SYNTAN 02			180'	3	
0,20%	SODIUM BICARBONATE			30'		
0,20%	SODIUM BICARBONATE			30'		
0,20%	SODIUM BICARBONATE			30'		
0,10%	SODIUM BICARBONATE			30'	4	
						SLOW, AUTOMATIC
	DAY AFTER				3.8	DRAIN WASH
150,00%	WATER		20°C			
0,50%	OXALIC ACID			30'		SCARICARE
NOTE						

The application and the use of the products are beyond our control and they shall be exclusively on the customer's responsibility.

Table 5. LIFE GOAST tanning procedure example #2

Articolo/Article:		LIFE GOAST TANNING EXAMPLE 2				
Tipo pelle/Type of Leather:		Bovine Hide		Spessore/Thyckness:		
				Peso/Weight [g]: 20.000		
Operatore/Operator:						
%	Prodotti Products	Quantità Q.ty [g]	Temp. [°C]	Tempo Time	pH	Operazione Operation
100,00%	WATER		30°C			
9,00%	NaCl			20'		6/7 Bè
3,25%	GOAST TANNING AGENT 8555/1			120'		
7,00%	SYNTAN 01					
10,00%	SYNTAN 02				3	
1,00%	SYNTAN 03			180'		
0,20%	SODIUM BICARBONATE			30'		
0,20%	SODIUM BICARBONATE			30'		
0,10%	SODIUM BICARBONATE			30'	4	
						SLOW, AUTOMATIC
	DAY AFTER				3.8	DRAIN WASH
150,00%	WATER		20°C			
0,50%	OXALIC ACID			30'		SCARICARE
NOTE						

The application and the use of the products are beyond our control and they shall be exclusively on the customer's responsibility.

Table 6. LIFE GOAST tanning procedure example #3

Articolo/Article:		LIFE GOAST TANNING EXAMPLE 3				
Tipo pelle/Type of Leather:		Bovine Hide		Spessore/Thyckness:		
				Peso/Weight [g]: 20.000		
Operatore/Operator:						
%	Prodotti Products	Quantità Q.ty [g]	Temp. [°C]	Tempo Time	pH	Operazione Operation
100,00%	WATER		30°C			
9,00%	NaCl			20'		6/7 Bè
5,00%	GOAST TANNING AGENT 8555/1			120'		
9,00%	SYNTAN 01					
9,00%	SYNTAN 02			180'	3	
0,20%	SODIUM BICARBONATE			30'		
0,20%	SODIUM BICARBONATE			30'		
0,10%	SODIUM BICARBONATE			30'	4	
						SLOW, AUTOMATIC
	DAY AFTER				3.8	DRAIN WASH

150,00%	WATER		20°C		
0.50%	OXALIC ACID			30'	SCARICARE
NOTE					

The application and the use of the products are beyond our control and they shall be exclusively on the customer's responsibility.

Table 7. LIFE GOAST retanning procedure car interior example #1

Articolo/Article:		CAR INTERIOR 1				
Tipo pelle/Type of Leather:		Tanned Bovide Hide from LIFE GOAST	Spessore/Thyckness:		1,1/1,2	
			Peso/Weight [g]:		7.000	
Operatore/Operator:						
%	Prodotti Products	Quantità Q.ty [g]	Temp. [°C]	Tempo Time	pH	Operazione Operation
200,00%	WATER	14.000	30°C			
0,50%	OXALIC ACID	35,0				
0,50%	SURFACTAN 1	35,0		60'		DRAIN WASH
		0,0				
100,00%	WATER	7.000	30°C			
1,00%	SODIUM ACETATE	70,0		60'	4	DRAIN WASH
		0,0				
100,00%	WATER	7.000	30°C			
1,00%	FATLIQUOR 1	70,0				
3,00%	FATLIQUOR 2	210,0		60'		
16,00%	SYNTAN 1	1.120,0				
6,00%	VEGETABLE TANNIN 1	420,0				
6,00%	SYNTAN 2	420,0		30'		
2,00%	FATLIQUOR 1	140,0		10'		
16,00%	SYNTAN 1	1,120.0				
7,00%	VEGETABLE TANNIN 1	490,0		90'		SLOW, OVERNIGHT
	DAY AFTER	0.0				
200,00%	WATER	14.000,0	50°C			
1,00%	FORMIC ACID	70,0		10'		
1,50%	FORMIC ACID	105,0		30'		COD 41900 mg O2/l
		0.0				DRAIN
150,00%	WATER	10.500,0	50°C			
5,00%	FATLIQUOR 2	350,0				
4,00%	FATLIQUOR 1	280.0		60'		
1,00%	FORMIC ACID	70.0		10'		
0,50%	Al2(SO4)3	35.0		60'		COD 28000 mg O2/l
		0.0				DRAIN
150.00%	WATER	10,500.0	50°C			DRAIN

			0.0						
200,00%	WATER		14.000,0	20°C	10'		DRAIN		
200,00%	WATER		14.000,0	20°C					
0,30%	OXALIC ACID		21,0						
NOTE	VACUUM 40°								
<i>The application and the use of the products are beyond our control and they shall be exclusively on the customer's responsibility.</i>									

It is then summarised a series of analyses and test-results for the characterisation of the retanned LIFE GOAST leather obtained with these specially designed protocols, which finalise the achievements accomplished throughout the implementation. The results are yet not fully satisfactory, and do not entirely meet the requirements in order to be correctly processed as car-interior leather (red), although they are still promising (see **Table 8**). It is necessary to underline that these results are referred to the GOAST TANNING-42 which is based on the tanning and retanning procedures reported in **Table 6** and **Table 7** respectively, and potential improvements are hypothesised for the entire process. Difficulties in the delivery of the functionalised polymer were experienced, although with modification at the addition rates and pH they were overcome. The final results were still satisfactory and prompted our investigation for the future leather tanning tests.

Table 8. Summary of the physical and chemical tests run on LIFE GOAST leather.

TEST	METODO	REQUIRED	FOUND
Thickness	ISO 2589	1,2-1,5	1,36 mm
Tear strength (traction)t	ISO 3376	≥130 N (average 3 values)	L=178,15 T=169,00
Elongation at break of leather (%)	ISO 3376	30-70% (average 3 values)	L=45,8 T=34,04
Softness (ST 300)	ISO 17235	3,5-4,5 mm	3,6 mm
Elongation at a specified load (100N)	ISO 3376	8-25% (average 3 values)	L=31,45 T=23,97
Single edge tear	ISO 3377-1	≥25 N average 3 values)	L=16 T=16,37
Gravimetric fogging	ISO 17071	≤ 3,00 mg	2,01 mg
Reflectometric fogging	SAE J1756	≥ 70%	68,25
Heat resistance	(48±1h;80±2°C)	≥ 4 GS	OK
VDA 277		< 100 ppm	76ppm

3.3 Waste-water Analysis from the LIFE GOAST process

Waste water generated through the tanning and retanning implementation were carried out; basic COD and metal content analyses were monitored (see 3.2).

Zahn-Wellens tests were carried out with the waste-water generated from the LIFE GOAST tanning process; this methodology is used to evaluate the potential biodegradability of water-soluble and non-volatile organic substances exposed to relatively high concentrations of microorganisms at static conditions. Furthermore, this study will allow to assess the pattern of use and degradation of carbon within 28 days under controlled pH, temperature and dissolved oxygen conditions by the active biomass coming from the biological reactors in our purification plant. This study is still under investigation, although preliminary results are herein described.

Preliminary investigation on waste-water generated from the tanning and retanning showed that biological degradation stopped at about 70%, thus meaning that an approximately 30% of the soluble carbon is not biodegradable within 28 days (*Fig. 1*). The result was found to be reproducible with two different set of experiments, which were carried out at the beginning of 2018; unfortunately, the results did not show complete degradation, possibly due to non-ideal conditions of degradation (choice of microorganism pool). However, the residual from the biological degradation was found still found to be organic, which led the hypothesis of an easier treatment *via* precipitation, sludge formation and thermal degradation without harmful by-products.

Table 9 reports the content for metal analysis carried out on a tanning and retanning experiment, named **GOAST TANNING-54**; this experiment used the procedure reported in **Table 6** followed by the application of retanning from **Table 7**. Each entry in the first bold column identifies a portion of the generated waste water, which were isolated for the determination; prefixes T and R stands for *tanning* and *retanning* respectively, whilst suffix S stands for SURNATANT. The results of metals analysis showed a low to a negligible amount of metals in the LIFE GOAST tanning liquor. The traces of chrome observed in the tanning water waste could be ascribed to a previously contamination of both tannery drum and used water. In addition to this, general parameters for water analysis were monitored (see **Table 10**). More efficient waste-water treatment is therefore required and is still under investigation.

Table 9. Results of metals analysis of the GOAST-TANNING-54

	Cd (ppm)	Ag (ppm)	Cu (ppb)	Co (ppm)	Pb (ppb)	Mn (ppm)	Cr (ppm)	Tl (ppm)	Ni (ppm)	Fe (ppm)	Al (ppm)
T-T54	n.d	<20 ppb	n.d	n.d	n.d	<20 ppb	4,3	n.d	n.d	-	2,1
T-sT54	n.d	<20 ppb	n.d	n.d	n.d	<20 ppb	4,5	n.d	n.d	-	2,1
R-T54	n.d	2,1	n.d	n.d	n.d	<20 ppb	3,9	n.d	3,7	-	<20 ppb
R-sT54	n.d	2,3	n.d	n.d	n.d	<20 ppb	2,8	n.d	5,3	-	<20 ppb
F-T54	n.d	<20 ppb	n.d	n.d	n.d	<20 ppb	<20 ppb	n.d	1,7	-	6,5
F-sT54	n.d	<20 ppb	n.d	n.d	n.d	<20 ppb	<20 ppb	n.d	2,4	-	6,0

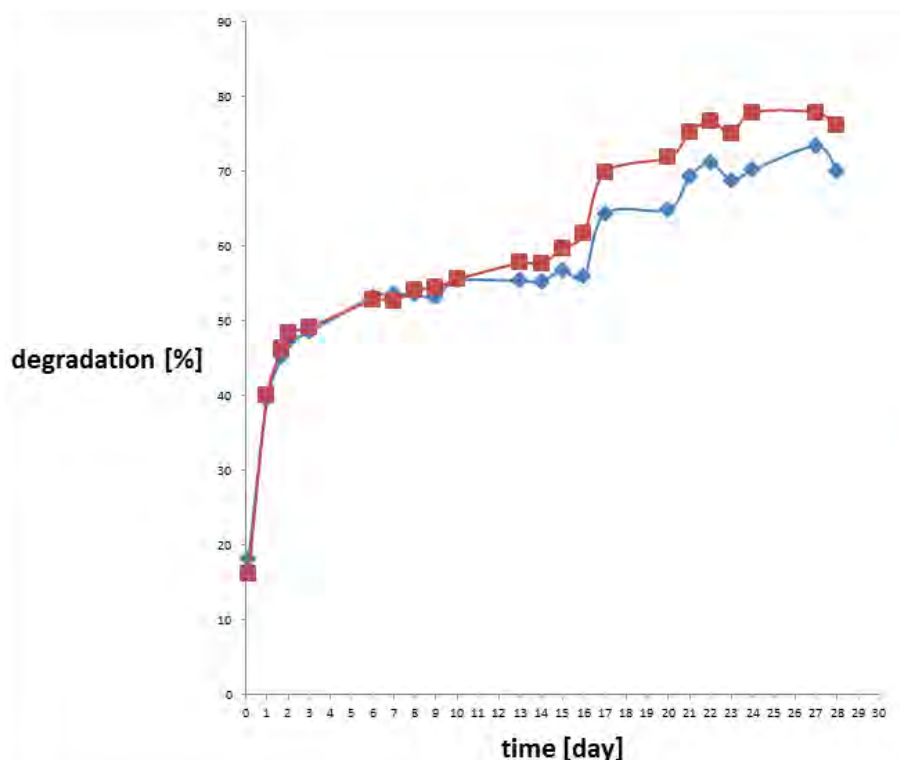


Fig. 1. Biological degradation of two sets of waste water generated from the LIFE GOAST tanning according to Zahn-Wellens tests

Table 10. Water parameters for LIFE GOAST effluent obtained from preliminary study.

Parameter	Waste-water
TKN (mg N/l)	571
COD (mg O ₂ /l)	44000
DOC (mg C/l)	14340
pH	6.28
Ammonia (mg NH ₄ /l)	384
Tn (mg N/l)	441
Chlorides (mg/l)	16574
Sulphates (mg/l)	4101
Nitrates (mg/l)	N.D.
Conductivity (µS/cm)	61000

3.4 Revaluation of the Shavings from the LIFE GOAST Process

Tanning hide into leather is a very complex process, which has a large number of steps and generates substantial quantities of solid and liquid wastes. As reported by Sundar *et al.* (Sundar, Gnanamani, Muralidharan, Chandrababu, & Mandal, 2011) processing of 1000 kg of rawhide produces on an average 200 kg of tanned leather, 450 kg of solid wastes and 50,000 kg of waste water. Therefore, due to this high environmental impact many efforts have been made in recent decades for the treatment of solid wastes from the pre-tanning, tanning and post-tanning processes in the leather industry (Jiang, Liu, & Han, 2016). In this context, pyrolysis could be considered one of the possible approaches for the treatment of solid wastes from the tanning industry.

Leather solid wastes produced by GOAST technology have the advantage of being Cr-free, which can be easier recyclable than chromium-tanned solid wastes. In view of this, an effective and sustainable process for the valorisation of leather waste produced by GOAST technology is under

investigation by Ca'Foscari University. The attention was focused on the enhancement of GOAST shaving waste for the production of "biochar" by pyrolysis and its application as soil improver or fertilizer (Yang , et al., 2016, p. 36:36), (Cha, et al., 2016). This project aims at avaluating the best pyrolysis conditions with the purpose to achieve the right compromise between bio-oil yield and bio-char yield, and to obtain a bio-char with best characteristics and agronomic properties for "soil improver" application. The optimal pyrolysis conditions have been investigated taking into account the effect of different parameters, such as temperature, heating rates, time, grinding size of raw material and inert flow rate, on the characteristics of biochar. In **Fig. 2** it is shown the distribution of the generated fractions (char, condensable and gas fraction) obtained in function of grinding size. The best pyrolysis conditions were found to be 600°C temperature, heating rate 10°C/min, hold temperature for 30 minutes; this process was carried out at 100 mL/min of nitrogen for the laboratory testing.

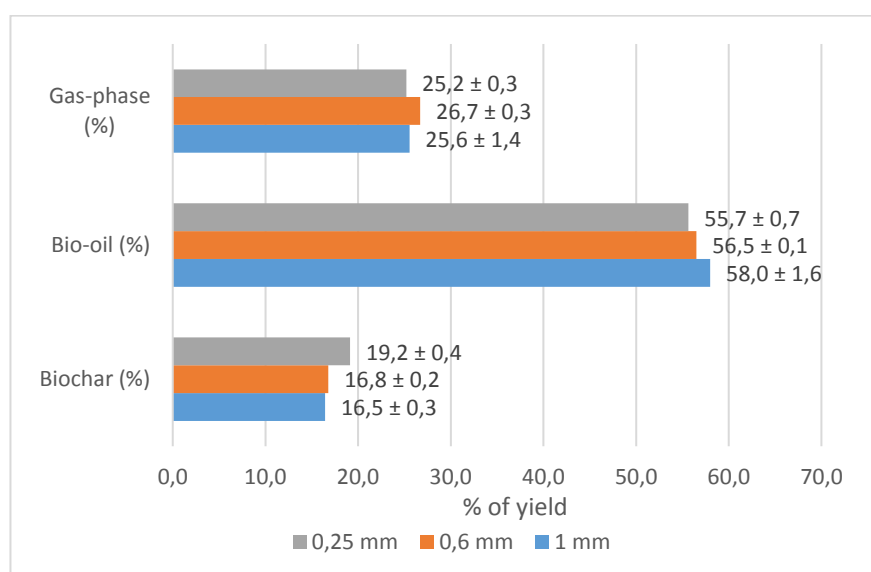


Fig. 2. Yield (%) of the generated fractions (char, condensable and gas fraction) vs grinding size (mm).

4 Conclusions

This investigation showed that LIFE GOAST technology could be used as an alternative to TCTP; despite the results achieved are not entirely satisfactory, LIFE GOAST produces leather is still promising and could lead to a less impacting tanning technology in the near future. LIFE GOAST leather showed a firm grain surface, sufficient softness and low emission (both VOC and medium volatile compounds).

The reported LIFE GOAST procedures for both tanning and retanning (**Table 4, Table 5, Table 6** and **Table 7**) are only examples obtained from the implementation and should not be set as the conclusive guidelines for our investigation. It is expected that by the end of the project, the procedure will be updated and improved in terms of shrinkage temperature and COD and leather performances due to the application of specially-designed leather auxiliaries. It is remarkable that, despite the different nature of the chemistry below LIFE GOAST, such technology could be simply applied within the previous procedure for TCTP, substituting the addition of the chrome salts, to give tanned leather. In addition, the leather auxiliary tested for this implementation in terms of fatliquors and retanning agents are simply the same used in the TCTP, which points out that LIFE

GOAST technology is definitely an alternative to TCTP which is based to a different completely organic-tanning system.

It is noteworthy that crust leather obtained by LIFE GOAST technology showed to be more environmental friendly than the TCTP counterpart, due to the absence of heavy metals in the tanning liquor (easier waste-water treatment) and a reduced contribution to the VOC emission. No chromium-salts were involved in the LIFE GOAST trials, and therefore the consequent waste-water, sludge and leather shavings did not contain this element; however, the investigation of the aqueous waste showed traces of chromium and nickel, although it was believed to be a contamination of the floats. Aluminium was found in the floats, sludge and in the leather shavings, which is in line with the contents from one of the retanning strategies of the leather developed in the investigation. Novel chemical auxiliaries for fatliquoring and retanning will be investigated in the future to improve the retanning stage of the process; in fact, it is believed that the utilisation of standard TCTP auxiliaries could not be suitable for the LIFE GOAST process since the basis of the tanning technology are completely different. Despite the satisfactory results accomplished since the beginning of the implementation, it is believed that the design of special auxiliaries will improve the COD of entire leather process and will lower the water demand.

Despite car-interior leather have highly demanding requirements, LIFE GOAST leather seemed to be suitable for this purpose; the implementation is still in progress, but the technology will be suitable for this application, especially in terms of VOC emission and firm leather.

Future work will be carried out on split leather, in order to include different articles and manufactures. In addition, the implementation on the leather shavings revaluation will be highly important for the project.

5 Acknowledgements

The LIFE GOAST team would like to acknowledge the EC for fundings (LIFE16 ENV/IT/000416) and the single partners for the remarkable job carried out since the beginning of the project. Special thanks should be done to *GSC Group spa, Conceria Pasubio, Medio Chiampo* and *Università 'Ca Foscari di Venezia*.

References

1. Buljan, Reich, & Ludvik. (1998). *Mass Balance in Leather Processing*. *Leder & Häutemarkt*, 4, 30; 5,25.
2. Cha, J., Park, S., Jung, S., Ryu, C., Jeon, J., Shin, Park, Y. (2016). *Production and Utilization of Biochar: A Review*. *Journal of Industrial and Engineering Chemistry*, 1-15.
3. Jiang, H., Liu, J., & Han, W. (2016). *The status and developments of leather solid waste treatment: A mini-review*. *Waste Manag Res.*, 399-408.
4. Reich. (1995). *Die Nutzung von Kollagen außerhalb der Lederindustrie, Teil I: Allgemeines und Einsatzgebiete mit hoher Leder*, 46, 2.
5. Sundar, V., Gnanamani, A., Muralidharan, C., Chandrababu, N., & Mandal, A. (2011). *Recovery and utilization of proteinous wastes of leather making : a review*. *Reviews in Environmental Science and Bio/Technology*, 151-163.
6. Taeger. (2003). *Innovative Chemie für einen alten Rohstoff—Erste Schritte auf dem Weg zur nachhaltigen Lederherstellung*. *Leder & Häute Markt*, 9, 33-38.
7. Yang, D., Yunguo, L., Shaobo, L., Zhongwu, L., Xiaofei, T., Xixian, H., Bohong, Z. (2016). *Biochar to improve soil fertility. A review*. *Agron. Sustain. Dev.*, 36.

A NEW SYSTEM TO MEASURE LEATHER SHRINKAGE TEMPERATURE

J. M. Morera^{1 a)}, B. Esteban¹, G. Baquero¹ and R. Cuadros¹

Department of Computer Science and Industrial Engineering, Universitat de Lleida (UdL), Av Pla de la Massa 8, 08700 Igualada (Spain)

a)Corresponding author: josepmaria.moreira@udl.cat

Abstract. A characteristic of leather is that if it is gradually heated in aqueous solution it reaches a temperature where sudden and irreversible shrinkage occurs (shrinkage temperature). This phenomenon is related to the denaturalization of the collagen protein that conforms the hide and is known as leather shrinkage. Specifically, the internal bonds break thus causing a shortening of the leather that can be up to a 35% from its original length. The method that describes the ISO 3380:2015 standard uses a device where the determination of the shrinkage temperature is performed visually by the laboratory technician. Consequently, the method tends to be imprecise and subjective. It should also be noticed that the device proposed by the standard does not allow differentiation between the different stages of the contraction process. There are other methods to determine leather shrinkage temperature including differential scanning calorimetry, microscopic hot table, thermogravimetric analysis, differential thermal analysis and thermomechanical analysis. All these methods involve complex devices and are only suitable for specialized personnel. In this work, a new device is developed to precisely measure the leather shrinkage temperature and to distinguish the different contraction stages. In addition, the proposed device is simple, easy to use and inexpensive, which facilitates its use in any industry. The developed system consists basically of a load cell to measure the strength produced by the shrinkage of the leather. With the logged data during the test a strength versus temperature graph is built. By means of its interpretation, the different stages of shrinkage can be determined. Different mathematical analysis of the logged data is proposed to determine the shrinkage stages temperatures, thus achieving a high degree of certainty and repeatability.

1 Introduction

One of the most used methods to check the quality of the leather tanning process is the determination of the shrinkage temperature according to the ISO 3380:2015 standard. This method measures the leather shrinkage when constantly increasing the sample temperature. The shrinkage temperature (T_s) corresponds to the temperature when the sample suddenly contracts. The value of this temperature indicates the degree of collagen stability and therefore, when higher, the leather will have better quality and resistance.

The process of leather shrinkage can be divided in different stages. Several authors discriminate temperature A1 (when the first fibre starts to shrinkage), temperature C (when there is a massive shrinkage) and finally temperature A2 (when the last fibres are contracted individually). [2,3]



Fig. 1. Temperatures defining each step according to fibers shrinkage: T_{Initial} (the material fibers are inactive), A1 (the first shrinkage of individual fibers is noticed), B1 (the individual fiber shrinkage is immediately followed by another fiber shrinkage consecutively), C (most fibers experience simultaneous shrinkage), B2 (the last fibers experience simultaneous shrinkage), A2 (the shrinkage of the last individual fibers is noticed), T_{Final} (fibers shrinkage is complete).

The device presented in this work is based on the isometric method that measures the fibers tension (in terms of strength) of a leather sample that occur when its temperature increases. This

method has been used by different authors to study the different types of cross bonds of collagen [4]. Other authors define the different stages of the strenght-temperature curve and place the shrinkage temperature where the curve tends to intersect with the abscissa axis or the onset temperature [5-7]. These methods do not consider that if the leather suffers a previous contraction, the results of the T_s differ from those obtained according to the ISO 3380:2015 method, as shown in Figure 2.

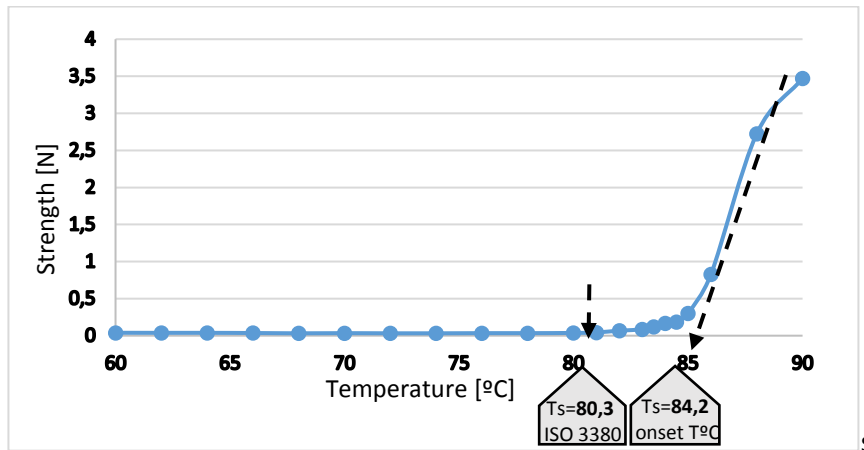


Fig. 2. Differences of T_s based on the determination method. Strenght vs. temperature of a vegetable tanned leather probe.

To avoid this differences in temperature the present work proposes to take into account the derivative of the presented curve and determine the point where it begins to increase. In this way, this method intends to find a way to determine if the T_s from the strenght-temperature curve is equivalent to the one obtained through the method according to the ISO 3380:2015.

2 Experimental design

In order to be able to verify the new measurement method of T_s , a new device has been prepared, which allows the T_s to be measured according to the ISO 3380:2015 method and at the same time registering the probe strenght to determine the T_s from the strenght-temperature curve. The two samples are tested simultaneously, submerged in a bath with agitation and temperature control. The strenght and temperature data are initially calibrated and then recorded and mathematically treated to obtain the strenght-temperature curve and its derivative. Figure 3 shows the device developed to measure T_s .



Fig. 3. Experimental device used to measure T_s and tanned leather probes.

The samples tested on the device are vegetable tanned leather probes. The sample 1 was from a leather tanned with mimosa and the sample 2 was from a leather tanned using quebracho and mimosa. Three repetitions have been performed and the T_s has been determined using the following methods:

- Method 1: T_s according to the ISO 3380:2015 method.
- Method 2: T_s Onset temperature
- Method 3: T_s from the strenght-temperature curve derivative, corresponding to the sampled data where the derivative starts to increase.

The value of the T_s according to the ISO 3380:2015 (method 1) is determined directly. However, to obtain the value of the T_s according to methods 2 and 3, it is necessary to register the value of the strenght vs temperature during the test.

3 Results and Conclusions

Figure 4 shows the table of results obtained from testing six different leather samples along with the calculation of the error " ε " and the arithmetic mean " \bar{x} ". The samples have been tested according to the methods described in the previous section and it can be seen that the results of method 3 proposed in this work are close to the results of method 1 (ISO 3380:2015).

		T_s method 1	T_s method 2	T_s method 3
		ISO:3380	On set	New
Sample 1	1	78,8	79,5	78,0
	2	77,5	79,3	77,7
	3	77,5	78,9	77,9
calf	\bar{x}	77,9	79,3	77,9
	err	0,8	0,3	0,1
Sample 2	1	81,5	84,3	79,0
	2	79,5	84,0	79,0
	3	81,8	84,2	78,0
cow hide	\bar{x}	80,9	84,1	78,7
	err	1,4	0,2	0,7
Sample 3	1	82,3	84,2	80,6
	2	81,3	84,6	81,5
	3	81,7	84,0	81,5
cow hide	\bar{x}	81,8	84,3	81,2
	err	0,5	0,3	0,6
Sample 4	1	74,5	79,4	73,5
	2	74,8	78,7	73,0
	3	75,3	78,1	72,0
calf	\bar{x}	74,8	78,7	72,8
	err	0,4	0,6	0,7
Sample 5	1	76,5	84,4	73,0
	2	73,3	84,6	74,0
	3	75,4	84,4	74,0
calf	\bar{x}	75,1	84,5	73,7
	err	1,8	0,1	0,7

Fig. 4. T_s results obtained using the three tested methods.

The T_s results using method 2 clearly show differences comparing to the ones according the ISO standard. Methods 3 shows T_s results similar to the ones from the ISO standard but some slight differences can be seen.

4 References

1. ISO. ISO 3380:2015. 'Determination of shrinkage temperature up to 100 °C. Geneva: International Organization for Standardization', (ISO), 2015.
2. Budrugaec, P., Cucos, A. and Miu, L. 'The use of thermal analysis methods for authentication and conservation state determination of historical and/or cultural objects manufactured from leather', *J. Therm. Anal. Cal.*, 104, 439–450, 2011.
3. Larsen, R. 'Experiments and observations in the study of environmental impact on historical vegetable tanned leathers', *Thermochim. Acta*, 365, 85–99, 2000.
4. Allain, J. C., Le Lous, M., Bazin, S., Bailey, A. J. and Delaunay, A. 'Isometric tension developed during heating of collagenous tissues. Relationships with collagen cross-linking.', *Biochim. Biophys. Acta*, 533, 147–55, 1978
5. Mitchell, T. W. and Rigby, B. J. 'In vivo and in vitro aging of collagen examined using an isometric melting technique', *Biochim. Biophys. Acta*, 393, 531–541, 1975.
6. Covington A. D. 'Tanning Chemistry the science of leather', Cambridge: RSC Publishing, 2011.
7. Allain, J. C., Le Lous, M., Cohen-solal, L., Bazin, S. and Maroteaux, P. 'Isometric tensions developed during the hydrothermal swelling of rat skin', *Connect. Tissue. Res.*, 73, 127–133, 1980.

OPTIMIZATION OF CHAMOIS OXIDATION PROCESS OF LEATHER USING BENZOYL PER OXIDE AS OXIDIZING AGENT

Bindia Sahu ¹, Jaya Prakash Alla ², Gladstone Christopher Jayakumar ¹, Kalarical Janardhanan Sreeram ³, Jonnalagadda Raghava Rao ²

1 Centre for Academic and Research Excellence

2 Inorganic & Physical Chemistry Laboratory

3 Centre for Analysis, Testing, Evaluation & Reporting Services (CLRI-CATERS),

Central Leather Research Institute, Council of Scientific and Research, Adyar, Chennai 600020, India

a Corresponding author - bindiya1480@gmail.com (Bindia Sahu)

Abstract. Chamois leathers are basically oil tanned leathers, usually requires 10 to 15 days to process from raw skins. In chamois making, air oxidation plays a major role, free radicals initiate the oxidation process in oil, which oxidizes the double bond of the fatty acid and then the oxidized oil interacts with collagen to stabilize the skin by coating the fibers. In the present study an attempt has been made to reduce the time for chamois leather processing. A common oxidizing agent (Benzoyl peroxide (BPO)) was utilized to enhance the oxidation of oil and reduce the time duration. It has been observed that the oxidation of oil in the presence of benzoyl peroxide has significantly reduced the duration of process from 15 to 4 days. Strength properties such as tensile and percentage elongation were found to be on par with control leather. The water absorption values of the experimental leathers improved by 1-26 %, compared with control leather.

1 Introduction

Tanning is where skin or shroud protein cooperates with tanning materials, for example, metal or vegetable tannoids or oil to change over it into leather. In metal tanning, fundamental chromium sulfate is utilized which at higher pH convert into poly chromium buildings which cross-connected with amino acids of collagen to tanned them.¹ In vegetable tanning, polyphenol astringent synthetic concoctions, got from normal sources like bark and leaves of plants, rejoins with amino acids of collagen to shape leather. In contrast to metal and vegetable tanning, chamois leathers are made utilizing oils.² Chamois leathers are commonly utilized for cleaning, because of their capacity to retain huge measure of water, oils and astounding soil expulsion abilities. These leathers additionally locate some top of the line applications, for example, filtration of fuel, cleaning optical instruments, glass windows, in making gloves, pieces of clothing, and footwear.³⁻⁵

Oil is principally connected on the outside of skin and are presented it to the environment for oxidation, the procedure is tedious and as a rule takes around nine to fourteen days.⁶⁻⁸ The way toward making chamois is tedious. There are not many literary works answering to diminish the time required for oil tanning utilizing some oxidation quickening agents, for example, hydrogen peroxide, sodium per carbonate and ozone.⁹⁻¹⁴ However, treatment of these materials needs care because of their solid oxidizing capacity and destructive nature. Thus there is a requirement for option oxidizing agents which needs negligible consideration in taking care of and successful oxidation.

In the present examination, Benzoyl peroxide was utilized as an oxidizing specialist and utilized for the streamlining for chamois leathers preparing with fish oil.

2 Materials and Methods

2.1 Materials

Indian sheep skins were procured from the local slaughter house, Chennai, India. Glutaraldehyde (BASF, Chennai), Benzoyl peroxide (BPO) (Himedia, Chennai), Fish oil (Chennai) and all other leather chemicals were of commercial grade.

2.2 Oil Tanning Using Fish Oil

Partially pickled skins were pre tanned using glutaraldehyde. Mixture of fish oil (20%), soda ash (0.5%) and benzoyl peroxide (X %) for experimental process were pre mixed in a beaker and the mixture was applied on the leather in a rotating drum so that the oil is distributed throughout the surface. The process was carried out for 90 min continuously. The skins were hanged up for oxidation in open drying stands. The completion of oil tanning was visually judged by the colour of the skins turning to golden yellow. Then, the leathers were washed with water (100%), soda ash (1%) and wetting agent (1%) for the complete removal of unfixed oil. Final leathers were dried and subjected to staking, buffing and milling. Control chamois leather was made in the similar manner as explained above without the use of benzoyl peroxide. Detail description of leather processing is seen in Table 1.

Table 1. Detail description of process for making chamois leather.

Process	Chemical	Percentage (%)	Time (min)	Remarks
Washing	Water	100	10	Wash and drain
Deliming	Water	100		
	Ammonium chloride	2	40	Check de-liming using phenolphthalein
	Alkaline bate	0.5	30	Drain
Washing	Water	200	10	Wash and drain
Partial pickling	Water	80		
	Salt	8	30	
	Formic Acid	0.5	30	In 1:10 dilution with water
	Sulphuric Acid	0.2		In three feeds with 1:10 dilution with water, adjust pH to 3.5-4
	Glutaraldehyde	1	60	Drain, pile for overnight
Next day	Fish oil	20		
	Benzoyl per oxide (experiment)	X		
	Sodium carbonate	0.5		Mix using stirrer, make paste. add to drum along with skin

X= 0.20, 0.40,0.60, 0.80, 1.00

2.3 Shrinkage Temperature Measurement

Aqueous dependability of chamois leather was surveyed so as to comprehend the leather opposition towards warmth. Shrinkage temperature of leather was done according to standard test procedure.¹⁵

2.4 Estimation of Physical Strength Properties

Physical quality parameters of leather were considered subsequent to testing, rigidity and rate prolongation properties were dissected by the standard procedures.^{16,17}

2.5 Water Absorption Analysis

Water ingestion is the leather capacity to ingest water per unit weight of leather and communicated in rate. Estimation of water retention was done according to the standard procedure.¹⁸

3 Results and Discussion

3.1 Plausible Mechanism of Oil Tanning and the Effect of Oxidizing Agent in Chamois Making

Poly unsaturated fat are exceedingly responsive to oxidation. Unsaturated oils are slanted to autoxidation, which is the prompt reaction of atomic oxygen with hydrocarbons of unsaturated fats of oil. The utilization of benzoyl per oxide improved the convergence of oxygen radical by breaking of inner oxygen-oxygen bond appeared in Fig. 1.

Unsaturated aldehydes produced amid proliferation step with their free aldehyde groups connects with amino groups of amino acids of collagen by means of Schiff base arrangement alongside hydrogen bond development with carboxylic acid group of collagen. This give a system of cross connection of oxidized oil with collagen appeared in Fig. 2.

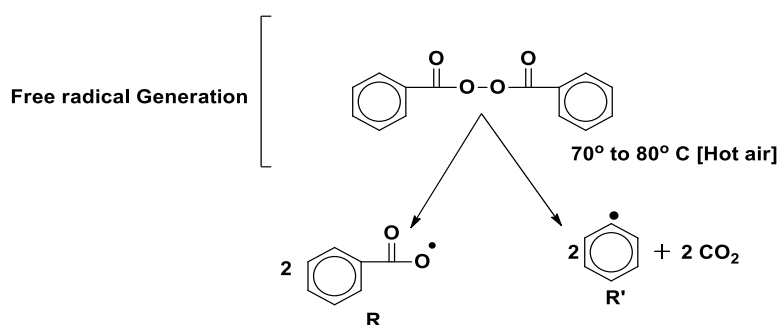


Fig. 1. Benzoyl peroxide free radical generation.

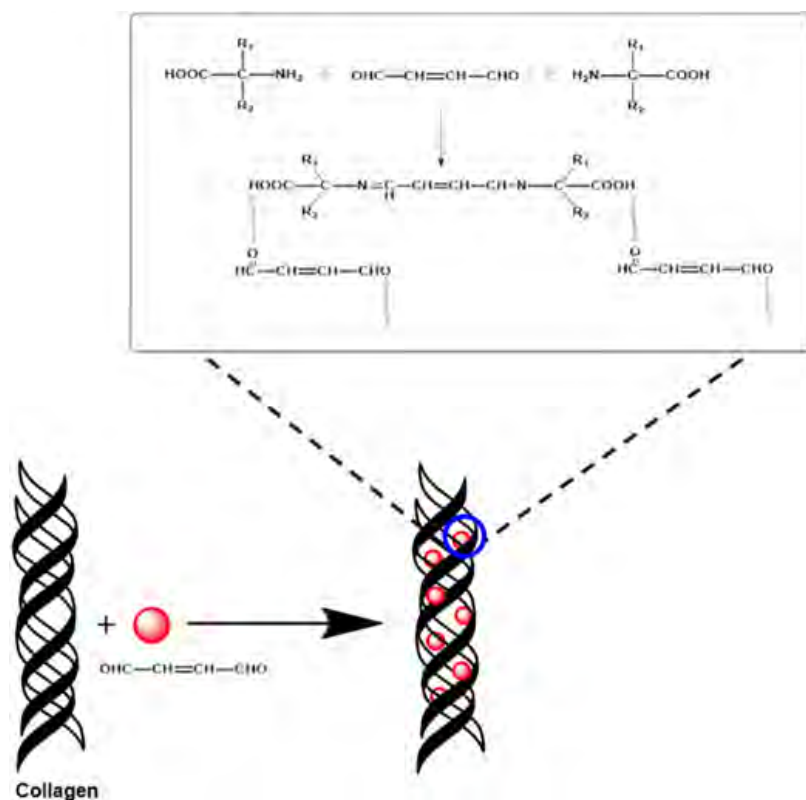


Fig. 2. Plausible interaction of Unsaturated aldehydes, generated from oil oxidation with collagen as a tanning agent.

3.2 Hydrothermal Stability of Chamois Leathers

Shrinkage temperature measurement of chamois leather provides the information about the leather resistance towards load due to hydrothermal shrinkage, which in turn gives the idea of oil tanning occurred due to the treatment of fish oil. From table II, shrinkage temperatures of experimental leathers were in the range of 78-79 °C, which is comparable to conventional oil tanning.

Table 2. Shrinkage temperature measurement of chamois leather.

S No	Sample	Shrinkage temperature (°C)
1	Control	78±1
2	BPO (0.20%)	78±1
3	BPO (0.40%)	78±1
4	BPO (0.60%)	78±1
5	BPO (0.80 %)	79±1
6	BPO (1.00 %)	79±1

3.3 Physical Strength Properties of Chamois Leathers

Chamois leathers were tried for quality and water ingestion capacities. Elasticity of the chamois leathers expanded with increment in benzoyl peroxide rate. This might be a result of the total oxidation of the fish oil and improving the tanning proficiency. The elasticity of the chamois leathers expanded with increment in grouping of the benzoyl peroxide. Rate prolongation of the leathers tests were similar with control leathers. (Table III) Likewise, chamois leathers are known for their water engrossing capacity, water retention test was completed to comprehend the impact of

oxidizing agents in chamois making. Water assimilation by the exploratory leathers expanded in the range 1 to 26 % when contrasted with control. Higher water assimilation by chamois was shown at benzoyl peroxide convergence of 1%.

Table 3. Physical testing data of chamois leathers.

S. No	Sample	Tensile Strength N/mm ²	Elongation (%)	Water Absorption (%)
1	Control	11±0.5	73±2	464±10
2	BPO (0.20%)	12±0.5	70±5	463±10
3	BPO (0.40%)	14±0.5	75±2	501±10
4	BPO (0.60%)	15±0.5	78±2	539±10
5	BPO (0.80%)	17±0.5	76±1	575±10
6	BPO (1.00 %)	18±0.5	72±5	587±10

4 Conclusions

In the present study, we have shown the use of Benzoyl peroxide as an accelerant to oxidize fish oil in chamois making. It was also shown that the time required for making chamois leather was significantly reduced from 15 to 4 days with the use of benzoyl peroxide as oxidation aid. Water absorption capability increased by 1 to 26 % compared to convention chamois leathers. Further, shrinkage temperature of the chamois leathers was comparable with control leathers along with other organoleptic properties such as softness, colour and odour. It can be concluded that the use of benzoyl peroxide in chamois making not only reduces time but also have positive benefits on final quality of leathers.

5 Acknowledgements

Author acknowledge financial support from CSIR-CLRI.

References

1. Covington, A.: *Modern Tanning Chemistry*, Chemical Society Review, 26, 111–126,1997
2. Covington, A. D.: *The chemistry of tanning materials, Conservation of leather and related materials*, 2006
3. Suparno, O. Sa'id, E.G. Kartika, E.A. Muslich, Shiva, A.: *Chamois leather tanning accelerated by oxidizing agent of hydrogen peroxide*, Teknik Kimia Indonesia, 11(1), 9-16, 2012
4. Prakash, A. J. Aravindhan, R. Nishad, N. F. Rao, J. R.: *Dyeing of chamois leather using water soluble sulphur dyes*, JALCA, 111, 383-388, 2016
5. Smith, E. R.: *Eyeglass- cleaning kit and method of cleaning eyeglasses*, US 5,000, 204, 1991
6. Marshall, W.: *Lower body garment apparatus: US 5, 706, 523. 1998*
7. Vedaraman, N. Muralidharan, R. Sundar, V. J. Velappan, K.C. Muralidharan, C.: *Modified jatropa oil for making chamois leather*, BTAIJ, 9, 203-205, 2014
8. Tony Covington.: *Tanning chemistry, the science of leather*, RSC Publishing, 2009
9. Sandhya, K. V. Vedaraman, N. Sundar, V. J. Mohan, R. Velappan, K.C. Muralidharan, C.: *Suitability of different oils for chamois leather manufacture*, JALCA, 110, 221-225,2015
10. Suparno, O. Kartika, I.A. Muslich.: *Chamois leather tanning using rubber seed oil*, JSLTC, 93, 158-161, 2009
11. Suparno, O. Kartika, I.A. Muslich, Amwaliya, S.: *Chamois leather tanning accelerated by oxidizing agent of hydrogen peroxide*, Jurnal Teknik Kimia Indonesia, 11, 9-16 2012
12. Hongru, W. Yuanyue, M. Yue, N.: *An oil tanning process accelerated by oxidation with sodium percarbonate*, JSLTC, 92, 205-209, 2008

13. Hongru, W. Yuanyue, M. Yue, N.: *An oil tanning process accelerated by oxidation with sodium percarbonate, JSLTC, 92, 205-209, 2008*
14. Sundar, V. J. Vedaraman, N. Balakrishnan, P. A. Muralidharan, C.: *Chamois leathers - An approach for accelerated oxidation, JSLTC, 88(6), 256-259, 2004*
15. IUP 16, *Determination of shrinkage temperature up to 100 °C, JSLTC, 84, 359, 2000*
16. IUP 2, *Sampling, JSLTC 84, 303, 2000*
17. IUP 6, *Measurement of tensile strength and percentage elongation, JSLTC, 84, 317-321, 2000.*
18. IUP 7, *Determination of the static absorption of water, JSLTC, 84, 323, 2000*

STUDY OF THE APPLICATION OF WB600-KERT IN UNHAIRING PROCESS

Yiming Shen¹, Jinzhi Song¹, Yanchun Li^{1a}, Shan Cao^{1b}

¹School of Light Industry and Engineering, Qilu University of Technology(Shandong Academy of Sciences), Jinan, 250353, China,;

²Shandong Leather Industry Research Institute, Jinan, 250021, China

a) Corresponding author: qlulyc@126.com

b) another author: cs1988@foxmail.com

Abstract. Unhairing process is usually considered as the most polluted process in leather production. The conventional method of unhairing which using lime and sodium sulfide produces a large amount of sludge and waste water. In order to reduce pollution, we developed a novel unhairing enzyme and named as Wb600-KerT, which possesses low collagen-degrading ability and high keratin-degrading ability in previous study. The objective of this study is to study the properties and effect of Wb600-Kert to replace traditional chemicals in unhairing process. It found that the protease of Wb600-Kert exhibited optimum keratin activity at 40°C. Compared with commercial unhairing enzyme and conventionally sodium sulfide methods, Wb600 exhibited better unhairing effect and higher efficiency. The results indicated that goat skin unhairing with Wb600 achieve enough softness, shrinkage temperature and tear strength as well as conventionally sodium sulfide methods. Furthermore, if adding a small amount of sodium sulfide, the unhairing process could be accelerated while the unhairing effect was further improved. Generally speaking, this enzyme showed good application potential in unhairing process and was effective for reducing pollution which may promote the development of leather industry.

1 Introduction

Leather making is a significant manufacture over the world, however, it is facing the threat of closure because of environmental pollution problems day by day. The problems are mainly occupied by some chemicals utilized during the leather processing, and thence it is important to find cleaner technologies to improve the heavy pollution problems. Generally, unhairing is an indispensable process and it occupies fundamental pollution¹. The traditional method used lime and sodium sulfide led to solid waste and wastewater contained high levels of sulfur. When referring to this field, the usage of clean technology in unhairing process is urgent.

The hair preserving unhairing process was gradually accepted and replacing the position of conventional lime-sodium sulfide unhairing. Among these, Enzymatic unhairing is the most promising approach to decrease environment problems. Enzymes are specificity, toxic free and safe, it can accelerate the reaction rate by reducing the activation energy of the chemical reaction. As a representative alternative for lime-sulfide process, enzymatic unhairing attracted much attention in recent years. The biggest obstacle for the promotion of enzymes in unhairing was usage and time.

In this paper, a novel genetically modified protease named Wb600-KerT which exhibited low collagen-degrading ability and high keratin-degrading ability was applied in unhairing process. The combination of 0.5% sodium sulfide and 0.04% 2520 U/g Wb600-KerT can gain good unhairing effects. After normal tanning, the shrinkage temperature and tear strength of crust leather can achieve 96 °C and 15.06 N/mm, respectively. These results indicated that enzyme Wb600-KerT has a potential application in enzymatic unhairing.

2 Materials and methods

2.1 Reagents

Goat salt dry skin (Preparation from Shandong Juncheng Leather Industry Co., Ltd.), Enzyme Wb600-KerT (Preparation from Tianjin University of Science and Technology Microbial Deposit Center), Enzyme X-Zyme 4072 (Preparation from Langsheng Co., Ltd.), Enzyme Dowell UHE (Preparation from). Glacial acetic acid, glycine, tyrosine, trichloroacetic acid, chloramine T and anthrone were all analytical grades and obtained from Sigma-Aldrich (Shanghai, China).

2.2 Determination of protease activity

Protease activity was measured by using modified method of Songjian². Casein is used as the substrate. One unit of protease was considered as the amount of enzyme which catalyzes the release from casein to 1 µg of tyrosine per minute under certain temperature and pH conditions.

2.3 Determination of collagenase activity

Collagenase activity was estimated by the method of Qiangqiang Zhou³, using type I collagen as substrates prepared in 0.1 mol/L PBS buffer (pH=7.5). Reaction systems comprised of 10 mg substrate and 1 mL of appropriately diluted enzyme. Reaction mixtures were incubated at 37 °C for 40 min, stopped using 10% chilled TCA. The amount of released free glycine was measured by the ninhydrin colorimetry method. One unit of collagenase activity was defined as the amount of hydroxyproline enzyme that released 1 µg per minute under the conditions used.

2.4 Determination of keratinase activity

Keratinase activity was measured by using modified method of Gradisar⁴. Wool powder used as the substrate was grinded before the experiment. Insoluble residues were removed by centrifugation through TGC-16G high speed benchtop centrifuge (Shanghai, China). Assay mixture containing 10 mg substrate and 2 mL of enzyme was incubated at 40°C for 1 h, then the reaction was stopped using 10% TCA. One unit of protease was considered as the increase of 0.01 at 280 nm.

2.5 Goat hide unhairing assays

Before unhairing, the goat skins were soaked with water containing fungicide, degreaser and alkaline protease until they are in good conditions. Then the soaked hide was weighed and put into controllable drum, a variety of enzyme and chemicals was separately added into different drums for unhairing under 40 °C within 4 h. After the function of enzyme, 1.2% and 1.3% calcium hydroxide was added within 2 h in order. Finally, the hide was left overnight in the drum. Next day, the waste liquid was collected for further analysis.

2.6 Later process of goat hide

After unhairing, the hides were washed with 300% water for 10 min for twice to remove hair and de-hairing enzyme. The pelts were delimed with 2.5% ammonium sulfate and 150% water, the treatment was for 1 h. In the following pickling process, the pelts were treated with 0.3% formic acid, 1.5% sulfuric acid, 8% sodium chloride and 150% water for 3 h. The eventual pH value was adjusted to 3. Then 4% glutaraldehyde, 8% sodium chloride and 80% water were added together, subsequently 2.5% baking soda was added within 90 min in three times. After that, the skins were neutralized with 150% water and 1% ammonium sulfate for 1 h. When retaining, 100% water, 15% jing bark silicone

were taken for 2 h, then 0.5% diluted formic acid were used for fixing. At last, 4% sulfonated fats, 4% synthetic fats, 4% beef hoof and 150% water used for fatliquoring with running 2 h under 50°C.

2.7 Analysis of polysaccharide concentration

The waste liquid of unhairing were collected and filtered as samples. The proteoglycan concentration of samples was measured by using a modified method of Lin.⁵ The reaction of proteoglycan and anthrone was performed in a 10 mL test tube; the mixture was place at a boiling water bath for 15 min. After cooling down to room temperature by cold water for 10 min, the absorbance was measured at $\lambda=628$ nm in order to calculate the proteoglycan concentration of the samples.

2.8 Physical properties of crust leather

Samples from crust leathers were cut for various physical tests. Before tests, they were conditioned at 20 ± 2 °C and $65\pm 2\%$ R.H. over a period of 48 h. For certain tests, such as those performed to evaluate tear strength, shrinkage temperature and softness follow standard methods⁶.

3 Results and Discussions

3.1 Various enzyme activities in protease used in the experiments

Table 1. Different protease activities.

Protease activity	Wb600-KerT	X-Zyme 4072
Collagenase activity	260 U/g	7.14 U/mL
Casein activity	3720 U/g	26.86 U/mL
Keratin activity	2520 U/g	48.7 U/mL

As shown in table 1, the enzymes tested in the experiments exhibited a certain vitality. Enzyme unhairing mainly hydrolyze soft keratin and hair root sheath polysaccharide protein, which weakens the relationship between hair bags and hair shafts, and achieves hair removal effect by mechanical action eventually⁷. Therefore, keratin activity is a key point be considered. when under the same keratin activity, the collagenase activity of enzyme Wb600-KerT is inferior to X-Zyme 4072 because that the alternation of Wb600-KerT decrease the activity of collagenase lead to it suitable for unhairing. The post-sequence unhairing experiment was established according to the industrial routine method of X-Zyme 4072, further compared with conventional lime sodium sulfide unhairing to explore the application condition unhairing of Wb600-KerT.

3.2 Unhairing methods of different groups

Table 2. Different unhairing methods in the experiments.

methods of unhairing	the compoments of unhairing
A	0.006% 2520 U/g Wb600-KerT
B	0.01% 2520 U/g Wb600-KerT
C	0.04% 2520 U/g Wb600-KerT
D	0.1% 2520 U/g Wb600-KerT
E	0.04% 2520 U/g Wb600-KerT+0.5% Na ₂ S
F	2.5% Na ₂ S+2% Ca(OH) ₂
G	0.3% 48.7 U/mL X-Zyme 4072+1% Na ₂ S+0.5% NaHS

As presented in table 2, methods from A to D were unhairing by different dosage of keratin Wb600-KerT. In addition, method F was a conventional unhairing in the leather industry, method G was a common enzymatic unhairing used in industries. The keratin activity of method A and G was equality. For the early research, we know that 0.1% 2520 U/g of Wb600-KerT was safety for unhairing. While 1.5% sodium sulfide was used for enzymatic unhairing. Therefore, 0.5% sodium sulfide was used to assist the enzyme in this experiment for exploration the application of Wb600-KerT.

3.3 The observation of crust leathers

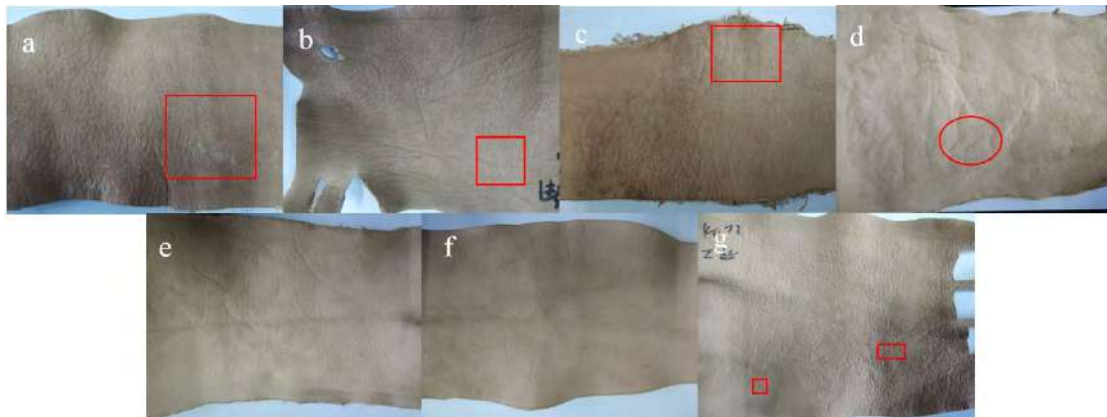


Fig. 1. The observation of crust leathers by different unhairing methods (a. Method A, b. Method B, c. Method C, d. Method D, e. Method E, f. Method F, g. Method G)

As shown in Figure 1, after the same tanning process, the surface of several methods of unhairing seemed to be more visible. In method A, certain hair can be found in the surface of the leather partly due to the lower dosage of Wb600-KerT. Along with the increasing of Wb600-KerT, the remain of hair become less to less even none. However, when the usage of 2520U/g Wb600-KerT gained to 0.1%, the grain surface of leather was damaged mainly because of the high activity of Wb600-KerT which lead to the high degradation of collagen in leathers. Compared with last three crust leather, little residual hair can be found, however, in unhairing method G, hair removal was not complete, it confirmed the possibility of incomplete unhairing by common enzymatic unhairing. Above all, the safety usage of 2520 U/g Wb600-KerT was 0.1%, the combination of 0.5% sodium sulfide and 0.04% 2520 U/g Wb600-KerT can achieve excellent unhairing.

3.4 Polysaccharide contents in waste liquid after different unhairing methods

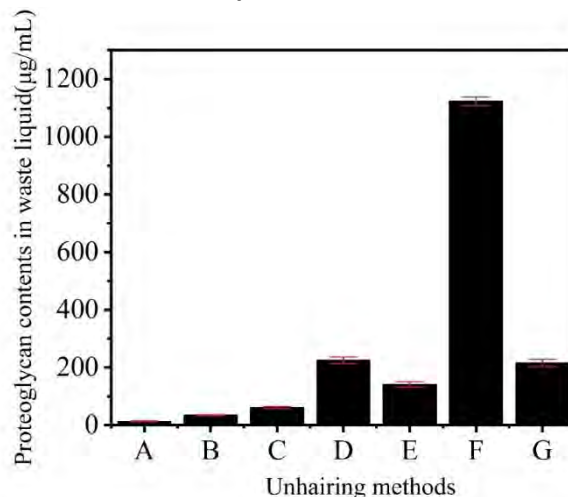


Fig. 2. Changes in polysaccharide contents in waste liquid after different unhairing methods.

As we all known, the proteoglycans are the main components of fibrous interstitial and were widely distributed in the hides. In addition, proteoglycans were also the core substance which connect the hair and the epidermis. Hence, the removal of proteoglycans was beneficial for unhairing and dispersion of enzymes. After different methods of unhairing, the polysaccharide of waste liquid was shown in Fig 2. It indicated that from Method A to D (increase the usage of enzyme Wb600-KerT), more and more proteoglycans were degraded by enzyme Wb600-KerT owing to the high activity which is consistent with former theory. In the method F, for one thing proteoglycans consist of several disulfide bonds, for another the sodium sulfide can hydrolyze the disulfide bonds. These factors lead to the highest content of proteoglycan. When the combination of 0.5% sodium sulfide and 0.04% 2520 U/g Wb600-KerT used for unhairing, sodium sulfide can dissolve part epidermis then accelerate the promotion of enzyme, degrade more plasmin, his method can get higher unhairing efficiency. Similarity, method G achieve unhairing by degrade plasmin. In the end, the combination of 0.5% sodium sulfide and 0.04% 2520 U/g Wb600-KerT for unhairing can gain good efficiency.

3.5 The physical analysis of crust leather

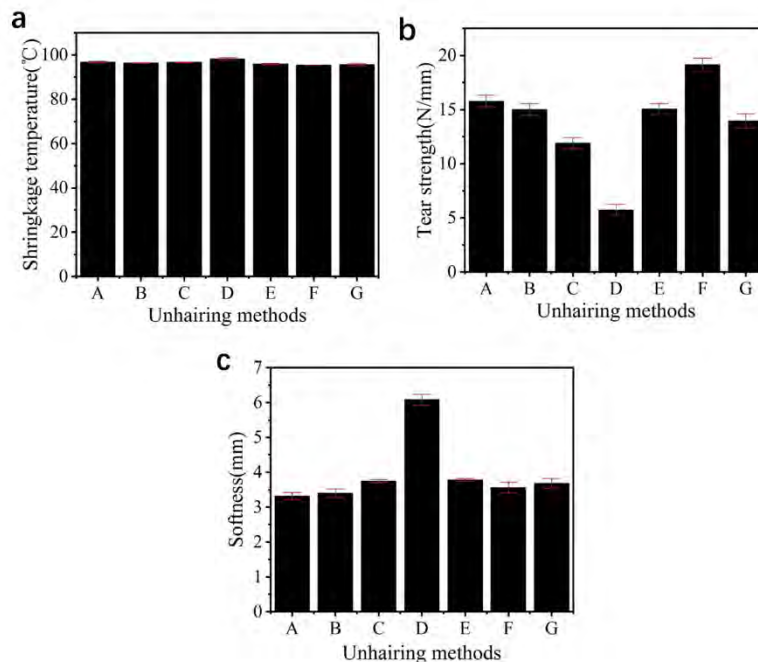


Fig. 3. The physical properties of crust leather (a. shrinkage temperature b. tear strength c. softness).

The most quickly and convenient way to determine the shrinkage temperature was to record the temperature when the leathers first shrinks in hot water. The skin after tanning, the tanning agent binds to reactive group in skin to form new crosslink, thereby the shrinkage temperature of leather increased. As shown in Fig.3.a, after seven methods of unhairing, the crust leather seemed little difference in shrinkage temperature. In method D, the shrinkage temperature of it higher than others. It possibility that excessive enzyme Wb600-KerT expose more binding sites, then combine tinctures to gain higher shrinkage temperature. However, this method degraded much collagen even caused the danger of losing the surface. The skin of unhairing by 0.5% sodium sulfide and 0.04% 2520 U/g Wb600-KerT, after tanning, it's shrinkage temperature up to 96°C revealed good thermal stability.

It's well known that tear strength is one of the important physical and mechanical properties of light leather. The higher the tear strength of the sample, the better quality of the crust leather. As

shown in Fig.3.b, with the usage of 2520 U/g Wb600-KerT increasing (from method A to D), the tear strength of crust leather decreased. It revealed that more enzyme can degrade more collagen which reduced the combined collagen and longer the distance between fibers. Therefore, the tear strength of crust leather declined. Method F and G attained normal effect. Apart from this, in method E, 0.5 % sodium sulfide assisted the enzyme Wb600-KerT, part of the epidermis was dissolved, the enzyme infiltrated into the skin which led to the amount of enzyme function on the epidermis decreased. The combination of collagen and tinctures become more and firm. The softness is an important hand feeling of leather, it revealed quality of crust leather. It was worth to pay attention to Fig.5, on the one hand, the softness of method D beyond normal level. It may be corresponding to previous theory, excessive enzyme Wb600-KerT degraded collagen and increase the distance between fibers eventually caused abnormal softness. Above all, the leather unhairing by 0.5% sodium sulfide and 0.04% 2520 U/g Wb600-KerT can acquire common requirements.

Conclusions

In this paper, the combination of 0.5% sodium sulfide and 0.04% 2520 U/g Wb600-KerT for unhairing can gain excellent unhairing efficiency without damaging the properties of leather. The sodium sulfide made contributions to the penetration of enzyme Wb600-KerT in skin by dissolving part epidermis. What's more, Na⁺ has a certain activation on the activity of Wb600-KerT. These factors led to the good results. The unhairing skin after normal tanning, it's shrinkage temperature can attain 96 °C and other properties near the leather unhairing by conventional lime-sodium sulfide. In addition, the amount of sodium sulfide used in this method is only one-third of the common dosage. It revealed enzyme Wb600-KerT has a potential application in unhairing.

Acknowledgements

This study was financially supported by the National Key Research and Development Program of China under contract No. 2017YFB0308402.

References

- 1 Pillai P, Archana G. Hide depilation and feather disintegration studies with keratinolytic serine protease from a novel *Bacillus subtilis* isolate. *Applied Microbiology & Biotechnology*. 2008, 78(4): 643-650.
- 2 Jian S, Tao W, Chen W. Kinetics of enzymatic unhairing by protease in leather industry. *Journal of Cleaner Production*. 2011, 19(4): 325-331.
- 3 Qiangqiang Z. Screening of collagenase-producing strain and studying on the characteristics of collagenase. Jilin University, 2009.
- 4 Gradišar H K S F J. Keratinase of *Doratomyces microsporus*. *Applied Microbiology & Biotechnology*. 2000, 2(53): 196-200.
- 5 Yi-Hua L. Determination of Polysaccharides in *Sarcopyramis Nepalensis* Wall by Anthrone-Sulfuric Acid Method. *Fujian Analysis & Testing*. 2017, 26(6): 52-55.
- 6 Sundararajan S K C N C. Alkaline protease from *Bacillus cereus* VITSN04: Potential application as a dehairing agent. *Journal of Bioscience & Bioengineering*. 2011, 111(2): 128-133.
- 7 E Berla T, G Suseela R. Purification and characterization of alkaline protease from *Alcaligenes faecalis*. *Biotechnology & Applied Biochemistry*. 2011, 35(2): 149-154.
- 8 Wei X. Determination of Variation of Components in Depilatory Liquors During the Process of Unhairing. *Leather Chemicals*. 2007, 1(1): 1-4.

CHARACTERISTICS OF TYPICAL POLLUTANTS IN TANNERY SITE SOIL: A REVIEW

XU Teng^{1 b)}, ZHANG Wen-hua^{1, 2a)} and SHI Bi¹

1 Key Laboratory of Leather Chemistry and Engineer of Ministry of Education, Sichuan University, Chengdu 610065, China;

2 National Engineering Laboratory for Clean Technology of Leather Manufacture, Sichuan University, Chengdu 610065, China.

a) Corresponding author: zhangwh@scu.edu.cn

b) xuteng6558@163.com

Abstract. This paper briefly introduced the process of leather manufacture and the potential pollution sources of soil in tannery sites. Pollutants are mainly derived from the use of a large number of various chemicals and organic matter decomposed by raw skin. The characteristics of typical pollutants in tannery sites soil were summarized, including tannery site soil pH, organic and inorganic compounds, and heavy metals, etc., especially the status of chromium contamination were reviewed. The pH of soil in the tanning workshop (6.65-7.8) is generally lower than tannery sludge dumping site (7.94-8.40). The main organic pollutants contained in the tannery site soil include nitrogen compound, grease, petroleum hydrocarbon. In tannery sludge dumping site soil, the content of nitrogen compound (10cm depth) is 28400 mg/kg, which is similar to tannery sludge. The content of petroleum hydrocarbon is 5-700 mg/kg, which partially exceed the limits of China agricultural land quality standard (<500 mg/kg). In tanning workshop soil, the content of grease is 220-62000 mg/kg. The main inorganic pollutants contained in the tannery site soil include sulfide, high concentration of salt, lime. The high salt content of tannery sludge (99000 mg/kg) leads to high salt content in soil (5500-17500 mg/kg). Total hardness (>450mg/L), total dissolved solids (>1000mg/L), sulfate ions (>250mg/L), nitrite nitrogen (>0.02mg/L) partially exceed the limits of China groundwater quality standard, which are found in groundwater below the tannery site. Heavy metal pollutants in the tannery sites soil have many characteristics and large differences in content, due to the different tanning processes. Among them, chromium (Cr) is the most used heavy metal and the highest content of pollutants. Cr content in tanning process wastewater, dyeing process wastewater and chromium-containing sludge are about 2000-3000 mg/L, 30-40 mg/L and 8500-25800 mg/kg, respectively. Total Cr content in the partial tannery sites soil are higher than 800 mg/kg, which exceed the limits of China agricultural land quality standard (<150mg/kg). Surprisingly, Cr(VI) appears in tannery sites soil and the contents are partly higher than 40 mg/kg, which exceed the limits of China development land quality standard (<3.0mg/kg). Furthermore, the more effort needs to be directed toward the chemistry of chromium-organic complex pollutants, and an understanding of the speciation of Cr in highly organics contaminated tannery site soil is essential for the development of suitable remediation strategies for contaminated soil.

1 Introduction

With the adjustment of industrial structure, China has developed into a world-recognized tanning country. The light leather production reached 735 million m² in 2016¹. The issuance of the "Industrial Structure Adjustment Guidance Catalogue (2011)" promoted the formation of a leather industry cluster area in which the upstream, middle and lower reaches products are mutually compatible. At the same time, some small and medium-sized tanneries with lower concentration are gradually shutting down. For example, Haining City dismantled the old factory building by 16,000 m², built and renovated factory building 49,900 m² and reclaimed 132,266 m² of tannery land. Xinji City established 1.73 million m² of tanning industrial zone and bringing together 106 companies^{2, 3}. Land used by the tannery may be re-planned as commercial and residential land in the process of industrial restructuring. As the consequence, the remediation and safety assessment before reuse makes the soil pollution problem of the tannery gradually attract people's attention^{4, 5}. This paper reviews the pollution characteristics of soils in tannery sites around the world., and puts forward relevant suggestions.

2 Source of Soil Pollution in Tannery

Leather processing technology can be roughly divided into preparation section, tanning section and dyeing and finishing section, and each section contains a plurality of processes. Leather processing has the characteristics of many processes steps and using a large amount of chemical raw materials. Among them, which attracts widespread attention is chromium. More than 80% of the light leather is made from basic chromium sulphate. Wastewater and solid waste are produced in the leather production process. The tannery sludge will be produced after the treatment of wastewater in each section and comprehensive tannery wastewater. According to the statistics, processing 1t cowhide raw material will need 700 ~ 720 kg of various chemical raw materials, produce 60 ~ 120 t wastewater, 150 kg sludge (water mass fraction 70%) and 400 kg meat residue, leather shavings, etc^{6, 7}. The typical chrome tanning process, as well as the process of producing wastewater, solid waste and sludge, is shown in Figure 1.

Obviously, heavy metals such as chromium coexist with oil, protein, aromatic, aliphatic, inorganic acid, alkali and salt during tanning. The tanning bath is repeatedly changed from alkaline to acidic according to the process, and the pH span is larger. This leads to complex interactions between chemicals and collagen fibers, and causes complex material transformation, absorption and release during the tanning process. The tannery sludge has a high moisture content and is rich in microorganisms and bacteria. Under natural conditions, the sludge composition is extremely unstable, which makes the migration and conversion of chromium and organic matter in the site more complicated. If the tanning bath leaks, or the tannery and waste shavings percolate during the stacking process, it will lead to complex pollution characteristics of the soil in the tannery.

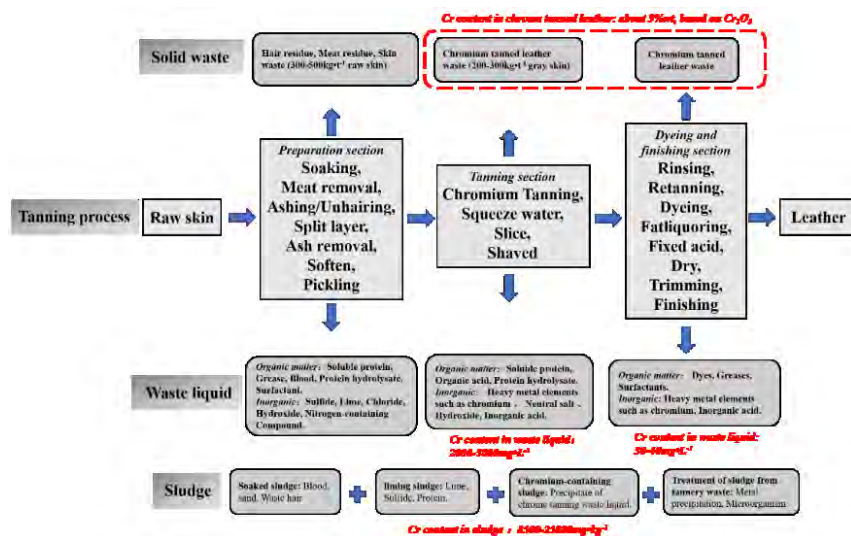


Fig. 1. Major wastes from cattle leather production⁸⁻¹².

3 Acidity and Alkalinity (pH) Characteristics of Contaminated Soil in Tannery

pH value is the main physical and chemical index of soil¹³. It not only affects the soil nutrient availability and soil fertility, but also is one of the main factors affecting the environmental effects of pollutants. The survey shows that the soil pH varies greatly in different areas and different depths of the tannery site. This is related to the distribution of tanning workshop, chemical reagents and solid waste dumping site. For example, the pH value of the site soil is found to be 4.57 ~ 7.80 according to the survey of an abandoned 81-year-old tannery in California¹⁴. The surface soil pH of the tanning

workshop is significantly lower than that of the deep soil, showing acidic characteristics. The pH value of the deep soil is closer to the background soil (7.56), indicating that the surface soil is more affected by the acid chrome tanning waste liquid. Kong investigated a site with a 1-year history of tannery sludge dumping in Xinji City, and found that the pH of soil at different depths is about 7.94 ~ 8.40¹⁵. The pH of the topsoil is similar to the pH of the sludge (7.67), while the pH of the deep soil is closer to the background value (8.30). It indicates that the surface soil is affected by the leachate produced by the tanning sludge stacking, so that the pH value is lower than the background value. A survey of the soil pollution of a tanning solid waste dumping site in Haining City found that the surface soil pH of the site is about 7 ~ 8, and significantly higher than the background surface soil pH (4.67)¹⁶. The investigation of groundwater in the tanning site area has found that the pH value of each area of groundwater was 6.58 ~ 8.04, and not exceed type of I-III Standard for Groundwater Quality in China¹⁷.

In the tannery site, the pH of the main process bath of chrome tanning is quite different, as shown in Table 1. Obviously, the waste liquid and solid waste pH generated by the tanning site vary with the progress of the process. If the bath droplets leak and the waste leachate enter the site soil, it will inevitably lead to a large difference between the soil pH of the site and the background soil, and present the spatial distribution characteristics of pH closely related to the pollution source of the tanning site. For example, the acidic waste liquid produced in the tanning section gives the contaminated soil an acidic character. During the tanning sludge stacking process, a large amount of alkaline leachate is infiltrated into the soil due to the influence of rainfall, so that the pH value of the soil is alkaline¹⁵.

Table 1. Typical chromium tanning process waste liquid pH.¹⁸⁻²⁰

Process	Soaking	Ashing/Unhairing	Ash removal	Pickling	Chromium tanning	Finishing	Integrated wastewater
pH	7.5 ~ 8.0	11 ~ 13	7.0 ~ 9.0	2.0 ~ 3.0	2.5 ~ 4.0	3.5 ~ 4.5	7.0 ~ 9.0

4 Characteristics of Typical Pollutants in the Soil of Tannery

The chemical pollution of the soil in the tannery site comes from two aspects. On the one hand, the leather processing requires the addition of chemical materials with a raw skin content of more than 40%. For example, inorganic salts such as sodium chloride, sulfide, lime, and chromium salts, and organic materials such as softeners, retanning agents, dyes and fatliquors. On the other hand, organic matter decomposition products brought by raw material skin during tannery production, including oils, animal hair, meat, etc. In leather processing, the combination of these chemical materials and leather fibers is physically or chemically combined, which leads to complex waste water and stacked solid waste components, and change with the process.

Mainly concerned with total chromium, hexavalent chromium, chlorides and sulfides in tannery wastewater and solid waste. In addition, it is generally characterized by comprehensive indicators such as COD, suspended solids, etc, as shown in Table 2. These materials or wastes enter the site soil, undergo complex physicochemical effects, and exhibit various pollution characteristics.

Table 2. Contaminant characteristics of wastewater and sludge in the main process of tanning.^{9, 21-25}

	Chloride	Sulfide	Total chromium	Grease	Total nitrogen	BOD ₅	COD _{Cr}	Suspended matter
Chromium tanning wastewater, mg•L ⁻¹	5000 ~ 12500	2 ~ 150	2500 ~ 3000	—	130 ~ 160	100 ~ 250	400 ~ 500	
Dyeing and finishing wastewater, mg•L ⁻¹	500 ~ 1000	—	30 ~ 40	20000 ~ 50000	400 ~ 500	1000 ~ 2000	2500 ~ 7000	600 ~ 1000
Tannery sludge, mg•kg ⁻¹	5800 ~ 14000	335 ~ 405	8500 ~ 25800	—	700 ~ 1700	—	10000 ~ 30000	—

Note: “—” No relevant values found

4.1 Typical Organic Pollution in Tannery Sites

The amount of organic materials used in the tannery site is large, and there are many organic residues, resulting in a high total amount of soil organic matter in the tannery. The TOC value in the surface soil (10cm) of the tannery sludge dump site is 14.3%, which is similar to the sludge TOC value. The TOC value in deep soil (100cm) is 0.2%, which is similar to the background soil. The total nitrogen concentration in the surface soil is as high as 28400mg•kg⁻¹. Due to soil adsorption and microbial degradation, the total nitrogen and ammonia nitrogen content in the soil decreases with increasing depth. When the depth reaches 70cm, the total nitrogen concentration is reduced to 700mg•kg⁻¹¹⁵. The oil and grease pollution in the soil of the tannery site is also serious. The content of oil and grease in the surface soil (15cm) can reach 62000mg•kg⁻¹. Due to the finer bay mud retardation effect, the oil and grease content was reduced to 220 mg•kg⁻¹ in soil with a depth of 137.16 cm¹⁴. Investigation of a tannery sludge dump in Haining revealed that the total petroleum hydrocarbon content in the surface soil is generally higher than that in the deep soil. The content of petroleum in soil is more than 700mg•kg⁻¹, which exceeds the Soil Environmental Quality Risk Control Standard for Soil Contamination of Development Land, and Guideline for Risk Assessment of Contaminated Sites^{26, 27}. There are many kinds of organic substances used in tannery sites, but there are few studies on the migration of complexes formed by interaction between different organic substances in soil. The chemical and physical interactions between different organic substances are complex and deserve further study.

4.2 Typical Inorganic Pollution in Tannery Sites

The amount of inorganic salt used in the pre-tanning treatment section is relatively large, among which the main environmental hazards are sulfides, high concentrations of sodium chloride and lime. Unlike organic pollution, inorganic salts are highly mobile and may cause soil and groundwater to be contaminated. The investigation found that the salt content in the surface soil (10 cm) of the tannery site was 17500 mg•kg⁻¹. The salt content in deep soil (200 cm) is still high, reaching 5000mg•kg⁻¹¹⁵. Groundwater survey on contaminated areas in tannery sites indicates that the inorganic matter of the groundwater is characterized by total hardness (256 ~ 606 mg • L⁻¹), solubility total solid (456 ~ 1116 mg • L⁻¹), sulfate (33 ~ 344 mg • L⁻¹), chloride (50 ~ 243 mg • L⁻¹), nitrate nitrogen (0.25 ~ 15.02 mg • L⁻¹), nitrite nitrogen (0 ~ 0.203 mg • L⁻¹) and ammonia nitrogen (0 ~ 0.031 mg • L⁻¹)¹⁷. Inorganic concentration at some sampling points exceed the national groundwater quality standards to varying degrees, and the polluted area is within 0.2km² of the tannery. Correlation analysis showed that the total hardness of groundwater increased, accompanied by an increase in the concentration of chloride, sulfate, and dissolved solids.

4.3 Typical Heavy metal Pollution in Tannery Sites

There are three sources of heavy metals in the tannery. First, the use of metal chemical materials in the tanning process, including inorganic tanning agent such as chromium, antibacterial agents for heavy metals such as silver, metal complex dyes such as cobalt, inorganic pigments such as cadmium sulfide, Metal flocculant such as polyaluminum chloride²⁸⁻³². The second is the entrainment of the chemical production process, such as organic retanning agents, dyes, pigment pastes^{33, 34}. Third, the heavy metals produced by the corrosion of production equipment. Heavy metal pollution in tannery sites varies by process. There are many types and large differences in content, but chromium pollution is the most prominent. For example, in the tannery sludge, Cr content is 11784 ~ 20490 mg · kg⁻¹, Zn content is 380 ~ 864 mg · kg⁻¹, Cu content is 70 ~ 179 mg · kg⁻¹, Ni content is 23 ~ 23.82 mg · kg⁻¹, Pb content is 13 ~ 280 mg · kg⁻¹, Cd content is 0.24 ~ 3 mg · kg⁻¹³⁵.

Deepali has found that the concentration of heavy metal elements in the soil of a tannery site are Cr(630.85 ~ 815.25 mg · kg⁻¹), Fe(37.45 ~ 37.95 mg · kg⁻¹), Mn(0.96 ~ 0.99 mg · kg⁻¹), Cu(0.03 ~ 0.05 mg · kg⁻¹) and Cd(0.03 ~ 0.05 mg · kg⁻¹), respectively³⁶. Cr contamination in groundwater samples (0.93mg/L) was observed only in samples collected from nearby areas of tannery. The findings also indicate that the Cr contamination was more than other metals. Rahaman has investigated the contents of Cr, Pb, Cd and Zn in the soil of the tannery site³⁷. The content of various heavy metals in each soil layer is quite different, and the Cr content is 31 ~ 561 mg · kg⁻¹, Zn content is 73 ~ 158 mg · kg⁻¹, Pb content is 24 ~ 70 mg · kg⁻¹, Cd content is 0.71 ~ 2.25 mg · kg⁻¹. It indicates that the concentration of these heavy metals in the soil of the tanning site is significantly higher than that of the background soil. Andy investigated the content of Cr in groundwater near the tanning site. The Cr content measured from some sampling points is 0.008-0.115 mg · L⁻¹³⁸. The reason for the occurrence of Cr in groundwater is that the organic matter produced by the tannery site forms chromium-organic complex, which increases the solubility of Cr in water. In addition, formation of chromium organic complex can prevent oxidation of Cr(III) to Cr(VI). Kashem has investigated the soil and plant heavy metal pollution in tannery sites³⁹. The concentrations of Mn, Zn, Cu, Ni, Pb and Cd in the soil are 218 ~ 577, 73 ~ 477, 35 ~ 217, 47 ~ 112, 20 ~ 89 and 0.87 ~ 1.8 mg · kg⁻¹, respectively. Heavy metal concentration decreases with increasing distance from the tannery. The total concentration of Cd, Cu, Mn, Ni, Pb and Zn in soil is positively correlated with the extractable concentration of DTPA. Araújo has used visible-near-infrared-infrared spectroscopy (VIS-NIR-mid) to study chromium-contaminated soil in tannery sites⁴⁰. It was found that the adsorption of Cr in the soil leads to a significant change in the spectrum, and the Cr content can be calculated by the spectral reflectance in the VIS-NIR-mid spectrum. Another survey found that some soil samples from the tannery site also detected the presence of Cr(VI)^{15, 16}, and the content (250 mg · kg⁻¹) far exceeded the Soil Environmental Quality Risk Control Standard for Soil Contamination of Development Land.

It should be noted that during the long-term aging process of heavy metals in polluted soils, there is almost no change in the total amount, but its bioavailability gradually decreases with the passage of time. Determination of the total amount of heavy metals in the soil is not suitable for evaluating the bioavailability, toxicity and migration of heavy metals⁴¹⁻⁴⁴. Therefore, more attention should be paid to the content of bioavailable heavy metals in the investigation of heavy metal pollution in contaminated soil at tannery sites⁴⁵⁻⁵⁰.

5 Conclusion and Outlook

High content and various of organic and inorganic salts in contaminated soil at tannery sites, which is closely related to the tanning process. Among them, Chromium is the main pollutant of concern.

Fractionation analysis showed that the content of effective chromium in the soil of the tannery was significantly higher than that in the background area, which significantly increased the mobility and bioavailability of chromium. Although tanneries use only trivalent chromium, higher levels of hexavalent chromium are found in the site soil. Therefore, when investigating the migration and transformation mechanism of chromium in the tanning site contaminated by compound pollution, attention should be paid to the influencing factors of available chromium and hexavalent chromium. Furthermore, it is necessary to clarify the formation mechanism of soil hexavalent chromium in tannery sites to determine the environmental risk composition of the site. It provides a basis for the development of remediation agents suitable for complex contaminated soil in tannery sites, and also provides an ecological reference for the selection and development of chemical materials for cleaning tanning.

Acknowledgement

Supported by the National Key Research and Development Program of China (No. 2018YFC1802201)

References

1. Prospective Industrial Research Institute: Analysis on market scale and competition pattern of China's leather industry development in 2017 (In Chinese). 2017-09-26[2019-01-23]. <https://www.qianzhan.com/analyst/detail/220/170925-b5cefb58.html>
2. Tang, Y. G., Gong, H. H.: 'Economic form analysis of Haining leather industry (In Chinese)', *Western Leather.*, 36(10), 8-11, 2014
3. Liu, P. J., Cheng, X. K., Cheng, G. P.: 'Re-launching of Ship-Xinji leather industry zone for environmental protection improvement (In Chinese)', *China Leather.*, 43(15), 51-57, 2014
4. Li, F. S.: 'Analysis on the decision-making and industrial development of China's contaminated site remediation under new situation (In Chinese)', *Environmental Protection.*, 20, 13-15, 2016
5. Jin, X. D., Ma, H. J., Yan, Z. G., et al.: 'Characteristics of heavy metal pollution on farmland soil surrounding representative tannery (In Chinese)', *Journal of Guangxi University (Nat Sci Ed).*, 43(5), 2079-2087, 2018
6. Tan, Q. T., Liu, W. T., Li, G. Y.: 'Current status and research progress of tannery sludge treatment technology (In Chinese)', *Leather and Chemical Industry.*, 27(4), 20-25, 2010
7. Chen, X. Q., Gu, Y. F.: 'Preliminary study on the disposal method of tannery sludge (In Chinese)', *Western Leather.*, 12, 31-36, 2006
8. Lin, W., Mu, C. D., Tang, J. H.: 'Tannery sludge treatment and resource utilization (In Chinese)', *Leather Science and Engineering.*, 15(4), 57-61, 2005
9. Jiang, H., Zhou, J. F., Liao, X. P., et al.: 'Wastewater pollution sources apportionment of cowhide processing based on equal—standard pollution load method (In Chinese)', *China Leather.*, 47(5), 39-45, 2018
10. Liu, D. J., Xie, J., Yang, F. Y., et al.: 'Development present situation of leather and fur processing industry in Henan province (In Chinese)', *Guangdong Chemical Industry.*, 44(9), 162-170, 2017
11. Ma, H. R., Hao, Y. Y., Wang, Q., et al.: 'Treatment effects compare of tannery secondary effluent with ozonation and electro-oxidation methods (In Chinese)', *China Leather.*, 47(2), 40-47, 2018
12. Chai, X. W., Gao, M. M., Wang, Y. N., et al.: 'Chrome concentration in wastewaters of post-tanning processes and the analysis of its origin (In Chinese)', *Leather Science and Engineering.*, 23(6), 40-42, 2013
13. Wang, C. W., Xu, M., Zhang, J. J., et al.: 'Effects of soil pH and Eh on longitudinal migration and transformation of heavy metal chromium(VI) (In Chinese)', *Journal of Environmental Engineering.*, 10(10), 6035-6041, 2016
14. Makdisi, R. S.: 'Tannery wastes definition, risk assessment and cleanup options, Berkeley, California,' *J. HAZARD. MATER.*, 29(1), 79-96, 1991
15. Kong, X. K., Huang, G. X., Han, Z. T., et al.: 'Vertical distribution characteristics of pollutants in typical soil profiles of tannery sludge storage sites (In Chinese)', *South-to-North Water Transfer and Water Conservancy Technology.*, 15(6), 96-100, 2017
16. He, Y. F., Wang, H. C., Chen, J., et al.: Preliminary investigation report on three tannery sludge dumps and their surrounding environment in Shanglin Village, Zhouwangmiao Town, Haining City (In Chinese), Zhejiang University, 2015
17. Zhang, D. Z., Li, H. M., Zhan, X. Y., et al.: 'Characteristics of groundwater salt pollution in typical tannery contaminated sites (In Chinese)', *Hydrogeological Engineering Geology.*, 41(2), 18-22, 2014
18. Li, W. X.: *Tanning pollution control and waste resource utilization (In Chinese)*, Chemical Industry Press, 2005
19. Zhang, C. K., Hao, Y. C., Hu, D. L., et al.: 'Research on the heavy metal trapping agent for the enhanced coagulation treatment of tannery wastewater (In Chinese)', *Industrial Water Treatment.*, 39(4), 41-44, 2019

20. Tang, Y. L., Zhou, J. F., Zhang, W. H., et al.: 'Existence of Cr in post-tanning wastewater and influencing factors on its removal (In Chinese),' *China Leather.*, 46(11), 7-12, 2017
21. Wu, H. T.: *Tanning industrial wastewater treatment technology and engineering examples (In Chinese)*, Chemical Industry Press, 2002
22. Zhou, J. J., Ma, H. R., Dong, H. X., et al.: 'Research progress on resourceful treatment and disposal of tannery sludge (In Chinese),' *China Leather.*, 47(4), 44-48, 2018
23. Zeng, G. Q., Jia, X. S.: 'Nitrogen removal performance of ANAMMOX ABR process in tannery wastewater treatment (In Chinese),' *Environmental Science.*, 35(12), 4618-4625, 2014
24. Zhang, X., He, S. Y., Wang, W. C., et al.: 'Recovery of chromium from tannery sludge by acid leaching (In Chinese),' *Energy Environmental Protection.*, 29(1), 12-15, 2015
25. Xia, H., Yang, D. M.: 'Review of tanning wastewater and its treatment situation (In Chinese),' *Leather and Chemicals.*, 31(1), 25-29, 2014
26. GB 15618-2008.: *Soil environmental quality standards (revised) (In Chinese)*, Ministry of Environmental Protection., 2008
27. DB 33/T 892-2013.: *Guidelines for risk assessment of contaminated sites (In Chinese)*, Zhejiang Quality and Technical Supervision Bureau, 2013
28. Zhao, Y.: 'Study on heavy metal elements in leather and its products (In Chinese),' *China Leather.*, 38(9), 33-37, 2009
29. Chen, W. Y., Wang, Y. H., Chen, J. P.: 'Preparation and application of chrome-valonia tannin retanning agent (In Chinese),' *China Leather.*, 34(17), 20-22, 2005
30. Li, J. X., Yuan, J. X., Lan, Y. J.: 'The preparation and use in the leather of the environmental friendly Fe complex dyes (In Chinese),' *China Leather.*, 34(23), 17-19, 2005
31. Yu, R. Q., Xiang, J., Li, K. J., et al.: 'The study of PEGylated chitosan/silver nanoparticle composite as antibacterial coating for leather (In Chinese),' *Leather Science and Engineering.*, 28(2), 44-48, 2018
32. Wan, X. C., Li, G. Y.: 'Preparation of chrome tanning agent using the chrome sludge from chrome shavings and its tanning properties (In Chinese),' *Leather Science and Engineering.*, 29(1), 11-15, 2019
33. Liu, W., Dan, N. H., Xiao, S. X., et al.: 'Composition and structure of tanning liquors of Zr-Al-Ti coordination complex tanning agent (In Chinese),' *China Leather.*, 46(9), 1-9, 2017
34. Hou, R. G., Su, H. K., Guan, P., et al.: 'Emission characteristics of heavy metals and pollution prevention in the leather industry (In Chinese),' *Guangdong Chemical Industry.*, 42(5), 87-89, 2015
35. Zeng, C. M., Wang, D. H., Chen, P. Q.: 'Study on physical and chemical properties of heavy metals in several typical hazardous wastes (In Chinese),' *Guangzhou Environmental Science.*, 24(2), 6-9, 2009
36. Deepali, K. K., Gangwar, K.: 'Metals concentration in textile and tannery effluents, associated soils and ground water,' *N. Y. Sci. J.*, 3(4), 82-89, 2010
37. Rahaman, A., Afroze, J. S., Bashar, K., et al.: 'A comparative study of heavy metal concentration in different layers of tannery vicinity soil and near agricultural soil,' *Am. J. ANAL. CHEM.*, 7(12), 880-889, 2016
38. Davis, A., Kempton, J. H., Nicholson, A., et al.: 'Groundwater transport of arsenic and chromium at a historical tannery, Woburn, Massachusetts, USA,' *APPL. GEOCHEM.*, 9(5), 569-582, 1994
39. Kashem, M. D. A., Singh, B. R.: 'Heavy metal contamination of soil and vegetation in the vicinity of industries in Bangladesh,' *WATER. AIR. SOIL. POLL.*, 115(1-4), 347-361, 1999
40. Araújo, S. R., Demattê, J. A. M., Vicente, S.: 'Soil contaminated with chromium by tannery sludge and identified by vis-NIR-mid spectroscopy techniques,' *INT. J. REMOTE. SENS.*, 35(10), 3579-3593, 2014
41. Lock, K., Janssen, C. R.: *Influence of aging on metal availability in soils*, Springer, 2003
42. Shi, R. Y., Li, J. Y., Xu, R., et al.: 'Effects of bio-ash ameliorating red soil in acidity (In Chinese),' *Acta Pedologica Sinica.*, 52(5), 1088-1094, 2015
43. Zhang, Y. Y., Sun, H., Gao, M., et al.: 'Pollution level and bioavailability of heavy metals in ginseng soil Jilin province (In Chinese),' *Acta Pedologica Sinica.*, 48(6), 1306-1313, 2011
44. Lan, M., Zhang, P., Gao, Y. C., et al.: 'The response of phytostabilization of polymetallic contamination soil to heavy metal leaching by a simulated acidic rainfall in the Dabao mountain mine dump (In Chinese),' *Chin. J. Appl. Environ. Biol.*, 1-14, 2019
45. Yang, M. L., Ye, M. L., Ma, Y. H., et al.: 'Review on heavy metal pollution evaluation in farmland soil based on bioavailable form of heavy metal (In Chinese),' *Adm. Techn. Envir. Monit.*, 31(1), 10-12, 2019
46. Wang, Z., Mi, Z. S., Zheng, C. L., et al.: 'Effect of biochar on the bioavailability and transformation of heavy metals in soil of mining area (In Chinese),' *Chem. Ind. Eng. Prog.*, 1-9, 2019
47. Yang, G., Zhao, L., Sun, Z. J., et al.: 'Study on passivation effects of multi-passivators on the cadmium (Cd) contaminated soils in sewage irrigation area (In Chinese),' *Applied Chemical Industry.*, 46(6), 1037-1041, 2017
48. Xu, J. C., Li, Y., Xiao, H. F., et al.: 'Effect of amendments on remediation of heavy metal compound contaminated soil (In Chinese),' *Chinese Journal of Environmental Engineering.*, 11(12), 6511-6517, 2017
49. Zou, F. Z., Long, X. X., Yu, G. W., et al.: 'In-situ remediation of a multi-metal contaminated acid using organic-inorganic mixed amendments evaluation by heavy metal fractions and phytoavailability (In Chinese),' *Journal of Agro-Environment Science.*, 36(9), 1787-1795, 2017
50. Wu, S. Y., Zhao, Z. Q., Xu, X. X., et al.: 'Passivation repair of heavy metal contamination soil by high magnesium phosphate rock (In Chinese),' *Hebei Agricultural Sciences.*, 56(21), 4046-4050, 2017

Ti(III)-TANNIN COMBINATION TANNING TECHNOLOGY BASED ON MICROWAVE IRRADIATION

JIACHENG WU^{1,2}, GUOQIANG NING^{1,2}, JINWEI ZHANG^{1,2}, WUYONG CHEN^{1,2}

*1Key Laboratory of Leather Chemistry and Engineering of Ministry of Education,
Sichuan University, Chengdu 610065, P. R. China, wuyong.chen@163.com*

*2National Engineering Laboratory for Clean Technology of Leather Manufacture,
Sichuan University, Chengdu 610065, P. R. China.*

a)Corresponding author: wuyong.chen@163.com

b)First author: 805263831@qq.com

Abstract. Microwave is a fast, efficient and energy-saving thermal resource, hence an attempt has been made for applying this technology in the combination tanning using titanium (III) and tannin extracts. In this work, the microwave effects on the complex reaction of Ti(III) with tannin extracts and leather products properties were investigated. The precipitation condition was used to characterize the complexation degree between Ti(III) and tannin extracts. And the shrinkage temperature, tear strength, SEM, and histological structure were used to characterize the changes in the physical and chemical properties of the combined tanned leather. The results showed that microwave irradiation can accelerate the complex reaction of Ti(III) with tannin extracts. At the room temperature, the mixture of tannin and Ti(III) kept stable at pH 3-4. In addition, microwave could increase the shrinkage temperature, tear strength, and fibrage of Ti(III)-tannin tanned leather, and it would not change the combination mode of the skins with tanning agents as well as the hierarchical structure of collagen. Therefore, these results inferred that microwave could promote the reaction between Ti(III) and tannins and the combination of tannins with collagen, which may provide a theoretical basis for the application of microwave in Ti(III)-tannin combination tanning technology.

1 Introduction

Microwave is an electromagnetic wave with a frequency between 300MHz and 300GHz, which can excite the transition of the rotational energy level of the molecule, thereby directly acting on the condensed matter molecules in the reaction system. Because of its convenience, rapidity, homogeneity, simple operation to control, small pollution, and low energy consumption, microwave heating is attracting more and more attention from chemists all over the world.^{1,3} A large number of experiments in recent years have confirmed that microwave could greatly increase the reaction rate of some chemical reactions.⁴⁻⁸ Therefore, leather chemists and technologists have tried to apply it in leather making, such as fat-liquoring, dyeing, drying and so on^{9,10}, where there was a positive effect on the performance of leather products compared to conventional heating^{11,12}.

In recent years, as the environmental pressures have increased, various strategies and methods have been tried for leather industry to replace traditional tanning processes. The combination method with metal salt and vegetable tannin was reported as a practical to manufacture leather with 'chrome-like' properties¹³, which may reduce the environmental pollution. Known by Covington¹⁴, tannin extract and titanium sulfate (Ti(III)) could be used as a combination tanning agent and corresponding leather products with high thermal stability were obtained after the treatment by using this method. After that, Bo¹⁵ analysed the complexation of Ti(III) and tannin extracts, and the results reported that

the temperature, system pH, complexation ratio, and tannin addition order had a huge effect on the complexation reaction, and Ti(III)-tannin agent could increase the shrinkage temperature of the leather.

Owing to the polarity of collagen, tannin and Ti(III), their composition and properties perhaps have a change in the microwave electromagnetic field, which may lead to the change of tanning process, technology and even tanning mechanism. However, the related application of microwave in the Ti(III)-tannin combination process has not been reported yet. In this work, the microwave effects on the complex reaction of Ti(III) with tannin extracts and leather products properties will be investigated, in order to provide a theoretical basis for the application of microwave in Ti(III)-tannin combination tanning technology.

2 Experimental

2.1 Materials

Pickled sheepskin was made in our laboratory according to conventional technology¹⁶. Titanium sulfate (Ti(III)) was purchased from ShandongXiya reagent Co. Ltd. Acacia Mangium extract (AME), Valonia extract (VE), Bayberry extract (BE) were industrial products, commercially purchased from Wu Ming tannin extract factory in Guangxi, China. All the other compounds used were analytical reagents commercially purchased from Chengdu Kelon Chemical Reagent Factory, China. 0.01g/mL of Ti(III) solution and 0.02g/mL of tannin extract solution were prepared respectively. And the pH of the Ti(III) solution was adjusted to 1.40 with sulfuric acid.

2.2 Complex at Different Temperature

Mixtures containing 10 mL $Ti_2(SO_4)_3$ and 5 mL tannin extract solution were diluted to 30 mL with water. And then they were kept in different temperature conditions at 30, 40 and 50 °C for 2 h respectively under microwave irradiation heating (MIH, produced by a Xian Yuhui MCR-3 microwave chemistry reactor). Corresponding procedure under water bath heating (WBH) acted as a control. After being centrifuged for 0.5 h with 6000 r/min rotating speed, the precipitations were dried at 120°C, and weighted.

2.3 Mixture under Different pH

Mixtures were composed of 15 mL of the tannin extract solution (4 g/L) and 15 mL of Ti(III) solution (0.4 g/L), and neutralized to a serious pH (1, 2, 3, 3.5, 4, 5, 6 and 7) with dilute sulfuric acid or sodium bicarbonate ($NaHCO_3$). After that, the samples were placed at room temperature for 4 h, observing the solution precipitation condition.

2.4 Tanning with Different Tannin Extract and Ti(III)

Two pickled sheepskin pieces were sampled (13cmx7cm) along the backbone and weighted (the following reagent dosage: 1.5 times of the pickled pieces mass). 30% tannin extract, 400% water, 6% sodium chloride and 3% Ti(III) were added into a beaker and then the solution was neutralized to pH 3.0-4.0 with $NaHCO_3$. After the pH was stable, the skin sample (2cmx6cm) was put into the beaker, and the tanning was performed at room temperature. After the tannin extract had completely penetrated into the skins, the samples were taken out. One test was carried out for 12 hours at 50 °C under MIH for the experiment, and the other served as a control being treated by WBH. After the tanning finished, the sample was taken out and collected for test.

2.5 Microscopy of Ti(III)-tannin Tanned Leather

Tissue staining microscopy is one of the more effective techniques for observing the histology structure of the leather. 2cmx2cm pieces of the Ti(III)-tannin tanned leather were first fixed in 10% neutral formaldehyde solution (100mL, v/v) for 48 hours. Next, the fixed piece was washed completely and sectioned (thickness, 12 μ m) using a CM-1950 freezing microtome (Leica, Germany); after this step the section was attached to the slide with protein glycerin, and dried for 72 hours in air. At the staining step, the section was placed in the solution containing hematoxylin alcohol solution (1%) and ferric chloride solution (29%, 4mL) with 95 mL of distilled water for 20 min, and then washed and staining again in picric acid saturated aqueous solution containing 1% acid magenta solution (85:15, v/v) for 3 min, washed and followed by 2 min of differentiation with ethanol (95%) for three times, and immersion in 95% alcohol, pure alcohol and xylene, respectively (2 times each of the alcohol liquids and once for xylene, 2 minutes each time). The final stained piece was observed under the microscope. The magnification was 15 \times .

2.6 Measurement of Physical and Mechanical Properties

To determine the shrinkage temperature (T_s), a 2.5cm x 1.0cm leather piece was heated in glycerin solution at 2 $^{\circ}$ C/min rate measured by a MSW-YD4 digital shrinkage temperature meter (Institute of Sunshine Electronics, Shaanxi University, China). The tensile and tear strength samples were conditioned at 20 \pm 2 $^{\circ}$ C (RH, 65 \pm 2%). The 4.5cmx1.0cm leather piece was measured with a thickness gauge and an AI7000S automatic tensile machine (GOTECH testing Machines Inc., China) was used for the tests. The tear strength was calculated using Formula 1:

$$T=F/t \quad (1)$$

where T is tear strength (N/mm), F is tear force (N) and t is average thickness of the sample (mm).

2.7 Measurement of Scanning Electron Microscope (SEM)

The cross-sections of the tanned leather were examined in a Jeol JSM-7500F scanning electron microscope. The samples were coated with a gold film before such measurement.

3 Results and Discussion

3.1 The Influence of Microwave Temperature on the Complexation

The precipitation amounts of the complexation under different temperature were shown in Table 1. Apparently, in the condition of both of MIH and WBH, the precipitation amounts were increased with the temperature, indicating that the complexation of the tannin with Ti(III) solution was enhanced as the temperature went up. However, MIH method promoted the reaction more strongly. From 30 $^{\circ}$ C to 50 $^{\circ}$ C, the precipitation amounts of the microwave group were 1.0 mg, 8.1 mg and 17.6 mg, respectively, which were more than that of control. It could be inferred that microwave had an ability to increase the collision of tannin particles and Ti³⁺, which made the complexation easier.

Table 1. The precipitation amounts of the complexation under different temperature.

Temperature (°C)	Precipitation amounts (mg)	
	MIH	WBH
30	6.6	5.14
40	31.2	23.1
50	68.4	50.8

3.2 The Influence of pH on the Stability of The Tannin and Ti(III) Mixed Solution

It can be seen from Fig. 1 that the mixed solution becomes cloudy immediately at pH 1 and 2, because pH deviates from the isoelectric point of tannin, the phenolic hydroxyl group reacted rapidly with Ti^{3+} . At pH 3 and 4, there is no precipitation in the mixed solution, thus the solution is stable, which may be because the phenolic hydroxyl of the tannin extract was hidden, and the tannin could not react with Ti^{3+} . Due to titanous sulfate is hydrolyzed to form precipitation at pH 5, 6, and 7, there are some white precipitates in the mixed solution. As it is shown from Fig. 2, the mixed solution is still clear and stable at pH 3, 3.5 and 4.0 after standing for 4 h. So, we could conclude that the complexation reaction is slow at pH 3-4 at room temperature.

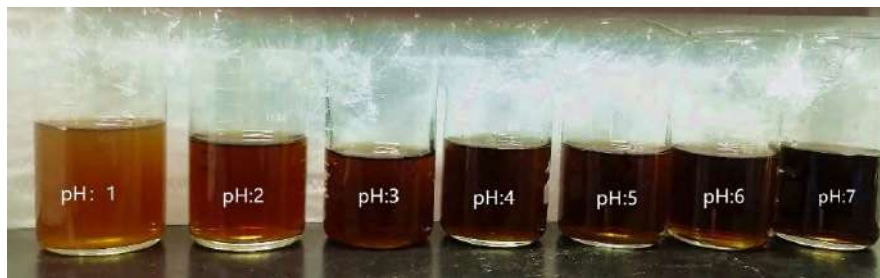


Fig. 1. The mixture of tannin and Ti(III) under different pH.



Fig. 2. The mixture of tannin and Ti(III) at pH 3.0, 3.5 and 4.0.

3.3 Histology Structure Analysis

The fibrous structure can be observed through the microscope. Fig. 3 is the histology structure of Ti(III)-tannin tanned leather. It can be found that the fibers of the experimental are closer and more evenly distributed than the control. The reason of this phenomenon could be explained by that the interaction of Ti^{3+} , tannin and collagen was accelerated in the microwave high frequency transformed electromagnetic field, thus making the crosslinking is more intense. Besides, because of the bulk-heating of the microwave, the collagen fibers' weave was more uniform.

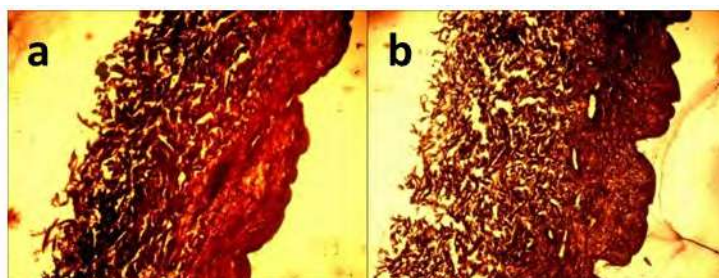


Fig. 3. The fibrage of the leather tanned under WBH (a) and MIH (b)(15×).

3.4 Ts Analysis

Table 2 shows Ts of the leathers obtained using different tanning processes. It can be seen from the Table 6 that both microwave heating and water bath heating methods can increase the Ts of the leather. Ts of the leather tanned under MIH was greater than that of WBH. Among the three types of tannin, Ts of VE tanned leather was most obviously improved, which increased by 5.6 °C after microwave heating. For BE tanned leather, the microwave promotion effect showed a little, and the Ts of the microwave group was only 1.2 °C higher than that of control. However, no matter what the tannin type is, the Ts could be increased under MIH. This may be because the microwave could not only promote the combination of tannin and Ti^{3+} with collagen, but also enhance the combination of tannin and Ti^{3+} , strengthening the crosslinking effect among tannin, Ti^{3+} , and collagen, producing a synergistic effect of tannin and Ti^{3+} .

Table 2. The Ts of Ti(III)-tannin tanned leather under different heating methods.

Heating method	AME	VE	BE
Before heating	84.0	74.8	79.1
MIH	93.5	90.4	86.2
WBH	90.8	84.8	85.0

3.5 Physical and Mechanical Properties

Table 3. The tear strength of Ti(III)-tannin tanned leather under different heating methods.

Tannin	AME		VE		BE	
	MIH	WBH	MIH	WBH	MIH	WBH
Heating method						
Tear force /N	39.48	32.81	43.80	35.11	56.41	37.69
Tear strength /N·mm ⁻¹	15.19	14.82	21.87	18.33	19.28	16.87

Tearing force is one of the important physical properties of the leather products. Due to the special woven structure of the leather, the leather not only has high tensile strength but also high tearing force, which is one of the rare and valuable properties of leather. Table 3 records the tear strength of Ti(III)-tannin tanned leather under different heating methods. It is observed that the tear strength of experimental sample is higher than that of control. That was, microwave irradiation might promote synergistic effect between tannin and Ti(III), thereby, the effective connection between the collagen fibres was enhanced and the strength of the collagen fiber weaving network was increased.

3.6 SEM Analysis

Fig. 4 shows the SEM image of Ti(III)-tannin tanned leather. It is obvious from the picture that the leather is woven from fibres apparently and the magnification is X 25. When it is further magnified (X 5000), the fibres of the samples are obviously woven from finer fibres. Moreover, there are bright and dark grainy stripes on the fibre bundle of the sample (X 20,000 and X 50,000), which is the performance of a quarter of the split structure of collagen fibres. These results reflected that both of the method (MIH and WBH) did not destroy the hierarchical structure of collagen in the tanned leather. However, microwave could promote the combination of tannins and collagen and make the fibre structure more compact.

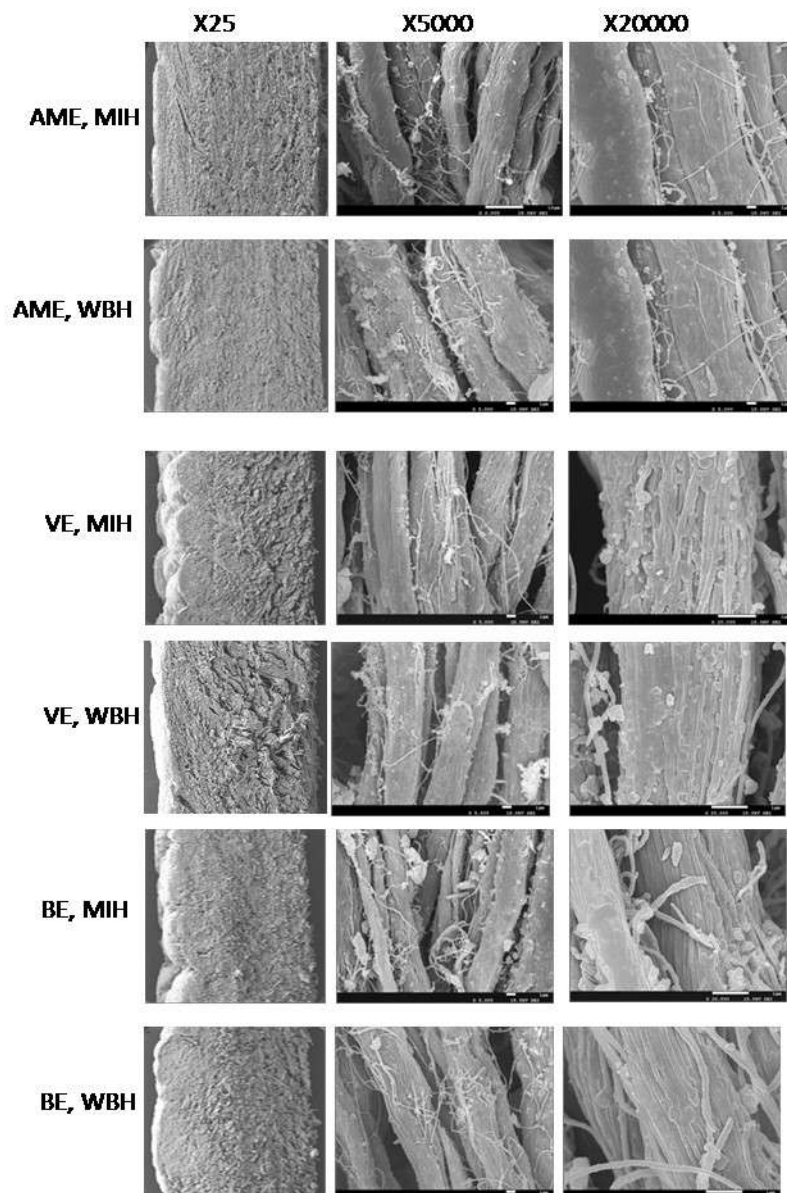


Fig. 4. SEM image of Ti(III)-tannin tanned leather.

4 Conclusion

In this study, the influence of microwave on the complex reaction of Ti(III) with tannin extracts and tanned leather products properties were investigated. The results showed that microwave irradiation can accelerate the complex reaction of Ti(III) with tannin extracts. At pH 3-4 and room temperature, the mixture of tannin and Ti(III) could be used as a combination tanning agent. Evidences indicated that microwave could increase the shrinkage temperature, tear strength, and fibrage of Ti(III)-tannin tanned leather, and it would not change the combination mode of the skins with tanning agents as well as the hierarchical structure of collagen. Hence, microwave may have an ability to promote the reaction between Ti(III) and tannins and the combination of tannins with collagen, providing a theoretical basis for the application of microwave in Ti(III)-tannin combination tanning technology.

Acknowledgement

The authors wish to thank the National Natural Science Foundation of China (No. 21576171) for financial support.

References

1. Jin, Q. H., Dai, S. S., Huang, K. M.: *Microwave Chemistry*, Science Press, Beijing, 1999
2. Zhu X. H., Hang Q.M.: 'Microscopical and physical characterization of microwave and microwave-hydrothermal synthesis products', *MICRON*, 44, 21-44, 2013
3. Aivazoglou, E., Metaxa, E., Hristoforou, E.: 'Microwave-assisted synthesis of iron oxide nanoparticles in biocompatible organic environment', *AIP Adv.*, 8(4), 048201, 2018
4. Gedye, R. N.: 'Microwave assisted syntheses in house hold microwave ovens', *Tetrahedron Letters*, 27(3), 279-283, 1986
5. Sezer, G. G., Yesilel, O. Z., Sahin, O., et al.: 'Synthesis of 2D Zn(II) coordination polymer and its crystal structure, selective removal of methylene blue and molecular simulations', *J Mol Struct.*, 1143, 355-61, 2017
6. Liu, X.C., Wan, Q., Zhao, Z., et al.: 'Microwave-assisted Diels-Alder reaction for rapid synthesis of luminescent nanodiamond with AIE-active dyes and their biomedical applications', *Mater Chem Phys.*, 197, 256-65, 2017
7. Alwin, S., Shajan, X. S., Karuppasamy, K., et al.: 'Microwave assisted synthesis of high surface area TiO₂ aerogels: a competent photoanode material for quasi-solid dye-sensitized solar cells', *Mater Chem Phys.*, 196, 37-44, 2017
8. Lu, Y. J., Zhao, Z. D., Chen, Y. X., et al.: 'Synthesis of allyl acrylpimarate by microwave irradiation and phase-transfer catalytic reaction and its UV-curing reactions as a new monomer', *Prog Org Coat.*, 109, 9-21, 2017
9. Gilet, J., Dynavac, G.: 'Drying without heat', *Journal of the American Leather Chemists Association*, 82, 61-64, 1987
10. Komanowsky, M.: 'Drying of leather with microwaves', *Journal of the American Leather Chemists Association*, 85(5), 131-141, 1990
11. Monzó-Cabrera, J., Díaz-Morcillo, A., Catalá-Civera, J. M., et al.: 'Kinetics of combined microwave and hot air drying of leather', *Journal of the Society of Leather Technologists and Chemists*, 84(1), 38-44, 2000
12. Bajza.: 'The influence of fatliquor concentration on microwave drying kinetics', *Journal of the Society of Leather Technologists and Chemists*, 81(1), 227-230, 1997
13. Covington, A. D.: 'The 1998 John Arthur Wilson memorial lecture: new tannages for the new millennium', *Journal of the American Leather Chemists Association*, 93, 168-183, 1998
14. Covington, A. D.: 'Lampard, G.S., Pennington, M., An investigation of titanium (III) as a tanning agent', *Journal of the Society of Leather Technologists and Chemists*, 82(2), 78-80, 1998
15. Teng B., Jian X. Y., Chen W. Y.: 'Effect of gallic acid content on Tannin-Titanium (III) combination tanning', *Leather & Footwear Journal*, 13(1), 389-394, 2012
16. Liao L. L., CHEN W. Y.: *Beamhouse. In Tanning Chemistry and Technology, 1st ed.; Science Press, China, Volume 1, 186, 2005*

A NOVEL COLLAGEN EXTRACTION METHOD BASED ON MICROWAVE IRRADIATION

YULIN CHENG^{1,2}, JIACHENG WU^{1,2}, JINWEI ZHANG^{1,2}, WUYONG CHEN^{1,2}

*1Key Laboratory of Leather Chemistry and Engineering of Ministry of Education,
Sichuan University, Chengdu 610065, P. R. China, wuyong.chen@163.com*

*2National Engineering Laboratory for Clean Technology of Leather Manufacture,
Sichuan University, Chengdu 610065, P. R. China.*

a) Corresponding author: wuyong.chen@163.com

b) First author: yulin.cheng@qq.com

Abstract. Microwave was used as a thermal source to extract collagen from the cattle hide in the present work. The effects of microwave on collagen extraction yields were studied under different irradiation temperature, time and solid-liquid ratio. The optimal extraction process was obtained by an orthogonal experiment. The results showed that the extraction yield of collagen was positively correlated with irradiation temperature. With the solid-liquid ratio decreased and the irradiation time, the extraction yield increased within limits. Under the condition of 37 °C, 7 h and 1:45 of solid-liquid ratio, the extraction yield was the highest (14.35 %). And the composition, structure and properties of the extracted collagen were characterized by amino acid analysis, FTIR, UV-Vis, and VP-DSC. Amino acid analysis confirmed that the composition of the products were similar to that of standard type I collagen. The UV absorption peak of the product conformed to the characteristics of collagen. Moreover, the absorption peak of the collagen products in the infrared spectrum did not migrate, indicating the triple helix structure of the collagen was stable. Furthermore, the VP-DSC results showed that the thermal denaturation temperature of collagen products was 38.82 °C. Therefore, these results proved that the natural structure of the product was still maintained, which provided a new choice for efficient extraction of collagen.

1 Introduction

Collagen is the most abundant protein in mammals, accounting for 25-30% of the protein weight. This fibrous structural protein consists of three left-handed spiral peptide chains with right-handed supercoil structures¹ Due to its excellent biophysical properties, it is widely used in medicine², food³, cosmetics⁴ and so on. And it has vast development potential and broad market application prospects. The development of extraction of collagen containing natural structure will bring huge commercial value and social benefits. At present, the methods for preparing collagen mainly include acid extraction⁵, enzymatic extraction⁶, alkali extraction⁷, hot water extraction⁸, neutral salt extraction¹⁰. Among these methods, the collagen extracted by acid method has complete structure and high purity, but the extraction rate is low⁹.

Since microwaves was used to treat nuclear waste in Harwell Laboratory at 1970, it had been widely used in various chemical fields as a transmission medium or heating energy source¹¹, gradually formed microwave chemistry. People began to pay attention to the excellent performance of microwave in chemical reaction process. At present, microwave irradiation has become an important technology to accelerate chemical reaction. Moreover, previous studies¹² proved that microwave-assisted method can shorten the time and increase the extraction rate while ensuring product quality.

In order to prepare structurally intact collagen more effectively, a new method for efficient extraction without affecting the activity of collagen molecules was explored. In this work, microwave was used

as heat source in the extraction process of extracting collagen by acid method under water bath heating was used as control group. The influence of solid-liquid ratio, microwave irradiation time and temperature on the extraction rate was investigated by single factor method. Then the extraction process was optimized by orthogonal method. The structure and properties of the product were characterized by FTIR, VP-DSC, UV-Vis. These results may offer theoretical supports for a new collagen extraction method based on microwave irradiation.

2 Materials and methods

2.1 Materials

Collagen was prepared from cattle hide made in laboratory. All other chemicals were commercially available of analytical grade from Chengdu Cologne Chemical Co., Ltd.

2.2 Methods

2.2.1 Preparation

The raw material was prepared according to the method of ZHONGKAI et al.¹⁴. Green hides which came from cattles were processed by conventional tanning process to prepare limed stock. After splitting, the samples with the size of 100 cm × 80 cm were taken symmetrically along the back line of the split and weighed as the basis of the following materials. Then the samples were delimed with 2% ammonium chloride and 0.5% hydrochloric acid for 1 h, followed by neutralizing with 0.5% hydrochloric acid solution which aimed to adjust the pH to 6.0-7.0. After that, the samples were rinsed with distilled water for 30 min and cutted into fragments of 0.5 cm × 0.5 cm. Finally, they were put into a dryer and set aside after air drying.

2.2.2 Extraction of collagen by microwave irradiation

3 g of the raw material was weighed accurately in a 100 mL beaker to extract collagen under certain conditions. Next, the crude extract was obtained by filtering the extract with 200 mesh gauze, and then centrifuged at 8000 r/min for 10 min by using desktop high speed centrifuge (TG-20; Sichuan Shuke instrument Co., Ltd; China). Subsequently, sodium chloride was added to the supernatant until the concentration was 3 mol/L. Afterward, collagen precipitation was collected by centrifugation again and dissolved in acetic acid solution of 0.5 mol/L. After the collagen was dialyzed with distilled water for 3 days, dialysis fluid was freeze-dried and put into the dryer for use. The product obtained by microwave extraction is called the experimental product (EP), while the product obtained under water bath heating was the control product (CP).

In order to optimize the experimental conditions, the single factor experiment was conducted. With the extraction yeild of collagen as indicator, collagen was extracted respectively at different irradiation temperatures (irradiation time 6 h, solid-liquid ratio 1:30), different solid-liquid ratio (irradiation temperature 35 °C, irradiation time 6 h) and different irradiation time (irradiation temperature 35 °C, solid-liquid ratio 1:40) to explore the effect of extraction conditions on the extraction yield of collagen. On the basis of single factor experiments, orthogonal experiment with 3 factors and 3 levels were carried out. Details on the orthogonal optimization, including irradiation temperature, time and solid-liquid ratio were given in Table 1.

Table 1. Details on orthogonal design.

Levels	Factors		
	A (°C)	B	C (h)
1	33	1:35	6
2	35	1:40	7
3	37	1:45	8

A: irradiation temperature; B: solid-liquid ratio; C: irradiation time

2.3 Analysis

2.3.1 Composition determination

A small part of the raw material was used to determine the proximate composition, including ash, moisture, crude fat and crude protein according to the method of AOAC ¹⁵.

2.3.2 Yield

Standard type I collagen solutions of 0, 0.25, 0.50, 0.75, 1.00, 1.25 and 1.50 mg/L were prepared with acetic acid solution of 0.5 mol/L. With acetic acid solution of 0.5 mol/L as reference, the absorbance of collagen solution were recorded over the range of 200-400 nm at the scanning speed of 400 nm/min by ultraviolet spectrophotometer (UV1900; Shanghai Flying Art instrument Co., Ltd.; China) to determine the characteristic absorption peak of collagen. According to the absorbance of collagen solution at the characteristic absorption peak, the standard curve which was used to calculate the concentration of collagen in the crude extract was made. Then the yield of collagen was calculated according to formula 1:

$$Y = \frac{C \cdot V \cdot 100}{M \cdot F} \quad (1)$$

Y---The extraction rate of collagen (%);

C---Collagen concentration in crude extract (mg/L);

V---Volume of crude extract (L);

M---the weight of raw material (mg);

F---percentage of protein in raw material skin (%).

2.3.3 Amino acid analysis

25.0 mg of the collagen products were completely hydrolysed in the presence of hydrochloric acid of 6 mol/L at 120 °C for 24 h. The solutions were filtered and diluted. Thereafter, the amino acid composition of filtrate was determined by amino acid analyzer (L-8900; Hitachi Co., Ltd.; Japan).

2.3.4 Fourier transform spectroscopy (FTIR)

2 mg of the products were mixed with potassium bromide (1:100) respectively, grounded and pressed evenly for spectrum recording. Subsequently, they were scanned in the Fourier transform infrared spectrometer (Nicolet iS10; Seymour Technology Co., Ltd.; America) for 32 times with a wave number range of 400-4000 cm⁻¹ at room temperature.

2.3.5 Differential scanning calorimetry (DSC)

0.5 mg/mL collagen solution were prepared with acetic acid solution of 0.5 mol/L. Acetic acid solvent of 0.5 mol/L was used as a reference control, and the solutions were degassed in the instrument

for 30 min followed by being tested in the temperature range of 20 °C to 60 °C by hypersensitive differential scanning calorimetry (VP-DSC; Microcal; USA) with the increasing rate of 1 °C/min.

3 Results and discussion

3.1 Composition of cattle hide

The composition of each component of the raw materials is shown in Table 2. It can be seen that the main components in the raw materials are protein and water, which together account for 89.3% of the tare weight, in addition to 7.26% fat and ash besides 3.44% other substances. Since the raw material is prepared from limed stock after degreasing, the fat contained only 6.4% of the tare weight. Followed on air drying, the moisture content of the raw material is reduced to 17.1%. After the pretreatment is completed, the content of protein in the material is as high as 72.2%, which is suitable for the extraction of collagen.

Table 2. Composition of material.

	Water	Ash	Protein	Fat
content g/100 g	17.1	0.86	72.2	6.4

3.2 Relationship between collagen concentration and absorbance

The standard curves of different concentrations of standard type I collagen solution were obtained at the characteristic absorption peak (234 nm) of collagen, as shown in Fig. 1. According to Lambert-Beer's law, there is a linear relationship between the UV absorption and the concentration in a certain concentration range Fehler! Verweisquelle konnte nicht gefunden werden.. It can be seen that the concentration and absorbance of collagen conform to the law, and the linear relationship is $y=0.5799x+0.0307$, besides, the linear relationship variance is 0.9955, which indicates that the concentration of collagen has a good linear relationship with absorbance and the obtained data are in good agreement with the fitting function.

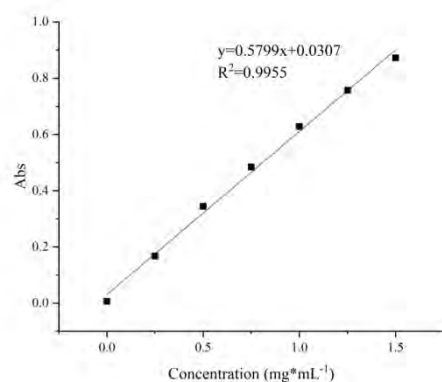


Fig. 1. Relationship between concentration and absorbance of standard type I collagen

3.3 Effect of microwave on collagen extraction yield

3.3.1 Effect of irradiation temperature on extraction yield

Collagen was extracted by microwave irradiation under the condition of solid-liquid ratio 1:30 for 6 h. The effect of irradiation temperature on the extraction of collagen was investigated by extracting collagen at different temperatures. Taking the temperature as the abscissa and the extraction yield as the ordinate, the relationship between the extraction yield and the irradiation temperature was obtained (figure 2).

It can be seen that the collagen extraction yield is the lowest at 15 °C. With the increase of irradiation temperature, the extraction yield increases rapidly, and the highest extraction yield is exhibited while the irradiation temperature was 40 °C. When irradiation temperature is 15 °C, the temperature is cool, therefore, corresponding microwave power is low, resulting in small effect on collagen. Simultaneously, the acidic condition destroys the Schiff bond (-C=N-) and salt bond between the collagen molecules Fehler! Verweisquelle konnte nicht gefunden werden., causing its compact structure to become loose and collagen molecules to be extracted. With the temperature went up gradually, the solubility of collagen molecules increased and the thermal motion fortified, besides the augment of microwave power. The molecular motion is more intense under the action of high-frequency electric field, which makes the collagen structure looser and more soluble. Therefore, as the temperature rises, the extraction yield increases. It is reported that the denaturation temperature of collagen is about 40 °C, and even lower when collagen is in an acidic environment, which is at 38-39 °C Fehler! Verweisquelle konnte nicht gefunden werden.. In order to extract collagen with natural structure, 35 °C was selected the optimum irradiation temperature.

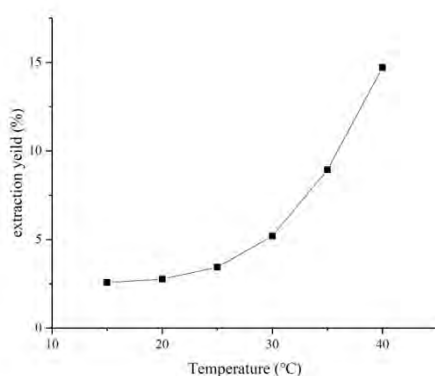


Fig. 2. Relationship between extraction temperature and extraction yield of Collagen

3.3.2 Effect of solid-liquid ratio on extraction yield

Under the conditions of irradiation temperature of 35 °C and irradiation time of 6 h, the collagen was extracted at different solid-liquid ratios. The relationship between the extraction yield and solid-liquid ratio was shown in figure 3. It is known that when the solid-liquid ratio is large, as the solid-liquid ratio decreases, the extraction yield rises, and with the solid-liquid ratio decreases gradually to 1:30, the extraction yield increases sharply. Till the solid-liquid ratio reaches 1:40, the maximum is reached; while the solid-liquid ratio is less than 1:40, the solid-liquid ratio decreases leading to the decrease of extraction yield, and finally reaches the relative equilibrium value. When the ratio is relatively large, there is little acetic acid solvent resulting in less amount of collagen. With the small solid-liquid ratio, more solvent exists since the probability of the material being irradiated becomes smaller, which is not conducive to collagen dissolution Fehler! Verweisquelle konnte nicht gefunden werden., and the increase of acetic acid content promotes the hydrolysis of collagen. Therefore, the solid-liquid ratio is the most suitable at 1:40.

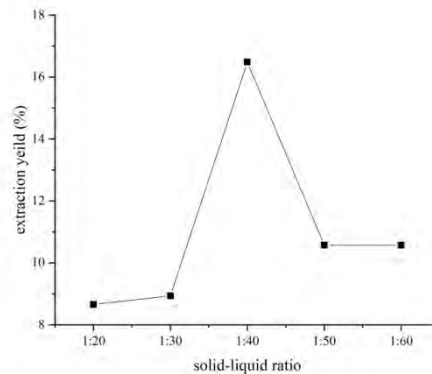


Fig. 3. Relationship between extraction yeild and solid-liquid ratio.

3.3.3 Effect of irradiation time on extraction yeild

On the basis of the above experiments, collagen was extracted at different times to explore the effect of irradiation time on collagen extraction under the solid-liquid ratio of 1:40 and the irradiation temperature of 35 °C. The relationship between the extraction yeild and the irradiation time is shown in Fig. 4. The extraction yeild of collagen increased with the prolongation of irradiation time, and the maximum value is reached between 6 and 9 hours. Afterwards, the extraction yeild of collagen decreased as the reduction of irradiation time. When the irradiation time is short, microwave can break the wall to a certain extent, and at the appropriate temperature, it can also loosen the triple helix structure of collagen to promote the dissolution of collagen Fehler! Verweisquelle konnte nicht gefunden werden. If the time is too long, molecular exercise is intense, causing collagen to hydrolyze, resulting in a decrease in extraction yeild at higher temperatures Fehler! Verweisquelle konnte nicht gefunden werden. Based on the results of single factor experiment, the experimental point with the highest extraction yeild was selected as the optimum extraction conditions, that is, the irradiation time was 6 h, the irradiation temperature was 35 °C, and the solid-liquid ratio was 1:40.

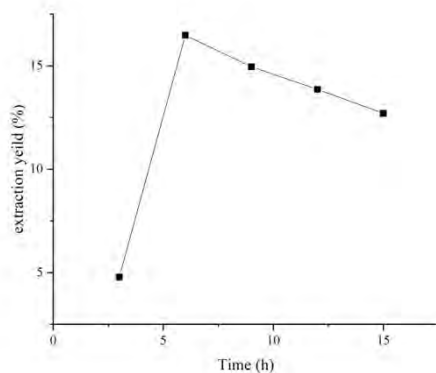


Fig. 4. Relationship between extraction yeild and solid-liquid ratio

3.3.4 Optimization of the collagen extraction based on microwave irradiation

According to the results of single factor experiment in which collagen was extracted by microwave irradiation, the extraction yeild was taken as the target parameter, and the orthogonal tests of three factors and three levels were carried out on the solid-liquid ratio (1:35, 1:40, 1:45), irradiation time (6, 7, 8 h) and irradiation temperature (33, 35, 37 °C). Wherein the extraction temperature

selected is no higher than the critical denaturation temperature which is 37 °C. The experimental results are shown in Table 3.

Table 3. Orthogonal test results of collagen extraction by microwave irradiation.

Number	A	B	C	Extraction yeild /%
1	33	1:35	6	5.98
2	33	1:40	7	10.77
3	33	1:45	8	8.59
4	35	1:35	7	11.65
5	35	1:40	8	7.78
6	35	1:45	6	10.38
7	37	1:35	8	11.48
8	37	1:40	6	10.80
9	37	1:45	7	11.49
K ₁	25.34	29.11	27.16	
K ₂	29.81	29.36	33.91	
K ₃	33.77	30.46	27.85	
R	8.42	1.36	6.75	
S	11.84	0.35	9.19	

According to the analysis of the orthogonal test, the extraction yeild of No. 4 test was the highest (11.65%), and the corresponding extraction conditions were A₂=35 °C, B₁=35, and C₂=7 h. S and R are the variance and range of K₁, K₂ and K₃, respectively. The larger the variance and the range difference, the more significant the influence of this factor on the test results. The analysis results in S₁>S₃>S₂ and R₁>R₃>R₂, illustrating that the order of the influence on the extraction yeild was as follows: irradiation temperature > irradiation time > solid-liquid ratio. Optimal level obtained by the combination is A₃B₃C₂, that is, the irradiation temperature is 37 °C, the ratio of material to liquid is 45:1, and the irradiation time is 7 hours. Under this condition, the verification experiment showed that the extraction yeild of collagen was 14.35%, and the corresponding product was called experimental product; while heated under the same condition by traditional water bath, the extraction yeild of collagen was 9.30%, and the corresponding product was called control product. In contrast, microwave irradiation extraction technology can significantly improve the extraction yeild of collagen, and has a good application prospect.

3.4 Structure and properties of collagen extracted by microwave irradiation

3.4.1 Amino Acid Composition

The molar percentages of the respective amino acids in the EP and the CP are shown in Table 4. Glycine, proline and alanine were the main amino acids of the two products, and among them, the content of glycine was the highest. The molar percentage of glycine in the experimental product and the control product was 33.90% and 34.38% respectively, which accorded with the proportion of glycine in bovine collagen²¹. Besides, the contents of proline and alanine were about 10% of the total molar content. The ratio of hydroxyproline to proline of the experimental product was 0.59, which was similar to that of the control product (0.63), indicating that the stability of the two products was comparable²². In addition, trace amounts of tyrosine showed the presence of terminal peptide residues in the product²³. The existence of a small amount of other amino acids (such as glutamic acid, arginine, aspartic acid, etc.) proved that the product was consistent with the primary structure of collagen, and its basic composition was collagen.

Table 4. Amino acid composition of experimental and control product.

Amino acid	Molar percentage /%	
	EP	CP
Asp	4.41	4.55
Thr	1.52	1.72
Ser	3.77	3.73
Glu	7.72	7.60
Gly	33.90	34.38
Ala	10.54	10.17
Val	1.32	0.22
Met	0.63	2.53
Ile	1.41	1.33
Leu	3.10	3.04
Tyr	0.22	0.43
Phe	1.89	1.96
Hylys	0.76	0.77
His	0.38	0.31
Lys	2.94	2.86
Arg	5.48	5.35
Hypro	7.40	7.42
Pro	12.60	11.64

3.4.3 UV-Vis Spectra

The absorbance of collagen solution in the range of 200-400 nm was measured by UV spectrophotometer with 0.5 mol/L acetic acid solution as the blank, and the EP, CP and standard type I collagen ultraviolet spectrum were obtained, shown in diagram 5. Collagen contains phenylalanine and tyrosine, which have sensitive chromogenic groups and characteristic absorption peaks at 258 nm and 278 nm, respectively. Their superposition of UV absorption gives collagen a maximum absorption peak below 300 nm Fehler! Verweisquelle konnte nicht gefunden werden.. The UV spectrum of the product showed that the standard type I collagen, experimental product and control product all had maximum absorption peak at 234 nm, which was accorded with the characteristics of collagen. At the same time, the results showed that microwave irradiation would not destroy the primary structure of collagen.

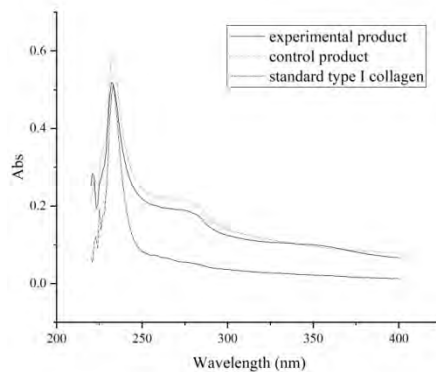


Fig. 5. Ultraviolet spectra of EP, CP and standard type I collagen.

3.4.4 FT-IR spectra

A scanning image by the Fourier transform infrared spectrometer of the EP, the CP and the standard type I collagen is shown in Fig. 7.

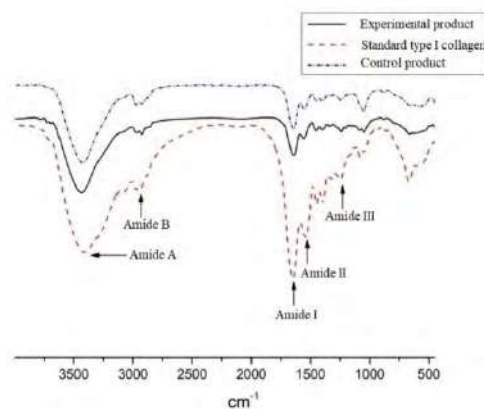


Fig. 6. Infrared spectra of EP, CP and standard type I collagen.

As can be seen from fig. 7, there is an absorption peak of the amide A band caused by the stretching vibration of NH at $3400\text{--}3440\text{ cm}^{-1}$. Absorption peak at $2800\text{--}3000\text{ cm}^{-1}$ is a stretching vibration peak generated by the asymmetric CH_2 of the amide B band. The amide I band absorption peak located between $1640\text{--}1660\text{ cm}^{-1}$ is the main characteristic absorption peak of collagen infrared spectrum, that is the vibration peak of the C=O group forming the hydrogen bond in the triple helix, which is often used for the secondary structure analysis of collagen ^{Fehler! Verweisquelle konnte nicht gefunden werden.}. Due to the C-N stretching vibration and N-H bending vibration of collagen, the absorption peak of the amide II band appeared at $1500\text{--}1600\text{ cm}^{-1}$, and the absorption peak of the amide III band was produced between $1200\text{--}1360\text{ cm}^{-1}$. Therefore, it can be speculated that the product possess a complete triple helix structure ²⁶. The absorption peaks of the experimental product, the control product and the standard type I collagen were almost in the same position, which indicated that the microwave irradiation extraction technology would not destroy the structure of the product.

3.4.5 Denaturation temperature

There are two endothermic peaks of predenaturation transition and main denaturation transition on the typical collagen VP-DSC curve, corresponding to the transition temperatures T_{m1} and T_{m2} , respectively. Among them, T_{m2} is an important indicator of the thermal stability of collagen, and

the greater the value, the higher the stability of collagen²⁷. Table 5 shows the thermal denaturation temperature of collagen products obtained by different extraction methods. The thermal denaturation temperatures of the experimental product, the control product and the standard type I collagen were 38.82 °C, 38.91 °C and 39.09 °C, respectively, which were consistent with the thermal denaturation temperature of cowhide reported in the literature^{Fehler! Verweisquelle konnte nicht gefunden werden.}. Compared with the control product, the thermal denaturation temperature of the experimental product did not change significantly, indicating that the extraction of collagen by microwave irradiation did not change its thermal stability. Based on the analysis of amino acid composition, and infrared spectrum, the collagen extracted by microwave irradiation can maintain the natural structure.

Table 5. Thermal denaturation temperature of the products and the standard.

Sample	EP	CP	Standard type I collagen
Denaturation temperature/°C	38.82	38.91	39.09

4 Conclusions

In this study, the collagen was extracted under the conditions of microwave irradiation by acetic acid with the traditional water bath heating as the control. The effect of microwave on the extraction yield of collagen was explored, and the optimum extraction process was obtained by orthogonal experiment. A variety of methods, including FTIR, VP-DSC, UV-Vis and amino acid analysis, demonstrated that microwave irradiation did not change the natural structure of collagen. The results displayed:

- (1) Irradiation temperature is positively correlated with extraction yield. Within a certain range, the extraction yield increases with the decrease of the solid-liquid ratio and the prolongation of irradiation time. And the optimum conditions for extracting collagen by microwave irradiation are 37 °C, 7 h and ratio of material to liquid 1:45. Moreover, extraction yield significantly increased by microwave irradiation was 1.5 times higher than that of traditional water bath heating, which was 14.35%.
- (3) Amino acid composition analysis confirmed that the basic composition of the product was collagen. Compared with the standard type I collagen, its UV absorption peak accorded with collagen characteristics and the absorption peak of infrared spectrum did not migrate. The thermal denaturation temperature was 38.82 °C. These results demonstrate that the product extracted by microwave irradiation was type I collagen with natural triple helix structure.

Acknowledgements

The authors wish to thank the National Natural Science Foundation of China (No. 21576171) for financial support.

References

1. Shoulders, M. D. Raines, R. T.: 'Collagen Structure and Stability', *Annual Review of Biochemistry*, 78 (1), 929-958, 2009
2. Peiren, L.: 'Collagen surgical suture', *Gelatin Science and Technology*, 21 (2), 79-82, 2001
3. Zhu, D. Y. Li, Y. C. Jin, L. Q. et al.: 'Study on the binding properties of collagen peptides to calcium', *Chinese Leather*, (03), 29-32, 2005
4. Liang, M. Z.: 'Application of protein in Cosmetics', *Guangdong Chemical Industry*, 36 (12), 104-105, 2009

5. Shen, J. Q. Tang, J. Shen, Y. L. et al.: 'Study on preparation of Kraft Collagen by Acid method and its structure and Properties', *Food Industry*, 43 / 46, 2009 (4)
6. Liu, D. Wang, L. Q. Ren, Y.: 'Study on Enzymatic extraction of Collagen from Porcine Achilles tendon', *Food Industry*, 72 / 77, 2017 (10)
7. Hu, J. P. 'Study on extraction and Properties of Fish scale Collagen by Acid method', *Food Science and Technology*, 37 (11), 141-148, 2012
8. Gu, Y. J.: 'Study on preparation and Properties of Grass Carp scale Frozen', *Shanghai Ocean University*, 2013
9. Qian, M. Wu, X. Z. Qiu, C. G. et al.: 'Study on extraction Technology and Properties of Fish scale Collagen by Thermal method and Enzymatic Hydrolysis', *Food Industry Science and Technology*, 70 / 72, 2007 (10)
10. Elstow, S. F. Weiss, J. B.: 'Extraction, isolation and characterization of neutral salt soluble type V collagen from fetal calf skin', *Collagen&Related Research*, 3 (3), 181-193, 1983
11. Huang, K. M. Yang, X. Q.: 'New progress in the study of non-thermal effects in microwave accelerated chemical reactions', *Progress in Natural Science*, 16 (3), 273-279, 2006
12. Zhong, C. H. Li, C. M. Liang, J. N. et al.: 'Optimization of extraction Technology of Collagen from Fish scal', *Food Science*, 162 / 166, 2006 (07)
13. Li, X. W. Li, H. Q.: 'Optimization of microwave-assisted extraction of collagen from pig skin', *Food Science*, 33 (6), 11-14, 2012
14. Zhang, Z. Li, G. Shi, B.: 'Physicochemical properties of collagen, gelatin and collagen hydrolysate derived from bovine limed split wastes', *Journal of the Society of Leather Technologists and Chemists*, 90(1), 23-28, 2006
15. AOAC.: 'Official methods for analysis', *Association of official analytical chemist Inc*, Arlington, 2000
16. Huo, R. G.: 'Application and limitation of Lambert-Beer's Law in Chemical Analysis' *Academic Weekly*, 14-15, 2013 (33)
17. Liu, Z. F. Lu, W. J. Dai, S. J. et al.: 'Progress in extraction, Modification and Application of Collagen', *Food and Drug*, 16 (6), 443 447, 2014
18. Gu, Q. S.: *Collagen and clinical medicine*, *Second military Medical University Press*, 2003.
19. Lin, S. R. Chen, B. Wang, Q. et al.: 'Research progress on properties and preparation methods of collagen', *Fisheries Research*, 40 (05), 73-81, 2018
20. Min, R.: 'Study on extraction of Collagen Peptide from Chondroitin Sulfate residue by Microwave-assisted Enzymatic Hydrolysis', *Food and Food Industry*, 51 / 54, 2016 (3)
21. Li, H. Liu, B. L. Gao, L. Z. et al.: 'Studies on bullfrog skin collagen', *Food Chemistry*, 84 (1), 65-69, 2004
22. Josse, J. Harrington, W. F.: 'Role of pyrrolidine residues in the structure and stabilization of collagen', *Journal of Molecular Biology*, 9(2), 269-287, 1964
23. Brown, E. M. Farrell, H. M. Wildermuth, R. J.: 'Influence of Neutral Salts on the Hydrothermal Stability of Acid-Soluble Collagen', *Journal of Protein Chemistry*, 19 (2), 85-92, 2000
24. Li, H. Liu, B. L. Chen, H. L. et al.: 'Enzymatic extraction of Pig skin Collagen and its structure characterization', *Chinese Leather*, 31 (23), 14-16, 2002
25. Zhong, C. H. Li, C. M. Gu, H. F. et al.: 'Effect of temperature on secondary structure of fish scale collagen', *Spectroscopy and Spectral Analysis*, 27 (10), 1970-1976, 2007
26. Plepis, A. M. G. Das-Gupta, D. K. Goisis, G.: 'Pyroelectric properties of anionic collagen and anionic collagen: P(VDF/TRFE) composites', *International Symposium on Electrets*, 2002
27. Ding, C. Zhang, M. Wu, K. et al.: 'The response of collagen molecules in acid solution to temperature', *Polymer*, 55 (22), 5751-5759, 2014

MINIMIZATION OF THE ENVIRONMENTAL IMPACT IN THE CHROME TANNING PROCESS BY A CLOSED-LOOP RECYCLING TECHNOLOGY

L. Jin¹, S. Xiu¹, Y. Wang¹, Z. Zhang², J. Fang³ and E. Shen³

1 Qilu University of Technology, School of Light Industry and Engineering, Jinan, China

2 BIOSK Chemicals Co., Ltd, Shangqiu, China

3 Shandong Juncheng Leather Industry Co., Ltd, Linyi, China

a) Corresponding author: jin-liqiang@163.com

Abstract. It is acknowledged that conventional chrome tanning in leather processing discharges significant amounts of chromium, dissolved solids and chlorides. The recycling technology is one of the effective solutions to reduce the environmental impact of chrome tanning waste water at source. In this work, a novel closed recycling technology of chrome tanning wastewater was applied in the tanning process of the goat skins at a pilot scale level. The properties of chrome tanning liquors obtained by the recycling technology and the resultant crust were analysed. The results show that this close recycling process works well. The contents of Cr₂O₃, total organic carbon, and ammonia nitrogen in the waste water tend to accumulate with the increase of recycling times, and finally reach a balance after 5 times of recycling. The obtained leather sample is full, soft and having a shrinkage temperature comparable to that of conventional chrome tanned leather. SEM images indicate that the resulting leather samples by this recycling technology show fine and clean grain and well-dispersed fibrils. Compared with conventional chrome tanning technology, water, salt and chrome tanning agent are saved in this process. The cleaner production technology exhibits promising application prospect for its economic and environmental benefits.

1 Introduction

Tanning operation in leather making is the most important process which converts the perishable hides and skins into useful and durable leathers [1-3]. In this step, many kinds of tanning agents, such as metal salts, aldehyde derivatives, syntans and vegetable tannins, are used single or combinedly to produce leather with different properties and styles. Nonetheless, not only the handing qualities but also the hydro-thermal stabilities of leathers tanned by other tanning agents cannot parallel to these of chrome tanned leather [4-5]. Up to now, 90% of the leathers were produced by chrome tanning method [6], which makes them more versatile. Hence, chrome tanning method will still keep its dominant position for a long time and not be replaced entirely in the future.

However, the conventional chrome tanning method is facing the pollution pressure of discharged chrome salt, which potentially negative effects on the environment and human health. Generally, less than 70% chrome tanning agent was fixed on the leather, resulting in the concentration of chrome in spent water is high to 2500-3000mg/L [7-8]. On the other hand, at least 6% of sodium chloride is used in the pickling process to protect the collagen matrix from acid swelling [4], and all of the chloride would be discharged in effluent at the end of tanning. It was reported that approximate 27.5 billion liters of chrome tanning wastewater containing 24 kilotons of chrome salt, 340 kilotons of chloride and 270 kilotons of sulphate are drained from tanneries in worldwide every year [6]. In order to protect our environment, strict statutory limits have been set for chrome, chloride as well as other contaminants in China. According to the Chinese "Discharge Standard of Water Pollutants for Leather and Fur Making Industry", the limits of total chrome discharged into sewage and chloride discharged into water bodies are 1.5mg/L and 3000mg/L, respectively. Therefore, developing much cleaner chrome tanning processing has drawn great attention of global leather technologists.

In order to resolve the chloride pollution, the salt-free or low-salt pickling technologies were developed, in which non-swelling acids were used to replace formic and sulphuric acid. The non-swelling acids are mainly aromatic sulfonic acids, and some aromatic sulfonic acids such as phenol sulfonic [9], phenol sulfone sulfonic [4], naphthalene sulfonic [10] and naphthol sulfonic acid [4] were applied in the pickling processes to reduce the dosage of chloride. Although a large proportion (at least 80%) of sodium chloride was reduced in these researches, the widely commercial applications of these technologies are limited by the dissatisfactory qualities of result leather.

In the case of the resolution of chrome pollution, the high-exhaustion chrome tanning methods and chrome recovery technologies from wastewater for reuse were reported. The application of varied high-exhaustion auxiliaries such as small molecules glyoxylic acid and aliphatic dicarboxylates [11], low molecular weight acrylic copolymers [12], and hydroxyl-terminated dendrimer [13] is a convenient method to increase the chrome uptakes. Besides of these, new nanocomposites with multiple carboxyl groups were prepared for enhancing the uptake of chrome salt [2, 7]. However, the concentrations of chrome in the spent float were much higher than the limit of 1.5mg/L [2]. In view of this, recovery of chrome from tanning effluents and its reutilization technologies were drawn much more attentions. Some researches on recovering and concentrating chromium salts from exhausted baths through membrane filtration (ultrafiltration and nanofiltration) on laboratory scale were carried out [14-15]. The properties of leathers tanned by recycled chrome were similar to these of leather tanned by traditional methods. Whereas, the high cost of membranes makes this technology difficult to be a popular option.

All of the researches above mainly focused on the eliminating of chemicals discharge, while the reduction of water usage in tanning industry has also to be considered. Hence, the recycling strategy of wastewater is considered as an alternative approach to both increase the utilization coefficients of leather chemicals and save a large quantity of water. In present recycling systems, chrome salts are mainly used indirectly, namely the chrome was precipitated firstly and then acidified for using in pickling, tanning, or re-tanning process [16-18]. However, the water bath quality would deteriorate after several recycles and pigmentation would appear on the grain layer, which has negative effect on the appearances of finished leather [16, 19].

In recent years, a closed cycle technology of chrome tanning wastewater developed by BIOSK chemical company has been gradually applied in some cattle tanneries in China. In present work, this novel closed recycling technology was applied in the tanning process of the goat skins at a pilot scale level, and the properties of chrome tanning liquors obtained by the recycling technology as well as the qualities of crust leather were analysed.

2 Experiments

2.1 Materials

The goat skins were supplied by a local tannery in China (Shandong Juncheng Ltd.), and about 105 pieces (150Kg, calculated according to the weight of limed pelts) of skins were used in single recycle. The fungicide DK and basifying agent BE were supplied by BIOSK CO., and other chemicals used in the experiments were industrial grade.

2.2 The recycling formulation of chrome tanning wastewater

The tanning process (the 6th recycle) using chrome tanning wastewater was shown in Table 1. The chrome-contained wastewater was collected at the end of tanning process, and about 90% of chrome tanning effluent was collected due to the limitation of practical conditions. One third of the collected chrome baths was used in the next pickling process and the rest was added into drum at basifying step.

Table 1. The pickling and tanning process of the 6th recycle by using spent liquors.

Process	Chemical	Dosage %	Temp. (°C)	Time (min)	Remark
Pickling	Residual water	20	18		
	salt	4.0			
	5063	0.2		10	Baume degree 5.8
	Formic acid (85%)	0.5		10	1:10 diluting
	Sulfuric acid (96%)	1.0		20	1:10 diluting, ×2
	Chrome tanning effluent (20°C) / Pickling auxiliary D	60/0.15		60	×3, pH 2.6, full penetration
Tanning	Sodium formate	0.5		30	
	Chrome powder	3.0		30	
	Chrome powder	3.0		60	full penetration
	Chrome powder	0.2		30	
	Basifying agent BE	0.25		60	pH ≥ 3.1
	Basifying agent BE	0.25		90	pH 3.4
	Sodium bicarbonate	0.2		20	pH ≥ 3.5
	Sodium bicarbonate	0.1		10	pH ≥ 3.6
	Chrome tanning effluent (70°C)	120		10	39 °C
	Mildew preventive DK	0.15			
Pickling auxiliary D	0.2		20	overnight, pH ≥ 3.6, Baume degree 8.4	

2.3 The chemical analysis of spent tanning wastewater

About 500 mL wastewater of each recycle was filtered twice by double layers of gauze for analysing. The pH values, Baume degrees, chrome contents, and ammonia concentrations of tanning wastewater of 9 cycles were investigated. Additionally, the waste liquors were diluted 500 times and filtered through filter membrane (0.45 µm) for the total organic carbon (TOC) (TOC-L CPH CN20, SHIMADZU) values analysis.

2.4 The characterization of the wet-blue samples

The contents of Cr₂O₃ and shrinking temperatures of wet blues were determined accordance to Chinese standard QB/T 2720-2005 and QB/T 2713-2005, respectively. The morphologies of the grain layers and cross sections of the wet blues were investigated by an Environment Scanning Electron Microscope (ZEISS EVO18, Germany). The L*, a*, b*, C*, and DE* coordinates of the wet-blue samples were measured using a X-rite 8200 spectrophotometer, and the viewing conditions used were illuminant D65, 10° standard observer.

2.5 The physical and mechanical properties crust leathers

The tensile strength, bursting strength, tear strength, and other related properties of the crust leathers were tested due to Chinese industrial standard QB/T 2710-2005, 2712-2005, 2711-2005, et al.

3 Results and discussion

3.1 The chemical analysis of spent tanning wastewater

The pH values and Baume degrees of the spent water from zero recycle (control) to the 9th recycle were shown in Fig. 1. It was observed that the pH values decreased slightly as increase of recycle times, and it

was stable at around pH 3.2. On the other hand, the Baume degrees of the wastewater increased gradually with the recycle times as the accumulation of the salts. The pH and Baume degree properties of wastewater make it be suitable for reusing in pickling and tanning processes. Thus we further investigated the chrome concentration, TOC and ammonia nitrogen values in the wastewater of the each recycle.

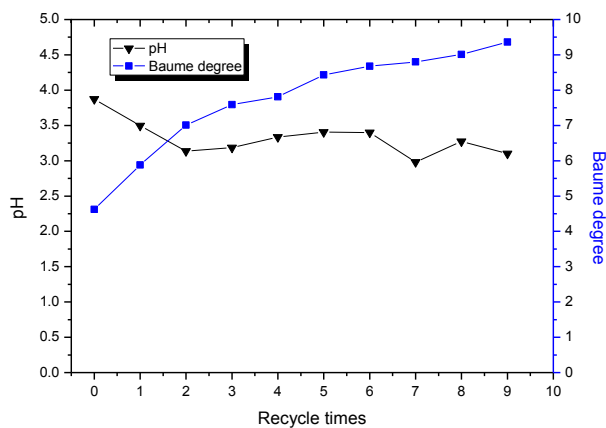


Fig. 1. The pH and Baume degree of wastewater from zero to the 9th recycle.

The Cr₂O₃ contents, TOC and ammonia nitrogen values of the wastewater from zero to 9th recycle were shown in Fig. 2. The Cr₂O₃ concentration increased greatly at the initial several recycles, it accumulated from about 2000mg/L to 4000mg/L. After 9 recycle times, the Cr₂O₃ concentration was stable at around 5000mg/L. It was because the chrome tanning agent could not be adsorbed absolutely by the skins and consequently the residual chromium accumulated in the wastewater. According to the chrome salt contents in the last used water, the dosage of chrome tanning agent was constantly adjusted in the next recycle. Therefore, the quality of the leathers would be guaranteed, while the chromium concentration in the effluents would be at balance. The changes of TOC and ammonia nitrogen values in the wastewaters were similar to that of chrome salts. The TOC values of the wastewater were stable at about 3000mg/L, and the ammonia nitrogen values were balance at around 230mg/L. In the pickling and tanning processes, the TOC and ammonia nitrogen might result from the slight dissolution of some protein of the goat skin, which hardly effected on the penetration and combination of chromium.

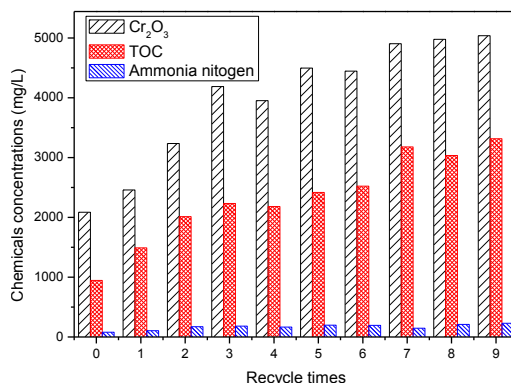


Fig. 2 The contents of Cr₂O₃, TOC and ammonia nitrogen in each recycle spent liquor

3.2 The characterization of the wet-blue samples

Some properties of the wet-blue sample were analysed to research the effect of the usage of wastewater on the qualities of the leather. Firstly, the Cr₂O₃ contents in wet-blue samples as well as

their shrinking temperatures (Ts) were measured, and the results were shown in Fig. 3. Totally, the Cr₂O₃ contents in the leather samples produced by recycle processes varied from 3.1% to 3.7%, which were close to that of the control (3.8%). All of the shrinking temperatures of leathers manufactured by this closed recycle process were higher than 104°C. These results proved that the closed recycle process of tanning wastewater was stable for leather making.

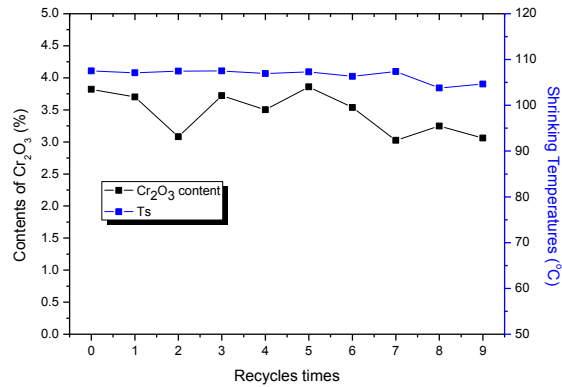


Fig. 3 The Cr₂O₃ contents in wet-blue samples produced by recycle process and the shrinking temperatures of leather samples

Besides of these, the appearances of the wet blue grain layers and the dispersion conditions of collagen fibers on cross sections of samples were observed by SEM, and the images of the wet blues produced in the 0, 5th and 9th recycles were shown in Fig. 4. Compared with the grain layer of the control (Fig. 4a-1), the hair pores on the wet-blue samples produced in the 5th and 9th recycle were also clearly, shown in Fig. 4b-1 and c-1 respectively. Meanwhile, their collagen fibers were opening well and dispersed evenly (shown as Fig.4 b-2 and c-2), which were very similar to that of the control which was shown in Fig. 4a-2. Basing on the SEM images, it can conclude that the close recycle process of tanning wastewater is feasible.

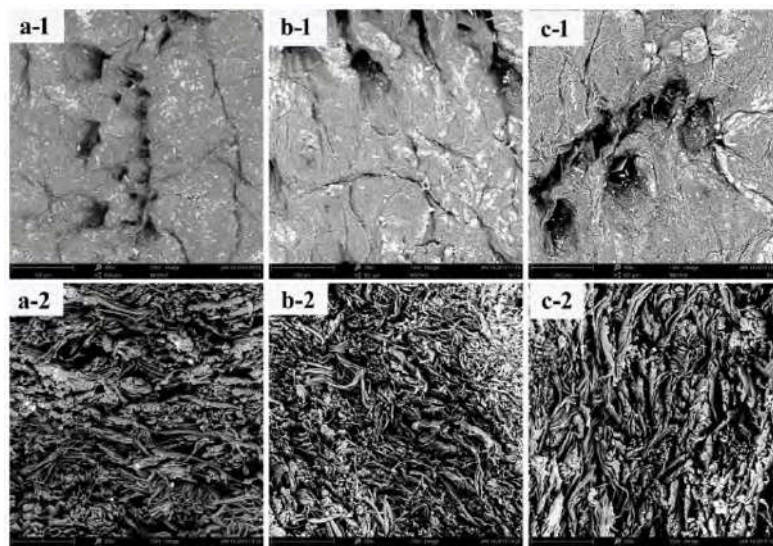


Fig. 4 The grain layer and cross-section SEM images of wet-blue produced in: (a) control, (b) the 5th recycle and (c) the 9th recycle

Table 2. The color coordinates of leather samples.

Samples	L^*	a^*	b^*	DE^*	\overline{DE}^a
0	59.00	-6.50	-6.50	42.02	41.89
	58.50	-6.10	-6.30	42.42	
	59.90	-6.70	-6.90	41.24	
1	58.50	-6.40	-7.10	42.59	41.99
	59.50	-6.20	-7.00	41.57	
	59.20	-6.10	-6.80	41.81	
2	58.30	-7.00	-8.00	43.03	42.86
	58.00	-6.90	-7.70	43.25	
	58.90	-6.70	-7.40	42.29	
3	59.80	-6.10	-6.10	41.12	41.56
	59.00	-5.40	-6.30	41.83	
	59.20	-5.80	-6.60	41.74	
4	60.40	-6.10	-7.20	40.71	41.02
	59.70	-6.20	-6.70	41.32	
	60.00	-6.20	-6.70	41.03	
5	60.20	-6.30	-7.50	40.99	41.10
	60.10	-6.40	-7.10	41.03	
	59.80	-6.10	-7.20	41.29	
6	59.90	-6.30	-7.10	41.21	41.10
	60.20	-6.20	-7.20	40.92	
	59.90	-6.10	-7.00	41.16	
7	61.90	-6.90	-7.70	39.48	40.34
	59.90	-6.30	-7.00	41.19	
	60.70	-6.20	-6.70	40.35	
8	61.40	-6.60	-7.80	39.93	40.33
	61.30	-6.50	-7.90	40.03	
	60.30	-6.40	-8.10	41.02	
9	63.00	-6.50	-8.20	38.45	38.84
	61.90	-6.40	-7.90	39.43	
	62.80	-6.50	-8.20	38.64	

a: the average of DE^*

Generally, the color of the wet-blue is a key quality standard in leather making. Hence, the colors of the wet blue samples produced by traditional tanning process and the closed recycle process of wastewater were characterized by color coordinates, namely L^* , a^* , b^* , and DE^* values. According to the definition of color coordinates, the L^* value reflects the brightness of the sample, while the negative b^* value indicates that the sample is blue. Principally, the L^* value and the absolute of b^* increased slightly with the increase of recycle time, as listed in table 2. It manifests that the blue appearance qualities of the wet-blues produced by the closed recycle process of wastewater had no obvious batch differences. Except the sample produced in the 9th recycle, the average of DE^* value was close to each other, which indicated that the color differences of these samples were hard to find by naked eyes. The SEM and color coordinates analysis above verified that the closed recycle process of tanning wastewater can run stably in pilot scale.

3.3 The characterization of the crust leather samples

Furthermore, the physical and mechanical properties of the crust leathers were measured to evaluate the effect of the closed recycle process of tanning wastewater on the performances of the crust leather, which results were listed in table 3. The tensile strength of the crust leathers were approximate to that of the leather produced by traditional chrome tanning method. However,

compared with the control, the variation of the tearing strength and bursting strength of the samples was much larger. It was probably because these mechanical properties were much closer to the fiber structure properties of individual goat skin.

Table 3. The physical and mechanical properties of the crust leathers.

Samples	Tensile strength (N/mm ²)	Bursting strength (N/mm)	Tear strength (N/mm)
0	23.75	399.02	39.40
1	24.11	392.15	38.85
2	23.01	391.40	38.28
3	23.22	366.88	29.35
4	22.46	343.41	28.43
5	20.48	310.94	30.96
6	22.85	308.04	45.55
7	21.84	379.75	29.14
8	19.68	321.27	36.82
9	21.05	319.97	45.32

3.4 Economic analysis

The advantages of the closed recycle process of tanning wastewater were saving water and chemicals dosage, meanwhile the discharge of wastewater was almost zero. The approximate dosages of main chemicals and fresh water in different tanning processes and their discharges of effluents were listed in table 4. In our experiments, about 1500kg goat skins were produced and about 270000Kg fresh water would be used in traditional tanning process. However, totally 51300Kg fresh water was used when the same amount of goat skins were produced by the closed recycle process of tanning wastewater. Above 4 fifths fresh water was saved. Moreover, the discharge of wastewater in the closed recycle process was only 1% of the traditional method, which was attributed to the technological limit. The closed recycle process can be considered as a zero discharge technology, which is very helpful to the sustainable development of the leather making industry and the protection of the environment. Additionally, the main chemicals such as sodium chloride and chrome tanning agent used in the tanning process of leather were saved greatly. Both the produce cost and the charge for wastewater treatment were decreased highly. Therefore, the closed-loop recycling technology of chrome tanning wastewater minimized the environmental impact in the chrome tanning process.

Table 4. The approximate dosages of main chemicals and fresh water in different tanning processes and their discharges of effluents.

Tanning Method	Weight of limed pelt (kg)	Water (Kg)	Sodium chloride (Kg)	Chrome powder (Kg)	Effluents (Kg)
Traditional	1500	270000	90	120	270000
Closed Recycle	1500	51300	30	90	2700

4 Conclusions

A closed-loop recycling technology of tanning wastewater was applied in the tanning process of the goat skins at a pilot scale level. It was found that the properties of the tanning wastewater were suitable for the reused in the pickling and tanning processes. The high contents of chrome salt, chloride sodium could save the dosage of relevant chemicals, while the TOC and ammonia nitrogen

values of the wastewater had little influence on the fixation of chrome according to the close shrinking temperatures of wet blue sampled produced in each recycle. The qualities of the wet blue were stable, which was estimated from the SEM and color coordinates results. Importantly, more than 4 fifths fresh water was saved and the discharge of wastewater in the closed-loop recycling process was only 1% of the traditional method in 10 times of tanning producing. It can be predicted that the water saving rate will be increased greatly with the recycling times, while the discharge of effluent will be decreased tremendously. Thus, this technology can minimize the environmental impact in the chrome tanning process and is deserved for researching deeply for further employing in large-scale tanning production.

References

1. Mengistie, E.: *Ultrasound assisted chrome tanning: Towards a clean leather production technology*, *Ultrasonics Sonochemistry*, 32, 204–212, 2016
2. Liu, M.: *Enhancement of chromium uptake in tanning process of goat garment leather using nanocomposite*, *J. Cleaner Prod.*, 133, 487-494, 2016
3. Nashy, E.H.A.: *Molecular spectroscopic study for suggested mechanism of chrome tanned leather*, *Spectrochim. Acta Part Mol. Biomol. Spectrosc.* 88, 171-176, 2012
4. Zhang, C.: *A salt-free and chromium discharge minimizing tanning technology: the novel cleaner integrated chrome tanning process*, *J. Cleaner Prod.*, 112, 1055-1063, 2016
5. John, S. V.: *Recovery and utilization of chromium-tanned proteinous wastes of leather making: a review*, *Crit. Rev. Environ. Sci. Technol.*, 41, 2048-2075, 2011.
6. Sathish, M.: *Cyclic Carbonate: A Recyclable Medium for Zero Discharge Tanning*, *ACS Sustainable Chem. Eng.*, 4, 1032–1040, 2016
7. Li, K.: *pH-Sensitive and Chromium-Loaded Mineralized Nanoparticles as a Tanning Agent for Cleaner Leather Production*, *ACS Sustainable Chem. Eng.*, DOI: 10.1021/acssuschemeng.9b00482, 2019
8. John, S. V.: *Cleaner chrome tanning emerging options*. *J. Clean. Prod.* 10, 69-74, 2002
9. Morera, J. M.: *Optimization of two low-salt chrome tanning processes without float*, *J. Soc. Leather Technol. Chem.*, 102, 121-128, 2007
10. Palop, R.: *Auxiliary agents with non-swelling capacity used in pickling/tanning process: Part 1*, *J. Soc. Leather Technol. Chem.*, 86, 139-142, 2002
11. Fuchs, K.: *Glyoxylic acid: an interesting contribution to clean technology*, *J. Am. Leather Chem. Assoc.*, 88, 402-413, 1993.
12. Luan, S.: *A novel pre-tanning agent for high exhaustion chromium tannage*, *J. Soc. Leather Technol. Chem.*, 91, 149-153, 2007.
13. Yao, Q.: *Mechanism and effect of hydroxyl-terminated dendrimer as excellent chrome exhausted agent for tanning of pickled pelt*, *J. Cleaner Prod.*, 202, 543-552, 2018
14. Cassano, A.: *Integrated Membrane Process for the Recovery of Chromium Salts from Tannery Effluents*, *Ind. Eng. Chem. Res.*, 46, 6825-6830, 2007.
15. Kiril Mert, B.: *Applicability of nanofiltration in the recovery of chrome tanning wastewater*, *Procedia Engineering*, 44, 1907-1909, 2012
16. Sundar, V.J.: *Cleaner chrome tanning emerging options*, *J. Cleaner Prod.*, 10, 69–74, 2002
17. Cao, S.: *Mechanism and Effect of High-Basicity Chromium Agent Acting on Cr-Wastewater-Reuse System of Leather Industry*, *ACS Sustainable Chem. Eng.*, 6, 3957–3963, 2018
18. Cao, S.: *Application of CRBD to Reducing Pollution of Leather Tanning Wastewater*, *Adv. Mater. Res.*, 800, 593–596, 2013
19. Morera, J. M.: *Minimization of the environmental impact of chrome tanning: a new process reusing the tanning floats*, *J. Cleaner Prod.*, 19, 2128–2132, 2011

THE CHARACTERIZATION OF VOLATILE ORGANIC COMPOUNDS (VOC) IN WET-WHITE AND METAL FREE LEATHER

Naviglio B.¹, Florio C.¹, Caracciolo D.¹, Gambicorti T.¹, Aveta R.¹, Girardi V., Scotti M.¹

1 Stazione Sperimentale Industria Pelli e Materie Concianti, Via Campi Flegrei, 34, 80078 - Pozzuoli - NA

Phone: 39-081-5979100, Fax: 39-081-265574

Corresponding author: c.florio@ssip.it; t.gambicorti@ssip.it

Abstract. In recent years, among the tanning sector, the so-called wet-white and/or metal-free concepts have had a certain increase. For example, in the automotive sector the wet-white tanning system, carried out with glutaraldehyde and tannins, has had widespread use. Automotive manufacturers, indeed, offer leather for interior furnishings not only for luxury cars but also in lower market segments. The components on which the leather upholstery is applied are mainly steering wheel, seats, dashboard and panels. Therefore, the use of leather also in this context must be able to meet both the aesthetic/performance criteria and the environmental ones; environmental criteria should also consider the air quality of the interior of a motor vehicle. In practice, the interior furniture consisting of finished leather should have to be able to release a few volatile substances and, at the same time, provide a typical smell of leather. Considering, therefore, the diffusion of alternative chrome tanning systems for the different uses, in this work, wet-white (glutaraldehyde and tannins) will be investigated, both from the point of view of the performance characteristics and from the ecotoxicological ones. Furthermore, leathers deriving from the latest generation of metal-free tanning, will be analysed. For the characterization of Volatile Organic Compounds (VOC) the GC-MS will be used coupled with the "Purge and Trap" technique with the aim of obtaining information on the new substances used in the wet-white / metal free production process and then avoiding undesired effects during use (eg bad smell, SVHC substances, etc.)

1 Introduction

Recently, an increase in the spread of leather tanned with alternative chrome systems and marketed under different names such as "wet-white", "chrome-free", "metal-free", etc. has been observed on the market; for example in the automotive sector the wet-white tanning system, carried out with glutaraldehyde and tannins, has had a widespread use.

In order to characterize these types of leathers (wet-white and latest generation tanning), various analytical investigations have been carried out to evaluate the presence of tanning metals and Volatile Organic Compounds (VOCs).

The evaluation of the tanning metals allowed to better define the type of tanning according to the current European Standard (EN 15987:2015) while the VOCs allowed to obtain information about any undesired effects concerning the bad smell and the possible presence of SVHC substances.

2 Materials and methods

The following leather samples have been analysed:

1. Bovine crust chrome tanned leather for automotive use
2. Bovine wet-white tanned crust leather for automotive
3. Bovine dyed crust leather tanned with latest generation of organic tanning for automotive
4. Sheep not dyed crust leather tanned with latest generation of organic tanning for leather goods

The bovine leathers were supplied by an Italian tannery of the Veneto district while the ovine one comes from the Solofra district. The samples were analyzed with the following instruments:

- *HP GC System/6890 - HP/5973 Mass Selective Chromatograph* equipped with a Purge & Trap *O.I.Analytical 4660* Sampler.
- *Thermo Fisher - ICAP RQ -Inductively Coupled Plasma Mass Spectrometry (ICP-MS)*.

3 Results and discussion

3.1 Tanning metals

Table 1 shows the analytical results relating to the tests carried out to evaluate the chemical characteristics of the samples, in order also to define the type of tanning in accordance with the standardize terminology of leather (EN 15987 European Standard).

Tab. 1. Chemical characteristics of the examined leathers

Parameter	Method	Sample 1 <i>Bovine crust chrome tanned leather for automotive</i>	Sample 2 <i>Bovine wet-white tanned crust leather for automotive</i>	Sample 3 <i>Bovine dyed crust leather with organic tanning for automotive</i>	Sample 4 <i>Sheep not dyed crust leather with organic tanning for leather goods</i>
Humidity and volatile substances (%)	EN ISO 4684	8,1	8,0	5,4	8,8
Mineral substances (%)	EN ISO 4047	5,1	1,1	1,6	2,5
Organic substances (%)	Residual substances at 102°C- 800°C	86,8	90,9	93,0	88,7
Determination of matter soluble in dichloro-methane (%)	EN ISO 4048	4,4	4,8	7,9	8,5
Determination of the pH of the aqueous extract	EN ISO 4045	3,70	4,80	5,10	3,70
Chemical determination of the Al content (mg/kg)	EN ISO 17072-2	1261	102	755	233
Chemical determination of the Cr content (mg/kg)	EN ISO 17072-2	31822	173	626	57
Chemical determination of the Fe content (mg/kg)	EN ISO 17072-2	286	52	122	123
Chemical determination of the Ti content (mg/kg)	EN ISO 17072-2	25	7	130	43
Chemical determination of the Zr content (mg/kg)	EN ISO 17072-2	-	-	-	5
Sum of tanning metals (mg/kg)	-	33394	334	1633	461

From the values found it is possible to gather that the dyed crust sample tanned with new generation tanning (sample 3), cannot be defined as "metal-free" considering that the sum of the tanning metals, equal to 1633 mg/kg, exceeds the value foreseen by the current standard (1000 mg/kg). Therefore, the adequate definition, from the European Standard point of view, is leather with organic tanning. In fact, in this case the sum of the tanning metals must be equal to or less than 0.3% (3000 mg/kg).

The other two not-chrome-tanned leathers examined (samples 2 and 4) show values of the total content of tanning metals less than 0.1% (1000 mg/kg). Therefore, in this case, leathers obtained with adopted tanning systems can be defined as "metal free".

3.2 VOC results

Figures 1, 2, 3 and 4 show the chromatograms obtained with the GC-MS Purge & Trap technique.

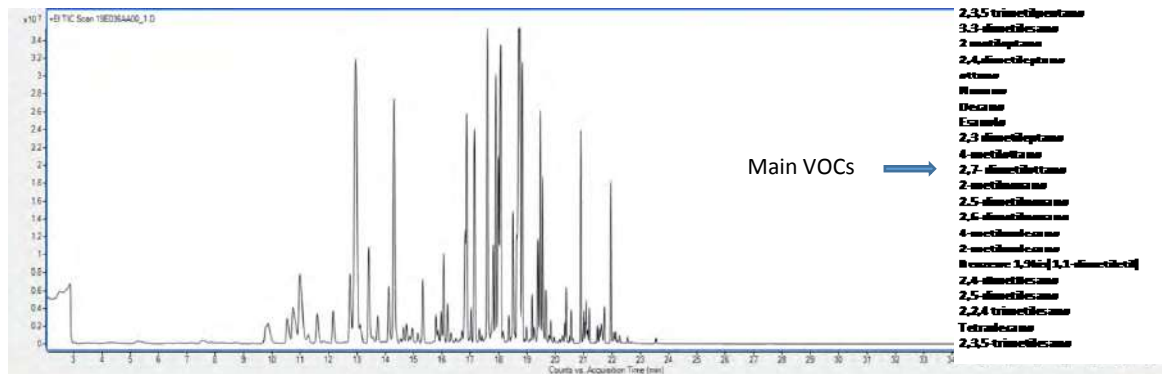


Fig. 1. Chromatographic profile of sample 1.

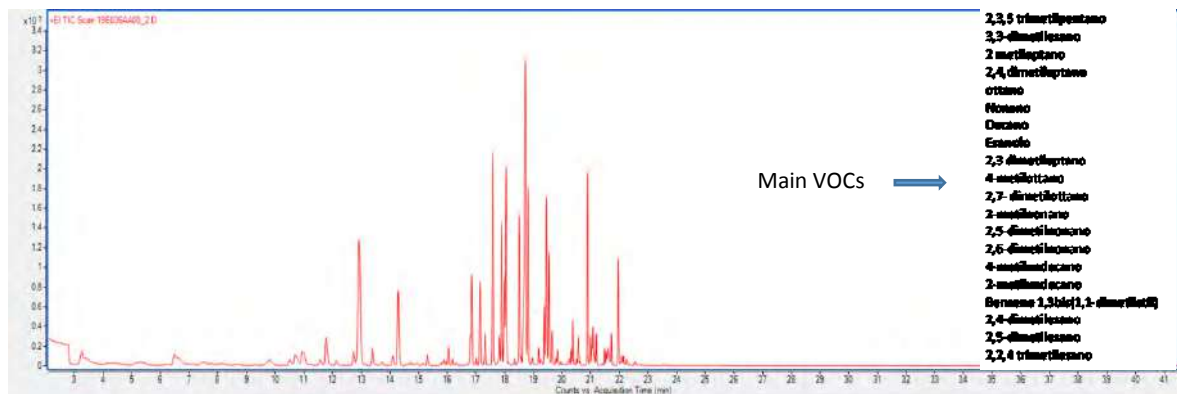


Fig. 2. Chromatographic profile of sample 2.

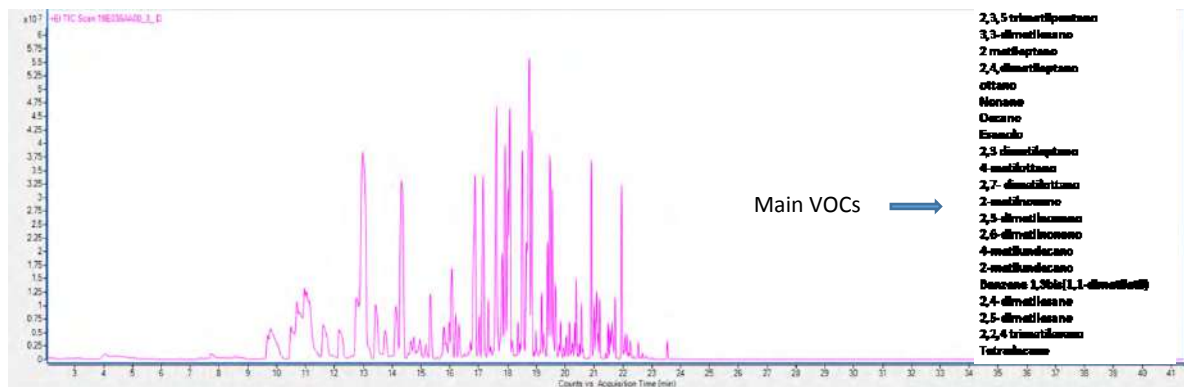


Fig. 3. Chromatographic profile of sample 3.

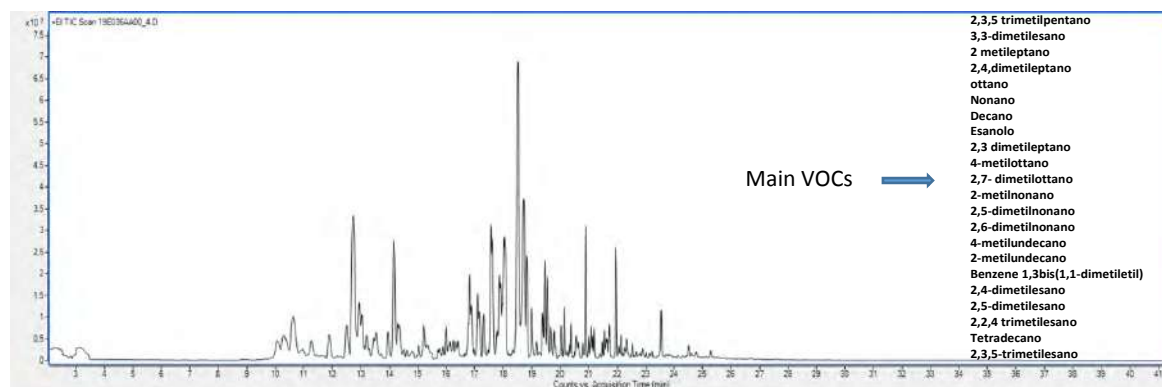


Fig. 4. Chromatographic profile of sample 4.

The results obtained can be summarized as follows:

Sample 1: The chrome leather crust shows the presence of volatile substances hydrocarbons based; in particular, the main constituents concern saturated aliphatic hydrocarbons such as 2,4 dimethyl heptane (CAS 2213-23-2) whose peak, retention time 12,959 minutes, has a higher% area (10.37%). The other families of volatile compounds that have an area greater than 1% are aldehydes (hexanal, Tr = 13413 min., A = 2.20%) and terpenes consisting predominantly of limonene (Tr = 18512, A = 1,93%).

Sample 2: Even the wet-white leather has predominantly VOCs made up mostly of alkanes such as 3.7 dimethyldecane whose peak, retention time = 18.720 min., Presents a higher% area (12.11%). The limonene, in this case, is present with an area% equal to about 4%. Unlike chrome leather, the presence of some aromatic hydrocarbons has also been found (eg toluene, Tr = 11773 min., A = 1.69%).

Sample 3: Bovine leather with new generation organic tanning agents similarly shows the preponderant presence of saturated hydrocarbons; the main component, in terms of area%, turns out to be, as in the previous case, 3.7 dimethyldecane (A% = 5.91). Terpenes such as limonene (A% = 2.61), aldehydes such as the hexanal (A% = 1.73) and long chain alcohols and 2.2 dimethyloctanol (A% = 1.25, Tr = 18650 min., CAS: 2370-14-1), are also present in a significant way. There are also traces of furans.

Sample 4: Finally, sheep's leather with new generation organic tanning agents as well as exhibiting volatile organic compounds such as alkanes of 2,4 dimethylheptane (A% = 7.12, Tr = 12732), aldehydes and limonene (A% = 9.37), it has peaks attributable to halogenated alkanes (eg 2-bromo dodecane, A% = 2.23, Tr = 18821). Also present aromatic hydrocarbons (eg para, ortho, meta xylene, 1,3-di.tert-butylbenzene).

4 Conclusion

The characterization of the leathers examined allowed to appropriately define the terminology of the type of tanning used; for example, according to the EN 15987 standard, metal-free leather must have a total content of tanning metals of less than or equal to 1000 mg/kg (0.1%), while that with organic tanning must not exceed 3000 mg/kg (0.3 %).

Concerning the characterization of Volatile Organic Compounds (VOCs), the analytical investigations have allowed to identify prevalently for all the samples examined the main families of compounds such as, for example, saturated hydrocarbons, aldehydes like the hexanal, terpenes like limonene. Aromatic hydrocarbons are sometimes present, in terms of A%, less significantly than in other families. In the case of sheep's leather with new generation organic tanning agents, the presence of halogenated hydrocarbons has also been highlighted.

Considering that the leathers examined are not finished it is possible to hypothesize that the families of volatile organic compounds identified with the Purge and Trap technique coupled with

GC-MS come from the fatliquoring phase. Future developments of the work may include the determination of VOCs after appropriate tests of artificial aging, for samples processed with different types of tanning.

References

1. B. Naviglio, M. Tomaselli, D. Naviglio, C. Raia, *Caratterizzazione gas-cromatografica delle componenti volatili di pelli e cuoi*, CPMC Anno 78 – n.2 marzo/aprile 2002
2. M. Tomaselli, B. Naviglio, D. Naviglio, G. Comite, G. Calvanese, *XXVIII IULTCS Congress-Firenze, March, 9-12 2005 The characterization of volatile organic compounds in leather*,
3. M. Tomaselli, B. Naviglio, G. Calvanese, G. Comite, D. Caracciolo, *Identification of volatile compounds in the vegetable tanned leather, II Eurocongrss IULTCS, Istanbul, 24-27 Maggio 2006*
4. Naviglio B., Calvanese G., Cipollaro L., Pierri G., *Caratterizzazione di prodotti chimici conciari: ingrassanti*, CPMC, 81(4), 231 (2005)
5. Naviglio B., Calvanese G., Caracciolo D., Florio C., Romagnuolo M., *L'odore del cuoio come parametro di qualità funzionale ed ecologica*, CPMC, 87, (4), 163-169 (2011)
6. M.Schropfer, M. Czerny, H. Schultz, P. Schieberle, *The Odor of Leather*, JALCA, 108, 94-107, 2013
7. R.M. Cuadros, A. Marsal, L.Ollè, A. Bacardit, J.Font, *Characterization of the volatile organic compounds by Hs-SPME-GC-MS in the leather sector*, JALCA,108, 420-427, 2013
8. E. Chorier, N. Blanc, J.C. Cannot, A. Berthod, *Headspace GC-MS for the determination of Halogenated Hydrocarbons, Ethers and Aromatic volatiles in fabric and leather*, Jalca, 109, 322-329, 2014

HIGH-EFFICIENCY CHROME TANNING USING PRE-TREATMENTS: SYNCHROTRON SAXS AND DSC STUDY

Yi Zhang, Jenna K. Buchanan, Geoff Holmes and Sujay Prabakar^a

Leather and Shoe Research Association of New Zealand, P.O. Box 8094, Palmerston North, 4472, New Zealand

a) Corresponding author: sujay.prabakar@lasra.co.nz

Abstract. Pre-treatments are widely used during tanning processes to improve the performance of the main tannage. To study the effect of each type of pre-treatment on chromium-collagen cross-linking reaction during tanning, synchrotron small-angle X-ray scattering (SAXS) and differential scanning calorimetry (DSC) were used to provide fundamental understanding of the overall performance of each process. Four common types of pre-treatment were investigated in this study: monodentate complexing agent (sodium formate, SF), chelating agent (disodium phthalate, DSP), covalent cross-linker (glutaraldehyde, GA) and nanoclay (sodium montmorillonite, MMT). Based on the structural and thermal analyses, the performance of chrome tanning with pre-treatments was presented considering five aspects: cross-linking, the level of hydration, hydrothermal stability, uniformity through leather cross-section and the uptake of chrome. At the same chrome offers, leather pre-treated using SF, DSP and MMT showed improved hydrothermal stability, uniformity and level of hydration, while GA showed decreased hydration. All of the pre-treatments reduce surface fixation by decreasing the reactivity of chromium with collagen. Insights into the structural changes of collagen during tanning with varied reaction conditions can guide the design of novel, benign tanning processes to reduce environmental impact.

1 Introduction

Pre-treatments such as masking or pre-tanning modify the collagen structure in skins and hides to improve the efficiency of the main tannage.¹ Chrome is one of the most common main tannages which is involved in around 90% of the world's leather production.²⁻³ However, its usage during tanning is so far inefficient, considering its excess usage to meet with the demanded production rate, leading to poorer uptake with the remainder discharged to the effluent.^{2,4} Many types of pre-treatments have been applied in chrome tanning to compensate for its weaknesses in efficiency via different mechanisms including complexing (masking), covalent cross-linking (pre-tanning) and electrostatic binding (filling or coating).¹ However, the molecular-level structure of collagen affected during the pre-treatments and chrome tanning are yet to be clarified.

Small-angle X-ray scattering (SAXS) has been applied to study the long-range ordered collagen structure in untanned skins and hides as well as leathers.⁵⁻⁹ During leather processing, the collagen fibrils in skins and hides showed significant changes that can be monitored using synchrotron-based SAXS. Differential scanning calorimetry (DSC) is used in combination with SAXS to study the hydrothermal stability of collagen in leather to provide an all-round image of the characteristic performance of each pre-treatment method. In this study, four mainstream pre-treatments were selected to represent different mechanisms including sodium formate (SF) as a monodentate complexing agent, disodium phthalate (DSP) as a chelating agent, glutaraldehyde (GA) as a covalent cross-linker, and sodium montmorillonite (MMT) as a nanofiller. A high-exhaustion chrome tanning process, "ThruBlu", was chosen as a model to highlight differences across the pre-treatments. The aim of this study is to establish an overall understanding of pre-treatments about their interactions with collagen and/or chromium, as well as the resulting properties of the leather products.

2 Materials and Methods

2.1 Leather processing

Pickled grain splits of cattle hide were processed using modified ThruBlu chrome tanning.⁷ Sodium bicarbonate was added to raise the pH to 7.5-8.0 before tanning. The pH is brought down to 4.0 by the acidity of chrome at the end of overnight processing.

For GA sample: pickled hides (uncross-linked hide, Col) were treated with 2.0% offer of 50% glutaraldehyde aqueous solution followed by neutralisation (Col-GA).

For other samples: pickled hides were neutralised (Col-STD), and then treated by different pre-treatments: 2.5% of Feliderm® DP solution (Col-DSP), 0.5% sodium formate (Col-SF) or 2.0% Cloisite® Na+ Nanoclay (Col-MMT).

Pre-treated samples were then tanned with Chromosal® B (basic chromium sulphate) at 3.0%, 4.5%, 6.0% offers overnight (named as Cr-1, Cr-2 and Cr-3, respectively). The wet blue leathers were then stored in a fridge (4°C) ready for further analyses.

2.2 Structural analysis using SAXS

Thin slices of hide samples were prepared using a microtome (Leica CM1850 UV, Leica Biosystems) to the same section size of 0.3 cm × 0.3 cm × 200 μm (L × W × H). Such slices were collected across grain, centre and corium layers of the leather cross-section and then air-dried at room temperature prior to SAXS measurement. SAXS measurements were carried out at beamline I22 at the Diamond Light Source. Dry leather slices were held between Kapton® tape to keep the moisture levels constant. The measurements were taken using 12.4 keV X-rays with a 9.7m sample-to-detector distance. The images were processed to q-plot ($q = 0.021 - 1.7 \text{ nm}^{-1}$) using Data Analysis Workbench (DAWN).¹⁰ SAXS data were then fitted to a combined population and fibre d-spacing model implemented using SAXSFit.¹¹ Relative peak intensity is calculated as $R_{i/j} = A_i/A_j$, where A_i stands for the area of peak order i .

2.3 Hydrothermal analysis using DSC

Samples were microtomed and rehydrated with DI water in sealed Tzero aluminium pans overnight, followed by ramping at 5°C/min from 30°C to 120°C under N₂ purge (DSC Q2000, TA Instruments). The temperature of the onset of the peaks on DSC curves were calculated as the denaturation temperature (T_d) of the hide sample. By carrying out measurements throughout the cross-section of leather, the lowest and highest T_d (i.e., T_{\min} and T_{\max}) were determined ($T_d = T_{\min}$). The range of T_d across the cross-section of each hide was calculated as: $R_T = T_{\max} - T_{\min}$.

2.4 Chrome uptake analysis using AAS

The percentage uptake of chrome (Up%) in leather samples as measured by Atomic absorption spectrophotometer (AAS) (SpectrAA 220FS, Varian). First, leather samples were hydrolysed using an excess amount of concentrated nitric acid and a mixture of perchloric acid and sulphuric acid to solubilise chromium species. Then, the mixtures were diluted with water followed by boiling for at least 10 min to eliminate the unreacted oxidising acids. The solutions were filtered and further diluted to an optimal concentration for AAS measurements (air/acetylene flame, wavelength = 357.9 nm, spectral bandwidth = 0.2 nm). Percentage uptake was then calculated as: $\text{Up}\% = 100\% * (\text{the amount of chromium in the leather after processing}) / (\text{the amount of chromium added during processing})$.

2.5 Overall performance

Overall performance of each pre-treatment method was compared according to the average ranking of (1) $R_{3/2}$; (2) T_d and (3) $Up\%$ by descending order, and (4) $R_{6/8}$ and (5) R_T by ascending order, of samples tanned with all three chrome offers.

3 Results and Discussions

3.1 SAXS: Structural analysis

Small-angle X-ray scattering of the standard chrome tanned hide sample showed a characteristic scattering pattern of fibrillar collagen (Fig. 1a), which originates from the long-range ordered packing of collagen molecules. The packing of collagen in hides follows a quarter-staggered arrangement with axial gap/overlap regions in a characteristic axial periodicity (D-period).¹² Due to the variation of electron density across the hide collagen matrix, the intensity of diffraction rings in the SAXS image changes amongst different orders.¹³ Therefore, SAXS allows us to study collagen structural changes during chemical cross-linking that disrupts the electron density distributions in the matrix. Tanning with 3.0%, 4.5% and 6.0% chrome offers (named as Cr-1, Cr-2 and Cr-3) changes the intensity of the diffraction peaks significantly (Fig. 1b).

To highlight the changes of each order peaks, the normalised intensity of all peaks was plotted across different processing stages (Fig. 2). While the 1st and 2nd order peaks showed a drastic decrease in intensity, the other peaks (3rd to 9th) increased to different extents. The overall peak intensity changes could be attributed to: (i) the enhanced electron density contrast due to the introduced chromium species to the matrix; (ii) the structural changes triggered by chromium-collagen covalent and non-covalent interactions.

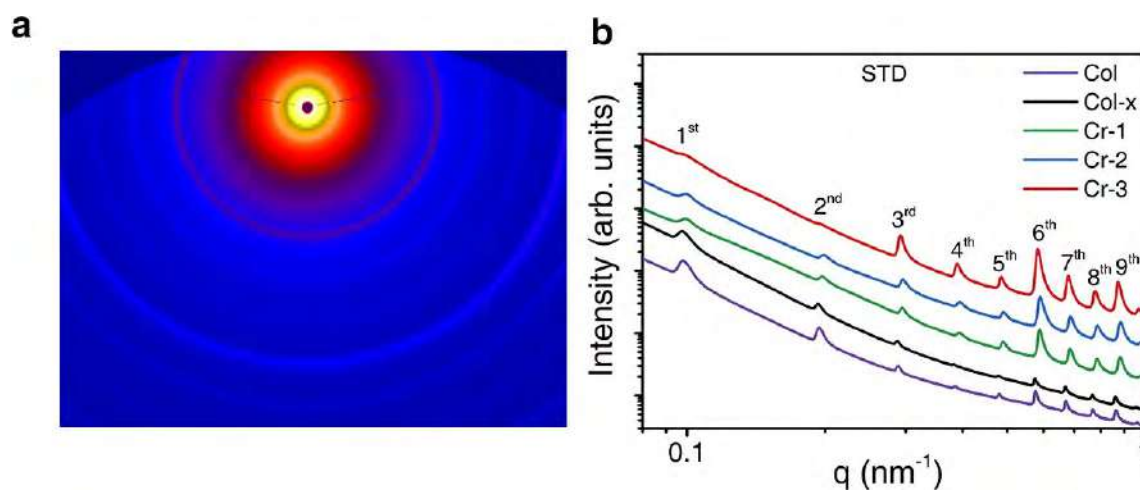


Fig. 1. (a) 2D SAXS image of chrome tanned leather. (b) Integrated 1D SAXS plots of untanned hide (Col), pre-treated hide through standard method (Col-x, where $x = \text{STD}$) and the subsequent chrome tanned leather (Cr-1, Cr-2 and Cr-3). Diffraction peaks are labelled according to $q = 2\pi n/D$ where n is the peak order and D is the D-period. © Int. J. Biol. Macromol. DOI: 10.1016/j.ijbiomac.2018.12.187.

Similar observations on the changes in peak intensity before and after tanning has been reported on both skins and hides from the 4th to 9th order peaks.^{6-7, 14} However, the 3rd order peak has shown a decrease in wet leather after chrome tanning,⁷ unlike what we have found in this study using dry leather. Previous reports showed that during drying, the intermolecular structure of collagen contracts and caused a decrease in the 3rd order peak,¹⁵ while cross-linking can provide resistance

to contraction, resulting in a stronger 3rd order peak in a dry state. Instead, the uncross-linked collagen can contract without the introduced restrictions to give a weaker 3rd order peak. On the other hand, a larger increase in the 6th order peak along with the increase in chrome offer was also observed over the other order peaks (Fig. 2). Stronger 6th order peak compared to the 3rd, 5th, 7th or 8th as previously found to relate to the drying of collagen.¹⁴⁻¹⁶ In this study, all samples have been dried equally in air at room temperature, so that the intensity changes of 6th over the other peaks showed insightful evidence into the binding environment of water with collagen, which varies amongst the different pre-treatments.

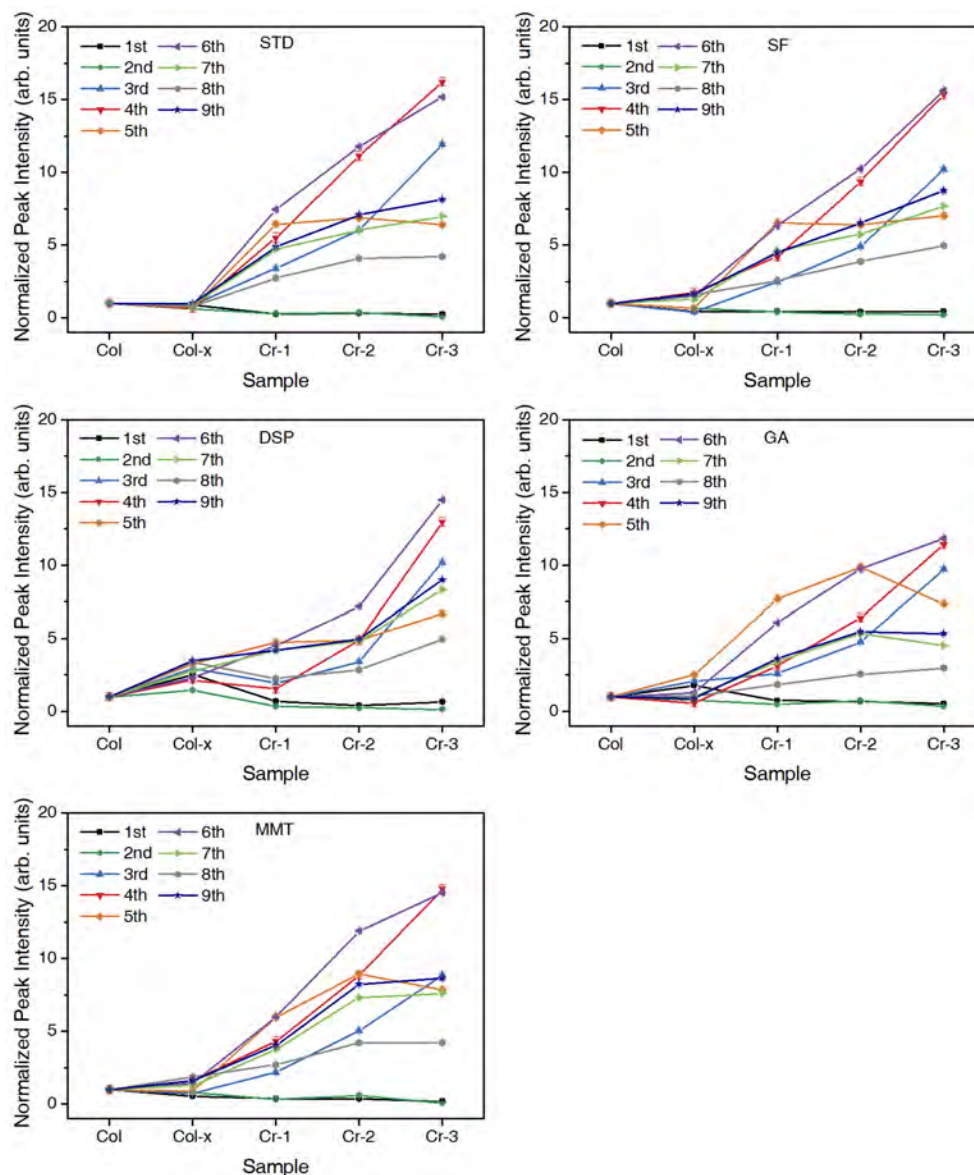


Fig. 2. Normalized 1st to 9th order peak intensity of each sample at different processing stages: untanned hide (Col), pre-treated hide (Col-x, x = STD, SF, DSP, GA and MMT) and the subsequent chrome tanned leather (Cr-1, Cr-2 and Cr-3). © Int. J. Biol. Macromol. DOI: 10.1016/j.ijbiomac.2018.12.187.

To study the effect of chromium cross-linking on collagen structure with various pre-treatments, the relative diffraction peak intensities of the 3rd to 2nd ($R_{3/2}$) and the 6th to 8th ($R_{6/8}$) order peaks (Fig. 3). $R_{3/2}$ indicates variations in the axial gap/overlap region of the collagen molecules, allowing investigation of the structural resistance to osmotic shrinkage.¹⁷ On the other hand, $R_{6/8}$ indicates

the level of hydration of the collagen molecules, which can affect the organoleptic properties of the leather products.¹⁷⁻¹⁸

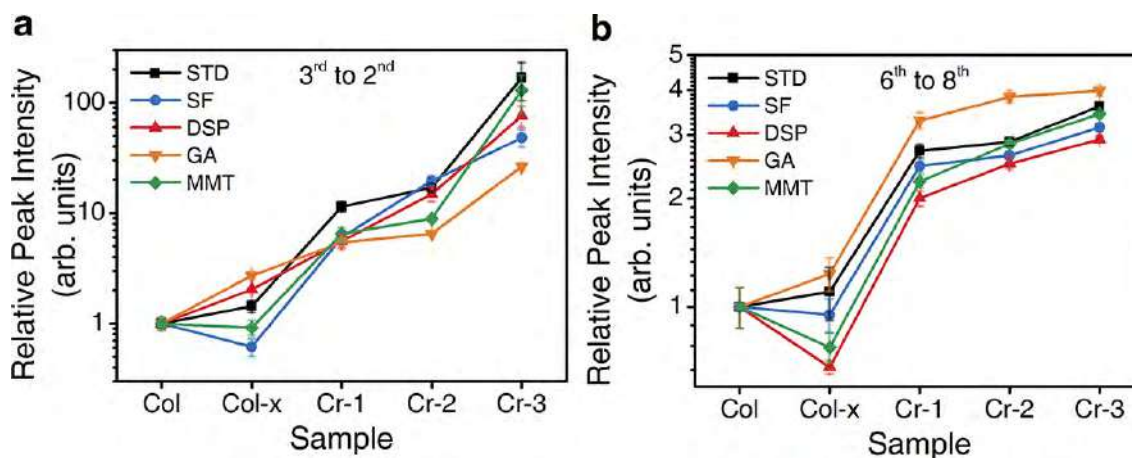


Fig. 3. Relative intensity ($R_{i/j}$, where i, j as peak orders) of (a) 3rd to 2nd and (b) 6th to 8th order peak of different samples: untanned hide (Col), pre-treated hide (Col-x, $x = \text{STD, SF, DSP, GA}$ and MMT) and the subsequent chrome tanned leather (Cr-1, Cr-2 and Cr-3). © Int. J. Biol. Macromol. DOI: 10.1016/j.ijbiomac.2018.12.187.

3.1.1 Cross-linking performance

One of the most important indicators of a successful tanning process is the cross-linking performance, which is revealed using $R_{3/2}$. According to the results (Fig. 3a), the pre-treatment step caused significant changes in $R_{3/2}$. GA caused the biggest change and this can be explained by its covalent cross-linking mechanism.^{1, 19} The other pre-treatments caused lesser changes in $R_{3/2}$ due to the non-covalent nature of their interactions with collagen.^{1, 20-22} After chrome tanning, all samples saw a significant increase in $R_{3/2}$. The covalent cross-linking of chromium with collagen constrained its intermolecular structure, thereby causing less fibril contraction when unbound water was removed.²³ The lower $R_{3/2}$ of GA samples after chrome tanning implied a minimised cross-linking effect from chromium, due to the more confined collagen structure after first covalently cross-linking it with GA.²⁴ Although higher than the GA samples, the $R_{3/2}$ of SF, DSP and MMT samples were also lower compared to STD samples after chrome tanning. This is in good agreement with their mechanisms: SF and DSP complex with chromium to reduce its cross-linking effect, while MMT has negatively charged silanol (Si-O⁻) and aluminol (Al-O⁻) groups that can also mask chromium species by binding electrostatically.^{1, 21-22}

3.1.2 Molecular hydration

Another performance indicator for the effect of chrome tanning, the molecular hydration of collagen, was demonstrated using $R_{6/8}$ (Fig. 3b). GA samples observed a higher $R_{6/8}$ over STD samples, confirming its covalent cross-linking mechanism that can lead to a decrease in hydrogen bonding sites in collagen and therefore, causes a less hydrated molecular structure.²⁵ Instead, SF, DSP and MMT brought carboxyl and hydroxyl groups into the collagen matrix and caused increased molecular hydration.²⁶⁻²⁷ When tanned using a low chrome offer (Cr-1), $R_{6/8}$ increased significantly and then plateaued at high offers (Cr-2 and Cr-3), implying decreasing efficiency per unit of chromium on its covalent cross-linking with collagen due to the shortage of active sites at the high chrome offers.⁷

3.2 DSC: Hydrothermal stability

DSC analyses of pre-treated and chrome tanned hide samples also provided important performance indicators such as hydrothermal stability and uniformity (Fig. 4).

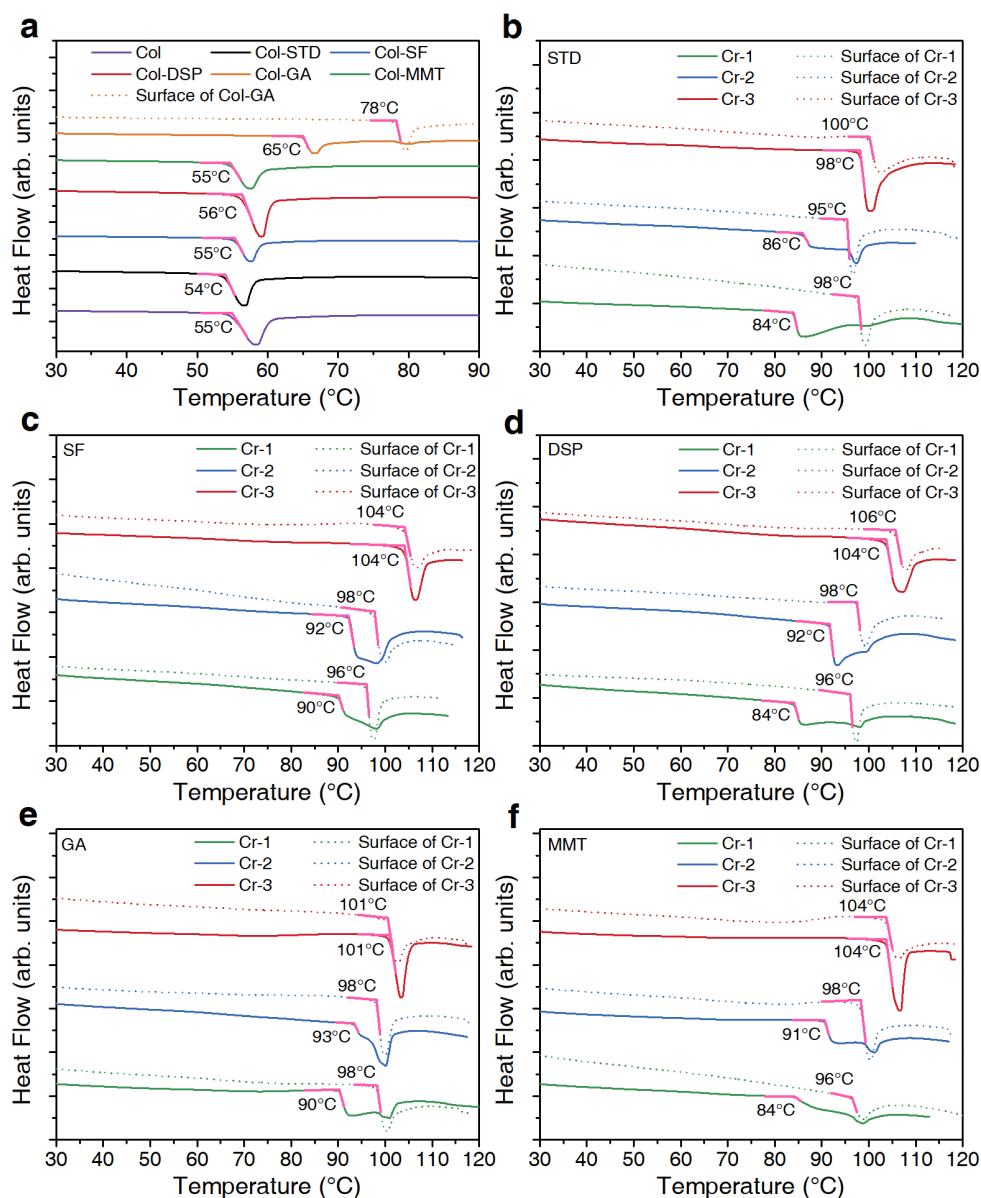


Fig. 4. DSC results of untanned hide (Col), pre-treated hide (Col-x, x = STD, SF, DSP, GA and MMT) and the subsequent chrome tanned leather (Cr-1, Cr-2 and Cr-3) throughout cross-sections (solid) or on the surfaces of the grain split hides (dotted). © Int. J. Biol. Macromol. DOI: 10.1016/j.ijbiomac.2018.12.187.

3.2.1 Hydrothermal stability

The most heat labile region of a tanned leather determines its overall denaturation temperature (T_d), which is also the minimum T_d throughout the cross-section of leather (T_{min}). Fig. 4a showed that there are only minor changes during pre-treatment using STD, SF, DSP and MMT, agreeing with their non-covalent interactions with collagen. On the other hand, covalent cross-linker, GA, caused an increment of T_d to 65°C. After chrome tanning (Fig. 4b-f), T_d increased significantly but the shapes

of endothermic peaks were different via each pre-treatment. Broad irregular shaped peaks were observed at low chrome offers (Cr-1 and Cr-2), while a high offer (Cr-3) produced sharper peaks. This highlighted the non-uniform penetration of chromium through the leather matrix.

Amongst all of the Cr-1 samples, a higher T_d at 90°C as observed in SF and GA samples, while MMT and DSP showed similar T_d at 84°C to the STD sample. Better penetration of chrome to the centre of the hide would provide a higher overall T_d of the collagen in leather. The masking effect of SF is again confirmed to assist the penetration of chrome. GA, on the other hand, limits the reaction of chromium with collagen on the surface via covalent cross-linking so as to improve the penetration. MMT and DSP samples showed no improvement in T_d in the centre, however, the shape of the endothermic peaks suggested a better distribution of chrome through the matrix. Stronger heat absorption at higher temperatures indicated a greater proportion of the collagen had improved hydrothermal stability. MMT can bind with chromium via electrostatic interactions to minimise the rapid cross-linking reaction to facilitate penetration. DSP contributed to penetration via bulk chelation with chromium to reduce its affinity to collagen.

Cr-2 samples showed higher T_d than Cr-1 samples with narrowed endothermic peaks. In addition, all of the pre-treated samples exhibited better hydrothermal stability than STD. Although the T_d were very similar among the different pre-treatments, the shape of the endothermic peaks varied. The GA sample displayed the largest proportion of higher T_d collagen, followed by MMT, SF and DSP, in descending order.

Similarly, in Cr-3 samples, the T_d of pre-treated leather is higher than the standard. However, GA produced the lowest T_d (101°C) amongst the four pre-treatments, which could be attributed to its nature of covalent cross-linking that hindered chromium from reacting with the collagen.

3.2.2 Uniformity through leather cross-section

Surfaces of leather were also measured for their T_d to identify the T_{max} throughout the leather cross-section, and their uniformity can be calculated based on the difference between T_{min} and T_{max} (R_T). A large R_T value (i.e., a wide range of T_d across the cross-section) indicates non-uniform penetration of chromium through the leather. Across the three chrome offers, the lowest overall R_T was observed in SF and GA treated samples. DSP and MMT also showed a slight improvement to R_T compared with STD. The overall results of R_T were generally consistent with improvements at low chrome offer.

3.3 AAS: percentage uptake of chrome

AAS analyses were conducted to quantify the uptake of chrome (Up%) for all pre-treatment methods (Table 1). In general, higher chrome offer was found to lead to a lower uptake, which agrees with previous observations. The percentage uptake of chromium was found to decrease with increasing chromium concentration, and is also in agreement with previous observations.⁷

Table 1. Percentage uptake of chrome during processing with different pre-treatments.

Chrome offer (%)	Chrome uptake (%)				
	STD	SF	DSP	GA	MMT
3.0 (Cr-1)	92 ± 2	84 ± 2	84 ± 1	99 ± 4	92 ± 2
4.5 (Cr-2)	82 ± 2	78 ± 2	76 ± 1	85 ± 1	81 ± 3
6.0 (Cr-3)	70 ± 2	61 ± 2	71 ± 2	67 ± 1	77 ± 2

© Int. J. Biol. Macromol. DOI: 10.1016/j.ijbiomac.2018.12.187.

GA provided an increased uptake compared to STD, whilst SF and DSP reduced uptake. GA improves chrome uptake at lower offers by facilitating more uniform penetration through the leather. However, its cross-linking also hinders the reaction of collagen with chromium at high offers therefore resulting in a lower uptake. SF and DSP complex with chromium to decrease its affinity

and ability to fix to the collagen molecules, hence providing reduced overall uptakes of chromium. MMT mitigates the reaction of chromium with collagen via its preferential adsorption of chromium species. Due to the affinity of chromium to collagen, it balances and prefers to fix to collagen at the end of the tanning process. In the presence of an excess of chrome, the active sites on collagen can be exhausted; with the rest of the chromium species therefore being adsorbed onto the MMT, resulting in a higher uptake in the highest chrome offer.

3.4 Overall performance of pre-treatments

The overall performance of four common pre-treatments was summarised according to their rankings across five key aspects. Cross-linking ($R_{3/2}$) and hydration ($R_{6/8}$) can greatly affect the organoleptic properties of leather. Hydrothermal stability (T_d) is also crucial, especially for the manufacturing of shoes. When it comes down to the practical manufacturing, the uptake of chrome (Up%) and its uniformity through the leather cross-section also needs to be considered to balance the cost and production efficiency. An evaluation is therefore demonstrated based on five aspects (Fig. 5). SF, DSP and MMT reduced chromium-collagen cross-linking and increased molecular hydration, hydrothermal stability and uniformity. GA introduced a decrease in both chromium-collagen cross-linking and hydration by covalently cross-linking with the collagen. The uptakes of chrome were improved by GA cross-linking and MMT adsorption. However, uptakes were reduced due to the complexing effect of either SF or DSP.

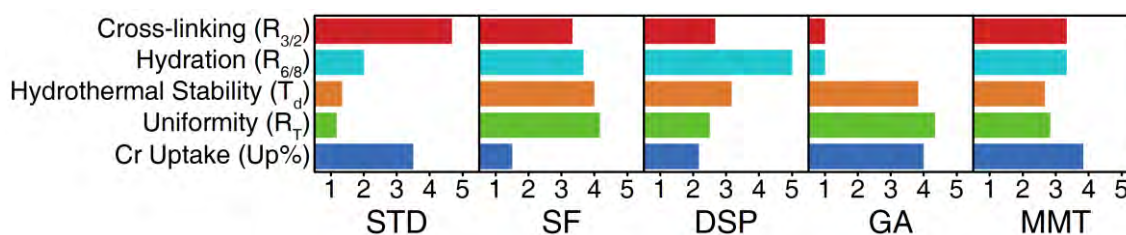


Fig. 5. Key aspects of the efficiency of chrome tanning through different pre-treatments. © Int. J. Biol. Macromol. DOI: 10.1016/j.ijbiomac.2018.12.187.

4 Conclusion

An efficient chrome tanning process can lead to a both economically and environmentally sustainable leather industry. Knowing the influence on performance of pre-treatments will allow us to improve the efficiency of chrome tanning, thereby improving collagen stability and the organoleptic properties of treated leather, alongside a reduction in chrome usage, mitigated environmental burden and diminished cost for the treatment of effluent. Our fundamental studies using SAXS and DSC provide a strategic guide to screen different combination tannages to design a more efficient chrome tanning processes. Such metrics can also be applied to the evaluation of cross-linkers for the biomedical industry to gauge their influence on collagen structure and hydrothermal stability.

5 Acknowledgements

S.P, Y.Z & G.H would like to thank the Ministry of Business, Innovation and Employment (MBIE) for providing funding through grant LSRX-1801. S.P & Y.Z would like to thank the Diamond Light Source, UK, for the granted access to SAXS beam time on the I22 beamline for this research.

References

1. Covington, A. D.: *Tanning chemistry: the science of leather*, Royal Society of Chemistry: Cambridge, 2009.
2. Sreeram, K.; Ramasami, T.: 'Sustaining tanning process through conservation, recovery and better utilization of chromium', *Resources, conservation and recycling*, 38, 185-212, 2003.
3. UNIDO Future Trends in the World Leather and Leather Products Industry and Trade; UNIDO: Vienna, 2010; pp 1-120.
4. Sundar, V.; Rao, J. R.; Muralidharan, C.: 'Cleaner chrome tanning—emerging options', *Journal of cleaner production*, 10, 69-74, 2002.
5. Zhang, Y.; Ingham, B.; Leveneur, J.; Cheong, S.; Yao, Y.; Clarke, D. J.; Holmes, G.; Kennedy, J.; Prabakar, S.: 'Can sodium silicates affect collagen structure during tanning? Insights from small angle X-ray scattering (SAXS) studies', *RSC Advances*, 7, 11665-11671, 2017.
6. Zhang, Y.; Ingham, B.; Cheong, S.; Ariotti, N.; Tilley, R. D.; Naffa, R.; Holmes, G.; Clarke, D. J.; Prabakar, S.: 'Real-Time Synchrotron Small-Angle X-ray Scattering Studies of Collagen Structure during Leather Processing', *Industrial & Engineering Chemistry Research*, 57, 63-69, 2018.
7. Zhang, Y.; Mansel, B. W.; Naffa, R.; Cheong, S.; Yao, Y.; Holmes, G.; Chen, H.-L.; Prabakar, S.: 'Revealing Molecular Level Indicators of Collagen Stability: Minimizing Chrome Usage in Leather Processing', *ACS Sustainable Chemistry & Engineering*, 6, 7096-7104, 2018.
8. Naffa, R.; Maidment, C.; Ahn, M.; Ingham, B.; Hinkley, S.; Norris, G.: 'Molecular and structural insights into skin collagen reveals several factors that influence its architecture', *International journal of biological macromolecules*, 128, 509-520, 2019.
9. Zhang, Y.; Snow, T.; Smith, A. J.; Holmes, G.; Prabakar, S.: 'A guide to high-efficiency chromium (III)-collagen cross-linking: Synchrotron SAXS and DSC study', *International journal of biological macromolecules*, 126, 123-129, 2019.
10. Pauw, B. R.; Smith, A.; Snow, T.; Terrill, N.; Thünemann, A. F.: 'The modular small-angle X-ray scattering data correction sequence', *Journal of applied crystallography*, 50, 1800-1811, 2017.
11. Ingham, B.; Li, H.; Allen, E. L.; Toney, M. F.: 'SAXSFit: A program for fitting small-angle X-ray and neutron scattering data', *arXiv:0901.4782*, 1-5, 2009.
12. Petruska, J. A.; Hodge, A. J.: 'A subunit model for the tropocollagen macromolecule', *Proceedings of the National Academy of Sciences*, 51, 871-876, 1964.
13. Hulmes, D. J.; Miller, A.; White, S. W.; Doyle, B. B.: 'Interpretation of the meridional X-ray diffraction pattern from collagen fibres in terms of the known amino acid sequence', *Journal of molecular biology*, 110, 643-666, 1977.
14. Maxwell, C. A.; Smiechowski, K.; Zarlok, J.; Sionkowska, A.; Wess, T. J.: 'X-ray studies of a collagen material for leather production treated with chromium salt', *Journal of the American Leather Chemists Association*, 101, 9-17, 2006.
15. Fratzl, P.; Daxer, A.: 'Structural transformation of collagen fibrils in corneal stroma during drying. An x-ray scattering study', *Biophysical Journal*, 64, 1210-1214, 1993.
16. Tomlin, S.; Worthington, C. In *Low-angle X-ray diffraction patterns of collagen*, *Proceedings of the Royal Society of London A: Mathematical, Physical and Engineering Sciences*, The Royal Society: 1956; pp 189-201.
17. Masic, A.; Bertinetti, L.; Schuetz, R.; Chang, S.-W.; Metzger, T. H.; Buehler, M. J.; Fratzl, P.: 'Osmotic pressure induced tensile forces in tendon collagen', *Nature communications*, 6, 5942, 2015.
18. Sasaki, N.; Odajima, S.: 'Elongation mechanism of collagen fibrils and force-strain relations of tendon at each level of structural hierarchy', *Journal of biomechanics*, 29, 1131-1136, 1996.
19. Damink, L. O.; Dijkstra, P. J.; Van Luyn, M.; Van Wachem, P.; Nieuwenhuis, P.; Feijen, J.: 'Glutaraldehyde as a crosslinking agent for collagen-based biomaterials', *Journal of materials science: materials in medicine*, 6, 460-472, 1995.
20. Prabakar, S.; Whitby, C. P.; Henning, A. M.; Holmes, G.: 'The Effect of Cloisite (R) Na plus Nanoclay Filler on the Morphology and Mechanical Properties of Loose Leather', *Journal of the American Leather Chemists Association*, 111, 178-184, 2016.
21. Drljaca, A.; Anderson, J.; Spiccia, L.; Turney, T.: 'Intercalation of montmorillonite with individual chromium (III) hydrolytic oligomers', *Inorganic Chemistry*, 31, 4894-4897, 1992.
22. Abollino, O.; Aceto, M.; Malandrino, M.; Sarzanini, C.; Mentasti, E.: 'Adsorption of heavy metals on Na-montmorillonite. Effect of pH and organic substances', *Water research*, 37, 1619-1627, 2003.
23. Bertinetti, L.; Masic, A.; Schuetz, R.; Barbetta, A.; Seidt, B.; Wagermaier, W.; Fratzl, P.: 'Osmotically driven tensile stress in collagen-based mineralized tissues', *Journal of the mechanical behavior of biomedical materials*, 52, 14-21, 2015.
24. Fein, M.; Filachione, E.; Naghski, J.; Harris Jr, E.: 'Tanning with glutaraldehyde III. Combination tannages with chrome', *The Journal of the American Leather Chemists Association*, 58, 202-221, 1963.
25. Liu, Y.; Ma, L.; Gao, C.: 'Facile fabrication of the glutaraldehyde cross-linked collagen/chitosan porous scaffold for skin tissue engineering', *Materials science and engineering: c*, 32, 2361-2366, 2012.
26. Madhan, B.; Muralidharan, C.; Jayakumar, R.: 'Study on the stabilisation of collagen with vegetable tannins in the presence of acrylic polymer', *Biomaterials*, 23, 2841-2847, 2002.
27. Holmgren, S. K.; Bretscher, L. E.; Taylor, K. M.; Raines, R. T.: 'A hyperstable collagen mimic', *Chemistry & Biology*, 6, 63-70, 1999.

EVALUATION OF ECOTOXICITY OF TYPICAL SURFACTANTS FOR LEATHER MANUFACTURE BY LUMINESCENT BACTERIA

W. M. Han¹, X. Zhou^{1,2}, J. Tan^{1,2}, L. Q. Peng² and W. H. Zhang^{1,2,a}

¹ The Key Laboratory of Leather Chemistry and Engineer of Ministry of Education, Sichuan University, Chengdu 610065, China.

² National Engineering Laboratory for Clean Technology of Leather Manufacture, Sichuan University, Chengdu 610065, China.

a) W. H. Zhang: zhangwh@scu.edu.cn

Abstract. Surfactants are used as auxiliaries in every wet processing process of leather production and discharged into wastewater, which would cause potential ecological risks. In this paper, fresh luminescent liquids were employed to evaluate the ecological toxicity of six surfactants, including anionic, cationic and non-ionic surfactants, and mixture of two typical ionic and nonionic surfactants after a 15-min exposure period. Non-ionic surfactants AEO and Tween80 showed slight light inhibition ie.10-35% to luminescent bacteria. The toxicity of anionic surfactants with polar sulfonic group was: penetrant T($EC_{50}=406.81\text{mg/L}$) > SDBS($EC_{50}=573.37\text{mg/L}$). The toxicity of cationic surfactants was: DTAB ($EC_{50}=10.68\text{mg/L}$) > SKC ($EC_{50}=73.96\text{mg/L}$). The addition of nonionic surfactants reduced the toxicity of ionic surfactants. 1-1 mixture of SKC and AEO: $EC_{50}=80.17\text{mg/L}$, 1-1 mixture of SDBS and AEO: $EC_{50}=624.34\text{mg/L}$. These results provided ecological parameters for the selection of surfactants in the process of ecological leather production.

1 Introduction

The process of leather production is heterogeneous physical chemical reaction. Therefore, the interfacial property has an effect on the leather processing and the product performances¹. Surfactants involving in interfacial properties were extensively used in the wet processing process of leather production to improve the permeation, diffusion, absorption or spreading of other leather chemicals²⁻⁴. According to the features of dissociation activity of polar groups, surfactants are divided into ionics and nonionics, in which the ionic surfactants are divided into anionics, cationics, zwitterionics. Anionic and nonionic surfactants are in widespread application in leather production, such as soaking, degreasing, liming, tanning, dyeing, and fatliquoring⁵⁻⁶. Meanwhile, cationic surfactants have been increasingly applied in leather production, due to the special properties of softening and sterilization⁷. Besides, surfactants compound are extensively used in leather production due to the excellent properties, such as strong surface/interfacial activities, low cost, low critical concentration (cmc), ect, compared to the single surfactant⁸⁻¹⁰.

It is generally viewed that the surfactants are non-covalently bonded to collagenous fibers in leather processing, resulting in that surfactants are discharged into the tannery wastewater¹¹⁻¹². It is widely acknowledged that surfactants will reduce the content of dissolved oxygen in water. For instance, anionic surfactant sodium dodecyl benzene sulfonate (SDBS, the COD value is up to 13g/L) has significantly effects on oxygen restoration process and physical chemical reactions of other organics in water body, which has potential ecological risks on the ecosystem¹³. Toxicity testings with several biological systems are used to evaluate aquatic toxicity, such as *algae*, *fish*, *Daphnia magna*, and luminous bacteria¹⁴. The bioluminescent bacteria assay is adopted in worldwide countries as standard method for its short test time and high sensitivity¹⁵⁻¹⁶.

In this paper, bioluminescence inhibition assay with luminous bacteria (*Photobacterium Phosphoreum*) was introduced to evaluate the ecotoxicity of nine common anionic, cationic, nonionic and mixed surfactants.

2 Materials and Methods

2.1 Test Chemicals

Stock solutions of anionic surfactants penetrant T (AR, Chengdu, China) and Sodium alkyl benzene sulfonate (AR, Chengdu, SDBS), cationic surfactants dodecyl trimethyl ammonium bromide (DTAB, AR, Chengdu, China) and benzyl dimethyl stearyl ammonium chloride (SKC, AR, Chengdu, China), nonionic surfactants fatty alcohol polyoxyethylene ether (AEO, CP, Chengdu, China) and Tween 80 (AR, Chengdu, China) were prepared in saline water solution (3% sodium chloride [NaCl]) in all of experiments. SDBS and AEO were mixed at different mass ratio 1:1, and the same to SKC and AEO. The mixed surfactants were also prepared in 3% NaCl. Water used in all the experiments was distilled.

2.2 Bacterial Culture

The freeze-dried *Photobacterium phosphoreum* (T3 mutation) was purchased from Shenzhen Langshi Biological Instrument Co., Ltd. (Shenzhen, China). The reagent was stored at -20 °C and rehydrated before inoculation. The bacteria were cultured in the complete liquid culture medium (5.00g tryptone, 5.00g yeast extract, 30.00g NaCl, 12.61g Na₂HPO₄·12H₂O, 1.31g K₂HPO₄·3H₂O, 3.00g glycerin, and 1000mL distilled water) with a shaking speed 200rpm at 20°C for 18h. Then the pre-culture *P. phosphoreum* was inoculated in new complete liquid medium again. And the bacteria were grown to the logarithmic growth stage after 18h¹⁷.

2.3 The Determination of Bacterial Density for Test

5mL fresh bacteria liquid in the logarithmic growth stage was diluted with 11mL 12mL 13mL 14mL 15mL 16mL 17mL 18mL 19mL 20mL 3% NaCl to obtain bacteria suspensions in different optical density (OD) which can be determined at 600nm with UV-vis spectrophotometer (Shanghai MAPADA Co. Ltd., China). 50μL bacteria suspensions in different optical density were added to the 950μL 0.10mg/L HgCl₂ (as standard controls) and 3% NaCl (as blanks). After an exposure for 15min at 20°C, the relative luminous intensity was detected by LumiFox 6000 (Shenzhen Langshi Biological Instrument Co., Ltd., China). All samples were tested in three parallel samples. The 50±5% bioluminescence inhibition of 50μL bacteria suspension served as a reference to verify the reliability of the experimental results.

2.4 Toxicity Test

According to the National Standard Method of China (GB/T 15441-1995, 1995), 50μL bacteria suspensions were added to 950μL test chemicals and the control (3% NaCl solution), respectively. At least 10 concentrations were prepared for every surfactant. The relative luminous intensities of the bacteria with an exposure of 15min at 20°C were measured. All samples were tested in triplicate.

2.5 Data Analysis

The relative luminous intensity *E* of sample could be calculated as follows:

$$E = \frac{I}{I_0} \times 100\%$$

where *I*₀ and *I* were average luminous intensity of *P. phosphoreum* exposed to the blank controls and test samples, respectively. The regression models were used to describe dose-effect relationships of the surfactants on the bacteria. Toxicity of the samples was evaluated by EC₅₀, the effective concentration corresponding to 50% bioluminescence inhibition calculated from the models. The higher EC₅₀ value indicated lower toxicity¹⁷⁻²⁰.

3 Results and Discussion

3.1 Bacteria Density and Sensitivity Measurement

The relationship between OD₆₀₀ value and the relative luminous intensity of the bacteria suspension after exposed to 0.10mg/L HgCl₂ was shown in Fig. 1

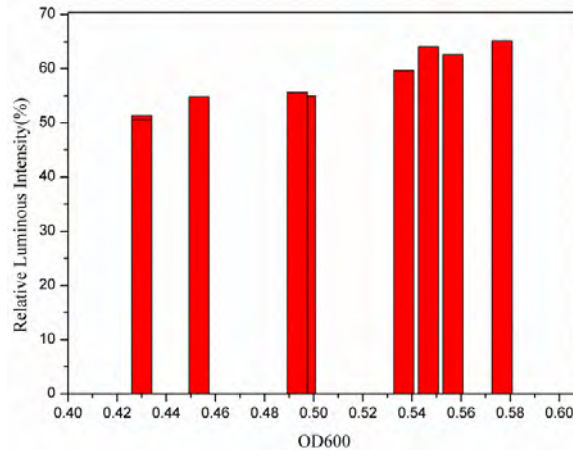


Fig. 1. The relationship between OD₆₀₀ and relative luminescence intensity of bacterial liquid.

Obviously, the density of the bacteria suspension affected the relative luminous intensity, thereby affecting the sensitivity and accuracy. As shown in Fig. 1, the relative luminous intensity of bacteria increased with the increase of bacteria density after the exposure of 0.10mg/L HgCl₂. There was no clear linear relationship between them, which may be one of sources of the errors. However, when the bacteria density within certain range, e.g. OD600 in 0.55~0.57, the relative luminous intensity of bacteria exposed to 0.10mg/L HgCl₂ fall in 50±5%, which meant that the results has excellent stability. Therefore, it is necessary to confirm the bacteria density by standard toxic substance (0.10mg/L HgCl₂) when the fresh bacteria liquid is used to detect the toxicity of chemicals.

3.2 Toxicity of Nonionic Surfactants

AEO and Tween 80 are polyethoxylated nonionic surfactants, which are widely applied in soaking, degreasing and pickling et al. in leather production. The dose-effect relationships of nonionic surfactants were displayed in Fig. 2.

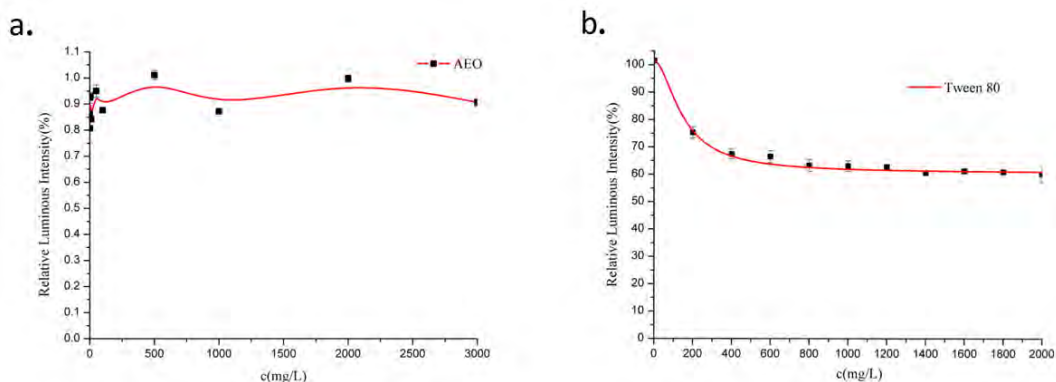


Fig.2. Dose-effect relationship of anionic surfactants on luminescent bacteria, a: AEO b: Tween 80.

As stated in Fig. 2, the inhibitory effects of the surfactants to *P. phosphoreum* were limited in the range from 0.1mg/L~2000mg/L. And there are differences among them in the laws of inhibitions. The relative luminous intensity always fluctuated around 85% with AEO concentration from 0.1mg/L to 3.0 g/L, which indicated little ecotoxicity on the bacteria. The relative luminous intensity of bacteria exposed to Tween 80 decreased to 68% with the concentration increasing from 1mg/L to 400mg/L and remained invariable as the concentration increased to 2.0 g/L. The EC₅₀ of the surfactants couldn't be obtained in the range of the testing concentration. Based on Microtox toxicity grading standard of America (the relative luminous intensity < 25% for very toxicity, 25~50% for moderately toxicity, 51-75% for toxicity, 75% for slightly toxicity), AEO and Tween 80 (<0.2g/L) showed slightly toxicity for *P. phosphoreum*.

3.3 Toxicity of Anionic Surfactants

SDBS (Sodium alkyl benzene sulfonate) and penetrant T (sulfonated aliphatic polyester) are sulfonate anionic surfactant and used in soaking, liming, dyeing, fat liquoring and so on. The dose-effect relationships of the two surfactants were stated in Fig. 3.

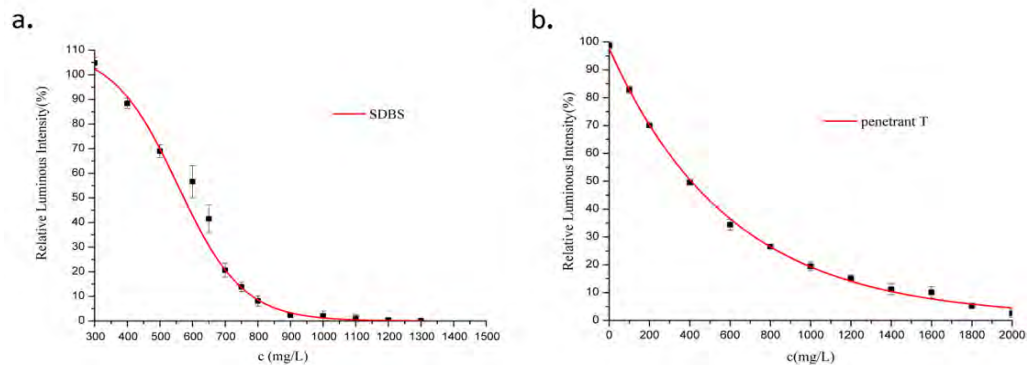


Fig.3. Dose-effect relationship of anionic surfactants on luminescent bacteria, a: SDBS; b: Penetrant T.

As displayed in Fig. 3, the bioluminescence inhibition values increased and the relative luminous intensities decreased with the increase of the concentration of the surfactants. When the mass concentration of SDBS increased to 1100 mg/L, the bioluminescence was inhibited completely and the relative luminous intensities decreased to 0%. The model DoseResp was used to fit the dose-effect curve of SDBS as follows:

$$y = 2.7834 \times 10^{-4} + \frac{1.1009 - 2.7834 \times 10^{-4}}{1 + 10^{(555.0962 - x) \times (-0.0044)}}$$

The correlation coefficient of the model was 0.9986 and EC₅₀ was 598.15mg/L. While, as the mass concentration of penetrant T increased to 2000mg/L, the bioluminescence was also inhibited and the relative luminous intensities of the bacteria decreased to 5%. The dose-effect relationship of penetrant T was described by the regression model ExpDec1 as follows:

$$y = 0.9649e^{-\frac{x}{598.3981}} + 0.0111.$$

The correlation coefficient of the model was 0.9995 and EC₅₀ was 406.81mg/L. According to the bioluminescence inhibition of the bacteria, penetrant T showed higher toxicity than SDBS. Based on the American Microtox toxicity grading standard, the relative luminous intensities was lower than 50% when the concentration of SDBS and penetrant T exceeded 200mg/L, indicating that the two surfactants showed moderately toxicity on the bacteria. However, on the basis of the toxicity standard of BASF SE, the chemicals of which EC₅₀ are greater than 100mg/kg are considered to be safe. So, SDBS and penetrant T are safe products.

3.4 Toxicity of Cationic Surfactants

SKC (benzyl dimethyl stearyl ammonium chloride) and DTAB (dodecyl trimethyl ammonium bromide) are quaternary ammonium cationic surfactants, applied in the soaking, pickling, tanning, fatliquoring, finishing et al. The dose-effect relationships of the two surfactants were shown in Fig. 4.

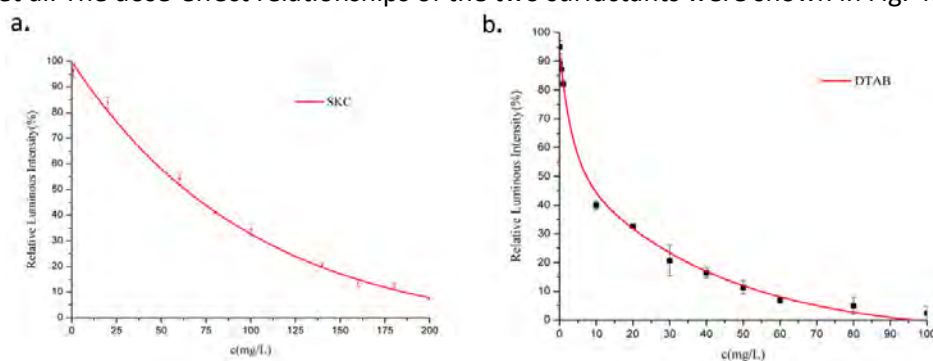


Fig.4. Dose-effect relationship of cationic surfactants on luminescent bacteria, a: SKC; b: DTAB.

As shown in Fig. 4, with the concentration of the three surfactants increasing, the bioluminescence inhibition increased significantly and the relative luminous intensities decreased rapidly. The relative luminous intensity decreased to 10%, when the concentration of SKC increased to 200mg/L. The dose-effect relationship of SKC was fitted by the model ExpDec3:

$$y = 66.6813e^{\frac{-x}{206.5416}} + 43.3805e^{\frac{-x}{206.4838}} + 30.8815e^{\frac{-x}{206.7109}} - 48.5245.$$

The correlation coefficient of the model was 0.9930 and EC₅₀ was 73.96mg/L. When the concentration of DTAB increased to 20mg/L, the decreasing trend of the relative luminous intensity became slower. And when the concentration increased to 120mg/L, the bioluminescence was inhibited almost completely. The model ExpAssoc was used to describe the dose-effect relationship of DTAB as follows:

$$y = 0.9540 - 0.5052(1 - e^{\frac{-x}{35.7272}}) - 0.4441(1 - e^{\frac{-x}{8.1927}}).$$

The correlation coefficient of the model was 0.9995 and EC₅₀ was 10.68mg/L. The values of EC₅₀ indicated that DTAB are more toxic than SKC. According to the toxicity standard of BASF SE, the chemicals of which EC₅₀s are greater than 100mg/kg are considered to be safe. It is meant that the surfactants in the range from 1~100mg/L can be used safely.

3.5 Toxicity of the Mixture of Surfactants

The toxicity of mixture of ionic surfactants (including anionics SDBS and cationics DTAB) and nonionic surfactant (AEO) was detected and the dose-effect relationships was shown in Fig. 5.

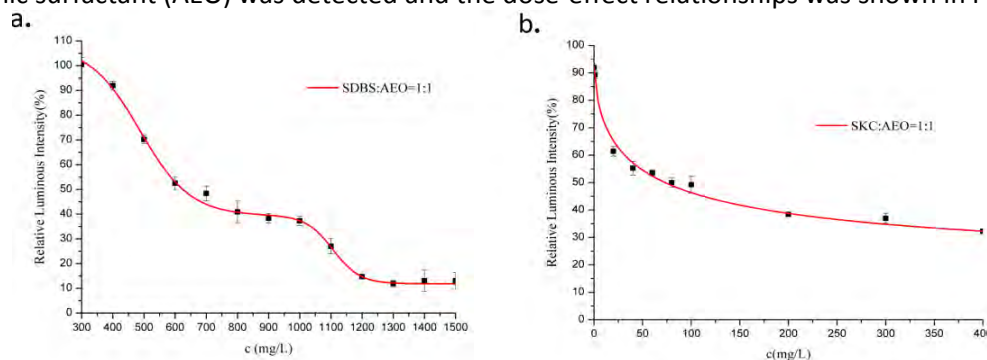


Fig. 5. Dose-effect relationship of the compound of surfactants on luminescent bacteria, a: mixed surfactants of SDBS and AEO; b: mixed surfactants of SKC and AEO.

As shown in Fig.5, the relative luminous Intensity decreased with the increase of concentration of the surfactants mixtures. In consideration of little toxicity of AEO, only concentrations of individual ionic surfactants were stated as x-axis in the dose-effect relationships of the mixed surfactants. The dose-effects relationship of the mixture of SDBS and AEO was fitted by BioDoseResp:

$$y = 0.1183 + (1.0811 - 0.1183) \left[\frac{0.7138}{1 + 10^{(487.2145-x) \times (-0.0054)}} + \frac{1 - 0.7138}{1 + 10^{(1106.4488-x) \times (-0.0100)}} \right]$$

The correlation coefficient of the model was 0.9994. The EC₅₀ was 624.34mg/L, lower than EC₅₀ of individual SDBS 598.15mg/L indicating that the composites of SDBS and AEO resulted in the lower toxicity of the surfactants. For the mixture of SKC and AEO, the relative luminous intensity decreased with the increase of the surfactant mixtures and maintained about 35% with the concentration increasing to 400mg/L. The dose-effect relationship was described by the model Logistic:

$$y = 14.1394 + \frac{93.7710 - 14.1394}{1 + \left(\frac{x}{52.5623}\right)^{0.6010}}$$

The correlation coefficient of the model was 0.9998. The EC₅₀ was 80.17mg/L. Though the EC₅₀ of the mixtures was closed to the EC₅₀ of individual SKC (73.96mg/L), the relative luminous intensity remained about 35% when the concentration exceeded 100mg/L, which meant that the individual SKC showed much higher toxicity than the mixtures of SKC and AEO. To sum up, the mixture of ionic and nonionic surfactants showed lower toxicity than individual ionic surfactants.

4 Conclusion

In this work, the ecotoxicity of the surfactants widely used in leather production were investigated using bioluminescence inhibition assay with *Photobacterium phosphoreum*. The cationic surfactants showed highest toxicity on the bacteria and the nonionic surfactants showed lowest toxicity. And the composites of ionic and nonionic surfactants could lower the toxicity of surfactants.

The testing results provide the evaluation parameters of the eco-friendliness for the selection of the surfactants in leather production. Meanwhile, the purity of the industrial chemicals can't meet the requirement of the experiment reagents. The coexisting chemicals have complicate impacts on the toxicity of the surfactants. Therefore, it is necessary to investigate the toxicity of the surfactants in practical application.

Acknowledgement

This work was financially supported by the National Natural Science Foundation of China (21476149).

References

1. Covington, A. D.: *Tanning Chemistry, the Royal Society of Chemistry, 2009.*
2. Han, M.: 'The Application of Surfactant in Leather Industry', *Science & Technology Vision, 1, 174, 2015.*
3. El-Sayed, R. et al.: 'Synthesis, Surface Parameters, and Biodegradability of Water-soluble Surfactants for Various Applications', *J. Oleo Sci., 67, 551-569, 2018.*
4. Wu, L. L. et al.: 'Performance and Applications of Surfactant (X X)-Applications of Surfactant in Leather Industry', *China Surfactant Detergent & Cosmetics, 45, 425-428, 2015.*
5. Lv, B. et al.: 'Application of Surfactants in Leather Industry', *Detergent & Cosmetics, 38, 48-52, 2015.*

6. Hankey, R. A. et al.: 'The Use and Subsequent Treatment of Surfactants for Leather Processing', *J. Am. Leather Chem. Assoc.*, 96, 205-213, 2001.
7. Lv, B. et al.: 'The Application of Cationic Surfactant in Leather Industry', *Leather Science and Engineering*, 24, 22-28, 2014.
8. Radulovic, J. et al.: 'Investigation of speeding of surfactant mixtures', *Chem. Eng. Sci.*, 64, 3227-3235, 2009.
9. Lu, S. H. et al.: 'Micellar evolution in mixed nonionic/anionic surfactant systems', *J. Colloid Interface Sci.*, 367, 272-279, 2012.
10. Danov, K. D. et al.: 'Micelle-monomer equilibria in solutions of ionic surfactants and in ionic-nonionic mixtures: A generalized phase separation model', *Adv. Colloid Interface Sci.*, 206, 17-45, 2014.
11. Lu, B. et al.: 'Measurement of Cytotoxicity and Irritancy Potential of Sugar-Based Surfactants on Skin-related 3D Models', *Toxicology in Viro*, 40, 305-312, 2017.
12. Jones, M. N.: 'Surfactant Interactions with Biomembranes and Proteins', *Chem. Soc. Rev.*, 21, 127-136, 1992.
13. Xu, R. S.: 'Evaluation of Pollution Sources and Pollution Degree of Surfactants in Rural Water Environment', *Fujian Agriculture Science and Technology*, 4, 53-54, 2005.
14. Dai, D., N. et al.: 'Ecotoxicity Reduction and the Dafety Assessment During the Wastewater Treatment and Reuse Process', *Journal of Safety and Environment*, 17, 1442-1447, 2017.
15. Eltzov, E. et al.: 'Flo-through Real Time Bacterial Biosensor for Toxic Compounds in Water', *Sens. Actuators, B*, 142, 11-18, 2009
16. Stefaniuk, M. et al.: 'Ecotoxicological Assessment of Residues from different biogas production plants used as fertilizer for soil' *J. Hazard. Mater.* 55, 32-38, 2018.
17. Zhu, W. J. et al.: *Luminous Bacteria and Environmental Monitoring*, first ed. China Light Industry Press, Beijing.
18. Ma, X. Y. Y. et al.: 'Study of the variation of ecotoxicity at different stages of domestic wastewater treatment using vibrio-qinghaiensis sp.-Q67', *J. Hazard. Mater.* 190, 100-105, 2011.
19. Zhang, J. et al.: 'Time-dependent hermetic effects of 1-alkyl-3-methykimidazolium bromide on *Vibrio qinghaiensis* sp.-Q67: Liminescence, redox reactants and antioxidases', *Chemosphere*, 91, 462-467, 2013.
20. Hernando, M. D. et al.: 'Toxicity evaluation with *Vibrio fisheri* test of organic chemicals used in aquaculture', *Chemosphere*, 68, 724-730, 2007.

NOVEL METHOD FOR PREPARING FISH COLLAGEN GELS WITH EXCELLENT PHYSICOCHEMICAL PROPERTIES VIA THE DEHYDRATION OF ETHANOL

Lirui Shen^{1b}, Songcheng Xu^{1c}, Kun Wu^{2d} and Guoying Li^{1a}

1 National Engineering Laboratory for Clean Technology of Leather Manufacture, Sichuan University, Chengdu 610065, PR China

2 Chengdu Textile College, Chengdu 610065, PR China

a)Corresponding author: liguoyings@163.com

b)leorexs@163.com

c)jsc3122212@163.com

d)wucbawuk@aliyun.com

Abstract. Fish collagen has been considered to be an alternative for mammalian collagen, however, physicochemical properties of fish collagen-based materials such as gels are so far not adequate for actual application. In the present study, we prepared two types of fish collagen gels with sufficient elasticity: i) dehydrated fibrillogenesis collagen gels (DFCG), which were fabricated via collagen self-assembly followed by immersion in different concentrations of ethanol solutions, and ii) dehydrated cross-linking collagen gels (DCCG), which were fabricated via collagen self-assembly and simultaneous cross-linking followed by immersion in ethanol solution. Furthermore, the physicochemical properties of DFCG and DCCG were analyzed by atomic force microscopy, differential scanning calorimetry and dynamic viscoelastic measurements. The microstructure of DFCG was consisted of characteristic D-periodic collagen fibrils and insusceptible of ethanol concentrations (20-100% (v/v)). However, the thermal stabilities and mechanical properties of DFCG distinctly increased with the increase of ethanol doses, possibly ascribing that ethanol with higher polarity might dehydrate partial free water of DFCG and strengthen the interactions of hydrogen bond. Especially, for the gel treated by 100% (v/v) ethanol, T_d increased by 32.7 °C and G' was 55-folds than those of undehydrated gel (43.1 °C and 239 Pa). In the case of DCCG, the formation of collagen fibrils was depended on the concentrations of *N*-hydroxysuccinimide adipic acid derivative (NHS-AA), which was converted to [NHS-AA]/[NH₂] ratios (calculated by the [active ester group] of NHS-AA and [ε-NH₂] of lysine and hydroxylysine residues of collagen). As the ratio= 0.05, the characteristic D-periodic fibrils were still formed and the treatment of 60% (v/v) ethanol increased the T_d (52.5 °C) and G' (7388 Pa) values of the gel compared with those of uncross-linked gel (49 °C and 2064 Pa, respectively), majorly resulting from the effects of covalent cross-linking bonds and hydrogen bonds. However, when the ratio= 0.2, the collagen self-assembly was intensively inhibited and the dehydration of free water within gel structure in the absence of thick fibrils led to the shrinkage of the gel and an obvious decrease in T_d (42 °C) and G' (432 Pa). Although the [NHS-AA]/[NH₂] ratio further increased to 0.8, the thermal stability and elasticity of the gel enhanced mildly suggesting that the presence of thick fibrils formed via the self-assembly was significantly crucial for reinforcing the gels.

Key words: fish collagen gel, self-assembly, cross-linking, thermal stability, dynamic viscoelasticity

1 Introduction

Hydrogels based on the self-assembly of natural proteins such as silk fibroin, elastin and collagen, which are three-dimensional, hydrophilic, polymeric networks capable of absorbing large amounts of water or biological fluids, have been widely applied to biomedical areas due to their inherent biodegradability and biocompatibility, tunable rigidity and toughness, flexible environmental responsiveness and abundant resources.¹⁻⁵ Collagen, as the major constituent of the extracellular matrix, is an attractive candidate for biomedical applications.^{2,6} Generally, collagen such as type I collagen with an approximate molecular weight of 300 kDa, which is composed of two α1 chains and one α2 chain in a right-handed triple helix, can undergo self-assembly via noncovalent bonds including hydrogen bonding, hydrophobic interaction, and electrostatic interaction to form the gels with an entangled network of thick D-periodic fibrils under physiological conditions.^{1,7-9} Recently, the fish collagen has been a potential alternative for the collagen from the mammals due to its

natural abundant resources, high yield, and absence of infections such as bovine spongiform encephalopathy, transmissible spongiform encephalopathy and foot-and-mouth disease.¹⁰⁻¹² However, the biomedical applications of the gels based on fish collagen are limited because of low denaturation temperature (T_d) and poor gelling properties, etc.^{13,14} For example, the T_d values of shark, salmon and grass carp collagen solution are approximately 30, 19 and 36 °C, respectively, which result in the low T_d values of their fibrillogenesis gels at 37, 28 and 39 °C, respectively.^{13,15,16} To effectively reinforce the physicochemical properties of fish collagen gels has attracted more attention of researchers.

The physicochemical properties of fibrillogenesis collagen gels depend on the thickness, length, and three-dimensional density of the collagen fibrils.^{17,18} In the last decades, a variety of chemical and physical methods based on different principles to reinforce the collagen gels were broadly developed. Firstly, there are many active amino residues (-NH₂) and/or carboxyl residues (-COOH) on the side chains of collagen molecule, which can be covalently cross-linked by adding cross-linking agents. Increasing the cross-linking number modifies the network architecture, thus reducing the distance between joints and creating denser and stiffer networks.¹⁸ In our previous study, we have investigated the physicochemical properties of fish collagen gels prepared by collagen self-assembly and simultaneously cross-linking with N-hydroxysuccinimide adipic acid derivative (NHS-AA), which could form long bridges between contiguous ε-NH₂ of collagen molecules with low toxicity.^{7,19} The results showed that the introduction of NHS-AA could inhibit the collagen self-assembly and the T_d and G' of the gel (47 °C and 420.7 Pa, respectively) increased by 8 °C and 198.3 Pa than those of uncross-linked gel due to the formation of abundant covalent cross-linking bonds. Secondly, the blending of collagen with natural and synthetic polymers (*e.g.*, chitosan, hyaluronic acid, alginate and poly(ethylene glycol), etc.) were also used to reinforce the gels by the introduction of non-covalent bonds including hydrogen bonds, electrostatic interactions, hydrophobic interactions.²⁰⁻²⁴ Thirdly, the effects of physical parameters such as compressing, extension, and irradiation (*e.g.*, UV irradiation, and gamma-ray irradiation and electron-beam irradiation, etc.) have been widely used to induce the intermolecular cross-linking of collagen.^{17,25,26} Nevertheless, the mechanical properties of the cross-linked collagen gels by chemical and physical methods are still not adequate to meet the demand for application, especially in the clinical fields of orthopedics, cardiovascular surgery, and neurosurgery.²⁷

It is important to note that the water enwrapped in the network structure plays a crucial role for reinforcing thermal stability and mechanical properties of the collagen gels because the water can not only affect the stability of polymeric backbone by non-covalent bonds, but also influence three-dimensional density of collagen fibrils. Recently, Mori et al. constructed the collagen gels with sufficient mechanical strength and elasticity by EDC/gamma ray cross-linking and sequentially heating for 30 min at 80 °C.¹⁷ They found that the density of collagen fibrils significantly increased due to the reduction of water during the heating process and the collagen gels sequentially cross-linked by 125 mM EDC after heating exhibited the highest G' value (7010 Pa), which was approximately 158-folds higher than that of uncross-linked gel without heating (G' , 44.1 Pa). However, there were partial collagen fibrils that were not cross-linked and were easily denatured during the heating process because of its low thermal stability. Furthermore, another method that was proceed by repeating the cycle of gel formation, cross-linking with EDC, freeze-drying, and heating, was developed to prepare collagen gels with high mechanical strength in the previous study described by Mori et al.²⁷ The collagen concentration could be significantly increased using repeated gel-formation inside the micropores of lyophilized collagen sponge, leading to the network structure consisting of densely packed fibrils. Especially, the collagen gel prepared by repeating the cycle for 3 times in which the heating was done only once after 125 mM EDC cross-linking in the first cycle (3-cycled collagen gel) exhibited an extremely high G' value (40200 Pa), which was approximately 911-folds higher than uncross-linked collagen gel. However, when 3-cycled collagen gel was sequentially heated once, the G' value decreased to 38500 Pa, attributing

that the uncross-linked collagen was denatured by heating. Although the dehydration by heating and gel-formation/lyophilization cycle can effectively reinforce the gels, it is worthy to note that their serious effects would denature partial collagen and break the original network structure of the gels consisting of periodic fibrils. The water-holding capacity of the gels depends on the capillary, osmotic and hydration interactions.²⁸ The bound water is important to sustain the stability of the collagen fibrils by maintaining the triple helix structures with the hydrogen bonding with collagen, in which the loosely-bound water can be removed by chemical dehydration with polar solvents such as methanol, ethanol and *n*-propanol.²⁹⁻³¹ Moreover, the replacement of polar solvents to the water could also establish stronger hydrogen bonds between the solvent and collagen to enhance the stability of network structure. Therefore, to study the effects of the dehydration of polar solvents on the preparation of the fish collagen gels with excellent physiochemical properties are extremely significant for expanding the medical applications of fish collagen.

In the present study, in order to establish a method to prepare the fish collagen gels with excellent physiochemical properties, we prepared two types of fish collagen gels: i) dehydrated fibrillogenesis collagen gels (DFCG), which were fabricated via collagen self-assembly followed by immersion in different concentrations of ethanol solutions; and ii) dehydrated cross-linking collagen gels (DCCG), which were fabricated via collagen self-assembly and simultaneously cross-linking followed by immersion in ethanol solution. Then, the microstructure, thermal stabilities, and dynamic viscoelasticity of collagen gels were analyzed.

2 Materials and methods

2.1 Materials

Southern catfish skin was purchased from a local market in Chengdu and was fleshing prior to cutting into small pieces. Then, the fish skins were thoroughly washed using deionized water and stored at -20 °C until used. The pepsin collagen was extracted according to the method as described in a previous paper.⁷ Briefly, the supernatants were extracted from the fish skins using 0.5 M acetic acid containing 1% (w/w) pepsin (EC 3.4.23.1, 1, 1:10000, Sigma–Aldrich, MO, USA) at 4 °C for 3 days after degreasing and decoloring procedures. Then, the precipitates were collected via adding 0.7 M NaCl into the supernatants and dissolved in 0.1 M acetic acid prior to dialyzed against 0.01 M acetic acid for 4 days. Finally, the collagen solution was finally lyophilized by a freezer dryer (Alpha 1-2 LDplus, Christ, Osterode, Germany). The purity and molecular weight of collagen were evaluated using sodium dodecyl sulfate polyacrylamide gel electrophoresis (SDS-PAGE) measurement. The SDS-PAGE pattern displayed two α bands (110 kDa for α_1 and α_2) and one β band (250 kDa), which are typical bands of type I collagen. NHS-AA was synthesized according to the method previously described by Chen et al.³² In brief, 2 M NHS and 1 M adipic acid were mixed in acetone for 15 min. Then, 2.2 M EDC was added into the mixed solution and reacted for 1 day at 20 °C. The acetone was removed using rotary evaporation prior to drying in vacuum at 50 °C. The structure of synthesized NHS-AA was evaluated by a fourier transform infrared spectrometer (FTIR) (Nicolet iS 50, Thermo Fisher Scientific, Waltham, USA). The FTIR spectra showed the typical peaks of ester group, which were at 1065, 1210 and 1739 cm^{-1} .

2.2 Preparation of DFCG and DCCG

Lyophilized collagen was dissolved in 10 mM phosphate-buffered saline solution (PBS, pH 7.4) containing 125 mM NaCl and centrifuged at 10000 \times g for 10 min at 4 °C to remove bubbles. For the preparation of DFCG, 5 mg/mL collagen solution was incubated at 30 °C for 5 h and then immersed in different concentrations of ethanol solutions (0, 20, 40, 60, 80 and 100% (v/v), respectively) for

24 h at a liquor ratio of 1:10 (w/v). Ethanol solutions were changed once every 2 h. The obtained gels were named DFCG(0), DFCG(20), DFCG(40), DFCG(60), DFCG(80) and DFCG(100). In the case of preparing DCCG, the collagen self-assembly and cross-linking of NHS-AA were simultaneously carried out, and then the gels were dehydrated by the treatment of ethanol solution. NHS-AA concentrations were converted to active ester groups of NHS-AA as molar ratios to the calculated ϵ -NH₂ in hydroxylysine and lysine residues ($[\text{NHS-AA}]/\text{NH}_2$).² 0.044, 0.175, 0.35 and 0.7 mM NHS-AA solubilized in dimethyl sulfoxide (DMSO) were respectively mixed with PBS-solubilized collagen solutions to obtain a series of 5 mg/mL collagen solutions with different $[\text{NHS-AA}]/\text{NH}_2$ ratios (0.05, 0.2, 0.4 and 0.8, respectively). Both uncross-linked and cross-linked samples were immediately incubated at 30 °C for 5 h to gel and immersed in 60% (v/v) ethanol solution at a liquor ratio of 1:10 (w/v) for 24 h. Ethanol solutions were replaced once every 2 h. The obtained collagen gels were called DCCG(0), DCCG(0.05), DCCG(0.2), DCCG(0.4) and DCCG(0.8).

2.3 Atomic force microscopy (AFM) measurements

The slices cut from DFCG and DCCG by scissors were dropped onto freshly cleaved mica substrates. Subsequently, the samples were air dried in a desiccator for 72 h at 20 °C. The surface topography of DFCG and DCCG was detected by an atomic force microscope (Dimension 3100 Nanoscope IV, Shimadzu Corporations' SPM 9600, Kyoto, Japan). The height images were recorded in the soft tapping mode using silicon cantilevers with a force constant of 42 N/m and a scanning rate of 1 Hz. Every image was obtained at three various points to confirm the consistency of the observed morphologies.

2.4 Differential scanning calorimetry (DSC) measurements

DSC measurements was conducted to evaluate the thermal stability of collagen gels using DSC 200PC (Netzsch, Selb, Germany). Approximate 8 mg DFCG and DCCG were accurately weighed and sealed in an aluminum pans while a sealed aluminum pan containing same solvent with the sample was used as the control. The temperature ranged from 30 to 90 °C with a heating rate of 5 °C/min under a nitrogen atmosphere. The transition temperature of endothermic peak in the DSC curves was taken as the denaturation temperature (T_d) of collagen gels.³³

2.5 Dynamic viscoelasticity measurements

DFCG and DCCG disks with a diameter of 35 mm were prepared for dynamic viscoelasticity measurements, which were carried out using a Rheometer System Mars III (Hakke, Karlsruhe, Germany) with a parallel plate ($\varphi = 35$ mm) at a constant strain of 2% within the linear viscoelastic region. The temperature was controlled at 20 °C using a Peltier temperature controller with an accuracy of ± 0.1 °C by a circulatory water bath. The storage modulus (G') and loss modulus (G'') were recorded as a function of frequency at a range from 0.01 to 10 Hz. Triplicate experiments were conducted for each sample and mean value was calculated.

3 Results and discussion

3.1 Appearance of the gels

Appearance of two types of collagen gels before and after dehydration of ethanol is shown in Fig. 1. As shown in Fig. 1, the fibrillogenesis gels without the dehydration of ethanol looked opalescent and shrank slightly to form turbid gels after dehydration using different concentrations of ethanol.

For the gels prepared by the self-assembly and simultaneously cross-linking, the appearance was dependent on the concentration of NHS-AA. Without the dehydration of ethanol, the appearance of gels changed from opalescent state to transparent state. The results were in agreement of those of the previous study.⁷ Upon the dehydration of ethanol, DCCG shrank slightly when the [NHS-AA]/NH₂ ratio lower than 0.05, while it shrank distinctly and changed opalescent when the [NHS-AA]/NH₂ ratio higher than 0.2, compared with the untreated collagen gels.

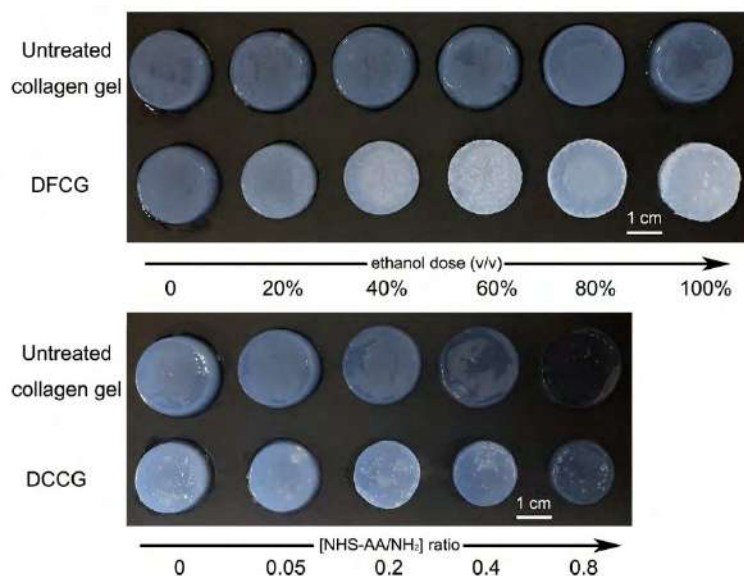


Fig. 1. Appearance of the DFCG and DCCG. Untreated and treated collagen gels are shown in the upper and lower rows, respectively.

In order to elucidate the variation on appearance of the gels, the microstructure of the gels was explored. The AFM images of DFCG and DCCG are shown in Fig. 2. As shown in Fig. 2A, the network structure of DFCG(0) was consisted of abundant D-periodic fibrils, which were formed by the self-assembly of collagen molecules through hydrogen bonding, hydrophobic and electrostatic interactions.^{6,9} The increase of ethanol concentration almost not changed the microstructure of DFCG, in which the diameter of fibrils was similar. The explanation was probably that the structure consisted of thick D-periodic fibrils was stable and different concentrations of ethanol only replaced free water and partial bound water within the structure of the gels owing to its higher polarity. Upon the addition of NHS-AA, the collagen self-assembly was slightly inhibited when the [NHS-AA]/NH₂ ratio lower than 0.05, but was distinctly hindered when the [NHS-AA]/NH₂ ratio higher than 0.2.⁷ For DCCG(0.5), the diameter of fibrils slightly decreased (Fig. 2B), but the gel was still constructed by the collagen self-assembly and had good stability to resist the dehydration of ethanol. However, as the [NHS-AA]/NH₂ ratio exceeded 0.2, the formation of gels was predominately depended on the covalent bonds between collagen molecules and NHS-AA, and exhibited an entangled network of tenuous fibrils (Fig. 2B), which could not resist the dehydration of ethanol. Furthermore, the shrinkage of the gels resulted in higher density of fibrils within the gels, which would hinder the transmittance of light and make DCCG(0.8) to become turbid.

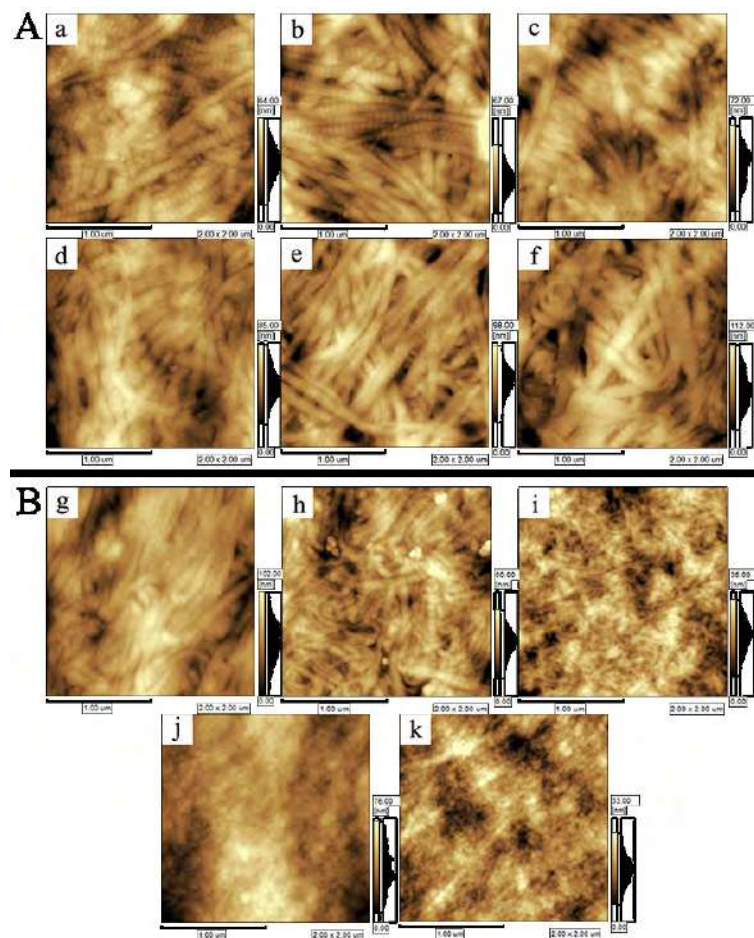


Fig. 2. AFM images of DFCG (A) and DCCG (B). The images from a to f are the fibrillogenesis collagen gels treated under the doses of ethanol of 0, 20, 40, 60, 80 and 100% (v/v), respectively. The images from g to k are the collagen fibrillogenesis and simultaneous cross-linking of NHS-AA treated by 60% (v/v) ethanol with the [NHS-AA]/NH₂ ratios of 0, 0.05, 0.2, 0.4 and 0.8, respectively.

3.2 DSC measurements

The potential application of fish collagen materials was restricted owing to its low thermal stability. The triple helix structure of collagen molecules is stabilized by intra-chain hydrogen bonds and cross-linking bonds. The thermal transition curves of DFCG and DCCG as detected by DSC are shown in Fig. 3. Both the self-assembly and cross-linking could improve the thermal stability of collagen. For DFCG, the dehydration of ethanol promoted the increase of thermal stability, which might be attributed that the different concentrations of ethanol replaced the water in the gels and stronger hydrogen bonds between collagen molecules and ethanol molecules were formed due to higher polarity of ethanol than water. Therefore, the T_d values increased with increasing ethanol concentrations, especially, the T_d value of DFCG(100) distinctly increased by 32.7 °C compared with that of DFCG(0) (Fig. 3A). For the collagen gels formed by the self-assembly and simultaneously cross-linking, the effects of NHS-AA on the thermal stability were similar to the results in our previous study. When the [NHS-AA]/NH₂ ratio was 0.05, the collagen self-assembly was slightly inhibited and the introduction of cross-linking bonds reinforced the structure of gels; as the [NHS-AA]/NH₂ ratio increased to 0.2, the collagen self-assembly was seriously hindered, but the cross-linking degree was low resulting in the decrease of thermal stability; as the [NHS-AA]/NH₂ ratio higher than 0.2, the increase of covalent cross-linking bonds promoted the increase of thermal

stability. Furthermore, compared with the gels without the dehydration of ethanol, the thermal stability of all DCCG samples increased. Interestingly, DCCG(0.05) exhibited a higher T_d value (52.5 °C), however, the T_d value of the gel formed at a [NHS-AA]/NH₂ ratio of 0.05 decreased by 2.7 °C than that of the gel formed at a [NHS-AA]/NH₂ ratio of 0.8 without the dehydration of ethanol. This phenomenon might be originated that the triple helix structure of partial collagen molecules denatured by 60% ethanol solutions when NHS-AA dosages was higher ([NHS-AA]/NH₂ ≥ 0.4). Consequently, the presence of thick D-periodic fibrils was more significant than the cross-linking for preparing the collagen gels with high thermal stability for application by the dehydration of ethanol.

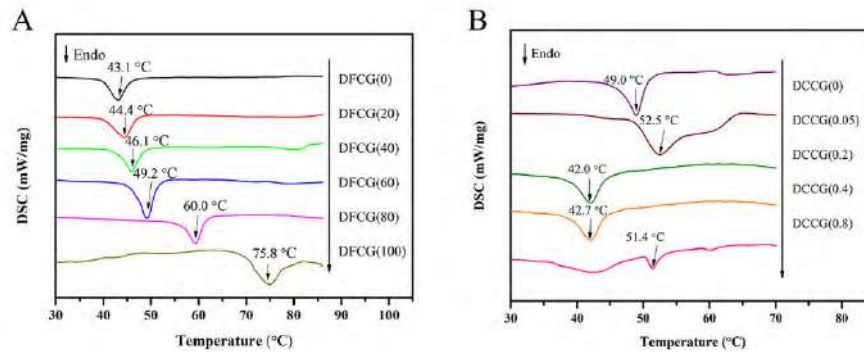


Fig. 3. DSC curves of DFCG (A) and DCCG (B). The curves from a to f are the fibrillogenesis collagen gels treated under the doses of ethanol of 0, 20, 40, 60, 80 and 100% (v/v), respectively. The curves from g to k are the collagen fibrillogenesis and simultaneous cross-linking of NHS-AA treated by 60% (v/v) ethanol with the [NHS-AA]/NH₂ ratios of 0, 0.05, 0.2, 0.4 and 0.8, respectively.

3.3 Dynamic viscoelasticity measurements

The technique of dynamic viscoelasticity measurement was frequently used capable of resolving the structural properties of materials into an elastic and a viscous response using the parameters of G' and G'' , respectively.³⁴ The values of G' and G'' of two types of collagen gels as a function of frequency at a range from 0.01 to 10 Hz are displayed in Fig. 6. For both DFCG and DCCG, the values of G' and G'' were nearly constant over the region of dynamic frequency and the values of G' were higher than that of G'' , characterizing high elasticity of these two types of collagen gels.^{19,35} The G' value at frequency of 1 Hz was assumed to be the shear modulus (G) value. The number of network points per cubic meter (ν) might be calculated using the following formula:^{17,27}

$$G = \nu kT$$

where T is the absolute temperature (293 K) and k is the Boltzmann constant (1.38×10^{-23} J/K).

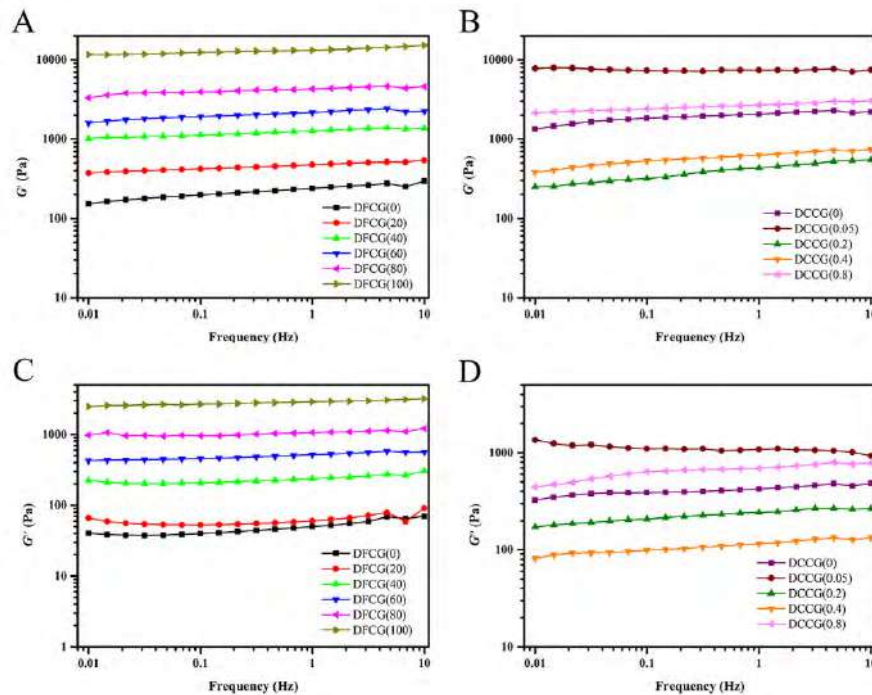


Fig. 4. The storage modulus (G') and loss modulus (G'') of the fibrillogenesis collagen gels dehydrated by ethanol at different concentrations (A and C) and the collagen fibrillogenesis and simultaneous cross-linking of NHS-AA treated by 60% (v/v) ethanol (B and D), respectively.

The values of G' and G'' at frequency of 1 Hz as well as ν value are summarized in Table 1. As shown in Fig. 6 and Table 1 and Table 2, the G' , G'' and ν values of DFCG increased with the increase of ethanol concentrations. In the case of DFCG, ethanol might majorly replace free water and partial bound water within the gel structure and stronger hydroxy bonds among ethanol, bound water and collagen molecules were established. Therefore, the network structure of the gels was reinforced, which was indicated by increasing ν values. Furthermore, slightly shrinkage of the gels owing to the exchange between ethanol and free water also improved the density of fibrils. As a result, when ethanol concentration was 100%, the values of G' and G'' were 13142.6 and 2893.8 Pa, respectively, which were approximately 55-folds than those of DFCG(0). For DCCG, the influence of NHS-AA dosages on dynamic viscoelasticity of the gels was in agreement of the results of DSC measurements. When the $[\text{NHS-AA}]/[\text{NH}_2]$ ratio was 0.05, the G' value was approximately 2-folds higher than that of DCCG(0) due to the introduction of the covalent cross-linking bonds in the presence of thick fibrils. As the $[\text{NHS-AA}]/[\text{NH}_2]$ ratio higher than 0.2, the collagen self-assembly was distinctly inhibited. Although there were abundant covalent cross-linking bonds among collagen molecules, free water was removed during the infiltration of 60% ethanol solutions, illustrating that the covalent cross-linking bonds could not maintain the stability of free water within the gel structure. Additionally, the triple helix might be broken during the process of ethanol permeation. Therefore, DCCG(0.8) exhibited lower G' and ν values than those of DCCG(0).

Table 1. The values of G' and G'' at frequency of 1 Hz as well as ν values of the fibrillogenesis collagen gels dehydrated by ethanol at different concentrations.

Samples	G' (Pa)	G'' (Pa)	ν ($\times 10^{23}$, number/m ³)
DFCG(0)	239.2 \pm 31.4	49.9 \pm 10.7	0.59
DFCG(20)	474.4 \pm 58.1	60.2 \pm 12.6	1.17
DFCG(40)	1265.9 \pm 103.4	236.2 \pm 29.4	3.13
DFCG(60)	2162.9 \pm 176.3	516.5 \pm 61.2	5.35
DFCG(80)	4285.0 \pm 249.5	1066.0 \pm 76.4	10.59
DFCG(100)	13142.6 \pm 528.2	2893.8 \pm 185.1	32.48

Table 2. The values of G' and G'' at frequency of 1 Hz as well as ν values of the collagen fibrillogenesis and simultaneously cross-linking of NHS-AA treated by 60% (v/v) ethanol.

Samples	G' (Pa)	G'' (Pa)	ν ($\times 10^{23}$, number/m ³)
DCCG(0)	2064.3 \pm 164.8	424.8 \pm 46.5	5.10
DCCG(0.05)	7388.0 \pm 319.7	1085.5 \pm 94.3	18.26
DCCG(0.2)	432.2 \pm 60.3	242.0 \pm 29.5	1.07
DCCG(0.4)	626.9 \pm 84.5	115.6 \pm 17.2	1.54
DCCG(0.8)	2699.18 \pm 192.8	692.12 \pm 92.7	6.67

4 Conclusions

In summary, two types of fish collagen gels were prepared by the dehydration of ethanol in the present study and we proved that the presence of thick D-periodic fibrils was distinctly significant to fabricate the gels with excellent physiochemical properties. For dehydrated fibrillogenesis gel, the three-dimensional structure of the gels was well maintained after the dehydration of different concentrations of ethanol, and stronger hydroxy bonds among ethanol, bound water and collagen molecules were established to improve the thermal stability and elasticity of the gels. The properties of the dehydrated cross-linking gels were dependent on the NHS-AA dosages. Low concentrations of NHS-AA ([NHS-AA]/[NH₂] ratio= 0.05) almost not affected the formation of thick D-periodic fibrils, and the gel exhibited the largest values of T_d and G' compared with the dehydrated fibrillogenesis gel owing to the introduction of covalent cross-linking bonds. As the [NHS-AA]/[NH₂] ratio higher than 0.2, thermal stability and elastic modulus of dehydrated cross-linking gels increased with the increase of NHS-AA dosage, however, the values of T_d and G' were lower than those of the gel formed when the [NHS-AA]/[NH₂] ratio was 0.05 due to the absence of thick fibrils.

5 Acknowledgements

This work was financially supported by the National Natural Science Foundation of China (No.21776184).

6 References

1. Wang H., Heilshorn S. C.: Adaptable hydrogel networks with reversible linkages for tissue engineering, *Adv. Mater.*, 27, 3717, 2015.
2. Xing R., Liu K., Jiao T., Zhang N., Ma K., Zhang R., Zou Q., Ma G., Yan X.: An Injectable Self-Assembling Collagen-Gold Hybrid Hydrogel for Combinatorial Antitumor Photothermal/Photodynamic Therapy, *Adv. Mater.*, 28, 3669, 2016.

3. Williams R. J., Hall T. E., Glattauer V., White J., Pasic P. J., Sorensen A. B., Waddington L., McLean K. M., Currie P. D., Hartley P. G.: *The in vivo performance of an enzyme-assisted self-assembled peptide/protein hydrogel*, *Biomaterials*, 32, 5304, 2011.
4. Kapoor S., Kundu S. C.: *Silk protein-based hydrogels: Promising advanced materials for biomedical applications*, *Acta Biomater.*, 31, 17, 2016.
5. Caló, E. Khutoryanskiy V. V.: *Biomedical applications of hydrogels: A review of patents and commercial products*, *Eur. Polym. J.*, 65, 252, 2015.
6. Yan M., Li B., Zhao X., Qin S.: *Effect of concentration, pH and ionic strength on the kinetic self-assembly of acid-soluble collagen from walleye pollock (*Theragra chalcogramma*) skin*, *Food Hydrocolloid.*, 29, 199, 2012.
7. Shen L., Tian Z., Liu W., Li G.: *Influence on the physicochemical properties of fish collagen gels using self-assembly and simultaneous cross-linking with the N-hydroxysuccinimide adipic acid derivative*, *Connect. Tissue Res.*, 56, 244, 2015.
8. Piechocka I. K., Van Oosten A. S., Breuls R. G., Koenderink G. H.: *Rheology of heterotypic collagen networks*, *Biomacromolecules*, 12, 2797, 2011.
9. Fang M., Goldstein E. L., Matich E. K., Orr B. G., Holl M. M.: *Type I collagen self-assembly: the roles of substrate and concentration*, *Langmuir*, 29, 2330, 2013.
10. Huang Y.-R., Shiao C.-Y., Chen H.-H., Huang B.-C.: *Isolation and characterization of acid and pepsin-solubilized collagens from the skin of balloon fish (*Diodon holocanthus*)*, *Food Hydrocolloid.*, 25, 1507, 2011.
11. Li Z., Wang B., Chi C., Zhang Q., Gong Y., Tang J., Luo H., Ding G.: *Isolation and characterization of acid soluble collagens and pepsin soluble collagens from the skin and bone of Spanish mackerel (*Scomberomorus niphonius*)*, *Food Hydrocolloid.*, 31, 103, 2013.
12. Jongjareonrak A., Benjakul S., Visessanguan W., Nagai T., Tanaka M.: *Isolation and characterisation of acid and pepsin-solubilised collagens from the skin of Brownstripe red snapper (*Lutjanus vitta*)*, *Food Chem.*, 93, 475, 2005.
13. Yamada S., Yamamoto K., Ikeda T., Yanagiguchi K., Hayashi Y.: *Potency of fish collagen as a scaffold for regenerative medicine*, *Biomed Res. Int.*, 2014, 302932, 2014.
14. Carvalho A. M., Marques A. P., Silva T. H., Reis R. L.: *Evaluation of the Potential of Collagen from Codfish Skin as a Biomaterial for Biomedical Applications*, *Mar. Drugs*, 162018.
15. Yunoki S., Nagai N., Suzuki T., Munekata M.: *Novel biomaterial from reinforced salmon collagen gel prepared by fibril formation and cross-linking*, *J. Biosci. Bioeng.*, 98, 40, 2004.
16. Zhai Z., Wang H., Wei B., Yu P., Xu C., He L., Zhang J., Xu Y.: *Effect of Ionic Liquids on the Fibril-Formation and Gel Properties of Grass Carp (*Ctenopharyngodon idellus*) Skin Collagen*, *Macromol. Res.*, 26, 609, 2018.
17. Mori H., Shimizu K., Hara M.: *Dynamic viscoelastic properties of collagen gels in the presence and absence of collagen fibrils*, *Mat. Sci. Eng. C-Mater.*, 32, 2007, 2012.
18. Valero C., Amaveda H., Mora M., Garcia-Aznar J. M.: *Combined experimental and computational characterization of crosslinked collagen-based hydrogels*, *Plos One*, 13, e0195820, 2018.
19. Duan L., Liu W., Tian Z., Li C., Li G.: *Properties of collagen gels cross-linked by N-hydroxysuccinimide activated adipic acid derivate*, *Int. J. Biol. Macromol.*, 69, 482, 2014.
20. Brindha J., Chanda K., Balamurali M M.: *Revisiting the insights and applications of protein engineered hydrogels*, *Mat. Sci. Eng. C-Mater.*, 95, 312, 2019.
21. Baniyasi, M., Minary-Jolandan, M.: *Alginate-Collagen Fibril Composite Hydrogel*, *Materials*, 8, 799, 2015.
22. Ma L., Gao C., Mao Z., Zhou J., Shen J., Hu X., Han C.: *Collagen/chitosan porous scaffolds with improved biostability for skin tissue engineering*, *Biomaterials*, 24, 4833, 2003.
23. Chen J. X., Yuan J., Wu Y. L., Wang P., Zhao P., Lv G. Z., Che, J. H.: *Fabrication of tough poly(ethylene glycol)/collagen double network hydrogels for tissue engineering*, *J. Biomed. Mater. Res. A*, 106, 192, 2018.
24. Pietrucha K.: *Changes in denaturation and rheological properties of collagen-hyaluronic acid scaffolds as a result of temperature dependencies*, *Int. J. Biol. Macromol.*, 36, 299, 2005.
25. Hara M.: *Various Cross-Linking Methods for Collagens: Merit and Demerit of Methods by Radiation*, *J. Oral. Tissue. Engin.*, 3, 118, 2006.
26. Van Oosten A. S., Vahabi M., Licup A. J., Sharma A., Galie P. A., MacKintosh F. C., Janmey P. A.: *Uncoupling shear and uniaxial elastic moduli of semiflexible biopolymer networks: compression-softening and stretch-stiffening*, *Sci. Rep-UK*, 6, 19270, 2016.
27. Mori H., Shimizu K., Hara M.: *Dynamic viscoelastic properties of collagen gels with high mechanical strength*, *Mat. Sci. Eng. C-Mater.*, 33, 3230, 2013.
28. Buwalda S. J., Boere K. W., Dijkstra P. J., Feijen J., Vermonden T., Hennink W. E.: *Hydrogels in a historical perspective: from simple networks to smart materials*, *J. Control. Release*, 190, 254, 2014.
29. Agee K. A., Prakki A., Abu-Haimed T., Naguib G. H., Nawareg M. A., Tezvergil-Mutluay A., Scheffel D. L., Chen C., Jang S. S., Hwang H., Brackett M., Gregoire G., Tay F. R., Breschi L., Pashley D. H.: *Water distribution in dentin matrices: bound vs. unbound water*, *Dent. Mater.*, 31, 205, 2015.
30. Usha R., Ramasami T.: *Role of aliphatic alcohols on the stability of rat - tail tendon (RTT) collagen fiber*, *J. Polym. Sci. Pol. Phys.*, 37, 1397, 1998.
31. Jee S. E., Zhou J., Tan J., Breschi L., Tay F. R., Gregoire G., Pashley D. H., Jang S. S.: *Investigation of ethanol infiltration into demineralized dentin collagen fibrils using molecular dynamics simulations*, *Acta Biomater.*, 36, 175, 2016.
32. Chen Y., Zhang M., Liu W., Li G.: *Properties of alkali-solubilized collagen solution crosslinked by N-hydroxysuccinimide activated adipic acid*, *Korea-Aust. Rheol. J.*, 23, 41, 2011.
33. Du T., Niu X., Li Z., Li P., Feng Q., Fan Y.: *Crosslinking induces high mineralization of apatite minerals on collagen*

- fibers, Int. J. Biol. Macromol., 113, 450, 2018.*
34. Kasapis S., Mitchell J. R.: *Definition of the rheological glass transition temperature in association with the concept of iso-free-volume, Int. J. Biol. Macromol., 29, 315, 2001.*
35. Anumolu S. S., Menjoge A. R., Deshmukh M., Gerecke D., Stein S., Laskin J., Sinko P. J.: *Doxycycline hydrogels with reversible disulfide crosslinks for dermal wound healing of mustard injuries, Biomaterials, 32, 1204, 2011.*

DESIGN OF EXPERIMENTS (DOE) FOR PRODUCT AND PROCESS IMPROVEMENTS: A PHENOLIC SYNTAN CASE STUDY

Eric Verlaan^{1a}, Wouter Hendriksen¹, Rob Meulenbroek¹, Devlin du Prie¹

¹ Smit & zoon, Nijverheidslaan 48, 1382LK Weesp, the Netherlands

a) Corresponding author: Eric.Verlaan@smitzoon.com

Abstract. For sustainable developments the chemical industry is continuously looking for technical innovations with wide potential implications. The Design of Experiments (DOE) approach has been proven to be a powerful tool in determining the relationship between factors affecting output variables. DOE is done to identify the first order effects and higher order interactions and eventually realize output optimization. Although we can influence properties by application, the effect a retanning agent has on leather originates to a large extent from the chemistry involved. To understand interactions and the possibilities of targeted improvements of the production process, a DOE factorial design approach was used to identify the control parameters and their interactions in our phenolic syntan recipes. Instead of trial-and-error or one-factor-at-a-time practices, DOE made it possible to limit the number of lab experiments and still quantify the first order effects and the higher order interactions. As a result, a much deeper and more consistent understanding of the building blocks' interactions and how these influence the chemical process of phenolic syntan synthesis has been gained. This includes the amount of different building blocks, their molar ratios as well as process conditions. Aiming at achieving optimal efficiency for various projects, right now we are looking at possibilities in implementing DOE within Smit & zoon.

1 Introduction

The production of chemical ingredients can be described by a process of multiple factors for example molar ratios of different raw materials and process conditions such as temperatures, pressure, stirring speed and process time. This process creates all kinds of measurable data labelled as response information (see figure 1). Using Design of Experiments (DOE) the impact of multiple factors on a response can be investigated by simultaneously adjusting levels of multiple factors in each test run. To optimize the process on a response, it is important to obtain the right factors and the interaction of different factors having their effect on a certain response.



Figure 1. Process overview from factors to responses.

A specific process is the production of a group of re-tanning agents which are so-called phenolic resins. These widely known polymer products are for instance produced by a condensation reaction of phenol-sulphonic acid with formaldehyde together with other building blocks like other aromatics or amines.

This article describes the case study of a small DOE model for obtaining control factors and interactions on the response of free phenol content in powder products.

2 Materials and Methods

2.1 Materials

Chemicals used for the analysis of free phenol are purchased from different lab chemical suppliers such as Sigma Aldrich (phenol $\geq 99\%$), Acros Chemicals (4-aminoantipyrine 98%) and Chem-Lab (potassiumhexacyanoferrate [III] p.a.). For the synthesis of a phenolic resin, chemicals like acids, caustic, aldehyde solutions, aryl- and amine compounds are used from own production stocks.

2.2 Analytical method to analyze phenol content

Emerson's reagent (4-aminoantipyrine – potassiumhexacyanoferrate [III]) is widely used for the determination of phenol. In this method the free phenols are released when syntan are dissolved and separated from interfering constituents by steam distillation. The phenolic compounds are buffered to a pH of 10 in order to prevent formation of quinonoid substitution products (antipyrine red). The free phenol present in the aqueous solution is then reacted with Emerson's reagent [1] to form a yellow-red complex, depending on amount of reacted phenol. This complex can then be quantitatively determined via spectrometry. Emerson's reaction has many advantages: speedy results, easy manipulation, use of stable reagents, applicability over a wide range of concentration of phenolic materials [1].

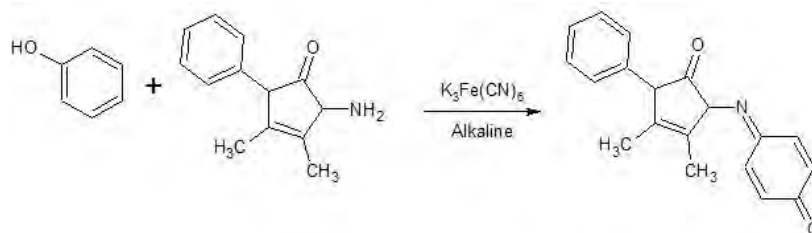


Figure 2. Emerson's reagent reaction with phenol

2.3 Full factorial design

The experiment is set up by using a full factorial design where three factors (A, B and C) will be investigated (see figure 3). Each factor will have an upper and a lower value (blue balls) and an additional experiment in the center of these factor settings (green ball). This center point helps to see whether the interactions between the factors are linear or not.

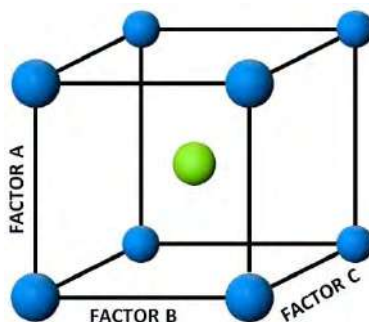


Figure 3. Cubic plot of factors with a center point in a full factorial design set up.

In table 1, an overview of 9 experiments is shown for the design set up in this study. Factor A and B are of chemical origin and factor C being a technical one.

Table 1. Expression of corner and center points of a cubic plot

Experiment	Setting Factor A	Setting Factor B	Setting Factor C
1	High	High	High
2	High	High	Low
3	High	Low	High
4	High	Low	Low
5	Medium	Medium	Medium
6	Low	High	High
7	Low	High	Low
8	Low	Low	High
9	Low	Low	Low

2.4 Preparation of a re-tanning agent

As an example for the investigation, a simple process for the synthesis of phenolic resins is used, comparable to the example used by E. Stiasny [2]. For the equipment a 2 ltr, three-necked round bottom flask with condenser and dropping funnel is used including stirring and thermometer. The first step in the reaction process is the sulphonation of phenol at 100°C, followed by the addition of water and an amine, like urea. At 65°C the condensation reaction with an aldehyde takes place. After this step the reaction mixture is partially neutralized. A second addition of phenol and aldehyde was used to continue the polymerization. Finally, the product was finalized by setting a required pH with sodium hydroxide. The liquid product is spray dried into a powder version by using a pilot spray dryer (Anhydro Lab 1). This product is analyzed on the amount of free phenol.

3 Results and Discussion

All nine syntheses resulted in powder products that made it possible to analyze their free phenol content in ppm (see table 2). This design inputs have been entered in the powerful calculation tool MiniTab®18 [3].

Table 2. Data overview of factors, level settings and response.

Experiment	Setting Factor A	Setting Factor B	Setting Factor C	Response Phenol content
1	0.09	2.00	120	< 50
2	0.09	2.00	15	601
3	0.09	1.25	120	2060
4	0.09	1.25	15	7047
5	0.045	1.63	68	1274
6	0	2.00	120	< 50
7	0	2.00	15	655
8	0	1.25	120	1800
9	0	1.25	15	6041

To show the effect of each factor, the average response of each low and high level factor is calculated for that specific factor (see figure 4). A large slope corresponds to a strong effect caused by that factor. When the graph has a small slope, or even a horizontal line, the effect is getting more and more negligible. From this graph it can be seen that factor B and C have a strong effect, while the response effect for factor A is almost negligible for the selected levels.

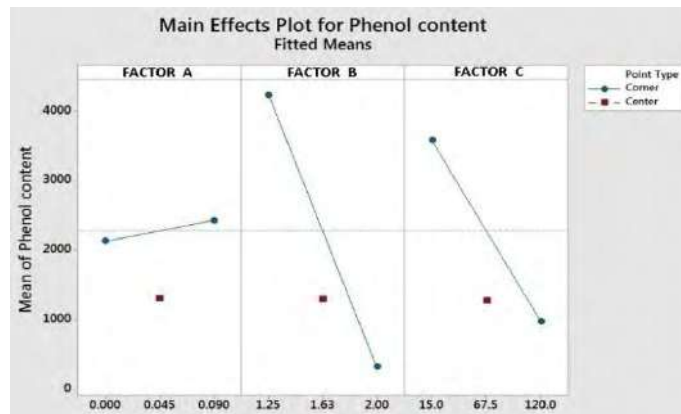


Figure 4. The effect of a single factor on the response.

In this design, there are three two-factor interactions, so-called 2nd order interactions, namely AB, AC and BC. For these interactions, it is also possible to calculate the effect of these factor-interactions, visualized in figure 5. When lines are parallel to each other, there is no interaction between two factors and therefore no additional effect. There is an interaction when lines will attend to cross each other, for example as for factor B with C, causing an additional effect on the response.

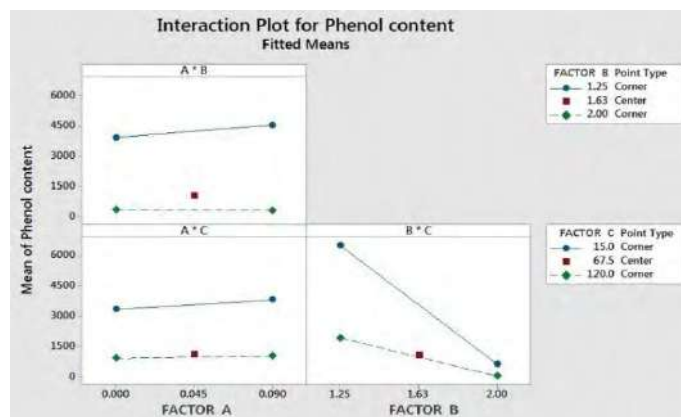


Figure 5. Interaction plot of different factors on response.

Besides the factors themselves and the 2nd order interactions, there is also a 3rd order interaction, mentioned as interaction ABC. The effect is calculated in the same way like the 2nd order interaction. To visualize the magnitude and the importance of all the effects from largest to smallest, a Pareto chart is made (see figure 6). In this case it is clear that factor B and C and the 2nd order interaction BC have the highest effect. The 3rd order interaction ABC is almost negligible in this case study.

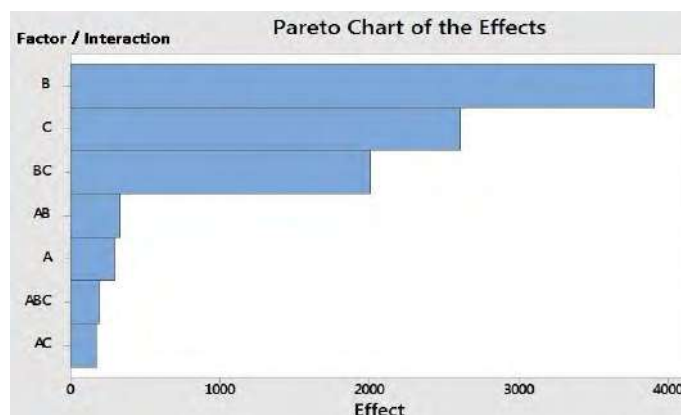


Figure 6. Effect impact for each factor and interaction

4 Conclusion

Design of Experiments (DOE) has been proven to be efficient and effective in product and process improvement in a phenolic syntan case study. From this case study, it is thought that decreasing the amount of free phenol in the product is possible, by increasing factor B and factor C within the recipe. The interaction of both factors (BC) even strengthens the effect. Factor A does not have a significant impact on the response, nor its interaction with other factors.

5 Outlook

DOE factorial design can be used to identify factors (control parameters) and especially their multiple order interactions in a wide range of (industrial) applications. The approach of large systems, high amount of factors, by using DOE is an effective and efficient way to obtain that knowledge. Increasing the amount of factors increases the amount of experiments tremendously, according to equation (1);

$$L^k = \text{number of experiments} \quad (1)$$

L is the number of levels for each factor
k is the number of different factors

In table 3 an overview is shown on the number of experiments required for the amount of factors in a 2-level system. Depending on the resources available, the amount of experiments can be reduced using fractional factorial design. This leaves out the highest order interactions, because the change of a big impact on the response is small. For that reason, the amount of experiments can be significantly reduced, while obtaining great amount of knowledge of factor and lower order interaction effects.

Table 3. Factorial designs in a 2-level system

# exp	Factors								
	2	3	4	5	6	7	8	9	10
4	Full	n.a.	n.a.						
8		Full	Fract	n.a.	n.a.	n.a.	n.a.		
16			Full	Fract	Fract	Fract	Fract	n.a.	n.a.
32				Full	Fract	Fract	Fract	Fract	Fract
64					Full	Fract	Fract	Fract	Fract
128						Full	Fract	Fract	Fract

Full: full factorial design, maximum of information (green)

Fract: fractional factorial design, high degree (green) or less degree (yellow) of information

n.a.: not applicable, too much loss of information (red)

References

1. Chitra V, G Tamilselvan, IVMV Enoch, Paulraj M S. Phenol Sensing Studies by 4-Aminoantipyrine Method—A Review. *Organic & Medicinal Chem IJ*. 2018; 5(2): 555657. DOI: 10.19080/OMCIJ.2018.05.555657
2. AT58405 (B) - Verfahren zur Darstellung gerbender Stoffe
3. <https://www.minitab.com/en-us/products/minitab/>

PREPARATION AND PROPERTIES OF MICROFIBRILLATED CHITIN/GELATIN COMPOSITES

Yifan Li¹, Caixin Cao, Ying Pei*, Xueying Liu, Keyong Tang*

*School of Materials Science and Engineering, Zhengzhou University
Zhengzhou 450001, P. R. China.*

*: Corresponding author E-mail: peiyang@zzu.edu.cn, kytangzzu@126.com

Abstract. Microfibrillated chitin/gelatin composite films were prepared by solvent casting method, and the nano-sized microfibrillated chitin as reinforce phase to improve oxygen resistance, water-resistant and mechanical performance in this system. The morphologies were analyzed by scanning electron microscope (SEM), and the mechanical properties were investigated by texture analyzer. Oxygen permeability property, optical property and swelling property were investigated. The results indicated that the elastic modulus and tensile strength of microfibrillated chitin/gelatin composite film reached 2.2 GPa and 74.5 MPa respectively when the content of microfibrillated chitin is 8 wt.%. The swelling ratio decreased to 11.63 with the 6 wt.% content of microfibrillated chitin. In addition, chitin microfibrils effectively enhanced the oxygen resistance of composite film without obvious loss of transmittance. This work expects to provide a pathway to improve gelatin performance.

1 Introduction

With sustainable development and increasing popularities of low carbon economy, the utilization of biomass from nature resources has aroused public attention^[1-2]. The usage of disposable plastic packings has aroused series of tricky environmental pollution problems. It is urgent to replace synthetic plastic by using biomass materials in the field of food packaging^[3-4]. Biomass such as proteins and polysaccharides which have been chosen by scientists to applied widely in biomedical or food packaging fields due to their biodegradability, sustainability and renewability^[5]. In particular, gelatin is a protein obtained from the partial denaturation of native collagen that existed in the bones, tendon and skin of animals, and can be obtained by a controlled hydrolysis reaction^[6-8]. Like most proteins, gelatin has good film-forming properties, excellent biocompatibility and biodegradability. Moreover, it features barrier properties against oxygen and aromas at low and intermediate relative humidity^[9-10]. In previous researches, soy protein isolate/gelatin composites were prepared by compression molding with being able to replace those environmentally unfriendly additives required in making packaging^[11]. Citric acid-incorporated fish gelatin/chitosan composite films were prepared as active food packaging with good UV barrier properties, showing the excellent ability to reduce the *E. coli* growth^[12].

However, there are some disadvantages of gelatin, which limited its applications. The weak interactions between gelatin molecules make its high brittleness^[13]. Molecules of hydrophilic nature induce that gelatin is sensitive to water or humid environment, resulting in non-ideal swelling property^[14]. Numerous efforts have been made to improve the mechanical properties or swelling properties of gelatin by various methods such as chemical crosslinking^[15-16], plasticizer and reinforcing modification^[17]. Chemical agents including glutaraldehyde, formaldehyde would bring healthy and security problems. Although plasticizers could greatly improve gelatin physical performance, they could easily migrate from gelatin matrix when the environment changes, which would have great influence on the modification effect.

Chitin, the most abundant natural polymer besides cellulose on the earth, is a kind of polysaccharide mostly from the shells of crustaceans, insects and other invertebrates^[18-19]. Chitin features excellent

biodegradability, antibacterial activity, biocompatibility and low immunogenicity. It's worth noting that microfibrillated chitin could be obtained by high-pressure homogenization, grinding and ultrasonic treatment to be a nano-size biomass material with high surface area and high aspect ratio. Furthermore, microfibrillated chitin possesses ability to form a dense network by inter- and intra-fibril hydrogen bonds. This network structure composed of nano-microfibers benefits the reinforcement of gelatin matrix because of its high strength and stiffness ^[20-21]. In this work, microfibrillated chitin was employed as reinforce phase to improve the performance of gelatin matrix. The structure and properties of composite films were investigated by SEM, texture analyzer, oxygen transmissivity tester and ultraviolet-visible spectrophotometer, expecting to provide a pathway to modify gelatin.

2 Materials and Methods

2.1 Materials

Gelatin derived from bovine skin (Type B, bloom 250, *pI* 5-5.5) was purchased from Shanghai Macklin Biochemical Co., Ltd. Chitin powder was supplied by Zhejiang Golden Shell Pharmaceutical Co., Ltd. All other reagents used were of analytical grade and used without further treatment.

2.2 Chitin Purification

The purpose of purification is to remove carbonate and protein in carb shells thoroughly, and the procedures were according to the method reported by Cai (2013) ^[22]. Firstly, chitin powder was treated by 5% sodium hydroxide solution for 6 h at room temperature, and then washed with deionized water to neutral. Subsequently, the powder was immersed into 7% hydrochloric acid aqueous solution for 1 day at room temperature. After rinsed with distilled water, the resulting powder was treated with 5% sodium hydroxide aqueous solution for 2 days. 1.7% sodium hypochlorite, 0.3 mol/L sodium acetate solution treated the above chitin powder for 6 h at 80 °C. The as-purified chitin powder was rinsed with distilled water and dried for the next use.

2.3 Microfibrillated Chitin (MFCh) Preparation

The purified chitin was dispersed into 10% sodium hydroxide solution under stirring for 2 h at 60 °C to a total swelling state. Chitin suspension was homogenized at 1000 bar for 20 times using a high-pressure homogenizer equipped with a cooling system (APV 2000, SPX Flow technology Rosista GmbH, German) until obtaining a white milky suspension. The solid content of microfibrillated chitin suspension was determined by dried and weighted.

2.4 Preparation of MFCh/Gel Composite

Gelatin was dissolved into distilled water for 2 h at 50 °C to obtain gelatin solution. Microfibrillated chitin suspension was mixed with the gelatin solution under agitation for 1 h. Then the mixture was poured into the polytetrafluoroethylene molds and dried at ambient condition (RH 50%) for 2 days. The composite samples were noted as MFCh/Gel. According to the amount of microfibrillated chitin in gelatin solution: 2, 4, 6, 8 and 10 wt.%, the samples were labeled as MFCh2/Gel, MFCh4/Gel, MFCh6/Gel, MFCh8/Gel, and MFCh10/Gel, respectively. Gelatin film (Gel) without chitin was prepared in the same method. All the film samples were conditioned at 25 °C and 70% RH in a climatic chamber before testing. The average thickness of films was 0.17±0.027 mm.

2.5 Characterization

The surface and cross section of samples were spilled with gold and observed through a scanning electron microscopy (SEM, Quanta 250, USA) at the accelerating voltage of 20 kV and 5 kV. Mechanical properties of the samples were tested with a Texture Analyzer (TAHD-PLUS) at a crosshead speed of 50 mm/min using a load cell of 750 N. Tensile modulus (E_t), tensile strength (σ_t) and elongation at break (ε_{break}) of samples were determined from stress-strain curves. The resulting values were the average values for every five samples. Swelling experiments were performed by immersing dry films in deionized water until swelling equilibrium. The initial samples were dried at 25 °C and weighted accurately, noted as W_0 . The weights of swelling samples were noted as W_e . The swelling capacity M_e of the composite was calculated as following:

$$M_e (\%) = \frac{W_e - W_0}{W_0} \times 100 \quad (1)$$

Oxygen Transmission Rate (OTR) measurements have been carried out using an Oxygen Permeability Tester (OX2/231, PERME, China) at 23 °C abiding by a standard of ASTM D 3985. The films were installed in a cell where 100% O₂ was flushed on the top side and 100% N₂ on the bottom side. The amount of O₂ transferred through the films was assessed by an oxygen sensor in the N₂ gas flow. Ultraviolet-visible spectrophotometer (TU-1950, PERSEE, China) was employed to characterize the optical transmittance of composite films in the wavelength range from 400 to 800 nm.

3 Results and Discussion

3.1 Morphology

Figure 1 shows the morphology of the chitin powder and the microfibrillated chitin. The morphology of chitin powder is irregular particles. It shows that the high-pressure homogenization achieved effective fiber fibrillation, and the aggregation structure of chitin was separated into smaller fibrils with large surface area (Figure 1a-b). It is observed that the chitin nanofibers display a network structure with the average fibers diameter of around 100 nm, which is distinguished from the morphology of chitin powder (Figure 1c). Effective improvement of matrix in mechanical property could be obtained by the addition of microfibers with higher aspect ratio and network structure^[23-24]. Therefore, chitin microfibrils could have been a promising reinforce agent for gelatin matrix. The morphologies of MFCh/Gel composites are showed in Figure 2. It is indicated that chitin microfibrils can be dispersed uniformly in the system, showing a very good interfacial adhesion. However, chitin microfibrils aggregated at high concentration, which is in agreement with the following mechanical results.

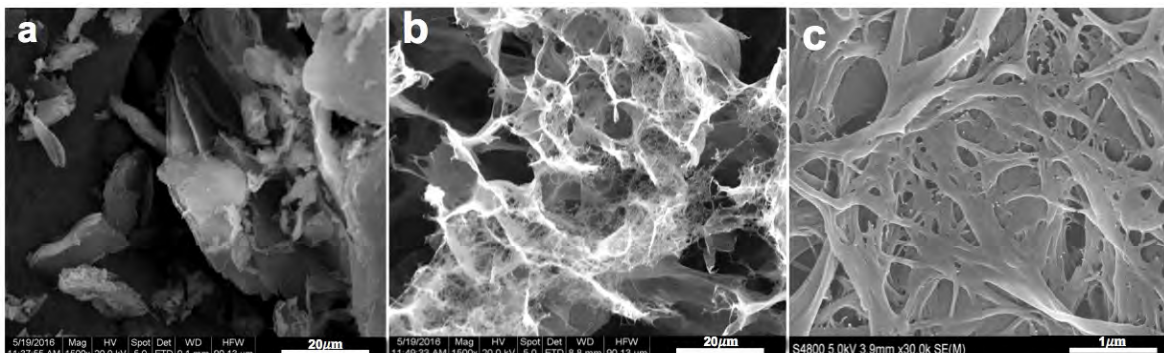


Fig. 1. SEM images of chitin microfibrils. (a) Chitin power, (b-c) microfibrillated chitin treated by high-pressure homogenization.

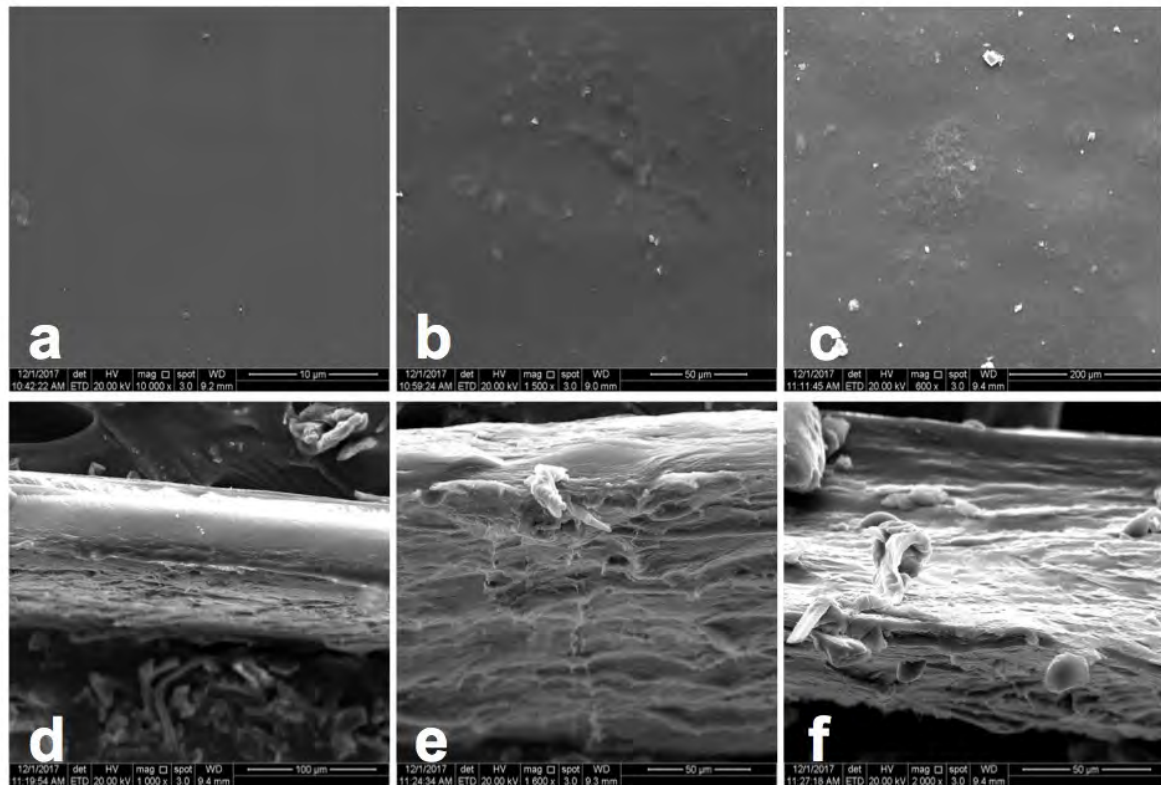


Fig. 2. SEM images of surface (a-c) and cross-sectional (d-f) morphology of MFCh/Gel composites. (a, d) Gel, (b, e) MFCh6/Gel, (c, f) MFCh8/Gel.

3.2 Tensile Properties of MFCh/Gel Composites

Figure 3a-c exhibits the effect of the amount of microfibrillated chitin on the tensile properties of the gelatin. The elastic modulus and tensile strength of gelatin are about 1.7 GPa and 61.3 MPa, respectively. It is shown that the tensile properties increase with the increase of chitin microfibrils content. When 8 wt.% microfibrils are incorporated, the optimal mechanical property (E_t , σ_t) is obtained. The tensile modulus reaches 2.2 GPa, and the tensile strength of CMFh/Gel is increased from 61.3 MPa to 74.5 MPa, an increase of 21.5%, suggesting a good improvement. Due to the high degree microfibrillation, chitin has large aspect ratio and specific surface area with a great quantity of polar hydroxyl groups on the fiber surface, which can have interactions with the amino groups and carboxyl groups of gelatin molecules. The chitin microfibrils not only can bear the load effectively but also prevent the crackle from propagating. When chitin content above 8 wt.%, the tensile strength of the composite films decreases gradually, properly resulting from the aggregations of chitin microfibrils at high concentration. More fibers cannot be dispersed uniformly in the system, and the agglomeration of microfibrillated chitin in the composite film may form stress concentration point when the material is loaded. Furthermore, the elongation at break increased by 26.9% with the addition of 6 wt.% microfibrillated chitin, the maximum value of ϵ_{break} was 7%. It is because some amounts of microfibrillated chitin increase the evenly distribution of stress and decrease the stress concentration.

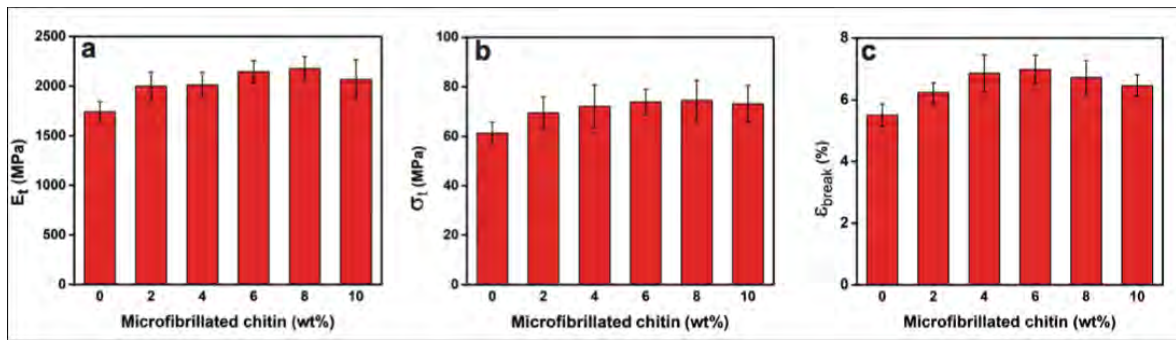


Fig. 3. Tensile properties of gelatin and MFCh/Gel (a) modulus (E_t), (b) strength (σ_t) and (c) elongation at break (ϵ_{break}).

3.3 Swelling Property

Gelatin has strong hydrophilicity due to the abundant hydrophilic groups such as hydroxyl, carboxyl and amino groups in molecules. It tends to swell or even dissolve when applied in water or humid environment. The swelling ability of the composites influences the physical properties such as shape and mechanical properties. Therefore, the investigation of the swelling ability is very necessary for gelatin system. Swelling ratios of gelatin and MFCh/Gel composites are shown in Figure 4. It is observed that with increasing chitin content, the swelling ratios of the composite films decrease at first and then increase. When the content of microfibrillated chitin is 6 wt.%, a minimum swelling ratio of 11.63 is obtained, which is 14.43% lower than that of gelatin film. Therefore, the addition of chitin microfibrils can decrease the swelling ratio and the water sensitivity of gelatin matrix. On one hand, the interactions between gelatin and chitin microfibrils replace some interactions between gelatin and water molecules, reducing the hydrophilic tendency of gelatin system. On the other hand, the network structure of microfibrillated chitin could effectively depress the water uptake through capillary action in gelatin matrix, resulting in the improvement of swelling property [25]. However, with the increase of microfibrillated chitin content, the swelling ratio of composite increases on the account of severe phase separation between chitin fiber and gelatin.

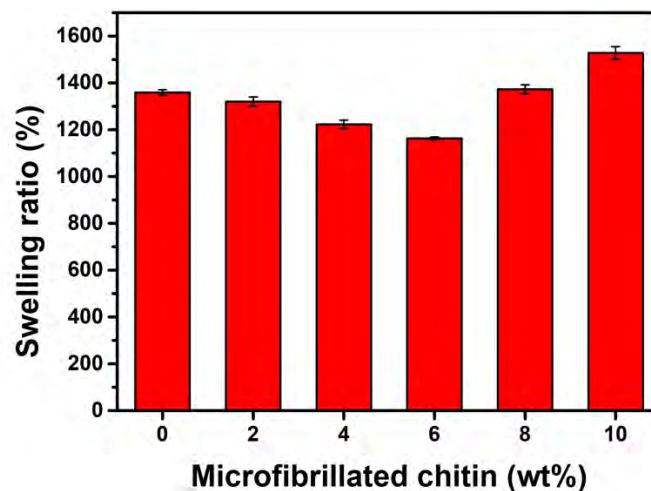


Fig. 4. Swelling property of gelatin and MFCh/Gel.

3.4 Oxygen Permeability Property

Gas barrier performance of packaging materials is a key parameter because good oxygen resistance can effectively help slow food deterioration and extend shelf life. Oxygen transmission rate (OTR)

of gelatin and composites is presented in Figure 5. The addition of chitin microfibrils significantly decreases OTR compared with that of the gelatin film especially for 10 wt.% microfibrillated chitin content. Microfibrillated chitin with network structure can create a longer diffusion path for oxygen permeation, resulting in the decreasing in the permeability of composites [26].

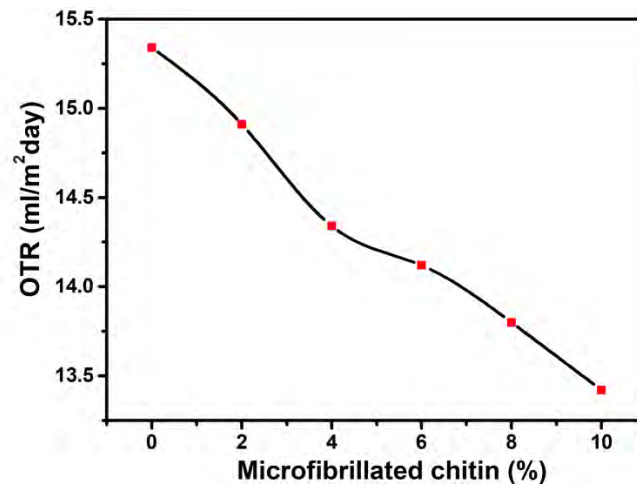


Fig. 5. Oxygen Transmission Rate (OTR) of gelatin and MFCh/Gel.

3.5 Optical Property

The optical property is of great importance for packaging materials. Light transmission of the MFCh/Gel films is shown in Figure 6. It indicates that the gelatin film has a high transmittance and can reach about 90% in the visible wavelength range from 400 to 800 nm. An obvious UV resistivity for gelatin and MFCh/Gel films appears in the wavelength range of 200-250 nm due to the ability of UV radiation absorbance for protein material. The films remain relatively high transparency with low content of microfibrillated chitin (less than 8 wt.%) due to microfibrillated chitin's homodisperse in the gelatin matrix [27]. With increasing the amount of microfibrillated chitin, the light transmittance of the composite film decreases gradually, which may be due to the agglomerations of microfibrillated chitin and phase separations in the composite system. However, the composite film can maintain a good light transmittance of above 60% when addition of 10 wt.% microfibrillated chitin content, which could be acceptable in packing applications.

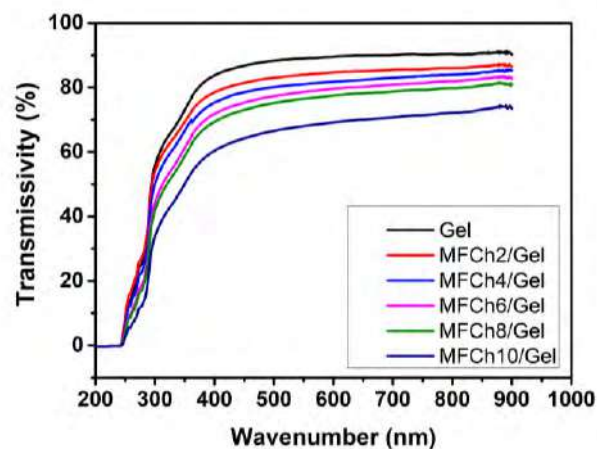


Fig. 6. Effect of microfibrillated chitin content on the optical property of the gelatin and MFCh/Gel.

4 Conclusions

Chitin can be separated into microfibrils successfully by high-pressure homogenization to obtain microfibrillated chitin with nanoscale diameter and network morphology. Owing to network structure and abundant hydroxyl groups, microfibrillated chitin played the role of a reinforcing agent in gelatin matrix to improve the mechanical properties. When the addition of microfibrillated chitin was 8 wt.%, the modulus and tensile strength increased to 2.2 GPa and 74.5 MPa, which improved 29.4% and 21.5% compared to that of gelatin film. The swelling ability of composite films dramatically decreased with 6 wt.% chitin microfibrils content, due to the interactions between gelatin and chitin microfibrils and the depression of water uptake by the network structure of microfibrillated chitin through capillary action. The incorporation of chitin microfibrils greatly improved oxygen barrier property of the biomass composites since that chitin microfibrils could create a longer diffusion path for oxygen permeation. Moreover, the composite film exhibited relatively good optical transmittance property in the visible range. This work expects to provide a pathway to improve gelatin performance and a new composite material for packaging applications.

References

1. Mu C, Guo J, Li X, et al. Preparation and properties of dialdehyde carboxymethyl cellulose crosslinked gelatin edible films, *J. Food Hydrocolloids*. 27(1) (2012) 22-29.
2. Pena C, D Caba K, Eceiza A, et al. Enhancing water repellence and mechanical properties of gelatin films by tannin addition, *J. Bioresour Technol*. 101(17) (2010) 6836-6842.
3. Vieira M G A, Silva M A D, Santos L O D, et al. Natural-based plasticizers and biopolymer films: A review, *J. European Polymer Journal*. 47(3) (2011) 254-263.
4. Wang J, Wang J, Zhang K, et al. Preparation and characterization of CST/CS/PVA/GEL blend membrane, *J. Materials Review*. 35(11) (2012) 2689-2693.
5. Chambi H, Grosso C, Edible films produced with gelatin and casein cross-linked with transglutaminase, *J. Food Research International*. 39(4) (2006) 458-466.
6. Cai Z, Kim J, Preparation and characterization of novel bacterial cellulose/gelatin scaffold for tissue regeneration using bacterial cellulose hydrogel, *J. Journal of Nanotechnology in Engineering and Medicine*. 1(2) (2010) 1-6.
7. Hashim D M, Man Y, Norakasha R, et al. Potential use of fourier transform infrared spectroscopy for differentiation of bovine and porcine gelatins, *J. Food Chemistry*. 118(3) (2010) 856-860.
8. Martucci J F, Ruseckaite R A, Biodegradation of three-layer laminate films based on gelatin under indoor soil conditions, *J. Polymer Degradation & Stability*. 94(8) (2009) 1307-1313.
9. Lu A, Ma Z, Zhuo J, et al. Layer-by-layer structured gelatin nanofiber membranes with photoinduced antibacterial functions, *J. Journal of Applied Polymer Science*. 128(2) (2013) 970-975.
10. Martucci J F, Ruseckaite R A, Biodegradation of three-layer laminate films based on gelatin under indoor soil conditions, *J. Polymer Degradation & Stability*. 94(8) (2009) 1307-1313.
11. Guerrero P, Stefani P M, Ruseckaite R A, et al. Functional properties of films based on soy protein isolate and gelatin processed by compression molding, *J. Journal of Food Engineering*. 105(1) (2001) 65-72.
12. Uranga J, Puertas A I, Etxabide A, et al. Citric acid-incorporated fish gelatin/chitosan composite films, *J. Food Hydrocolloids*. 86(2019) 95-103.
13. George J, Siddaramaiah, High performance edible nanocomposite films containing bacterial cellulose nanocrystals, *J. Carbohydrate Polymers*. 87(3) (2012) 2031-2037.
14. Karnnet S, Potiyaraj P, Pimpan V, Preparation and properties of biodegradable stearic acid-modified gelatin films, *J. Polymer Degradation & Stability*. 90(1) (2005) 106-110.
15. Kim S, Nimni M, Yang Z, et al, Chitosan/gelatin-based films crosslinked by proanthocyanidin, *J. Journal of Biomedical Materials Research Part B: Applied Biomaterials*. 75B(2) (2005) 442-450.
16. Matsuda S, Se N, Iwata H, et al. Evaluation of the antiadhesion potential of UV cross-linked gelatin films in a rat abdominal model, *J. Biomaterials*. 23(14) (2002) 2901-2908.
17. Fakhreddin H S, Rezaei M, Zandi M, et al. Preparation and functional properties of fish gelatin-chitosan blend edible films, *J. Food Chemistry*. 136(3-4) (2013) 1490-1495.
18. Chai P, Zhang W, Jin X, The new exploiting and researching trends of chitin/chitosan, *J. Chemistry*. (7) (1999) 8-11.

19. Simpson B K, Gagne N, Simpson M V, *Bioprocessing of chitin and chitosan*, in: AM Martin (Eds.), *Fisheries Processing*. London: Chapman and Hall, 1994, pp. 155-173.
20. Liu M, Huang J, Luo B, et al. *Tough and highly stretchable polyacrylamide nanocomposite hydrogels with chitin nanocrystals*, *J. International Journal of Biological Macromolecules*. 78 (2015) 23-31.
21. Salaberría A M, Díaz R H, Labidi J, et al. *Role of chitin nanocrystals and nanofibers on physical, mechanical and functional properties in thermoplastic starch films*, *J. Food Hydrocolloids* 46 (2015) 93-102.
22. Duan B, Chang C, Ding B, et al. *High strength films with gas-barrier fabricated from chitin solution dissolved at low temperature*, *J. Journal of Materials Chemistry A*. 1(5) (2013) 1867-1874.
23. George J, Siddaramaiah, *High performance edible nanocomposite films containing bacterial cellulose nanocrystals*, *J. Carbohydrate Polymers*. 87(3) (2012) 2031-2037.
24. Eichhorn S J, Dufresne A, Aranguren M, et al. *Review: current international research into cellulose nanofibres and nanocomposites*, *J. Journal of Materials Science*. 45(1) (2010) 1.
25. Zheng X, Liu J, Pei Y, et al. *Preparation and properties of sisal microfibril/gelatin biomass composites*, *J. Composites Part A Applied Science & Manufacturing*. 43(1) (2012) 45-52.
26. Belbekhouche S, Bras J, Siqueira G, et al. *Water sorption behavior and gas barrier properties of cellulose whiskers and microfibrils films*, *J. Carbohydrate Polymers*. 83(4) (2011) 1740-1748.
27. Ifuku S, Ikuta A, Egusa M, et al. *Preparation of high-strength transparent chitosan film reinforced with surface-deacetylated chitin nanofibers*, *J. Carbohydrate Polymers*. 98(1) (2013) 1198-1202.

STUDY ON THE DIFFERENCE OF COLLAGEN FIBRE STRUCTURE CAUSED BY EPOXY RESIN EMBEDDING

Lu Jianmei¹, Hua Yuai², Zhang Huayong², Cheng Jinyong², Xu Jing³, Li Tianduo³

1 School of Chemical and Material Engineering, Jiangnan University, Wuxi 214122, P. R. China

2 Qilu University of Technology (Shandong Academy of Sciences), Jinan 250353, P. R. China

3 Shandong Provincial Key Laboratory of Molecular Engineering, School of Chemistry and Pharmaceutical Engineering, Qilu University of Technology (Shandong Academy of Sciences), Jinan 250353, P. R. China

a) ylpt6296@vip.163.com

b) jianmei.lu@126.com

Abstract. The researches on collagen that possesses unique fibre structure are reported frequently. In this paper, the cross images of leather fibre of dried wet blue cowhide leather embedded with and without epoxy resin(E51) were investigated with the micro computed topography(MCT). The images obtained by MCT of leather fibre are original status without any damage, while the embedded leather can emerge distortion because the fibre was fixed during the solidifying and immersing of the resin. In this research, 1178 images of leather fibre were investigated on wet blue leather(original fibre) and the same piece of leather embedded by epoxy resin(embedded fibre). The total pixels number of the sections from the original fibre and the embedded fibre was examined for each image. The results showed that the fiber contraction rate of the embedded skin sample calculated by the MATLAB method is 7.93%, and the overall "panel" contraction rate of the embedded skin sample is 10.88%.The embedded skin sample has significant shrinkage. Otherwise, different denoising methods will produce different effects. In other words, there may be two problems of insufficient or excessive denoising. This will result in a deviation and it needs further analysis.

1 Introduction

Collagen is widely used in medical and cosmetic fields¹, so it is of great significance to study its internal structure. Collagen is the main component of animal support structure. As a natural polymer material, collagen has unique fiber structure, which is incomparable with other materials. Type I collagen accounts for 90% of total collagen and 20% of total protein². Many studies have shown that collagen molecules are extremely long, in relation to their cross-section, which are triple helix structures with a length of about 280nm, a diameter of 1.4 ~ 1.5nm, and a molecular weight of about 300,000³. By electron microscopy, the collagen fibrils were observed to have light and dark periodic transverse striations of about 60-68nm (D-spacing), and the lateral accumulation of microfibril was fibril with a diameter of 30-500nm which changes with the animal species, tissue origin and age⁴. However, the pattern of fibril forming fiber and the weaving law of fiber bundle are still not clear, which has a great influence on the physical and mechanical properties of collagen-based materials.

The study of microstructure requires the aid of microscanning technology. The microimage acquisition methods include: microscopic X-ray tomography (MCT), nuclear magnetic resonance (MRI), laser confocal scanning microscopy (CLSM), ultrasonic method and section method. MRI and ultrasound measurements have low resolution (8 ~ 50 μ m) and are mainly used for medical research and clinical examination. The scale of type I collagen molecule is at the nanometer level, the resolution of these two methods is far from enough. CLSM technology is suitable for transparent materials. For opaque materials, only surface scanning analysis can be performed, so it is not suitable for studying the internal structure of collagen. The method of slicing is to make ultra-thin slices of the sample and observe the fiber section under the microscope⁵. The resolution depends

on the microscope. However, we found that the slices were easily broken when the thickness was less than 3 μm . In addition, the fiber structure was deformed and the image was distorted due to the cutting pressure of the blade.

The research group improved the traditional slicing method, replaced the paraffin-embedded leather sample with rigid material-epoxy resin, layered and polished the sample, observed and analyzed the fiber section structure under the microscope, and obtained the sequence section image. However, certain deformation will occur after fiber embedding, which will affect the accuracy. Therefore, this study compared and studied the MCT images of embedded and non-embedded samples, and studied the deformation and image error, creating conditions for further study on the braided structure of fiber.

2 Experimental Procedures

Leather fibre was obtained from 2 years old American cowhide wet blue. Conventional beamhouse and tanning processes were used to generate the leather. A pelt was depilated using a caustic treatment, and then the residual keratinaceous material was removed. The pelt was splitted, and relimed using 2% (w chemical/w limed leather for all percent chemical additions unless otherwise stated) lime and 0.2% liming auxiliary LAB. After washing, 0.6% Deliming agent DF(TRUMPLER) and 1.8% Ammonium sulfate was added , which gradually increased the pH to 8.4–8.6. The pickled pelt was then chrome tanned and neutralized by sodium sulfate.

Leather fibre were investigated with MCT on wet blue leather(original fibre) after drying, which were taken from butt area according to the regular sample. 2357 imagines with 4032 \times 4032 pixels were got, then 1178 imagines with 2016 \times 2016 pixels were obtained from the same piece of leather which was embedded by epoxy resin(embedded fibre) and investigated with MCT.

3 Results

3.1 Imagine Processing

The 2037 MCT section images with 4032 \times 4032 pixels of the wet blue leather (original sample) was compressed into 2016 \times 2016 pixels, with 1,178 images first. Then the image denoising is processed by MATLAB, and the denoised images are shown as follows:

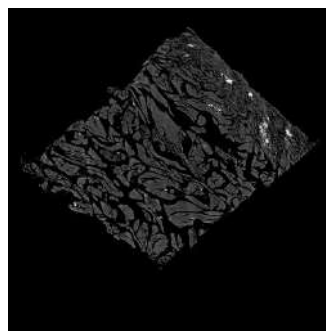


Fig. 1. Image of the wet blue leather (original sample) after denoising.

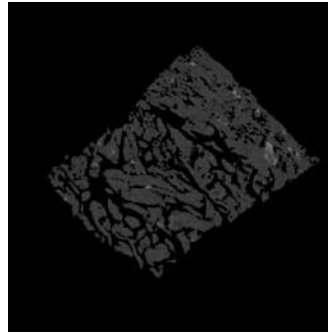


Fig. 2. Image of the embedded leather fibre after denoising.

3.2 Calculation for the Contraction Rate of Embedded Leather Fiber

3.2.1 Contraction rate of embedded leather sample fiber

Because the slice layers of the two types of images are of the same thickness, the same resolution, and the actual size of each pixel is the same, a simple way to compare the volume of the two types of leather sample fibers is to compare the total number of pixels occupied by the two types of fibers. Thus defined the calculation formula as follows:

$$\begin{aligned}
 P &= \frac{A-B}{A} \times 100\% \\
 &= \frac{\sum a - \sum b}{\sum a} \times 100\% \\
 &= \left(1 - \frac{\sum b}{\sum a} \right) \times 100\%
 \end{aligned}$$

P: contraction rate of embedded skin sample

A: volume of in situ MCT slice image

B: volume of embedded MCT slice image

a: pixels of in situ MCT slice image

b: pixels of embedded MCT slice image

The total pixel amount of in situ compressed 1178 MCT slice images of 2016×2016 pixels and embedded 1178 MCT slice images of 2016× 2016 pixels were calculated by MATLAB software as follows:

Total pixels of in situ MCT slice image: 1.0070×10^9 pixels.

Total pixels of embedded MCT slice image: 0.9271×10^9 pixels.

$$P = \left(1 - \frac{0.9271 \times 10^9}{1.0070 \times 10^9} \right) \times 100\% = 7.93\%$$

3.2.2 Contraction rate of "Panel"

The "panel" is obtained by filling the interior of the compressed 1178 in-situ MCT slice images of 2016×2016 pixels and the embedded 1178 MCT slice images of 2016×2016 pixels with MATLAB software, as shown in the following figure:



Fig. 3. In-situ MCT slice image "panel" after denoising.



Fig. 4. Embedded MCT slice image "panel" after denoising.

The total number of pixels in the image "panel" is calculated as follows:

Total number of pixels of in-situ MCT slice images "panel": 1.4663×10^9 pixels.

Total number of pixels of embedded MCT slice image "panel": 1.3068×10^9 pixels.

$$Px = \left(1 - \frac{1.3068 \times 10^9}{1.4663 \times 10^9} \right) \times 100\% = 10.88\%$$

Px: contraction rate of "panel"

3.3 Discussion

3.3.1 Contraction rate of the embedded skin sample

The fiber contraction rate of the embedded skin sample calculated by the above method is 7.93%, and the overall "panel" contraction rate of the embedded skin sample is 10.88%. This indicates that the embedded skin sample has significant shrinkage.

The reason might be the reduction of interval space among the fibre filled with epoxy resin, otherwise the conglutination of fibre caused by the evaporation of solvent (acetone used in embedding) in the course of the resin solidifying. Likewise, it can be the adhesion of the tiny fibre with the larger fibre that will diminish the area calculated. The factors will be studied further on embedding to achieve a method with minimum deformation on cross image of fibre.

3.3.2 Deviation

Due to the strong noise of the embedded leather sample and the difficulty in controlling the denoising scale, different denoising methods will produce different effects. In other words, there may be two problems of insufficient or excessive denoising. This will result in a deviation between the calculated expansion rate of the embedded leather sample and the expansion rate of the "panel" of the embedded leather sample. This needs further analysis.

This work was supported by the National Natural Science Foundation of China (Grant No. 21776143, 21606138) and Program for Li Tianduo Taishan Scholar Team of Shandong Province.

References

1. Dan Weihua.:*'Skin Collagen and Tissue Engineering'*, *Leather Science and Engineering*,12(2):12-16,2002
2. Jiang, Tinda.:*Collagen and Collagen-based Biomaterials*, Chemical Industry Press, 2005
3. Haines,B.M.:*'Review the Anatomy of Leather'*,*Journal of Materials Science*,10,525-538,1975
4. Li, Zhiqiang.:*The Chemistry and Histology of Animal Skins*, China Light Industry Press, 2009
5. Zhang, Huayong.:*'A Novel Technique for Getting Leather Section Image Based on Metallographic Sample Preparation'* *Journal of the American Leather Chemists Association*, 108(5):166-170,2013

ADDED FUNCTIONS OF LEATHER SURFACE BY Ag/TiO₂ NANOPARTICLES USE AND SOME CONSIDERATIONS ON THEIR CYTOTOXICITY

C. Gaidau¹, M. Calin², D. Rebleanu² and C. Constantinescu²

¹The R&D National Institute for Textiles and Leather (INCDTP)-Division Leather&Footwear Research Institute (ICPI) Bucharest, 93, Ion Minulescu Str., 031215,

Bucharest, Romania

²Institute of Cellular Biology and Pathology "Nicolae Simionescu" of Romanian Academy,

8, BP Hasdeu Str., 050568, Bucharest, Romania

a) carmen.gaidau@icpi.ro

b) manuela.calin@icbp.ro

Abstract. Nanoparticles showed a huge potential for new properties development in many economic sectors like electronics, medicine, textile, waste water treatment etc. The modification of surface functionality by using low concentrations of nanomaterials opens the possibility of lowering the ecological impact of chemical materials based on volatile organic compounds. The objectives of our research were related to the use of commercial nanoparticles based on Ag and TiO₂ with average particle size of 8 nm for leather surface functionalization and the investigation of the cytotoxicological impact of nanoparticle concentrations on human skin cells. The practical implications of the approach consist of multifunctional leather surface development, leather durability and comfort increase by generating antimicrobial and self-cleaning properties. The relation between leather functionality and the cytotoxicity concentration limit of nanomaterials was the hypothesis of our research. The main procedures for leather surface covering followed the classical recipes based on surface spraying with film forming composites with nanoparticle content. The optimized technology was evaluated by leather surface analyses regarding the antimicrobial (SR EN ISO 20645) and self-cleaning properties under visible light exposure as compared to leather surface covered without nanoparticles. The cytotoxicity tests were performed by incubation of keratinocytes (Human immortalized keratinocytes- HaCaT) with different concentrations of nanoparticles for 48 hours and measurement of cell viability by MTT (3-[4,5-dimethylthiazol-2-yl]-2,5-diphenyltetrazolium bromide) assay protocol. Other tests were devoted to leather wearing simulation in order to estimate the potential transfer of nanoparticles on human skin and the health and safety impact. These simulations were based on rubbing test (SR EN ISO 11640) followed by scanning electron microscopy with energy dispersive X-ray spectroscopy (SEM/EDX) analyses and by leachability tests (SR EN ISO 4098) performed in artificial perspiration solution followed by inductively coupled plasma -mass spectrometry (ICP-MS) according to SR EN ISO 17294-2 and SR EN ISO 16171. The main conclusions of our research showed that it is possible to add multifunctional value to leather surface by using Ag and TiO₂ nanoparticles with low impact on safety and health.

1 Introduction

Nanoparticles offer a great area for innovation because their properties differ significantly from ion or bulk materials through their unique chemical, electrical, optical, and biological activity which are mainly determined by the size, shape, composition, crystallinity or other structural properties [1]. The studies regarding the antimicrobial properties of nanoparticles [2] are the most numerous due to their efficiency on a large spectrum of bacteria and fungi. Silver, zinc oxide, titanium oxide, silica, carbon based nanoparticles or compounds of these showed promising functionalities regarding antimicrobial [3], photocatalytic [4, 5], conductive [6] properties or heat/fire resistance [5]. The potential of nanoparticles is still under research for leather industry and no commercial dedicated products are on the market.

The balance between efficiency and added cost can be improved by multifunctional properties generation under leather surface. Another limitation is the lack of information regarding the potential risk associated with specific nanomaterials and the need to evaluate every kind of treated

material [7]. Our previous studies showed that nanosilver doped nitrogen-titanium dioxide (Ag/N-TiO₂) has enhanced antimicrobial and photocatalytic properties and cytotoxicity tests on lung and skin human cells found that the concentration risk limits are of 500 µg/mL [8] which is very high as compared to other reference [9] with values of 10-25 µg/mL.

In the present research we have investigated the multifunctional properties of leather surface finished with commercial Ag/TiO₂ nanoparticles in solution, the scenarios regarding the potential nanoparticle releasing in wearing conditions and the potential nanoparticles cytotoxicity impact on human skin cells.

2 Experimental

2.1 Materials and Methods

2.1.1 Leather finishing with Ag/TiO₂ nanoparticles

Sheepskins were prepared by using an ecological commercial technology based on aldehydes and syntans in pilot plant station of Leather Research Department of ICPI.

Silver-doped titanium dioxide nanoparticles with average primary particle size <8nm [10], in solution (Ag425), were purchased from TIPE® AG, China. The composition of Ag425 solution was found to be 0.86% Ag and 0.72% Ti after the analyses performed by ICP-MS (Aurora M90, Bruker) according to SR EN ISO 17294-2:2017 and SR EN ISO 16171:2017.

The application of leather finishing (Figure 1) was performed by integration of Ag425 solution in base and top coat binders using classical finishing method by spraying [11].



Fig. 1. Leather finishing by spraying

2.1.2. Added functions and performance of new leather surface

Antibacterial properties of leather surfaces finished with Ag425 were assessed according to SR EN ISO 20645 against *Staphylococcus aureus* (gram-positive bacteria) and *Escherichia coli* (gram-negative bacteria). The photocatalytic (self-cleaning) properties were evaluated by simulation of leather surface staining with organic dyes, methylene blue (MB) and orange II (OII), known in literature as model stains for photocatalytic nanoparticles testing.

Leather sample and control surfaces were stained with the same quantity (0.5 µL) of dye solutions of 200 ppm (OII) and 1000 ppm (MB) concentration. The samples and control were exposed up to 5 hours to visible light (500W halogen lamp with irradiation between 400-700 nm) and were monitored in time by taking pictures and by measuring the stain discoloration with DATA Color Check Plus II portable device assisted by CIELab color management software.

2.1.3. Nanoparticles leachability

The leachability test was performed with **artificial** perspiration solution (SR EN ISO 4098) **at pH=8, followed by Ag and Ti quantification with the** inductively coupled plasma -mass spectrometer (ICP-MS, Aurora M90, Bruker) according to SR EN ISO 17294-2 and SR EN ISO 16171.

Other tests were performed by analyzing the rubbed and unrubbed areas of leather surfaces (SR EN 11640:2003) by using Scanning electron microscopy (FEI QUANTA 450 FEG) with energy dispersive X-ray spectroscopy (SEM-EDX).

2.1.4. Evaluation of nanoparticles cytotoxicity

The assessment of cell viability was based on induced cytotoxicity by Ag425 on keratinocyte (Human immortalized keratinocytes- HaCaT), using MTT (3-[4,5-dimethylthiazol- 2-yl]-2,5-diphenyltetrazolium bromide) technique described by Mosmann T in 1983 [12].

The viable cells with active metabolism have the ability to convert the tetrazolium salt MTT in formazan (which can be spectrophotometrically detected), by breaking the tetrazolium ring at the mitochondrial level by dehydrogenase enzymes. The cells which have not active metabolism, lose the ability to convert MTT in formazan, such that the color reaction serves as a marker for viable cells. The experimental protocol was the following: the cells were seeded at a density of 10,000 cells / well in a 96-well plate and incubated at 37 ° C in atmosphere of 5% CO₂ in order to be attached to the plate.

After 24 hours, the cells were treated with different concentrations of Ag425 (10, 50, 100, 200, 300, 400, 500, 750, 1000 µg/mL) and the cell viability was assessed after 24 and 48 hours of incubation. The nanoparticle medium was removed and 0.1 mL / well of MTT solution (Sigma Aldrich) was added, the concentration being 0.5 mg / mL. After 2 hours of incubation, the MTT solution was removed and the cells were lysed with 0.1 mL / lysis buffer (0.1 N HCl in isopropanol).

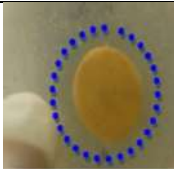
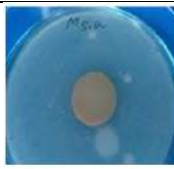
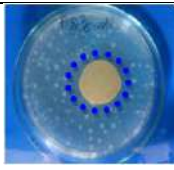
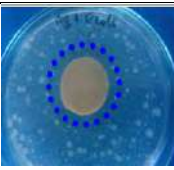
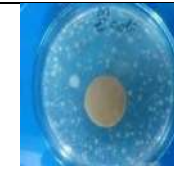
Absorbance was measured using a plate reader (Tecan GENios) at 570 nm wavelength with a reference wavelength of 690 nm. The results were expressed as percentages of control (cells incubated in the medium in the absence of Ag425).

3 Results and discussions

3.1 Added Value for New Leather Surfaces

The evaluation of antibacterial properties of leather surfaces was performed on different samples in different stages of research stages and showed that they have satisfactory level of protection with inhibitory area development as compared to the untreated surfaces (Table 1). According to the standard SR EN ISO 20645 the satisfactory level shows that the treatment has antibacterial effect.

Table 1. Antimicrobial properties of leather surfaces treated with Ag425

Test against <i>Staphylococcus aureus</i>		
Sample 1 with inhibitory area	Sample 2 with inhibitory area	Control sample without inhibitory area
		
Test against <i>Escherichia coli</i>		
		

The photocatalytic properties of new finished leathers were evaluated and showed that under the visible light exposure the rate of stain decomposition is higher for the treated surfaces as compared to untreated leathers (Figures 2 and 3). The discolouration of MB stains was more efficient as compared to Oil stain, the effect was evaluated for many samples with reproducible results (Figures 4 and 5 show the results for two samples, Ag1 and Ag2).

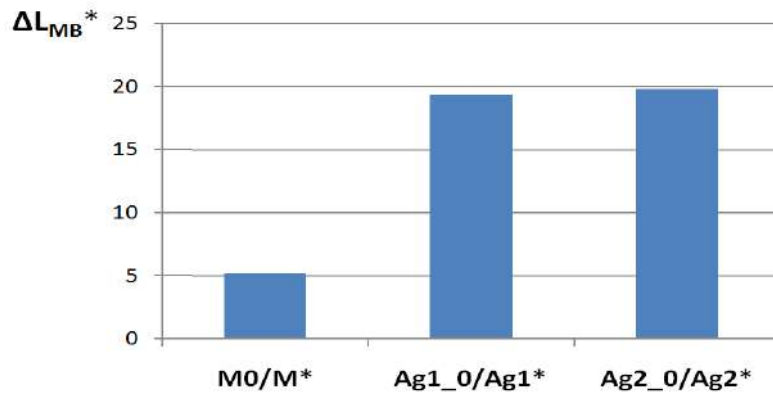


Fig. 2. Lightness difference of MB stain in initial state and after visible light exposure

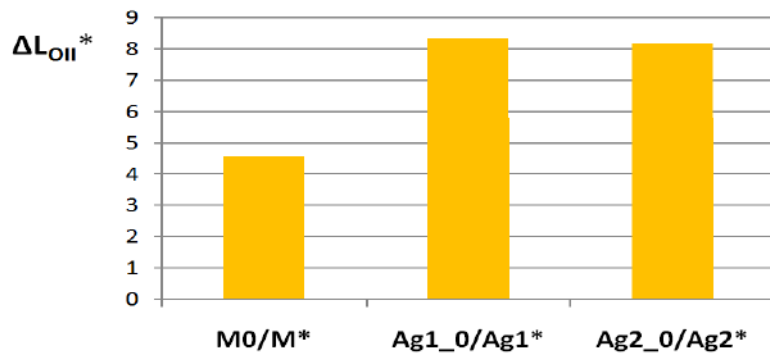


Fig. 3. Lightness difference of Oil stain in initial state and after visible light exposure

Table 2. Self-cleaning effect after 30 minutes of visible light exposure

Control sample		Ag1 sample		Ag2 sample	
Initial stain	After 30' exposure to Vis light	Initial stain	After 30' exposure to Vis light	Initial stain	After 30' exposure to Vis light

3.2 Wearing Simulation Tests and Nanoparticle Leachability Evaluation

The aim of the tests was to set the concentration of nanoparticles which can detach from the leather surface in conditions of wearing. The evaluation of nanoparticles by washing the leather in perspiration solution [13] has taken into consideration the leather surface of 13.5 dm² which can be in contact with foot skin and a volume of 20-100 mL perspiration [14] which can be released in footwear wearing conditions. In Table 3 can be seen the average values of 3 analyses for Ag and Ti

which show that 8% of silver and 32% of titanium are released from the leather surface in perspiration solution.

Table 3. Leached nanoparticles and concentration in perspiration solution

Ag, µg/mL		Ti, µg/mL	
Initial concentration	Leached concentration	Initial concentration	Leached concentration
0.76-3.75	0.06-0.31	89-445	29-145

The other investigations were performed after the leathers were tested for rubbing fastness on rubbed surface and on unrubbed surface just next to the analysed area by mapping the elements with SEM-EDX such as semi quantitative results to offer a scenario for nanoparticles releasing and to supply reliable information regarding the potential impact on human skin. In this case the rubbing with perspiration solution leads to silver nanoparticles releasing by 33.3% and no releasing of titanium (Table 4). We can consider that the released concentration of nanosilver after the rubbing test with perspiration solution is still very low and according to the data of Table 3 can reach values of 0.25-1.25 µg/mL. In conditions of dry rubbing test, after 100 dry cycles, the nanoparticles were not released from the leather finishing (Table 5).

Table 4. SEM-EDX mapping of nanoparticles on rubbed surface of leather with perspiration solution in comparison with no rubbed surface

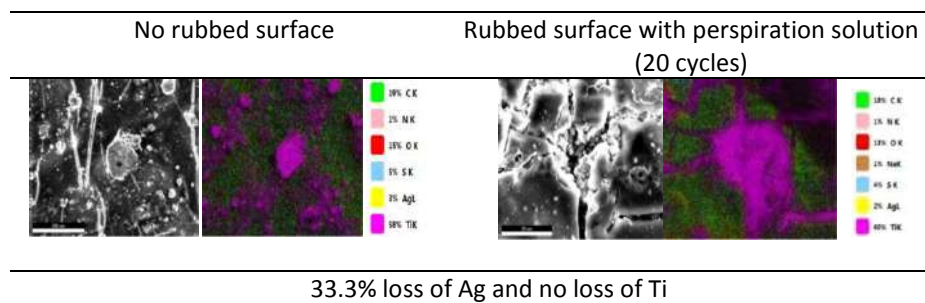
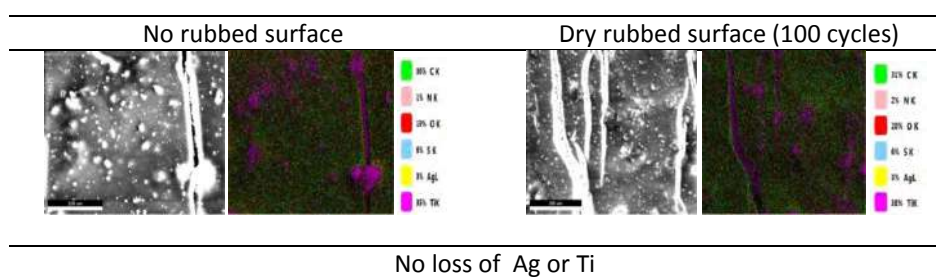


Table 5. SEM-EDX mapping of nanoparticles on dry rubbed surface of leather in comparison with no rubbed surface



3.3 Ag425K Nanoparticle Cytotoxicity

HaCaT cells have been treated with different concentrations of Ag425K for 48 hours, and the cellular viability was measured by MTT technique. The results of cellular viability test for nanoparticle concentrations of 10 µg/mL, 50 µg/mL, 100 µg/mL, 200 µg/mL, 300 µg/mL, 400 µg/mL, 500 µg/mL, 750 µg/mL and 1000 µg/mL in comparison with the cells without nanoparticles (C) are presented in Figure 4.

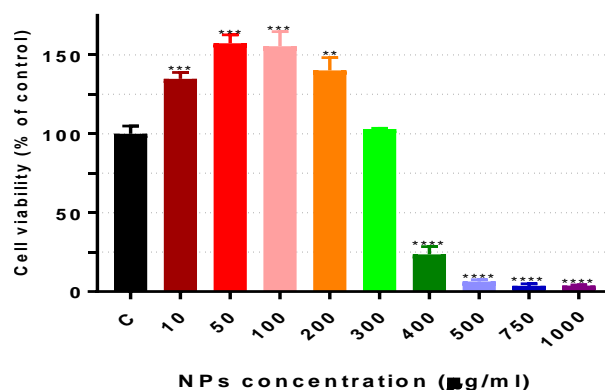


Fig. 4. Keratinocyte viability after 48 hours incubation with different concentrations of Ag425K in comparison with control sample. The average \pm deviation of values are presented, the statistic was carried out with Anova test and the comparison was done with control sample and with every concentration of nanoparticles (* $P < 0.05$, ** $P < 0.005$, *** $P < 0.0008$, **** $P < 0.0001$).

In figure 4 it can be seen that Ag425K has an increased cytotoxic effect starting with the concentration of 400 $\mu\text{g}/\text{mL}$. Concentrations between 10 and 200 $\mu\text{g}/\text{mL}$ of nanoparticles induce the proliferation of HaCaT cells by 134% at 10 $\mu\text{g}/\text{mL}$ concentration and by 155% at 50 and 100 $\mu\text{g}/\text{mL}$ respectively, whereupon the proliferation decreases at 140 and 200 $\mu\text{g}/\text{mL}$ (relative to the control cells). At the concentration of 300 $\mu\text{g}/\text{mL}$ no change was observed compared to control cells grown in the absence of nanoparticles. At concentrations greater than 300 $\mu\text{g}/\text{mL}$, there was a significant and dramatic decrease in the number of viable cells. Thus, keratinocytes exposed to Ag425K exhibit significantly reduced viability up to 23% at 400 $\mu\text{g}/\text{mL}$, 6% at 500 $\mu\text{g}/\text{mL}$ and 3% at 750 and 1000 $\mu\text{g}/\text{mL}$. MTT results indicate that this type of nanoparticles stimulates the proliferation of HaCaT human keratinocytes at low concentrations (below 250 $\mu\text{g}/\text{mL}$) but becomes toxic to cells if they exceed 350 $\mu\text{g}/\text{mL}$.

The wearing simulation and tests showed that the concentration of leached nanoparticles are of maximum 145 $\mu\text{g}/\text{mL}$ which is under the cytotoxicity limit of 350 $\mu\text{g}/\text{mL}$ for human skin cells and the risk for consumer health can be avoided.

4 Conclusions

Many recent studies were devoted to smart leather processing with new nanomaterials with potential to be used in low concentrations for new properties development or as alternative to volatile organic compounds. The impact of new materials and processed products on human health and environment are of high interest the more they are at the nano scale. The use of commercial nanoparticles with particle size under 8 nm was found to be efficient in terms of antimicrobial properties and with photocatalytic potential for leather surface finishing. The wearing simulation tests and cytotoxicological evaluation on human skin cells showed that the released concentrations of nanoparticles can be managed by leather processing below cytotoxicological risk limits.

Acknowledgements

The works were funded by Romanian Ministry of Research and Innovation, CCCDI - UEFISCDI, project no 15/2015 under the frame of the ERA-NET for a Safe Implementation of Innovative Nanoscience and Nanotechnology program, project no 44 PHYSforTeL/2018 and project no 4PERFORM-TEX-PEL/2018 within PNCDI III.

References

1. Simoncic B. and Tomsic B.: Structures of Novel Antimicrobial Agents for Textiles –A Review, *Textile Research Journal*, 80, 16, 1721–1737, 2010
2. Kaygusuz M. (Koizhaiganova): Application of Antimicrobial Nano-Materials on Leather: A Review, *J SOC LEATH TECH CH*, 101,173-178, 2017
3. Yorgancioglu A., Bayramoglu E. E. and Renner M.: Preparation of Antibacterial Fatliquoring Agents Containing Zinc Oxide Nanoparticles for Leather Industry, *J. Amer. Leather Chem. Ass.*, 114, 172-179, 2019
4. Bitlisi B. O., Yumurtas A.: Self cleaning leathers-the effect of nano TiO₂, *J. Soc. Leather Technol.Chem*, 92, 5, 183-186, 2008
5. Gaidau C., Ignat. M., Piticescu R.M., Piticescu R. R., Popescu M., Ionescu M.: Leather with self-cleaning and resistance to heat/fire and method of obtaining thereof, EP 3 173 493 A1, 2017, *Bulletin* 2017/22
6. Wei L., Zhang W., Ma J., Bai S.-L., Ren Y., Liu C., Simion D., Qin J.: π - π stacking interface design for improving the strength and electromagnetic interference shielding of ultrathin and flexible waterborne polymer/sulfonated graphene composite, *Carbon*, 149, 679-692, 2019
7. Milieu Ltd. and AMEC Environment & Infrastructure UK Ltd. for DG Environment of the European Commission, *Review of Environmental Legislation for the Regulatory Control of Nanomaterials under Contract No 070307/2010/580540/SER/D*, 2011.
8. Rebleanu D., Gaidau C., Voicu G., Constantinescu C. A., Mansilla C., Rojas T. C., Carvalho S. Calin M.: The impact of photocatalytic Ag/TiO₂ and Ag/N-TiO₂ nanoparticles on human keratinocytes and epithelial lung cells, *Toxicology*, January 2019, DOI: 10.1016/j.tox.2019.01.013
9. Andor B., Tischer (Tucuina) A.A., Berceanu-Vaduva D., Lazureanu V., Cheveresan A., Poenaru M.: Antimicrobial Activity and Cytotoxic Effect on Gingival Cells of Silver Nanoparticles Obtained by Biosynthesis, *REV.CHIM.(Bucharest)*, 70, 3, 781- 3, 2019
10. GB/T 19591-2004, 纳米二氧化钛[Nano-titanium dioxide] (AQSIO) (Effective on 1 April 2005)
11. Petica A., Gaidau C., Ignat M., Sendrea C., Anicai L.: Doped TiO₂ Nanophotocatalysts for Leather Surface Finishing with Self-Cleaning Properties, *J. Coat. Technol. Res.*, 12, 6, 1153-1163, 2015
12. Mosmann T.: Rapid colorimetric assay for cellular growth and survival: application to proliferation and cytotoxicity assays, *J Immunol Methods.*, Dec 16;65(1-2):55-63., 1983
13. Kulthong K., Srisung S., Boonpavanitchakul K., Kangwansupamonkon W. and Maniratanachote R.: Determination of silver nanoparticle release from antibacterial fabrics into artificial sweat, *Particle and Fibre Toxicology*, 7:8, <http://www.particleandfibretoxicology.com/content/7/1/8>, 2010
14. Kuklane K., Holmer I., Giesbrecht G.: Change of Footwear Insulation at Various Sweating Rates, *Applied Human Science*, 18, 5, 161-168, 1999.

RESOURCE UTILIZATION: PREPARATION AND APPLICATION OF A SULFITED FAT-LIQUOR BASED ON WASTE BEEF TALLOW FROM TANNERY

LUO RU-HUI , WU WEI-XIAO , CEHN DE-YAN , LUO JIAN-XUN

Department of Light Chemistry Engineering, College of Material & Textile Engineering, Jiaying University, Jiaying 314001, P. R. China.

Corresponding author: jianxunluo986@126.com

Abstract. Leather industry is one of many traditional and characteristic industries in China. During the process of Leather manufacture, the problem of a certain the waste of resources and environmental pollution has been yielded. The waste tallow is one of the problems should be solved quickly. Based on the problem of the waste of resources and environmental pollution form the waste tallow of the leather industry, act waste beef tallow from tannery as raw material, determination of its physical and chemical properties, de-colorization, deodorization, amidation, esterification and sulfitation were done successively. Results showed that the acid value and the saponification value of the waste beef tallow was 45mgKOH/g, 207mgKOH/g respectively. When 10% hydrogen peroxide and 6% activated clay were successively used to decolorization and deodorization, the best effect was obtained. When n(ethanolamine) : n(waste beef tallow) is 4:1, the reaction temperature was 130-140°C and time was 2hrs respectively by 1.5% sodium formate as a catalyst, the acid value and hydroxyl value of the treated beef tallow was 15-30mgKOH/g, about 280mgKOH/g respectively. When the optimum dosage of sodium pyrosulfite is 20%, the fat-liquor obtained light yellow and good stability. The sheepskin garment leather fat-liquored by this fat-liquor is very soft.

1 Introduction

Fat-liquoring process is one of the most important processes in leather manufacture, which can give the leather certain physical, mechanical properties and properties of use¹. The common fat-liquoring materials are modifiers of natural animal fat/oil, vegetable oil modified by sulfated, sulfited, oxisulphited, sulphonated and synthetic polymer¹. Based on their different sources and modified methods, there are differences in emulsion particles, emulsion stability and so on so as to give different properties for Leather.

Because the raw hide or skins contain a certain fat/oil, it is necessarily removed by de-fleshing and de-greasing process in order to promote the penetration and combination of water-soluble materials in hide or skins, which produces lots of hide/skin scrapings. However, bad smell and odor will be produced if these hide/skin scrapings and grease can't be reused in time so as to cause environment pollution. According to statistics, the annual output of waste fat/oil from Tannery is about 3.8Mt in China, which can produce 0.45Mt refined oil according to 15% extraction rate of waste oil². If the fat/oil were reused, it can not only make up the shortage of natural oil resources and save the resources, but also reduce the environmental pollution.

Some studies were carried out on the resource utilization of waste oil, which were used as emulsifier of diesel, stearic acid, bio-diesel and fat-liquor etc. Acted the waste tallow from Tannery the as materials, Fatty acid methyl-ester was prepared and ethanol-diesel emulsifier of alcohol- diesel was further prepared. When n(fatty acid methyl-ester)/n(di-ethanolamine) was 1.0, the reaction temperature was 130°C, the dosage of catalyst KOH was 1.0% and the reaction time was 5h, the emulsifying performance of the emulsifier was very good. The ethanol-diesel mixture prepared by adding the emulsifier is stable in the range of zero and 70°C with uniform particle size distribution and stable morphology³. Acted waste cooking waste oil as the material, firstly it was de-colored by activated clay and was de-hydrated, then the de-colored oil was saponified by sodium hydroxide on the condition of boiling, then white particles was obtained by the method of salting out which reacted with Pb(NO₃)₂, filtered and acidified by hydrochloric acid and oleic acid and stearic acid were obtained⁴. Acted the hogwash oil as raw materials, it was treated by a two-step esterification process, that is, Firstly

the free fatty acids in the hogwash oil were converted into fatty acid methyl-ester by concentrated sulfuric acid, and its acid value was reduced below 4mg/g. Then, the triglycerides in the hogwash oil were converted into fatty acid methyl-ester by acid as a catalysis⁵. The flash point and cold filter point of bio-diesel obtained by this way are better than 0# diesel, which is beneficial for storage and transportation. The hogwash oil was oxidated and sulfited and was prepared to leather fat-liquor which can give good elongation at break, tensile strength and softness for the fat-liquored leather⁶.

In this paper, waste beef tallow was taken as raw materials, its physical and chemical indexes were measured. Then, it was modified by de-odorization, de-colorization, amidization, esterification and sulfite successively and the fat-liquor was obtained so as to achieve the purpose of resource utilization.

2 Experimental procedures

2.1 Materials

Waste tallow was used as raw materials which origins from a tannery located in Zhangpu city, Fujian province, China. Sodium pyrosulfite, p-toluene sulfonic acid, maleic anhydride, hydrogen peroxide solution, sodium methoxide were obtained from Shanghai lianshi chemical re-agent co., Ltd. Activated clay was obtained from Zanyu S&T co., Ltd, Zhejiang province, China. PASTOSOL BCN60, TRUPON SWS, TRUPON DB were obtained from TRUMPLER Chemicals s.p.a, Germany. All chemicals used for leather processing were of commercial grade, others are analyzed grade.

2.2 Plan of modification of waste tallow from Tannery and its application

Waste beef tallow is shown in Fig.1. Based on its color and smell, modified scheme of waste beef tallow is also shown in Fig.2. The main content of modification and application includes testing of some indexes of waste beef tallow from Tannery, de-coloring and de-odorization of waste tallow from Tannery, aminification reaction, esterification & Sulfite reaction of waste tallow from Tannery, etc, which can make Waste tallow into fat-liquor. Then emulsion stability, application properties of the fat-liquor will be tested.



Fig. 1. Waste tallow from Tannery.

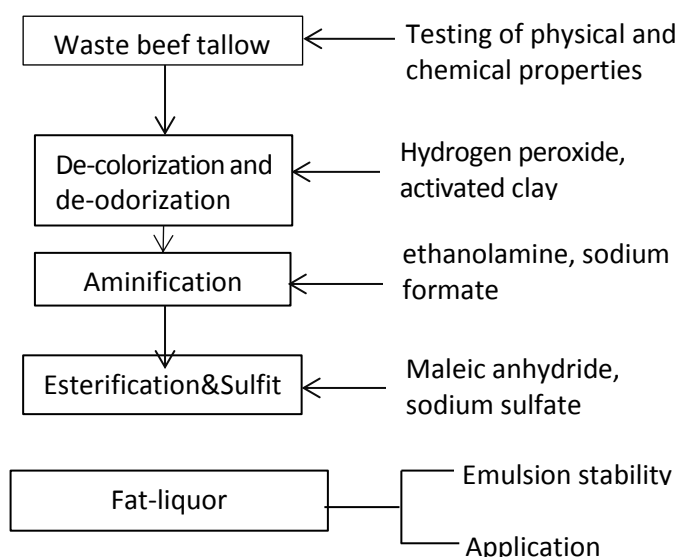


Fig. 2. Modification and application technology of waste tallow for Tannery.

2.3 Testing of some indexes of waste tallow from Tannery

The saponification value, acid value and hydroxyl value of Waste beef tallow were tested according to GB/T5534--200,GB/T5530--2005/ISO660:1996 and SN/T0801.20-1999 standards respectively, which can become references of modification methods based on the appearance, smell and structural characteristics of Waste tallow.

2.4 De-coloring and de-odorization of waste tallow from Tannery

The methods of de-coloration and de-odorization of oil include oxidation, reduction and physical adsorption, etc. According to the appearance and smell of the waste beef tallow, physical adsorption method and oxidation method were combined to achieve better de-colorization and de-odorization. Therefore, hydrogen peroxide solution and activated clay were used as de-coloring and de-odorizing materials. The experimental scheme is shown in Table 1.

Table 1. Experimental scheme for decolorization and deodorization of Waste tallow from Tannery.

Hydrogen peroxide/%	Amount of activated clay/%	Clay first and then hydrogen peroxide	Hydrogen peroxide before clay
5	4	A certain amount of clay +5% H ₂ O ₂	A certain amount of H ₂ O ₂ +4% clay
10	6	A certain amount of H ₂ O ₂ +4% clay	A certain amount of H ₂ O ₂ +6% clay
15	8	A certain amount of clay +15% H ₂ O ₂	A certain amount of H ₂ O ₂ +8% clay

2.4.1 De-coloration and deodorization of Activated clay

- 100g Waste beef tallow was put in a 250mL three-mouth flask and was heated to 110°C on the condition of stirring.
- 4%-8% active clay was added and continue stirring for 30min. Then it was filtered on the condition of vacuum.
- The filtered oil was placed in the divide funnel and stayed overnight. Then the water was separated the next day.

2.4.2 De-coloration and deodorization of hydrogen peroxide

- a. 100g Waste beef tallow was put in a 250mL three-mouth flask and was heated to 65-75°C on the condition of stirring.
- b. Hydrogen peroxide was slowly added dropwise and the time was 30-40min. then it has been reacted for 3h at 75-80°C.
- c. The de-colored oil was placed in the divide funnel and stayed overnight. Then the water was separated the next day.

2.4.3 De-coloration and deodorization of hydrogen peroxide & Activated clay

- a. Firstly the optimal amount of active clay was used to decolorization and deodorization. Then different amount of hydrogen peroxide was used. The operation procedure is the same as 2.4.1 and 2.4.2.
- b. Firstly the optimal amount of hydrogen peroxide was used to decolorization and deodorization. Then different amount of active clay was used. The operation procedure is the same as 2.4.1 and 2.4.2.

2.4.4 Test methods of effect of De-coloration and deodorization

Color and smell of de-colored and de-odored were tested by the manual scoring method. The score is in the range of 1 and 5. The higher is the score, the lighter is the color and the lighter is the smell.

2.5 Amideation reaction of waste beef tallow from Tannery

In order to increase the number of hydroxyl groups of Waste beef tallow from Tannery, ethanolamine was used to react with Waste beef tallow. According to the influence of reaction time, molar ratio of reactants and dosage of catalyst on ester exchange reaction, the orthogonal experiment was carried out. Scheme design and experiment are shown in Table 2, Table 3 and Table 4⁷.

Table 2. Levels of different factors

level	A/n (Waste beef tallow) : n (ethanolamine)	B/time/h	C/ Dosage of Catalyst /%
1	1:2	4	0.5
2	1:3	3	1
3	1:4	2	1.5

Table 3. Experimental scheme of Aminification reaction

No.	A/n (Waste beef tallow) : n (ethanolamine)	B/time /h	C/ Dosage of Catalyst /%
1	1:2	4	0.5
2	1:3	4	1
3	1:4	4	1.5
4	1:2	3	1
5	1:3	3	1.5
6	1:4	3	0.5
7	1:2	2	1.5
8	1:3	2	0.5
9	1:4	2	1

A certain amount of de-colored and de-odorized waste beef tallow was placed in a three-necked flask, and a certain amount of ethanolamine and sodium methylate was added. The temperature was raised to 130-140°C, and the condensation reflux had been conducted for 2-4hrs. The test method for the acid value and hydroxyl value of the aminated waste tallow is the same as 2.3.

2.6 Esterified & Sulfite reaction of aminated waste beef tallow

The aminated waste beef tallow was esterified with maleic anhydride and then modified with sodium pyrosulfite. A certain amount of aminated waste tallow was placed in a three-neck flask. When the water bath temperature reached 65-70°C, p-toluene sulfonic acid, maleic anhydride were added, and then heated to 80-90°C for 2h. Then drop the temperature to 65-70°C, add a certain amount of 30% sodium hydroxide solution, and adjust its pH to 4-5. Then a certain amount of sodium pyrosulfite was slowly added to a three-necked flask whose dosage of sodium pyrosulfite was 10%, 15%, 20%, 25% and 30% respectively. Then the pH was adjusted to 6.5-7.0 with 30wt% sodium hydroxide solution, and the oil content of the fat-liquor was adjusted to 60%. At last, the degree of sulfite of the aminated waste beef tallow and the emulsion stability of the fat-liquor were determined⁸.

2.7 Application of the fat-liquor originated from Waste beef tallow of Tannery

The fat-liquor was applied in the fat-liquoring process of shaved sheepskin wet blue. The process is shown in Table 4. The softness, fullness and other characteristics of the fat-liquored leather were tested.

Table 4. Fat-liquoring process of the fat-liquor in shaved sheepskin wet blue.

Process	T/°C	Material	Dosage /%	Time/min	Note
washing	35	water	200		
		PASTOSOL BCN-60	0.3		
		formate acid	0.3	60min	pH3.7-3.8 , washing
retanning	normal temperature	water	200		
		chrome tanning agent	4		
		chrome tannins	3	120min	
		sodium formate	0.5		
		baking soda	0.5	30min	pH4.0 , stop/overnight
neutralization	30	water	200		
		Sodium formate	1.0	30min	
		Baking soda	2.0	3×20min	pH6.0 , washing
fatliquoring	50	water	200		
		fatliquor	18	90min	
		formate acid	1.2	3×20min	pH3.5, washing hang dry

3 Results and Discussion

3.1 Some indexes of Waste tallow from Tannery

Testing results of relevant indexes of waste beef tallow from Tannery is shown in Table 5. As can be seen from Table 5, the acid value of the oil is 45mgKOH/g which is higher than normal natural oil and show that it has high content of free fatty acids. The saponification value of Waste tallow is 207mgKOH/g and the relative molecular weight is 813g/mol, which is in the range of 650 to 970g/mol. In addition, Waste beef tallow (18-22°C) appearance of dark-brown solid at room temperature and odor.

Table 5. Related indexes of Waste beef tallow from Tannery.

Test project	Test results
Outside view	Dark-brown solid
Acid value / mgKOH/g	45
Saponification value / mgKOH/g	207
Relative molecular mass	813g/mol

3.2 Results of deodorization and decolorization of Waste beef tallow from Tannery

Results of active clay, hydrogen peroxide and their combination are shown in Table 6, Table 7, Table 8 and Table 9. As can be seen from Table 6, the color of Waste beef tallow is significantly changed with the amount of activated clay. When the amount of activated clay is 6%, the color is the lighter than others. However, the smell of Waste beef tallow is still large. So the de-odorization effect of activated clay is not good. In addition, the acid value of Waste beef tallow treated with clay decreased slightly, which show that it had little influence on the acid value of Waste tallow. As can be seen from Table 7, the color of the oil becomes obviously lighter with the increase in the amount of hydrogen peroxide, which is lighter than that of activated clay. The deodorization effect of hydrogen peroxide is better than that of activated clay. Therefore the optimal amount of hydrogen peroxide is 10%.

Table 6. De-colorization and de-odorization effect of activated clay for Waste beef tallow.

Amount of activated clay/%	Color	Smell	Acid value (mgKOH/g)	Stability (24)
4	3	1	42.0	good
6	4	1	40.5	good
8	2	1	41.8	good

Table 7. De-colorization and de-odorization effect of Hydrogen peroxide for Waste beef tallow.

Hydrogen peroxide/%	Color	Smell	Acid value (mgKOH/g)	Stability (24h)
5	3	3	43.2	general
10	4	3	42.3	good
15	4	3	41.1	good

Table 8. De-colorization and de-odorization effect of activated clay and hydrogen peroxide for Waste beef tallow.

Amount of decolorizing material	Color	Smell	Acid value (mgKOH/g)	Stability (24h)
10%H ₂ O ₂ +4% clay	4	3	44.3	good
10% H ₂ O ₂ +6% clay	5	3	41.0	good
10% H ₂ O ₂ +8% clay	5	3	41.2	good

As can be seen from Table 8 and Table 9, the color, when hydrogen peroxide and activated clay are along used for de-coloration and de-odorization, the color and smell of Waste beef tallow is lighter than one of hydrogen peroxide and activated clay. Among them, the use of hydrogen peroxide, then the use of clay, de-colorization & deodorization effect is good. Considering the effect and cost of de-colorization and de-odorization, 10% hydrogen peroxide and 6% activated clay was used.

Table 9. De-colorization and de-odorization effect of hydrogen peroxide and activated clay for Waste beef tallow.

Amount of decolorizing material	Color	Smell	Acid value (mgKOH/g)	Stability (24h)
6% clay +5% H ₂ O ₂	3	2	45.3	good
6% clay +10% H ₂ O ₂	4	2	42.3	good
6% clay +15% H ₂ O ₂	4	2	41.7	good

3.3 Results of Amidation reaction of of de-colored & de-odored waste beef tallow from Tannery

Results of amidation reaction of the de-colored& de-odored waste beef tallow are shown in Table 10. As can be seen from the Table, the order of affecting factor is mole ratio of the reagent, the reaction time and the dosage of catalyst. The acid value of Waste beef tallow decreased from 45mgKOH/g to 15-30mgKOH/g after it is amidated. At the same time, the hydroxyl value of Waste beef tallow changed little with the change of reaction time, which shows that the reaction time had little effect on amidation reaction. From the results of the orthogonal experiment, the most appropriate reaction time is 2h. As the molar ratio of ethanolamine and Waste tallow increased, the hydroxyl value of it rise. Therefore, the optimal molar ratio of ethanolamine and Waste beef tallow was 1:4. In addition, with the increase of the amount of catalyst, the hydroxyl value of Waste tallow changes less. From the orthogonal experiment, the acid value of modified Waste beef tallow is smaller than others when the amount of catalyst is 1.5%.

Table 10. Results of orthogonal experiment of amidation reaction of de-colored waste beef tallow.

No.	A/n(Waste tallow):n (Ethanol-amine)	B/reaction time/h	C/Dosage of Catalyst/%	Acid value/ (mgKOH/g)	Hydroxyl value/ (mgKOH/g)
1	1:2	4	0.5	31.1	206.8
2	1:3	4	1	26.6	222.6
3	1:4	4	1.5	27.3	213.2
4	1:2	3	1	38.0	202.3
5	1:3	3	1.5	25.5	216.7
6	1:4	3	0.5	29.9	217.6
7	1:2	2	1.5	15.5	204.6
8	1:3	2	0.5	21.5	246.0
9	1:4	2	1	26.4	288.3
K1	84.6 (613.7)	85 (642.6)	82.5 (670.4)		
K2	73.6 (685.3)	93.4 (636.6)	91 (713.2)		
K3	83.6 (719.1)	63.4 (738.9)	68.3 (634.5)		
k1	28.2 (204.6)	28.3 (214.2)	27.5 (223.5)		
k2	24.5 (228.4)	31.3 (212.2)	30.3 (237.7)		
k3	27.9 (239.7)	21.3 (246.3)	22.7 (211.5)		
R	3.7 (35.1)	10 (34.1)	7.6 (26.2)		

3.4 Results of Esterified & Sulfito reaction of aminated waste beef tallow

Effects of different amounts of sodium pyrosulfite on the stability, sulphiting degree and state of Fat-liquor emulsion are shown in Fig.3 and Table 11. As can be seen from Fig.3, the 1:9 sulfite emulsions have good stability. As can be seen from Table 11, the color of the fat-liquor gradually lightens with the increase of the amount of sodium sulfite, which maybe that more $-SO_3Na$ groups in the butter increases improves the hydrophilic and emulsifying properties of the sulfite fat-liquor. The sulphiting degree of the fat-liquor rise with the dosage of sodium pyrosulfite increases.when

the dosage of is sodium pyrosulfite 20%~30%, the degree of sulfite reaches more than 18% and the sulphiting degree of the fat-liquor is high.



Fig. 3. Stability of 1:9 sulfited fat-liquor emulsion.

Table 11. Emulsion stability, sulphiting degree and state of the sulfited fat-liquor.

Heavy sodium sulfite dosage	10%	15%	20%	25%	30%
1:9 emulsion stability	Not layered	Not layered	Not layered	Not layered	Not layered
Sulphiting degree	2.9%	6.5%	18.3%	20.9%	25.6%
State	Yellow paste	Yellow paste	Light yellow paste	Light yellow paste	Light yellow paste

3.5 Results of application of the sulfited fat-liquor

The sheepskin garment leather fat-liquored by the sulfited fat-liquor is soft and full, which shows that it has good fat-liquoring properties.

4. Conclusion

During the process of Leather manufacture, cleaner production and resource utilization of solid waste are the requirements for the sustainable development of leather industry. Waste beef tallow is one of the solid wastes whose refined oil is dark brown solid and bad smell. The acid value, saponification value of the refined oil of Waste beef tallow is 45mgKOH/g and 207mgKOH/g. The fat-liquor was prepared from Waste tallow by de-colorization with hydrogen peroxide and active clay, amidation, esterification and sulfited, which has light color and good fat-liquoring performance.

When Waste beef tallow was de-colored and de-odorized with 10% hydrogen peroxide and 6% activated clay, the color and smell of the de-colored ,de-ordorized waste tallow are light. Ethanolamine was used for the amidation reaction of the decolorized and deodorized waste beef tallow. The optimal conditions were that 1.5% catalyst (sodium methanol), n(ethanolamine):n(oil) at 4:1, 2h, and 130~140°C. The acid value, hydroxyl value of the amidated oil was 15-30mgKOH/g and 280mgKOH/g respectively.

By esterified reaction with equal molar maleic anhydride & Sulfited reaction with 20% sodium pyrosulfite successively, the modified fat-liquor has high sulphiting degree, yellow paste appearance and good emulsion stability which can give good softness for leather.

References

1. Shan, Z. H. Chen, H. Luo, J. X. et al.: 'Tanning Chemistry and Technology', Beijing: Science press, 2017
2. Yu, C. Z. Chen, Y. F. Ma, X. Y. et al.: 'Countermeasures of Environmental Pollution of Leather Industry', The environmental condition of world leather industry, 2004,33(17):31-36
3. Ma, J. Z. Ma, D. Lv, B. et al. 'Preparation of Ethanol-diesel Emulsifier from Leather Waste Oil'. Petroleum refining and chemical industry, 2011, 42(10):73-77.
4. Guo, T. Du, L. L. Wan, H. et al. 'Study on Preparation of Stearic Acid and Oleic Acid from Waste Food Oil'. Food science and technology, 2009, 34(8):109-112
5. Zhang, Y. 'Preparation of Biodiesel from Gutter Oil'. China oils and fats, 2008,33(11):48-50
6. Duan, B. R. Tan, S. Z. Wang, Q. J. et al. 'Preparation of Fatliquor from Waste Oil by Sulfite Oxidation and Its Application in Leather Making'. China leather, 2012,41(1):43-47
7. Li, Y. Y. Hu, C. R. 'Experimental Design and Data Processing'. Beijing: chemical industry press,2015.
8. Luo, X. M. Ding, S. L. Zhou, Q. F. 'Physical and Chemical Analysis of Leather'. Beijing: China light industry press,2013

OBSERVATION AND ANALYSIS OF LEATHER STRUCTURE BASED ON NANO-CT

Huayong Zhang^{1, b}, Jinyong Cheng², Tianduo Li^{2, a}, Jianmei Lu², Yuai Hua²

¹ State Key Laboratory of Biobased Material and Green Papermaking, Qilu University of Technology (Shandong Academy of Sciences), Jinan, 250353

² Shandong Provincial Key Laboratory of Fine Chemicals, Qilu University of Technology (Shandong Academy of Sciences), Jinan, 250353

a) Corresponding author: ylpt6296@vip.163.com

b) headingzhy@126.com

Abstract. The composition, working principle and the image acquisition procedure of nano-CT were introduced. A dried piece of blue stock of chrome-tanned cattle hide was chosen for this work and a sequence of 2357 images was obtained. 3D visible digital models of leather fiber bundle braided network and the interspace between fiber bundles were reconstructed. The inner structure and composition of leather were shown accurately and intuitively in the form of 2D sectional images and 3D image. Based on the 3D model, the diameter, volume, surface area and other parameters of the fiber bundles, the pore structure and inclusions were measured and calculated.

1 Introduction

Leather is formed by tight weaving of collagen fiber bundles. The three-dimensional (3D) weaving network of collagen fibers is the structural basis of physical and mechanical properties of leather. Recognizing and studying this three-dimensional weaving network of collagen fibers can facilitate researches on structure-performance relationship of leathers effectively and promote improvement and development of leather production techniques^[1]. There are many methods to acquire the 3D weaving structure of leather, including microtomy, layered polishing method of metallographic preparation sample, magnetic resonance imaging (MRI) imaging method and micro-CT method^[2-5]. Among them, the first two methods are time and labor-consuming ones. Although MRI imaging method won't cause damages to samples, it has low resolution and high cost. In this study, micro-CT method which causes no damages to samples and has high resolution was applied.

CT is the short for computed tomography. Micro-CT generally refers to CT with the spatial resolution reaching $1\ \mu\text{m}\sim 10\ \mu\text{m}$. It is a non-invasive and non-destructive imaging technique and scans samples by X-ray to acquire internal structural information of samples, without damaging samples^[6]. Later, it composes the 3D structural images of samples based on analysis and processing, thus getting thorough three-dimensional structural information of samples. Micro-CT is widely applied in many research fields, such as medicine, materials, biology, archaeology, electronic engineering and geology^[7-10].

The small size of leather fiber bundles and complicated weaving structure proposed high requirements on performance and parameter setting of instruments. So far, there are few studies on three-dimensional structure of leather based on micro-CT. In 2014, E.Bittrich et al. studied structure of leather by micro-CT and acquired the 3D structure of vegetable tanned leather under the resolution of $3.3\ \mu\text{m}$. However, they failed to get clear structure images of chrome tanned leather, which were attributed to influences of tanned metals^[5].

In this study, scanning steps and imaging observation method of high-resolution micro-CT to chrome tanned leather were explored and introduced systematically. Research conclusions can provide certain assistances and references to further study 3D structure of leather.

2 Experimental Materials and Instruments

Dried pieces of blue stock of chrome-tanned cattle hide provided by Qilu university of technology leather laboratory was chosen for this work.

The micro-CT Equipped with CCD detector and analysis software was Bruker SkyScan2211, Belgium.

3 Experimental methods

3.1 Composition and principle of micro-CT

The major component of micro-CT is composed of X-ray source, rotating sample platform and high-resolution detector (Fig. 1). In addition, it covers the control system and computer processor, etc. Structure of micro-CT is shown in Fig. 1.

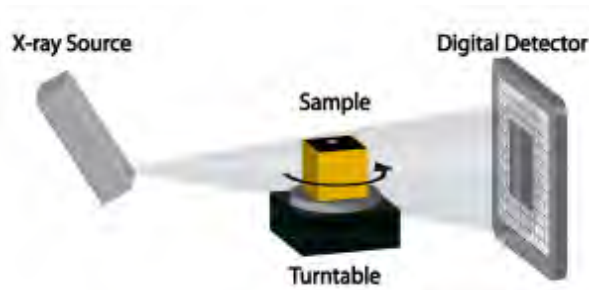


Fig. 1. Schematic diagram of micro-CT system.

X-ray emission source and detector were fixed, while samples rotated between X-ray source and detector. Besides, samples could move vertically and horizontally. The conical X-ray bundles which are produced continuously by X-ray source penetrate samples and images of the sample was produced on the X-ray detector. Since the penetrability of X-ray in different substances is difference, light intensity at different positions of the detector varies. According to light intensity produced gray image^[11], projection image of sample from this perspective is acquired. The X-ray projection images of the sample from different perspectives are gained by rotating it at a certain angular rate. After series of projection images are acquired, data of these projection images were processed by certain mathematical algorithm, thus getting three-dimensional information of the sample. Processing and analysis of data formed by micro-CT scanning requires the use of special three-dimensional analysis software.

3.2. 2D images Acquisition by micro-CT

3.2.1 Determination of scanning parameters

In this experiment, resolution was set $1.5\mu\text{m}/\text{pixel}$ and the leather sample size was about $5.4\text{mm}\times 3.5\text{mm}\times 3.9\text{mm}$. According to structural properties of leather, image qualities under different parameters were observed and compared. With comprehensive consideration to efficiency and quality, CCD detector was chosen. Scanning parameters were set: Voltage and current of the light tube were 50KV and $320\mu\text{A}$, respectively. The exposure time was 1000ms and the focusing current was 620.9mA . The scanning step length was 0.2° and each step had 8 scans. The scanning angle was 180° . The scan took a total of 3h and 38 minutes, getting 970 projection images. The image pixel size was 4032×2688 (bmp format, 10.3M). Four images are shown in Fig. 2. Since projection image was gained after ray penetrating through the whole sample, it superposed multiple layers of sample information and couldn't reflect the leather structure intuitively.

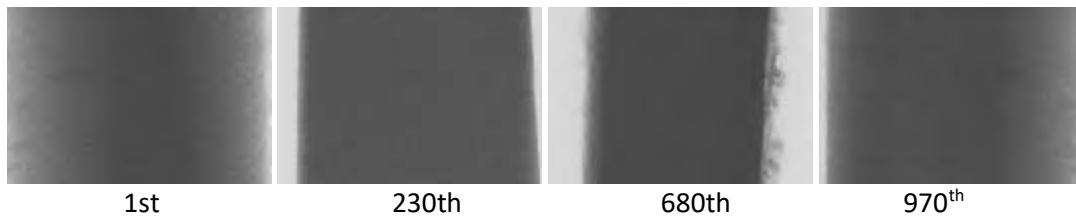


Fig. 2. Leather projection images acquired by micro-CT.

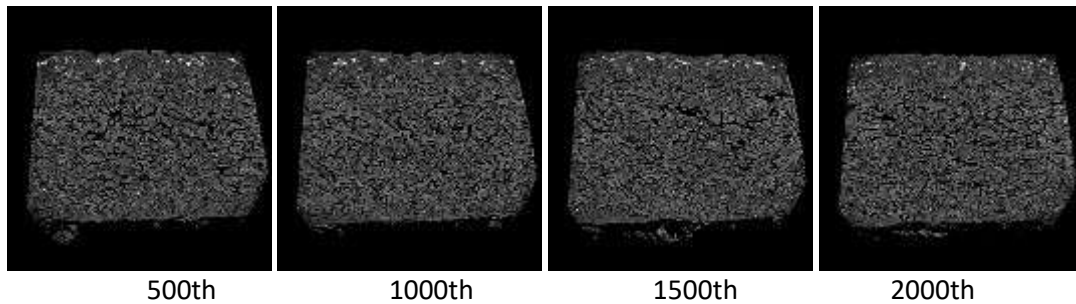


Fig. 3. Leather section images reconstructed from the series CT projection images.

3.2.2 Reconstruction and observation of 2D section images

Section images of leather were reconstructed from the series projection images by the NRecon software. Firstly, the series projection images were aligned and eliminated negative influences of ring artifact and beam hardening, accompanied with appropriate smoothing. Next, 2D sections were reconstructed and 2357 series images of 2D section (x-y) were produced. Pixel size of each section image was 4032×4032(bmp format, 15.5M) and the interlayer distance was 1 pixel (1.5µm). Four section images are shown in Fig.3. It can be seen from Fig.3 that the grain surface and reticular layer of this leather sample were distinguished obviously. In the grain layer, fiber bundles are thin and weaved tightly. In the reticular layer, fiber bundles of the middle portion are thick and weaved loosely, showing big spaces between fiber bundles. Some fiber bundles close to the grain layer and meat layer are thin and weaved slightly tightly. Many white bright spots in Fig.3 are high-density crystals which are not processed cleanly. There are many large white bright spots in the grain layer, but there are few small spots on the reticular layer.

Three orthogonal section images centered at any point of the reconstructed space were displayed by the DataViewer software. Pixels were expressed in different colors according to the gray value. For example, in Fig.4, three orthogonal section images which passed through one point were clear. The same structure could be observed from different perspectives to reflect fiber bundles and pores intuitively. In addition, all structures can maintain the original shape completely by using the digital slicing method, without deformation and falling.

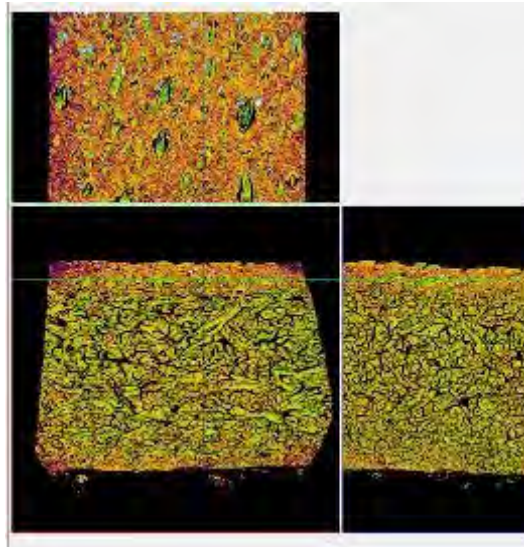


Fig. 4. Three orthogonal section images of leather.

3.2.3 Reconstruction, observation and measuring quantitative parameters of 3D images

Series 2D section images were reconstructed into 3D images by the volume rendering software CTVOX. By setting transparency of pixel points with different gray values and certain color the three-dimensional structure of overall structure or one substructure was reflected intuitively (Fig.5a). When the fiber bundles and pores were set transparency, 3D distribution of high-density crystals was observed (Fig.5b). Moreover, random digital cutting could be carried out and one part of the result was displayed and processed. For example, the 3D digital model of the selected part position was shown in Fig.6. Obviously, the part surface of grain layer was cut off, which exposed the pores or veins clearly (Fig.6a). The high-density white crystals were exposed (Fig.6b).



(a) leather fiber bundle braided network



(b) interspace between fiber bundles

Fig. 5 3D volume rendering reconstruction images of leather (5.4mm×3.5mm×3.9mm).

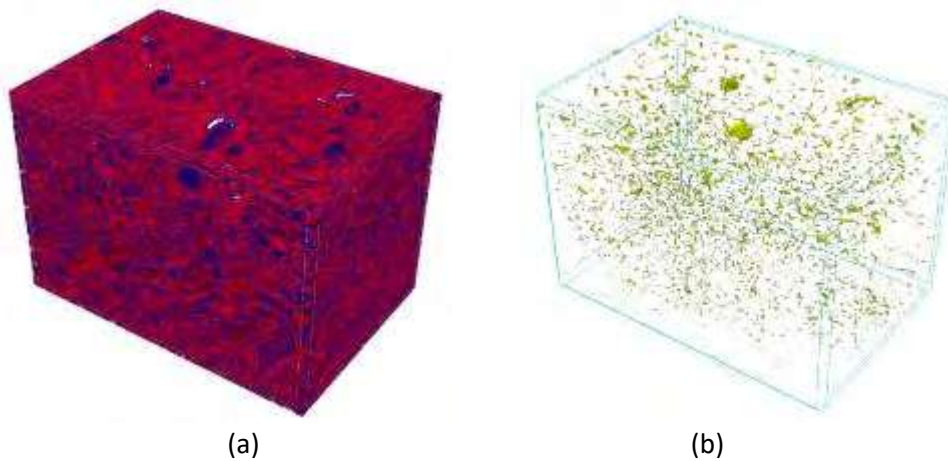


Fig.6 Selected part position of 3D digital model (3mm×1.5mm×2mm).

Based on the 3D model, the diameter, volume, surface area and other parameters of the fiber bundles, the pore structure and inclusions were measured and calculated by CT-analyser software. Partial 3D analysis based on the 3D model of Fig. 5a see Table 1, and the structure thickness (Diameter of fiber bundles) distribution see Table 2.

Table 1. 3D analysis of the 3D model.

Description	Value	Unit
Total VOI volume	70239387385	um ³
Object volume	46193939033	um ³
Percent object volume	65.77	%
Total VOI surface	152146821	um ²
Object surface	4053470740	um ²
Intersection surface	53355506	um ²
Object surface / volume ratio	0.08775	1/um
Object surface density	0.05771	1/um
Number of objects	14027	
Number of closed pores	361841	
Volume of closed pores	504048841	um ³
Surface of closed pores	214219493	um ²
Closed porosity (percent)	1.08	%
Volume of open pore space	23541399511	um ³
Open porosity (percent)	33.52	%
Total volume of pore space	24045448352	um ³
Total porosity (percent)	34.60	%

4 Conclusions

A method to acquire and observe 3D weaving structure of leather through micro-CT was introduced. The composition and principle, parameter settings and data acquisition steps of micro-CT were introduced thoroughly. Images were processed by corresponding software accordingly, thus getting the series 2D and 3D images of chrome-tanned leather. The gained 3D digital structure has following purposes and significance: it is not only beneficial to further study the morphology of 3D structure

of leather accurately and thoroughly, but also to explore the relationship between structure and performance of leather. Assisted by corresponding image processing tool, any slices or internal structure of 3D volume can be analyzed deeply through a series of cutting, enhancing and measurement functions, such as measuring morphological parameters of leather fiber bundles and pores (e.g. diameter, length, specific surface and volume), studying distribution pattern of fiber bundles, observing connectivity of spaces among fiber bundles, and calculating physical parameters (e.g. porosity, volume density and fractal dimension) of leather. Further studies on these aspects will be carried out in future.

Table 2. Structure thickness distribution.

Range	Mid-range	Volume	Percent volume in range
um	um	um ³	%
1.50 - 4.50	3	22374160.5	0.0485
4.50 - 7.50	6	201329951.5	0.4361
7.50 - 10.50	9	345494838.7	0.7484
10.50 - 13.50	12	968296506.9	2.0974
13.50 - 16.50	15	1683379913	3.6463
16.50 - 19.50	18	2090130837	4.5274
19.50 - 22.50	21	3156601127	6.8374
22.50 - 25.50	24	3430937981	7.4317
25.50 - 28.50	27	3561692161	7.7149
28.50 - 31.50	30	3707121253	8.0299
31.50 - 34.50	33	3814585777	8.2627
34.50 - 37.50	36	3273281346	7.0902
37.50 - 40.50	39	3271279391	7.0858
40.50 - 43.50	42	2982358271	6.46
43.50 - 46.50	45	2425641873	5.2541
46.50 - 49.50	48	2146793315	4.6501
49.50 - 52.50	51	1925423249	4.1706
52.50 - 55.50	54	1562657940	3.3848
55.50 - 58.50	57	1307396731	2.8319
58.50 - 61.50	60	1020285284	2.21
61.50 - 64.50	63	807400344.4	1.7489
64.50 - 67.50	66	635641526.3	1.3768
67.50 - 70.50	69	474858622.4	1.0286
70.50 - 73.50	72	362268497.3	0.7847
73.50 - 76.50	75	258186644.4	0.5593
76.50 - 79.50	78	194791460	0.4219
79.50 - 82.50	81	144638910.8	0.3133
82.50 - 85.50	84	109573726.7	0.2373
85.50 - 88.50	87	77387817.79	0.1676
88.50 - 91.50	90	56490527.97	0.1224
91.50 - 94.50	93	38037136.99	0.0824
94.50 - 97.50	96	28998738.37	0.0628
97.50 - 100.50	99	16561532.43	0.0359
100.50 - 103.50	102	13055085.92	0.0283
103.50 - 106.50	105	11628597.39	0.0252

Acknowledgements

This work was supported by the Project of Natural Science Foundation of Shandong Province (No. ZR2017LB024), the National Natural Science Funds of China (No. 211776143), and Program for Li Tianduo Taishan Scholar Team of Shandong Province.

References

1. Yuan, J.J., *Leather Sci. and Eng.* 21, 19-21, 2011
2. Luo, L. S., *Materials Rev.* 24(09), 1-5, 2010.
3. Zhang, H. Y., *J. Amer. Leather Chem. Ass.*, 2014, 109, 1.
4. Zhang, H. Y., *J. Amer. Leather Chem. Ass.*, 2018, 113,248
5. Zhang, H. Y., *J. Soc. Leather Technol. Chem.*, 2015, 99, 23.
6. Bittrich E. J. *Amer. Leather Chem. Ass.*, 2014,109,367
7. Moreno-Atanasio R, *Particuology*, 2010 (8): 81
8. Kariem H, *J Materials Sci.*, 2018:1.
9. Zhou M, *Energies*, 2018, 11(6):1409.
10. Heyndrickx M, *Mater Charact.* 2018, 139:259.
11. Zauer M, *Wood Sci. Technol*, 2014, 48(6):1229.
12. Sukop M C, *Phys. Rev. E*, 2008, 77: 026710.

EFFECTS OF CHOLINE CHLORIDE, UREA AND THEIR DEEP EUTECTIC SOLVENTS ON THE MODIFICATION OF LEATHER

Letian Qi^{1,a)}, Lihong Fu²

1 State Key Laboratory of Biobased Material and Green Papermaking, Qilu University of Technology, Shandong Academy of Sciences, Jinan, 250353.

2 School of Light Industry Science and Engineering, Qilu University of Technology, Shandong Academy of Sciences, Jinan, 250353.

a)Corresponding author: lqi01@qlu.edu.cn

Abstract. The application of split leather is an important issue in leather industry as most of them was not properly treated and wasted. In this study the application of choline chloride ([Ch][Cl]), urea (U) and corresponding deep eutectic solvents (DES) on the modification of thermal stability and mechanical strength of mink split leather was investigated. TGA and DSC results indicated DES treatment enhanced thermal stability of split leather, and [Ch][Cl] treatment reduced the stability. While, U treatment provided a kinetic inhibition during the thermal-decomposition. In terms of the mechanical strength, both [Ch][Cl] and U treatment reduced burst intensity and extended height. While, after DES treatment the burst intensity and extended height increased significantly. In terms of the dosage, 7% DES provided best performance. Results mentioned above illustrated that DES formed by simply mixing [Ch][Cl] and U provided strong interaction with fiber, enhanced the crosslinks. A hypothesis of [Ch(Urea)]+[Cl(Urea)]- type structure was proposed, as it enabled DES forming strong hydrogen bonds with functional groups on leather fiber, enhancing the crosslinks and therefore improving the thermal stability and mechanical strength. The DES treatment on leather fibers improved their overall performance and thereby broaden their applications.

1 Background

The split leather is an important leather and bio-based material in tanning industry, whose physical properties can be improved to expand applications. However, it was not properly treated during the tanning process and a great portion was wasted. For example, split mink leather was discarded during the shaving process, for its small area, low physical strength and poor thermal stability. This caused the waste of high-quality collagen materials and a pollution to the environment.

The utilization of split leather requires thermal treatment either directly or after a chemical pretreatment to improve the physical strength. In which, thermo-treatment was commonly used in the direct processing. However, the poor thermal stability and extensibility prohibit the application of mink split leather. In addition, the thermal decomposition and denature of collagen also cause problem during the utilizations. Retanning and ester addition are the most widely used chemical treatments, which improve the leather performance, thereby broad its applications. Chrome tanning is the most commonly used tanning technic, which enhances the crosslink between collagen fibers. As the crosslink directly related to the thermal stability and physical strength, chrome tanning helps improving the thermal and physical properties of the leather. However, the major concern is environmental pollutions induced by chrome containing chemicals. Fat liquoring agent improves the softness of leather but decreases the physical strength of leather. The other draw back includes the large dosage and poor biodegradability, which causes problems in the downstream processes. Thereby, both academic and industrial side focused on developing a greener, environmental-friendly approach to enhance the physical strength and thermal stability of the leather.

Ionic liquids (IL) are nova green solvents with merits of good solubility, nonvolatile, easy to recycle, low toxicity, environment friendly, and tunable. Therefore, it was extensively studied in chemistry, chemical engineering, material, biology field. The strong electronic effect and H-bonding

was found in ionic liquids, thereby it is ideal to improve the physical strength of leather. Jayakumar et al.¹ firstly reported that [BMIM][Cl] ionic liquid loosened the leather fibers, pointing out the potential of applying IL in the dehairing process. Latterly, Alla et al.² successfully applied [BMIM][BF₄] ionic liquid in the dehairing and fiber loosening process. In addition, Ranganathan et al.³ reported that quaternary ammonium based ionic liquids could disturb the disulfide bond in keratin/certain, cause the dehair effect and improve the physical strength of leather. However, the study of IL application on tanning process are still limited to the commercial availability of ILs, which are usually expensive and prevented their further applications.

Choline based ionic liquids are generally cheap and environment friendly. Therefore, it is an ideal bio-based material treatment agent. It contains multiple H-bonding sites such as halogen anions and hydroxide groups on cations, which act as H-bond acceptors and donors, respectively. These H-bonding sites could interact with functional groups on collagen fibers, forming multiple H-bonds. At the main time, as an ampholyte the leather fiber also interacts with IL cations and anions through coulomb force. Thereby, the application of choline based ILs should be able to improve the crosslinks of the collagen fibers, resulting in an enhancement of leather physical strength and thermal stability. On the other hand, urea (U) is an important additive in leather industry, which was usually used in liming treatment process⁴. Urea molecule interacts with collagen fibers through H-bonds on amino and carbonyl groups. Therefore, it could disturb the collagen-water interactions in leather and modify the leather properties⁵.

Mix [Ch][Cl] with urea at 1:2 molar ratio generates deep eutectic solvent (DES) with melting point as low as 12 °C. In comparison, the melting point of [Ch][Cl] and urea under atmosphere pressure are 300 and 133 °C, respectively. The decrease of melting point indicates the present of strong H-bonds. Liquid state also makes pumping and injecting more convenient to achieve in process. Therefore, [Ch][Cl]-U DES is an ideal leather fiber treatment agent, as it may provide dual function from both [Ch][Cl] and urea side and may also present some new features. Abbott et al.⁶ reported that DES present high electronic interactions that makes tanning agent much easier getting into leathers. Thereby, the application of DES based ionic liquids can be used to replace traditional solvent. This work was the first to ingratiate the application of DES on mink split leather. [Ch][Cl]-U (A), [Ch][Cl] (A0), and urea (U) was applied for mink split leather treatment, in order to study their effect on physical strength and thermal stability. The study provides important information over the mechanism of DES-collagen fiber interactions.

2 Experimental

2.1 Materials

Mink split leather was obtained from a leather company in Shandong Province, P. R. China. Chemicals used for leather treatment and DES synthesis, including source and grade, were as following:

Choline chloride (AR, 98-101%, Sinopharm Chemical Reagent Co., Ltd.), urea (AR, 99.0%, Tianjin Da Mao Chemical Co.). [Ch][Cl]-U DES was synthesized by mixing choline chloride and urea at 1:2 molar ratio under 60 °C for 4 hr. Ultra-pure water (18 MΩ·cm) was supplied by JNLC Water Purification System, P. R. China.

2.2 Chemical Treatment on Mink Leather

The mink split leather was washed and squeeze-dried 3 times with ultra-pure water, followed by stabilizing in polyethylene bag for 30 min (water content 55.95%). Then, water ($w_{wet\ leather}:w_{water} = 1:10$) was added into stabilized leather samples, with or without the

addition of treatment chemicals. Chemicals were added basing on the dry weight of leather, and 5 different treatment conditions were listed as following:

0% (blank test), 7%[Ch][Cl]-U, 14% [Ch][Cl]-Cl, 7% [Ch][Cl] and 7% U.

Treatment was carried out under room temperature (19 °C) for 37.5 hr, ceased by removing leather samples from the aqueous solutions. The samples were air-dried for 24 hr, prior thermal analysis and physical strength tests.

2.3 Thermal Analysis

Thermal characterization of treated and untreated leather samples included thermal gravimetric (TG), differential thermal gravimetric (DTG) and differential scanning calorimeter (DSC) techniques.

TG/DTG analysis was performed using TGA-Q50 apparatus, produced by TA Instruments, US, in N₂ atmosphere and 20-500 °C temperature range, at a heating rate of 5 °C/min.

DSC analysis was performed using DSC-Q20 apparatus, produced by TA Instrument, US, in N₂ atmosphere and 30-350 °C temperature range, at a heating rate of 10 °C/min. Samples weighted 5–6 mg was placed in aluminium pan to perform the test.

2.4 Mechanical Strength Analysis

Air-dried leather samples were conditioned at 20 °C, RH 65% for 24 hr, in a YG751D constant temperature and humidity incubator, produced by Shanghai Jing Hong Laboratory Instrument Co., Ltd. Burst intensity and extended height was analysed by XK-3055 burst intensity tester, produced by Xiangke Testing Instrument Co., Ltd. Following equations were used during the determinations of the mechanical strengths:

$$\text{Burst intensity} = F/\delta \tag{1}$$

$$\text{Extended height} = h \tag{2}$$

Where, F is the load at fracture (N), h is the extended height at fracture (mm), δ is the thickness of testing samples (mm).

3 Results and Discussions

3.1. Thermal Gravimetric Analysis (TGA)

Thermal gravimetric analysis of leather samples treated by different chemicals were illustrated in Fig.1 (a). All the samples viewed a 5% weight loss between 30 to 125 °C, followed by sharp drop from 250 °C. Leather pretreated by [Ch][Cl]-U presented TG curve of the same trend but above the blank test, thereby its thermal stability was slightly better than the blank test. TG curve of 7% A0 is lower than blank test, thereby this treatment reduced the thermal stability of the leather sample. However, the 7% U treatment results moved towards the upper right corner, indicating an enhancement in thermal stability.

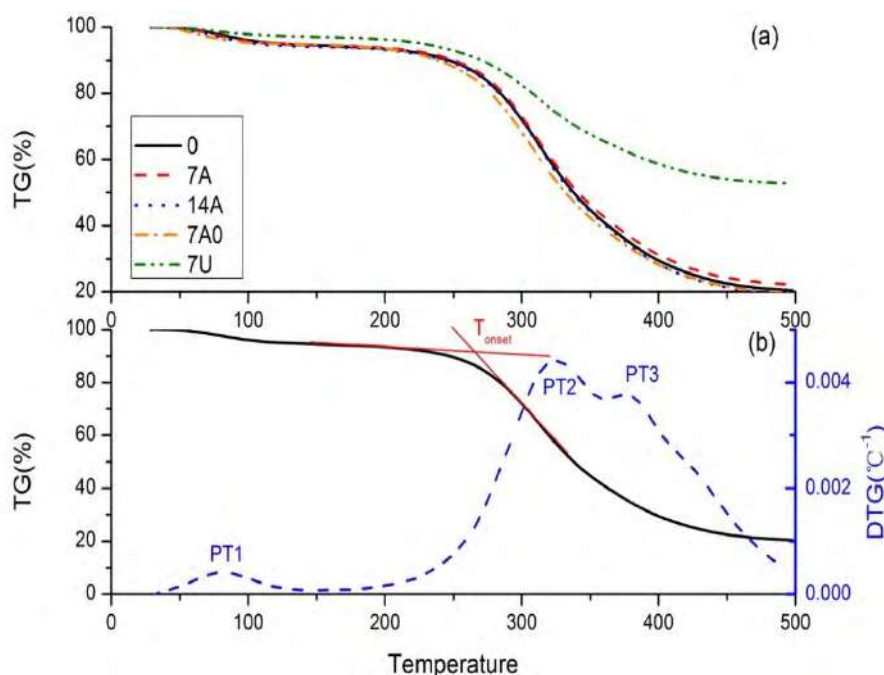


Fig. 1. Thermal gravimetric (a) and differential thermal gravimetric (b) of mink split leather. Note: 0, blank test; 7 A, 7% [Ch][Cl]-U; 14 A, 14% [Ch][Cl]-U; 7 A0, 7% [Ch][Cl]; 7 U, 7% urea.

Differential thermal gravimetric analysis provided more detailed information. Taking the blank test data in Fig. 1 (b) for example, the mass change of leather sample under N₂ environment could be classified into 2 stages: the first stage is dehydration of leather sample, which was shown as peak PT1 at 82 °C; the second stage was the thermal decomposition of collagen, which was PT2, PT3 at 325 and 376 °C, respectively. T_{onset} can be considered as the cut-off point of the two stages mentioned above. Details of TG, DTG analysis can be found in Table 1.

Table 1. Effect of different treatment on the thermal stability of mink split leather.

	0%		7% [Ch][Cl]-U		14% [Ch][Cl]-U		7% [Ch][Cl]		7% U	
	T (°C)	Weight loss (%)	T (°C)	Weight loss (%)	T (°C)	Weight loss (%)	T (°C)	Weight loss (%)	T (°C)	Weight loss (%)
PT1	82.3	2.5	77.9	2.5	78.7	2.9	65.2	2.3	77.5	1.3
T _{onset}	265.0	7.3	267.0	6.8	266.8	7.4	257.6	7.7	257.7	4.3
PT2	325.2	43.2	325.0	41.8	321.1	41.5	316.0	41.5	315.0	22.5
PT3	375.8	64.2	378.6	63.2	380.2	66.3	370.7	64.4	379.1	38.0

As shown in Table 1, the IL treatment shifted the appearance of dehydration peak (PT1), and all of which were lower than the normal boiling point of water (100 °C). Thereby, the mass loss at PT1 could attribute to the removal of free water. PT1 of blank sample occurred at 82.26 °C, and the treated samples moved towards lower temperature, where PT1 of 7% and 14% [Ch][Cl]-U occurred at 78 °C, the 7% [Ch][Cl] peak occurred at 65 °C. Under the same dosage (7 wt% loading) the PT1 appearance temperature from high to low was: [Ch][Cl] – U ≥ U >> [Ch][Cl] Which indicates the various effect of leather fiber holding onto water molecular. It should be noticed that, although 7% U presented similar dehydration temperature with 7% [Ch][Cl]-U, its weight loss was much lower. The shift of PT1 towards lower temperature after chemical treatment could attribute to the formation of hydrogen bond and electronic interactions between chemicals and collagen fibers.

These interactions occupied the H-bonding sites for water-fiber interactions, thereby reduced the overall fiber-water interactions through its functional groups. This phenomenon caused the increase of water activity, leading to an easier removal of water molecule, thereby moved the PT1 peak towards lower temperatures. To this point, the dehydration temperature illustrated the strength of interaction between the collagen fiber and treatment agent. The PT1 temperature of treated sample from high to low ranked: 7% [Ch][Cl] << 7% U ≤ 7% [Ch][Cl] – U < 14% [Ch][Cl] – U < 0%. These results indicate that A0 could form stronger interactions than A and U.

T_{onset} was the temperature that samples started thermal decompositions, which represented the thermal stability of leather. The T_{onset} of blank test was 265.0 °C, samples treated by 7% and 14% [Ch][Cl]-U were having T_{onset} of 267 °C, while 7% [Ch][Cl] and U treatment reduced the T_{onset} to 258 °C. 7% U treatment gives leather a different thermal performance, as only 4.3% weight loss was observed. In comparison, the 7% [Ch][Cl] and [Ch][Cl]-U treatment lost 7.7% and 6.8%, respectively. In addition, with the increase of the dosage of [Ch][Cl]-U from 7% to 14%, the weight loss increased from 6.8% to 7.4%. These results indicated that the treatment chemicals applied in this research presented different effects: [Ch][Cl]-U treatment improved the crosslinks between fibers, thereby improved the thermal stability; [Ch][Cl] interacted with collagen fiber but formed limited crosslinks with fibers due to its small size, resulting in a decrease in thermal stability, and achieved a high thermal decomposition ratio; U treatment failed to bring up the T_{onset} of the leather, however, delayed the decomposition process. The ratio of leather samples decomposed was only half of the amount in other samples. Therefore, it presented more a kinetic inhibition effect. It may possibly be caused by the small molecule size of urea allowing it to be inserted between fibers and enlarged the fiber distance, thereby inhibiting the crosslink between fibers, resulting in a decrease in thermal stability. Hereby, [Ch][Cl] and U have synergistic effects, which made [Ch][Cl]-U an efficient treatment chemical in improving the thermal stabilities of leather.

PT2 and PT3 were rapid decomposition peaks. From Fig.1 and Table 1, [Ch][Cl]-U and [Ch][Cl] treatment presented similar thermal behavior with the blank test during this period, while 7% [Ch][Cl]-U treatment presented a better thermal stability. U treatment did not shift the peak position of PT2 and PT3 towards higher temperatures. However, Fig. 1 illustrated that the decomposition process in this temperature range was also significantly delayed after U treatment. The results supported the previous proposal that U treatment inhibited the thermal decomposition process of collagen fibers.

3.2 Differential Scanning Calorimeter Analysis

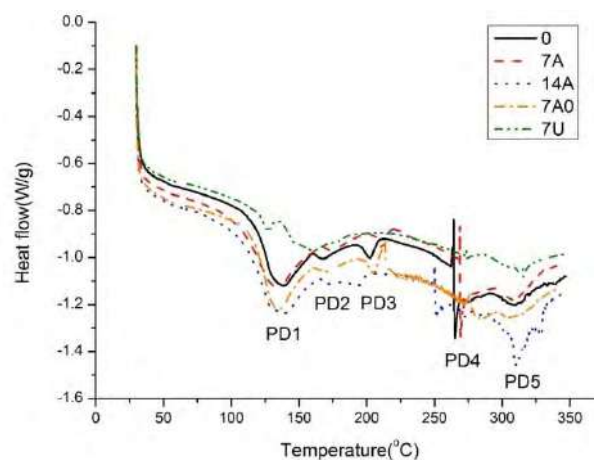


Fig. 2. Effect of different treatment on the DSC of leather with or without treatment. Note: 0, blank test; 7 A, 7% [Ch][Cl]-U; 14 A, 14% [Ch][Cl]-U; 7 A0, 7% [Ch][Cl]; 7 U, 7% urea.

Table 2. Assignment of DSC peaks of treated and untreated leather.

Peak / (°C)	Blank	7% [Ch][Cl]-U	14% [Ch][Cl]-U	7% [Ch][Cl]	7% U
PD1	138.8	134.7	139.2	135.6	127.5
PD2	167.4	173.8	172.2	169.2	161.3
PD3	202.9	212.1	194.2	205.1	NA
PD4	265.0	269.2	254.9	285.6	274.5
PD5	310.4	310.1	310.1	305.9	315.7

Previously, TGA results illustrated thermal decomposition of leather has 3 stages, which was in line with that reported by Cheng et al.⁷. Corresponding DSC results was shown in Fig. 2 and details of peak assignments was presented in Table 2, in which the first stage was the dehydration stage from 30 to 125 °C, including PD1. The second stage from 125 to 250 °C, including PD2 and PD3, represented the thermal behavior before the decomposition. In this stage, a melting of crystalline collagen in amorphous occurred⁸, as only minor weight loss was observed. The third stage was the rapid decomposition stage from 250 to 350 °C, including PD4 and PD5.

Thermal behavior of leather in the first stage was closely related with combined water, which played an important role while stabilizing the collagen fibers. In Fig. 2 leather samples presented a trend of an endothermic peak (PD1) followed by two small peaks (PD2, PD3), which was similar with that reported by Budrugaec et al.⁹. Therefore, the occurrence of PD1 at 135 °C could be attributed to the dehydration of leather, which represented the removal of bonded water. In addition, the enthalpy changes (ΔH) at PD1 was related to the strength of water molecules bonded with collagen fibers. Higher ΔH value indicated the requirement of more energy for water removal, thereby, a stronger water-fiber exists. As shown in Table 3, the ΔH value of tested leather samples from high to low ranked as: 7% [Ch][Cl] \gg 7% [Ch][Cl] – U > 14% [Ch][Cl] – U \gg 0% \gg 7% U.

Table 3. Effect of different treatment on the enthalpy changes (ΔH) of treated and untreated leather.

ΔH (J/g)	Blank	7% [Ch][Cl]-U	14% [Ch][Cl]-U	7% [Ch][Cl]	7% U
PD1	-32.55	-49.08	-47.58	-61.23	-3.12
PD2	-1.94	-1.78	-0.52	-2.27	-21.88
PD3	-3.20	-2.70	-1.81	-4.03	NA

Varies H-bonding sites on [Ch][Cl] allowed it to form strong interaction with water molecules, made the bonded water difficult to remove. Thus, [Ch][Cl] treatment requires the most energy for water removal. This also illustrated that only limited crosslink was caused between fibers after [Ch][Cl] treatment, as most of [Ch][Cl] molecules just remained in the fiber gaps and was not bounded with fibers. In the same manner, [Ch][Cl]-U molecule also have multiple H-bond sites, but due to the large molecular size, it can form more effective crosslinks between fibers. Thereby, a lower ΔH was required to remove water in 7% [Ch][Cl]-U treated leather sample than the [Ch][Cl] treated one. The addition of [Ch][Cl]-U resulted in an increase formation of intermolecular interactions with each other, instead of fiber crosslinks. Therefore, excess [Ch][Cl]-U enlarged the gap between fiber, which helped with the dehydration process, resulting in a decrease of ΔH value. In terms of U, it has a relatively weaker interaction with water molecules¹⁰, thereby require less energy, leaving the dehydration process occurs at a lower temperature than other samples.

At PD2 and PD3, endothermal phenomenon occurs but no significant weight loss was viewed in TGA. This could be attribute to the rearrangement of crystalline and amorphous structure of collagen. Budrugaec⁸ reported that the well-organized collagen triple helix was immersed in the

amorphous region, and the endothermal phenomenon viewed was caused by the transfer of crystalline collagen towards amorphous state. It was reported that collagen melt at 230 °C⁹, which was close to the PD3 in this work. At this temperature dry thermal shrinkage occurred^{11,12}, where microcosmic melting of crystalline region resulting in a macrocosmic collapse of leather matrix structure¹³. In this work, the PD2 temperature of treated samples from high to low ranked as: 7% [Ch][Cl] – U > 14% [Ch][Cl] – U > 7% [Ch][Cl] > 0% > 7% U. While for PD3: 7% [Ch][Cl] – U > 7% [Ch][Cl] > 0% > 14% [Ch][Cl] – U. 7% U sample had no PD3. Higher PD2, PD3 value indicates better thermal stability. Thereby, 7% [Ch][Cl]-U treated sample presented highest temperature at PD2 and PD3, and presented the best thermal stability. It should be point out that U treatment, again, presented different thermal behavior than others. Although its PD2 appeared at a relative lower temperature, this peak was rather flat in comparison with other samples. Therefore, it provided more kinetic decomposition inhibition effect during the test, and this finding again supported the previous proposed mechanism.

PD4 occurs at 255-286 °C, at which point the collagen was denatured¹⁴. Combining TG results analyzed previously, leather samples started thermal decomposition. DSC curve presenting a trend of sharp increase followed by a significant decrease. This may due to the rearrangement of hydrophobic bonds¹³. The cleavage of hydrophobic bonds releases energy, followed by the formation of new bonds, consume energy¹³. PD5 is the rapid thermal decomposition of leather. Interestingly, thermal behavior of U treated leather at PD4, PD5 are again different with other samples, indicating their different effect.

To summarize up, [Ch][Cl] treatment slightly decreased the thermal stability of leather, whereas, [Ch][Cl]-U generated by mixing [Ch][Cl] with U, caused crosslinks with fibers, improved the thermal stability of leather. 7% [Ch][Cl]-U treated leather presented good thermal stability, however excess application of 14% [Ch][Cl]-U, reduced the thermal stability. In terms of U, it worked as a kinetic inhibitor during the decomposition, mainly filled in the collagen fiber gaps. Although, it did not lift the thermal decomposition temperature, the decomposition rate was significantly delayed. Thereby, although [Ch][Cl]-U was synthesized by [Ch][Cl] and U, it provided both strong ionic charge center and various H-bond sites and presented very different effect than either of them. Comparing with [Ch][Cl] and U, [Ch][Cl]-U has a more suitable molecule size to form crosslinks between fibers, and to enhance the leather properties.

3.3 Mechanical Strength Analysis

Burst intensity reflected the strength of fibers in all directions and its crosslink intensities, while extended height indicated the mobility of fibers. Higher burst intensity was related to higher crosslink between fibers, and higher extended height was related to better molecule movements. It can be seen in Fig. 3, [Ch][Cl] and U treatment reduced the extended height and burst intensity, which could attribute to the small molecular size that allowing them to get into leather fibers. The enlargement of fiber gaps inhibited the formation of crosslinks between fibers and reduced the burst intensity. Applying U on its own formed multiple H-bonds with fiber, resulted in an increase in stiffness and brittleness of leather, and reduced the extended height significantly. In terms of [Ch][Cl]-U, it formed H-bonds and electrovalent bonds with leather fibers, improved fiber crosslink and enlarged the fiber distance. Therefore, [Ch][Cl]-U treatment improved extended height and burst intensity at the same time.

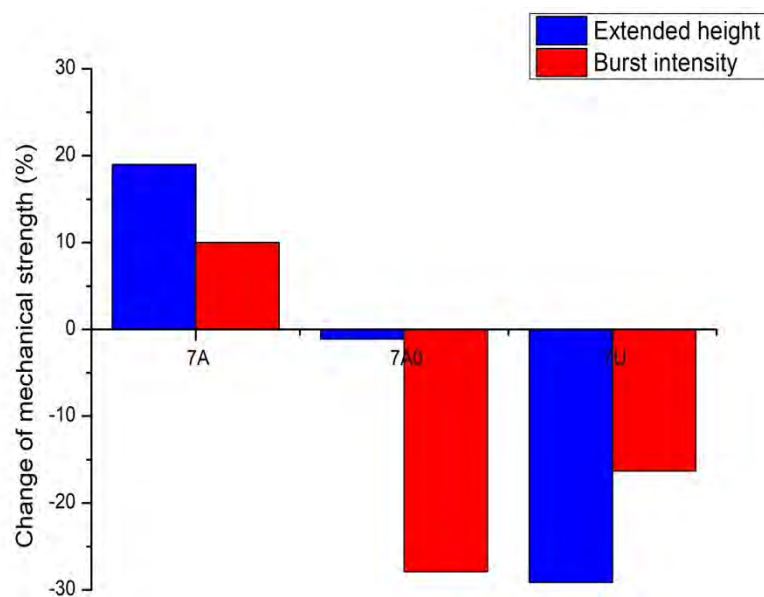


Fig. 3. Effect of different treatment on the burst intensity and extended height of leather. Note: 7 A, 7% [Ch][Cl]-U; 14 A, 14% [Ch][Cl]-U; 7 A0, 7% [Ch][Cl]; 7 U, 7% urea.

In this work, both the physical strength test and thermal stability tests results illustrated that [Ch][Cl]-U treatment provided different effect than [Ch][Cl] and U. This should attribute to their different molecular structures: choline chloride was a quaternary ammonium-based IL, its anion had strong H-bond accepting ability. The quaternary ammonium based ILs was used for synthesizing deep eutectic solvents (DES) by simply mixed with H-bond donors, such as urea. In terms of the molecular structure, it was commonly considered that in this [Ch][Cl]-2Urea DES system, two urea molecules was complexed with chloride anion, appeared as $[\text{Ch}]^+ [\text{Cl}(\text{Urea})_2]^-$ type structure¹⁵. However, this theory cannot well explain the phenomenon that was found in this work. The anion of [Ch][Cl] provided strong H-bond accepting ability, which was considered as main contribution of H-bonding abilities. The combination of two urea with chloride anion formed a complex anion but consumed the H-bond accepting sites on $[\text{Cl}]^-$, reduced the overall H-bond accepting ability. In terms of cation, the cation of $[\text{Ch}]^+ [\text{Cl}(\text{Urea})_2]^-$ DES is similar to that of [Ch][Cl]. Therefore, the overall H-bonding ability of [Ch][Cl]-U should be lower than [Ch][Cl]. The crosslinks that endured by [Ch][Cl]-U should be less or weaker than [Ch][Cl]. In addition, if two urea molecules were inserted onto the anion, the H-bond donor and H-bond acceptor center will mainly be located on the complex anion. The existence of steric hindrance inhibited the formation of crosslink with collagen fibers. But all these theoretical analyses were different from that observed experimentally. Thereby, this theory may not properly explain the experimental phenomenon in this work.

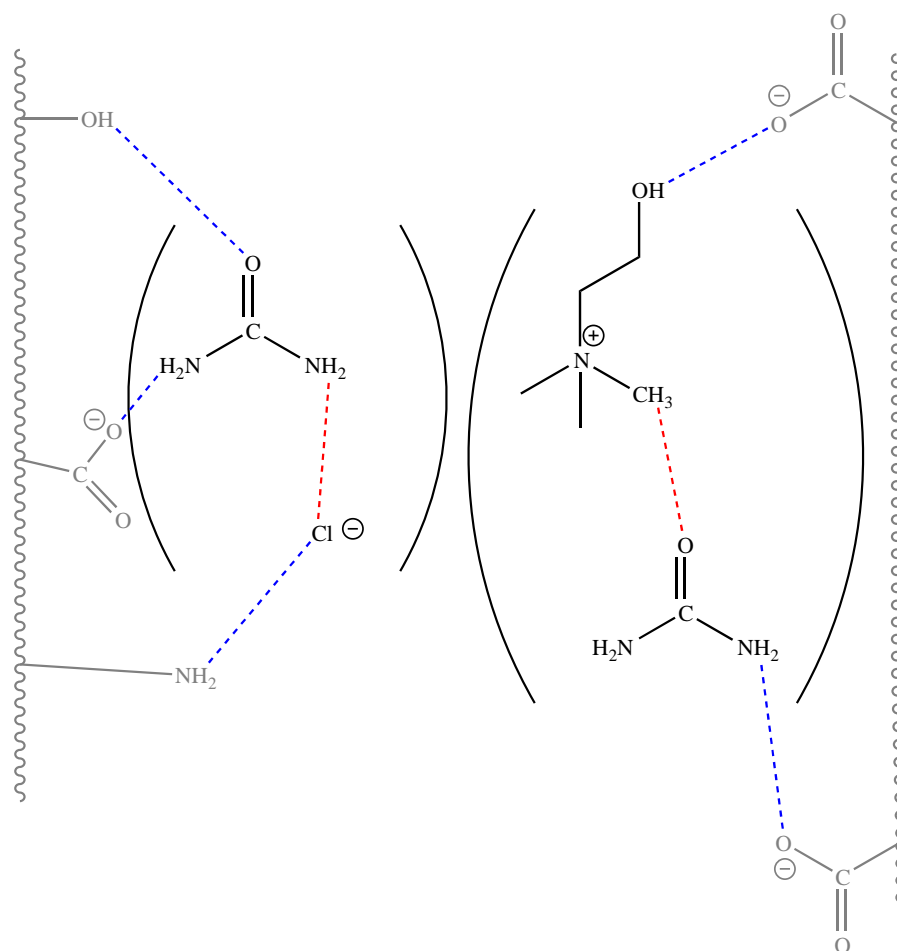


Fig. 4. Schematic diagram of interactions between ChCl-2urea DES and leather fibers. Note: grey curve, collagen fibers; red dash, intramolecular H-bonds; blue dash, intermolecular H-bonds.

The $[\text{Ch}(\text{Urea})]^+ [\text{Cl}(\text{Urea})]^-$ type structure⁴⁵ proposed by Ashworth provided an alternative approach, in which urea interacted with choline cation through carbonyl group. The complex cation formed were still able to provide strong H-bond donor ability. Whereas, after complexed with a urea molecule, the chloride still provided strong H-bond accepting ability and H-bond donating ability at the same time. Fig. 4 shown the schematic diagram of the DES-fiber interactions basing on Ashworth's theory. The complex cation and anion of DES was formed by chloride anion forms H-bond with urea molecule through amino group, and choline cation H-bonded with urea through its alkyl hydrogen. The grey chain on both sides represented the collagen fibers, which contained virous functional groups. The H-bond donor groups such as amino group and hydroxide group could interact with the complex anion. While, carboxyl groups on the fibers could interact with complex cation. The complex cation and anion paired through coulombic interaction. Therefore, multiple H-bond sites and various interactions formed between DES and collagen fibers could contribute to the formation of crosslinks. The formation of effective crosslinks improved the thermal stability and mechanism strength of leather. Therefore, this approach can be further investigated over the applications on collagen fibers.

4 Conclusions

In this work, [Ch][Cl]-U, [Ch][Cl] and U was applied for the treatment of leather. TG, DSC, burst intensity and extended height was applied for analyzing the thermal stability and mechanism strength of leather. Due to the ionic charges and H-bond effect of the treatment chemicals. Free water in treated samples could be removed at lower temperature, whereas, the removal of the bonded water requires more energy. It was found that [Ch][Cl] and U filled in the gaps of fibers, without forming efficient crosslinks. Therefore, it presented minor effect in thermal stability improvement and reduced the mechanism strength. In comparison, [Ch][Cl]-U improved the thermal stability and mechanism strength at the same time. Through the mechanism analysis, it was found that [Ch][Cl]-2Urea DES system interacted with collagen fiber through [Ch(Urea)]+[Cl(Urea)]- type structure. The DES improved crosslink with collagen fiber through amino and carboxyl groups, and therefore enhanced the thermal stability and physical strength of leather.

References

1. Jayakumar, G. C., Mehta, A. L., Jonnalagadda, R. R., & Fathima, N. N.: *Ionic liquids: new age materials for eco-friendly leather processing*. *Rsc Adv.*, 5(40), 31998-32005, 2015
2. Alla, J. P., Rao, J. R., & Fathima, N. N.: *Integrated depilation and fiber opening using aqueous solution of ionic liquid for leather processing*. *Acs Sustain. Chem. Eng.*, 5(10), 2017
3. Ranganathan, V., Vedaraman, N., Chellappa, M., Mandal, A. B., & Macfarlane, D.: *Aqueous ionic liquid solutions as alternatives for sulphide-free leather processing*. *Green Chem.*, 17(2), 1001-1007, 2015
4. Feng, W. P., Wang, F., Tang, K. Y., Pan, H. B.: *Influence of urea process on the dry heat shrinkage behavior of collagen fibers*. *China Leather*, 39(11), 19-21, 2010
5. Tang, K. Y., Feng, W. P., Wang, F., Pan, H. B.: *Influence of urea process on thermal degradation behavior of collagen fibers*. *China Leather*, 39(13), 9-12, 2010
6. Abbott, A. P., Alaysuy, O., Antunes, A. P. M., Douglas, A. C., Guthrie-Strachan, J., & Wise, W. R.: *Processing of leather using deep eutectic solvents*. *Acs Sustain. Chem. Eng.*, 3(6), 1241-1247, 2015
7. Cheng, F., Jiang, L. Y., Gong, Y., Chen, W. Y.: *Analysis of pyrolysis performance of leather retanned with different retanning agent by TG-DSC*. *Leather Science and Engineering*, 22(3), 18-21, 2012
8. Budrugaec, P., Carşote, C., Miu, L.: *Application of thermal analysis methods for damage assessment of leather in an old military coat belonging to the history museum of braşov—romania*. *J. Therm. Anal. Calorim.*, 1-8, 2017
9. Budrugaec, P., Miu, L.: *The suitability of dsc method for damage assessment and certification of historical leathers and parchments*. *J. Cult. Herit.*, 9(2), 146-153, 2008
10. Wang, X. A., Fu, L. H.: *A preliminary study on buffer effect of carbamide to pH value of the liming liquor*. *West Leather*, 31(11), 10-12, 2009
11. Zhang, Y. C., Fu, L. H.: *Variety of wet blue hydrothermal properties in dechroming process*. *China Leather*, 37(19), 14-17, 2008
12. Zhang, Y. C., Fu, L. H.: *Dry heat properties of fibers in dechroming process of wet blue*. *China Leather*, 38(9), 12-14, 2009
13. Chahine, C.: *Changes in hydrothermal stability of leather and parchment with deterioration: a dsc study*. *Thermochim. Acta*, 365(1-2), 101-110, 2000
14. Cucos, A., Budrugaec, P., Miu, L.: *Dma and dsc studies of accelerated aged parchment and vegetable-tanned leather samples*. *Thermochim. Acta*, 583(14), 86-93, 2014
15. Ashworth, C. R., Matthews, R. P., Welton, T., Hunt, P. A.: *Doubly ionic hydrogen bond interactions within the choline chloride-urea deep eutectic solvent*. *Phys. Chem. Chem. Phys.*, 18(27), 18145, 2016

DEVELOPMENT OF A NOVEL METHOD TO REDUCE THE IMPACT OF CUTANEOUS CHEMICAL ATTACKS

S. J. Davis^{1a}, W. R. Wise^{1b}, A. D. Covington¹, J. Petter^{2c} and P. Reip²

1 Institute for Creative Leather Technologies, University of Northampton, University Drive, Northampton, NN15P, UK

2 Hydro Navitas Solutions LTD, Lakeside House, The Lakes, Bedford Road, Northampton NN4 7HD, UK

a) Corresponding author: Stefan.davis@northampton.ac.uk

b) Will.Wise@northampton.ac.uk

c) James@hydronavitas.com

Abstract. Chemical attacks are a global problem: from 2011 to 2016 there were 1,464 incidents involving a corrosive substance in London alone. The most common chemicals used in these attacks are sulfuric, nitric and hydrochloric acids. Concentrated solutions of strongly alkaline substances including sodium hydroxide and sodium hypochlorite are also used. Current first-aid advice suggests diluting the exposed area with water and transfer to a hospital for further treatment. An immediate neutralisation treatment is avoided as incorrect identification of the corrosive could worsen the damage. In addition, there are concerns the enthalpy of solvation and neutralisation causes secondary burns. These limitations demonstrate the need for an amphoteric neutralising treatment with a low enthalpy of neutralisation. Aqueous formulations of natural water-based surfactants with natural plant-based substances have been trialled as neutralisers of sulfuric acid, sodium hydroxide and sodium hypochlorite. pH titrations demonstrated that the natural formulations are amphoteric, capable of effectively neutralising acidic and alkaline corrosives with minimal heat of neutralisation and no gas evolution. In addition, the studies have shown that the formulations can reduce oxidising compounds such as sodium hypochlorite. The experiments compared intact collagen with attacked but untreated collagen and collagen that had a corrosive applied but followed by treatment at different time intervals. Scanning electron microscopy (SEM) showed the reaction with concentrated sulfuric acid is rapid; significant collapse and gelatinisation of the fibre structure was observed within 5 seconds. Pigskin was utilised to model human skin: the observations demonstrated the importance of the epidermis in protecting the skin from chemical damage. Five minutes exposure to sulfuric acid, sodium hydroxide and sodium hypochlorite did not penetrate the epidermis, although damage was observed. The formulations of natural products recently tested at the University of Northampton have been shown to mitigate secondary chemical burns, whereas treatment with water alone resulted in secondary burns due to residual corrosive in the skin structure not being neutralised. The trials indicate that the product could be usefully applied by first responders and emergency services personnel.

1 Introduction

Chemical attack is defined as the act of throwing a corrosive substance onto the body of another with intent to harm the eyes, skin and deeper body tissues.ⁱ The possible long-term physical consequences of these attacks include blindness, scarring of the skin tissue.ⁱⁱ The most common types of acid used in these attacks are sulfuric and nitric acid.ⁱⁱⁱ Hydrochloric acid is sometimes used, but is much less damaging.ⁱⁱⁱ Concentrated solutions of strongly alkaline materials including sodium hydroxide can also be used.

Although chemical attacks occur all over the world, the UK has one of the highest rates of chemical attacks per capita in the world, according to Acid Survivors Trust International (ASTI).^{iv} From 2011 to 2016 there were 1,464 crimes involving a corrosive substance in London.^{iv} Work by the UK government to reduce the frequency of attacks is ongoing but this is unlikely to prevent their occurrence completely, therefore the need for a suitable neutralising system is required.⁵

Current recommended first-aid advice suggests flooding the exposed areas with water for at least 20 minutes and transfer to a hospital for further treatment.^v General first-aid advice recommends first-responders do not attempt to neutralise burns as the time taken to identify the corrosive and

an appropriate antidote would facilitate further damage compared to dilution with water.^v Water does not provide a neutralising mechanism for acid or alkaline materials; it remedies the burn by dilution and mechanical action removing the corrosive from the afflicted area.^{vi} It is possible to use weak acids such as 5% acetic acid to neutralise alkaline burns, whereas acid burns can use dilute solutions of weak sodium bicarbonate.^{vii} However, there are concerns over the enthalpy of reaction associated with these neutralisation processes causing secondary thermal burns.^{vii} Also, these treatments would have to be kept separate and identification of the corrosive would be required before selecting an appropriate treatment. This suggests a treatment system for chemical attacks needs to be amphoteric.

Other materials have similar potential advantages, however their application requires application within the first minute of exposure to a corrosive.^{vi} This target would be difficult to achieve given average response times for category 1 (life threatening) emergency calls is 7 minutes in the UK.^{viii} This suggests there is still a need for development of an amphoteric neutralising agent that can be effective in the average first-responder response times

The current study aimed to trial aqueous formulations developed from modified tree saps with biodegradable and non-toxic properties, referred to as sap-formulation A and sap-formulation B, as a counter to an attack with corrosive substances. These formulations have been shown to neutralise both acids, alkalis and chemical oxidisers, and demonstrate potential to be an effective tool for first responders when called to an attack.

2 Methodology

Sap-formulation A and B were formulated by Hydro Navitas Ltd. Dilution of sap-formulation A and sap-formulation B to a 10% v/v solution was achieved by adding the agent to water under magnetic stirring. 50% v/v sulfuric acid was prepared by adding 95% sulfuric acid to water under constant magnetic stirring with the receiver flask in a cold-water bath. 30% w/v sodium hydroxide and saturated sodium bicarbonate solutions were prepared by the same method.

2.1 pH Titrations

25 ml of a corrosive substance were pipetted into an insulated flask. The pH and temperature were recorded using separate probes: Mettler-Toledo Multi Seven, and Fisher Scientific ECOTEMP respectively. The pH probe was calibrated using standard pH 1.2, 4 and 7 buffers for acidic corrosives and pH 4, 7 and 9.22 for alkaline corrosives. The temperature probe was encased in glass filled with glycerol. The neutralising agent was dispensed in small aliquots from a burette and magnetically stirred for 5 seconds; a probe reading was taken after 60 seconds.

2.2 Residual Free-Cl₂ Titrations

Aliquots of sodium hypochlorite (technical grade) were neutralised with the theoretical quantity of neutraliser required to reach the equivalence point of the treatment. A 25 ml sample of treated sodium hypochlorite was pipetted into a 250 ml volumetric flask (dilution factor 10). A 5 g sample was taken and diluted with 50 ml of deionised water, 10 ml of 50% v/v acetic acid solution and 2-3g of potassium iodide were added. The solution was titrated against 0.1M sodium thiosulfate in the presence of a starch indicator. The oxidising capacity of the bleach was quoted as grams Cl₂ per litre of bleach solution.

2.3 Preparation of Pickled Sheepskins

Salted sheepskins (Buitelaar, IRL) were beamhouse processed to the pickled stage. The sheepskins were depickled, sammed and cut into 2.5 x 2.5 x 0.1 cm samples using a hydraulic clicking press (CPR, F60).

2.4 Sheepskin Chemical Burn Trials

Pelt sections were exposed to 2 ml of corrosive for 5 seconds to 1 hour after which, the sample was washed in 100 ml of treatment for 2 minutes. Samples were transferred to a vial containing 20 ml of buffered formaldehyde solution (3.8% v/v formaldehyde, 2.30 g l⁻¹ Na₂HPO₄, 8.73g l⁻¹ KH₂PO₄).

2.5 Scanning Electron Microscope Sample Preparation

Formaldehyde-preserved samples were submersed in acetone for 1 hour. The acetone was replaced with clean acetone for a further 30 minutes. The acetone was drained, and the samples dried for 12 hours. The samples were submersed in molten camphene (Sigma Aldrich, 50 °C) for 12 hours in sealed containers. Excess camphene was discarded, and the samples were refrigerated at 3 °C for 1 hour. The hardened samples were sectioned in the direction of the hair follicle crosssection the using a clean razor blade. Specimens were left in open air at room temperature for camphene sublimation for 12 hours. Specimens were then mounted using adhesive carbon pads (Agar Scientific). The samples were gold-coated using a Quorum Technologies SC7620 splutter coater.

2.6 Scanning Electron Microscope Procedure

Specimens were imaged by scanning electron microscopy (Hitachi, SEM-3000N).

2.7 Preparation of Raw Pigskins

Salted pigskins (DEVRO, UK) were washed and degreased at 35 °C (Trumpler, Pastasol BZ, Pastasol F). Skins were shaved using an electric hair clipper set to 1 mm. Shaved skins were cut into 75 x 200 mm samples and stored at 3 °C.

2.8 Pigskin Corrosive Burn Trials

4 ml of corrosive substance was dispensed over the pelt surface from an auto pipette (Socorex 1-10 µl). The corrosion process was recorded using a Nikon D7000 with an 18-200 mm f/3.5-5.6 lens at 200 mm, f/8 and a focal distance of 1 m. Photographs were also taken with a thermal imaging camera (FLIR, i7) throughout recording. After an exposure time of either 30 seconds or 5 minutes, the skin was neutralised.

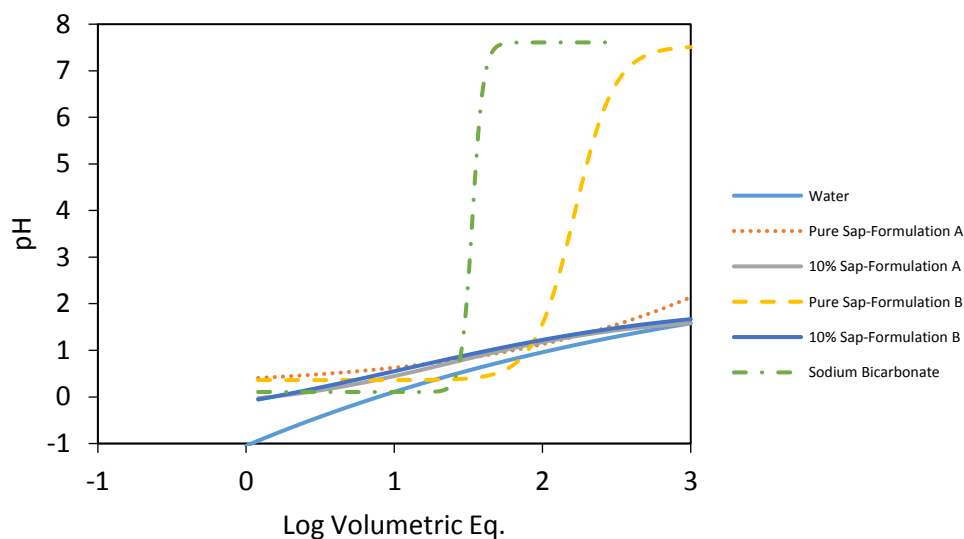
2.9 Pig skin and Sheepskin Volatiles Contents

A 2 x 2 cm sample of pigskin or sheepskin was accurately weighed and was dried in an oven (Abinghurst, UK) at 102 ± 2 °C for 12-16 hours. The samples were weighed and returned to the oven at the same temperature for one hour. The process was repeated until the sample weight remained constant. Volatile matter content was carried out in accordance with BS EN ISO 4684, and it has been assumed that the volatile matter content is equivalent to the moisture content.

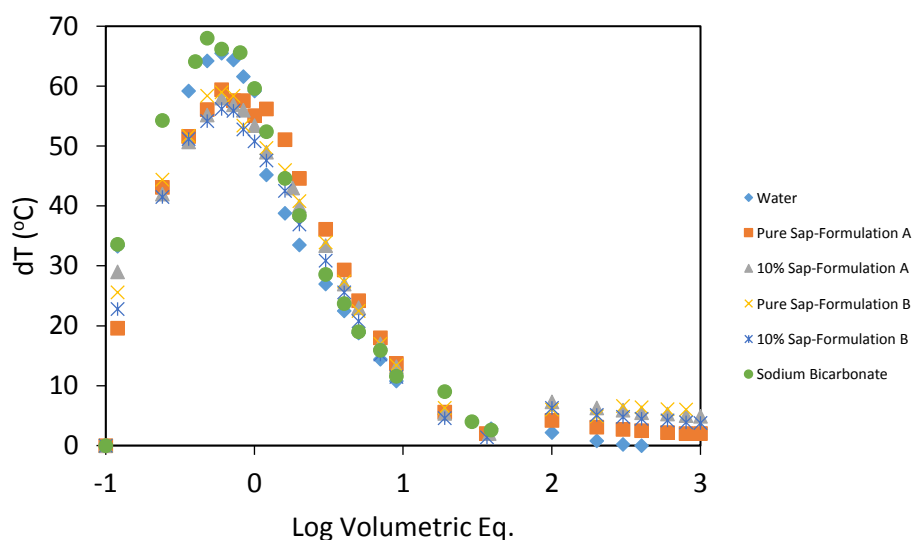
3 Results and Discussion

3.1 pH Titrations: Neutralising Agent into Corrosive

Figures 1 A and B show the pH and temperature profiles respectively of the neutralisation of 95% sulfuric acid. Diluted sap-formulation and water did not neutralise sulfuric acid within addition of 1000 volumetric equivalents of the neutralising agent. sap-formulation B and saturated sodium bicarbonate solutions show neutralising capability requiring 165 and 34 volumetric equivalents respectively.



A



B

Figure 1. pH (A) and temperature (B) profiles of 95% sulfuric acid during neutralisation as a function of volume of neutralising agent. X-axes are equivalent for cross-referencing.

The temperature increase is a result of hydration of the concentrated acid when an aqueous solution or water is added.^{ix} All neutralising systems were found to dissipate the resultant heat of hydration equally with 10 volumetric equivalents required to bring the change in temperature down

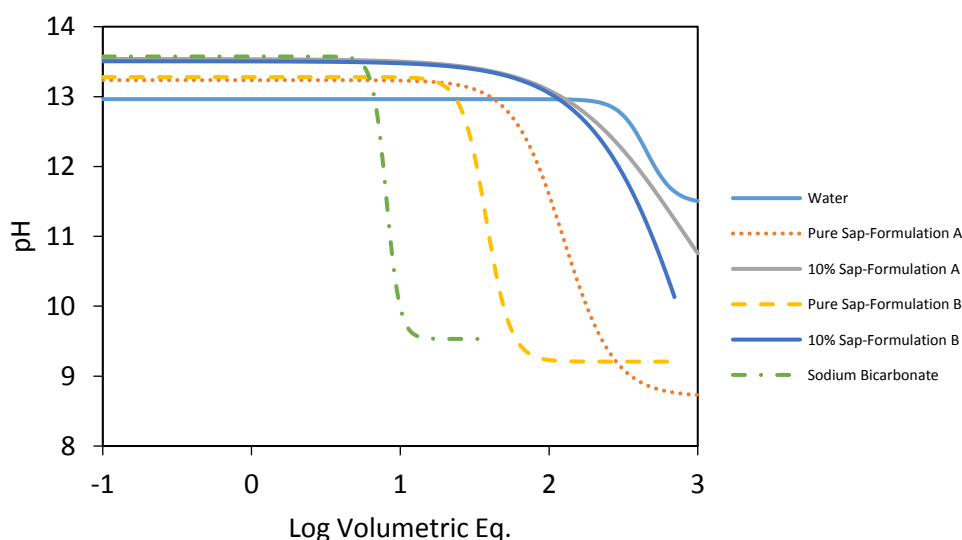
to +10 °C. This temperature change would equate to a real temperature of 35-40 °C, which is below the denaturation temperature of raw skin. Water and the saturated sodium bicarbonate solution reached peak temperatures of 7-9 °C greater than the sap-formulations.

Figure 1 demonstrates sap-formulation B and sodium bicarbonate neutralise strong acids, however, sodium bicarbonate reacts very violently with strong acids with rapid evolution of CO₂ and excess heat of neutralisation (typically 50 to 60 kJ mol⁻¹).^x Sodium bicarbonate solutions also have a limited shelf life, as decomposition into CO₂ and water occurs.^{x,xi} The key benefit of the sap-formulation B is the ability to neutralise strong acids without a violent reaction or significant evolution of neutralisation heat, and a long shelf life. The obvious advantage of sap-formulation B compared to water is the capacity to neutralise a strong acid, whereas, water solely functions by a dilution mechanism.

The pH and temperature profiles of 30% (w/v) sodium hydroxide, as shown in **Figure 2**, illustrate diluted sap-formulations and water did not neutralise within an addition of 1000 volumetric equivalents. The concentrated sap-formulations and saturated sodium bicarbonate show neutralising capability requiring 125 (sap-formulation A), 38 (sap-formulation B), and 8 volumetric equivalents respectively.

All neutralising systems were found to dissipate the resultant heat of hydration equally. The peak temperature changes recorded were 2°C therefore, heat dissipation not a significant concern for sodium hydroxide solutions. The exception to this is the saturated sodium bicarbonate system with a peak change of 6°C, which is likely to be due to the heat of neutralisation, however this change is still regarded as insignificant.

Both sap-formulations neutralise strong alkaline substances, but are not as efficient as a saturated sodium bicarbonate. However, due to the violent reaction between sodium bicarbonate and sulfuric acid, and the requirement for an amphoteric neutralising agent, sap-formulation B has the potential to be a suitable alternative to sodium bicarbonate.^{xii} The advantage of the sap-formulations compared to water is the capacity to neutralise a strong alkaline. Water does not have this capacity and solely functions by a dilution mechanism. Sap-formulation B presents an amphoteric behaviour, which is a fundamental characteristic of any single component treatment system. Although sodium bicarbonate is also amphoteric, the severity of the reaction with strong acids would mean identification of the corrosive during a chemical attack may be required.



A

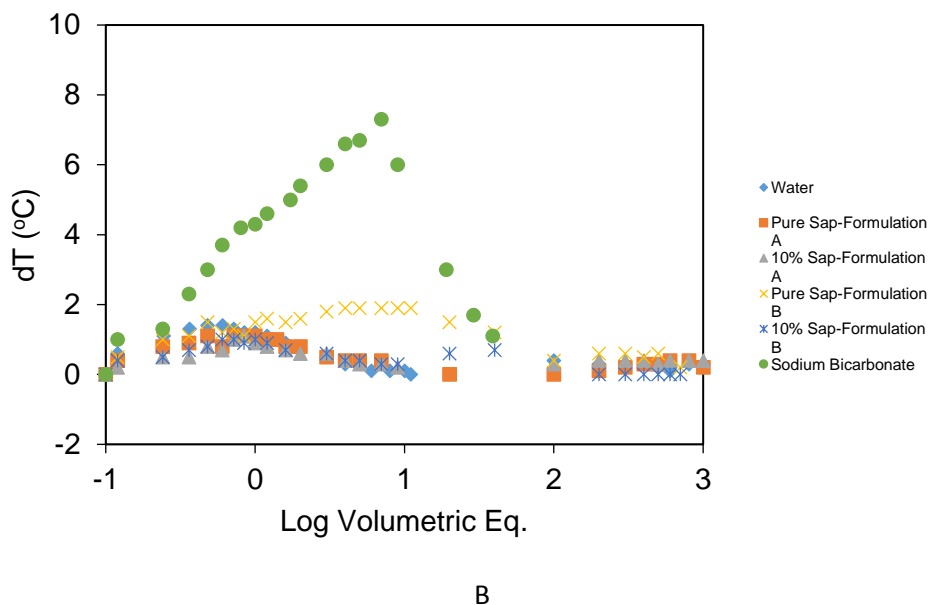


Figure 2. pH (A) and temperature (B) profiles of 30% (w/v) sodium hydroxide during neutralisation as a function of volume of neutralising agent.

3.2 Residual Sodium Hypochlorite Reduction Titrations

As alkaline pH, bleach formulations containing sodium hypochlorite also have an oxidising potential that requires neutralisation to prevent damage to skin in an attack situation.^x Agents capable of neutralising pH may not reduce oxidising agents, therefore, the residual free Cl₂ of pH neutralised sodium hypochlorite was analysed, as shown in **figure 3**. 1000 volumetric equivalents of water were used for the water reference, as no equivalence point was observed.

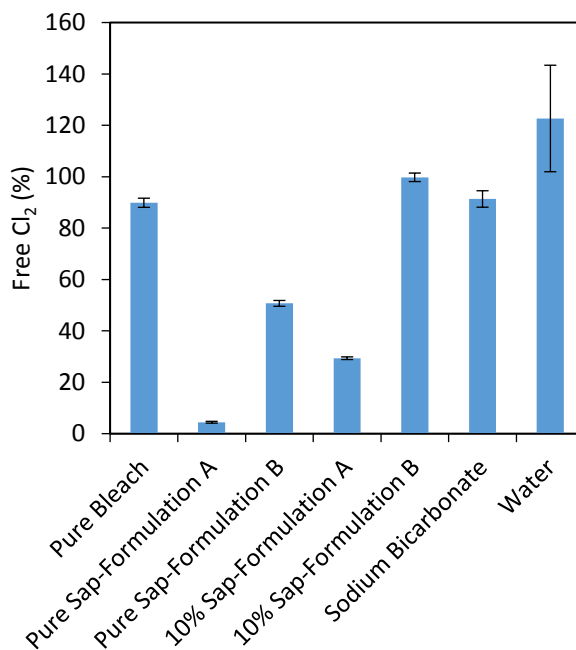


Figure 3. The free Cl₂ concentrations of pH neutralised sodium hypochlorite solutions.

Both sap-formulations can reduce significant quantities of the available free Cl_2 with sap-formulation A reducing 95% of the available free Cl_2 . Diluted sap-formulation B, saturated sodium bicarbonate and water do not have any significant reducing capacity. Sap-formulation B was expected to show more significant reducing properties compared to sap-formulation A, as sap-formulation B was more efficient at neutralising pH, however, this was not observed. The chemical composition of sap-formulation B and sap-formulation A are not publicly known, and it is not possible to explicitly attribute the difference in bleach reducing properties. Water does not reduce sodium hypochlorite and only acts through dilution mechanisms.

3.3 Chemical Attack Trials

Sections of beamhouse-processed sheepskins were exposed to corrosives for different timed periods and neutralised by submersion into a neutralising agent. Scanning electron microscopy (SEM) was used to assess the skin structure and damage. **Figure 4 A** is a micrograph of the complete cross-section of an undamaged control sample showing the presence of: hair follicles blood vessels, sweat glands, and cavities due to the removal of fat within the skin cross-section.^{xiii} **Figure 4 B** shows scanning electron micrographs of a full cross-section of sheepskin exposed to 95% sulfuric acid for 5 seconds prior to neutralisation in a pure sap-formulation A solution showing a complete collapse of the inherent collagen fibre structure. There was no evidence of hair follicles, blood vessels, sweat glands or cavities in the upper (grain) section and no evidence of the inherent fibre structure in the lower (corium) sections. This observation was made for all neutralisers tested after a 5-second exposure to 95% sulfuric acid.

Figure 4 C displays scanning electron micrographs of a cross-section of sheepskin exposed to 95% sulfuric acid for 5 seconds prior to neutralisation in a saturated sodium bicarbonate solution and shows inherent fibre structure in the middle of the cross-section. However significant damage to the upper (grain) and lower (corium) sections was evident. Damage to lower corium has been attributed to some of the 95% sulfuric acid contacting the underside of the sample in error. More significantly it provides evidence the rate of neutralisation between 95% sulfuric acid and saturated sodium bicarbonate is faster than the sap-formulations. **Figure 4 C** also indicates the presence of spherical cavities in the grain and lower corium sections. A postulated cause for this observation is the reaction mechanism between sulfuric acid and sodium bicarbonate which, results in the evolution of gaseous CO_2 .^x It is possible neutralisation is occurring within the skin cross-section and releasing trapped CO_2 , which could expand the surrounding fibre matrix leaving a spherical cavity upon release of the trapped CO_2 . Sodium bicarbonate was the only neutralising agent to demonstrate this behaviour and highlights a potential issue with its application as a pH treatment in an chemical attack scenario. The sap-formulations do foam during the neutralisation of sulfuric acid; however, the reaction is significantly less vigorous compared to sodium bicarbonate and damage like sodium bicarbonate was not observed.

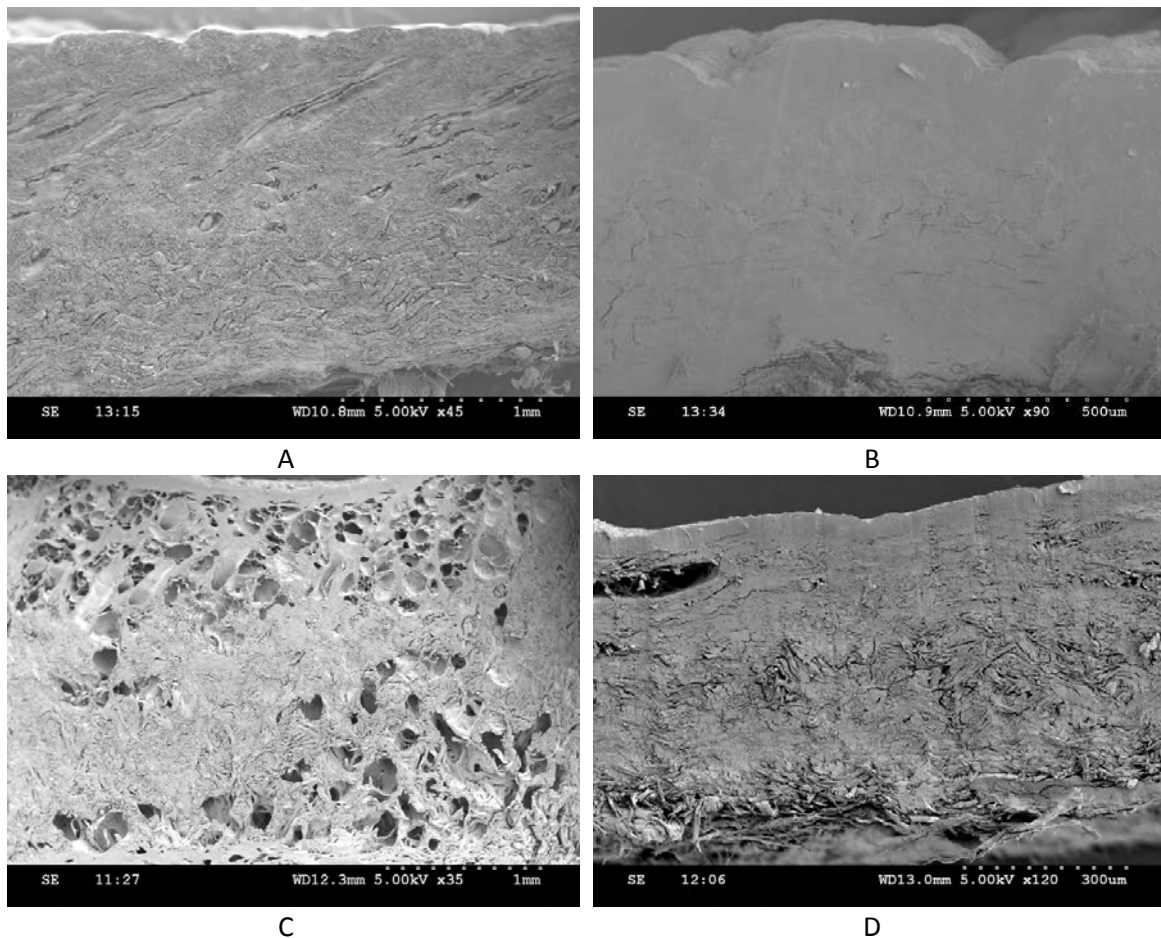


Figure 4. Scanning electron micrographs of neutralised sheepskin cross-sections: Undamaged (A) 5s exposure to 95% sulfuric acid (B) 5s exposure to 95% sulfuric acid neutralised with sodium bicarbonate (C) 1-hour exposure to sodium hypochlorite (D).

The reaction between sodium hypochlorite and collagen is significantly slower compared to 95% sulfuric acid and 30% sodium hydroxide, as significant parts of the inherent fibre structure was still evident after a 1-hour exposure and neutralisation with sap-formulation B, as shown in **figure 4 D**. In all cases, only limited collapse of the fibre structure, was observed within 1 hour of exposure to sodium hypochlorite, thus suggesting dermal and corium layers of the skin cross-section have intrinsic resistance to hydrolytic damage. **Figure 4 D** show the upper most layer has completely collapsed showing no inherent fibre structure. In all cases, the presence of a neutralising agent does not reverse the damage cause to the sub-epidermal layers. Although significant parts of the inherent fibre structure are observable, the sodium hypochlorite solution does cause damage. This damage will be imparted via an alkaline hydrolysis mechanism analogous to sodium hydroxide, but significantly slower due to a lower solution pH. Under the current methodology, damage caused by the oxidative capacity of sodium hypochlorite cannot be differentiated against the damage caused by alkalinity. However, it is suspected not to be significant, as the overall damage observed is limited compared to sulfuric acid. Exposing sheepskin to sodium hydroxide resulted in comparable observations to the effect of 95% sulfuric acid.

Topographical thermographs were taken using a thermal imaging camera to compare an unexposed area of a skin sample with an exposed area. **Figure 5** is an example of an unexposed section of pigskin. **Figure 5 B-D** are thermographs showing the increase in temperature around the burn area during exposure and after neutralisation of 95% sulfuric acid. **Figure 5 B** confirms the

immediacy of the exothermic dehydration reaction, however the observed increase in temperature was not as significant as suggested by the titrations reported earlier. This may be a consequence of the moisture and fat content of the skin. The heat observed upon exposure of the skin to sulfuric acid is a consequence of the reaction between sulfuric acid and the skin's water content. The moisture content of the pigskins used for these trials was 58-60 %, which qualitatively matched the moisture content of living skin tissue. It would be expected, skin samples with a lower moisture content would show a lower maximum temperature, whereas skin samples with a higher moisture content would be expected to have a higher maximum temperature upon exposure to sulfuric acid. The maximum temperature observed during pigskin trials involving sulfuric acid was 40 °C. **Figure 5 C** confirms the heat of dehydration is still evident after 5 minutes of exposure, however the maximum temperature was below 30 °C, thus suggesting heat dissipation to the surroundings occurred and the dehydration reaction has significantly slowed down.

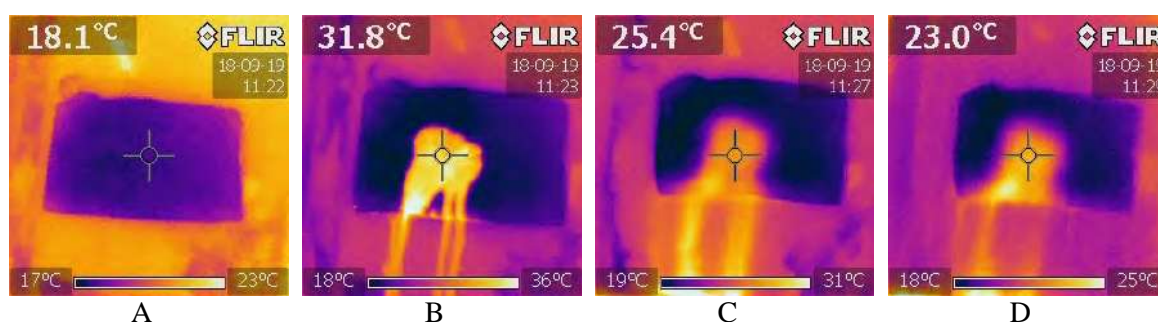


Figure 5. Thermographs of pigskin exposed to 95% sulfuric acid for 5 minutes and neutralised with sap-formulation A: before exposure (A) at exposure (B) after 5 minutes exposure (C) 1 minute after neutralisation (D).

Figure 5 D is a thermal photograph taken 1 minute after neutralisation by aspirating pure sap-formulation A over the burn area. The burn area is still distinguishable, but the maximum temperature observed was less than 25 °C. During neutralisation, there was no observable rise in temperature due to the enthalpy of neutralisation, which suggests the benefits of a neutralising mechanism are not compromised by a temperature increase due to the thermodynamics of neutralisation. This observation is significant, as it demonstrates a fundamental advantage compared to using water as a neutralising agent. The above observations apply to all neutralising agents being tested for 30-second and 5-minute exposure times. All trials involving 30% sodium hydroxide showed no significant change in skin temperature during exposure or neutralisation. This observation also applied to the trials involving sodium hypochlorite, which agree with the titrations mentioned earlier.

In addition to chemical burns caused by the initial exposure, it is possible for further skin damage to occur from long-term incomplete neutralisation; these are referred to as secondary burns. The application of pH treatments in the case of a chemical attack scenario should consider the mitigating properties against secondary burns as well as their effect on the immediate, primary burns. **Figure 6** compares the burn areas of pigskin exposed to 95% sulfuric for 20 seconds and neutralised with: water (A & D), sap-formulation B (B & E) and saturated sodium bicarbonate solution (C & F) 4 hours after neutralisation.

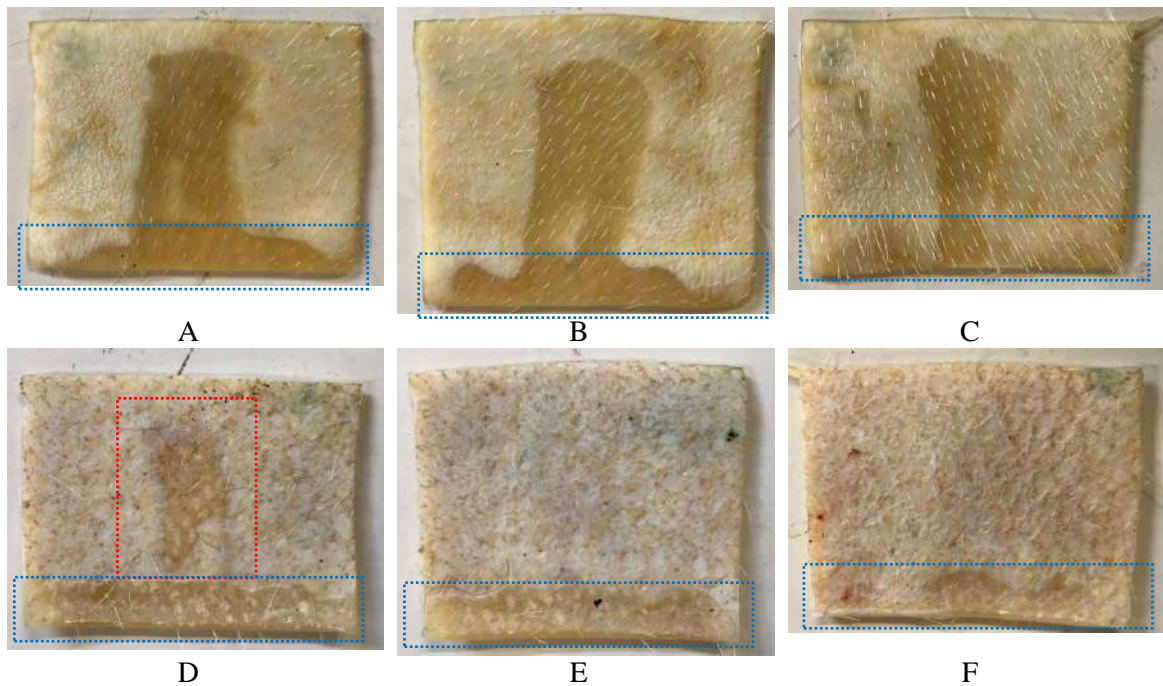


Figure 6. Photographs showing secondary burns 4 hours after neutralisation with a range of agents: Water topside (A), water underside (D), sap-formulation B topside (B), sap-formulation B underside (E), Sodium bicarbonate topside (C), sodium bicarbonate underside (F)

Figure 6 D shows a clear secondary burn has developed on the underside of the skin sample neutralised using water, highlighted in red. In comparison, the skin samples neutralised with sodium bicarbonate and sap-Formulation B did not develop a secondary burn on the underside within the same timeframe. This is a significant observation, as it provides evidence sap-Formulation B and sodium bicarbonate can mitigate against secondary burns. The areas highlighted in blue appear on both sides of all 3 samples and are edge effects caused by sulfuric acid encountering the underside of the sample and burning from underneath: edge effects should not be considered when reviewing secondary burns.

4 Conclusions

The amphoteric formulations, based on natural products, have been shown to be efficacious in treating acid, alkali and oxidising attacks: they do not exhibit the disadvantages of pure water or bicarbonate solution. Therefore, they could be used by first responders, who can safely use the solutions *ad lib.* without fear of causing more harm. Similarly, the products can be carried by the police and fire services; moreover, they can be held by organisations or institutions where there is a perceived risk of attack, such as night clubs.

References

-
1. L. M. Taylor, *Ga. Journal Int'l & Comp. Law.*, 2000, 29, 395–419.
 2. M. Bandyopadhyay, M. R. Khan, in: *Violence against women in Asian societies*, Routledge Curzon, Abingdon, Editors: L. Manderson and L. R. Benjnett, 2003, Chapter: *Loss of face: Violence against women in South Asia*, 61-75
 3. J. Welsh, *It was like burning in hell: A comprehensive exploration of acid attack violence*, Carolina Papers on International Health, Center for Global Initiatives, University of North Carolina, 2006
 4. <http://www.asti.org.uk/a-worldwide-problem.html> [Accessed Oct 2018]
 5. <https://www.sja.org.uk/sja/what-we-do/latest-news/first-aid-for-acid-attacks.aspx> [Accessed Oct 2018]
 6. *Diphoterine® Solution: Captures the Corrosive and Eliminates it*, Prevor, www.prevor.com [Accessed Oct 2018]
 7. K. L. Andrews, A. Mowlavi, S. M. Milner, *Plast. Reconstr. Surg.*, 2003, 111, 1918-21.
 8. <http://www.qualitywatch.org.uk/indicator/ambulance-response-times> [Accessed Oct 2018]
 9. G. Hill, J. Holman, *Chemistry in Context*, ITP, Surrey, 4th Ed., 1995, Ch. 23, 360 -380
 10. E. N. Ramsden, *A-level Chemistry*, Thornes Publisher, Cheltenham, Illustrated edition, 1985, Ch. 18, 352
 11. <http://www.td-bkh.ru/en/products/35> [Accessed Oct 2018]
 12. J. S. Fordtrana, S. G. Morawski, C. A. Santa Ana, F. C. Rector Jr., *Gastroenterology*, 1984, 87, 1014–1021
 13. A. D. Covington, *Tanning Chemistry: The Science of Leather*, RSC Publishing, Cambridge, 1st Ed., 2009, Ch 2, 29 - 71

MONITORING OF BIOGAS PRODUCTION AND REDUCTION OF BIODEGRADABILITY FROM TANNERY SOLID WASTES ANAEROBIC CO-DIGESTION

C. B. Agustini¹, A. C. C. Pena¹, M. Costa², and M. Gutterres¹

1 Laboratory for Leather and Environmental Studies – LACOURO, Chemical Engineering Department, Federal University of Rio Grande do Sul, Brazil.

2 Bacteriology Laboratory, Microbiology Department, Institute of Basic Health Sciences – ICBS, Federal University of Rio Grande do Sul, Brazil.

a)agustini@enq.ufrgs.br

Abstract. The understanding of how chemical, physical and environmental parameters work during anaerobic digestion production and waste treatment is an important step in improving the efficiency and process stability. This study provides the biogas production and the reduction of biodegradability of the treatment of the anaerobic digestion of solid wastes of tanneries. Leather shavings and sludge from wastewater treatment plants substrates were considered in the study. The findings suggest that the biodegradability of the residues practically did not change during the biodegradation tests, since the biodegradable part was transformed into microbial biomass.

1 Introduction

Renewable energy deriving from biomass sources has great potential for growth to meet our future energy demands. Biogas is a very important source of renewable methane. It is produced from anaerobic digestion (AD) of biomass in the absence of oxygen¹. Compared to other renewable energy sources such as wind energy or photovoltaics, biogas is generated independently from weather phenomena and can be stored, making it available on demand. Furthermore, bio-methane is a valuable substitute for limited natural gas using the same, already well established gas distribution system. Additionally, in view of the waste management, biogas is more favorable than composting, since fossil fuels can be substituted and the CO₂ emissions can be reduced².

Raw biogas consists mainly of methane (CH₄, 40-75%), with lower heating value between 15 and 30 MJ/Nm³, and carbon dioxide (CO₂, 15-60%). Trace amounts of other components such as water (H₂O, 5-10%), hydrogen sulfide (H₂S, 0.005-2%), siloxanes (0-0.02%), halogenated hydrocarbons (VOC, <0.6%), ammonia (NH₃, <1%), oxygen (O₂, 0-1%), carbon monoxide (CO, <0.6%) and nitrogen (N₂, 0-2%) can be present and might be inconvenient when not removed³.

AD is the consequence of a series of metabolic interactions among various groups of microorganisms: hydrolytic, acidogenic, acetogenic and methanogenic². The process is carried out in digesters that are maintained at temperatures ranging from 30 to 65°C, where the mesophilic range (30-35 °C) is the most cost-effective. Co-digestion – the digestion of two or more substrates – is a very attractive solution for improving the process, as it results in better distribution of nutrients and trace elements, supporting microbial activity and providing potential for higher methane yield^{4,5}.

The leather making process generates substantial quantities of solid waste (cuts of hides and skins, fats, shavings and trimmings, buffing dust) and sludge from wastewater treatment plants, which in most cases contain chromium, the main chemical used in the tanning process^{6,7}. These residues are usually disposed of in hazardous industrial landfills, which are characterized as places of waste confinement where the residues undergo undesired and uncontrolled biological treatment⁸. As they are organic matrices, they also correspond to an interesting substrate for the implementation of AD⁹. This research attempts to evaluate the feasibility of the AD of tannery solid wastes (mixtures of shavings and sludge) in co-digestion processes. The aim of this work is the assessment of biogas production and

reduction of BOD/COD ratio in the anaerobic co-digestion of leather shavings and sludge from wastewater treatment plants.

2 Materials and Methods

2.1 Biodegradation assays

Biodegradation assays on a scale five times smaller than Agustini¹ were performed in 50 mL vials and biogas production was monitored with the aid of a graduated syringe, as shown in Fig. 1.



Fig 1. Biodegradation test in 50 mL flask with monitoring of biogas production with graduated syringe.

The proportion of biogas components was accessed weekly through a gas chromatograph (GC-2014 Shimadzu) equipped with a ShinCarbon column (ST 100/120 2 m 1 mmID 1/16" OD Silco) and TCD detector. Helium (White Martins 5.0) was used as the carrier gas at a flow rate of 10 ml/min. The injector and detector temperatures were held at 200 and 250 °C, respectively. The oven program was: 40 °C (3 min), ramp at 15 °C/min to 150 °C, and hold for 0.67 min.

2.2 Biochemical oxygen demand - BOD

The microorganisms present in a liquid sample containing biodegradable organic matter consume oxygen for their metabolic activity and produce an equivalent amount of carbon dioxide. If the process occurs in a closed system and the carbon dioxide is absorbed by a strong alkali, a progressive reduction of internal pressure can be observed. The determinations of the biochemical oxygen demand (BOD) were carried out with a pressure sensor (BOD Sensor) from VELP Scientifica equipped with a

system of agitation (System 6). The composition of materials and reagents for the analyzes is shown in Table 1. After assembly, the vials were incubated at 20°C for 5 days. A sample with only water (blank) was always performed to obtain the BOD value relative to the seed only.

Table 1. Composition of solutions for BOD analysis.

Solution	Amount
Sample (dilution 1:20)	
Water	237.5 mL
Sample	12.5 mL
Sample pretreatment	
Sodium sulphate 1.58 g/L - removal of chlorides	1 mL
2-Chloro-6 (trichloromethyl) pyridine 350 g/L - inhibition of nitrifying agents	1 mL
Seed	
Sludge from tanning wastewater treatment plant that used chrome salts and vegetable tannins in the tanning process	2 mL
Nutrient Solution	
FeCl ₃ · 6 H ₂ O 0.25 g/L	0.25 mL
CaCl ₂ 27.5 g/L	0.25 mL
MgSO ₄ · 7 H ₂ O 22.5 g/L	0.25 mL
KH ₂ PO ₄ 8.5 g/L	
Na ₂ HPO ₄ · 7 H ₂ O 33.4 g/L	0.25 mL
K ₂ HPO ₄ 1.7 g/L	

2.3. Chemical Oxygen Demand - COD

Chemical oxygen demand (COD) measurements were performed using the closed-loop colorimetric method (5220 - Standard Methods) where the organic and inorganic materials present in the sample are oxidized by means of the oxidizing agent potassium dichromate (K₂Cr₂O₇). The COD is quantified because it is linearly proportional to the color change of the medium as the chromium is reduced (Cr⁶⁺ to Cr³⁺).

The composition of materials and reagents for the analyzes is shown in Table 2. After addition of the solutions in glass tubes with digestion threads, the tubes were closed and arranged in a heating plate model ECO25 from VELP Scientifica for 2 h at 150°C. After cooling, the absorbance of the sample was read on a spectrophotometer model T80 + UVVis Spectrometer from PG Instruments at 600 nm. A sample with only water (blank) was always performed. The calculation of the COD concentration was performed using the equation of the straight line obtained from the standard calibration curve with potassium biftalate (1000 ppm = theoretical COD of 1000 ppm of O₂).

Table 2. Composition of solutions for COD analysis.

Solution	Amount
Sample (dilution 1:2)	
Water	1 mL
Sample	1 mL
Digestive solution	
Potassium dichromate (K ₂ Cr ₂ O ₇) 10.216 g in 500 mL of distilled water	
Sulfuric acid (P.A.) 167 mL	
Mercury Sulfate II (HgSO ₄) 33.3 g	1.2 mL
Avolume in 1000 ml of distilled water	
Catalytic solution	
Silver Sulfate (Ag ₂ SO ₄) 10.12 g/L in sulfuric acid (P.A.)	2.8 mL

3 Results and discussion

3.1 Biogas production

The daily production and composition of the biogas produced are shown in Fig. 2. The triplicate assays yielded on average 10.18 mL of accumulated biogas/g SVS added (mean value of triplicate \pm standard deviation) with a maximum percentage of methane of $40.9 \pm 0.05\%$ (by volume). This maximum percentage, however, did not remain until the end of the experiment and the oxygen concentration did not remain at zero throughout the experiment, showing that the flask was not able to seal the oxygen inlet and, because it was a small scale experiment, oxygen was able to penetrate the reaction medium and partially inhibited methanogenic activity.

The analysis of the results of the accumulated biogas production is shown in Fig 3. Comparing these results with the that obtained from scale studies of Agustini¹, by statistical inference of variance (F test with a significance level of 0.05), it was found that there was a significant difference ($F_{\text{biogas}} (34.32) > F_{\text{critical}} (5.14)$) between this scale in relation to the others, so that the linear consistency was not maintained, proving that these tests were partially inhibited by the oxygen present. The log phase of these trials (slope of 0.142) was 1.6 times lower than the laboratory scale (slope of 0.2375) and ended approximately 20 days later, maintaining the ratio that the solids concentration influences the DA velocity.

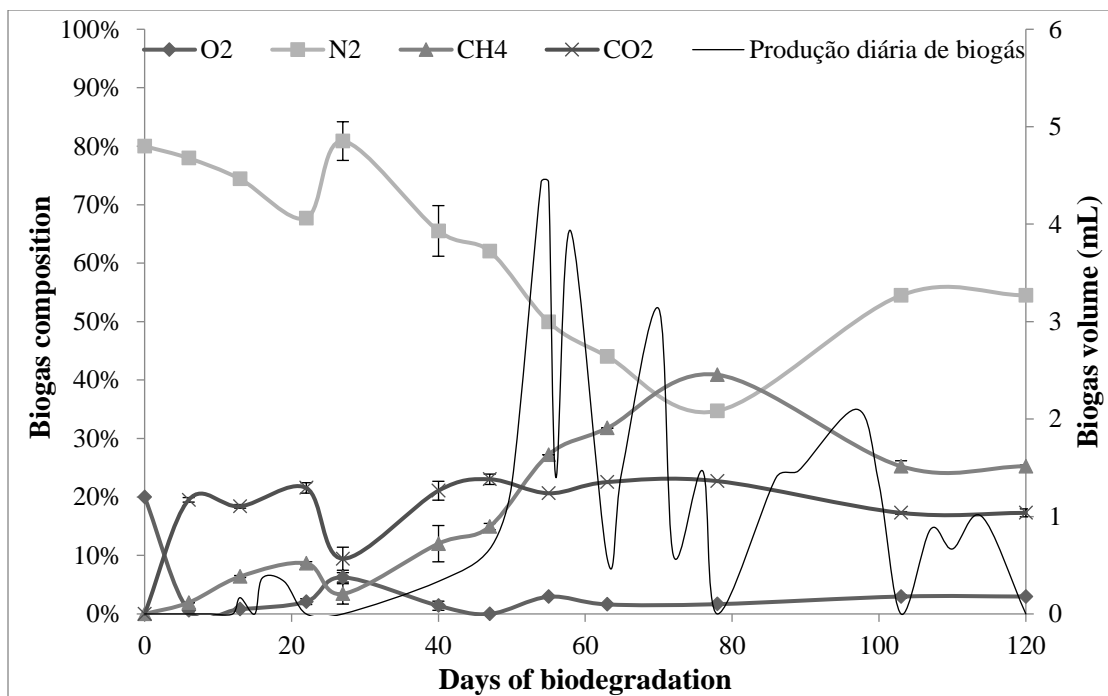


Fig. 2. Average composition and daily production of biogas.

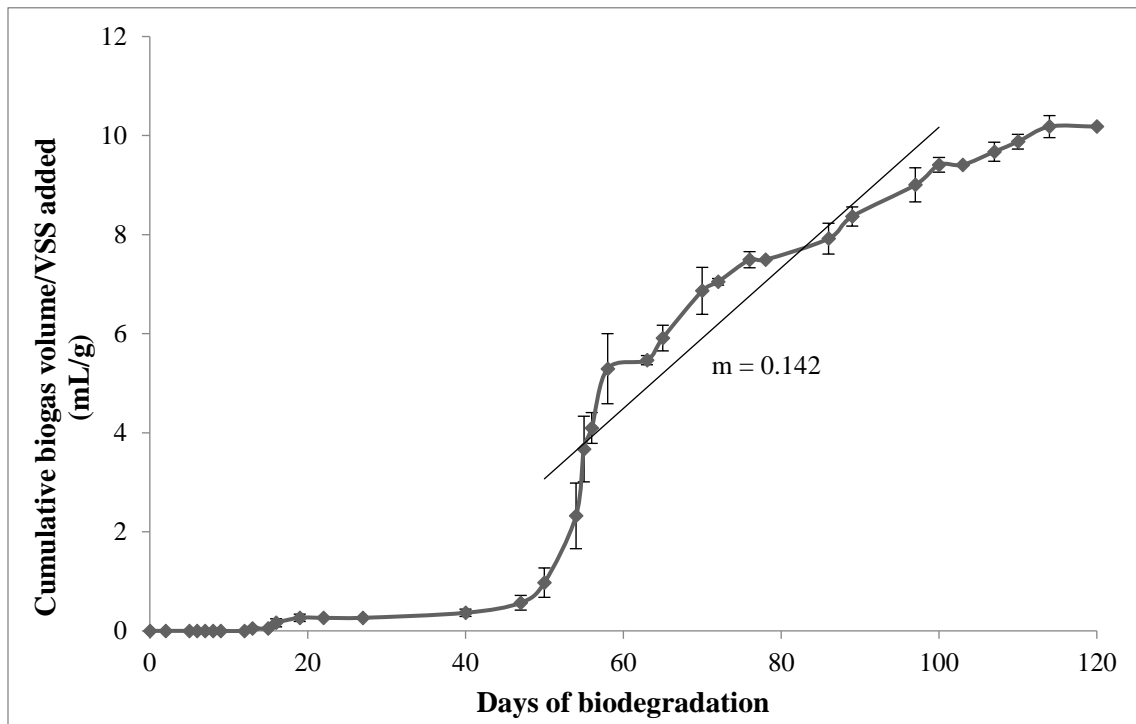


Fig. 3. Cumulative biogas production and indication of slope of the log phase.

The variation of VDS and VSS is shown in Fig 4. VDS, as expected, remained constant. The triplicate assays reduced $13.4 \pm 0.6\%$ SVD (mean value in three replicates \pm standard deviation). VSS, as expected, reduced. The triplicate assays reduced $39.3 \pm 1.0\%$ SVS (mean value in three replicates \pm standard deviation). Despite the large reduction, VSS remained approximately 30% at the end of the experiment, while on the larger scales¹, VSS almost reached zero, confirming that AD was partially inhibited by aerobiosis and that very small reaction volumes are more easily influenced by the presence of oxygen.

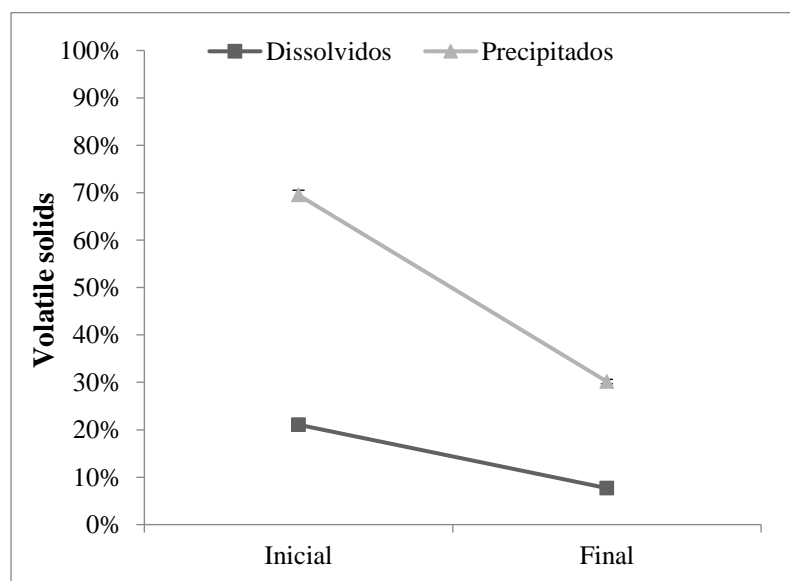


Fig. 4. Volatile solids dissolved and precipitated.

3.2 Reduction of biodegradability – BOD/COD ratio

Table 3 shows the BOD, COD and BOD/COD values before and after DA.

Table 3. Comparison between the BOD and COD parameters.

	Initial	Final
BOD (ppm)	2.040 ± 110	1.090 ± 65
COD (ppm)	2.519 ± 17	1.131 ± 7
BOD/COD	1.23	1.04

Dissolved COD, like BOD, reduced by more than half. A reduction of $1,388 \pm 30$ ppm (55%) COD concentration (mean value of triplicate \pm standard deviation). The analysis of the COD reduction results obtained, using statistical inference of variance (F test with significance level of 0.05), did not show significant differences ($F_{COD} (0.46) < F_{critical} (18.51)$). The COD is related to many parameters of the biodegradable and recalcitrant organic matter, so that no difference between the COD reductions was detected.

The BOD/COD ratio is an indicator of biodegradability and tends to decrease throughout the AD process. For tannery residues, typical BOD/COD values range from 0.6 to 1.7¹⁰. The initial BOD/COD value obtained of 1.23 is within the range expected for tannery waste. A reduction of 0.20 ± 0.01 (16%) BOD/COD ratio (mean value of triplicate \pm standard deviation) was observed. The analysis of the results of the reduction of the BOD/COD ratio obtained, using statistical inference of variance (F test with a significance level of 0.05), showed no significant differences ($F_{COD/BOD} (7.70) < F_{critical} (18.51)$). The small reduction of the BOD/COD ratio for the high amount of biogas that left the system may be due to the formation of microbial biomass that kept the BOD values close to that of COD.

4. Conclusions

The findings suggest that small production scales can be impaired by the possible entry of O₂ to affect the process, due to the oxygen penetration power being sufficient, in small scale means, to reach the anaerobic zones and, thus, inhibit the methanogenic activity. The biodegradability of the residues practically did not change during the biodegradation tests, since the biodegradable part was transformed into microbial biomass.

References

- ⁸AGUSTINI, C. B. et al. Biodegradation of leather solid waste and manipulation of methanogens and chromium-resistant microorganisms. *Journal of The American Leather Chemists Association*, v. 112, p. 7–14, 2017.
- ¹AGUSTINI, et al. Biogas production from tannery solid wastes - Scale-up and cost saving analysis. *JOURNAL OF CLEANER PRODUCTION*, v. 187, p. 158-164, 2018.
- ⁹FIORE, S. et al. Scale-up evaluation of the anaerobic digestion of food-processing industrial wastes. *Renewable Energy*, v. 96, p. 949–959, 2016.
- ⁴FOTIDIS, I. A.; LARANJEIRO, T. F. V. C.; ANGELIDAKI, I. Alternative co-digestion scenarios for efficient fixed-dome reactor biomethanation processes. *Journal of Cleaner Production*, v. 127, p. 610–617, 2015.
- ²GALLERT, C.; HENNING, A.; WINTER, J. Scale-up of anaerobic digestion of the biowaste fraction from domestic wastes. *Water Research*, v. 37, p. 1433–1441, 2003.
- ⁶GUTTERRES, M. et al. Water reuse in tannery beamhouse process. *Journal of Cleaner Production*, v. 18, n. 15, p. 1543–1550, 2010.
- OLADIPO, A. A. et al. *Journal of Water Process Engineering Bio-derived MgO nanopowders for BOD and COD*

- reduction from tannery wastewater. Journal of Water Process Engineering, v. 16, p. 142–148, 2017.*
8. ³POESCHL, M.; WARD, S.; OWENDE, P. *Environmental impacts of biogas deployment - Part I: Life Cycle Inventory for evaluation of production process emissions to air. Journal of Cleaner Production, v. 24, p. 168–183, 2012.*
 9. ⁷PRIEBE, G. P. S. et al. *Anaerobic digestion of chrome-tanned leather waste for biogas production. Journal of Cleaner Production, v. 129, p. 410–416, 2016.*
 10. ⁵ZIGANSHIN, A. M. et al. *Microbial community structure and dynamics during anaerobic digestion of various agricultural waste materials. Applied Microbiology and Biotechnology, v. 97, p. 5161–5174, 2013.*

MICROENCAPSULATION OF CLOVE ESSENTIAL OIL WITH GELATIN AND ALGINATE

V. V. Kopp¹, C. B. Agustini¹, J. H. Z. dos Santos² and M. Gutterres¹

1 Laboratory for Leather and Environmental Studies – LACOURO

Post-Graduation Program in Chemical Engineering, Federal University of Rio Grande do Sul, Brazil

a)Corresponding author: koppvictoria1@gmail.com

b)mariliz@enq.ufrgs.br

Abstract. Clove essential oil has antioxidant and antimicrobial properties. To prevent chemical changes the oil is microencapsulated. The method used was emulsion extrusion, using a cross-linking agent, calcium chloride. The encapsulated materials can be used in leather industry. The wall material is build of alternative, inexpensive and natural polymeric, like gelatin and sodium alginate. Two microcapsules were developed: E130 and E131, with concentrations of 1% clove essential oil, 3% alginate and 0 - 1% gelatin, respectively. The microcapsules were characterized throughout morphology, encapsulation efficiency (EE), functional groups present and thermogravimetric analysis. Clove essential oil showed great antioxidant capacity of 85.37%, even with low content of total phenolic compounds (6.35 EAG mg g⁻¹). FTIR confirmed the incorporation of clove oil into the microcapsules and the chemical stability of the clove oil after encapsulation. The EE was 63% and 61% for E130 and E131, respectively. Furthermore, FTIR and thermogravimetric analysis indicated an interaction between the wall material and clove oil. Encapsulation process of clove essential oil by emulsion extrusion is an efficient technique to maintain the oil in the capsule.

1 Introduction

Essential oils have received commercial interest primarily because of their potential antimicrobial, antifungal and antioxidant properties and for being of natural origin, which generally means lower risk to the environment and human health¹. But they are instable compounds and can suffer oxidation or volatilization or react with other formulation components². Clove essential oil (CEO) not only contains many kinds of biological active substances but also has highly effective and comprehensive antibacterial functions, based on its constituents of phenolic compounds. Its essential oil contains mainly phenylpropanoids, such as eugenol, β -caryophyllene, and α -humulene organic compounds³. The high levels of eugenol contained in CEO are responsible for its strong biological and antimicrobial activities against a wide range of pathogenic microorganisms^{4,5}. The CEO can replace some biocides, conventionally used in the leather industry, that are toxic and generate environmental risks. These biocides are used to prevent the development and growth of fungi in pickled hides, tanned leathers (from chromium or vegetable tannin) and finished products during their storage and shipping⁶.

To prevent chemical changes in the essential oil, it is microencapsulated. The encapsulated materials are utilized in pharmaceutical, food, agricultural, cosmetic, textile, paper, paint, and printing industries, among others⁷. Microcapsules comprise an active agent surrounded by a natural or synthetic polymeric membrane providing isolation, entrapment, protection or controlled release. This controlled release allows to prolong its useful life, avoiding its rapid evaporation and improving its performance⁸.

Emulsion extrusion is considered as the most common approach of microencapsulation and might be achieved by emulsifying or dispersing the hydrophobic components in an aqueous solution where gelation occur (ionotropic or thermal)⁹. By using emulsion extrusion for microencapsulation, abroad selection of polymer coatings ("shell") and methods of deposition are available, which are

easily adaptable to large-scale production¹⁰. Polysaccharides and proteins are the most widely used wall materials for microencapsulation in industry.

Sodium alginate is a linear copolymer composed of α -L-guluronic and β -D-mannuronic acids, synthesized by brown algae found in coastal sea regions. This polymer has been used in the encapsulation of essential oils¹¹. Gelatin is a biodegradable biomaterial¹² that can be extracted through the hydrolysis of hide and chromium tanned leather wastes¹³. Using this materials as wall for the microcapsule, is produced a new material from renewable sources, replacing synthetic polymers^{14,15}.

Microcapsules with natural antibacterial substances can be use in smart leather, which have additional functionalities. Smart scented leathers using orange and lavender oil encapsulates were developed¹⁶ and a functional antimicrobial leather using polyurethane-microencapsulated clove oil was investigated¹⁷, which can lead to value addition to leather.

The performance of antimicrobial agents against different fungus was evaluated⁶. For chrome leather, the antimicrobial agents 2-thiocyanomethylthio benzothiazole (TCMTB) and Aqueous dispersion of 2-n-octyl-4-isothiazolin-3-one + methyl-Nbenzimidazol-2-ylcarbamate (OIT+BMC/water) showed antifungal capacity against different fungi tested applied in concentration of 0.2% (weight leather base). However, for vegetable tanned leather⁶, the results revealed a low antifungal capacity of selected microbicides when applied at an offer of 0.2% (mass hide base) fungicides. Treatment with OIT+BMC/water (0.75%) showed satisfactory fungal protection against different fungi tested and proved to be the most suitable for the preservation of vegetable tanned leather. Thus, the development of ecological and effectively antimicrobial bactericides is essential.

The aim of this study was to develop essential oil microcapsules from sodium alginate and gelatin. The microcapsules will be characterized as morphology, encapsulation efficiency (%), functional groups present and thermogravimetric analysis.

2 Materials and Methods

2.1 Materials

Sodium alginate (Dinâmica, Brazil), Clove essential oil (Delaware, Brazil), Calcium chloride (Dinâmica, Brazil), were purchased and used as received. Gelatin type B (bloom 240), was donated from Gelita (Brazil). All other reagents were analytical grade and used without further purification.

2.2 Methods

2.2.1 Microencapsulation process

Microencapsulation of oil was performed using emulsion extrusion technique¹⁰. For the microcapsule with sodium alginate wall only, sodium alginate was dissolved in distilled water to produce alginate solutions with concentration of 3 w/v%. Afterwards, sodium alginate suspension and clove oil (1 w/v%) were homogenized into a 200 mL beaker with stirring at a speed of 300 rpm for 15 min by a magnetic stirrer. The oil was gradually added to the alginate suspension mixing until the desired oil loading was obtained. The alginate-oil emulsion was then dropped into a collecting water solution containing calcium chloride solution 1 w/v% using a syringe. The resulting microcapsules were allowed to harden in the CaCl₂ solution for 5 min. The oil-loaded alginate capsules were rinsed with distilled water and filtered. The microcapsule with sodium alginate and gelatin wall, the difference was the addition of the solution gelatin 1 w/v% in the water solution containing calcium chloride solution 1 w/v% (Table 1).

Table 1. Composition of the wall materials.

Assay	Wall material (g.100g ⁻¹ solution)	
	Alginate	Gelatin
E130	3	0
E131	3	1

Core material - clove essential oil: 1 g.100g⁻¹ solution

2.2.2 Total phenolic content of essential oil

The total phenolic content of clove essential oil was determined by the Folin-Ciocalteu method¹⁸. Thus, 0.1 g of CEO was diluted in 10 mL of methanol and allowed to stand for 24 h. After that the sample was centrifuged and 500 µL of the supernatant was mixed with 4 mL of distilled water and 250 µL of Folin-Ciocalteu solution 10% (v/v) and react for 3 min. After, 500 µL of 1 M Sodium Carbonate solution was added. The reaction was stored in the dark for 1 h and was analysed at 725 nm in spectrophotometer T80+ UV/Vis (PG Instruments) using as a blank water and reagents only. Results were expressed as mg of gallic acid equivalents per gram of sample (GAE mg g⁻¹) and was determined in triplicate.

2.2.3 Antioxidant activity of essential oil

The antioxidant activity was determined using the scavenging of DPPH (2,2-diphenyl-1-picrylhydrazyl) radical, a spectrophotometric methodology, according to the proposed method¹⁹. Antioxidant activity was expressed as percentage of DPPH scavenging and calculated using the following equation (1):

$$AA (\%) = \frac{Ac-As}{Ac} * 100 \quad (1)$$

where Ac is the absorbance of the control which contains control reaction (containing DPPH solution and methanol except the CEO), and As is the absorbance in the presence of CEO.

2.2.4 Encapsulation efficiency

The efficiency of encapsulation (EE) was determined by the presence of phenolic compounds in CEO, using the method proposed¹⁹. The amount of CEO encapsulated into the microbeads was quantified by extracting the loaded oil from 0.1 g of capsules via their dissolution with 10 mL of methanol and left for 24 h. After this period, the solution was centrifuged at 4000 rpm, for 15 min at room temperature, and 0.5 mL of the supernatant was collected for the analysis. Total phenolic content of collected fractions were evaluated as described in item 2.2.3. The EE was calculated according Equation 2, giving the percentage of phenolic compounds:

$$EE (\%) = \frac{\text{Phenolic content of oil} - \text{Phenolic content of capsules}}{\text{Phenolic content of oil}} * 100 \quad (2)$$

2.2.5 Characterization of the microcapsules

Fourier Transform Infrared spectroscopy of the microcapsules were recorded in the range 650-4000 cm⁻¹ with 32 scans and 4 cm⁻¹ of resolution on a Frontier ATR-FTIR spectrophotometer (Perkin Elmer, USA). Thermal analyses were carried out under N₂ atmosphere. Both the thermogravimetry (TG) and differential scanning calorimetry (DSC) (DSC 6000, Perkin Elmer) were used to investigate the thermostability of CEO and microcapsules. The temperature ranges were 40-800°C and 0-300°C, respectively, and the heating rate was 10°C min⁻¹. The morphology of microparticles was observed using stereo microscope (Model SZX16, Olympus) attached to a digital camera. Microparticles were placed onto a glass slide, observed under microscope and captured.

3 Results and Discussion

3.1 Characterization of clove essential oil

The total phenolic compounds content in the essential oil and its antioxidant capacity is presented in Table 2. Total phenolic compounds found is lower than 9.07 EAG mg g⁻¹¹⁹ but was higher than 2.41 mg EAG g⁻¹, that showed a small concentration of phenolics²⁰. These different values suggest that the concentration of phenolic compounds is dependent on the oil extraction method and characteristics of the sample. Antioxidant capacity of CEO at the concentration of 488 µg mL⁻¹ was high. For instance, the literature report 45.27% of scavenging of DPPH at the concentration level of 500 µg mL⁻¹²¹, while 94.86% was reported for the scavenging of DPPH at 484.7 µg mL⁻¹¹⁹. The high DPPH scavenging activity observed for the CEO can be explained by a synergistic effect between phenolic compounds, even at low concentrations¹⁹.

Table 2. Total phenolic compounds and antioxidant capacity (%) of CEO.

Assay	Total phenolic (EAG mg g ⁻¹)	Antioxidant capacity (%)
CEO	6.35±0.5	85.37

3.2 Characterization of microcapsules

The microcapsules E130 and E131 (Fig. 1a and 1b) were regular and spherical and measured 2 mm.

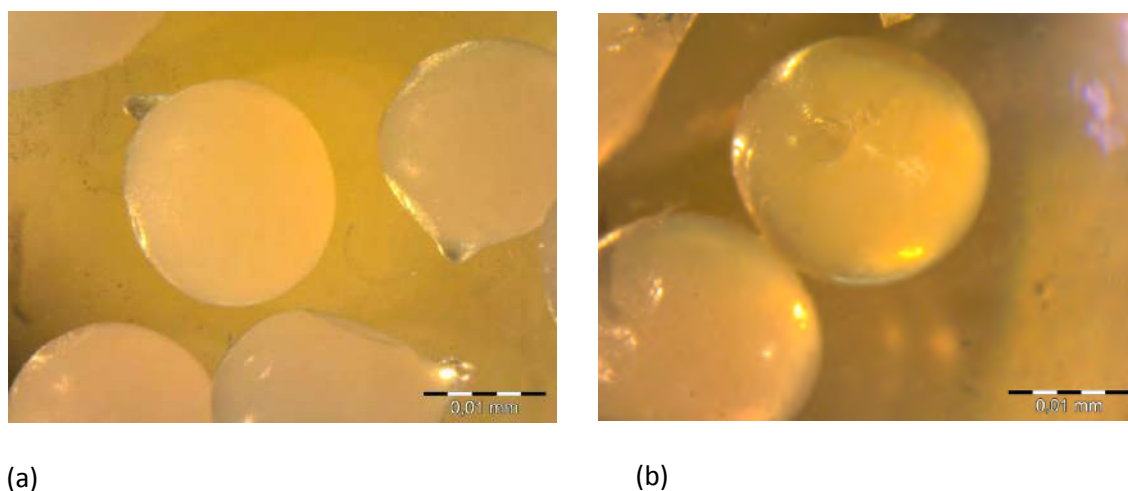


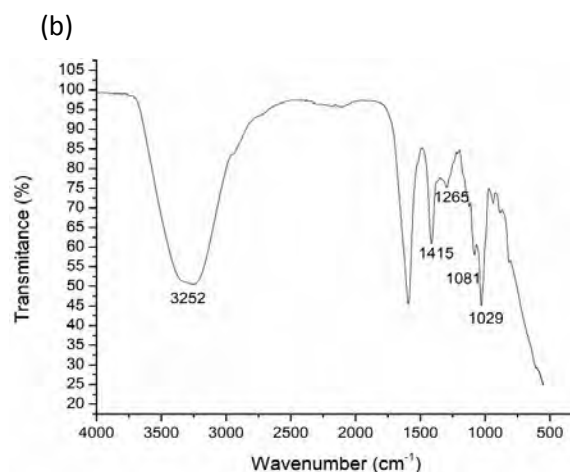
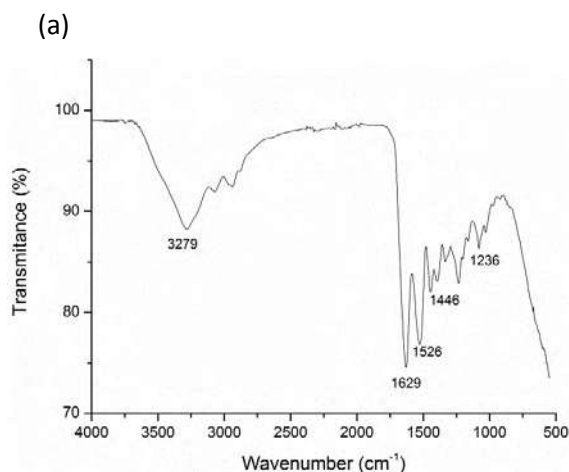
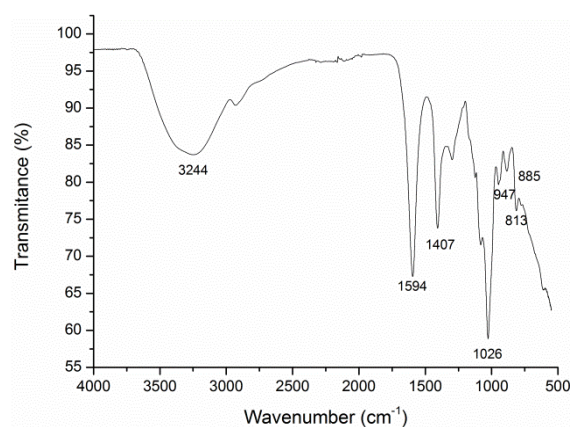
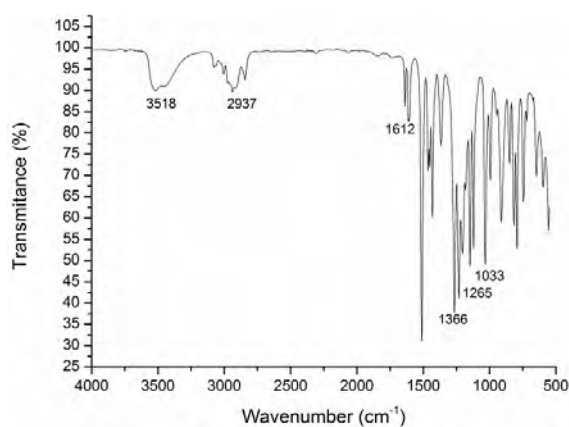
Fig. 1. Microscopy images (x40 magnification) of microcapsules: (a) E130; (b) E131.

The encapsulation efficiency (EE) of microcapsules is presented in Table 3. Microcapsule without gelatin shows better EE. EE results reported in the literature are dependent of the wall material, emulsifier and encapsulated oil. Clove essential oil was encapsulated with alginate (2%) and obtained EE of 90.02%¹⁹, but when encapsulated with soybean phospholipids EE was 57.9% to 84.6%⁵.

Table 3 – Encapsulation efficiency of microcapsules

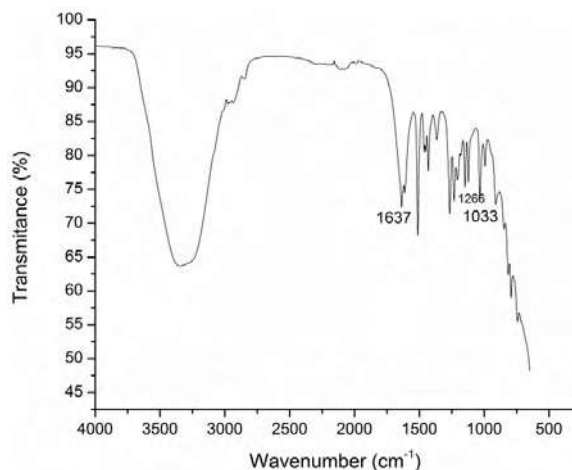
Assay	EE (%)
E130	63.09
E131	61.92

The Fourier transform-infrared (FTIR) was used to confirm the presence of CEO, sodium alginate and gelatin in the microcapsules. FTIR spectra of CEO show (Fig. 1a) peaks at 3518 cm^{-1} of stretching vibrations O-H, at 2937 , 1612 , 1366 cm^{-1} attributed to C-H, C=C, O-H, respectively and some special peaks at 1265 cm^{-1} (C-OH axial)²² and at 1033 cm^{-1} (C-O-C axial symmetric)¹⁷. The FTIR spectrum of gelatin is shown in Fig. 1b. The band appearing at 3279 cm^{-1} represented the N-H stretching vibrations of amide groups designated as amide A. The carbonyl C=O stretching vibrations with contributions from in-phase bending of the N-H bond and stretching of the C-N bond occurred at 1629 cm^{-1} and are referred as the amide I band. The amide II band appeared at 1526 and 1446 cm^{-1} . The small peak representing the amide III band was also found at 1236 cm^{-1} ²³. The FTIR spectrum of sodium alginate (Fig. 1c) showed characteristic absorption bands at 3244 , 1594 , 1407 and 1026 cm^{-1} that corresponded to stretching vibration of O-H, COO- (asymmetric), COO- (symmetric) and C-O-C. These similar findings were reported in the literature²⁴. Besides, peaks at 947 , 885 and 813 cm^{-1} are attributed to the C-H vibration of the pyranose (ring of the alginate) group²⁵. Microcapsule E130 (Fig. 1d) presented peak at 3252 cm^{-1} (O-H vibration) due to the presence of the great amount of water. The peak at 1415 cm^{-1} is attributed to the asymmetrical stretching of COO-. The bands at 1081 and 1029 cm^{-1} correspond to guluronic units of C-H stretching present in sodium alginate. The peak at 947 cm^{-1} corresponds to the C-H group of the ring pyranose. The CEO is present at 1265 cm^{-1} (C-OH axial). In case of microcapsule E131, the spectra (Fig. 1e) showed peaks 1266 and 1033 cm^{-1} , the same peaks present in CEO, showing that the encapsulation did not alter the structure of the oil's main assets. In addition, the peak at 1637 cm^{-1} is characteristic of the CONH₂ group and indicate the interaction between alginate and gelatin. The results indicate the successful incorporation of clove oil into the microcapsules and the chemical stability of the clove oil after encapsulation.



(c)

(d)



(e)

Fig. 1. FTIR spectra of (a) CEO, (b) sodium alginate, (c) gelatin, (d) E130 and (e) E131.

Thermal analysis (TGA and DSC curves) of E130 and E030 are given in Figure 3. TGA curve (Fig. 3a) showed the weight loss. This is related to moisture, corresponding to water hydrogen bounded to the saccharide structure of polymeric system²⁶. The end of the thermal event occurs at a temperature above 100°C and this event may be associated with a bound water molecule. According to Lopes *et al.*²⁵, sodium alginate has two types of water in its structure, a portion of unbound water related to moisture and another portion of water bound to the polymer. The curve indicates that up to 100°C the samples contained a low relative tenor of organic matter, and starting from this temperature the samples degraded quickly during the heating up to 800°C. The presence of gelatin in the composition of microcapsules didn't improve the chemical stability of the microcapsules. DSC curve (Fig. 3b) indicates a thermal event between 30 and 100°C, characteristically endothermic. Thermal data of capsules analyzed by TGA was consistent with their DSC behavior. Initially, by increasing temperature, the samples lost weight until about 160°C. Accordingly, DSC measurements show the first endothermic peak below 150°C (Fig. 3a). Endothermic peak of sodium alginate is presumably due to the cleavage of the carboxylate-calcium bond, formed in the reaction between sodium alginate and calcium chloride during encapsulation process¹⁹. Thus, an appropriate microencapsulation assures that the CEO remain viable throughout storage.

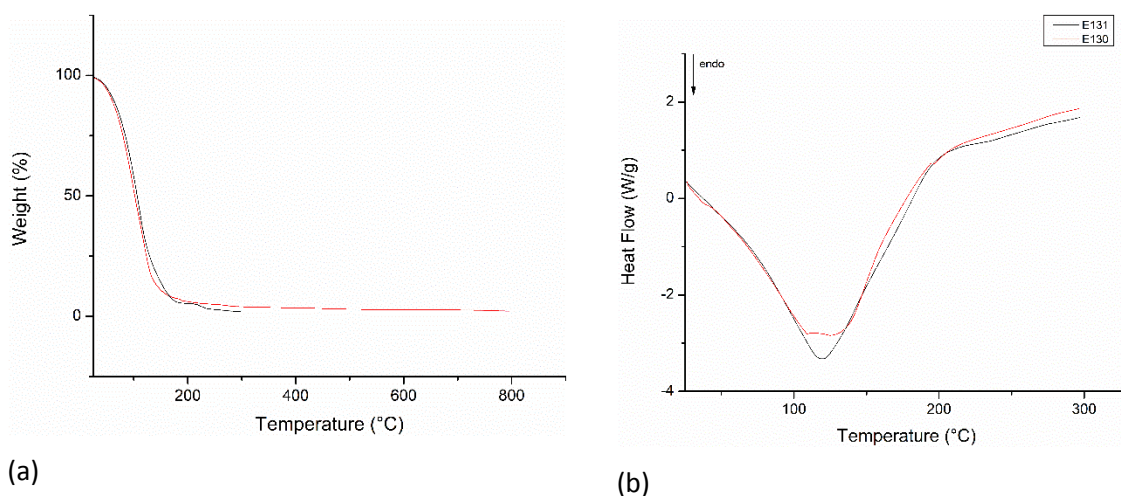


Fig. 2. TGA (a) and DSC (b) curves of E130 and E131.

4 Conclusion

Clove essential oil has a great antioxidant capacity of 85.37%, even with low content of total phenolic compounds (6.35 EAG mg g⁻¹). Sodium alginate and gelatin showed great efficiency of clove essential oil encapsulation, 63.09% for E130 and 61.92% for E131. FTIR confirmed the incorporation of clove oil into the microcapsules and the chemical stability of the clove oil after encapsulation. Furthermore, FTIR and thermogravimetric analysis indicated an interaction between the wall material and clove oil. Encapsulation process of clove essential oil can be considered as inexpensive and efficient technique to maintain the oil in the capsule.

References

1. de Oliveira, M. S.; da Costa, W. A.; Pereira, D. S.; Botelho, J. R. S.; de Alencar Menezes, T. O.; de Aguiar Andrade, E. H.; da Silva, S. H. M.; da Silva Sousa Filho, A. P.; de Carvalho, R. N. Chemical Composition and Phytotoxic Activity of Clove (*Syzygium Aromaticum*) Essential Oil Obtained with Supercritical CO₂. *J. Supercrit. Fluids* **2016**, *118*, 185–193. <https://doi.org/10.1016/j.supflu.2016.08.010>.
2. Leimann, F. V.; Gonçalves, O. H.; Machado, R. A. F.; Bolzan, A. Antimicrobial Activity of Microencapsulated Lemongrass Essential Oil and the Effect of Experimental Parameters on Microcapsules Size and Morphology. *Mater. Sci. Eng. C* **2009**, *29* (2), 430–436. <https://doi.org/10.1016/j.msec.2008.08.025>.
3. Gulçin, I.; Elmastaş, M.; Aboul-Enein, H. Y. Antioxidant Activity of Clove Oil - A Powerful Antioxidant Source. *Arab. J. Chem.* **2012**, *5* (4), 489–499. <https://doi.org/10.1016/j.arabjc.2010.09.016>.
4. Adel, A. M.; Ibrahim, A. A.; El-Shafei, A. M.; Al-Shemy, M. T. Inclusion Complex of Clove Oil with Chitosan/β-Cyclodextrin Citrate/Oxidized Nanocellulose Biocomposite for Active Food Packaging. *Food Packag. Shelf Life* **2019**, *20* (May 2018), 100307. <https://doi.org/10.1016/j.fpsl.2019.100307>.
5. Carine Sebaaly, Alia Jraij, Hatem Fessi, Catherine Charcosset, H. G.-G. Preparation and Characterization of Clove Essential Oil-Loaded Liposomes. *Food Chem.* **2015**, *178*, 52–62. <https://doi.org/10.1016/j.foodchem.2015.01.067>.
6. Fontoura, J. T.; Ody, D.; Gutterres, M.; Alegre, P. Performance of Microbicides for the Preservation of Vegetable Tanned Leather. *Am. Leather Chem.* **2016**, *111*, 259–266.
7. Ghayempour, S.; Mortazavi, S. M. Preparation and Investigation of Sodium Alginate Nanocapsules by Different Microemulsification Devices. *J. Appl. Polym. Sci.* **2015**, *132* (17), 1–8. <https://doi.org/10.1002/app.41904>.
8. Martins, I. M.; Barreiro, M. F.; Coelho, M.; Rodrigues, A. E. Microencapsulation of Essential Oils with Biodegradable Polymeric Carriers for Cosmetic Applications. *Chem. Eng. J.* **2014**, *245*, 191–200. <https://doi.org/10.1016/j.cej.2014.02.024>.
9. Yuliani, S.; Torley, P. J.; D'Arcy, B.; Nicholson, T.; Bhandari, B. Extrusion of Mixtures of Starch and D-Limonene Encapsulated with β-Cyclodextrin: Flavour Retention and Physical Properties. *Food Res. Int.* **2006**, *39* (3), 318–331. <https://doi.org/10.1016/j.foodres.2005.08.005>.
10. Soliman, E. A.; El-Moghazy, a. Y.; El-Din, M. S. M.; Massoud, M. A. Microencapsulation of Essential Oils within Alginate. *J. Encapsulation Adsorpt. Sci.* **2013**, *03* (01), 48–55. <https://doi.org/10.4236/jeas.2013.31006>.
11. Natrajan, D.; Srinivasan, S.; Sundar, K.; Ravindran, A. Formulation of Essential Oil-Loaded Chitosan-Alginate Nanocapsules. *J. Food Drug Anal.* **2015**, *23* (3), 560–568. <https://doi.org/10.1016/j.jfda.2015.01.001>.
12. Hayashi, K.; Tabata, Y. Preparation of Stem Cell Aggregates with Gelatin Microspheres to Enhance Biological Functions. *Acta Biomater.* **2011**, *7* (7), 2797–2803. <https://doi.org/10.1016/j.actbio.2011.04.013>.
13. De Matos, E. F.; Scopel, B. S.; Dettmer, A. Citronella Essential Oil Microencapsulation by Complex Coacervation with Leather Waste Gelatin and Sodium Alginate. *J. Environ. Chem. Eng.* **2018**, *6* (2), 1989–1994. <https://doi.org/10.1016/j.jece.2018.03.002>.
14. Vieira, E. F. S.; Cestari, A. R.; Airoidi, C.; Loh, W. Polysaccharide-Based Hydrogels : Preparation , Characterization , and Drug Interaction Behaviour. **2008**, 1195–1199.
15. Salem, D. M. S. A.; Sallam, M. A. E.; Youssef, T. N. M. A. Synthesis of Compounds Having Antimicrobial Activity from Alginate. *Bioorg. Chem.* **2019**, *87* (March), 103–111. <https://doi.org/10.1016/J.BIOORG.2019.03.013>.
16. Velmurugan, P.; Ganeshan, V.; Nishter, N. F.; Jonnalagadda, R. R. Encapsulation of Orange and Lavender Essential Oils in Chitosan Nanospherical Particles and Its Application in Leather for Aroma Enrichment. *Surfaces and Interfaces* **2017**, *9*, 124–132. <https://doi.org/10.1016/j.surfin.2017.08.009>.
17. Zhiyuan, W.; Haibin, G. U.; Wuyong, C. Polyurethane-Microencapsulated Clove Oil for Antimicrobial Leather: Preparation, Characterization and Application. *Soc. Leather Technol. Chem.* **2013**, *97* (July 2013), 154–165.
18. Hillis, T. S. W. E. H. The Phenolic Constituents of *Prunus Domestica*. *J. Sci. Food Agric* **1959**, *10*.
19. Radünz, M.; da Trindade, M. L. M.; Camargo, T. M.; Radünz, A. L.; Borges, C. D.; Gandra, E. A.; Helbig, E. Antimicrobial and Antioxidant Activity of Unencapsulated and Encapsulated Clove (*Syzygium Aromaticum*, L.) Essential Oil. *Food Chem.* **2019**, *276*, 180–186. <https://doi.org/10.1016/j.foodchem.2018.09.173>.
20. Muhson, I.; Mashkor, A. Al. Evaluation of Antioxidant Activity of Clove (*Syzygium Aromaticum*). *Int. J. Chem. Sci* **2015**, *131* (1), 23–30.

-
21. Silvestri, J. D. F.; Paroul, N.; Czyewski, E.; Lerin, L.; Rotava, I.; Cansian, R. L.; Mossi, A.; Toniazzi, G.; Oliveira, D. de; Treichel, H. Perfil Da Composição Química e Atividades Antibacteriana e Antioxidante Do Óleo Essencial Do Cravo-Da-Índia (*Eugenia Caryophyllata* Thunb.). *Rev. Ceres* **2012**, 57 (5), 589–594. <https://doi.org/10.1590/s0034-737x2010000500004>.
 22. Cabral, I. S. R.; Oldoni, T. L. C.; Prado, A.; Bezerra, R. M. N.; De Alencar, S. M.; Ikegaki, M.; Rosalen, P. L. Composição Fenólica, Atividade Antibacteriana e Antioxidante Da Própolis Vermelha Brasileira. *Quim. Nova* **2009**, 32 (6), 1523–1527. <https://doi.org/10.1590/S0100-40422009000600031>.
 23. Sutaphanit, P.; Chitprasert, P. Optimisation of Microencapsulation of Holy Basil Essential Oil in Gelatin by Response Surface Methodology. *Food Chem.* **2014**, 150, 313–320. <https://doi.org/10.1016/j.foodchem.2013.10.159>.
 24. Arab, M.; Marzieh, S.; Nayebzadeh, K.; Khorshidian, N.; Youse, M. Microencapsulation of Microbial Canthaxanthin with Alginate and High Methoxyl Pectin and Evaluation the Release Properties in Neutral and Acidic Condition. **2019**, 121, 691–698. <https://doi.org/10.1016/j.ijbiomac.2018.10.114>.
 25. Lopes, S.; Bueno, L.; Júnior, F. D. A.; Finkler, C. Preparation and Characterization of Alginate and Gelatin Microcapsules Containing *Lactobacillus Rhamnosus*. In *Annals of the Brazilian Academy of Sciences*; 2017; Vol. 89, pp 1601–1613. <https://doi.org/http://dx.doi.org/10.1590/0001-3765201720170071>.
 26. Anbinder, P. S.; Deladino, L.; Navarro, A. S.; Amalvy, J. I.; Martino, M. N. Yerba Mate Extract Encapsulation with Alginate and Chitosan Systems : Interactions between Active Compound Encapsulation Polymers. *J. Encapsulation Adsorpt. Sci.* **2011**, 2011 (December), 80–87. <https://doi.org/10.4236/jeas.2011.14011>.

SUSTAINABILITY DISCLOSURE IN THE LEATHER INDUSTRY: A CONTENT ANALYSIS OF SELECTED SUSTAINABILITY REPORTS

O. Omoloso^{1,2, a}, W.R. Wise^{1, b}, K. Mortimer^{2, c} and L. Jraisat^{2, d}

1 - University of Northampton, Institute for Creative Leather Technologies, Northampton, NN1 5PH, United Kingdom.

2 - University of Northampton, Faculty of Business and Law, Northampton, NN1 5PH, United Kingdom.

a) Corresponding author: oluwaseyi.omoloso@northampton.ac.uk

b) will.wise@northampton.ac.uk

c) kathleen.mortimer@northampton.ac.uk

d) luai.jraisat@northampton.ac.uk

Abstract. This study identifies good practices of sustainability reporting and discusses the details of sustainability reporting from a selected number of companies in the leather supply chain. A content analysis was used to extract sustainability information from either the website, annual report, sustainability report or corporate social responsibility report of six leather-related companies. A review of existing literature assisted in categorising different practices under social, economic and environmental sustainability, while an identification of patterns among practices followed. The results show that the companies are observing a good practice of either dedicating a section of their website to revealing their sustainability activities or utilising their sustainability reports or annual reports. Additionally, these companies follow a good practice of reporting their activities based on the economic, social and environmental sustainability dimensions, rather than focusing on just one of the aspects. Energy efficiency, waste management and reduction in greenhouse gases emission were the most occurring environmental sustainability practices. On the other hand, health and safety occurred as the dominant social sustainability practice, while economic sustainability practices have not been well defined, providing an opportunity for future research. Conclusively, the study provides a useful resource for managers and companies in the leather supply chain to learn from brands that have been embarking on sustainability efforts and assist them to a better understanding of the concept, in readiness for strategy formulation, implementation and reporting.

1 Introduction

Over the years, the subject of sustainability reporting has gained prominence in industrial contexts. Previously, the need for sustainability actions and reporting was borne out of the need to meet legal and regulatory compliances. Now, business stakeholders such as suppliers, customers and investors are the main drivers for the communication of sustainability credentials¹⁻³. Furthermore, being transparent about revealing sustainability credentials has also been a source of competitive advantage for businesses⁴. This study focuses on the leather industry, where present literature on sustainability has often significantly focused on the environmental aspect, with social and economic sustainability aspects having gained less attention.

Few studies relating to sustainability reporting in the leather industry exist. A recent study by⁵ revealed the “impacts of CSR reporting on pro-ecological actions of large and small tanneries” but does not delve into the specificity of what is contained in the reports of companies surveyed in their study.⁶ Sustainability reports and reporting play a crucial role in improving the understanding of sustainability amongst companies. Thus, this paper proceeds from the above perspective, owing to the need for a long-established industry, like leather, with a complex global supply chain and presence of several small and medium enterprises to understand the practices relating to the sustainability dimensions.

Several authors have discussed different topics relating to sustainability reporting but none of the previous studies have made a comparison between companies on how reporting is done and what is being reported, in the context of the leather industry. Hence, the aim of this study is to

compare the areas of focus of social, economic and environmental sustainability practices, using the sustainability reports of selected leather-based companies. This paper contributes to the literature in a major way - it focuses on a 'sustainability-sensitive' industry like leather where sustainability reporting is crucial but understudied, compared to other industries.

2 Literature Review

Sustainability reporting is described as a voluntary activity that has become prominent among business enterprises^{2,5}. Though a voluntary endeavour, its adoption is seeing exponential growth by organisations across the globe⁴. In 2017,⁷ revealed that three quarters of 4900 (large and middle-sized) companies studied now issue corporate responsibility reports. Given the recent EU directive 2014/95/EU that necessitates corporations (with at least 500 employees) to disclose information relating to their sustainability credentials⁸, it can be argued that in the near future, the practice of reporting could become a necessity for small, medium and large companies. Furthermore, in different organisational contexts, sustainability reporting has been similarly referred to corporate social responsibility (CSR) reporting, triple bottom line reporting, non-financial reporting, sustainable development reporting, environmental, social and governance (ESG) reporting^{1,4}. However, sustainability reporting is pragmatically used in this study as it conforms to the subject of the paper.

Sustainability reporting has been identified to provide organisations with several benefits.^{5,7} posits that it contributes to the enhancement of organisations' reputation, thereby attracting investors. Similarly,⁹ also argues that reporting drives value and companies preparing reports manage liquidity better than their counterparts who do not. Understanding the practical aspect of sustainability in the leather industry context in relation to the three sustainability dimensions could enable related organisations to reap the possible benefits.

Social sustainability, also known as the "people" aspect of sustainability is often regarded as the least explored dimension of sustainability. Owing to the labour-intensive nature of the leather industry¹⁰ and the multiplier effects that poor environmental practices can have, social sustainability is an important issue. For example,¹¹ found out that people of both genders, working in the tanning industry, have an increased risk of developing some form of cancer during their lifetime, if protective measures are inadequate. These suggests a dire need for actors to take the issue of occupational and community health and safety, as crucial. Intuitively, only healthy work and happy workers could adequately contribute to the economic or environmental sustainability of a company or industry over the long run.

On the other hand, economic sustainability, also referred to as the "profit" dimension takes into consideration an organisation's effort to improve the value it generates and delivers, at the same time reducing the cost of its supply chain related activities¹². In becoming economically sustainable, organisations are suggested to gear considerable efforts towards making maximum profit while ensuring the most efficient use of all resources and raw materials¹³.

Finally, the "planet" aspect of sustainability, known as environmental sustainability, is based on the notion that for humans to continually enjoy the ecosystem services the environment provides (such as renewable and non-renewable resources and capacity for waste absorption), there is a need to live within the boundaries of "biophysical environment"¹⁴. The leather industry, characterised by its high volume of solid and liquid effluents takes the issue of environmental sustainability seriously¹⁵. In fact, if adequate environmental management systems are not installed, the tanning industry could pose a threat, both environmentally and socially, due to the chemical intensive production processes, energy consumption and solid and liquid wastes⁵. Considering this as a stand-alone factor necessitates the importance of revealing how leather-related companies

are (and can) gear efforts towards being environmentally friendly, socially responsible and economically viable.

The International Council of Tanners (ICT), an organisation of world’s leather trade associations defines the three sustainability aspects as in **Table 1**:

Table 1. Sustainability Practices (Source:¹⁶⁾

Environmental sustainability	Social sustainability	Economic sustainability
Complete compliance with environmental regulations that encapsulates water, air emissions, solid waste.	Complete compliance with product safety regulations.	Commitment to fair trade practices.
Obligation to energy efficiency.	Health and safety compliance.	Traceability of raw material hides.
Life Cycle Assessment (LCA) identification, environmental footprint of the leather industry.	Compliance with employers’ regulations (e.g. no use of forced or child labour, respect of human rights).	Observing and promoting correct labelling of leather and its products.
Application of best practices during processing to anticipate future environmental controls and carbon footprint reduction.	Commitment to the principles of animal welfare.	Transparency on origin of leather production.

The table provides a comprehensive and useful insight into what being sustainable depicts, in terms of the leather industry and serves as a basis of comparison to what is being reported by leather companies.

3 Materials and Methods

To achieve the aim of the research, secondary data in form of the sustainability/CSR reports or statements of six leather-related companies in Europe were used. These companies were purposely selected based on the criteria that they are involved in some form of sustainability actions and there is ease of access to their CSR/Sustainability report or statements. The content analysis method was used to analyse the contents of these reports because of its suitability for analysing information from documents¹⁷. This approach was also followed by^{18–20} in similar studies. Content analysis is defined as the “systematic reading of a body of texts, images and symbolic matter, not necessary from an author’s or user’s perspective”²¹. The reports were carefully examined to extract word clusters that suitably explain the constituents of their efforts in relation to the three sustainability dimensions. The identity of the companies used in the study was also anonymised.

The nature of sustainability concept requires that an understanding of contextual meanings and phrases are taken into consideration in order to extract necessary information. Hence, human coding method was used. Additionally, human coding is appropriate for small volumes of data²² and in this case, six sustainability reports/websites were reviewed. Latent and manifest analysis i.e. what is evident and obvious from the reports as well as underlying meanings from textual data from the reports²³, were the approaches to analysis. Thus, the unit of analysis is the words or group of words that state each sustainability practice. Furthermore, the “emergent” method of coding was used rather than the “a priori” method²⁴. This meant the categories of words coded were identified after carefully reading through the sustainability reports or statements to identify key words or

group of words related to the three sustainability dimensions. Existing literature was used to verify the efficacy of the coding categories.

4 Results and Discussion

Results show that that companies have a range of ways through which they publish their sustainability efforts as shown in **Table 2**.

Table 2. Source of data analysed (Source: authors' compilation)

Company	Year of Report	Source
Tannery A	2018	Sustainability report
Tannery B	2017	Sustainability report
Tannery C	2019	Website
Manufacturing A	2018	Annual report
Manufacturing B	2017	Annual report
Manufacturing C	2017	CSR report

While some companies published separate sustainability reports apart from their annual reports, some other companies have adopted an integrated approach of including their sustainability activities within their annual report without publishing a separate sustainability report. The latter is called integrated reporting, and this signifies one of the growing trends of sustainability reporting⁷. The latest report from these organisations was selected and practices from the three sustainability dimensions were carefully identified and results presented in **Table 3** below:

Table 3. Degree of focus of leather companies on three aspects of Sustainability (Source: Authors' compilation based on reports of mentioned companies)

Coding Categories	List of Companies – Tan = Tannery; Man = Manufacturing					
	Tan A	Tan B	Tan C	Man A	Man B	Man C
Environmental sustainability practices						
Energy Efficiency	○	○	○	○	○	○
Emission reduction of greenhouse gases	○	○	○	○	○	○
Efficient water management	○	○		○	○	○
Waste Management	○	○	○	○	○	○
LCA Assessment identification		○			○	○
Reduced noise and olfactory emissions					○	
Social Sustainability practices						
Health and safety	○	○	○	○	○	○

Employee development	○	○		○	○	○
Diversity and equal opportunities at the workplace	○	○		○	○	○
Social Sustainability practices (continued)						
Coding Categories	Tan A	Tan B	Tan C	Man A	Man B	Man C
Respect and protection of human/workers' rights	○	○		○	○	○
Local community engagement	○	○		○	○	○
Work-life balance	○	○			○	○
Job security		○				○
No use of forced or child labour	○	○		○	○	○
Animal welfare	○	○			○	
Economic Sustainability practices						
Investment in innovative technologies.	○	○				
Traceability of raw skin and hides.	○	○		○		○
Efficiency of resource use.		○	○			○
Profitability.		○	○			

From the analysis, some companies stated their holistic approach towards sustainability. For example, in Tannery A, what sustainability means to the company was well captured in a statement in their sustainability report:

“Sustainability is not just about continuing business as usual. Rather, it is an evolution towards a sustainable future in which environmental priorities, economic prosperity and social justice are pursued simultaneously”.

Similarly, in Tannery B, a holistic approach towards sustainability is captured on their website as thus:

“achieving sustainability means bringing the environmental, financial, and social aspects of our commercial operations together in a permanently balanced and harmonious relationship”

These clear statements suggest how crucial the focus on the three sustainability aspects is, rather than a focus on just one aspect. However, it is important to note that failure of companies to indicate some practices in their report does not necessarily mean an absence of these practices, more so, since the absence of a sustainability report does not translate to the absence of sustainability practices⁵. Furthermore, it was found out that some brands use the concept of sustainability and CSR interchangeably as shown in **Table 2** and this conforms to the literature in form of ^{1,4}.

The findings reveal that energy efficiency, waste management and reduction in greenhouse gases emission represented the most reported environmental sustainability practices, occurring in all the analysed reports. Efficient water management and evaluation of the environmental footprint of activities (in form of LCA identification) were other key practices. The uniformity of practices

among these actors suggests a sound understanding of environmental sustainability among the organisations. This finding reflects with the literature on the prevalence and dominant focus on the environmental aspect.

With regards to social sustainability, health and safety occurred in all the reports analysed. The authors posit that this could be because of the nature of the industry. Additionally, in five of six companies, employee development; diversity and equal opportunities at the workplace; respect and protection of human/workers' rights; local community engagement and compliance to labour regulations (in form of no use of forced or child labour) featured as important social sustainability practices. Work-life balance was also a point of emphasis in four of the companies. While animal welfare was also deemed as an important practice, it should be understood that the leather industry does not take responsibility for the impacts of animal rearing (an agricultural activity) in relation to sustainability²⁵. Nevertheless, some companies seek to ensure that their relevant upstream supply chain partners treat animals with utmost care. Conclusively, the recurrence of these practices amongst the companies suggests a good level of awareness and understanding of the social dimension of sustainability.

Finally, traceability of the raw materials used in production of the leather products is the most recognised economic practice. Traceability is a crucial aspect of the leather supply chain, as some of the regulating bodies and associations (like the LWG – Leather Working Group and COTANCE – European Confederation of the Leather Industry) constantly push for transparency on the origin of hides and skin and other raw materials to improve the image of the leather industry²⁶. Efficiency of resource use (an important economic problem due to scarcity) was also highlighted in half of the reports analysed, as an important consideration. This factors into some important initiatives related to resource efficiency like the United Nations Environment Programme²⁷ and part of Europe 2020's strategy called "Resource-efficient Europe"²⁸. Lastly, profitability (a traditional business indicator that reflects the health of a business) and investment in innovative technologies least featured. Largely, economic sustainability practices were found to be dissimilar and under-reported. In fact, there appears to be a non-convergence on the areas of focus on economic sustainability practices when compared to the environmental and social aspects. Hence, future research to investigate the causes of disparity in focus may be necessary to set the foundation for unification on related practices.

To reiterate, companies not highlighting specific practices in their reports or website does not necessarily mean an absence. For example, the statement of Tannery C focuses significantly on their environmental responsibility efforts. However, this does not translate that they are not making efforts relating to economic and social sustainability, since the company falls under the EU directive previously mentioned. An absence of a sustainability report may thereby be a reason for under-expression of their sustainability credentials. Conclusively, the recent trends suggest that companies should publish some form of report that succinctly explains their sustainability efforts, as this information is increasingly demanded by investors, among other business stakeholders⁷. The understanding of these practices is useful because the brands used in this study are well known in their supply chain and thus, could have significant level of control in terms of urging their global supply chain partners towards more sustainable business practices.

5 Conclusion, Implications and Recommendations for Future Research

The importance of sustainability in the leather industry has continually increased over time but in practice, there is a need to foster the holistic understanding of this concept in the supply chain as a significant focus has been on the environmental aspect. This paper attempted to uncover some of the practices relating to the dimensions of sustainability, providing a useful resource for actors

in the leather supply chain. This study is part of a larger study that broadly focuses on social and economic sustainability in the leather supply chain.

The study has its limitations. The companies whose reports were analysed are all Europe based and fall under the EU directive 2014/95/EU. Hence, the results from this research may not reflect the practices in other non-European countries. Future research may investigate the practices in leather-related companies in other countries for comparative purposes. The data analysed in this study was obtained solely from the company reports and as such, the “face value” of information acquired was adopted but not backed up with primary research. Thus, the validity of findings could be reduced. While this research focuses on particular organisations in different supply chain levels, the transcendence of practices among their supply chain partners can also be investigated to identify best practices and gaps in order to ensure a sustainable leather supply chain.

The findings from this study could assist managers in leather-related companies to better integrate the information on the three sustainability dimensions into their sustainability strategy which could allow for a multiplier effect on better sustainability credentials of actors in the leather supply chain. Furthermore, while metrics usually exist to measure environmental and economic sustainability, the social aspect still suffers from the use of limiting qualitative metrics, such as “yes and no” that does not reveal the true extent of progress. Further research could delve into developing robust metrics which could be qualitative or quantitative in nature and specific to the leather industry. Given the global nature of the leather supply chain, some form of regularised standards could be instituted to ensure the uniformity of sustainability reports in the global industry.

References

1. Thijssens, T., Bollen, L., and Hassink, H. : *Managing sustainability reporting: many ways to publish exemplary reports*, *J. Clean. Prod.*, 136, 86–101, 2016.
2. Braam, G.J.M., Uit de Weerd, L., Hauck, M., and Huijbregts, M.A.J. : *Determinants of corporate environmental reporting: the importance of environmental performance and assurance*, *J. Clean. Prod.*, 129, 724–734, 2016.
3. Nobanee, H., and Ellili, N. : *Corporate Sustainability Disclosure in Annual Reports: Evidence from UAE Banks: Islamic Versus Conventional*, *SSRN Electron. J.*, 2016.
4. Siew, R.Y.J. : *A review of corporate sustainability reporting tools (SRTs)*, *J. Environ. Manage.*, 164 2015.
5. Śmiechowski, K., and Lament, M. : *Impact of Corporate Social Responsibility (CSR) reporting on pro-ecological actions of tanneries*, *J. Clean. Prod.*, 161, 991–999, 2017.
6. Higgins, C., and Coffey, B. : *Improving how sustainability reports drive change: a critical discourse analysis*, *J. Clean. Prod.*, 136, 18–29, 2016.
7. KPMG : *Edge of Page - The KPMG survey of corporate responsibility reporting 2017*, *KPMG Surv. Corp.*, 2017.
8. European Commission : *EUR-Lex - 32014L0095 - EN - EUR-Lex*, Available at: <https://eur-lex.europa.eu/legal-content/EN/TXT/?uri=CELEX:32014L0095>[Accessed: April 9, 2019], 2014.
9. Kuzey, C., and Uyar, A. : *Determinants of sustainability reporting and its impact on firm value: Evidence from the emerging market of Turkey*, *J. Clean. Prod.*, 143, 27–39, 2017.
10. ILO : *Textiles, clothing, leather and footwear sector*, Available at: <http://www.ilo.org/global/industries-and-sectors/textiles-clothing-leather-footwear/lang--en/index.htm>[Accessed: May 8, 2018], 2018.
11. Decouple, P. : *Cancer Risks Associated with Employment in the Leather and Leather Products Industry*, *Arch. Environ. Heal. An Int. J.*, 34, 33–37, 2013.
12. Closs, D.J., Speier, C., and Meacham, N. : *Sustainability to support end-to-end value chains: the role of supply chain management*, *J. Acad. Mark. Sci.*, 39, 101–116, 2011.
13. Singh, S.C., and Gupta, D. : *Sustainability: A Challenge for Indian Leather Industry*, *J. Supply Chain Manag. Syst.*, 2, 37–43, 2013.
14. Moldan, B., Janoušková, S., and Hák, T. : *How to understand and measure environmental sustainability: Indicators and targets*, *Ecol. Indic.*, 17, 4–13, 2012.
15. Daniels, R., and Landmann, W. : *The framework for leather manufacture.*, *World Trades Pub*, 2013.
16. International Council of Tanners : *Sustainability of the Tanning industry | ICT Leather*, Available at: <https://leathercouncil.org/introduction-to-leather/sustainability-of-the-tanning-industry/>[Accessed: October 12, 2018], 2018.

17. Bell, J. : *Doing your Research Project. Fourth Edition*, 2005.
18. Tate, W.L., Ellram, L.M., and Kirchoff, J.F. : *Corporate Social Responsibility Reports: A Thematic Analysis Related To Supply Chain Management*, *J. Supply Chain Manag.*, 46, 19–44, 2010.
19. Jose, A., and Lee, S.-M. : *Environmental Reporting of Global Corporations: A Content Analysis based on Website Disclosures*, *J. Bus. Ethics*, 72, 307–321, 2007.
20. Brandenburg, M., and Seuring, S. : *Quantitative models for sustainable supply chain management: Developments and directions*, *Eur. J. Oper. Res.*, 233, 299–312, 2014.
21. Krippendorff, K. : *Content analysis : an introduction to its methodology*, 2018.
22. Su, L.Y.-F., Cacciatore, M.A., Liang, X., Brossard, D., Scheufele, D.A., and Xenos, M.A. : *Analyzing public sentiments online: combining human- and computer-based content analysis*, *Information, Commun. Soc.*, 20, 406–427, 2017.
23. Erlingsson, C., and Brysiewicz, P. : *A hands-on guide to doing content analysis*, *African J. Emerg. Med.*, 7, 93–99, 2017.
24. Elliott, V. : *Thinking about the Coding Process in Qualitative Data*, 2018.
25. *Leather Naturally : Leather Naturally - Mission*, Available at: <http://www.leathernaturally.org/About/Mission.aspx>[Accessed: June 7, 2018], 2018.
26. *MVO Nederland : Sustainability in the leather supply chain*, 2013.
27. *UNEP : Resource efficiency | UN Environment*, Available at: <https://www.unenvironment.org/explore-topics/resource-efficiency>[Accessed: May 7, 2019], 2019.
28. *Eurostat : Resource efficient Europe - Eurostat*, Available at: <https://ec.europa.eu/eurostat/web/europe-2020-indicators/resource-efficient-europe>[Accessed: May 7, 2019], 2019.

STUDY ON SELF-CROSSLINKING OF HYDROGEN PEROXIDE OXIDATING COLLAGEN

Yujie Zhang ^{b)}, Li hong Fu ^{a)}, *

Qilu University of Technology, School of Light Industry Science and Engineering, Jinan, China

a) Corresponding author: flh891006@163.com

b) another author: 913480760@qq.com

Abstract. The utilization of mink waste generated through the industrial process attracted both industry and academia interests. In this study, the use of hydrogen peroxide as an oxidizing agent onto collagen producing self-crosslinking which extracting from mink solid waste was studied by infrared spectrum, fluorescence spectrum and thermal properties. The effect of hydrogen peroxide dosage and reaction temperature on the degree of oxidative self-crosslinking of collagen was analyzed by the changes of molecular structure and thermal stability. It was found that, hydroxide groups on the collagen side-chains can be oxidized to aldehyde groups and carboxyl groups by hydrogen peroxide in alkaline environment. These oxidized groups can crosslink with functional groups on collagen by covalent bond and ionic bond, changing collagen molecular structure and improving thermal stability. When the dosage of hydrogen peroxide was 14.74% and reaction temperature was 40°C ±, the oxidative self-crosslinking of collagen was the strongest. This study provided theoretical basis for the high-value utilization of mink wastes.

1 Introduction

Mink is one of the most important products in the international fur trade market with “king of fur” name¹. In production and the treatment of shabby goods exists the problems of resource utilization of protein waste including hide fiber and wool fiber. Extracting collagen from protein-containing wastes and utilizing it as a resource has become a research hotspot in related fields.

Green and biodegradable oxidants acting on the active groups of collagen molecular chain can form new crosslinking in the system, thus increasing the structural stability of collagen. As a strong oxidant, potassium permanganate has been used in environmental pollution control, tap water treatment and chemical industry²⁻⁵. However, due to the color of the reaction products, the use of potassium permanganate is limited. Although the price of sodium hypochlorite is low, the chlorine released in the process of oxidation and decomposition will not only cause environmental pollution, but also endanger human health. The oxidation reaction of hydrogen peroxide produces water and oxygen⁶. It is a strong oxidant that meets the ecological requirements and has almost no pollution, it is called "the cleanest" chemical product⁷. At present, it has been widely used in textile, paper-making, food, medicine, electronics and chemical industries⁸. Gong Juxia⁹ discussed the effect of hydrogen peroxide treatment on the structure and properties of collagen type I. They believed that hydrogen peroxide played a dual role in crosslinking and degradation of collagen type I. Lu Xingfang¹⁰ studied the effect of hydrogen peroxide on shrinkage temperature and isoelectric point of raw skin during dehairing and the effect of hydrogen peroxide on gelatin. The results showed that the liming skin shrinkage temperature of dehairing by hydrogen peroxide was higher than that of dehairing by sodium sulfide, but the isoelectric point of collagen was lower, moreover, the glass transition temperature of gelatin was increased by hydrogen peroxide. These results indicated that hydrogen peroxide can react with collagen and collagen hydrolysates, but the self-crosslinking of mink collagen by hydrogen peroxide has not been reported. In this paper, the collagen extracted from mink solid waste was taken as the research object and hydrogen peroxide was used as oxidant, discussing the effects of the amount of hydrogen peroxide and reaction temperature on the oxidation and self-crosslinking of collagen from the changes of molecular structure and thermal

stability of collagen by infrared spectroscopy, ultraviolet spectroscopy and differential scanning calorimetry, in order to provide basis for the treatment and resource utilization of the solid waste containing collagen in mink solid waste.

2. Experiments and Methods

2.1 Materials

Collagen was extracted from mink waste by using pepsin. Glacial acetic acid was purchased from Dasen chemical company (Tianjin, China). Sodium hydroxide was purchased from Xinda chemical company (Shanghai, China). 5 mg/ml collagen solution was prepared dissolving the freeze-dried collagen in 0.01 mol/L HAC.

2.2 Sample preparation

2.2.1 Effect of NaOH on reaction solution pH

20 ml collagen solution (5 mg/ml) and 2.5 ml 0.1 mol/L NaOH were mixed evenly, placing for 3h at 18°C And then the pH (Acidometer, PHS-3C, Shanghai Precision Science Co., China) and absorbance at 280 nm (Ultraviolet spectrophotometer, UV-2000, Unico, USA) of the solution were measured at different time.

2.2.2 Effect of H₂O₂ dosage on the self-crosslinking of oxidating collagen

20 ml collagen solution (5 mg/ml) and 2.5 ml 0.1 mol/L NaOH were mixed by gently stirring for 30s, then adding various dosage H₂O₂ (0.00%, 6.31%, 10.53%, 14.74%, 18.95%, 21.06%) by water bath shaking for 3h at 18°C. The emission and synchronous fluorescence spectra of the solution were measured, then the freeze-dried collagen was tested by Fourier transform spectrometer and Differential scanning calorimetry.

Freeze-drying conditions: pre-freeze for 24h at -18°C, then freeze-dry for 36h at -38°C.

2.2.3 Effect of temperature on the self-crosslinking of oxidating collagen

20 ml collagen solution (5 mg/ml) and 2.5 ml 0.1 mol/L NaOH were mixed by gently stirring for 30 s, then adding 14.74% H₂O₂ by water bath shaking for 3h at different temperature (20°C 25°C 30°C 35°C 40°C 45°C). The blank sample was prepared by 20 ml collagen solution (5mg/ml). The emission and synchronous fluorescence spectra of the solution were measured, then the freeze-dried collagen was tested by Fourier transform spectrometer and Differential scanning calorimetry. The freeze-drying conditions is the same as 2.2.2.

2.3 Fourier transform infrared (FTIR) spectroscopy

FTIR (Fourier transform spectrometer, IRA-1S, Shimadzu, Japan) spectra have been achieved from the samples containing 1 mg collagen in approximately 200 mg potassium bromide with the frequency range from 4000 to 400 cm⁻¹, scanning time was 20, resolution rate was 4.

2.4 Fluorescence measurements

The measurement was carried out using the Cary Eclipse (Agilent, Australia). Both the excitation and the emission slit openings were set as 5 nm. In the case of the synchronous fluorescence spectra, the initial (excitation) wavelength was set at 280 nm and the wavelength shift ($\Delta\lambda$) was equal to 15 nm

and the scan interval was set between 200~400 nm. The fluorescence emission spectra of collagen, the wavelength was set as 280 nm and the scan interval was set between 290~400 nm.

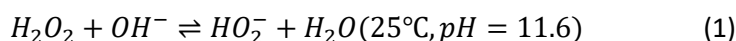
2.5 Differential scanning calorimetry (DSC)

The measurement was carried out using the DSC 25 (TA, USA). The samples (4.0~5.0 mg) were weighed accurately into aluminum pans and sealed. Aluminum pans were scanned over a temperature range of 20~200 °C with a heating rate 5 °C/min under N₂ atmosphere.

3. Result and Discussion

3.1 Effect of NaOH on reaction solution pH

Collagen is oxidized by H₂O₂ to produce self-crosslinking which took advantage of the oxidizability, H₂O₂ could easy form HO₂⁻ under alkaline conditions ¹¹.



Formula (1) shows that strong alkali causes the above equilibrium to move to the right, but excessive pH will accelerate the ineffective decomposition of H₂O₂. In order to ensure the self-crosslinking effect of collagen oxidized by H₂O₂, it is necessary to determine the pH of solution when adding H₂O₂, and the solution pH is regulated by NaOH generally. However, NaOH can hydrolyze collagen, the hydrolysis will not only consume alkali but also produce collagen hydrolysate which will affect the pH of solution and the effect of H₂O₂. In this experiment, 2.5 ml NaOH (0.1mol/L) was first added to the collagen solution to make the oxidative self-crosslinking reaction of collagen with H₂O₂ proceed under alkaline conditions. The change of reaction pH with time is shown in Fig. 1.

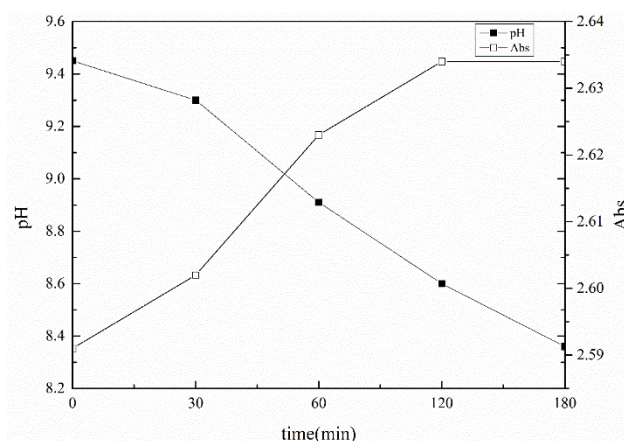


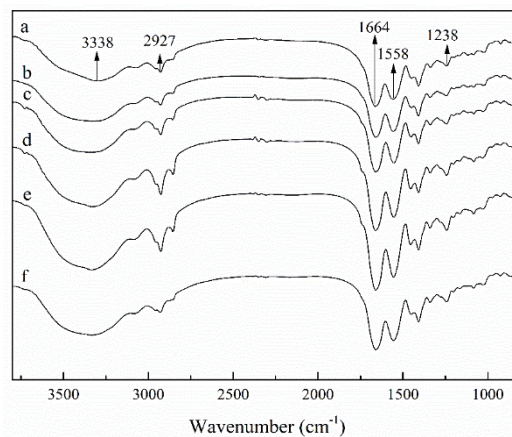
Fig. 1. The relationship between the reaction solution pH and time (2.5 ml NaOH, 18°C)

As can be seen from Fig. 1, with the increase of reaction time, the solution pH decreased but not significant, and remained in the alkaline range within 180 minutes. The initial pH of reaction solution was 9.45, then decreased to 8.36 after 180 minutes. From the absorbance curve of the solution, it can be seen that the hydrolysis of sodium hydroxide breaks some collagen molecular chains and produces polypeptides or amino acids. These exposed amino acids will bind to OH⁻ in the solution and H⁺ will be increased in the solution. Therefore, the solution pH decreased slowly within 180 minutes.

3.2 Effect of H₂O₂ dosage on the self-crosslinking of oxidating collagen

3.2.1 FTIR spectroscopy

The collagen functional groups can be qualitatively and semi-quantitatively analyzed by infrared spectroscopy to understand the effect of H₂O₂ on collagen. Infrared Spectrum of oxidized mink collagen with different dosage of H₂O₂ is shown in Fig. 2.



a~f, m H₂O₂ / m col (%)= 0.00, 6.31, 10.53, 14.74, 18.95, 21.06

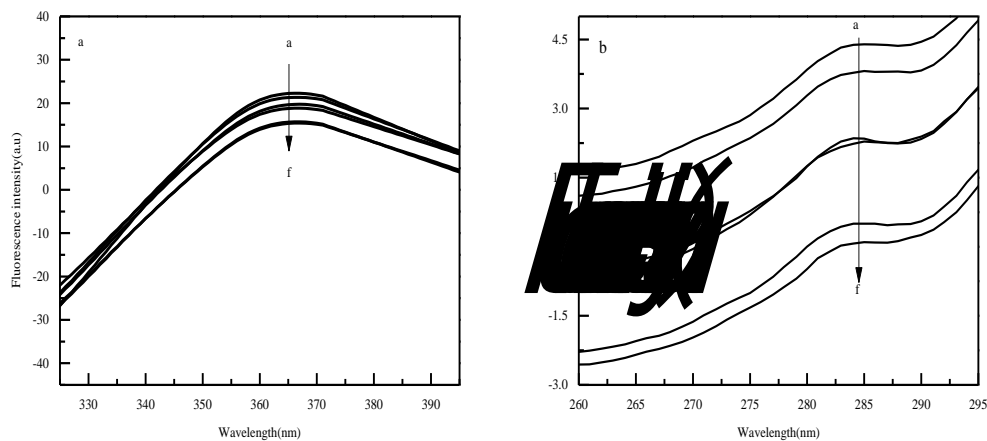
Fig. 2. Infrared Spectrum of Oxidized mink collagen with different dosage of H₂O₂ (18°C, 3h)

As can be seen from Fig. 2, the characteristic absorption peak of collagen amide A band of mink skin before and after oxidation is at 3338 cm⁻¹, and it is mainly related to the stretching vibration of hydrogen bond in molecule, and the characteristic absorption peak of amide B band is 2927 cm⁻¹. The amide bond is the characteristic functional group for characterizing and analyzing the secondary structure of proteins by infrared spectroscopy¹²⁻¹³. The characteristic absorption peaks of amide I band are 1630~1680 cm⁻¹, amide I band of mink collagen is at 1664 cm⁻¹, which is C=O stretching vibration peak of amide I band and COO⁻ antisymmetric contracting vibration peak. 1558 cm⁻¹ and 1238 cm⁻¹ are characteristic absorption peaks of amide II band and amide III of mink collagen respectively, amide band II is caused by C-N stretching vibration and heterogeneous N-H bending vibration, while amide band III is mainly caused by in-phase N-H bending vibration and C-N stretching vibration¹⁴.

It can be seen from the comparison that the absorption area of the characteristic peak (amide band) of mink collagen increased significantly with the increase of the dosage of H₂O₂ (a~f). This is because hydroxide groups on the collagen side-chains can be oxidized to aldehyde groups and carboxyl groups by hydrogen peroxide in alkaline environment. The oxidation enhanced with the increase of hydrogen peroxide dosage, so the amount of H₂O₂ increased, and the characteristic absorption peak of mink collagen protein in amide band strengthened.

3.2.2 Fluorescence spectrum

Tryptophan (Trp), tyrosine (Tyr) and phenylalanine (Phe) residues in protein molecules can absorb and emit fluorescence, so proteins have endogenous fluorescence. Fluorescence spectrum of oxidized mink collagen with different dosage of H₂O₂ is shown in Fig. 3.



a: a~f, m H₂O₂ / m col (%) = 6.31, 18.95, 14.74, 21.06, 10.53, 0.00; b: a~f, m H₂O₂ / m col (%) = 10.53, 0.00, 18.95, 6.31, 14.74, 21.06

Fig. 3. Emission fluorescence spectra (a) and synchronous fluorescence spectra (b) of Oxidized mink collagen with different dosage of H₂O₂ (18°C, 3h)

When the excitation wavelength is 280 nm, tryptophan and tyrosine are the main factors for the intrinsic fluorescence of proteins¹⁵. Because the mink collagen does not contain tryptophan, so the intrinsic fluorescence of collagen solution is mainly produced by tyrosine at 280 nm. The intrinsic fluorescence of proteins decreases the fluorescence signals intensity due to the interaction with solvents or solute molecules. This phenomenon is called fluorescence quenching which is a common phenomenon in protein fluorescence analysis. Fig. 3 (a) shows that when the excitation wavelength is at 280 nm, the absorption peak of mink collagen is about 365 nm. When the amount of H₂O₂ increased from 0.00% to 21.06%, the fluorescence intensity of mink collagen from high to low was 6.31%, 18.95%, 14.74%, 21.06%, 10.53%, 0.00%.

Synchronous fluorescence spectroscopy can be used to study the polarity around protein amino acid residues and the change of protein conformation. When $\Delta\lambda=15$ nm, the change of microenvironment around tyrosine residues can be obtained¹⁶. Fig. 3 (b) shows that the characteristic absorption peak of collagen is 287 nm when the dosage of H₂O₂ is 0% while the characteristic absorption peak of collagen is 285 nm when the dosage of H₂O₂ is increased from 6.31% to 14.74%. It is suggested that the interaction between H₂O₂ and collagen molecules can slightly reduce the microenvironment polarity of tyrosine. When the dosage of H₂O₂ increased from 18.95% to 21.06%, the absorption peak shifted from 284 nm to 285 nm, and the polarity of tyrosine microenvironment increased. This is because when the amount of H₂O₂ is less than 14.74%, H₂O₂ acts on collagen molecules oxidizing hydroxyl groups on collagen side chains to aldehyde or carboxyl groups, these aldehyde or carboxyl groups bind with active groups in the form of covalent bonds or ionic bonds, embedding tyrosine residues and destroying the conformation of microenvironment. When the dosage was more than 18.95%, the oxidative hydrolysis of collagen by H₂O₂ increased which further broke the peptide chain and shortened the molecular chain, resulting in more exposure of tyrosine residues, thus increasing the polarity of the microenvironment.

3.2.3 DSC thermogram

Collagen molecules are composed of three helices. When collagen is heated, its secondary, tertiary and quaternary structure will be destroyed and degenerated. When the temperature continues to rise, collagen will undergo thermal degradation, collagen peptide chain will break, the primary structure will be destroyed, and decomposed into gelatin. The thermal denaturation temperature and thermal degradation temperature of collagen can be characterized by DSC. DSC curves of Oxidized mink collagen with different dosage of H₂O₂ is shown in Fig. 4.

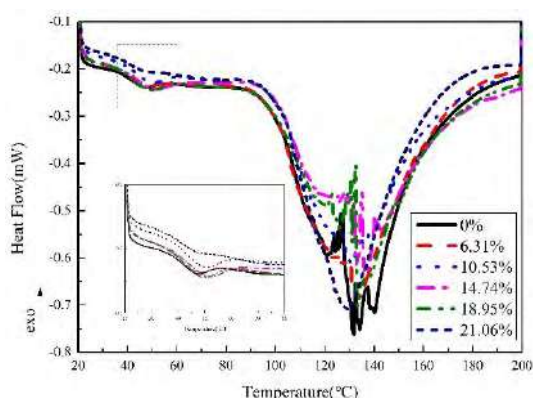


Fig. 4. DSC curves of Oxidized mink collagen with different dosage of H₂O₂ (18°C, 3h)

As can be seen from Fig. 4, there were two obvious endothermic peaks on DSC curves of mink collagen before and after oxidation with H₂O₂. When the amount of H₂O₂ increased from 0% to 14.74%, the peak value of thermal denaturation temperature gradually moved to the right, and when the amount of H₂O₂ was more than 14.74%, the peak value moved to the left. The effect of H₂O₂ on thermal stability of mink collagen is shown in Table 1.

Table 1. The effect of c on thermal stability of mink collagen (18°C, 3h).

	H ₂ O ₂ (%)					
	0.00	6.31	10.5	14.7	18.9	21.0
Denatured temperature (°C)	46.91	47.27	49.4	51.2	48.7	46.8
Degradation temperature (°C)	131.7	133.8	130.	136.	133.	129.
Heat content (J/g)	490.7	482.1	421.	406.	441.	443.
	3	3	18	24	90	73

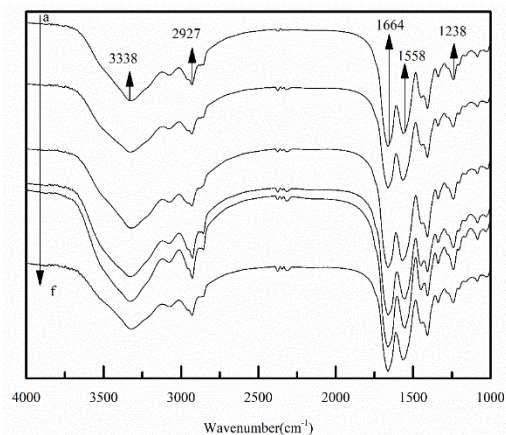
The thermal stability of collagen is provided by the polar interaction between polar groups on the molecular chain and the hydrogen bond formed¹⁷. Table 1 shows that with the increase of H₂O₂ dosage (0%~21.06%), the thermal denaturation temperature and degradation temperature of collagen increases first and then decreases, reaching the maximum when the dosage is 14.74%. It is suggested that H₂O₂ at higher concentration can oxidize hydroxyl groups of collagen side chains to aldehyde or carboxyl groups, and bind with active groups in molecular chains by covalent or ionic bonds. Covalent bond energy is much larger than hydrogen bond and polar bond energy¹⁷, and it was proved that H₂O₂ oxidation had cross-linking effect and improved the thermal stability of collagen. When the amount of H₂O₂ was more than 14.74%, the oxidative hydrolysis of collagen peptide chains dominated, resulting in the decrease of the thermal denaturation temperature of collagen. In conclusion, under alkaline conditions, when the amount of H₂O₂ was 14.74%, the self-crosslinking effect of oxidized mink collagen was the best.

3.3 Effect of temperature on the self-crosslinking of oxidating collagen

3.3.1 FTIR spectroscopy

Infrared Spectrum of Oxidized mink collagen with different reaction temperature is shown in Fig. 5. As can be seen from Fig. 5, when the reaction temperature was increased from 20°C to 25°C the peak shape of the characteristic absorption peak of collagen in infrared spectra remained almost unchanged. When the reaction temperature increased from 30°C to 40°C the absorption peaks of

collagen at 3338 cm^{-1} , 2927 cm^{-1} and 1664 cm^{-1} increased, while the other peaks did not change significantly, the absorption peaks of collagen at the above three points were weakened at 45°C . The results showed that the increase of appropriate temperature was beneficial to the oxidation of collagen by hydrogen peroxide, and increased the content of aldehyde or carboxyl groups in the collagen molecular chain. When the temperature is too high ($>40^\circ\text{C}$), hydrogen peroxide decomposes excessively, which reduces the oxidation.

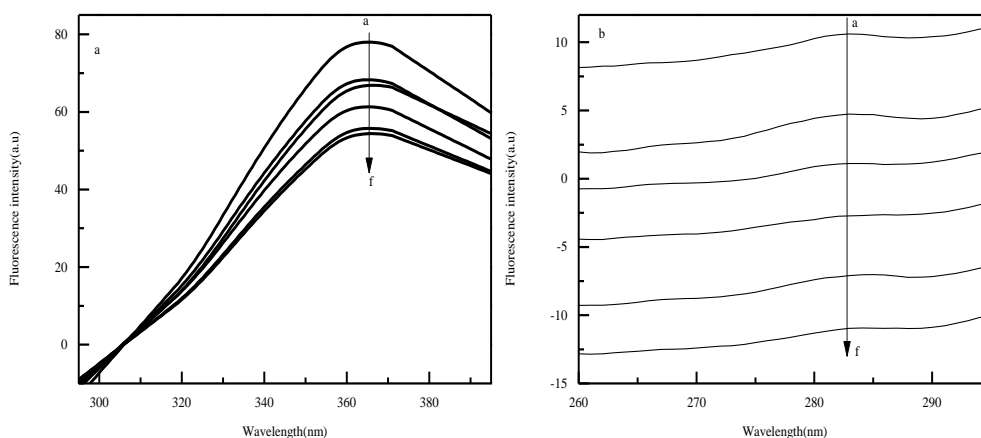


a~f, T ($^\circ\text{C}$) = 20, 25, 30, 35, 40, 45

Fig. 5. Infrared Spectrum of Oxidized mink collagen with different reaction temperature (14.74% H_2O_2 , 3h)

3.3.2 Fluorescence spectrum

Infrared Spectrum of Oxidized mink collagen with different reaction temperature is shown in Fig. 6. As can be seen from Fig. 6, when the excitation wavelength was 280 nm, the absorption peak of collagen protein appeared at 362 nm. The fluorescence intensity decreases with the increase of reaction temperature. It is suggested that the reaction of collagen self-crosslinking with hydrogen peroxide is extremely sensitive to temperature. Appropriate increase of temperature (35°C) is beneficial for hydrogen peroxide to oxidize hydroxyl groups in collagen molecular chains to aldehyde or carboxyl groups, and bond with covalent or ionic bonds of active groups. Tyrosine is encapsulated resulting in a reduction of fluorescent sources quantity. The absorption peaks of collagen synchronous fluorescence spectra remained almost unchanged at different reaction temperatures.



a: a~f, T ($^\circ\text{C}$) = 30, 20, 40, 25, 45, 35; b: a~f, T ($^\circ\text{C}$) = 30, 20, 45, 35, 25, 40

Fig. 6. Emission fluorescence spectra (a) and synchronous fluorescence spectra (b) of Oxidized mink collagen with different reaction temperature (14.74% H_2O_2 , 3h)

3.3.3 DSC thermogram

DSC curves of oxidized mink collagen with different reaction temperature is shown in Fig. 7.

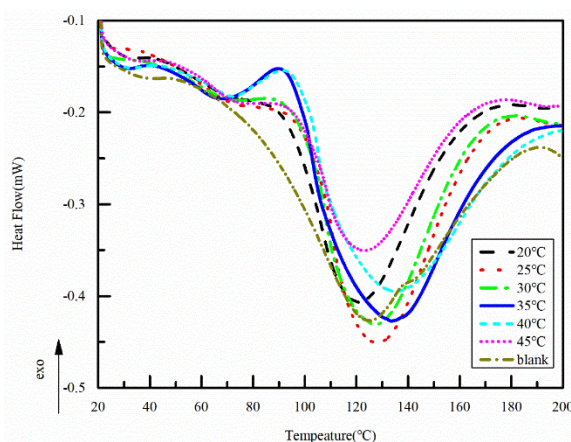


Fig. 7. DSC curves of oxidized mink collagen with different reaction temperature (14.74% H₂O₂, 3h)

As can be seen from Fig. 7, the self-crosslinking samples of collagen peroxide showed obvious endothermic peaks at different reaction temperatures. There are two endothermic peaks on the DSC curve of collagen when the temperature is 35°C and 40°C. The effect of denatured temperature on thermal stability of oxidized mink collagen is shown in Table 2.

Table 2. The effect of denatured temperature on thermal stability of oxidized mink collagen (14.74% H₂O₂, 3h).

	Reaction temperature (°C)						Blank
	20	25	30	35	40	45	
Denatured temperature (°C)	-	-	-	65.89	71.25	-	-
Degradation temperature (°C)	119.9	126.7	126.2	132.6	133.4	121.2	123.4
Heat content (J/g)	273.7	294.8	285.9	296.5	285.7	249.3	306.5

Note: The blank sample was untreated collagen, i.e. without NaOH and H₂O₂.

As can be seen from Table 2, the denaturation temperatures of collagen at 35°C and 40°C were 65.89°C and 71.25°C respectively. With the increase of reaction temperature, the thermal degradation temperature increases first and then decreases, reaching the maximum at 40°C (133.43°C), indicating that the peptide chain of collagen molecules breaks and the amino acid residues are destroyed. This is because when hydrogen peroxide acts on collagen molecules, hydroxyl groups are oxidized to aldehyde or carboxyl groups, which bind to the active groups on the molecular chain by covalent bonds or ionic bonds, thus increasing the thermal stability of collagen. Increasing the temperature properly can decompose hydrogen peroxide into more hydrogen peroxide radicals (H₂O), promoting the oxidation self-crosslinking reaction and enhancing the stability of the peptide chains. When the reaction temperature is higher than 40°C hydrogen peroxide produces more ineffective decomposition and the oxidation decreases. In conclusion, the self-crosslinking effect of collagen peroxide is better when the reaction temperature is 40°C.

The thermal degradation temperature of collagen treated with hydrogen peroxide was higher than that of blank sample (123.47°C) when the reaction temperature was raised from 25°C to 40°C. The low reaction temperature (20°C), the weak oxidation of collagen side chain hydroxyl by hydrogen peroxide, and the hydrolysis of collagen to a certain extent, resulting in the thermal

degradation temperature of collagen which is oxidized at 20°C is lower than that of blank samples. The higher the reaction temperature (> 40°C), the more ineffective decomposition of hydrogen peroxide was produced, and the hydrolysis of collagen molecular chain itself was intensified, the main chain structure was destroyed. Therefore, the thermal degradation temperature of collagen oxidized at 45°C is lower than that of blank samples.

4. Conclusion

The self-crosslinking mechanism of hydrogen peroxide collagen oxidating was studied by analyzing the mink collagen thermal properties, infrared spectrum and fluorescence spectrum. Infrared spectrum showed that hydroxide groups on the collagen side-chains can be oxidized to aldehyde groups and carboxyl groups by hydrogen peroxide in alkaline environment; Fluorescence spectrum showed that hydrogen peroxide changes protein conformation and tyrosine microenvironment; The change of thermal stability of collagen proved that hydrogen peroxide can make new crosslinks between collagen molecular chains and increase the thermal denaturation temperature of collagen. Under alkaline conditions, when the dosage of hydrogen peroxide was 14.74% and reaction temperature was 40°C, the oxidative self-crosslinking of collagen was the strongest.

Acknowledgement

This work was financially supported by the National Natural Science Foundation of China (No.21606139).

Reference

1. Li, Y. L.: 'Mink and Its Economic Value', *Heilongjiang Animal Science and Veterinary Medicine*, 12, 114, 2011 (in Chinese)
2. Li, C. M.: 'Effect of Potassium Permanganate on Algal Cells and Extracellular Organics Control', *Chinese Journal of Environmental Engineering*, 12, 1879-1887, 2018 (in Chinese)
3. Zhao, X.: 'Application of Potassium Permanganate Activated Carbon in Iron and Manganese Removal from Domestic Drinking Water Treatment', *Water & Wastewater Engineering*, 54, 12-14, 2018 (in Chinese)
4. Zhang, S. Y.: 'Experimental Investigation on the Preparation of Adipic Acid by Potassium Permanganate Oxidizing Cyclohexanol', *Chemical Enterprise Management*, 22, 41-42, 2018 (in Chinese)
5. Zhao, S. H.: 'Preparation and Properties of Pd-Ni Catalysts Supported by KMnO₄ Modified Carbon Black', *Fine Chemicals*, 36, 01-10, 2019 (in Chinese)
6. Shen, H. X.: 'Study on the Application of Hydrogen Peroxide in Organic Chemical Synthesis', *Chemical Engineering & Equipment*, 02, 227-229, 2017 (in Chinese)
7. Wang, D. R.: 'Development and Application Progress of Hydrogen Peroxide Production', *Fujian Paper Making*, 02, 21-27, 2002 (in Chinese)
8. Fan, X. Y.: 'Present Situation and Application of Hydrogen Peroxide Production Technology', *Chemical Enterprise Management*, 27, 144, 2017 (in Chinese)
9. Gong, J. X.: 'Effect of Hydrogen Peroxide Treatment on Structure and Performance of Type I Collagen', *China Leather*, 44, 10-13, 2015 (in Chinese)
10. Lu, X. F.: 'Effect of Hydrogen Peroxide on the Properties of Collagen', *Journal of Shaanxi University of Science & Technology*, 02, 06-09, 2003 (in Chinese)
11. Xu, Z. Z.: 'Analysis of Influencing Factors on Hydrogen Peroxide Decomposition', *Textile Dyeing and Finishing Journal*, 01, 33-35, 2006 (in Chinese)
12. Liu, F. M.: 'Purification of Collagen from Pacific Cod Skin by Isoelectric Precipitation Processing and The Study of Its Structure Properties', *Science and Technology of Food Industry*, 01-15, 2018 (in Chinese)
13. Muyonga, J. H.: 'Fourier Transform Infrared (FTIR) Spectroscopic Study of Acid Soluble Collagen and Gelatin from Skins and Bones of Young and Adult Nile Perch (*Lates niloticus*)', *Food Chemistry*, 86, 325-332, 2004
14. Hou, H.: 'Collagen Fibers Morphology and Physical and Chemical Properties of Collagen of Sea Cucumber', *Modern*

- Food Science and Technology, 29, 1491-1495, 2013 (in Chinese)*
15. Kanakis, CA.: 'Milo β -lactoglobulin Complexes with Tea Polyphenols', *Food Chemistry, 127, 1046-1055, 2011 (in Chinese)*
 16. Shen, B. J.: 'Study on the binding mode of naringenin to human serum albumin by fluorescence and ultraviolet spectroscopy', *Chinese Journal of Analysis Laboratory, 35, 41-46, 2016 (in Chinese)*
 17. Tang, K. Y.: *Physics and Chemistry of Collagen, Science Press, 2016 (in Chinese)*

NEW WET WHITE/CHROME FREE PROCESS OFFERING SIGNIFICANT ENVIRONMENTAL AND PHYSICAL PROPERTY ADVANTAGES FROM BEAMHOUSE TO CRUST

Julian Osgood¹, Michel Deville² and Wolfram Scholz³

1 ATC Tannery Chemicals

2 Tannery Chemicals

3 W2O Environment

a) Corresponding author: josgood@atc.fr

b) mdeville@atc.fr

c) wolfram@w2oenvironment.net

Abstract. A combination of processing techniques and speciality chemicals has been developed to target environmental issues and legislation in the European leather industry, especially for automotive upholstery leather. This process combines new techniques in the beamhouse process through to the tanning process. Initial work on several different individual concepts showed some excellent improvements, but when these concepts have been brought together to form a single strategic process the advantages and improvements have exceeded expectations. The process demonstrates a reduction in the use of salt, formic acid and sulphuric acid. After more than two years of trials from small scale to full production in an automotive leather production environment, we are able to present independently test results showing the benefits of following this system.

1 Introduction

ATC Tannery Chemicals have been promoting a pickle free chrome tanning process for a number of years, with excellent results in removing sulphuric acid, formic acid, salt and magnesium oxide from the tanning process, at the same time total chrome used is reduced by up to 1/3 and the resultant effect of chrome in the effluent after the tanning process is greatly reduced. Now, a recent study has shown that the use of the same technology can also apply to wet-white production as well as wet-blue. Resulting in the elimination of sulphuric acid from this tanning process as well. As the automotive leather industry is very aware the popularity of wet-white tanning has increase massively over the years and in some automotive plants, chrome leather production has been stopped, or at least significantly reduced in favour of wet-white.

2 The Paper in full

Mankind has known for years the harmful effect that many chemicals can have on the environment, we hear about these issues daily. All tanners and especially those that specialise in the automotive industry are well aware that many of the products they have to use on a daily basis are often classed as hazardous and polluting. Add to this the worldwide growth in employee welfare and the ever-increasing amount of legislation required to maintain a legal manufacturing presence and the pressure on a leather manufacturing facility to provide a viable, quality product and maintain the safety and health of their workforce becomes almost impossible.

Obviously, this pressure to consider the people and environment of our planet is a good thing, any improvement in general health and safety and better manufacturing processes can only be

applauded. However, the question of “how” to do this is being repeated in almost every responsible leather manufacturing facility around the world. The Automotive sector is under even greater scrutiny as compliance with ISO14001 is seen as a must.

For this article ATC wanted to consider just one chemical and inform the reader of a cost effective, safe, easy method to take one of the most dangerous chemicals from the warehouses of tanneries for ever. Sulphuric Acid has been widely used within leather tanning for many hundreds of years. It is considered an essential product to manipulate the acidity of processes such as the tanning process. It is almost universally used for vegetable tanning, aldehyde tanning, chrome and other metal tanning processes.

As a young leather technician fresh from school I can still remember what happens to my own skin when sulphuric acid comes into contact with it. I still have the scars. The fumes from the sulphuric acid storage tanks are also not good to experience. If we also consider recent work on the effects of sulphuric acid on collagen it can be shown that one of the products we rely on so heavily, is actually causing damage to the very substance we are trying to preserve.

A recent paper given at the **VGCT 7th Freiberg Leather Days** by **Dr Rafea Naffa from LASRA entitled. Skin Strength: A critical analysis of strength differences of sheep, goat, deer skins and cow hides** discusses how much damage that tanners are doing to natural collagen during the many processes involved in making a piece of leather. One of the primary areas of concern was the pickling process, just before tanning, where quite high quantities of sulphuric acid are used and a large number of natural crosslinking bonds within the fibre structure are destroyed, thus weakening the resultant leather.

ATC Tannery Chemicals have been promoting a pickle free chrome tanning process for a number of years, with excellent results in removing sulphuric acid, formic acid, salt and magnesium oxide from the tanning process, at the same time total chrome used is reduced by up to 1/3 and the resultant effect of chrome in the effluent after the tanning process is greatly reduced. Now, a recent study has shown that the use of the same technology can also apply to wet-white production as well as wet-blue. Resulting in the elimination of sulphuric acid from this tanning process as well. As the automotive leather industry is very aware the popularity of wet-white tanning has increase massively over the years and in some automotive plants, chrome leather production has been stopped, or at least significantly reduced in favour of wet-white.

However, one of the draw backs of wet-white leather has been that this tanning method does not produce a product that is as physically strong as a chrome tanned leather. Physical properties of wet-white leather often show poor results in typical physical properties tests required by the automotive manufactures, such as the following:

Strength	Determination of distension and strength of grain (ball burst test)	Internal methodology	Ball burst
Softness	Determination of softness	ISO 17235	ST 300
Determination of tear load	Determination of tear load – Single edge tear	ISO 3377-01	Dynamometer
Strength	Determination of tensile strength and percentage extension	ISO 3376	Dynamometer

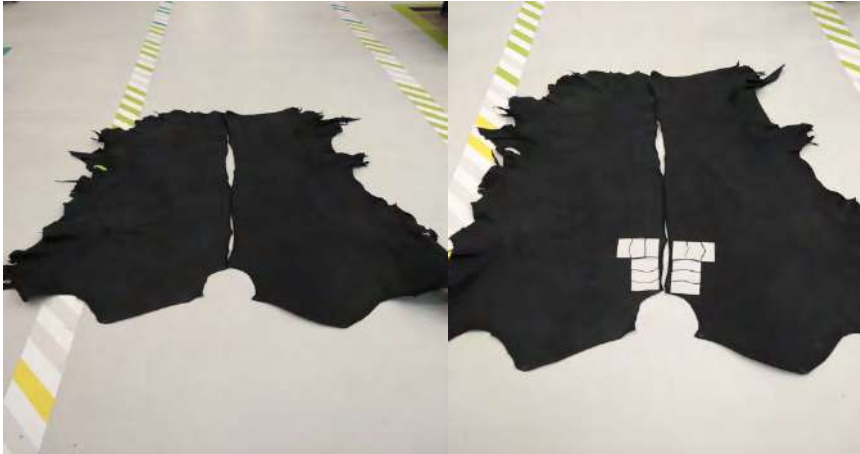
ATC wanted to answer the question of what improvement could be seen in a typical wet-white upholstery leather by removing the pickling process and therefore sulphuric acid from the method.

- We took lime split full hides.
- After delimiting and bating as normal, the hides were cut in two parts :

SAMPLE 1 - the Right side was pickled with sulphuric acid (normal process, with brine)

SAMPLE 2 - the Left side was prepared with Actipickle NSA (without any acid)

- Pretannage was done with Actidial GTA (modified dialdehyde)
- After 48 hours shrinkage temperature was taken:
Sample 1 = 80°C
Sample 2 = 82°C
- The two sides were put together and processed with an automotive style dyeing and retanning system
- Dried, conditioned and staked, identically



3 Results

Average Strength (N) Average of 3 values	Transverse	Parallel
Side 1 (no NSA)	65.6	65.6
Side 2 (NSA)	80.9	101.6
Gain	+23%	+55%

The results have been extremely dramatic and the improvements in the trial were exceptional. The next steps were to scale up the trials and finally try this in full production sized lots. Various further experimental and bulk trials have been performed with the assistance of several tanneries around the world and results have been extremely positive. Although due to the sensitive nature of these trials and to maintain the wishes of our customers, we are not prepared to add these results to this paper.

3.1 Environmental Improvement Results

3.1.1 Chrome Tanning Environmental Results

Independent testing of effluent liquors by the UK company W2O Environment Ltd. from trial tannages-running side by side, gave the following results and conclusions:

ADVANTAGES

Improved clarification with 86% less suspended solids in the samples
Reduced COD and higher biodegradability COD/BOD from 9.5 to 3.5
Less than ½ of chrome in the sample, reduced by 57%
Less than 1/2 of the TDS in the supernatant reduced by 56%
Chloride content reduced by 99% in the sample.
1/5 of sludge generation TDS reduced by 79%
1/5 of chrome content in the sludge (-79%)
Less organic residues derived from the hides (-95%)

DISADVANTAGES

None

3.1.2 Chrome Free/Wet White Tanning Environmental Results

Independent testing of effluent liquors by the UK company W2O Environment from trial tannages running side by side, gave the following results and conclusions:

ADVANTAGES

Improved clarification with low suspended solids of 22 mg/l in the sample
Chloride content reduced by 54% in the sample
29% less TDS and environmental salt impact
Less organic residue derived from the hide, (-10%)

DISADVANTAGES

None

4 Conclusion

In final conclusion, the system developed over many years for ATC Tannery Chemicals using the product Actipickle NSA and incorporating techniques and methods gained from trial and production testing has demonstrated without doubt, the many benefits of using this system to give improvements in quality of the final leather, to reduce the amount of chemicals consumed in the tannery process, while significantly reducing the environmental impact at the tannery, on both, Chrome tanned leather and chrome free, wet white leather. If more information is required, please contact ATC Tannery Chemicals.

References

1. VGCT 7th Freiberg Leather Days by Dr Rafea Naffa from LASRA entitled. *Skin Strength: A critical analysis of strength differences of sheep, goat, deer skins and cow hides.*

HYGIENIC PROPERTY AND WATER RESISTANCE OF WATERBORNE POLYACRYLATE/FLOWER-LIKE ZnO COMPOSITE COATINGS

Yan Bao^{1,a}, Lu Gao¹ and Jianzhong Ma^{1,b}

¹ College of Bioresources Chemical and Materials Engineering, Shaanxi University of Science and Technology, Xi'an, 710021, PR, China,

Corresponding author: baoyan@sust.edu.cn

Another author: majz@sust.edu.cn

Abstract: Polyacrylate as film-forming materials has been widely used in leather finishing, but its compactness significantly obstructs the hygienic property of upper leather. Therefore, considerable efforts have been made to endow polyacrylate with required properties. In this study, we demonstrated a facile and rapid sonochemical process to synthesis the flower-like ZnO nanostructures. The related morphology and structure of product were characterized by X-ray diffraction (XRD), scanning electron microscopy (SEM) and transmission electron microscopy (TEM). Afterwards, flower-like ZnO were introduced into the polyacrylate matrix by physical blending method and the morphology, latex stability, water vapor permeability and water resistance of polyacrylate/flower-like ZnO composites were studied. The results showed that flower-like ZnO assembled by ellipsoid-like nanorods with the length of about 600 nm was successfully fabricated. The average size of flower-like ZnO was 1.2 μm . According to SEM images, flower-like ZnO evenly dispersed were observed in composite matrix. Compared with pure polyacrylate, polyacrylate/flower-like ZnO composites exhibited superior stability. Meanwhile, its water vapor permeability and water resistance were increased by 52.91% and 53.13%, severally. The reason for this is that ZnO with rough structure can increase voids in polyacrylate film and thus improving hygienic property of polyacrylate film. Additionally, the hydrophilic groups on surface of ZnO can crosslink with polyacrylate chains, which contributed to the enhancement of water resistance. Thus, a promising coating with hygienic property and water resistance for leather finishing agent was approved.

Keywords: Polyacrylate/flower-like ZnO composites, hygienic property, water resistance, leather finishing.

1 Introduction

Significant efforts have been devoted to developing waterborne polyacrylate due to the strict environmental regulations. Waterborne polyacrylate coating, possessing good adhesion, transparent coating and aging resistance, is attractive for leather finishing^[1]. However, the hygienic property of leather finished by polyacrylate might be decreased due to its compactness. Besides, the polyacrylate offers weak water resistance under lots of hydrophilic groups^[2]. In recent years, the modification of polyacrylate is of great interest and importance. To the best of our knowledge, various methods have been employed to modify polyacrylate, mainly including introducing functional monomers, modifying by polyurethane and introducing inorganic nanomaterials (e.g., SiO₂, ZnO, TiO₂, etc.)^[3~8]. Our research group has been engaging in the study on polyacrylate/inorganic nanocomposites^[9~13]. Previous research showed that the properties enhancement of polyacrylate film was associated with the morphology of nanomaterials.

In this study, we developed an ultrasonic route to prepare flower-like ZnO, which was acted as a fortifier to the modification of polyacrylate. A serious characterizations of XRD, SEM and TEM were carried out to demonstrate flower-like ZnO and polyacrylate/flower-like ZnO composites. The results indicated that the water vapor permeability, water resistance, mechanical properties and UV resistance of polyacrylate/flower-like ZnO composite film were enhanced by introducing flower-like ZnO.

2 Experimental Section

2.1 Materials

All reactants were of analytical grade and used as received without any further purification. Zinc acetate ($\text{Zn}(\text{CH}_3\text{COO})_2 \cdot 2\text{H}_2\text{O}$, 98%, Tianjin FuChen Chemical) and ammonium hydroxide ($\text{NH}_3 \cdot \text{H}_2\text{O}$, 99%, Hongyan) were used as zinc cation and hydroxide anion precursors, respectively. And Ethylene glycol (EG) was obtained from Tianjin Kemiou Chemical Reagent Co., Ltd. Deionized (DI) water and polyacrylate latex were prepared in the laboratory.

2.2 Synthesis of Flower-like ZnO and Polyacrylate/Flower-like ZnO Composites

For synthesis of flower-like ZnO, 5 mmol of zinc acetate was added into a mixture solution of EG and deionized water (EG:DI=1:1) under magnetic stirring to form a transparent solution. Then, $\text{NH}_3 \cdot \text{H}_2\text{O}$ was dropped into the zinc acetate solution with regulating pH to 8 under continuously stirring for 30 min. The precursor slurry was then transferred into ultrasonic grinder with 2 s pulse-on and 1 s pulse-off in one pulse cycle. The precursor slurry was irradiated for 30 min. Ultimately, the precipitation was centrifuged, washed thoroughly with deionized water and absolute ethanol, and then dried at 60 °C for 6 h to obtain a dried ZnO powder.

For synthesis of polyacrylate/flower-like ZnO composites, the synthetic method was mentioned in the previous work^[13].

2.3 Characterizations and Measurements

X-ray diffraction (XRD) patterns of flower-like ZnO were recorded by a D/max 2550 V diffractometer with Cu K α radiation. The morphology and high resolution structure of flower-like ZnO were determined by scanning electron microscope (FE-SEM, Hitachi S-4800, Japan) and transmission electron microscopy (TEM, Tecnai G2 F20S-TWIN, America). Besides, SEM was also used to observe the existence status of flower-like ZnO in polyacrylate matrix.

For properties measurements, the W30/060 water vapor transmission rate test system was employed to measure the water vapor permeability of composite film. Water resistance of composite films was determined according to GB/T2223.1996. And Gotech AI-3000 servo control testing machine was applied to test the tensile strength and elongation at break of composite film. The UV transmittance curves of film were obtained by using Cary-5000 ultraviolet-visible-near infrared spectrophotometer.

3 Result and discussion

3.1 Structure and morphology

The structure and chemical composition of flower-like ZnO were confirmed by XRD patterns (Fig. 1). The obtained diffraction peaks located at $2\theta = 31.6^\circ, 34.3^\circ, 36.2^\circ, 47.5^\circ, 56.5^\circ, 62.7^\circ, 67.9^\circ$ and 76.8° matched with (100), (002), (101), (102), (110), (103), (112) and (202) plane of ZnO (JCPDS No.36-1451), respectively. Furthermore, there was no extra peak in the XRD patterns, suggesting the prepared flower-like ZnO sample showed high purity. Fig.2a showed SEM image of flower-like ZnO. It can be observed that an integral flower-like ZnO was spliced by ellipsoidal-like ZnO with the length of about 600 nm, together with some isolated 1D spheroid and twin-spheres. The size of flower-like ZnO was around 1.2 μm .

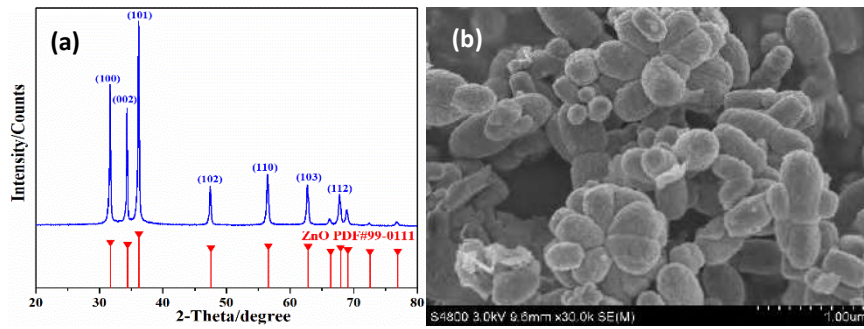


Fig. 1. (a)XRD pattern of flower-like ZnO, (b) SEM image of flower-like ZnO.

The prepared flower-like ZnO nanoparticles were introduced into polyacrylate emulsion to form composite film. Above all, the existence status of flower-like ZnO in polyacrylate matrix was investigated. It can be seen that cross-section of pure polyacrylate film was smooth without obvious cracks and bulges in Fig.2a. Different with pure polyacrylate film, the evenly dispersed flower-like ZnO nanostructures (bumps) were observed in composite matrix (Fig.2b).

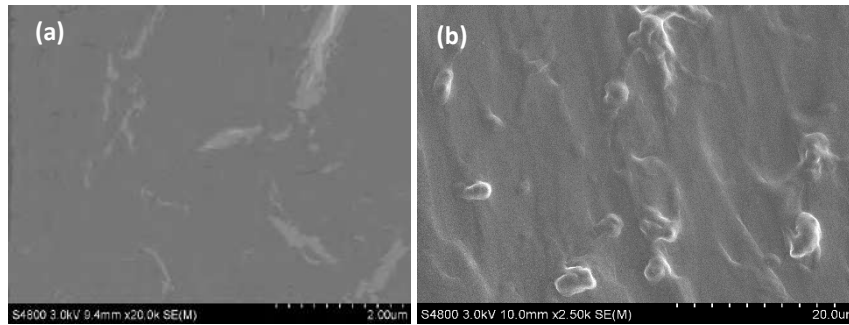


Fig. 2. SEM images of (a) polyacrylate film and (b) polyacrylate/flower-like ZnO composite film.

The investigation of the water vapor permeability, water resistance, mechanical properties and UV transmittance are necessary to evaluate the nature of composite film. Fig. 3 depicted the water vapor permeability and water resistance of composite film. It can be found the water vapor permeability and water resistance of composite film including ZnO were simultaneously enhanced. The reason of this result was that a rough structure of flower-like ZnO can produce abundant interface gaps between flower-like ZnO and polyacrylate matrix, which promoted water vapor across the film. For water resistance, this can be interpreted that the hydroxyl groups and positive charge on the surface of flower-like ZnO could react with the carboxyl groups on polyacrylate chains, which reducing the number of hydrophilic groups of film. Compared with pure polyacrylate film, the water vapor permeability and water resistance of composite film were increased by 52.91% and 53.13%, severally.

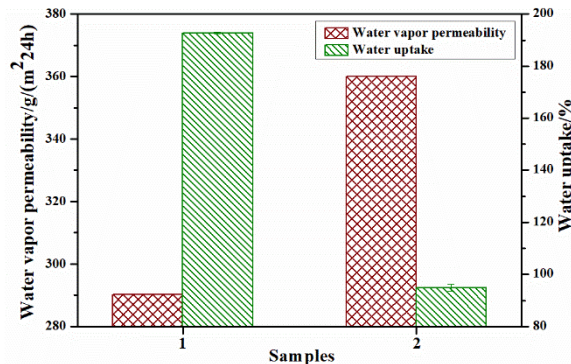


Fig. 3. Water vapor permeability and water resistance of polyacrylate film (Sample 1) and polyacrylate/flower-like ZnO composite film (Sample 2).

As leather finishing agent, the mechanical properties of film plays an important role for leather performance. In this work, the mechanical properties of composite film were inspected by testing its tensile strength and elongation at break. As shown in Fig. 4a, the tensile strength of composite film was better than that of pure film, but the elongation at break was lower, which was consistent with the results of polyacrylate/hollow ZnO nanospheres in our previous work^[13]. Due to the enhancement of interface effect between flower-like ZnO and polyacrylate film, the tensile strength of composite film was increased. But as inorganic matter, ZnO nanoparticles with certain rigidity cause the crazes in the film, resulting in the decline of elongation at break. In conclusion, polyacrylate/flower-like ZnO composite film can meet the needs of leather finishing. In addition, the UV transmittance of both samples was determined in Fig. 4b. Polyacrylate/flower-like ZnO composite film had a lower UV transmittance than polyacrylate film, suggesting the composite film possessed a higher UV resistance. This result might be explained by well-known mechanism that ZnO nanoparticles possess absorption and scattering for UV light. When the UV light irradiated on the composite film, the intensity of UV irradiation for the film was reduced through flower-like ZnO absorbing and dispersing UV light in all directions.

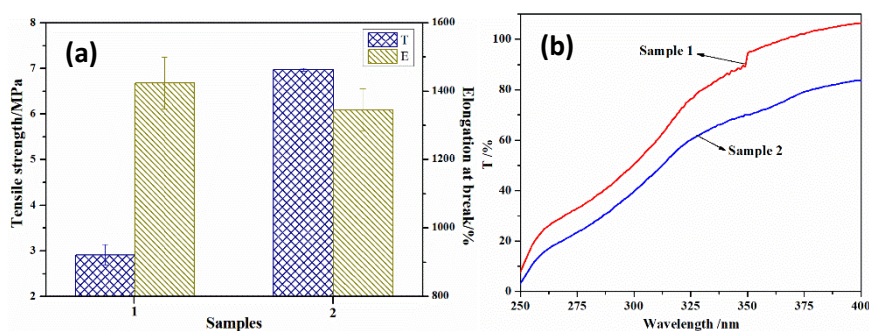


Fig. 4. (a) Mechanical properties of polyacrylate film (Sample 1) and polyacrylate/flower-like ZnO composite film (Sample 2), and (b) UV transmittance of the corresponding film.

4 Conclusions

In summary, we have developed an ultrasonic method for fabricating flower-like ZnO nanostructures with an average diameter of $\sim 1.2 \mu\text{m}$. The as-synthesized ZnO products were introduced into polyacrylate matrix whose water vapor permeability, water resistance, mechanical properties and UV resistance were improved. Compared with the pure polyacrylate film, the water vapor permeability, water resistance and tensile strength of composite film were increased by 52.91%, 53.13% and 58.85%, respectively.

References

1. Zhang K, Shang S, Sun P, et al. Hydrogenated rosin ester latexes/waterborne polyacrylate blends for pressure-sensitive adhesives, *J. Appl. Polym. Sci.*, 133(6), 2016.
2. Bao Y, Feng C, Wang C, et al. Hygienic, antibacterial, UV-Shielding performance of polyacrylate/ZnO composite coatings on a leather matrix, *Colloids Surf., A*, 518, 232-240, 2017.
3. Zhu B, Liu J, Chen Y, et al. Superhydrophobic coating with multiscale structure based on crosslinked silanized polyacrylate and nanoparticles, *Surf. Coat. Technol.*, 331, 40-47, 2017.
4. Lü T, Qi D, Zhang D, et al. Fabrication of self-cross-linking fluorinated polyacrylate latex particles with core-shell structure and film properties, *React. Funct. Polym.*, 104, 9-14, 2016.
5. Huang K, Liu Y, Wu D. Synthesis and characterization of polyacrylate modified by polysiloxane latexes and films, *Prog. Org. Coat.*, 77(11), 1774-1779, 2014.

6. Wang X, Shen Y, Lai X. Micromorphology and mechanism of polyurethane/polyacrylate membranes modified with epoxide group, *Prog. Org. Coat.*, 77(1), 268-276, 2014.
7. Miklečić J, Blagojević S L, Petrič M, et al. Influence of TiO₂ and ZnO nanoparticles on properties of waterborne polyacrylate coating exposed to outdoor conditions, *Prog. Org. Coat.*, 89, 67-74, 2015, .
8. Sheng X, Xie D, Wang C, et al. Synthesis and characterization of core/shell titanium dioxide nanoparticle/polyacrylate nanocomposite colloidal microspheres, *Colloid Polym. Sci.*, 294(2), 463-469, 2015.
9. Bao Y, Shi C, Yang Y, et al. Effect of hollow silica spheres on water vapor permeability of polyacrylate film, *RSC Adv.*, 5(15), 11485-11493, 2015.
10. Liu J, Ma J, Bao Y, et al. Polyacrylate/surface-modified ZnO nanocomposite as film-forming agent for leather finishing, *Int. J. Polym. Mater. Polym. Biomater.*, 63(16), 809-814, 2014.
11. Liu J, Ma J, Bao Y, et al. Nanoparticle morphology and film-forming behavior of polyacrylate/ZnO nanocomposite, *Compos. Sci. Technol.*, 98(16), 64-71, 2014.
12. Kang Q, Bao Y, Li M, et al. Effect of wall thickness of hollow TiO₂ spheres on properties of polyacrylate film: Thermal insulation, UV-shielding and mechanical property, *Prog. Org. Coat.*, 112, 153-161, 2017.
13. Bao Y, Feng C, Wang C, et al. One-step hydrothermal synthesis of hollow ZnO microspheres with enhanced performance for polyacrylate, *Prog. Org. Coat.*, 112, 270-277, 2017.

A RESEARCH ON THE USE OF ALUMINUM SULPHATE IN PARCHMENT PRODUCTION AND ITS EFFECTS ON AGEING AND COLOR

Nilgün Kayahan Kolan¹, Eser Eke Bayramođlu²

1,2 Department of Leather Engineering, Faculty of Engineering, Ege University, 35100 Bornova-Izmir, Turkey

Abstract. In this study, different proportions 2.5%, 5%, 10% of Aluminum sulfate were used as tanning agents during parchment production. The research was carried out on goat skin and also there were no usage of any tanning agents as control groups. Finished leathers have been exposed to ageing conditions. Before and after ageing color measurements on all finished leathers have been conducted with Konica Minolta CM-3600d brand spectrophotometer. The impacts of the aluminum sulfate utilized in the research on light fastness were also inspected by using an ATLAS-XENOTEST ALPHA+ test instrument. Visible whitening on the color of parchment was observed when tanning process with aluminum sulphate was performed.

1 Introduction

Parchment is a material invented to write on it. It is a material that made by skin of certain animals such as lamb and goat. Firstly, the hair is removed from the skin by liming, then it is cleaned by washing and dried by stretching and rubbing. The importance in carrying and transcription of information made parchment a milestone in science and art history (Bayramođlu and Yılmaz, 2018).

It is known that, citizens of Pergamum are the first community that invent parchment and used it. Also it is supported by historical documents. Moreover, it is indicated that, the name parchment is coming from Pergamum (Dađtaş, 2017; Yıldız,2003). The story of invention of parchment in Pergamum lies within outgrown Pergamum library. The Egyptians who are owners of Alexandria Library have become so jealous about Pergamum library and put a ban on sending papyrus to Pergamum. Thus, citizens of Pergamum invented parchment and developed it (Bayramođlu and Yılmaz, 2018).

Actually, İsmail Araç is the last tanner (87 years old) who produces parchment in a traditional method. İsmail Araç trained two apprentices who become masters through Ahi-order traditional ceremony. The Ahi-order ceremony is performed according to its original style and traditionally symbolized after 107 years and attracted quite a lot of attention (Figure 1). Important endeavors of Journalist Lütfü Dađtaş and Mehmet Gönenç, mayor of Bergama, who are architects of this ceremony, can be traced on the book they published and offered as a cultural service (Dađtaş, 2017).



Figure 1. Traditional Ahi ceremony held in Bergama on 2017 (Photo: Prof. Dr. Eser Eke Bayramođlu).

Parchment is manufactured in this research by applying aluminum sulfate to the pelts with various ratios and light-fastness is examined. Moreover, color values specimens of Parchment manufactured with different methods are measured before ageing process and after 24 hours and 96 hours of ageing processes. According to data obtained and with the use of aluminum sulfate, visible bleaching and temporal variations on light-fastness are determined.

2 Material and Method

2.1 Material

Domestic goat skin, aluminum sulfate, ammonium sulfate, CaCO₃ and Na₂S are used for the process.

2.2 Method

Skins, while they are treated according to Parchment treatment formula, following stages are processed after the liming:

- 1st group is washed after liming and left for drying by stretching.
- 2nd group's lime is eliminated after liming process, it is processed by acids and enzymes, pH 3 is decreased and they are tanned with 2.5% of aluminum sulfate for 12 hours and they are washed and left for drying.
- 3rd group's lime is eliminated after liming process, it is processed by acids and enzymes, pH 3 is decreased and they are tanned with 5% of aluminum sulfate for 12 hours and they are washed and left for drying.
- 4th group's lime is eliminated after liming process, it is processed by acids and enzymes, pH 3 is decreased and they are tanned with 10% of aluminum sulfate for 12 hours and they are washed and left for drying.

Dried parchments are taken from the drying bench, are scraped and their sides are cleaned. Light-fastness Test of specimens of Parchment obtained is done according to EN ISO 105-B02 method whereas Color Measurement Test is done with Konica Minolta CM-3600d model spectrophotometer (In-House Method).

2.2.1 Light-fastness Test

Light-fastness Test is done according to EN ISO 105 B02 Normal: 2002. Discoloring on leathers' colors and leathers' surfaces are observed during the time due environmental impacts. This formation is accelerated with Light-fastness Test and results are obtained.

Test samples are cut and prepared with 1 cm x 4 cm dimensions. Samples prepared are properly placed on panels. Test selected is started according to specialties, after panels are placed by an expert on the ATLAS Xenotest Alpha+ model machine. Samples are treated for 72 hours. Samples taken out from the machine are measured on grey scale and blue scale and fastness degrees are determined.

2.2.2. Ageing Test – Color Change Test

Manufactured Leathers – Light-fastness Test: it is done according to International Standard ISO 17228 ULTCS/IUF 412, concerning Ageing Test and Color Change Test.

Samples of 15 x 15 dimensions are cut from all leather samples for this test. Ageing Test is done in three different ways. These standards are respectively the following: the first one is solely ageing with heat, the second one is ageing with heat and humidity and the third one is ageing with heat

and humidity cycles on different degrees. In this standard, extended general purpose ageing method, 96 hours, 50°C and 90% humidity is applied.

Colors of samples are measured before starting the ageing test with Konica Minolta CM-3600d model spheroidal spectrophotometer. Measurements are processed according to CIE Lab color system. Second Minolta color measurement is done after having applied first standard of ageing test and impacts of ageing are observed. Leather samples are again exposed to ageing process and color is again measured on Minolta. Increase on “L” value indicates an augmentation of brightness and whiteness whereas a decrease on “L” value indicates a diminution of brightness and whiteness. Color measurements are done on different points of 4 different leather samples and mean value of values measured are considered. Only “L” values elaborated, for dyestuff is not used in the research.

2.2.3. Statistical Analyses

Data obtained from color measurement done after the Ageing Test is analyzed with Wilcoxon Signed Ranks Test and Kruskal Wallis Test. Statistical difference before and after the Ageing Test is considered. Besides, color changes observed on the leather with application in different rates of aluminum sulfate to the leather is analyzed with Kruskal Wallis Test.

3 Results and Discussion

Whereas a visible whiteness occurs on leathers tanned with aluminum sulfate, a slight decrease is determined when light-fastness is considered. This difference is not observed among groups which include aluminum sulfate. Results of both grey scale and blue scale are coherent among them (Table 1).

Table 1. Light fastness results of the parchments.

	Groups	Grey scale	Blue scale
0 % Aluminum sulfate	Control 1	4	2/1
	Control 2	4	2/1
	Control 3	5	1
2.5 % Aluminum sulfate	4. Parchment	4	2
	5. Parchment	3	3/2
	6. Parchment	4/5	2/1
5 % Aluminum sulfate	7.Parchment	4/5	3/2
	8. Parchment	4/5	2
	9. Parchment	3/4	4
10 % Aluminum sulfate	10 .Parchment	3/4	4
	11. Parchment	5	4
	12.Parchment	4/5	4/3

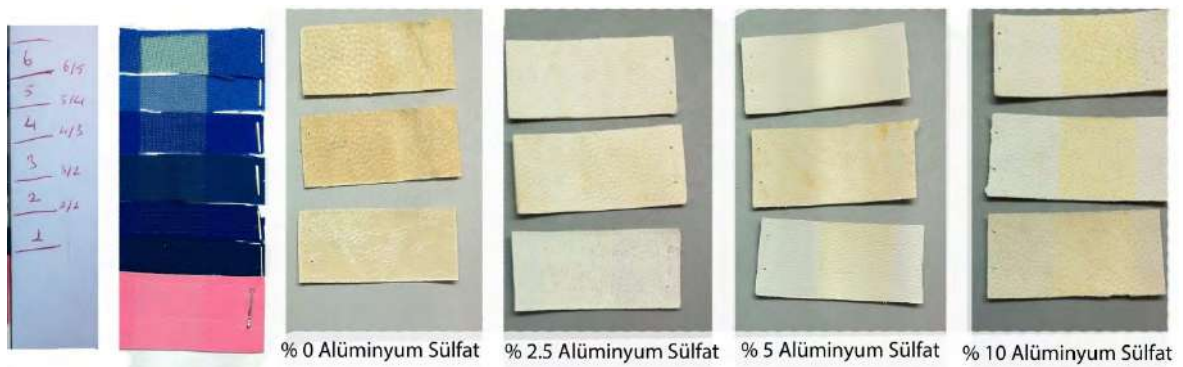


Figure 3. Comparison on blue scale of Light-Fastness Test results.

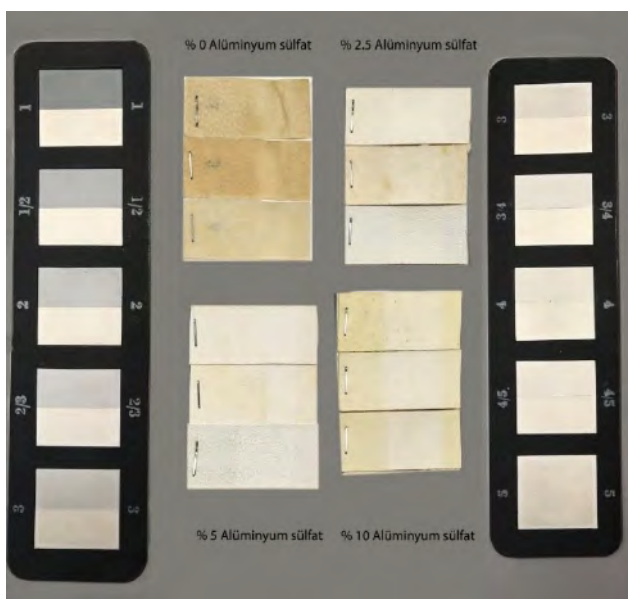


Figure 4. Comparison on grey scale of Light-fastness Test results.

3.1. Ageing Test – Color Change Test Results

Table 2. Color Change Test Results by Minolta.

	Groups	First Measurement	Second Measurement (after the first ageing: 50°C, 90% humidity, 24 hours)	Third Measurement (after the second ageing: 50°C, 90% humidity, 96 hours)
0 % Aluminum sulfate	Control 1	72,35	70,37	70,70
	Control 2	70,47	68,97	69,22
	Control 3	78,95	77,36	77,56
2.5 % Aluminum sulfate	4. Parchment	91,36	90,90	90,36
	5. Parchment	90,07	89,39	89,48
	6. Parchment	92,01	91,8	91,55

5 % Aluminum sulfate	7.Parchment	92,89	92,58	92,16
	8. Parchment	89,62	88,62	88,46
	9. Parchment	91,68	91,33	91,01
10 % Aluminum sulfate	10 .Parchment	92,31	91,83	91,81
	11. Parchment	92,74	92,50	93,37
	12.Parchment	85,53	88,03	88,37

State of specimens of Parchment before and after ageing is observed on figures.

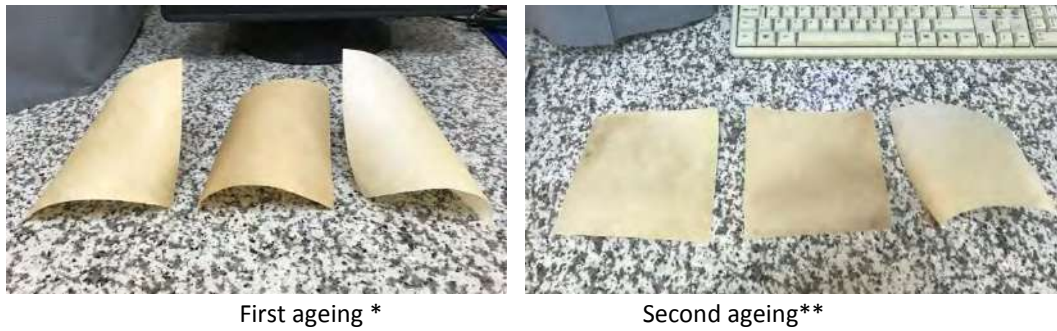


Figure 5. Control 0% Aluminum sulfate.



Figure 6. 2.5 % Aluminum sulfate.



Figure 7. 5 % Aluminum sulfate.



Figure 8. 10 % Aluminum sulfate.

- * **First ageing:** Second Measurement (after the first ageing: 50°C, 90% humidity, 24 hours)
- ****Second ageing:** Third Measurement (after the second ageing: 50°C, 90% humidity, 96 hours)

Discoloration on leather surface, color changes and deterioration on physical forms occurred after the Ageing test (Figure 5,6,7,8)

Statistically significant difference among values read before ageing and after the first ageing is determined ($p < 0.05$); however, no statistical difference is found between the second ageing and the first ageing ($P > 0.05$). Besides, whereas there exists a significant difference ($p < 0.05$) between the Kruskal Wallis Test and the Control Group, in other words parchments which do not include aluminum sulfate and leathers tanned with aluminum sulfate, no significant difference is determined among groups concerning leathers tanned with different rates of Aluminum sulfate ($P > 0,05$).

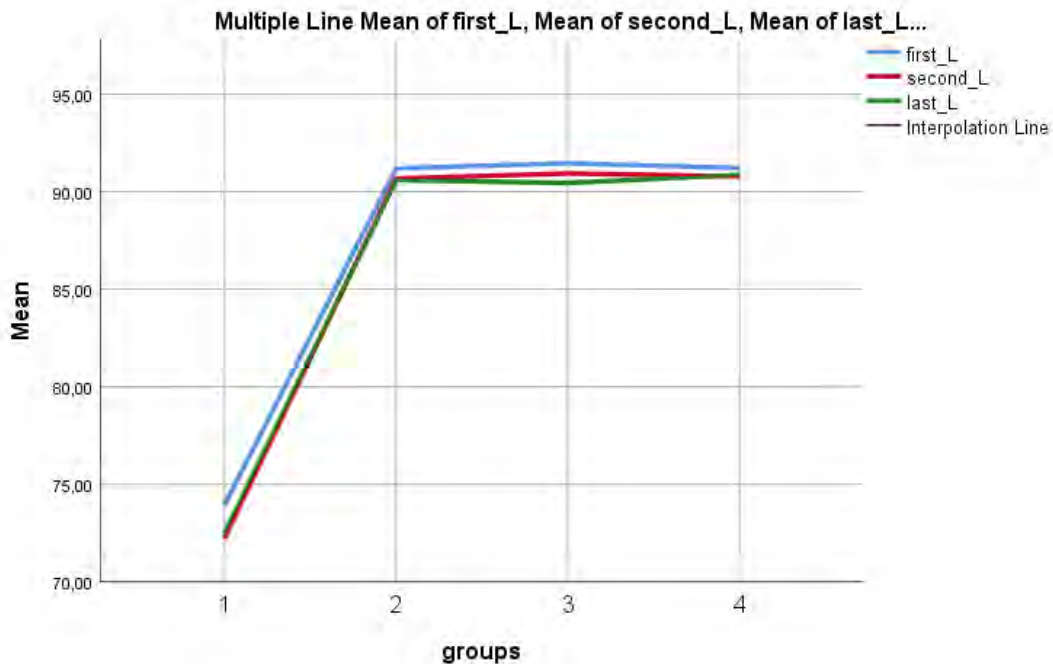


Figure 9. Statistical diagram graph of the color changing before and after ageing.

4 Conclusion

Discoloration and color changes with close rates occurred on all leather groups; however, whereas physical deformation is much more in the control group, we have observed that is lesser on leather samples treated with Aluminum sulfate. Close results are obtained on physical tests applied on leathers tanned in different groups, in terms of leathers treated with 2.5%, 5% and 10% rates. To conclude, we can say that a physical difference occurred between the control group and parchments tanned with Aluminum sulfate but the use in different rates of aluminum sulfate did not generate quite a difference in itself. Significant bleach on the parchment is determined with the use of aluminum sulfate.

Acknowledgement

The authors would like to thank to Nilay Örk Efendioğlu for statistical evaluation. The authors also acknowledge the project of “Industrial Doctorate Program of Textile and Leather–2007 DPT 001” supported by T.R. Ministry of Development.

References

1. Bayramoğlu E.E. and Yılmaz S.,: *Academia Journal of Social Sciences, Special Issue 1, 242-251,2018*
2. *Determination of Light Fastness, EN ISO 105-B02*
3. *Determination of Ageing , TS EN ISO 17228 – 7B*
4. Dağtaş, L.,: *Adını Bergama'dan Alan Pergament ve Anadolu'nun Son Karatabağı Bergamalı İsmail Araç,96 s. 2017*
5. Düzgüneş, O., Kesici, T. ve Gürbüz, F.,: *İstatistik metotları I, Ankara Üniversitesi Ziraat Fakültesi yayınları, no: 861, Ders Kitabı, Ankara, 1983*
6. Yıldız, N.,: *Antikçağ Kütüphaneleri, Arkeoloji Ve Sanat Yayınları, İstanbul,2003*

DEVELOPMENT AND PRACTICAL APPLICATION OF UNHAIRING METHOD WITHOUT USING SULFIDE

K. Takase¹, M. Terashima¹ and K. Yoshimura²

1 Tokyo Metropolitan Leather Technology Center, 3-3-14, Higashisumida, Sumida-ku, Tokyo, 131-0042, Japan, +81-3-3616-1671,a)

takase.kazuya@hikaku.metro.tokyo.jp b) terashima.mariko@hikaku.metro.tokyo.jp

*2 Japan Leather and Leather Goods Industries Association, 1-12-13, Komagata, Taito-ku, Tokyo, 111-0043, Japan, +81-3-3847-1451,
yoshimurak@leather.onmicrosoft.com*

Abstract. Leather manufacturing industry uses a lot of water and chemicals, and it discharges large amounts of wastewater. The processing a large amounts of wastewater requires a huge cost. Therefore, reduction of amount of a pollution load in wastewater is a theme in many countries around the world. During the leather process, a lot of pollutants occur in the unhairing process. Some estimate that the amount of pollution generated in the unhairing process accounts for 70% of the entire leather manufacturing process. In this unhairing process, usually a large amount of sulfide is used. Sulfide is known to generate hydrogen sulfide and cause damage to the drain pipe. In Tokyo, strict criteria are set for draining sulfide to sewers. Therefore, reducing the amount of sulfide used is an important task for tanner. In addition, since sulfide has no degreasing effect, a large amount of surfactant is required in the unhairing process. However, to reduce the cost and the load of the wastewater, it is also required to reduce the amount of the surfactant used. Therefore, development of a method of effectively removing hair loss and degreasing without using a sulfide is urgent for the leather manufacturing industry. On the other hand, pelts are widely used as raw materials for foods such as gelatin and collagen casing, cosmetics, and pharmaceuticals. However, sulfides are not recognized as food additives in Japan. Sulfides are not recognized as food additives in Japan. Therefore, some companies are concerned about using pelts as a raw material for food using sulfide in the unhairing process. Also from this point of view, it is necessary to develop an unhairing method without using sulfides. The method using sodium hydroxide has been studied for a long time. However, this method is hard in handling, and is difficult to set conditions such as concentration and temperature. That is, while successful at the experimental level, it has not been put to practical use. Therefore, we studied a method to solve the above problem using sodium hydroxide. The method developed this time can reduce the pollutant in waste water, and the amount of water used in the unhairing process to 1/10 or less of the conventional one. Moreover, since it is not influenced by water temperature, it made it possible to stably remove hair irrespective of the season. The finished leather kept sufficient strength. In addition, sodium hydroxide reacts with fat in the skin and turns it into soap, so it shows the degreasing effect and contributes to reduce the dosage of degreasing agent.

1 Introduction

At present, production with reduced environment load is one of the most important issues for the manufacturing industry. In reducing environment load, there are various issues such as resource saving, effective use of waste, and the use of safe substances in the manufacturing process. Emphasis on reducing environment load affects the evaluation criteria of companies and may change consumers' buying behavior.

Also for tanners, it is required to make products with reduced environment load. The environment-friendly issues in the leather manufacturing industry include various things such as resource saving, water saving, reduction of wastewater pollution load, efficient wastewater treatment, and effective use of waste. In particular, in order to continue making leather stably even in developing countries where wastewater treatment facilities are not sufficiently developed, establishing a recipe that contains less waste and is easy to treat wastewater is an extremely important issue .

However, these problems span each process, and it is extremely difficult to solve them at one time. Also, among these tasks, there are many that are difficult to cope with immediately. For

example, when there is no substitute, or when there is a cost increase. Nevertheless, environmental-friendly corporate activities are a global trend, and the formulation of measures is urgently needed.

In this study, we focused on the unhairing process, which is considered to have the highest wastewater pollution load among the leather making processes, and examined methods to minimize the load in this process.

In the unhairing process, it is said that it accounts for 70% of the wastewater pollution drained in the leather making process. By reducing the wastewater pollution in this process, the reduction effect of the whole process can be expected. The treatment of the wastewater generated in the unhairing process is one of the difficult problems. The cause of the high wastewater pollution load in the unhairing process includes the use of sodium sulfide and sodium hydrosulfide. Sodium sulfide has long been used in the unhairing process. It is considered that the cost of medicine is lower than other methods, and it is easy and effective. However, iodine consumption is greatly increased by using sodium sulfide. When a sulfide is used, it is about 20,000 mg/L. On the other hand, in Japan's sewers, drainage standards are set at less than 220 mg / L. The reference value of the iodine consumption is determined because, if the value is high, hydrogen sulfide generated from the waste water is oxidized to change to sulfuric acid. The generated sulfuric acid corrodes due to chemical reaction such as metal and concrete, which causes a big problem in maintaining and managing the sewerage. If the corrosion and deterioration of the pipeline facilities proceed, not only the maintenance cost will increase but also the loss of the pipe will cause the depression of the road and the contamination of ground water. In order to reduce iodine consumption, it is known that the oxidation method by aeration processing is effective. However, aeration of wastewater with high iodine consumption may generate toxic gas such as hydrogen sulfide. Therefore, it may cause problems at the sewage treatment plant. Sodium sulfide is disliked also from this point.

It is conceivable that the most reliable way of suppressing the generation of hydrogen sulfide is not to use sodium sulfide. A variety of enzymatic unhairing methods have been investigated as an alternative method that does not use sulfides. Since enzyme unhairing generally does not dissolve hair, reduction of COD and BOD other than iodine consumption can be expected. However, the fallen hairs need to be recovered and become an obstacle in the operation. In addition, since the hair is removed by loosening the hair roots, no effect can be expected on skins without reticular layers such as pigs.

On the other hand, the hair removal method by sodium hydroxide has been studied for a long time. Although, the formulation used in the past is not practical because the amount of water used is so large as 300%, and the drum is loaded. Also, according to our previous experiments, it was extremely difficult to produce stable quality products throughout the seasons, as it is influenced by water temperature when there is much quantity of water. Therefore, in the present study, we investigated the unhairing method for pig skins, using sodium hydroxide and potassium hydroxide with small amount of water.

We applied this method and tried to remove hair and make leather on a pilot scale.

2 Materials and Methods

2.1 Materials

Pig skins were purchased from raw material traders in Tokyo. Sodium hydroxide was used as a commercially available 48% solution (w / w), and potassium hydroxide was used as a 50% solution (w / w) in granular form. For unhairing, these solutions were used undiluted or diluted with a small amount of water.

2.2 Unhairing and tanning prescription

The methods from unhairing to tanning are shown in Table 1. 6.5 to 20% of sodium hydroxide was added per weight of raw hide. The amount added was determined based on the season and temperature. At this time, the molecular weight of potassium hydroxide was about 1.4 times that of sodium hydroxide, so the amount added was also 1.4 times that of sodium hydroxide. In addition, sodium chloride was added for sodium hydroxide and potassium chloride was added for potassium hydroxide in the reaction step in order to suppress skin swelling. Furthermore, in order to establish unhairing conditions, the relationship between the concentration of the aqueous solution and the reaction temperature was examined.

Table 1. Unhairing with sodium hydroxide and tanning process.

Process	Dosage(%)	Chemicals	Temperature(°C)	Time (minutes)
Flush		Water		10
Unhairing	7.5	Sodium hydroxide.aq(48%)	28	40
	10	Sodium chloride	28	60
Flush				5
Liming	250	Water	25	
	3.0	Slaked lime		
	0.4	Surfactant		180
Stirring				30
Flush				5
Deliming	100	Water	32	
	3.0	Ammonium chloride		
	0.4	Surfactant		30
Flush				5
Pickling	10	Water	25	
	6.0	Sodium chloride		10
	0.4	Surfactant		
	6.0	Formic acid		
		1/3		10
		1/3		10
		1/3		60
Tanning	8.0	Chrome tanning agent	30	
	1.6	Sodium hydrogen carbonate		
		1/3		10
		1/3		10
		1/3		20
	0.1	Antifungal agent		
Stirring				30
pH adjustment	1.0	Sodium hydrogen carbonate	25	20
Horse up				

2.3 Physical property measurement

Tensile strength, elongation and tear strength of the leathers made from the above-mentioned recipe were measured based on JIS K 6550 (Japanese Industrial Standards). Six pig leathers were prepared for the test. For each leather, six test samples were cut out for each test from the site defined by JIS K 6550. That is, the test sample was 6 sheets × 6 points / sheet = 36 points. The same test was also performed on leathers made of depilated skin using sodium sulfide and sodium hydrosulfide.

3 Results and Discussion

3.1 Results of unhairing

Unhairing was completed approximately 40 minutes after adding sodium hydroxide. Figure 1 shows the appearance of pelt after unhairing has been completed. Pelts depilated with sodium hydroxide had a higher degree of whiteness compared to the one using sulfide (Figure 2). This may be due to the low sulfur content. This feature is considered to be advantageous for making white or light colored leather.



Fig. 1. The appearance of pelt after unhairing



Fig. 2. Pelts depilated with sodium hydroxide

3.2 Relationship between sodium hydroxide concentration and reaction temperature

The relationship between the sodium hydroxide concentration and the reaction temperature was examined based on the successful depilatory recipe. As a result, it was shown that the relationship is almost linear (Figure 3). It is thought that unhairing will be successful near the straight line.

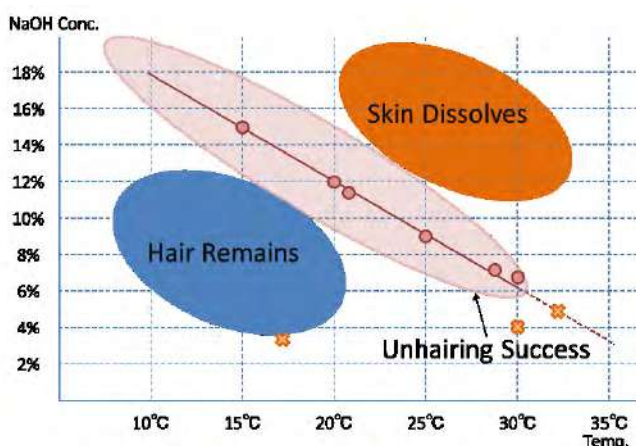


Fig. 3. Relationship between the sodium hydroxide concentration and temperature

3.3 Physical property (tensile strength, elongation, tear strength)

The results of physical property measurement are shown in Table 2. The numbers in parentheses indicate the standard deviation.

The difference between the two was tested by t-test. The tensile strength was not significantly different at a t value of $0.07274 > 0.05$. As for the elongation, there was a significant difference between the two at a t value of $2.4332 \times 10^{-17} < 0.05$. Tear strength was significantly different between the two at a t value of $2.1342 \times 10^{-8} < 0.05$. That is, there was no significant difference in tensile strength between the two. On the other hand, regarding the elongation and tear strength, the leather made of sodium hydroxide was shown to be easy to stretch and flexible, and to be superior in tear strength.

Table 2. Effect of the chemicals for unhairing on physical properties

Chemicals for unhairing Test item (unit)	Sodium Hydroxide	Sodium Sulfide
Number of sample	36	36
Tensile Strength (MPa)	10.6(2.1)	11.7(3.1)
Elongation (%)	54.2(10.8)	36.2(7.8)
Tear strength (N/mm)	24.1(2.8)	19.2(3.6)

4 Conclusion

We have developed a different method of unhairing. That is, a method using sodium hydroxide with small amount of water for pig skins. The features of the method developed this time are water saving, shortening of the unhairing process, simplification of wastewater treatment and reduction of degreasing agent usage. Methods developed in the past used a large amount of water, with a float of 300%. Therefore, it was extremely difficult to control the temperature, and it was hard to stably remove hair using only sodium hydroxide.

As mentioned above, in this formulation, when the water temperature exceeded 20 °C., the pelts tended to become weak. Moreover, when the ratio of the float was large, the skin swelled in alkali, and it was not avoided that the grain of the skin was damaged. These problems could be achieved by using a high concentration sodium hydroxide solution and reducing the amount of float. At this

time, since a commercially available liquid medicine was used as a stock solution or diluted with a small amount of water, the float was about 30%, and it was possible to significantly reduce the amount of water used. Also, the time required for unhairing could be significantly reduced compared to sodium sulfide.

The sodium hydroxide used in the unhairing process reacts with the fat in the skin and turns into a soap, so that a degreasing effect was also exhibited. In particular, pig skin is more fat than other animal species.

Therefore, a large amount of surfactant is required for degreasing, which causes an increase in manufacturing cost. Since it is possible with inexpensive sodium hydroxide, cost reduction can also be expected.

In the prescription used this time, the bating process using an enzyme was omitted. In general, it is considered that, by performing bating, it is possible to make the leather flexible, stretchable, and smooth grain. Although the smoothness of the grain was not examined, the elongation showed a high value as compared with that of the depilated by sodium sulfide. That is, it has been suggested that a leather with high elongation can be produced without the bating process. Also in this respect, it has been shown that the use of sodium hydroxide can contribute to simplification of the working process. By applying this method, it may be possible to make leather in a way with less environmental load than the recipe we implemented this time.

From now on, by examining the effective utilization of wastewater, we would like to realize saving of water in the leather making process and reduction of wastewater treatment cost.

It is also possible to make gelatin and collagen peptide from pelts that has been depilated by this formulation, and it can be expected to make food safer than before. We plan to develop this matter as well.

EFFECT OF GRAPHENE OXIDE ON THE THERMAL PROPERTIES OF BOVINE HIDE POWDERS

Lan Luo, Hao Zhang, Jie Liu*, Keyong Tang*

College of Materials Science and Engineering, Zhengzhou University, Henan Zhengzhou, 450001.

a) Corresponding author: liujie@zzu.edu.cn, kytangzzu@hotmail.com

b) other authors: xixiliyaxue@163.com, 1825604345@qq.com

Abstract. Graphene oxide (GO) is one of the most interesting two-dimensional nanomaterials in recent years. In order to explore its potential application in leather making process, a study on evaluating the effects of GO on the thermal stability and thermal decomposition kinetics of bovine hide powders (HP) was performed by thermogravimetry. The results revealed that GO-doped hide powders (GO-HP) exhibit better thermal stability than those of raw hide powders. The kinetic and mechanism of the decomposition process were analyzed by using an integrated procedure involving model-free methods and universal master-plots method. Three methods were employed to determine the apparent activation energy of the samples, including the Flynn-Wall-Ozawa (FWO), Modified Kissinger-Akahira-Sunose (MKAS), and Friedman methods. The activation energy values of HP and GO-HP samples were found to be 240.45 and 184.66 kJ/mol, respectively. Comparison of the experimental and theoretical master plots of various reaction mechanisms indicated that when the conversion values are below 0.5, the most probable decomposition mechanism for both HP and GO-HP is One-dimensional diffusion (D1). Above 0.5, the decomposition mechanisms of HP and GO-HP are most probably described by Random Nucleation and nuclei growth (A3) and Phase boundary controlled reaction (R3) models, respectively.

Keywords. Graphene oxide, hide powder, thermal kinetic, activation energy

1 Introduction

Collagen is the most abundant structural protein in hides and skins, which has a rod-like triple-helical structure. The multilevel hierarchical structure of collagen and the presence of crystallization zone help to stabilize collagen fiber. However, when heated to a certain temperature, the triple helix chain is transformed into a disordered structure and denaturation occurs. Generally, when raw hides and skins are heated to above their denaturation temperature, they will shrink and a reduction of the area of collagen materials can be observed. For leathers, several tens or more than one hundred degrees centigrade could also induce irreversible denaturation, although collagen fibers were crosslinked by tanning agents. Higher temperatures will further result in decomposition and pyrolysis of leather. Therefore, improving the thermal stability of leather has been an important purpose during leather production. To achieve this goal, one should preferably have in-depth understanding of the thermal degradation kinetics and mechanism before any attempts are made to enhance the thermal stability of leather. Kronick et al. studied the thermal deformation behaviour of bovine skin collagen, and proposed that raw skin contains two different types of collagen [1]. Sundar et al. studied the effect of copolymer dispersions on properties of leather, they found that thermal stability increased with the increase of ionic content of dispersion [2]. Olivares et al. studied the effect of sodium montmorillonite on the thermal stability on leather [3].

Graphene oxide (GO) can be obtained by oxidation of graphene using strong acid and has the similar structure to graphene, which contains a two-dimensional network structure. It differs from graphene in the surface which contains more oxygen-containing functional groups such as -OH, C=O, and -COOH. As a result, GO is highly amphiphilic and can soluble in water and organic solvents, but the presence of these functional groups will also destroy the large π bond on the surface, reducing the electron transporting ability [4]. Also due to the presence of these reactive polar

groups and adsorbed water molecules on the surface of the graphene oxide, the single layer graphene oxide is thicker than the single layer graphene.

The use of graphene oxide as reinforcing filler can bring about improvements in mechanics, electricity, and thermal stability for polymer composites. Many researchers have studied the effect of GO on different kinds of polymers. Mo et al. [5] modified graphene oxide with cetyltrimethylamine and then added it into polyacrylic acid, resulting in composites with better conductivity. Kai et al. [6] filled polycaprolactone (PCL) with graphene oxide and found that the thermal stability and mechanical properties of PCL were significantly improved. In this work, GO was incorporated into hide fibers in order to improve their thermal properties. The activation energies of thermal decomposition of the fibers were first evaluated using several model-free methods, and then the degradation mechanisms were further analyzed using the master-plots method.

2 Materials and Experiences

Hide powders (HP) used in this work was prepared in our laboratory using delimed bovine split hide as the raw materials. Graphene oxide dispersion (0.05mg/ml) was purchased from Jining Leadernano Tech. Co., Ltd., China. GO doped hide powders (GO-HP) were fabricated by immersing hide powders into GO dispersions under gently magnetic stirring for 24 h. After washing in distilled water for several times, the fibers were freeze-dried and conditioned in a desiccator over silica gel for 1 week before analysis.

Thermogravimetry tests were performed on a Mettler Toledo thermogravimetric instrument (TGA/DSC 1), which allowable range of sample quality is 8-15mg. In each test, around 10 mg of GO-HP sample was spread uniformly on the bottom of the alumina crucible. The pyrolysis experiments were performed at heating rates of 5, 10, 20, and 30 °C/min in a dynamic high purity nitrogen flow of 40 ml/min. The temperature of the furnace was programmed to rise from room temperature to 600 °C.

2.1 Kinetic methods

ICTAC Kinetics Committee recommends the appropriate ways for calculating kinetic data and kinetic computations like apparent activation energy (E), pre-exponential factor (or the frequency factor, A) and mechanism function [7]. The single-step kinetic equation of solid sample at isothermal prerequisite is described as Eq. (1).

$$\frac{d\alpha}{dt} = k(T)f(\alpha) \quad (1)$$

Where α is the extent of conversion (Eq. (2)), and m_t , m_0 , and m_f are the weight at time t , initial and final mass of the sample, respectively.

$$\alpha = \frac{m_t - m_0}{m_f - m_0} \quad (2)$$

The kinetic constant k can be expressed using the Arrhenius model, which is a function of the temperature with the universal gas constant R and activation energy E .

$$k = Ae^{-\frac{E}{RT}} \quad (3)$$

The kinetic parameters E and A can be determined by differential method. This involves introducing β , the linear heating rate:

$$\beta = \frac{dT}{dt} \quad (4)$$

Thus, substituting for Eq. (3) and (4) in Eq. (1) gives:

$$\beta \left(\frac{d\alpha}{dT} \right) = Af(\alpha) \exp \left(-\frac{E}{RT} \right) \quad (5)$$

which is the commonly used kinetic equation of the heterogeneous reaction.

It is known that the model-free isoconversional or non-isoconversional methods are very useful for estimating apparent activation energy regardless of the reaction mechanism. Three model-free methods were used in this study. Through each given α corresponding to temperatures of the weight loss data at four different heating rates, $\ln(\beta/T^{1.92})$, $\ln(\beta)$ and $\ln(d\alpha/dt)$ against $1/T$ can be straight lines and the apparent activation energy can be calculated from the slope.

$$\ln \left(\frac{\beta_i}{T_{\alpha,i}^{1.92}} \right) = Const - 1.0008 \left(\frac{E_\alpha}{RT_\alpha} \right) \quad (6)$$

$$\ln \beta_i = Const - 1.052 \left(\frac{E_\alpha}{RT_\alpha} \right) \quad (7)$$

$$\ln \left(\frac{d\alpha}{dt} \right)_\alpha = \ln [f(\alpha)A_\alpha] - \frac{E_\alpha}{RT_\alpha} \quad (8)$$

2.2 Generalized master plots method

The generalized time (θ), introduced by Ozawa, was used for the universal master plots and was valid for experimental data recorded under any heating profile [8], which was defined as:

$$\theta = \int_0^t e^{(-E/RT)} dt \quad (9)$$

Another form can be obtained by differentiating Eq. (9):

$$\frac{d\theta}{dt} = e^{(-E/RT)} \quad (10)$$

The substitution of Eq. (10) into Eq. (1) leads to:

$$\frac{d\alpha}{d\theta} = Af(\alpha) \quad (11)$$

$\alpha=0.5$ was used as a reference point, then Eq. (11) becomes:

$$\frac{d\alpha/d\theta}{(d\alpha/d\theta)_{0.5}} = \frac{f(\alpha)}{f(0.5)} \quad (12)$$

Eq. (12) indicates that, for a given α , the expression $(d\alpha/d\theta)/(d\alpha/d\theta)_{\alpha=0.5}$ would be equivalent to $f(\alpha)/f(0.5)$. From Eq. (10) and (11), the relationship between the generalized reaction rate and the experimental data can be established:

$$\frac{d\alpha/d\theta}{(d\alpha/d\theta)_{0.5}} = \frac{d\alpha/dt}{(d\alpha/dt)_{0.5}} \frac{e^{(E/RT)}}{e^{(E/RT_{0.5})}} \quad (13)$$

where $T_{0.5}$ is the temperature corresponding to $\alpha=0.5$. This function implied that the experimental mater plots need a predetermined activation energy value under non-isothermal conditions. Table 1 lists the most frequently used reaction models and functions, including the recently proposed random scission model [8].

Table 1. $f(\alpha)$ kinetic functions for the most frequently used reaction mechanisms of solid state processes.

Symbol	Reaction mechanism	$f(\alpha)$
A2	Random Nucleation and nuclei growth (Avrami-Erofeev, n=2)	$2(1-\alpha)[- \ln(1-\alpha)]^{1/2}$
A3	Random Nucleation and nuclei growth (Avrami-Erofeev, n=3)	$3(1-\alpha)[- \ln(1-\alpha)]^{2/3}$
A4	Random Nucleation and nuclei growth (Avrami-Erofeev, n=4)	$4(1-\alpha)[- \ln(1-\alpha)]^{3/4}$
An	Random Nucleation and nuclei growth	$n(1-\alpha)[- \ln(1-\alpha)]^{(n-1)/n}$
D1	One-dimensional diffusion	0.5α
D2	Two-dimensional diffusion (Valensi)	$[- \ln(1-\alpha)]^{-1}$
D3	Three-dimensional diffusion (Jander)	$3(1-\alpha)^{2/3}/2[1-(1-\alpha)^{1/3}]$
D4	Three-dimensional diffusion (Ginstling - Brounstein)	$(3/2)[1-(1-\alpha)^{1/3}]^{-1}$
F1	First-order reaction	$1-\alpha$
F2	Second-order reaction	$(1-\alpha)^2$
F3	Third-order reaction	$(1-\alpha)^3$
R2	Phase boundary controlled reaction (contracting area)	$2(1-\alpha)^{1/2}$
R3	Phase boundary controlled reaction (contracting volume)	$3(1-\alpha)^{2/3}$
L2	Random scission	$2(\alpha^{1/2} - \alpha)$

3 Results

The thermogravimetric experiments were carried out at four different heating rates (5, 10, 20 and 30 °C/min) at an inert atmosphere of nitrogen. The continuous shift of TG and DTG curves to higher temperatures can be observed with the increase in heating rate. This is typical for all nonisothermal experiments within a range of heating rate due to the existence of temperature gradient throughout the cross-section of the samples. From Fig. 1 and Fig. 2, the thermal decomposition process of both HP and GO-HP can be divided into three stages of weight loss for a heating rate of 10°C min⁻¹ in the temperature range from room temperature to 600 °C. The first stage goes from room temperature to around 150°C. There are many hydrophilic groups on collagen molecules, which will inevitably absorb a certain amount of water during storage. This weight loss stage is most likely due to the evaporation of water absorbed from the fibers. The second stage, from 150 to 550°C, showing the obvious weight loss corresponding to the main composition of the collagen fibers. A high DTG peak can be found at around 330°C. A small shoulder peak appeared on DTG curves of HP at about 230°C. A more prominent shoulder peak can be observed at about 200°C on DTG curve of GO-HP. This could be attributed to the degradation of free GO, as reported by Song et al. [9] and Guo et al. [10]. The third stage, from 550 to 600°C, is the slow decomposition of carbonaceous matters accounting for less than 5% of the total mass loss.

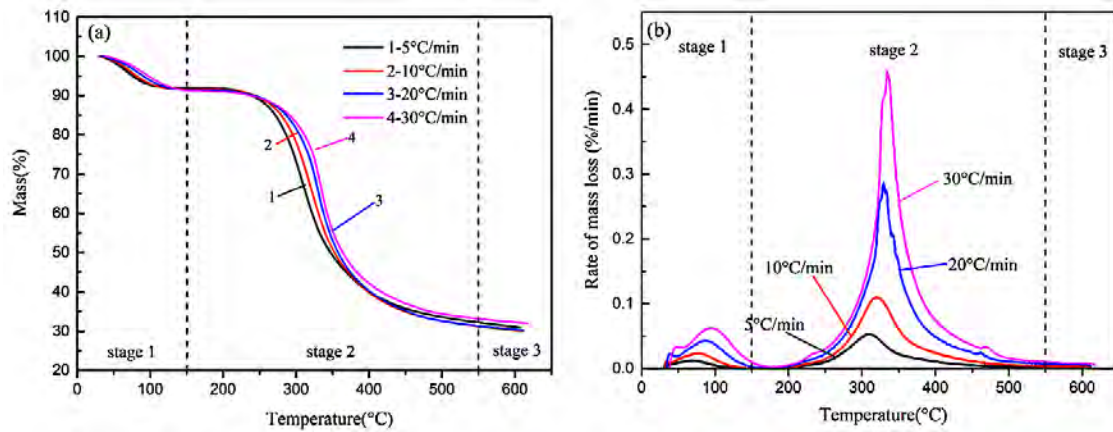


Fig. 1. (a) TG and (b) DTG curves of HP at heating rates of 5, 10, 20, 30°C /min.

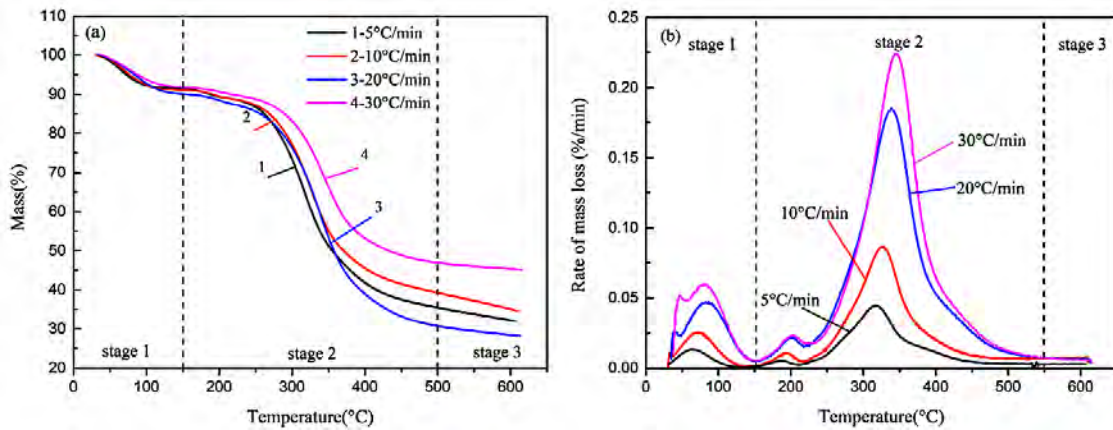


Fig. 2. (a) TG and (b) DTG curves of GO-HP at heating rates of 5, 10, 20, 30°C /min.

Fig. 3 shows a comparison of the TG and DTG curves of HP and GO-HP at a heating rate of 10°C/min. In order to further evaluate the effect of GO on thermal stability of hide fibers, we considered the temperature of the maximum rate of degradation as the decomposition temperature (T_{max}), onset temperature of decomposition (T_{onset}), the temperature of the degradation process at which 50% weight loss occurs ($T_{50\%}$) and the solid residues remaining at 600°C (Table 2). It can be found that the T_{onset} and T_{max} , which are considered as indicators for structural destabilization of polymers, increased after the incorporation of GO into the hide fibers. The $T_{50\%}$ value of GO-HP is higher than that of the HP, suggesting that GO can delay the degradation of hide fibers and improve the thermal stability in the initial stage of thermal decomposition. The improvement of thermal stability of hide fiber is more likely related to the strengthening effect of GO, which can restrict the molecular mobility of the macromolecular (collagen) chains in the solid state.

Table 2. The temperature corresponding to the onset temperature of the main degradation (T_{onset}), maximum rate of mass loss (T_{max}), the temperature corresponding to 50% mass loss ($T_{50\%}$) and the residue at 600°C at a heating rate of 10°C min⁻¹.

Samples	T_{onset} (°C)	T_{max} (°C)	$T_{50\%}$ (°C)	Residues remaining at 600°C (%)
HP	279.17	322.89	353.46	30.13
GO-HP	283.45	326.89	372.51	35.04

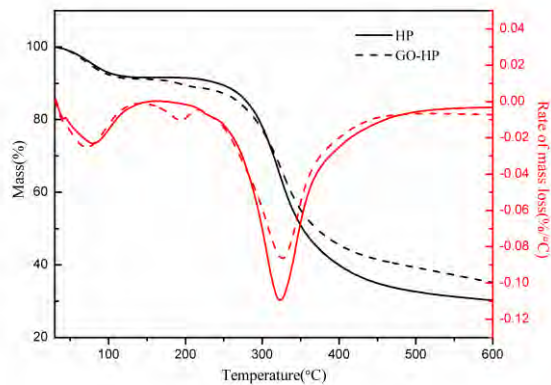


Fig. 3. TG and DTG curves of HP and GO-HP at a heating rate of 10°C /min.

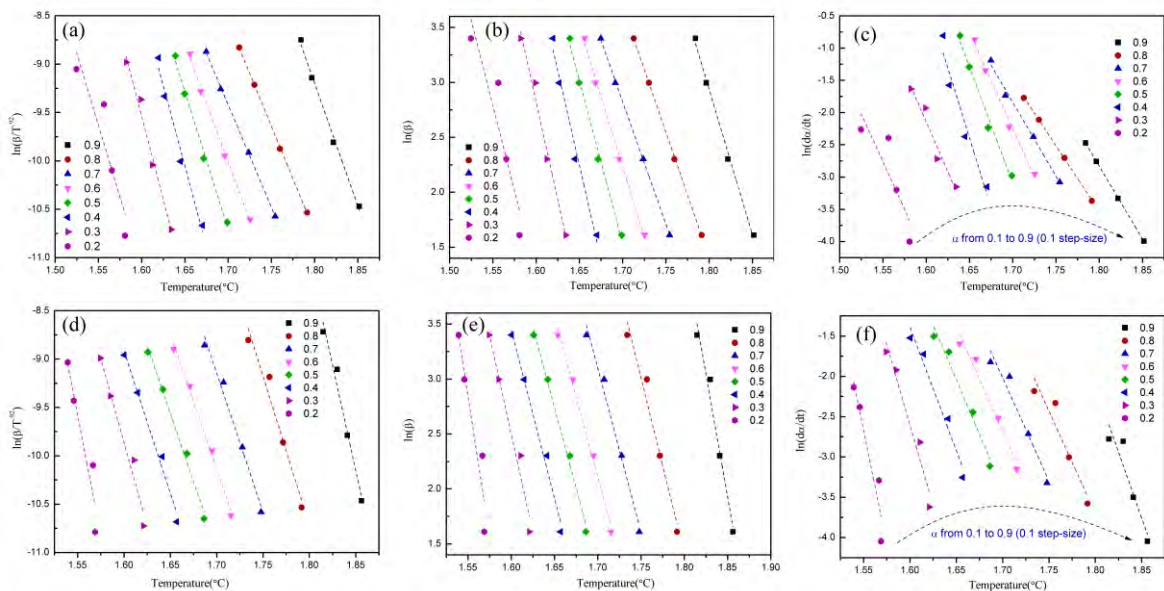


Fig. 4. Typical iso-conversional plots of (a,d) MKAS, (b,e) FWO and (c,f) Friedman methods of (a,b,c) HP and (d,e,f) GO-HP.

Activation energy is considered as a measurement of the energy barrier to a controlling (rate limiting) bond rupture or bond redistribution step. According to the plots of $\ln(\beta/T^{1.92})$, $\ln(\beta)$, and $\ln(d\alpha/dt)$ against $1/T$ (Fig. 4), the linear fitting can be straight lines, and the activation energy values can be obtained from the slopes. The E results of HP and GO-HP obtained by MKAS, FWO and Friedman methods are shown in Table 3. The results calculated based on MKAS method was chosen in the following mechanism analysis, according to the suggestion of Criado et al. [11]. The average thermal degradation activation energy of HP is calculated to be 226.88 kJ/mol, and that of GO-HP is 283.30 kJ/mol. It can be concluded that the incorporation of GO into hide fibers increases the activation energy of thermal degradation of HP by around 25%. From the activation energy results as well as other thermal degradation parameters, it can be concluded that the graphene oxide can enhance the thermal stability of raw hide materials. That may be due to that a large amount of graphene oxide adsorbs on the surface of collagen, forming a protective shell-like structure, which protects collagen from thermal degradation during the heating process.

Table 3 Activation energy (E) results of HP and GO-HP based on MKAS, FWO and Friedman methods.

α	HP (kJ/mol)			GO-HP (kJ/mol)		
	MKAS	FWO	Friedman	MKAS	FWO	Friedman
0.2	247.02	244.77	244.81	412.00	401.70	470.46
0.3	285.45	280.98	257.35	287.40	282.90	331.67
0.4	276.42	272.18	360.32	245.22	242.60	254.12
0.5	236.43	234.01	301.04	233.47	231.27	225.51
0.6	202.42	201.54	248.34	232.38	230.07	216.57
0.7	175.83	176.12	190.97	238.44	235.67	212.91
0.8	180.79	180.65	169.05	256.39	252.52	210.99
0.9	210.65	208.74	187.97	361.08	351.77	271.21
Average	226.88	224.87	244.98	283.30	278.56	274.18

Fig.5 shows the theoretical generalized master plots corresponding to the kinetic models calculated by $f(\alpha)/f(0.5)$ using the expressions in Table 1, and the experimental results obtained at different heating rates. When the conversion is less than 0.5, the model of both HP and GO-HP is close to the D1, indicating that the degradation mechanism of them refers to one-dimensional diffusion model. However, when $\alpha > 0.5$, degradation of HP is most probably regulated by random nucleation and nuclei growth (A3), and GO-HP changed the kinetic model to phase boundary controlled reaction (R2). Liang et al. [12] reported a similar degradation model of graphene nano-platelets composite materials. The results of the present study provide useful information for fabricating high-performance leather.

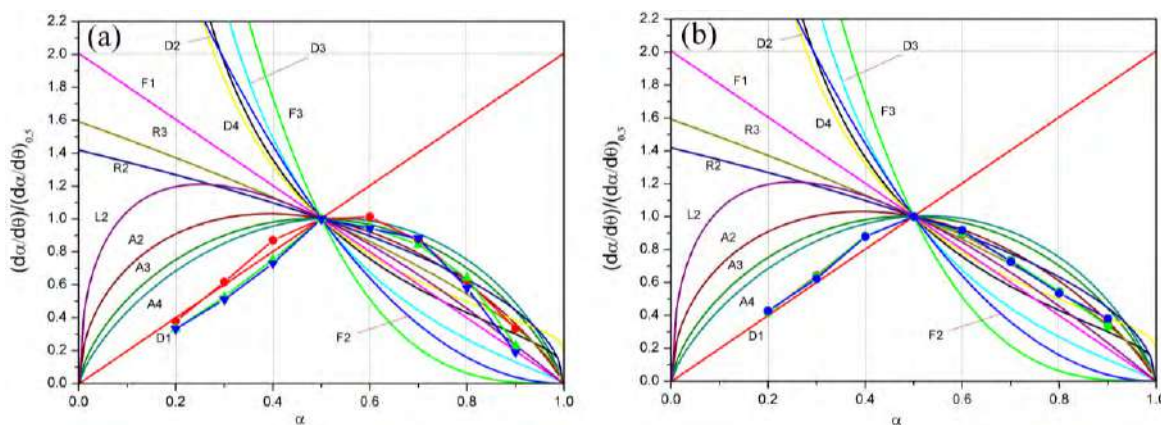


Fig. 5. Master curves and experimental data obtained for (a) HP and (b) GO-HP at different heating rates.

4 Conclusions

The thermal degradation process of the HP and GO-HP can be divided into three stages: water loss stage, thermal degradation stage and slow decomposition stage. The obtained GO-HP sample shows an enhancement in the thermal properties in the temperature range from room temperature to 600 °C. The isoconversional kinetic study of the thermal decomposition was performed using Flynn-Wall-Ozawa (FWO), Modified Kissinger-Akahira-Sunose (MKAS), and Friedman methods. The

most probable mechanism of thermal decomposition was suggested by comparison between experimental and theoretical master plots. The reaction model for both HP and GO-HP is D1 when the α is less than 0.5. When $\alpha > 0.5$, the degradation models for HP and GO-HP are corresponding to A3 and R2, respectively.

References

1. Paul Kronick, Beverly Maleeff & Robert Carroll.: 'The Locations of Collagens with Different Thermal Stabilities in Fibrils of Bovine Reticular Dermis', *Connect. Tissue Res.*, 18,123-134, 2009.
2. Steffen Maier, Alexander Sunder, Holger Frey et al.: 'Synthesis of poly (glycerol) - block - poly(methyl acrylate) multi-arm star polymers', *Polymer Crystallization*, 21, 226-230, 2000.
3. G.Sanchez-Olivares, A.Sanchez-Solis, F.Calderasb, et al.: 'Sodium montmorillonite effect on the morphology, thermal, flame retardant and mechanical properties of semi-finished leather', *Appl. Clay Sci.*, 102, 254-260, 2014.
4. P. Budrugaec, Andrei Cucos, Lucreția Miu.: 'The use of thermal analysis methods for authentication and conservation state determination of historical and/or cultural objects manufactured from leather', *J. Therm. Anal. Calorim.*, 104, 438-450, 2011.
5. Jinpeng Mo, Wenshi Ma, Guorong Qiu et al.: 'Mesoporous silica coated graphene oxide: fabrication, characterization and effects on the dielectric properties of its organosilicon hybrid films', *J. Mater. Sci. - Mater. Electron.*, 30, 130-146, 2019.
6. Weihua Kai, Yuuki Hirota, Lei Hua et al.: 'Thermal and mechanical properties of a poly (ϵ -caprolactone)/graphite oxide composite', *J. Appl. Polym. Sci.*, 107, 1395-1400, 2008.
7. Sergey Vyazovkin, Alan K.Burnham, José M.Criado et al.: 'ICTAC Kinetics Committee recommendations for performing kinetic computations on thermal analysis data', *Thermochim. Acta*, 520, 1-19, 2011.
8. Starink MJ.: 'The determination of activation energy from linear heating rate experiments: a comparison of the accuracy of isoconversion methods', *Thermochim. Acta*, 404, 163-176, 2003.
9. Pingan Song, Zhenhu Cao, Yuanzheng Cai, et al.: 'Fabrication of exfoliated graphene-based polypropylene nanocomposites with enhanced mechanical and thermal properties', *Polymer*, 52, 4001-4010, 2011.
10. Sheng Guo, Gaoke Zhang, Yadan Guo, et al.: 'Graphene oxide-Fe₂O₃ hybrid material as highly efficient heterogeneous catalyst for degradation of organic contaminants', *Carbon*, 60, 437-444, 2013.
11. Criado JM, Pérez-Maqueda LA, Gotor FJ, et al.: 'A unified theory for the kinetic analysis of solid state reactions under any thermal pathway', *J. Therm. Anal. Calorim.*, 72, 901-906, 2003.
12. J.Z.Liang, J.Z.Wang, Gary C.P et al.: 'Thermal decomposition kinetics of polypropylene composites filled with graphene nanoplatelets', *Polym. Test.*, 48, 97-103, 2015.

EFFECTS OF SOLUBLE SOYBEAN POLYSACCHARIDE AS FILLING AGENT ON THE PROPERTIES OF LEATHERS

Zhenye Tang¹, Jide Zhong², Xianqing Feng², Yafei Zhang¹, Yadi Hu¹, Hui Liu¹, Jie Liu¹, Cem Emre Ferah³, Keyong Tang^{1*}

1. School of Materials Science and Engineering, Zhengzhou University, Zhengzhou 450001, P. R. China.

2. Henan Prosper Skin & Leather Enterprise Co., Ltd., Jiaozuo 454791, P. R. China

3. Engineering Faculty, Leather Engineering Department, Ege University, Bornova, Izmir 35100, Turkey.

*Corresponding author: kytangzsu@hotmail.com

Abstract. After a series of chemical treatments and physical operations, the hides are finally turned into leathers. Nowadays, filling is one of the most important processes in leather manufacture, the filled leather has good performances such as fullness, flexible. According to the different ways of operation, the filling methods are generally divided into wet filling and dry filling. Most commonly used fillers are polyurethane resins and acrylic resins for dry filling. However, so few reports have focused on wet filling with polysaccharide macromolecules. In this work, soluble soybean polysaccharide (SSPS) was applied on leather wet filling. SSPS is good in emulsification, and stable emulsion may be formed with the addition of SSPS in fatliquoring agents. Therefore, wet-blue leather was used as raw materials, then retanned and neutralized, fatliquoring and filling with SSPS were carried out at the same time, with different amounts of SSPS, i.e., 1%, 3%, 5%, 7% in weight. Finally, leather samples were dried at room temperature. The effect of SSPS amounts on the thickness, air permeability and water vapor permeability of the crust leather were studied. Also, the tensile property of the leathers filled with SSPS were analyzed. The results indicated that with increasing the amounts of SSPS, the thickness and the water vapor permeability of the leathers increases, while the air permeability decreases. The maximum stress-strain capacity of leathers decreases with increasing the SSPS amount. At the SSPS amount of 3%, the leather is good in softness, as well as in physical and mechanical properties.

1 Introduction

In the process of leather-making, the filling can make the leather feel fuller and the grain surface tighter, and at the same time, the grain layer relaxation and partial loosening surface which may occur in the tanning process can be improved. When the tanners produce leather from hide, the non-collagen components are removed after a series of physical and chemical operations, which causes voids between the fiber bundles^[1]. The purpose of filling is to make the filling agents into the voids, finally make the leather get various properties. Currently, little information has been done for wet filling of leather. Taylor et al. already studied that effect of enzymatically modified protein as filler^[2-4], the results showed that it had no significant effect on properties of leather. Oksana Kozar et al. used natural minerals as filler for shoe upper, this provided a new filling agent for shoe production of leather^[5].

With the development of economy, people are increasing demanding for safe and natural leather products, so it is very important to research natural chemical fillers. A potential development direction of the filling industry is the use of natural, renewable and ecologically friendly soybean polysaccharide as filler. SSPS is an acidic polysaccharide whose backbone consists of long-chain rhamnogalacturonan, short-chain homogalacturonan and neutral sugar of galactose and arabinose as side chains^[6]. In addition, it is found that SSPS has a highly branched structure^[7] and its molecular conformation is global in aqueous solution^[8]. Properties are determined by structure, SSPS has high water solubility, resistance to acid, alkali and temperature, as well as emulsification. The emulsifying properties of SSPS are stable between pH 3 and 7^[9]. Therefore, SSPS can be used with fatliquoring agent in the same process because they can form a stable emulsion and SSPS can enter

the internal space of the collagen fiber bundles with the MK fatliquoring agent together, meanwhile it will not be removed in the subsequent processes.

Mechanical properties are important qualities that determine the final use of leather. The research showed that the effective length stretch increase should be less than 10% [10]. The larger the stretch ratio, the worse the performance of the leather. Tang Keyong and Wu Dacheng reported the stress stain behavior of pigskin [11]. When subjected to stress, the weaker fibers of pigskin were broken first, then the stress was concentrated on the fibers that were not broken until all the fibers broke. The previous papers from our laboratory reported the effect of constant stress and cyclic stress on mechanical properties of leather [12-15]. It is found that the role of force in leather processes has a great influence on leather products and that may benefit tanners to get the desired product by controlling the mechanical operations.

In this paper, we first focused on the amounts of SSPS that may have an impact on the properties of leather. After filling, the leather requires to obtain its final uniformity. the use of soluble soybean polysaccharide as a filler for leather was researched and the effect of filling with SSPS on the thickening ratio, air permeability and water vapor permeability and mechanical properties of leathers were investigated.

2 Materials and Methods

2.1 Preparation of samples

SSPS was kindly provided by Pingdingshan Jinjing Biotechnology Co., Ltd. Wet blue leather was obtained from Henan Prosper Skin & Leather Enterprise Co., Ltd. All samples were cut along the symmetrical area of the leather backbone. Then they were retanned by glutaraldehyde (50% water solution), neutralized with 1%wt NaHCO₃ solution, MK fatliquored and filled with different amounts of SSPS in a five-drum tanning machine (DJD-350, Wuxi Derun Light Industry Machinery factory, China). The obtained leather samples were dried at room temperature. After drying, chose the samples of similar thickness(1.3mm-1.4mm), then the leather samples were stored in a glass dryer at 25°C and 60% RH for 48h according to HG/T 2765.5-2005. All other chemicals were analytical grade and made in China.

There were five different amounts of SSPS for filling: Blank group (0%); 1% SSPS by wet weight of leather (1%); 3% and 5% mean that the amounts of SSPS are 3% and 5% by wet weight of leather samples.

2.2 Thickening ratio

Samples of 10cm× 20cm before filling were marked in the top left corner, The thicknesses were measured with a thousand gauge thickness gauge (Gotech Testing Machines INC., China), and each sample was measured at three points from the top, middle, and bottom of the marked portion. After filling, measured the thickness at the same position. Finally, the thicknesses were averaged. So, the calculation formula of thickening rate was:

$$R(\%) = \frac{T_2 - T_1}{T_1} \times 100 \quad (1)$$

T₂ is the average thickness after filling; T₁, average thickness before filling; R is thickening ratio.

2.3 Air permeability

The round leather samples whose radius was 3.5cm were cut by the sampler. TQD-G1 air permeability testing machine (Labthink instrument co., ltd) was employed to measure the air permeability of different samples. Each sample was measured three times, then averaged as results. The maximum air permeability was tested at pressure difference of 800Pa. The equation for calculating the air permeability was shown as follow:

$$P_s = \frac{V}{\Delta P \times S \times t} \quad (2)$$

P_s is air permeability, ml/(Pa×m²×s); V is the amount of air passing through the sample during the measurement time, ml; ΔP is pressure difference between the two sides of the sample; $S(38.48\text{cm}^2)$ is test area; t is testing time.

2.4 Water Vapor Permeability

Water Vapor Permeability (WVP) was measured by evaporation method, 20ml distilled water was added to the round mouth glass cup. The cup was sealed with leather sample and weighed as W_1 . Then the cup was put into a dryer containing color-changing silica gel and weighed as W_2 24 hours later at 25°C. Then the calculation formula of water vapor Permeability was:

$$\text{WVP} = \frac{W_1 - W_2}{A \times t} \times 10 \text{ (g / (10cm}^2 \times 24\text{h))} \quad (3)$$

Where W_1 is weight of the leather sample and the cup with distilled water before placed into the dryer, W_2 is weight of leather sample and the cup with distilled water after placed into the dryer for 24h, $A(10.179\text{cm}^2)$ is the test area.

2.5 mechanical properties

The mechanical properties of leather samples parallel to the backbone were tested with SMSTA.XT Plus Texture analyzer (Lotun Science Co. Ltd., Britain). According to GB/T 1040.3-2006 standard, the leather samples were cut into dogbone-shaped as shown in figure 1.

Table 1. Size of dogbone-shaped sample.

Position	d	w	e	r
Value(mm)	4	30	75	12.5

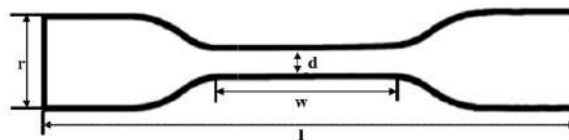


Fig. 1. Schematic diagram of dogbone-shaped sample.

2.6 Scan electron microscopy (SEM) observation

The samples filled with different amounts of SSPS were cut along parallel to the backbone, fixed on the sample stage with conductive adhesive, the samples should keep dry enough, then surface was

sprayed with a thin layer of gold, and finally the cross section was observed with the scanning electron microscopy (JSM-7001F, made in Japan).

3 Results and Discussion

3.1 Effect of filling with SSPS on thickening ratio of leather samples

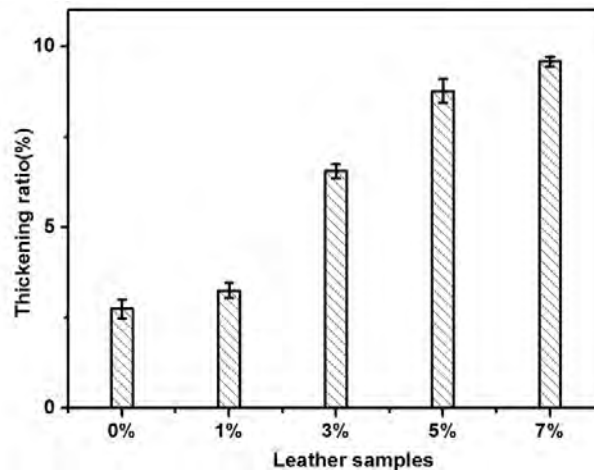


Figure 2. The thickening ratio of different filled leather samples

The leather is woven from collagen fiber bundles. The fiber bundles of partial leather will be loose after soaking, tanning and retanning process. Filling can improve these areas to obtain uniform thickness. Fig. 2 shows that the thicknesses of samples increase when the amounts of SSPS increase, the 0% is effect of fatliquoring agent on thickening ratio. After subtracting the effect of fatliquoring agent on thickness, we found that the effect of SSPS dosage on thickness was non-linear. However, we tested the hand feeling of filled leather and found that 5%, 7% of the samples were poor texture and hard, 0% and 1% of the samples were extremely soft, 3% of the sample ensured the softness and texture.

3.2 Effect of filling with SSPS on air permeability

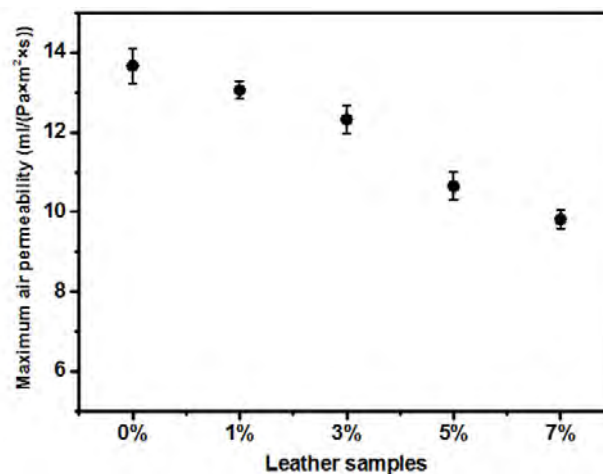


Figure 3. The maximum air permeability of different filled leather samples

The air permeability of leather is mainly determined by the thickness and porosity. Fig. 3 showed that the maximum air permeability of leather samples decreases with the amounts of SSPS increase. The larger amount of filling with SSPS caused the worse air permeability of leather. The reason maybe that filling of SSPS into the gaps of the collagen fiber bundles resulted in a tightly woven structure. And the Leather porosity also reduced. Therefore, the air permeability of the leather is decrease.

3.3 Effect of filling on water vapor permeability

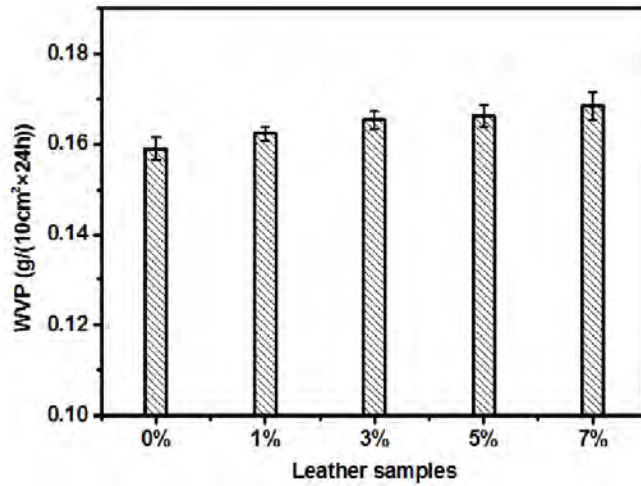


Fig. 4. The water vapor permeability of different filled leather samples.

Many voids between collagen fibers interwoven and the fibers themselves, and many hydrophilic groups on the collagen molecular chain endow the excellent water vapor permeability of the natural leather. The filling also introduced some hydrophilic groups on the molecular chain of SSPS into the leather. It can be seen from fig. 4 that the filling of SSPS increased the water vapor permeability of leather, but it only caused very limited change.

3.4 Effect of filling with SSPS on stress-strain behavior

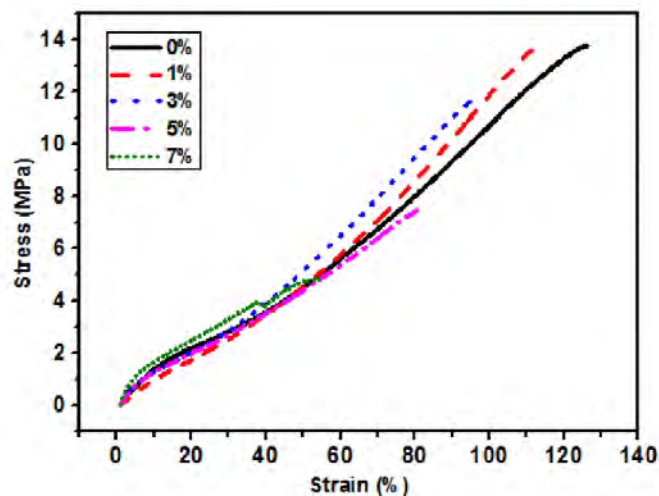


Fig. 5. Stress-strain curves of different filled leather samples.

There are many important mechanical properties on the stress-strain curve of leather. The maximum stress value on the curve is the tensile strength, and the strain at break is the elongation at break, which determines the end use of the leather. Fig. 5 showed that the filling of SSPS reduced the tensile strength and elongation at break of leather. The reason may be that SSPS will cause the fibers to stick together and affect the relative slip motion between the fiber bundles, so causing changes in mechanical properties.

3.5 SEM observation

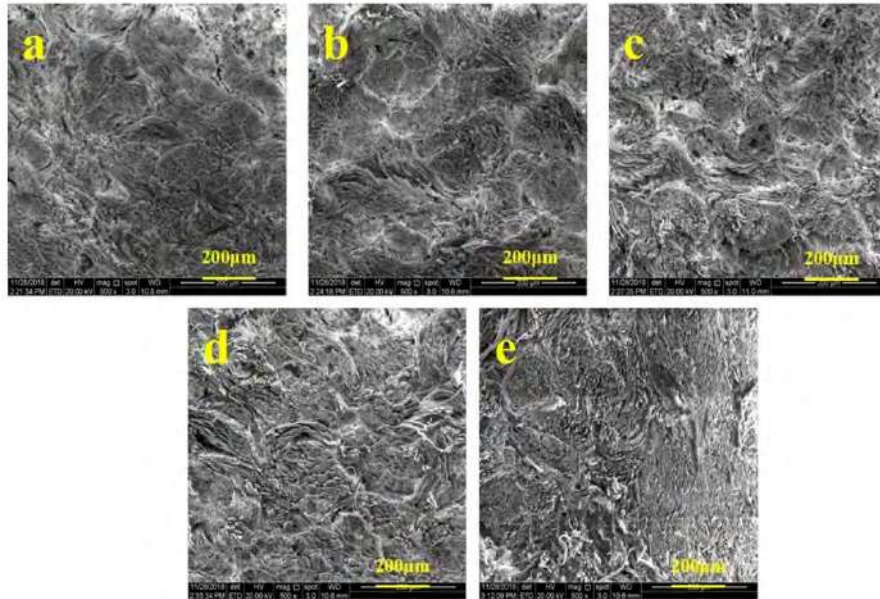


Fig. 6. the SEM microscopy of Cross sections of different filled leather samples (a, blank sample (0%); b, 1%; c, 3%; d, 5%; e, 7%).

Fig. 6 showed the cross sections of the leather fiber structure. In the blank sample, the fiber bundles exhibited a loose structure (figure 1a), the leather fiber bundles were relatively dispersed after retanning and fatliquoring, therefore the leather was soft. We found that as the amounts of SSPS increased, the leather samples became tighter and the fiber bundles were wrapped closer together. The 1% sample was relatively close to the 0%. The reason may be that the amount of the SSPS is less to fill completely the gaps of the collagen fiber bundles. The gaps of 3% sample was narrowed, then the hand feeling test was carried out. It was found that the sample had better texture than the blank sample, which not only maintained good softness, but also made the leather uniform. The collagen fiber bundles of 5% and 7% were severely spliced together. This is mainly because that the amount of SSPS was overfull, resulting in excessive adhesion of collagen fiber bundles.

4 Conclusion

As the filling amount of the SSPS increased, the thickness of leather gradually increased, and the hydrophilic groups on SSPS were the main reason for increased water vapor permeability of leathers, but the porosity of the leather collagen fiber was lowered, so the air permeability was gradually decreased. When it was present in the bundle of collagen fibers, the slip between the fibers becomes difficult, so the more filling amount, the worse mechanical properties. The results show that the optimal dosage of soybean polysaccharide for leather filling is 3%. Therefore, SSPS may be used in the leather filling process to replace polyurethane and acrylic obtained from petroleum as potential filler.

Acknowledgement

This project is financially supported by National Key R & D Program of (ChinaNo.2017YFB0308500) and the National Natural Science Foundation Commission (NO.51673177) are greatly appreciated.

References

1. Liu C K, Latona N P, Lee J, et al. Microscopic observations of leather looseness and its effects on mechanical properties[J]. *Journal of the American Leather Chemists Association*, 2009, 140: 230-6.
2. Taylor M M, Bumanlag L, Marmer W N, et al. Use of enzymatically modified gelatin and casein as fillers in leather processing[J]. *Journal of the American Leather Chemists Association*, 2006, 101(5):169-178.
3. Taylor M M, Marmer W, Brown E. Evaluation of polymers prepared from gelatin and casein or whey as potential fillers[J]. *Journal of the American Leather Chemists Association*, 2007, 102(4):111-120.
4. Taylor M M, Marmer W N, Brown E M. Effect of fillers prepared from enzymatically modified proteins on mechanical properties of leather[J]. *Journal of the American Leather Chemists Association*, 2008, 103(4):128-137.
5. Kozar O P, Mokrousova O, Wozniak B. Deformation characteristics of leather for shoe upper, filled with natural minerals[J]. *Journal of Chemistry and Chemical Engineering (USA)*, 2014, 8: 47-53.
6. Maeda H, Nakamura A. Soluble soybean polysaccharide[M]. *Handbook of hydrocolloids*. Woodhead Publishing, 2009: 693-709.
7. Wang Q, Huang X, Nakamura A, et al. Molecular characterisation of soybean polysaccharides: an approach by size exclusion chromatography, dynamic and static light scattering methods. [J]. *Carbohydr Res*, 2005, 340(17): 2637-2644.
8. Chivero P, Gohtani S, Ikeda S, et al. The structure of soy soluble polysaccharide in aqueous solution[J]. *Food Hydrocolloids*, 2014, 35: 279-286.
9. Nakamura A, Takahashi T, Yoshida R, et al. Emulsifying properties of soybean soluble polysaccharide[J]. *Food Hydrocolloids*, 2004, 18(5): 795-803.
10. Liu C K, Latona N P, DiMaio G L, et al. Viscoelasticity studies for a fibrous collagen material: chrome-free leather[J]. *Journal of Materials Science*, 2007, 42(20): 8509-8516.
11. Tang Keyong, Wu Dacheng. Study on the Stress Strain Behavior of Soft Leather from Pigskin. *China Leather* 1998(6):10-11.
12. Wang Fang, Du Jing, Tang Keyong, Zhao Kang. Effects of Stress State while Dried on Leather Mechanical Properties. *China Leather* 43(3): 31-35, 2014.
13. Du Jing, Tang Keyong, Zhao Kang. Influence of Stress State while Dried on the Yield and Water Vapor Permeability of Leathers. *China Leather* (1): 23-28, 2014.
14. Tang Keyong, Du Jing, Wang Fang, He Xichan. Influence of Setting Stress State on Thermostability of Leather and Collagen Fibers. *China Leather* 43(3): 41-43, 2014.
15. Huang J, Liu J, Tang K, et al. Effect of Cyclic Stress while Being Dried on the Mechanical Properties and Thermostability of Leathers[J]. *Journal of the American Leather Chemists Association*, 2018, 113(10): 318-325.

COMPARISON ON THE THERMAL DEGRADATION KINETICS AND MECHANISM OF HIDES BEFORE AND AFTER FORMALDEHYDE-TANNING

Yadi Hu, Lan Luo, Jie Liu, Fang Wang, Haolin Zhu, Keyong Tang*

*School of Materials Science and Engineering, Zhengzhou university
Zhengzhou, Henan 450001 China*

**Corresponding author: kytangzsu@hotmail.com*

Abstract. The thermal degradation kinetics of hides before and after being tanned with formaldehyde were investigated using thermogravimetric analysis (TGA) at four different heating rates of 5, 10, 20, 30°C/min. Such model-free methods as Flynn-Wall-Ozawa and Friedman as well as model-fitting method of Criado were employed to determine the thermal degradation active energy and degradation mechanism. Based on the Flynn-Wall-Ozawa and Friedman methods, the average active energy (E_a) of formaldehyde-tanned leather was 223.1 kJ/mol and 230.7 kJ/mol respectively. Results from general master curves showed diffusion processes in the thermal degradation of formaldehyde-tanned leather. Neither the thermal degradation activation energy nor the degradation mechanism is affected by the formaldehyde tanning. Nevertheless, the results obtained by thermogravimetric analyzer coupled with Fourier transform infrared spectrometry (TG-FTIR) indicated difference in the relative amounts of evolved products. According to the 3D-FTIR analysis, the dominant components of evolved gas for both untanned and tanned hides are CO_2 , CH_4 , H_2O , NH_3 along with small amount of HNCO . However, after formaldehyde tanning, the evolved NH_3 by the decomposition of free $-\text{NH}_2$ groups and peptide $-\text{NH}-$ groups from different amino acids and CH_4 by the cleavage of $-\text{CH}_3$ and $-\text{CH}_2-$ in collagen slightly increases.

Key words: Formaldehyde-tanned leather, Thermal degradation kinetics, TG-FTIR, Evolved gases

1 Introduction

Tanning process can convert collagen in raw hides into stable fibre structure (leather) due to formation of additional cross-links [1]. Aldehyde and vegetable tanning agents have already been applied to produce leather in ancient China. Nowadays, chrome tanning agent is the most frequently used in leather industry [2, 3]. Since formaldehyde tanning agent is cheaper and cleaner than vegetable tanning agent [4] and leather tanned with formaldehyde exhibits excellent sweat resistance, laundry resistance and alkali resistance, it is still used in fur skin tanning. However, comparing with chrome-tanned leather, the thermal stability of leather tanned with formaldehyde is poor because the combination of collagen in leather with formaldehyde is weaker than that with chrome [5]. For this reason, formaldehyde-tanned leather will likely decompose under certain conditions. Generally, thermal stability is an extremely significant indicator during use and processing of leather and can be evaluated by Micro hot table (MHT), thermogravimetric analysis (TGA) and differential scanning calorimeter (DSC). Thus, researchers applied these methods in comparing the thermal stability of leather tanned with different agents. Budrugaec P et al [6] found that the shrinkage temperature of combined (vegetable + Cr) tanned leathers is higher than that of vegetable-tanned leathers. Carçote C et al [7] investigated the effect of tannins species on the thermal stability of vegetable leather using micro DSC and found that resistance against deterioration of quebracho calf leather was higher than that of chestnut calf leather. In view of these, tanning effect can be well reflected by thermal stability of leather based on the values of shrinkage temperature (T_d) or denature temperature (T_s). Meanwhile, leather tanned with different tanning agents may show difference in thermal stability due to different combined mechanisms between collagen in leather and tanning agents, which has been confirmed by Onem E et al [8]. In addition, Rosu L et al [9] reported that wet-white leather exhibited lower thermal

stability and temperatures of evolved gases than wet-blue leather and stated that this difference is caused by the nature of used tanning agent.

This paper aims at the study of thermal degradation kinetic and mechanism of leather before and after formaldehyde tanning. Thermal decomposition kinetics may be applied in investigating the theoretical reaction mechanisms and in estimating degradation properties in applications^[10]. Apparent active energy (E_a), pre-exponential factor (A) and mechanism function ($f(\alpha)$) are three elements of thermal degradation kinetics. Wherein E_a was calculated by Flynn-Wall-Ozawa (FWO) and Friedman methods in our paper. Then theoretical reaction mechanisms of samples were identified based on obtained E_a value and Criado method. TG analysis have been proved extremely suitable to calculate the thermal degradation kinetics of materials according to the TG data obtained at different heating rates. Nevertheless, it cannot provide the information of evolved gases during decomposition. Therefore, TG combined with FTIR are also employed to further analyse the degradation mechanism during decomposition. This work established the degradation mechanism of formaldehyde-tanned leather. Furthermore, the main degradation pathway of hides before and after formaldehyde-tanning is also discussed with the help of TG-FTIR analysis.

2 Materials and methods

2.1 Materials

Calf hides after deliming are obtained from Henan Prosper Skin & Leather Enterprise Co., Ltd., Jiaozuo. In order to obtain leather samples, dry calf hides were first soaked in water and then immersed for 2 h in neutral protease solution with concentration of 0.05 wt.% for bating treatment. It is noteworthy that the percentage is based on the weight of hides after soaking in water and the liquid ratio is 1:2. After rinsing a few times, pickling was followed. Before pickling, calf hides should be soaked in a solution containing 7.0 wt.% sodium chloride for 1 h to avoid acid swelling. Pickling was performed using 2.0 wt.% sulfuric acid solution (1mL, 98.0 wt.% sulfuric acid diluted with 10 mL distilled water). Before tanning, pickling hides was dipped into 0.3 wt.% sodium carbonate for about 1 h to adjust the pH to 6-8. Finally, 3.0 wt.% formaldehyde solution with 37.0 wt.% concentration was added for tanning. Then the obtained formaldehyde-tanned leather was washed with distilled water to remove the remaining tanning agents on the sample surface and dried in the air. A few days later, they were kept in the drier to a constant weight.

2.2 Methods

2.2.1 Thermogravimetric Analysis (TGA)

The thermogravimetric analysis was undertaken using TGA/DSC1 (METTLER TOLEDO, Switzerland) with argon gas flow of 40 mL/min. Approximately 8-15 mg of each sample placed in open aluminium crucible was heated from 30 to 600°C at heating rates of 5, 10, 20, 30°C/min respectively.

2.2.2 Thermogravimetric -Fourier transform infrared spectroscopy (TG-FTIR)

The evolved gas analysis was conducted using a TGA/DSC (STA499F3 Jupiter, NETZSCH, Germany) coupled with FTIR spectrometer (Bruker Tensor II, Germany). Approximately 8-10 mg of each sample was used and performed in open corundum crucible by heating from 40 to 900°C under flowing nitrogen at 60 mL/min with a heating rate of 10°C/min. The balance adapter, transfer line and the FTIR gas cell should be kept at 200°C to avoid the condensation of the evolved gases. The FTIR spectra were scanned in the mid-IR region from 4000 to 400 cm^{-1} at a resolution of 2 cm^{-1} .

2.3 Thermal degradation kinetics

Generally, the reaction rate equation of solid-state materials during non-isothermal degradation can be described as follows [11-13]:

$$\frac{d\alpha}{dt} = A \exp\left(-\frac{E_a}{RT}\right) f(\alpha) \quad (1)$$

$$\alpha = \frac{m_0 - m_t}{m_t - m_f} \quad (2)$$

where α is the conversion extent and defined in eq. (2); m_0 and m_f is the initial and final sample mass respectively; m_t is the sample mass at any time of t (given in min). A is the pre-exponential factor; E_a is the apparent active energy; R is the gas constant; $f(\alpha)$ is the mechanism function.

The heating rate $\beta = dT/dt$ is introduced to eq. (1) and then obtained eq. (3). Integrating eq. (3) yields to eq. (4).

$$\beta \frac{d\alpha}{dT} = A \exp\left(-\frac{E_a}{RT}\right) f(\alpha) \quad (3)$$

$$g(\alpha) = \int_0^\alpha \frac{d\alpha}{f(\alpha)} = \frac{A}{\beta} \int_0^T \exp\left(-\frac{E_a}{RT}\right) dT = \frac{AE_a}{\beta R} P\left(\frac{E}{RT}\right) \quad (4)$$

In order to calculate the thermal degradation kinetics, two different methods were used in this paper, namely model-free methods (FWO and Friedman) and model-fitting method (Criado). FWO equation is shown in eq. (5). E_a can be determined by plotting $\ln \beta$ vs. $1000/T$ without any information of thermal degradation mechanism in advance.

$$\ln \beta = \ln \frac{AE_a}{g(\alpha)R} - 5.331 - 1.052 \frac{E_a}{RT} \quad (5)$$

Friedman method is another commonly used differential isoconversional method. It is obtained by taking logarithm to eq. (4), which is shown in eq. (6). Therefore, E_a values at conversion ranges from 0.1 to 0.8 can be evaluated based on the slope of straight lines obtained by plotting $\ln(\beta \cdot d\alpha/dT)$ vs. $1000/T$.

$$\ln\left(\beta \frac{d\alpha}{dT}\right) = \ln[Af(\alpha)] - \frac{E_a}{RT} \quad (6)$$

Criado method is usually used to identify the degradation mechanism of solid-state materials, which is defined by eq. (7) [14].

$$Z(\alpha) = \frac{d\alpha/dt}{\beta} \pi(\chi)T \quad (7)$$

Where $\chi = E_a/RT$ and $\pi(\chi)$ is an approximation of the temperature integral which cannot be expressed in a simple analytical form. Based on previous literatures, $\pi(\chi)$ is generally expressed by the fourth rational expression of Senum and Yang, namely $p(\chi)$, which gives errors of lower than 10^{-5} % when $\chi > 20$ [15,16]. Simple rearrangement of eq. (7) gives rise to the following eq. (8), which is used to plot the experimental curve. The master curves corresponding to different models listed in **Table 1**, are obtained based on eq. (9). By comparing the experimental curve with master curves, the degradation mechanism of samples can be identified.

$$Z(\alpha) = \frac{d\alpha}{dT} \left(\frac{E_a}{R}\right) \exp\left(\frac{E_a}{RT}\right) P(\chi) \quad (8)$$

$$Z(\alpha) = f(\alpha)g(\alpha) \quad (9)$$

Table 1. Function expressions of the most common reaction mechanisms in solid-state reactions. [17-19]

Kinetic mechanism	$f(\alpha)$	$g(\alpha)$	order	
Nucleation and growth	$2(1-\alpha)[- \ln(1-\alpha)]^{1/2}$	$[- \ln(1-\alpha)]^{1/2}$	1/2	A2
	$3(1-\alpha)[- \ln(1-\alpha)]^{2/3}$	$[- \ln(1-\alpha)]^{1/3}$	1/3	A3
	$4(1-\alpha)[- \ln(1-\alpha)]^{3/4}$	$[- \ln(1-\alpha)]^{1/4}$	1/4	A4
Phase boundary reaction	1	α	1	R1
	$2(1-\alpha)^{1/2}$	$[1-(1-\alpha)^{1/2}]$	2	R2
	$3(1-\alpha)^{2/3}$	$[1-(1-\alpha)^{1/3}]$	3	R3
One-dimensional diffusion	$1/2\alpha$	α^2	1	D1
Two-dimensional diffusion	$[- \ln(1-\alpha)]^{-1}$	$[(1-\alpha)\ln(1-\alpha)] + \alpha$	Valensi equation	D2
Three-dimensional diffusion	$3(1-\alpha)^{2/3} / [2(1-(1-\alpha)^{1/3})]$	$[1-(1-\alpha)^{1/3}]^2$	Jander equation	D3
Chemical reaction	$1-\alpha$	$-\ln(1-\alpha)$	1	F1
	$(1-\alpha)^2$	$(1-\alpha)^{-1} - 1$	2	F2
	$(1-\alpha)^3$	$[(1-\alpha)^{-2} - 1] / 2$	3	F3

3 Results and discussion

3.1 TGA analysis under argon atmosphere

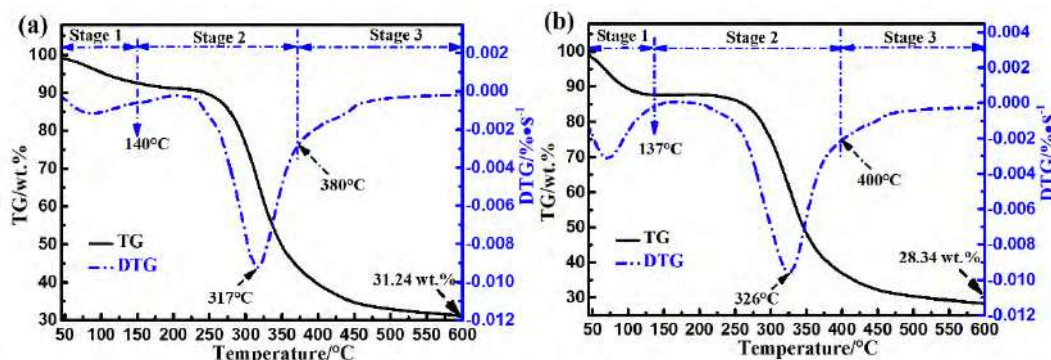


Fig. 1. Comparison of the TG/DTG curves of (a) untanned hide, (b) formaldehyde-tanned leather.

Fig. 1 is the comparison of the TG/DTG curves of hides before and after formaldehyde-tanning with a heating rate of 10°C/min. Based on the DTG curves, it can be seen that the thermal degradation process is composed of three stages, namely dehydration, fast devolatilization and carbonization stage. The temperature ranges of each stage are also marked in **Fig. 1**. In the dehydration stage, the mass loss is small (7.47 wt.% before tanning and 12.25 wt.% after tanning) mainly due to the release of moisture in samples. However, in the fast devolatilization stage, the mass loss of samples reach maximum (50.96 wt.% before tanning and 51.15 wt.% after tanning). This stage was attributed to the devolatilization of samples. In the third stage, a small part of samples (about 10.00 wt.%) could continue to be volatilized and finally the residue was bio-char.

After tanning, no obvious changes were observed from **Fig. 1** except that the peak temperature where the mass loss is the highest slightly raise, indicating that the thermal degradation stability of hides wasn't significantly improved by formaldehyde tanning which may because formaldehyde combined with collagen in hides through single site way other than crosslink with collagen like chrome.

3.2 Kinetics analysis under argon atmosphere

TG curves at different heating rates under argon atmosphere were used to calculate apparent active energy of hides before and after formaldehyde tanning. In **Fig. 2 and 3**, the curves shifted to higher temperature with the increase of heating rates. However, the pattern of curves didn't change, due to the similar thermal degradation mechanism at different heating rates^[20]. It should mention here that single-step reaction is assumed to take place during thermal degradation in our work due to single peak observed in DTG curves shown in **Fig. 1** and the single-step overall apparent active energy is calculated based on FWO and Friedman methods.

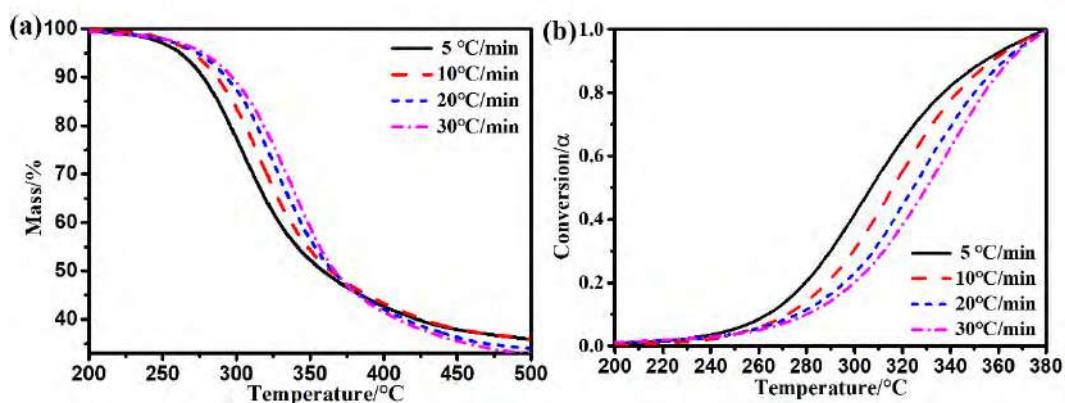


Fig. 2. TG analysis results of untanned hides at different heating rates: (a) mass loss and (b) relative conversion extent.

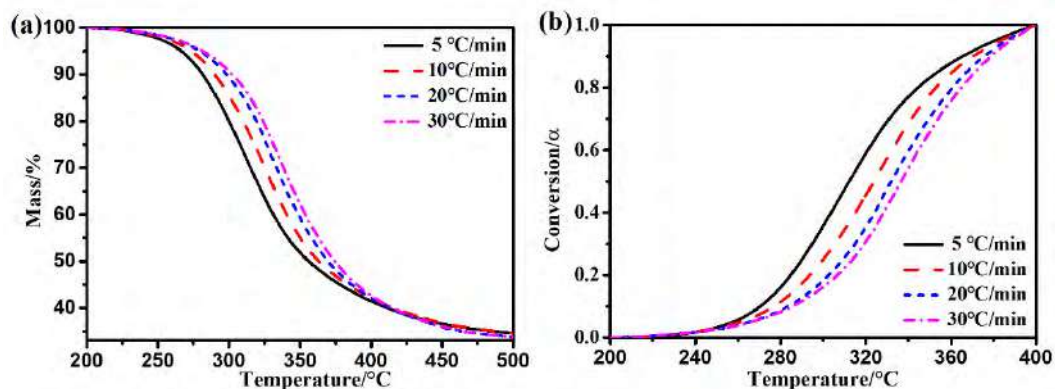


Fig. 3. TG analysis results of leather samples tanned with formaldehyde at different heating rates: (a) mass loss and (b) relative conversion extent.

Following, the plots of $\ln\beta$ vs. $1000/T$ and $\ln(\beta \cdot d\alpha/dT)$ vs. $1000/T$ are shown in **Fig. 4** and **Fig. 5**. From the slope of these fitting lines, apparent active energy of samples at conversion of 0.1-0.8 are calculated and listed in **Table 2**. Results showed that the mean active energy of hides before tanning is 229.8 kJ/mol while is 223.1 kJ/mol for that formaldehyde tanning one based on FWO method. Moreover, the values of E_a obtained by Friedman method are higher than that obtained by FWO method. It is well-known that formaldehyde would combine with the free $-NH_2$ groups in collagen through Schiff base reaction, thereby improving the shrinkage temperature of hides^[21]. However, this combination is weaker than the coordinate covalent bonding formed between collagen and chrome and extremely vulnerable during thermal decomposition. Thus, formaldehyde tanning has no significant positive effect on the mean values of apparent active energy during thermal decomposition.

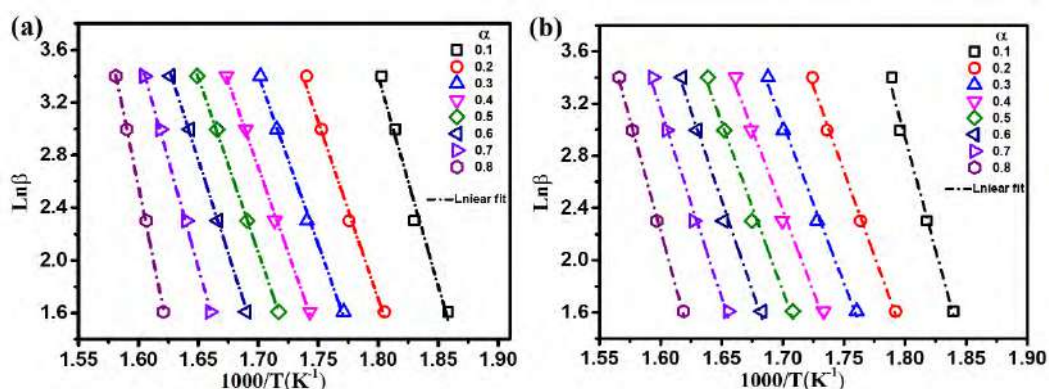


Fig. 4. Typical plots of $\ln \beta$ vs. $1000/T$ according to FWO method for (a) untanned hides and (b) formaldehyde-tanned leather.

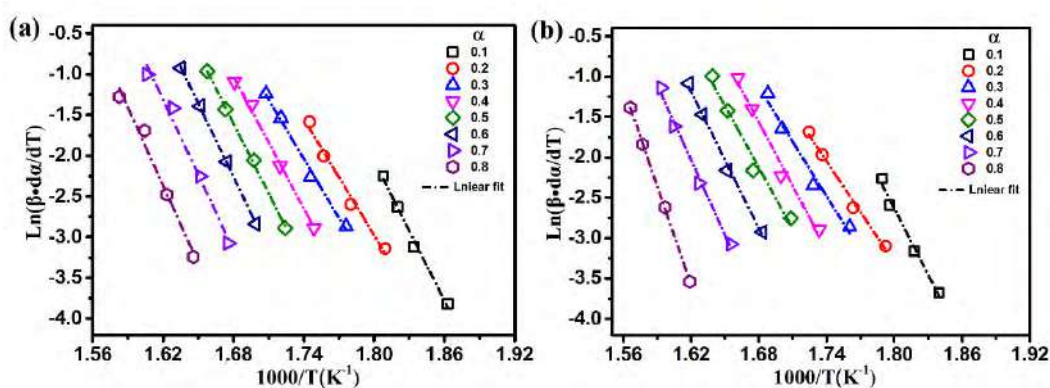


Fig. 5. Typical plots of $\ln(\beta \cdot d\alpha/dT)$ vs. $1000/T$ according to Friedman method for (a) untanned hides and (b) formaldehyde-tanned leather.

Table 2. Active energy values (E_a) obtained by FWO and Friedman methods for studied samples.

Conversion (α)	$E_a/kJ \cdot mol^{-1}$ (Before tanning)		$E_a/kJ \cdot mol^{-1}$ (After tanning)	
	FWO	Friedman	FWO	Friedman
0.1	261.2	238.1	272.3	226.6
0.2	218.9	197.6	205.6	174.6
0.3	206.2	201.2	193.0	187.0
0.4	209.4	225.0	195.5	219.0
0.5	214.6	238.0	204.0	211.1
0.6	224.0	249.2	216.7	234.6
0.7	246.1	255.2	228.9	257.7
0.8	258.4	265.7	269.0	335.3
Mean	229.8	233.7	223.1	230.7

Furthermore, the E_a values calculated according to FWO method were applied in Criado method to determine the thermal degradation mechanism of samples. As shown in Fig. 6, the experiment curves of untanned hides and formaldehyde-tanned leather tend to overlap with D_n mechanism, associate with the diffusion process. Moreover, the $Z(a)$ values of samples are closer to D_3 mechanism at low conversion ($\alpha < 0.4$). This behaviour may attribute to the ease of the heating diffusion at relative low temperature, which can promote the random domains or small chain sides in collagen of hides degraded with the heating transferring throughout the sample. However, not only the heating diffusion would be restrained but also the diffusion of evolved gases formed throughout the sample become difficult because of high ordered parts of collagen^[14]. Therefore, at relative high temperature, the degradation mechanism of samples turns to D_2 , the diffusion process in two dimensions.

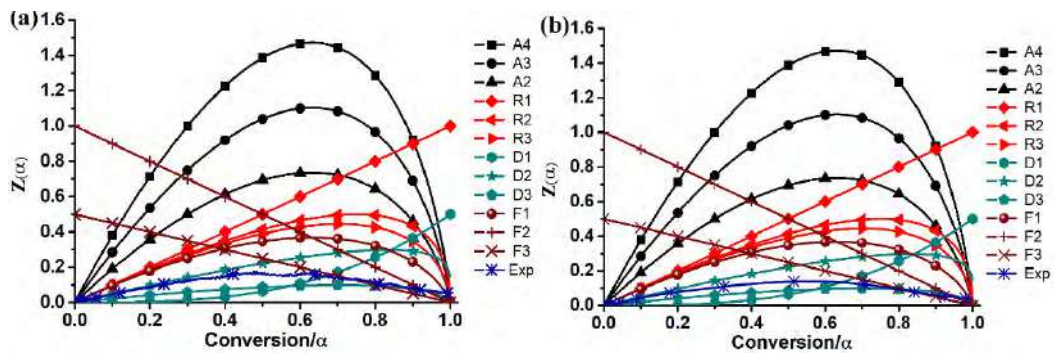


Fig. 6. Master curves and experimental values obtained using the Criado method for (a) untanned hide and (b) formaldehyde-tanned leather.

3.3 TG-FTIR analysis

Fig. 7 illustrates the 3D-FTIR spectra of untanned hide and formaldehyde-tanned leather, which recorded the gases evolved in thermal decomposition process. Three remarkable characteristic absorbance bands are clearly observed. In order to identify the components of evolved gases, 2D FTIR spectra of studied samples are shown in Fig. 8. The FTIR spectra in Fig. 8 (a) and (b) represent the absorbance peak of evolved gases at the temperature where the mass loss rate is the highest for hides before and after formaldehyde-tanning respectively. Some permanent gaseous component can be identified by their characteristic infrared absorbance bands, such as CO₂ (2400-2250 cm⁻¹ and 671 cm⁻¹), H₂O (4000-3400 cm⁻¹ and 2000-1300 cm⁻¹) and NH₃ (985 cm⁻¹ and 925 cm⁻¹) [22-24]. The small absorbance bands at 2982 cm⁻¹ and 2930 cm⁻¹ correspond to C₂H₆ and CH₄ respectively [25]. The FTIR band at 2254 cm⁻¹ observed in Fig. 8 (b) is the absorbance peak of HNCO [22-24,26].

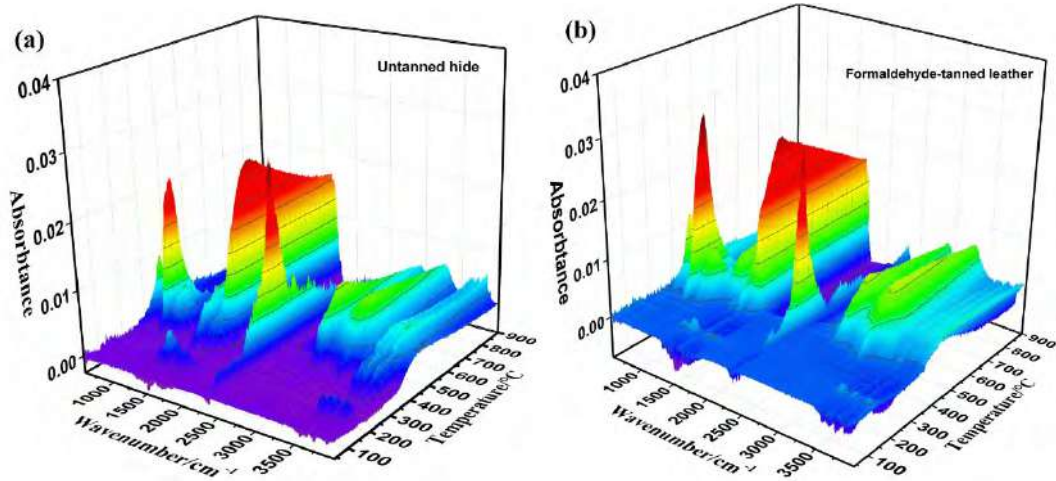


Fig. 7. 3D-FTIR spectra of evolved gases in the decomposition of (a) untanned hide and (b) formaldehyde-tanned leather.

Previous researches have reported that the evolution of H₂O mainly relates to the moisture release of sample and the peak intensity is generally weak [22-24]. However, the intensity of absorbance peak at around 1700 cm⁻¹ is even as strong as that of CO₂ band and reach the highest at temperature of 400°C based on the results in Fig. 7. By close examination of the absorbance peaks in range of 2000-1300 cm⁻¹ at 400°C shown in Fig. 8 (c) and (d), it is obtained that the strong peak is at about 1694 cm⁻¹ relating to the stretching vibration of C=O, which is possibly attributed to the ketones or organic acid [27,28]. In addition, as temperature increased to 400°C, the absorption peak of HNCO becomes obvious and characteristic bands of CO at 2190 cm⁻¹ and pyrrole at 720 cm⁻¹ are observed, suggesting that these two products may be evolved at high temperature.

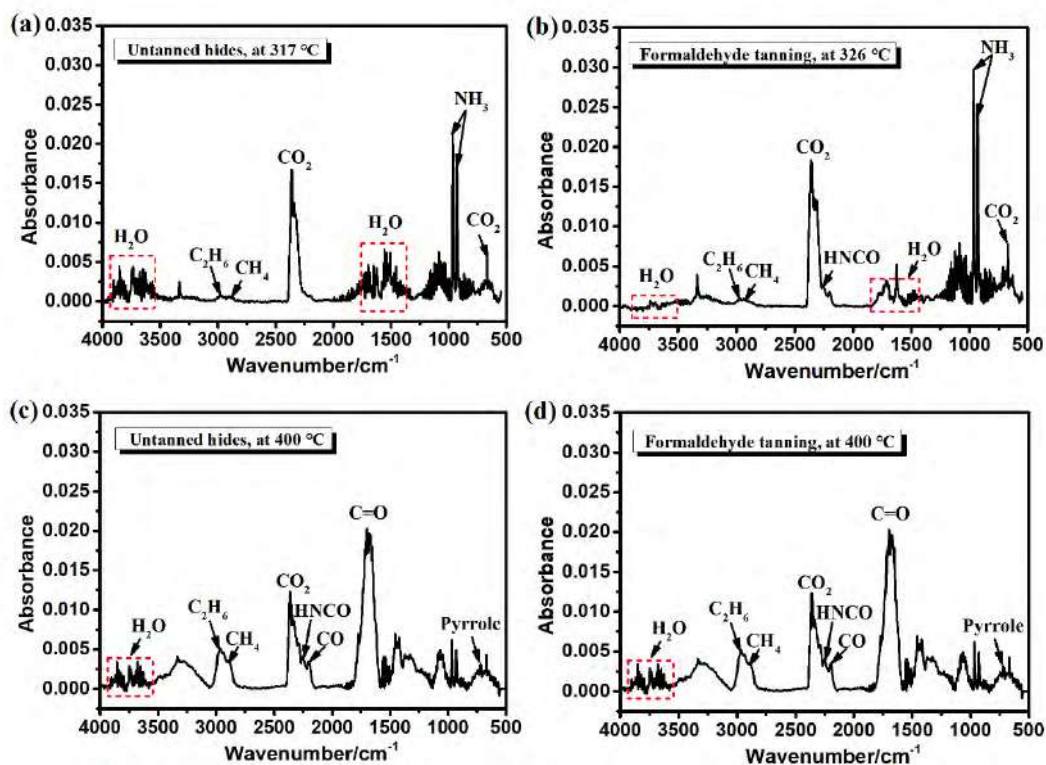


Fig. 8. 2D-FTIR spectra of evolved gases in the decomposition of (a) and (c) untanned hide, (b) and (d) formaldehyde-tanned leather.

It is evident that there is no significant difference in the components of evolved gases but in the intensity and width of gaseous evolved peaks between untanned hide and formaldehyde-tanned leather. Consequently, the evolution of CO_2 , CH_4 , NH_3 , HNCO and Pyrrole with the increase of temperature was also investigated and presented in **Fig. 9**. It is observed that CO_2 evolved at temperature range of 200-400°C. Generally, the initial release of CO_2 was mainly attributed to the decarboxylation of free $-\text{COOH}$ groups from glutamic and aspartic acids [29,30]. As temperature increased, the evolution of CO_2 may be caused by condensation reactions involving peptide $-\text{CO}-$ groups and by internal oxidation of other organic groups [25,29-30]. According to **Fig. 9**, the evolution peak of CO_2 for untanned hide was broader than that for formaldehyde-tanned leather. It may be because that the uniformity of collagen structure increased after formaldehyde tanning. Therefore, the release of CO_2 was restrained. Whereas the evolved content of NH_3 after formaldehyde-tanning increased and the initial evolved temperature decreased compared with untanned hide, which illustrates an easier release of ammonia. Ammonia can be produced by the deamination reaction of free $-\text{NH}_2$ groups and peptide $-\text{NH}-$ groups. As mentioned above, the aldehyde can combine with free $-\text{NH}_2$ groups in collagen through Schiff base reaction. Therefore, the increasing evolution of NH_3 after formaldehyde-tanning may be because the deamination reaction of peptide $-\text{NH}-$ groups occurs more easily. Apart from this, CH_4 caused by the cleavage of $-\text{CH}_3$ and $-\text{CH}_2-$ also slightly increases. These results again prove that formaldehyde-tanning didn't improve the thermal degradation stability of hide. As temperature is above 300°C, HNCO and pyrrole were detected, with a peak at about 355°C. Nevertheless, HNCO and pyrrole bands always overlap with the band of CO_2 at 2368 cm^{-1} and 671 cm^{-1} respectively. Therefore, their intensity may be greater than the actual [25].

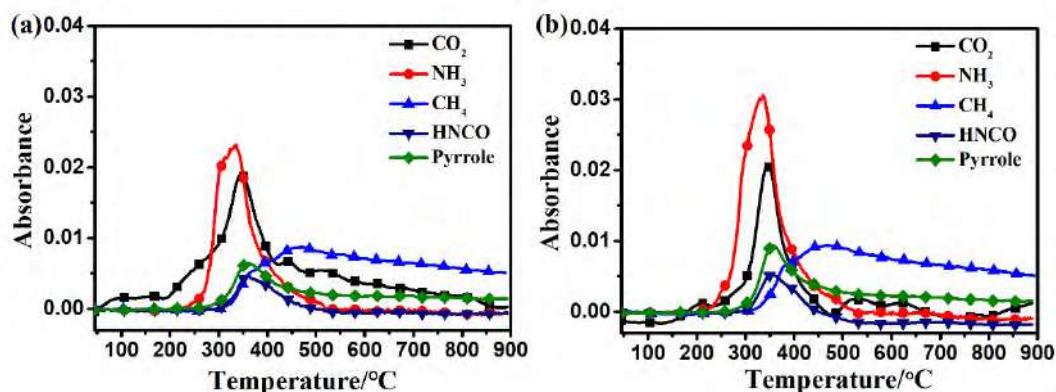


Fig. 9. Evolution of some major components in the decomposition of (a) untanned hide (b) formaldehyde-tanned leather.

4 Conclusions

Hides before and after formaldehyde-tanning were investigated by TG and TG-FTIR to analyze the thermal degradation kinetics and monitor the changes in the thermal degradation behaviours. The results of TG analysis showed that the active energy of untanned hide based on FWO and Freidman is 229.8 kJ/mol and 233.7 kJ/mol respectively while is 223.1 kJ/mol and 230.7 kJ/mol after formaldehyde-tanning, suggesting that formaldehyde-tanning has no significant effects on the mean apparent active energy. Moreover, the thermal degradation mechanisms of untanned hide and formaldehyde-tanned leather are the same, complying the diffusion type. According to the results of TG-FTIR analysis, it is obtained that formaldehyde-tanning also didn't change the composition of evolved gases. CO_2 , NH_3 , and $\text{C}=\text{O}$ are the dominant components during thermal degradation in nitrogen, together with the characteristic bands of CH_4 , C_2H_6 , H_2O , HNCO , and pyrrole. However, the width of CO_2 peak decreased and the intensity of NH_3 and CH_4 peaks increased after formaldehyde-tanning. Based on our findings, at low conversion (below 300°C), both the thermal degradation of untanned hide and the formaldehyde-tanned leather mainly are the release of CO_2 by the decarboxylation of free $-\text{COOH}$ groups from glutamic and aspartic acids accompanying with the deamination reaction of free $-\text{NH}_2$ groups and peptide $-\text{NH}-$ groups. As conversion increased ($300-400^\circ\text{C}$), the more ordered parts in collagen started to degradation, which may restrain the diffusion process. Nevertheless, the temperature is high. Therefore, organic components with small molecular, such as CH_4 , C_2H_6 , HNCO and $\text{C}=\text{O}$ start to evolve.

Acknowledgements

This work was supported by the National Key R & D Program of China (No.2017YFB0308500), the National Natural Science Foundation of China (Grant No. 51373158) and Weng Hongwu Research Foundation of Peking University.

References

1. Yao, Q., Li C., Huang, H., et al: 'Waterborne Carboxyl-terminated Hyperbranched Oligomer polyester Ligand: Synthesis, Characterization and Chelation with Chromium (III)', *J. Mol. Struct.*, 1143, 371-377, 2017
2. Nashy, E. H. A., Osman, O., Mahmoud, A. A., et al: 'Molecular spectroscopic study for suggested mechanism of chrome tanned leather', *Spectrochim. Acta. A. Mol. Biomol. Spectrosc.*, 88, 171-176, 2012

3. Sunda, r V. J., Rao, J. R., Muralidharan, C.: 'Cleaner chrome tanning - Emerging options', *J. Clean. Prod.*, 10, 69-74, 2002
4. Sun X., Jin Y., Lai S., et al: 'Desirable retanning system for aldehyde-tanned leather to reduce the formaldehyde content and improve the physical-mechanical properties', *J. Clean. Prod.*, 175, 199-206, 2018
5. Onem E., Yorgancioglu A., Karavana H. A., et al: 'Comparison of different tanning agents on the stabilization of collagen via differential scanning calorimetry', *J. Therm. Anal. & Calorim.*, 129, 615-622, 2017
6. Budrugaec P., Miu L.: 'The suitability of DSC method for damage assessment and certification of historical leathers and parchments', *J. Cult.Herit.*, 9, 146-153, 2008
7. Carşote C., Badea E., Miu L., et al: 'Study of the effect of tannins and animal species on the thermal stability of vegetable leather by differential scanning calorimetry', *J. Therm. Anal. & Calorim.*, 124, 1255-1266, 2016
8. Onem E., Yorgancioglu A., Karavana H A., et al: 'Comparison of different tanning agents on the stabilization of collagen via differential scanning calorimetry', *J. Therm. Anal. & Calorim.*, 129, 615-622, 2017
9. Rosu L., Varganici C., Crudu A., et al: 'Influence of different tanning agents on bovine leather thermal degradation', *J. Therm. Anal. & Calorim.*, 134, 583-594, 2018
10. Sergey, B., Alan K., et al: 'ICTAC Kinetics Committee recommendations for performing kinetic computations on thermal analysis data', *Thermochim. Acta*, 520, 1-19, 2011
11. Danon B., Mkhize N. M., Van d G. P., et al: 'Combined model-free and model-based devolatilisation kinetics of tyre rubbers', *Thermochim. Acta*, 601, 45-53, 2015
12. Holland B. J., Hay J. N., 'The value and limitations of non-isothermal kinetics in the study of polymer degradation', *Thermochim. Acta*, 388, 253-273, 2002
13. Wight, C. A., 'Model-free and model-fitting approaches to kinetic analysis of isothermal and nonisothermal data', *Thermochim. Acta*, 340, 53-68, 1999
14. Poletto M., Zattera A. J., Santana R. M. C.: 'Thermal decomposition of wood: Kinetics and degradation mechanisms', *Bioresour. Technol.*, 126, 7-12, 2012
15. Pérez-Maqueda L. A., Criado J. M.: 'The Accuracy of Senum and Yang's Approximations to the Arrhenius Integral', *J. Therm. Anal. & Calorim.*, 60, 909-915, 2000
16. Al-Salem S. M., Sharma B. K., Khan A R., et al.: 'Thermal Degradation Kinetics of Virgin Polypropylene (PP) and PP with Starch Blends Exposed to Natural Weathering', *Ind. & Eng. Chem. Res.*, 56, 5210-5220, 2017
17. Saha B., Reddy P. K., Ghoshal A. K.: 'Hybrid genetic algorithm to find the best model and the globally optimized overall kinetics parameters for thermal decomposition of plastics', *Chem. Eng. J.*, 138, 20-29, 2008
18. Aboukhas A., Harfi K. E., Bouadili A. E.: 'Thermal degradation behaviors of polyethylene and polypropylene. Part I: Pyrolysis kinetics and mechanisms', *Energ. Convers. Manage.*, 51, 1363-1369, 2010
19. Ma Z., Wang J., Yang Y., et al.: 'Comparison of the thermal degradation behaviors and kinetics of palm oil waste under nitrogen and air atmosphere in TGA-FTIR with a complementary use of model-free and model-fitting approaches', *J. Anal. Appl. & Pyrol.*, 134, 12-24, 2018
20. Saha B., Ghoshal A. K.: 'Model-free kinetics analysis of ZSM-5 catalyzed pyrolysis of waste LDPE', *Thermochim. Acta*, 453, 120-127, 2007
21. Krishnamoorthy G., Sadulla S., Sehgal P. K., et al: 'Greener approach to leather tanning process: d-Lysine aldehyde as novel tanning agent for chrome-free tanning', *J. Clean. Prod.*, 42, 277-286, 2013
22. Zhu H M., Yan J. H., Jiang X. G., et al: 'Study on pyrolysis of typical medical waste materials by using TG-FTIR analysis', *J. Hazard. Mater.*, 153, 670-676, 2008
23. Marcilla A., García A. N., León M., et al: 'Study of the influence of NaOH treatment on the pyrolysis of different leather tanned using thermogravimetric analysis and Py/GC-MS system', *J. Anal. Appl. & Pyrol.*, 92, 194-201, 2011
24. Mocanu A. M., Moldoveanu C., Odochian L., et al: 'Study on the thermal behavior of casein under nitrogen and air atmosphere by means of the TG-FTIR technique', *Thermochim. acta*, 546, 120-126, 2012
25. Cucos A., Budrugaec P.: 'Simultaneous TG/DTG-DSC-FTIR characterization of collagen in inert and oxidative atmospheres', *J. Therm. Anal. & Calorim.*, 115, 2079-2087, 2014
26. Li J., Wang Z., Yang X., et al: 'Evaluate the pyrolysis pathway of glycine and glycyglycine by TG-FTIR', *J. Anal. Appl. & Pyrol.*, 80, 247-253, 2007
27. Ma Z., Chen D., Jie G., et al: 'Determination of pyrolysis characteristics and kinetics of palm kernel shell using TGA-FTIR and model-free integral methods', *Energ. Convers. & Manage.*, 89, 251-259, 2015
28. Ma Z., Sun Q., Ye J., et al: 'Study on the thermal degradation behaviors and kinetics of alkali lignin for production of phenolic-rich bio-oil using TGA-FTIR and Py-GC/MS', *J. Anal. Appl. & Pyrol.*, 117, 116-124, 2016
29. Steven F. S., Jackson D. S.: 'Purification and amino acid composition of monomeric and polymeric collagens', *Biochem. J.*, 104, 534-536, 1967
30. Si L., Yan F., Wang Y., et al: 'Thermal degradation behavior of collagen from sea cucumber (*Stichopus japonicus*) using TG-FTIR analysis', *Thermochim. Acta*, 659, 166-171, 2018

NANO-BIO ALDEHYDE SYSTEM FOR LEATHER MANUFACTURE

A. Yasothai^{1,2}, G. C. Jayakumar², S. Angayarkanny¹, N. K. Peter², V. K. Swarna²

1 Anna University, Department of Chemistry, Chennai, India

2 CSIR-Central Leather Research Institute, CHORD, Chennai, India

Corresponding authors: swarna@clri.res.in

Abstract. Development of eco-friendly chemicals from natural renewable resources are widely explored owing to their eco-acceptability and sustainability. Exploring biopolymers is the need of the hour to combat the sustainability in leather processing. Currently, the use of biopolymers is undergoing intense study since it enables a more sustainable leather manufacturing. Finishing is an imperative step that enhances the aesthetic appeal of the final leather during which protein finishing systems known for its glazing properties are applied. Commonly used cross-linkers such as formaldehyde and glutaraldehyde are restricted owing to biocompatibility issues. However, the use of crosslinker is inevitable for protein finish system. In the present research, nano-bio polyaldehyde (NBP) system is established through selective oxidation of starch; the size of the system is fine-tuned in the nano range for effective and efficient crosslinking through emulsion technique. From the characterization studies, the architectural design of NBP is ascertained as a good crosslinking agent for leather finishing chemicals. A particle size of the NBP system is found to be in the range of 80-110 nm. The leather samples showed an improved hydrophobicity nature and also enhanced wet, rub fastness, color fastness, and adhesion strength. The study provides an insight on tunability of known biopolymers for developing sustainable technology.

1 Introduction

Nowadays, nanotechnology holds enough promise to be one of the major drivers of technology. Indeed, using nanoparticles can potentially help achieve higher performance materials, intelligent systems and new production methods. With the rapid discoveries made in the nanotechnology field, shortly enough, nanoparticles will be ubiquitous and used to their full potential. In the past few decades, the leather industry has gained a negative image due to its use of highly polluting chemicals and the discharge of toxic tannery effluents. Thus, recently research has been focused on manufacturing sustainable leather with the use of nanoparticles. Nanotechnologies are considered in leather manufacturing process since they can offer cost-effective improvements to the quality of finished leather. The enhancement of the properties of the leather is owed to the increased surface area to volume ratio. During leather finishing processes, the reactions occur at the surface of the chemical or the material; hence, for the same volume, the greater the surface, the greater the reactivity. And nanotechnology allows just that, as particles get smaller, the surface area to the volume ratio increases effectively.

The previously mentioned advantageous property of nanoparticles can be put to use (effective) during coating processes for leather goods such as garments, furniture, car seats or even for footwear leather. Moreover, this would allow for a more eco-friendly, biologically safe finishing process requiring lower maintenance and cleaning. The improved chemical bonding between the nanoparticles and leather surface provides for a more durable and high quality leather. Indeed, furniture upholstery needs to be stain resistant and resistant to the effects of continued sunlight exposure. Leather car upholstery needs light fastness, resistance against UV radiation and a high degree of rub fastness properties. These necessary properties for high quality leather can be achieved through incorporation of suitable metal nanoparticle in finishing formulations. Hence, the primary ambition of this project is to attain superior quality of high-performance leather by combining the fields of leather technology and nanotechnology.

The present study aims specifically to develop a leather coating agent incorporating nanoparticles to form a layer that provides the different required properties. There by developing a novel nano-finish formulation for a flexible substrate with multi-function properties like leather. The polyaldehyde nanoparticles embedded in leather coating chemicals will exhibit enhanced wet and dry rub fastness, color fastness and perspiration and color migrations. Additionally, further properties such as resistance, abrasion resistance...etc will also be allotted, allowing leather to be used for high-end leather applications like automobile upholstery, high performance upper leather...etc.

2 Experimental

2.1 Material and methods

Soluble Starch powder (st), Span80, ethanol and Acetic acid was obtained from SRL Chemicals, India. Sodium Periodate (NaIO_4), Hydroxylamine hydrochloride, Chloroform, Toluene, All the chemicals used were of analytical reagent grade obtained from SD Fine chemicals(India). All the leather finishing chemicals were procured from TFL, Chrompet, Chennai, India and Stahl India. Pvt. Ltd, Nagalkeni, Chennai, India. Cow crust leather was obtained from Tannery Division, CLRI, and India. All the characterizations were done the CSIR- CLRI, Caters Lab.

2.2 Synthesis of Dialdehyde Starch Nanoparticle

Aqueous soluble starch solution of 1% was heated and hydrolyzed until the solution got clarified. Toluene and Chloroform were mixed in the ratio 3:1 to make as a solvent. 2% Span 80 was prepared by dissolving in the above solvent. The clarified starch solution was mixed with the centrifuged solution in a beaker and placed in a magnetic stirrer. 1.52% of Sodium periodate was added and stirred for 40 minutes, and than 0.05% of cross-linking solution, was added and stirred for 1.5 hours. During this period, the micro-emulsion was broken with Ethanol and washed with dilute hydrochloric acid once. Then again it was washed with acetone and water alternatively. The stirred solution was then subjected to centrifugation. The resultant precipitate was freeze-dried to obtain the final product of dialdehyde starch nanoparticles.

2.2.1 FT-IR

The powder samples were analysed using JASCO FTIR 4100 FTIR spectrometer. The powder samples were directly taken for FTIR analysis. The spectra were recorded between $400\text{-}4000\text{ cm}^{-1}$ with average of four scans and 4 cm^{-1} .

2.2.2 SEM Analysis

Morphological features of the dialdehyde starch nanoparticles and starch solution was done using Scanning Electron Microscopy (SEM). The samples were mounted on the sample grid and examined by the microscope at 10.00 kV with a range of magnitudes. SEM analysis provided the morphological details of the various samples.

2.2.3 Preparation of Leather Finishing Formulation

Compact Binder of 7.5 g were taken in beaker and add 1.25g of pigments was added and stirrer for 20 minutes and followed by water and commercial cross linker (AKU) and stirred for 10 minutes than applied on the goat upper leather the same process is followed by the experimental also The above formulation was sprayed by High Volume Low Pressure (HVLP) Spray gun. Then the leather was subjected to 80°C and 80 kg/cm^2 pressure in hydraulic press.

2.3 Physical Properties of formulated leather

The physical properties of finished leather sample from both control and experimental goat upper leather were taken for physical testing measurements. The samples were taken from official sampling position by IUP testing method (ref). For all physical strength analysis of leather samples were conditioned at $20\pm 2^\circ\text{C}$ and $65\pm 4\%$ humidity for 48h. The Measurement of Wet, dry rub, color fastness and fastness test carried out according to IUF 450 by veslic C-4500, and the results are given in Table 4.

3 Results and Discussions

3.1 Functional group analysis of ATIR-FTIR

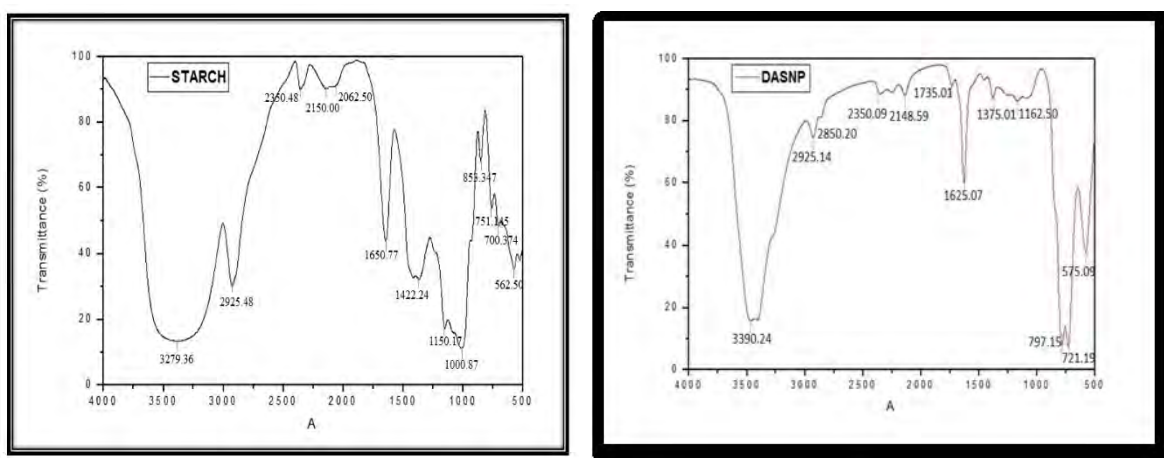


Fig. 2. FT-IR spectra of Starch and DASNP.

The FT-IR peaks of the control-starch and the dialdehyde starch nanoparticles were compared. From the FTIR analysis, the compounds mainly present in Starch were found to be alcohols, phenols and hydrocarbons such as alkanes and alkenes. On conversion of starch to DASNP by periodate oxidation most of the alkanes and alkenes were seen to be converted to alcohols, amines and carbonyl groups. The introduction of carbonyl stretching around 1735cm^{-1} indicates the formation of dialdehyde derivative. The hydroxy (-OH) stretching was narrowed due to the conversion of hydroxyl to carbonyl.

3.2 Morphology structure (SEM) of Synthesised DASNP

The morphology of the prepared nanoparticles was examined using scanning electron microscopy. Fig. 2 (a) shows that the surface morphology and shapes of the particles are nearly crystalline structure and Fig. 2 (b) shows the surface morphology and shapes are nearly spherical and clearly show a slight aggregation of the particles. The aggregation occurred probably during the process of drying [23, 24].

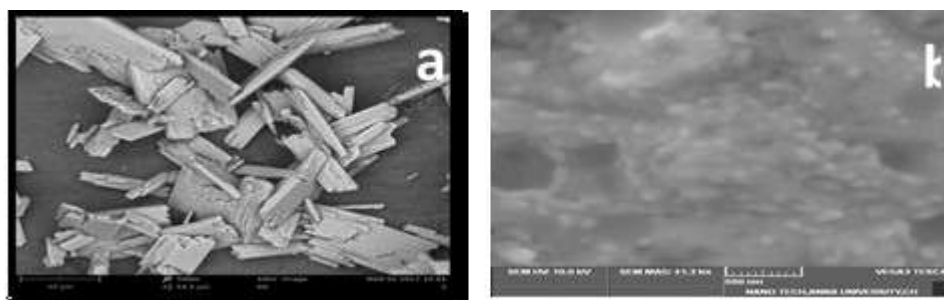


Fig. 3. SEM images of (a) starch and (b) Dialdehyde starch nanoparticles.

3.3 Effect of Physical Properties of Formulated Leather

The goat upper leather finishing formulation prepared as per Table 1 i.e., with water, compact binder, AKU commercial cross linker and pigment was sprayed on the standard goat upper leather crust by HVLP gun at 30 psi. 8 grams of season mix was deposited on one sq.ft of leather by four cross coat spray with intermediate drying. The same formulation as followed by experimental like DASNP. Then the leather was subjected to 80°C and 80 kg/cm² pressure in hydraulic press and the results are given in Table 1. Measurement of fluxing is carried out by SATRA STM 601/12 12 and the values are given in Table.

S.No	Wet Rub	Dry Rub	Color fastness	Perspiration Resistance	Color Migrations
Control	3/4	3/4	3/4	3/4	3/4
Expt.	4/4	4/4	4/4	4/4	4/4

4 Conclusions

The present study establishes novel nano bioaldehyde system for leather finishing. Finished leather characteristic of NBP system crosslinker is similar commercially used cross-linker. The study provides new insight in using eco-friendly and sustainable chemical as a crosslinker for leather finishing.

5 Acknowledgements

Authors thank the support from Department of Leather Technology, A.C. Tech, and Department of Chemistry, College of Engineering, Anna University, India.

References

1. R.Y. Hong, J.Z. Qian, J.X. Cao, *Powder Technol.* 163 (2006) 160.
2. R.Y. Hong, J.H. Li, L.L. Chen, D.Q. Liu, H.Z. Li, Y. Zheng, J. Ding, *Powder Technol.* 189 (2009) 426.

EFFECTS OF DIFFERENT SALT-ENZYMES ON OPENING UP OF COLLAGEN FIBER BUNDLES FOR LEATHER MAKING

Yafei Zhang¹, Zhenye Tang¹, Hui Liu¹, Cem Emre Ferah², Keyong Tang^{1,*}

1. School of Materials Science and Engineering, Zhengzhou University, Henan, Zhengzhou, 450001, P. R. China

2. Engineering Faculty, Leather Engineering Department, Ege University, 35100 Bornova, Izmir, Turkey

*Corresponding author: kytang@126.com

Abstract. Traditional leather industry involves mechanical, chemical and biological processes, and a lot of leather chemicals are widely used annually. In the beamhouse, especially in liming and re-liming, enormous pollution is usually released because of the traditional use of Na₂S and lime. Many researchers have devoted to clean production for leather making. In this study, salt-enzyme liming process was studied in modern leather process to remove the inter-fibrillary matter. Three such salts as Na₂SO₄, NaCl, and MgCl₂ were used with such enzymes as neutral protease and cellulase. The enzyme activity was evaluated by Folin Method. The opening up degree of collagen fiber bundles was observed by SEM and microscopic image of histological staining. The waste water was analyzed. The tannin absorptivity of the samples was evaluated by colorimetry. It was demonstrated that enzyme activity is not affected by salt, but it helps the action of enzymes on hides. Salt might accelerate the penetration of enzymes into the hide to promote the removal of inter-fibrillary and the opening up of collagen fiber bundles. The best fiber opening result was found by SEM at the MgCl₂ content of more than 0.4 wt.% in liming. Microscopic observation by histological staining as well as waste water analysis indicated a good removing effect for the inter-fibrillary. This work may provide a cleaner leather making technology.

1 Introduction

Traditional processing industries directly cause adverse changes for environment and are, therefore, being challenged severely by mankind^[1]. Among them that leather industry as a traditional industry in the world^[2], many leather products are produced each year. However, the environment has been seriously polluted and people's health also threatened due to the use of many chemicals and lime during leather making processes.

The important stages in the leather-making process are beam-house operation, tanning operation and finishing operation^[3], and the beam-house operation is the most critical stage among them. Traditional beam-house operation involves lots of water, lime, sulfide and other chemicals, which produced waste water, silt, solid waste and so on. About 60%-70% of total pollution such as biological oxygen demand (BOD), chemical oxygen demand (COD) and total dissolved solids (TDS) are released from beam-house operation^[4; 5]. The preparation sections for unhairing and removal of interfibrillar substance cause nearly 40% of biochemical oxygen demand (BOD) and 50% of chemical oxygen demand (COD)^[6]. In past few decades' years, many scientific workers have been committed to the cleaner production of leather the sake of protecting the environment from harm and study the leather making method sustainability. With the growth of biotechnology has achieved remarkable results in the production and application such as biological products in leather-making processing such as unhairing, liming and re-liming^[4; 7]. Several bio-products have been developed for leather making, in which such as neutral protease, keratinase, amylase and lipase been used for unhairing, fiber opening and fat removal from hide and the leather produced by these methods have achieved the similar properties to those traditional leather properties, which can absolutely replace lime and sodium sulfide^[8]. In leather making, more and more enzyme-based processes have been reported recent years^[9].

Enzyme have been widely used in many industries especially for leather process due to its characteristics of high efficiency and specificity. Usually, enzyme-assisted beam-house process is being used in many leather factories to replace lime, sulfide and calcium hydroxide^[10]. Over the past decade, enzyme-assisted materials such as ionic liquids^[11; 12], hydrogen peroxide^[13] and organic solvents^[14] have been developed for leather making and achieved the similar result to traditional methods. In present study, an attempt that salt-assisted enzymatic for fiber opening has been studied to as far as possible dispersed the collagen fiber, and then tanning experiments been carried out to explore its absorption in tannic acid by leather. The results proved that salt could promote fiber dispersion without destroying enzyme's activity. This method of beam-house operation make it possible to achieve the clean production.

2 Materials and methods

2.1 Materials

Dry salted cow skin chosen from Henan Prosper Skin & Leather Enterprise Co., Ltd., Jiaozuo 454791, P. R. China was used for leather process. Neutral protease with its CAS of 9068-59-1 (Commercial grade, from Nanning Donghenghuadao Biotechnology Co., Ltd., activity 100000U/g), cellulase (BR, from Macklin, activity 10000U/g), sodium chloride (NaCl, AR, Aladdin), sodium sulphate (Na₂SO₄, AR, Macklin), magnesium chloride (MgCl₂, AR, Macklin). All the other chemicals in leather process were analytical purity bought by Macklin. Tannic acid bought from Macklin was used as tanning operation.

2.2 Activity of neutral protease

The activity of neutral protease with different sodium sulphate concentrations and different times were assessed by the Folin-reagent method in this study^[13]. 2.0 wt.% enzyme solution was mixed with different concentration of sodium sulfate solutions. 1 mL samples were collected from the enzyme mixed solution, added 1 mL of casein and 2 mL of trichloroacetic acid in sequence. After standing for 15 minutes, the supernatant was filtered and 1 mL was collected to add 5 mL sodium carbonate solution and 1 mL Folin reagent to incubate for 20 minutes, and then the absorbance at 660 nm was measured compared to the blank group. The concentration of tyrosine was further calculated by standard curve. 1 U of protease activity is defined as the amount of enzyme required to produce 1 μmol of tyrosine/min^[7].

2.3 Fiber opening

The soaked cow pelt was taken for unhairing and fiber opening. After unhairing and fat removal from hide operation the hide was divided into several uniform pieces. 2.0 wt.% of protease and 0.1 wt.% of cellulase of mixed solution were prepared, and then six different concentrations of sodium sulphate solutions (which 0, 0.2 wt.%, 0.4 wt.%, 0.6 wt.%, 0.8 wt.% and 1.0 wt.%) were added to the mixed solutions. The other mixed solutions of magnesium chloride and sodium chloride with enzyme were prepared the same as the method of mixed solution of sodium sulfate with enzyme. The hide pieces were treated by above solutions for removal of interfibrillar substance and fiber opening for 24 h. These samples treated by different salt-enzyme solutions were thoroughly washed and subjected for tanning operation using tannic acid.

2.4 Tanning

The salt-enzyme treated samples were washed thoroughly and taken for tanning process. Tannin tanning was done to turn the pelt to leather in this study. All the experimental samples were tanned using tannic acid of 45 wt.% of the sample mass, which the tannic acid was added in three portions (10 wt.%, 15 wt.% and 20 wt.%). The time interval for each addition was 2 hours, and the tanning continued for 48 hours after the last addition.

2.5 Proteins dissolution analysis

The proteins dissolution from hide samples treated with salt-enzyme at different time intervals (which 4, 8, 12, 20 and 24 h) were measured during the fiber opening process. All the liquors were collected the filtrate and tested. The quantification of the proteins was done by matching the absorbance values at 562 nm with the standard curve derived by the mucin standards.

2.6 Scanning electron microscope (SEM)

For scanning electron microscope analysis, the samples were prepared after treatment with above salt-enzyme solutions and stored in a deep freezer (-50°C) for 24 hours, and thereafter lyophilized. The freeze dried samples were cut into 2×2 mm² sections and placed on the conductive adhesive of sample stand and then gold coated. The surface morphology of fiber-opened samples was observed using FEI's field scanning electron microscopy, and SEM images were obtained in the working voltage of 10 kV, at a room temperature 20°C and 50% relative humidity.

2.7 Histological staining evaluation

In order to evaluate the effect of different salt-enzyme in fiber opening of the skin, the samples of 1 cm² were cut from pelt treated with different methods at similar positions and fixed in 4% formaldehyde solution for more than 24 hours. Samples sections of 6 μm were obtained using microtome. The tissue specimens obtained were dehydrated with ethanol from low to high (up to 100%) and stained with hematoxylin and eosin. The images were observed and collected under a bright field microscopy.

2.8 Estimation of Absorption of Tannic acid

Subsequent to tanning, Ultraviolet-visible spectrophotometry was carried out to estimate the absorbance of tannic acid at 275 nm. Tannic acid solutions were diluted to 10000 times and the absorbance was measured by standard curve, and the absorption amount of leather to tannin tanning reagent was calculated.

3 Results and discussion

3.1 Enzyme activity

The activity of neutral protease in different sodium sulfate solutions were evaluated firstly in this study in order to assess the effect of different salt concentrations on enzyme-based fiber opening. Hence, to study the influence of sodium sulfate on enzyme activity, the changes of activity of the mixed salt-enzyme solutions with the increased of time were tested and combined the results in

Figure 1. It is very interesting to conclude that the enzyme activity would not obviously affected when different concentrations of sodium sulfate were mixed with protease. As time goes on, the activity of the mixed solution decreased and 70% of enzyme activity was preserved after 10 days. Nevertheless, there was somewhat different from previous reported^[15] that the activity of enzymes decreases considerably in the presence of salt. This situation might be due to the lower concentration of salt used in this study so that there was not evidently reduction at protease activity. Protease essentially is protein, the prolongation of the retention time of the mixed solution will cause partial denaturation of the protein, resulting in partial loss of the enzyme activity, which is consistent with common sense. This activity study proved that the protease activity would not affected greatly when sodium sulfate was mixed with the neutral protease, so the efficiency of the enzyme in the fiber opening process will not be affected.

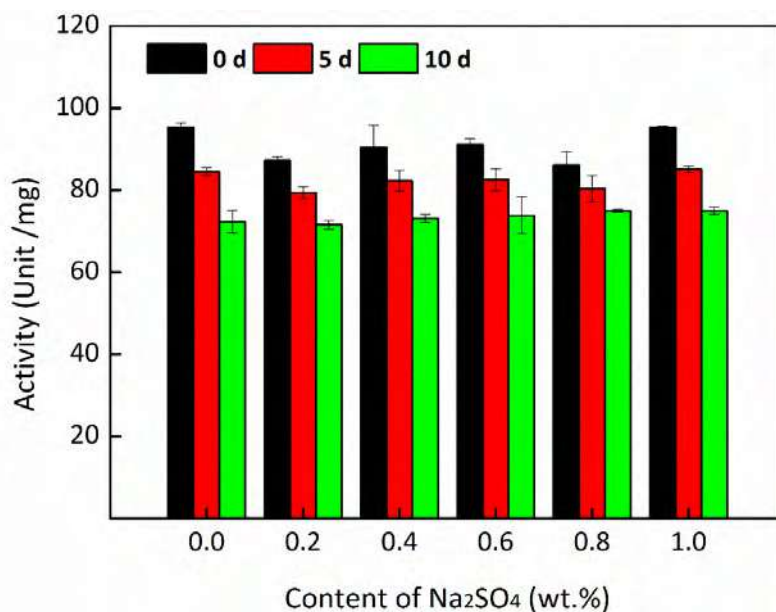


Fig. 1. Neutral protease activities at different sodium sulphate concentrations and different times.

3.2 Scanning electron microscope (SEM)

In general, SEM is a very important method to characterize the dispersion of collagen fibers in leather study. Great majority of the reported about leather industry have used this method. The dispersion of collagen fiber could be observed by SEM. In present study, three different salt-enzyme (which sodium sulfate-enzyme, magnesium chloride-enzyme and sodium chloride-enzyme) systems had been used for removal of interfibrillar substance and fiber opening. The effects of different kinds of salt-enzyme and different salt concentrations on fiber opening were discussed.

The results of SEM images of fiber opened by different concentrations of sodium sulfate (which 0, 0.2 wt.%, 0.4 wt.%, 0.6 wt.%, 0.8 wt.% and 1.0 wt.%) with 2.0 wt.% protease and 0.1 wt.% cellulase were showed in **figure 2**. It can be obviously inferred from the **figure 2** that the enzyme-based fiber opening would be improved distinctly at the presence of sodium sulfate compared with the method of without sodium sulfate, and the maximum dispersion of collagen fiber was observed when the concentration of sodium sulfate was 0.4 wt.%. Nevertheless, an appearance of inhibiting fiber opening was appeared when the sodium sulfate arrived above 0.6 wt.%.

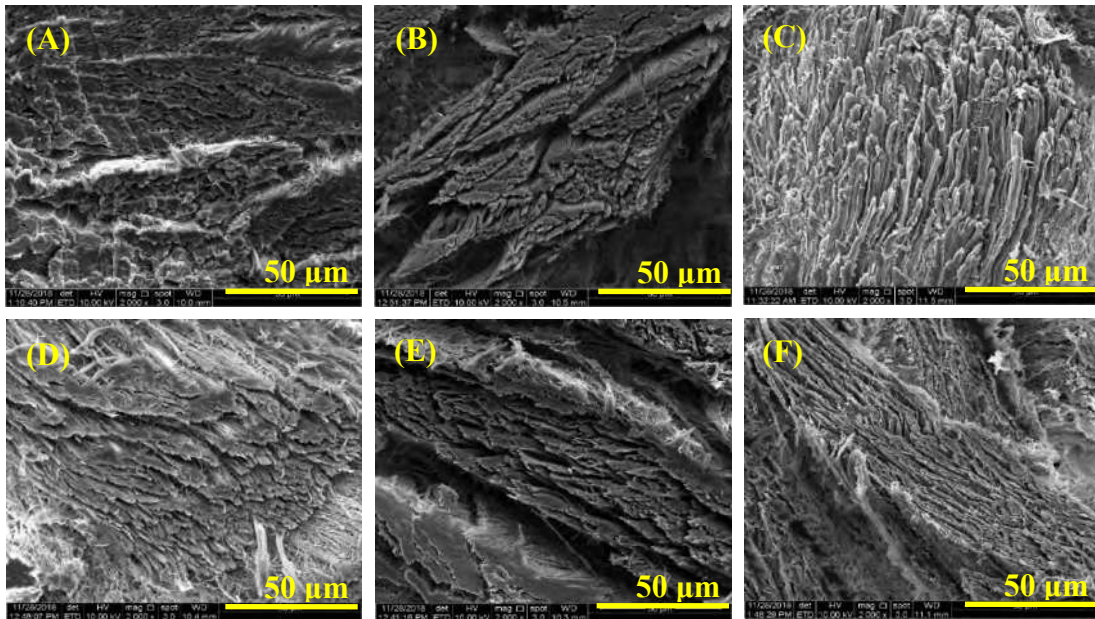


Fig. 2. Scanning electron microscopy images after fiber opening. (Content of Na₂SO₄: (A) 0 (B) 0.2 wt.% (C) 0.4 wt.% (D) 0.6 wt.% (E) 0.8 wt.% (F) 1.0 wt.%. Neutral protease: 2.0 wt.%. Cellulase: 0.1 wt.%)

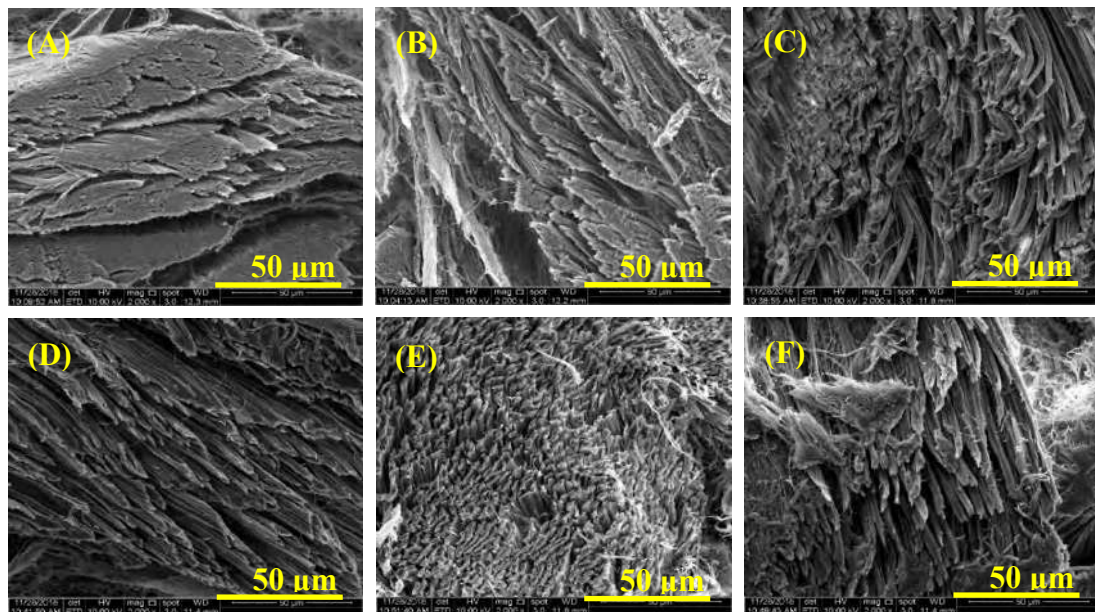


Fig. 3. Scanning electron microscopy images after fiber opening. (Content of MgCl₂: (A) 0 (B) 0.2 wt.% (C) 0.4 wt.% (D) 0.6 wt.% (E) 0.8 wt.% (F) 1.0 wt.%. Neutral protease: 2.0 wt.%. Cellulase: 0.1 wt.%)

The SEM images showing the different concentrations of magnesium chloride (which 0, 0.2 wt.%, 0.4 wt.%, 0.6 wt.%, 0.8 wt.% and 1.0 wt.%) mixed with 2.0 wt.% protease and 0.1 wt.% cellulase for fiber opening were showed in **figure 3**. The magnesium chloride assisted enzyme-based treated skin showed better opened up structure of collagen fiber and formed the single bundle of fibers with the increase of salt concentration. Hence, the maximum dispersion of collagen fiber would be observed when the concentration of magnesium chloride was 0.4 wt.%. On the contrary, with the concentration of salt was further increased, the degree of opened collagen fiber has been not increased significantly. This results may be due to the fact that magnesium chloride could promote

the protease into the skin to open the collagen fiber more thoroughly, and the most effect of the enzyme-based opened up structure was exhibited in the SEM when the concentration of salt was 0.4 wt.%. Therefore, the dispersion of collagen fiber opened by enzyme would not be further improved through the concentration of salt was increased.

The cross section of leather produced by experiments with different concentrations of sodium chloride (which 0, 0.2 wt.%, 0.4 wt.%, 0.6 wt.%, 0.8 wt.% and 1.0 wt.%) mixed with 2.0 wt.% protease and 0.1 wt.% cellulase for fiber opening were still observed by a SEM, and the results were showed in **figure 4**. As can be seen from **figure 4** that sodium chloride promoted the protease on the opening of collagen fiber less than sodium sulfate and magnesium chloride. However, it is worthwhile mentioning that the obviously opened up fiber structure has been observed by SEM when the concentration was 0.8 wt.% and with the concentration of sodium chloride further increased until to 1.0 wt.%, the opened up structure of fiber could not be observed clearly.

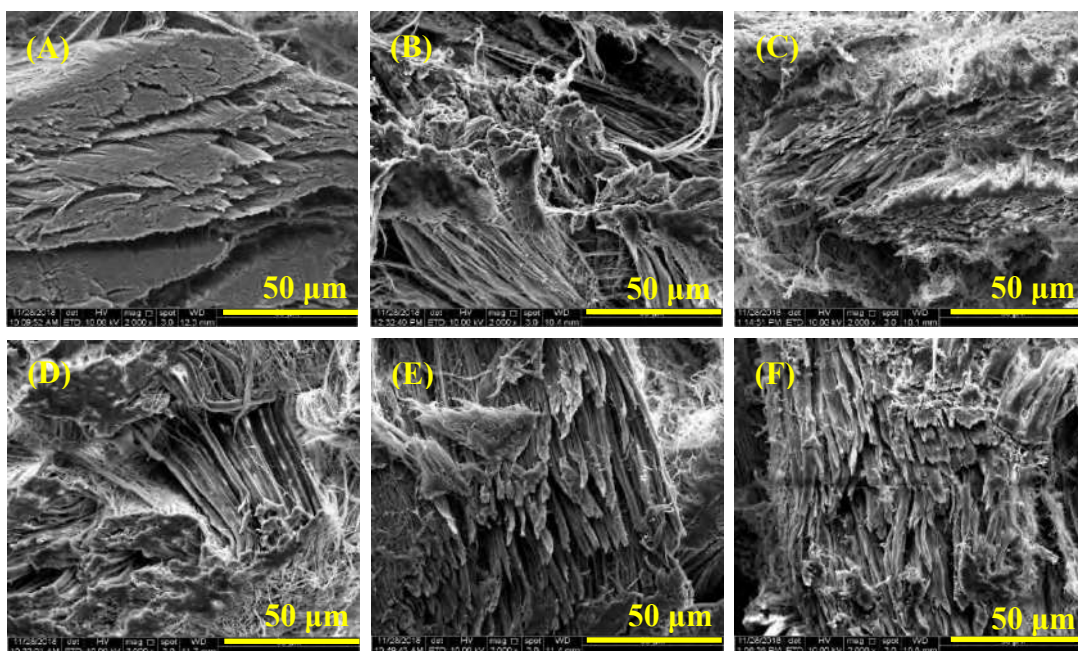


Fig. 4. Scanning electron microscopy images after fiber opening. (Content of NaCl: (A) 0 (B) 0.2 wt.% (C) 0.4 wt.% (D) 0.6 wt.% (E) 0.8 wt.% (F) 1.0 wt.%. Neutral protease: 2.0 wt.%. Cellulase: 0.1 wt.%)

In general, the effect of different salt-assisted enzyme on fiber opening were different. It can be clearly inferred from SEM images above that magnesium chloride had a better effect compared with other two salts. And sodium sulfate also could promote fiber opening as we could observed in **figure 2**. On the contrary, the effect of sodium chloride-assisted enzyme was not as well as that of the other two salts. It can be concluded that different salt-assisted enzymes had a same rule on fiber opening, which was that when the salt concentration reached a certain value, there was a little difficult to increase the salt concentration on promote the enzyme-based fiber opening, somewhat even inhibit the dispersion of fiber. The reasons are related to the ion radius of salt and the effect of different kinds of salt on the skin.

3.3 Total proteins dissolution analysis

The interfibrillar substance is mainly composed by interstitial-protein and proteoglycan, which is not conducive to the later tanning operation, so it is necessary to remove it. In beamhouse, the dissolution of interstitial-protein indirectly reflects the effect of salt-enzyme system on hide. Hence, it is need to determine the amount of protein released from hide. By measuring the protein content in solution before and after the experiment, which could indirectly determine the situation of

protein dissolution from hide and the effect of enzymes on removal of interfibrillar substance. In present study, the enhanced BCA Protein Assay Kit^[16] was used to determine the content of protein.

Figure 5 (A) shows the mass of protein dissolution per gram of skin after fiber opening using different concentrations of sodium sulfate mixed with 2.0 wt.% protease and 0.1 wt.% cellulase and **Figure 5 (B)** shows the mass of protein dissolution in different treatment periods. It could be clearly concluded from results that different concentrations of salt have the different effects on protein dissolution. It could be observed the maximum dissolution of proteins when the concentration of sodium sulfate was 0.4 wt.%, however, with further increased the concentration of sodium sulfate, the dissolution of protein was inhibited. From which can be indicated that a low concentration of sodium sulfate could promote the enzyme on dissolution of proteins, while if the concentration was more than 0.4 wt.%, it will inhibit them. It could be extracted that low concentration of sodium sulfate accelerates the enzymatic penetration into the skin and accelerate the enzymatic action on removal of interfibrillar substance, which dynamic process can proved from **Figure 5 (B)**.

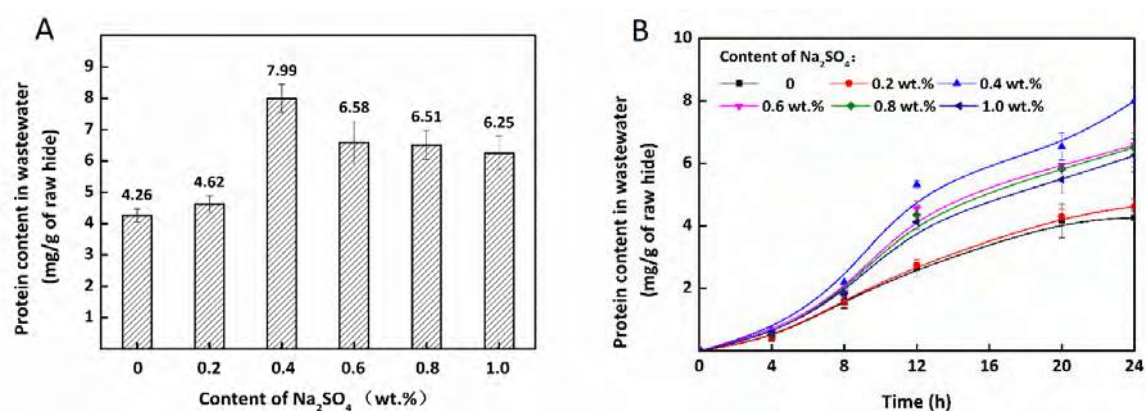


Fig. 5. Values of proteins of the liming process (A) and dynamic process (B) at different sodium sulphate concentrations. (Neutral protease: 2.0 wt.%. Cellulase: 0.1 wt.%)

Figure 6 (A) shows the mass of protein dissolution per gram of skin after fiber opening using different concentrations of magnesium chloride solution mixed with 2.0 wt.% enzymes and 0.1 wt.% cellulase, and **Figure 6 (B)** shows the dissolution of protein at different periods. It can be seen from **Figure 5** and **Figure 6** that the effect of protein dissolution as similar as sodium sulfate that different concentrations of magnesium chloride also had the different effect on protein dissolution. Nevertheless, there were also some difference that when the concentration of magnesium chloride was 0.4 wt.%, the protein dissolution was 10.73 mg/g and when the concentration of magnesium chloride was further increased, the phenomenon of neither accelerating protein dissolution nor inhibiting protein dissolution occurred, reaching a relatively balanced amount. Enzymatic fiber opening played a full role when the concentration of magnesium chloride was 0.4 wt.%, hence, the enzymatic action could not be improved further more by increasing the concentration of salt. Compared with sodium sulfate, magnesium chloride mixed with enzyme had a better removal of interfibrillar substance, which was indicated that magnesium chloride had better effect on promoting enzyme into the skin. From **Figure 6 (B)**, it can be seen that the dissolution ratio of proteins in the first 12 hours was improved evidently when using magnesium chloride assisted enzyme for fiber opening faster than that with using sodium sulfate, which indicated that the mixed action of magnesium chloride with enzyme can not only promoted the increase of the amount of protein dissolution, but also improved the dissolution rate. When this mixture was mixed for fiber opening, magnesium chloride could quickly promote the enzyme into the skin. The slope of the protein dissolution curve for the first eight hours shown in **Figure 6 (B)** also proved this. With time goes on, the dissolution of protein gradually reaches a saturation value.

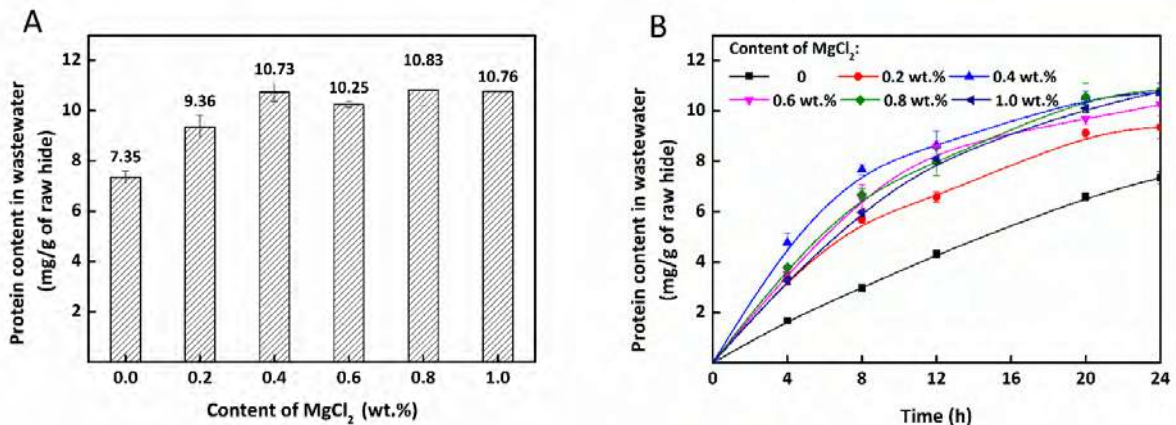


Fig. 6. Values of proteins of the liming process (A) and dynamic process (B) at different magnesium chloride concentrations. (Neutral protease: 2.0 wt.%. Cellulase: 0.1 wt.%)

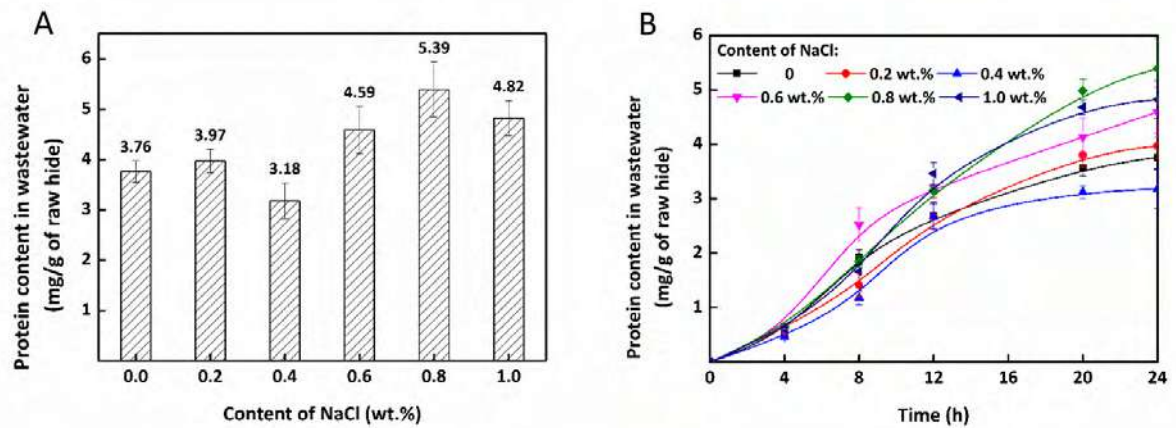


Fig. 7. Values of proteins of the liming process (A) and dynamic process (B) at different sodium chloride concentrations. (Neutral protease: 2.0 wt.%. Cellulase: 0.1 wt.%)

Different concentrations of sodium chloride mixed with enzyme were used to removal of interfibrillar substance and the situation of the protein dissolution were shown in **Figure 7**. By comparing **Figure 5**, **Figure 6** and **Figure 7**, it can be easily concluded that the effect of sodium chloride with enzyme on removing interfibrillar substance was obviously weaker than that of sodium sulfate and magnesium chloride mixed with enzyme. The maximum dissolution of protein was only 5.39 mg/g as the concentration of sodium chloride was 0.8 wt.%. Besides, with the further increased of NaCl concentration, protein dissolution was inhibited.

3.4 Histological staining

The histological staining analysis method is a very practical method for characterizing the dispersion of collagen fiber. After fiber opening, the degree of removal of interfibrillar substance could be judged by histological staining. In present study, histological stained cross section of skins after fiber opening were performed and observed using EVG staining. This stained method can provide the information about collagen and non-collagen materials present in the skin. **Figure 8 (A)** shows the tissue staining image of the raw skin without fiber opening, while **Figure 8 (B)**, **(C)** and **(D)** show the histological stained cross section of skin after fiber opening using three different salts mixed with enzyme.

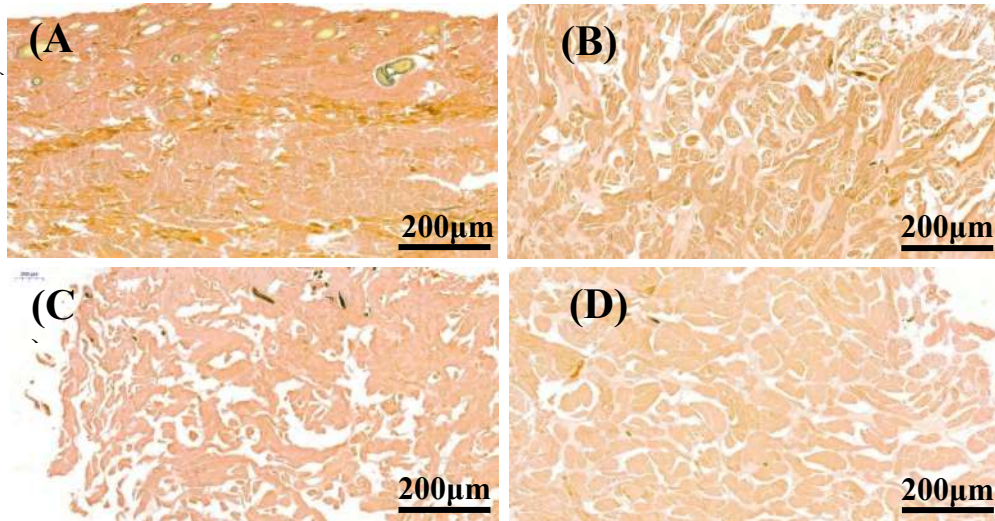


Fig. 8. EVG staining images of hides. ((A) Untreated (B) Na₂SO₄ (C) MgCl₂ (D) NaCl Neutral protease: 2.0 wt.%. Cellulase: 0.1 wt.%)

The non-collagen materials present in the skin could be clearly seen from **Figure 8** (A). Compared with the raw skin without fiber opening, **Figure 8** (B), (C) and (D) clearly demonstrate the effectiveness of enzyme-driven fiber opening process and different salt-assisted enzyme have different effects on fiber opening. The dispersion of collagen fiber could be assessed in terms of the interfibrillar spacing. It can be obviously inferred from **Figure 8** (C) that, after fiber opening using magnesium chloride mixed enzyme, the collagen fiber was split apart, which could be observed in the opened up structure. And this is consistent with the observation from SEM (**Figure 3**). On a comparative note, the fiber opening of samples using sodium sulfate assisted enzymes and sodium chloride assisted enzymes for fiber opening were slightly worse than those with magnesium chloride-assisted enzymes for fiber opening, as it could be seen from **Figure 8** (C) and (D).

3.5 Tannin Absorption

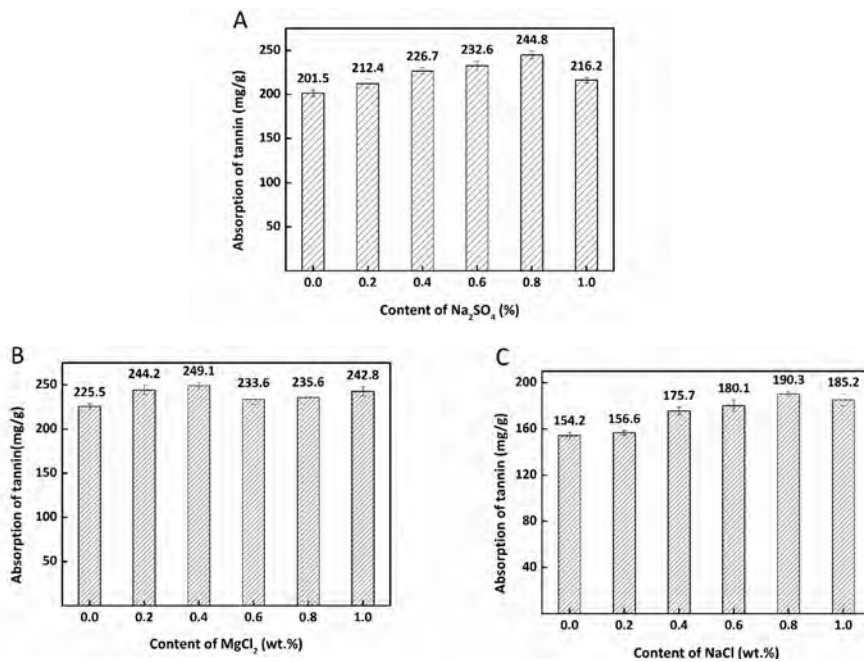


Fig. 9. Absorption of tannin after fiber tanning using different salt-enzyme for fiber opening. (Neutral protease: 2.0 wt.%. Cellulase: 0.1 wt.%)

Tanning process is a very important operation in which animal skin turn into leather^[17]. After fiber opening operation, many active groups would be exposed on the collagen molecule. Tanning process usually is mainly through the penetration of tanning agent molecules into the skin and combine with the active group of collagen molecule in which would happen the qualitative change. In present study, the tannic acid was used to tanning operation. In the tanning process, the tannin molecule and the collagen molecule were linked by hydrogen bonds and formed a stable large network structure^[18]. To some extent, the better the dispersion of collagen fiber, the more active groups exposed on the collagen molecule, and the more tannic acid molecules which could bind to collagen molecules. Therefore, the dispersion of collagen fiber can be indirectly judged by evaluating the amount of tannic acid binding to collagen molecules. **Figure 9** shows the amount of tannic acid absorbed by skin after tanning of the experiment samples. The more tannic acid was absorbed by per unit mass of skin, the better opened up structure of collagen fiber. It can be observably concluded from **Figure 9** that the absorption of tannic acid by skin was exactly related to the degree of fiber opening. The experiment samples which after fiber opening treated with sodium sulfate assisted enzyme and magnesium chloride assisted enzyme, the absorption of tannic acid absorbed by skin reached more than 200 mg/g, which indicated that the collagen fiber had a preferable opened structure and the evidence also could be obtained from the SEM (**Figure 2** and **Figure 3**). When the concentration of magnesium chloride was 0.4 wt.%, the content of tannic acid absorbed by the skin reached to 249.1 mg/g, indicating the best opened up structure, which was also verified by SEM (**Figure 3** (C)). On the contrary, the tannic acid absorbed by the sample treated by sodium chloride mixed enzyme was less than above two methods, and the poor opened up fiber structure was also observed.

4 Conclusion

In this study, three kinds of salts (sodium sulfate, magnesium chloride and sodium chloride) were selected to assist enzyme for fiber opening operation in the leather making. The results have shown that salt can be used to promote enzyme into skin to remove the interfibrillar substance and open the collagen fiber, furthermore the degree of fiber opening was related to the kind and concentration of salt assisting. Magnesium chloride had the best effect of promoting fiber opening, and the enzyme could play its full role in the process when the concentration of salt was 0.4 wt.% and at the same time the maximum protein dissolution and tannic acid could be measured. Compared with sodium sulfate and magnesium chloride, sodium chloride had a slightly poor effect on promoting fiber opening, nevertheless the dispersed fiber structure could be observed at 0.8 wt.% concentration. The degree of dispersion of fiber was related to the amount of tannin tanning agent absorbed by skin. The better dispersed structure could absorb more tannic acid. This beamhouse method provides a more efficient reference for the removal of interfibrillar substance and fiber opening by use salt-enzyme mixture.

Acknowledgement

The financial supports from the National Natural Science Foundation Commission of China (No. 51673177) and National Key R & D Program of China (No.2017YFB0308500) are greatly appreciated.

References

1. Thanikaivelan P, Rao J R, Nair B U, et al. Progress and recent trends in biotechnological methods for leather processing. *TRENDS BIOTECHNOL*, 22(4), 181-188, 2004
2. Durga J, Ranjithkumar A, Ramesh R, et al. Replacement of lime with carbohydrases – a successful cleaner process for leather making. *J CLEAN PROD*, 112, 1122-1127, 2016
3. Saravanabhavan S, Aravindhan R, Thanikaivelan P, et al. Green solution for tannery pollution: effect of enzyme based lime-free unhairing and fibre opening in combination with pickle-free chrome tanning. *GREEN CHEM*, 5(6), 707-714, 2003
4. Pandi A, Ramalingam S, Rao J R, et al. Inexpensive α -amylase production and application for fiber splitting in leather processing. *RSC ADV*, 6(39), 33170-33176, 2016
5. Nazer D W, Al-Sa'ed R M, Siebel M A. Reducing the environmental impact of the unhairing–liming process in the leather tanning industry. *J CLEAN PROD*, 14(1), 65-74, 2006
6. Rao R J, Thanikaivelan P, Nair B. An eco-friendly option for less-chrome and dye-free leather processing: in situ generation of natural colours in leathers tanned with Cr–Fe complex. *CLEAN TECHNOL ENVIR*, 14(2), 115-12, 2002
7. Saran S, Mahajan R V, Kaushik R, et al. Enzyme mediated beam house operations of leather industry: a needed step towards greener technology. *J CLEAN PROD*, 54, 315-322, 2013
8. Murugappan G, Zakir M J A, Jayakumar G C, et al. A Novel Approach to Enzymatic Unhairing and Fiber Opening of Skin Using Enzymes Immobilized on Magnetite Nanoparticles. *ACS SUSTAIN CHEM ENG*, 4(3), 828-834, 2016
9. Durga J, Ramesh R, Rose C, et al. Role of carbohydrases in minimizing use of harmful substances: leather as a case study. *CLEAN TECHNOL ENVIR*, 19(5), 1567-1575, 2017
10. Ranjithkumar A, Durga J, Ramesh R, et al. Cleaner processing: a sulphide-free approach for depilation of skins. *ENVIRON SCI POLLUT R*, 24(1), 180-188, 2017
11. Vijayaraghavan R, Vedaraman N, Muralidharan C, et al. Aqueous ionic liquid solutions as alternatives for sulphide-free leather processing. *GREEN CHEM*, 17(2), 1001-1007, 2015
12. Alla J P, Rao J R, Fathima N N. Integrated Depilation and Fiber Opening Using Aqueous Solution of Ionic Liquid for Leather Processing. *ACS SUSTAIN CHEM ENG*, 5(10), 8610-8618, 2017
13. Andrioli E, Petry L, Gutterres M. Environmentally friendly hide unhairing: Enzymatic-oxidative unhairing as an alternative to use of lime and sodium sulfide. *PROCESS SAF ENVIRON*, 93, 9-17, 2015
14. Aravindhan R, Monika V, Balamurugan K, et al. Highly clean and efficient enzymatic dehairing in green solvents. *J CLEAN PROD*, 140, 1578-1586, 2017
15. Yongchao Liang. Effects of silicon on enzyme activity and sodium, potassium and calcium concentration in barley under salt stress.pdf. *PLANT SOIL*, 209, 217–224, 1999
16. Piercer. BCA Protein Assay Kit product information (Fisher Scientific GmbH, 2010).
17. Zhang H, Chen X, Wang X, et al. A salt-free pickling chrome tanning approach using a novel sulphonic aromatic acid structure. *J CLEAN PROD*, 142, 1741-1748, 2017
18. Tambi L, Frediani P, Frediani M, et al. Hide tanning with modified natural tannins. *J APPL POLYM SCI*, 108(3), 1797-1809, 2008

LEATHERS FOR MARINE APPLICATIONS: INSTIGATING PHYSICO-CHEMICAL PROPERTIES OF CONVENTIONAL LEATHER

Gladstone Christopher Jayakumar^{1,2}, Jotheisvaran Abishek^{1,2}, Shahabudeen Sheik Sharukh^{1,2},
Jonnalagadda Raghava Rao^{1,2,3}

1 Anna University, Leather Technology, Chennai, India

2 CSIR-CENTRAL LEATHER RESEARCH INSTITUTE, Centre for Academic and Research Excellence, Chennai, India

3 CSIR-CENTRAL LEATHER RESEARCH INSTITUTE, Inorganic & Physical Chemistry, Chennai, India

Corresponding authors: jayakumarclri@gmail.com

Abstract. Leather and leather products are known for its durability and luxuries which makes it more unique amongst the other synthetic materials. Breathability and visco-elastic properties make leather unique choice of biomaterial. Utilization of leathers in marine based applications is limited owing to reactivity of leather towards salt and weather conditions. Moreover, the choice of raw materials and chemicals used during leather manufacture has greatly influence the properties of the leather. An attempt has been made to understand the influence of sea conditions on leathers. Conventional chrome tanned and vegetable tanned leathers were incubated in sea water and subsequently processed into post tanning to evaluate the physical properties. To understand, the leaching of chemicals, dyed leathers are incubated at different humidity and saline conditions. Interestingly, chrome tanned leathers found to be friendlier to marine conditions whereas, vegetable tanned leathers lead to leaching of chemicals. Furthermore, leaching of chromium is negligible, and crust leathers resulted in soft leathers. Prolonged exposure of chrome tanned leathers under salt stress leads to more softness. This might be due to saline stress to the skin matrix. Moreover, the compatibility of conventional leather chemicals was also tested using sea water. The research provides a new insight on fine tuning the chemicals to suit marine based applications.

1 Introduction

Leather is a natural material processed from animal skins mainly from goat, sheep, cow and buff. Viscoelastic and breathability are the unique properties of natural leathers which makes it more comfort and luxurious than synthetic materials. Leathers are widely used to manufacture footwear, garments, upholstery and goods. Understanding the physical properties of leathers in marine conditions is less reported. Research is carried out to utilise sea to manufacture leathers. However, the compatibility of conventionally tanned leathers such as chrome and vegetable tanned leather in sea water has not been reported. Leather for marine based application is seems to be challenging because of its major intricate physico-chemical properties like Fading due to weather conditions and salt concentration leading to corrosion (metal tanned leathers). Moreover, the consequences of salt interaction with leather are monitored for its hardness, shape retention, loss in physical strength and loss of moisture leading to fibre drying. Hence, this study is carried out to understand the various basic parameters in order to respond the above mentioned consequences. This study focuses on assessing the influence of sea water on chemical stability and leather characteristics.

2 Material and Methods

Chrome tanned, Vegetable tanned and Crust leathers (Dyed and undyed) of goat origin were used for the study. Sea water from Bay of Bengal was collected and used for the study without any further modification. Commercial and analytical grade chemicals were used for the compatibility testing with sea water and analysis respectively.

3 Results and discussion

In the present work the various parameters are chosen for selecting materials for marine applications are evaluated for their resistance behaviour to corrosion by seawater and by external environment (Humidity and Temperature) over a wide range of operating conditions, Figure 1. It is also monitored for its antifungal activity towards marine bio fouling and their mechanical properties of the material with increased life expectancy. Commercial chrome tanning and vegetable tanning (wattle) agents are mixed with sea water and checked for the stability. Vegetable tannins readily precipitated whereas the stability of chrome tanning agents is evaluated through visual assessment. Similarly, vegetable tanned leathers showed leaching of chemicals in the presence of sea water whereas, chrome tanned leathers showed no leaching of chromium which has been confirmed through Cr estimation in the liquor.

From the physico-chemical parameters it can be inferred that metal complex based tanning system shows much resistant to marine water.

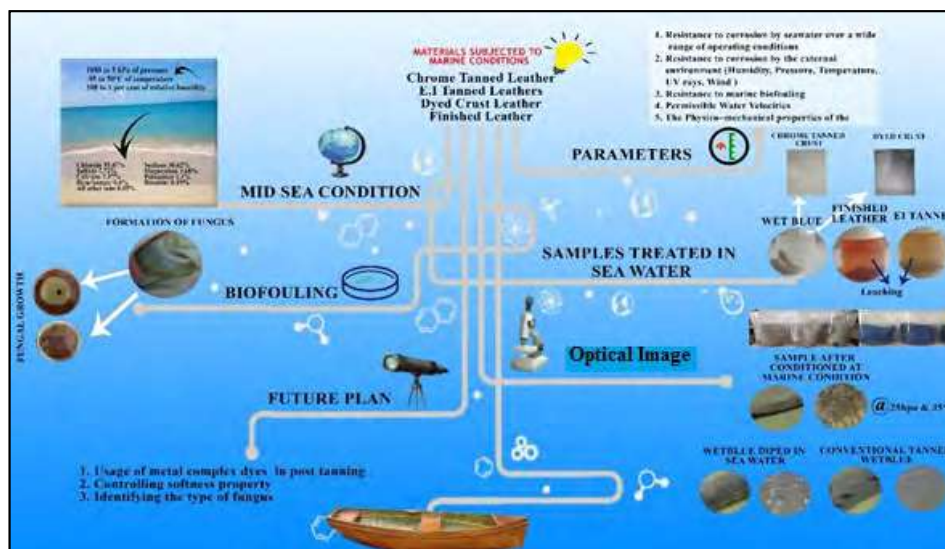


Figure 1. Schematic representation of the results.

This confirms the use of wet blue leathers are best suited for marine application. With the various post tanning chemicals, precipitation behavior has been studied and exhibited better dilution behaviour for fat liquors in marine water. In case of natural tanning system, precipitation occurs mainly due to the salt linkage formation at higher concentration in sea water during the post tanning processes. The crust leather without natural tannins soaked in sea water has been processed and evaluated for their physical strength properties. We observe that it has influenced softness in the white crust leather and leaching of dye seems to be minimal in case of dyed crust leathers. Similarly, in the case of dyeing characteristics, metal complex dyes are stable in marine sea water conditions. In case of marine bio fouling property, they show no fungal growth in the presence of preservatives and slight growth of *Aspergillus* without added preservative has been observed.

4 Conclusion

The present work confirms the wider usage range of chrome tanned leather with properly chosen post tanning chemicals would be a better and an appropriate material for marine based applications like marine boots and marine gloves.

5 Acknowledgements

Authors thanks the financial support from Department of Science and Technology (DST)- Promotion of University Research and Scientific Excellence (PURSE)II, Government of India and Department of Leather Technology, A.C. Tech, Anna University, India.

Reference

1. N Vedaraman, K Iyappan, S Ramalingam, C Muralidharan & P G Rao. (2003). Use of seawater in leather processing. *Journal of the American Leather Chemists Association*. 98. 333-336.
2. EL-Shahat H. A. Nashy & Ghada A. Abo-ELwafa. Highly Stable Nonionic Fatliquors Based on Ethoxylated Overused Vegetable Oils. *Journal of the American Oil Chemists' Society*. 88(10). 2011. 1611-1620
3. S Michael S & M Michael. Dimensional and structural stability of leather under alternating climate Conditions. *Journal of asociación de químicos españoles de la industria del cuer*. 63. 2012. 1-8.
4. Meyer, M., Schröpfer, M. and Trommer, A. Effects of temperature and humidity on different crosslinked collagen structures. *Proceedings of the XXXIX IULTCS Congress, Istanbul, 2006*

STRIDING TOWARDS SELF-SUSTAINABILITY USING ALUMINIUM FROM TANZANIAN KAOLIN FOR COMBINATION TANNING SYSTEM

^aC. R. China^{1,2}, G. C. Jayakumar², A. Hilonga¹, S. V. Kanth², K. N. Njau¹

¹ The Nelson Mandela African Institution of Science and Technology, Materials Science and Engineering (MaSE) P. O. Box 447, Arusha, United Republic of Tanzania

² Tanzania Industrial Research and Development Organization, Division of Textile and Leather Technology, P. O. Box 23235, Dar es Salaam, Tanzania.

³ CSIR-Central Leather Research Institute, Centre for Human and Organizational Resources Development (CHORD), Chennai, India.

a) Corresponding authors: ceciliac@nm-aist.ac.tz and jayakumarclri@gmail.com

Abstract. Sustainability is a key factor which controls future leather manufacture. Developing several new technologies is one of the primary agendas for sustainability. However, developing countries are facing several challenges which not only limited to best practice technologies but also finding self-sustainability in maximizing the available resources. In the present study, an attempt has been made to explore the potential resource of aluminium sulphate from kaolin of Pugu hills, Tanzania for combination tanning. Though, extraction of aluminium sulphate from several resources are available, there is limited literature pertaining to Tanzania resources. Therefore, aluminium sulphate extracted from kaolin was basified and studied for its tanning efficiency. Diffraction and vibrational spectroscopic studies were carried out to assess the confirmation of extracted aluminium. Combination tanning has been carried out with vegetable tannins, which are from natural resources. Leathers tanned with aluminium sulphate and mimosa resulted with a hydrothermal stability temperature beyond 100°C as compared to vegetable tannin alone showed 78°C. Physical strength characteristics met the standard norms. Fiber separation was good, which has been confirmed through microscopic studies. The study provides a new insight on accomplishing self-sustainability through available resources and manufacture eco-friendly system.

Key words: Pugu kaolin, Combination tanning, Aluminium sulphate, mimosa, leather manufacturing

1 Introduction

Sustainability is a key factor, which controls future leather manufacture. Today's leather industry is dominated by use of chromium salt as tanning agent. However, Chromium tanning is being debatable owing to reported toxicity of chromium (VI) and associated disposal issues [1]. A new tanning system without using chromium salt is an immediate need for sustainable leather industry. Studies revealed that combination tanning, whereby vegetable tannins are coupled with Aluminium Sulphate [Al₂(SO₄)₃], produce good quality leather mimicking the properties of chrome-tanned leather [1-10]. Al₂(SO₄)₃ currently used in combination tanning is industrially produced by the Bayer and Hall-Herault processes, using bauxitic rocks as raw materials, which contain between 20 and 30% of aluminium [11, 12]. However, bauxite is globally diminishing and also it is often completely absent in known commercial quantity in most developing countries [13]. Kaolin, which is richly available in most developing countries, containing between 10-20% aluminium, can be a reliable source of aluminium for production of Al₂(SO₄)₃ for various applications [12].

Tanzania is endowed the largest kaolin deposit in Africa that entails possible production of Al₂(SO₄)₃ for combination tanning. About 2.3 billion metric tons kaolin deposit of high standard is located in Pugu Hills, 35 km from Dar es Salaam, Tanzania [14-16]. The potentials of Pugu kaolin for industrial use is still untapped [14, 15]. In the present study, an attempt has been made to explore the potential resource of aluminium from kaolin of Pugu hills, Tanzania for combination tanning.

2 Material and Methods

2.1 Materials

Kaolin was collected from Pugu hills, Kisarawe in the coast region of Tanzania, by using quarter sampling technique as described by Sempeho [17]. All chemicals used were of analytical grades purchased from Sigma Aldrich Ltd, India. Industrial chemicals used were of commercial grade, Goatskins pelts were generously donated by CSIR-CLRI pilot tannery, pre-tanning section.

2.2 Extraction of kaolin

Raw kaolin was grounded to fine particles, activated by heating and dissolved in concentrated sulphuric acid at a definite ratio for 90 minutes. Resultant filtrate was concentrated to obtain white crystals of aluminium sulphate. The latter was analysed by XRD AND FTIR to assess the confirmation of extracted aluminium.

2.3 Combination tanning trials

Sample goatskins were treated with mimosa in combination with basified and masked $\text{Al}_2(\text{SO}_4)_3$ from kaolin. The recipe for tanning process was adopted from CSIR-CLRI pilot tannery. In summary, 15% of mimosa was used in combination with varying concentrations of $\text{Al}_2(\text{SO}_4)_3$ expressed as % Al_2O_3 . Control skin sample treated with mimosa alone.

2.4 Determination of shrinkage temperature

The shrinkage temperature test was carried out as per SATRA STD 114 method. A strip of about 2 cm^2 leather were cut from tanned leather sample clamped between jaws of the clamp that in turn was suspended in a solution of water: glycerol mixture (3:1). The mixture was gradually heated and the temperature at which leather sample shrinks to one third of its original length was recorded as a shrinkage temperature. All analyses were done in duplicate.

2.5 Post tanning process

After tanning the samples were shaved to uniform thickness of 1.1 mm and conventional post tanning processes were carried out by 13% syntans and 8% fatliquor. Thereafter, leather samples were set, toggled to dry, staked and buffed.

2.6 Physical characterization of crust leather

Experiment and control crust leather samples were subjected to physical testing to determine the influence of $\text{Al}_2(\text{SO}_4)_3$ from kaolin on physical properties of leather. Tear strength water vapour permeability tests were carried out using SATRA TM 162:1992. All test samples were conditioned at 20°C and 65% relative humidity. Duplicate analyses were performed for each sample.

2.7 Scanning Electron Microscopic analysis of Leather Samples

Experiment and control crust leather samples were cut into predefined sampling position and shaped into uniform thickness, coated with gold using Edwards E306 sputter coater followed by scanning process. The micrographs for cross section were obtained by operating the SEM at an accelerating voltage of 5 KV with 150X magnification.

3 Results and discussion

In the present study, Combination tanning using mimosa and $Al_2(SO_4)_3$ extracted from kaolin was carried out with the main goal of exploring potential utilization of kaolin resource in leather industry (Fig. 1).

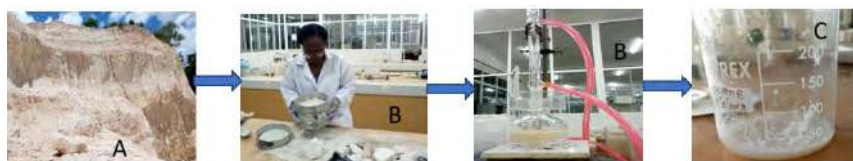
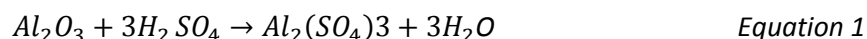


Figure 1. Step by step preparation of aluminium sulphate from Pugu kaolin (A=Kaolin deposit, B=Preparation and extraction, C=Aluminium sulphate)

3.2 Analysis of $Al_2(SO_4)_3$ from Pugu kaolin

During extraction process, Al_2O_3 present in kaolin is leached and react with sulphuric acid used for dissolution to form $Al_2(SO_4)_3$ and water (eq. 1). XRD and FTIR spectra of extract have displayed most characteristic peaks of $Al_2(SO_4)_3$ signifying that $Al_2(SO_4)_3$ was formed during extraction process.



3.3 Determination of shrinkage temperature

The shrinkage temperature of the samples was determined to assess the tanning effect. It was observed that addition of $Al_2(SO_4)_3$ resulted in significant increase in shrinkage temperature in the order of 78, 115, 118, 114°C for 0, 2, 5 and 10% Al_2O_3 , respectively.

3.4 Physical properties of leather samples

It is important to study the influence of the tanning system on the strength properties of leathers. Physical properties analyses carried out are tearing strength and water vapour permeability. Physical characteristic data for leather samples tanned with different concentrations of Al_2O_3 meet standard values recommended by CLRI. Micrographs of leather samples tanned with combination system show better fiber dispersion than those tanned using mimosa alone.

4 Conclusion

In the present work, investigation was made to study potential of Pugu kaolin as source of $Al_2(SO_4)_3$ for combination tanning. $Al_2(SO_4)_3$ was successful obtained from kaolin using sulphuric acid as dissolution agent. Its application in combination tanning with mimosa gave leathers with shrinkage temperature beyond 100°C that can be achieved with as low concentration as 2% Al_2O_3 . Produced leather showed physical properties above recommended values and good fiber structures separation. This study provides useful information on accomplishing self-sustainability through available resources in Tanzania for eco-friendly leather manufacturing.

5 Acknowledgements

This work was financed by the Centre for Science and Technology of the Non-Aligned and Other Developing Countries (NAM S&T Centre) under Research Training Fellowship for Developing Countries Scientists (RTF-DCS) 2016-2017 Scheme [Grant number NAM – 05/74/2015] and Africa Development Bank through The Nelson Mandela African Institution of Science and Technology [Grant number 2100155032816]

Reference

1. Madhan, B., et al., *Interaction of aluminum and hydrolysable tannin polyphenols: An approach to understand the mechanism of aluminum vegetable combination tannage*. Vol. 101. 2006. 317-323.
2. Musa, A. and G. Gasmelseed, *Combination tanning system for manufacture of shoe upper leathers: cleaner tanning process*. *Journal of the Society of Leather Technologists and Chemists*, 2012. **96**(6): p. 239-245.
3. Musa, A. and G. Gasmelseed, *Development of eco-friendly combination tanning system for the manufacture of upper leathers*. *International Journal of Advance Industrial Engineering*, 2013. **1**(1): p. 9-15.
4. Musa, A. and G. Gasmelseed, *Eco-friendly vegetable combination tanning system for production of hair-on shoe upper leather*. *Journal of Forest Products & Industries*, 2013. **2**(1): p. 5-12.
5. Musa, A., et al., *Studies on combination tanning based on henna and oxazolidine*. *Journal of the American Leather Chemists Association*, 2009.
6. Choudhury, S.D., S. DasGupta, and G.E. Norris, *Unravelling the mechanism of the interactions of oxazolidine A and E with collagens in ovine skin*. *International journal of biological macromolecules*, 2007. **40**(4): p. 351-361.
7. Hassan, E.A. and M.T. Ibrahim, *Innovation of New Cleaner Technology: Tannage by Local Tanning Agent Acacia Nilotica (Garad) and Aluminum Retannage*. 2014.
8. Mahdi, H., et al., *Vegetable and aluminium combination tannage: aboon alternative to chromium in the leather industry*. 2008.
9. Covington, A.D., *Modern tanning chemistry*. *Chemical Society Reviews*, 1997. **26**(2): p. 111-126.
10. E Musa, A. and G. A Gasmelseed, *Combination Tanning System for Manufacture of Shoe Upper Leathers: Cleaner Tanning Process*. Vol. 96. 2013. 239-245.
11. Pinna, E.G., et al., *Hydrometallurgical extraction of Al and Si from kaolinitic clays*. *REM-International Engineering Journal*, 2017. **70**(4): p. 451-457.
12. Chigondo, F., B.C. Nyamunda, and V. Bhebhe, *Extraction of water treatment coagulant from locally abundant kaolin clays*. *Journal of Chemistry*, 2015. **2015**.
13. Aderemi, B.O., L. Edomwonyi-Otu, and S.S. Adefila, *A new approach to metakaolin dealumination*. *Australian Journal of Basic and Applied Sciences*, 2009. **3**(3): p. 2243-2248.
14. Akwilapo, L.D. and K. Wiik, *Ceramic properties of Pugu kaolin clays. Part I: Porosity and modulus of rupture*. *Bulletin of the Chemical Society of Ethiopia*, 2003. **17**(2).
15. Kimati, B., *Massive kaolin deposits untapped at Pugu hills*, in *Daily News*. 2012, Tanzania Standard Newspapers Ltd: Dar es Salaam.
16. Schwaighofer, B. and H. Muller, *Mineralogy and genesis of the pugu hill kaolin deposit, Tanzania*. *Clay Minerals*, 1987. **22**(4): p. 401-9.
17. Sempeho, S., E. Lugwisha, and L. Akwilapo, *Suitability of kaolin and quartz from Pugu and feldspar from Morogoro as raw materials for the production of dental porcelain [MS thesis]*. University of Dar es Salaam, Dar es Salaam, Tanzania, 2012.

LEATHER PROPERTIES AS A FUNCTION OF CATTLE BREED

S. Stenzel^{1,a}, M. Schroepfer¹, I. Prade¹ and M. Meyer^{1,b}

1 Research Institute of Leather and Plastic sheeting (FILK) gGmbH, Meißner Ring 1-5, 09599 Freiberg, Germany. .

a)Corresponding author: sandra.stenzel@filkfreiberg.de

b)michael.meyer@filkfreiberg.de

Abstract. Since hundreds of years, tanners share the opinion that hides from different cattle breeds lead to varying leather characteristics. Especially European hides from the alpine region (e. g. Simmentaler or brown origin) are preferred by tanners. These leathers feature a higher thickness, a maximum utilisation induced by a minor thickness difference over the whole area and a lower tensile strength in contrast to leathers from other breeds. However, are these alpine hides better because of their breed affiliation or because they are kept in special regional conditions? It is known that, besides the breed, also other factors can influence the rawhide and leather quality like age, gender, nutrition and climate conditions. In addition, present dairy and beef cattle are high-performance cattle by breeding, which leads to more crossbreeds than 100 years ago. Our intention was to find out, whether leather characteristics nowadays are still a function of breed or not. For that purpose, 50 rawhides from four different cattle breeds (Angus, Charolais, Simmentaler, Limousin, Holstein) were collected from the Saxon region. For characterization, the physical parameters tensile strength, elongation at maximum force and stitch tear strength were detected for all breeds. In summary, only minor differences between leathers from different cattle breeds were found for the tensile strength, the elongation at maximum and the stitch tear strength. In addition, the intra-group variation within the breeds was constantly on a high level. Interestingly, we observed that older skin donors show a higher variance of the tensile strength and of the elongation at maximum force. Nevertheless, this tendency to equal leather properties between the breeds must be confirmed by a larger quantity of test individuals.

1 Introduction

It is an unwritten law for tanners, that hides from different cattle breeds lead to varying leather characteristics. Especially European hides from the alpine region (e. g. Simmentaler or brown origin, so called “south german raw hides”) are preferred by tanners. On the rawhide market, such raw hides achieve higher prices in contrast to hides from north German regions, where breeds such as Holstein prevail.

Leathers with south German origin should feature a higher thickness, a maximum utilisation induced by a minor thickness difference over the whole area and a lower tensile strength in contrast to leathers from other breeds (1). This tanners opinion is raised over hundreds of years but is only underlined by one scientific publication, which is over 60 years old. Since then, cattle breeds have extremely changed by genetic breeding programmes to raise their economic traits (e. g. milk yield, maternal ability, feed efficiency) (2). Additionally, present dairy and beef cattle are high-performance cattle, which leads to more crossbreeds than 100 years ago. However, there is the question whether these alpine hides are better because of their breed affiliation or because their regional husbandry conditions. It is known that, besides the breed, also other factors can influence the rawhide and leather properties like age, gender, nutrition and climate conditions (3,4).

We wonder if this deep-rooted opinion from high-quality –leathers of alpine origin is still up-to-date. The intention of our study is to investigate if leather properties are still dependent on the cattle breed.

2 Materials and Methods

Collection of skin samples

Skins were collected from the following breeds: Simmentaler, Holstein, Angus (widespread occurrence in Germany), Limousin and Charolais.

All skins have their origin from small farms located in the Saxon region. Ten rawhides were collected from every breed. Preservation was achieved by salting. Table 1 shows the age and gender for all skins. For every breed, 5 skins of male and 5 skins of female individuals were collected. All individuals were younger than 4 years and 10 months. All female individuals were heifer, which means, that no female individual was pregnant during lifetime.

Table 1.

Breed	hide	Age (months)	gender	Breed	hide	Age (months)	gender
Angus	A1	20	♂	Limousin	L1	25	♂
	A2	24	♀		L2	30	♀
	A3	28	♀		L3	24	♀
	A4	23	♀		L4	30	♀
	A5	25	♀		L5	29	♀
	A6	12	♀		L6	46	♀
	A7	41	♀		L7	16	♀
	A8	27	♀		L8	34	♀
	A9	34	♀		L9	11	♀
	A10	41	♀		L10	12	♀
Charolais	C1	19	♀	Simmentaler	F1	24	♀
	C2	22	♀		F2	23	♀
	C3	19	♀		F3	21	♀
	C4	19	♀		F4	24	♀
	C5	21	♀		F5	17	♀
	C6	19	♀		F6	22	♀
	C7	19	♀		F7	24	♀
	C8	18	♀		F8	20	♀
	C9	16	♀		F9	22	♀
	C10	17	♀		F10	23	♀
Holstein	S1	56	♀				
	S2	36	♀				
	S3	13	♀				
	S4	25	♀				
	S5	13	♀				
	S6	17	♀				
	S7	39	♀				
	S8	17	♀				
	S9	15	♀				
	S10	15	♀				

Leathers and test samples

All skins were halved from neck to tail along the backbone and were prepared equally. The leather was produced by using conventional processes: First, the skins were subjected to a lime-sulfide liming, followed by a mechanical flesh removing, a formic and sulphuric acid pickling and chrome tanning. Skins from one breed were tanned in one lot. The skins were then fatliquored, dyed and dried.

The samples for the physical measurements were cut from the same area along the backbone in the lower third, which is the official testing side for leathers or so called DIN-area.

Tensile strength and elongation at maximum force

Measurements of tensile strength and elongation at maximum force were performed according to standard methods (DIN EN ISO 3376) on a LLOYD Instrument (Erichsen Prüftechnik Wuppertal). The thickness of the rawhides was measured with the same instrument. The tensile strength and the elongation at maximum force were normalized for thickness of the leathers. For every individual, two leather samples from the DIN-area was taken from the right and left hide. Six samples were taken from each hide sample for the measurements, respectively. Every individual leather contributes with 12 data values to the overall of data set.

Stitch tear strength

Measurements of stitch tear strength were performed according to standard methods (DIN EN ISO 23910) and normalized for leather thickness. For each leather, three test samples were cut parallelly and perpendicularly to the backbone, respectively. Therefore, one leather contributes with 12 data values (left and right hide) to the overall data set.

All parallel and perpendicular measurements of one leather were averaged for the stitch tear strength. Because the stitch tear strength depends mainly on the orientation of the collagen fibrils (5), an adjusted stitch tear strength (ATS) is introduced. The ATS is the quotient between the stitch tear strength parallel to the backbone and the strength perpendicular to the backbone. An ATS of 1 indicates the same force is needed to tear the leather parallelly and perpendicularly to the backbone. An ATS over 1.0 indicates that a higher force is needed to tear the leather parallelly than perpendicularly to the backbone. Moreover, an ASR under 1.0 indicates lower forces for leather rupture parallel in contrast to perpendicular to the backbone are needed.

Data analysis

Data were submitted to analysis of variance using R (6) and mean values were compared by Tukey's test (7) at 5 % level of significance.

3 Results and Discussion

The collected 50 rawhides have their origin in the saxon region. The thickness of these rawhides was compared to get a first overview over the hide samples. Figure 1 shows the thickness of all sampled hides grouped by breed or gender.

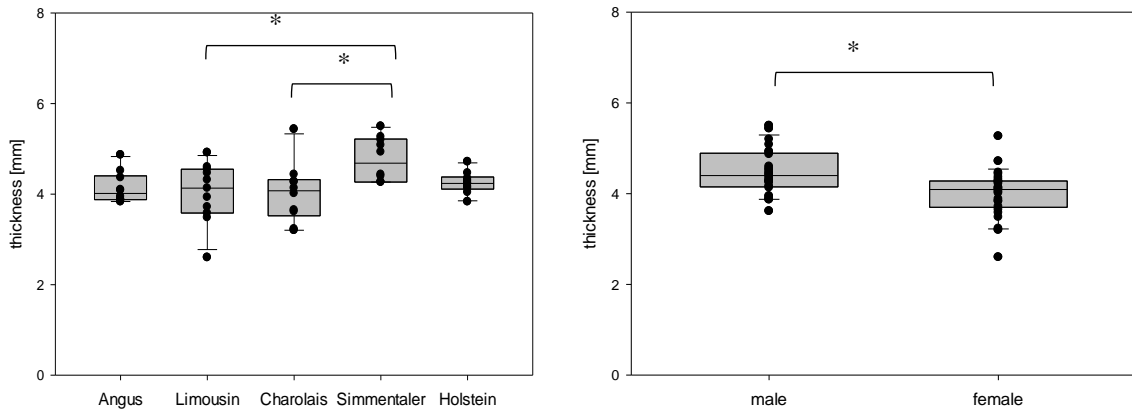


Figure 1. Thickness of all sampled hides (left: grouped by breed, right: grouped by gender, Significance code: ‘*’ 0.05.) Every point is a mean value of 12 data values for one hide.

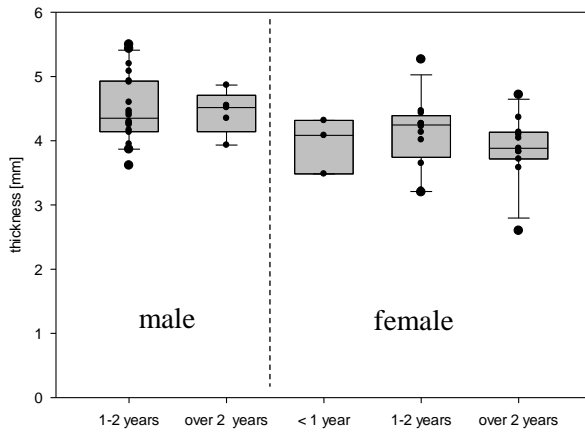


Figure 2. Thickness of the rawhides in dependence of the age of the donor (Every point is a mean value of 12 data values for one hide).

Simmentaler rawhides show the highest thickness compared to the other tested breeds. This is in accordance to the measurements of the workgroup of Hausam from 1952 (1), who also showed, that breeds with south german origin (such as Simmentaler) have a higher thickness in contrast to other breeds.

For Holstein rawhides, the variance was the smallest (Figure 1, left), which means that Holstein individuals deliver hides of mostly constant thickness independent from gender or age (age variance 13 months up to 56 month, see table 1). Except from Holstein, male and female rawhides differ significantly in thickness (Figure 2). However, the age of the donor did not affect the thickness (Figure 2). In summary, the thickness of the rawhides depends on breed and gender.

All rawhides were tanned equally, because any change in the leather manufacture process influences derma structure and the final properties of leather (8). The produced leathers were subjected to tensile strength measurements. Figure 3 and 4 show the resulting values for the tensile strength in dependence of breed, gender or age.

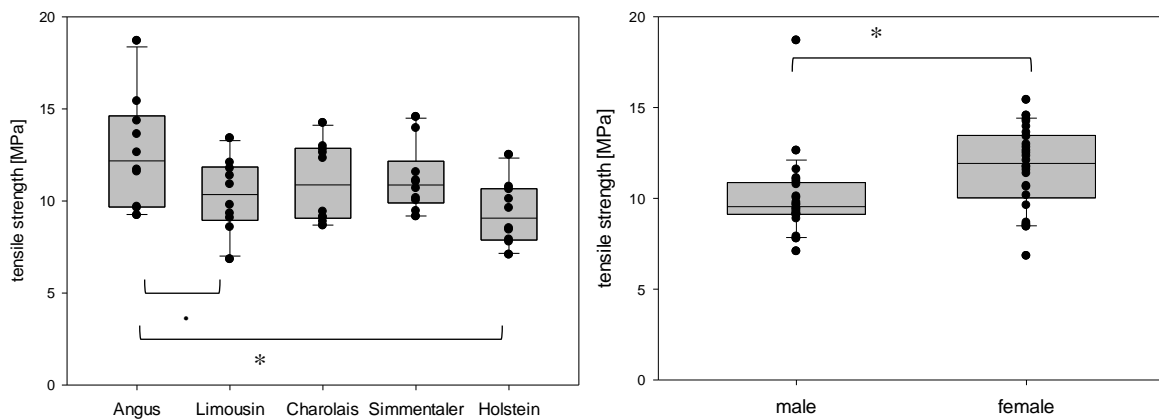


Figure 3. Tensile strength in dependence of breed (left) and gender (right) (Significance codes: ‘.’ 0.1, ‘*’ 0.05). Every point is a mean value of 12 data values for one leather.

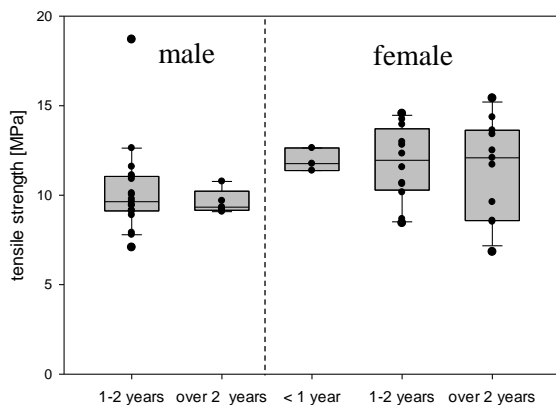


Figure 4. Tensile strength in dependence of the age of the donor. Every point is a mean value of 12 data values for one leather.

The major skin component is the protein collagen, which is therefore responsible for many properties of the skin and also of the leather such as flexibility and strength (9). The stability of leather and therefore its tensile strength depends mainly on the produced crosslinks by tanning (10) and on the collagen matrix of the rawhide. Leathers with Limousin or Holstein origin feature the lowest tensile strength (in dependence of the chosen tanning procedure) (Figure 3, left). This is not in accordance with fewer results, because as described by Hausam (1), the breeds with south German origin (e. g. Simmentaler) should have the lowest tensile strength. In our study, leathers with Angus origin showed the highest tensile strength when compared to Limousin or Holstein. However, the variation within the breeds are mostly higher than between the breeds.

In addition, there is a significant difference of the tensile strength between leathers with male and female origin (Figure 3, right). Leathers with female origin show higher tensile strengths than leathers with male origin. But this result must regard with caution, because of the existing sub-grouping by breed in the male and female group.

Figure 4 shows the dependence of the tensile strength in dependence of different age categories. No significant differences were found between the different groups, but leathers with female origin show the more variation, the older they are. Obviously, external influences on the skin stability, such as nutrition and husbandry conditions, increase over time. This effect is not confirmed in the

groups of male leathers, but here only 5 individuals account to the group of leathers from over- 2- years- old individuals.

For the produced leathers, also the elongation at maximum force was measured. The elongation of maximum force was normalized for thickness because of local thickness changes between the leathers. Of course, the elongation at maximum force depends not only on the thickness. The elongation at maximum force is mainly a function of the density because of the heterogeneity of the leather material. However, the existing data were plotted against thickness, and under the given conditions, the elongation at maximum force became a linear function of the thickness (in the range of 1.3 mm to 2.2 mm) [data not shown]. Therefore, the normalization for thickness is a good approximation for interpretation of the existing data. Figure 5 and 6 show the normalized data in dependence of breed, gender or age.

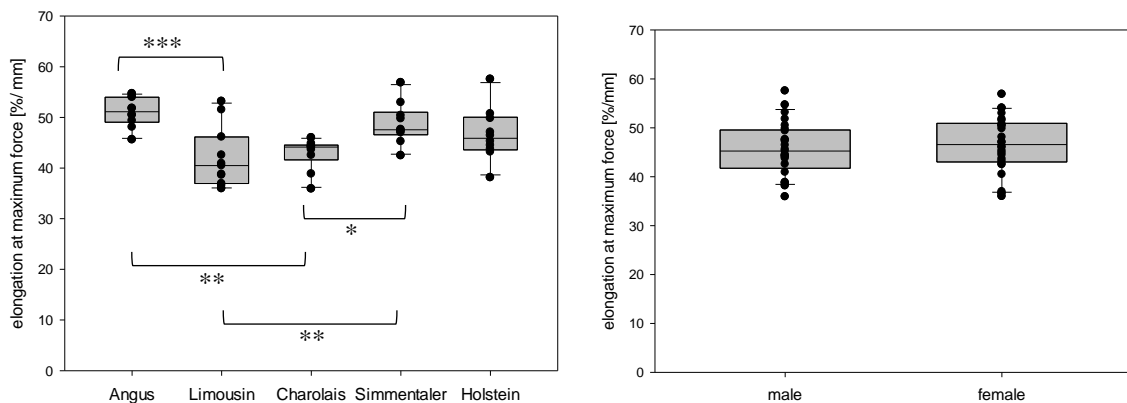


Figure 5. Elongation at maximum force in dependence of breed (left) and gender (right). (Significance codes: '.' 0.1, '*' 0.05, '**' 0.01, '***' 0.001). Every point is a mean value of 12 data values for one leather.

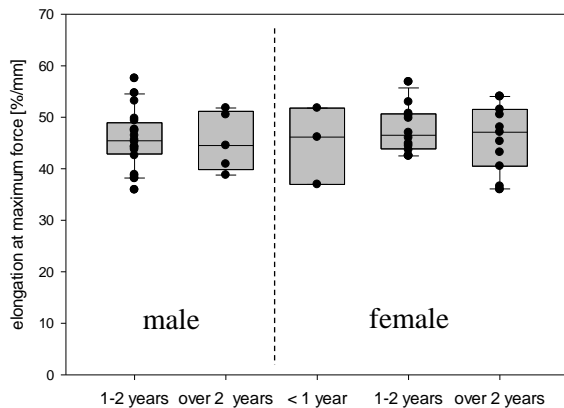


Figure 6. Elongation at maximum force in dependence of the age of the donor. Every point is a mean value of 12 data values for one leather.

Leathers with Limousin and Charolais origin feature the lowest elongation at maximum force (Figure 5, left). Although, the variation within the breeds are quiet high, significant differences of both breeds compared to Angus and Simmentaler could be observed.

There is no significant difference between leathers with male or female origin (Figure 5, right). But the male and female group are also structured, which means that differences between breeds could be balanced out by each other. Therefore the male and female group must be divided in breed- dependent sub-groups, which is handicapped by the low number of individuals.

Figure 6 shows that the elongation at maximum force has the lowest variation in 1-2 years- old individuals. Similar to the tensile strength, the variation of the elongation is higher in older donors. Females younger than one year are not considered because of the low number of samples.

Finally, besides tensile strength and elongation at maximum force, the stitch tear strength was analysed. Figure 7 and 8 show the stitch tear strength in dependence of breed, gender or age.

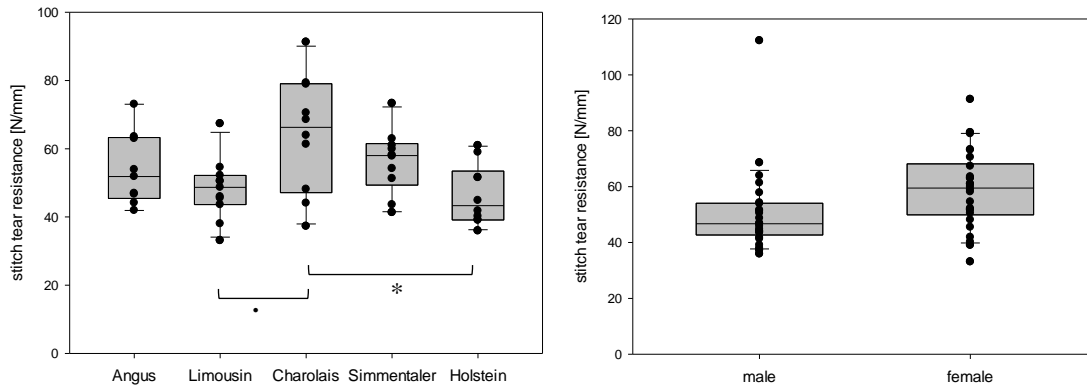


Figure 7. Stitch tear strength in dependence of breed (left) and gender (right). (Significance codes: ‘.’ 0.1, ‘*’ 0.05, ‘**’ 0.01, ‘***’ 0.001). Every point is a mean value of 12 data values for one leather.

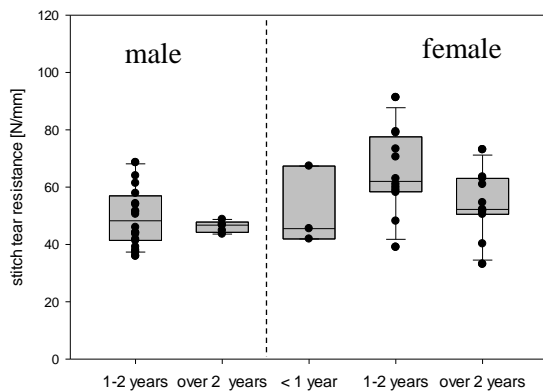


Figure 8. Stitch tear strength in dependence of the age of the donor. (Significance codes: ‘.’ 0.1, ‘*’ 0.05, ‘**’ 0.01, ‘***’ 0.001). Every point is a mean value of 12 data values for one leather.

Leathers with Charolais origin feature the highest stitch tear strength, but also the highest in- group- variation (figure 7, left). The lowest stitch tear strength was measured in the Limousin and Holstein group. However, the variation within the breeds are again mostly higher than between the breeds. There is no significant difference between leathers with male or female origin (Figure 7, right) for the stitch tear strength. The high variance of older donor individuals was not present here (see Figure 8). However, the stitch tear strength is higher for female leather in the age category 1- 2- years- old donor individuals than for male leathers of the same age category.

Because the stitch tear strength depends mainly on the orientation of the collagen fibrils (5), measurements parallel and perpendicular to the backbone were performed and the ATS was calculated for every breed (Figure 9).

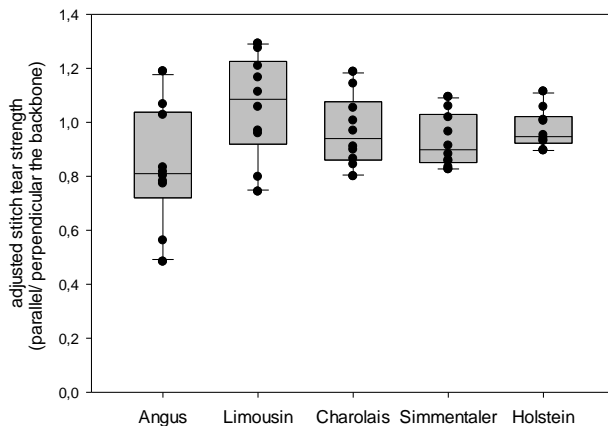


Figure 9. Adjusted stitch tear strength (ATS) in dependence of cattle breed.

The average ATS for all leathers except for leathers with Limousin origin showed values below 1.0, that means a lower force is needed to tear the leathers parallel than perpendicular to the backbone. Why Limousine leathers have a different behaviour compared to the other breeds is unknown. Maybe a different collagen fibril orientation is present. But more analyses are needed to verify this assumption (e. g. small angle X-ray scattering studies, SAXS(5,11)).

4 Conclusions

In summary, the results indicate, that the over- hundreds- of- years- raised tanners opinion can be partially disproved. Simmentaler rawhides have the highest thickness, but differences in physical tests are mostly negate when transformed to leathers. The tensile strength, the elongation at maximum force and the stitch tear strength of different leathers showed only minor differences between the cattle breeds. The variation within the breeds were mostly higher than between the breeds. However, this evaluation is based only on 10 individuals per breed, and the measured tendency must be confirmed by a larger quantity of test individuals. For this purpose, an analysis is planned with 100 individuals from different breeds and crossbreeds.

5 Acknowledgements

The project no. 19368BR of the research association “Leder und Kunststoffbahnen, Meißner Ring 1, 09599 Freiberg” was funded on behalf of the Federal Ministry of Economics and Technology by the AiF in the framework of the program “Industrielle Gemeinschaftsforschung” (IGF) based on a resolution of German Bundestag. We would like to thank for the support granted.

6 References

1. Hausam W. *Die Bedeutung der Rinderrassen für die Lederherstellung. Wissenschaftl. Verl.-Ges.*; 1952. 148 p.
2. Spiller A, Gauly M, Balmann A, Bauhus J, Birner R, Bokelmann W, et al. *Wege zu einer gesellschaftlich akzeptierten Nutztierhaltung. Berichte Über Landwirtsch - Z Für Agrarpolit Landwirtsch [Internet]. 2015 Jul 20 [cited 2019 Mar 28];0(221). Available from: <http://buel.bmel.de/index.php/buel/article/view/82>*
3. Schroer T. *Zur Hautproduktivität der einheimischen Rinder und der Einfluss der Rinderproduktion auf die Rohwarenqualität. Leder- und Häutemarkt. 1989;16:86–113.*

4. Naffa R, Maidment C, Ahn M, Ingham B, Hinkley S, Norris G. Molecular and structural insights into skin collagen reveals several factors that influence its architecture. *Int J Biol Macromol.* 2019;128:509–520.
5. Basil-Jones MM, Edmonds RL, Cooper SM, Haverkamp RG. Collagen fibril orientation in ovine and bovine leather affects strength: A small angle X-ray scattering (SAXS) study. *J Agric Food Chem.* 2011;59(18):9972–9979.
6. RStudio. *RStudio: Integrated development environment for R (Version 1.2.1335) [Computer software].* Boston, MA. 2012;
7. Steel RG, Torrie J. *Principales And Pricedures Of Statistics.* Mcgraw-Hill Book Company, Inc.; New York; Toronto; London; 1960.
8. Valeika V, Širvaityt J. *Estimation of Chrome-free Tanning Method Suitability in Conformity with Physical and Chemical Properties of Leather.* :8.
9. Goldsmith LA. *Biochemistry and Physiology of the Skin.* Oxford University Press; 1991.
10. Heidemann E. *Fundamentals of leather manufacture.* Darmstadt: Roether; 1993. 647 p.
11. Kelly SJ, Edmonds RL, Cooper S, Sizeland KH, Wells HC, Ryan T, et al. Mapping Tear Strength and Collagen Fibril Orientation in Bovine, Ovine and Cervine Hides and Skins. *J Am Leather Chem Assoc.* 2018;113(1):1–11.

DEVELOPMENT OF A TANNING TECHNOLOGY WITH TANNING AGENTS FROM *LIGUSTRUM VULGARE*

M. Schröpfer^{1), a)}, M. Meyer¹⁾

¹⁾ Research institute for leather and plastic sheeting, Freiberg gGmbH, FILK

^{a)} Corresponding author: michaela.schroepfer@filkfreiberg.de

Abstract. A technology for the production of leathers was developed using exclusively privet tanning agents as pre-tanning agents. The development includes production, characterization and optimization of the plant extracts, the development of the pre-tanning technology and the adaptation of the wet end for the corresponding application areas. The leathers which have been manufactured show high shrinkage temperature and good mechanical properties. They show an inherent colouring, but seem to be suitable for use in automotive interiors, as shown by a comparison of the test results with the technical delivery conditions of automobile manufacturers.

1 Introduction

The sole use of vegetable tanning agents for pre-tanning as an alternative to synthetic or chromium-containing tanning agents is one way of improving sustainability and ecology in leather production. In recent years, a new group of secondary plant compounds, the iridoids and secoiridoids, has been discovered to be used as tanning agents.

Currently, a tanning agent from olive leaves with active cross-linking substances deriving from the secoiridoid Oleuropein is commercially available¹. In order to extend the product range of alternative vegetable tanning agents with covalent cross-linking mechanisms by indigenous raw material, we screened a number of further plants for such covalently cross-linking active substances. Extracts from privet leaves showed a particularly high cross-linking activity.

Privet belongs to the *Oleacea* family and is common in Asia with several species. In Europe, the species *Ligustrum vulgare* can be found everywhere, especially as a hedge plant for gardens. The main Secoiridoids in privet leaves² are drawn in Figure 1:

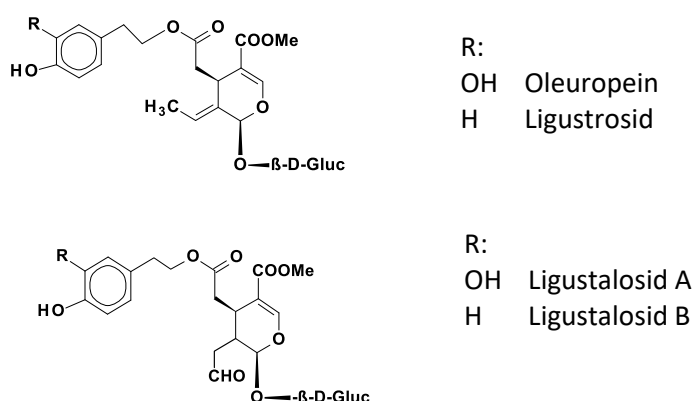


Figure 1. Main Secoiridoids found in extracts of privet leaves.²

In order to cross-link proteins such as collagen by secoiridoids, plant-specific enzymes (β -glucosidase) first cleave off the glucose molecules bound to the secoiridoid. This causes a ring opening and the formation of reactive aldehyde groups. The proposed reaction mechanism for the cross-linking of

collagen is a covalent Michael addition to basic amino groups³. In addition, these secoiridoids contain phenolic hydroxyl groups which can also react covalently with the basic amino groups after oxidation to quinones by plant polyphenol oxidases, or via hydrogen bonds.

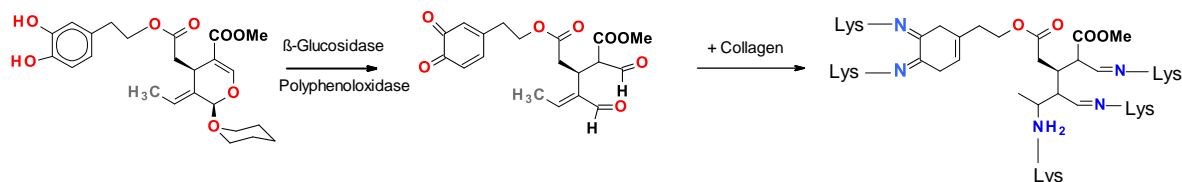


Figure 2. Proposed chemical reaction of oleuropein and collagen.³

The reaction mechanism is similar to the cross-linking mechanism of collagen with glutaraldehyde. Compared to other plant based cross-linkers, cross-linking with secoiridoid results in cross-linking products with the highest chemical stability.⁴

The following questions were considered in the development of tanning technology:

- use of privet leaf extracts or ground privet leaves
The suitability of ground leaves without the need for prior extraction would result in significant economic advantages.
- During the production of extracts, the optimum production parameters need to be determined and methods found to assess cross-linking activity. These investigations were carried out with skin powder, as there are no problems with the diffusion but only the binding on the collagen can be evaluated.
- determination of the required concentrations of the tanning agent and the pH control of the tanning process. For this purpose, small pelt pieces were used on a laboratory scale.
- investigation of the interplay of diffusion and binding of the tanning agent to skins on a pilot plant scale
- the production of finished leathers with various retanning technologies.

2 Experimental

Extraction of plant material

The plant material was collected from the cut of garden hedges and dried. Leaves and stems were mechanically separated. The extraction was carried out on a laboratory and pilot scale. The parameters used were part of optimization process (see results).

Investigation of extract composition

The extracts were analysed by reverse phase liquid chromatography (LC, Shimadzu) with a photodiode array detector (PDA).

- Stationary phase: C18 (Supelco)
- Mobile Phase: Gradient ACN/ Water

Calibration was performed with the reference substance oleuropein (Sigma-Aldrich). The substances ligustalosite A and ligustrosid were identified by fractionation of the extract after separation via the stationary phase and determination of the characteristic mass peaks with a mass spectrometer (QTrap400, Episcix).

Test of cross-linking activity

In order to assess the cross-linking activity of the extracts and leaves, an indirect method must be used, since the cross-linking active substances (deglycosylated and degraded secoiridoids) cannot

be determined analytically. Therefore, hide powder was treated with the extracts according to a standardized procedure and the cross-linking parameters of the hide were determined. The use of hide powder offers the advantage over the use of intact pelts that diffusion is of minor influence and only information on cross-linking activity is obtained.

Hide powder was soaked in a defined volume of 0.4 M McIlvain buffer at pH 7. The plant extract was solved in water and added to the buffered hide powder in a volume ratio of 1:1 (final concentration 10 % mass_{Extract}/mass_{buffer}). Samples were shaken for 6 h at 30 °C, then centrifuged. The supernatant was discarded and the samples were washed 3 times with excess of water and finally soaked in phosphate buffer at pH 7.

The cross-linking degree of the treated hide powder was measured via the increase of denaturation temperature and by the determination of the amount of bound amino-groups. The denaturation temperature was measured with a DSC 1 device (Mettler-Toledo). Approximately 6 mg (calculated on dry weight) of wet cross-linked hide powder at pH 7 were placed in an aluminum pan and hermetically closed. Temperature scans were run from 10 – 125 °C with a rate of 5 Kmin⁻¹. From the endotherms T_{onset} and T_{peak} were calculated.

The amount of bound amino-groups was measured by amino-acid-analysis (Biochrom 30+). The samples were hydrolysed with 6 N HCl at 110 °C for 20 h, dried and resolved in lithium citrate buffer and analyzed by pre-column derivatisation with ninhydrin according to standard protocols. The percentage of amino groups, that formed an acid-stable bond, was calculated from the area below the lysine, hydroxylysine or arginine peaks and normalised to the area under the peaks from alanine and valine (not involved in cross-linking). The resulting factor was related to the same factor calculated from a non-cross-linked sample.

Development of a tanning technology on a laboratory scale

The laboratory-scale tanning tests were carried out on pelt pieces (de-limed cow skin, standard liming protocol) of approx. 200 g and 1,8 mm thickness in a parallel dyeing machine (diameter approx. 50 cm). Pelt mass, treatment time (36 h) and float volume were kept constant. The tanning results were evaluated by the determination of denaturation temperature of the cross-linked pelts with DSC. Therefore samples were thoroughly washed with water and buffered to pH 7 to ensure comparability of the denaturation temperature.

Production of leathers on a pilot scale

The crusts were produced in a 1 m-diameter tanning drum (Dosemat). Half croupions were used. Cow hides of mass class 20-25 kg were limed according to a standard protocol. Technologies with and without pickle were investigated.

Pre-tanning was carried out with privet extracts from privet leaves ground to various degrees and ground privet leaf powder. The quantity of used tanning agent was kept constant. The degree of cross-linking across the cross-section of the skin was estimated by DSC measurement. Crusts with two different wet-end technologies (wet end 1 and wet end 2) from the automotive sector were produced from the semi-finished products. The crusts were dried, staked and milled. Leathers with glutaraldehyde pre-tanning with the same wet end technology were produced as references. Thickness was average 1,5 mm. The mechanical and chemical properties of the crusts were tested with standardized testing norms.

3 Result and discussion

Optimization of plant extraction procedure

Optimization parameters were

- plant part
- temperature
- extracting agent

- degree of grinding of plant material
- time
- amount of extractant
- number of extraction steps
- drying process

The main influence parameters on cross-linking activity of extracts of *ligustrum vulgare* are the temperature of extraction, the solvent, the part of the plant used for extraction and its grinding degree. In contrast to privet leaves, the stems show no cross-linking activity.

Figure 3 shows the dependence of cross-linking activity on hide powder on the temperature of extraction (A + B). The dependence of the Oleuropein and Ligustalosisid A content of the respective privet leaf extract on the temperature of extraction is shown in Figure 3C. As can be seen, the cross-linking activity drops rapidly to near zero at extraction temperatures above 60 °C. Correspondingly, the non-cross-linking glycosylated secoiridoids Oleuropein and Ligustalosisid A were detected at extraction temperatures above 60 °C. Since the cross-linking active deglycosylated form of the secoiridoids could not be observed by chromatography, the rise of the glycosylated form above 60 °C gives evidence for deglycosylation below this temperature, hence cross-linking should be observable as proved by the rise in denaturation temperature and crosslinked lysine.

We assume that under suitable conditions a spontaneous activation of the secoiridoids (deglycosylation, oxidation to quinoid structures) takes place during extraction by the plant's own enzymes such as glucosidases or polyphenoloxidases.³ It is assumed that the enzymes are inhibited if the extraction temperatures are too high. Unfortunately, no substances could be analyzed in the activated extracts (e.g. aglycones or their degradation products) to which a cross-linking activity could be assigned.

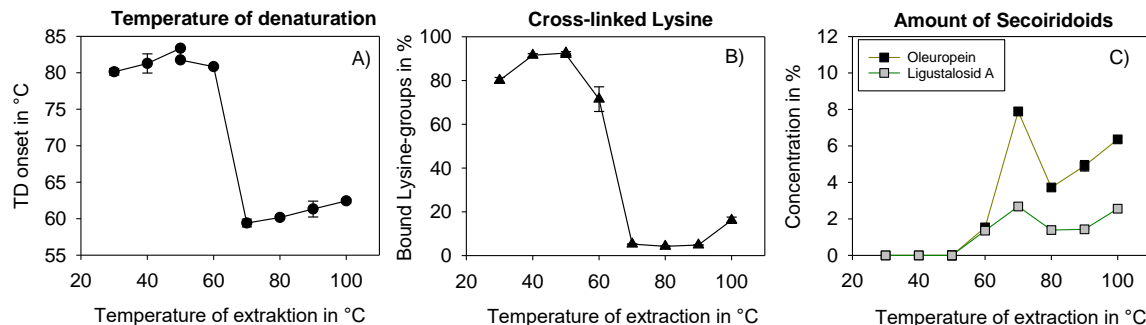


Figure 3. Denaturation temperature (A) and degree of bound Lysine-groups (B) in hide powder tanned with privet leaf extract, and amount of Oleuropein and Ligustalosisid depending on the temperature of extraction.

A similar result is observed when using ethanol or mixtures of ethanol and water as extractants: the higher the proportion of non-aqueous extractant, the higher the cross-linking activity and the lower the content of secoiridoides.

The degree of grinding of the privet leaves also plays a role in the cross-linking activity. The leaves were ground and the particle size distribution was determined by sieve analysis. The categories "coarse" and "fine" include particles with diameters between 300 and 1500 µm and between 30 and 90 µm, respectively. Figure 4 shows the cross-linking activity of the extracts from the various ground leaves and the cross-linking activity of the unextracted leaves as a function of the used cross-linker concentration.

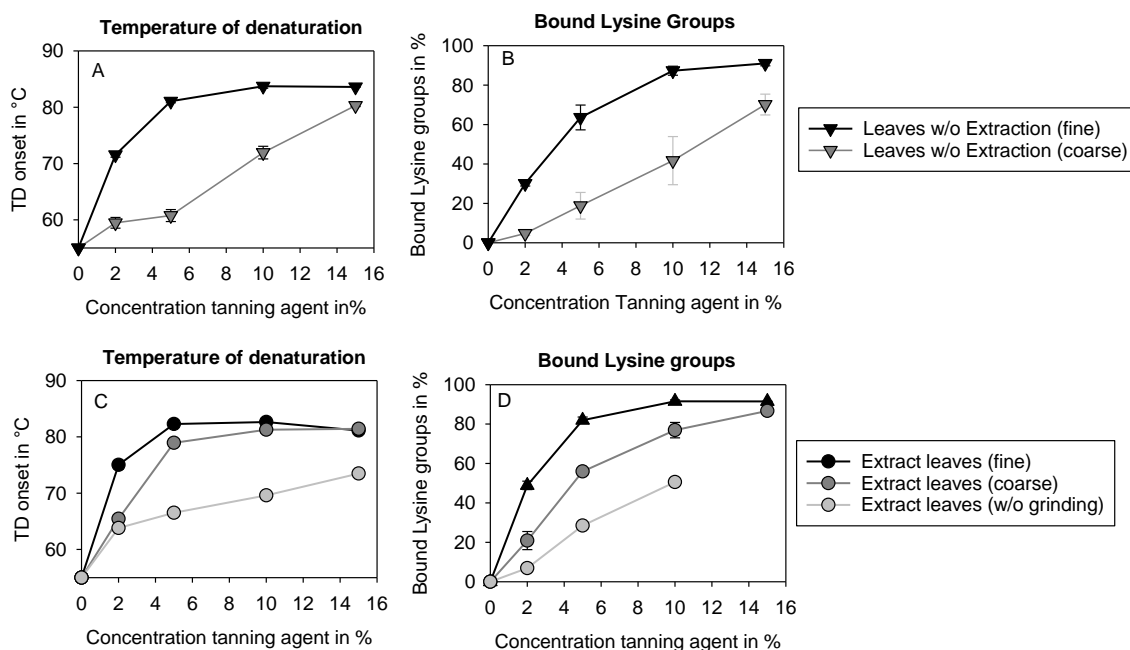


Figure 4. Cross-linking of hide powder with privet leaf tanning agents: Influence of the degree of grinding of the extracted leaves on denaturation temperature TD (A, C) influence of the concentration on the proportion of cross-linked lysine groups in tanned hide powder (B,D).

The cross-linking activity increases with increasing degree of comminution. However, the colour intensity of the extract solutions and of the tanned skin powder is also increased.

Interestingly, the cross-linking activity of the finely ground leaves is almost as high as that of the extracts produced from them. This makes it possible to tan with the finely ground leaves without any additional upstream extraction step.

The influence of the other optimization parameters was less significant. In summary, the following parameter ranges were defined for scaling up the extraction:

- Temperature < 60 °C
- Extraction agent Water
- $m_{\text{water}} : m_{\text{leaves}} 20:1$
- one extraction step
- Time 4h
- Drying by means of freeze drying or spray drying

The production of extracts was scaled up to the technical scale. The achieved average yield is 35 % of the leaf mass. To check the extract quality, cross-linking tests were carried out by the hide powder method with each batch.

Optimization of tanning process in lab scale

When tanning hide, the diffusion of the tanning agent inside of the skin is a main optimization parameter to be considered beside the cross-linking activity. The progress of diffusion and binding is usually controlled and regulated by the pH value. The investigation of the dependence of the cross-linking activity of privet leaf extract on pH revealed a high cross-linking activity in all pH ranges⁴. This could be an indication that not only the covalent bond (nucleophilic Michael addition) is responsible for cross-linking, but also electrostatic interactions with phenolic hydroxyl groups, which are more active in the acidic range. This cross-linking ability over a wide pH-range could have a negative effect on diffusion and uniform distribution of the tanning agent.

Full penetration and tanning across the cross-section of the skin was evaluated by the denaturing temperature and the shape of the DSC-Peak of the semi-finished products. If tanning is incomplete, the denaturing peaks are wide. Sometimes the scans show two peaks, which corresponds to a more strongly tanned outer area and a less tanned inner area (Figure 5). The distance between the lowest and highest denaturing peaks can be used as a rough evaluation criterion for tanning, whereby the differently tanned areas are not necessarily clearly separated as shown in Figure 5B. A good homogeneous tanning result is represented as single sharp denaturation peak (Figure 5A).

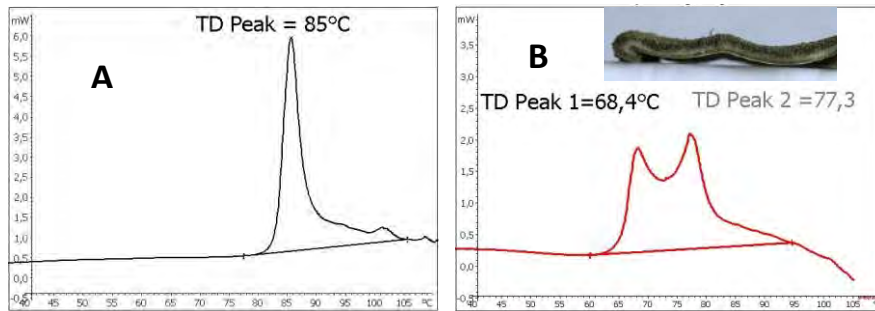


Figure 5. Example of denaturation Peaks of homogeneous A) tanned hide (Glutaraldehyde) and B) non homogeneous tanned hide (Privet leaf powder), x-axis: Temperature in °C, y-axis: Heat-flow in mW).

For optimisation, the following parameters were varied with small pelt pieces on a laboratory scale:

- concentration of the privet tanning agents
- pH value at the beginning and end of the tanning process
- Extracts or leaves (finely ground)

The tanning agent was added in two steps. Figure 6 shows the lowest peak temperatures of denaturation of the tanned pelts as a function of the concentration of tanning agent.

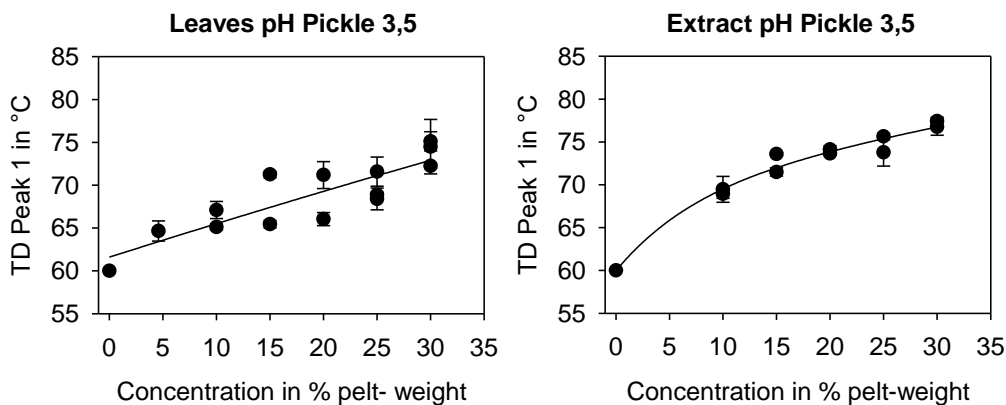


Figure 6. Denaturing temperatures inside the tanned pelts with extracts from privet leaves and ground leaves as a function of concentration (pH pickle 3.5, pH end 4.1), total tanning time: 36 h, (n=3 DSC measurements per semi-finished product, washed and buffered to pH 7).

Acceptable denaturation temperatures inside the pelt (> 70 °C) are achieved at concentrations of 25 % extract based on pelt weight and higher, and 30 % ground leaves, resp. The tanning is not perfectly uniform in most cases. The reproducibility of the tanning results is significantly better with extracts than with ground leaves.

Figure 7 shows the tanning results in dependence of pH before tanning. The pH was adjusted during pickling. In the tests with pH < 4.5, the pH value was raised to 4.2 after tanning.

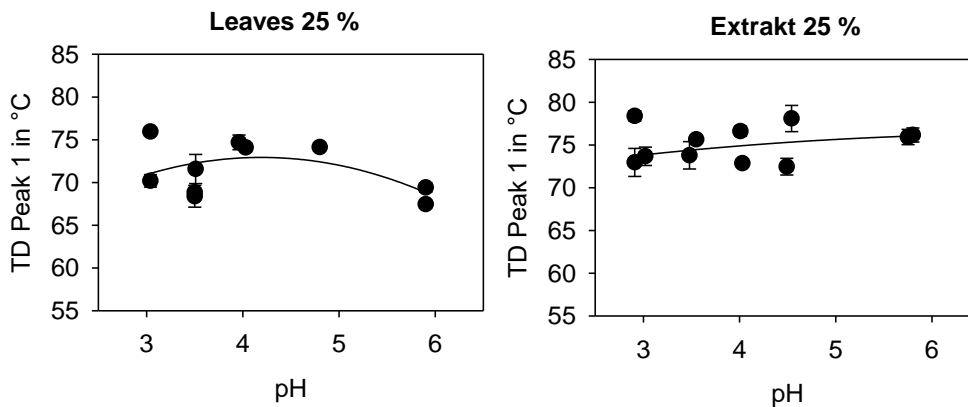


Figure 7. Denaturation temperatures inside the tanned pelts with extracts from privet leaves and ground leaves depending on the pH of the pickle, $C_{\text{Extract}} = 25\%$, total tanning time: 36 h, (n=3 DSC measurements per semi-finished product), washed and buffered to pH 7.

The pH of pickle has only minor influence on the cross-linking results as shown by the denaturing temperature of the semi-finished products considering the variation of the results from triplicate tests. In the case of extracts, the denaturing temperatures increase slightly with increasing pH, since the proportion of unprotonated amino groups as reaction partners increases with increasing pH. During the production of the leather, however, dead-tanned leather with partial grain breakage could result if the process was carried out without pickling or with a high starting pH. Additionally, the pH value has an influence on the intensity of the coloring of the semi-finished products: the higher the pH value, the darker the color and the more pronounced the grain. If extracts are used, the color of the pelts is brown, if ground leaves are used, the semi-finished products are green.

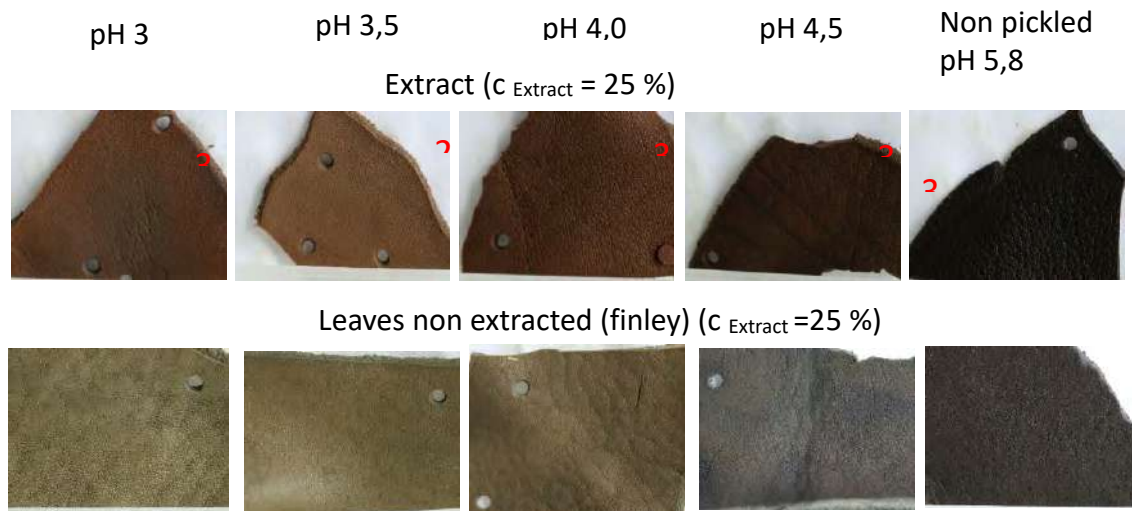


Figure 8. Colours of pelts, tanned with different tanning agents from privet leaves at different pH values, semi-finished.

Production of leathers in pilot scale

The production of leathers was performed with half croupions limed, delimed and pickled after standard protocols in a drum for labscale (Dosemat VGI). Finely ground leaves and extracts from finely ground leaves were used as tanning agents. The diffusion progress was estimated by determination of the denaturing temperatures in dependence of the tanning time. Figure 9 shows exemplarily the temporally course of the first peak temperature of the denaturation peak for leave powder and extract.

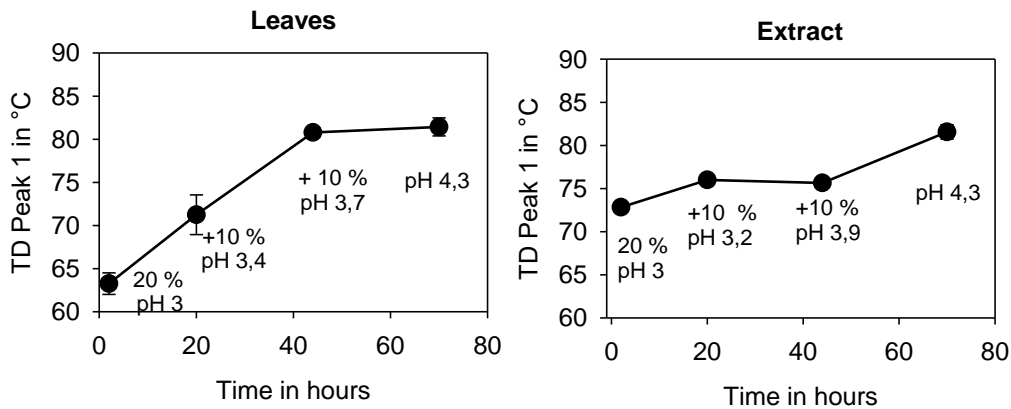


Figure 9. Time course of the denaturing temperatures of inner (TD Peak 1) areas of the hide during tanning privet leaves finely ground, and extract from finely ground leaves, adding point of different rates of tanning agent and the pH during tanning, samples are buffered to pH 7 before DSC measurement.

The colour of the semi-finished products before wet end differs depending on the privet tanning agent used. It could be brightened by the use of syntans in the wet end. The resulting colours are shown in Figure 10. The leathers produced with extract of finely ground leaves are slightly brown, whereas the leathers produced with extract of coarsely ground leaves are lighter. Leathers tanned with ground leaves are slightly green.



Figure 10. Photos and microscopic images (50x) of leathers of tanning agents from privet leaves and glutaraldehyde.

Various mechanical and chemical parameters of the privet tanned leathers were tested, and the chemical composition determined.

The tensile strength of leather tanned with ground leaves is significantly higher than that of glutaraldehyde leather and leather tanned with privet leaf extract.

Parameters such as tear load, stitch tear resistance, static and permanent elongation, bending stiffness, density, weight per unit area and softness show good values that meet the requirements for leather in automotive interiors.

4 Conclusion

Tanning agents from privet leaves contain Secoiridoids, which can be used to produce leather. The leathers show good mechanical properties, in some cases even better, as the leather tanned with glutaraldehyde and the same wet end technologies. Furthermore, it has been shown that privet leaves that are finely ground are just as suitable for tanning as extracts from ground leaves. Some mechanical properties like the tensile strength could be improved by tanning with the finely ground leaves.

5 References

1. Zotzel, J., Sarafeddin, A. C.-D., Marx, S. & Germann, H.-P. Agent and methods for tanning pelts and skins. in (WO Patent WO/2009/065,915, 2009).
2. Romani, A. et al. HPLC analysis of flavonoids and secoiridoids in leaves of *Ligustrum vulgare* L. (Oleaceae). *J. Agric. Food Chem.* **48**, 4091–4096 (2000).
3. Konno, K., Hirayama, C., Yasui, H. & Nakamura, M. Enzymatic activation of oleuropein: a protein crosslinker used as a chemical defense in the privet tree. *Proc. Natl. Acad. Sci.* **96**, 9159–9164 (1999).
4. Schroepfer, M. & Meyer, M. Investigations towards the binding mechanisms of vegetable tanning agents to collagen. *Res J Phytochem* **10**, 58–66 (2016).

APPLICATION OF SILANES IN LEATHER TANNING

J. Benvenuti^{1a)}, S. Griebeler¹, J. H. Z. Dos Santos² and M. Gutterres^{1b)}

1 Laboratory for Leather and Environmental Studies (LACOURO), Chemical Engineering Post-Graduated Program (PPGEQ), Federal University of Rio Grande do Sul (UFRGS), Av. Luiz Englert s/n°, Porto Alegre-RS, Brazil, 90040-040, + 55 51 3308-3954

2 Chemistry Institute, Federal University of Rio Grande do Sul (UFRGS), Av. Bento Gonçalves, 9500, Porto Alegre-RS, Brazil, 91501-970, +55 51 3308-6295

a) Corresponding author: jaque08@enq.ufrgs.br

b) mariliz@enq.ufrgs.br

Abstract. This work investigates the potentialities and limitations of the use of alkoxysilanes in leather tanning, introducing silica nanoparticles in the hides, aim for process and product innovation in leather industry. The synthesis of silica nanoparticles was carried out by a typical sol-gel Stöber process. From the silica precursor tetraethoxysilane (TEOS), ammonium hydroxide as catalyst, ethanol and water, the formation of nanoparticles dispersion takes place. Vegetable tanning process was explored by introducing the silica nanoparticles in this stage starting from pickled cattle hide. Shrinkage temperature, tensile strength, softness and colour fastness to light were evaluated in the leather samples. The results achieved shown that the tanning experiment with only silica, without other tanning agent, did not reach the minimum shrinkage temperature required to be labelled as tanned leather. Conversely, in the presence of vegetable tannin, the shrinkage temperature reached 80°C. The physical-mechanical properties indicated that the enhanced on the tensile strength of vegetable leathers with nanosilica was about 50% and their softness was not affected by the introduction of silica. A lighter coloured leather was generated with silica but less stable to light. The tanning chemistry involving silica nanoparticles and collagen is complex, therefore, more studies are needed to explore the influence of silanes on hide stabilization.

1 Introduction

The collagen stabilization of the hides with silicon compounds has been investigated for many years with the intention of developing a sustainable and low-cost route for tanning^{1,2}. These compounds are studied as an alternative to wet-blue leather tanning – which is still the predominant method used in tanneries³ – in the context of manufacturing chromium-free wet-white leathers. Usually employed in the form of silicates, these substances can interact with collagen via hydrogen bonding and electrostatic attraction. However, studies have shown that there is no significant effect on the hydrothermal stability of the hides, which indicates that silicates, acting as sole tanning agent, are not effective for tanning^{2,4-6}.

Although the silicon compounds do not stabilize the hide irreversibly, they can act as auxiliaries, being their best application as pre-treatment for vegetable tanning. By occupying reaction sites in collagen structure and, consequently, reducing the reaction rate between polyphenolic plant tannins and collagen, silica facilitates penetration, improving the absorption of tannins in the hide^{3,7}.

However, the synthesis of nanometric silica particles has been exploited for possible application in tanning, due to their small size and ability to combine with polymeric substrates⁸. An in-situ route to produce nanosilica has been established to facilitate the introduction of the nanoparticles into the hide in order to achieve a real tanning effect. In this route, a silane precursor of the nanoparticles is dispersed in the hide. Under a special condition such as pH change, heat, radiation, among others, the nanosilica precursor undergoes hydrolysis and condensation in the organic matrix of the collagen, producing in situ the inorganic silica nanoparticles. Thus, a strong interaction between the organic and inorganic phases is obtained due to the high reactivity of the nanoparticles, favouring the increase of the shrinkage temperature of the leather and conferring

improvement in the mechanical properties⁹⁻¹¹. In addition, the surface of silica nanoparticles can be modified by adding reactive groups of various organosilanes in order to control particle size, obtain chemical stability and homogeneous dispersion of nanoparticles in the medium^{12,13}.

Other benefits achieved with the use of silicon compounds in leather process include the use of silicates as lime substitutes in the liming process¹⁴, the improvement in dye and auxiliaries absorption, the decrease in suspended solids, COD, BOD and total N levels, and reduction of chrome content in the effluent, in addition to saving water and chemicals. These hides may also present resistance to fungi and provide a better biodegradability of the organic compounds present in the effluent when compared to the chrome tanning. Further advantages of nano-tanning include studies that omitted the pickle stage and performed the simultaneous tanning and fatliquoring steps, reducing process time^{9,10}. Moreover, silica can also add properties such as increased UV light protection and high-quality gelatine recovery from leather shavings^{8,15}. Table 1 presents some works in the field of silica application in leather tanning.

Table 1. Application of silica products in leather tanning report in the literature.

Silica precursor	Substrate	Silica synthesis	Tanning agents combined
Tetraethoxysilane - TEOS	Bated pelt	TEOS + modified oil/polymer-based dispersion supporter	Oxazolidine ⁹
TEOS + (3-Glycidyoxypropyl) trimethoxysilane	Goatskin (pickled)	Direct contact with the hide in the drums	Cr ₂ O ₃ 24% B=33% ¹¹
TEOS	Goatskin (squeezed and shaved)	NanoSiO ₂ , 50-150 nm (patented synthesis) + modified animal/vegetal oil	Oxazolidine (as pre-tanning agent) ¹⁶
Sodium silicate (20% SiO ₂ content)	Goatskin (pickled)	Direct contact with the hide as pre-tanning agent	Chromium salts ¹⁷
TEOS (redistilled)	Sheepskin (pickled)	Stöber method + modified oil	Tetrakis(hydroxymethyl) phosphonium chloride ¹⁸
Sodium metasilicate	Goatskin (pickled)	Mixed with the other tanning agents in acidic medium	Sodium dichromate, zinc sulphate ¹⁹
Sodium metasilicate	Goat and sheepskin (delimed)	Direct contact with the hides after the other tanning agents	Aluminium sulphate, tannic acid ²⁰
Sodium metasilicate	Goatskin (pickled/delimed)	Direct contact with the hide (sodium metasilicate previously neutralized)	Aluminium sulphate, Tetrakis(hydroxymethyl) phosphonium sulphate ²¹
TEOS + [3-(Methacryloyloxy)propyl]trimethoxysilane	Sheepskin (pickled)	Modified Stöber method	Methacrylic acid, Diallyl dimethyl ammonium chloride, acrylamide acrylonitrile ²²

The results achieved so far are of great value in exploring chrome-less tanning or future chromium-free tanning technology with the use of silica and help promote the sustainable development of the leather industry. However, the tanning chemistry between nanomaterials and collagen is complex and still not fully understood to date²³.

Then, the objective of this work was to investigate the potentialities and limitations of the use of silanes in leather tanning. It was explored the vegetable tanning step by introducing nanometric silica particles produced by the Stöber method. This study searches for improvements in the properties of the leather or a gain in time, cost of process or less use of chemicals, working on process/product innovation.

2 Materials and methods

The following precursors were used for the synthesis of the silicas: tetraethoxysilane ($\text{Si}(\text{OCH}_2\text{CH}_3)_4$, TEOS, Acros, > 98%), (3-Aminopropyl)triethoxysilane ($\text{H}_2\text{N}(\text{CH}_2)_3\text{Si}(\text{OC}_2\text{H}_5)_3$, APTES, Sigma-Aldrich, 99%) and octadecylsilane ($\text{CH}_3(\text{CH}_2)_{17}\text{SiH}_3$, ODS, Sigma-Aldrich, 97%). Ammonium hydroxide (NH_4OH , Nuclear, 29%) was used as catalysts in the sol-gel process.

2.1 Synthesis of the silica nanoparticles dispersion

The synthesis of silica nanoparticles was performed based on the Stöber method²⁴ by diluting 5.0 mL of TEOS in 50.0 mL of ethanol, adding to the reaction 1.0 mL of 0.5 mol L^{-1} NH_4OH as the basic catalyst, and 3.0 mL of distillate water. The reaction medium was kept under slow stirring for at least 4 h. This synthesis results in the formation of a dispersion of nanometric silica particles. In another experiment, 1.0 mL of the organosilanes APTES and ODS were added to the synthesis, separately, for the functionalization of the nanoparticles with amino groups and long carbon chains, respectively. Fig. 1 presents a scheme of the synthesis with TEOS.

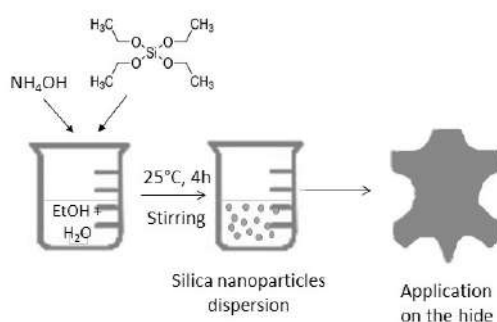


Fig. 1. Scheme of the silica nanoparticles dispersion synthesis and application.

2.2 Tanning process with the silica nanoparticles

The incorporation of the silica nanoparticles to the hides was carried out in the tanning step. Vegetable tannin from *Acacia mearnsii* was used as tanning agent combined with the nanosilicas. The tanning process was started from a pickled bovine hide. The hide weight employed in all experiments was 200 g in each drum. Table 2 shows the formulation used for the three initial tanning experiments with the nanosilica dispersions (nano-SiO₂). The percentage of products used was based on pelt weight. In the Experiment I (E-I) the nanosilica dispersion was employed without the organosilanes and without the fatliquoring step. In the Experiment II (E-II) the organosilane APTES was added in the synthesis of the silica nanoparticles. In the Experiment III (E-III), the organosilane ODS was used to the silica functionalization. Control samples – without nanosilica – were also performed for the experiments. The rotation of the bench drums was set at 25 rpm for the whole process.

Table 2. Tanning process formulation for the three experiments with the silica nanoparticles dispersion.

Step	Product	%	t (min)	Remarks	
Conditioning	H ₂ O	200.0	15	25°C	
	NaCl	5.0			
	HCOONa	1.5			
Washing	H ₂ O	200.0	10	Drain	
Tanning	H ₂ O	50.0		35°C	
	Experiment I	Nano-SiO ₂	2.3 ^b		
	Experiment II	Nano-SiO ₂ + APTES	2.8 ^b	30	
	Experiment III	Nano-SiO ₂ + ODS	2.8 ^b		
		VT ^a	7.0		
		VT	8.0	60	
		VT	10.0	120	
		VT	10.0	120	
		VT	10.0	overnight	
Fatliquoring ^c	sulphited fatliquor	7.0	30	36°C	
	sulphated fatliquor	6.0	30		
Fixing	H ₂ O	100.0	60	Drain	
	HCOOH (1:10 v/v diluted)	1.0			

^a VT: vegetable tannin

^b percentage of the silica precursors

^c step only carried out on the experiments II and III

After that, the following tanning experiment, Experiment IV (E-IV), was carried out with an additional step, the pre-tanning, where phenolic synthetic tannin was employed to facilitate the penetration of the tanning agent. Table 3 shows the formulation for this case.

Table 3. Formulation for the Experiment IV with a pre-tanning stage and the silica nanoparticles dispersion.

Step	Product	%	t (min)	Remarks	
Pre-tanning	H ₂ O/NaCl 6°Bé	50.0		25°C	
	Fungicide	0.1	120		
	Synthetic tannin	5.0			
		NaHCO ₃	2.0		
Washing	H ₂ O	200.0	10	Drain	
Tanning	H ₂ O/NaCl 10°Bé ^a	200.0		35°C	
	Nano-SiO ₂	2.3 ^b	60		
	VT	5.0			
	Nano-SiO ₂	2.3 ^b	120		
	VT	10.0			
		VT	15.0	120	
		VT	5.0	overnight	
Fatliquoring	Sulphited fatliquor	7.0	30	36°C	
	Sulphated fatliquor	6.0	30		
Fixing	H ₂ O	100.0	60	Drain	
	HCOOH (1:10 v/v diluted)	4.0			

^a for the control sample it was 6°Bé

^b percentage of the silica precursor TEOS

2.3 Leather proprieties analyses

The thickness of the samples was measured via an analogue thickness gauge (Wolf). The average thickness was obtained according to IULTCS/IUP 4. The measurement of tensile strength and

percentage extension was carried out according to the IULTCS/IUP 6 in a universal tensile testing machine (AME-5, Oswaldo Fisola).

For the analysis of softness, a softometer (KWS Basic, Wolf-Messtechnik) was employed and leather samples with the dimensions of 7.5 × 5.0 cm was used for the measurements²⁵. The outcome of this measure is the surface tension of the sample. The leather shrinkage temperature was measured according to the IULTCS/IUP 16, where a sample of leather with the dimensions of 10.0 × 2.0 cm was used to evaluate the hydrothermal stability of the samples.

The colour fastness to UV light of the leather samples was analysed, where the samples had 50% of their surface exposed to an UV lamp with 300 W for 24h. After that, the colour change of the leather samples was evaluated with the use of a colorimeter (Colorium, Delta Color) and the Lab7[®] software. The measured values were distributed into three-dimensionally colorimetric coordinates that describes the psychometric colour space of CIE Lab lightness (L*), coordinate a* (red content (+), green (-)) and coordinate b* (yellow content (+), blue (-)). The obtained coordinates of each sample were converted into numerical values, providing relative values to the colour differences between the materials:

ΔL^* = represents the difference in lighter and darker (positive = lighter, negative = darker)

Δa^* = represents the difference in red and green axis

Δb^* = represents the difference in yellow and blue axis

The total colour difference (ΔE) is defined by the equation:

$$\Delta E = (\Delta L^2 + \Delta a^2 + \Delta b^2)^{1/2} \quad (1)$$

The water contact angle (WCA) analysis was performed on the drop shape analyser (DAS 100, Krüss GmbH) equipped with a video camera. Using the sessile drop method, where a drop (3-6 μL) of deionized water at room temperature was deposited on the surface of the leather by means of a micro syringe. The image of the drop on the leather was captured and the angle formed between the drop and the surface was measured.

The 3D Optical Profiler (Contour GT-K, Bruker) was used to measure roughness in nanometric scale (1 nm of vertical resolution) and fast obtaining 2D and 3D surface images of the leather samples.

3 Results and discussion

Preliminary experiments were carried out to generate silica *in situ* in the leather tanning process as a tanning agent. Silica nanoparticles from the Stöber process were added to the hides and the drums were run for extended time in order to ensure the silica formation for all routes. Initially a large amount of silica precursor (TEOS) was used in relation to the hide weight, which results in rigid hides. Although the experiment was kept running for a long time, the shrinkage temperature reached by the hides was 55°C, concluding that the hide was not tanned. This indicated that the silica produced cannot be considered as a single tanning agent. For this reason, it was investigated in the following experiments if the silicon compounds could act as auxiliaries in the process, in order to aggregate properties of strength, colour, and filler, among others.

Therefore, in Experiment I (E-I) the nanosilica dispersion was incorporated in the hides at the tanning step of the leather process with vegetable tannin as tanning agent. The results (Table 4) demonstrate that the control sample and the sample with the nanosilica achieved the same shrinkage temperature, indicating that the presence of the nanosilica did not compromise the hydrothermal stability of the leather.

The tensile strength at the breaking point for the leather with the nanosilica dispersion was 52% higher than the control sample. The results of elongation at break for the sample with the nanosilica were also greater than the control sample (without silica), demonstrating that the nanosilica added resistance properties to the leather. From the softness analysis it was found similar values of surface tension, revealing that the quantity of the nanosilica provided in this experiment did not affect the

softness of the leather. Regarding the increase in the thickness between the initial hide and the final leather, it was higher for the leather with silica compared to the control, suggesting greater filling provided by the silica.

In the Experiment II (E-II) and III (E-III), the presence of the organosilanes APTES and ODS, respectively, and the addition of the fatliquoring step in the tanning formulation result in significant variations in the physical-mechanical properties analysed (Table 4).

The main function of the fatliquoring step is to ensure softness to the leather, an important quality requirement, especially in the case of upholstery leathers. In relation to the softness, the experiment with the presence of the organosilane APTES (E-II) resulted in the most rigid sample, with the highest surface tension. In the literature, the values found for leather without fatliquoring step were 5.27 N/mm and ranged between 2.36 and 3.11 N/mm in leather with fatliquor²⁶. These values are in line with that found in this work, when compared the E-I (without fatliquoring) with the experiments E-II and E-III (with fatliquoring).

A satisfactory shrinkage temperature was achieved for all the samples, but the one with APTES (E-II) was lower than the others because the vegetable tannin diffusion was not complete in this experiment. For vegetable tannin, the shrinkage temperature achieved after tanning ranges between 70 and 85°C²⁷.

The tensile strength was higher for the control sample and the lowest for the sample with APTES, possibly for the incomplete diffusion of the vegetable tannin. Conversely, the percentage extension revealed that the samples with the organosilanes (E-II and E-III) elongated more than the control sample before the breaking point. The thickness increase after the tanning process was similar for the control sample and the sample with APTES (E-II) and lower for the E-III.

Table 4. Results for the leathers from Experiment I, II and III.

Parameter	Experiment I		Experiments II and III		
	Control sample	E-I	Control sample	E-II	E-III
Shrinkage temperature (°C)	76	76	80	74	80
Tensile strength – breaking point (MPa)	17.9	27.2	42.7	27.6	36.6
Elongation at break (%)	45.8	58.5	48.8	51.8	54.5
Surface tension (N/mm)	4.86	5.01	1.3	2.2	1.4
Thickness increase (%)	-	25	46	40	22

Contact angle and optical profile analysis were performed for the leathers resulting from the experiments II and III in order to verify the influence of the organosilanes on the hides. For contact angle analysis, the leather without nanosilica (control sample) absorbed the water very fast and it was not possible to capture the image of the drop. Instead, the leather samples with the organosilanes took more time to absorb the drop of water, being possible to capture the image. The results were for the E-II with APTES, an angle of 84.8° in the left side, and 82.4° in the right side (Fig. 2a). For the E-III with ODS, the angles were 69.2° for the left side and 70.5° for the right side (Fig. 2b). This suggests that the leather surfaces with the organosilanes are more hydrophobic than the surface of the control sample. However, as the measured contact angle was less than 90°, all the samples presented hydrophilic surface.

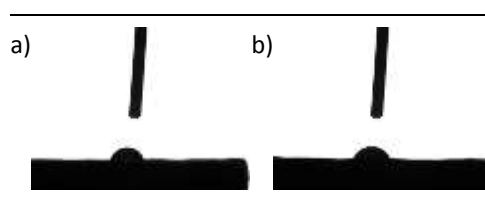


Fig. 2. Contact angle images of a drop of water on leathers with organosilanes. Sample (a) E-II with APTES and (b) E-III with ODS.

From the optical profile analysis (Fig. 3), which shows the roughness of the surface, we can see the red regions, which indicate peaks and the blue ones, which indicate valleys. The leather sample with the organosilane ODS (Fig. 3b) presented the red region more homogeneous than the control sample (Fig. 3a), as can be better observed in the 2-D image. This analysis is useful to compare the roughness of treated leather with silica and leathers without silica, looking for more uniform surfaces, since smooth leathers are of great value for the consumer market.

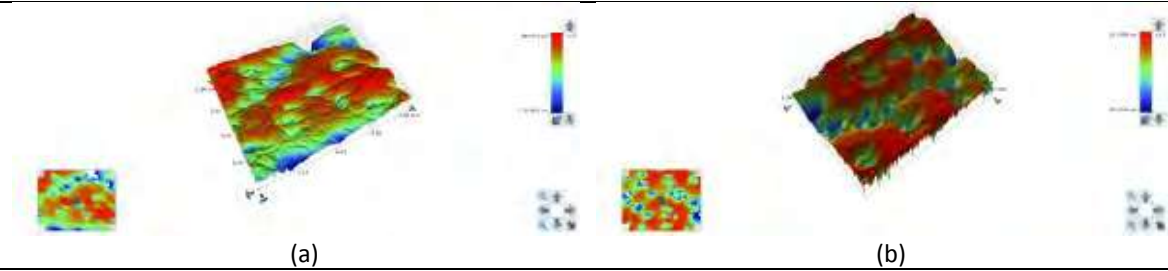


Fig. 3. Optical profiler images from (a) control sample and (b) E-III with ODS.

In the Experiment IV (E-IV), a pre-tanning formulation was used to facilitate the diffusion of the vegetable tannin. In this experiment there were two additions of the nanosilica dispersion in order to maximize the effect of silica on the properties of leather. The leathers resulting from this experiment were tested for their physical-mechanical properties and the results are presented in Table 5.

Table 5. Results from the Experiment IV.

Parameter	Control sample	E-IV
Shrinkage temperature (°C)	78	78
Tensile strength – breaking point (MPa)	19	23
Elongation at break (%)	47	54
Surface tension (N/mm)	1.33	1.54
Thickness increase (%)	85	115
Total colour difference (ΔE) – lightening	-	3.25
Total colour difference (ΔE) – UV-light exposition	-	3.87

According to Table 5, the presence of silica did not impair the stabilization of the hide, since the shrinkage temperature was the same for the control sample and the leather with silica. From the tensile and percentage extension test, leather with silica showed 22% higher tensile strength when compared to the control. The percentage of extension was also higher for the leather with silica. From the softness analysis it was found that the introduction of silica did not compromise the softness of the leather. The thickness increase revealed the greatest filling for the leather sample with silica.

The total colour difference (ΔE) indicated that the Experiment IV produced lighter coloured leather than the control, which can also be observed visually in Fig. 4. Light hides are interesting for the industry once which facilitate dyeing with lighter colours.

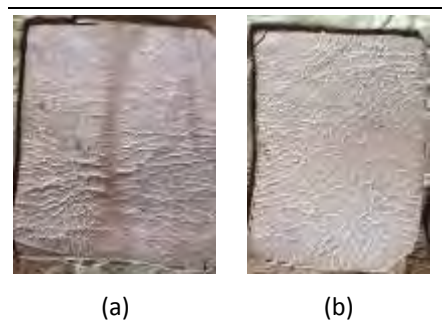


Fig. 4. Leather samples from experiment IV: (a) control sample (b) E-IV.

The stability of the leather - with and without nanosilica - to ultraviolet light was also evaluated. The colour variation before and after exposure to UV light was higher for the silica samples, indicating that the leather obtained in this experiment was less stable to UV light.

From the Experiment IV, it was also concluded that there was an increase in the amount of salt required for the vegetable tanning due to the alcohol existent in the synthesis of the nanosilica dispersion that reduces the density of the tanning liquour. On the other hand, in the same experiment, the addition of 5% of pre-tanning agent reduced in 10% the vegetable tannin amount needed to complete the tanning process.

4 Conclusions

This work investigated the use of silanes in leather tanning, where variations in the nanosilica synthesis from the precursors TEOS, APTES and ODS were tested. The shrinkage temperature to consider the hide tanned was only achieved in the presence of vegetable tannin as tanning agent. The physical-mechanical properties varied according to the formulations used. There was improvement in the tensile strength in the most cases and the softness was not altered by the introduction of the silica. Lighter coloured leather was produced with the introduction of the nanosilica dispersion. However, it was less stable to UV light and demanded more salt in the process. On the other hand, the vegetable tannin amount required to complete diffusion decrease representing considerable savings of product. Therefore, to explore the influence of organosilanes on hide stabilization, further studies are needed because the tanning chemistry between nanomaterials and collagen is complex even so promising.

References

1. Rose, A. A NEW TYPE OF SILICA TANNAGE. *Can. J. Res.* **17b**, 385–389 (1939).
2. Zhang, Y. et al. Can sodium silicates affect collagen structure during tanning? Insights from small angle X-ray scattering (SAXS) studies. *RSC Adv.* **7**, 11665–11671 (2017).
3. Covington, T. *Tanning chemistry : the science of leather.* (Royal Society of Chemistry, 2011).
4. Sreeram, K. . & Ramasami, T. Sustaining tanning process through conservation, recovery and better utilization of chromium. *Resour. Conserv. Recycl.* **38**, 185–212 (2003).
5. Munz, K. H. Soluble Silicates in Leather Products. *J. Am. Leather Chem. Assoc.* **98**, 159–167 (2003).
6. Saravanabhavan, S., Thanikaivelan, P., Rao, J. R., Nair, B. U. & Ramasami, T. Sodium Metasilicate Based Fiber Opening for Greener Leather Processing. *Environ. Sci. Technol.* **42**, 1731–1739 (2008).
7. Munz, K. H. & Sonnleitner, R. Application of Soluble Silicates in Leather Production. *J. Am. Leather Chem. Assoc.* **100**, 66–75 (2005).
8. Lu, Y. et al. NaNO-SiO₂/oxazolidine combination tannage: Potential for chrome-free leather. *J. Soc. Leather Technol. Chem.* **92**, 252–257 (2008).
9. Fan, H., Shi, B. & He, Q. Tanning Characteristics and Tanning Mechanism of Nano-SiO₂. *J. Soc. Leather Technol. Chem.* **88**, 139–142 (2004).
10. Fan, H. J., Ling, L. I., Shi, B. I., Qiang, H. E. & Peng, B. Y. Characteristics of leather tanned with nano-SiO₂. *J. Am. Leather Chem. Assoc.* **100**, 22–30 (2005).
11. Li, Y., Wang, B., Li, Z. & Li, L. Variation of pore structure of organosilicone-modified skin collagen matrix. *J. Appl. Polym. Sci.* **134**, (2017).
12. Pan, H., Zhang, Z. & Zhang, J. Preparation and Application of a Nanocomposite Tanning Agent - MPNS/SMA. *JOURNAL- Soc. LEATHER Technol. Chem.* **89**, 153–156 (2005).
13. Pan, H., Qi, M. & Zhang, Z. Preparation and Application of a Nanocomposite Tanning Agent -- RNS/P(MAA-BA). *J. Soc. Leather Technol. Chem.* **92**, 34 (2008).
14. Liu, Y., Chen, Y. & Fan, H. Environment-friendly Lime-free Liming. *J. Soc. Leather Technol. Chem.* **93**, 56–60 (2009).
15. Liu, Y. et al. An environmentally friendly leather-making process based on silica chemistry. *J. Am. Leather Chem. Assoc.* **105**, 84–93 (2010).
16. Lu, Y., Chen, Y., Fan, H. J., Peng, B. Y. & Shi, B. A novel nano-SiO₂ tannage for making chrome-free leather. in *32nd Congress of the International Union of Leather Technologists and Chemist Societies, IULTCS 2013* (2013).

17. Hao, L., Wang, X. & Xu, W. High Exhaustion Chrome Tanning Process Aided by Sodium Silicate. in 30th International Union of Leather Technologists & Chemists Societies (2009).
18. Yang, J. et al. Study on the In situ Preparation of Nano-SiO₂/THPC Nano-composite Tanning Agent. in 30th International Union of Leather Technologists & Chemists Societies (2009).
19. Fathima, N., Madhan, B., Rao, J. & Nair, B. Mixed metal tanning using chrome-zinc-silica: A new chrome-saver approach. *Journal- American Leather Chemists Association* **98**, (2003).
20. Fathima, N., Subramani, S., Rao, J. & Nair, B. An Eco-Benign Tanning System Using Aluminium, Tannic Acid, and Silica Combination. *Journal of the American Leather Chemists Association* **99**, (2004).
21. Fathima, N., Prem Kumar, T., Ravi Kumar, D., Rao, J. & Nair, B. Wet white leather processing: A new combination tanning system. *Journal of the American Leather Chemists Association* **100**, (2005).
22. Pan, H., Li, G.-L., Liu, R.-Q., Wang, S.-X. & Wang, X.-D. Preparation, characterization and application of dispersible and spherical Nano-SiO₂@Copolymer nanocomposite in leather tanning. *Appl. Surf. Sci.* **426**, 376–385 (2017).
23. Chen, Y., Fan, H. & Shi, B. Nanotechnologies for leather manufacturing: A review. *J. Am. Leather Chem. Assoc.* **106**, 260–273 (2011).
24. Stöber, W., Fink, A. & Bohn, E. Controlled growth of monodisperse silica spheres in the micron size range. *J. Colloid Interface Sci.* **26**, 62–69 (1968).
25. KELLERT, H. J. & WOLF, H. Neues Biegesteifheitsprüfgerät "Softometer KWS". *Das Leder* **41**, 138–142 (1990).
26. Gutterres, M. Absorción de los Agentes de Curtición y Engrase y Modificación de la Matriz de Colágeno. *Boletín Técnico la Assoc. Química Española la Industria del Cuero* **54**, 207–2015 (2003).
27. BASF. *Vade-mécum do curtidor.* (2004).

INVESTIGATION OF THE REACTION MECHANISM BETWEEN BOVINE COLLAGEN AND A TRIAZINE-BASED COUPLING REAGENT

G. Pozza^{1,a}, S. Mammi², A. Cattazzo², T. Carofiglio²

¹ Gruppo Mastrotto SPA, via IV Strada, 7 - 36071 Arzignano (VI), Italy

² Department of Chemical Sciences, via Marzolo 1 - 35131 Padova, Italy

a) Corresponding author: pozza@mastrotto.com

Abstract. The triazine-based coupling reagent 4-(4,6-dimethoxy-1,3,5-triazin-2-yl)-4-methylmorpholinium chloride (DMTMM) is a promptly water-soluble white solid commonly used in chemical synthesis, which is proven to act as effective tanning agent. This research work provides an experimental evidence that the tanning ability of DMTMM is associated to an increase of the cross-linking density in the collagen molecule. As a result of the coupling reaction, DMTMM is converted into water-soluble by-products that can be removed by washing.

1 Introduction

The compound 4-(4,6-Dimethoxy-1,3,5-Triazin-2-yl)-4-Methylmorpholinium Chloride (DMTMM) is a versatile triazinic coupling agent¹ used in organic synthesis to promote the formation of carboxamides via direct condensation of carboxylic acids with amines.^{2,3} Although several chemical species are available for the same purpose,^{4,5} DMTMM is attractive for green chemistry industrial applications because it is highly water-soluble^{6,7} and is commercially available in the form of air- and moisture-stable solid powder (melting point 116 – 117 °C).⁸ It can be stored at room temperature for up to a month or for several months in the refrigerator without detectable decomposition.⁹

This research work provides experimental evidence to the hypothesis that the powerful tanning effect of DMTMM is due to an increase of amide cross-link density in the collagen molecule. The reaction is investigated here using soluble collagen and DMTMM in aqueous solution; furthermore, the coupling reaction has been modelled by condensing a carboxylic acid and an amine with DMTMM in water.

2 Materials and Methods

DMTMM, acid soluble Calf Skin Type I Collagen and D₂O (99.9 % D), amylamine (≥ 99%) and propionic acid (ACS reagent, ≥ 99.5%) were purchased from Sigma Aldrich. Thermogravimetric analyses were performed with a Q5000 IR instrument with a temperature gradient set at 10 °C/min, in the interval 50 - 700 °C. A Q20 DSC calorimeter was used for differential scanning calorimetry measurements; both were supplied by TA Instruments. The ¹H-NMR spectra were recorded at room temperature (298 K) with a Bruker DRX-400 (400 MHz) spectrometer. The Fourier transform infrared spectroscopy of samples was performed with a JASCO FT/IR-4100 Type A spectrometer equipped with a PIKE MIRacle ATR accessory (Ge crystal); spectra were recorded with 128 scans per spectrum at 2 cm⁻¹ resolution. MS spectra of all samples were collected with an Agilent Technologies LC-MSD-Trap-SL 10367 system. A 1:1 mixture of H₂O and acetonitrile (ACN), both acidified with 0.1% CH₃COOH, was used as eluent.

An unexpected, massive presence of citric acid was detected in the commercial collagen sample, likely attributable to the extraction procedure from the biological material.^{10,11} By means of TGA measurements, it was possible to estimate a content of about 18 % wt. of citric acid. In order to purify the product, a solution was prepared in milliQ water (28.8 mg in 5.76 mL, pH \approx 4) and subjected to dialysis in a Pur-A-Lyzer Purg10010 Dialysis Kit (Sigma-Aldrich) with a MW cut-off of 1000 Da. The solution was dialysed versus 500 mL of milliQ water, periodically replaced, at room temperature under continuous stirring for 6 days. The solution was eventually freeze-dried in a Lio-5 P Freeze-Drier (CiK Solutions) at $T \approx -50$ °C and $p \approx 0.5$ mbar, obtaining 20.0 mg of solid collagen (yield 69%). Elimination of citric acid was confirmed by the disappearance of the corresponding signal in the $^1\text{H-NMR}$ spectrum of a collagen solution in D_2O (figure 1).

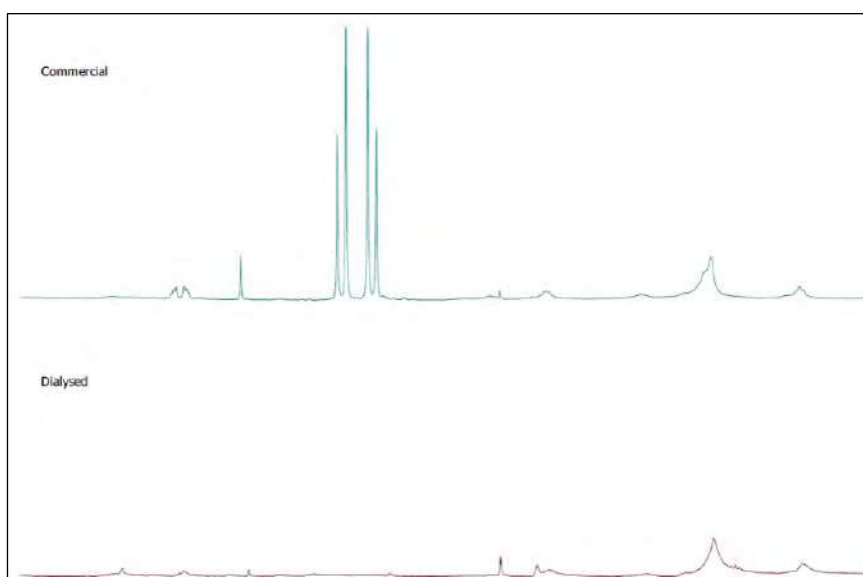


Figure 1. $^1\text{H-NMR}$ spectra of commercial and purified collagen.

3 Results

3.1 Cross-linking reaction in water soluble collagen

An aqueous solution of collagen was prepared dissolving 20.0 mg of pristine solid collagen (see Materials and Methods) in 4000 μL of milliQ water and maintaining it under stirring for 8 hours at room temperature. An amount of 22.1 mg of DMTMM was then added while keeping the solution under stirring. Three hours later, the formation of small aggregates was observed, and an additional quantity (22.1 mg) of DMTMM was added to the mixture at this point. After other 2 hours, a whitish gel-like agglomerate appeared within the solution (figure 2). The liquid mixture was subsequently dialysed with the protocol described above in order to remove by-products and residual DMTMM. After freeze-drying, 7.7 mg of solid was recovered. The by-products of the reaction are expected to be DMT-OH (Figure 3) and N-methylmorpholine (NMM), both water-soluble.⁴

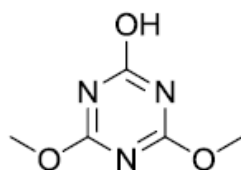


Figure 2. DMT-OH

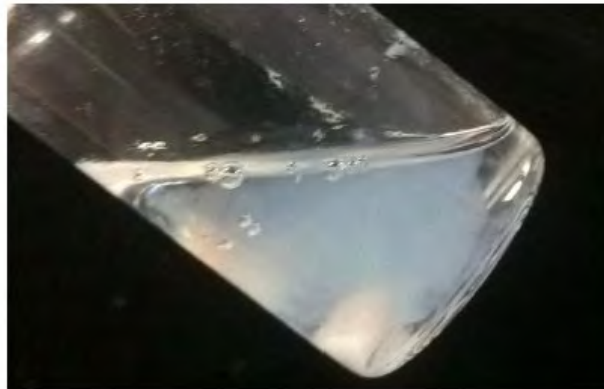


Figure 3. Gel-like agglomerate in the collagen solution after reaction with DMTMM.

3.2 Thermal Gravimetric Analysis (TGA)

The comparative TGA analysis was performed under air flux with 0.340 mg of purified collagen and 0.499 mg of cross-linked product. The results (figure 4) show that the bound water content is 7.9% for the pristine sample and 3.6% for the cross-linked collagen, indicating that, after the reaction with DMTMM, the collagen matrix becomes less hydrophilic. Since the formation of amide bonds takes place at the expense of the highly hydrophilic carboxylic and amino moieties in the collagen side chains, a lower affinity of the substrate for water is expected as one consequence of the crosslinking reaction, in line with the result of TGA measurements.

Another notable outcome of the comparison of TGA curves is that the reaction product starts to decompose at a lower temperature than pristine collagen (see figure 3), indicating that it is slightly less stable. Because of the structural role of water in the collagen molecule,^{12,13,14} this may correlate with the lesser content of bound water resulting from TGA measurements.

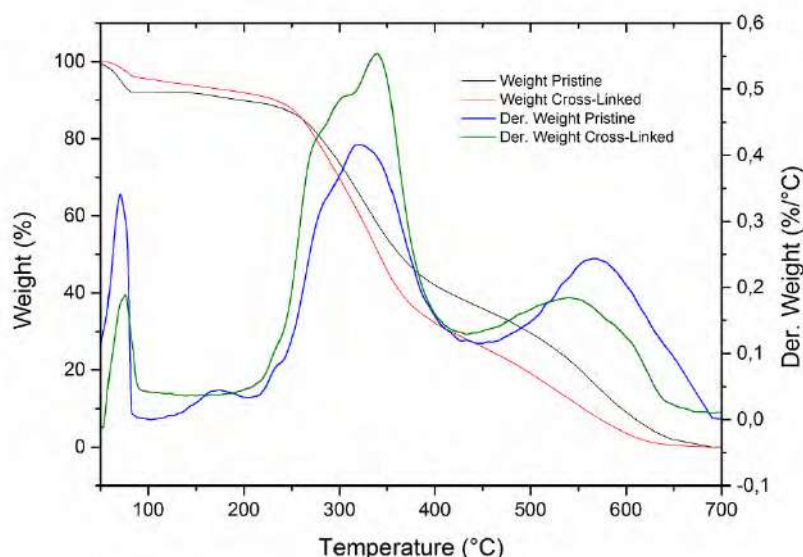


Figure 4. TGA and D-TGA curves of pristine (black and blue) and cross-linked (red and green) collagen.

3.3 Fourier transform infrared spectroscopy

Infrared spectroscopy is thoroughly exploited in the investigation of protein structure.¹⁵ Specifically, resonances related to the peptide bonds are classified as Amide I, Amide II, Amide III, Amide A, etc. based on their position in the spectrum, and they are influenced by the structural features of the protein. For the collagen molecule, the Amide I band falls at around 1650 cm^{-1} , the Amide II at 1550 cm^{-1} , the Amide III at 1245 cm^{-1} ,¹⁶ while overtones and Fermi resonances (Amide A and B) are found at 3293 cm^{-1} and 3097 cm^{-1} , respectively.¹⁷

FT-IR spectra of both freeze-dried pristine and cross-linked collagen are shown in figure 5. The similarity between band frequencies for the two samples indicates that the transformations undergone by collagen do not affect its chemical composition, although some structural modifications occurred. The most notable differences regard Amide A and Amide II bands. The Amide A band is independent on the backbone conformation but is very sensitive to the strength of hydrogen bonds (note that it is superimposed to the O-H stretching band of collagen-bound water). For quantitative comparison, the spectra were normalized using the intensity of the C=O band (Amide I), assuming that the amidation reaction has no effect on it. The decrease of the Amide A band in the cross-linked collagen indicates the disappearance of amino groups; since the cross-linking degree is correlated to the ratio A_i/A_A , the increase of this ratio from 2.90 to 3.73 in the final product confirms that DMTMM promotes cross-linking in collagen and suggests that the reaction product contains less bound water. The decrease of both Amide II and the carboxylate symmetric stretching band at around 1401 cm^{-1} in the reaction product indicates the reduction of amino and carboxyl groups, consistent with an increase of cross-linked collagen.

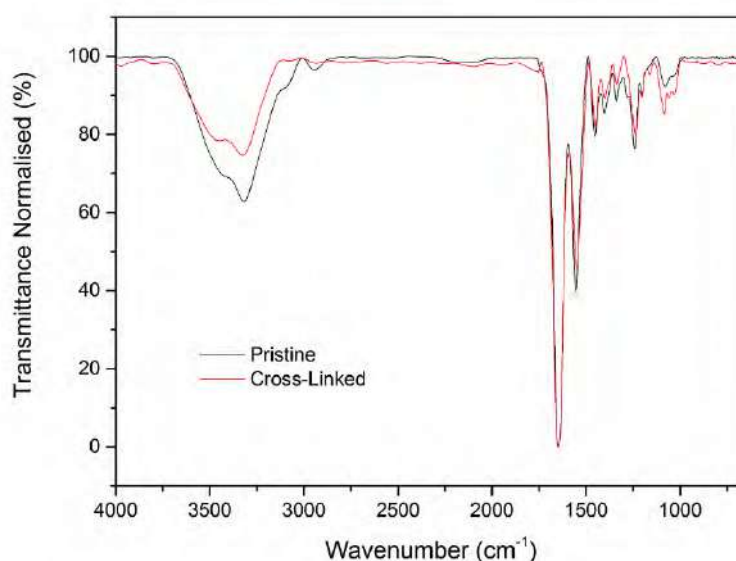


Figure 5. Superimposed FT-IR spectra of collagen before (black line) and after (red line) reaction with DMTMM.

The last observation regards the difference between the frequencies of Amide I and II, which denotes the presence of denatured collagen for $\Delta\nu > 100\text{ cm}^{-1}$.¹⁸ In this case, the values are 94 cm^{-1} for the original sample and 95 cm^{-1} for the reaction product, indicating that no denaturation occurred after reaction of collagen with DMTMM.

3.4 Amide condensation in a homogeneous aqueous system

The water-based amidation that leads to increasing the cross-linking density in collagen has been further investigated by reacting the two water-soluble substrates propionic acid ($pK_a = 4.9$) and amylamine (n-pentylamine, $pK_a = 10.2$) in presence of DMTMM. To this purpose, 100 μL of amylamine and 64.4 μL of propionic acid were dissolved in 400 μL of water and thoroughly mixed. An appropriate amount of HCl 0.1 M was added to the mixture until the pH was lowered from the initial value (about 9) to 6.5, at which value both amino and carboxylic functional groups are electrically charged; in these conditions, the most effective nucleophile in solution is the deprotonated acid.

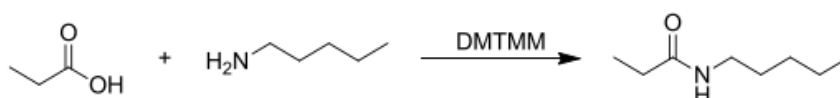


Figure 6. Amide coupling reaction between propionic acid and amylamine.

An amount of 0.2348 g of DMTMM was subsequently added to the mixture while keeping it under stirring. Within a few minutes a white precipitate appeared, and the pH spontaneously decreased to about 4. A small aliquot of the suspension was dissolved in ACN/ H_2O 1:1 and, after properly dilution, it was characterised by ESI-MS technique. The resulting mass spectrum (figure 7) demonstrates that N-pentylpropanamide is formed, as expected.

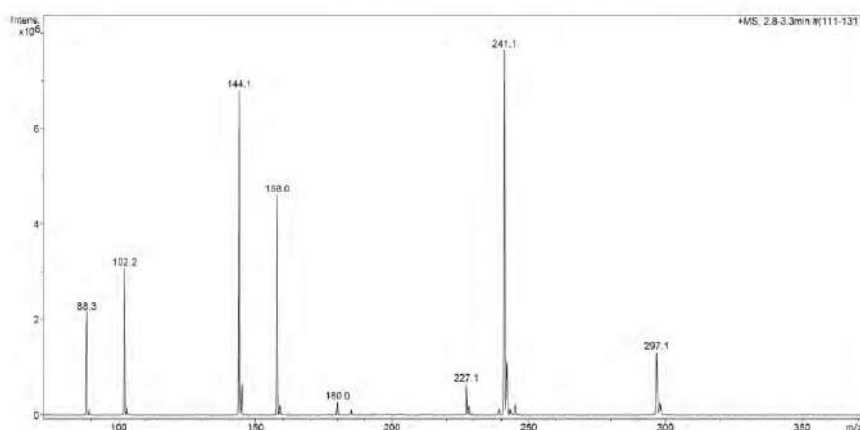


Figure 7. ESI-MS spectrum of the reaction mixture between propionic acid and amylamine.

The assignment of the signals in the spectrum are as follows: 88.3 m/z [amylamine- H^+], 102.2 m/z [NMM- H^+], 144.1 m/z [N-pentylpropanamide- H^+], 158.0 m/z [DMTOH- H^+], 180.0 m/z [DMTOHNa $^+$], 227.1 m/z [DMTM- H^+], 241.1 m/z [DMTMM $^+$] and 297.1 m/z [(DMT) $_2\text{O}$ - H^+]. Propionic acid was not detected. Thus, ESI-MS confirms that the coupling reaction was successful both for the presence of the amide and of all the expected by-products of DMTMM (NMM and DMT-OH) signals. The mass of the demethylated DMTMM is also present, indicating that de-methylation represents a spontaneous decay route for DMTMM in aqueous environment. Finally, the mass at 297.1 m/z, which could be assigned to bis(4,6-dimethoxy-1,3,5-triazin-2-yl) ether, (DMT) $_2\text{O}$, confirms the occurrence of a solvolysis side reaction. A plausible reaction pathway that leads to the formation of the triazine ether is the nucleophilic attack of the negative charged oxygen of DMT- O^- towards the partially positively charged carbonyl carbon of the keto form of DMT-OH (figure 8).

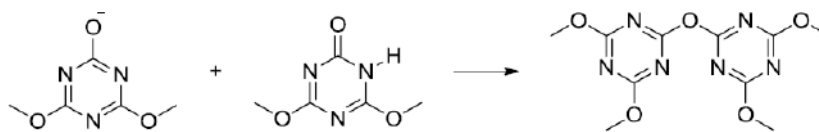


Figure 8. Proposed mechanism for the formation of (DMT)₂O.

4 Conclusion

This research work contributes to elucidating the tanning mechanism of DMTMM in aqueous medium. It was demonstrated by means of various techniques (TGA and DSC, but especially with FT-IR) that the cross-linking density in soluble collagen increases after reaction with DMTMM. The mediating role of DMTMM in water-based amide synthesis was further confirmed with a simple model reaction where reagents (propionic acid and amylamine) are both water-soluble. It was also shown that DMTMM in water undergoes demethylation via solvolysis.

References

1. Kamin'ski, Z. J.: 'Triazine-Based Condensing Reagents', *Biopolymers*, 55, 140–164, 2000
2. Kunishima, M., et al.: 'Formation of carboxamides by direct condensation of carboxylic acids and amines in alcohols using a new alcohol- and water- soluble condensing agent: DMT-MMT', *Tetrahedron*, 57, 1551-1558, 2001
3. Hojo K., et al.: 'Aqueous microwave-assisted solid-phase peptide synthesis using Fmoc strategy. III: Racemization studies and water-based synthesis of histidine-containing peptides', *Amino Acids*, 46, 2347-2354, 2014
4. Montalbetti, C. A. G. N., Falque, V.: 'Amide bond formation and peptide coupling', *Tetrahedron*, 61, 10827–10852, 2005
5. El-Faham A., Albericio, F.: 'Peptide Coupling Reagents, More than a Letter Soup', *Chem. Rev.*, 111, 6557-6602, 2011
6. Shieh, W.-C., et al.: 'Synthesis of sterically-hindered peptidomimetics using 4-(4,6-dimethoxy-1,3,5-triazine-2-yl)-4-methyl-morpholinium chloride', *Tetrahedron Lett.*, 49, 5359-5362, 2008
7. Parmentier, M., et al.: 'Switching from organic solvents to water at an industrial scale', *Curr. Opin. Green Sustain. Chem.*, 7, 13-17, 2017
8. Armitt, D.J.: '4-(4,6-Dimethoxy-1,3,5-triazin-2-yl)-4-methylmorpholinium Chloride (DMTMM)', *Aust. J. Chem.*, 54, 469, 2001
9. Blotny, G.: 'Recent applications of 2,4,6-trichloro-1,3,5-triazine and its derivatives in organic synthesis', *Tetrahedron*, 62, 9507-9522, 2006
10. Xiong, X., et al.: 'A new procedure for rapid, high yield purification of Type I collagen for tissue engineering', *Process Biochem.*, 44, 1200–1212, 2009
11. Song, W., et al.: 'Extraction Optimization and Characterization of Collagen from the Lung of Soft-Shelled Turtle *Pelodiscus Sinensis*', *Int. J. Food Sci. Nutr.*, 3, 270-278, 2014
12. De Simone, A., et al.: 'Role of hydration in collagen triple helix stabilization', *Biochem. Biophys. Res. Commun.*, 372, 121–125, 2008
13. Bella, J., et al.: 'Hydration structure of a collagen peptide', *Structure*, 3, 893–906, 1995
14. Brodsky, B., Persikov, A. V.: 'Molecular Structure of the Collagen Triple Helix', *Adv. Protein Chem.*, 301–339, 2005
15. Krimm, S., Bandekar, J.: 'Vibrational Spectroscopy and Conformation of Peptides, Polypeptides, and Proteins', *Adv. Protein Chem.*, 181–364, 1986
16. De Campos Vidal, B., Mello, M. L. S.: 'Collagen type I amide I band infrared spectroscopy', *Micron*, 42, 283–289, 2011
17. Doyle, B. B., et al.: 'Infrared spectroscopy of collagen and collagen-like polypeptides', *Biopolymers*, 14, 937–957, 1975
18. Albu, M. G., et al.: 'Chemical functionalization and stabilization of type I collagen with organic tanning agents', *Korean J. Chem. Eng.*, 32, 354–361, 2014

EFFECTIVE USE OF ENZYMATIC PROCESSES IN BEAMHOUSE THROUGH NANOPARTICLE IMMOBILIZATION

Gunavadhi Murugappan¹, Kalarical Janardhanan Sreeram^{1*}

¹(CATERS Division, CSIR- Central Leather Research Institute, Adyar, and Chennai-600020)

*Corresponding author: Dr. Kalarical Janardhanan Sreeram, CATERS Division, CSIR-Central Leather Research Institute, Adyar, Chennai 600 020, Tamil Nadu, India, Ph
No. +91-44-24437216, Email id: kjsreeram@clri.res.in

Abstract. One of the well-explored alternatives to the lime – sulphide approach for dehairing and fibre opening is the enzymatic approach. In the approach, using a drum method, about 2.5 – 5.0%, on the soaked weight of the skin/hide, of the protease and amylase are sequentially employed, with each operation run for about 6 h. An extensive washing between the two steps required as the activity of one enzyme may be compromised in the presence of the other, especially during the long running of the drum. Though a combination approach, through the use of a bifunctional enzyme has been reported in the past for single step dehairing and fibre opening, this process is likely to have limited applications as there are reports that the storage stability of combination enzymes comprising of protease, amylase and lipase is low, which is generally circumvented by employing higher concentration of amylase and lipase over protease. The individual enzyme activities are also compromised in the presence of detergents and chelators. A similar scenario has also been observed in other industries such as food, laundry etc. The applicability of nanoparticle-based approach to immobilization of enzymes (individual) has been reported in areas such as catalysis and our earlier work immobilization of enzymes on iron oxide nanoparticles has been well received. In this paper, the immobilization of multiple enzymes on copper oxide nanoparticle surfaces is reported. The immobilization, the stability of the enzyme immobilized nanoparticles and the activity of the enzymes present in the immobilized system has been confirmed using various analytical techniques. The extended storage stability of the protease – amylase – nanoparticle system has been studied. A comparative study between protease – amylase combination (in the absence/presence of nanoparticles) indicated that in the absence of nanoparticles, the amylase activity was reduced, possibly due to denaturation of the amylase by the protease. The mechanism by which copper oxide nanoparticles prevent the denaturation of amylase has been studied through computational methods. From the leather processing point of view, the use of protease – amylase – nanoparticle system for combined dehairing and fibre opening has been established and the intact nature of the collagen fibres confirmed through histopathological studies. A comparison between lime-sulphide, protease followed by amylase, protease-amylase-nanoparticle systems for dehairing – fibre opening has been made and the effectivity of the nanoparticle immobilization demonstrated.

1 Introduction

In biological systems, the biotransformation and bioconversion process are carried by biocatalyst called Enzymes. Enzymes are proteins with particular conformation having one or more active sites where catalysis will occur. They are being produced inside a cell of a living organism. Currently enzymes are produced, isolated, characterised and tested for carrying out green-chemistry synthesis in multiple industries.¹

In leather industry, enzymes are being used extensively which substitutes hazardous chemicals used in the processing of leather. Leather Tanning is a series of events which converts the raw skin/hide to stable leather. There are three main stages in tanning process: pre-tanning, tanning and post-tanning. Dehairing and fibre opening are two main processes during pre-tanning of skins and hides. The conventional method for dehairing and fibre opening is through the usage of Lime and Sulphide paste. Lime and Sulphide let out hazardous solid sludge discharge and toxic wastes into the environment. In addition to harmful by-products, the chemical method consumes copious amount of water.² As a bioremediation solution, enzymes like Amylase, Protease, and Lipase are used as substitutes for Lime and Sulphide.³

However, in an Industrial application, there are few drawbacks of using enzymes. The enzymes have inferior stability. They get degraded easily. Change in temperature, pH and other factors affects the enzymatic activity. Significant issues with enzymes include poor thermal and chemical stability, high cost, requires skilled labor.⁴ Enzyme immobilization is carried out to overcome these drawbacks. Enzyme Immobilization is a process where the enzyme molecules are attached or conjugated onto solid support or matrix. There are many advantages of enzyme immobilization.⁵⁻⁷

Nanoparticles have extended their application in the field of enzyme immobilization. Nanoparticles are used as a carrier molecule to immobilize the enzymes.⁸ They have a high surface to volume ratio, better-withstanding capability during high pressure applications and flexible platform for surface modification. Among the nanostructures, metal oxide nanoparticles are found to be very efficient in enzyme immobilization, bio-sensing, drug delivery etc. Unique physical and chemical properties of metal oxide nanoparticles which differs from the bulk material has found its application in various facets.⁹

Cupric Oxide nanoparticle (CuO Nps) is one of the oxide compounds of Copper. Copper Oxide nanoparticles is a brownish black powder with 6.3-6.49 g/cm³ density and melting point of 1201°C. It is soluble in dilute acid, ammonium chloride, ammonium carbonate and potassium cyanide solution. It is insoluble in water. One of the leading property which will help in retrieving the CuO nanoparticles from the reaction system. Enzyme immobilized CuO can be easily recovered. CuO is used in the field of catalysis, superconductor, rocket fuel, active electrode potential etc. The particle size of nano copper oxide should be between 1-100 nm. CuO nanoparticles have additional peculiar properties like surface effect, Quantum size effect, optical absorption, chemical activity, thermal resistance, catalysis, and quantum tunnelling effect.¹⁰

2 Materials and methods

The CuO Nps were prepared using Sol-Gel method as described in the "Synthesis and Characterization of CuO Nano Particles by Novel Sol-Gel Method"¹¹ with slight modifications. After the synthesis of Copper Oxide nanoparticles, they were subjected to X-Ray diffraction analysis by Rigaku Mini Flux X-Ray Diffractometer to confirm the elements present are Copper and Oxygen and to determine the crystalline size and crystal system. The hydrodynamic diameter of the sample was measured by Dynamic Light Scattering (DLS) technique after dispersing the nanoparticles in water under sonication. The Zeta Potential of nanoparticles to enzyme coating using Malvern Zetasizer Nano ZS.

For immobilization studies, 1mg/mL α -Amylase-Protease solution and 1mg/mL CuO nanoparticle solution were prepared. 1mL of CuO solution was added to all the tubes. The supernatant was collected, and protein content was estimated through Lowry Protein estimation method.¹² Further, with the pellet containing the CuO and immobilized enzymes, Amylase and Protease assay were performed.

As per the industrial requirement, 4% Protease, 1% α -Amylase and 1% CuO nanoparticles were used to obtain the immobilized product. The CuO nanoparticles were dispersed in water by sonication. The enzyme mixture was added to the CuO solution drop wise. The mixture was stirred continuously at 800 rpm for 1hour. The mixture was washed for 3 times by centrifugation. The pellet was dried in vacuum to obtain the immobilized product.

For leather trials, the skin was taken from the vertebral region of the goat. The skin was washed thoroughly to remove blood, dirt and other undesirable particles. The adipose tissue layer was removed with the knife. The wet skin was cut into five pieces each weighing around 100g.

Five different samples were taken for the study – 5% of Lime and 5% of Sodium Sulphide. The second sample consisted of 5% of Immobilized product (α -Amylase+ Protease+ CuO nanoparticles). The third sample consisted of 5% of Immobilized product (α -Amylase+ Protease+ CuO nanoparticles)

and 5% of Lime. The fourth sample consisted of 5% of enzyme mixture (α -Amylase+ Protease) and 5% of Lime. The fifth sample consisted of 5% of enzyme mixture (α -Amylase+ Protease).

Each sample was made into a paste by adding 10% of distilled water. Each piece of skin was treated with the respective sample paste, by applying the paste on the flesh side of the skin. The skin pieces were incubated for 16 hrs. After the incubation, the dehairing process was carried to remove the hairs from the skin pieces. The treated skins were thoroughly washed and subjected for conventional tanning procedures.¹³

Proteoglycan Assay was carried to quantify the proteoglycan released from each piece of treated skin. After dehairing, the skin pieces were put into a respective shaker flask containing distilled and were kept in shaker at 160 rpm for 2 hours. The liquor was collected for the analysis.

Copper Oxide nanoparticles have anti-bacterial properties. Mostly Gram-negative bacteria are more susceptible to Copper Oxide nanoparticles. The mechanism is not yet known.

The anti-microbial assay was carried out using Gram-negative Escherichia coli (ATCC 8739). The Bacterial culture was purchased from CSIR-IMTech, Chandigarh. Disc diffusion method was used for this assay. Autoclaved Luria Bertani- Agar media was used for plating. The 100 μ L of bacterial suspension of 1×10^6 was inoculated on the plate. Gentamycin (30 μ g/disc) was used as positive control for antimicrobial activity.¹⁴ 50 μ L of CuO nanoparticles solution having the concentration of 1mg/mL and Immobilized CuO solution having 1mg/mL nanoparticle and 1mg/mL enzyme mixture were loaded on to the respective wells. The plate was incubated overnight in the incubator at 37°C. The zone of inhibition around the wells were measured.

3 Results and Discussion

The Figure 1. Shows the XRD pattern of Copper Oxide Nanoparticles. Sharp peaks formation exhibits crystalline structure. The peaks corresponding to the following 2θ values: 33, 36, 39, 49, 54, 62, 66, 72, 75 confirms the CuO formation.¹⁰ TEM image indicates that the synthesized sample possess rod-shaped particles with homogeneous nature.

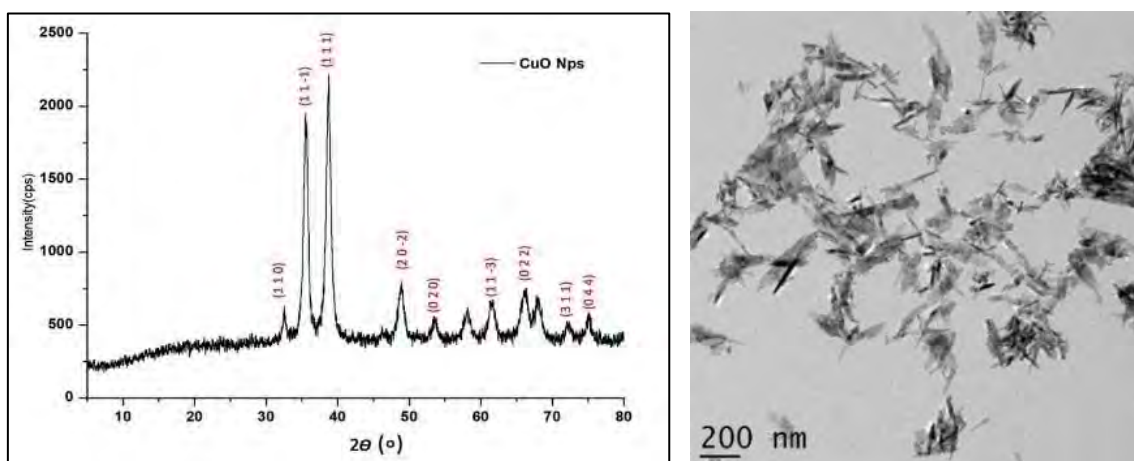


Fig. 1. XRD and TEM of synthesized CuO Nps

From Lowry, the protein content in Blank enzyme and immobilized samples were quantified. The Blank enzyme contained around 992 μ g. The supernatant from the immobilized sample comprised around 943 μ g. From the above results, protein content in the pellet was calculated. It was 48.8 μ g. This shows that the protein loading capacity of CuO nanoparticles is quite weak when the concentration of the enzyme is high (i.e. around 1000 μ g).

But from the α -amylase activity assay, it is clear that the activity of the immobilized enzyme is retained. Whereas in Blank Enzyme sample, over the time, the amylase enzyme is getting degraded by the protease enzyme. Thus, immobilization prevents Protease from cleaving Amylase enzyme. These results thus support the fact that multiple enzymes can be loaded on to one carrier without affecting the enzymes activity.

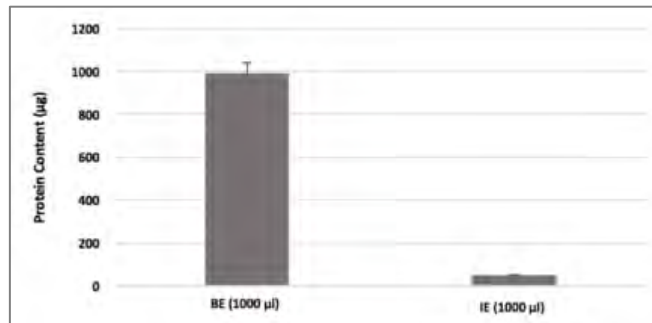


Fig. 2. Protein quantification by Lowry analysis

The Protein content in Blank Enzyme and immobilized samples are 748µg and 133.3µg respectively. The protein loading capacity of CuO nanoparticles is poor. But comparing with the 1000µg sample, the 750µg sample has got more protein immobilized on to the CuO nanoparticles. Thus, the loading efficiency of the CuO nanoparticles is better at lower enzyme concentrations.

From Protease assay, the activity of the immobilized enzyme is comparatively higher than that of blank enzyme. In immobilized enzyme sample, for 18% of protein content it is having 44% of enzymatic activity. Thus, the activity of the enzyme is increased due to immobilization.⁵



Fig. 3. Skins before and after dehairing. [5% of Lime and 5% of Sodium Sulphide- (1), 5% of Immobilized- (2), 5% of Immobilized +5% of Lime- (3), 5% of bare enzyme mixture +5% of Lime - (4), 5% of bare enzyme mixture]

From the leather dehairing studies it was clear that sample 2(Immobilized enzyme can perform proper dehairing to that of control sample (5% lime+ 5% Sodium Sulphide). Nevertheless the presence of lime in the sample 3 along with immobilized enzyme shows a phenomenal setback in the performance of the sample by incomplete dehairing. On the other hand, skins treated with sample 4 and 5 with 5% bare enzymes started to decay, which was indicated by strong putrefaction smell.

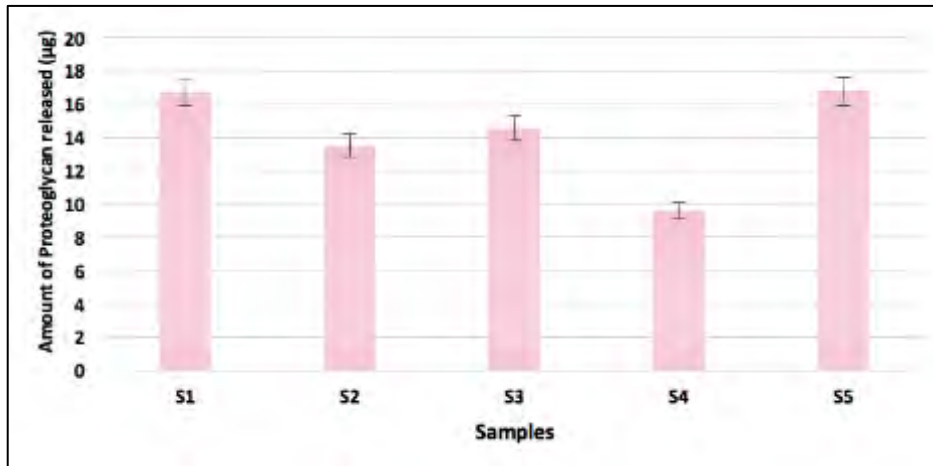


Fig. 4. Proteoglycan release assay.

The proteoglycan released were quantified through proteoglycan assay. The Figure. 4 Represent the amount of proteoglycan released from each skin pieces. The types of Proteoglycans released are Heparan Sulphate, Chondroitin and dermatan. Compared with the other samples, the Proteoglycan released is higher in Sample 1 where Lime and Sulphide was used. Comparable or similar result is observed in Sample 5 where only 5% of enzyme mixture is used. In Sample 4, the proteoglycan release is quite low due to presence of Lime along with enzyme mixture. This is because the enzymes got denatured in the presence of Lime. Although, in Sample 3 containing Immobilized enzyme and Lime, the proteoglycan released from the sample is higher than Sample 4. This shows that denaturation of enzymes by Lime is minimized due to the immobilization. Sample 2 contains only 2.5% of enzyme mixture (along with 2.5% of CuO nanoparticle). For the amount of enzyme (2.5%) provided, Proteoglycan released from Sample 2 is comparably higher. This is because, activity of the enzymes has increased significantly due to immobilization. The CuO nanoparticles because of their small size, can easily penetrate through the skin pores and acts as a vehicle to make enzymes accessible in the hair follicle regions, thus there is higher removal of proteoglycans and hairs from the skin.

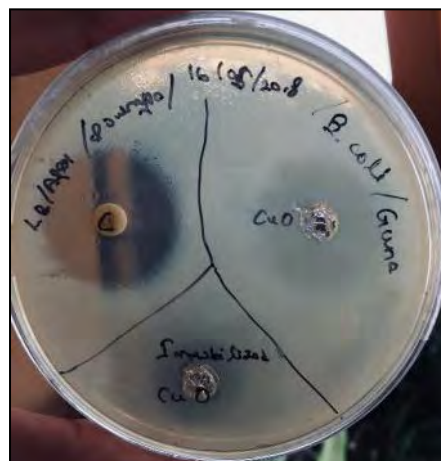


Fig. 5. Anti-microbial assay.

For this study, E. coli gram negative bacterial culture was used. The zone of inhibition around the antibiotic gentamycin formed was measured to be 30mm. The zone of inhibition formed for CuO sample and Immobilized enzyme sample does not have a clear distinct boundary. For CuO nanoparticles, the zone of inhibition was measured to be 25mm. And for immobilized enzyme, the zone of inhibition was measured to be 21mm. This shows that CuO has some effect on gram negative bacteria. By increasing the concentration of the CuO nanoparticles, toxicity level will increase resulting in the formation of clear and distinct zone of inhibition.

4 Conclusion

In this study, we have successfully demonstrated that Cupric Oxide nanomaterials can be employed as a support material for enzymes. Immobilization of enzymes with nanoparticles were done through adsorption with 80% yield, which addresses the possible transition from chemical to bio-based leather processing. Also Nano delivery carriers increase the acceptability of enzymatic approaches as known lacunae are overcome. Thus Nanotechnology paves the way for sustainable beam house operations.

References

1. Gurung, N.; Ray, S.; Bose, S.; Rai, V., *A broader view: microbial enzymes and their relevance in industries, medicine, and beyond*. *BioMed research international* 2013.
2. Chowdhury, M.; Mostafa, M. G.; Biswas, T. K.; Mandal, A.; Saha, A. K., *Characterization of the Effluents from Leather Processing Industries*. *Environmental Processes* 2015, 2 (1), 173-187.
3. Saran, S.; Mahajan, R. V.; Kaushik, R.; Isar, J.; Saxena, R. K., *Enzyme-mediated beam house operations of leather industry: a needed step towards greener technology*. *Journal of Cleaner Production* 2013, 54, 315-322.
4. Wälti, M.; Roulin, S.; Feller, U., *Effects of pH, light and temperature on (1→3, 1→4)- β -glucanase stability in wheat leaves*. *Plant physiology and Biochemistry* 2002, 40 (4), 363-371.
5. DiCosimo, R.; McAuliffe, J.; Poulouse, A. J.; Bohlmann, G., *Industrial use of immobilized enzymes*. *Chemical Society Reviews* 2013, 42 (15), 6437-6474.
6. Guzik, U.; Hupert-Kocurek, K.; Wojcieszńska, D., *Immobilization as a strategy for improving enzyme properties-application to oxidoreductases*. *Molecules* 2014, 19 (7), 8995-9018.
7. Rodrigues, R. C.; Ortiz, C.; Berenguer-Murcia, Á.; Torres, R.; Fernández-Lafuente, R., *Modifying enzyme activity and selectivity by immobilization*. *Chemical Society Reviews* 2013, 42 (15), 6290-6307.
8. Kaushik, A.; Khan, R.; Solanki, P. R.; Pandey, P.; Alam, J.; Ahmad, S.; Malhotra, B., *Iron oxide nanoparticles-chitosan composite based glucose biosensor*. *Biosensors and bioelectronics* 2008, 24 (4), 676-683.
9. Shah, E.; Mahapatra, P.; Bedekar, A. V.; Soni, H. P., *Immobilization of Thermomyces lanuginosus lipase on ZnO nanoparticles: Mimicking the interfacial environment*. *RSC Advances* 2015, 5 (33), 26291-26300.
10. El-Trass, A.; ElShamy, H.; El-Mehasseb, I.; El-Kemary, M., *CuO nanoparticles: Synthesis, characterization, optical properties and interaction with amino acids*. *Applied Surface Science* 2012, 258 (7), 2997-3001.
11. Tran, T. H.; Nguyen, V. T., *Copper Oxide Nanomaterials Prepared by Solution Methods, Some Properties, and Potential Applications: A Brief Review*. *International scholarly research notices* 2014, 2014, 856592-856592.
12. Lowry, O. H.; Rosebrough, N. J.; Farr, A. L.; Randall, R. J., *Protein measurement with the Folin phenol reagent*. *The Journal of biological chemistry* 1951, 193 (1), 265-75.
13. Gladstone Christopher, J.; Ganesh, S.; Palanivel, S.; Ranganathan, M.; Jonnalagadda, R. R., *Cohesive system for enzymatic unhairing and fibre opening: an architecture towards eco-benign pretanning operation*. *Journal of Cleaner Production* 2014, 83, 428-436.
14. Azam, A.; Ahmed, A. S.; Oves, M.; Khan, M. S.; Habib, S. S.; Memic, A., *Antimicrobial activity of metal oxide nanoparticles against Gram-positive and Gram-negative bacteria: a comparative study*. *International journal of nanomedicine* 2012, 7, 6003-6009.

A PROTEIN BASED POLYMERIC SYNTAN FROM LEATHER WASTE: RETANNING AGENT FOR SUSTAINABLE LEATHER PROCESSING

J. Kanagaraj^{1a*}, R. C. Panda^{2b}, R. Prasanna¹ and M. Javed¹

1Sr Principal Scientist, Leather Process Technol., CSIR-CLRI, Chennai, India

2Sr Principal Scientist, Department of Chemical Engineering CSIR-CLRI

a)Corresponding author: jkraj68@yahoo.co.uk

b)rcpanda@yahoo.com

Abstract. A copolymer has been synthesized from leather waste and monomer and its application has been studied for improved exhaustion in tanning and post-tanning processes. After synthesizing, the product has been analyzed and found to have particle size of 810 nm, pH of 4.0, relative viscosity of 0.8872 cp, polydispersity index (Mw/Mn) of 0.555 and percent solid as 23%. The weakly anionic character of the co-polymer is supported by zeta potential of -0.0403 mV. The stability of the particle was also studied using TGA, DSC. Functional groups of the polymer were analyzed by FT-IR which revealed the presence of carboxylic acid, amide I & II, hydroxyl groups and ester groups in the product. The product can be used for increasing exhaustion and leather-properties in chrome tanning and post-tanning processes. It improves belly filling, provides fullness, softness and dye exhaustion in post-tanning process. It also shows better fullness and body in chrome tanning processes. The color properties found to be better and strength properties were comparable in experimental leather as compared to conventionally produced leather. This product can be applicable for manufacturing different types of leather where fullness and tightness are necessary. The present process helps in mitigating pollution problem of liquid and solid wastes of leather industry. A cost benefit analysis shows that the process is feasible for up-scaling.

1 Introduction

About 0.6 million tonnes of solid wastes/annum are generated from leather industry globally. Out of this, 40-50% contribute raw trimming and chrome shaving waste. In India, there are about 2000 tanneries which process 700,000 tonnes of hides and skins per annum. During leather processing, 500-600 kg of the solid waste is generated per tonne of the raw material. In total, this contributes nearly 70,000 tonnes of trimming plus chrome shavings of solid wastes per annum. Hence, there is a need to develop a suitable technology from solid waste for minimizing the pollution problem. The leather industry requires a suitable technology/aid for increasing the chrome exhaustion in chrome tanning because conventional chrome tanning generates nearly 30-40% of chromium in the effluent that has to be addressed immediately. Application of suitable exhaustion aid to improve the exhaustion level more than 90% is the need of the hour.

Cr(III) is widely used in tanning process for tanning the pelt. The conventional process of chrome tanning employs Basic Chromium Sulphate (BCS) at the level of 6-10% in tanning process. In tanning process BCS at the level of 60-70% is absorbed while the remaining goes with effluent containing 2000-4000 ppm of Cr(III) which poses potential problems to environment. The efficiency of the tanning process could be increased by improving the exhaustion through employing high performance aids/ modifying the tanning process itself. The application of various aids/ compounds such as amino acids, fibrous sheets based on acrylate, polymeric materials (Phely-Bobin et al., 2002), insulators or building material and then animal feed etc. while indirect use of these protein based wastes is used either to separate or to enhance exhaustion of Cr(III) on the collagen matrix for stabilization of leather (Kresalkova et al., 2002). It has been reported from literature that protein hydrolysate obtained from various leather wastes were also very useful for increasing the exhaustion of chrome tanning process. One of the major solid wastes of leather industry namely fleshing wastes were hydrolyzed and the hydrolyzates were copolymerized using acrylic acid for the

application of enhancement of Cr(III) exhaustion while nano-particle based polymer was prepared from keratin hydrolyzate and acrylic ester for application in dyeing (Kanagaraj et al., 2008). In another approach, the chrome shaving wastes were used as reducing agent for Cr(VI) in preparation of chrome(III) tanning salt. The polymeric products obtained from leather wastes were also used after several hydrolysis for the preparation of tanning agent to provide a zero discharge of chrome in leather waste.

In the present approach, protein based retanning agent has been prepared from raw skin trimming wastes. Initially the wastes were hydrolyzed by alkali hydrolysis and then polymerized with poly ethylene glycol (PEG) to get low molecular weight retanning agent (Kanagaraj et al., 2015). This retanning agent was used as an exhaust aid in the tanning process and post tanning process and the leather properties were studied.

2 Materials and Methods

2.1 Materials

Raw skin trimming wastes were collected from the tannery division of CLRI. Basic chromium sulphate (BCS), PEG, acetone, potassium persulfate was purchased from Sigma Aldrich. The wet salted skins weighing 1.5kg/skin were procured from local vendor. Pelt (ready for tanning) and wet-blue were prepared from wet salted skin.

2.2. Methods

2.2.1 *Synthesis of retanning agent from skin trimming wastes*

Retanning agent from skin trimming wastes was synthesized as follows. 250 mL of distilled water was taken in a three necked round bottom reaction flask attached to magnetic heating system at 90°C with constant stirring. Then 20 g of skin hydrolysate (prepared by alkali hydrolysis using 4% sodium hydroxide followed by thermal heating at 90°C for 4 h) was added and stirred for 60 min with heating to make homogenous mixture. 40 g of PEG (was dissolved in sufficient amount of methanol) was added in drops through one of the necks of the flask while initiator, potassium persulfate weighing 1.5 g dissolved in 50 mL of water, was also added in installments through the other neck of the flask. The reaction was allowed to proceed for 3 h with constant heating at 85-90°C and with constant stirring. The pH of the resultant product was recorded as 2.5 which was adjusted further to pH of 4 with aqueous solution of sodium bi carbonate. Finally, the product was cooled (using desiccators) at room temperature and was stored. The characteristic feature of the product was analyzed for various parameters using standard methods.

2.2.2 *Characterization of retanning agent*

The product prepared from leather wastes was characterized for particle size, Differential scanning calorimetry (DSC) and Thermogravimetric analysis (TGA) using standard procedures. The % solid level was found out by conventional evaporation method.

2.2.3 *Application of protein based retanning agent in chrome tanning and post tanning processes*

The retanning agent prepared from the raw trimming wastes was applied at the level of 5% in the tanning process and the % uptake of chromium was studied. For this, the pickled pelt (with pH about 3.0) were treated with 6% of BCS (chromium (III) tanning agent) in a rotating drum/vessel for a period of 2 h and were followed by basification using sodium formate and bicarbonate where the

pH of the leather was adjusted to 4.0. The spent liquors were collected. Then retanning agent at the level of 5% was added with the chrome-treated leather with constant stirring in the rotating vessel for a period of 1 h for completion of reaction and penetration. The collected spent liquors were recharged and the process was continued for another hour. The spent liquors were collected and analyzed for the % uptake of chromium. Similarly, the retanning agent was applied in post-tanning process along with dye, fatliquor and other retanning agents and the organoleptic properties of the leather were assessed.

2.2.4 FT-IR analysis

The sample after tanning was collected and dried in the water bath. They were mixed with potassium bromide (1:20; 0.02g of sample with KBr at a final weight of 0.4g) separately. The sample was then ground, desorbed at 60°C for 24 h and pressed to obtain IR-transparent pellets. The FT-IR was first calibrated for background scanning signal against a control sample of pure KBr. FT-IR Spectra of the samples was recorded using an FT-IR spectrum 2000 Perkin-Elmer spectrophotometer within the scanning range of 400-4000 cm⁻¹. Then the experimental sample was also scanned in similar way.

2.2.5 Color properties

The leather samples after tanning with retanning agent were processed into leather and were subjected to study difference in color properties using Gretag Macbeth Spectrolino Spectrophotometer with measurement geometry of 45°/0°. The parameters L, a, b, c and H of the measurement were obtained using the standard procedures.

2.2.6 Physical testing

The experimental and control crust leathers samples were performed for various physical tests and the data were obtained as per IULTCS method. Specimens were conditioned at 80±4°C and 65±2%RH. Over a period of 48 hours, physical properties such as tensile strength, % elongation at break, tear strength and grain crack were examined for both experimental and control samples.

3 Results and Discussion

The retanning agent from raw trimming wastes has been prepared using suitable monomer through polymerization technique. PEG possess important characteristics such as good binder, high permeability and retention factor, good osmotic pressure, hydrophilic properties. Besides, it is also used as a preservative for many substances. These qualities have motivated the authors to select PEG as one of the monomer for the preparation of retanning agent. The retanning agent exhibited the following characteristics.

Table 1. Characteristics of Retanning agent.

Product characteristics	
pH	4.0
% solid content	23
Particle size	810 nm
Molecular weight	2490 D
Viscosity	0.8872 cp

The characteristic properties of the retanning agent is presented in Table 1. The retanning agent showed pH of 4.0, % solid of 23 %, particle size of 810 nm, molecular weight of 2490 D and viscosity of 0.8872cp. The above characteristics of retanning agent showed the possibility of better reactivity with collagen to bring about increased exhaustion. The retanning agent is readily soluble in aqueous medium as its low-viscosity helps in dispersing the co-polymer in water medium easily promoting better penetration of co-polymer to the leather matrix. Percent solid level of the product is found to be 23 which help the retanning agent for dispersing in aqueous medium speeding the diffusion. In the present investigation, retanning agent is added after the chrome tanning process in the same environment which helps to increase the uptake of chromium from the bath. This is due to plenty availability of reactive sites in the retanning agent that helps to increase the uptake and reactivity of the collagen.

TGA and DSC analysis

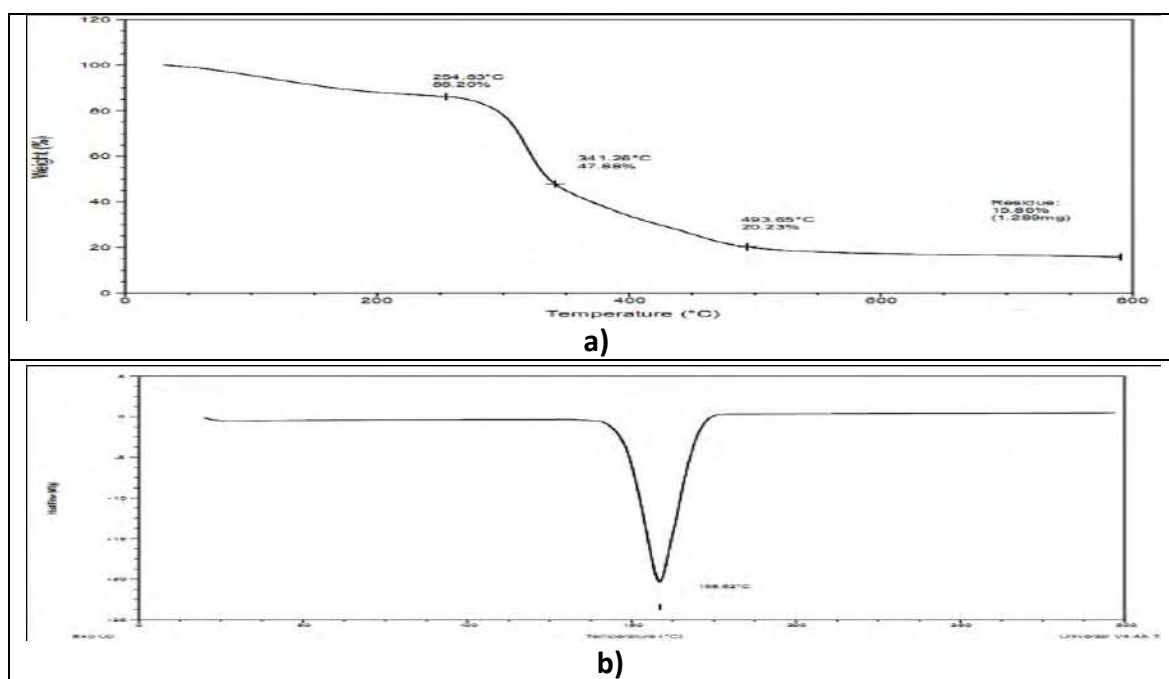


Fig. 1. Characterization of retanning agent a) TGA; b) DSC.

The stability of the retanning agent was tested by DSC and TGA analysis (Fig.1). DSC curve shows peak at 160°C where as TGA showed peak at 264, 341 and 493 °C. Weight loss of these materials as a function of temperature was recorded using this study. One can see that there are three stages in the curve. The first stage occurs between 100°C to 264°C indicating about 14 % losses in weight of the sample. The weight losses in this stage are because of loss in moisture. The second part of the curve represents the maximum weight loss because of the thermal degradation of the sample that happens at 341°C with weight losses of 52% for the copolymer sample. The third part of decomposition occurred at 493°C with a weight loss of about 80% which are mostly due to evaporation of volatile compounds. The final stage of decomposition curve is because of formation and evaporation of some volatile compounds from the sample.

Table 2. Chromium content in the tanned leather samples.

Raw material	Product offered		Chromium content		% Exhaustion	
	BCS	Retanning agent	Experiment	Control	Experiment	control
Cow	6%	5%	3.48	3.37	91%	74%
Goat	6%	5%	3.62	3.50	93%	77%

(Control: Absence of retanning agent)

The retanning agent has been applied in the chrome tanning process at the level of 5% and the exhaustion of chromium has been studied and presented in the Table 2. The chrome content was found to be slightly higher in the leather obtained from goat as compared to cow sample. The chrome content is found to be 3.48 and 3.37 for the experiment and control cow-wet-blue leather samples. Similarly, the chrome content is found to be 3.62 and 3.50 for the experiment and control goat-wet- blue leather samples. The percentage exhaustion of the experimental tanned sample showed 91 and 93% (cow and goat respectively) as compared to 74 and 77% for the control sample. The reason for the increase uptake of chromium was due to free functional carboxylic groups present in the copolymer which helps for the exhaustion of chromium. The free carboxylic acids of retanning agent may form hydrogen bonding at multipoint in providing additional adsorption and exhaustion to the complex. The other reason behind this improved adsorption may be due to the fact that -OH groups of PEG that forms H-bonding with carboxyl groups of collagen. In addition to that a physiochemical property of ester is responsible for masking the Cr complexes that indirectly helps in stabilizing Cr complex in adsorption process. Masking reduces the potency of the chromium thereby increases the reactivity of chromium with the collagen matrix. Masking also favors in uniform distribution of chrome complexes and to stabilize all the reactive groups of collagen, thereby higher exhaustion of chrome is achieved.

Table 3. FT-IR findings.

Peaks	Functional groups
3390 cm ⁻¹	Stretching frequency O–H and NH groups
1715 cm ⁻¹ and at 1650 cm ⁻¹	C=O stretching and N-H bending frequency
1340 cm ⁻¹	C-N stretching frequency of the amide group
1555 cm ⁻¹	Amide-II
1644 cm ⁻¹	Ester groups

The retanning agent was characterized for FT-IR and presented in the Table 3. It is seen from the table that the peak observed at 3390 cm⁻¹ is due to presence of protein containing OH and NH groups for the retanning agent. The peaks visible at 1715 cm⁻¹ and at 1650 cm⁻¹ are due to C=O stretching and to N-H bending frequency of the co-polymer. The functional groups present in the co-polymer envisaged that it is an amide co-polymer. It is further evident from the peak at 1340 cm⁻¹ representing C-N stretching frequency of the amide group of the co-polymer. The C=O- and the N-H bonds present in the amide group provide stability to the collagen matrix by hydrogen bonding that is very helpful in the present investigation for the effective crosslinker of the chromium in the tanning process. Moreover, peak at 1555 cm⁻¹ represents presence of amide-II and 1644 cm⁻¹ represents ester groups.

Table 4. Color analyses of the leather sample.

Sample	L	a	b	c	H
Control (cow)	29.31	5.19	5.81	7.79	48.23
Experiment (cow)	20.45	3.45	2.66	4.35	37.6

The dyed crust leather produced using retanning agent was subjected to color analyses and presented in Table 4. The leather showed better uptake of dye that resulted in higher intensity of color as compared to control sample. The color values such as L, a, b,c and H values were better in the experimental leather indicating improved dyeing/ color properties.

Further, the leathers analysed for color fastness & resistance to hot contact and are presented in Table 5. The results indicated that color fastness and resistance to hot-contact of the experiment sample was comparable to control leather.

Table 5. Color fastness & resistance to hot contact.

S. NO.	Property	Result		CLRI recommendation	Test method
		Control	Experiment		
1.	Colour fastness circular to rubbing (Grey scale rate) Dry 512 rubs Wet 256 rubs	Grade 4/5 Grade 4/5	Grade 4/5 Grade 4/5	Min. 3.0	SATRA
2.	Resistance to hot contact	No finish damage at 175 °C Moderate finish damage at 225 °C	No finish damage at 175 °C Slight finish damage at 250 °C	No melting/fusing/ breaking of finish and no colour change upto 175 °C	SATRA TM 49 : 1995

The leathers obtained by the application of retanning agent were analyzed for the performance in terms of strength properties by standard physical testing methods and are presented in Table 6. The leathers obtained from experiment showed comparable strength values with that of control leather. Physical strength properties such as tensile strength, elongation at break, tear strength, load at grain crack and distension at grain crack were comparable to the control leather with repetition of 5 times for obtaining the standard results.

Table 6. Physical strength properties using retanning agent.

Parameters	Experiment	Control
Tensile strength (kg/cm ²)	246±4.0	222 ±4.0
Elongation at break (%)	56±1.0	55±1.0
Tear strength (kg/cm)	50±1.0	50±1.0
Load at grain crack (kg)	40±1.0	38±1.0
Distension at grain crack (mm)	14±0.2	12±0.1

4 Summary

A retanning agent has been synthesized from raw trimming waste and PEG for studying improved exhaustion of chromium in the chrome tanning process. Application of protein based retanning agent at the level of 5% showed 91 and 93% exhaustion of chromium for cow and goat sample respectively in the chrome tanning process. The FT-IR analysis confirmed the reason for improved exhaustion of chromium. It was due to the fact that the functional groups present in the retanning agent envisaged that it was an amide co-polymer. It is further evident from the peak at 1340 cm^{-1} representing C-N stretching frequency of the amide group of the retanning agent. The C=O- and the N-H bonds present in the amide group provide stability to the collagen matrix by hydrogen bonding that is very helpful in the present investigation for the improved uptake of the chromium in the tanning process. The main advantages of using the protein based retanning agent in the tanning and post-tanning processes are improved dye uptake, improved body and tightness in the belly area, good softness, spongy and fluffy leathers, improved fullness, smoother grain, excellent exhaustion of other post-tanning chemical. The color analyses also showed improved dye/color uptake in the experimental leather. The physical strength properties were also comparable to the control sample.

References

1. Phely-Bobin, T.; Chattopadhyay, D.; Papadimitrakopoulos, F.: Characterization of mechanically attired Si/SiO_x nanoparticles and their self-assembled composite films, *Chem. Mater.*, 14 (3), 1030–1033, 2002
2. Kresalkova, M.; Hnankova, L.; Kupec, J.; Kolomaznik, K.: Application of protein hydrolysate from chrome shavings for polyvinyl alcohol based biodegradable material, *J. Amer. Leather Chem. Assoc.*, 7, 143-149, 2002
3. Kanagaraj, J.; Gupta, S.; Baskar, G.; Reddy, B. S. R.: High exhaust chrome tanning using novel copolymer for eco-friendly leather processing, *J. Amer. Leather Chem. Assoc.*, 103, 36, 2008
4. Kanagaraj, J, Panda, R.C and Sumathi, V.: Water Soluble Graft Copolymer Synthesized from Collagenous Waste and PEG with Functional Carboxylic Chains: A Highly Efficient Adsorbent for Chromium (III) with Continuous Recycling and Molecular Docking Studies, *Industrial Engineering Chemistry Research.*, 54, 7401--7414, 2015

IS SCREENING OF GENUINE LEATHER POSSIBLE?

Priya Narayanan¹, Kalarical Janardhanan Sreeram^{1*}

¹ CATER'S DEPARTMENT, CSIR-CENTRAL LEATHER RESEARCH INSTITUTE, ADYAR CHENNAI-600020, INDIA

*Corresponding author: Dr. Kalarical Janardhanan Sreeram, CATER'S Division, CSIR-Central Leather Research Institute, Adyar, Chennai 600 020, Tamil Nadu, India, Ph
No. +91-44-24437216, Email id: kjsreeram@clri.res.in

Abstract. The value chain of leather is complex and originates from the animal husbandry system to meat processing, pre tanning, tanning, post tanning and product manufacturing processing. The imbibed properties of the material gained from the environmental conditions under which the animal grew to the range of human skills and processing chemicals determines how best the leather products meet the customer desires. The customer desire for feel and handle is ultimately traced back to the origin of the animal itself. Leather thus is a unique product whose properties such as visco-elasticity, breathability etc. remained unmatched by synthetics. Industrialization activities, reduced farming, the vegan culture all have contributed to reduced availability of hides and skins for meeting the quantity of leather required for various end products. This in essence contributed to the growth of a new market for synthetics, wherein the manmade fabrics tried to reproduce all the features of leather, synthetically. Commercially, these products came to be known through various names such as leatherette, faux leather, vegan leather, PU leather, pleather etc. Advancement in material science led to a range of products and manufacturing methods has today ensured that conventional identification techniques such as rough edges, imperfect surfaces, wrinkle test, water absorption, burnability, uneven stitch holes, structure retention, smell, grain pattern can no longer be used to distinguish between leather and similar artificial products. Advancement in technology for the manufacture of various types of leather like materials has made it difficult to identify genuine leather from other leather like materials. With leather like materials meeting most of the conventional methods of identifying genuine leather there is today a need for a new methodology for identifying genuine leather. This paper addresses to a study of a statistically relevant number of samples of leather and non-leather materials through a range of iterative instrumental techniques leading to the establishment of a protocol for identification of genuine leather. The methodology starts with the FTIR-ATR based (non-destructive) identification of signature bands of collagen – the amide I, II and III. After the first level screening, iterative analysis of samples that have the amide bands matching with that of collagen would be screened through techniques such as hydroxyproline estimation, thermogravimetric analysis, fibre structure assessment etc. The paper would report the results, the positives and negatives associated with the first level screening for genuine leather using FTIR.

1 Introduction

In recent years, synthetic leather has seen major improvements as they become more comparable to genuine leathers. Synthetic leather is dyed and treated to make it look and feel like a real leather. These synthetic leathers are less expensive and do not require a tedious process for the manufacturing, since genuine leather has to go through many processes before reaching the final product. It's not easy to differentiate between a genuine leather product and a synthetic leather product. Nowadays the genuine leather is slowly occupied by the synthetic leather as upholstery, clothing and fabric. So the identification of leather genuinity becomes essential.

Leather is made from raw hide by tanning process. The tanning process makes the leather durable and flexible. Tanning process keeps the protein fibre (collagen) intact. The making of leather from raw skin is considered to be time and money consuming process.

Synthetic leather, which is a polymer (Poly Urethane or Poly Vinyl Carbonate) based product. The feel and look of synthetic leather resemble to that of original leather. These synthetic leather are marketed in various names like leatherette, faux leather, vegan leather, PU leather and pleather.

The leather whose protein fibre is kept intact is differentiated by the marker collagen. Collagen is found in our various types of connective tissues such as cartilage, tendons, bones, and ligaments. There are about 30 types of collagen present in the body of a mammal. Every collagen type consists

of three polypeptide chains, each one composed of at least one Gly-X-Y sequence structured in left-handed α -like helices and where the X and Y positions are often proline and hydroxyproline, respectively. In the skin of mammals the type I collagen is present in abundance. Both destructive and non-destructive methods to identify the leather genuinity is scanty. Determination of nitrogen content in leather is a destructive method. In recent trends, the sophisticated instruments like Scanning Electron Microscopy (SEM), Transmission Electron Microscopy (TEM), and Fourier Transform Infrared spectroscopy (FT-IR) are used in identification leather matrix and some salient feature of leather which is said to be a non-destructive method.

This study focuses on the non-destructive techniques for confirming the genuinity of the leather with some of its markers like collagen, using some latest available sophisticated instruments like FT-IR-ATR, FT-IR-imaging, and FT-Raman. To pick the signature characters of the marker collagen, and to compare these signals with the synthetic.

2 Material and methods

FTIR a non-destructive technique considered to a major tool for differentiating the leather from synthetic leather. The collagen marked peaks of amide I, II and III at 1600 cm^{-1} (C=O), 1525 cm^{-1} (CH₂), 1400 , 1300 , 1200 cm^{-1} (C-N and N-H) respectively. The synthetic leathers which are considered to be the polymer based product the collagen (protein fibre) and its significant IR absorption are expected to be absent. Collagen was considered to be a marker for the identification of the leather. The FTIR Analysis was performed using JASCO 4700 series(Japan) IR Spectrophotometer using the ATR mode. The crystal used is ZnSe. ZnSe has a Refractive Index of 2.4; long wavelength cut off of $525\text{ }\mu\text{m}$, Depth of penetration in microns@ 1000 cm^{-1} of 2.0 and the working pH range of 5-9. Pure Reference Type I Collagen was obtained from Sigma-Aldrich. Hide powder was purchased from BLC international. Finished leather was collected from various species and different tanneries was collected and analyzed. Synthetic leather was collected from Hong Kong fare. Several polymer-based materials(synthetic leathers)like PU, PVC, etc., were analyzed.

3 Results and Discussion

FTIR spectrum of collagen (Fig.1) the signatory amide peaks and its wavenumber (cm^{-1}) was noted down. The C=O stretch at 1627 cm^{-1} (amide I) and the CH₂ bending at 1547 cm^{-1} (amide II)and the cluster of peaks at $1451,1336,1234\text{ cm}^{-1}$ (amide III) were also found in the collagen reference materials. Leather (Fig.5-a)and hide powder (purest form of leather) IR spectrum(fig.2 &3) was compared with the reference IR spectrum of Type I collagen. It was found that the signatory peak of amide I, II, III was found in both the leather and hide powder. The IR spectrum of the leather had a wavenumber shift of 2 cm^{-1} to 5 cm^{-1} because of the interference of the chemical that was used for finishing. The hide had a good match to that of collagen standard.

Synthetic leather(Fig.5-b) which was similar in look to that of leather was taken for the IR analysis. Its spectrum (Fig.4) failed to show any of the signatory amide peaks. This gives a clear intimation of differentiating synthetic leather from a original leather.

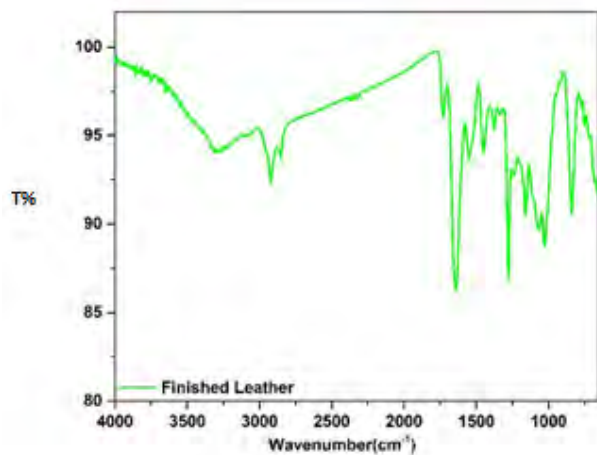


Fig. 1. IR spectrum of Type I collagen.

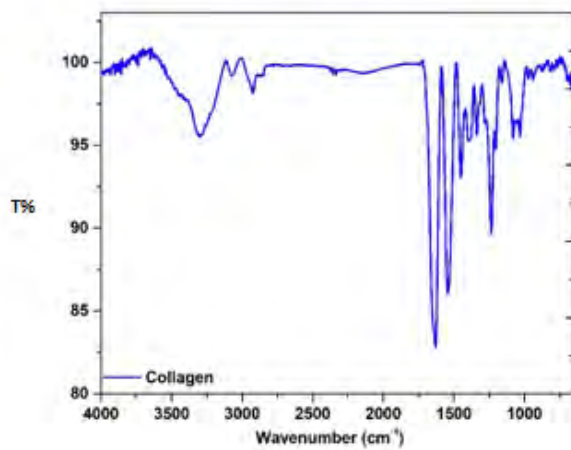


Fig. 2. IR spectrum of Finished leather.

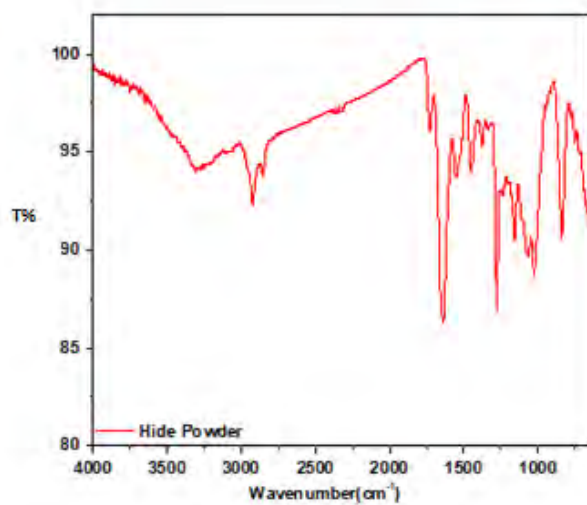


Fig. 3. IR spectrum of Hide powder.

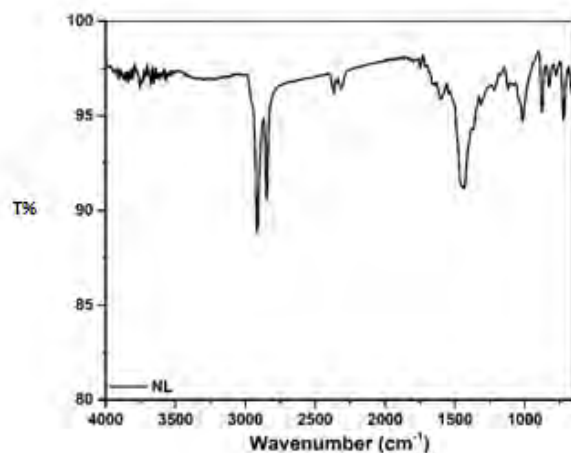


Fig. 4. IR Spectrum of Synthetic leather.

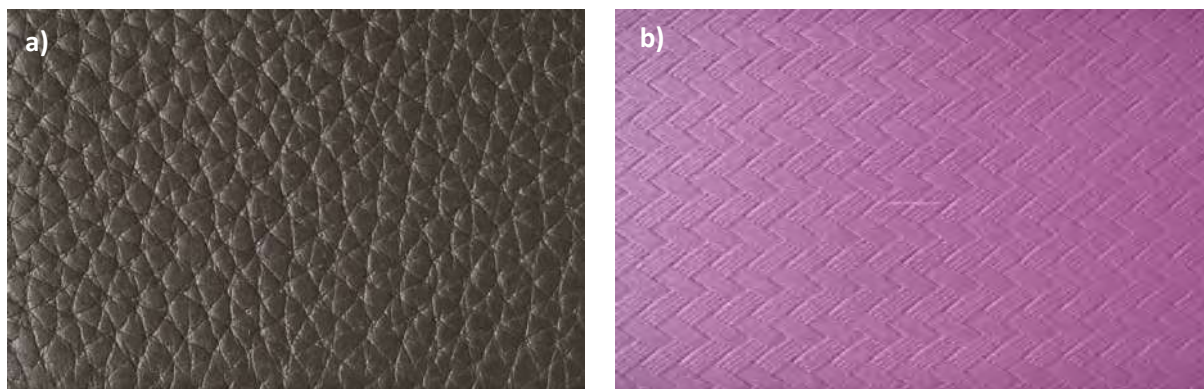


Fig. 5. a) Genuine leather b) Synthetic Leather.

4 Conclusion

FTIR-ATR helped in screening 30% of leather from that of leather like material by utilizing the characteristic features of collagen. Further studies are required to distinguish materials carrying collagen products (composites based on hydrolysates) from genuine leather.

Reference

1. Alejandro Heredia, Maria Colin-Garcia, Miguel A. Peña-Rico⁴, Luis F. L. Aguirre Beltrán, José Grácio, Flavio F. Contreras-Torres, Andrés Rodríguez-Galván, Lauro Bucio⁴, Vladimir A. Basiuk¹ "Thermal, infrared spectroscopy and molecular modeling characterization of bone: An insight in the apatite-collagen type I interaction" *Advances in Biological Chemistry*, 2013, 3, 215-223
2. R. Cantero, J. R. Riba, T. Canals, L. L. Izquierdo and H. Iturriaga "Characterization of leather finishing by ir spectroscopy and canonical variate analysis" *Journal of the Society of Leather Technologists and Chemists*,. 93 p.12.
3. Stamatis C. Boyatzis¹, Marina Kehagia¹, Katerina Malea "Evaluation of Effectiveness of Tanned Leather Cleaning with SEM-EDX and FTIR Spectroscopy" *Analytical Bioanalytical Chemistry*
4. Elshahat H.A.Nashy Osama Osman³ Abdel AzizMahmoud³ MedhatIbrahim "Molecular spectroscopic study for suggested mechanism of chrome tanned leather" *Spectrochimica Acta Part A: Molecular and Biomolecular Spectroscopy* 88, 2012, 171-176.

SOME COMPARISONS OF THERMAL ENERGY CONSUMPTION IN A TEMPERATE VERSUS A SUBTROPICAL ZONE

J. Buljan¹, M. Bosnić² and I. Král'³

1) Mlinovi 62; 10000 Zagreb, Croatia; 2) A. Starčevića 17a/IV, 23000 Zadar, Croatia; 3) United Nations Industrial Development Organization, Wagrammerstrasse 5, P.O.Box 300, 1220 Vienna, Austria

a) Corresponding author: buljan.jakov@gmail.com

b) mladen.bosnis@zd.ht.hr

c) i.kral@unido.org

Abstract. Due to different ambient temperatures many would expect that the overall thermal energy consumption in a tannery in a hot climate zone is considerably lower than in a temperate zone. In reality it is somewhat more complex and worth comparing. The aim of this desk study is to compare consumption of thermal energy in temperate vs. (sub)tropical climate for two representative processes: float heating (bating and dyeing) and chamber drying, with the view of contributing towards overall assessment of thermal energy consumption for tanneries operating under rather different conditions. The energy consumption is calculated for 1 t of wet salted hides and assuming that 1000 kg of wet salted weight corresponds to 1100 kg of pelt weight containing 838 kg of water and 262 kg of collagen subsequently segregated into grain leather and usable splits. Float rates (200% on pelt/shaved weight), average inlet water temperatures (15 oC vs. 25 oC), process float temperatures for bating (35 oC) and dyeing (60 oC) have been defined. Similarly, for computation of thermal energy for chamber drying, identical initial (45 %) and target leather humidity (20 %) are set and average respective fresh air temperature (15 oC vs. 30 oC) and fresh air relative humidity (50% vs. 70%) estimated and operating conditions such as exhaust air temperature and relative humidity defined. Based on such parameters and assumptions, specific ratios for thermal energy consumption for float heating (bating & dyeing) and for chamber drying have been calculated and comparisons made; the results might not quite coincide with common perceptions. The energy needs computed are net amounts, i.e. regardless of the source and without taking into account any losses and disregarding energy consumption for ambient heating and/or cooling. Thus, the total energy needs are much higher. The ratios computed for grain leather are valid for split leather as well. However, if the solar energy is used to support water heating, the conditions in the tropic zone are substantially more favourable, due to higher insolation and higher efficiency factor (i.e. difference of the final vs. inlet water temperature). In any case, two very important factors, (i) temperature and (ii) humidity of inlet air are often overlooked in estimation of energy required for the crust and/or leather drying.

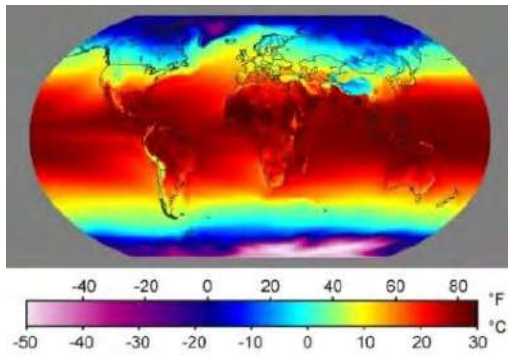


Fig. 1. World climate zones – annual mean temperatures (Source: <http://www.wattsupwiththat.com>)

The baseline data and/or assumptions:

The energy consumption is calculated for 1 t of wet salted hides and assuming that 1000 kg of wet salted weight corresponds to 1100 kg of pelt weight and 262 kg of grain leather and 88 kg of usable splits.

1 Float Heating

1.1 Temperate zone

1.1.1 Bating

Limed (pelt) weight: $G = 1100$ kg, the water being 838 kg, leather substance (collagen) 262 kg

Float 200%

$G = 2200$ litres = 2200 kg

Inlet water temperature:

$tw = 15$ oC

Process float temperature $t_f = 35$ °C
 Dry leather specific heat capacity: $c_l = 1.5$ kJ/kg/°C
 Water specific heat capacity: $c_w = 4.1814$ kJ/kg/°C

The thermal energy necessary to heat the water for the bating float:
 $Q_{\text{bating, float}} = G * c * (t_f - t_w) = 2200 * 4.1814 * (35 - 15) = 2200 * 4.1814 * 20 = 184000$ kJ
 The thermal energy necessary to warm the pelt:
 $Q_{\text{bating, pelt}} = G * c * (t_f - t_w) = 262 * 1.5 * (35 - 15) = 262 * 1.5 * 20 = 7860$ kJ
 The thermal energy necessary to heat the water contained in the pelt:
 $Q_{\text{bating, water in pelt}} = G * c * (t_f - t_w) = 838 * 4.1814 * (35 - 15) = 838 * 4.1814 * 20 = 70080$ kJ
 $Q_{\text{bating total}} = 184000 + 7860 + 70080 = 261940$ kJ = 262 MJ/t wet salted hides

1.1.2 Dyeing, fatliquoring

Shaved weight, grain: $G = 262$ kg containing about 130 kg of water, leather substance (collagen) 132 kg
 Float 200%: $G = 524$ litres = 524 kg
 Inlet water temperature: $t_w = 15$ °C
 Process float temperature: $t_f = 60$ °C
 Dry leather specific heat capacity: $c_l = 1.5$ kJ/kg/°C
 Water specific heat capacity: $c_w = 4.1814$ kJ/kg/°C

The thermal energy necessary to heat the water for the dyeing and fatliquoring float:
 $Q_{\text{dyeing, float}} = G * c * (t_f - t_w) = 524 * 4.1814 * (60 - 15) = 524 * 4.1814 * 45 = 98600$ kJ
 The thermal energy necessary to heat the leather:
 $Q_{\text{dyeing, leather}} = 132 * c * (t_f - t_w) = 132 * 1.5 * (60 - 15) = 132 * 1.5 * 45 = 8910$ kJ
 The thermal energy necessary to heat the water contained in the leather:
 $Q_{\text{dyeing, water in leather}} = 130 * c * (t_f - t_w) = 130 * 4.1814 * (60 - 15) = 130 * 4.1814 * 45 = 24460$ kJ
 $Q_{\text{dyeing, total}} = 98600$ kJ + 8910 kJ + 24460 kJ = 132 MJ/ t wet salted hides

1.2 Subtropical zone

1.2.1 Bating

Limed (pelt) weight: $G = 1100$ kg, the water being 838 kg, collagen 262 kg
 Float 200% $G = 2200$ litres = 2200 kg
 Inlet water temperature: $t_w = 25$ °C
 Process float temperature $t_f = 35$ °C
 Dry leather specific heat capacity: $c_l = 1.5$ kJ/kg/°C
 Water specific heat capacity: $c_w = 4.1814$ kJ/kg/°C

The thermal energy necessary to heat the water necessary for the bating float:
 $Q_{\text{bating, float}} = G * c * (t_f - t_w) = 2200 * 4.1814 * (35 - 25) = 2200 * 4.1814 * 10 = 92000$ kJ
 The thermal energy necessary to warm the pelt:
 $Q_{\text{bating, pelt}} = G * c * (t_f - t_w) = 262 * 1.5 * (35 - 25) = 262 * 1.5 * 10 = 3930$ kJ
 The thermal energy necessary to heat the water contained in the pelt:
 $Q_{\text{bating, water in leather}} = G * c * (t_f - t_w) = 838 * 4.1814 * (35 - 25) = 838 * 4.1814 * 10 = 35040$ kJ
 $Q_{\text{bating total}} = 131$ MJ/t wet salted hides

1.2.2 Dyeing, fatliquoring

Shaved weight, grain: $G = 262$ kg containing about 130 kg of water, leather substance (collagen) 132 kg
 Float 200%: $G = 524$ litres = 524 kg

Inlet water temperature: $t_w = 25\text{ }^\circ\text{C}$
 Process temperature $t_f = 60\text{ }^\circ\text{C}$
 Dry leather specific heat capacity: $c_l = 1.5\text{ kJ/kg/}^\circ\text{C}$
 Water specific heat capacity: $c_w = 4.1814\text{ kJ/kg/}^\circ\text{C}$

The thermal energy necessary to heat the water for the dyeing and fatliquoring float:

$$Q_{\text{dyeing, float}} = G * c * (t_f - t_w) = 524 * 4.1814 (60 - 25) = 524 * 4.1814 * 35 = \mathbf{76700\text{ KJ}}$$

The thermal energy necessary to heat the leather for dyeing and fatliquoring:

$$Q_{\text{dyeing, leather}} = G * c * (t_f - t_w) = 132 * 1.5 * (60 - 25) = 132 * 1.5 * 35 = \mathbf{6930\text{ kJ}}$$

The thermal energy necessary to heat the water contained in the leather for dyeing and fatliquoring:

$$Q_{\text{dyeing, water in leather}} = G * c * (t_f - t_w) = 130 * 4.1814 * (60 - 25) = 130 * 4.1814 * 35 = \mathbf{19025\text{ kJ}}$$

$$Q_{\text{dyeing, total}} = 102.6\text{ MJ/t wet salted hides}$$

2 Leather Drying

As said earlier, the energy consumption is calculated for the input of 1 t of wet salted hides giving 262 kg of grain leather and 88 kg of usable splits; it is also assumed that both in temperate and hot climate the leather humidity before drying is 45 % and after drying 20 %.

Thus, the base values for grain leather are:

Dry leather substance in 262 kg of wet leather:

$$262 * 0.55 = 144.1\text{ kg of dry leather}$$

$$\text{Water content in the leather before drying: } 262 - 144.1 = 117.9\text{ kg}$$

$$\text{Dried leather weight with 20 \% humidity: } 144.1/0.8 = 180.1\text{ kg}$$

$$\text{Water content in the dried leather: } 180.1 - 144.1 = 36.0\text{ kg}$$

$$\text{Water evaporated: } 262 - 180.1 = \mathbf{81.9\text{ kg}}$$

2.1. Temperate zone

The necessary data for the humid air are taken from the hx diagram and tables for humid air.

$$\text{Fresh air temperature: } t_f = 15\text{ }^\circ\text{C}$$

$$\text{Fresh air relative humidity: } \varphi_f = 50\text{ \%}$$

$$\text{Fresh air absolute humidity: } x_f = 0.005\text{ kg H}_2\text{O/kg dry air}$$

$$\text{Fresh (humid) air enthalpy: } h_f = 28\text{ kJ/kg dry air}$$

$$\text{Volume of fresh air: } v_f = 0.833\text{ m}^3/\text{kg humid air}$$

$$\text{Exhaust air, temperature: } t_e = 60\text{ }^\circ\text{C}$$

$$\text{Exhaust air, relative humidity: } \varphi_e = 90\text{ \%}$$

$$\text{Exhaust air, absolute humidity: } x_e = 0.135\text{ kg H}_2\text{O/kg dry air}$$

$$\text{Exhaust (humid) air, enthalpy: } h_e = 415\text{ kJ/kg dry air}$$

$$\text{Volume of humid exhaust air: } 1.16\text{ m}^3/\text{kg humid air}$$

The air capacity to absorb the evaporated water from wet leather:

$$x_e - x_f = 0.135 - 0.005 = 0.130\text{ kg H}_2\text{O/kg dry air}$$

Theoretic quantity of the air (expressed as dry air) needed to absorb the evaporated water:

$$81.9/0.130 = 630\text{ kg of dry air}$$

$$\text{The volume of fresh air needed: } 630 * 0.833 = \mathbf{525\text{ m}^3}$$

The specific thermal energy necessary for water evaporation from the wet leather and air heating:

$$\Delta h = h_e - h_f = 415 - 28 = 387\text{ kJ/kg dry air: } 630 * 387 = 243810\text{ kJ} = \mathbf{243.8\text{ MJ}}$$

$$\text{Dry leather specific heat capacity: } c_l = 1.5\text{ kJ/kg/}^\circ\text{C}$$

$$\text{Water specific heat capacity: } c_w = 4.1814\text{ kJ/kg/}^\circ\text{C}$$

The heat (energy) necessary to heat the leather from the ambient temperature (15 °C) to outlet temperature (60 °C) :

fully dry leather: $144.1 * 1.5 * (60 - 15) = 144.1 * 1.5 * 45 = 9726.8 \text{ kJ} = \mathbf{9.73 \text{ MJ}}$

remaining humidity in dried leather: $36 * 4.1814 * 45 = 6774 \text{ kJ} = \mathbf{6.77 \text{ MJ}}$

The heat (energy) necessary for leather heating (15 - 60°C): $9.73 + 6.77 = \mathbf{16.5 \text{ MJ}}$

The net amount of thermal energy needed to dry leather: $243.8 + 16.5 = \mathbf{260.3 \text{ MJ}}$

2.2 Subtropical zone

2.2.1 Average air temperature 30 oC, relative humidity 70%

The necessary data for the humid air are taken from the hx diagram and tables for the humid air.

Fresh air temperature: $t_f = 30 \text{ °C}$

Fresh air relative humidity: $\varphi_f = 70 \%$

Fresh air absolute humidity: $x_f = 0.019 \text{ kg H}_2\text{O/kg of dry air}$

Fresh (humid) air enthalpy: $h_f = 76 \text{ kJ/kg of dry air}$

Volume of fresh air: $v_f = 0.895 \text{ m}^3/\text{kg}$

Exhaust air, temperature: $t_e = 60 \text{ °C}$

Exhaust air, relative humidity: $\varphi_e = 90 \%$

Exhaust air, absolute humidity: $x_e = 0.135 \text{ kg H}_2\text{O/kg of dry air}$

Exhaust air, enthalpy: $h_e = 415 \text{ kJ/kg of dry air}$

Volume of exhaust air: $1.16 \text{ m}^3/\text{kg of air}$

The capacity to absorb evaporated water: $x_e - x_f = 0.135 - 0.019 = 0.116 \text{ kg H}_2\text{O/kg of dry air}$

The theoretical quantity of air (expressed as dry air) needed to absorb the evaporated water:

$81.9/0.116 = 706 \text{ kg of dry air}$

The volume of fresh air needed: $706 * 0.895 = \mathbf{632 \text{ m}^3}$

The specific thermal energy necessary for the evaporation of the water from the wet leather and air heating:

$\Delta h = h_e - h_f = 415 - 76 = 339 \text{ kJ/kg dry air}; 706 * 339 = 239346 \text{ kJ} = \mathbf{239.3 \text{ MJ}}$

Dry leather specific heat capacity: $c_l = 1.5 \text{ kJ/kg/°C}$

Water specific heat capacity: $c_w = 4.1814 \text{ kJ/kg/°C}$

The heat (energy) necessary to heat the leather from the ambient temperature (30°C) to outlet temperature (60°C):

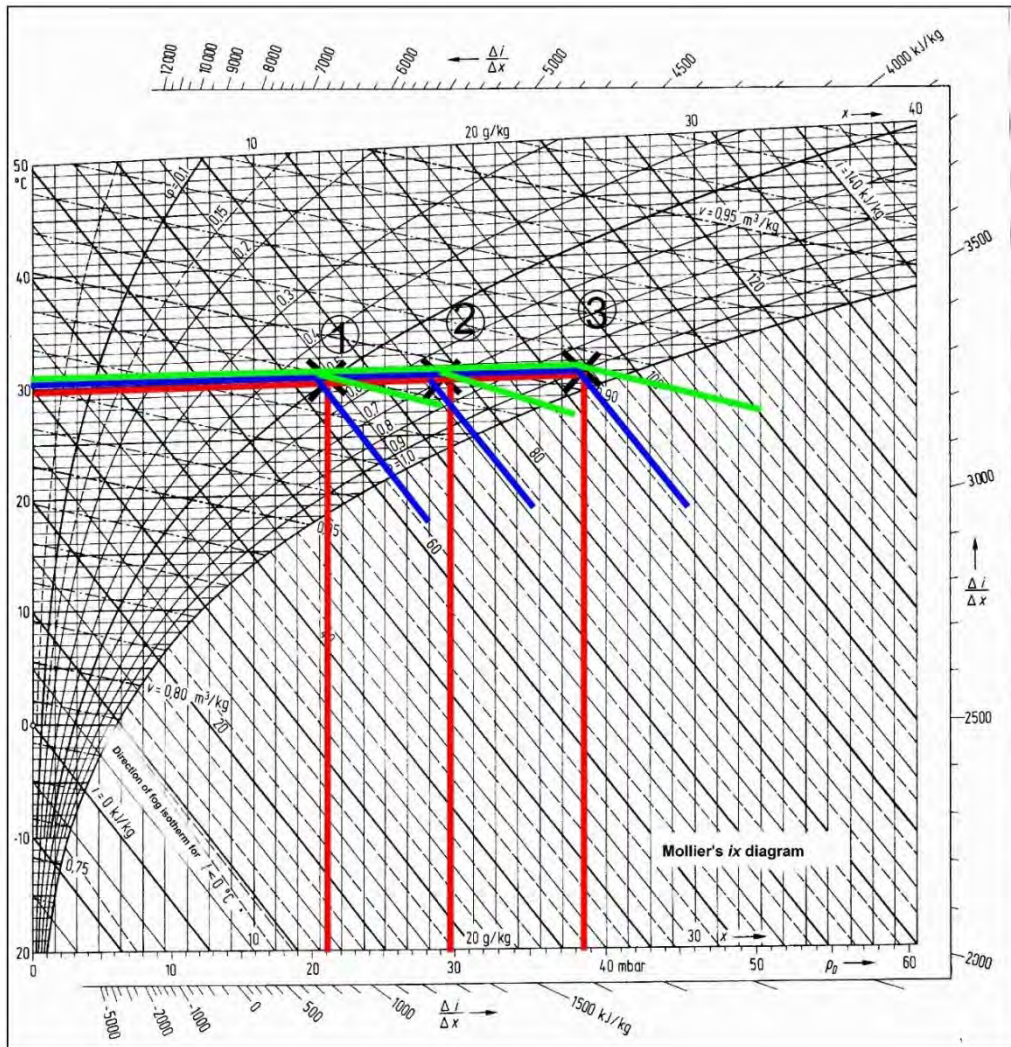
fully dry leather: $144.1 * 1.5 * (60 - 30) = 144.1 * 1.5 * 30 = 6484 \text{ kJ} = \mathbf{6.5 \text{ MJ}}$

the remaining humidity in dried leather: $36 * 4.1814 * 30 = 4516 \text{ kJ} = \mathbf{4.5 \text{ MJ}}$

The heat (energy) necessary for leather heating (30 - 60 °C): $6.5 + 4.5 = \mathbf{11.0 \text{ MJ}}$

The net amount of thermal energy needed to dry leather: $239.3 + 11.0 = \mathbf{250.3 \text{ MJ}}$

Water vapour with molecular mass of 18.04 g/mol is lighter than dry air ($\approx 29 \text{ g/mol}$). Thus, the increase of water vapour content (humidity) results in lower air density because of Avogadro's law, which states "equal volumes of all gases, at the same temperature and pressure, have the same number of molecules." The higher number of water vapour molecules, the lower number of (heavier) air molecules.



1. Fresh Air 30°C, 50 % relative humidity

- Fresh air, absolute humidity 0.0135 kg H₂O/kg of dry air
- Enthalpy of fresh (humid) air 65 kJ/kg of dry air
- Volume of fresh air 0.890 m³/kg

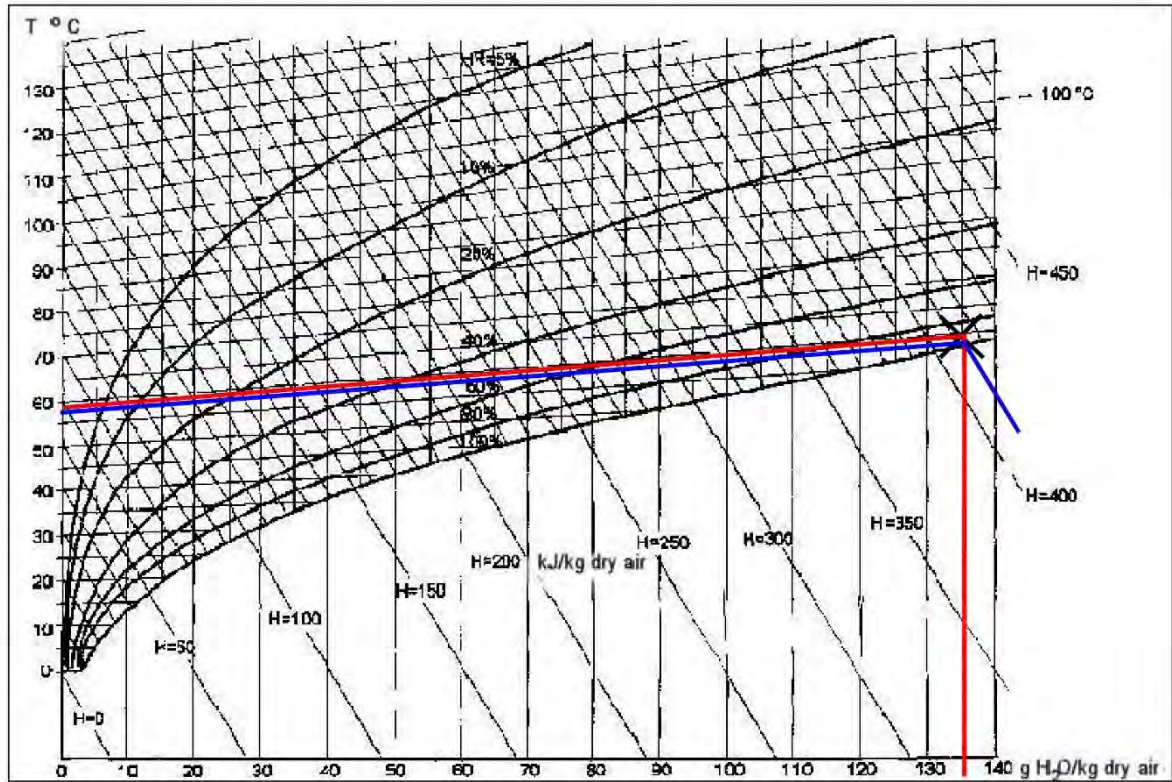
2. Fresh Air 30°C, 70 % relative humidity

- Fresh air, absolute humidity 0.019 kg H₂O/kg of dry air
- Enthalpy of fresh (humid) air 76 kJ/kg of dry air
- Volume of fresh air 0.895 m³/kg

3. Fresh Air 30°C, 90 % relative humidity

- Fresh air, absolute humidity 0.025 kg H₂O/kg of dry air
- Enthalpy of fresh (humid) air 93 kJ/kg of dry air
- Volume of fresh air 0.900 m³/kg

Fig. 2. The main parameters of wet air (Mollier's diagram) – subtropical zone (Chart reading by M. Bosnić)



— Exhaust air, absolute humidity 0.135 kg H₂O/kg of dry air
— Exhaust air, enthalpy 415 kJ/kg of dry air

Fig. 3. The main parameters of wet (exhaust) air – 60 °C, relative humidity 90 % (Chart reading by M. Bosnić)

The following table contains a summary of data and the corresponding computations.

Table 1. Comparative overview of thermal energy needs for leather drying for different ambient temperatures and air humidity

Parameter	Ambient/inlet air temperatures and humidity			
	Temperate zone	Subtropical zone		
Fresh air temperature, t_f	15 °C	30 °C	30 °C	30 °C
Fresh air relative humidity, φ_f	50 %	50 %	70 %	90 %
Fresh air absolute humidity, x_f , kg H ₂ O/kg of dry air	0.005	0.0135	0.019	0.025
Fresh (humid) air enthalpy, h_f , kJ/kg of dry air	28	65	76	93
Volume of fresh air, v_f , m ³ /kg	0.833	0.890	0.895	0.900
Exhaust air, temperature, t_e	60 °C	60 °C	60 °C	60 °C
Exhaust air, relative humidity, φ_e	90 %	90 %	90 %	90 %
Exhaust air, absolute humidity, x_e , kg H ₂ O/kg of dry air	0.135	0.135	0.135	0.135
Exhaust air, enthalpy, h_e , kJ/kg of dry air	415	415	415	415
Volume of exhaust air, m ³ /kg of air	1.16	1.16	1.16	1.16
The capacity to absorb water, $x_e - x_f$, kg H ₂ O/kg of dry air	0.130	0.1215	0.116	0.110

Parameter	Ambient/inlet air temperatures and humidity			
	Temperate zone	Subtropical zone		
The theoretical quantity of air needed (expressed as dry air), kg of dry air	630 kg	674 kg	706 kg	745 kg
Thermal energy needed for water evaporation, $\Delta h = h_e - h_f$	243.8	236 MJ	239.3 MJ	240 MJ
The volume of fresh (humid) air needed	525 m ³	600 m ³	632 m ³	671 m ³
Dry leather specific heat capacity, kJ/kg/°C	$c_l = 1.5$	$c_l = 1.5$	$c_l = 1.5$	$c_l = 1.5$
Water specific heat capacity, kJ/kg/°C	$c_w = 4.18$	$c_w = 4.18$	$c_w = 4.18$	$c_w = 4.18$
The energy needed to heat the leather from the ambient to the outlet temperature of 60 °C and humidity 20 %:				
- fully dry leather	9.73 MJ	6.5 MJ	6.5 MJ	6.5 MJ
- the remaining humidity in leather	6.77 MJ	4.5 MJ	4.5 MJ	4.5 MJ
The energy needed for leather heating	16.5 MJ	11.0 MJ	11.0 MJ	11.0 MJ
The total amount of thermal energy needed to dry leather	260.3 MJ	247.0 MJ	250.3 MJ	251.0 MJ

3 The comparison of net thermal energy needs

3.1 Float heating

3.1.1 Bating

$Q_{\text{bating total subtropical zone}} = 131 \text{ MJ/t of wet salted hides}$
 $Q_{\text{bating total temperate zone}} = 262 \text{ MJ/t of wet salted hides}$
 Ratio: $131/262 = 50 \% \text{ or } 1: 2$

3.1.2. Dyeing, fatliquoring

$Q_{\text{dyeing total, subtropical zone}} = 103 \text{ MJ/t of wet salted hides}$
 $Q_{\text{dyeing, fatliquoring total, temperate zone}} = 132 \text{ MJ/ of wet salted hides}$
 Ratio: $103/132 = 0.78 = 78 \% \text{ i.e. nearly } 20 \% \text{ less}$

Table 2. The comparison of net thermal energy needs for chamber drying

	Ambient/inlet air temperatures and humidity			
	Temperate zone	Subtropical zone		
		15 °C, 50 %	30 °C, 50 %	30 °C, 70 %
The total thermal energy needed to dry leather	260.3 MJ	247.0 MJ	250.3 MJ	251.0 MJ
The ratio subtropical vs. temperate climate	-	95 %	96.2 %	96.4%
The volume of fresh air needed, m ³ /t of w. s. hides	525 m ³	600 m ³	632 m ³	670 m ³
The ratio subtropical vs. temperate climate	-	114 %	120 %	128 %

The energy needs computed here are net amounts, i.e. regardless of the source and without taking into account any losses. Thus, the total energy needs are much higher. The ratios computed for grain leather are valid for split leather as well.



Fig. 4. A pole-drying tunnel (Source: Demaksan)

4 Conclusions

A simple computation based on estimated average yearly fresh water and air (ambient) temperatures shows that the amount of net thermal energy needed for heating the float in (sub)tropical zone (South India) is from 20% (dyeing) to about 50 % (bating) of that in the temperate zone (Middle Europe).

Chamber drying in (sub)tropical zone benefits from the higher ambient (air) temperature but at the same time it is negatively affected by high relative humidity and consequently much higher volume of fresh air required. However, the fact that the energy required for water evaporation¹ does not change much with water temperature ultimately prevails over parameters such as ambient (air) temperature and air humidity. Accordingly, energy consumption for chamber drying in (sub)tropical zone with average air temperature of 30°C and relative humidity in the span of 50-90 % is only about 5 % less than in the temperate zone.

However, if the solar energy is used to support water heating, the conditions in the tropic zone are substantially more favourable, due to two factors:

- insolation
- efficiency factor (depends on the temperature difference of the *final vs. inlet water temperature*)

The insolation in the temperate zone (Europe) is approx. 1500 kWh/m²/y (4.1 kWh/m²/d), and in the tropical zone (South India) approx. 2200 kWh/m²/y (6.0 kWh/m²/d), so that the factor of proportionality is 1.5. Since the efficiency ratio case can be estimated as 1.05 it means that the solar based production of thermal energy in a hot climate country is about 1.6 times more favourable than in temperate climate.

¹ The **(latent) heat of vaporization** is the amount of energy (enthalpy) that must be added to a liquid substance to transform a quantity of that substance into a gas. The enthalpy of vaporization is a function of the pressure at which that transformation takes place.

References

1. *Energieeinsatz in der Lederindustrie*, Pfisterer H, *Bibliothek des Leders*, Band 9, 1986
2. *Tehnologija kože i krzna*, Grgurić H, Vuković T, Bajza Ž, 1985
3. *Nauka o toplini (Heat science -Thermodynamics)*, F. Bošnjaković, *Tehnička knjiga Zagreb*, July 1986

THE USE OF NATURAL PRODUCTS IN THE LEATHER INDUSTRY: DEPILATION WITHOUT DAMAGE

Y. Tu^{1,2*}, M. Ahn^{1,2}, M. L. Patchett¹, R. Naffa², D. Gagic¹, and G. E. Norris¹

1 School of Fundamental Sciences, Massey University, Colombo Road, Palmerston North 4442, New Zealand

2 Leather and Shoe Research Association of New Zealand, P.O. Box 8094, Palmerston North 4410, New Zealand

*Corresponding author: Y.H.Tu@massey.ac.nz

Abstract. Sheepskin, a by-product of the meat industry, is often processed to leather and used for fashion items including jackets, coats and gloves. Where the tanneries are distant from the abattoirs and freezing works, the raw skins have to be transported long distances to be processed and in warm weather, there is the potential for putrefaction of the skins which are then of no commercial value. Before they can be tanned, the wool is removed by a process that traditionally uses strong alkali and sulfides both of which are environmentally unfriendly. We have found a natural product that prevents putrefaction, preserving the skin for days at room temperature. In addition, it allows easy removal of the wool from the skin, eliminating a need for most of the beamhouse processes that produce toxic waste.

1 Introduction

The chemicals used in the pre-tanning processes are significant contributors to environmental pollution.¹ Large quantities of both solid and liquid waste are produced during various pre-tanning processes, with one-third of the pollution produced from the leather industry being due to the sulfide and alkaline water waste from the depilation process.²⁻³ Conventional depilation and collagen fibre-opening processes for sheep skins require painting a thick solution containing calcium or sodium hydroxide and sodium sulfide, on the flesh side of the pelt which allows the wool to be mechanically removed from the skin.⁴ The chemicals are removed by washing the depilated skins with copious volumes of water which then has to be treated before it can be fed into the waste stream. As environmental compliance becomes more demanding such processes will place a significant financial burden on tanneries and the industry.⁵

To address this problem, research efforts have been aimed to depilate skins using enzymes as these are recyclable and environmentally friendly. Various enzymes, such as keratinases, proteases and lipases have been shown to successfully remove hair from skin, but usually damage it.⁶⁻⁹ Furthermore, in some cases, the addition of sulfide to the enzyme mixture is necessary to provide depilation efficiency.¹⁰ Hence, at present, although significant advances have been made, the use of enzymes has not been effective on an industrial scale.

We have found a natural product that when incubated with fresh sheepskin prevents putrefaction and preserves the skin for up to five days at room temperature (20 °C). In addition, it allows easy removal of the wool from the skin through gentle thumb pressure. Microscopic examination of the depilated product showed no sign of damage to the surface of the skin. This innovative procedure not only depilates, but also preserves the skins over the time required for transport or processing. This paper describes the progress that has been made to understand the science behind this phenomenon and to compare the properties of skins depilated using this method with those depilated using the traditional beamhouse process.

2 Materials and Methods

2.1 Natural product survey

All fresh sheepskin was obtained with the help of New Zealand Leather and Shoe Research Association (LASRA). Unwashed skins were cut into 20 cm x 6 cm sections using a sterile scalpel blade. These were then placed in sterilised sealed containers before being submerged in sufficient volume of sterilised natural product to ensure the wool was completely covered. The process of depilation was followed by monitoring the pH of the liquid, the smell, the condition of the skin and the ease of depilation twice a day until the wool could be removed from the skin with gentle thumb pressure. Controls included sterile water, water at pH 4.0 and water that was maintained at pH 4.0 during the experiment.

2.2 Identification of microorganisms that could contribute to the depilation process

To assess whether the microbiome of the depilation liquid was changing throughout the process, samples were taken for identification of the organisms present before and after depilation. It should be noted that in all these experiments, the skin samples were not washed or treated in any way before the experiment.

2.2.1 Isolation of the microorganisms after successful depilation with natural products

One hundred μL of the natural product that was used to incubate and depilate sheepskin were taken and plated on five different nutrient agar plates: Tryptone soya broth (TSB), Luria broth (LB), *Lactobacilli* MRS broth (MRS), malt and fungal minimal growth media (Wilson's media)¹¹ agars. Distinctive colonies were isolated and re-plated on their respective nutrient agar plates.

2.2.2 Identification of the microorganisms isolated from depilation trials

Standard procedures were used to extract microbial genomic DNA¹² from cultures grown from each single colony, which was then subjected to the colony polymerase chain reaction (PCR) using the primers listed in Table 1. The PCR products were purified using ethanol precipitation¹³, then sequenced using a capillary ABI3730 DNA Analyser (ThermoFisher; USA) with the BigDye Sequencing Ready Reaction Mix (ThermoFisher; USA). The results were analysed using the Nucleotide Basic Local Alignment Search Tool (BLASTn); <http://blast.ncbi.nlm.nih.gov/Blast.cgi> online search engine.

Table 1. PCR primer sets for the amplification of the bacterial 16s and fungal 18s rRNA.

Primer name	Sequence	Gene to be amplified	Reference
fd1 rD1	AGAGTTTGATCCTGGCTCAG AAGGAGGTGATCCAGCC	16S rRNA	14
Eub338F Eub518R	ACTCCTACGGGAGGCAGCAG ATTACCGCGGCTGCTGG	16S rRNA	15
nu-SSU-0817 nu-SSU-1196	TTAGCATGGA ATAATRRRAATAGGA TCTGGACCTGGTGAGTTTCC	18S rRNA	16

2.3 Fractionation experiment

To detect any compound that may contribute to the preservation of the skins, the liquid used for depilation was subjected to size fractionation and screened for differences in protein content by denaturing gel electrophoresis (SDS-PAGE). The fractions were also tested for antimicrobial properties using traditional plate assays and ability to depilate sheepskin.

2.3.1 Fractionation of the natural product

The natural product used to successfully depilate skin samples was first passed through a 0.2 µm filter to remove any particulate material, then subjected to sequential ultrafiltration using different molecular weight cut-off (MWCO) membranes (100, 30, 10 and 3 kDa (Millipore; USA)), in a pre-sterilised pressure-based stirred cell (Amicon 8400; USA). Both the filtrate and retentate of each fraction were collected in sterilised bottles and stored at 4 °C before they were analysed by tricine SDS-PAGE. Samples were also tested for antimicrobial activity against a number of different microorganisms. This involved making indicator plates with different bacterial species embedded in the agar forming wells in the plate with a hole cutter, then adding 50 µL of each filtrate or retentate into each well and incubating at 37 °C overnight. Fresh skins were also incubated in each filtrate and retentate fraction to assess their ability to depilate.

2.4 Chemical analysis of the depilated sheepskin

Collagen crosslink and glycosaminoglycan (GAG) analyses were done on sheepskin before and after depilation with product A. Extraction and quantitation of the collagen crosslinks were done as described by Naffa *et al.* (2016).¹⁷ Glycosaminoglycan analyses were done as described by Naffa (2017).¹⁸

2.5 Scanning electron microscopy (SEM) analysis of the depilated sheepskin

Sheepskin samples that were depilated with the natural product were analysed with the FEI Quanta 200 Environmental Scanning Electron Microscope (ThermoFisher; USA) at an accelerating voltage of 20 kV. Samples were dried to critical point using liquid CO₂ as the critical point fluid and absolute ethanol as the intermediary with the Polaron E3000 series II (Quorum Technologies; UK) critical point drying apparatus. Samples were then mounted onto aluminium stubs using double sided tape and sputter coated with approximately 100 nm of gold with a Baltec SCD 050 sputter coater (Capovani Brothers Inc.; USA). The surface of the samples was then examined.

3 Results and Discussion

3.1 Natural product A depilates and preserves sheepskin

The results of the depilation experiment with 8 natural products showed that only one sample, named product A, could successfully depilate sheepskin within 3 – 5 days. The skins treated with product A appeared pink in colour, were plump and smelled slightly fermented after depilation, whereas the skin treated with other solutions, appeared grey and had an unpleasant odour due to the onset of putrefaction. A change in the pH of the media during the process was also observed. Product A had an initial pH of 7.0 that continued to drop as the incubation progressed and stabilised when it reached 4.5 at which point, the wool could be easily removed. In contrast, the pH of the other samples increased over the course of the experiment, eventually reaching 7.5 – 8.0.

3.2 Four main microorganisms identified in the media after depilation

The change in the pH and the smell during the process of depilation was indicative of the success of the process (*i.e.* if the pH of the media dropped to 4.5 and smelled slightly fermented and musty, the sheepskin could be successfully depilated). It has been shown that an increased pH in meat is a sign of putrefactive bacterial growth and subsequent product spoilage.¹⁹ This was also seen in our

depilation trials as the increased pH of the media after depilation was concomitant with a rotten smell. The question therefore arises, what is in product A that enables depilation to occur, and at the same time prevents the skins from putrefying. Control experiments showed that skins on their own in acidified water or in pure water putrefy quickly, even at low temperatures. Product A also deteriorates quickly if exposed to the air at room temperature. It is therefore possible that compounds and/or microorganisms in product A combined with those on the skins create an environment that suppresses the growth of putrefying microorganisms while encouraging the growth of others. It is feasible that both produce enzymes responsible for depilation and perhaps other antimicrobial compounds that control the microbiome.

To identify the microorganisms from depilation trials, the liquid after depilation was plated and differences in the colony morphologies of the microorganisms grown on nutrient agar plates were observed. It was not surprising to see a large variety of microorganisms present on the plates swabbed with fresh sheepskin or samples from water incubated with the skin (**Fig. 1**). Product A was also plated before and after the incubation with fresh sheepskin (**Fig.2**). After skin had been incubated with product A, the number of different colonies was drastically reduced to three to four types. The common morphologies are shown in **Fig. 3**.

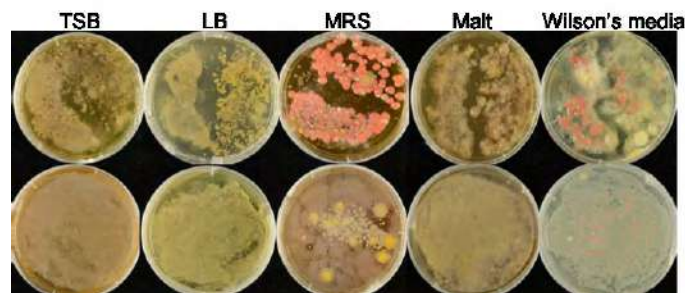


Figure 1. Agar plates that were swabbed with fresh sheepskin (top row) and the H₂O that was incubated with sheepskin (bottom row).

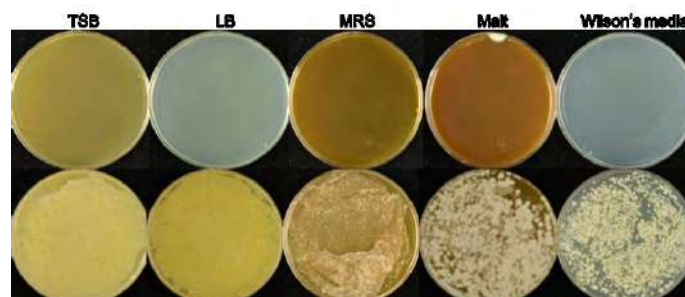


Figure 2. Agar plates spread with sterilised product A (top row) and the liquid that was incubated with sheepskin after depilation (bottom row).

After treatment with product A (Fig. 1-3) the number of colony types decreased significantly, compared to those cultured from the fresh sheepskin. The reason for the apparent survival of only a few species is not yet understood and is part of the investigation of this study. To identify the microorganisms, DNA from the individual colonies were isolated, and used as template to amplify phylogenetic markers encoding 16S rRNA and 18S rRNA genes. The amplicons were subsequently sequenced and analysed using the standard bioinformatic tool NCBI BLASTn. Two dominant fungal and two dominant bacterial species were identified. Out of these, three are known to produce antimicrobial substances, including bacteriocins. It is, therefore, possible that they are responsible for the reduction in the number of microbial species that occurs during depilation.

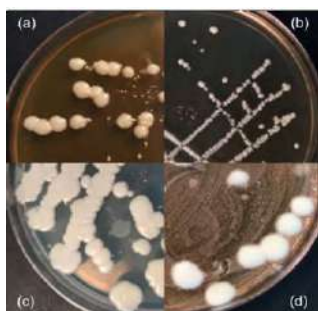


Figure 3. Examples of the common morphologies of microorganisms seen on nutrient agar plates after depilation with product A. (a) cream-coloured large circular colonies (b) cream-coloured small circular colonies (c) cream-coloured irregular-shaped colonies (d) large white fluffy colonies.

Using culture-based methods only the species that grow rapidly under standard laboratory conditions (*i.e.* incubation temperature, types of nutrients in the growth media) can be identified. Hence, it is possible that some of the microorganisms that are involved in this complex interplay between the sheepskin microbiome and product A remain unidentified using these methods. Therefore we used metabarcoding as a culture-independent method to obtain microbial community profiles of the sheepskin before and after depilation alongside that of product A *post* depilation. The sequencing data is currently being analysed through a bioinformatic pipeline.²⁰

3.3 Fractionation of sterilised product A and its depilation effect

All retentate and filtrate fractions were able to depilate sheepskin within 4-5 days without obvious damage to the skin. The pattern of depilation was identical to that observed when unfractionated product A was used; skins depilated in all fractions smelled slightly fermented, and had a pH of 4.5. Furthermore, tricine SDS-PAGE analysis showed that the peptide/protein concentration of all fractions was low and their profile was identical (**Fig. 4**). The protein concentrations of all fractions were around 0.03 to 0.08 mg/mL. As all fractions of retentates and filtrates of product A were able to depilate and preserve sheepskin, it is likely that the antimicrobial substance is contributed by one or more metabolites produced by the bacterial population. A metabolomics analysis of the liquid pre and post depilation will further identify metabolites that have the potential for antimicrobial action.

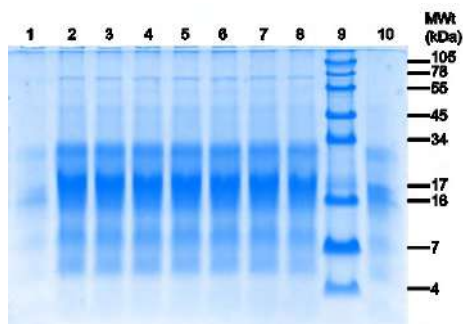


Figure 4. Tricine-SDS gel (16.5 %) of sterilised product A fractions. Lane 1, 100 kDa MWCO retentate; lane 2, 100 kDa MWCO filtrate; lane 3, 30 kDa MWCO retentate; lane 4, 30 kDa MWCO filtrate; lane 5, 10 kDa MWCO retentate; lane 6, 10 kDa MWCO filtrate; lane 7, 3 kDa MWCO retentate; lane 8, 3 kDa MWCO filtrate; lane 9, molecular weight marker; lane 10, sterilised product A filtered through 0.8 um filter.

3.4 Biochemical analysis of the depilated sheepskin reveals differences in the skin molecular composition after depilation with our method

3.4.1 Glycosaminoglycans (GAGs) analysis

Glycosaminoglycans were extracted from three biological samples of raw and sterilised product A depilated sheepskin. Skin 3 appeared to have a significantly higher concentration of GAGs compared to skins 1 and 2, although this difference was attenuated in the depilated skins (**Fig. 5**). The raw sheepskin GAG concentrations were also similar to previous reports.²¹ Although the GAG content of the skins decreased by half after depilation by sterilised product A, they were still 20 times higher than those measured in pickled sheepskin.²¹ Many reports have shown through the processing steps of liming, deliming, bating and then pickling, significant amounts of GAGs are removed.²² Further experiments will show whether this higher concentration of GAGs remaining in the skins has any effect, either beneficial or detrimental on the physical properties of the final leather product.

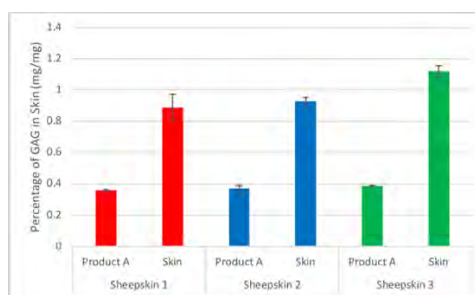


Figure 5. Percentage of sulfated glycosaminoglycan in raw and sterilised product A depilated sheepskin. Error bars represent standard deviation.

3.4.2 Collagen crosslink analysis

Collagen crosslinks were extracted from three biological samples of raw and sterilised product A depilated sheepskin. All skin samples were shown to contain mature collagen crosslinks histidine-hydroxylysinonorleucine (HHL) and histidinohydroxymerodesmosine (HHMD), and immature crosslinks hydroxylysinonorleucine (HLNL) and dihydroxylysinonorleucine (DHLNL). The ratio between the mature to immature crosslinks was calculated (**Fig. 6**) and decreased two to three fold after depilation with product A. Preliminary results showed that the process of soaking raw sheepskin in product A to depilate removed three to five folds of the skins' total crosslinks. Future experiments will compare the crosslink concentration of product A depilated sheepskin with conventionally pickled skin. It has been reported that there is a relationship between the total crosslink concentration and the strength of skin. Sheepskin, is a relatively weak skin, compared to cow skins, and already has the lowest crosslink content.²¹ Reducing it further may not provide a good outcome. Further testing on leather made from skins depilated with product A will be carried out to determine the effect of this reduction.

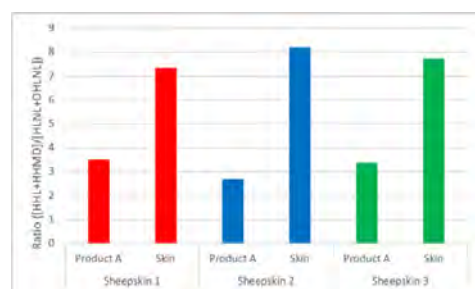


Figure 6. The ratio of mature crosslinks to immature crosslinks in sheepskin before and after depilation with product A.

3.5 Microscopy analysis of the depilated skins showed no signs of damage

SEM was used to examine the surface of the skin after depilation with product A. The depilation treatment did not appear to damage the surface of the skin, and the wool was cleanly removed without damage to the follicle (**Fig. 7**). Bacterial species could be seen on the surface of the skin and the hair follicle, which was not unexpected as two dominant bacterial and a few other bacterial species could be cultured from product A *post* depilation.

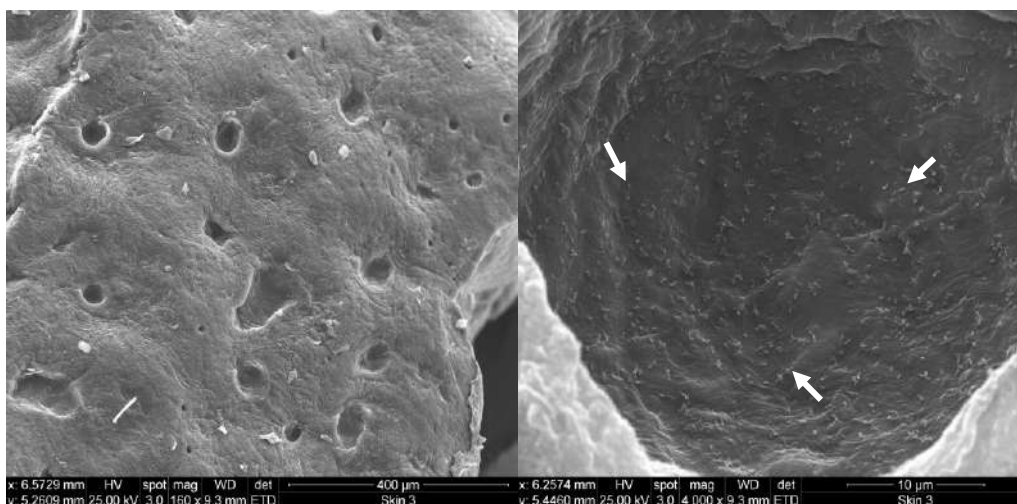


Figure 7. SEM images of the sheepskin that was incubated with sterilised product A and was successfully depilated. (a) The surface of the skin (b) the empty hair follicle; white arrows indicate the presence of bacteria.

Conclusions

We found a natural product that not only depilates sheepskin but also prevents putrefaction of the skin for a significant period of time. The investigation into understanding this phenomena has produced a number of interesting and unpredictable results.

- 1) Skins exposed to product A, have a pH of approximately 4.5 after depilation. Hence, it is possible they could be tanned without further treatment (*i.e.* bate and pickle).
- 2) Four main microbial species were identified from the liquid after depilation was complete. It is possible that they secrete metabolites that are responsible for preserving the skins as well as enzymes responsible for the depilation.
- 3) Microscopy analysis of the depilated skins showed no signs of damage. A full biochemical analysis of the skin components is being carried out to compare the molecular differences between skins depilated with product A and skins depilated with lime-sulfide.
- 4) We have developed a method for depilating sheepskin that avoids the production of toxic waste and is environmentally friendly.

Acknowledgements

The authors would like to thank the Massey University Agricultural and Life Sciences Trust for the financial support (Project number RM 3000028979) and the New Zealand Leather and Shoe Research Association (LASRA) for financial and technical support through the Ministry of Business, Innovation and Employment (MBIE) grant number LSRX1801. The authors would also like to thank the Manawatu Microscopy and Imaging Centre (MMIC) for microscopic technical support.

References

1. Dixit, S., Yadav, A., Dwivedi, P. D. & Das, M.: Toxic hazards of leather industry and technologies to combat threat: a review, *Journal of Cleaner Production*, 87, 39-49, 2015
2. Kanagaraj, J., Senthilvelan, T., Panda, R. C. & Kavitha, S.: Eco-friendly waste management strategies for greener environment towards sustainable development in leather industry: a comprehensive review, *Journal of Cleaner Production*, 89, 1-17, 2015
3. Kamini, N. R., Hemachander, J., Geraldine Sandana Mala, J. & Puvanakrishnan R.: Microbial enzyme technology as an alternative to conventional chemicals in leather industry, *Current Science*, 77(1), 80-86, 1999
4. Covington, A. D: *Tanning chemistry: the science of leather*, RSC Publishing, 112-133, 2009
5. Thanikaivelan, P., Rao, J. R., Nair, B. U. & Ramasami, T.: Progress and recent trends in biotechnological methods for leather processing, *Trends in Biotechnology*, 22(4), 181-188, 2004
6. Fang, Z., Yong., Y., Zhang, J., Du, G. & Chen, J.: Keratinolytic protease: a green biocatalyst for leather industry, *Applied Microbiology and Biotechnology*, 101(21), 7771-7779, 2017
7. Ranjithkumar, A., Durga, J., Ramesh, R., Rose, C. & Muralidharan, C.: Cleaner processing: a sulphide-free approach for depilation of skins, *Environmental Science and Pollution Research*, 24, 180-188, 2017
8. Saran, S., Mahajan, R. V., Kaushik, R., Isar, J. & Saxena, R. K.: Enzyme mediated beam house operations of leather industry: a needed step towards greener technology, *Journal of Cleaner Production*, 54, 315-322, 2013
9. Sujitha, P., Kavitha, D., Shakilanishi, S., Babu, N. K. C. & Shanthi, C.: Enzymatic dehairing: a comprehensive review on the mechanistic aspects with emphasis on enzyme specificity, *International Journal of Biological Macromolecules*, 118, 168-179, 2018
10. Kandasamy, N., Velmurugan, P., Sundarvel, A., Raghava, R. J., Bangaru, C. & Palanisamy, T.: Eco-benign enzymatic dehairing of goatskins utilizing a protease from a *Pseudomonas fluorescens* species isolated from fish visceral waste, *Journal of Cleaner Production*, 25, 27-33, 2012
11. Wilson, K., Padhye, A. A. & Carmichael, J. W.: Antifungal activity of *Wallemia ichthyophaga* (= *Hemispora stellate* Vuill. = *Torula epizoa* Corda), *Antonie van Leeuwenhoek*, 35(1), 529-532, 1969
12. Güssow, D. & Clackson, T: Direct clone characterization from plaques and colonies by the polymerase chain reaction, *Nucleic Acids Research*, 17(10), 4000, 1989
13. Green, M. R. & Sambrook, J.: Precipitation of DNA with ethanol, *Cold Spring Harbour Protocols*, 2016 (12), [pdb.prot093377](https://doi.org/10.1101/093377), 2016
14. Weisburg, W. G., Barns, S. M., Pelletier, D. A. & Lane, D. J.: 16S ribosomal DNA amplification for phylogenetic study, *Journal of Bacteriology*, 173, 697-703, 1991
15. Fierer, N., Jackson, J. A., Vilgalys, R. & Jackson, R. B.: Assessment of soil microbial community structure by use of taxon-specific quantitative PCR assays, *Applied and Environmental Microbiology*, 71, 4117-4120, 2005
16. Borneman, J. & Hartin, R. J.: PCR primers that amplify fungal rRNA genes from environmental samples, *Applied and Environmental Microbiology*, 66, 4356-4360, 2000
17. Naffa, R., Holmes, G., Ahn, M., Harding, D. & Norris, G. E.: Liquid chromatography-electrospray ionization mass spectrometry for the simultaneous quantitation of collagen and elastin crosslinks, *Journal of Chromatography A*, 1478, 60-67, 2016
18. Naffa, R.: *Understanding the molecular basis of the strength differences in skins used in leather manufacture: a dissertation presented in the partial fulfilment of the requirements for the degree of Doctor of Philosophy at Massey University, Palmerston North*, 2017
19. Lee, H. S., Kwon, M., Heo, S., Kim, M. G. & Kim, G. B.: Characterization of the biodiversity of the spoilage microbiota in chicken meat using next generation sequencing and culture dependent approach, *Korean Journal for Food Science and Animal Resources*, 37(4), 535-541, 2017
20. Bolyen, E., Rideout, J. R., Dillon, M. R., Bokulich, N. A., Abnet, C., Al-Ghalith, G. A., Alexander, H., Alm, E. J., Arumugam, M., Asnicar, F., et al.: QIIME 2: Reproducible, interactive, scalable, and extensible microbiome data science, *PeerJ Preprints* 6, e27295v2, 2018, <https://doi.org/10.7287/peerj.preprints.27295v2>
21. Naffa, R., Holmes, G. & Norris, G. E.: Insights into the molecular composition of the skins and hides used in leather manufacture, *Journal of the American Leather Chemists Association*, 114(1), 29-37, 2019
22. Sizeland, K. H., Edmonds, R. L., Basil-Jones, M. M., Nigel, K., Hawley, A., Stephen, M. & Haverkamp, R. G.: Changes to collagen structure during leather processing, *Journal of Agricultural and Food Chemistry*, 63(9), 2499-25-5, 2015

A NEW FUNGAL ISOLATES APPLICATED TO BOVINE SKIN IN BEAMHOUSE PROCESSES

B. Galarza¹, L. Garro¹, N. Ferreri², L. Elíades², R. Hours³

¹Research Center for Leather Technology (CITEC), INTI-CICPBA, Camino Centenario y 508, (1897) Gonnet, Argentina

²Institute of Botany Carlos Spagazzini, CONICET, FCNM, UNLP, 53 n°477 (B190BAJ), La Plata, Argentina

³Research and Development Center for Industrial Fermentations (CINDEFI), CONICET, UNLP, La Plata, Argentina

a) Corresponding author: betinagal@hotmail.com

b) mariagarro12@gmail.com

c) nati_f@live.com.ar

d) lorenaeliades@yahoo.com; e) hours@biotec.org

Abstract. Some new fungal enzyme extracts were applied on submerged bovine skin in the soaking and unhairing steps. *Clonostachys rosea* (CR), *Emericellopsis minima* (EM), *Purpureocillium lilacinum* (PL), *Penicillium* sp (Psp), *Fusarium oxysporum* (FO), *Acremonium* sp (A) and an unidentified filamentous fungal strain with sterile yellow mycelium (SYM) enzymatic extracts from submerged culture demonstrated a different unhairing capacity observed by SEM.

1 Introduction

Beamhouse area is an important step in leather technology, either in the final quality of the leather or in the contribution to the contamination of effluents. The process of unhairing assisted with enzymes compared to the traditional method brings a decrease of 50% in the effluent sulfide content as well as the suspended solids by 40%, reducing the emission of odors and allowing by oxidation to convert sulfur to sulfate in concentrations that meet established specifications and reduce the cost of effluent treatment (1). The hydrogen sulfide gas generated in the traditional unhairing process can reach maximum values of 2000 ppm after deliming (both at acid and alkaline pH and with organic or inorganic acids, ammonium salts or combinations), while concentrations close to 10-40 ppm were detected in the area near the drum (2). For example, at low concentrations of sodium sulfide, at pH 9 the concentration of gaseous H₂S is higher than the allowed values in work environments (Table 1).

Table 1. Allowed values of SH₂ in effluents and work environments.

	Allowed values in the effluents	Allowed values in work environments			Traditional unhairing
		MAC	VLA-ED	VLA-EC	
Liquid effluent	1 mg/l as S ⁻² [1]				50-120 mg/l de S ⁻² [7,8]
Gaseous effluent	0.008 ppm SH ₂ [2]				20-40 ppm SH ₂ [7,8] 2000 ppm SH ₂ [9]
Solid waste	500 mg SH ₂ /kg [3]	10 ppm [4]	5 ppm [5]	10 ppm [6]	500-1500 mg SH ₂ /kg [7,8]

^[1](3); ^[2]Ministry of the Argentina Nation, National Law N°24.051, decree N°831/1993, (1993) Hazardous Waste Law, Annex II, table 10, Air quality guide levels; ^[3]Annex V, 1-1.7, Physical parameters of sludges; ^[4]MAC (Maximum permissible concentration to which a worker can be exposed 8 h a day, 5 days a week); ^[5]VLA-ED (Environmental Limit Value, for an exposure for 40 h per week); ^[6]VLA-EC (Environmental Limit Value for a short-term exposure) (4);^[7](5);^[8](6);^[9](2).

Enzyme use brings advantages for the environment but its application is limited. Sometimes the mechanism of proteolysis cannot be controlled totally because the enzymatic action on the structure of the collagen reticular layer lasts, influencing remarkably the properties of the finished leather.

The enzymatic unhairing mechanism consists of two simultaneous processes: sulfitolysis mediated by keratinolytic enzymes and proteolysis by proteases, especially of the endopeptidase type. The characterization of enzymatic extracts allows controlling the proteolysis mechanism so that its action does not attack the reticular structure.

However, keratinases would be the specific enzymes capable of acting as proteolytic depilating agents and degrading keratin. They have been isolated, characterized and purified from different microorganisms such as fungi, actinomycetes and other bacteria.

Especially the fungi belonging to the three types of dermatophyte group: *Microsporum*, *Trichophyton* and *Epidermophyton* and other genera belonging to the fungi imperfecti genre (*Chrysosporium*, *Aspergillus*, *Alternaria*, *Trichuris*, *Curvularia*, *Cladosporium*, *Fusarium*, *Geomyces*, *Gliomastix*, *Paecilomyces*, *Scopulariopsis*, *Penicillium* y *Doratomyces*) have been reported as good producers of keratinolytic enzymes (7; 8).

This document provides a template and guidelines for authors using MS Word or similar word-processor to prepare a conference proceedings paper. Please save this file and amend the dummy text for your needs.

2 Objectives

New fungal species with potential industrial application isolated from soil with high keratinolytic activity *in vitro*, were applied in bovine skin in the soaking and unhairing stages. Morphological changes were observed by SEM.

3 Materials and methods

3.1 Isolation, culture and characterization of fungal extracts

Fungal strains were isolated from crabs dwell at alkaline soils of coast of Buenos Aires province by soil washing method (9) and further drying in filter paper (10). Strains were isolated in malt extract agar with antibiotics.

Acremonium sp Link 1809: (A), *Clonostachys rosea* (Preuss) Mussat 1901: (CR), *Emericellopsis minima* Stolk 1955: (EM), *Purpureocillium lilacinum* (Thom) Samson (Luangsa-ard et al.): (PL), *Penicillium* sp Link 1809: (Psp), *Fusarium oxysporum* Schltdl. 1824: (FO) and an unidentified filamentous fungus strain with sterile yellow mycelium (SYM) were the selected fungal strains from keratinolytic screening between other twenty isolated.

Fungal crude enzyme extracts (EE) were obtained by submerged liquid culture (batch) with 1% hair waste substrate from the hair-saving unhairing process in Sabouraud breeding ground. Cultures

were incubated 8 days at $30\pm 1^\circ\text{C}$ in orbital agitation at 180 rpm and biomass was separated by filtration through a $0.45\ \mu\text{m}$ membrane.

3.2 Assay of keratinolytic activity

Keratinolytic activity was assayed by using hair waste as substrate (washing with tensioactives, dried at 45°C , ground, autoclaved at 121°C and retained with $850\ \mu\text{m}$ sieve, USA Standard ASTM E 11-61).

Reaction mixture containing $150\ \mu\text{l}$ of EE and the 1% (w/v) substrate in buffer Tris-HCl 0.1 M, pH 9 (11), Isogras AN 0.1% $50\ \mu\text{l}$, Baymol AZ 0.5% $50\ \mu\text{l}$ and biocide TCMTB (relation biocide/enzyme (w/w): $100\ \mu\text{g}$ biocide/ $1\ \mu\text{g}$ CE protein) was incubated at 37°C with agitation (100 rpm) for 60 min. Reaction was stopped by addition of 1 ml of trichloroacetic acid (TCA) 10% (w/v), centrifuged ($5000\ \times\ \text{g}$, 15 min) and the supernatant was measured at 280 nm (triplicate). Reaction blanks were performed by incubation 60 min: substrate, tensioactives and buffer. After that EE, biocide and TCA 10% (w/v) were added and procedure was the same as before. Keratinolytic activity unit (U_{ker}) was defined as the amount of enzyme that, under the test condition, causes an increase of $0.01\ \text{Abs}_{280\text{nm}}$ per minute.

3.3 Assay with submerged skin bovine in fungal extracts

Pieces of fresh bovine skin from the butt of 1 cm by 1 cm were placed in glass tubes of 11 cm length and 2.5 cm width with 5 ml of different solutions and reagents. In the soaking step, EE of different fungal cultures with 0.1% Isogras AN and the biocide TCMTB (0.2% w/w wet skin) were incubated for 4 h at 25°C with agitation (40 rpm). In the unhairing step, after soaking, 0.5% Baymol AZ was added in each reaction mixture, incubated for 48 h at 25°C with agitation (40 rpm).

Controls: a. 5 ml Buffer 0.1 M Tris-HCl, biocide TCMTB (0.2% w/w wet skin); b. 5 ml Buffer Tris-HCl (0.1 M, pH 9), 0.1% p/v Isogras AN, 0.5% Baymol AZ and biocide (0.2% w/w wet skin); a and b incubation was done during 48 h at 25°C with agitation (40 rpm); c. fresh skin without treatment and incubation.

3.4 SEM observation

After completion of the treatments, samples of skin were fixed, post-fixed in 4% formaldehyde and dehydrated in ethanol 30%, 50%, 70% and 100% (12). After critical point drying and metalized, samples were observed by Scanning Electron Microscope (FEI-Quanta 200, LIMF Research Laboratory on Physical Metallurgy, School of Engineering, National University of La Plata, Argentina).

4 Results and discussion

4.1 Assay of keratinolytic activity

The behavior of the selected fungal extracts in relation to its keratinolytic activity is shown in Figure 1. Enzymatic activities decreased in the following order: SYM>FO>CR>>Psp>PL>A. SYM produced an EE with the highest enzymatic activity: $9.06\ U_{\text{ker}}$ while EM produced the less ($1.5\ U_{\text{ker}}$). The other strains, A, FO, CR, Psp, PL, presented intermediate keratinolytic activities, in decreasing order, respectively. These last strains have been reported as keratinolytic strains (13; 14; 15; 16; 17).

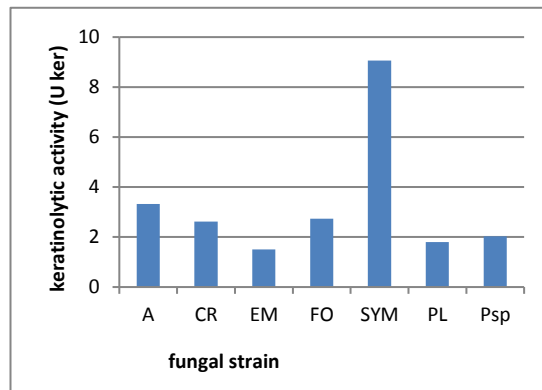


Fig. 1. Keratinolytic activity (U_{ker}) of different fungal enzyme extract (see text for details).

4.2 SEM observation

In Fig. 2 skin control with buffer and biocide, epidermis and hair without modification is observed. Changes in the skin were observed depending on the fungal strain. FO EE showed the greatest effect. In Fig. 3 the absence of epidermis, visible dermal papilla and empty hair follicles are appreciated. In Fig. 4 y 5, *Fusarium oxysporum* EE and *Acremonium* sp EE, respectively, caused strong changes: epidermis removed, papillary layer exposed and hair layers detached.

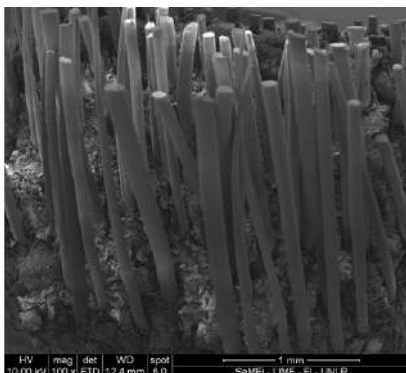


Fig. 2. Control 100 X

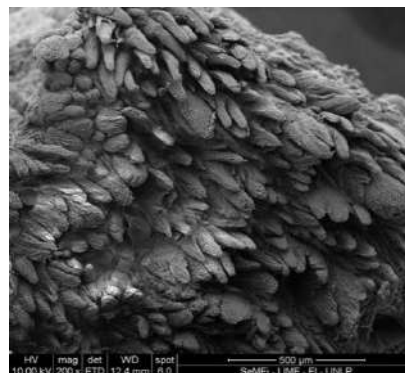


Fig. 3. *Fusarium oxysporum* EE 200X

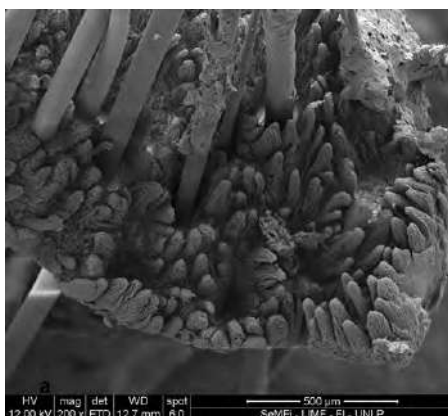


Fig. 4. *Fusarium oxysporum* EE 200 X

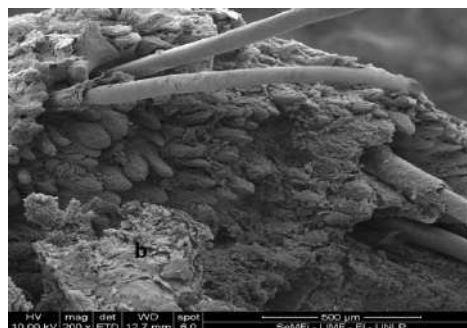


Fig. 5. *Acremonium* sp EE 200 X

In Fig. 6 and 7, PL EE has not produced changes in the skin: hair and epidermis remained intact, while with SYM EE, detachment of epidermis and removal of hairs.

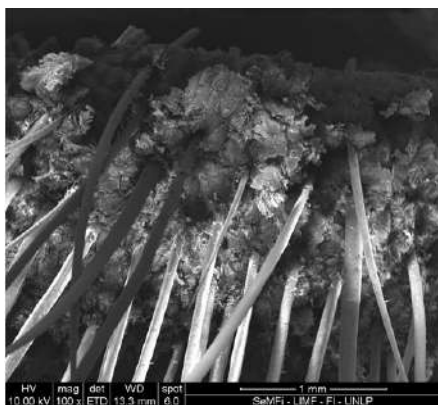


Fig. 6. *Purpureocillium lilacinum* EE 100 X

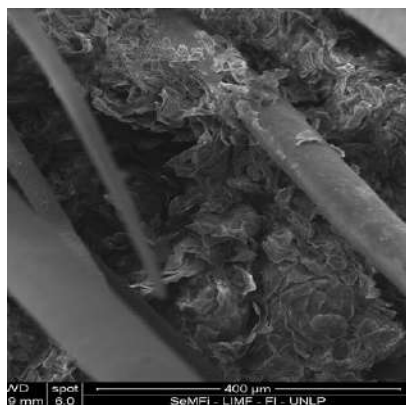


Fig.7. Sterile yellow mycelium strain EE 400 X

Psp EE (**Fig. 8**) and CR EE, skin presented normal characteristics, hair and epidermis with normal patterns. In **Fig. 9**, EM EE produced a detachment of hair follicle sheath.

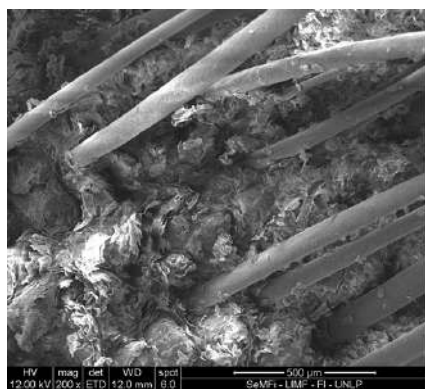


Fig. 8. *Penicillium* sp EE 200 X

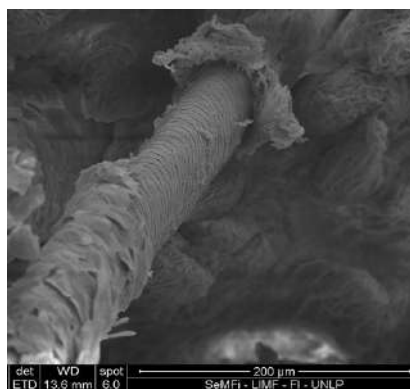


Fig. 9. *Emercicellopsis minima* 800 X

5 Conclusions

Submerged liquid culture with keratin as inductor produced keratinolytic enzymes useful for unhairing step. *Fusarium oxysporum* enzymatic extract showed the greatest effect on the skin, thus the relationship between keratinolytic activity and depilatory effect was found. However, it is necessary to find the optimal conditions to avoid the damage of collagen and enable its application as a sustainable technology.

References

1. Crispim, A. & Mota, M.: *Unhairing with enzymes*, *Journal of the Society of Leather Technologists and Chemists*, 87 (5), 198-202, 2003.
2. Skrabs, R.: *Über die Gefahren des Schwefelwasserstoffs bei der Lederherstellung*, *Das Leder*, 27, 153-157, 1976.
3. ACUMAR (Cuenca Authority Matanza Riachuelo): *Resolutions: 001/2007-336/2003, Entity for the environmental sanitation plan*, Government of the Nation, Argentina, 2003.
4. Instituto Nacional de Seguridad e Higiene en el Trabajo (INSHT). (2015). *Professional exposure limits for Chemical Agents in Spain*. doi: www.insht.es/Inshtweb/contenidos/documentacion, 2015.
5. Frentrup, W. & Buljan, J. (2000). *Hair-save-unhairing methods in leather processing*. United Nations Industrial Development Organization (UNIDO), US/RAS/92/120, 1-37, 2000.

-
6. Galarza, B., Garro, M., Martegani, J. & Hours, R.: Characterization and Evaluation of Fungal Enzymatic Pool with Unhairing Activity. *Journal of the Society of Leather Technologists and Chemists*. 100 (5), 257-262, 2016.
 7. Friedrich, J., Gradišar, H., Mandin, D. & Chaumont, J.: Screening fungi for synthesis of keratinolytic enzymes. *Letters of Applied Microbiology*, 28, 127-130, 1999.
 8. Galarza, B., Garro, M., Gortari, C., Bonfranceschi, A., Hours, R. & Cantera, C.: From a problem of solid waste to an useful product in beamhouse process, *Journal of AQEIC*, 65 (2), 49-55, 2014.
 9. Parkinson, D. & Williams, S.: A method for isolating fungi from soil microhabitats, *Plant and Soil*, 13, 347-355, 1961.
 10. Widden, P. & Parkinson, D.: Fungi from coniferous forest soils. *Canadian Journal of Botany*, 51(12), 2275-2290, 1973.
 11. Yamamura, S., Morita, Y., Hasan, Q., Yokohama, K. & Tamiya E.: Keratin degradation: a cooperative action of two enzymes from *Stenotrophomonas* sp., *Biochemical and Biophysical Research Communications*, 294, 1138-1143, 2002.
 12. Garro, L., Galarza, B., Greco, C. & Hours, R.: Unhairing of Bovine Skin with Fungal Enzymes by Immersion and Spread Throughout the Epidermis, *Journal of the Society of Leather Technologists and Chemists*, 103, 28-34, 2019.
 13. Singh, I.: Extracellular keratinase of some dermatophytes, their teleomorphs and related keratinolytic fungi, *European Journal of Experimental Biology* 4(4):57-60, 2014.
 14. Kumar, J. & Kushwaha, R.: Screening of fungi efficient in feather degradation and keratinase production, *Archives of Applied Science Research* 6 (1):73-78, 2014.
 15. Dalee, A., Chehama, M., Sali, K., Hayeeyusoh, N. & Hayeewangoh, Z.: Keratinase-producing fungi from local environmental samples of Far South Thailand and their efficiency in hydrolyzing keratinous wastes, *IOP Conf. Series: Journal of Physics: Conf. Series* 1097, 012036, doi :10.1088/1742-6596/1097/1/012036, 2018.
 16. Wang, Q. & Liao, M.: Biodegradation of feather wastes and the purification and characterization of a concomitant keratinase from *Paecilomyces lilacinus*, *Applied Biochemistry and Microbiology*, 50(3), 279–285, 2014.
 17. Eliades, L. Cabello, M., Voget, C., Galarza, B. & Saparrat, M.: Screening for alkaline keratinolytic activity in fungi isolated from soils of the biosphere reserve "Parque Costero del Sur" (Argentina), *World Journal of Microbiology and Biotechnology* 26(11), 2105-2111, 2010.

MEASUREMENT OF LEATHER SURFACE: VARIABILITY IN THE MEASUREMENT USING ELECTRONIC AND PIN WHEEL DEVICES ON DIFFERENT KIND OF LEATHERS

R. Mascolo¹, G. Calvanese¹, C. Bruno², P. De Rosa-Giglio², F. Pepe², G. Zorzi²

1 Stazione Sperimentale per l'Industria delle Pelli e delle Materie Concianti - Via Campi Flegrei, 34, 80078 Pozzuoli (NA) - Italy

2 UNIC - Italian Tanneries - Via Brisa, 3, 20123 Milano- Italy

a) r.mascolo@ssip.it

Abstract. The measurement of the surface of leather represents the most important measure for tanneries and their customers. From tanneries point of view, the entire tanning process is economically quantifiable by the amount and value of the surface of the leather sold. However, compared to the other goods and raw materials whose value is defined by a measure, the determination of leather surface is not univocal. Many different aspects do not allow a clear and accurate measurement. For leather area, in fact, there are no certified reference materials, the measurements can be performed with different devices and there is a high variability in measurements depending on the product characteristics of the different items on the market (e.g. leather for gloves, automotive, footwear, etc). The reference tolerances for leather are defined in the International Contract No. 7 established between ICT and ICHLSTA. These tolerances are simply assessed by the percentage difference between the value of the purchased surface and the area checked by an institution from the list agreed between ICT and ICHLSTA on a batch sample. The main problem is that the same contract prescribes the pin-wheel machine as the control device in the event of legal disputes and the ISO 11646:2014 as reference standard for measurement with the consequent difficulties in comparing results, due to the obsolescence of pin-wheel machines that are no longer in use by tanneries in favour of optoelectronic machines. From the other side it is only recently available a standard for area measurement using these machines, that is the ISO 19076:2016. So, with the aim to provide data to clarify area measurement issues, a wide data collection campaign was organized, involving the leather supply chain stakeholders with the aim of qualifying the behaviour of the different leather articles with the different measuring machines, including the pin-wheel machine.

1 Introduction

Finished leather is a material purchased by dimensional measurements. Compared to other goods or raw materials, which value is defined by a measure (weight, flow, power, volume), for leather there is no certified reference material able to represent the numerous kinds of articles on the market. From the metrological point of view, the only possible operation is actually a verification of the calibration status of the measurement machines through rubber calibrated templates. Further complication is the existence of different measuring machines using different measurement principles, with the consequent difficulties in data comparison.

As far as the devices available are concerned, the pin-wheels machine was the most used device until the 1960s, period after which the increasingly massive diffusion of electronic machines began. Due to the high costs of maintenance and management, today, the pin-wheel machines have been completely dismissed by tanneries and their customers in favour of conveyor, roller, scanner and digital machines. Roller and conveyor machines are now the most used devices by tanneries and by their customers, moreover, cutting tables with digital image acquisition and scanners are quite common among leather users. Except for leather for automotive and furniture, whose surface is measured almost exclusively with roller machines, for other intended uses (i.e. gloves, leather goods, apparel, footwear, etc.) there was a random spread of different devices, not necessarily consistent with the final use. It often happens, therefore, that sellers and customers measure the same item with different machines.

As regards documents on the measurement of leather surface, the reference is still in the International Contract No. 7¹ between the International Council of Tanners and The International Council of Hides Skins and Leather Traders Associations, finalized in the 90s, establishing the tolerances allowed in

leather trading. The contract defines the general tolerance of 2% and also accepts a tolerance of 3% for softer, stretcher leathers, such as gloving and clothing leathers, light-weight suedes, chamois leathers, bellies, and upholstery leather. While the International Contract has regulated the leather trade, on the other hand it has severely limited the development of updated technical standards to new electronic equipment. The contract, in fact, requires that the reference equipment to be used in the event of legal disputes is the pin-wheel machine and the measurement method ISO 11646^{2,3} (Area Measurement using pin-wheel machine, last updated in 2014). Except for some national standards (eg. Italy⁶ and Spain^{4,5}) only in 2016, in fact, an international standard for the determination of the leather area using optoelectronic machines was published, that is ISO 19076⁷. This standard provides general characteristics of the modern devices and general procedures for area assessment.

However, the obligation of verification with pin-wheel machines remains, despite only a few units (3-4) are still fully functional among the Institutes agreed between ICT and ICHSLTA for arbitration purposes as at 31st December 2001⁸. Moreover, the entry into force of the MID Directive⁹ in 2016, where machines for dimensional measurements are treated, with all consequent requirements regarding maintenance, calibration and test reporting. For the above, an extensive data collection campaign has been carried out involving all the industrial stakeholders of leather. Starting from the participants to Italian Technical Committee for Leather, UNI/CT13, the project was subsequently shared within CEN/TC 289 with the participation of other European partners. 44 participants have been involved: tanneries, brands and users, laboratories, research institutes and devices manufacturers took part in the project, including 4 Institutes agreed for arbitration purposes by ICT and ICHSLTA.

51 series of tests were carried out using all machines defined in ISO 19076 Section 5.1: n. 15 roller machines (Type A), n. 15 conveyor machines (Type B), n. 1 flatbed scanning machine (Type C) and n. 3 bi-dimensional static measuring devices (Type D). The tests have been carried out on n. 9 conveyor machines with air aspiration and N. 8 pin-wheel machines according ISO 11646.

16 different kind of leather articles, representative different leather uses (gloves, apparel, footwear, leather goods, furniture, automotive), were measured using all the machines above. Thousands of data are now available to qualify the behaviour of the leather for each type of machine with its specific characteristics.

The aim of this work is providing a general frame about how measurements change from a statistical point of view with different devices and according to test results of ISO 11646 and ISO 19076. The purpose is providing objective technical data aimed at updating the regulations and standard in force.

2 Materials and Methods

2.1 Materials

In table 1 samples selected for the project are reported. Each sample consists in a small batch of n. 4 leathers. Samples cover all typical leather destination of use. Different size, shape, origin and tanning process have been chosen.

The calibration and verification of all electronic devices have been carried out using the same 65 dmq and 130 dmq certified templates. These were not suitable for pin-wheel calibration. So different certified templates were used (50, 70, 100 dmq).

Table 1. Samples.

ID.	ARTICLE	ORIGIN	TANNING	SHAPE	DESTINATION
1	Washed	Bovine	Vegetable	Whole	Footwear
2	Wrinkled	Bovine	Chrome	Whole	Footwear
3	Calf	Bovine	Chrome	Side	Leather goods
4	Calf	Bovine	Vegetable	Whole	Leather goods
5	Goat	Caprine	Chrome	Whole	Leather goods
6	Lamb	Ovine	Chrome	Whole	Glove
7	Suede	Caprine	Chrome	Whole	Footwear
8	Washed	Ovine	Chrome	Whole	Footwear
9	Wrinkled	Ovine	Chrome	Whole	Footwear
10	Calf	Bovine	Chrome	Whole	Apparel
11	Calf	Bovine	Chrome	Side	Footwear
12	Interior Upholstery	Bovine	Glutaraldehyde	Whole	Automotive
13	Sofa	Bovine	Chrome	Whole	Upholstery
14	Suede (split)	Ovine	Chrome	Whole	Apparel
15	Ovine	Ovine	Chrome	Whole	Apparel
16	Ovine with hairs	Ovine	Chrome	Whole	Apparel

2.2 Apparatus and Devices

The following devices for assessment of surface have been used:

- Roller machines (Type A, ISO 19076): EDA, GER, WEGA, Selin devices
- Conveyor machines (Type B, ISO 19076): GER, Selin and Mostardini devices
- Flatbad scanner (Type C, ISO 19076): Muver
- Bi-dimensional devices (Type D, ISO 19076): Teseo, Atom and Comelz
- Pin-wheel machine (ISO 11646): Gozzini, Tomboni and Turner

The assessment of physical and mechanical properties of samples have been carried out by:

- tensile testing machine with a 1000 N loading cell class 0,5 according to ISO 7500-1
- thickness gauge accordance with to ISO 2589.

2.3 Procedures and Methods of Analysis

Where possible, all samples have been stored for conditioning for 48 hours in standard (20/65) or alternative (23/50) environment in accordance with ISO 2419:2012.

After conditioning, measuring devices have been calibrated and for each sample calibration procedures have been carried out as specified respectively in ISO 19076 and ISO 11646. Samples have been measured according to ISO 19076, section 8.5 and 8.6. The results, if required, have been corrected using the correction factor F as reported in point 9.3 of ISO 19076.

For the comparison of results, as specified in International Contract No. 7, surface values have been reported as total area to simulate the batch. A batch consisted in three leathers. The fourth one of each sample has been mechanically characterized for identify a possible correlation of results with leather properties.

All three leathers of each sample have been measured 10 times in repeatability conditions for subsequent statistical analysis. From the operative point of view, for each device, parameters with no prescriptions in the standards that could affect the measurement have been identified.

About conveyor machines, it must be noticed that ISO 19076 does not make any reference to air aspiration system. Nevertheless, the tests were performed with and without air aspiration, to verify the effects on area measurement.

For roller machines, both the effects of rollers speed and feeding side have been assessed to determine whether or not they affect the measure. Moreover, for sides leathers (cut in halves on the backbones), the direction of feeding have been evaluated not only as reported in ISO 19076, i.e. the straight edge should form an angle of 10° to 20° with the feeding direction, but also with a 0° angle to the feeding direction.

For flatbed scanner machines, sensor line array could touch samples with evident wrinkles during translation. In these cases, it's usual to flatten the sample disposing a transparent glass over them. This sample manipulation is not expected in ISO 19076, but however additional tests have been carried out.

The effects of all the above have been assessed only for leather n. 1 of each sample. Moreover, in order to verify that the 44 surface measurements did not modify the physical characteristics of samples (i.e. permanent deformation or leather damage), SSIP has carried out the batches measurement both at the beginning and at the end of the trials, with subsequent data comparison.

Finally, a mechanical characterization of samples has been carried out to verify any correlation between the results variability and deformability of the material, due to the application of a specific load, according to ISO 13934-1:2013.

2.4 Statistical Analysis

The behaviour of each leather sample has been defined through a robust analysis, as specified in ISO 13528:2015 *Statistical methods for use in proficiency testing by interlaboratory comparison*. For each device, percentage repeatability and reproducibility (r and R) have been assessed for each n. 1 leather of samples. Before the robust analysis, a normal distribution test, according to Anderson-Darling, has been carried out on each set of data. Finally, a t -test has been used to determine if the averages of two sets of data were significantly different, to evaluate possible differences between the first and the last trial (both carried out in SSIP).

3 Test Results

3.1 Robust Analysis

In table 2 are summarized the results of robust analysis for all samples with reference to pin-wheel machine and electronic devices. For scanning machines, only 1 participant attended to the project, so no statistical assessment was possible.

Where:

- p is the number of participants
- $Mean$ is the average value assessed in the robust analysis
- r is the percentage repeatability
- R is the percentage reproducibility

It is evident that for big leathers (automotive and upholstery) is not possible yet any comparison as only roller machine measurements were available.

Table 2. Robust analysis for pin-wheel, roller, conveyor and bi-dimensional machines.

ID.	PIN-WHEEL MACHINE				ROLLER MACHINE (TYPE A)				CONVEYOR MACHINE (TYPE B)				BI-DIMENTIONAL MACHINES (TYPE D)			
	p	MEAN (dmq)	R (%)	r (%)	p	MEAN (dmq)	R (%)	r (%)	p	MEAN (dmq)	R (%)	r (%)	p	MEAN (dmq)	R (%)	r (%)
1	8	66	12,1%	1,9%	15	63,1	12,1%	2,4%	15	60,7	3,2%	1,7%	3	61,4	3,1%	0,5%
2	8	69	4,3%	1,5%	14	68,0	3,9%	1,5%	15	66,9	1,6%	0,9%	3	68,1	5,2%	0,3%
3	8	158	2,4%	0,7%	14	157,1	1,8%	0,5%	14	157,3	1,4%	1,1%	3	158,0	2,8%	0,2%
4	8	90	1,3%	0,0%	14	89,8	2,0%	0,0%	15	89,0	2,0%	0,9%	3	90,1	2,2%	0,1%
5	8	59	4,7%	1,5%	14	57,2	4,0%	1,9%	15	56,3	2,8%	1,4%	3	57,9	6,3%	0,5%
6	8	36	4,4%	2,0%	15	36,4	7,4%	2,2%	15	35,4	3,3%	1,5%	3	36,2	5,3%	0,6%
7	8	46	8,3%	1,9%	15	44,3	7,5%	2,5%	15	43,0	1,8%	0,9%	3	43,7	4,7%	0,5%
8	8	49	12,0%	2,5%	15	47,2	9,3%	2,8%	15	46,9	1,3%	0,8%	3	47,4	3,9%	0,3%
9	8	83	6,5%	1,3%	14	81,1	5,6%	1,9%	15	80,3	1,6%	0,7%	3	81,0	4,0%	0,1%
10	8	51	9,8%	2,3%	15	49,7	8,1%	2,6%	15	48,5	2,8%	1,7%	3	48,9	2,5%	0,6%
11	8	150	2,9%	0,9%	14	147,9	2,4%	1,1%	14	147,8	1,5%	0,7%	3	147,8	2,9%	0,2%
12	-	-	-	-	14	464,6	1,9%	0,4%	-	-	-	-	-	-	-	-
13	-	-	-	-	14	553	2,8%	0,9%	-	-	-	-	-	-	-	-
14	8	53	10,6%	2,0%	15	53,1	9,5%	2,6%	15	51,9	2,1%	0,6%	3	53,1	6,2%	0,5%
15	8	56	8,6%	1,7%	14	56,2	2,7%	0,2%	15	55,9	0,6%	0,6%	3	56,4	2,9%	0,2%
16	8	39	4,6%	2,9%	14	39,3	7,1%	3,5%	15	37,3	6,2%	2,9%	2	40,4	3,4%	1,2%

3.2 Pin-Wheel Results

As demonstrated by results, roller machines show the same behaviour of the pin-wheel ones in terms of repeatability and, above all, reproducibility. It is also evident a systematic overestimation of the results when the pin-wheel machines are used. These higher values are probably due to the absence of a temporary feeding blocking system of wheels (e.g. by manual holding) during measurement, as in many roller machines. This determines a significant alteration of the measurement due to the consequent stretching of leather in the direction of feeding.

Moreover, some pin-wheel machines showed a different feeding of leathers, resulting in a different deformation effect on samples. In general, the results seem to be affected by flexibility, presence of wrinkles and deformability of leathers. It should be noticed that, according to ISO 11646, the side of feeding is always with the flesh side upward.

3.3 Roller Machines Results

The results are very similar to those obtained with pin-wheel machines in terms of *r* and *R*. The lower values of surface measured, as explained above, are related to the possibility to avoid alteration of results when the feeding is blocked (i.e. manual blocking for flatten wrinkles).

It was observed that, as it occurs using pin-wheel machines, the lateral distention of wrinkles and the eventual blocking of samples to prevent folding of edges, represent the operation that most influences the results.

As shown in table 3, the direction of feeding and the rotation speed of the roller determine a systematic variation in results. Different series of area measurement were carried out changing the speed from about 25 m/min to 35 m/min and inverting the side of feeding. The results showed that higher speed determines higher values of area and feeding samples with flesh side upward (as carried out by laboratories to be consistent with ISO 11646 principles) causes an increase of measured area as well. In the first case, the higher values are related to the stretching of samples,

while in the second one the differences are probably be related to the different friction behaviour of leather surfaces. More investigations are needed on these issues.

Table 3. Percentage variations due to roller speed increase and inversion of feeding side.

ID.	SPEED	SIDE
1	+4,2%	+1,7%
2	+0,9%	0,0%
3	0,0%	-0,8%
4	0,0%	-0,8%
5	0,0%	-0,6%
6	+2,5%	0,0%
7	+4,2%	0,0%
8	+2,3%	-1,5%
9	0,0%	-1,0%
10	+3,2%	0,0%
11	+0,9%	-1,2%
12	0,0%	-0,8%
13	+2,0%	-0,6%
14	+7,0%	0,0%
15	-3,0%	-1,9%
16	+1,6%	0,0%

Other interesting results are related to half leathers (side leathers). ISO 19076 standard defines a direction of feeding forming an angle between 10° and 20°. Measuring in such a way, in some cases it was observed that the weight of sample, suspended from the plane down to the floor, can generate an angular momentum with the consequential slippage of leather over the sensors. This slippage could determine a light overestimation of the results.

3.4 Conveyor, Digital and Scanner Results

For conveyor machines, the repeatability and reproducibility are lower but, during the measurements, wrinkles and folding on edges can determine an underestimation of the leather surface. The activation of air aspiration flattens wrinkles and avoids folds, resulting in small area increments. It shall be noticed that air aspiration is needed for big half leathers. For these samples (i.e. n. 3 and n. 11) the weight of leather outside the wires o belts of the machine could determine a slippage under the sensors provoking bad results.

As for flatbed scanner devices, the results are very similar to conveyor machines ones. The application of glasses to flatten wrinkles shows a similar effect of the air aspiration of conveyor machine. Table 4 shows the average values of conveyor, bi-dimensional and flatbed scanner machines that are the devices where surface is approximated to the projection of the sample on the horizontal plane.

On the other hand, as for bi-dimensional machines, some problems have been noted during measurements. Image acquisition depends from the identification of the edges and the borders of leathers by the software used and it is strictly related with the colour contrast between the samples and the plane of the device (e.g. white leather on white surface).

Moreover, there have been observed problems in the assessment of the surface of sample n. 16, that is an ovine leather with long hair. During the detection of the borders, hair has been always confused with leather so that the measured area results higher.

Table 4. Percentage variations due to roller speed and side feeding.

ID.	ARTICLE	CONVEYOR MACHINE	CONVEYOR WITH ASPIRATION	DIGITAL MACHINES	SCANNER MACHINE	SCANNER MACHINE WITH GLASS PLATES
		MEAN (DMQ)	MEAN (DMQ)	MEAN (DMQ)	MEAN (DMQ)	MEAN (DMQ)
1	WASHED	60,7	61,5	61,4	60,3	61,8
2	WRINKLED	66,9	67,2	68,1	66,8	67,2
3	CALF	157,3	157,4	158,0	157,6	0,0
4	CALF	89,0	89,3	90,1	89,3	89,4
5	GOAT	56,3	56,5	57,9	56,2	56,4
6	LAMB	35,4	35,9	36,2	35,0	35,3
7	SUEDE	43,0	43,5	43,7	42,8	43,3
8	WASHED	46,9	47,1	47,4	46,6	47,2
9	WRINKLED	80,3	80,8	81,0	80,4	80,7
10	CALF	48,5	49,1	48,9	48,4	48,6
11	CALF	147,8	147,9	147,8	147,7	0,0
12	BOVINE	-	-	-	-	-
13	BOVINE	-	-	-	-	-
14	SUEDE	51,9	52,6	53,1	51,7	52,4
15	OVINE	55,9	56,1	56,4	55,9	55,9
16	OVINE WITH HAIRS	37,3	37,9	40,4	37,6	38,3

3.5 Physical properties of samples

To assess any relation between reproducibility in area measurement and the physical properties of leathers, flexibility and deformability characteristics of materials have been investigated. In particular, the following parameters have been determined:

- Percentage elongation at 100 N, in accordance with ISO 13934-1:2013
- Flexibility, according to an SSIP internal method. In this method, a stripe of leather measuring 300 mm x 50 mm is moved on the border of a horizontal plane to another plane at 45°. The length in millimetre of test piece that folds under its weight till touch the 45° plane is the flexibility of leather. The greater this length, the lower is the flexibility.

The results reported in table 5 are only referred to pin wheel and roller machines, that are the devices whose higher values of reproducibility have been assessed and where the feeding of leather in a stretched mode or in tension could determine more evident variation in the results.

Table 5. Physical performances of samples.

ID.	PIN-WHEEL MACHINE		ROLLER MACHINE		PHYSICAL PARAMETERS		
	MEAN	R (%)	MEAN	R (%)	THICKNESS (MM)	FLEXIBILITY (MM)	%ELONGATION
1	66	12,1%	63,1	12,1%	1,0	40,0	20%
2	69	4,3%	68,0	3,9%	1,2	16,3	8%
3	158	2,4%	157,1	1,8%	1,5	6,4	3%
4	90	1,3%	89,8	2,0%	0,9	8,1	4%
5	59	4,7%	57,2	4,0%	2,0	22,1	11%
6	36	4,4%	36,4	7,4%	0,8	56,2	28%
7	46	8,3%	44,3	7,5%	1,2	35,4	18%
8	49	12,0%	47,2	9,3%	1,1	25,3	13%

9	83	6,5%	81,1	5,6%	1,1	27,8	14%
10	51	9,8%	49,7	8,1%	0,7	60,5	30%
11	150	2,9%	147,9	2,4%	1,3	20,2	10%
12	-	-	464,6	1,9%	1,7	18,0	9%
13	-	-	553	2,8%	1,0	34,3	17%
14	53	10,6%	53,1	9,5%	0,5	23,4	12%
15	56	8,6%	56,2	2,7%	1,2	36,7	18%
16	39	4,6%	39,3	7,1%	0,9	49,7	25%

3.6 Data Comparison ISO 11644 vs ISO 19076

Finally, in Table 6 are reported the area measurement of the samples considered as a batch, in accordance with ISO 11644 and ISO 19076 for electronic devices.

Table 6. Area of the samples as a batch according to ISO 11646 and ISO 19076.

ID.	PIN-WHEEL (DMQ)	ROLLER (DMQ)	%Δ	CONVEYOR (DMQ)	%Δ	CONVEYOR ASP. (DMQ)	%Δ	DIGITAL (DMQ)	%Δ	SCANNER (DMQ)	%Δ
1	199	192	-4%	183	-8%	185	-7%	185	-7%	182	-9%
2	210	209	-1%	205	-3%	206	-2%	209	-1%	205	-3%
3	512	509	-1%	509	-1%	511	0%	511	0%	508	-1%
4	265	264	0%	261	-1%	262	-1%	265	0%	262	-1%
5	162	159	-2%	155	-4%	156	-3%	160	-1%	155	-4%
6	115	115	0%	112	-3%	113	-2%	114	-1%	110	-4%
7	126	123	-3%	119	-5%	121	-4%	121	-4%	119	-6%
8	146	143	-2%	141	-3%	141	-3%	142	-3%	139	-4%
9	214	209	-2%	207	-3%	207	-3%	209	-2%	206	-4%
10	174	170	-2%	165	-5%	167	-4%	167	-4%	165	-5%
11	422	417	-1%	415	-2%	417	-1%	416	-2%	416	-1%
12	-	1409	-	-	-	-	-	-	-	-	-
13	-	1679	-	-	-	-	-	-	-	-	-
14	156	155	0%	151	-3%	153	-2%	155	-1%	150	-4%
15	182	181	0%	180	-1%	181	0%	182	0%	181	-1%
16	98	100	2%	95	-3%	97	-1%	102	5%	95	-2%

As reported in the International in section 17.2 of the International Contract N. 7, in the table a percentage comparison between the average values from robust analysis for electronic devices with pin-wheel ones has been simulated. Data are the mean of the results of the participants. In table 6 is evident that in some cases, depending on leather type, the percentage difference is not compliant with the tolerances.

4 Conclusions

On the basis of the data of interlaboratory trials, the feedback of participants and the direct observations of measurement activities, the following remarks can be made:

- the pin-wheel machine shows a variability in results like the roller machine;
- the data are strongly affected by the measurement device principle and procedures, so that the comparison between area measurements carried out with different machines could be inconsistent, notably for small, elastic and flexible leathers for which even small differences in measure could determine percentage variations near to the prescribed International Contract N. 7 tolerances.

- the interlaboratory trials revealed the need to update the ISO 19076. The standard should be revised to reduce the variability factors identified in this trial and the measurement procedure should be accurately specified for each device.

However, in general, the aim of this work is not the identification of the best couple leather/machine or indicating a suitable machine. Each machine on the market is suitable for an effective area measurement for any leather as it is evident by data collected.

We would like to thank all participants: electronic machines manufacturers, tanneries, clients, research centres and industrial associations for their availability in this trial. As the list is very long and it impossible to be included in this work, we are going to thank each one personally.

References

1. *International contract No. 7 — Finished leather*
2. *ISO 11646:1993 (IULTCS/IUP 32) Leather - Measurement of area*
3. *ISO 11646: 2014 (IULTCS/IUP 32) Leather - Measurement of area*
4. *UNE 59050:1993 Leather. Measurement of area*
5. *UNE 59050:2012 Leather. Strain-free surface area measurement using optoelectronic equipment*
6. *UNI 11380:2010 Guideline for the measurement of leather surface by means of optoelectronic machine*
7. *ISO 19076:2016 (IULTCS/IUP 58) Leather - Measurement of leather surface - Using electronic techniques*
8. *Measurement Institutes Agreed Between ICT and ICHSLTA for Arbitration Purposes as at 31st December 2001*
<https://leathercouncil.org/what-we-do/measurement-institutes/>
9. *Measuring Instruments Directive 2014/32/UE*



WE THANK ALL OUR BUSINESS PARTNERS AND SUPPORTERS

CONGRESS PARTNERS



TEGEWA e.V. German Chemical Industry Association for Textile-, Tanning Chemicals and Detergents



FILK Freiberg gGmbH German Leather and Collagen Research and Testing Institute



VdL German Tanners Association



COTANCE Confederation of National Associations of Tanners and Dressers of the European Community

MEDIA PARTNERS



ProLeder (German)



International Leather Maker (English)



Leather Age (Indian)



Arsutoria Tannery (Italian)



china leather.org (Chinese)



ABQ TIC Revista Do Couro (Brazilian)



World Leather



BUSINESS PARTNERS

PLATINUM



GOLD



SILVER



BRONZE



This project is co-financed by budgetary resources on the basis of a resolution of the Saxon State Parliament.

Supported by WIRTSCHAFTSFÖRDERUNG SACHSEN